THE ASTROPHYSICAL JOURNAL

THE UNIVERSITY OF CHICAGO PRESS
CHICAGO, ILLINOIS

THE CAMBRIDGE UNIVERSITY PRESS
LONDON

THE MARUZEN-KABUSHIKI-KAISHA
TOKYO, OSAKA, KYOTO, FUKUOKA, SENDAI

THE MISSION BOOK COMPANY
SHANGHAI

~~Astron~~
~~A~~

THE
ASTROPHYSICAL JOURNAL

111

An International Review of Spectroscopy and Astronomical Physics

EDITORS

GEORGE E. HALE
Mount Wilson Observatory of the Carnegie Institution of Washington

EDWIN B. FROST
Yerkes Observatory of the University of Chicago

HENRY G. GALE
Ryerson Physical Laboratory of the University of Chicago

COLLABORATORS

JOSEPH S. AMES, *Johns Hopkins University;* ARISTARCH BELOPOLSKY, *Observatoire de Poulkova;* WILLIAM W. CAMPBELL, *Lick Observatory;* HENRY CREW, *Northwestern University;* CHARLES FABRY, *Université de Paris;* ALFRED FOWLER, *Imperial College, London;* CHARLES S. HASTINGS, *Yale University;* HEINRICH KAYSER, *Universität Bonn;* ALBERT A. MICHELSON, *University of Chicago;* HUGH F. NEWALL, *Cambridge University;* ERNEST F. NICHOLS, *Nela Laboratory, Cleveland;* ALFRED PEROT, *Paris;* CARL RUNGE, *Universität Göttingen;* HENRY N. RUSSELL, *Princeton University;* SIR ARTHUR SCHUSTER, *Twyford;* FRANK SCHLESINGER, *Yale Observatory*

VOLUME LV

JANUARY–JUNE, 1922

185610
29.11.23

THE UNIVERSITY OF CHICAGO PRESS
CHICAGO, ILLINOIS

QB
1
A9
V55-56
Cop.2

Published
January, March, April, May, June, 1922

Composed and Printed By
The University of Chicago Press
Chicago, Illinois, U.S.A.

CONTENTS

NUMBER I

PAGE
Color-Transparency of Ray-Filters in Use at Yerkes Observatory. Ernest C. Bryant 1
Systematic Corrections to Spectroscopic and Trigonometric Parallaxes. Gustaf Strömberg 11
New Measurements of Stellar Radiation. W. W. Coblentz . . 20
Solar Constant, Sun-Spots, and Solar Activity. Anders Ångström. 24
The Orbits of the Spectroscopic Binaries 1 Hydrae and 75 Cancri. R. F. Sanford 30
An Investigation of the Constancy in Wave-Length of the Atmospheric and Solar Lines. Charles E. St. John and Harold D. Babcock. 36
The Wave-Length in Astronomical Interferometer Measurements. J. A. Anderson 48
Minor Contributions and Notes: On the System of Procyon. Joseph Lunt 71

NUMBER II

The Spectrum of the Corona as Observed by the Expedition from Lowell Observatory at the Total Eclipse of June 8, 1918. V. M. Slipher. 73
Spectrophotometric Methods for Determining Stellar Luminosity. Bertil Lindblad 85
The Theory of Ionization and the Sun-Spot Spectrum. Henry Norris Russell 119

NUMBER III

The Excitation of the Enhanced Spectra of Sodium and Potassium in a Low Voltage Arc. Paul D. Foote, W. F. Meggers, and F. L. Mohler 145
The Vacuum-Spark Spectra of the Metals. Edna Carter. . . 162
The Masses and Densities of the Stars. Frederick H. Seares. . 165

PAGE

ON THE CALCULATION OF MASSES FROM SPECTROSCOPIC PARALLAXES. Henry Norris Russell 238

ON THE UPPER LIMIT OF DISTANCE TO WHICH THE ARRANGEMENT OF STARS IN SPACE CAN AT PRESENT BE DETERMINED WITH SOME CONFIDENCE. J. C. Kapteyn and P. J. Van Rhijn 242

A CORRECTION. F. H. Seares 272

NUMBER IV

THE QUANTUM THEORY OF BAND SPECTRA AND ITS APPLICATION TO THE DETERMINATION OF TEMPERATURE. Raymond T. Birge . . 273

THE ARC SPECTRA OF GALLIUM AND INDIUM. H. S. Uhler and J. W. Tanch 291

FIRST ATTEMPT AT A THEORY OF THE ARRANGEMENT AND MOTION OF THE SIDEREAL SYSTEM. J. C. Kapteyn. 302

A CONTINUOUS SPECTRUM FROM MERCURY VAPOR. C. D. Child. . 329

FORMATION AND LIFE OF METASTABLE HELIUM. Fabian M. Kannenstine 345

NOTES ON IONIZATION IN THE SOLAR ATMOSPHERE. Henry Norris Russell 354

NOTICE TO CONTRIBUTORS 360

NUMBER V

PARTIAL EXPLANATION, BY WAVE-LENGTHS, OF THE K-TERM IN THE B-TYPES. Sebastian Albrecht 361

EFFECTIVE WAVE-LENGTHS OF 129 STARS WITHIN 0°5 OF THE NORTH POLE AND OF THE Σ COMPANION OF POLARIS. Ejnar Hertzsprung. 370

ELECTRIC FURNACE EXPERIMENTS INVOLVING IONIZATION PHENOMENA. Arthur S. King 380

CARBON DIOXIDE ABSORPTION IN THE NEAR INFRA-RED. E. F. Barker 391

THE BROADENING OF THE BALMER LINES OF HYDROGEN WITH PRESSURE. E. O. Hulburt 399

THE DISTANCE OF THE ANDROMEDA NEBULA. E. Oepik . . . 406

NOTE ON THE THICKNESS OF AIR REQUIRED TO PRODUCE THE ATMOSPHERIC ABSORPTION BANDS A, *a*, and B. Arthur S. King . . 411

SPECTROPHOTOMETRIC METHODS FOR DETERMINING STELLAR LUMINOSITY. A CORRECTION. Bertil Lindblad 413

INDEX 414

THE
ASTROPHYSICAL JOURNAL
AN INTERNATIONAL REVIEW OF SPECTROSCOPY
AND ASTRONOMICAL PHYSICS

VOLUME LV JANUARY 1922 NUMBER 1

COLOR-TRANSPARENCY OF RAY-FILTERS IN USE AT YERKES OBSERVATORY

By ERNEST C. BRYANT

ABSTRACT

Spectro-photometric transmission curves for two ray-filters in use at Yerkes Observatory, and for three colored glasses used in the Hess-Ives tint photometer are given for 400 to 750 $\mu\mu$. The filters investigated are J 1, M 1, December 1907, Beta 7 and Beta 10; the glasses are a red, a green and a blue-violet.

Lemon-Brace spectro-photometer.—Suggestions as to the adjustment and calibration of this instrument, which was used in obtaining the foregoing curves, are given, and also measurements of the *relative selective absorption of nicol prism and silver strip* from 475 to 750 $\mu\mu$.

Color-curve of the 40-inch objective at Yerkes Observatory is reproduced in Figure 5.

The 40-inch refractor at Yerkes Observatory, although designed only for visual observations, has been available for astronomical photography since 1900 by means of a method at that [illegible] perfected by G. W. Ritchey and described by him in the *Astrophysical Journal* for December of that year. The method consists of the use of a ray-filter which absorbs those waves of short lengths for which the objective is uncorrected, combined with photographic plates which are especially sensitive to the yellow, a color which the ray-filter transmits freely, and which comes in the region for which the color-curve of the 40-inch objective is very nearly flat.

The filters first used by Ritchey were made by Carbutt, of Philadelphia. R. J. Wallace came to Yerkes in 1906 and immediately began fitting filters to the various telescopes, especially to give photo-visual results in connection with the isochromatic plates in use, mainly the Cramer Isochromatic and Trichromatic.

After several trials the 8×10 filter marked "Dec. '07," consisting of a colored gelatine film between two sheets of optical glass, was put into regular use in the parallax program and other work with the 40-inch telescope. After some years the gelatine began to deteriorate at the edges of the film, and the filter was finally superseded by a similar one made by Mees, of the Eastman Research Laboratory. He planned to duplicate the former filter as closely as possible. Of the two which he made, that called "M 1" was put into use in the parallax work in May 1920.

Wallace made similar filters for the 2-foot reflector and the 6-inch ultra-violet camera. On the reflector, filter "Beta 7" 3×3 inches in size, was used from July 1906 until it was accidentally broken in July 1917. On the camera, "Beta 10," 4×5 inches, has been in use from February 1907 till the present time. Both have been shown to give substantially correct photo-visual magnitudes when used with Cramer Isochromatic plates. By comparison with photographic magnitudes found with ordinary plates on the same instruments, color-indices are obtained and spectral types inferred (see *Astrophysical Journal*, **27**, 169, April 1908).

After the accidental breaking of "Beta 7," several others were tried, both Wallace and Eastman; but none was satisfactory. In 1917 Petitdidier furnished two tinted Jena glass filters, No. F [illegible] inches which replaced "Beta 7"; and one 6×6 inches [illegible], called "J 1," has been used on the reflector since 1917.

Photographic determinations of the spectral intensity-curves for Seed 27 plates without ray-filter and for Cramer Trichromatic plates with ray-filter have been made, but no direct measurements of the color transmission of the filters themselves have previously been obtained. The loan of a Lemon-Brace Polarization Spectrophotometer from the Ryerson Physical Laboratory has enabled these determinations to be made this summer, and the following results have been obtained. This instrument has been described in this *Journal*, January 1900, September 1902, and April 1914, but a brief statement of the method used by the author for adjusting and calibrating it may be helpful to those having their first experience with the process.

Referring to Figure 1, the instrument when in adjustment must fulfil the following conditions: (1) slits S_1, S_2, and S_3 must be at the principal foci of their respective objectives; (2) optical axes of collimators C_1 and C_2 and of the telescope T must be in the same plane, which must be perpendicular to the refracting edges of the Brace prism AEI; (3) light from S_1 must strike prism at B, making $AB = 1/4AE$, at the angle of minimum deviation for the Fraunhofer lines D, emerging at F, making $IF = 1/4IE$; (4) light from S_2 similarly must strike the prism at D, making $ED = 1/4EA$, at the angle of minimum deviation for the D lines. It must meet the division plane CI at H, the same place where the light from S_1 meets it, and that part reflected by the silver strip on CI must follow the same direction HF, FJ as the light from S_1. In the instrument used, the Brace prism merely rested on its platform with nothing to locate its position on the platform or its orientation.

After making adjustments (1) and (2), beams of sunlight were reflected into S_1 and S_2, directed so as to emerge through the centers of their objectives. This latter condition was carefully maintained throughout the process. The prism was oriented for minimum deviation of D lines, the slits were opened and coincidence of emerging beams at F was tested by placing a piece of white paper against the face of the prism at that point. The prism was moved parallel to line S_1B, retaining minimum deviation of D lines, until the beam from S_2 reflected at H emerged at F exactly between the beams from S_1 which passed above and below the silver strip at H. Coincidence in direction of emergent beams was tested by receiving them on the white paper held in front of the telescope objective and then beyond the eyepiece J. If not coincident in direction, collimator C_2 must be swung on its axis to obtain coincidence. This will require a repetition of the preceding adjustment. These two adjustments must be thus repeated until the three beams emerge at F in the same vertical line, enter the telescope and emerge at the eyepiece likewise in the same vertical line. The final adjustment of C_2 is made by narrowing S_1 and S_2 and testing for coincidence of Fraunhofer lines. The lines given by light through S_2 should be exact continuations of the lines given by light through S_1. For this test the "*b*" lines were found most favorable. If the slight motion of C_2 to secure this last step displaces the central emergent beam at *F* the prism must be moved enough to restore it and the last step repeated. When the adjustments are finally secured, collimator C_2 is clamped, and prism *AEI* is secured in its position. The instrument is then ready for calibration. The author did this by using the Fraunhofer lines of the solar spectrum, and determining the reading of the scale attached to the telescope when sighted on each of nineteen lines.

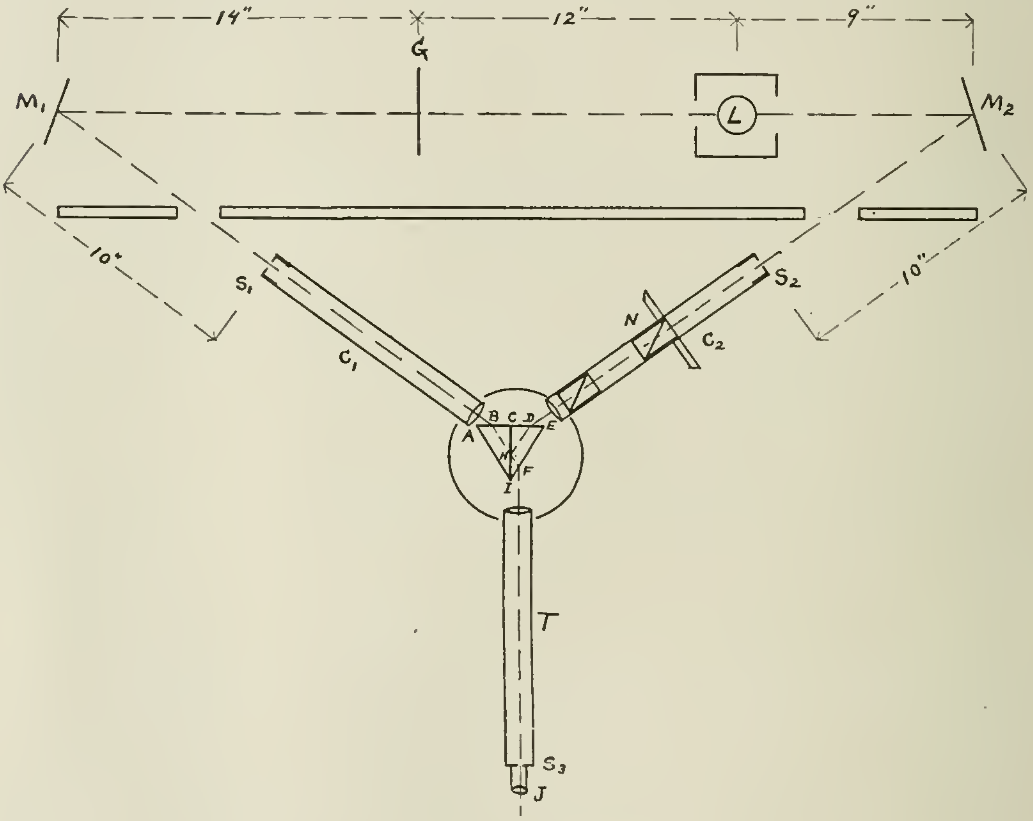

FIG. 1.—Lemon-Brace spectro-photometer

After calibration, the instrument was set up as shown in Figure 1. *L* is a 50-watt, nitrogen-filled, electric lamp of white glass. It is inclosed in a box with openings as shown. M_1 and M_2 are mirrors adjustable about vertical and horizontal axes so as to reflect the light from *L* along the optical axes of C_1 and C_2.

In order that the illumination of the silver strip by M_2 might be brighter than that of the background by M_1 when the nicols were parallel, it was necessary to have L much nearer M_2 than M_1 and also to place a piece of ground glass, G, in position as shown. An improvement could be made by the use of a lamp of higher power with an adjustable rheostat. This would give better illumination at the ends of the spectrum and also enable one to reduce the brightness at the middle of the spectrum. With the present arrangement the ends are too faint for accurate measurement, while the middle is too bright for comfort.

While making measurements, the room was darkened and the lamp, mirror, etc., were covered with black cloth. Slits S_1 and S_2 were opened to a width of $\frac{1}{2}$ mm. Eyepiece J was removed, and slit S_3 made as narrow as possible without producing diffraction fringes. The telescope was set at such a scale-reading as to bring light of the desired wave-length to S_3. Without having the ray-filter in place, five settings of nicol N were made, balancing the illumination of the silver strip against its background. The average $\sin^2$ of these readings gave the fractional part of the light of the chosen wave-length entering S_2 necessary to balance that entering S_1. The ray-filter was then put in front of S_1 and five other settings of N were made. The average sine^2 of these readings gave the fractional part of the light entering S_2 now necessary to balance that transmitted by the ray-filter. The ratio between the two averages gave the fractional part of the incident light of the chosen wave-length which was transmitted by the ray-filter. By making the measurements in this way, the percentage of transmission at any particular wave-length could be obtained at any time with no necessity of taking any other measurements in the series.

The current through the lamp L sometimes dropped to 50 per cent, or less, of its normal value, when the motor raising the floor in the big dome was started, but no perceptible effect on the balancing of illuminations in the Brace prism was produced thereby.

The five ray-filters already described were examined for their color-transmission and the percentages of transmission of the selected wave-lengths are given in the following table. The curves for filters "Dec. '07" and "M 1" appear in Figure 2. It will be seen how closely the filters "Dec. '07" and "M 1" correspond in their transmission to the flat part of the color-curve of the 40-inch objective shown in Figure 3, which is taken from the investigation published by Philip Fox in this *Journal*, 27, 237, May 1908. The fact that the filters transmit the longer wave-lengths for which the color-curve slopes upward is neutralized by the lack of sensitiveness of the photographic plates to those wave-lengths. The combination of the three elements thus enables the great light-gathering power of the 40-inch telescope to be employed photographically with practically no troublesome effects due to chromatic aberration.

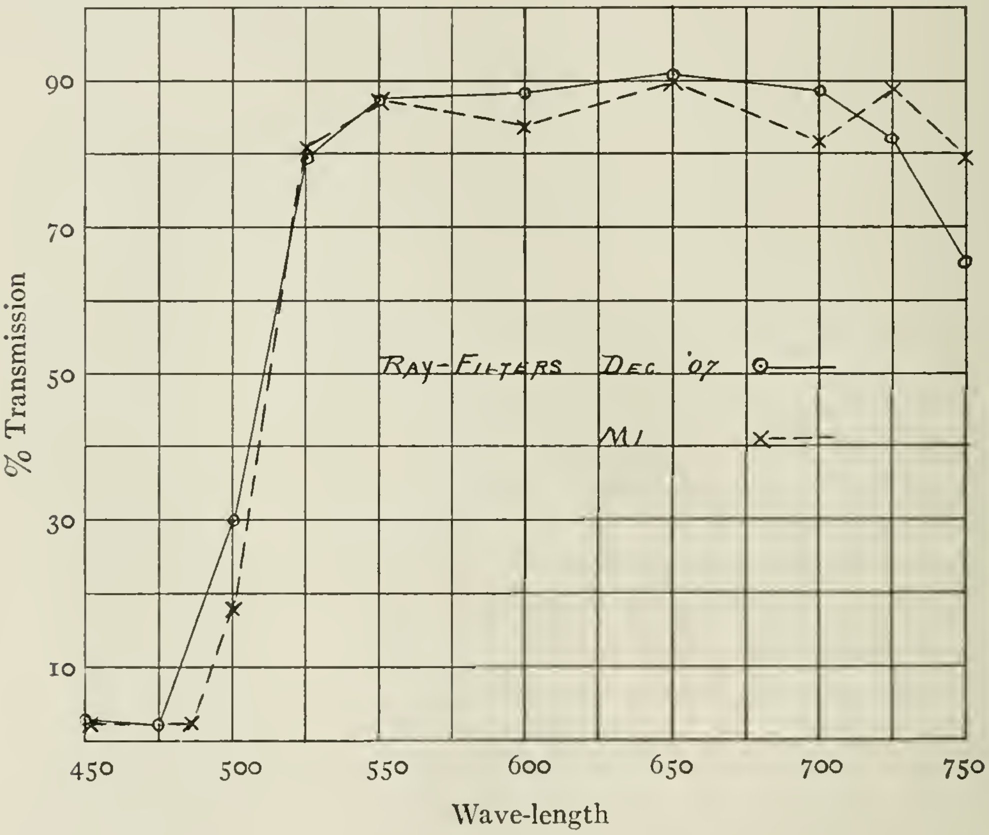

FIG. 2

The ray-filter possessing these transmission characteristics, combined with a plate having a maximum sensitiveness to the yellow, gives a combination whose position of maximum sensitiveness corresponds to that of the retina of the human eye. This is one of the reasons why the determinations of stellar magnitudes

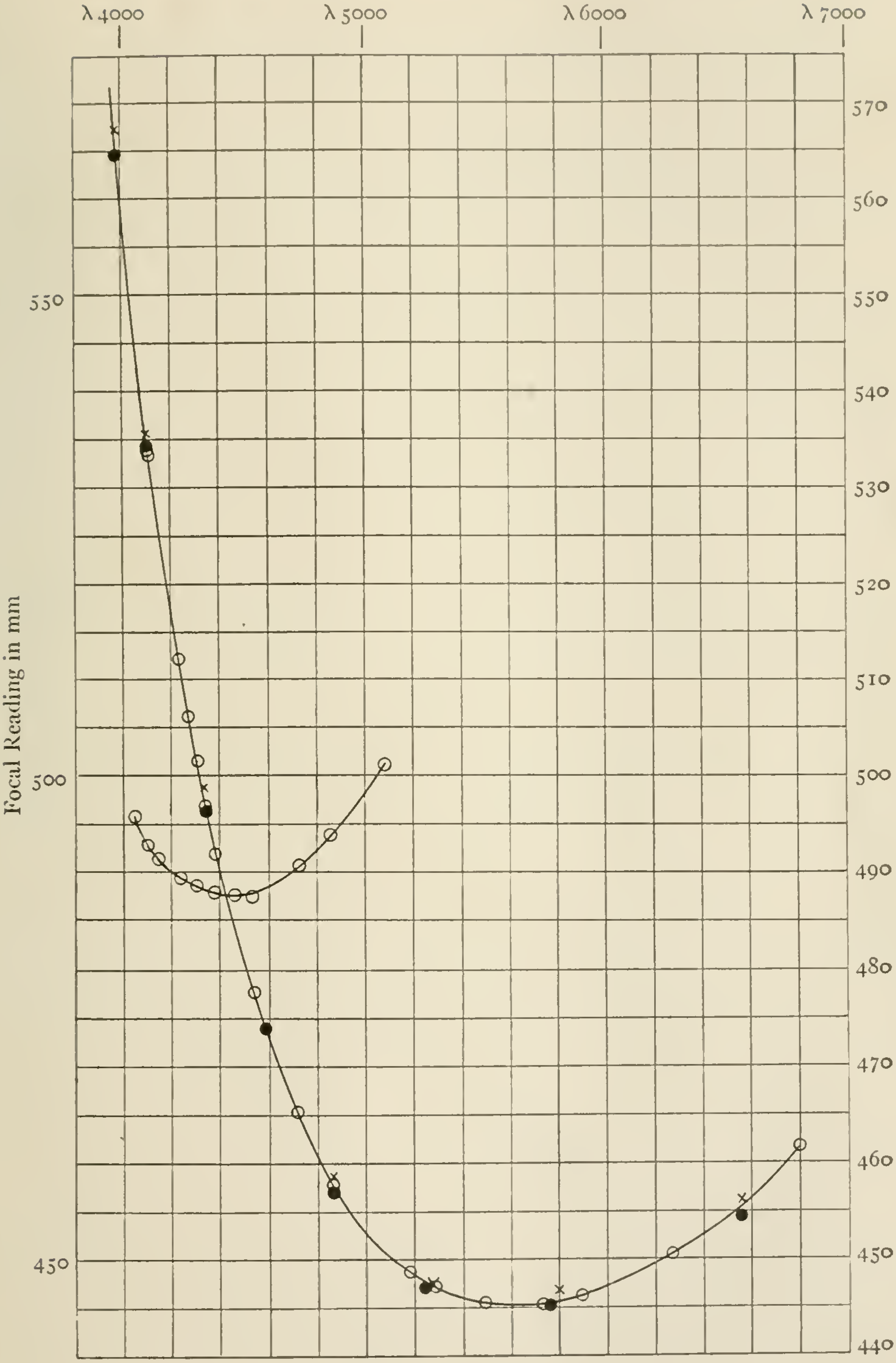

FIG. 3.—Color-curve of the 40-inch objective

made by Professor J. A. Parkhurst by his photographic method have such close correspondence to the visual magnitudes.

TABLE I

TRANSMISSION-PERCENTAGES OF RAY-FILTERS

Wave-Length	J 1	M 1	Beta 10	Dec. '07	Beta 7
750	87.1	79.4	82.0	64.8	72.2
725	85.5	89.2	73.9	81.8	79.3
700	89.3	81.8	74.0	88.7	78.0
650	92.6	90.3	82.2	91.0	87.1
600	87.7	84.0	86.2	88.5	83.5
550	88.7	87.8	88.8	87.6	87.8
525	87.3	81.1	85.3	79.6	81.5
500	57.6	18.5	40.0	29.8	40.8
486	7.9	2.0	14.4	....	....
475	2.5	0.6	6.0	2.0	12.5
450	....	....	....	2.3	4.9

The three colored glasses in use with a Hess-Ives Tint Photometer were also examined for their color-transparency. The results appear in the following table and in Figure 4.

TABLE II

TRANSMISSION-PERCENTAGES OF COLORED GLASSES, HESS-IVES TINT PHOTOMETER

RED GLASS		GREEN GLASS		BLUE-VIOLET GLASS	
Wave-Length	Percentage	Wave-Length	Percentage	Wave-Length	Percentage
766	0.0	628	0.0	495	0.0
750	11.7	610	0.04	486	0.8
725	57.7	590	1.1	475	3.9
700	73.0	570	6.0	465	9.2
675	78.7	550	15.9	455	14.4
650	78.4	530	19.5	445	19.1
625	65.0	510	10.5	435	20.9
600	3.4	490	0.8	425	18.7
489	0.0	468	0.0	415	0.0

It will be seen that the red glass has a maximum transmission of 78.7 per cent for light of wave-length 675 $\mu\mu$. Its average transmission in the region for which it transmits appreciably, i.e., between 766 $\mu\mu$ and 589 $\mu\mu$ is 51.5 per cent of the incident light. In the same way the maximum transmission for the green glass is 19.5 per cent for light of wave-length 530 $\mu\mu$, and its average transmission for the region between 628 and 468 $\mu\mu$ is 6.7 per cent. The blue-violet glass has a maximum transmission of 20.9 per cent for light of wave-length 435 $\mu\mu$, and an average transmission for the region between 495 $\mu\mu$ and 415 $\mu\mu$ of 10.9 per cent. It is very noticeable how little overlapping there is in the light transmitted by either pair of adjacent glasses.

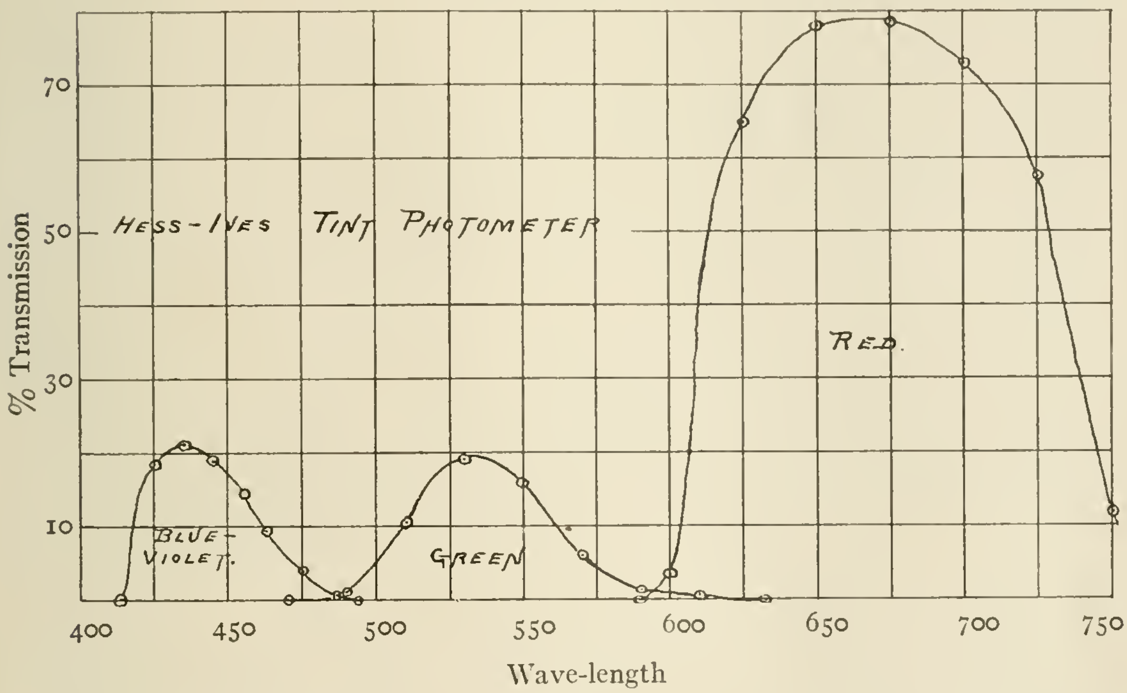

FIG. 4

An interesting piece of incidental information is the relative selective absorption exerted by the nicol prisms and the silver strip. When the readings are taken with no ray-filter in front of S_1, the angle through which the nicol N must be rotated to produce a balancing of illuminations is not the same for all wave-lengths. At first it increases as wave-length decreases, remains practically uniform from $\lambda = 600$ $\mu\mu$ to $\lambda = 525$ $\mu\mu$, and then decreases with the wave-length, showing that there is selective absorption corresponding in relative values to the $\sin^2$ of the angle of rotation of the nicol. The table below is computed from the average values obtained in the measurements of filters "M 1," "Beta 10," and "J 1."

The measurements on ray-filters "Dec. '07" and "Beta 7" were made after the instrument had been taken down, readjusted and calibrated, and therefore could not be included. Figure 5 gives the curve corresponding to this table.

TABLE III

Wave-length	750	700	650	600	550	525	500	485	475
Sin²	0.246	.415	.563	.613	.610	.611	.575	.535	.513

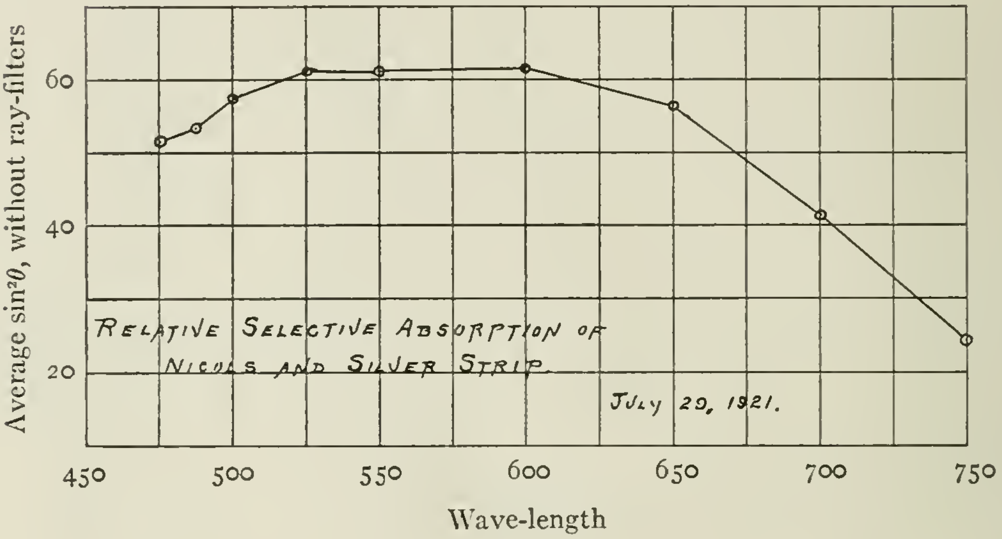

FIG. 5

The author is greatly indebted to Professor J. A. Parkhurst for suggesting the investigation and for his kind assistance during its progress and in the preparation of this report.

MIDDLEBURY COLLEGE
October 1, 1921

SYSTEMATIC CORRECTIONS TO SPECTROSCOPIC AND TRIGONOMETRIC PARALLAXES[1]

By GUSTAF STRÖMBERG

ABSTRACT

Systematic corrections to reduce spectroscopic and trigonometric parallaxes to absolute parallaxes.—The fact that the systematic and accidental errors of spectroscopic parallaxes are proportional to the parallaxes themselves, while the errors in trigonometric parallaxes are independent of the values of the parallaxes, makes it possible, theoretically at least, to determine from a comparison of the two systems the true systematic corrections for each system and even for each observer. The basis of grouping the stars must be independent of each system and therefore Kapteyn's mean parallaxes, derived from apparent magnitudes and proper motions, were used. The factorial correction (x) for the spectroscopic parallaxes and the additive correction (s) for the trigonometric parallaxes, connected by the fundamental equation $x\pi_s=\pi_t+s$, were thus determined. For dwarfs x ranges from 0.97 to 1.07 for different spectral types; for giants the range is from 0.89 to 1.13, the extreme values being rather uncertain. The corresponding systematic correction to absolute magnitudes averages only about 0.1 for dwarfs, but may be somewhat larger for the giants. *For the separate observatories*, McCormick, Allegheny, Yerkes, and Mount Wilson, the reductions from relative to absolute parallaxes come out, respectively, $+0''.0053$, $+0''.0076$, $+0''.0084$ and $-0''.0010$ within about $\pm 0''.002$. These values agree well with those obtained by van Maanen and Miss Wolfe. Hence the list of 1646 spectroscopic parallaxes recently published from Mount Wilson probably gives the absolute parallaxes without any appreciable systematic error.

The large number of spectroscopic parallaxes now available enables us to determine fairly accurate values of the systematic corrections for both spectroscopic and trigonometric parallaxes. In the derivation of the reduction tables for converting line intensities into absolute magnitudes used in the recent list of 1646 parallaxes[2] no corrections were applied to the trigonometric parallaxes, but it was found that if the corrections deduced by van Maanen and Miss Wolfe[3] had been used, the effect due to these corrections would have been less than 0.1 magnitude. The method used by van Maanen and Miss Wolfe consisted in comparing the means of the trigonometric parallaxes found by different observers for groups of stars of nearly the same mean apparent magnitude and mean proper motion. Their corrections represent the deviations of the results by individual observers from the mean system defined by all the trigonometric parallaxes. Since the systematic errors of individual observers must compensate each other to a large extent in the mean system, the corrections of van Maanen and Miss Wolfe are presumably close approximations to the true systematic errors.

---

[1] *Contributions from the Mount Wilson Observatory*, No. 220.

[2] *Mt. Wilson Contr.*, No. 199; *Astrophysical Journal*, 53, 1, 1921.

[3] *Mt. Wilson Contr.*, No. 189.

Other determinations of systematic corrections of trigonometric parallaxes have been made by Flint[1] and B. Boss,[2] the former reducing his corrections to a system based upon the Yale parallaxes, the latter comparing the spectroscopic parallaxes published in *Mt. Wilson Contribution*, No. 142 (*Astrophysical Journal*, **46**, 313, 1917) with the different series of trigonometric parallaxes.

The comparison of spectroscopic and trigonometric parallaxes enables us, theoretically at least, to determine the true systematic corrections for each observer and for the spectroscopic system as well. This depends upon the fact that the systematic and accidental errors of the spectroscopic parallaxes are proportional to the parallaxes themselves, while the errors in the trigonometric parallaxes are independent of the size of the parallax. Hence, for any series of trigonometric parallaxes, when compared with the spectroscopic system, we have, as shown more in detail below, an equation of the form

$$x\pi_s = \pi_t + s,$$

from which the systematic correction s, and the correction factor x for the spectroscopic parallaxes, can be determined. The successful use of the equation of course presupposes a considerable range in the values of the parallaxes compared. Another important advantage of the method is that any error in the assumed values of the mean parallax of the comparison stars used for the reduction of the relative trigonometric parallaxes to absolute values goes over into s and is determined as a part of the systematic correction. In principle, therefore, the comparison permits us to establish an absolute system of parallaxes.

The principal object of this investigation being to determine systematic corrections of the spectroscopic parallaxes as a whole, taking into account the possibility of constant corrections to the trigonometric parallaxes, only the larger lists of trigonometric parallaxes, viz., those derived at the McCormick, Allegheny, Yerkes, Mount Wilson, Sproul, and Yale observatories, have been discussed.

---

[1] *Astronomical Journal*, **29**, 189 (No. 696), 1916.

[2] *Ibid.*, **33**, 17 (No. 771), 1920.

The following notation has been used:

M = Absolute magnitude as published in *Mt. Wilson Contribution*, No. 199.

ΔM = Systematic correction to M to obtain the most probable absolute magnitude.

T = Accidental error of $M+\Delta M$.

π = True parallax.

π_1 = Spectroscopic parallax based on the absolute magnitude M.

π_0 = Trigonometric parallax.

s = Systematic correction to π_0

ϵ = Accidental error of π_0+s.

We have then (cf. *Mt. Wilson Contribution*, No. 199, p. 4)

$$\left.\begin{array}{ll} & \pi=10^{0.2(\Delta M+T)}\pi_1=\pi_0+s+\epsilon \\ \text{or} & \sigma\tau\pi_1=\pi_0+s+\epsilon \\ \text{where} & \sigma=10^{0.2\Delta M}, \qquad \tau=10^{0.2T} \end{array}\right\} \tag{1}$$

Expanding τ in a power series,

$$\left.\begin{array}{l} \tau=1+E+\tfrac{1}{2}E^2=A+E \\ E=\dfrac{0.2T}{\text{Mod}} \\ A=1+\tfrac{1}{2}E^2 \end{array}\right\} \tag{2}$$

Thus

$$\sigma A\pi_1-s-\pi_0=\epsilon-E\sigma\pi_1 \tag{3}$$

As the right-hand side of this equation must be assumed equal to zero, we cannot group the stars according to the size of π_0 or π_1. If we group the stars according to values of π_0 the quantity $\bar{E}$ could be assumed zero,[1] but $\bar{\epsilon}$ would show a continuous decrease from positive to negative values as $\bar{\pi}_0$ increases. The same holds for $\bar{E}$ if we group the stars according to π_1, and furthermore the weight of the unknown quantity σ would be systematically affected by the accidental errors in π_1. These circumstances correspond to the difference in slope of the two regression lines in the correlation theory. A neutral basis of grouping according to the size of the parallaxes must therefore be used, i.e., one for which we can assume the errors in the parallaxes to be independent of the errors in the measured quantities M and π_0. Such an independent basis of grouping is afforded by Kapteyn's mean parallaxes, which are a function of apparent magnitude and proper motion. For each star the mean parallax was therefore computed from Kapteyn's formula in *Groningen Publication*, No. 8, and groups of stars were then formed having mean parallaxes within certain limits. The mean spectroscopic and trigonometric parallax was then found for each group. Each of these groups then furnished an equation of condition.

---

[1] A bar above a symbol denotes throughout this paper an algebraic mean.

From equation (3) we find

$$\sigma\bar{A}\bar{\pi}_1 - s - \bar{\pi}_0 = \bar{\epsilon} - \sigma\overline{E\pi_1}\,.$$

For a neutral basis of grouping we have $\bar{\epsilon}=0$ and $\bar{E}=0$. The second term on the right-hand side, however, is not quite zero, as E is to some extent dependent on π_1 and thus $\overline{E\pi_1}$ is not exactly equal to $\bar{E}\bar{\pi}_1$.

To reduce the right-hand side of the equation of condition to zero, we multiply equation (1) by

$$\frac{1}{\tau} = 1 - E + \tfrac{1}{2}E^2 = A - E$$

and find

$$\sigma\pi_1 = A(\pi_0 + s + \epsilon) - E(\pi_0 + s + \epsilon).$$

Thus

$$\frac{\sigma}{A}\pi_1 - s - \pi_0 = \epsilon\left(1 - \frac{E}{A}\right) - \frac{E}{A}(\pi_0 + s).$$

For a neutral basis of grouping, we have, including terms of second order of E,

$$\frac{\sigma}{\bar{A}}\pi_1 - s - \bar{\pi}_0 = \bar{\epsilon}(1 - \bar{E}) - \bar{E}(\bar{\pi}_0 + s) = 0.$$

The equations of condition thus become

$$\left.\begin{aligned} x\pi_1 - s - \pi_0 &= 0 \\ \text{Weight} = \frac{1}{\overline{\epsilon^2} + \overline{E^2}\,\overline{\pi^2}} &= \frac{N}{\bar{\epsilon}^2 + \overline{E^2}\,\bar{\pi}^2} \end{aligned}\right\} \qquad (4)$$

TABLE I

SYSTEMATIC CORRECTIONS—SEPARATE SOLUTION FOR EACH TYPE

Spectrum	M	x	McCormick s_1	Allegheny s_2	Yerkes s_3	Mount Wilson s_4	Sproul s_5	Yale s_6
A6 to F9....	1.0 to 5.5	1.056 ± .035	+0″.0037 (53) ± .0020	+0″.0020 (92) ± .0015	+0″.0013 (25) ± .0019	−0″.0009 (24) ± .0015	−0″.0068 (35) ± .0021	−0″.0008 (46) ± .0022
G0 to G9....	≦3.0	1.095 ± .134	+0.0012 (35) ± .0033	+0.0011 (69) ± .0031	+0.0052 (10) ± .0055	−0.0040 (13) ± .0036	−0.0114 (11) ± .0062	+0.0085 (11) ± .0082
G0 to G9....	≧3.1	0.975 ± .053	−0.0055 (36) ± .0044	+0.0038 (60) ± .0032	−0.0048 (27) ± .0034	+0.0221 (8) ± .0040	−0.0130 (10) ± .0054	−0.0008 (74) ± .0031
K0 to K9....	≦4.0	1.075 ± .113	−0.0028 (25) ± .0034	+0.0058 (54) ± .0025	+0.0181 (7) ± .0050	−0.0085 (26) ± .0017	−0.0090 (8) ± .0040	+0.0198 (7) ± .0056
K0 to K9....	≧4.1	1.030 ± .064	+0.0040 (39) ± .0061	+0.0069 (27) ± .0062	+0.0109 (30) ± .0052	−0.0012 (7) ± .0092	+0.0133 (20) ± .0067	+0.0054 (70) ± .0050
A6 to K9....	....	....	+ .0012 (188) ± ″.0016	+0.0030 (302) ± ″.0011	+0.0026 (99) ± ″.0014	−0.0024 (78) ± ″.0010	−0.0069 (84) ± ″.0016	+0.0018 (208) ± ″.0016

where $x=\frac{\sigma}{A}$ is the quantity by which the spectroscopic parallaxes must be multiplied in order to obtain the best agreement with π_0+s. N is the number of stars in the group.

Assuming only that the quantities x and s are constant for a certain group of stars, we can determine them separately without introducing any limitation as to their size. The value of s found in this way is the systematic correction which reduces π_0 to *absolute* parallax.

We have assumed that the external accidental probable error in the trigonometric parallaxes determined at the McCormick, Allegheny, Yerkes, and Mount Wilson observatories is $\pm 0\rlap{.}''010$. The probable errors of the spectroscopic parallaxes have been assumed to be $\pm 0.20\,\pi_1$. The weights of the equations of condition are therefore proportional to $N/(0.09\overset{2}{\pi}+0.000225)$ where for $\bar{\pi}$ we have used $\frac{1}{2}(\bar{\pi}_1+\bar{\pi}_0)$, x being nearly equal to unity.

The following provisional reductions to absolute parallaxes were applied before the computations were made: For McCormick, Allegheny, and Yerkes observatories, $+0\rlap{.}''005$; for Mount Wilson, $+0\rlap{.}''002$; for Sproul and Yale the reductions were computed from the table given by Kapteyn in *Groningen Publications*, No. 24, page 15. The Sproul and Yale parallaxes were given half-weight.

The value of x was determined separately for giant and dwarf stars of different spectral types. For the first solution the systematic correction s was determined for each of the above-mentioned groups of trigonometric parallaxes. The results are given in Table I. The first column indicates the limits of spectral type, the second the division according to absolute magnitude. The probable errors for x and s are below the numbers to which they belong. The numbers of stars used are given in parentheses. The last line shows the weighted means of s for all types and absolute magnitudes.

Using these mean systematic corrections to the trigonometric parallaxes and recomputing the correction factor of the spectroscopic parallaxes, we find the values of x and ΔM_1, given in Table II. The quantity ΔM_1 is the correction that must be applied to M in

TABLE II

CORRECTION FACTORS FOR SPECTROSCOPIC PARALLAXES

Spectrum	M	x	ΔM_1
A6 to F9	1.0 to 5.5	1.059 ± .012	+0.12 ± 0.02
G0 to G9	≦3.0	1.121 ± .040	+0.25 ± 0.08
G0 to G9	≧3.1	0.999 ± .029	0.00 ± 0.06
K0 to K9	≦4.0	1.001 ± .059	0.00 ± 0.13
K0 to K9	≧4.1	0.960 ± .019	−0.09 ± 0.04
F0 to F9	≦0.0	0.149 ± .103	+0.30 ± 0.20
Ma to Md	<3.0	0.892 ± .081	−0.25 ± 0.20
Ma to Md	>7.0	1.089 ± .086	+0.18 ± 0.17

order to obtain the most probable parallax and is determined by the equation

$$\Delta M_1 = 5 \log x = \Delta M - 5 \log \bar{A}.$$

Another solution was made, using all the spectral types, A6 to Md, and solving all the equations as a simultaneous set of conditions, assuming the correction s to be constant for each observer. The results of this solution are given in Table III.

TABLE III

SIMULTANEOUS SOLUTION FOR ALL TYPES

	s		s
McCormick	−0″.0015 ± 0″.0018	Mount Wilson	−0″.0038 ± 0″.0014
Allegheny	+ .0010 ± .0015	Sproul	− .0085 ± .0025
Yerkes	+ .0019 ± .0021	Yale	+ .0004 ± .0021

Spectrum	M	x	ΔM_1
A6 to F	1.0 to 5.5	1.015 ± .040	+0.03 ± 0.08
G	≦3.0	1.037 ± .078	+0.08 ± .16
G	≧3.1	0.969 ± .033	−0.07 ± .07
K	≦4.0	0.922 ± .074	−0.18 ± .17
K	≧4.1	0.940 ± .029	−0.14 ± .07
F	≦0.0	0.962 ± .247	−0.08 ± .57
M	<3.0	0.750 ± .154	−0.63 ± .45
M	>7.0	1.082 ± .045	+0.17 ± .09

From van Maanen's investigation we know, however, that the Sproul and Yale parallaxes have a considerable magnitude correction. Such an error would affect appreciably the determination of the factor x, and for this reason a final solution was made, omitting the Sproul and Yale parallaxes. The results of this solution, which are given in Table IV, are probably the most trustworthy. They are in good agreement with those found by van Maanen and Miss Wolfe, which, reduced to the same system of corrections for reduction to absolute parallaxes as used here, are given in the last column of Table IV.

TABLE IV

Simultaneous Solution (Sproul and Yale Omitted)

	s	s (van Maanen)
McCormick	+0″.0003±0″.0021	−0″.0016
Allegheny	+ .0026± .0017	+ .0027
Yerkes	+ .0034± .0022	+ .0036
Mount Wilson	− .0030± .0014	− .0020

Spectrum	M	x	ΔM_1
A6 to F	1.0 to 5.5	1.041±.045	+0.09±0.09
G	≦3.0	1.135±.092	+0.27± .18
G	≧3.1	0.987±.037	−0.03± .08
K	≦4.0	1.012±.086	+0.03± .18
K	≧4.1	0.972±.034	−0.06± .08
F	≦0.0	1.090±.254	+0.19± .52
M	<3.0	0.888±.167	−0.26± .41
M	>7.0	1.068±.052	+0.14± .11

Using the systematic corrections resulting from this final solution, we find the following reductions from *relative* to *absolute* parallax.

McCormick	+0″.0053±0″.0021	Yerkes	+0″.0084±0″.0022
Allegheny	+0″.0076±0″.0017	Mount Wilson	−0″.0010±0″.0014

The systematic corrections to the absolute magnitudes are in general very small except in the case of the giant G and M stars and the very brightest F stars, most of which are Cepheids or pseudo-Cepheids. For these stars, however, the probable errors are rather large on account of the smallness of the parallaxes. In the previous derivation of the reduction tables for the determination of absolute magnitudes it was found that in the case of the giant G stars the results from trigonometric parallaxes and parallactic motion differed considerably. The determination of the mean absolute magnitudes based on parallactic motion would make these stars considerably brighter than the results from the trigonometric parallaxes indicate. A weighted mean was accordingly used. The discordance is now nearly eliminated by the application of the systematic corrections to the trigonometric parallaxes. The same holds for the brightest F stars, for which originally the measured parallaxes were not used at all, the result from parallactic motion having much higher weight. For the giant M stars the original determination was based mainly on the peculiar motion, and the present results seem to indicate that for these stars as a whole the system is nearly correct.

As the final result of this investigation, we may say that the system of spectroscopic parallaxes in *Mt. Wilson Contribution,* No. 199, as a whole, is correct within the errors of the quantities involved, and that there is no need at present to apply corrections to the system. The systematic corrections to the trigonometric parallaxes determined at the McCormick, Allegheny, Yerkes, and Mount Wilson observatories have been found to agree satisfactorily with those of van Maanen and Miss Wolfe, and, as the method used here gives absolute corrections, it can be regarded as probable that after these corrections have been applied there remain no appreciable outstanding constant errors in the resulting absolute parallaxes.

MOUNT WILSON OBSERVATORY
September 1921

NEW MEASUREMENTS OF STELLAR RADIATION

By W. W. COBLENTZ

ABSTRACT

Relative total radiation of 27 bright stars, down to magnitude 3.8.—New measurements which were recently made with the 40-inch reflector of the Lowell Observatory at Flagstaff, using a vacuum thermo-couple, are given in a table. These confirm the result obtained at Mount Hamilton in 1914 that the total radiation from red stars is 2.5–3 times as much as that from blue stars of the same visual magnitude.

Distribution of energy in the spectra of some bright stars was determined by the use of a series of filters which isolated various spectral regions. In this *preliminary note* merely the general result is reported that the *maximum emission* lies in the infra-red (0.7–0.9 μ) for stars of types K and M, and in the ultra-violet for stars of types B and A. The corresponding *black body temperatures* vary from 3000° C., for the red M stars to 9000° or 10,000° C., for the blue B stars. The *percentage transmission through 1 cm of water* is given for 22 stars and varies from 81 for B stars to 40 for M stars.

In a previous paper[1] data were given on a comparison of stellar radiometers and radiometric measurements of stars as observed at an altitude of about 4000 feet at Mount Hamilton, California, with the Crossley 36-inch reflector of the Lick Observatory. Quantitative measurements were made of stars down to magnitude 5.3 and qualitative measurements to magnitude 6.7. It was found that red stars emit from 2.5 to 3 times as much *total* radiation as blue stars of the same visual magnitude.

These observations were verified by an independent method which consisted in measuring the transmission of stellar radiation through a 1-cm cell of water, having quartz windows. By this means it was shown that, of the *total* radiation emitted, blue stars have about two times as much *visible* radiation as yellow stars, and about three times as much *visible* radiation as red stars.

At various times during the past seven years attention was given to the improvement of the stellar radiometers,[2] galvanometers, etc. The various subsidiary data will be published in a complete paper dealing with the whole subject.

The object of this paper is to give a preliminary survey of the results of new stellar radiometric measurements, made at a much higher altitude, 7300 feet, at Flagstaff, Arizona, with the 40-inch reflector of the Lowell Observatory. This was made possible through the generosity of Drs. V. M. Slipher and C. O. Lampland. Not only was an otherwise busy program interrupted, but furthermore, Dr. Lampland personally operated the telescope, thus insuring speed and efficiency in accomplishing results. It is a pleasure to record here my grateful acknowledgments for the many courtesies accorded by various members of the staff of the Lowell Observatory.

---

[1] Coblentz, *Bulletin of the Bureau of Standards*, **11**, 613, 1914.

[2] *Bulletin of the Bureau of Standards*, **13**, 423, 1916; **14**, 532, 1918; **16**, 253, 1920; *Journal of the Washington Academy of Sciences*, **6**, 473, 1916.

The object of the present investigation was (1) to verify previous results; (2) to measure the intensities of radiation of bright stars in the region of 0 hours to 12 hours in right ascension, not previously measured; and (3) to determine the feasibility of the method of obtaining the distribution of spectral energy of stars by means of transmission screens which, either singly or in combination, are placed in front of the vacuum thermo-couple. By means of these thermo-couples, measurements were made on the intensities of radiation of thirteen bright stars not observed in 1914, thus completing the survey of the whole sky. A total of thirty celestial objects was measured, including Venus and Mars.

By means of a series of transmission screens (of yellow and red glass, of water, and of a thick plate of quartz) wide spectral regions were isolated and the intensities of radiation in the spectrum from 0.3 μ to 0.43 μ; 0.43 μ to 0.6 μ; 0.6 μ to 1.4 μ; 1.4 μ to 4 μ; and 4 μ to 10 μ were determined. In this manner the distribution of energy in the spectra of sixteen stars was determined, and thus was obtained for the first time an insight into the intensities of radiation in the complete spectrum of a star.

By means of this device it was found that in the stars of types B and A the maximum intensity of radiation lies in the ultra-violet (0.3 μ to 0.4 μ) while in the cooler stars of types K and M the maximum emission lies at 0.7 μ to 0. 9 μ in the infra-red. From this it appears that the black-body temperature (i.e., the temperature which a black body would have to attain in order to emit a similar distribution of relative spectral energy) varies from 3000°C. for red M stars to 9000° or 10,000°C. for blue B stars.

The observing station being much higher than previously used, the atmospheric scattering of light was greatly reduced and consequently the transmissions in the violet are somewhat higher than previously observed when the water-cell was interposed.

TABLE I

Transmission of Stellar Radiation through a 1-Cm Layer of Water

Star	Magnitude Harvard Revision	Deflection for a Galvanometer Sensitivity of $i=1\times10^{-10}$ Amperes	Spectral Type	Percentage of Transmission	Remarks
θ Orionis (Nebula)	....	±0.02 cm	......	......	
ε Orionis........	1.75	0.66	B	81	
γ Orionis........	1.70	0.64	B2	82	
α Leonis.........	1.30	0.77	B8	......	
β Tauri..........	1.78	0.78	B8	79	
β Canis Minoris..	3.09	0.38	B8	......	
β Orionis........	0.34	2.89	B8p	63*	Rigel, spectroscopic binary
β Lyrae.........	Var.	0.26	B8p	......	
α Geminorum....	1.99 2.85	0.78	A	82	Castor
α Lyrae.........	0.14	3.60	A	75	Vega
γ Geminorum....	1.93	0.71	A	......	
α Canis Majoris..	−1.58 8.5	10.62	A	65*	Sirius, binary
α Cygni.........	1.4	1.34	A2	76	Deneb
α Aquilae........	0.9	1.88	A5	71	Altair
α Persei.........	1.90	0.75	F5	74	
α Canis Minoris..	0.48 13.5	2.67	F5	64*	Procyon, binary
α Aurigae........	0.21	4.91	G	57	Capella
ε Geminorum....	3.18	0.58	G5	66	
β Geminorum....	1.21	2.19	K	58	Pollux
α Boötis.........	0.24	8.10	K	47	Arcturus
γ Leonis.........	2.61 3.80	0.99	K	......	
α Tauri..........	1.06	6.03	K5	42	Aldebaran
λ Aquarii........	3.84	0.75	Ma	47	
μ Geminorum....	3.19	2.11	Ma	41	
β Andromedae....	2.37	2.45	Ma	41	
α Orionis........	0.92	15.00	Ma	34	Betelgeuse
α Scorpii........	1.22	8.82	Map	33*	Antares, spectroscopic binary
β Pegasi.........	2.61	2.96 cm	Mb	38	

However, all the data verify previous measurements showing that blue stars emit less infra-red radiation than do red stars of the same visual magnitude. Moreover, observations made on the same night (same weather conditions) are consistent in showing small gradations in the infra-red component of the radiation, corresponding with the small gradations (say B2 and B8) in spectral types.

For binary stars having companions of low luminosity, transmissions of the water-cell are low, indicating that the companion stars emit considerable infra-red radiation. See Table I.

It was found that even in red stars the component of spectral radiation of wave-lengths greater than 4 μ is only from 1 to perhaps 10 per cent of the total. From this it would appear that in future work it may be permissible to use vacuum thermo-couples with thin quartz windows instead of fluorite, thus saving expense and possible leakage by constructing the container of quartz.

WASHINGTON, D.C.
October 24, 1921

SOLAR CONSTANT, SUN-SPOTS, AND SOLAR ACTIVITY

By ANDERS ÅNGSTRÖM

ABSTRACT

Variation of solar constant with number of sun-spots.—A study of 205 observations for 1915–1917 furnished by C. G. Abbot suggests that the solar constant S does not increase regularly with any power of the sun-spot number N, but rather reaches a maximum value for N between 100 and 160, approximated in accordance with the formula $S=1.903+0.011\sqrt{N}-0.0006N$. The number of observations for high value of N is, however, too small to be decisive.

A comparison of the values of the solar constant computed by Abbot and his collaborators with the sun-spot numbers given by Wolfer shows, if mean values for the separate years are considered, a close connection between the two phenomena. Thus a high sun-spot number seems to correspond to a high value of the solar constant and vice versa. The relation is apparently not a linear one; and inquiring into the exponent which applied to the sun-spot numbers gives the highest correlation between the two phenomena, I have found this exponent to be very nearly equal to $\frac{1}{2}$.[1]

If we consider only yearly mean values, the solar constant S seems then to be given with good approximation by the relation:

$$S=1.903+0.0055\sqrt{N}\,, \qquad (1)$$

where N is the number of sun-spots according to Wolf-Wolfer. The mean difference between observed and computed values during the epoch 1905–1917 is less than 0.01, i.e., less than 0.5 per cent of the value of the solar constant itself, as may be seen from Table I.

As the question regarding the probable connection between solar constants and sun-spot numbers is an important one for the solution of many problems connected with the climate of past epochs and with the constitution of the sun, it seems worth while to enter a little more closely into the question.

---

[1] *Geografiska Annaler*, H. 1, 1920.

For the low values of N which are obtained by taking averages during a considerable time the relation (1) seems to hold with good approximation. But is this true also for a wider range of values of N? If we consider the values of S and N corresponding to individual days, what will be the relation between them?

In order to answer these questions, I have divided the values of the solar constant during the years 1915–1917, kindly put at my disposal by Dr. Abbot, in groups according to the corresponding sun-spot numbers, as is seen from Table II. The years named are selected from the point of view that the sun-spot numbers have varied during that time over a considerable range ($0 < N < 256$), and also because the variation in the yearly mean values is small, and consequently should not have introduced any complications. The values of the solar constant corresponding to the various groups of sun-spot frequencies are given in Table II together with the numbers of values of which they represent the means. On the basis of this table, Figure 1 has been drawn, where the values of the solar constant are plotted against sun-spot numbers.

The table and figure seem now to suggest the following conclusions. With increasing sun-spot numbers, the solar constant first increases in order to reach a maximum, which seems to correspond to a sun-spot number of between 100 and 160 (maximum difficult to locate exactly); thereafter, the solar constant decreases with an increase in sun-spot numbers. The relation between solar constant and sun-spot numbers is apparently governed by two separate phenomena. The one causes an increase of the solar constant with increasing sun-spot numbers, and this effect predominates for the small values of N; the other effect goes in the opposite direction, and predominates for large values of N. Let us start from the assumption that the relation between solar constant and sun-spots for small values of N may be given by the expression

$$S = 1.903 + k\sqrt{N}\,, \tag{2}$$

obtained in its general features by the study of the yearly mean values. We may assume the other effect, which evidently must depend upon a function of higher order of N than $N^{\frac{1}{2}}$, to be of the form N^a, where a is to be determined from the observations. The expression for the relation then takes the form:

$$S = 1.903 + k\sqrt{N} - cN^a. \tag{3}$$

A comparison with the tabulated values gives us the following approximate values for the constants:

$$k = 0.011,\ c = 0.0006,\ a = 1 \text{ (approx.)}.$$

The smooth curve of Figure 1 is computed from (3) on the basis of these values of a, k, and c.

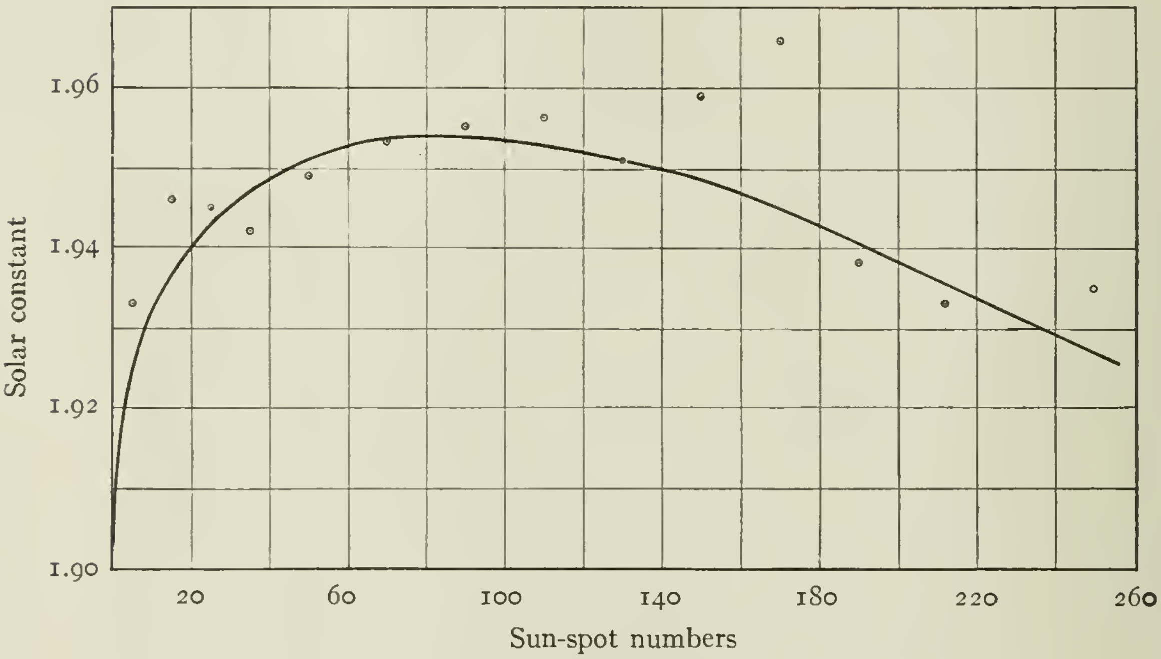

FIG. 1.—Solar constant and sun-spot numbers

It is clear that too much weight ought not to be attached to a result based upon a number of observations which, especially for large values of N, is very limited. In fact, the decrease of the solar constant with increasing N after a maximum value is reached is based upon ten observations, of which, according to Abbot, four are excellent (*e*), two very good (*vg*), three good (*g*), and one poor (*p*). It is to be noted, however, that the value marked (*p*) is the highest one of them all, namely 1.971, and consequently it has raised and not lowered the mean value. But, on the other hand, the result seems to me to be in remarkable agreement with consequences to be expected from the nature and constitution of sun-spots. The sun-spots themselves are dark relative to the surrounding parts of the sun's disk. The decrease in brightness varies between wide limits, but according to E. Liais[1] and M. Gouy and L. Thollon,[2] the larger sun-spots generally have a brightness less than 20 per cent of the normal. The percentage of heat radiation is somewhat larger. S. P. Langley[3] gives it as about one-half of the normal for the photosphere. It is evident that the spot-covered area itself cannot contribute to the increase in the solar constant. The observations of individual sun-spots show, however, that the dark area of the spot generally is surrounded by an outer region, where the brightness for a number of special lines is more intense than the normal for the surface. At this area the protuberances and flocculi are especially strongly developed, surrounding the inner and darker part by a kind of luminous corona of more or less symmetric form. If we assume the point of view expressed by Abbot, Fowle, and Aldrich, namely, that the increase in the solar constant is caused mainly by an increase in the vertical convection through which hot material is carried to the surface of the sun, we must conclude that the seat of this "intensified" radiation must be located especially at peripheric rings round the sun-spots. It seems very natural, then, that the areas of these rings must increase less rapidly than the area of the sun-spots, viz., the Wolf-Wolfer sun-spot numbers. On the other hand, it seems as natural that the simultaneous decrease of the solar constant is proportional to the spot area, which as we know represents dark regions of the sun's surface for luminous as well as dark heat radiation. The measured area of the sun-spots is, it is true, scarcely more than a few thousandths of the sun's disk. But to this area we must probably add a great part of smaller spots of granular structure which never are counted as real sun-spots, but the area of which increases and decreases with the sun-spot number itself.

The data available at present are too few to give a very definite idea of the form of the relation between solar constant and sun-spot number. It is with all probability a function dependent not only on the area of sun-spots, but also on their number, intensity, and constitution in general. *So much seems clear, however, from the previous discussion, that this function is not a linear one; the opinion that an increase of sun-spots is also accompanied by an increase in the solar constant must be subjected to a revision. In all probability the solar constant passes through a maximum with increasing sun-spot area*, after which a continuous decrease of the solar constant takes place when the area increases.

---

[1] *Mémoires de la Société des Sciences de Cherbourg*, 12, 1866.

[2] *Comptes Rendus*, **95**, 1834–1836, 1882.

[3] *Monthly Notices*, **37**, 5, 1876.

From our material at present it therefore does not seem permissible to assume that very high values of the solar constant in the past have accompanied a very high value of the frequency of sun-spots, but, on the contrary, that the solar constant at certain epochs possibly may have had a very low value on account of a great frequency of sun-spots. If we dared to extrapolate the function given above to represent the conditions at very high sun-spot frequencies, we should find that a sun-spot number of 1,000 corresponds to as low a solar constant as about 1.66, or a decrease from the normal by about 15 per cent. As such high sun-spot frequencies have not yet occurred, so far as we have observed, we then enter into the region of hypotheses.

Further determinations of the solar constant, especially at the times of maxima of sun-spots, will be of great interest in throwing more light upon the questions raised above. The foregoing discussion seems to the author to form an additional support for the opinion that the variations of the solar constant, observed by Abbot and his collaborators, are real and the sun consequently is a variable star.

Recently doubts as to the reality of the variations of the solar constant have been raised by G. Granqvist on account of a correlation found to exist between the values of the solar constant and the values of the atmospheric transmission[1]. In a recently published paper[2] I consider that I have shown: (1) that in the case of Abbot's values the correlation pointed out by Mr. Granqvist practically disappears, if one accounts for the probable variation of the solar constant itself during the time of observations; and (2) that the connection between solar constant and transmission in the case of the observations of Mr. Granqvist probably is caused by variations in the atmospheric transmission during the time of observations, i.e., too high a value of the solar constant is obtained when, in view of the increasing transmission, too low a value is computed for the transmission, and vice versa.

---

[1] *Kosmos*, Stockholm, 1921.

[2] "Är solens strålning variabel?" *Tidskrift för elementär matematik fysik och kemi.* Alb. Bonnier, Stockholm, 1921.

TABLE I

Years	Solar Constant (S)		Sun-Spot Numbers (N)	O.−C.
	Observed	Computed	(Wolfer)	
1905	1.956	1.946	63	+0.010
1906	1.942	1.945	58	−0.003
1908	1.936	1.944	55	−0.008
1909	1.918	1.940	46	−0.022
1910	1.921	1.928	21	−0.007
1911	1.921	1.922	3	−0.001
1913	1.904	1.909	1	−0.005
1914	1.956	1.919	9	+0.037
1915	1.952	1.946	62	+0.006
1916	1.946	1.942	50	+0.004
1917	1.960	1.961	113	−0.001
Mean difference	....	....	....	0.009

TABLE II

Sun-Spot Number (N)	Mean Solar Constant (S)	Number of Observations (n)
0–9	1.933	5
10–19	1.946	12
20–29	1.945	17
30–39	1.942	17
40–59	1.949	35
60–79	1.953	33
80–99	1.955	27
100–119	1.956	23
120–139	1.951	11
140–159	1.959	10
160–179	1.966	5
180–199	1.938	2
200–224	1.933	3
225–275	1.935	5

STOCKHOLM
May 1921

THE ORBITS OF THE SPECTROSCOPIC BINARIES 1 HYDRAE AND 75 CANCRI[1]

By R. F. SANFORD

ABSTRACT

Orbits of the spectroscopic binaries, Boss 2227 = 1 Hydrae and Boss 2447 = 75 Cancri. —These stars are of classes F1 and G2 and of visual magnitudes 5.7 and 6.0, respectively. Twenty-seven spectrograms of each give for the periods, 1.563 and 19.46 days; for e, 0.05 and 0.206; for K, 30.3 and 20.2 km/sec.; and for γ, +71.3 and +12.3 km/sec., respectively. Attention is called to the large γ for Boss 2227, and to the fact that Boss 2447 is a dwarf star. Radial velocity-curves are shown.

A previous paper[2] discusses the orbits of seven spectroscopic binaries; the present note gives the orbits of two additional binaries. The general remarks which precede the discussions of individual stars in the first paper are equally applicable here and need not be repeated.

The data in Table I, except for the last column which gives the number of revolutions of the star in its orbit between the first and last observations, are taken from the list of spectroscopic parallaxes of 1646 stars.[3] Figures 1 and 2 show the radial velocity-curves. In the following pages the derivation of the orbits of these two spectroscopic binaries is discussed.

TABLE I

Name	Vis. Mag.	α (1900)	δ (1900)	Spectral Class	Vis. Abs. Mag.	μ	$\pi_{\mathrm{sp.}}$	No. Rev.
Boss 2227–1 Hydrae	5.7	$8^{\mathrm{h}}19^{\mathrm{m}}.6$	$-3^{\circ}26'$	F1	+3.6	$0''.216$	$0''.038$	340
Boss 2447–75 Cancri	6.0	9 2.9	+27 3	G2	+4.1	0.404	0.042	59

BOSS 2227

Measures of the first two spectrograms of this star by Professor H. C. Wilson showed that its radial velocity is variable. Accordingly observations were started immediately for the determination of the elements of its orbit. Twenty-seven suitable spectrograms are listed in Table II. The derivation of the correct period presented some difficulty at first because of its shortness. Finally, all observations were gathered into one period in a satisfactory manner when $P = 1.562975$ days was used. Since approximately 340 revolutions of the star in its orbit occurred between the first and last observations it seemed needless to endeavor to correct the period, and therefore the value given above has been taken as final.

---

[1] *Contributions from the Mount Wilson Observatory*, No. 221.

[2] *Mt. Wilson Contr.*, No. 201; *Astrophysical Journal*, 53, 201, 1921.

[3] *Mt. Wilson Contr.*, No. 199; *Astrophysical Journal*, 53, 13, 1921.

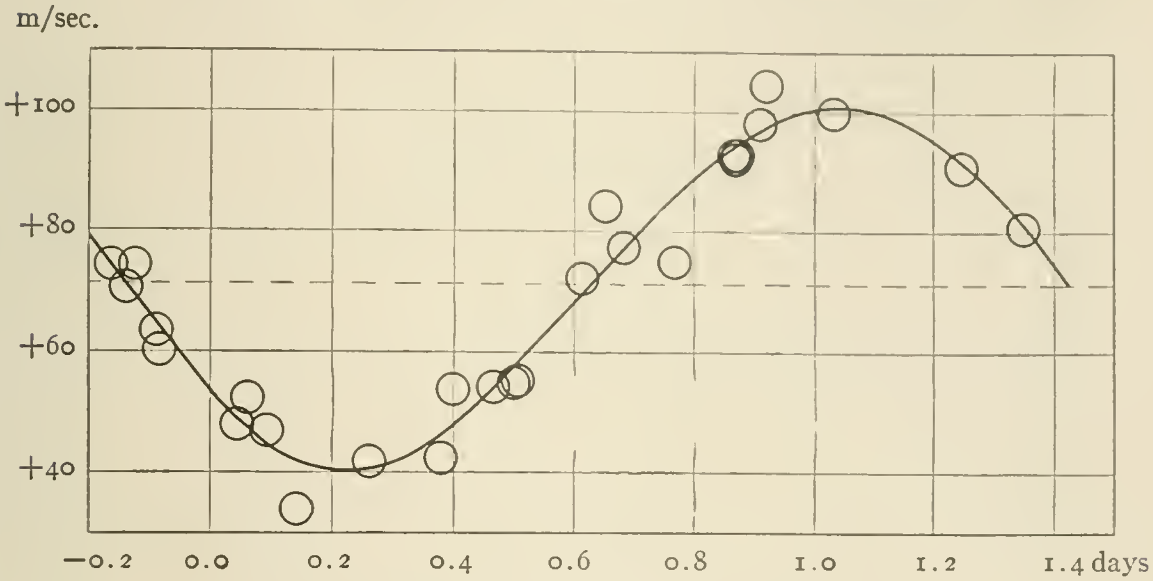

FIG. 1.—Radial velocity-curve for Boss 2227

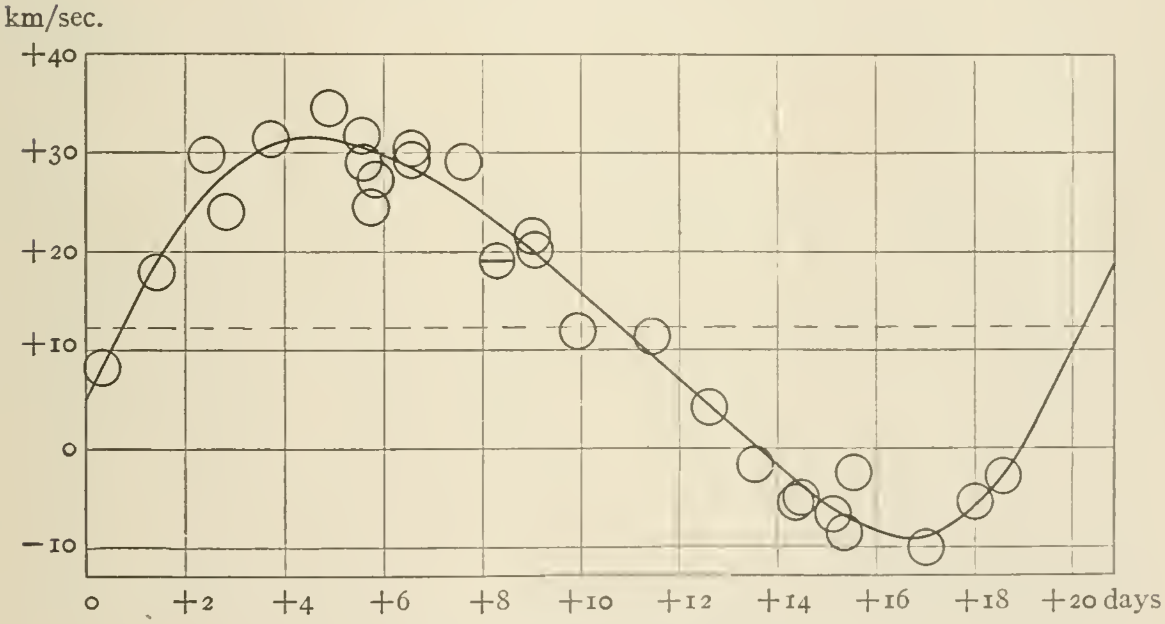

FIG. 2.—Radial velocity-curve for Boss 2447

With preliminary elements derived by Russell's method, an ephemeris was computed and the residuals (O–C) derived. The spectrum is of Class F1, with only one set of lines which at best yields a velocity of only fair precision and which varies so in quality from plate to plate that it has seemed advisable to assign weights to the measures of different plates. The best have been given weight unity and the rest weight 0.75 to 0.50, according to the inherent quality of the lines, or their quality as affected by photographic density, focus, etc., or a combination of these circumstances. The twenty-seven observations were converted into seventeen normal places, assigned proper weights and then used to correct the preliminary elements by the method of least squares. With the elements thus corrected the quantity Σpv^2 is about 75 per cent

TABLE II

Observations of Boss 2227

Plate No.	Date	G.M.T.	Phase	Weight	Velocity	O−C
					km/sec.	km/sec.
γ 8860......	1919 Nov. 12	0^h43^m	$0\overset{d}{.}062$	0.75	+ 52.2	+ 4.9
9109......	1920 Apr. 4	15 11	0.870	0.75	+ 92.6	− 1.8
9666......	Oct. 26	0 19	0.501	1.00	+ 54.6	− 2.7
9687......	29	0 24	0.380	0.75	+ 42.4	− 3.9
C 741......	Nov. 1	0 40	0.262	0.75	+ 41.8	+ 1.3
γ 9705......	2	0 13	1.246	1.00	+ 90.6	− 1.2
9723......	20	0 36	0.506	0.50	+ 55.0	− 2.8
9732......	20	23 58	1.479	0.75	+ 60.3	− 3.6
9738......	21	22 47	0.867	1.00	+ 92.8	− 1.4
9747......	23	1 06	0.401	0.50	+ 53.7	+ 5.8
C 778......	24	1 28	1.416	1.00	+ 70.9	− 0.8
γ 9809......	Dec. 22	22 55	0.614	1.00	+ 72.1	+ 2.4
9893......	1921 Feb. 15	16 47	0.653	0.50	+ 84.0	+ 9.9
9897......	17	15 22	1.031	0.75	+ 99.9	− 0.7
9934......	21	18 20	0.466	0.75	+ 54.1	+ 0.4
C 897......	22	18 29	1.473	1.00	+ 63.5	− 1.2
γ 9940......	23	18 32	0.910	1.00	+ 98.0	+ 1.2
9957......	25	19 46	1.400	0.75	+ 74.2	− 0.2
9995......	Mar. 16	14 50	1.439	1.00	+ 74.4	+ 5.2
9999......	16	18 52	0.045	1.00	+ 48.0	− 0.9
10003......	17	14 42	0.871	1.00	+ 92.8	− 1.6
10012......	19	15 42	1.349	0.75	+ 80.6	− 0.2
10046......	24	15 19	0.095	1.00	+ 46.9	+ 1.8
10091......	Apr. 17	16 25	0.682	0.50	+ 77.3	+ 0.1
10099......	18	17 03	0.143	0.50	+ 33.9	− 8.0
10124......	25	17 40	0.920	1.00	+104.4	+ 7.0
10139......	28	17 04	0.768	0.75	+ 75.0	−11.0

of its value when derived with the preliminary elements. The residuals obtained by substitution of the unknowns in the equations of condition agree satisfactorily with the residuals from an ephemeris based on the final elements. In Table III are to be found preliminary elements, corrections, final elements, and their probable errors. The probable error of a single observation of velocity of weight unity is ±2.64 km/sec. The absolute magnitude (+3.6) is very nearly that of Class F stars of greatest frequency and is therefore typical.

TABLE III

	Preliminary Elements	Corrections	Final Elements
P		....	1.562975 days
e	0.08	−0.029	$0.051 \pm .035$
ω	119°	$+4^{\circ}.92$	$123.92 \pm 34^{\circ}.4$
K	30.5 km/sec.	−0.22 km/sec.	30.28 ± 1.38 km/sec.
T	J.D. 2422650.073	$+0^{d}.009$	$2422650.082 \pm 0^{d}.132$
γ	+71.7 km/sec.	−0.40 km/sec.	+71.3 km/sec.
$a \sin i$		....	650000 km
$\frac{m^3 \sin^3 i}{(m+m_1)^2}$		....	0.0045 ⊙

BOSS 2447

This was announced as a spectroscopic binary in a list published by Adams and Joy.[1] The single set of lines appearing on its spectrograms, which show that its class is G2 and its absolute magnitude +4.1, is quite satisfactory for measurement on properly exposed plates. Table IV gives the data for the twenty-eight plates which have been obtained. With $P = 19.4589$ days all observations arranged themselves satisfactorily within a single period and furnished the basis for the preliminary elements. Since the observations extend over an interval of approximately sixty revolutions of the star in its orbit, this period was taken as definitive. By the method of least squares the other five elements were corrected, equal weights being given to all of the twenty-seven plates which were used. Plate γ 6662, whose residual stood out as the only large one, was arbitrarily rejected from the least-squares solution, and Plate γ 9997 was obtained after the elements were derived. Data for both plates are given in Table IV, however. The quantity Σpv^2 derived from the elements, corrected as indicated by the solution given above, is 18 per cent less than for the preliminary elements, and substitution of the unknowns into the equations of condition gave residuals comparable with those derived from an ephemeris calculated with the corrected elements, which are therefore adopted as final. The preliminary elements, corrections, final elements, and probable errors are given in Table V. The probable error of a single observation of velocity of weight unity is ±1.74 km/sec. The barred circle in Figure 2 represents the velocity from Plate γ 9997.

---

[1] *Publications of the Astronomical Society of the Pacific*, 31, 41, 1919.

TABLE IV

OBSERVATIONS OF BOSS 2447

Plate No.	Date	G.M.T.	Phase	Velocity	O−C
				km/sec.	km/sec.
γ 6396	1917 Nov. 27	0^h01^m	9^d021	+21.6	+ 1.5
6591	1918 Jan. 22	22 51	7.598	+29.1	+ 3.8
6662*	30	22 19	15.574	+ 4.3	+11.8
6706	Feb. 28	20 43	5.589	+29.0	− 1.4
6894	May 1	16 59	9.057	+20.2	+ 0.3
6943	30	16 43	18.589	− 2.8	− 0.3
C 346	1920 Apr. 3	15 02	11.456	+11.4	+ 1.8
352	4	18 43	12.609	+ 4.2	− 0.1
356	5	17 00	13.537	− 1.6	− 1.8
γ 9123	6	15 22	14.469	− 5.0	− 1.2
9130	7	17 04	15.540	− 2.5	+ 4.9
9179	May 6	15 39	5.563	+31.7	+ 1.2
9186	7	15 35	6.560	+30.4	+ 2.0
C 410	7	15 35	6.560	+29.3	+ 0.9
γ 9255	June 4	16 16	15.130	− 6.7	− 0.5
9266†	6	15 58	17.017	−10.1	− 1.2
9272	7	15 56	18.016	− 5.4	+ 0.6
9667	Oct. 26	0 52	2.813	+24.0	− 3.9
9688	29	1 03	5.821	+27.3	− 2.7
9767	Nov. 26	1 05	14.367	− 5.5	− 2.1
9774	27	0 53	15.359	− 8.6	− 1.8
9876	1921 Jan. 28	20 14	0.326	+ 8.2	− 0.1
9886	29	22 21	1.414	+17.9	− 0.8
9889	30	22 33	2.422	+29.8	+ 3.9
9927	Feb. 20	16 36	3.716	+31.4	+ 0.8
9935	21	20 56	4.896	+34.5	+ 3.3
C 896	22	17 10	5.739	+24.4	− 5.7
γ 9969	26	21 46	9.930	+11.9	− 4.4
9997‡	Mar. 16	17 06	8.277	+19.2	− 3.7

* Not used in least-squares solution.

† Poor plate.

‡ This plate obtained after elements were derived.

TABLE V

	Preliminary Elements	Corrections	Final Elements
P		....	19.4589 days
e	.200	+ .006	0.206 ± .002
ω	248°5	+4°00	252°5 ± 7°70
K	20.5 km/sec.	−0.29 km/sec.	20.21 ± 0.49 km/sec.
T	J.D. 2422426.555	$+0\overset{d}{.}079$	$2422426.634 \pm 0\overset{d}{.}384$
γ	+12.49 km/sec.	−0.16 km/sec.	+12.3 km/sec.
$a \sin i$		....	5295900 km
$\frac{m^3 \sin^3 i}{(m+m_1)^2}$		....	0.0157 ⊙

Mount Wilson Observatory
October 1921

AN INVESTIGATION OF THE CONSTANCY IN WAVE-LENGTH OF THE ATMOSPHERIC AND SOLAR LINES[1]

By CHARLES E. ST. JOHN and HAROLD D. BABCOCK

ABSTRACT

Constancy in wave-length of atmospheric lines in the solar spectrum.—In 1915 Perot reported having found the wave-length of an O line considerably longer at noon than at sunrise and sunset. Since these lines are constantly used as standards of wave-length in solar observations, a study of the *wave-length as a function of the altitude of the sun* was made for a number of atmospheric lines in the B group at λ 6867, in the α group at λ 6276, and in the water-vapor band near λ 5900. Measurements of 25 plates show no indication of a variation greater than the accidental error. Moreover, spectrograms and data accumulated at Mount Wilson since 1911 give wave-lengths, some determined with reference to solar lines and some with reference to arc lines, which agree very closely, the difference from the general mean shown by any plate seldom exceeding 0.001 A. This negative result indicates the absence of high velocity *radial currents in the earth's atmosphere* and justifies the use of atmospheric lines as a reliable standard of reference even in work requiring the highest precision.

Constancy in wave-length of lines from the center of the solar disk.—While Evershed reported in 1919 remarkable variations amounting to several thousandths of an angstrom, the experience at Mount Wilson is that the more carefully the solar wave-lengths are compared with standard arc lines, the smaller the deviations from spectrogram to spectrogram become. Evidence from 13 plates is presented. These results prove that the *radial convection currents in the sun*, while not absent, are remarkably constant, apparently downward at high levels and upward, but small, at low levels.

In spectrographic observations on the solar spectrum for determining wave-lengths and displacements of the Fraunhofer lines with high precision, a desideratum is some means of procuring a simultaneous comparison spectrum under the same conditions of illumination as those obtaining for the spectrum under investigation. Provided their wave-lengths are constant, ideal conditions occur when atmospheric lines are used for reference in solar observations, since in the instrument the path of the light is identical for both classes of lines.

It has been generally assumed that under all practical conditions of solar observation the velocities of terrestrial atmospheric movements are of such an order that no measurable Doppler effect is produced. It would require motion in the line of sight of approximately 125 miles an hour to cause a displacement of 0.001 A at λ 6000. Some observations reported by Perot,[1] however, give very remarkable and surprising results, and if confirmed would show that the atmospheric lines are not constant in wave-length and hence not reliable as standards of reference. He measured with an interferometer the wave-length of an oxygen line in the B group at different hours of the day and concluded that the wave-length increased from morning to noon and decreased from noon to evening. He interprets his results as showing a recession of the absorbing centers from the surface of the earth with a radial velocity of about 3 km per second.

---

[1] *Contributions from the Mount Wilson Observatory*, No. 223.

In view of the importance of the atmospheric lines in solar observations we have examined for change in wave-length during the day the atmospheric lines in three spectral regions, namely, in the B group at λ 6867, in the α group at λ 6276, and in the water-vapor band near λ 5900, and have supplemented these observations from spectrograms taken for other purposes through a series of years. For much of the measurement and reduction we are under obligation to Miss Ware, Miss Miller, and Miss Keener.

Oxygen lines in the B group.—On two occasions grating spectrograms of the center of the sun were taken in the first order of the 75-foot spectrograph of the 150-foot tower at intervals from sunrise to sunset. The wave-lengths of eight oxygen lines were obtained from solar lines whose wave-lengths were corrected for the earth's motions. The statistical results are given in Table I. The lines are identified by their Rowland wave-lengths in the first and fourth columns and in the other columns are given the deviations from the mean for the hours of observation. In Figure 1*A* the average deviations from the general mean are plotted against the corresponding altitudes of the sun.

From our investigation on solar wave-lengths in the international system we extract the data given in Table II. These measurements were made during June, 1919, with the interferometer attached to the Snow telescope. Our unpublished international values of solar lines were used as standards. The first column contains the preliminary wave-lengths in the international system of 28 oxygen lines in the B group. In the other columns are shown

---

[1] *Comptes Rendus*, 160, 549, 1915.

TABLE I

Relative Wave-Lengths of Oxygen Lines of the B Group at Different Hours of the Day. Grating Spectrograms

(Unit for residuals=0.001 A)

λ Rowland	February 25–26, 1919, P.S.T.			λ Rowland	June 5, 1919, P.S.T.						
	7:00	12:00	4:37		6:27	9:12	11:56	2:57	3:02	5:41	5:50
6879.288	+2	−3	0	6877.882	+4	0	−2	−2	0	0	0
6880.172	+6	+2	−7	6880.172	+4	+2	−2	−1	+1	−2	−2
6884.076	0	+2	−3	6884.076	+4	−4	−5	0	+1	+1	0
6886.000	+1	+2	−3	6900.199	+2	−4	−3	+2	+2	−2	+4
6913.448	−7	+5	+1	6905.271	+2	−2	+1	−1	0	−3	0
6914.337	−5	0	+6	6909.676	+1	0	0	−3	+1	−1	−1
6918.370	....	+1	−1	6913.448	+2	0	−1	−3	−1	0	−4
6919.250	....	−1	+2	6918.370	+1	0	+3	0	+2	−2	−1
Mean	−0.5	+1.0	−0.6	Mean	+2.5	−1.0	−1.1	−1.0	+0.6	−1.1	−0.5
Altitude	7°00′	46°40′	10°20′	Altitude	17°40′	51°30′	78°10′	49°40′	48°40′	16°10′	14°20′

the deviations from the mean values for altitudes varying from 12°50′ to 75°40′. The observed mean wave-length at the highest altitude is 0.0012 A less than the general mean.

Oxygen lines of the α group.—On June 7 and 9, 1919, spectrograms of the center of the sun were taken with the 75-foot spectrograph at intervals from 6:00 A.M. to 6:00 P.M. Eight oxygen lines of the α group were measured in terms of solar standards. After correction of the reference lines for the earth's motions, the mean wave-length at noon exceeded the mean for the two lowest altitudes by 0.0016 A. The numerical data are given in Table III; the relative results are plotted in Figure 1*B* against the hours of observation.

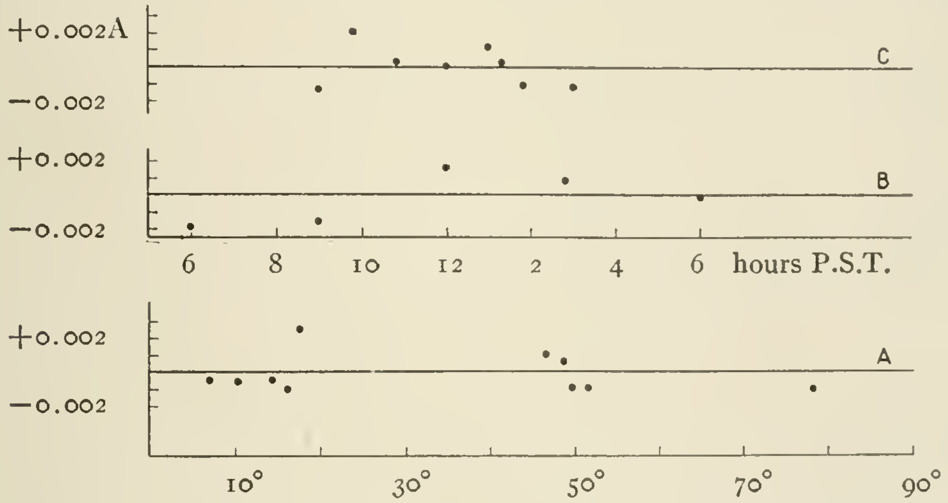

FIG. 1.—*A*. Deviations of oxygen lines in B group from mean wave-length; for different altitudes of sun.

B. Deviations of oxygen lines in α group from mean wave-length; at different hours of the day. Solar standards.

C. Same as *B*, referred to absorption lines of iodine as standards.

In order to eliminate solar standards and obtain an independent determination, spectrograms of sunlight filtered through iodine vapor were taken with an interferometer using two absorption lines of iodine as the fixed references. These observations were made in the Pasadena laboratory in April, 1919, with an etalon of 20 mm separation giving a mean order of interference of 63400 for the eight measured oxygen lines of the α group. The deviations from the mean wave-length at the hours of observation are plotted in Figure 1*C*. The wave-length at noon shows no deviation from the mean of the series.

TABLE II

Relative Wave-Lengths of Oxygen Lines of the B Group at Different Hours of the Day. Interferometer Spectrograms

(Unit for residuals=0.001 A)

June 6, 15, 16, 1919, P.S.T.

λ I.A.	June 6 9:08	June 6 10:32	June 6 12:36	June 16 3:40	June 15 5:11	June 16 6:03
6872.265	−3	−1	+1	+2	+3	−3
6872.861	+1	−3	−3	+3	0	....
6873.816	−2	0	0	0	+4	−2
6874.671	−2	+1	−3	−2	+5	0
6875.608	0	0	0	0	+3	−5
6876.733	−2	+3	0	−2	−2	+1
6877.655	+2	+2	−2	−3	+1	−1
6879.058	+2	+3	−3	+2	−1	−10
6879.947	+4	0	−3	−1	−1	−5
6883.850	+1	+1	0	−1	+1	−6
6885.772	−1	+1	−1	−1	+4	−4
6886.761	−1	+1	−2	0	+3	−3
6888.967	+1	+1	−1	0	0	−3
6889.921	−2	0	0	+2	−3	....
6892.389	−6	+3	−3	+2	−1	....
6893.328	0	0	−5	−2	+6	−4
6896.056	0	+2	+2	−2	−3	−2
6896.984	+1	0	0	+1	−3	−3
6899.972	−1	0	−1	+2	−1	+2
6900.887	−2	+1	−4	+0	+4	−5
6904.137	−1	+2	−2	−2	0	....
6905.137	−1	+2	−2	−2	0	....
6908.553	+1	+1	−3	−1	+3	−2
6909.450	−1	+2	−2	−1	+1	−3
6913.219	0	+3	+1	−4	+1	....
6914.109	0	+5	0	−4	+1	....
6918.140	−2	+2	−2	+1	−3	....
6919.022	+1	0	−1	−1	+3	....
Mean	−0.4	+1.1	−1.4	−0.5	+1.0	−2.9
Altitude	50°40′	67°20′	75°40′	41°10′	22°30′	12°50′

From spectrograms and data accumulated since 1911, when the *a* band was first studied at Mount Wilson, a yearly record is available. The results for eight lines are given in Table IV. The mean wave-lengths for the eleven-year period are in the first column and those for the separate years in the succeeding columns. The mean wave-length of the group is shown at the bottom of the table. The spectrograms were taken in various months, on various days, and at various hours. It would seem that frequently occurring disturbances should have been detected; but on none of the scores of spectrograms measured is there definite evidence of radial movements of the absorbing regions of the atmosphere. The difference from the general mean shown by any plate seldom exceeds 0.001 A.[1]

TABLE III

WAVE-LENGTHS OF OXYGEN LINES OF THE a GROUP AT DIFFERENT HOURS OF THE DAY. GRATING SPECTROGRAMS

June 7–9, 1919, P.S.T.

λ I.A.	June 7 6:00	June 7 9:00	June 7–9 12:00	June 9 2:50	June 9 6:00
6280.404	.403	.402	.406	.404	.403
6281.187	.185	.186	.189	.189	.186
6281.964	.962	.962	.966	.966	.963
6290.230	.229	.230	.232	.230	.229
6295.187	.185	.184	.188	.187	.188
6295.969	.967	.968	.970	.971	.968
6302.009	.006	.006	.010	.009	.010
6302.770	.768	.769	.772	770	.771
Mean .215	.2131	.2134	.2166	.2158	.2148
No. of plates	2	1	3	2	4
Altitude	12°30′	49°10′	78°40′	51°20′	12°40′

Water-vapor lines near λ 5900.—To complete the investigation on atmospheric lines, grating spectrograms of the center of the sun's disk were taken at high and low sun in the region of the rainband near D_1 and D_2. The results of the measures of eleven lines on twenty-four spectrograms are shown in Table V. Solar lines were used as standards. The mean wave-lengths in the international system are in the first column, weighted according to the number of exposures. For the eleven lines the wave-length at high sun exceeds the mean at low sun by 0.001 A.

---

[1] This confirms and extends in time other observations on the a group. Royds, *Annual Report, Kodaikanal Observatory*, 1917; St. John and Babcock, *Publications of the Astronomical Society of the Pacific*, 31, 178, 1919.

TABLE IV

YEARLY RECORD FOR ATMOSPHERIC LINES OF THE a GROUP

MEAN WAVE-LENGTHS I.A. UNITS	STANDARDS OF REFERENCE										
	Solar Lines Corrected for the Earth's Motions								IRON ARC LINES USED AS STANDARDS		
	At Center			At Limb, Corrected for Limb-Center Shift							
	1911	1912	1913	1914	1915	1916	1917	1918	1919	1920	1921
6280.400	.400	.400	.403	.403	.400	.397	.400	.402	.402	.398	.403
6281.186	.183	.185	.185	.186	.184	.183	.185	.185	.186	.187	.188
6281.963	.961	.960	.963	.964	.966	.962	.963	.963	.963	.963	.964
6290.229	.230	.229	.228	.230	.229	.228	.226	.229	.229	.229	.229
6295.186	.187	.183	.184	.186	.185	.184	.187	.182	.187	.185	.185
6295.968	.970	.967	.968	.969	.968	.967	.967	.965	.968	.968	.970
6302.008	.009	.007	.010	.012	.006	.008	.005	.005	.008	.007	.009
6302.771	.771	.771	.769	.776	.772	.768	.771	.767	.770	.772	.772
Mean .214	.214	.213	.214	.216	.214	.212	.213	.212	.214	.214	.215
No. of plates	8	2	2	3	4	2	2	2	22	13	2

TABLE V

WAVE-LENGTHS OF WATER-VAPOR LINES AT DIFFERENT HOURS OF THE DAY (March and June 1921)

λ I.A.	P.S.T. of Observation			
	7:03	11:40	3:16	5:40
5885.982	.980	.983	.984	.980
5887.227	.226	.227	.230	.226
5887.665	.664	.668	.663	.664
5892.402	.396	.405	.403	.402
5909.001	.998	.000	.004	.002
5913.999	.998	.996	.004	.999
5919.058	.056	.059	.059	.057
5919.646	.644	.647	.646	.646
5924.276	.275	.275	.278	.276
5932.097	.096	.097	.098	.097
5932.788	.788	.788	.788	.788
Mean .4675	.466	.468	.469	.467
Altitude	16°	61°	35°	13°

When the observations on atmospheric lines at high sun are compared with the mean for all altitudes, the residuals, high sun *minus* mean, are as follows:

Source	Lines Observed	Altitude High Sun	Residuals
Table I	B group	78°10′	−0.0010 A
Table II	B group	75 40	−0.0012
Table III	α group	78 30	+0.0016
Table IV	Water-vapor	61 20	+0.0005
Mean			0.0000

We are unable to account for the wide divergence between our measures and those of Perot. Within the error of measurement our series of observations show no variation in the wave-lengths of the terrestrial lines with the altitude of the sun. It will be recalled that Dunér,[1] in his determination of solar rotation in 1887–1889, used the terrestrial line λ6302.209 as a fixed point of reference, and in 1899–1901 the other component of the pair, λ6302.975. If the terrestrial atmosphere in the absorbing region is subject to radial velocities of 3 km per second his consistent

[1] *Über die Rotation der Sonne*, Upsala, 1906.

values are remarkable, particularly for the highest latitude where the observed rotational velocity was only 0.39 km per second. It must be admitted that radial velocities in the earth's atmosphere of the order of 3 km per second, if they do occur, are extremely rare and very local. It seems to us more probable that a different interpretation should be sought for Perot's observations. His interpretation requires for the absorbing centers a radial velocity of 6700 miles per hour. That such enormous radial velocities occur even in attenuated regions of the earth's atmosphere is open to question, and it is more doubtful still that the radial component would remain constant for a month over a given locality. From our observations we feel justified in using the atmospheric lines as reliable standards of reference, even in work requiring the highest precision.

On constancy of wave-length of solar lines.—Jewell[1] was the first to raise the question of variability in the wave-lengths of the solar lines. He says,

> Another effect of this investigation may be to make the lines of the solar spectrum step down from the commanding position which they have occupied, as standards of reference.

At the period of Jewell's investigation the instability of many lines in the arc spectra of metals had not been recognized. Moreover, the records of the spectrograms taken by Rowland and used by Jewell were not sufficiently detailed to determine corrections depending upon the earth's motions. Under these conditions the conclusion reached by Jewell loses much of its weight. Evershed[2] reports that

> a continuous series of sunlight and Fe spectra was taken to test the constancy of the sun-arc displacement. Confining attention to the region 4337–4531 and to lines not subject to pole-effect in the arc, it was found that some remarkable variations occurred amounting to several thousandths of an angstrom. The variations are of two kinds: a general change for all the lines in the region studied, and a change affecting particular lines or groups of lines.

He says,

> These displacements may be observed at the center of the disk, but up to the present they have not been found very near the limb. It appears therefore that, unlike the displacements in the penumbra of spots, they may be

---

[1] *Astrophysical Journal*, 3, 113, 1896.

[2] *Annual Report, Director, Kodaikanal and Madras Observatories*, 1919, p. 2.

due to movements normal to the surface or having a component normal to the surface.

At Mount Wilson it has been found that in the determination of solar wave-lengths from arc standards, the more carefully the iron arc is controlled, the more completely instrumental displacements are eliminated, the more accurately the image of the sun is centered,[1] and the more exactly the axes of the light-cones incident upon the grating are made to coincide, the smaller the deviations from spectrogram to spectrogram become.

A comparison of four observations with the grating spectrograph from April to June, 1921, and the mean of measures in 1917 for the 13 solar lines common to all plates gives for the fractional part of the mean wave-length the following:

		1917, Mean	1921, April 21	1921 April 29	1921 May 1	1921 June 1
13 lines...........	λ 4337–λ 4401	0.5545	0.5552	0.5550	0.5565	0.5554

The three April-June observations for the other common lines also show good agreement in the fractional part.

		1921, April 21	April 29	May 1
17 lines................	λ 4489–λ 4607	0.5574	0.5594	0.5593
15 lines................	λ 4615–λ 4688	0.3942	0.3941	0.3945
20 lines................	λ 4707–λ 4784	0.5217	0.5217	0.5216

These wave-lengths are determined from the arc standards, not by measuring the displacements between the center of the sun and arc, but by using the arc lines as standards of reference. Five interferometer spectrograms likewise referred to arc standards, taken on August 5, 1920, at intervals from 10:44 A.M. to 5:03 P.M. P.S.T. and one taken a year later on August 8, 1921, give deviations from the mean of the six as follows for a group of 38 solar lines:

		August 5, 1920					August 8, 1921
		10:44	2:34	3:30	4:22	5:03	4:50
38 lines...	λ 5497–λ 5862	.0000	+.0011	+.0003	−.0020	+.0005	.0000 A

---

[1] *Observatory*, **43**, 260, 1920.

The degree of constancy of the solar wave-lengths at the center of the sun shown by these determinations is further evidenced by considering the data in Table IV from this point of view.

The wave-lengths of the oxygen lines in the table, except for the years 1920–1921, were referred to solar standards determined as above. In 1911, 1912, 1913, and 1919 the wave-lengths of the solar lines at the center of the disk were used. For the years 1920–1921 the oxygen lines were referred directly to the iron-arc standards. This completes the cycle: arc–sun–atmospheric lines–arc. The closing of the cycle is practically perfect. Unless it is assumed that continuously compensating changes in the wave-lengths of the solar and terrestrial lines occur, the agreement between the first and last sections of Table IV may be taken as a measure of the constancy in wave-length of the atmospheric lines and of the solar lines at the center of the disk, and also of the accuracy of their determination in terms of the international iron-arc standards. In 1914–1918 the results are less dependable, as the measures were made upon spectrograms of the limb and it was necessary to apply a correction for the limb-center shift, a somewhat uncertain quantity for a single observation. From an extended series the mean limb-center shift for solar lines in this spectral region is 0.007 A with a range of 0.002 to 0.010 A.

In view of the probable existence of radial convection currents on the sun the relative constancy of wave-length at the sun's center is somewhat surprising. At any given level, the radial velocity appears to reach a comparatively steady state, differing from level to level and in widely different levels even opposite in direction. For the strong lines—high-level lines—the motion is apparently downward. The great intensity of these lines at high levels is probably dependent on the increased ionization under the low pressures at the high elevations.[1] As yet too little is known of the ionizing potentials of the elements involved for a definite conclusion. For very low-level lines the motion is small but upward. At both low and high levels we appear, however, to be dealing with remarkably steady states. In this regard there is a marked difference between the center and the limb, the range of deviation from plate to plate at the limb being four- to five-fold that at the center. Though the causes of the motions in the solar and terrestrial atmospheres are different, there may be common characters in the general atmospheric movements due to the similar damping influences. In both cases centrifugal velocities are opposed by gravitation, very powerfully so in the sun, while tangential movements are damped by the smaller forces of friction. Thus through a kind of selective action the tangential components would tend to persist and the radial components to be quenched, so that in both the solar and terrestrial atmospheres the prevalent atmospheric flows would tend to be tangential. In the sun the opposing effects of light-pressure and gravitation may have influence in producing the steady state at any given level, the different levels of the absorbing centers being again a selective result as the equilibrium between light-pressure and gravitation depends upon the ratio between the mass and diameter of the centers.

---

[1] Megh Nad Saha, *Philosophical Magazine*, 40, 472, 1920.

From these observations it is evident that differences between solar wave-lengths at the sun's center and in terrestrial sources may be determined with an accuracy comparable to that for the terrestrial lines. Upon the magnitude of these differences, their variation over the solar disk, from element to element, from line to line, and from wave-length to wave-length, rests the possibility of disentangling the causes of the displacement of solar lines, a formidable but far from hopeless undertaking.

Mount Wilson Observatory
October 1921

THE WAVE-LENGTH IN ASTRONOMICAL INTERFEROMETER MEASUREMENTS[1]

By J. A. ANDERSON

ABSTRACT

Effective wave-length in measurements with astronomical interferometer.—The separation of double stars and the diameters of stellar disks are measured by the interferometer in terms of an effective wave-length λ which is such that if the stellar object emitted monochromatic light of wave-length λ the setting of the interferometer would be that actually found. The accuracy of setting obtainable in these measurements is such that in each case λ should be known to a few tenths of 1 per cent. *For any star*, the normal effective wave-length may be computed from the effective temperature corresponding to its spectral type, by combining the Planck radiation law with the mean transmission curve for the atmosphere and with the A.I.S. visibility-curve for the normal eye. The corrections required for variations of atmospheric absorption and of eye sensitivity from the assumed values may best be obtained experimentally by observations on sunlight, since in any case the correction is equal to the difference between the observed and computed effective wave-lengths for sunlight under the same conditions. The method and apparatus used in the *determination of the effective wave-length for sunlight* are described, and the results of some observations on the *variation of λ with zenith distance and atmospheric conditions* are given. On Mount Wilson the values found vary from 5660 A at sunrise and sunset to 5510 A for zenith distances up to 60°; at Pasadena the variation with zenith angle was more rapid. The wave-length was greater on cloudy days and least after a rain.

Astronomical interferometer.—The distribution of intensity in the interference patterns, for both circular and rectangular apertures, is fully discussed, and in the particular case of a double star is given mathematically for all points of the focal plane, for all orientations of the apertures. *The effect of the size of the apertures on the setting* is nil when rotation is used and also when the setting is made for minimum visibility of the fringes; but when the apertures are separated until minimum intensity at the center is obtained, it is found both theoretically and experimentally that for apertures of width a and separation D, the effective separation is very closely equal to $D/[1+K\,(a/D)^2]$ for D/a greater than 3.5, where K is 0.223 instead of 0.765 as given by Hamy.

The interferometer as used in astronomical measurements consists of two apertures alike in shape and size, placed either in front of the objective or in the converging beam a short distance in front of the focal plane. The idea of using a telescope in this manner appears to have originated with Fizeau,[2] and the first actual trials were made by Stephan.[3] Michelson[4] carried both the theory and applications of the method considerably farther than his predecessors; he gave an analytical treatment for the case of a pair of narrow slits, and applied it to the determination of the diameter of Jupiter's satellites. Hamy[1] treated the case of narrow slits, and also that of rectangular apertures whose width cannot be neglected in comparison to their separation, and applied his results to a measurement of the diameter of Jupiter's satellites and of some of the brighter asteroids. Comstock[2] used the method for a determination of the effective wave-length of star light. The work of the past two years is so recent that references to it need not be given here in detail.

---

[1] *Contributions from the Mount Wilson Observatory*, No. 222.

[2] *Comptes Rendus*, 66, 934, 1868.

[3] *Ibid.*, 78, 1008, 1874.

[4] *Philosophical Magazine*, 30, 1, 1890.

The purpose of the present paper is to call attention to the necessity of knowing quite accurately the effective wave-length of the source which is studied; to describe and illustrate a method for determining this quantity quickly and accurately; and to discuss in some detail the effect of using apertures of different shapes and sizes.

Consider first the determination of the diameter of a star, assumed to appear as a uniformly luminous circular disk. If the apertures are narrow in comparison with their separation, the angular diameter is given by

$$\beta=\frac{1.22\lambda}{D} \tag{1}$$

where β is the angular diameter, D the distance between the centers of the apertures corresponding to the first vanishing of the interference fringes as the distance is increased, and λ the wave-length of light. The two quantities which determine β are λ and D. Experience indicates that the probable error in the determination of D under good conditions is of the order of 1 per cent; and accordingly if the uncertainty of the true value of λ exceeds a few tenths of 1 per cent, the probable error of β will be larger than that of D.

Again, consider a double star whose angular separation is to be measured. This is given by

$$a=\frac{\lambda}{2D} \tag{2}$$

where a is the angular separation, the other quantities being the same as in (1). In this case, under good conditions, the uncertainty in the value of D is considerably less than 1 per cent.

[1] *Bulletin Astronomique*, 16, 257, 1899.

[2] *Astrophysical Journal*, 5, 26, 1897.

Other cases might be given, but always the quantity to be measured will be expressed in the form $K\lambda$, where K is determined by the actual observation, while λ in general must be found by some other means, and since λ is always a simple multiplier, it is necessary or at least desirable to know its value with a probable error considerably smaller than that involved in K.

At present all observations with the interferometer are made visually, and hence the value of λ will fall somewhere near the middle of the visibility curve of the eye, at least for sources emitting white light; or, we may say that λ will have a value lying somewhere within the range 5400 A to 6000 A. It follows from what has just been said that, if possible, λ should be known for a given source within 10 A to 20 A.

Definition of the effective visual wave-length.—*a*) Let an artificial double star be illuminated with the white light whose effective visual wave-length is required; let this double star be viewed with an interferometer, and the latter adjusted so that the interference fringes just disappear according to equation (2). Leaving the interferometer unchanged we now illuminate the double star with the monochromatic light whose known wave-length can be varied at will. The value of λ which just makes the fringes disappear is defined as the effective visual wave-length of the white source in question.

b) Analytically[1] the definition may be given as follows: Take rectangular co-ordinates in the focal plane with the origin on the axis of the telescope. Let the geometrical images of the components of a double star fall at $(+c, 0)$ and $(-c, 0)$. Let the apertures be narrow slits separated by a distance D, and the focal length of the objective be F.

If $I(\lambda)d\lambda$ be the visual effect of the radiation of the source lying between the limits λ and $\lambda+d\lambda$, the intensity along the x-axis is given by

$$J=\int_0^\infty I(\lambda)d\lambda\left[\cos^2\frac{\pi D(x-c)}{F\lambda}+\cos^2\frac{\pi D(x+c)}{F\lambda}\right] \tag{3}$$

---

[1] This statement was first suggested to the writer in a letter from Dr. C. M. Sparrow.

When D is very small, J has a maximum at $x=0$. As D increases, J diminishes for $x=0$, reaching a value of zero when D is somewhere near $F\lambda_0/2c$ where λ_0 is an arbitrary value of λ near the middle of the range for which $I(\lambda)$ has an appreciable value. Both for D small and for D having a value near $F\lambda_0/2c$, J oscillates as x is varied; but for a value of D in the neighborhood of $F\lambda_0/4c$, these oscillations become very small, and in particular at $x=0$, $J(x)$ will have a stationary value for some particular value of D. The condition for this is

$$\frac{\partial^2 J}{\partial D^2}=0; \quad \text{for } x=0 \tag{4}$$

Solving (4) we have $D=F\lambda_0'/4c$, where λ_0' is the effective visual wave-length required.

For a source such as a given star, $I(\lambda)$ is defined as follows: Let $E(\lambda)$ represent the energy-curve of the star, as determined outside our atmosphere; let $T(\lambda)$ be the transmission-curve of the atmosphere at the time and place of the observation; and let $V(\lambda)$ be the visibility-curve of the eye of the observer; then

$$I(\lambda)=E(\lambda)T(\lambda)V(\lambda).$$

Some questions now naturally arise, among which the following are important enough to state:

1. If in (*a*), instead of using an artificial double star, we use an artificial star disk, would the same value of λ be obtained?

2. If the components of a double star are of different spectral types, or, what amounts to the same thing, if the effective wave-length of the components is not the same, what wave-length is to be used in calculating the angular separation from the data given by an observation with the interferometer?

3. In case of a star disk darkened toward the limb, if this darkening is accompanied by a color change, what value of λ is to be used?

It is important to remember that when the observations are made visually, different observers will not in general find the same effective wave-length for a given source. In (*b*) above this is provided for by the factor $V(\lambda)$, which may differ slightly for different observers. In (*a*) it is automatically provided for by reason of the fact that the same observer is supposed to make both the adjustments. Again, since $T(\lambda)$ enters as a factor in $I(\lambda)$, an observer will not obtain the same value of λ for a given source under different conditions of observations as to time and place.

Only a beginning has thus far been made in the application of the interferometer to astronomical measurements, and it is too early to predict what its future may be; yet it will undoubtedly be valuable in certain restricted fields; for example, in the direct determination of star diameters and in the measurement of very close double stars of particular types. No doubt it will be applied successfully also in other fields. Now, as has already been pointed out, the result of any interferometer measure[1] will be expressed in the form

$$\theta = K\lambda \tag{5}$$

where K is given by the observation, and λ depends upon the object observed. If λ did not depend upon local conditions such as the observer, the time and place of the observation, and the instruments employed, the reduction would be a relatively simple matter; for this case the value of λ could be found, once and for all, for stars of all spectral types. It is clear, however, from what has already been said, that this may involve errors very much larger than the errors of observation. On the other hand, it will obviously be quite impracticable for each observer to determine independently the value of λ for every observation he makes. The following plan will, it is hoped, remove most of the difficulties. We will leave out of account objects such as the planetary nebulae, that is, objects having discontinuous spectra, for in such cases there is no difficulty in determining the value of λ with sufficient accuracy. Consider then only objects like the great majority of the stars, having continuous spectra, more or less similar to spectra of black bodies at various temperatures. The fact that no star radiates exactly like a black body is of little importance, because the black-body temperature will be used merely as an auxilliary in the general scheme. The black-body temperature of stars has been determined for all or nearly all the brighter stars, and these include nearly all of the spectral types that it will be necessary to consider.

[1] The position-angle of a double star is an exception.

Using Planck's law, the mean transmission-curve of the atmosphere, and the adopted *A.I.S.* visibility-curve of radiation, we may compute by equation (4) the value of λ_0' for a few temperatures from 3000° to 20,000° absolute. A curve passed through the computed points will enable one to read off λ_0' for any temperature within the range. The absolute value of the wave-lengths thus derived may not be correct, but this does not matter, for their relative values will be sensibly right. To illustrate the use of such a curve in practice, suppose that an observer has made an interferometer measure of a star of spectral type F0; assume also that he has made a determination of the effective wave-length of sunlight by the method given later in this paper. From tables giving the effective temperatures of stars of different spectral types, he reads off the temperature for an F0 star and for a star of the same spectral type as the sun. Let these temperatures be, respectively, T_1 and T_2. From the curve the corresponding wave-lengths are λ_1 and λ_2. If now the measured wave-length of sunlight is λ_0, the proper wave-length for the F0 star will be

$$\lambda=\lambda_0+\lambda_1-\lambda_2 \tag{6}$$

Of course, as the determination of λ_0 is necessarily made in daytime while the observation of the star is made at night, it is probable that the atmospheric conditions will have changed in the interval. But as different determinations of λ_0 will soon show about what correction is required for variations in observing conditions, this difficulty is not very serious.

Experimental determination of effective wave-length.—In Figure 1 let *A* be an artificial double star, consisting of two small pinholes

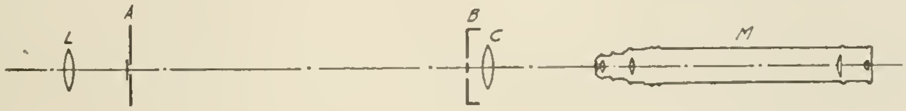

FIG. 1

whose linear separation is δ, illuminated by white light such as sunlight. At *B* are two circular apertures separated by the distance *D*, so mounted that they can be rotated about the axis of the telescope *C*. Observations are made through the compound microscope M. The distance A to B will be denoted by L. The angular separation of the pinholes as viewed from B is δ/L. The value of D for the first disappearance of the interference fringes, if the line joining the pinholes is parallel to that joining the apertures at B, is, by equation (2),

$$\frac{\delta}{L}=\frac{\lambda}{2D}$$

or, if the two lines make an angle θ with each other,

$$\frac{\delta}{L}=\frac{\lambda}{2D\cos\theta} \tag{7}$$

All the quantities in the equation except λ are directly measurable, and hence λ can be determined.

In order to form some idea of the accuracy to be expected in this determination, we will now examine in detail the measurement of each of the quantities entering into equation (7).

In the present experiments δ was of the order of 0.6 mm. The two pinholes were made in tinfoil, as follows: A fine needle was selected and mounted in a mechanics' pin-chuck. A small piece of tinfoil was smoothed out on a flat, smooth piece of soft metal such as brass or aluminum. A small round hole was made by resting the needle point on the tinfoil, the needle and chuck being vertical, and then carefully turning the chuck a few times. By always taking care to have the pressure about the same, holes of very nearly the same diameter may be made, and if care is used in rotating the chuck and in lifting the needle after the operation, the holes will be quite perfectly round. The diameter of the pinholes used was between 0.035 and 0.050 mm. Under a microscope the distance between such a pair of openings can be determined with a probable error of about 0.0002 mm. Since δ is about 0.6 mm, this corresponds to a probable error of the order of 1 in 3000. Before measurement the tinfoil is mounted on a metal plate through which a hole about 2 mm in diameter has been drilled, the apertures in the tinfoil being directly over this hole.

Two sources of error are to be noted in using such an arrangement as an artificial double star:

1. The plane of the apertures will not in general be exactly perpendicular to the line of sight from the observing telescope, but will make an angle ϕ with this line. The apparent separation will then be not δ but $\delta \sin \phi$. With ordinary care in mounting the tinfoil and adjusting the plate, ϕ should not differ from 90° more than a degree, which would at most cause an error of 15 parts in 100,000, which is negligible.

2. When an image of the sun is formed on the apertures, the tinfoil becomes heated somewhat, causing δ to increase. The rise in temperature to be expected may be roughly estimated. The image-forming lens has an area of 16 cm^2, and its focal length was 1 meter, so the diameter of the image was roughly 1 cm. Of this $\frac{1}{25}$ fell on the tinfoil, which is equal to the amount of sunlight falling on $\frac{16}{25}$ cm^2, or 1 calorie per minute. Assuming that the tinfoil reflects 80 per cent of this, we have $\frac{1}{5}$ calorie per minute taken up by the tinfoil or 0.003 calorie per second. When equilibrium is established, the greater part of this energy passes by conduction from the tinfoil to the brass plate, which is so large that its temperature never rose appreciably above room temperature. A temperature gradient of 3° per centimeter in the tinfoil would more than suffice to carry this amount of energy to the brass plate—and hence we may conclude that, within a very few degrees, the tinfoil was always at room temperature, and that the error due to thermal expansion was less than 1 in 10,000, which is negligible.

The value of D was usually between 6 and 7 mm. The apertures were round holes made with a drill in a brass plate; they were always sensibly equal in diameter, and the determination of their distance apart could always be made with an error less than 1 part in 5000. Various diameters were used, from about 1 mm up to 2.5 mm. The effect of using apertures of different sizes will be discussed more fully below.

The value of L was about 900 centimeters, and with a good steel tape this distance could always be measured to a millimeter.

It follows that, as far as the quantities δ, D, and L are concerned, the sum of the errors made in their evaluation should never affect the result by as much as 1 part in 1000; and, since the wave-length of the light used was near 5500 A, the uncertainty arising from the instrumental constants is not more than 5 A.

It remains now to discuss the value of θ, which is the only quantity directly measured in an actual experiment. In order to make the discussion of θ intelligible it is necessary to describe and explain the appearance of the diffraction pattern and its system of interference fringes in some detail.

Consider the distribution of intensity in the focal plane, due to a single distant point source, when the objective is covered by a screen perforated by a single circular aperture of radius r. Denote the focal length by F, and let the origin of rectangular co-ordinates coincide with the optical axis. The intensity is given by

$$I=K\frac{4J_1^2\dfrac{2\pi r\sqrt{x^2+y^2}}{F\lambda}}{\left(\dfrac{2\pi r\sqrt{x^2+y^2}}{F\lambda}\right)^2} \tag{8}$$

where J_1 is a Bessel function of the first order.

This well-known expression states that at $x=0$, $y=0$, the intensity is a maximum and equal to K; as we move away from the origin, the intensity diminishes at first very slowly, then more rapidly, and reaches a value zero, when the argument of J_1 is equal to about 219°33′. For larger values of the argument the intensity increases, reaching a second maximum whose value is $0.0175\,K$ near 292°, and a second zero value near 401°, etc. This is, of course, simply the ordinary diffraction pattern of a circular aperture, or the so-called spurious star disk. In ordinary telescopic observations with relatively large apertures the entire disk and diffraction rings are apparently very small; but in interferometer work, on account of the small apertures and the very high magnification employed, the pattern may cover the larger part of the field of view.

The appearance is independent of the location of the aperture, as long as this falls entirely within the objective. Hence we will assume that it is placed so that its center is at a distance $D/2$ from the axis. Now let an equal aperture be uncovered, at the same distance from, but on the other side of, the axis. This second aperture alone would give exactly the same intensity as the first, namely that expressed by equation (8); but if we use both apertures together, the result will be the sum, not of the intensities as given by (8), but of the amplitudes formed by taking the square root of the right-hand side of (8), with proper attention to the relative phases of the two disturbances.

Let the apertures be so placed that the line joining their centers is parallel to the x-axis; in this case the amplitudes and phases will be equal at $x=1$. At $x=\pm F\lambda/2D$ the phases will differ by 180°, and since the amplitudes are equal, the resultant amplitude is zero. At $x=\pm F\lambda/D$, the phases differ by 360°, that is, they are in phase, and the amplitude will be the sum of the two, and so on.

It follows that the resultant intensity is now given by

$$I=I_0 \frac{4J_1^2 \dfrac{2\pi r\sqrt{x^2+y^2}}{F\lambda}}{\left(\dfrac{2\pi r\sqrt{x^2+y^2}}{F\lambda}\right)^2} \cos^2 \frac{\pi D x}{F\lambda} \tag{9}$$

I_0 being the intensity at the origin.

Hence the general outline of the pattern is the same as that given by a single aperture; we still have the central disk surrounded by diffraction rings; but the effect of using two apertures is to break up the disk and rings into a series of equally spaced interference fringes parallel to the y-axis—that is, perpendicular to the line joining the apertures. Along a line parallel to the y-axis the distribution of relative intensity is exactly the same as that in the pattern given by a single aperture; parallel to the x-axis we have this intensity multiplied by the factor $\cos^2 \pi Dx/F\lambda$.

Figure 2 gives a graphical representation of the intensity along the x-axis. The dotted curve is the intensity due to a single aperture, multiplied by the factor 4.

If we retain the apertures, but use two point-sources separated by an angular distance α, there will be two such patterns, whose centers are separated by the distance $2c=F\alpha$. If the centers fall at $(-c, 0)$ and $(+c, 0)$, respectively, the expression for the intensity becomes

$$I=I_0\left\{\frac{4J_1^2\left(\frac{2\pi r\sqrt{(x-c)^2+y^2}}{F\lambda}\right)}{\left(\frac{2\pi r\sqrt{(x-c)^2+y^2}}{F\lambda}\right)^2}\cos^2\frac{\pi D(x-c)}{F\lambda}+\frac{4J_1^2\left(\frac{2\pi r\sqrt{(x+c)^2+y^2}}{F\lambda}\right)}{\left(\frac{2\pi r\sqrt{(x+c)^2+y^2}}{F\lambda}\right)^2}\cos^2\frac{\pi D(x+c)}{F\lambda}\right\} \tag{10}$$

If the line joining the apertures makes an angle θ with the x-axis, then, letting $m=\tan\theta$, the expression for the intensity will be that given by equation (10), except that we write $x+my$ instead of x in the cosine factors. Figure 3 is a sketch showing the pattern for such a double point-source, the line joining the apertures making the angle θ with x-axis. The centers of the patterns are at P and P' respectively; the pattern centered at P' is shown in dotted lines. The straight lines represent the centers of the bright fringes, AA being the central fringe for P', $A'A'$ that for P'. The angle θ has been so chosen that the fringes due to P' are just midway between those due to P. If θ is diminished, the similarly lettered fringes will approach each other and the visibility will be increased; and similarly, if θ is increased, AA will approach $B'B'$, etc., and the visibility will again increase. The position represented is that of minimum visibility.

Remembering that the intensity in a pattern diminishes from the center outward, it is clear that at all points on the y-axis the intensity of one pattern is the same as that of the other, except for the changes due to the interference, and since the maxima in one pattern fall on the minima of the other, the result is very nearly uniform intensity along this line. To the right of the y-axis the intensity of P' is greater than that of P, and hence the maxima of the P' pattern become more and more prominent as we go to the right. To the left of the y-axis the P pattern is stronger and hence its maxima become increasingly prominent in this direction. The observer will therefore see two sets of fringes meeting just out of step near and along the y-axis. (*a*) If θ is decreased a certain amount, so that the distance between AA and $A'A'$ becomes smaller than the adjacent intervals, the corresponding bright fringe will start at A' on the right and run in a sensibly straight line to A on the left, crossing the y-axis exactly at the origin. (*b*) If θ is increased, we shall have a dark fringe running from A on the right in a nearly straight line to A' on the left, also crossing the y-axis at the origin. The change in θ necessary to pass from condition (*a*) to condition (*b*) depends upon the number of fringes in the pattern as here represented, being the smaller, the larger the number of fringes. For a case such as that in Figure 3, with 6 fringes across the central disk, the total required change in θ is about 5°. With 12 to 15 fringes it will be from 2° to 3°. It is evident, therefore, that a setting for the exact bisection can be made quite accurately—in general to a few tenths of a degree.

We can now estimate the probable error in the determination of θ. In one rotation of the aperture plate there are four values of θ which give the appearance just described, and a "set of observations" in the present experiments has consisted of five complete rotations. As a typical example we may take the measures made on Mount Wilson on June 18, 1921. Fourteen sets of observations were made of which only eleven were complete. The probable error of each set was calculated in the usual way, and the sum of these probable errors found to be $0\overset{\circ}{.}48$, or an average of about $0\overset{\circ}{.}035$ for a set. Taking $\theta = 45^\circ$, the percentage error of $\cos\theta$ is 0.05 per cent or 1 part in 2000.

Hence the experimental method should be capable of giving λ to at least 1 part in 1000, or to about 5 A.

Effect of the size of the apertures.—Hamy[1] derived a formula for the correction to be applied to observations made with apertures of finite width. The apertures were assumed to be rectangular, of width a and separation D: The source was assumed to be a uniformly luminous circular disk of angular diameter β. The fringes will disappear near the center of the pattern when

$$D = \frac{1.22\,\lambda}{\beta}\left\{ 1 + 0.765\left(\frac{a}{D}\right)^2 \; . \; . \; . \; . \; \right\} .$$

---

[1] *Bulletin Astronomique*, 16, 257, 1899.

No other cases were treated. It would seem reasonable to assume, however, that if the source is a double star of angular separation α, the corresponding formula would be

$$D=\frac{\lambda}{2\alpha}\left\{1+0.765\left(\frac{a}{D}\right)^2 \ldots\ldots\right\}$$

since the correction must depend upon some property of the observing instrument. For circular apertures, a further modification would no doubt be required, and we may reasonably assume that this would be the substitution of $a'/1.22$ for a where a' is the diameter of the circular aperture.

Observations were made on the artificial double star with circular apertures of various sizes, using the method of rotating aperture plate. These gave the *same* value of θ for all sizes of apertures, well within the errors of observation, thus indicating that for this method of observing and with this kind of a source no correction whatever is required. This result was so surprising that it seemed worth while to make a theoretical examination of the problem, using a method somewhat different from that employed by Hamy.

The method adopted, while being very simple, has the advantage of giving a clear physical picture of the phenomenon so that the need for a correction, if required, is made evident.

Let us consider rectangular apertures having a width a, and a length b, and let their centers be separated by a distance D. When the line joining the apertures is parallel to the x-axis the intensity in the focal plane due to a distant point-source is

$$I=I_0\frac{\sin^2\frac{\pi ax}{F\lambda}}{\left(\frac{\pi ax}{F\lambda}\right)^2}\frac{\sin^2\frac{\pi by}{F\lambda}}{\left(\frac{\pi by}{F\lambda}\right)^2}\cos^2\frac{\pi Dx}{F\lambda} \tag{11}$$

If a double point-source is used, the angular separation being α, we have, writing $2c=F\alpha$

$$I=I'_0\left\{\frac{\sin^2\frac{\pi a(x-c)}{F\lambda}}{\left(\frac{\pi a(x-c}{F\lambda}\right)^2}\,\frac{\sin^2\frac{\pi by}{F\lambda}}{\left(\frac{\pi by}{F\lambda}\right)^2}\cos^2\frac{\pi D(x-c)}{F\lambda}\right.$$
$$\left.+\frac{\sin^2\frac{\pi a(x+c)}{F\lambda}}{\left(\frac{\pi a(x+c)}{F\lambda}\right)^2}\,\frac{\sin^2\frac{\pi by}{F\lambda}}{\left(\frac{\pi by}{F\lambda}\right)^2}\cos^2\frac{\pi D(x+c)}{F\lambda}\right\} \qquad (12)$$

If circular apertures of radius r be employed, we have equation (10) instead of the foregoing.

These expressions hold for monochromatic light of wave-length λ, and hence by definition (*a*) they are also valid for white light of visual effective wave-length λ. If we limit ourselves to the phenomena on the x-axis, which in no way restricts the generality of the treatment, we can place the factors involving y equal to 1 in equation (11) and write x for $\sqrt{x^2+y^2}$ in equation (10). Writing $D/a=n$, equation (12) may be put in the form

$$I=I'_0\left\{\frac{\sin^2\frac{z-c'}{n}}{\left(\frac{z-c'}{n}\right)^2}\cos^2(z-c')+\frac{\sin^2\frac{z+c'}{n}}{\left(\frac{z+c'}{n}\right)^2}\cos^2(z+c')\right\} \qquad (12a)$$

in which $c'=\pi Dc/F\lambda$.

When n is very large, the intensity near the center of the pattern is given very nearly, by

$$I=I'_0\{\cos^2(z-c')+\cos^2(z+c')\}.$$

The visibility will be zero when $z-c'=z+c'-\frac{\pi}{2}$, or, $2c'=\frac{\pi}{2}$, or, applied to equation (12), we find that for a small in comparison to D, the fringes will vanish when

$$\frac{2\pi Dc}{F\lambda}=\frac{\pi}{2}$$

whence $2c=F\lambda/2D$, or, since $2c/F=a$,

$$a=\frac{\lambda}{2D}$$

which is the ordinary formula, equation (2).

In order to form a clear idea of what happens when a is increased, let us refer to Figure 2, and for this purpose we will assume that the dotted curve represents

$$\frac{\sin^2\frac{z-c'}{n}}{\left(\frac{z-c'}{n}\right)^2}$$

instead of

$$\frac{4J_1^2\left(\frac{2\pi rx}{F\lambda}\right)}{\left(\frac{2\pi rx}{F\lambda}\right)^2}$$

which really makes very little difference.

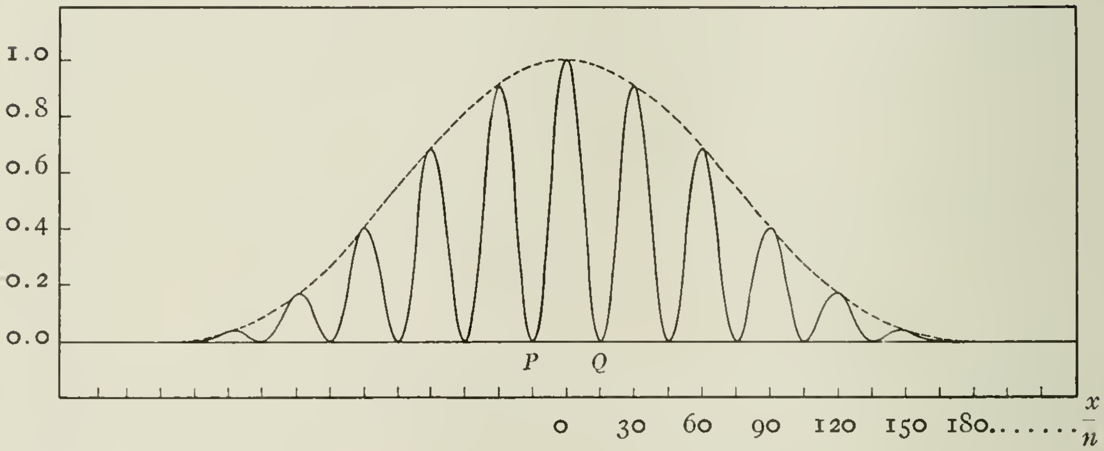

FIG. 2.—Dotted curve; $y=\frac{\sin^2\frac{x}{n}}{\left(\frac{x}{n}\right)^2}$ $(n=6)$

Full curve: $y=\frac{\sin^2\frac{x}{n}}{\left(\frac{x}{n}\right)^2}\cos^2 x$

With this understanding, we have then $2n$-loops of the inscribed curve in the central loop of the dotted curve. If n is very large, or a very small, the loops of the inscribed curve near the origin all have very nearly the same height, the dotted curve approaching a straight line parallel to the x-axis, and the inscribed curve approaching a true cosine-square curve more and more closely as

n is increased. If, under these conditions, we superpose two patterns displaced in the x direction by one-quarter of a period, the maxima of one will fall upon the minima of the other, and the sum will be a constant, which leads directly to equation (2).

When n is not large, the inscribed curve may be regarded as a distorted cosine-square curve, the distortion becoming more and more pronounced the more the dotted curve deviates from a straight line parallel to the axis. Since with white light the fringes are observable only near the center of the pattern, it follows that we need consider only the loops of the inscribed curve which are near the origin, and when n is small we have to confine our attention to the central fringe only, or to the portion of Figure 2 between the points P and Q. Let the ordinate at $x=0$ be taken as unity, and expressing x in degrees, we have for the undistorted curve ($n=\infty$) the value 0.500 at $\pm 45°$ and the value 0 at 90°. For the distorted curve we have unity at $x=0$, and zero at 90°, but a value less than 0.500 at 45°. Hence if we superpose two such curves, 90° apart, there will be a minimum at 45°, or at the point midway between them, which will disappear only if their distance apart is made less than 90°. This makes it clear why equation (2) requires modification for small values of n, at least if we regard only the center of the pattern. It is necessary to remember, however, that when the minimum at 45° for the superposed curves disappears, the minimum at 135° has been made more prominent, and accordingly the "correction" that we employ to remove the minimum at 45° is really somewhat too large.

In order to calculate the angular displacement necessary to fill up the minimum at the center of the superposed curves, we need only equate the second derivative of (12) with respect to c, equate it to zero, and solve for c on the assumption that $x=0$. The factor in y is of course placed equal to unity. Table I gives the results of this calculation for a few values of n.

Here we have written the formula applicable to double stars in the form

$$D=\frac{\lambda}{2a}(1+K)$$

where K according to Hamy is $0.765\left(\frac{a}{D}\right)^2$.

Experimental verification of the results given in Table I.—In Table I we have applied Hamy's formula to a case which was not considered in his investigation, namely that of double stars. The difference between our calculated values and those given by Hamy's formula as here applied is so great that it seemed worth while to test both the case of double stars and that of a star disk experimentally, to see if there is really any difference between the two.

TABLE I

n	c	K(Calculated)	K by Hamy's Formula	Ratio $\frac{K(\text{Hamy})}{K(\text{Calc.})}$
∞	45°.000	0	0	....
11.5	44.9234	0.0017	0.00577	3.395
5.75	44.6938	0.0068	0.02314	3.403
4.60	44.5275	0.0106	0.03615	3.411
3.45	44.1721	0.0187	0.06427	3.437

The experimental arrangement was as follows: A screen having a horizontal slot 2 mm in width was placed in front of the objective of the observing telescope. A plate was arranged to slide in a vertical direction directly in front of and in contact with this screen. This plate had two parallel slots 5 mm apart, each tapering from $\frac{1}{2}$ mm in width at one end to $2\frac{1}{2}$ mm at the other end, the length being 55 mm. This arrangement provided two nearly rectangular openings in front of the objective, at a constant distance apart; by sliding the plate up and down the width of each opening could be varied continuously from $\frac{1}{2}$ mm to $2\frac{1}{2}$ mm, or, what amounts to the same thing, n could be varied from $n=2$ to $n=10$ in a continuous manner.

Observations were made both on an artificial double star, and on an artificial star disk. The disk was illuminated with approximately monochromatic green light, in order to avoid the variations in color which are troublesome with white light, especially when the visibility of the fringes is low.

The observations were made by finding the distance between the observing telescope and the source which gave the minimum visibility for $n=10$, and also the distance at which the central minimum for $n=2$ just vanished. Since the results were the same as far as the correction factor is concerned, whether a star disk or a double star was used, we will record only the observations made on the star disk:

Wave-length of green light (mean) 5400 A.
Diameter of artificial star disk (δ) 0.650 mm.
Distance between centers of rectangular apertures $(D)=5.0$ mm.
Minimum visibility $n=10$, at 492 cm ± 2 cm.
Minimum in central fringe just disappears $(n=2)$ at 478 *cm* ± 2 cm.

Using $L=D\delta/1.22\,\lambda$ for the distance at which fringes should vanish with $n=\infty$ and substituting, we get $L=493.3$ cm, which, considering the uncertainty in the value of λ used, is sufficiently near 492 cm.

From this we find an experimental value of K for $n=2$, namely, $\frac{492}{478}-1$ or $\frac{493.3}{478}-1$, according to whether we use the observed or calculated value of L_∞. The first gives $K=0.0293$, the second $K=0.0320$, while by Hamy's formula, which is strictly applicable to this case, K should equal 0.19125. An extrapolation of the values in Table I to $n=2$ gives a value of K slightly larger than 0.03, which is in good agreement with the observations. We must conclude that the formula given by Hamy is incorrect, and that if the observations are made directly on the vanishing of the minimum in the central fringe, the values given in Table I are correct. It must be borne in mind, however, that if the observations are made simply on the minimum visibility of the pattern as a whole, which on account of seeing, will generally be the case in astronomical work, the simple formulae (1) and (2) are to be used without any corrections. It has already been shown (see p. 64) that, with the method of rotating apertures, no correction to the simple formula is required.

Determination of the effective wave-length of sunlight.—We will first consider some general questions which bear directly on the problem. It may be assumed that the quality of sunlight outside of our atmosphere is constant or very nearly so. In passing through the atmosphere it is modified by selective absorption and scattering to an extent which depends both on the thickness of the air layer and upon its character, such as water-vapor content, smoke, haze, etc. Most of these factors will reduce the intensity of the short wave-lengths more than that of the red end of the spectrum. Water-vapor is, however, an exception. It is very transparent to the short wave-lengths, while absorption begins somewhat below 6000 A and increases rapidly toward the red. Since its absorption lies almost entirely on the red side of the maximum of the sensitivity curve of the human eye, it appears that the

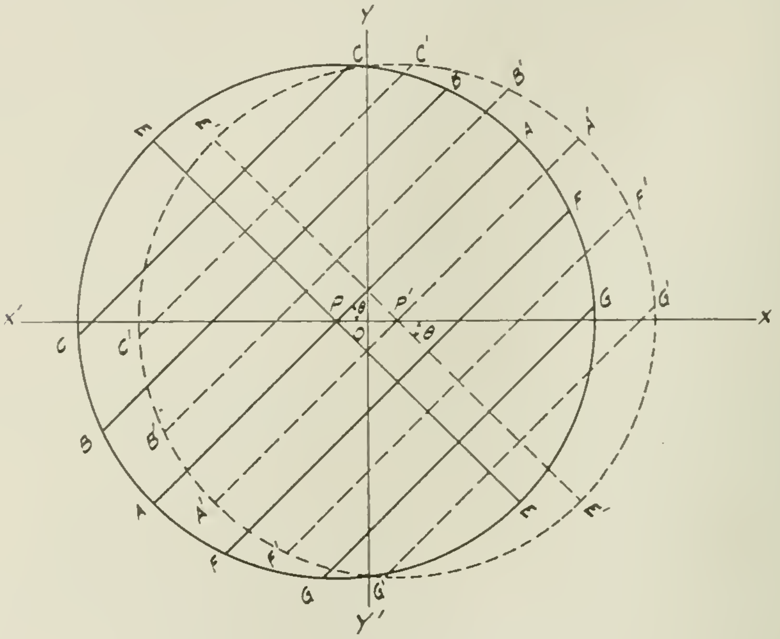

FIG. 3.—Pattern for double star

effect of water-vapor by itself is to move the value of the effective wave-length toward the violet. Dust, smoke, haze, and increased thickness of the atmosphere due to large zenith distances might be expected to shift the wave-length to the red. A priori, then, a given observer would not expect to find a constant value for the wave-length.

Apparatus.—Figure 1 gives a schematic diagram of the apparatus, and Figure 4 is a drawing of the observing telescope and aperture plate. The lens *C* is a theodolite objective of 22 mm aperture and of about 20 cm focus. The miscroscope consists of an 8-mm objective and a 7.5-power eyepiece, giving a linear magnification of about 125×. The circle *B* is graduated in degrees and can be read easily to 0°.1. It carries the aperture plate *AA*, and is rotated by a worm *DW*, so arranged that one revolution of the worm gives a rotation of 10°. The whole instrument is mounted on a solid brass base plate, *K*, which is easily clamped to a table or other convenient support. The slot *S* was designed to hold a plane parallel quartz plate, cut at 45° to the optic axis. Viewed through this plate, a single distant pinhole appears as an artificial double star, whose angular separation depends only on the thickness of the quartz plate. A slight difficulty arises in the use of such a quartz plate, on account of the fact that one of the emergent beams of light is colored, due to the dispersion of the quartz. A great deal of time was spent in the calibration of the plate by the use of monochromatic light, and a few observations were made using it in conjunction with the 100-inch Hooker telescope on some of the brighter stars, but the results were not entirely satisfactory. When the quartz plate is not used the slot *S* is covered by a suitable cap. In the determination of the wave-length of sunlight the source was always a pair of pinholes made and mounted as described above; the sunlight was reflected into the quartz projection lens *L*, Figure 1, by a two-mirror coelostat, the mirrors being freshly silvered and polished every two or three weeks.

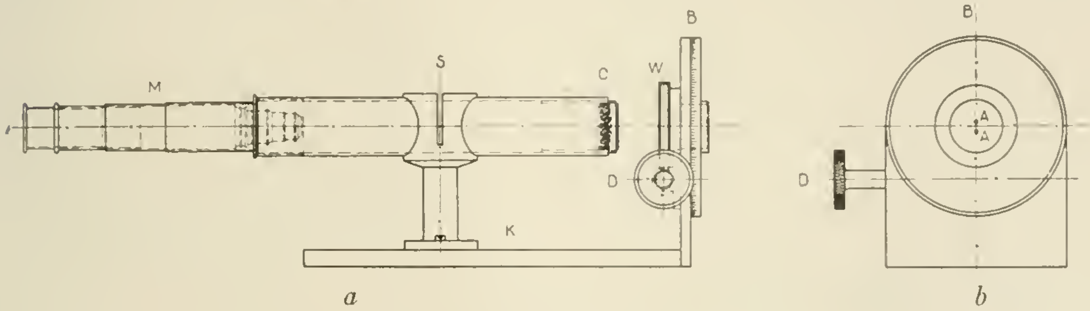

FIG. 4.—Laboratory apparatus
a. Side view. *b*. End view

In Tables II and III are collected the observations which have been made with the apparatus shown in Figure 4. Table II gives the observations made on Mount Wilson, June 15 to June 18, while in Table III are collected all the miscellaneous observations made under all sorts of conditions of sky in Pasadena. The first two columns give the date and hour of the observation. Since each complete observation required about 10 minutes, the time given refers to the middle of the observation. The third column gives the zenith distance of the sun to the nearest degree at the time. The fourth column gives the number of settings in each determination, which was always 20, excepting for the first observation on Mount Wilson which was stopped by fog, and for the three early observations on June 18, when the available time did not permit a complete set. The only observations calling for special comment are those of April 5 and 6 in Pasadena. These were made immediately after a rain, and the abnormally low value for the wave-length may be due to a relatively large amount of water-vapor; this, as mentioned above, would tend to displace the effective wave-length to the violet.

TABLE II

MOUNT WILSON OBSERVATIONS

Date	Mean Time	ζ	No. of Settings	λ	Remarks
June 15.....	8:35 A.M.	45°	16	(5546)	Incomplete. Fog blowing over. Image drifting badly.
June 16.....	5:14 A.M.	85	20	5631	
June 16.....	5:46 A.M.	79	20	5574	
June 16.....	6:35 A.M.	69	20	5542	
June 16.....	7:53 A.M.	53	20	(5535)	Fog coming over. Foggy remainder of day.
June 17.....	6:32 A.M.	69	20	5554	
June 17.....	7:52 A.M.	53	20	5515	
June 17.....	8:34 A.M.	45	20	5519	Faint haze.
June 17.....	9:18 A.M.	35	20	5519	
June 17.....	10:06 A.M.	25	20	5520	
June 17.....	10:49 A.M.	17	20	5515	Clouded over at 11:00 A.M.
June 17.....	4:50 P.M.	65	20	5546	Clouds. Haze as high as mountain tops. Sky blue.
June 17.....	5:22 P.M.	71	20	5579	Clouds. Haze as high as mountain tops. Sky blue.
June 17.....	6:13 P.M.	82	20	5596	Through very thin clouds. Haze.
June 17.....	6:37 P.M.	86	20	5625	Haze only.
June 18.....	4:58 A.M.	87	8	5656	Sky clear all day.
June 18.....	5:06 A.M.	86	8	5629	Sky clear all day.
June 18.....	5:07 A.M.	85	8	5619	Sky clear all day.
June 18.....	5:17 A.M.	83	20	5593	
June 18.....	5:47 A.M.	78	20	5561	
June 18.....	6:12 A.M.	73	20	5546	
June 18.....	6:44 A.M.	67	20	5528	
June 18.....	7:43 A.M.	55	20	5523	
June 18.....	8:12 A.M.	48	20	5512	
June 18.....	9:10 A.M.	37	20	5512	
June 18.....	10:11 A.M.	25	20	5515	
June 18.....	10:56 A.M.	17	20	5513	
June 18.....	11:20 A.M.	14	20	5510	
June 18.....	11:58 A.M.	11	20	5509	

TABLE III

Pasadena Observations

Date	Mean Time	ζ	No. of Settings	λ	Remarks
March 27...	10:11 A.M.	40	20	5537	
March 27...	11:41 A.M.	32	20	5521	
March 28...	9:05 A.M.	48	20	5568	
March 28...	9:57 A.M.	42	20	5531	
March 28...	11:03 A.M.	34	20	5515	
March 28...	2:03 P.M.	42	20	5555	
March 29...	9:19 A.M.	48	20	5556	
March 29...	9:50 A.M.	42	20	5542	
March 29...	10:29 A.M.	36	20	5522	
March 29...	11:30 A.M.	31	20	5525	
March 29...	1:10 A.M.	36	20	5559	Sky very thick.
March 30...	8:30 A.M.	56	20	5562	Sky thick toward east.
March 30...	9:10 A.M.	49	20	5537	
March 30...	9:40 A.M.	45	20	5542	
March 30...	10:03 A.M.	41	20	5547	
March 30...	10:27 A.M.	37	20	5528	Clearing rapidly.
March 30...	11:01 A.M.	33	20	5522	
March 30...	11:25 A.M.	31	20	5515	
March 30...	1:00 P.M.	34	20	5519	
March 30...	1:30 P.M.	38	20	5522	
March 30...	2:05 P.M.	43	20	5526	
March 30...	2:50 P.M.	51	20	5526	Cirrus developing rapidly.
April 2...	10:10 A.M.	28	20	5553	Some fog. Light unsteady.
April 2...	10:38 A.M.	34	20	5547	White sky, haze.
April 2...	11:10 A.M.	31	20	5524	
April 2...	11:30 A.M.	30	20	5524	
April 2...	1:35 P.M.	37	20	5527	
April 4...	8:30 P.M.	55	20	5524	After a rain. Cumulus clouds. Sky clear. Windy.
April 4...	8:56 P.M.	50	20	5527	
April 4...	9:48 P.M.	40	20	5524	
April 4...	10:42 P.M.	34	20	5533	
April 4...	11:17 P.M.	31	20	5531	Observer P.W.M.
April 5...	9:10 P.M.	46	20	5517	Thin cirrus here and there.
April 5...	10:12 P.M.	37	20	5494	Through cirrus.
April 5...	11:13 P.M.	30	20	5503	Clear.
April 6...	8:05 A.M.	59	20	5515	Clear.
April 6...	9:46 A.M.	39	20	5513	Clear.
April 6...	11:22 A.M.	29	20	5506	Clear.
June 21...	8:50 A.M.	40	20	5560	Haze obscuring mountains. White area around sun. Sky blue otherwise.
June 21...	9:26 A.M.	33	20	5545	
June 21...	10:12 A.M.	24	20	5533	
June 21...	11:05 A.M.	14	20	5524	
June 21...	11:40 A.M.	11	20	5522	

Figure 5 gives a graphical representation of the Mount Wilson results. This shows that on clear days for purposes of interferometer measurement the wave-length is sensibly constant if the zenith distance is less than 60°, while for greater zenith distances it rises rapidly. The Pasadena observations in general show that for zenith distances less than 40° there is not much change in the wave-length. For small zenith distances the Pasadena observations indicate a value not far from 5520, while the Mount Wilson observations indicate 5510. The difference of 10 A, though perhaps real, is so small that it may be said to be negligible as far as ordinary astronomical interferometer work is concerned.

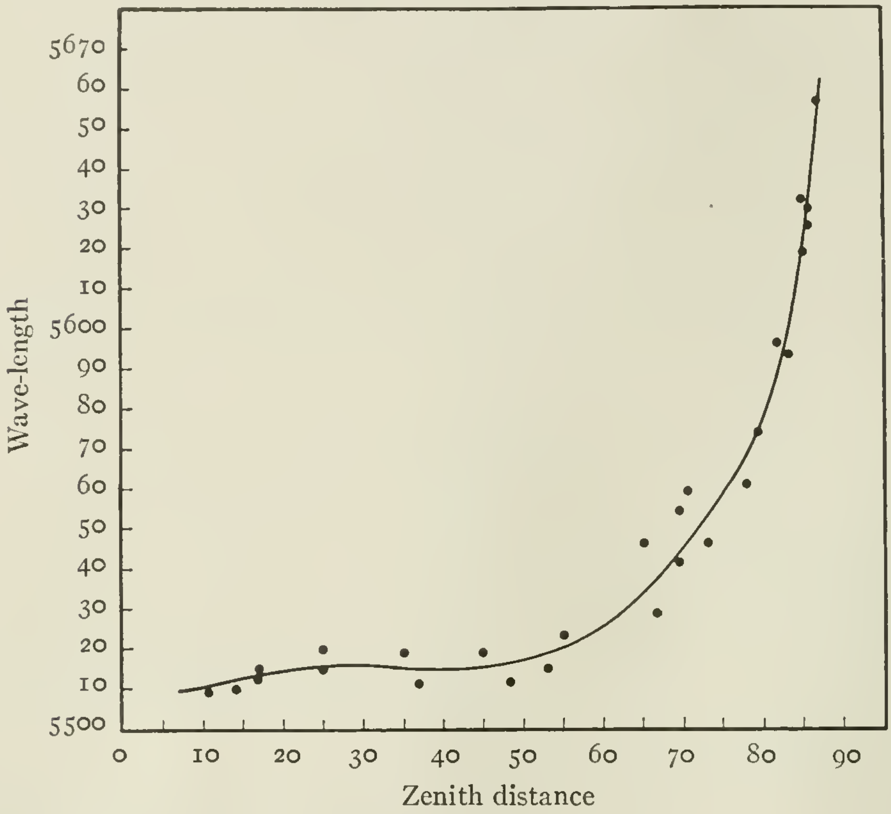

Fig. 5.—Mount Wilson observations
June 16–18, 1921

Mount Wilson Observatory
October 1921

MINOR CONTRIBUTIONS AND NOTES

ON THE SYSTEM OF PROCYON

ABSTRACT

Radial and orbital velocities of the system of Procyon.—A series of forty-five plates made from 1908 to 1913 give for V_0, after correction for the orbital velocity, the value -3.52 ± 0.057 km/sec. Taking the parallax at 0″.33 and the masses as 2.70 and 0.89, K comes out 0.60 km/sec. The sign of the inclination is assumed to be positive, but is not definitely known. In order that more accurate information as to the orbit may be obtained, it is hoped that other observatories will co-operate in measuring radial velocities during the next few years, since as favorable an opportunity will not occur again for thirty-nine years.

The most recent orbit of this well-known and interesting binary is due to Lewis Boss[1] who gave the following elements of the orbit of the faint star about the brighter one:

$$T = 1886.5$$
$$P = 39^{\rm y}.0$$
$$\Omega = 150^\circ.7$$
$$i = \pm 14^\circ.2$$
$$\omega = 36^\circ.8$$
$$a = 4''.05$$
$$e = 0.324$$

Aitken[2] gives the masses of the two stars in terms of the sun's mass as $m = 2.70$, $m' = 0.89$.

The following values of the parallax have been published: L. Boss[1] (adopted) 0″.33; Kapteyn and Weersma[3] 0″.324; Adams,[4] spectroscopic, 0″.347; trigonometric, 0″.309. There is considerable uncertainty in the foregoing elements owing to the difficulty of the observations and the short length of the arc described by the faint companion since its discovery by Schaeberle in 1896.

As observations of radial velocity, if sufficiently numerous and differential, promise results of value, it is opportune at the present time to call attention to them and to invite the co-operation of other observatories in an attack on the problem of the spectroscopic orbit.

---

[1] *Preliminary General Catalogue of 6188 Stars.*

[2] *Popular Astronomy*, 18, 485, 1910.

[3] *Groningen Publications*, 24.

[4] *Astrophysical Journal*, 53, 51, 1921.

Cape observations point to a + sign for the inclination; a series of plates taken during the next apparition, when the ascending node is being closely approached, will remove any doubts.

Assuming the sign positive we have the following values for V_0 based on unpublished details of my measures made from 1908 to 1913, viz.:

Mean Date	Number of Plates	Radial Velocity	Correction for Orbital Velocity	V_0
		km	km	km
1909.35...	13	−3.74	+0.19	−3.55
1910.73...	7	−3.74	+0.13	−3.61
1911.46...	12	−3.51	+0.09	−3.42
1912.49...	13	−3.56	+0.04	−3.52
Means 1911.03...	(45)	−3.63	+0.11	−3.52±0.057

Adopting −3.5 km/sec. as the value of V_0, 0''33 as the parallax, $\frac{m}{m+m'}$ as $\frac{0.89}{3.59}$, and the elements of Boss, the value of K becomes 0.60 km/sec. and the following radial velocities are calculated:

Date	$i+$	$i-$	Difference
	km	km	km
1921.0...........	−2.87	−4.13	+1.26
1922.0...........	−2.79	−4.21	+1.42
1923.0...........	−2.75	−4.25	+1.50
1923.5...........	−2.74	−4.26	+1.52 (max.)

It is important to take the opportunity of observing the radial velocities at the approaching node, an opportunity which will not again occur for thirty-nine years, in order to obtain a more accurate value of K when the observations are combined with others made at the node due in 1938. During the next seventeen years the velocity-curve shows the most rapid variations in the radial velocity. It is proposed to take three plates on each of seven nights for the determination of a normal place. Corrected for the solar motion, the system is approaching the sun with a velocity of 19 km/sec. in a path inclined 14° to the line joining sun and star.

JOSEPH LUNT

ROYAL OBSERVATORY
Cape of Good Hope
September 3, 1921

PLATE I

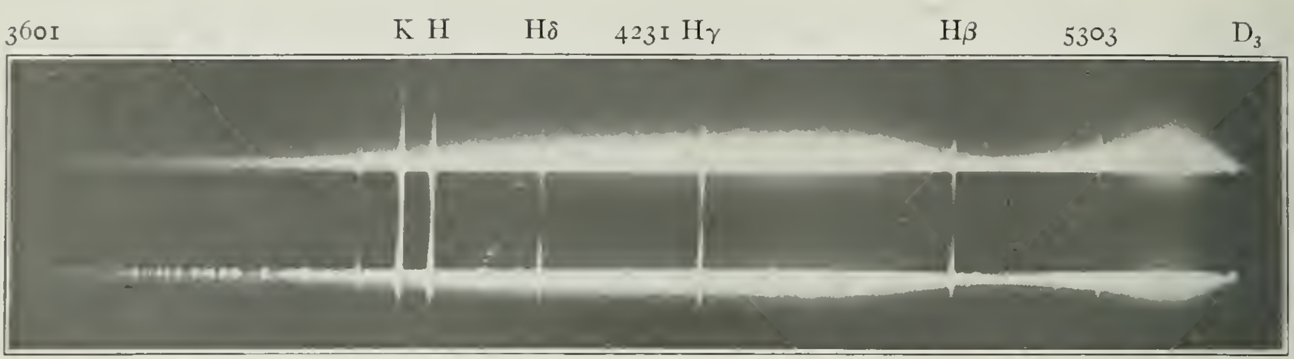

Fig. 1.—General spectrum of the corona. Single prism. Top W

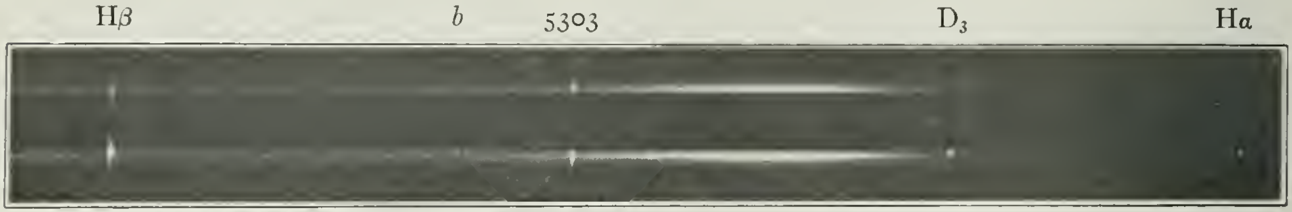

Fig. 2.—Spectrum of inner corona. Three prisms. Top E

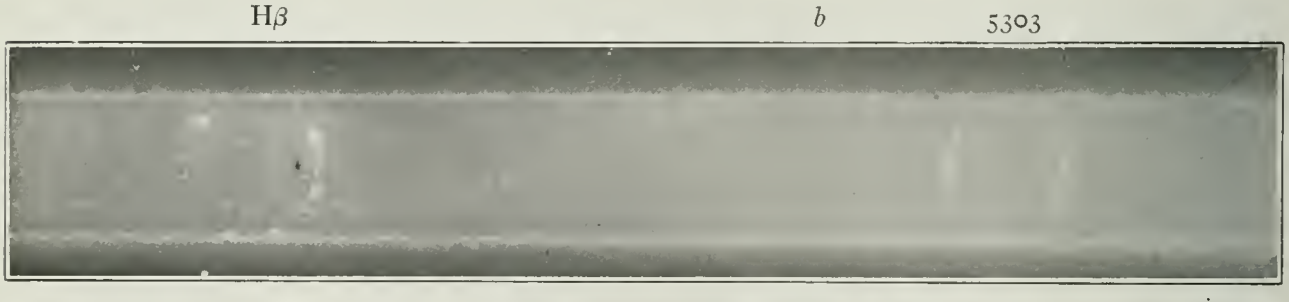

Fig. 3.—Hβ ring and green coronium ring. Top N

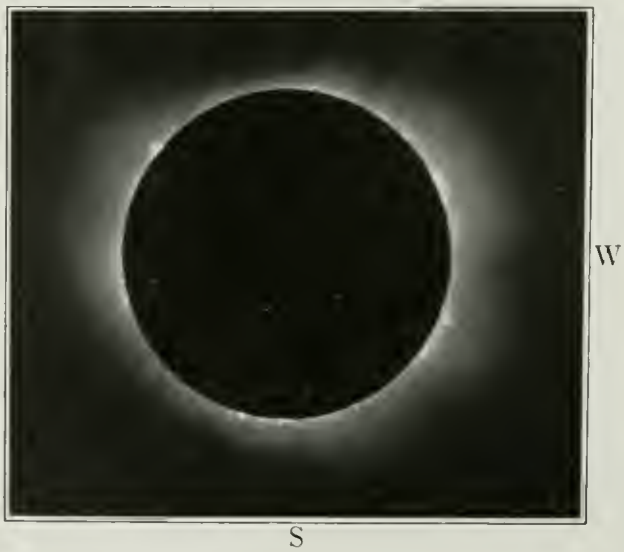

Fig. 4.—Prominences and inner corona with 39-foot camera.

Eclipse of June 8, 1918

73

THE
ASTROPHYSICAL JOURNAL
AN INTERNATIONAL REVIEW OF SPECTROSCOPY
AND ASTRONOMICAL PHYSICS

VOLUME LV MARCH 1922 NUMBER 2

THE SPECTRUM OF THE CORONA AS OBSERVED BY THE EXPEDITION FROM THE LOWELL OBSERVATORY AT THE TOTAL ECLIPSE OF JUNE 8, 1918

BY V. M. SLIPHER

ABSTRACT

Spectrum of corona observed at total eclipse of June 8, 1918.—The Lowell Observatory party, located near Syracuse, Kansas, obtained photographs with the following four spectrographs: (1) with single prism, 49 cm camera, slit E–W; (2) with single prism, 8.3 cm camera, slit N–S, then E–W; (3) with three prisms, 9-inch camera, slit E–W; (4) with three prisms, edges N–S, 47 cm camera, no slit. Weather conditions somewhat interfered with preparations; and thin haze veiled the sun during the eclipse, causing some scattering of light that rendered less certain the interpretation of some of the results. Yet useful plates were obtained with all the instruments. These show the usual prominence and chromospheric lines, the chief lines of coronium, the continuous spectrum of the corona, with weak dark lines whose origin is not quite certain; and strips of continuous spectrum coincident with certain prominences and sections of the inner corona uncovered by depressions of the moon's limb.

Distribution of coronium.—The coronium line λ5303.0 indicates that this substance extended about a solar diameter above the sun's surface. The slitless spectra show many condensations in the green coronium ring. These are not related to the prominences. Coronium was fairly abundant generally along the sun's limb under those major extensions of the outer corona, and scarce where the coronal rays typical of the polar regions occupied the limb.

The Lowell Observatory station for observing the solar eclipse of June 8, 1918, was located about eight miles north and one mile east of Syracuse, Kansas. Points along the path to the west of Denver offered somewhat better conditions as regards weather prospects, higher altitude of the sun and somewhat longer period of totality; but the advantages of accessibility and wider distribution of the expeditions along the eclipse path were sufficiently weighty to determine upon a station where the main line of the

Santa Fe Railroad was intersected by the eclipse path in western Kansas. This region is only one day by direct train from Flagstaff. Thus shipments of apparatus could be depended upon to go through more promptly and with less danger of injury than where changes in transit are involved. Then, too, this choice placed the Lowell station the farthest eastward of any of those prepared to undertake general observations of the eclipse.

In the autumn of 1917, Messrs. C. O. Lampland and E. C. Slipher looked over the general conditions in western Kansas with a view to finding a station site, and early in May, 1918, Mr. E. C. Slipher went to Syracuse, chose a site, found its latitude and the meridian and made all necessary arrangements, secured the needed help and materials, and went forward with the preparations. Others proceeded to Syracuse later as their rôles required, until the membership of the expedition was constituted thus: Mr. and Mrs. V. M. Slipher, Mr. and Mrs. C. O. Lampland, Mr. E. C. Slipher, Mr. Stanley Sykes, and Mr. E. C. Mills, of the Lowell Observatory; Mr. George R. Agassiz, of Boston, Massachusetts, and Mr. and Mrs. O. H. Truman, of the University of Iowa; and, on June 8, Mrs. Percival Lowell joined the expedition for the eclipse.

During the last week preceding eclipse day the weather was, for the most part, unfavorable. There were frequent showers and the sky was clouded much of the time, day and night. From what had been learned from weather records it had been expected that some clouds and rain would be encountered, but not so much as was experienced the last week. Thus the preparations and rehearsals could not be completed in the manner originally planned.

On eclipse day the sky at sunrise was only partly clear, and soon became completely overcast. However, in the late forenoon the clouds dissipated and by mid-day the sky was mostly clear. Throughout the afternoon some veil-like clouds of haze were present and at eclipse time one of these covered the region of the sun. This haze somewhat reduced the light and rather seriously limited the effectiveness of the small-scale cameras in recording the extreme outer extensions of the corona, by its direct action, and also by its scattering the light of the prominences and bright inner corona over the faint outer parts of the corona. However, although the haze must have affected to some extent the photographs of the inner corona and the spectrograms, its ill effects were not always manifest. Indeed, the two large-scale cameras, particularly, secured a number of negatives of the brighter parts of the corona that in comparison with other eclipse results are seen to be of a high degree of excellence. This valuable and extensive material will be published later by Messrs. Lampland and E. C. Slipher, who were responsible for that part of the eclipse program and deserve full credit for the success of the results.

It was thought wise to confine the studies of the spectrum to that of the corona. For this work serviceable instruments could be arranged from the stellar and nebular spectrographic equipment of the observatory. High linear dispersion was not considered vital in the observations to be undertaken and in arranging the different spectrographs questions of choice between dispersion and light-power were decided to favor light-power, in order that the instruments might be quick enough under good conditions to get a strong record of the spectrum and still to get some record even should the conditions be poor. The mountings of the instruments were made largely of wood, but metal was employed where most needed to give the optical parts proper support. The weather at Syracuse made clear the weakness of wood and the wisdom of making all essential parts of metal. At the eclipse camp Mr. O. H. Truman assisted me for several days before the eclipse, and he and Mrs. Slipher shared with me the operation of the instruments during the eclipse.

The single-prism spectrograph.—A spectrograph of one 63° flint glass prism and a 380-mm camera of 33-mm aperture was used in recording the general spectrum of the inner corona from D to the ultra-violet. It was supplied with an image-forming lens of about the same aperture and focus as the collimator, which was of 490-mm focus and 32-mm aperture. The slit was east and west over the sun's diameter and long enough to include the corona to some distance off the east and west limbs of the sun. The exposure ran from count 2 to 78 of the 83 seconds of the total phase. A Cramer Isochromatic plate was used, and recorded the spectrum from D_3 to about λ 3650 in the ultra-violet.

The exposure began soon enough after second contact to register a great number of chromospheric bright lines on the east edge of the sun, but it stopped too early to show these on the west edge.

The prominence lines of calcium, hydrogen, and helium are long, especially so those of calcium. The chief coronium line, that near λ 5303.0 is also strong and, like the lines mentioned above, it extends across the space occupied by the moon's image, owing to scattering of the light in the earth's atmosphere. The coronium line near λ 4231 is present and also weak impressions of the lines λ 4086 and 3601. The continuous spectrum of the inner corona extends from D almost to λ 3650, with the general variations of intensity that are to be expected from the variations in color sensitiveness of the photographic plate used. In its strongest portion—in the blue—it is recorded outward from the sun's east limb to a distance of about 10 minutes of arc and to about 14 minutes from the west limb. In the outer margin of the continuous spectrum there are irregularities, especially between Hδ and λ 4500, which I am more inclined to believe are the weak beginnings of the dark-line solar spectrum rather than that they are bright lines of a true coronal origin. This plate is reproduced in Figure 1, Plate I.

Low-dispersion spectrograph.—A slit spectrograph of high light-power having a 66° prism of dense but clear flint glass and a camera of 35-mm aperture and 83-mm focus, was used in photographing the spectrum of the corona to as great distances from the sun's surface as possible. This spectrograph with its image-forming lens was mounted so that it could be rotated through 90° in order to obtain two spectrograms: one with the slit N–S, for the outer corona off the north and south limbs of the sun; the other, with slit E–W, to cover the corona to the east and west of the sun. Thus, with a long slit it was planned to compare the spectra of two of the most dissimilar parts of the corona, the polar, and the equatorial regions. The slit was long enough to cover the corona out on each side to about 1.2 times the solar diameter. Unfortunately we did not have time, under the weather conditions, to perfect the adjustments for rotation so as to have the slit cover the desired portions of the corona for the polar and the equatorial comparisons.

In consequence, for the first exposure the slit which was east and west crossed the moon's image near the south limb. The exposure started two seconds after the second contact and continued during the first half of totality. Then at mid-totality the instrument was rotated through 90°—which brought the slit north and south and about 10′ west of the sun's west limb—the plate was shifted and the second exposure continued up to within about two seconds of third contact.

The plate used was a Cramer Trichromatic. It has a good impression of the continuous spectrum, over the full length of the slit, and from the violet down to the D line. The exposure with the slit crossing the sun's image near the south limb shows many prominence and chromospheric emission lines, including the red line of hydrogen. The green coronium line is clearly recorded by the first exposure and faintly by the second. This record of the coronium line will be of interest later in connection with the slitless spectrogram. A few of the strongest groups of solar absorption lines are discernible toward the edges of the spectrum of the first exposure and traceable across the full width of the second one.

The variation of intensity of these spectra across their width is in full accord with what the direct photographs indicate for light intensities along lines over the corona occupied by the slit: i.e., the first exposure slit E–W, shows more extension and density to the west than to the east of the sun, and the second more uniform density across its width. The ends of the slit for the first exposure reached distances of about 1.2 diameters from the sun's limb and for the second exposure about 1.3 diameters. The two exposures overlap by about one-eighth of their combined width and the plate was somewhat fogged by extraneous light from too early drawing of the slide. These faults and the incorrect placing of the slit for the two spectra made them unsuitable for the comparison of the coronal spectrum of the polar with the equatorial region.

The presence of the cloud of haze over the sun raises a question as to the extent reflected sunlight contributed to the dark-line spectrum. The direct photographs and also the slit spectra bear evidence of light scattered from the prominences and bright inner corona. The great extension of the calcium and hydrogen prominence lines and their presence over the moon's image is clear proof that prominence light was widely scattered. Some years ago the late Lord Rayleigh showed how rapidly the power of our atmosphere in scattering sunlight increased as the wave-length was decreased, and previous eclipse spectra have shown the effect with clear skies. Hence our air must have greatly aided the cloud in scattering the violet rays among which the dark lines, in the present case, were observed. It does not seem possible to determine just how great the effect of the haze was, but the presence of the prominence emissions over these spectrograms leaves no doubt that the strictly continuous spectrum of the bright inner corona was likewise spread over that of the outer corona, which would tend to cover up any dark lines it possessed. It is not possible to know to what extent these two opposing effects of the haze balanced each other, and hence we cannot say certainly that the dark lines observed were of true coronal origin although they appear to be such.

Three-prism spectrograph.—The Brashear stellar spectrograph of three prisms, supplied with a camera of nine inches focus, was adjusted for the visual end of the coronal spectrum with the hope of photographing more of the red region than is usually done. I had planned to sensitize a plate to the extreme red, but conditions did not permit my doing that and a Cramer Trichromatic plate was finally used.

The exposure ran from count 2 to 80. The slit was placed east and west. The plate records well the continuous spectrum from the blue down to D_3, where it rapidly weakens owing to the diminished sensitiveness of this emulsion in that region. On the shorter wave-length side of D_3 there are present the usual hydrogen and helium prominence lines and also a number of chromospheric lines. The C line of hydrogen is registered, but no other bright lines are evident on the red side of the D_3 line. The green coronium line λ 5303.0 is strongly impressed upon the plate (Fig. 2), but I have recognized no other true coronal lines.

The green line is long and nearly equally intense on the east and the west of the sun. Prominence and chromospheric lines, however, are much stronger on the east than on the west side, implying that the exposure began a little nearer second contact than the ending was to third contact. The comparison spectrum was unfortunately accidentally omitted from this plate, but the wavelength of the green line was determined with fair accuracy from measures of it relative to nearby prominence and chromospheric lines, the resulting value being λ 5303.0. Owing to scattering of light the green coronium line, like $H\beta$ and $H\gamma$, is traceable across the moon's image.

The slitless spectrograph.—A battery of three 63° dense flint prisms and a camera of 35-mm aperture and 472-mm focus served as a prismatic camera for investigating the spectrum of the corona with special regard to the green coronium ring. The adjustments were such as to include the spectrum from D_3 to beyond F in the blue, in order to have these helium and hydrogen radiations for comparison with the coronium ring in studying the distribution of this substance around the sun's surface. The prisms were not at minimum for λ 5303 and the green ring is somewhat elliptical. The edges of the prisms were set north and south instead of east and west, the more usual position. This orientation was the more favorable for recording the coronal ring clearly along the east and west limbs where it shows most intensity and detail. In this case the east and west limbs are in the middle of the spectral band and the north and south limbs at its edges, where details are of course confused. On account of the persistent clouds on the last few days and nights I did not get the focus sharply adjusted; and, too, the instrument received a slight jar when the small spectrograph described above was rotated at mid-totality, the two being mounted on the same polar axis. In consequence the objective spectra are not quite sharp, but it seems that nothing of importance was thereby lost.

The solar image on the plate of the prismatic camera had a diameter of 4.3 mm.

Three exposures were made with this instrument on isochromatic plates; one from the signal "go," for three seconds; the second (on the same plate shifted) for seventy seconds; and the third (on a separate plate) for about a second near third contact, for the flash. This last exposure was a little late and owing to the low dispersion is overexposed and probably does not merit any further consideration and description here.

The first of these exposures records the eastern crescents of F and D_3 together with a faint impression of the green coronal crescent. The second, the long exposure, secured a good impression of the green ring and of the irregular, broken rings of hydrogen F and helium D_3. The plate is of course considerably fogged by scattered light and by the light of the bright inner corona. There is sharp increase in the intensity of the continuous spectrum of the corona at its edges corresponding to the north and south limbs of the sun. These margins are strikingly sharp. They of course mask the coronium ring near the north and south points of the sun's disk; but as the ring becomes weak before reaching the edges except in the southwest quadrant, probably not much detail of the ring was thereby covered. However, it is strongly advised in such observations of future eclipses that the observer provide himself with a pair of instruments of this simple type and mount them so that for one the refracting edge of the prism (or grating rulings) is north and south, and for the other east and west. In this way, between the two, he will secure the whole of the sun's limb without masking, and for the most part he will thus also secure the much-to-be-desired duplicate records of the coronium spectrum.

The second exposure, with this instrument, of seventy seconds, began and ended about equally near second and third contacts, respectively, but it ended a very little nearer third contact. This negative shows that the green coronium ring is not uniformly intense around the sun. Its strength is much greater along the east and west limbs, generally, than about the north and south ones, yet its stronger parts do not coincide with the equatorial regions or its fainter parts with the polar regions. It occupies a greater extent of the west limb than it does of the east one, and on that side it extends in considerable strength farther to the south of the equator than it does to the north, in fact it seems traceable to the south pole. On the east limb, on the other hand, the ring stops quite suddenly nearer the equator on the south than on the north. That is, the coronium ring is faint or absent along the sections of the sun's limb occupied by the bristling streamers typical of the polar regions. The spectrogram, compared with direct photographs, shows that the coronium substance was relatively abundant generally in those regions of the sun's limb from which flowed the great extensions of the corona. While there seems to be this general correspondence in the distribution of the coronium substance and the main features of the corona, the nature of the relationship is a problem for further investigation.

In addition to these main variations in intensity of the coronium ring it has numerous local irregularities, its stronger portions being found in the zones of spots and prominences, generally; yet these do not coincide with individual prominences. The presence on the same plate of the F ring of hydrogen and the D_3 ring of helium, one on either side of the coronium ring, rendered comparison and study easy and definite. It is evident at a glance that the coronium ring is not at all like those of hydrogen and helium. The distribution of coronium thus is different from that of hydrogen and helium, and so no obvious relationship of coronium to these other substances is indicated. It is true only in a general way that the green ring is strong throughout regions including the zones frequented by sun-spots and prominences. The condensations in the coronium ring, none of which are definitely limited, stand in striking contrast to those of hydrogen and helium due to the prominences. The spectrogram shows the green radiation to fade, at first rather rapidly, outward from the sun's surface. While this negative gives no direct evidence on the question whether or not coronium is concerned in the arches over the prominences, it reveals a distribution of coronium favorable to its presence there. The coronium line on the plate of low dispersion, already described, extends outward fully a solar diameter into the corona. It is stronger off the southwest limb than off the southeast one—both of which were similarly included by the slit—thus conforming to the intensity-distribution of the coronium ring shown on the objective-prism plate. Of course we must consider here the effect that scattering of light in the earth's atmosphere has upon the extension of the line. Some assistance on this point is furnished by the negative for the general coronal spectrum, the first to be described of the series. This negative contains a good record of the emissions of hydrogen, helium, calcium, and coronium from the yellow to the ultra-violet, and, as it is without a comparison spectrum, it is well adapted to comparing the emission lines inside the moon's limb, where scattering is wholly responsible for their presence, with their extensions outward from the same limb into the corona, where the effect is a combination of scattering of light and the distribution of the substances involved. Inside the moon's disk the coronium line is as weak as, or weaker than, the helium line λ 4472 and, of course, weaker than any of the hydrogen lines; but when compared with the same lines at, say, half the solar radius outside the moon's limb, on the west, the coronium line is as strong as the strongest hydrogen line. Lord Rayleigh investigated the scattering of light in the atmosphere and found it to increase inversely as the fourth power of the wave-length. The effect is clearly disclosed by this spectrogram, the coronium line showing less spreading over the moon's image than do the blue and violet lines of hydrogen and helium. But outside the sun's limb over the corona something more than scattering is at work, for the coronium line gains strength relatively to these same H and He lines of shorter wave-length. This seems to imply that some coronium was present high above the sun's surface, as high apparently as the arches over the prominences.

These arches seemed unusually well developed at this eclipse and it is unfortunate that the presence (or absence) in them of coronium could not be cleared up. The presence of the coronium line high above the sun raises the question whether its luminescence may not be, as has been suggested, an electro-magnetic phenomenon similar to that of the aurora: the arches over the prominences have some resemblance to magnetic lines of force. One might further remark upon the fact that coronium and "aurorium" each has its distinguishing radiation in the same general region of the spectrum. Much remains to be learned of coronium and its relationships, at future eclipses.

This objective-prism plate, Figure 3, has further interest in that it shows strips of well-defined, continuous spectrum which run longitudinally through the main spectral background of the inner corona. Three of these are quite distinct and rather definitely limited in width. It appears evident that two of them coincide with the two strong prominences of the northern hemisphere, one on the east limb, the other on the west. The third is in the southern hemisphere and is somewhat wider and apparently related to some small prominences and an elevated region of the photosphere. Comparison of the maxima of the coronium ring with those of the H and He rings with regard to the strips of intensified continuous spectrum led me to the conclusion that the bands are related to the prominences and photosphere and not in any direct way to the substance of the green ring. In addition to what has been stated, the facts pointing to this conclusion are that the maxima of the ring are not definitely limited, as are the strips of continuous spectrum and there is not that correspondence between the two that would be expected were the ring maxima and the strips due to the same origin. It is noted that where the bands cross the ring it is generally denser, but it seems not more so than would result from the action of the blended light of the two.

It seems to be definitely established that some prominences possess a continuous spectrum, and brief computation shows that a depression of the moon's limb, moderate in depth among those known to exist[1], would have been equivalent to starting the exposure as much as 5 seconds early—or to stopping it that much late—which is ample time, near second or third contact, to expose sections of the photosphere and so introduce continuous spectrum. Observations clearly bear this out, as such lunar depressions have caused sharp strips of continuous spectrum on eclipse spectra in numerous cases. Both the causes mentioned above seem to have been concerned in the strips of continuous spectrum described here for the 1918 eclipse.

To Mrs. Percival Lowell, for her generous provision for the expedition and interest in its success; to Mr. Guy Lowell, the Trustee of the Lowell Observatory, who early proposed the undertaking; to Professor W. W. Campbell, Director of the Lick Observatory, for expert advice on plans and equipment; to Professor

---

[1] *Astronomische Abhandlungen der Hamburger Sternwarte in Bergedorf*, **3**, No. 1; *Selenographische Koordinaten von Friedrich Hayn.* IV Abhandlung des XXXIII Bandes, K. Sternwarte, Leipzig; *Astronomische Nachrichten*, No. 4615 (**193**, 118, 1912).

John A. Miller, Director of the Sproul Observatory, and Professor W. A. Cogshall, Director of the Kirkwood Observatory, for counsel and the loan of apparatus; to Mr. George R. Agassiz, Boston, Massachusetts, for the loan of a large lens; to the Naval, Flower, and Haverford observatories, for the loan of equipment, and to a number of citizens of Syracuse for their kind interest and assistance before and on eclipse day, it is a pleasure to make grateful acknowledgments.

Lowell Observatory
Flagstaff, Arizona
October 1921

SPECTROPHOTOMETRIC METHODS FOR DETERMINING STELLAR LUMINOSITY[1]

By BERTIL LINDBLAD

ABSTRACT

Two spectrophotometric methods for determining absolute magnitudes.—(1) *Relative intensity of spectral regions on either side of λ 3907.* Using the 10-inch Cooke refractor with 6° objective prism, a series of images of decreasing density was obtained for each star on each plate, making each exposure 0.707 times the preceding, and from these images the exposure ratio ($E=t_2/t_1$) required to give the same density in the two adjacent spectral regions was determined for stars in well-known groups with common proper motions and hence common parallaxes—the Hyades, the Pleiades, the Ursa Major stream, and Praesepe—and also for some stars with known spectroscopic parallaxes, in all, 107 stars of types A and B and 74 stars of later types. The results show that, especially *for stars of type B8 to A3*, there is a definite correlation between E and M, the variation being such that even with the small dispersion here used the probable error of a determination of M for a star within this range of type and of absolute magnitude 0 to 4 is only $0^{\mathrm{M}}.4$. (2) *Relative intensity of cyanogen bands and adjacent spectral regions.* Using the same instrument and method as above, the relative density on either side of λ *3889* was determined for 16 stars of known parallax, and (since the band at λ 4216 though weak is more favorable for the redder stars) the relative density in regions λλ 4144–4184 and λλ 4227–4272 was determined for 78 late stars. The absorption was found to be strongest *for the giants of types G5–K5* and much weaker for dwarfs; in fact all stars with log $E>0.17$ are giants. Figures 3–5 show the variation of log E with M for various types.

Relation of spectra of A and B stars to absolute magnitude.—A study of some spectra made with the 60-inch showed that the increase in the density of the region λλ 3889–3907 with reference to λλ 3907–3935 is caused by a widening of the Hζ line and also of some arc lines of Fe and Si, which may be due to a greater density gradient in the outer layers of the less luminous stars of this type. α Cygni and the faint companion of o_2 Eridani represent extreme types.

Spectral type and luminosity of 137 faint stars of magnitudes 10 to 14, in Messier 11, Messier 13, and Selected Areas 63 and 64, were determined from 10 plates made with a small focal-plane spectrograph attached to the 60-inch. Dwarfs and giants were distinguished by applying the spectrophotometric results reported above.

Spectrophotometric parallax determinations.—The concordance of the results for log E as a function of M, as determined from the various groups of stars, indicates that the assumed parallaxes for the *Hyades, Pleiades, and Praesepe*, $0''.023$, $0''.010$, and $0''.0072$, respectively, are accurate to within 10 per cent. The value found for *Messier 11* is $0''.00025$.

Schwarzschild's constant p for Seed 23 plates was determined for images made with the 10-inch refractor and 6° prism and found to be equal to: $0.97-0.026\,(m-5)$, where m is apparent magnitude ranging from 4 to 8. X-ray developer was used.

I. A CRITERION OF ABSOLUTE LUMINOSITY FOR STARS OF SPECTRAL TYPE A

The faint companion of the star o_2 Eridani of apparent magnitude 9.5 and absolute magnitude $+10.3$ was found by Adams[2] to be of spectral type Ao, and, intrinsically, is by far the faintest A-type star known. Some photographs of this object, taken with an objective prism on the 10-inch refractor and with a focal-plane spectrograph in conjunction with the 60-inch reflector, showed some peculiarities in the energy-distribution of the spectrum, when compared, for instance, with the spectrum of Sirius. The most conspicuous feature is the very strong widening of the wings of the hydrogen lines, connected with a decided weakening of the high-numbered members of the Balmer series. On the spectrograms of low dispersion taken here, $H\eta$ is the last hydrogen line to be identified with certainty. Seemingly as a consequence of this weakening of the extreme hydrogen lines, the photographs show a faint extension of the continuous spectrum much farther into the ultra-violet than is the case for an ordinary A-type star. A further difference between this star and Sirius was found in the distribution of energy between $H\epsilon$ and $H\zeta$, apparently consisting in a considerable decrease of intensity in the region λ 3889–λ 3907 as compared with the region λ 3907–λ 3935. This phenomenon may be caused partly by the expansion of the wings of $H\zeta$, but there was seemingly also some other cause; in particular, a widening of the silicon arc line λ 3905.6 was suspected. This line is well developed in the spectrum of Sirius, though probably it is to some extent a blend with an enhanced line of chromium. In order to see whether the last mentioned phenomenon might be a general criterion of intrinsic brightness for A-type stars, an investigation was begun on the Hyades which was later extended to include other groups of common proper motion.

---

[1] *Contributions from the Mount Wilson Observatory*, No. 228.

[2] *Publications of the Astronomical Society of the Pacific*, **26**, 198, 1914.

The instrument used was the 10-inch Cooke refractor with an objective prism of 6°. The scale of the spectra thus obtained, about 340 A per mm in the region of the K line, is probably near the lower limit possible for a successful investigation of the effect. No widening of the spectra was undertaken. Satisfactory images of an A star of photographic magnitude 6.5 were thus obtained in one minute. Seed 23 plates were used, with X-ray developer. Owing to the steep color-curve of the objective for the extreme violet, only a small region of the spectrum can be in good focus for a given setting; that used corresponded to the interval λ 3889–λ 3920.

In order to measure the decrease of intensity at λ 3907 the following process was used. For each object a series of exposures was made on the same plate with exposure-times decreasing in the ratio $\sqrt{2}:1$. Each star thus produced a sequence of images of decreasing photographic density; that is, a scale of images which may be represented by the numbers 0, 1, 2, 3, etc., corresponding to the exposure-times t_0, t_1, t_2, t_3 . . . . , where $t_i:t_{i+1}=\sqrt{2}$. The density in the region λ 3895 to λ 3907 of a certain image, for instance, the first, was compared with that in the region λ 3907 to λ 3925 of the following images. The point in the scale of images for which the density in the second region equaled that of the first region in the reference image, was estimated by interpolation to a tenth of an interval. Suppose the exposure-time corresponding to this "scale-reading" to be t. The logarithm of the ratio $t_0:t$, denoted by log E, is then a measure of the energy-fall in the spectrum near λ 3907. The successive images define a scale with intervals of logarithmic exposure-ratio equal to 0.15, and the "scale-reading" observed is therefore readily converted into log E. As many estimations as possible were made from each series of images, starting with each of the spectra in succession as a reference image. The process is analogous to that used by Seares[1] in determining the color of a star by the method of exposure-ratios. Distorted images, as well as very dense or very weak images, have not been measured. Whenever possible, measurements were made with the plate in two opposite positions. In some of the measurements, especially of very bright stars, like Sirius, for which sufficiently short exposures could not be made with the accuracy necessary to form a reliable scale, the value of log E was estimated directly from the difference of density between the two regions in the same image. Apart from the influence of possible changes of gradation from one plate to another, the two methods, if checked against each other, should give equivalent results. This follows from Kron's[2] results for the law of photographic density as a function of intensity and exposure-time. If the gradation in a time-scale is constant, a difference in density obtained during the same exposure for two different light-sources will always correspond to the same ratio of exposure-times giving the same density, independently of the order of magnitude of the intensities, in this case, of the apparent magnitude of the star.

---

[1] *Proceedings of the National Academy of Sciences*, 2, 521, 1916.

[2] *Publikationen des Astrophysikalischen Observatoriums zu Potsdam*, 22 (No. 67), 1913.

The wave-length λ 3907, separating the two regions, is easily identified with sufficient accuracy from its position relative to the lines Hζ, Hε, and K. The abrupt fall of intensity near this wave-length for low-luminosity A-type stars was confirmed by these observations and also on spectrograms of higher dispersion, as will be seen later. With the low dispersion used, the rapid change in intensity leaves the density fairly uniform in the two regions, λ 3895–λ 3907 and λ 3907–λ 3925. In fact, the success of the process depends on this circumstance. On the other hand, the smallness of the dispersion entails relatively large accidental errors, thus necessitating the use of a rather large number of images in order to get a reliable mean result.

Because of the juxtaposition of the two regions in the spectrum, it is evident that the influence of slight changes in the sensibility-curve of the plate, as well as of a variation in zenith-distance within reasonable limits from one object to another, will be negligible. The same will hold for a difference of gradation for the two regions. Further, if we use the law of density in Schwarzschild's form, $S=\phi\ (It^p)$, we may assume the value of p to be the same for the two regions. Suppose I_1 and I_2 to be the acting intensities for the first and second regions, respectively, and suppose S_1, t_1, S_2, t_2, to be corresponding values of density and exposure-time for the two regions. Then for equal densities we have $S_1=S_2$, and

$$I_1 t_1^p = I_2 t_2^p$$

$$\log \frac{I_2}{I_1} = p \log \frac{t_1}{t_2} = p \log E\,.$$

If we use the same kind of plates and the same developer, we have reason to assume p to be tolerably constant, though experience shows that large deviations may occur.

Since we may certainly disregard any difference in gradation for the two regions, there cannot, according to Kron's results, be any change of log E with the density of the images, a result which seems to be confirmed by the measures. This follows from the parallelism of the curves log It against log I for different degrees of density in Kron's diagrams. Two values of log I giving the same density will demand the same difference of log t for all values of the density. There may be, however, a slight change of log E with the absolute value of the acting intensity, that is, with the apparent magnitude of the star, due to the bending of the curves mentioned, corresponding to a change of the exponent p with the intensity.

The method described here admits a determination of Schwarzschild's constant p for a certain intensity, as soon as we have on a single plate the series of images of two different stars whose magnitudes are accurately known. The method of measurement is simply to interpolate the density of the successive images of one star into the scale defined by the images of the second star. In this way p has been determined from the relation $p=\frac{\Delta \log I}{\Delta \log t}$ for nearly all of the plates used here; in some cases p was determined for very different intensities on the same plate. The results seem to confirm Kron's conclusions. There is a decided decrease of p with the apparent magnitude. The mean from five plates is

$$\frac{\Delta p}{\Delta m}=-0.026\pm 0.002 \text{ (P.E.)},$$

for photographic magnitude 6.5.

Assuming a linear relation between p and m to hold for the variation of intensity met with in this investigation, we have as a mean for the first seventeen plates measured $p=0.97-0.026\,(m-5)$. Individual plates were assumed to differ from this equation by a constant ϵ, which in so far as possible was determined for each plate. The probable deviation in p from the formula for one plate, computed as a probable error for the seventeen plates mentioned, was found to be ± 0.03. A few Seed 23 plates of a later emulsion give, in the mean, lower values of p. One plate of the Pleiades was discarded by reason of an abnormally low value of p. The values of log E were reduced, as far as possible, to $p=0.97$. As a rule the corrections were small.

From stars measured on more than two plates it appears that the probable error of log E from a series of four measured images on a single plate is ± 0.025. The residuals of different plates indicate a probable systematic error of about ± 0.02. A considerable part of the probable error in log E for one plate must therefore be due to causes common to all the stars on the plate taken in the same exposure. For the greater part these are probably connected with irregularities in the images caused by imperfect guiding. From the foregoing discussion it seems unlikely that varying quality of the plates contributes appreciably. In computing the final values of log E, weights were therefore assigned equal to the number of images measured on the respective plates.

Attention was given first to members of well-known groups of stars with common proper motions, the Hyades, the Pleiades, the Ursa Major stream, and Praesepe, for which values of the parallaxes have been derived from the stream-motion or other plausible considerations. The large number of early-type stars in these clusters makes it much easier to establish the relation of spectral intensity to absolute magnitude than is the case for later types. Tables I–IV contain the results for stars of these groups; in addition, Table V gives results for some stars of types B5 to B9 of Kapteyn's groups in Orion and Scorpius, and for the two stars α Cygni and Comp. o_2 Eridani, which may be considered as representing extreme limits for the luminosities of A-type stars.

For the Hyades the parallax used for computing the luminosities is that of Kapteyn-Küstner,[1] $\pi = 0\overset{''}{.}023$. The Ursa Major stars are given according to Bottlinger.[2] Thirteen of the fifteen A-type stars which are certainly members of the group have been observed for this investigation. The absolute magnitudes of ϵ and ζ_1 Ursae Majoris, spectroscopic binaries with composite spectra of nearly equal intensities, have been increased by $+0\overset{M}{.}75$ in order to reduce to the absolute magnitude of each component. For the Pleiades a list of probable members brighter than $9\overset{M}{.}5$ photographic has kindly been communicated by Dr. Trumpler of the Lick Observatory. The value of the parallax adopted is Trumpler's[3] result, $\pi = 0''.010$, derived by means of the orbital motion of ten visual binaries belonging to the group. Some stars of the list are not measurable on the plates because of overlapping images. The maximum exposures for the four plates used were 30 minutes, 10 minutes, 2 minutes, and 30 seconds, respectively. For the Praesepe cluster Kohlschütter's[1] value $\pi = 0''.0072$ was adopted. This was derived by a comparison of the relations between apparent magnitude and spectrum for the early-type stars in the Hyades and Praesepe. This value is at least consistent since it gives for the four bright K stars of Praesepe a mean absolute magnitude nearly equal to that of the corresponding stars in the Hyades. For one of the Praesepe stars mentioned, B.D. $+20°2166$, Mr. Adams has kindly secured a spectrogram, from which he estimates the absolute

---

[1] *Publications of the Astronomical Laboratory at Groningen*, No. 23, 1909.

[2] *Astronomische Nachrichten*, **198**, 153, 1914.

[3] *Publications of the Astronomical Society of the Pacific*, **33**, 214, 1921.

TABLE I

HYADES, $\pi = 0''.023$

STAR		VIS. MAG.	SPECTRUM	LOG E	N	n	M_π	M_s	ΔM	Δ LOG E
Gron. 23	B.D.									
—	$+15°632$	3.62	F0	0.14	1	2	0.43			
—	18 640	3.63	G9	0.09	1	8	0.44			
28	15 612	3.86	G7	0.05	3	17	0.67			
79	17 712	3.93	G9	0.05	3	27	0.74			
224	15 631	4.04	G9	0.05	4	26	0.85			
143	17 719	4.24	A2	0.15	3	18	1.05	0.8	+0.3	−2
170	15 625	4.60	A5	0.17	4	27	1.41	1.1	+0.3	−2
315	14 720	4.75	A5	0.19	3	15	1.56			
107	17 714	4.84	A5	0.19	3	28	1.65			
385	15 666	4.85	A3	0.25	2	12	1.66	3.6	−1.9	+5
251	15 637	4.84	A5	0.22	2	9	1.65			
38	14 682	5.27	F0	0.19	3	23	2.08			
255	15 639	5.49	A5	0.20	3	16	2.30			
34	13 663	5.59	F0	0.19	3	13	2.40			
87	16 586	5.68	A2	0.22	3	18	2.49	1.9	+0.6	−2
245	15 636	5.70	F0	0.23	2	11	2.51			
64	13 668	5.76	A3	0.25	3	14	2.57	3.6	−1.0	+2
371	15 661	5.80	F0	0.19	2	10	2.61			
222	14 702	5.97	F0	0.19	3	10	2.78			
282	15 645	6.04	F0	0.17	3	16	2.85			
44	13 665	6.14	F2	0.11	3	12	2.85			
1	15 603	6.35	F5	0.15	2	6	3.16			
150	$+15$ 621	6.39	F8	0.12	4	15	3.20			

---

[1] *Astronomische Nachrichten*, 211, 289, 1920.

magnitude to be -0.4. A result of the same order is indicated by the strong absorption in the "cyanogen" bands shown by a spectrogram of the same star, taken by the writer with the Crossley reflector, which places the luminosity near that of β Geminorum ($M=+1.7$). The value $M=+0.69$ found with $\pi=0''.0072$ is in fairly good agreement with these results. The stars from Kapteyn's lists have been combined into groups having the same spectral type and nearly the same values of log E. The absolute magnitude was assumed to be the same within each group, and was calculated from the means of Kapteyn's values of the parallaxes.

TABLE II

URSA MAJOR STREAM

Star	Vis. Mag.	Spectrum	log E	N	n	M_π	M_s	ΔM	Δ log E
α Cor. Bor.	2.31	A0	0.12	2	19	0.37	0.4	0.0	0
ϵ Ursae Maj.	1.68	A0*p*	0.15	2	10	0.55	0.8	-0.2	$+2$
β Serpentis	3.74	A2	0.13	2	13	0.56	0.5	$+0.1$	0
γ Ursae Maj.	2.54	A0	0.14	3	22	0.60	0.6	0.0	0
78 Virginis	4.93	A2*p*	0.13	2	12	0.66	0.5	$+0.2$	-1
β Ursae Maj.	2.44	A2	0.15	3	11	0.80	0.8	0.0	0
α Canis Maj.	-1.58	A0	0.20	2	14	1.32	1.5	-0.2	-1
ζ_1 Ursae Maj.	2.40	A0*p*	0.20	2	8	1.44	1.5	-0.1	$+1$
76 Cygni	6.05	A0	0.19	1	6	1.62	1.4	$+0.2$	-1
ξ Eridani	5.23	A2	0.20	1	9	1.63	1.5	$+0.1$	0
δ Ursae Maj.	3.44	A2	0.21	4	29	1.71	1.7	0.0	0
g Ursae Maj.	4.02	A5	0.18	3	18	2.14	.....	......	......
ζ_2 Ursae Maj.	3.96	A0	0.23	1	4	2.25	2.2	0.0	0

The fourth column of the tables contains the final values of log E, corrected to $p=0.97$; the fifth and sixth give respectively the number of plates and the total number of images on which these values are based. The seventh column gives the absolute magnitude M_π, derived from apparent magnitude and parallax by the relation $M=m+5+5\log\pi$. The eighth column gives the absolute magnitude M_s, read by means of log E from the curves in Figure 1. The ninth and tenth columns give the residuals in M and log E from these curves.

The visual apparent magnitudes for the Hyades, the Ursa Major stars, and for Kapteyn's stars are from the Draper catalogue.

TABLE III

PLEIADES, $\pi = 0''.010$

Star		Vis. Mag.	Spectrum	log E	N	n	M_π	M_s	ΔM	Δ log E
Bessel	B.D.	Distance from Alcyone ≦ 1°								
η	+23°541.....	2.94	B5*p*	0.06	1	4	−2.06	.....	......	......
f	23 557.....	3.73	B8	0.06	2	8	−1.27	.....	......	......
b	23 507	3.76	B5*p*	0.11	3	12	−1.24	.....	......	......
c	23 516	3.93	B5	0.08	2	7	−1.07	.....	......	......
e	23 547.....	4.34	B5	0.09	2	11	−0.66	.....	......	......
d	23 522.....	4.28	B5	0.06	1	3	−0.72	.....	......	......
h	23 558.....	5.15	B8*p*	0.11	3	10	+0.15	0.2	0.0	+1
g	23 505.....	5.53	B5	0.11	1	4	0.53	0.2	+0.3	−2
28	22 563.....	5.54	B8	0.16	2	9	0.54	0.9	−0.4	+3
m	24 546.....	5.68	B8	0.09	2	11	0.68	.....	......	−5
k	24 553.....	5.83	B8	0.12	2	8	0.83	0.4	+0.4	−3
34	23 563.....	6.23	B8	0.19	3	12	1.23	1.4	−0.2	+1
32	23 561.....	6.66	B9	0.17	1	4	1.66	1.1	+0.6	−4
38	23 569.....	6.82	B9	0.24	3	15	1.82	2.5	−0.7	+3
12	24 562.....	6.88	B9	0.22	3	12	1.88	2.0	−0.1	0
24	23 540.....	6.93	B9	0.22	3	11	1.93	2.0	−0.1	+1
40	23 570.....	6.98	A0	0.23	3	17	1.98	2.2	−0.2	+1
29	23 553.....	6.99	A0	0.22	3	14	1.99	2.0	0.0	0
19	23 537.....	7.04	A0	0.24	3	16	2.04	2.5	−0.5	+2
22	23 538.....	7.19	B9	0.25	3	12	2.19	2.8	−0.6	+2
10	23 523.....	7.37	A0	0.24	3	15	2.37	2.5	−0.1	0
37	23 567.....	7.44	A0	0.22	3	13	2.44	2.0	+0.4	−2
39	24 578.....	7.46	A2	0.23	3	11	2.46	2.2	+0.3	−1
31	23 560	7.54	A0	0.28	1	3	2.54	3.6	−1.1	+4
20	24 566.....	7.68	A2	0.26	2	6	2.68	3.1	−0.4	+1
	24 540.....	7.79	A3	0.26	2	7	2.79	4.0	−1.2	+3
23	23 539.....	7.81	A2	0.24	2	5	2.81	2.5	+0.3	−1
7	23 517.....	7.87	A2	0.27	2	8	2.87	3.3	−0.4	+2
33	23 562	8.01	A2	0.23	2	5	3.01	2.2	+0.8	−3
1	23 510.....	8.06	A2	0.27	3	6	3.06	3.3	−0.2	+1
	23 496.....	8.07	A5	0.21	2	7	3.07	.....	......	......
	23 524	8.13	A2	0.29	2	7	3.13	3.9	−0.8	+3
30	23 559.....	8.14	A3	0.25	2	6	3.14	3.6	−0.5	+1
	23 504.....	8.22	A5	0.22	2	6	3.22	.....	......	......
	22 573.....	8.24	A3	0.23	2	6	3.24	2.6	+0.6	−1
	23 495	8.29	A5	0.19	2	9	3.29	.....	......	......
13	23 528.....	8.46	A5	0.24	2	5	3.46	.....	......	......
	23 508.....	8.51	A3	0.24	2	4	3.51	3.1	+0.4	−1
	22 565.....	8.53	A5	0.21	2	6	3.53	.....	......	......
	+24 563.....	8.59	A5	0.20	2	5	3.59	.....	......	......

TABLE III—*Continued*

Star: Bessel	Star: B.D.	Vis. Mag.	Spectrum	log E	N	n	M_π	M_S	ΔM	Δ log E
		Distance from Alcyone 1° to 3°								
	+21°535	6.0	B9	0.15	3	17	1.0	0.8	+0.2	−1
	22 523	6.7	A0	0.17	3	18	1.7	1.1	+0.6	−4
	22 545	6.9	A0	0.22	3	17	1.9	2.0	−0.1	+1
	22 572	6.9	B9	0.22	3	16	1.9	2.0	−0.1	0
	24 527	7.1	A0	0.21	3	18	2.1	1.7	+0.4	−2
	21 492	7.4	A0	0.20	3	16	2.4	1.6	+0.8	−4
	24 537	7.6	A3	0.23	3	14	2.6	2.6	0.0	0
	20 624	7.7	A2	0.20	3	9	2.7	1.6	+1.1	−5
	22 569	7.8	A2	0.29	3	13	2.8	3.9	−1.1	+4
	25 631	7.8	A2	0.24	3	12	2.8	2.5	+0.3	−1
	22 544	8.0	A2	0.22	3	10	3.0	2.0	+1.0	−4
	24 554	8.2	A3	0.26	2	8	3.2	4.0	−0.8	+2
	24 568	8.4	A3	0.21	2	8	3.4	1.9	+1.5	−4
	22 556	8.5	A2	0.27	2	7	3.5	3.4	+0.1	−1
	21 530	8.3	F0	0.13	2	6	3.3	.....	......	......
	24 528	8.9	A5	0.22	2	4	3.9	.....	......	......
	+25 615	8.9	A3	0.25	2	4	3.9	3.6	+0.3	−1

TABLE IV

PRAESEPE, $\pi = 0''.0072$

Star	Vis. Mag.	Spectrum	log E	N	n	M_π	M_S	ΔM	Δ log E
B.D.									
+20°2171	6.23	A2	0.17	2	14	0.52	1.1	−0.6	+4
20 2149	6.39	F0	0.15	2	10	0.68	.....	......	......
20 2166	6.40	G5	0.05	2	2	0.69	.....	......	......
20 2158	6.48	K0	0.08	2	5	0.77	.....	......	......
20 2159	6.48	A0	0.11	2	6	0.77	0.2	+0.6	−4
19 2069	6.54	F0	0.14	2	9	0.83	.....	......	......
19 2053	6.58	A5	0.13	2	13	0.87	.....	......	......
20 2175	6.60	A3	0.17	2	10	0.89	1.1	−0.2	+1
20 2172	6.77	A5	0.19	2	9	1.06	.....	......	......
20 2185	6.98	K0	0.10	2	3	1.37	.....	......	......
20 2143	7.09	F0	0.20	2	5	1.38	.....	......	......
20 2152	7.26	A0	0.16	2	8	1.55	0.9	+0.7	−4
20 2163	7.41	A0	0.24	1	4	1.70	2.5	−0.8	+3
20 2153	7.52	A0	0.18	2	6	1.81	1.2	+0.6	−3
19 2064	7.54	A3	0.17	2	7	1.83	1.1	+0.7	−4
20 2148	7.57	A3	0.21	2	6	1.86	1.9	+0.0	0
20 2132	7.72	A0	0.26	2	6	2.01	3.1	−1.1	+4
20 2165	7.74	A0	0.20	2	6	2.03	1.6	+0.4	−2
19 2078	7.77	A3	0.21	2	5	2.06	1.9	+0.2	−1
+19 2084	7.88	A5	0.20	2	6	2.17	.....	......	......

Those of the Pleiades are by Miss Parsons,[1] or by Müller and Kempf with the reduction −0.30 to the Harvard scale. For a few Pleiades stars Münch's photographic magnitudes have been used, reduced to the visual scale by means of color-indices inferred from the spectral type, which is not far from A0. The first part of Table III contains members of the group within 1°; the second, between 1° and 3° from Alcyone. For the latter stars the photographic magnitudes derived by Trumpler have been reduced to the visual scale in the same way as those by Münch. For Praesepe the photographic magnitudes by Kohlschütter on the Göttingen system were similarly reduced to visual magnitudes. The spectra are given according to Harvard with the exceptoin that for Pleiades stars fainter than $7\overset{\mathrm{M}}{.}5$ the spectral types have been revised on the basis of the strength of the K line.

TABLE V

KAPTEYN STARS, COMP. o_2 ERIDANI, α CYGNI

Star	Vis. Mag.	Spectrum	log E	Mean	N	n	M_π	M_s	ΔM	$\Delta \log E$
Boss 4018......	4.11	B9	0.11	......	1	7	....	....	.....	.....
1438......	4.92	B9	0.10	......	2	12	....	....	.....	.....
1455......	5.57	B9	0.11	0.12	3	19	0.01	0.4	−0.4	+2
1448......	6.61	B9	0.16	......	3	11	....	....	.....	.....
Boss 1944......	3.09	B8	0.08	......	1	5	....	....	.....	.....
4465......	4.65	B8	0.08	......	1	5	....	....	.....	.....
2071......	5.11	B8	0.08	......	1	5	....	....	.....	.....
4058......	5.41	B8	0.07	0.08	1	5	−0.16	....	.....	.....
4006......	5.61	B8	0.07	......	1	6	....	....	.....	.....
4573......	5.79	B8	0.06	......	1	5	....	....	.....	.....
1788......	5.88	B8	0.08	......	1	6	....	....	.....	.....
Boss 1262......	3.68	B5	0.04	0.05	1	8	....	....	.....	.....
926......	5.25	B5	0.06	......	1	7	−1.27	....	.....	.....
Comp. o_2 Eridani	9.5	B9	0.31	......	2	2	10.3	....	.....	.....
α Cygni........	1.33	A2p	0.08	......	1	8	....	....	.....	.....

Table VI contains the results of measurements on later-type stars from the list of spectroscopic parallaxes by Adams, Joy, Strömberg, and Burwell, made in connection with an investigation of the "cyanogen" absorption beyond λ 3889. The means were taken for limited intervals of spectral type and absolute magnitude; *N* is the number of stars in each group. No correction was made for a variation of Schwarzschild's constant, and the measurements for the individual stars are not as accurate as for the A-type stars in the preceding tables. In fact, with the decrease in intensity of Hζ and the general strengthening of the metallic lines in later spectral types the region λ 3895–λ 3907 has no longer the same uniform appearance as for the early types. The results in the table show, however, that the effect still persists to some extent in the later types, in spite of the vanishing of Hζ.

---

[1] *Astrophysical Journal*, 47, 38, 1918.

TABLE VI

Mean Results for Stars with Determined Spectroscopic Parallaxes

Spectral Range	Mean Type	*N*	Mean Abs. Mag.	Mean log *E*
F5*p*–G3*p*	G0*p*	4	−2.5	0.05
F4 –G8	G1	3	−1.7	0.04
A8 –F9	F4	3	0.3	0.09
F1 –G1	F7	15	3.9	0.15
G1 –K2	G8	12	0.9	0.05
G4 –K2	G9	6	5.7	0.16
K3 –Ma	K5	7	0.6	0.12
K3 –K7	K5	3	7.3	0.24

Figures 1 and 2 illustrate the result in the tables, log *E* being plotted against M_π, with different symbols for the different groups. α Cygni and Comp. o_2 Eridani are represented by arrows. The absolute magnitude of α Cygni can only be estimated qualitatively as very bright from exceedingly small proper motion. Comp. o_2 Eridani with $M = 10.3$ falls below the margin of the diagram. Figure 1 gives the results for spectral types B5–A3; Figure 2 for types from A5 on. From B8 to A2 there is no certain evidence of a change in the curve; but the A3 curve for lower luminosities evidently falls below the B8–A2 curve, and forms a transition to the A5 curve in Figure 2. The degeneration of the curves for types A5–F is clearly a consequence of the decreasing intensity of Hζ with advancing type.

It is evident from these results that the increase of log *E* with decreasing luminosity can be used for determining absolute magnitudes for stars of spectral types B8–A3, but that the curves for later types cannot give very trustworthy results. The curves further show that for very bright stars log E approaches a limiting value representing a very smooth run of the energy-curve between

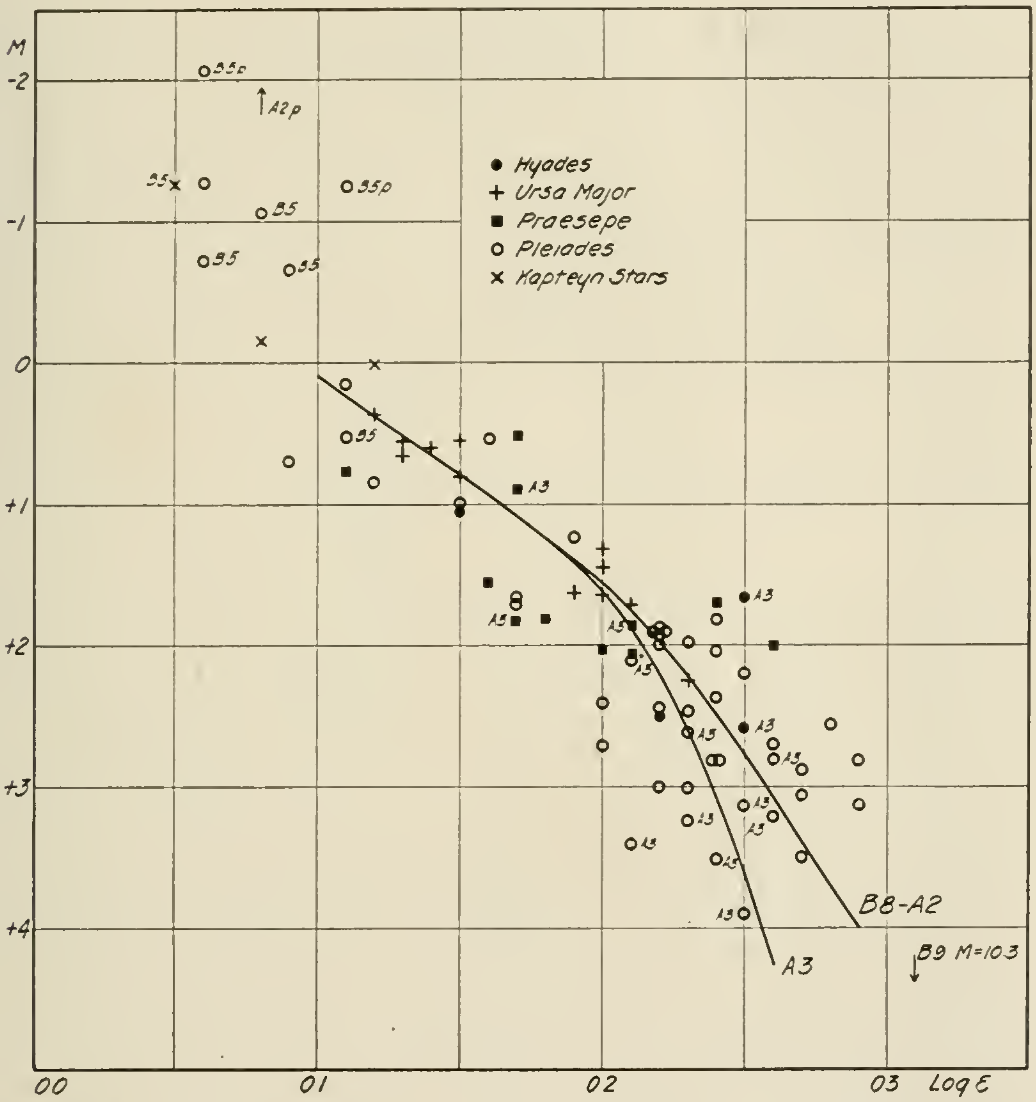

FIG. 1.—Logarithmic exposure-ratio for the regions λλ 3895–3907, 3907–3925, and absolute magnitude. Spectral types B5–A3.

Hζ and K, a consequence of the extreme narrowness of all absorption lines. This phenomenon seems to be more or less independent of type, α Cygni, A2*p*, falling in with the B5 stars of the Pleiades. The Cepheids and Pseudo-Cepheids and the very bright F4–G8 stars in Table VI also fall near the same point of the diagram. The steepness of the curve for stars brighter than $M = 0$ is such that only

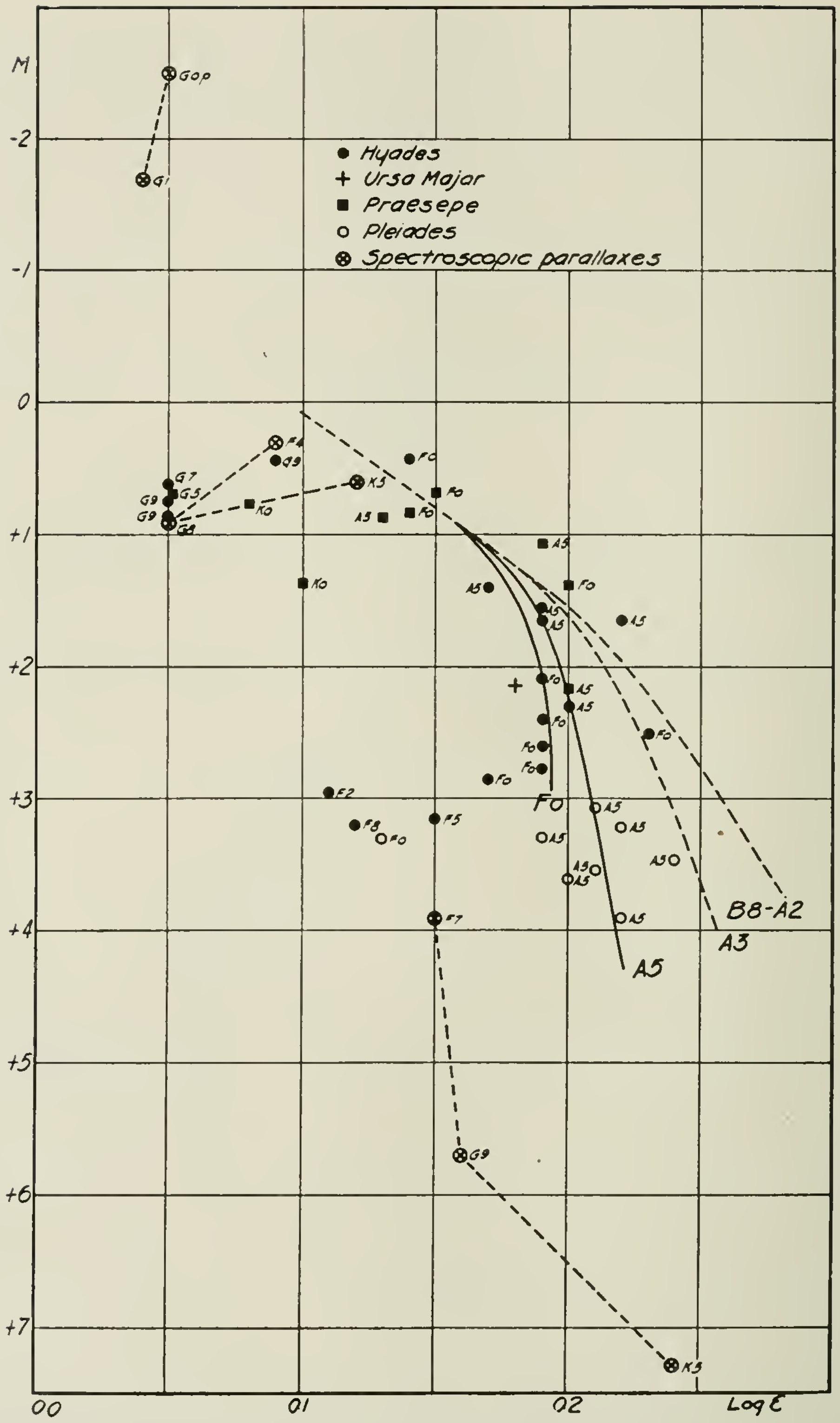

FIG. 2.—Logarithmic exposure-ratio for the regions λλ 3895–3907, 3907–3925, and absolute magnitude. Spectral types later than A5.

qualitative estimates of the luminosity can be made from values of log E less than 0.10.

To form the B8–A2 curve, means of log E for certain intervals of M were taken for both Ursa Major and Pleiades stars. Between $M=0$ and $M=+2$ the curve was drawn to represent the Ursa Major stars. A comparison with the eleven Pleiades stars in this region observed on three plates gave a systematic difference of +0.002 in log E, which is negligible. The remaining parts of the curves were then drawn in accordance with the results for the Pleiades, attention being given also to the Hyades and Praesepe stars in forming the A3 and A5 curves. The co-ordinates of the curves in Figure 1 then run as follows:

	B8–A2				
log E	0.10	0.15	0.20	0.25	0.28
M	+0.08	0.80	1.55	2.77	3.68
	A3				
log E	0.10	0.15	0.20	0.22	0.25
M	+0.08	0.80	1.62	2.20	3.60

The F0 curve in Figure 2 is drawn mainly from stars in the Hyades.

The absolute magnitudes corresponding to log E, M_s, have been read from these curves for all B8–A3 stars having log $E>0.10$; the two A5 stars in Figure 2 with log $E<0.18$ are included.

Errors in the assumed values of the parallaxes evidently combine with residual systematic errors in the measurements. From the discussion of systematic errors it seems that the reliability of any correction to the parallax that might result from the mean residuals for a group will probably depend more on the number of images measured for the individual stars than on the number of stars. The absolute magnitudes of the Ursa Major stars derived from stream-motion are probably but little affected by systematic errors. This likely is also true of the values of log E, because these stars were observed individually on a rather large number of different plates. As there seems to be no appreciable systematic difference between the Ursa Major stars and the Pleiades we may conclude that Trumpler's value of the parallax, $\pi = 0''.010$, is very good. With allowance for a possible systematic error of about 0.01 in log E the error may amount to about 10 per cent, or $\pm 0''.001$. For the Hyades and Praesepe we can determine the parallax which causes the systematic difference in log E to vanish. For the Hyades we find $\pi = 0''.023$, the value initially adopted; and for Praesepe, $\pi = 0''.0068$, differing by only $0''.0004$ from Kohlschütter's value. An uncertainty of 10 per cent is probably to be admitted for both these values. The Kapteyn stars of types B8 and B9 seem to agree with the curve as well as can be expected.

The residuals ΔM for the individual stars are seen to be very small for the Ursa Major stars, but are rather large for some of the A3 stars of low luminosity in the other groups. This is to be expected from the steepness of the curve. In all, the residuals for seventy-one stars give a probable deviation of $\pm 0^{M}.40$, which is comparable with the probable error of the spectroscopic method for late-type stars. With weights equal to the number of images, n, the probable deviation in log E from the curves is found to be ± 0.026 for a value based on four measured images. This value is to be compared with ± 0.025 previously derived from the residuals in log E from the mean for different plates. The latter value, it was concluded, was produced to a considerable extent by systematic errors common to a large number of stars in a certain group. In the new value, on the other hand, the systematic errors are combined with errors in the parallaxes, and may be partly eliminated in drawing the curves. The close agreement of the two results suggests, however, that the correlation between the energy distribution around λ 3907 and the absolute magnitude is close.

An investigation of spectra of higher dispersion for some selected A stars of different luminosities, photographed with a focal-plane spectrograph in the Newtonian focus of the 60-inch reflector, and with the Cassegrain spectrograph and an 18-inch camera, and also with a slitless quartz spectrograph used in conjunction with the Crossley reflector of the Lick Observatory, throws some light on the question of the physical cause of the effect investigated here. Undoubtedly the increase of log E with decreasing luminosity is to a considerable degree caused by a widening of the wings of the Hζ line, the extreme limits being represented by very bright stars such as α Cygni and α Leonis with narrow hydrogen lines and the very faint companion of o_2 Eridani, which has exceedingly wide lines. But there seems also to be evidence of another cause. It appears as though certain arc lines of iron and silicon in the region λ 3889–λ 3907 increase appreciably in width and intensity with decreasing luminosity. The lines suspected are λλ 3895.8, 3899.9, 3903.1, 3906.6 of iron, and λ 3905.6 of silicon. With the exception of λλ 3903.1 and 3905.6, these lines are classified by King[1] as belonging to Class IB. The exceptions are in classes II and III, respectively. A widening of these lines with decreasing luminosity seems to contribute perceptibly to the depression of the intensity in the region Hζ–λ 3907. There seems to be a similar effect, though much weaker, in the region λ 3914–λ 3923, including the two iron lines λλ 3920.4 and 3923.1 of Class IB. On the whole, in stellar spectra the region between λ 3907 and K is certainly affected by heavy arc lines to a much smaller degree than the region Hζ–λ 3907.

In some spectra of Sirius photographed by Nicholson with the Snow telescope, with a dispersion of 3 A per mm, the lines mentioned between λλ 3889 and 3907 are plainly visible, except the iron line λ 3906.6. The line λ 3905.6 is relatively strong, of about the same strength as the enhanced titanium lines λλ 3900.7 and 3913.7. We probably have here a blend of the silicon line with an enhanced line of chromium, but an indication that the blend is to a considerable part due to silicon may be found in the circumstance that the Kensington observers[2] state that it is somewhat weaker in the spectrum of ε Ursae Majoris than in the spectrum of Sirius, in spite of the fact that of thirty enhanced chromium lines all are found stronger in the former star, except one which is given as of the same intensity in both spectra. In the case of α Lyrae and α Coronae, which are stars of A0 type more luminous than Sirius, λ 3905.6 is still to be seen in the spectrograms taken with the Cassegrain spectrograph; of the iron lines only λ 3903.1 can be traced with certainty. On the other hand, in ζ_2 Ursae Majoris with $M = +2.25$, λ 3903.1 is strong, and λλ 3895.8 and 3899.9 are clearly visible; in the position of λ 3906.6 there is a very broad line seemingly including λ 3905.6 as a blend. The prominent arc lines of iron between Hζ and Hη are very broad and well marked, probably affecting to a perceptible extent the integrated intensity of the region between these two lines, at least from λ 3860 to Hη. To the red of λ 3907 no effects of similar importance for the variation of the integrated intensity of wide patches of the continuous spectrum can be seen, though the spectrum is evidently rich in lines. The K line, which indicates that the spectral type lies between A0 and A2, is weaker and sharper than in the spectrum of β Serpentis, type A2, $M = 0.56$, in which the iron arc lines are faint. The visibility of the broad arc lines is therefore not likely to be interpreted as due to an increase in spectral type. In addition to these comparisons made with the Cassegrain spectrograph, the slitless spectrograms taken with the quartz spectrograph on the Crossley reflector, and the low dispersion slit spectra obtained with the 60-inch reflector, show an abrupt fall of intensity near λ 3907 for ζ_2 Ursae Majoris, as well as for Nos. 10, 20, and 31 of the Pleiades, types A0, A2, A0, $M = +2.37$, 2.68, 2.54, respectively, for No. 64 of the Hyades, A3, $M = +2.57$, and the Praesepe star B.D. +20°2165, A0, $M = +2.03$. The difference relative to the brighter Pleiades and Ursa Major stars is plainly recognizable. A very marked depression near λ 3906 is shown on a spectrogram of Comp. o_2 Eridani taken with the quartz spectrograph. From the appearance of the K line this star ought probably to be classified a little earlier than A0.

---

[1] *Mt. Wilson Contr.*, No. 66; *Astrophysical Journal*, **37**, 239, 1913; *Publications of the Astronomical Society of the Pacific*, **33**, 106, 1921.

[2] Solar Physics Committee, *Chemical Origin of Various Lines in Solar and Stellar Spectra*, p. 49, 1910.

The effect in question persists for later types, as shown by Table VI and is confirmed by results from spectra of other kinds. The energy-fall in a slitless spectrogram at λ 3907 is much more pronounced for a dwarf than for a giant. This fact confirms our results just derived, because the importance of the hydrogen line Hζ for the effect must be negligible in these types. On the other hand, the degeneration of the effect toward type F shows that Hζ probably causes a large part of the phenomenon in the A type.

The facts dealt with here are probably best understood from the standpoint of an increased density-gradient in the outer layers of a star of certain type with decreasing luminosity, which follows because the change in luminosity is in all probability due chiefly to a change of the mean density. For a layer of certain temperature the density will be appreciably greater in a star of low luminosity than in a more luminous one, a condition which may be thought to favor the strength and width of the arc and flame lines.

The eclipsing binaries offer an opportunity to derive a relation between the effect at λ 3907 and the mean density of the star. From some preliminary results obtained here it has been found that the energy-fall near λ 3907 is strong for RZ Cassiopeiae and RR Draconis, whose brighter components have especially high mean densities, and seems to be much smoother for the low-density stars examined. For RZ Cassiopeiae a value of M between $+2$ and $+3$ inferred from the spectrum is in fair agreement with Dugan's[1] results for the dimensions of the brighter component of this star.

II. THE "CYANOGEN" ABSORPTION IN SPECTRA OF TYPES G–M

Miss Maury[2] makes the statement in her classification of stellar spectra that the sudden decrease of general intensity in the spectrum from λ 3889 toward the ultra-violet found in types XIV and XV, as well as the degree of absorption in the regions λ 4055–λ 4078 and λ 4144–λ 4216, is developed to a different degree for different stars within these types. The variation of intensity in these regions is further thought to be correlated to some extent with the strength of the lines $\lambda\lambda$ 4215.7, 4227, and the compound line λ 4076.8–λ 4077.9. Kapteyn[3] showed that stars with heavy absorption in the violet and ultra-violet regions mentioned have on the average much smaller proper motions than stars with comparatively slight absorption. This result was thought by him to bear upon the problem of selective absorption in inter-stellar space. In more recent years, however, the influence of differences in the absolute magnitudes of the stars on the appearance of their spectra has been recognized, especially by Adams and Kohlschütter in the development of the spectroscopic method for deriving stellar parallaxes. In this method the lines λ 4216 and λ 4078 are two of the most important variable lines. That the energy-fall beyond λ 3889 is intimately connected with the spectroscopically determined absolute magnitude was found by the writer by using very short objective-grating spectra.[1] The color-effect of the absolute magnitude was found to be much more strongly developed at the inner limit of the spectra in the "minimum wave-length" than in the "effective wave-length" measured by bisecting the images. It was then suspected that the effect could be due to an increase of absorption with stellar luminosity in the heavily winged lines of iron in the region λ 3870–λ 3890.

---

[1] *Contributions from the Princeton Observatory*, No. 4, 1916.

[2] *Harvard Annals*, **28**, 38, 1897.

[3] *Mt. Wilson Contr.*, No. 31; *Astrophysical Journal*, **29**, 46, 1909.

It has been found recently, however, that the effect is without doubt due to a variation in strength with stellar luminosity in the strong "cyanogen" band with its first head at λ 3883. On spectra of stars of different types and luminosities photographed with a slitless quartz spectrograph[2] on the Crossley reflector of the Lick Observatory three similarly behaving absorption regions were found to coincide with the three "cyanogen" bands with first heads at λλ 4216, 3883, and 3590. The band at λ 3883 is by far the strongest; the point most sensitive to changes in luminosity seems to be the region around and between the two heads at λ 3871 and λ 3883. Of the two other bands, that at λ 3590 seems to be somewhat stronger. The band at λ 4606 seems to be too faint to be identified with certainty.

The spectra of the following stars were photographed; the spectral types and absolute magnitudes are from the new list of spectroscopic parallaxes[3] by Adams and his collaborators.

---

[1] *Astrophysical Journal*, **49**, 289, 1919; *Upsala Universitets Årsskrift*, 1920.

[2] This instrument is described by W. H. Wright in the *Lick Observatory Bulletin*, **9**, 52, 1917.

[3] *Mt. Wilson Contr.*, No. 199; *Astrophysical Journal*, **53**, 13, 1921.

χ Leonis	F5,	0.8
39 Leonis	F8,	3.7
Lal 19896	G1,	4.5
Boss 2338	G3,	−1.0
Lal 21008	G6,	5.2
ε Virginis	G6,	0.0
ε Geminorum	G8,	−1.4
β Geminorum	G9,	1.7
θ_1 Tauri	G9,	1.4
o_2 Eridani	K1,	6.2
Cin. 1712	K3,	6.4
α Tauri	K4,	1.0
β Cancri	K4,	0.4
Lal 13284	K5,	7.1
Boss 2935	Ma,	10.5
Boss 1868	Ma,	−0.2
α Orionis	Ma,	−3.8

The development of the bands is at a maximum for giant stars of types between G5 and K5, and diminishes strongly toward the F and M types. In the dwarf stars of all types the bands are only faintly developed.

The absorption in the band at λ 3883 has been investigated here for stars of known spectroscopic parallax by means of the 6° objective prism on the 10-inch refractor. The method employed is analogous to that used for the A stars described in the first part of this paper. This investigation was carried out before the identification with the "cyanogen" band had been made. The two regions of the spectrum immediately adjacent to λ 3889 were compared in series of images taken with decreasing exposure-time to determine the exposure-ratio for equal photographic density in the two regions. The maximum effect seems to be in spectral types G8–K0, where the difference in exposure-ratio between average giants and dwarfs corresponds to nearly a magnitude. The effect decreases rapidly from G5 to G0. The Cepheids and pseudo-Cepheids have a somewhat peculiar position with even less contrast at λ3889 than dwarfs of the same spectral type. The smoothness of the spectrum around the Hζ line for these stars is probably due to the disappearance of the wings of the strong absorption lines following the advance of the spectrum toward Miss Maury's *c*-stage.

There is a very decided disadvantage, however, in the fact that the region in question is situated so far in the violet that for the redder stars the exposures must be made considerably longer. The band at λ 4216, though weaker, is much more favorable in this particular, and an investigation of it was therefore begun with the same instrumental arrangement. The region most strongly affected by this band lies between λλ 4144 and 4184.

This region of 40 A width, corresponding to about 0.09 mm on the plate, has been compared with that at λ 4227–λ 4272 as standard. The regions in question are easily identified with sufficient accuracy by estimating the distances from the G-band and the line λ 4227, which are conspicuous features of the spectra even with very low dispersion. For the dwarfs of types K5–M the intensity in the second region mentioned is probably somewhat modified by the wings of λ 4227 which produce an additional effect of luminosity on the exposure-ratio in the same direction as the effect of the "cyanogen" absorption in the first region. No special efforts were made to determine Schwarzschild's constant for the plates. The results obtained from the investigation of the A stars indicate that generally the changes in the constant are small and do not increase materially the probable error of the measured exposure-ratio, but that rather large changes may occur, especially from one emulsion to another. In this case several stars were measured on each plate, and systematic errors of large size ought to show in the residuals from the curves. The means of the residuals for the individual plates are found to be small, however.

As before, the plates used were Seed 23, size 8×10 inches, with X-ray developer. Images more than 3.6 inches from the center were excluded. The focus was set near λ 4200, and is tolerably constant over most of this area. Even within the adopted limit of distance, however, some images must be excluded by reason of distortion or bad focus, because the field has not exact symmetry of rotation with reference to the plate center.

A scheme for classifying the objective-prism spectra was developed by using types determined by Adams and his collaborators as standards. The classification is based on the appearance and relative strength of the hydrogen lines, the K line of calcium, the λ 4227 line of calcium, the titanium-oxide bands, and the general energy-distribution in the spectrum. Since the decrease of the hydrogen lines and the increase of λ 4227 with advancing spectral type proceed more rapidly in the dwarf series, while the increase of redness takes place faster in the giant series, and since λ 4227 has enormous strength in dwarfs of types K5–M, these characteristics

TABLE VII

Boss or Cin. No.	Harv. Vis. Mag.	Spectrum	M	log E	n	Spectrum Obj. Prism
3274	6.5	G8	0.4	0.25	6	G8*g*
3298	4.8	K3	0.6	0.27	8	K0*g*
3326	5.9	K0	4.2	0.16	4	K2
3344	6.5	G8	0.9	0.26	7	G8*g*
3362	4.9	Ma	−0.3	0.18	8	Ma*g*
C 1657	7.7	K2	6.4	0.14	4	K0*d*
3408	6.2	K4	0.5	0.25	4	K5*g*
3537	5.7	K3	0.4	0.25	4	K2*g*
3554	6.3	F9	4.3	0.12	6	G5*d*
4131	5.5	K2	1.1	0.27	5	K2*g*
4137	5.6	G2	4.7	0.12	7	G5*d*
4147	3.3	G6	0.0	0.19	5	G5*g*
4257	6.7	G8	4.7	0.13	7	K0*d*
4264	5.4	K5	0.8	0.24	7	K5*g*
4315	3.4	K2	0.6	0.26	5	K0*g*
4318	5.9	Ma	0.2	0.22	4	Ma*g*
4323	5.0	K5	0.2	0.29	5	K2*g*
4327	4.4	G2	−1.4	0.27	4	G5*g*
4342	7.9	K5	7.9	0.05	6	K5*d*
4370	5.3 5.3	K1 K2	6.3 6.3	0.12	7	K0*d*
4372	6.7	K4	7.3	0.08	5	K5*d*
4414	6.3	K1	1.3	0.24	3	K2*g*
4420	4.3	A9	1.6	0.12	4	F2
C 2322	7.9	K5	8.0	−0.02	4	K5*d*
Lal 31905	7.2	K2	2.1	0.25	4	K5*g*
4571	4.3 5.0	K0 K4	5.8 7.8	0.10	6	G8*d*
4580	4.7	G6	−0.1	0.27	6	G8*g*
4595	5.7	F4	2.8	0.12	6	F5
4618	6.1	G2	−0.3	0.20	6	G5*g*
4635	4.9	G5	−0.5	0.20	9	G0*g*
4638	3.4	G8	2.5	0.15	5	G8
A. G. Leip. 8449	7.6	K2	0.8	0.33	5	K2*g*
4660	5.7	G0	−0.8	0.22	9	G0*g*
C 2420	7.9	G5	5.5	0.11	5	G5*d*
C 2421	8.5	G9	5.2	0.10	6	G5*d*
A. G. Leip. 8507	8.9	G2	5.7	0.14	5	G5*d*
4678	5.4	G9	1.7	0.21	5	K0*g*
A. G. Leip. 8585	7.6	Ma	1.5	0.16	3	Ma*g*
4688	6.5	G8	2.8	0.22	3	K0*g*
4713	5.4	F0	1.6	0.11	6	A–F

TABLE VII—*Continued*

Boss or Cin. No.	Harv. Vis. Mag.	Spectrum	*M*	log *E*	*n*	Spectrum Obj. Prism
C 2456	8.8	Mb	10.7	−0.09	3	Mb*d*
4800	4.5	Mb	−1.2	0.15	8	Mb*g*
4817	5.4	F8	0.3	0.13	5	F8
4823	4.2	K1	1.0	0.28	11	K0*g*
C 2495	6.0	G4	3.7	0.10	10	G5*d*
4892	6.8	G4	5.5	0.13	3	G2*d*
4893	6.6	G6	5.7	0.12	3	G2*d*
4898	5.7	G8	−1.4	0.28	12	G8*g*
4910	6.3	G8	1.5	0.24	2	G5*g*
4912	4.5	K0	0.2	0.29	8	K2*g*
4920	6.0	F4	2.8	0.12	3	F8
4940	4.6	K4	0.5	0.26	4	K3*g*
4950	5.2	G8	5.1	0.13	5	G5*d*
5009	4.8	G9	5.8	0.09	6	G8*d*
5027	4.4	G8	0.0	0.22	6	G8*g*
5052	3.8	Ma	0.2	0.11	5	Ma*g*
5079	4.0	G2	0.7	0.13	6	G5*g*
5089	4.9	G9	0.8	0.18	5	G8*g*
5093	3.9	G8	3.9	0.13	5	G8
5098	5.8	G1*p*	−2.5	0.20	4	G5*pg*
5118	3.7	K6	0.5	0.25	6	K5*g*
5125	5.6	Mc	0.5	0.14	5	Mb*g*
5129	4.6	Mb	0.3	0.13	8	Mb*g*
C 2616	7.2	G8	5.6	0.13	2	G8*d*
5143	5.6	G8	0.0	0.27	2	K0*g*
5180	5.7	K2	5.9	0.13	6	K2*d*
5187	4.0	G9*p*	−2.0	0.23	4	G*pg*
5219	6.1	G2	5.2	0.06	3	G5*d*
5229	2.3	G0*p*	−3.0	0.24	5	G*pg*
C 2672	6.3	G8	6.2	0.12	4	G8*d*
5321	6.0	F5	3.6	0.13	2	F5
5346	3.6	G8	3.2	0.18	5	G8*g*
C 2707	8.6	Ma	9.4	−0.01	3	M*d*
C 2718	6.6	F7	3.9	0.10	9	F5
5420	6.2	G8	1.5	0.26	7	K0*g*
5431	3.9	K2*p*	−2.9	0.24	4	K*pg*
5433	5.6	K7	8.3	0.09	9	K5*d*
5434	6.3	K8	8.7	0.05	7	Ma*d*

alone will suffice in a great number of cases to determine the spectral type and to decide whether the star is a giant or a dwarf. From type G0 on, however, the degree of the "cyanogen" absorption must be taken into account, and the approximate luminosity will be obtained with the aid of log *E*. The spectra used are narrow and, in what concerns the visibility of the lines, are inferior to widened images, but this has been at least partly compensated by the large number of images with different intensities usually available. For spectral types Go–Ko both the hydrogen lines and λ 4227 are only faintly visible, but a fairly good discrimination between the stages Go, G5, and G8–Ko seems to be possible. Four Cepheids and pseudo-Cepheids among the stars observed were recognized as peculiar stars mainly by the abnormal strength of the hydrogen lines.

The results of the measurements and classifications are given in Table VII. The first four columns contain data from the list of spectroscopic parallaxes. The fifth column gives log *E*, the logarithmic exposure-ratio for equal intensities in the two regions λ 4144–λ 4184 and λ 4227–λ 4272, the former being situated in the densest part of the "cyanogen" band; *n* is the number of images used for determining log *E*. The last column gives the spectral type as determined from the objective-prism spectra, in most cases without knowledge of the more accurate values of the type in the third column. An added *g* or *d* indicates a giant or a dwarf, respectively. This estimation of luminosity is made mainly from the value of log *E* according to the curves in Figures 3 and 4, the value of the spectral type estimated from the objective-prism spectra being used as argument. The individual results given in the last column are therefore directly dependent only on the data secured from the low dispersion spectra. The good agreement between these results and the spectral type and absolute magnitude in the third and fourth columns seems to give promise of the usefulness of the method.

Figure 3 gives the relation between log *E* and the absolute magnitude for stars of types A9 to K2, Figure 4 for types K2–Mc. The curves drawn representing the different types have only provisional significance. Figure 5 gives log *E* as a function of the spectral type, different degrees of luminosity being represented by different notations. It is evident from these diagrams that the effect of the "cyanogen" band reaches a maximum near Type K2 and decreases toward Go and M. The analogy between

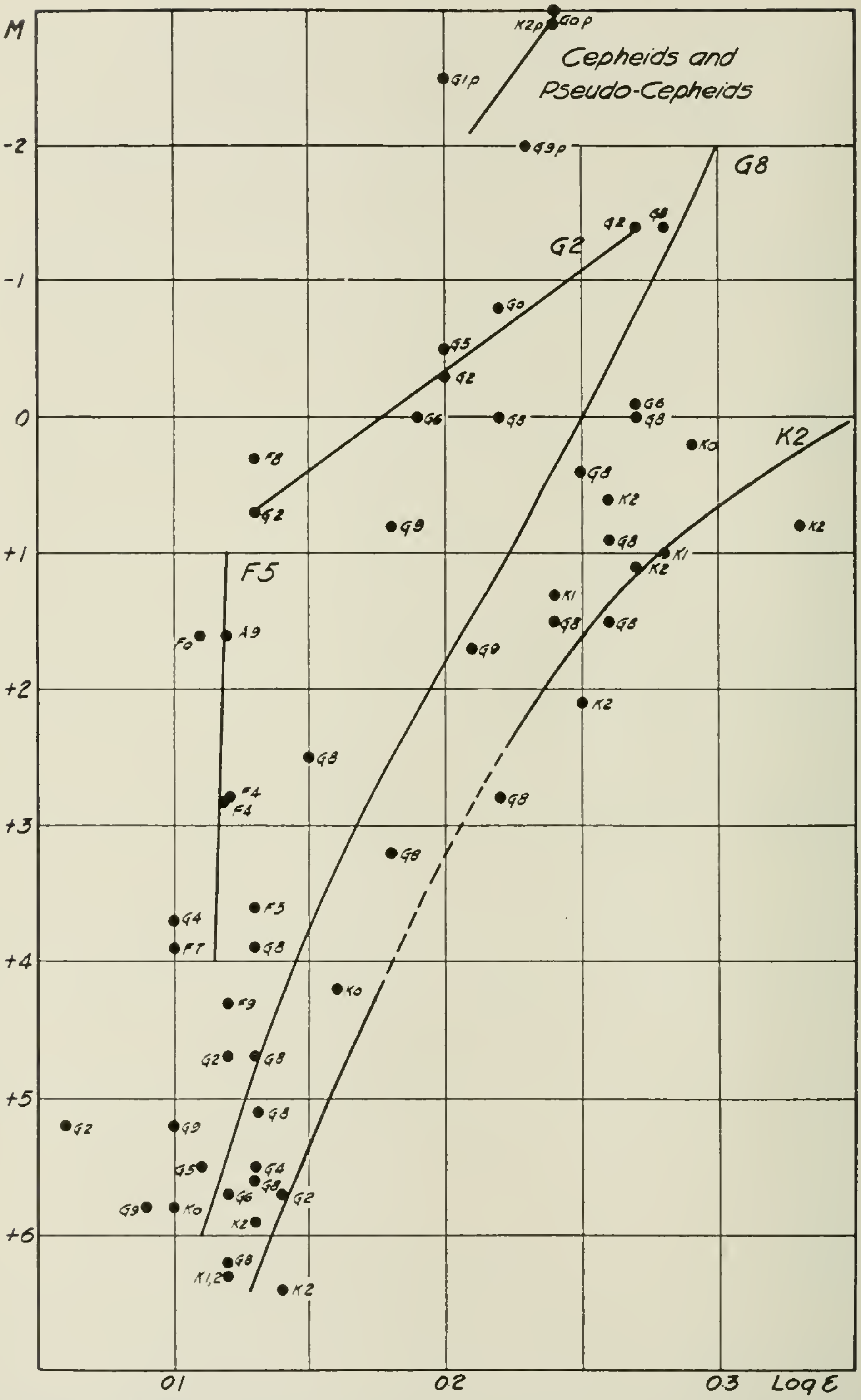

FIG. 3.—Logarithmic exposure-ratio for the regions λλ 4144–4184, 4227–4272, and absolute magnitude. Spectral types A9–K2.

Figure 5 and the diagram for the minimum wave-length of the grating-spectra[1] is very striking. The advantage of the present diagram, however, lies in the circumstance that the effect of the

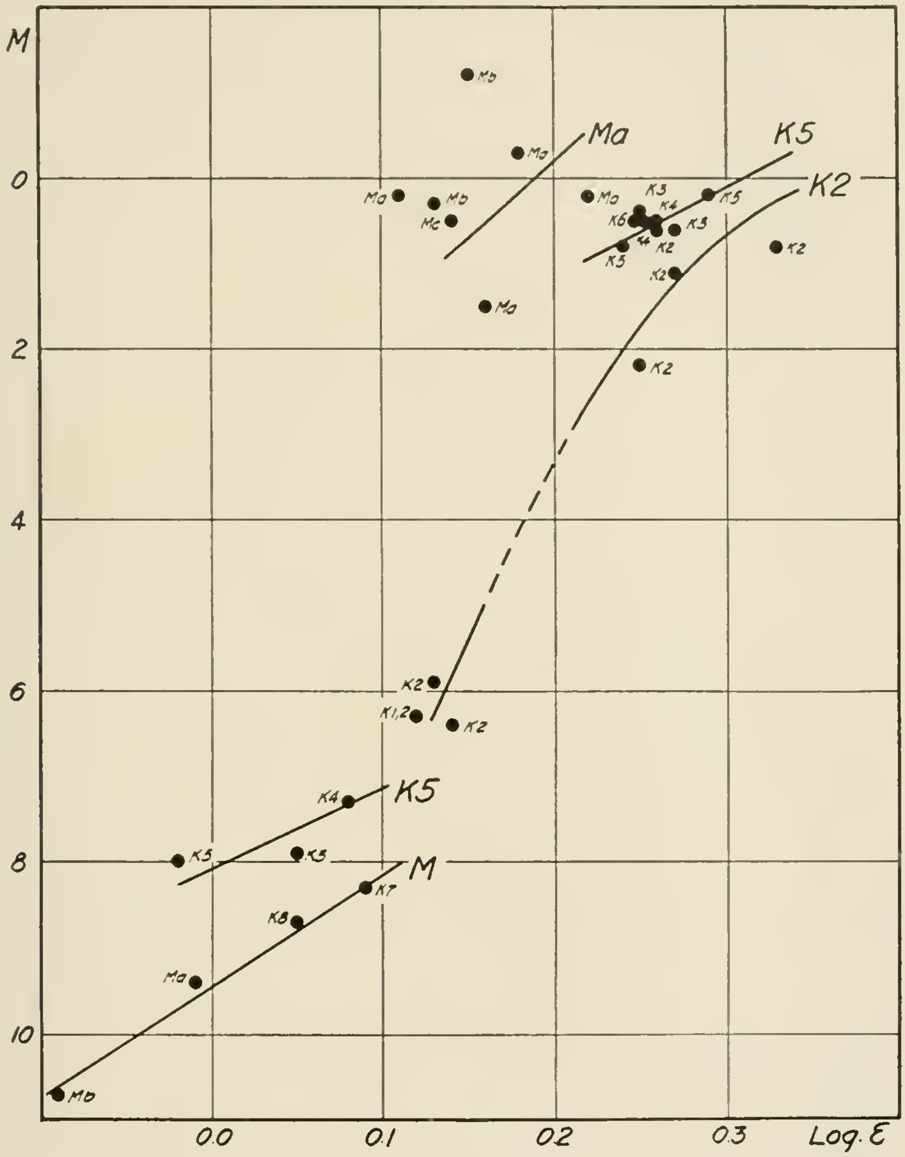

FIG. 4.—Logarithmic exposure-ratio for the regions λλ 4144–4184, 4227–4272, and absolute magnitude. Spectral types K2–Mc.

regular change in the energy-distribution in the spectrum due to the change of temperature in the spectral series has practically no effect on log E, owing to the closeness of the two compared regions. Except for the position of the Cepheids and pseudo-Cepheids the correspondence is nearly perfect between Figure 5 and a similarly arranged diagram for the absorption in the λ 3883 band. The variation in log *E* for the stronger ultra-violet band is, however, about 2.3 times as large as for the λ 4216 band. The increase of the effect from G8 to K2 probably explains the correlation of the absorption in the bands with the line λ 4227 found by Miss Maury in type XV.

---

[1] *Loc. cit.*

The rapid decrease of the effect toward G0, especially for stars with *M* between 0 and $+1$, is a disadvantage for a more accurate determination of luminosity. On the other hand, stars of this brightness, between types F0 and G2, seem to be very scarce. Most of the giants in this interval of spectral type given in the list of 1646 spectroscopic parallaxes, for example, are Cepheids or pseudo-Cepheids and of much higher luminosity.

The Cepheid variables and the pseudo-Cepheids seem to have an abnormally small absorption in the regions of the "cyanogen" bands; it is somewhat stronger, however, in the region of the λ 4216 band than in that of the λ 3883 band. In the case of the former band the stars still fall among the ordinary giants in the diagram in Figure 5, but in the case of the ultra-violet band, as mentioned before, they lie even below the dwarfs.

From K2 to M there is a general decrease of log *E;* the difference between giants and dwarfs is still well accentuated. The extent to which this difference is still due to "cyanogen" absorption in type M seems to be uncertain. For this type the line λ 4227, strong in the dwarfs, and the hydrogen lines, which are strong in the giants,[1] give a reliable criterion of the order of magnitude of the luminosity. The titanium-oxide bands characterizing type M are generally well developed in the objective-prism spectra. An observation of importance to be made from Figure 5 is that stars with $\log E > 0.17$ are giants.

An application of the preceding principles to stars of faint apparent magnitudes in a few rich regions has been made with a small focal-plane spectrograph attached to the 60-inch reflector. The spectrograph has a 64° U.V. prism; the focal lengths of collimator and camera are about 6 inches. The dispersion gives 1.51

---

[1] See various papers by Adams and his associates on the spectroscopic method.

mm between Hγ and Hδ, and is 2.8 times that of the objective-prism spectra. The slit was removed, thus giving a field about 9′×9′, of which about two-thirds is in good enough focus to be used. The objects investigated were the clusters M 11 and 13, and a few fields in Selected Areas Nos. 63 and 64 in the Cygnus region. A list of the photographs is given in Table VIII. Seed 30 plates were used, except for No. 33, which is Seed 23. All the plates were taken during good seeing, estimated about 5 and 6 on a scale of 10 in most cases. The last column gives for the Selected Area plates the number of the star in the Harvard Durchmusterung[1] which is nearest to the center of the field.

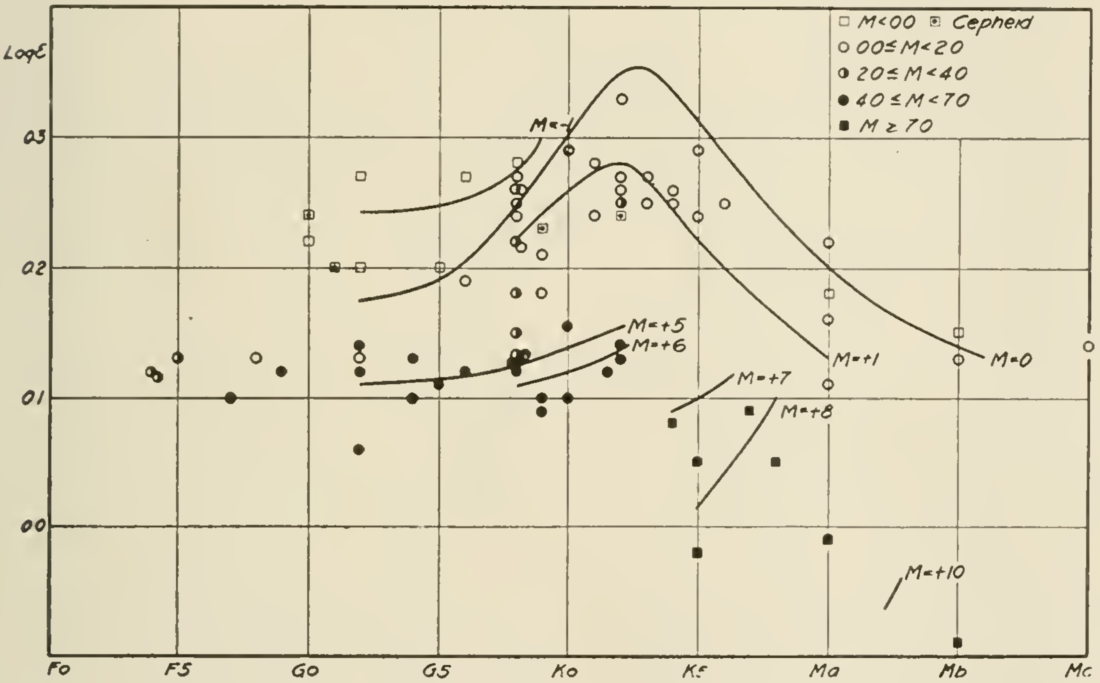

FIG. 5.—Logarithmic exposure-ratio for the regions λλ 4144–4184, 4227–4272, and spectral type.

Messier 11, R. A. 18ʰ46ᵐ, Decl. −6°23′ (1900).—This well-known open cluster, situated in the bright galactic clouds in Scutum Sobieski, is very rich in stars, several hundred being brighter than the fourteenth magnitude. Magnitudes and colors for a large number of stars in the cluster have been determined by Shapley.[2]

---

[1] "Durchmusterung of Selected Areas," *Harvard Annals*, 101, 1918.

[2] *Mt. Wilson Contr.*, No. 126; *Astrophysical Journal*, 45, 164, 1917.

Table IX gives the results of the classification of spectra for eighty-five stars in the cluster. A great many stars which are sufficiently bright have their images superposed, thus making estimates of their spectral types impossible. For early types the classification is based on the strength of the K line relative to the hydrogen lines; for the late types the spectra have been compared with spectrograms of stars with known spectroscopic parallaxes, photographed with the same instrumental arrangement on the same kind of plates. The numbers are those of Stratonoff[1]; the photographic magnitudes are according to Shapley. The letter *d* after the spectral type means for an A-type star that the spectrum shows a marked energy-fall at λ 3907, thus indicating a relatively low luminosity ($M > 1.5$); for later types a *g* indicates giant characteristics, in this case strong "cyanogen" absorption in the region λ 4144–λ 4184.

TABLE VIII

List of Plates

Plate No.	Object	Date	Exposure-Time	Harvard No.
33	Sel. Area 63	1921 May 10	$1^h 43^m$	527
35	Sel. Area 63	May 11	2 55	527
46	Messier 11	Aug. 2	30	....
47	Messier 11	Aug. 2	2 0	....
48	Messier 11	Aug. 2	5 1	....
49	Sel. Area 64	Aug. 2	4 0	666
50	Messier 13	Aug. 3	1 30	....
51	Sel. Area 64	Aug. 3	4 2	509
65	Sel. Area 64	Sept. 4	3 30	1029
75	Sel. Area 64	Sept. 5	4 37	454

The giants of types K0–K2 in Table IX have nearly the same apparent magnitude. The estimate $M = 0$ for their absolute magnitude seems to be fair, judging from the very marked "cyanogen" absorption in their spectra. The mean photographic magnitude of the four stars Nos. 252, 423, 666, 674, is 13.32. With a mean color-index somewhat exceeding unity, we find the modulus $M - m$ to be nearly equal to -12.

---

[1] *Publications de l'Observatoire de Tachkent*, No. 1, 1899.

The two brightest A stars in Table IX, Nos. 545 and 437, show sharp lines suggesting very high luminosity. With the value $M-m=-12$ their absolute magnitudes would be −2.8 and −0.5,

TABLE IX

Messier 11

No.	Pg. Mag.	Spectral Type	No.	Pg. Mag.	Spectral Type	No.	Pg. Mag.	Spectral Type
193	....	A0	365	13.32	A0	571	13.16	A0
197	....	A2	366	13.02	A0	579	(Triple)	A0*d*
204	13.38	A0	375	12.54	A0	581	11.85	A0
214	13.48	A0	377	13.64	A0	583	13.84	A2*d*
221	13.07	A0	381	12.44	A0	590	13.04	(G8*g*)?
224	13.56	A0*d*	405	13.18	A0	592	14.22	A0*d*
227	12.06	A0	407	11.93	A0	597	12.78	A2
232	12.22	A0	423	13.46	K2*g*	598	13.02	G8*g*
236	13.07	A0	425	12.62	A2	599	12.40	A0
237	11.74	A0	426	13.21	A0*d*?	601	11.69	F?
245	12.15	A0	437	11.46	A0	616	13.89	A2*d*
252	13.08	K*g*	439	13.64	A0	617	13.25	A0
267	13.26	A0	460	12.97	A0	630	13.54	A0
273	13.00	A0	462	12.79	A0	631	12.46	A0
274	14.32	A2*d*?	464	13.94	A0	633	13.37	A0
280	13.01	G8*g*	468	13.91	A2*d*?	635	13.23	A0
285	13.08	A0	486	12.85	A0	647	12.66	A0
288	12.75	A3	487	12.39	A2	662	12.47	A0
297	12.44	A0	490	13.12	A0	663	11.90	A5*d*
307	14.20	A2*d*	491	12.33	A0	666	13.45	K0*g*
310	13.04	A0*d*?	494	12.32	A0	672	12.50	A0
322	13.46:	A0	511	....	G8*g*	674	13.28	K2*g*
325	13.04	A2	519	13.30	A0	704	....	A0*d*?
331	12.24	A0	525	12.08	A0	715	....	A0
336	12.08	A0	529	13.48	A0*d*?	762	....	K2*g*
341	12.42	A0	545	9.3:	A5	....	....	....
345	12.06	A0	548	12.23	A0	....	....	....
356	12.60	A0	552	14.20	A0*d*?	....	....	....
362	13.68	A0	568	13.31	A0	....	....	....
364	12.73	G8*g*	569	13.26	A0	....	....	....

respectively. The remaining A stars have fairly broad hydrogen lines. Between photographic magnitude 11.8 and 13.5 the energy-distribution around λ 3907 was found to be smooth, except for star No. 663; with the value of $M-m$ found above, those limits will correspond to $M=-0.2$ and $M=+1.5$. The faintest A stars in the tables show indications of a more abrupt fall of intensity at λ 3907. For Nos. 224, 307, 592, 616, where this is most noticeable, we find for M the values of 1.6, 2.3, 2.2, 2.1, respectively, which are in good agreement with the results for the A stars in the first part of this paper. The A5 star No. 663, photographic magnitude 11.90, is probably a relatively near star, superposed on the cluster. The spectra of the four faint A stars just mentioned are rather weak, and no definite conclusions can be drawn from those stars alone, but the indications are that the value $M-m=-12$ deserves a fair degree of confidence. Adopting this value we find for the parallax of the cluster $\pi=0''.00025$, corresponding to a distance of 4000 parsec or 13,000 light-years. Shapley,[1] obtaining a value by an entirely different method, finds $\pi=0''.00014$. In view of the uncertainties affecting the two determinations the difference cannot be considered as by any means excessive.

Globular clusters.—On Plate No. 50 three of the brightest stars in the globular cluster Messier 13 are sufficiently well separated from other stars to permit an examination of their spectra. They are the Scheiner Nos. 47, 63, 127. Shapley[2] gives the photographic magnitudes 13.45, 13.70, 13.58, and the color-indices 1.41, 1.16, 1.42. With the parallax $=0''.000090$[3] the absolute magnitudes are -3.19, -2.69, -3.07, respectively. These stars seem to be of a spectral type not far from K0, but show a much smaller absorption in the region of the "cyanogen" band than the late-type stars in Messier 11. This agrees with the degree of luminosity found by Shapley, if the stars are pseudo-Cepheids; if they are ordinary giants we should estimate the absolute magnitude around $+1$. Low dispersion slit spectrograms of some stars in Messier 13 on a plate taken by Mr. Pease, and of stars in Messier 3 on a plate taken by Mr. Sanford, exposure-times 30^h and 20^h, respectively, seem rather to confirm the high degree of luminosity. The stars of earlier type on the first mentioned plate seem to have no appreciable change of intensity at λ 3907, and for the late-type stars on the latter plate, especially for the star von Zeipel No. 752, photographic magnitude 13.96, color-index 1.42, absolute magnitude according to

---

[1] *Proceedings of the National Academy of Sciences*, 5, 344, 1919.

[2] *Mt. Wilson Contr.*, No. 116.

[3] Shapley, *Mt. Wilson Contr.*, No. 152; *Astrophysical Journal*, 48, 154, 1918.

Shapley −3.18, the depression between λ 4100 and λ 4227 seems to be centered around Hδ and λ 4172 rather than in the "cyanogen" band, observations in favor of a classification in the Pseudo-Cepheid type.

Selected Areas

No. 63, R.A. 19^h0^m, Decl. +30°0′, (1900)
No. 64, R.A. 19^h58^m, Decl. +30°0′.

TABLE X

SELECTED AREAS 63 AND 64

Harv. No.	Pg. Mag.	Spectral Type	Harv. No.	Pg. Mag.	Spectral Type	Harv. No.	Pg. Mag.	Spectral Type
Area 63			504....	14.5	A0	710...	12.87	A0
511....	13.20	K3*g*	524....	14.0	A2	719...	14.40	K2*g*
513....	12.61	G5*d*	535....	12.5	A0	726...	14.26	K2*g*
518....	9.61	A0	581....	12.5	B9	733...	11.70	A0
519....	10.50	A5	583....	12.0	A0	744...	13.06	F8
535....	12.43	G0*d*						
			603....	13.6	A2	748...	13.31	A0
539....	11.86	A5*d*	611....	13.8	F8	767...	12.10	G5*d*
546....	13.43	K2*g*	619....	14.6	A0	1005...	11.3	A0
			623....	14.2	A0	1007...	10.6	A0
Area 64			629....	13.7	A0	1017...	13.1	K0*g*
430....	14.6	A						
435....	13.2	K2*g*	646....	11.3	G8*g*	1020...	13.9	K2*g*
438....	13.8	F5*g*	661....	14.1	A0	1021...	13.6	B?
442....	13.2	G8*d*	667....	14.18	K5*g*	1026...	10.9	F0
443....	14.0	F8*d*	668....	13.0	F8*d*	1027...	13.8	G0*d*
			671....	14.22	K0*g*	1028...	13.3	A0
445....	14.0	K5*g*						
448....	13.9	G5*d*	677....	13.31	A0	1104...	11.8	A2*d*
476....	13.5	G5*d*	680....	13.86	K0*g*			
479....	14.1	A0	682....	13.64	G5*d*			
486....	12.7	G5*d*	702....	13.81	K2*g*			
			706....	10.52	A2			

The results of classification for fifty-two stars in Selected Areas 63 and 64 are given in Table X. The numbers are according to the Harvard Durchmusterung. The photographic magnitudes for the central fields are according to unpublished Mount Wilson measures; for stars more distant from the center of the area the Harvard magnitudes have been reduced to the Mount Wilson system, and are given to only one decimal.

These two areas are situated in very rich galactic regions. There are eleven late-type stars classified as dwarfs in Table X, which as a group may be considered to be the nearest stars in the region. Of the remaining more distant stars twenty-eight are fainter than the thirteenth magnitude, twelve of which are found to be giants of types K0–K5, a remarkably high percentage. These late-type giants range in photographic magnitudes from 13.1 to 14.4, with a mean of 13.8. With a mean color-index of 1.2 and an absolute visual magnitude of 0.5 they should be at the same distance as M 11, about 4000 parsecs. If M 11 is associated with the galactic clouds in Scutum, the inference would be that these giant stars together with some of the A stars are members of the distant galactic cloud in Cygnus.

I wish to express my deep feeling of obligation to Director Hale for the opportunity to undertake this investigation during a stay of more than a year at the Observatory, and also to several members of the staff, especially Mr. Adams and Mr. Seares, for much valuable information and advice. I also wish to express my gratitude to Director Campbell for a month's stay at the Lick Observatory, and to Mr. Wright for his kind help and instruction in the work with the Crossley reflector.

Mount Wilson Observatory
October 1921

THE THEORY OF IONIZATION AND THE SUN-SPOT SPECTRUM[1]

BY HENRY NORRIS RUSSELL[2]

ABSTRACT

Saha's theory of temperature ionization, assuming the ionization to be due to temperature alone, leads to the relation: $Px^2/(1-x^2)=K$; that is, the ratio of the fraction of atoms ionized (x) to the fraction un-ionized ($1-x$), times the partial pressure of the free electrons $[Px/(1+x)]$, is equal to K, a function only of the ionization voltage I and of the absolute temperature T, namely: $\log_{10} K=-5036\ I/T+2.5\log_{10} T-6.5$. The theory is here *extended to mixtures of elements* by putting the partial pressure of the electrons equal to $P\bar{x}/(1+\bar{x})$ where $\bar{x}$ is the fraction of ionization for all the atoms present, and P, as before, is the total pressure. Hence, $Px_1\ \bar{x}/(1-x_1)(1+\bar{\ })=K_1$; $Px_2\,\bar{x}/(1-x_2)(1+\bar{x})=K_2$; etc.; and the ratio of $x_1/(1-x_1)$ to $x_2/(1-x_2)$ is merely K_1/K_2. Therefore the degree of ionization is always higher for an element of easy than for one of difficult ionization, and the relation between the two depends only on (I_2-I_1) and on T, and not on the pressure or on the relative concentrations. Saha's *formulae for second-stage ionization* are corrected. Only two successive stages of ionization can be present in any considerable proportions at the same time. Strong *evidence in favor of the theory* is afforded by a comparison of the sun-spot and the solar spectrum, since the predictions of the theory with reference to the relative intensity in the hotter and the cooler spectrum, of lines associated with ionized and un-ionized atoms, are found to be in general agreement with the facts. However, discrepancies such as the presence of too large a fraction of ionized Ba atoms, suggest the need of some modification of the theory; and it is evidently incomplete, since it neglects the effects of radiation on ionization.

Relative intensity in solar and sun-spot spectra of series lines.—The lines of the *alkali metals* (all of which are due to the neutral atoms) are *greatly strengthened* in the spot spectrum. Na ($I=5.11$ volts) exhibits its principal and subordinate series, K (4.32) the principal series alone, and Li (5.37) and Rb (4.16) the leading pair of the principal series, and only in the spot spectrum. The corresponding lines of Cs are out of reach in the infra-red.

Among the *alkaline earths* the lines of the *neutral atom* for Ca (6.08 volts) are strengthened in the spots to a degree which is greatest for the principal series and least for the combination series. The corresponding lines of Sr (5.67) are faint in the sun and much strengthened in spots. For Ba (5.12 volts) they are absent both in sun and spots. The *enhanced lines* arising from the ionized atoms (Ca+, Sr+, Ba+) are strong in both spectra.

For Mg (7.65 volts) the lines of the *neutral atom* are little affected, except that the fundamental line $1S-2p_2$ is stronger, while for Zn (9.4 volts) the arc lines are much weaker in the spot spectrum.

These results are all in agreement with Saha's theory. The lines of Li and Ba, however, are much weaker than the theory indicates.

Relative intensity of arc and enhanced lines.—It is pointed out that enhanced lines of easily ionized elements can be produced with less excitation than arc lines of difficultly ionized elements. This fact explains many apparent anomalies in astrophysical spectra.

Ionization potential of the elements as a function of atomic number.—Since from the relative behavior in sun, spot, and furnace spectra, of the lines of *Ca, Sc, Ti, V, Cr,*

---

[1] *Contributions from the Mount Wilson Observatory*, No. 225.

[2] Research Associate of the Mount Wilson Observatory.

Mn, Fe, Co, Ni, Cu, and Zn, the elements as arranged in the order of their atomic numbers, are progressively more difficult to excite spectroscopically, the ionization potential probably increases regularly from 6 volts for Ca to 9.4 volts for Zn, and this result combined with other data suggests that, *in general*, the ionization potential is a periodic function of the atomic number.

Identification of certain solar lines.—Lines of Rb have been detected in the sun for the first time. Also several faint Na lines have been identified and Datta's identifications of Na and K lines have been partly confirmed, partly not.

Tables of the series lines of Li, Na, K, Rb, Cs, Ca, Sr, Ba, Mg, and Zn are given with intensities in sun and spot, and wave-lengths in international units to 0.01 A.

Dr. Megh Nad Saha, in an important series of papers,[1] has shown the great importance of the modern thermodynamic theory of ionization in astrophysical and spectroscopic researches. In particular, he makes certain predictions about the behavior of the lines of the alkali metals in the spectra of sun-spots. The present communication deals with certain points connected with the theory, especially when many kinds of atoms are present at the same time, and with the observational verification of the predictions, which has been complete.

I. THE THEORY OF IONIZATION WHEN ATOMS OF SEVERAL KINDS ARE PRESENT

The equation of the "reaction isobar" as given by Saha[2] in the case of the ionization of a gas consisting of atoms of but a single kind is

$$\log \frac{x^2}{1-x^2}P = \log K = -\frac{U}{4.571\,T} + 2.5 \log T - 6.5 \qquad (1)$$

where the logarithms are to the base 10, P is the pressure of the gas, x the fraction of all the atoms which are ionized, T the absolute temperature centigrade, and U the "heat of ionization" in calories per gram-molecule. For the gas in question, the latter is proportional to the ionization potential, I, being 23,020 calories if I is one volt, so that we may also write

$$\frac{x^2}{1-x^2} = \frac{K}{P}, \qquad \log K = -\frac{5036\,I}{T} + 2.5 \log T - 6.5. \qquad (2)$$

---

[1] "Ionization in the Solar Atmosphere," *Philosophical Magazine*, **40**, 472, 1920; "Elements in the Sun," *ibid.*, **40**, 809, 1920; "On the Temperature Radiation of Gases," *ibid.*, **41**, 267, 1921; "On a Physical Theory of Stellar Spectra," *Proceedings of the Royal Society*, A, **99**, 135, 1921.

[2] *Philosophical Magazine*, **40**, 479, 1920.

If atoms of several different kinds, all capable of ionization, are present, the situation is somewhat more complicated. To use equation (1), introducing for P the value of the partial pressure of the vapor of each element separately, is inadmissible, since one of the products of the reaction—free electrons—is produced by all the ionizations. But if p' is the partial pressure of the ionized atoms of any sort, p that of the corresponding non-ionized atoms, and p'' that of the free electrons, we will always have

$$\frac{\mathrm{p}'\mathrm{p}''}{\mathrm{p}}=K \tag{3}$$

when K is given by (2).

If now atoms of several kinds are present in the relative numbers a_1, a_2, a_3 . . . . and the fractions x_1, x_2, x_3 . . . . of these are ionized, the whole number of atoms and free electrons present will be $a_1(1+x_1)+a_2(1+x_2)$ . . . . and the partial pressures for element 1 will be

$$\mathrm{p}_1'=\frac{a_1x_1}{\Sigma a+\Sigma ax}P \qquad \mathrm{p}_1=\frac{a_1(1-x_1)}{\Sigma a+\Sigma ax}P$$

(P being as before the whole pressure of the gas), while for the free electrons we will have

$$\mathrm{p}''=\frac{\Sigma ax}{\Sigma a+\Sigma ax}P=\frac{\bar{x}}{1+\bar{x}}P$$

where

$$\bar{x}=\frac{\Sigma ax}{\Sigma a}. \tag{4}$$

$\bar{x}$ is therefore the fraction of all the atoms present which are ionized, and may be regarded as a weighted mean of the values of x for the individual elements.

Equation (3) then becomes for the various elements

$$\frac{x_1}{1-x_1}\frac{\bar{x}}{1+\bar{x}}=\frac{K_1}{P}, \qquad \frac{x_2}{1-x_2}\frac{\bar{x}}{1+\bar{x}}=\frac{K_2}{P}, \quad . \; . \; . \; . \tag{5}$$

where K_1, K_2 are given by (2) with the ionization potentials for the elements concerned.

We then have

$$\frac{x_1}{1-x_1}=\frac{K_1}{K_2}\frac{x_2}{1-x_2}, \qquad \log\frac{K_1}{K_2}=5036\,\frac{I_2-I_1}{T} \tag{6}$$

or, expressed verbally: *The ratios of the number of ionized atoms to that of non-ionized atoms for any two elements in a gaseous mixture bear a fixed proportion to one another, which depends only on the temperature, and is independent of the pressure, the relative abundance of the two elements, or the presence of other elements.*

These latter conditions affect the amount of ionization, without modifying this proportion. The element of lower ionization potential is always the more highly ionized.

We may write (5) in the form

$$\frac{x_1^2}{1-x_1^2}=\frac{K_1}{P_1},$$

where

$$P_1=P\frac{\bar{x}}{x_1}\,\frac{1+x_1}{1+\bar{x}}\,. \tag{7}$$

If $x_1>\bar{x}$, that is, if the element is more easily ionized than the average, P_1 will be less than P, and the percentage of ionization will be greater than it would be if this element alone were present, with the same total pressure. For elements ionized with more difficulty than the average, the reverse will be the case.

The ionization will in all cases be less than if this element were present alone with its actual partial pressure, for p'', in equation (3), will always be greater than the partial pressure p_1' of the electrons arising from the dissociation of this one component of the mixture.

When ionization is just beginning all the x's will be small, and we will have approximately

$$x_2=\frac{K_2}{K_1}x_1,\text{ etc.}\qquad \bar{x}=\frac{x_1\Sigma aK}{K_1\Sigma a}$$

$$P_1=P\frac{\bar{x}}{x_1}=P\frac{a_1}{\Sigma a}\left(1+\frac{K_2a_2}{K_1a_1}+\frac{K_3a_3}{K_1a_1}\;\dots\dots\right).$$

The factor outside the parentheses is the partial pressure of constituent 1. It follows that at the beginning of ionization the constituent of lowest ionization potential behaves very nearly as if it alone were present at its actual partial pressure. For constituents more difficult of ionization the initial ionization is less, and may be very much smaller.

When the ionization of any element is nearly complete, we may set $x_1 = 1$ in (7) and find

$$P_1 = P\frac{2\bar{x}}{1+\bar{x}}.$$

The effective pressure for this element is therefore nearly equal to the total pressure (unless a large proportion of atoms of more difficult ionization is present).

For an element of easy ionization the range of temperature or pressure within which both ionized and uncharged atoms will be present in sensible proportions is therefore extended by the presence of other constituents in the mixture.

For an element of difficult ionization, x_1 will be much less than $\bar{x}$ and P_1 greater than P, when ionization is beginning. The range within which both phases are present will in this case be reduced.

If we set

$$\frac{\bar{x}^2}{1-\bar{x}^2} = \frac{\bar{K}}{P}$$

we find easily

$$\bar{K}\frac{1-\bar{x}}{\bar{x}} = K_1\frac{1-x_1}{x_1} = K_2\frac{1-x_2}{x_2} \quad . \; . \; . \; . \quad = \frac{\Sigma a K(1-x)}{\Sigma a x}$$

$$\bar{K} = \frac{\Sigma a K(1-x)}{\Sigma a(1-x)}$$

so that $\bar{K}$ is the mean of the individual K's, weighted in proportion to the number of non-ionized atoms remaining. At low temperatures, the atoms of easy ionization, which have the largest values of K, will contribute most to this mean; but at high temperatures these will be ionized, and the atoms of difficult ionization will contribute most. The effective mean ionization potential, corresponding to the value of $\bar{K}$, will therefore increase with the temperature.

Successive ionization.—Consider now atoms of the same kind, which are susceptible of the loss of two successive electrons. Let the ionization potential for the removal of the first be I and the additional potential for the second be I'. If x is the proportion of singly-ionized and y of doubly-ionized atoms, that of free electrons will be $x+2y$, and we will have[1]

$$\left.\begin{aligned}\frac{x(x+2y)}{(1-x-y)(1+x+2y)}=\frac{K}{P}\\ \frac{y(x+2y)}{x(1+x+2y)}=\frac{K'}{P}\end{aligned}\right\}. \tag{8}$$

The first of these equations may be written

$$\frac{(x+y)^2}{1-(x+y)^2}=\frac{K}{P}\,\frac{(x^2+2xy+y^2)(1+x+2y)}{(x^2+2xy)(1+x+y)}>\frac{K}{P}$$

also

$$\frac{x^2}{1-x^2}=\frac{K}{P}\left(1-\frac{y(2-x+x^2+2xy)}{(1-x^2)(x+2y)}\right)<\frac{K}{P}$$

while the second may be written

$$\frac{y^2}{1-y^2}=\frac{K'}{P}\,\frac{x}{1-y}\,\frac{2y^2+xy+y}{2y^2+xy+2y+x}<\frac{K'}{P}\,.$$

It follows that the numbers of both neutral and singly-ionized atoms are less than they would be if the second ionization did not occur—the draft upon the singly-ionized atoms being partly made up by fresh ionization of neutral ones; but the number of doubly-ionized atoms is less than it would be if the second ionization was the only one which occurred.

Dividing the second of the equations (8) by the first we find

$$\frac{y(1-x-y)}{x^2}=\frac{K'}{K}. \tag{9}$$

Now

$$\log\frac{K'}{K}=-5036\frac{I'-I}{T}$$

and in all cases which have so far been investigated $I'-I$ is positive, and equal to at least five volts.

---

[1] These equations differ from Saha's (*Proceedings of the Royal Society*, A, **99**, 143, 1921) which contain x^2 and y^2 in the numerators; but the latter formula would appear to involve the inadvertent assumption that an atom can combine only with an electron previously liberated by another atom which happens to be in the same state of ionization.

Hence K'/K is usually a small quantity, and it is impossible for y and $1-x-y$ to be considerable at the same time; that is, there will not simultaneously be any noticeable proportion of atoms in all three states of ionization. When the temperature is high K'/K increases; but in this case x is small and the number of neutral atoms very small.

At low temperatures we may set $y=0$, when the ordinary equation for single ionization is obtained; at high temperatures we may set $x+y=1$ and have

$$\frac{y^2+y}{2-y^2-y}=\frac{K'}{P}\,.$$

One or the other of these formulae will always give a good first approximation, provided that a third electron is not lost.

In a mixed gas, containing other constituents, we will have

$$\frac{x\bar{x}}{(1-x-y)(1+\bar{x})}=\frac{K}{P}\,;\quad \frac{y\bar{x}}{x(1+\bar{x})}=\frac{K'}{P}\,;\quad \bar{x}=\frac{\Sigma a(x+2y)}{\Sigma a}\,. \tag{10}$$

Since the potential for the second ionization is always high, the presence of other elements will in general diminish its amount; but equation (9) will hold in all cases.

Instead of equation (6) we will have

$$\frac{x}{1-x-y}=\frac{K}{K_2}\frac{x_2}{1-x_2}\qquad \frac{y}{x}=\frac{K'}{K_2}\frac{x_2}{1-x_2} \tag{11}$$

where x_2 is the percentage of ionization for any singly ionized element.

2. THE ALKALIES AND ALKALINE EARTHS IN THE SUN-SPOT SPECTRUM

Saha has shown[1] that sodium should be considerably ionized in the reversing layer, potassium almost completely, and rubidium and caesium entirely. As the familiar lines of these elements are absorbed by the neutral atoms only, the faintness of the lines of potassium in the solar spectrum and the absence of those of rubidium and caesium is immediately explained. At the lower temperatures which prevail in the spots he predicts that the lines of potassium should be strengthened, and that those of rubidium should show faintly.

---

[1] *Philosophical Magazine*, 42, 812–815, 1920.

Observations upon the behavior of sodium in sun-spots have been published by Adams[1] and the presence of lithium has been determined by King.[2] The study of the other alkali metals, which have their lines principally in the red, has been made very easy by the publication of extensive and accurate tables of wave-lengths in the red and infra-red, both in the solar spectrum[3] and in the arc,[4] and by the existence at Mount Wilson of an excellent series of plates of the spot spectrum, extending to λ 8200, taken by Mr. Brackett with the 150-foot tower telescope and 75-foot spectrograph, in the first order, with nicol prism and compound quarter-wave plate. All the available lines of the alkali metals were examined on these plates (or on the photographic map of the spot spectrum for the wave-lengths less than 6600 A) and some additions to the data for sodium and lithium were made.

The results, including those of the earlier observers, are given in Table I. In this table the first column gives the element and series designation of the line (after Sommerfeld). The leading pair of the principal series is denoted by 1s–2p, the next pair by 1s–3p, and so on. The corresponding pairs for the diffuse series are 2p–3d, 2p–4d, and for the sharp series 2p–3s, etc. Lines lying too far in the infra-red to be observed, or too far in the ultra-violet to be observable in spots, are in general omitted, as are also the fainter members of a series when the stronger earlier members are invisible.

The second column gives the wave-lengths found in the laboratory by Datta or by Meggers (or, in one or two cases, by others); and the third, the wave-length of the corresponding solar line derived from Rowland's tables, from Meggers, or from measurements made at Mount Wilson. All wave-lengths are given in

---

[1] *Mt. Wilson Contr.*, No. 40; *Astrophysical Journal*, **30**, 108, 1909.

[2] *Mt. Wilson Contr.*, No. 122; *Astrophysical Journal*, **44**, 169, 1916.

[3] W. F. Meggers, "Solar and Terrestrial Absorption in the Sun's Spectrum from 6500 A to 9000 A," *Publications of the Allegheny Observatory*, **6**, 12–44, 1919.

[4] W. F. Meggers, "Wave-Length Measurements in Spectra from 5600 A to 9600 A," *Bulletin of the Bureau of Standards*, **14**, 371–397, 1916; S. Datta, "The Vacuum Arc Spectra of Sodium and Potassium," *Proceedings of the Royal Society*, A, **99**, 69–78, 1921.

TABLE I

LINES OF THE ALKALI METALS

ELEMENT	WAVE-LENGTHS		INTENSITY		AUTHORITY	NOTES
	Arc	Sun	Sun	Spot		
Lithium						
1s–2p	6707.82	07.83	abs	5	King	1
2p–2s	8126.52	....	abs	abs	Russell	
2p–3d	6103.53	....	abs	abs	King	
Sodium						
1s–2p	5895.94	95.94	20	60	Adams	
	5889.97	89.97	30	90	Adams	
2p–3d	8194.82	94.84	2	7	Russell	
	8183.30	83.27	3	10	Russell	
2p–4d	5688.22	88.22	6	12	Adams	
	5682.67	82.65	5	12	Adams	
2p–5d	4982.86	82.82	2	4	Russell	2
	4978.61	78.56	0	1	Russell	3
2p–6d	4668.60	68.57	1*N*	3	Russell	4
	4664.86	....	....	....	Russell	5
2p–7d	4497.72	97.73	abs	0	Wilson	6
	4494.27	....	abs	abs	Russell	7
2p–4s	6160.72	60.75	3	8	Adams	
	6154.21	54.23	2	9	Adams	
2p–5s	5153.85	....	abs	abs	Russell	8
	5149.27	....	abs	abs	Russell	9
2p–6s	4751.89	51.83	00	2	Adams	
	4748.02	47.98	000	0	Adams	
Potassium						
1s–2p	7699.00	99.01	5	13	Russell	
	7664.92	64.92	6	15	Russell	10
1s–3p	4047.20	47.19	00*Nd*	0	Russell	11
	4044.14	44.14	0	2	Russell	
2p–4d	6965.0	....	abs	abs	Russell	12
	6936.0	....	abs	abs	Russell	
2p–5d	5832.31	....	abs	abs	Russell	
	5812.71	....	abs	abs	Russell	
2p–4s	6939.50	....	abs	abs	Russell	13
	6911.80	....	abs	abs	Russell	
2p–5s	5802.16	....	abs	abs	Russell	
	5782.77	....	abs	abs	Russell	

TABLE I—*Continued*

Element	Wave-Lengths In		Intensity In		Authority	Notes
	Arc	Sun	Sun	Spot		
Rubidium						
1s–2p.........	7947.64	47.63	abs	0	Russell	14
	7800.29	00.29	abs	1	Russell	
1s–3p.........	4215.57	....	abs	abs	Russell	
	4199.85	....	abs	abs	Russell	
2p–4d.........	7757.80	....	abs	abs	Russell	
	7619.12	....	abs	abs	Russell	
Caesium						
1s–2p.........	8943.46	....	abs	Unknown	....	15
	8521.12	....	abs	Unknown	....	
1s–3p.........	4593.22	....	abs	abs	Russell	
	4555.31	....	abs	abs	Russell	
	8079.4	....	abs	abs	Russell	16
	8016.2	....	abs	abs	Russell	

NOTES TO TABLE I

1. Much widened in the spot, and showing strong Zeeman effect.

2. Rowland's line 4982.994, for which he gives no origin. Identified by Datta.

3. Rowland 4978.732. Shows, like the last, a conspicuous Zeeman effect. Clearly separated from the iron line 4978.785 which is erroneously identified by Datta as the sodium line.

4. Rowland 4668.749. Shows Zeeman effect. Identified by Datta.

5. Masked by the chromium line 4664.965 (Rowland).

6. A faint line, visible only in the spot, and showing conspicuous Zeeman effect. Measured by Wilson (unpublished) 4497.900 on Rowland's scale. Datta identifies this with Rowland 4497.842, a titanium line which is clearly separated.

7. Datta identifies this with Rowland 4494.356 (00) which is not strengthened in the spot, and is probably not the sodium line. No trace of the latter could be seen. The character of the foregoing lines, and their strong intensification in the spots, support their identification as sodium lines. It is very difficult to get these lines sharp in the laboratory, and Datta's measures, though much superior to earlier ones, demanded long exposures.

8. Datta identifies as Rowland 5153.848 (000). This is a band line showing no Zeeman effect.

9. Datta identifies as 5149.267 (000) Rowland C. This is very little strengthened in the spot and shows no Zeeman effect. No trace of the sodium lines could be found in this vicinity.

10. Practically coincident with a strong atmospheric line in the tail of the A band, but identified by Meggers by means of the sun's rotation. The intensification of this line in the spot spectrum and the Zeeman effect are conspicuous in spite of this blending, which has been allowed for in the estimates of intensity.

11. Identification by Rowland and Datta confirmed.

12. Wave-lengths from Saunders. These lines are abnormally faint in the arc spectrum. Datta identifies as Rowland 6965.320 (000 N) which shows no Zeeman effect and 6926.290 (0000) which is invisible both in sun and spot on the Mount Wilson plates.

13. Identified by Datta as 5832.490 (000) and 5812.942 (0000). These lines are too faint to be visible on the Mount Wilson plates, either in sun or spot.

14 Typical spot lines, diffuse and showing strong Zeeman effect, and greatly resembling the lithium line at λ 6708. Measured by the writer, the first on one plate, the second on two. Probable error of measurement about ±0.01 A. One of the Zeeman components of 7947.63 is clearly separated from the atmospheric line at 7947.766 (Meggers). The other is blended with it.

15. These lines, which are the first pair of the principal series, lie beyond the limits of the region so far photographed at Mount Wilson, and attempts to secure plates showing the spot spectrum in this region have not yet been successful. They are not present in the solar spectrum (Meggers). The absence of the second pair of this series might have been anticipated.

16. This relatively narrow pair is strong in the arc, but does not belong to the known series. There are no strong lines of the subordinate series of caesium in favorable positions for investigation.

International units and Rowland's values have been reduced to this standard with the aid of a correction-curve which was kindly furnished by St. John.

The fourth and fifth columns give the intensity of the lines in sun and spot. The values in the former are taken from Rowland or Meggers; the latter, for the lines previously observed, from Adams or King. For lines newly observed, estimates have been made on the original plates, as nearly as possible upon the same scale as that used by Rowland or Meggers. Cases in which a line is certainly invisible are denoted by "abs." The sixth column gives the authority for the data concerning the spot spectrum (including measures of wave-length when the line does not appear in the spectrum of the photosphere), and the last provides references to the notes which follow.

These results may be summarized as follows:

Sodium is represented in the sun by the principal, diffuse, and sharp series, and all its lines are much strengthened in the spot spectrum. Some of Datta's identifications of faint lines have been confirmed and others modified. The absence of the pair λλ 5153, 5149 in both sun and spot is remarkable, since the following and fainter pair of the series appears to be present.

Potassium is represented by the principal series only. Its lines are greatly strengthened in the spots. Datta's identifications of faint solar lines as belonging to the subordinate series of this element are not confirmed.

Lithium shows in the spot spectrum alone, and only through the leading line of the principal series.

Rubidium, previously undetected in the sun, is definitely proved to be present by the appearance of both members of the leading pair of the principal series in the spot spectrum.

The corresponding lines of caesium lie far in the infra-red, and satisfactory photographs of the spot spectrum have not yet been obtained in this region.

The alkaline earths (for which the ionization potentials are likewise known) are of special interest, because the fundamental members 1s–2p, of the series of enhanced lines, absorbed by the ionized atoms, lie within the accessibie portion of the solar spectrum

TABLE II

LINES OF ALKALINE EARTHS IN SUN-SPOTS

ELEMENTS	WAVE-LENGTH	INTENSITY IN		NOTES
		Sun	Spot	
Mg				
1S–2P	2852.13	....	....	Out of reach
1S–$2P_2$	4571.11	5	7	1
2P–4D	5528.47	8	8	1
2P–5D	4703.07	10	10	1
2P–6D	4351.94	5	4	1
2P–4S	5711.13	6	6	1
2p–3s	5183.62	30	30	1
	5172.68	20	22	1
	5167.33	15	17	1
2p–4d	3838.28	25	....	
	3832.31	15	....	7
	3829.36	10	....	
Mg+				
1s–2p	2802.70	....	....	Out of reach
	2795.52	....	....	
Ca				
1S–2P	4226.73	20	25	2
1S–$2p_2$	6572.78	1	10	3
2P–3D	7326.10	2	5	4
2P–4D	5188.85	3	4	4
2P–4S	5512.98	4	5	4
2P–5S	4847.29	0	1	4
3D–4F	4878.13	3	3	4
3D–2P	6717.19	5	8	4
2p–4d	4556.61	2	4	2
	4555.88	3	5	2
	4554.77	5	7	2
	4535.67	4	6	2
	4534.95	5	7	2
	4525.43	4	6	2
2p–2s	6162.18	15	25	2
	6122.22	10	20	2
	6102.72	9	20	2
3d–4f	4585.92 }	4	6	4
	4585.87 }	....	....	
	4581.41	4	6	4
	4578.57	3	6	4
Ca+				
1s–2p	3968.08	700	700	3
	3933.68	1000	1000	3
2p–3d	8662.42	15	....	
	8542.48	16	....	
	8498.32	12	....	
2p–2s	3736.92	5	....	7
	3706.03	6	....	7
Sr				
1S–2P	4607.35	1	3	4
1S–$2p_2$	6892.36	abs	abs	4
2p–3s	7070.7	abs	abs	4
	6878.8	abs	abs	4
	6791.4	abs	abs	4

TABLE II—*Continued*

Elements	Wave-Length	Intensity in		Notes
		Sun	Spot	
Sr				
2p–4d	4971.68	abs	abs	4
	4967.94	....	....	5
	4962.28	000	00	4
	4876.06	abs	abs	4
	4872.49	abs	000	4
	4852.06	abs	abs	4
Sr+				
1s–2p	4215.50	8	8	2
	4077.73	5	5	2
2p–4d	10915.0	....	....	
	10328.3	....	....	Out of reach
	10038.7	....	....	Out of reach
2p–2s	4305.44	(3)	(5)	5
	4161.79	1	00	2
Ba				
1S–2P	5535.53	abs	abs	6
1S–2p$_2$	7911.36	abs	abs	4
Ba+				
1s–2p	4934.07	7	7	4
	4554.04	8	10	4
2p–4d	4166.01	0	0	4
	4130.65	2	2	4
	3891.83	....	....	5
2p–2s	4899.97	(2)	(2)	5
	4524.95	0	0	4
Zn				
1S–2P	2139.33	....	....	Out of reach
1S–2p$_2$	3075.90	1	....	7, 8
2P–3D	6362.35	1	0	9
2p–2s	4810.54	3	0	4
	4722.16	3	0	4
	4680.14	1	00	4
2p–4d	3346.02	0	....	7
	3345.58	1	....	7
	3345.12	2	....	7
	3303.37	....	....	5
	3303.59	1	....	7
	3282.33	....	....	5

NOTES

1. Adams, *Mt. Wilson Contr.*, No. 40, p. 20; *Astrophysical Journal*, **30**, 105, 1909.
2. Adams, *Mt. Wilson Contr.*, No. 22; *Astrophysical Journal*, **27**, 45–55, 1908.
3. Adams, *Mt. Wilson Contr.*, No. 40, p. 7; *Astrophysical Journal*, **30**, 93, 1900.
4. From examination of the map of the sun-spot spectrum or of original plates for wave-lengths greater than 6600. Many of these lines have previously been studied at Mount Wilson, but they have been re-examined because the later plates are probably better.
5. Masked by other lines.
6. This line (according to the accurate measures of Schultz (*Zeit. für Wiss. Phot.*, **11**, 209, 1912) lies at 5535.755 on Rowland's scale, and falls in a very confused region between the iron line 5535.644 (intensity 2) and the line 5535.778 (intensity 0), for which Rowland gives no origin. Between these two there is a faint line which is confined to the spot, in which it is of intensity 0 and shows Zeeman effect. It was measured and found to be at 5535.703. There is also a faint band line close by showing no Zeeman effect, but nothing which can be identified as the barium line. It is either absent, or masked by 5535.778.
7. Too far to the violet to show changes in the spot spectrum.
8. Rowland's line 3076.002, for which he gives no origin. Kayser and Runge find 3075.99 in the arc; Exner and Haschek, 3076.02.
9. But little weakened in the photographic map. Weakening confirmed on an original negative. Zeeman effect stronger over penumbra of spot than over umbra. May be blended with a band line. These are numerous in this region.

(except for magnesium) which is not known to be the case for any other elements. They are also noteworthy for possessing two radiation potentials, corresponding to the shift of an electron from its normal position in the neutral atom to the position corresponding to the limits of the subordinate series of single lines and of triplets.

These lines afford the most delicate tests for the presence of the ionized or neutral atoms of these elements. Their behavior in spots is indicated in Table II. Various other lines of these elements and the observable lines of zinc are included.

This table exhibits the well-known fact that the strongest lines of the alkaline earths (except magnesium) are enhanced lines.

The series of calcium and magnesium, both of triplets and of single lines, are conspicuous in the solar spectrum, and only some of the more prominent lines are given in the table. The calcium lines are considerably strengthened in the spot spectrum; those of magnesium are not, with one exception.

In the case of strontium, only the strongest lines of the neutral atom appear in the sun; these are very faint, but are intensified in spots, while not one of the strong low-temperature lines of barium appears either in the sun or the spots. This has been confirmed by examining a number of those which did not belong to known series and are therefore not given in the table.

3. APPLICATION OF THE THEORY OF IONIZATION TO THESE DATA

The ionization potentials of a number of elements of astrophysical importance are as follows:

	Volts		Volts		Volts
Caesium.........	3.81	Barium........	5.12	Ba+...........	9.86
Rubidium........	4.16	Strontium......	5.67	Sr+...........	10.70
Potassium........	4.32	Calcium........	6.08	Ca+..........	11.86
Sodium..........	5.11	Magnesium.....	7.65	Mg+..........	15.02
Lithium.........	5.37	Zinc...........	9.4	Zn+...........	18.20
Hydrogen........	13.54	Helium.........	25.2	He+............	53.4

The last column gives the potentials corresponding to the additional energy required to remove a second electron after the first is already gone.

We may now proceed to calculate the percentages of the atoms of various elements which are neutral, singly-ionized, and doubly-ionized, in a gaseous mixture at the temperature of the reversing layer and of a sun-spot—which we will take in round numbers as 6000° and 4000° respectively—and at various pressures.

Since the pressure in the solar atmosphere is unknown within very wide limits (except that it is probably small) we may save trouble by computing for assigned values of the "effective pressure" P_1, for sodium, using equations (2) and (7). The difference between the effective pressure and the true pressure will be much less than the range of uncertainty of the latter. We may then find the percentages of ionization of other elements by (5) or (11).

The results are given in Table III. Neutral atoms are denoted as usual by Ca; singly-ionized, by Ca+; and doubly-ionized, by Ca++ (taking calcium as an example). The percentage of atoms in the highest stage of ionization for each element is not given, except for hydrogen, since it can easily be found by subtracting the sum of the others from 100, and also because atoms of the elements given in the table, when in these states, absorb no known lines in the visible spectrum.

It should be remembered that the equations from which these tables have been calculated are based upon certain assumptions, as yet unverified, namely, that the chemical constant for the electron may be derived by an extrapolation of the Sackur-Tetrode relation (which gives this constant as a function of the atomic weight of an element) to the electron, considered as having an atomic weight of 0.00055, and also that the chemical constant is the same for the neutral and ionized atoms of any element.[1] An error in the former assumption could be corrected by multiplying all the tabular pressures by a constant factor; one in the second, by multiplying the pressure for each element by an appropriate factor before entering the table.

What is more important, the tabular numbers depend on the assumption that temperature alone is effective in producing ionization. This is certainly not the case in the solar atmosphere, where the absorption of radiation, though it does not completely ionize the absorbing atoms, must undoubtedly get them into a state in which ionization by some other stimulus becomes easier.[1] This should operate to increase the ionization in the reversing layer to a considerable degree.

---

[1] See Saha, *Philosophical Magazine*, 40, 479, 1920.

TABLE III

PERCENTAGES OF NEUTRAL AND IONIZED ATOMS

ELEMENT	*P* IN ATMOSPHERES						
	1	10^{-1}	10^{-2}	10^{-3}	10^{-4}	10^{-5}	10^{-6}
	Reversing Layer—Temperature 6000° C.						
Cs......	22.6	6.1	0.87	0.09	0.01	0.001	0.0001
Rb......	37.2	12.3	1.7	0.18	0.02	0.002	0.0002
K.......	44.7	14.8	2.2	0.19	0.02	0.002	0.0002
Na......	79.3	44.4	9.6	1.1	0.11	0.011	0.0011
Li.......	86.1	57.0	15.0	1.9	0.19	0.019	0.002
Ba......	79.1	45.0	9.7	1.1	0.10	0.005	0.0001
Ba+....	10.9	55.0	90.2	98.0	91.3	48.3	9.6
Sr.......	91.7	70.2	23.8	3.2	0.3	0.03	0.001
Sr+.....	8.3	29.8	76.2	96.4	97.9	84.6	35.8
Ca......	96.1	84.0	41.0	6.8	0.7	0.07	0.007
Ca+....	3.9	16.0	59.0	93.2	99.1	98.0	83.6
Mg.....	99.8	99.1	93.5	60.4	13.2	1.5	0.15
Mg+....	0.2	0.9	6.5	29.6	86.8	98.5	99.8
Zn......	99.99	99.96	99.7	96.9	75.6	23.7	3.1
Zn+....	0.01	0.04	0.3	3.1	24.4	76.3	96.9
H+.....	2×10^{-6}	1×10^{-5}	8×10^{-5}	8×10^{-4}	0.008	0.08	0.76
	Sun-Spot—Temperature 4000° C.						
Cs......	54.9	27.0	9.3	2.2	0.30	0.032	0.003
Rb......	77.0	50.0	21.9	5.7	0.83	0.089	0.009
K.......	84.2	61.5	30.9	8.8	1.3	0.14	0.014
Na......	98.1	94.1	81.5	48.9	11.6	1.37	0.14
Li.......	99.2	97.1	90.3	66.9	21.8	2.95	0.29
Ba......	98.2	94.1	81.8	49.5	11.8	1.42	0.14
Ba+....	1.8	5.9	18.2	50.5	88.2	98.58	99.86
Sr.......	99.63	98.76	95.8	82.9	40.0	6.6	0.72
Sr+.....	0.37	1.24	4.2	17.1	60.0	93.4	99.28
Ca......	99.89	99.62	98.7	94.1	68.5	18.7	2.3
Ca+....	0.11	0.38	1.3	5.9	31.5	71.3	97.7
Mg.....	99.999	99.996	99.975	99.93	99.52	95.6	69.0
Mg+....	0.001	0.004	0.025	0.07	0.48	4.4	31.0
Zn......	100.00	100.00	100.00	100.00	99.995	99.95	99.51
Zn+....	1.3×10^{-5}	4.3×10^{-5}	1.6×10^{-4}	7.2×10^{-4}	0.005	0.05	0.49
H.+....	4.7×10^{-11}	1.6×10^{-10}	5.7×10^{-10}	2.6×10^{-9}	1.9×10^{-8}	1.8×10^{-7}	1.8×10^{-6}

In applying these results to the interpretation of the spot spectrum, it is probably safe to work on the assumption that the more abundant elements in the solar atmosphere are present in amounts much greater than is necessary to produce strong lines and that, for the principal lines of these elements (at least) the absorption is substantially "saturated" so that a considerable change in the amount of element would produce little change in these lines, except in the strength of the wings. It is also important to remember that, according to modern theory, the atoms of a given element, in their normal state, are ready to absorb certain fundamental lines (those of the principal series, denoted by 1s–2p, etc., above) while, in order that they may absorb other lines (such as those of the subordinate series) they must first have absorbed energy enough to shift the electrons within them to some other definite state, less stable than the normal one. Saha, who has discussed this matter in detail, states that the relative numbers of atoms which are in condition to absorb lines of these various groups probably depend upon the temperature alone—high temperature favoring the absorption of the subordinate lines. It is obvious that "high" temperature must here be a relative term, the scale for any element being roughly proportional to the temperature at which ionization becomes large.

---

[1] The existence of such an effect for iodine has been experimentally proved by Smythe and Compton (*Physical Review*, 16, 501, 1920). Its importance in the solar atmosphere was suggested to the writer, in conversation, by Dr. Lindblad.

The main features of the behavior of the lines of the alkali metals in spots, as Saha has shown, may be accounted for by the relative ease of ionization, sodium being considerably ionized, potassium still more, and rubidium completely so, except in spots. But the fact that lithium, like rubidium, appears only in the spots, cannot be explained on the basis of ionization potentials alone, for it is harder to ionize than sodium, and the percentage of neutral atoms should be greater.

A solution may be found in the probable difference in the relative abundance of the elements. Sodium and potassium are among the most abundant of terrestrial metals, being present in the earth's crust in nearly equal amount (each about 2 per cent of the whole). Lithium is relatively rare on the earth, and, if the proportion present in the solar atmosphere is sufficiently small, it may well be that the number of neutral atoms which remain is insufficient to produce perceptible absorption lines, except in the spots, where the ionization is less. Among the far more numerous sodium atoms the number which escape ionization, though a smaller percentage of the whole, is so great that there are enough of them in a condition to absorb the subordinate series fairly strongly, and the principal series heavily. In potassium the percentage of neutral atoms is much less, and only the lines of the principal series appear, with moderate intensity, but much strengthened in the spots.

It remains somewhat puzzling, however, why rubidium, which is much easier to ionize than lithium, should show nearly the same behavior in the spot spectrum. According to Table III the percentage of neutral rubidium atoms should be less than one-tenth as great as in the case of lithium. The increase in this percentage in spots is great enough for both elements to account for the appearance of their lines there, and not on the disk, provided that we assume that the pressure in the region where the lines are absorbed is 0.01 atmospheres or less (which seems reasonable). But it is hard to see why the rubidium lines should appear at all, unless it is considerably more abundant in the sun than lithium is, which does not at all seem to be the situation on the earth.

Passing to the alkaline earths we find improved opportunities. While the ionized atoms of the alkali metals give no recognized lines in the visible spectrum, those of calcium and its congeners are unique in that the fundamental lines of the ionized atom lie within the region accessible to astrophysics. The great importance of these lines (H and K of calcium and λλ 4078, 4215 of strontium) is thus explained. They enable us to detect the ionization of these easily ionized atoms as soon as it occurs. The ionized atom of calcium is at once capable of absorbing the H and K lines.

From Table III it appears that, under the pressures which probably prevail in the reversing layer, the greater part of the calcium is in the singly-ionized condition.

H and K, therefore, are the lines which the atoms of one of the most abundant constituents of the solar atmosphere absorb most powerfully, when in that state in which under solar conditions they are most likely to occur. There are no other lines in the visible spectrum, so far as known, for which these three maximal conditions are all satisfied.

It is not surprising, therefore, that they are exceptionally conspicuous, and that few other lines play so important a part throughout almost the whole of the sequence of stellar spectra. A great deal of the calcium must be ionized, even in the spots, and this, coupled with the fact that the absorption in the H and K lines is probably far more than saturated, makes it easy to understand why these lines are not perceptibly weakened in the spots. The same remark applies, with even greater force, to the corresponding enhanced lines of strontium and barium.

Magnesium should also be considerably ionized in the reversing layer; but the only line by which we can detect the presence of ionized magnesium (λ 4481) is absorbed only by atoms which have undergone two internal changes subsequent to ionization, corresponding to the shifting of an electron from its normal position to the states denoted symbolically by 2p and 3d, and demanding the absorption of large amounts of energy. The temperature of the reversing layer, compared with that at which a considerable percentage of these $Mg+$ atoms would lose a second electron, is undoubtedly low. Hence very few such atoms indeed should be in a state to absorb λ 4481, and it is not surprising that it is excessively faint in the solar spectrum, if it appears at all, or that it becomes conspicuous only in the hotter stars.

If the earth's atmosphere transmitted light of short enough wave-length, we would probably find that the fundamental pair of enhanced magnesium lines near λ 2800 were rivals of H and K in intensity and astrophysical importance.

The very strong infra-red lines of calcium at λλ 8498, 8542, 8662, belong to the diffuse series and represent a stage of excitation intermediate between H and K and λ 4481. King[1] has found that they cannot be produced in the furnace, at temperatures at which H and K appear strongly. It may safely be predicted that they are weakened in the spot spectrum, and the matter will be investigated when suitable photographs can be obtained. The corresponding group for strontium is hopelessly far in the infra-red; but the leading pair of the sharp series of enhanced lines is accessible. One line is concealed by a blend; the other is greatly weakened in spots.

---

[1] *Mt. Wilson Contr.*, No. 150; *Astrophysical Journal*, 48, 13, 1918.

For barium, which is easier to ionize a second time, the enhanced lines of the diffuse series are not perceptibly weakened in spots.

The behavior of the lines due to the neutral atoms is also in accordance with this theory. Beginning with zinc, which has the highest ionization potential, we find that the prominent triplet in the blue is greatly weakened in spots, and the line in the red is also weakened, though to a less degree. These lines belong to the sharp series of triplets and the diffuse series of single lines, both of which are absorbed by atoms in which the electron has been shifted one step from its normal position (to 2p or 2P). Measured by a scale appropriate to the zinc atom, the temperature of the photosphere must be low and that of the spots very low; hence the weakening of these subordinate lines is just what should be expected.

It is of interest to note that the lines of hydrogen, which also belong to a subordinate series and to an element for which the ionization potential is high, are much weakened in the spot spectrum.[1]

The lines of magnesium are very little affected in spots. In this case the effects of higher excitation and greater ionization at the higher temperature of the reversing layer appear very nearly to balance one another except in the case of λ 4571, which is a characteristic low-temperature line, and is the easiest of all magnesium lines to excite in the laboratory.[2] This line, as might be expected, is strengthened in the spots, but only to a moderate degree.

For calcium, all the important lines of the neutral atom are strengthened in spots, indicating that the controlling factor is the diminution of ionization at the lower temperature, which increases the number of neutral atoms. Where allowance is made for the general increase toward the red of the degree to which lines are affected in spots, it appears that the strengthening is greatest for the lines absorbed by atoms in which the electron is in the normal state, 1S; less for those of the subordinate series, in which the electron starts from the state 2P (for single lines) or 2p (for triplets); and least of all for those of the Bergmann or combination series in which it starts from 3D or 3d. According to Saha[1] the ratio of the number of atoms which are in any one of these states to the number which are in the preceding stage should increase with the temperature. Hence the effect of the diminished number of neutral atoms in the hotter regions is almost neutralized for the lines of the "outer" series (3D–4F and 3D–2P) and increased for the fundamental lines (1S–2P), and 1S–2p.[2] The first of these, λ 4227, is so far to the violet that the effect in spots is not conspicuous, though great for a line in this region. This is very prominent in the cooler stars. The second, λ 6573, is one of the most remarkable of all sun-spot lines. It is an exact analogue of λ 4571 of magnesium, which likewise shows the greatest strengthening of any line of the element to which it belongs.

---

[1] Adams, *Mt. Wilson Contr.*, No. 40, p. 10; *Astrophysical Journal*, **30**, 95, 1909.

[2] Foote and Mohler, *Philosophical Magazine*, **37**, 40, 1919.

For strontium, the ionization is still greater, and the amount of the element present in the solar atmosphere probably much less, if we may judge by the earth's crust, in which strontium and barium are much rarer than calcium and magnesium. It is not surprising, therefore, that only the strongest lines of the neutral atom appear in the solar spectrum, or that these should be strengthened in the spots, especially the fundamental line λ 4607. λ 6892, which is analogous to λ 6573 of calcium, is absent even in the spot spectrum.

The probable reason for this is that the temperature, even in the spots, is high on the scale which it is necessary to use for the neutral strontium atom, and that, under this high excitation, the proportion of atoms in which the electron undergoes the corresponding change is small.

For barium the final stage appears to have been reached. The lines of the neutral atom do not appear at all either in the spectrum of the sun or of the spots. Even the fundamental line 1S–2P (λ 5535) is gone. This can be explained only on the assumption that barium is completely ionized in the sun, leaving not a trace of the neutral atoms, for the element is abundant enough, as is shown by the strength of its enhanced lines.

---

[1] *Proceedings of the Royal Society*, A, **99**, 142, 1921.

From the qualitative standpoint this explanation is quite satisfactory, but a quantitative study brings out difficulties. The ionization potentials for sodium and barium, as determined from their spectral series, should be practically identical. Hence, by the theory developed above, the atoms of both should be ionized to the same degree. But the direct spectroscopic evidence indicates that barium is ionized to a much greater extent than sodium. The absence of the flame lines even in spots, and the fact that the enhanced lines of the diffuse series are not sensibly weakened, would indicate a decidedly lower ionization potential both for Ba and Ba+.

A similar discrepancy, though less marked, exists in the case of strontium.

As the theory of the subject is still in an early stage of development, these facts may be taken as the results of an experiment performed by nature upon a grand scale, which may be used in improving our theories; but speculation as to the exact form of this improvement would at present be premature.

4. GENERAL COMMENTS

The data detailed above cover all the cases in which elements, for which the ionization potentials and spectral series are known, possess lines of any notable strength within the region in which the sun-spot spectrum can be satisfactorily investigated. It is evident that they are all in striking agreement with Dr. Saha's theory of ionization and that they confirm it in a very conclusive fashion, both in the matters in regard to which he has made predictions, and in various others which are here discussed for the first time.

There are many other elements whose lines show conspicuous changes in the spots; but no data are at present available regarding the ionization potentials. Most of these elements have spectra rich in lines, for which the series relations are known very incompletely or not at all.

The behavior of these lines in the spot spectrum,[1] coupled with that in the furnace, arc, and spark, makes it possible to arrange them in a decidedly definite order.

---

[1] Adams, *Mt. Wilson Contr.*, No. 40, pp. 6–26; *Astrophysical Journal*, **30**, 91–111, 1909.

A few of the elements already discussed are added for comparison. Lines which are relatively strong at the lowest temperatures (King's Class I) are called flame lines for brevity.

Calcium.—All lines strong in sun. Flame lines much strengthened in spots. Arc lines considerably strengthened in spots. Enhanced lines produced at medium temperature in furnace,[2] very strong in arc, and not weakened in spots.

Scandium.[1]—Flame lines very faint or absent in sun, greatly strengthened in spots. Arc lines faint in sun, much strengthened in spots. Enhanced lines produced in furnace at high temperature, strong in arc, and slightly weakened in spots.

Titanium[2] *and Vanadium*[3]—These elements behave in a very similar fashion, both in the laboratory and in sun-spots. The furnace lines are greatly strengthened in spots and the arc lines strengthened. Practically all the arc lines may be obtained in the furnace. The enhanced lines can be obtained in the furnace only with great difficulty, and are weakened in spots.

Iron,[4] *manganese,*[5] *and chromium*[3].—These again are similar in their behavior. The flame lines are strengthened in the spot spectrum, the arc lines little affected, and the enhanced lines much weakened. Many arc lines are very hard to produce in the furnace, and the enhanced lines cannot be produced there at all, and are faint in the arc. The percentage of lines which are strengthened in the spot spectrum is greater for chromium than for manganese and still smaller in the case of iron.

Cobalt and nickel.[6]—The number of lines weakened in spots is nearly as great as that of the strengthened lines in the case of cobalt, and much greater for nickel. The number of arc lines which cannot be obtained in the furnace is greater for nickel than for cobalt.

---

[1] King, *Mt. Wilson Contr.*, No. 214; *Astrophysical Journal*, **54**, 28, 1921.

[2] King, *Mt. Wilson Contr.*, No. 76; *Astrophysical Journal*, **39**, 139, 1914.

[3] King, *Mt. Wilson Contr.*, No. 94; *Astrophysical Journal*, **41**, 86, 1915.

[4] King, *Mt. Wilson Contr.*, No. 66; *Astrophysical Journal*, **37**, 239, 1913.

[5] King, *Mt. Wilson Contr.*, No. 198; *Astrophysical Journal*, **53**, 133, 1921.

[6] King, *Mt. Wilson Contr.*, No. 108; *Astrophysical Journal*, **42**, 344, 1915.

A number of cobalt lines and one nickel line described by Lockyer as enhanced appear in the furnace, but King gives good reason for supposing that these are not enhanced lines of the regular type.

Copper reveals itself in the sun by the first pair of the principal series, λλ 3274, 3247, which are produced when mere traces of the metal are present. They are recorded as of intensity 10 by Rowland, yet no trace of the lines of the subordinate series appears; although λλ 5782, 5700 are furnace lines.[1] The limit of the principal series, 1605 A,[2] corresponds to an ionization potential of 7.7 volts.

For *zinc*, as has already been noted, the arc lines are fairly strong in the sun, but greatly weakened in the spots. Finally, at the end of the series, come *silicon*, for which all the solar lines are greatly weakened in spots, and *oxygen*. The triplet of the latter in the extreme red, λλ 7772–7775, is faintly present in the arc, stronger in the spark, and, though fairly strong in the sun, is completely obliterated in the spot spectrum.[3] Yet the series relations of these lines, which belong to a combination series 2s–mp, show conclusively that they are produced by the neutral atom.

Part of the effect observed in the spots, however, is probably due to the formation of titanium oxide, which must diminish considerably the amount of free oxygen in the solar atmosphere.

The foregoing list shows a definite sequence in the behavior of the elements, alike in furnace, arc, and sun-spots, which suggests strongly that we have to do with a series in which the ionization potential steadily increases (except perhaps in the case of copper, for which the data are very meager). It cannot be a matter of chance that the list, from calcium, and, indeed, from potassium to zinc in order of increasing difficulty of spectroscopic excitation, is a complete list of the intervening elements in the order of their atomic numbers. It appears highly probable that in this region at least the ionization potential increases with the interval in the periodic table which separates the element from the preceding noble gas. Whether this relation holds good more generally cannot be known until further data become available, but it is of interest to note that silicon and oxygen, which are evidently decidedly hard to ionize, fit in very well, since, in the known cases, the ionization potential falls steadily for corresponding elements in each successive period of the periodic table.

---

[1] King, *Astrophysical Journal*, 21, 250, 1904.

[2] Konen, *Das Leuchten der Gase* (Braunschweig, 1913), p. 146.

[3] Merrill, *Mt. Wilson Contr.*, No. 183, p. 7; *Astrophysical Journal*, 51, 247, 1920.

The behavior in the spot spectrum of most of the elements in this list is intermediate between that of calcium and that of zinc. It may therefore be surmised that the ionization potentials for these metals lie between six and nine volts, as Saha has suggested[1] without specifying his reasons.

One further comment may be made on the foregoing. It is evident that the enhanced lines of an easily ionized element, such as barium or calcium, may be produced with a weaker excitation than the arc lines of an element of difficult ionization, such as zinc or silicon; the intervening elements present all degrees intermediate between these extremes. The mere fact that an enhanced line appears in a given spectrum is therefore not a proof that the temperature, for example, is high on an absolute scale, but only that it is high relative to the scale appropriate for the element in question. It would probably be fairly safe to assume that temperatures proportional to the various ionization potentials produce similar effects upon different atoms, but further knowledge is necessary before we can be sure of this.

The principles of the ionization theory will evidently be of great importance throughout the whole field of astrophysics, and Dr. Saha[2] has made an application of the highest interest to the question of the physical meaning of the sequence of stellar spectra. The writer hopes to present a discussion of many features of this problem at some time in the not distant future.

The possibilities of the new method appear to be very great. To utilize it fully, years of work will be required to study the behavior of the elements mentioned above and of others, in the stars, in laboratory spectra, and by the direct measurement of ionization, but the prospect of increase of our knowledge, both of atoms and of stars, as a result of such researches, makes it urgently desirable that they should be carried out.

---

[1] *Philosophical Magazine*, **40**, 822, 1920.

[2] *Proceedings of the Royal Society*, A, **99**, 135, 1921.

Mount Wilson Observatory
August 1, 1921

Note.—An admirable summary of the theory of ionization by Mr. E. A. Milne, in the *Observatory* for September (44, 261, 1921), has appeared since the completion of the foregoing discussion. He points out the influence of the free electrons resulting from the dissociation of easily ionized atoms in diminishing the ionization of other atoms, and gives the correct equation for second-stage ionization. Section 1 of the present paper was prepared independently and carries the analysis somewhat further, so that it appears sufficient to call attention here to Mr. Milne's prior publication.

THE
ASTROPHYSICAL JOURNAL
AN INTERNATIONAL REVIEW OF SPECTROSCOPY
AND ASTRONOMICAL PHYSICS

VOLUME LV APRIL 1922 NUMBER 3

THE EXCITATION OF THE ENHANCED SPECTRA OF SODIUM AND POTASSIUM IN A LOW VOLTAGE ARC[1]

By PAUL D. FOOTE, W. F. MEGGERS, and F. L. MOHLER

ABSTRACT

Variation of the spectra of Na and K with energy of electronic impact.—The quantum theory, as developed by Bohr and Sommerfeld, leads to the conclusions: that all the arc lines are emitted by neutral atoms and should be excited at voltages above the ionization voltages, 5.1 for Na and 4.3 for K, and that the enhanced lines are emitted by singly ionized atoms and, in the case of the alkalies, should be excited when (*b*) the valence electron is knocked out of its orbit, after (*a*) an electron from the outer ring (*L*-ring for Na, *M*-ring for K) has been removed. In the case of Na, the ionization (*a*) requires 35 volts if it is complete, giving $L\alpha$-radiation, or 30 volts if the electron goes to the $L\alpha$ orbit; and since the displacement (*b*) requires a maximum of 14 volts, the enhanced spectrum for Na should be excited by two successive impacts at 35 volts and possibly at 30 volts, and the highest frequency should correspond to about 14 volts. The corresponding figures for K are: 23 volts for the excitation of the $M\alpha$-radiation, possibly 20 volts for $M\alpha$ and the enhanced spectrum, and 11 volts for the energy corresponding to the highest frequency. Since these conclusions contradict the general belief that high potentials are necessary to excite these enhanced spectra, a series of *spectrograms* was made, with a large quartz spectrograph, of the light excited by low voltage electrons in a special cylindrical tube in which the distance between the central tungsten filament, which supplied the electrons, and the accelerating grid was so short and the vapor pressure used was so low (0.1 to 0.2 mm of Hg) that practically all the electrons entered the force-free space surrounding the grid, with the same energy. The voltages used varied from 3.5 to 5000 for Na, and from 3.5 to 40 for K. The results completely verify the theoretical conclusions. Tables and photographs are given which clearly show the *three-stage development* in the spectra of these elements: (1) Single pair stage: 2.1 to 5.1 volts (Na); 1.6 to 4.3 volts (K). (2) Arc spectrum stage: 5.1 to 30 volts (Na); 4.3 to 20 volts (K). (3) Enhanced spectrum stage: above 30 volts (Na); above 20 volts (K). With a heavy current (1 ampere) at 7 volts in K, the pair λ 4642 becomes very prominent, though it has the

---

[1] Published by permission of S. W. Stratton, Director, Bureau of Standards.

series notation ($1s-3d$). Its presence cannot be due to incipient Stark effect, and accordingly furnishes an exception to the principle of selection as applied by Sommerfeld. The *wave-lengths in I.A. and the series notations*, when known, are given for 250 lines.

The quantum theory of spectra attributes enhanced lines to ionized atoms. In the case of simply ionized helium the Bohr theory, as generalized by Sommerfeld, not only gives the correct wave-lengths of the observed enhanced lines, but their fine structure as well.

In applying the quantum theory to heavier atoms certain simplifying assumptions must be made in order to carry out the mathematical analysis. Thus Sommerfeld[1] considers the case where the atom has one electron in an outer orbit and where as an approximation the other electrons may be treated as though lying in a circular coplanar orbit. These electrons, as far as their action on the outer orbit is concerned, may be assumed equivalent to a ring of electricity of equal total charge.

Evaluating the kinetic energy of the outer electron, and applying the integral $\int pdq=nh$ both in respect to azimuth and radius as independent variables, in accordance with the quantum theory, Sommerfeld derives the following expression for the variable term of a spectral series, identical in form with the familiar Ritz equation:

$$(m,a)=\frac{N(E/e)^2}{[n_a+n_r+a-\alpha(m,a)]^2} \qquad (1)$$

where E is the excess in charge of the core over that of the ring, n_a the azimuthal and n_r the radial quantum numbers characterizing the outer orbits, and a and α constants which are approximately proportional to E and are functions of n_a but not of n_r.

An atom of an alkali metal has one electron in its outer orbit while that of an alkali earth has two, accounting for the monovalent and bivalent properties respectively For the neutral atom of an alkali metal $(E/e)^2=1$, and equation (1) represents the variable terms of the arc spectra. If one of the outer electrons of an atom of an alkali earth is permanently removed, that is, if the atom is simply ionized, equation (1) likewise applies except that $(E/e)^2=4$ and the values of a and α are altered in a definite manner.

---

[1] *Atombau* (2d ed.), p. 506.

Hence if the enhanced spectrum of magnesium is due to the simply ionized atom, it should resemble the arc spectrum of sodium. Such is the case, even to the appearance approximately of $4N$ and $a^* = 1.5\,a$ instead of N and a in the spectral formulae representing the enhanced lines.[1] A similar relation exists between the spectra of the other elements of these two groups. From the above and further considerations Kossel and Sommerfeld[2] concluded that in so far as enhanced spectra arise in *simply* ionized atoms the enhanced spectrum of any element should resemble the arc spectrum of the element of next lower atomic number. Very likely higher types of enhanced spectra may be produced by atoms which have suffered multiple ionization.

Now, as is well recognized, the complete arc spectrum of any monatomic vapor may be excited by electronic collision with a normal atom when the energy of the impacting electron is eV, where V is the ionization potential. Furthermore for all monatomic vapors not exhibiting metastable modifications[3] the voltage V is related to the highest convergence frequency ν of the arc spectrum by the quantum condition $ch\nu = eV$. The highest frequency in the arc spectra of the alkali earths is $1S$ and of the alkali metals $1s$, corresponding to ionization potentials from 4 to 10 volts. Similarly in the enhanced spectrum of an alkali earth, the highest frequency is $1\mathfrak{S}$, and accordingly at the corresponding voltage V^* the complete simple enhanced spectrum should be excited. We have verified this experimentally for magnesium.[4]

---

[1] Sommerfeld neglected to consider the shrinkage of the ring when the number of electrons in the ring is maintained constant while the charge on the core is increased by one unit. If this is taken into account we find for sodium and potassium $a^* = 1.5\,a$ instead of $a^* = 2\,a$ given by Sommerfeld. The former relation is well satisfied if we assign values of 1, 2, 3, etc., instead of 1.5, 2.5, etc., to m in the (ms) terms. Cf. *Journal of the Optical Society of America and Review of Scientific Instruments*, January, 1922.

[2] *Verh. d. Phys. Ges.*, 21, 240, 1919.

[3] From spectroscopic and other considerations there appear to be two modifications of helium, possibly one in which the two electrons are in crossed orbits and the other in which the orbits are coplanar. In polyatomic vapors the ionization potential may involve the work of dissociation in addition to the ionization of one or more atoms.

[4] The enhanced spectrum of magnesium is produced by electronic impact of 14.97 volts corresponding to the wave-number $1\mathfrak{S} = 121{,}270$, in which case the impact occurs with a simply ionized atom, with the result that the second valence electron

These voltages again are all small, of the order of 10 to 20 volts for the elements in this group of the periodic table.

The simple enhanced spectra of the alkali metals should resemble the complicated arc spectra of the rare gases. Since only recently attempts to correlate the latter in series[1] have been successful it is not surprising that nothing is known of series relations in the enhanced spectra of the alkali metals.

It is possible, however, to estimate roughly the voltages at which the enhanced spectra of sodium and potassium should be excited. In the case of sodium we have the K-ring with 2 electrons, the L-ring with 8 electrons, and the outer ring with the valence electron. There are two direct ways in which the atom may be ionized. First, the valence electron may be removed requiring an amount of work equivalent to 5.1 volts;[2] then a second collision of X volts may expel an electron from the L-ring. Secondly, an electron may be ejected from the L-ring requiring 35 volts,[3] followed by a collision of Y volts expelling the valence electron. X must be somewhat greater than 35, but, since the orbit of the valence electron is much larger than that of the L-ring, it is not evident that the repulsive force of the outer electron can materially assist in the expulsion of an electron from the L-ring. Hence to doubly ionize sodium by the first method should require electronic impacts of maximum value $La+\delta La$ volts where δLa is a small quantity and δ is a factor. The total work of double ionization is then $(La+\delta La+5)$ volts. In the second method of ionization accordingly $Y=\delta La+5$ which must be less than 35 volts. Hence by the first method of excitation, the enhanced spectrum of sodium should appear at $35(1+\delta)$ volts and by the second method at 35 volts, and in both cases should accompany its L-radiation.

---

is removed. This paper, *Phil. Mag.*, **42**, 1002, December, 1921, is of especial interest since De Gramont and Hemsalech, *C.R.*, **173**, 505, 1921, have just published a report of experiments in which they found that a potential gradient of 500 volts/cm was required to excite the enhanced spectrum of magnesium.

[1] For example, neon: Paschen, *Annalen der Physik*, **60**, 405, 1919.

[2] Tate and Foote, *Phil. Mag.*, **36**, 64, 1918.

[3] Mohler and Foote, "Soft X-Rays from Arcs in Vapors," *Journal of the Optical Society of America*, **5**, 328, 1921. For sodium $La=35$ volts.

Similar considerations for potassium show that its enhanced spectrum should be excited by direct impact at about 20 volts and should accompany its *M*-radiation.[1]

It is possible to arrive at an approximate estimate of the value of δ in the foregoing formulae. After expulsion of an electron from the *L*-ring, the ring shrinks, and provided the valence electron does not fall into the *L*-ring—a condition which would curtail the emission of the enhanced lines—it assumes a new orbit where the angular momentum is unity. This orbit represents a higher energy level. Following Sommerfeld's method of derivation except that two coplanar rings of electrons are assumed and their shrinkage is given consideration, we find for sodium and potassium:

$$\left.\begin{array}{ll} a^*=\dfrac{2(r+x)}{r+y}a & x=\dfrac{112}{(9-s_7)^2} \\ r=\dfrac{Z-9}{(Z-s_{Z-9})^2} & y=\dfrac{128}{(9-s_8)^2} \end{array}\right\} \qquad (2)$$

where a^* and a are the values of a in the Ritz formula, equation (1), for the enhanced and arc lines respectively, Z the atomic number and s_n the nuclear defect of the ring, i.e., effect of the interaction of the electrons. To an approximation, omitting terms beyond a in the Ritz formula:

$$V=\frac{13\cdot 55}{(1+a)^2} \qquad (3)$$

$$V^*=\frac{54}{(1+a^*)^2} \qquad (4)$$

where V is the simple ionization potential and V^* the voltage corresponding to the work required to remove the valence electron from its new quantized orbit, after the removal of an electron from the *L*-ring. V^* accordingly corresponds to the highest convergence frequency in the spark spectrum.

Equation (2) gives $a^*=1.5\,a$ for sodium and potassium. Computing a from equation (3) and the known ionization potentials, we obtain from (4) the following:

$V^*=14$ for sodium

$V^*=11.5$ for potassium.

---

[1] Mohler and Foote, *loc. cit.*, observed two *M*-limits for potassium one at 20 volts and one at 23 volts.

The total work of double ionization is accordingly:

$$\begin{aligned}\text{Total work} = La + V^* &= 35 + 14 = 49 \text{ volts for sodium}\\ &= 23 + 11 = 34 \text{ volts for potassium.}\end{aligned}$$

Hence for sodium

$$\begin{aligned}La + \delta La + V &= 49\\ \delta La &= 9\\ \delta &= 0.3.\end{aligned}$$

Similarly for potassium

$$\delta = 0.3.$$

These values of δ confirm the estimates made above from more qualitative considerations. It is of interest to note that in sodium, for example, although it requires but 14 volts to excite the enhanced spectrum, this spectrum cannot be produced at this voltage since as a prerequisite the displacement of an electron from the *L*-ring is essential, which necessitates electronic impact of higher energy value. This is in contradistinction to the phenomena observed in the case of the alkali earths. Here the removal of the valence electron at the simple ionization potential leaves the atom in the fundamental state for the emission of enhanced lines (just as the normal, unexcited atom is in the fundamental state for the emission of arc lines) and further impacts of even less energy value are sufficient to excite the "single-line" *enhanced* spectrum $1\mathfrak{S} - 2\mathfrak{P}$. However, with the alkalis, the simple ionization does not leave the atom in the fundamental state for the emission of enhanced lines, but rather in the state for the emission and even absorption of $L\alpha$ and other X-ray lines.

In the X-ray spectra of elements of higher atomic number it is known that $K\alpha$ cannot be produced except when the limit Ka is reached, under which condition all *K*-lines appear simultaneously. If a similar condition held for the *L*-radiation of sodium, it would be impossible to excite the enhanced spectrum below the voltage corresponding to the limit $La = 35$ volts. However, although a single-line X-ray spectrum has never been observed, it must be a possible phenomenon for elements of low atomic number where the ring concerned is the outermost "saturated" orbit. Hence $La = 35 - V = 30$ volts might be produced at 30 volts instead of at

La=35. Such being the case the enhanced spectrum could be excited by successive impact at the voltage corresponding to *La*, the first impact (or equivalent absorption of radiation) displacing the electron to the *La* orbit, where a second impact is more than sufficient to doubly ionize. Still further, Mohler and Foote observed a new series of critical potentials of lower value than *La*, for several of the elements of low atomic number, which may be related to the *L*-series. If so, the enhanced spectra of sodium might be excited by successive impact in an arc at the voltage corresponding to this new limit.

In view of the fact that heretofore all investigators have employed and believed requisite an exciting field of many thousand volts for the production of the enhanced spectra of sodium and potassium, the low values above estimated necessitated experimental verification.

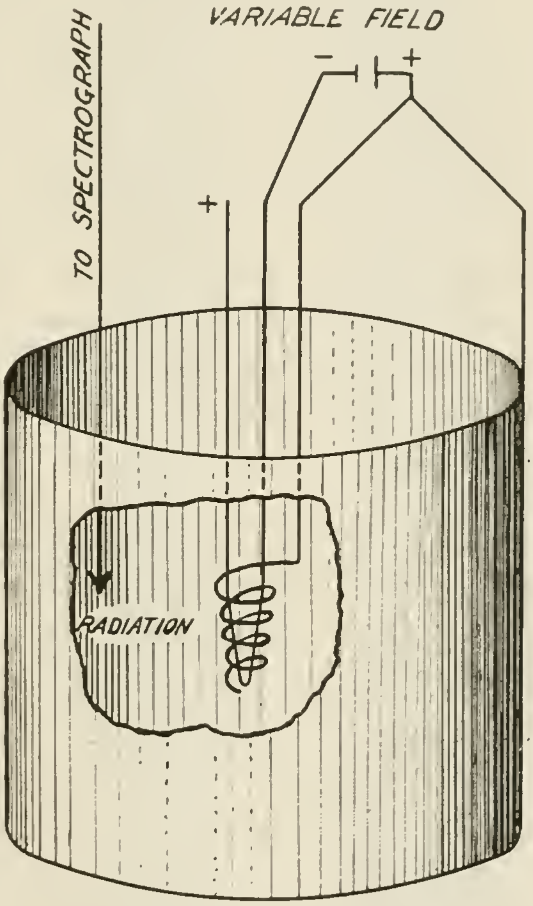

FIG. 1.—Discharge tube. The electrons attain the full velocity of the impressed field.

The form of the discharge tube employed is illustrated by Figure 1. Its novelty consists in the use of a grid (helical coil) mounted extremely close to a tungsten hot wire cathode (or in some cases an equipotential surface heated inside) and in metallic contact with a concentric hollow cyclinder of relatively large diameter. By properly regulating the temperature of the sodium or potassium vapor, a vapor pressure may be maintained for which relatively few electronic-atomic collisions occur over the short accelerating field between the cathode and grid, and the majority of electrons falling into the large force-free space between the grid and plate have, at the instant of collision, a velocity corresponding to the impressed field. The gas pressure registered by the gage was less than 0.001 mm of mercury and the vapor pressure was of the order 0.1 to 0.2 mm of mercury.

The arcs at various exciting voltages were photographed with a large Hilger Type C quartz-spectrograph. Plate II shows the results for sodium and Plate III for potassium. Ordinary Seed 30 plates were used for all exposures except the 3.5 volt potassium arc in which case the plate was made red sensitive by bathing in dicyanin. The pair λ 7699–7664, although present in the spectra at the higher voltages, was not recorded by the "blue-sensitive" plates used for the other spectrograms. The lines on all the plates were carefully measured and reduced to wave-lengths by the method of the Hartmann-Cornu interpolation formula, using lines of a mercury comparison spectrum and known arc and spark lines as normals.

SODIUM

Plate II shows the three successive stages in the sodium spectrum. The single-line spectrum consisting of the pair D_1 and D_2 is excited above the resonance potential, 2.1 volts, and below the ionization potential 5.1 volts. From 5.1 volts to about 30 volts the arc lines appear alone. At 30 volts numerous spark lines begin to appear while above 40 volts the complete enhanced spectrum is excited.

The lower spectrogram was obtained by connecting a small 5000-volt transformer between the hot wire and grid. The vapor was too rare for a discharge to pass except when the cathode was heated to give a copious emission of electrons. Since the effective resistance of the discharge gap must have been small compared to the impedance of the transformer, the actual applied voltage was undoubtedly much less than 5000 volts. Very few enhanced lines not excited at 50 volts were observed in this source but their intensity was considerably greater. All of the spectrograms of sodium were made with a very narrow slit and much of the detail readily apparent on the negatives is obscured in the reproduction. On this account reference must be made to Table I for a more careful consideration of the excitation of the enhanced lines, and verification of the foregoing statements.

PLATE II

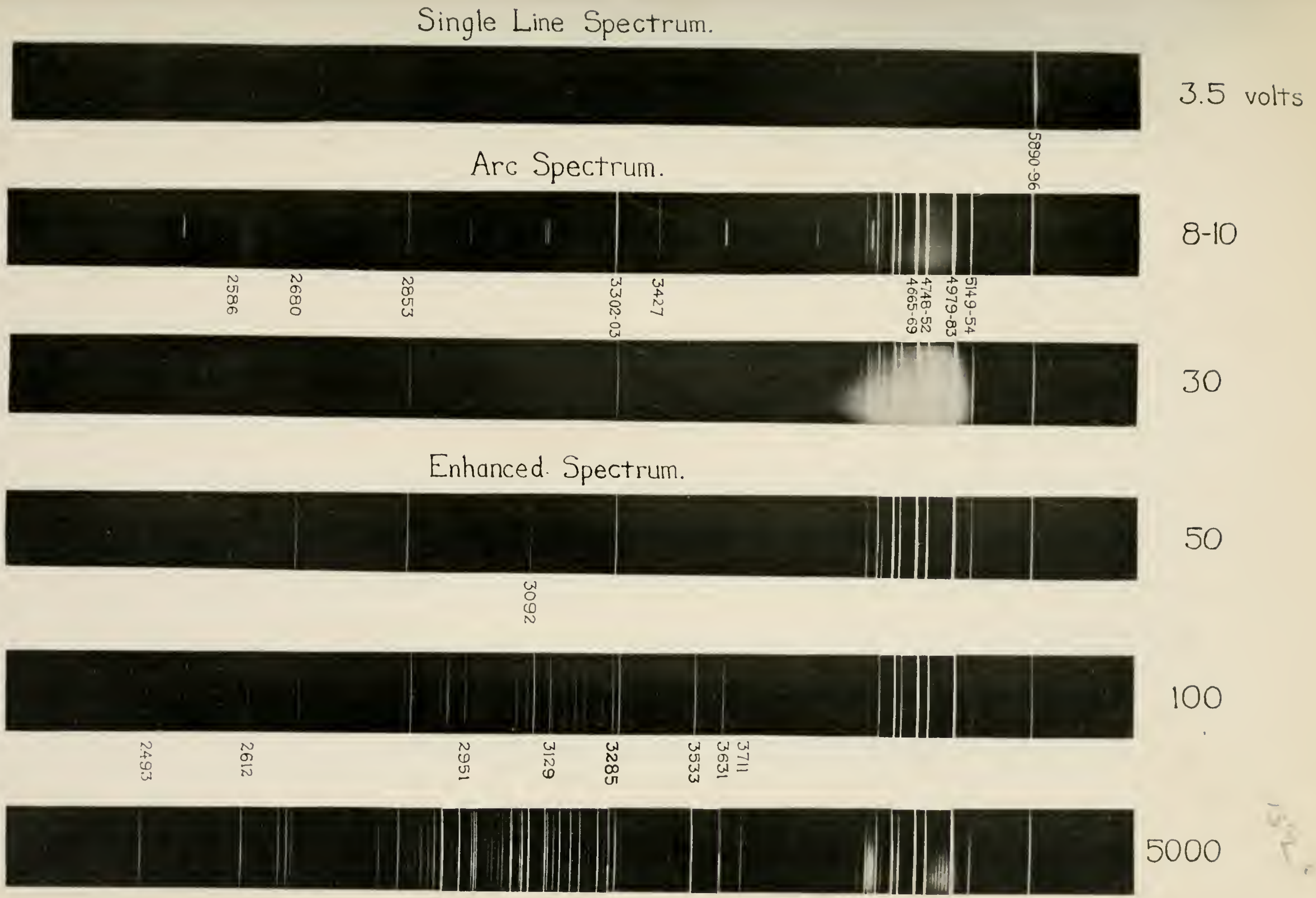

Spectra of Sodium

TABLE I

SPECTRA OF SODIUM

Wave-Length	5000 Volts	100 Volts	50 Volts	20 Volts	10 Volts	Notation for Arc Lines
2318.0	1—	1—	...	...	...	...
2475.51	...	...	...	...	1—	$1s-10p_{1,2}$
90.61	...	...	...	1—	1—	$1s-9p_{1,2}$
2493.36	4	4	2	1	...	...
2497.3	2	...	...	1	...	...
2506.40	1	1	...	...	...	...
12.14	1—	1—	1—	1	1	$1s-8p_{1,2}$
15.50	1	1	...	...	...	...
31.54	3	2	1	...	...	...
43.80	1—	1	1	2	2	$1s-7p_{1,2}$
86.27	1	1	...	...	...	...
93.89	1	2	2	3	3	$1s-6p_{1,2}$
2595.0	1—	1—	...	...	...	...
2612.18	5	4	1	1	...	...
61.72	4	3	1	1	...	...
71.94	5	3	1	1	...	...
78.2	3	2	1	...	...	...
2680.37	1	3	3	4	3	$1s-5p_{1,2}$
2809.76	4	3	1	1	...	...
18.5	1	1	...	...	...	...
30.0	1	1	...	...	...	...
39.36	1	1	...	...	...	...
41.99	6	4	2	...	...	...
52.80	3	4	4	5	5	$1s-4p_{1,2}$
59.56	3	2	1	...	...	...
61.2	1—	1—	...	...	...	...
70.89 } 71.39 }	3	2	1	...	...	...
73.0	1—	1—	...	...	...	...
81.33	4	3	2	1	...	...
86.46	3	2	1	...	...	...
2894.15	4	3	1	1	...	...
2901.39	3	2	1	...	...	...
05.16	6	4	3	2	...	...
17.76	4	3	3	2	...	...
19.46	3	3	2	1	...	...
21.14	3	3	2	1	...	...
23.65	2	2	1	...	...	...
31.44	1—	1—	...	...	...	...
34.42	1	1	...	...	...	...
2938.11	3	2	1	...	...	...
45.83	2	1	...	...	...	...
47.51	3	2	1	...	...	...
51.53	8	5	2	2	...	...
60.10	1	1	1—	...	...	...

TABLE I—*Continued*

Wave-Length	5000 Volts	100 Volts	50 Volts	30 Volts	10 Volts	Notation for Arc Lines
71.1	1—	1—	....	....	....	....
75.20	5	3	2	1	....	....
77.52	1	1	....	....	....	....
79.92	7	4	2	1	....	....
2984.44	6	4	2	1	....	....
3007.71	2	2	1	....	....	....
15.81	3	2	1	1	....	....
29.70	3	3	1	1	....	....
37.29	4	3	1	1	....	....
50.48	3	1	1—	....	....	
53.97	4	3	1	....	....	....
56.34	7	5	3	2	....	....
61.75	1—	....	....	....	....	....
64.8	2	1	1—	....	....	....
66.74	2	2	1—	....	....	....
74.63	4	3	1	1	....	....
78.51	5	4	3	....	....	....
80.58	2	2	....	....	....	....
92.91	12	8	6	3	....	....
3104.6	2	2	1	....	....	....
07.6	1—	1—	....	....	....	....
24.63	2	2	1—	....	....	....
29.57	7	5	4	2	....	....
35.65	5	4	3	1	....	....
38.11	1	1	....	....	....	....
46.07	1	2	....	....	....	....
49.48	5	4	3	1	....	....
64.11	7	5	2	2	....	....
75.38	1	1	....	....	....	....
79.19	3	2	....	....	....	....
3189.94	7	5	3	2	....	....
3212.42	7	5	3	2	....	....
16.5	1	1	....	....	....	....
26.1	2	2	....	....	....	....
35.1	3	2	1—	....	....	....
51.3	1	1	....	....	....	....
58.36	7	4	2	1	....	....
60.4	1	1	....	....	....	....
74.27	3	2	....	....	....	....
85.76	8	7	4	2	....	....
3302.33	3	4	3	4	10	$1s-3p_1$
02.93	2	3	2	3	8	$1s-3p_2$
05.2	2	2	....	....	....	....
18.2	3	2	....	....	....	....
20.7	1—	1	....	....	....	....

TABLE I—*Continued*

Wave-Length	5000 Volts	100 Volts	50 Volts	30 Volts	10 Volts	Notation for Arc Lines
3327.9	3	2	....	....	....	....
3400.2	1−	1−	....	....	....	....
27.1	1	1	1	4	7	$1s-3d$
3462.58	2	2	1	....	....	....
3533.08	12	8	5	3	....	....
3631.31	5	4	2	1	....	....
34.3	1	1	....	....	....	....
3711.15	4	3	1	....	....	....
3745.6	1−	1−	....	....	....	....
3881.0	1	1−	....	....	....	....
4124.0	2	2	....	....	....	....
4141.0	....	....	....	....	1−, *d*	$2p-18d$
48.0	....	....	....	....	1−, *d*	$2p-17d$
56.0	....	....	....	....	1−, *d*	$2p-16d$
65.0	....	....	....	....	1−	$2p_2-15d$
67.8	....	....	....	....	1−	$2p_1-15d$
77.4	....	....	....	....	1−	$2p_2-14d$
80.2	....	1−	....	1−	1	$2p_1-14d$
92.6	....	....	....	....	1−	$2p_2-13d$
4195.5	....	1	....	1	1	$2p_1-13d$
4212.4	....	....	....	....	1	$2p_2-12d$
15.4	....	1−	1−	1	2−	$2p_1-12d$
22.8	....	....	....	....	1, *d*	$2p-11s$
38.6	1−	....	....	....	1	$2p_2-11d$
41.6	1−	1	1	1	2	$2p_1-11d$
49.4	....	....	....	....	1−	$2p_2-10s$
52.4	....	1−	1−	1−	1−	$2p_1-10s$
73.2	1−	....	....	....	2	$2p_2-10d$
4276.3	1	1	1	1	3	$2p_1-10d$
87.5	....	1−	1−	1−	1−	$2p_2-9s$
4290.6	1−	1	1	1	1	$2p_1-9s$
4321.1	1	1	1	1	3	$2p_2-9d$
24.3	2	2	2	2	4	$2p_1-9d$
41.3	....	1	1	1	1	$2p_2-8s$
44.5	1	1	1	1	2	$2p_1-8s$
90.14	3	2	2	2	4	$2p_2-8d$
4393.45	4	3	3	3	6	$2p_1-8d$
4419.94	1−	1	1	1	2−	$2p_2-7s$
23.31	1	2−	2−	2−	3	$2p_1-7s$
94.266	5	4	4	4	5	$2p_2-7d$
97.724	6	5	5	5	7	$2p_1-7d$
4541.671	2	1	1	1	2	$2p_2-6s$
4545.218	3	2	2	2	4	$2p_1-6s$
4664.858	7	4	4	4	7	$2p_2-6d$
4668.597	9	6	6	6	9	$2p_1-6d$

TABLE I—*Continued*

Wave-Length	5000 Volts	100 Volts	50 Volts	30 Volts	10 Volts	Notation for Arc Lines
4748.016	4	2	2	2	3	$2p_2 - 5s$
4751.891	5	2	2	2	4	$2p_1 - 5s$
4978.608	9	6	6	7	9	$2p_2 - 5d$
4982.864	10	8	8	9	10	$2p_1 - 5d$
5149.090	2	2	2	2	5	$2p_2 - 4s$
5153.645	3	3	3	3	6	$2p_1 - 4s$
5682.675	1	1	1	1	2	$2p_2 - 4d$
5688.222	1	1	1	1	2	$2p_1 - 4d$
5889.965	15	10	10	8	15	$1s - 2p_1$
5895.932	10	8	8	6	10	$1s - 2p_2$
6154.214	1	....	....	....	1	$2p_2 - 3s$
6160.725	1	....	....	....	1	$2p_1 - 3s$

DATA FOR TABLE I

Exposure Number	Volts	Milliamperes	Time of Exposure
23	5000	....	4 hours
16	100	150	30 min.
17	50	40–140	50 min.
21	30	65	65 min.
20	8–10	2000	125 min.

The wave-lengths in Table I are in international angstrom units. The spark lines given by Schillinger,[1] having been corrected from the Rowland to the international scale, are represented by six significant figures while the values for the arc lines from λ 4390.14 to λ 6160.725 are those recently measured by Datta.[2] The remaining values are given to four or five figures and are the means of several determinations from the quartz prism spectrograms; they are probably not in error by more than one unit in the last place. Approximate values for the wave-lengths of many subordinate series lines were given by Zickendraht[3] and our numbers are in fair agreement with his for the higher terms.

It is seen from this table that the critical voltage for the excitation of the enhanced spectrum of sodium is about 30 volts, in the neighborhood of the values for *La* and *La*.

---

[1] Schillinger, *Sitzungsberichte der Kais. Akad. d. Wiss.*, **118**, 605, 1909.

[2] Datta, *Proc. Roy. Soc.* (A), **99**, 69, 1921.

[3] *Annalen der Physik*, **31**, 233, 1910.

PLATE III

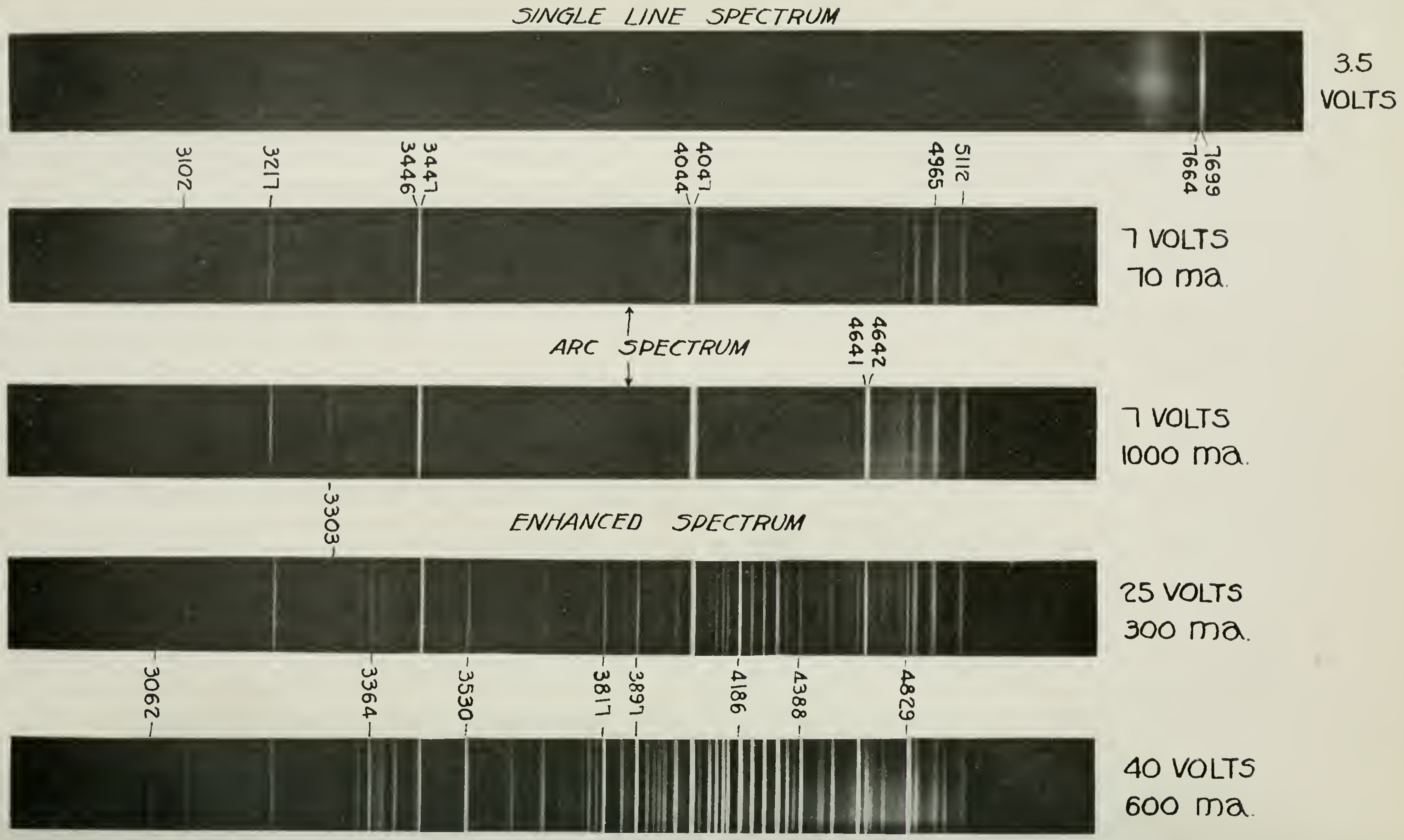

Spectra of Potassium

POTASSIUM

Plate III shows the three stages in the development of the potassium spectrum. Table II contains the wave-lengths and estimated intensities of the lines at various exciting voltages from 3.5 to 40 volts. From the resonance potential, 1.6 volts, to the ionization potential, 4.3 volts, the single-line spectrum is emitted, consisting of the pair λ 7699 and λ 7664. Above the ionization potential the complete arc spectrum is excited while in the neighborhood of 20 volts (viz., near *Ma* and *Ma*) the enhanced lines are prominent. A wider slit was used for this series of exposures than for sodium and the results are therefore more favorable for reproduction although less advantageous for precise measurement of wave-lengths. The values for the wave-lengths in Table II are compiled from the measurements of Shillinger and Datta. Only the stronger spark lines are listed, as these serve sufficiently to show how the intensity of the enhanced spectrum rapidly increases when the critical voltage is exceeded. A great many faint spark lines were observed in addition to those given by Shillinger, a fact also noted by McLennan,[1] but their wave-lengths are not known with sufficient accuracy to justify publication.

While the main issue of the present paper concerns the excitation of enhanced spectra, the second and third spectrograms of Plate III, showing the arc spectrum of potassium, are of considerable interest. Both of these exposures were made at 7 volts, the only difference being that an ionization current of 70 milliamperes was employed for the upper spectrogram and 1000 milliamperes for the lower. In the latter case the pair λ 4642 and λ 4641 appears as one of the most prominent lines in the spectrum. This pair has the notation $\nu = 1s - 3d$, representing an interorbital transition where the change in azimuthal quantum number is according to Sommerfeld two units.[2] It accordingly contradicts the Bohr or Rubinowicz principles of selection as applied by Sommerfeld to spectra of the non-hydrogenic type While the line

---

[1] *Proc. Roy. Soc.* (A), 100, 182, 1921.

[2] In a paper by Foote, Mohler, and Meggers, to appear in the *Philosophical Magazine*, this and other exceptions to the principle of selection are considered in more detail.

TABLE II

Spectra of Potassium

Wave-Length	40 Volts	25 Volts	20 Volts	16 Volts	6 Volts	3.5 Volts	Notation for Arc Lines
2992.21	....	....	....	1—	1—	....	$1s-8p_{1,2}$
3034.8	....	1	1	1	1	....	$1s-7p_{1,2}$
3062.44	3	2	2—	....	....	....	....
3102.03 02.25	1	3	3	2	2	....	$1s-6p_1$ $1s-6p_2$
05.31	2	1	1	....	....	....	....
29.39	1	1—	1—	....	....	....	....
69.89	1	1	1—	....	....	....	....
87.91	2	1	1	....	....	....	....
3190.42	2	1	1	....	....	....	....
3201.96	1	1—	....	....	....	....	....
17.01 17.50	4	5	5	5	5	....	$1s-5p_1$ $1s-5p_2$
20.80	1	1	....	....	....	....	....
3290.93	2	2—	1	....	....	....	....
3312.63	2	1	1—	....	....	....	....
45.7	5	4	2	....	....	....	....
58.33	1	1	....	....	....	....	....
60.16	1	1	....	....	....	....	....
63.25 64.56	6	5	3	....	....	....	....
73.84	2	2	1	....	....	....	....
80.97	2	2	1	....	....	....	....
3385.24	2	2	1	....	....	....	....
3404.57	5	4	2	....	....	....	....
22.26	1	1	1—	....	....	....	....
33.61	1	1—	....	....	....	....	....
40.36	2	1	1—	....	....	....	....
46.722 3447.701	5	6	8	8	8	....	$1s-4p_1$ $1s-4p_2$
3530.83	5	5	3	1	....	....	....
3609.26	2	1	1—	....	....	....	....
18.43	3	2	1	....	....	....	....
68.91	1	....	....	....	....	....	....
76.01	2	1	....	....	....	....	....
3681.52	4	3	2	....	....	....	....
3716.51	1	1	....	....	....	....	....
21.93	1	1	....	....	....	....	....
39.13	1	1—	....	....	....	....	....
44.62	1—	1—	....	....	....	....	....
67.37	3	2	1	....	....	....	....
3783.19	4	3	2	1—	....	....	....
3800.60	3	2	1	....	....	....	....
17,99	6	5	3	1	....	....	....
61.87	4	2	1	....	....	....	....

TABLE II—*Continued*

Wave-Length	40 Volts	25 Volts	20 Volts	16 Volts	6 Volts	3.5 Volts	Notation for Arc Lines
73.78.....	1	1	....	....	....	....	....
3878.31.....	1	....	....	....	....	....	....
3897.86.....	7	5	3	2	....	....	....
3923.65.....	3	2	1—	....	....	....	....
42.86.....	3	2	1	....	....	....	....
55.27.....	3	2	1	....	....	....	....
66.75.....	2	1	1	....	....	....	....
72.61.....	2	1	....	....	....	....	....
3995.08.....	2	1	....	....	....	....	....
4001.20.....	5	3	2	1	....	....	....
12.07.....	1	....	....	....	....	....	....
25.20.....	1	....	....	....	....	....	....
44.140....	6	7	8	8	8	....	$1s-3p_1$
47.201....	4	5	6	6	6	....	$1s-3p_2$
57.95.....	3	1	....	....	....	....	....
4114.96.....	5	4	2	1—	....	....	....
34.72.....	5	4	2	1	....	....	....
49.24.....	5	4	2	1	....	....	....
4186.23.....	9	8	4	2	....	....	....
4210.21.....	2	1	1	....	....	....	....
22.99.....	5	4	2	1	....	....	....
25.60.....	5	4	2	1	....	....	....
4263.32.....	6	5	2	1	....	....	....
4305.01.....	5	4	2	1	....	....	....
09.08.....	7	6	4	2—	....	....	....
4388.13.....	5	4	2	1	....	....	....
4423.72.....	1	....	....	....	....	....	....
4466.66.....	2	....	....	....	....	....	....
4505.39.....	4	2	1	....	....	....	....
4608.31.....	4	2	....	....	....	....	....
41.585 42.172 ...	2	4	5	4	8	....	$1s-3d'$ $1s-3d$
4659.58.....	1	....	....	....	....	....	....
4741.6.....	....	....	....	....	1—	....	$2p_2-10s$
45.58.....	....	1	1	1	1	....	$2p_2-11d$
54.5.....	....	....	....	....	1—	....	$2p_1-10s$
59.31.....	....	1	1	1	1	....	$2p_1-11d$
86.89.....	....	1	1	1	1	....	$2p_2-\ 9s$
4791.08.....	....	1	1	1	2	....	$2p_2-10d$
4800.16.....	....	1	....	1	1	....	$2p_1-\ 9s$
05.19.....	....	1	1	1	2	....	$2p_1-10d$
28.99.....	5	3	2	....	....	....	....
49.88.....	1—	1	1	2	2	....	$2p_2-\ 8s$
56.03.....	1	2	2	3	3	....	$2p_2-\ 9d$
63.61.....	1—	1	1	2	2	....	$2p_1-\ 8s$

TABLE II—*Continued*

Wave-Length	40 Volts	25 Volts	20 Volts	16 Volts	6 Volts	3.5 Volts	Notation for Arc Lines
4869.70.....	1	2	2	3	3	....	$2p_1-9d$
4941.964....	1	2	2	2	2	....	$2p_2-7s$
43.02.....	1	....	....	....	....	....	....
50.816....	2	3	3	3	3	....	$2p_2-8d$
56.043....	1	2	2	2	2	....	$2p_1-7s$
4965.038....	2	3	3	3	3	....	$2p_1-8d$
5005.34.....	2	....	....	....	....	....	....
55.78.....	1	....	....	....	....	....	....
84.212....	2−	3−	3−	3−	4−	....	$2p_2-6s$
97.144....	2	3	3	3	4	....	$2p_2-7d$
5099.180....	2−	3−	3−	3−	4−	....	$2p_1-6s$
5112.204....	2	3	3	3	4	....	$2p_1-7d$
5323.228....	2−	3−	3−	4−	4−	....	$2p_2-5s$
39.670....	2−	3−	3−	4−	4−	....	$2p_1-5s$
42.974....	2	3	3	4	4	....	$2p_2-6d$
5359.521....	2	3	3	4	4	....	$2p_1-6d$
....	....	....	....	....	....	....	....
....	....	....	....	....	....	....	....
7664.94.....	....	....	....	....	....	6	$1s-2p_1$
7699.01.....	....	....	....	....	....	4	$1s-2p_2$

DATA FOR TABLE II

Exposure Number	Volts	Milliamperes	Time of Exposure
2.................	40	500–600	10 min.
7.................	25	0–300	32 min.
5.................	20	100–700	15 min.
8.................	16	0–500	20 min.
18.................	6	1200	15 min.
26.................	3.5	12	7 hours

is well known, its excitation has been thought to be occasioned by the presence of the electrostatic field—an incipient Stark effect.[1] However, in the present case, with the special form of discharge tube employed, the radiation was observed only in the space shielded from the applied electrostatic field—itself only 7 volts. On referring to Table I and Plate II, it will be noted that the corresponding line λ 3427 appears in sodium. Its intensity increases very rapidly as the ionization current is increased, independently of the voltage, provided this exceeds the ionization potential.

---

[1] Sommerfeld, *Annalen der Physik*, 63, 249, 1921.

The importance of this result has been pointed out in the paper referred to above, in which we suggest that the explanation may involve a reconsideration of the method whereby single azimuthal quantum numbers have been assigned to each of the s, p, b, and d terms.

The following table summarizes the values of the critical voltages characterizing the three-stage development in the spectra of sodium and potassium.

Element	Volts	Notation	Spectrum
Sodium...........	2.09	$1s-2p$	Single pair
	5.11	$1s$	Arc lines
	35–30	....	Enhanced lines and L-radiation, $La=35$, $La=30$
Potassium.........	1.60	$1s-2p$	Single pair
	4.32	$1s$	Arc lines
	$\left.\begin{matrix}23\\20\end{matrix}\right\}$	....	Enhanced lines and M-radiation

Highest frequency in enhanced spectrum: sodium = 14 volts; potassium = 11 volts. Total work of double ionization: sodium = 49 volts; potassium = 34 volts.

Bureau of Standards
December 1, 1921

THE VACUUM-SPARK SPECTRA OF THE METALS[1]

By EDNA CARTER

ABSTRACT

Vacuum-spark spectrograms of Ca, Mg, Cd, Ti and Fe were obtained *with comparison arc and spark spectra*, on portrait films, using for the most part a 20-cm concave grating spectrograph. The Fe spectrum was also photographed with a dyed film from λ 4000 to λ 6600 A. The new spectra show no striking new characteristics. In the case of Ca and also of Mg (see Plate IV), the vacuum-spark spectrum is practically identical with the spark spectrum in air; in the case of Cd (see Plate V), the arc lines are somewhat more intense; with Ti this tendency to strengthen the arc lines is even greater, and the vacuum-spark spectrum of Fe is more like the arc spectrum than the spark. In general these spectra resemble the luminescence spectra produced by cathode-ray bombardment in a high vacuum, and it is probable that the conditions of emission are very similar in the two sources.

I. INTRODUCTION

The production of a brilliant spark between electrodes very close together in a high vacuum was observed by Rowland[2] and also by Wood.[3] The nature of the discharge was studied by Loving.[4] He concludes in regard to the spectrum produced that it is characteristic of the anode, the cathode having no effect, and that it is not analogous to either the spark or the arc. The spectra which he obtained were not sufficiently intense for an exact determination of their character.

Millikan[5] developed independently a method of producing this discharge; and, by using it as a source in a vacuum spectrograph, succeeded with his co-workers in extending the spectra of various elements into the extreme ultra-violet.

It was of interest to see whether a careful study of this source would disclose any peculiarities of metallic spectra in the usual photographic region. A comparison of the vacuum-spark spectra with the arc and the spark spectra of typical metals was therefore undertaken.

---

[1] *Contributions from the Mount Wilson Observatory*, No. 219.

[2] Rowland, *Physical Papers*, p. 574.

[3] *Physical Review*, **5**, 1, 1897.

[4] *Astrophysical Journal*, **22**, 285, 1905.

[5] *Ibid.*, **52**, 47, 286, 1920; **53**, 150, 1921; *Physical Review*, **12**, 168, 1918. *Science*, **19**, 138, 1919.

2. EXPERIMENTAL METHOD

The vacuum sparks were produced in a glass bulb about 12 cm in diameter provided with a quartz window, which in the case of the more easily vaporized metals was removed to a distance of 30 cm on account of the sputtering. The iron electrodes consisted of cylinders about one cm long and one cm in diameter, tapering to blunt points. These cylinders were screwed on the ends of aluminum rods, which projected to the outside through side tubes and were sealed in with sealing wax. The iron electrode was retained as cathode throughout the experiments, while anodes of the other metals were made by wedging a piece of the metal into a hole in the end of the aluminum rod. The distance between the electrodes was about 1.5 mm in the case of iron, but it amounted to 3 or 4 mm with some of the other metals, which were largely vaporized during the exposure.

Evacuation was effected with a Langmuir diffusion pump, the mercury vapor being kept away from the discharge by a trap immersed in solid CO_2 and ether.

The discharge was produced with a large induction coil used with an electrolytic interrupter. A current of from 15 to 20 amperes was passed through the primary. To secure the necessary capacity across the secondary, four parallel plate condensers, consisting of copper plates about 56 by 61 cm separated by 5-mm glass plates, were connected in series. The whole was immersed in oil to prevent leakage.

About eight hours were required to obtain a spectrogram of iron, because of the tendency of the discharge to pass over into an ordinary gas discharge, with the liberation of gas from the electrodes, and because it was necessary to keep the sealing wax joints cool. The total duration of the spark discharge was estimated at about thirty-five minutes for iron and not more than ten minutes in the case of cadmium. The iron required a much higher potential gradient between the electrodes for the production of the spark than the other metals.

A spectrograph with concave grating of 20-cm radius and ordinary portrait films were used in obtaining most of the spectrograms. The iron spectrum was photographed in the region 4000–6600 A by using an aesculin filter and films sensitized with a Wallace three-dye solution. Fairly rich spectra of iron and titanium were obtained also with a one-meter concave grating spectrograph.

The vacuum-spark spectra of magnesium and cadmium with comparison arc and spark spectra are reproduced in Plates IV and V.

3. DISCUSSION OF RESULTS

The vacuum-spark spectra of calcium and magnesium are practically identical with the spark spectra in air.

The cadmium vacuum-spark spectrum retains arc lines in somewhat greater relative intensity than they possess in the ordinary spark. The line λ 3261 is an example. This line came out also with marked intensity in the luminescence spectrum produced by cathode-ray bombardment.[1]

Titanium shows an even greater tendency to retain the arc lines. The spectrum is plainly an enhanced one, however, as is evidenced by the brightness of the lines λλ 4164 and 4172, for example, the ratios of whose intensities in the spark and the arc, as given by Exner and Haschek, are 20:2 and 15:1, respectively.

The vacuum-spark spectrum of iron, on the other hand, seems to resemble more closely the arc spectrum. The low-temperature lines found in the arc are missing, and the lines which are stronger at the poles and in the core of the arc are relatively more intense in this source. Even in this spectrum a close examination reveals the presence of the enhanced lines, such as λλ 4508, 4515, 5018, and 5316. Hα comes out very strongly and sharply in the photographs of the iron spectrum made in this region.

The varying tendency exhibited by these different metals toward the production of enhanced lines suggests a resemblance of the vacuum-spark spectra to the luminescence spectra produced by cathode-ray bombardment in a high vacuum. It is probable that the conditions of emission are very similar in the two sources. The difficulties in the way of obtaining rich spectra are considerably less in the case of the vacuum-spark.

Mount Wilson Observatory
September 1921

---

[1] *Astrophysical Journal*, 44, 303, 1916; 49, 224, 1919.

PLATE IV

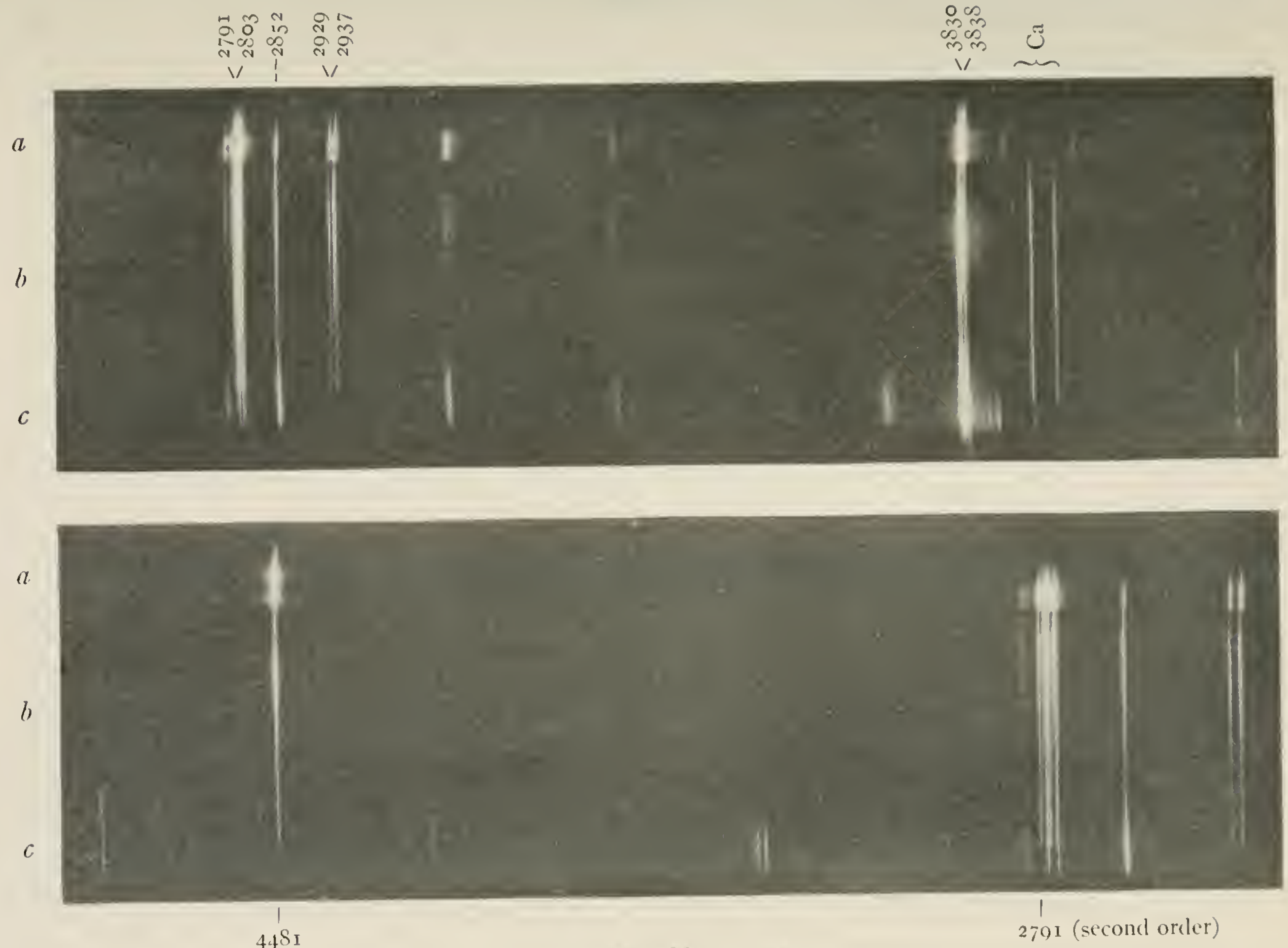

SPECTRUM OF MAGNESIUM
a Spark in air
b Vacuum-spark
c Arc

PLATE V

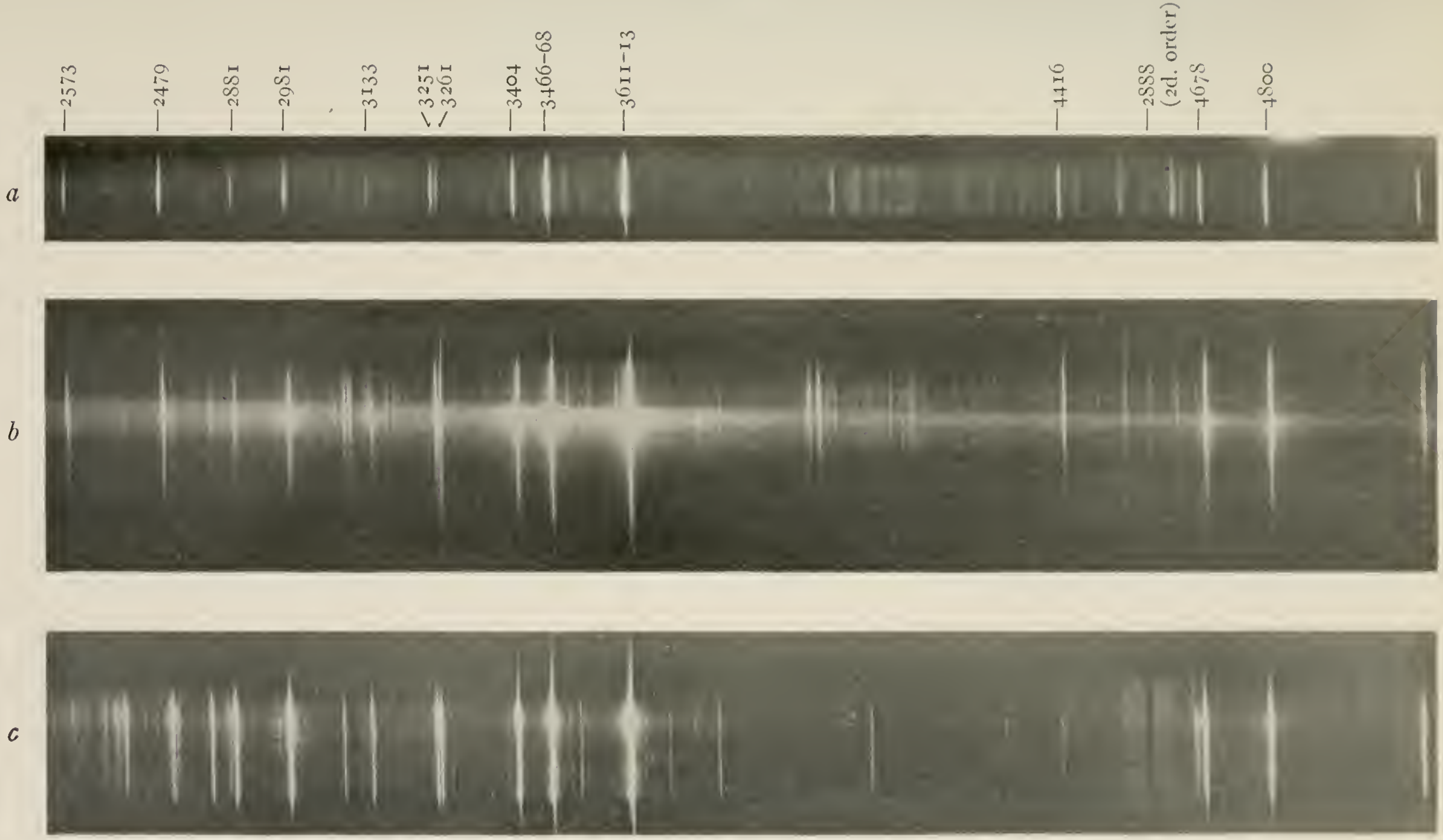

Spectrum of Cadmium

a Spark in air
b Vacuum-spark
c Arc

THE MASSES AND DENSITIES OF THE STARS[1]

By FREDERICK H. SEARES

ABSTRACT

Mean magnitudes and masses of visual binaries and dwarf stars of the different spectral types.—A statistical comparison of the absolute magnitudes (M_b) of 105 visual binaries, the hypothetical magnitudes (M_c) of these and 400 other visual binaries (computed by Jackson and Furner, assuming the combined mass, $\mu = \mu_1 + \mu_2$, of each binary to be 2), and the absolute magnitudes (M_s) of 1152 single stars (including some binaries) by Kapteyn and Adams, gives the mean difference $(\overline{M}_b - \overline{M}_c) = (\overline{M}_s - \overline{M}_c) - 0.3 \pm 0.1$ for each type; that is, $\overline{M}_b = \overline{M}_s - 0.3 \pm 0.1$. This indicates that the selection used is sufficiently homogeneous, also that the variation of the mean magnitude of binary star components with spectral type is the same as that of single stars. The values of $\overline{M}_s$ (Table IV and Fig. 1) for dwarf stars of types B0, A0, F0, G0, K0, and Ma are -1.60, $+0.70$, 2.40, 4.35, 5.90, and 9.80 respectively. The geometric mean mass for each spectral type of visual binary was next computed from the formula $\log \mu = \log 2 - 0.6\ (\overline{M}_s - 0.3 - \overline{M}_c)$. The values of μ, slightly corrected for the effect of selection as determined by a study of the binaries of known parallax, give, when multiplied by $\frac{4}{7}$ to reduce to single stars, a first approximation to the geometric mean masses of single stars along the dwarf branch of Russell's diagram, the values for types B0, A0, F0, G0, K0, and Ma, coming out 10, 6.0, 2.5, 1.0, 0.68, and 0.59, respectively, in terms of the sun's mass (Table IV). The data for visual binaries of known parallax indicate that the distribution of $\log \mu$ is approximately Gaussian and that the *dispersion in mass* is small, probably half the stars of each type having masses between 0.7 and 1.5 times the mean (Table VIII).

Mean velocity and energy of dwarf stars of different spectral types.—The mean square space-velocity corresponding to the mean magnitude was determined from the available data for each type, and these values were multiplied by the corresponding mean masses. The mean energy for each type so obtained is practically the same for all types from A0 to Ma, in spite of a 10 to 1 variation in mass (Table IX). The logarithm of the *mean kinetic energy constant* is 3.27 ± 0.036 (average deviation per type) in terms of sun's mass and km/sec., corresponding to 3.5×10^{46} ergs. The mean radial energy is also approximately constant for all except the B-type stars, which seem to be abnormal in this as in other respects. Whatever the cause may be, the distribution of energy among these stars seems to approximate equipartition.

Masses of stars as functions of magnitude and spectral type were then computed from the values of the mean velocity for each magnitude and type, assuming the mean energy independent of magnitude as well as of type (Table X). In Figure 2, curves are given showing M as a function of type for various constant values of the mass. To get more reliable data for the giants, the masses of 28 Cepheids were computed from the period, magnitude, and surface brightness of each, using a formula based on the pulsation theory (Table XVI), and Figure 2 was revised to agree with these values, giving Figure 3. If the masses computed in accordance with Eddington's theory of Cepheids (Table XIX) are adopted, a further slight revision will be necessary. The constant mass lines would be less irregular if bolometric magnitudes were used instead of visual. For the Cepheids, the probable *dispersion in mass* for a given M and type is only about 20 per cent. This result taken with the data for visual binaries indicates that in general the luminosity of a star is very closely determined by its spectral type (temperature) and its mass.

Effective temperature, color index, and surface brightness of stars of different spectral types.—The effective or black-body temperatures of the giants as determined from

---

[1] *Contributions from the Mount Wilson Observatory*, No. 226.

Wilsing's spectrophotometric measures of c/T for 199 stars, vary from 2890° for Mc to 10,500° for B0, while those of the dwarfs as determined from Mount Wilson color indices (provisional values, hitherto unpublished, also given for the giants) reduced to the same system, vary from 3330° for Ma to 6080° for F5 (Table XII). The difference between dwarfs and giants of the same type is too great to be neglected, the later-type dwarfs being considerably hotter. The surface brightness j as a function of temperature may be computed (1) from the difference between visual and bolometric magnitudes as determined by Eddington ($j=M-M_B-10 \log T+\text{const.}$) and (2) from Hertzsprung's formula derived from Planck's radiation law ($j=2.3\,(c/T)^{0.93}+\text{const.}$), both formulae giving practically the same results (Table XI). Combining these values with the temperatures of the stars of various types, we get the surface brightness as a function of spectral type, the results varying from 4.81 for $T=2890°$ to -2.28 for $T=10,500°$, expressed in magnitudes, sun $=0$ (Table XII). As a check on these values, the surface brightness of three stars, α Orionis, α Boötis, and α Scorpii, whose diameters have been determined directly by Pease, were computed and found to agree with the interpolated values within $\pm 0\overset{M}{.}2$ in each case (Table XIII).

Diameter and density of stars as a function of magnitude and spectral type were readily computed from the surface brightness, absolute magnitude, and mass (Table XIV). For dwarfs the diameter decreases from 6.8 to 0.54 (sun $=1$) and the density increases from 0.045 to 5.4 (water $=1$) as the type changes from B0 to Ma, while for giants of zero magnitude the corresponding changes of diameter and density are from 3.2 to 66 and from about 0.3 to 10^{-5}. When M is plotted as a function of type for various constant values of the density (Fig. 2), the equidensity lines are straight and nearly parallel and quite regularly spaced, so that the equation: $\log \rho=-1.22\,S+0.57\,M+1.11$, where S is the type number beginning with 0 for B0, represents the results quite closely for a wide range of density. For dwarfs of types B to F, the values agree satisfactorily with the values found by Shapley for the densities of eclipsing variables of these types. The giant part of the diagram, however, is less reliable, and is later modified in Figure 3 to agree with the values for 28 Cepheids (Table XVI) computed from their periods by the use of the theoretical formula: $\log \rho=-2 \log P+\text{const.}$ Adoption of Eddington's formula for Cepheids would lead to only a slight further modification (see Table XVII).

Relation of the observed variation of mean mass and of M with spectral type to the problem of stellar evolution.—For the dwarf branch, the decrease in mass from 10 for B0 to 0.6 for Ma may be partly, and perhaps wholly, accounted for by selection, the earlier and brighter stars being observed throughout a larger volume; further, only massive stars can attain high temperatures. The possibility that *mass may decrease with loss of energy by radiation* is also suggested, a possibility which agrees with the theory of relativity and does not necessarily conflict with Newtonian mechanics. For the giants, the observed change in M with spectral type (mass constant) is difficult to account for. Probable changes in mean atomic weight are insufficient. Changes in the opacity are doubtless involved, and likely also the source of energy, which almost certainly is not wholly gravitational and probably not independent of the time; for instance, the probable degree of ionization involves an amount of energy greater than seems to be available from gravitational forces. The intersection of equal-mass lines with the dwarf branch at large angles (Figs. 2, 3), however, does not conflict with the gravitational contraction hypothesis.

Eddington's radiative equilibrium theory of giants.—Although this involves the assumption that the ratio of the energy flow to the gravitational acceleration is constant throughout a star, whereas the ratio probably decreases considerably from center to outside surface, the calculated variation of magnitude with mass for a given spectral type is in fair agreement with observed values (Table XXII), but for a given mass the absolute magnitude is not constant as required by theory. *For Cepheids*, the theory gives the formula: $\log \rho=-2 \log P-2 \log (\gamma\alpha)^{\frac{1}{2}}+\text{const.}$, and this combined with the empirical relation, mass is proportional to radius, which Eddington's results suggest as a *condition for Cepheid variation*, gives: $M=-5 \log P+j-5 \log (\gamma\alpha)^{\frac{1}{2}}+\text{const.}$, which agrees with the observed variation of M with P for $P>2$ days, quite closely (Table XVIII and Fig. 5). This shows the consistency of Eddington's theory of Cepheids with his theory of radiative equilibrium and tends to confirm the relation of mass to radius, which is equivalent to the condition that the average heat content per unit mass is constant. Various consequences of this condition are given. The theoretical values of mass and density given by the pulsation theory are close to those indicated by Figure 3 (Table XVII).

Ionization and mean atomic mass inside stars.—Theoretical computations indicate that the temperature and pressure at various points inside a star change in such a way as to keep the degree of ionization of the same order throughout (Table XX); hence the mean atomic mass is also about constant. When we consider giant stars of constant mass but of increasing temperature, we find that while the densities change very greatly, the high degree of ionization in the earliest stages is maintained with but little change (Table XXI), so that the mean atomic mass should decrease but slowly as development proceeds.

Comparison of spectroscopic parallaxes of visual binaries with the hypothetical parallaxes of Jackson and Turner shows systematic differences for their Table II (Table III).

Information on the masses of stars has its origin in what can be learned of the masses of binary systems, spectroscopic and visual. Any discussion of spectroscopic binaries from the standpoint of mass is complicated by lack of definite information on the inclination of orbital planes, while in the case of visual binaries the lack is that of accurate knowledge of stellar distances. Approached from either standpoint, the problem, with rare exceptions, must be treated by statistical methods whose application presupposes an abundance of data. Any solution is therefore involved in some uncertainty, which is not lessened by the fact that a transfer of results thus obtained to the stars at large involves assumptions of comparability: we do not know, for example, how the mass of an average binary is related to that of an average single star of the same type and luminosity, or even that the relation is the same for all classes of stars. The uncertainty, however, is probably not great; at any rate, we can proceed only by making such assumptions.

The following discussion is based on the visual binaries. These lead to values of the masses of stars along the dwarf branch of the Russell diagram, including those of B-type spectra. The average mass decreases continuously with advancing spectral type. The combination of these results with the space velocities of large numbers of stars recently published by Adams, Strömberg, and Joy shows that the mean kinetic energy of translation of the A's and the dwarfs is approximately constant. The principle of equipartition is then used to derive values of the masses of stars of other luminosities. The distribution curves thus obtained for mass as a function of spectral type and absolute magnitude are a first approximation in so far as they concern stars of highest luminosity, but in the vicinity of the dwarf branch they should be reliable within a moderate percentage.

Valuable information on density has at various times been obtained from the eclipsing variables, but it has been difficult to correlate these results with other stellar characteristics, except loosely, because here again the distances, and hence the luminosities, of individual stars are inadequately known. Density, however, depends in a simple way on mass, total luminosity, and surface brightness. The surface brightness can be computed from radiation formulae, the results being checked in part by their agreement with Pease's measures of angular diameters. Hence with mass once known as a function of spectral type and absolute magnitude, the values of the density follow as a matter of course. The results thus found for mass and density are subject to control and readjustment with the aid of the Cepheid variables, whose relative densities and masses can be calculated directly from their periods, spectra, and surface brightness.

The lines of equal mass for the giant stars in Russell's diagram are irregular curves, considerably inclined to the axis of zero absolute magnitude. If therefore a giant star in its evolutionary development follows an equal-mass line, its luminosity does not remain constant during the giant stage as has often been supposed. The curves of equal density are approximately linear and parallel to the line of maximum frequency for the dwarfs. The correlation of mass with spectral type along the dwarf branch can be explained, in part at least, as a consequence of selection, although other factors may also enter. The concluding sections of the paper discuss the relation of these results to certain phases of Eddington's theory.

I. THE METHOD

The mean masses of the visual binaries of different spectral types may be found by a statistical comparison of the absolute magnitudes corresponding to their hypothetical parallaxes with the absolute magnitudes of stars of known parallax. The relation

$$\mu=\mu_1+\mu_2=\frac{a^3}{\pi^3 P^2} \tag{1}$$

leads at once to

$$\log \mu = k - 0.6M \tag{2}$$

where

$$k = 3 \log a - 2 \log P + 0.6m + 3$$

and where the absolute magnitude is defined by

$$M = m + 5 + 5 \log \pi. \tag{3}$$

For a hundred systems of known orbital elements Jackson and Furner[1] have used equation (1) to calculate the hypothetical parallax π_c corresponding to an assumed mass $\mu = 2$. For about 450 systems of unknown elements they have calculated hypothetical parallaxes from a formula depending on changes in position angle and distance, the assumption for the mass again being $\mu = 2$. The absolute magnitudes M_c corresponding to the hypothetical parallaxes for the two groups of stars are given in Tables I and II of their paper.

For any system of known elements, by (2),

$$0.30 = k - 0.6\,M_c$$

and by combination with (2) itself,

$$\log \mu = 0.30 - 0.6\,\Delta M \tag{4}$$

where $\Delta M = M - M_c$. Hence for a group of stars[2]

$$\left.\begin{aligned} \overline{\log \mu} = \log \underline{\mu} &= 0.30 - 0.6\,\overline{\Delta M} \\ \overline{\Delta M} &= \overline{M} - \overline{M}_c \end{aligned}\right\} \tag{5}$$

in which $\underline{\mu}$ represents the geometrical mean mass.

Equations (4) and (5) are the basis of the present discussion. Since the hypothetical parallaxes derived from changes in position angle and distance involve the mean inclination of the orbit-planes, the individual values of π_c thus found will differ from those obtained with the rigorous relation (1). Equation (4) therefore holds for individual stars only in the case of systems of known elements. Formulae (5), however, are valid for any representative group of stars, whether their elements are known or not, and can therefore be applied to objects in both the lists of Jackson and Furner.

---

[1] *Monthly Notices*, **81**, 2, 1920.

[2] Upon re-reading Russell's address, "Relations between the Spectra and Other Characteristics of the Stars," *Publications of the American Astronomical Society*, **3**, 22; *Popular Astronomy*, **22**, 275, 331, 1914, I find that in principle the method is essentially one used by him.

To determine the mass from equations (4) and (5), the values of M, or at least of $\overline{M}$, must be known for the various spectral types. For a certain number of systems direct determinations of distance are available. Hence, M is known, and the use of (4) gives at once values of μ for the individual stars. These results will be affected by large uncertainties, but the means for groups of stars should be accurate within a small percentage. For most of the binaries, however, only the hypothetical absolute magnitude M_c is known; no other approximation for M is available, and we must proceed indirectly. This we might do by using values of $\overline{M}$ derived from single stars of known parallax whose selection with respect to the stars as a whole presents the same characteristics as those of the binaries themselves. Similarity of selection in the two lists of stars—binaries and single stars—is, however, difficult to attain in practice. It will be sufficient if we can find a list of single stars whose differences in selection as compared with the binaries are the same for all spectral types.

Let $\overline{M}_s$ represent the mean absolute magnitude for a given spectral type of the single stars of known parallax, and let $\overline{M}$ be the corresponding magnitude of the binaries of the same type. We may then write

$$\overline{M}=\overline{M}_s+\delta M \tag{6}$$

where δM indicates the influence of difference in selection. If this difference is the same for all types, δM will be constant, and we shall then speak of the selection as homogeneous.

The second of (5) then becomes

$$\overline{\Delta M}=\overline{M}_s-\overline{M}_c+\delta M=\overline{\Delta M}_s+\delta M \tag{7}$$

where $\overline{M}_c$ is the mean hypothetical absolute magnitude of the binaries of the spectrum under consideration. The value of $\overline{\Delta M}_s=\overline{M}_s-\overline{M}_c$ is found by comparing the two lists of stars for which it is presupposed that the selection for different spectral types is homogeneous, while the constant δM is given by

$$\delta M=\overline{\Delta M}-\overline{\Delta M}_s=\overline{M-M_c}-\overline{\Delta M}_s \tag{8}$$

applied to the systems of independently determined parallax referred to above. M represents here the magnitude corresponding to the measured parallax of a binary whose hypothetical absolute magnitude is M_c. In other words, we derive δM by (8) from the hundred or more binaries of measured parallax, calculate $\Delta\overline{M}_s$ for each type by comparing the five hundred and fifty-odd stars in the lists of Jackson and Furner with the homogeneously selected single stars of known parallax, form $\overline{\Delta M}$ by (7), and, finally, solve for μ by means of the first of equations (5). Since the question of homogeneity of selection can be put to a direct test, the only assumption underlying this procedure is that the relation of mass to luminosity is the same for both binaries and single stars, which may be accepted as plausible at least.

The values of $\overline{M}_s$ and $\overline{M}_c$, whose difference is $\overline{\Delta M}_s$, are readily found by a graphical process. Plotting the values of M_c against spectral type, we find for the binaries a frequency diagram similar to that first given by Russell. The late-type giants are not numerous, but the dwarf branch is well defined. The points of maximum frequency for the dwarfs define a curve which joins smoothly with the line of modal values of the B- and A-type stars. This curve expresses the variation of $\overline{M}_c$ with spectral type, the giants of late type being disregarded altogether for the present. For $\overline{M}_s$ a similar curve was found from the data in the list of spectroscopic parallaxes,[1] supplemented by those for about 430 helium stars whose parallaxes have been determined by Kapteyn.[2] These two curves are shown in the central part of Figure 1. Their ordinates and differences in ordinates are given in the second, third, and fourth columns of Table IV. The data for the $\overline{M}_s$ curve could have been greatly increased by including results from trigonometric parallaxes. Little would have been gained in precision, however, for, as it is, the number of stars entering into the $\overline{M}_s$ curve is more than twice that for the $\overline{M}_c$ curve.

---

[1] Adams, Joy, Strömberg, and Burwell, *Mt. Wilson Contr.*, No. 199; *Astrophysical Journal*, **53**, 13, 1921.

[2] *Mt. Wilson Contr.*, Nos. 82, 147; *Astrophysical Journal*, **40**, 43, 1914; **47**, 146, 255, 1918.

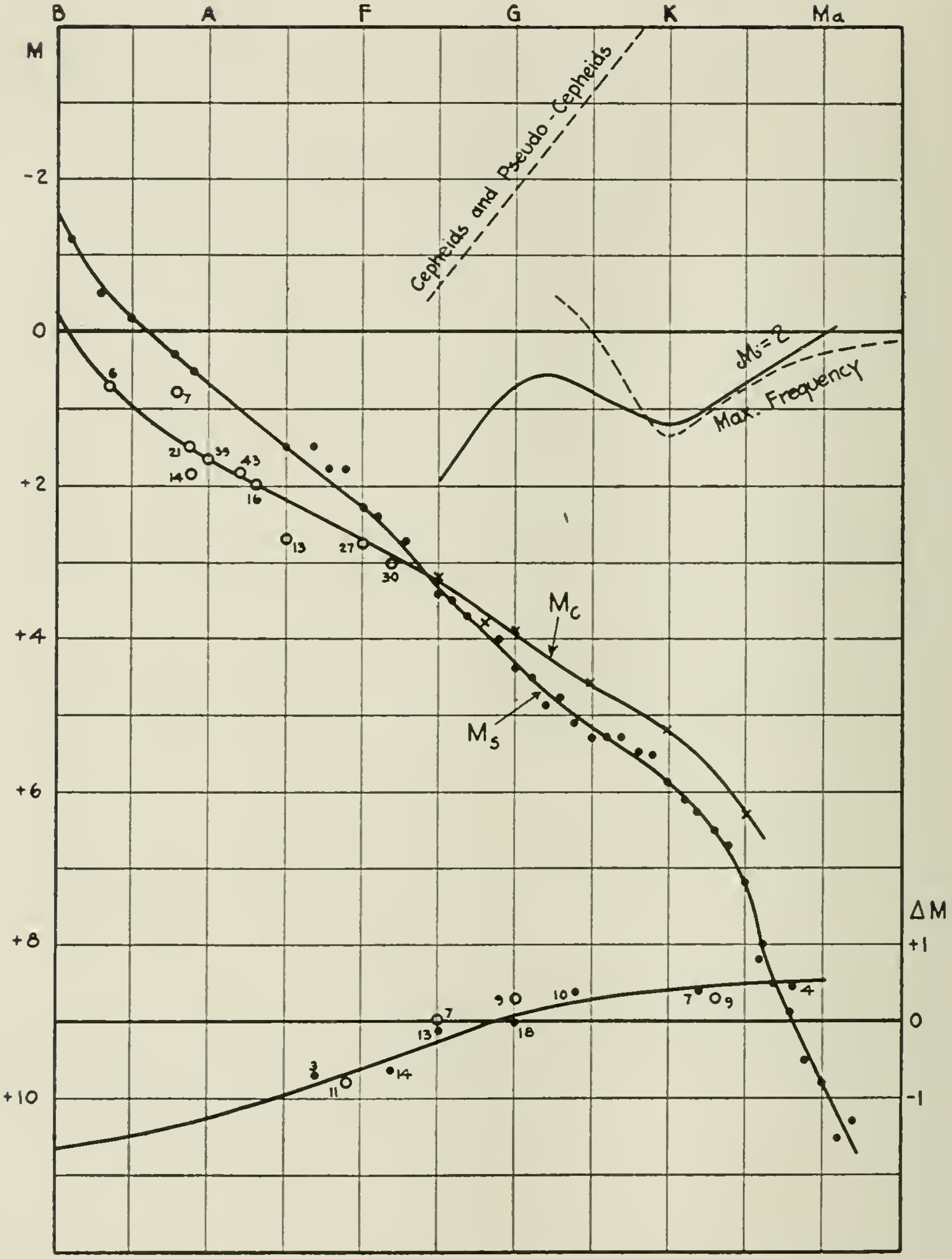

FIG. 1.—The curve M_s is the line of maximum frequency of M for the B stars of Kapteyn and the dwarfs from the list of spectroscopic parallaxes. M_c is the similar curve for the hypothetical absolute magnitudes of Jackson and Furner. The differences in the ordinates, corrected for zero point, are shown by the curve below (ΔM). The remaining curves refer to the discussion in section 16.

If we may assume that the selection for different spectral types is homogeneous, the differences in the ordinates of the two curves represent the values $\overline{\Delta M}_s$ as a function of spectrum. Irregularities of selection, or a progressive change in selection with type, will produce deformations or a tilt of the curve for $\overline{\Delta M}_s$. The curve for $\overline{\Delta M}$, formed directly from the curves for $\bar{M}_c$ and $\bar{M}_s$ and corrected for δM, is shown in the lower part of Figure 1 (the points are explained later). Since the curve is smooth, we conclude that there are no marked irregularities of selection, or at least that their influence has been minimized in drawing the curves for M_s and M_c.

2. INFLUENCE OF SELECTION ON THE STATISTICAL COMPARISON

To examine the question of selection more closely, consider the numbers of binaries and single stars of known parallax in each interval of apparent magnitude. Excluding the late-type giants and a few scattering stars at the ends of the sequence of apparent magnitudes, we find the data in the first two divisions of Table I. If the selection for the two lists were the same (not merely homogeneous), the ratios of the corresponding numbers for each type would not vary with the magnitude. Difference in selection for the binaries and single stars of any type implies a change in ratio with increasing magnitude; and, if the selection is homogeneous, the ratios for different types will show the same change. Absolute values of the ratios are of no significance, and for ease of comparison the ratios for each type have been multiplied by a constant factor which reduces that for median magnitude 6.5 to unity. Further, the numbers for the G5–K5 binaries have been combined with the mean numbers for single stars of F0–F9 and K0–K9 types.

The results in the third division of Table I indicate a satisfactory degree of homogeneity. The irregularities affecting the bright G5–K5 stars are unimportant, since the individual groups include only two or three stars each. The only deviations requiring comment are those shown by the faint G5–K5 stars and the faint B's. The latter arise from the fact that Kapteyn's lists of B stars include none fainter than the 6th magnitude. The binaries involved are ten in number, all of the 7th magnitude or fainter, and all but one or two of types B8 or B9. Any error in the corresponding $\overline{\Delta M_s}$ must be small, for there is no pronounced irregularity in the curve. The value of $\overline{M}_s$ for Kapteyn's earlier B's

TABLE I

NUMBERS OF STARS—INFLUENCE OF SELECTION

Spectrum	Median Apparent Magnitude								Total No.
	2.5	3.5	4.5	5.5	6.5	7.5	8.5	9.5	
	Binaries—Jackson and Furner								
Oe5–B9	1	1	7	7	7	8	2	0	33
A0 –A9	4	3	12	32	42	25	15	1	134
F0 –G0($M>+1$)	0	6	15	36	66	78	54	2	257
G5 –K5($M>+3$)	0	1	3	4	9	24	39	1	81
Total	......	......	......	......	......	......	......	......	505
	Single Stars*—Kapteyn and Adams								
Oe5–B9	23	42	137	194	30	0	0	0	426
A0 –A9	0	7	11	11	8	3	(2)	(1)	43
F0 –F9($M>+1$)	2	14	48	105	63	50	29	3	314
G0 –G9($M>+3$)	0	5	10	35	57	54	40	8	209
K0 –K9($M>+4$)	0	1	2	14	26	43	62	12	160
Total	......	......	......	......	......	......	......	......	1,152
	Ratio—Binaries/Single Stars								
B	......	0.1	0.2	0.2	1.0	∞	∞	......	......
A	......	0.1	0.2	0.6	1.0	1.6	1.5	0.2	......
F	......	0.4	0.3	0.3	1.0	1.5	1.8	0.7	......
G5–K5	......	1	3	0.8	1.0	2.2	3.5	0.5	......
	Ratio—Jackson and Furner/Pickering								
B	......	......	7	2	1.0	0.52	0.08	0.00	......
A	......	......	3	2	1.0	0.29	0.04	0.00	......
F	......	......	3	2	1.0	0.38	0.10	0.01	......
G5–K5	......	......	3	2	1.0	0.80	0.54	0.02	......
	Ratio—Kapteyn and Adams/Pickering								
B	......	......	34	13	1.0	0.00	0.00	0.00	......
A	......	......	17	4	1.0	0.18	0.03	0.02	......
F	......	......	12	6	1.0	0.25	0.05	0.01	......
G	......	......	3	4	1.0	0.33	0.08	0.02	......
K	......	......	0.4	1.5	1.0	0.46	0.34	0.12	......

* The "single stars" include the brighter members of a few binaries.

can scarcely have been affected by the limitation in apparent magnitude, for these stars are all so luminous that the limitation is of little consequence.

Among the stars fainter than $m=7.0$ there is an excess of G5–K5 binaries which represents a considerable fraction of the total number of G5–K5 stars. The corresponding M_c may be slightly too large. But, if appreciable, this effect must also be small, for as the stars actually observed in the intervals of fainter apparent magnitude are successively added, the value of $\overline{M}_c$ increases very slowly. A direct test is afforded by the binaries of measured parallax considered in a later paragraph.

The number of A stars in the spectroscopic list is small, but this does not seriously interfere with the determination of the curve of modal values because there are well-determined points for the early B's and for the F's. It does suggest, however, the advisability of an independent test of the selection of the much larger group of A's among the binaries, whose numbers can be considerably changed without greatly affecting the ratios in the middle section of Table I. To cover this point and as a further general test, both groups of stars have been compared with the counts of W. H. Pickering.[1] Using means of his values for the galactic poles and the galaxy itself (except for the B's, for which the galactic counts alone have been employed), we find the ratios in the last two sections of Table I. There is here some progression with type due to the fact that Pickering's counts include the late-type giants; but the ratios for the A-type binaries are in general agreement with those of the adjacent classes, which answers the question as to the selection of the A's. The large ratios for the bright B's in the last section of the table show merely what appears directly from the counts, namely, that Kapteyn's lists are not complete beyond the 6th magnitude. There seems also to be a defect of fainter A's in the spectroscopic list, a conclusion apparently confirmed by the fact that the points for these stars lie above the smooth $\overline{M}_s$ curve shown in Figure 1. It seems clear that none of the questions raised is serious and that we may accept the values of $\overline{\Delta M_s}$ found in the manner described and proceed to the determination of δM.

---

[1] *Publications of the Astronomical Society of the Pacific*, 33, 140, 1921.

3. ZERO POINT OF THE CURVE FOR MASS AND SPECTRUM

It will be noted that the values of $\overline{\Delta M_s}$ determine the rate of change of mass with spectral type, while the constant, δM, determines the zero point. For the calculation of δM only the spectroscopic parallaxes have been used, since these are based on a homogeneous system and are sufficiently numerous to afford an excellent determination. In forming values of $M-M_c$ for individual stars to be substituted into (8), two points must be borne in mind: First, the values of M given in the spectroscopic list correspond to the most probable values of the parallaxes, and, because of the logarithmic relation connecting absolute magnitude and parallax, are not the most probable magnitudes themselves. To obtain the latter, a small constant correction of $+0.08$ mag. must be applied to the tabular values.[1] Second, the values of M_c given by Jackson and Furner usually represent the total luminosity of the system. To make them comparable with values of M in the spectroscopic list, they must be reduced to the brighter component.

A summary of the results for δM is given in Table II, the two lists of Jackson and Furner being treated separately. The values of $\overline{\Delta M_s}$ required for equation (8) were interpolated from the fourth column of Table IV. The adopted result is $\delta M = -0.3$, whence equation (7) becomes

$$\overline{\Delta M} = \overline{\Delta M_s} - 0.3. \qquad (9)$$

It will be noted that there is no marked progression in the values of δM with type, which confirms, in part at least, the foregoing conclusion as to homogeneity of selection. This is also shown by the lower part of Figure 1, in which the curve is that representing equation (9), while the points correspond to the values of $\overline{M-M_c}$ in Table II. With the exception of the constant term, the curve depends wholly upon the statistical comparison, while the points are derived from values of M and M_c referring to the same star and are uninfluenced by any possible dissimilarity in selection. The agreement of the points with the curve is, however, within the uncertainty affecting their positions.

---

[1] *Mt. Wilson Contr.*, No. 199, p. 15; *Astrophysical Journal*, **53**, 27, 1921.

TABLE II

ZERO POINT OF CURVE FOR $\overline{\Delta M_s}$

J and F, Table I					J and F, Table II				
Sp.	$\overline{M-M_c}$	$\Delta\overline{M}_s$	δM	No. Stars	Sp.	$\overline{M-M_c}$	$\Delta\overline{M}_s$	δM	No. Stars
A7.....	−0.7	−0.5	−0.2	3	A9....	−0.8	−0.4	−0.4	11
F2.....	−0.6	−0.2	0.4	14	F5....	0.0	0.0	0.0	7
F5.....	−0.1	0.0	0.1	13	G0....	+0.3	+0.4	−0.1	9
G0....	0.0	+0.4	0.4	18	K3....	+0.3	+0.8	−0.5	9
G4....	+0.4	+0.6	0.2	10					
K2....	+0.4	+0.7	0.3	7					
K8....	+0.5	+0.8	−0.3	4					
Mean and total......			−0.29	69	Mean and total......			−0.27	36

A further detail bearing on the question of selection is the circumstance that the constant δM arises almost wholly from the use of the tabular values of M_c for the derivation of the curve for $\overline{M}_c$. Since these generally represent total luminosity, the reduction to the brighter component appears in δM, and in the mean is nearly equal to the value found for this constant. The effect upon $\Delta\overline{M}_s$ of the obvious differences in selection shown in Table I is therefore very small. Consequently, the influence of small deviations from homogeneity in selection in passing from type to type may be regarded as altogether negligible.

4. SYSTEMATIC DIFFERENCES IN THE HYPOTHETICAL PARALLAXES

Although the two mean values of δM given in Table II are practically identical, this was not the case when the calculation was originally made, the difference then amounting to several tenths of a magnitude. This discordant result has been traced to a systematic difference between the parallaxes of the two lists of Jackson and Furner, the character of which may be seen from the comparisons shown in Table III. For systems of known elements (J and F, Table I) the agreement of the mean hypothetical parallaxes with the spectroscopic results is excellent; the one large difference +0.″014 is only 7 per cent of the corresponding π_c and would be reduced to +0.″004 by the rejection of a single star, Bu 2109.

TABLE III

COMPARISON OF SPECTROSCOPIC AND HYPOTHETICAL PARALLAXES

π_c	J AND F, TABLE I			J AND F, TABLE II			J AND F, TABLE I—TABLE II		
	Mean π_c	$\pi-\pi_c$	No.	Mean π_c	$\pi-\pi_c$	No.	Mean π_c*	$\pi-\pi_c$	No.
<0.″020	0.″016	+0.″001	7	0.″015	−0.″002	8	0.″015	−0.″001	6
0.020–0.049........	0.030	−0.001	28	0.036	−0.009	16	0.024	−0.007	12
0.050–0.099........	0.065	−0.003	22	0.064	−0.012	13	0.043	−0.012	8
>0.100	0.198	+0.014	10	0.209	−0.071	1	......	....	....

* The intervals for π_c are $\lesseqgtr$0.″020, 0.″021–0.″029, and $\gtreqless$0.″030.

For the stars in the second list, however, the agreement for the first group alone is within the uncertainty; for the others the differences are systematic and an important percentage of the parallaxes themselves. Further, the same difference is shown by a direct comparison of the hypothetical parallaxes of twenty-six stars which occur in both the lists of Jackson and Furner. The means, arranged in three groups, are in the last division of Table III. For half of these stars no spectroscopic parallaxes are available, and to that extent the second comparison is independent of the first.

The difference, which is about 20 per cent of the parallax, corresponds to a difference of 0.4 mag. in the two values of δM and fully accounts for the discordance. For the final determination of δM, the hypothetical parallaxes from the second list were reduced to the spectroscopic system in accordance with the indications of Table III, in order that all the results may refer consistently to this system. The resulting value of δM is that given in the right-hand division of Table II.[1]

---

[1] I am greatly indebted to Mr. Adams for the spectroscopic parallaxes of nineteen binaries in the first list of Jackson and Furner (six stars also occur in the second list) which have been obtained since the reductions described in the text were finished. These reductions have not been revised, but I have satisfied myself that the inclusion of the new data would not change the results in section 4 or the following sections

5. PROVISIONAL MASSES—EFFECT OF SELECTION

The derivation of values of the masses now requires only the substitution of $\overline{\Delta M}$ from (9) into the first of (5). The results for log $\underline{\mu}$ are in the fifth column of Table IV. The first and last values depend upon extrapolations, and it is possible that those for B5 and A0 are also affected by considerable uncertainty. So far as the statistical comparison is concerned, the remaining values should be dependable within 5 or 10 per cent.

TABLE IV

ADOPTED GEOMETRICAL MEAN MASS ($\odot = 1$), SPECTRAL TYPE AND ABSOLUTE MAGNITUDE

SP.	M_s	M_c	$\overline{\Delta M_s}$	PROVISIONAL LOG $\underline{\mu}$	CORR. FOR SELECTION	VIS. BINARIES		SINGLE STARS	
						Log $\underline{\mu}$	$\underline{\mu}$	Log $\mathcal{M}$	$\mathcal{M}$
B0	−1.60	(−0.25)	(−1.35)	1.29	−0.04	1.25	18	1.01	10
B5	−0.20	+1.00	1.20	1.20	− 4	1.16	14	0.92	8.3
A0	+0.70	1.65	0.95	1.05	− 3	1.02	10.5	0.78	6.0
A5	1.50	2.15	0.65	0.87	− 3	0.84	6.9	0.60	4.0
F0	2.40	2.70	−0.30	0.66	− 2	0.64	4.4	0.40	2.5
F5	3.32	3.27	+0.05	0.45	− 2	0.43	2.7	0.19	1.5
G0	4.35	3.95	0.40	0.24	− 1	0.23	1.7	9.99	1.0
G5	5.20	4.60	0.60	0.12	0	0.12	1.3	9.88	0.76
K0	5.90	5.20	0.70	0.06	+ 1	0.07	1.2	9.83	0.68
K5	7.10	6.30	0.80	0.00	+ 3	0.03	1.1	9.79	0.62
Ma	+9.80	(+8.95)	(+0.85)	9.97	+0.04	0.01	1.0	9.77	0.59

These results can be accepted, however, only with some reservation, for it is easily seen that the visual binaries are a selected class of stars in the characteristic of mass itself, and especially is this true of the more distant objects. Since motion is detected only with difficulty, or not at all, in case the period is very long, equation (1) shows that the selection of large masses is favored to an increasing degree as more and more distant stars are considered. For a given value of a the factor a^3/π^3 increases rapidly with increasing distance; the smaller masses are therefore excluded in succession because they correspond to periods so long that motion has not been observed. For large values of π a wide range in mass

---

in any essential particular. Thus the first two differences in the first division of Table III would be +0.″002 and −0.″002 for seventeen and thirty-seven stars, respectively. The differences in the third division would not be changed by the inclusion of the six stars also occurring in the second list.

will be included, but since there is a practicable lower limit to a, only the most massive among the more distant stars will appear in our lists.

Another and perhaps even more important form of selection arises from the fact that only the most luminous of the distant stars get into our lists; the others are too faint to be seen. This, too, excludes in succession the smaller masses with increasing distance, and is related to the correlation of mass with spectral type discussed in section 16.

The influence of distance on the selection of mass seems to be shown by the data now available. To test the matter, consider the sixty-nine binaries of known parallax[1] in the first list of Jackson and Furner. For these, the individual masses, μ, can be calculated by (4). Comparing these values with the mean mass for stars of the same spectrum, as interpolated from Table IV, we obtain a series of residuals $\Delta \log \mu = \log \mu - \log \underline{\mu}$. When grouped according to parallax, these lead to the mean systematic deviations shown in Table V. A progression with increasing parallax, in the direction anticipated, is evident, the negative sign of the differences associated with the more distant stars indicating that the corresponding

TABLE V

DEPENDENCE OF MASS ON PARALLAX

π_S	Mean Sp.	No. Stars	$\overline{\Delta \log \mu}$	Curve
0″018	F2	10	−0.08	−0.11
.026	F6	10	−0.12	−0.08
.032	G1	10	−0.08	−0.07
.046	F7	10	+0.03	−0.03
.061	G3	10	−0.04	0.00
.102	G1	10	+0.04	+0.04
0.270	G8	9	+0.12	+0.12

---

[1] The thirty-six stars of known parallax in the second list are not included because of the systematic difference in the parallaxes of the two lists. In the preparation of Table II, where only a mean result for all the stars was finally used, the systematic difference can be corrected with sufficient precision. Here, however, we are concerned with individual stars, or at most with small groups, and it is not certain that the mean correction is applicable. Then, too, the fact that the second list of Jackson and Furner is based on a statistical formula, renders these data unsuitable for the present discussion.

mean masses in Table IV are too large. The character of the progression is best seen from the smoothed values of the differences given in the last column of Table V. Considered as corrections, these differences are such as would reduce the masses to values representing the selection for $\pi = 0''.06$. Even at this moderate distance the smallest masses will still be excluded; hence some further correction, a constant, is required. This cannot be accurately specified; but in general it may be said that, if we regard the selection for the two nearest groups in Table V as approximately representative of the visual binaries as a whole, the data of this table would indicate that the mean masses of the binaries actually observed at distances corresponding to $\pi = 0''.02$ are roughly 50 per cent larger than those of a representative collection.

This result at once suggests that the variation of log $\underline{\mu}$ with spectral type found above has been influenced by selection, for in general the mean parallax of the earlier-type stars, which are all highly luminous, is less than that of the late-type dwarfs. Forming the mean parallax for each of the spectral groups in the first half of Table II, we find in fact a progression in distance as shown in Table VI. If the data of Table V may be accepted, the values of log $\underline{\mu}$ in Table IV must be corrected as indicated in the last column of Table VI, in order to obtain the true variation of log $\underline{\mu}$ with spectral type. To make the results fully representative, the additional constant correction referred to above must also be applied. This seems to be of the order of −0.08.

TABLE VI

CORRECTIONS TO LOG $\underline{\mu}$

(To Eliminate Selection in Mass)

Sp.	$\bar{\pi}_s$	No. Stars	Correction to log $\underline{\mu}$
A7	(0″.133)	3	−0.03
F2	0.051	14	−0.02
F5	0.038	13	−0.05
G0	0.055	18	−0.01
G4	0.069	10	0.00
K2	0.114	7	+0.06
K8	0.229	4	+0.11

Unfortunately, however, the results in Table V are not as reliable as could be wished. The individual values of the masses are affected by large uncertainties, and the number of stars in the separate groups is small. Further, the residuals $\log \mu - \log \underline{\mu}$ depend upon the ordinates of the curve for ΔM shown in Figure 1. Any error in the curve, in the nature of a tilt with respect to the axis, must therefore have introduced a progression in the residuals which only partially disappears when they are grouped according to parallax, because such a grouping, in part at least, is also a grouping with respect to spectral type. This uncertainty is probably not very serious, for Table V shows that the relative effect on the corrections to $\log \mu$, for the two extremes of distance, is the differential error in the ordinates of the ΔM curve for F2 and G8. Since these ordinates are not widely separated, the influence of incorrect slope in the curve cannot be great.

6. ADOPTED MASSES

On the basis of the evidence in Table VI, the corrections given in the sixth column of Table IV were finally adopted. These are the smoothed values of the results in Table VI, extrapolated to B0 and slightly modified in the case of type K because of the small number of these stars. The small constant correction referred to above is ignored, because of its uncertainty and relative unimportance. It merges with the uncertainty involved in the assumptions of comparability which must be made in extending the results for the masses of the binaries to the stars at large.

The differential correction, affecting the relative values of the masses as it does, is of more interest. The present determination is to be considered as only a first approximation; the results are at least in the right direction, and it is believed that they do not represent an over-correction.

We have, finally, as adopted values of the geometrical mean masses of the visual binaries, the data in the seventh and eighth columns of Table IV. These results refer mainly to dwarf stars and correspond to the mean absolute magnitudes given in the second column of the table.

Owing to the small number of late-type giants in the lists of visual binaries, it is not possible to use the statistical method for a determination of the masses of these stars. Some indication of their values is afforded, however, by the application of equation (4) to such of these objects as occur in the spectroscopic list. For 14 G and K stars, with a mean absolute magnitude of 0.0,

$$\log \underline{\mu} = 0.47 \pm 0.16$$

whence $\underline{\mu} = 3.0$ with an uncertainty of about 40 per cent.

The use of the geometrical mean makes it difficult to compare the masses thus found with other results,[1] for which the arithmetical mean has usually been employed. For a Gaussian distribution of the logarithms of the mass, which seems to be that indicated by the available data, the conversion formula would be[2]

$$\log \bar{\mu} = \log \underline{\mu} + 2.53\, r^2$$

where $\bar{\mu}$ is the arithmetical mean, and r the probable dispersion, i.e., the median value of the differences $\log \mu - \log \underline{\mu}$, arranged in order without regard to sign. The value of r is difficult to determine. For the dwarf stars it is certainly small, probably not larger than 0.15 (see page 185), whence, approximately, $\bar{\mu} = 1.14\, \underline{\mu}$.

Applied to the present data, this relation would lead to arithmetical mean masses a little larger than those previously found, but close comparisons are not possible. The change in mass with spectral type is of the general character of that resulting from other investigations and is certainly well established, although the variation given here is not as large as that derived by Ludendorff[3] from a discussion of spectroscopic binaries.

Strictly speaking, the present results refer only to the particular group and class of stars upon which the conclusions are based.

---

[1] Russell, *loc. cit.; Publications of the American Astronomical Association*, **3**, 327; *Popular Astronomy*, **25**, 666, 1917. Aitken, *The Binary Stars*, pp. 206 ff., 1918. Van Maanen, *Publications of the Astronomical Society of the Pacific*, **31**, 231, 1919. Ludendorff, *Astronomische Nachrichten*, **189**, 145, 1911; **211**, 105, 1920.

[2] Adams, Strömberg, and Joy, *Mt. Wilson Contr.*, No. 210, p. 17; *Astrophysical Journal*, **54**, 25, 1921. Although derived for use in another connection the formula is generally applicable.

[3] *Loc. cit.*

Their applicability to any other class of stars presupposes some assumption. Thus in passing from the combined masses of the visual binaries to those of single stars, we can make use of the average mass-ratio of the two components and associate the resulting average values for the central stars with that for the non-binaries of the same spectra; but it is by no means certain that the stars so associated are strictly comparable. For the further discussion we make this assumption. Presumably the uncertainty is not large, for we thus arrive at a mean mass for the solar-type stars which is the same as that of the sun itself. To give this conclusion force it must be added that the average deviation of the mass of a dwarf star from the mean mass for the type in question is small (see next section).

There is some evidence that the mass-ratio varies with the type.[1] Adopting, however, the mean value 0.75 for the ratio of secondary to principal component, we find for the stars at large the geometrical mean masses ($\mathcal{M}$) in the last two columns of Table IV.

7. DISPERSION IN MASS

The residuals in log μ for the sixty-nine stars discussed above throw some light on the dispersion in mass. Freeing the individual residuals from the influence of selection in mass, we find the frequencies shown in Table VII. In spite of the small numbers of

TABLE VII

DISTRIBUTION OF Δ LOG μ

INTERVAL OF Δ LOG μ	NO. RESIDUALS		TOTAL	
	+	−	Obsd.	Theor.
0.00–0.09..........	8	4	12	17
0.10–0.19..........	10	8	18	15
0.20–0.29..........	6	7	13	12
0.30–0.39..........	5	7	12	10
0.40–0.49..........	5	5	10	6
0.50–0.59..........	0	1	1	4
0.60–0.69..........	1	1	2	3
0.70–0.79..........	0	0	0	1
0.80–0.89..........	1	0	1	0
Sums..........	36	33	69	68

---

[1] Aitken, *The Binary Stars*, pp. 206, 216, 1918.

stars, it is seen from the second and third columns that the frequency curve is approximately symmetrical. Further, the last two columns show that, within the uncertainty of the data, the values of log μ follow a Gaussian distribution.

The probable dispersion (dwarfs F0 to M) is

$$r(\Delta \log \mu) = \pm 0.22. \tag{10}$$

This, however, is not a true measure of the dispersion in log μ, for the result has been derived with the aid of equation (4) and includes, therefore, the influence of errors in M and M_c. Those in M_c arise from the factor a^3/P^2 and are relatively small. Bearing on the accuracy of M are the data in *Contribution* No. 199, p. 15, from which for the spectral types and luminosities involved, $r(M) = \pm 0.36$ mag. By (4), the contribution to the calculated dispersion in log μ arising from errors in M is therefore ± 0.22, which is the same as the calculated value of $r(\Delta \log \mu)$ itself. Since the dispersion in the masses presumably is not zero, the adopted value of $r(M)$ is probably too large. This unfortunately makes it impossible to gain any definite information as to the dispersion, and we can only indicate, as in the second column of Table VIII, the probable values corresponding to various assumed values of $r(M)$. The last column of the table gives the limits within which it is an even chance that the mass of any visual binary will be found. Thus, if we assume that the true probable error of the spectroscopic absolute magnitude is ± 0.25, the masses of one-half of the stars should be between 0.7 and 1.5 times the mean mass.

TABLE VIII

PROBABLE DISPERSION IN MASS

$r(M)$	Probable Dispersion in Log μ	Limits for Prob. = ½
±0.35	±0.07	0.85μ–1.18μ
0.30	0.13	0.74 –1.35
0.25	0.16	0.69 –1.45
0.20	0.18	0.66 –1.51
±0.15	±0.20	0.63 –1.58

Apparently the range in the masses of the dwarf stars from Fo on must be small. Further evidence is given on page 214. These results are in general agreement with the earlier findings of Russell and Eddington.[1]

8. EQUIPARTITION OF ENERGY

A possible analogy between the dynamical behavior of the stars and that of the molecules of a gas has frequently been mentioned.[2] Applicability of the kinetic theory would imply an equipartition of the energy of translation such that

$$\mu_1\overline{v_1^2}=\mu_2\overline{v_2^2}= \ . \ . \ . \ =\mu_n\overline{v_n^2} \tag{11}$$

where the individual values in $\overline{v_n^2}$ include all the velocities associated with a definite class of masses μ_n. In a gas this final state is brought about very quickly; in a collection of stars the period of relaxation, if the term has any meaning at all, obviously must be enormously long.

As a matter of fact, the theory for a collection of stars is much simpler than that of a gas, because the occurrence of collisions and close encounters is so rare that they may be neglected.[3] The effective agency for the transfer of energy is therefore only that arising from the attraction of the great mass of stars as a whole upon the individual members of the group. But this simplification of the theory and the consequent restriction of the mechanism for the redistribution of energy so enormously lengthens the interval required for the attainment of statistical equilibrium that Eddington[1] rejects altogether the analogy with a gas and proceeds on the principle that the motions of the stars do not mutually interfere.

---

[1] *Monthly Notices*, 77, 30, 1916; 604, 1917. Russell, in this connection, makes the important suggestion that the real dispersion in mass may be largely concealed in a discussion based upon spectroscopic data. This would be the case if the spectral characteristics used for the determination of a star's absolute magnitude are functions of its surface brightness (temperature) and density alone. For Russell's discussion of this interesting point see the following note on page 238.

[2] See for example Poincaré, *Hypothèses Cosmogoniques*, p. 257, 1911; Halm, *Monthly Notices*, 71, 634, 1911; Eddington, *Stellar Movements*, pp. 159, 247, 1914; Jeans, *Problems of Cosmogony and Stellar Dynamics*, pp. 224 ff., 1919.

[3] Jeans, *op. cit.*, p. 229.

As far as the present state of the universe is concerned, Jeans[2] concurs in this opinion, but points out that the conditions of an earlier stage in its history may have been entirely different. Following his conjecture that the system has evolved from a rotating nebula of dimensions much less than those of its present configuration, he shows that the earlier stages of development would be favorable to a rapid redistribution of energy, and that the system may have proceeded far on the way toward equipartition before its gradual expansion reduced the rate of transfer to its present negligible amount. The fact that readjustments are now inappreciable does not therefore demonstrate the absence of equipartition, which must be put to an observational test.

Although a certain type of systematic motion is not incompatible with a steady state, the phenomenon of star-streaming shows that equipartition has not been completely attained. Within the individual streams, however, there may be an approach to this state, just as in the case of two intermingling streams of gas. Further, if the stream motion is small as compared with the peculiar velocities of the stars, it will have little influence on the statistical averages in (11). For a decade or more some correlation of mass with velocity of the type hereby implied has been suspected, for it has been known that in general the most massive stars are the most luminous, and the most luminous stars have on the average the smallest velocities.[3] Now, however, we are in possession of data which admit of a more definite test.

For the B and A stars, whose extreme range in luminosity is small, we have the determinations of mean radial velocity by

---

[1] Eddington, *loc. cit.*, p. 254. See also *Astronomische Nachrichten, Jubiläumsnummer*, p. 9, 1921.

[2] *Op. cit.*, p. 237.

[3] Campbell, *Stellar Motions*, p. 207, 1913. Kapteyn, *Mt. Wilson Contr.*, No. 45; *Astrophysical Journal*, **31**, 258, 1910. Russell, *Observatory*, **37**, 174, 1914. Kapteyn and Adams, *Mt. Wilson Comm.*, No. 1; *Proc. Nat. Acad. of Science*, **1**, 14, 1915. Adams and Strömberg, *Mt. Wilson Contr.*, No. 131; *Astrophysical Journal*, **45**, 293, 1917.

Campbell.[1] For the remaining types, within which the differences in luminosity are much greater, we have the recent Mount Wilson results,[2] giving both radial and space velocities for each of these types as a function of absolute magnitude. Since the values of the masses in the last column of Table IV are probably representative of the stars at large, they may be combined with the mean velocities of the different types, in conformity with (11), to determine the degree to which the condition of equipartition is satisfied.

The values of the velocities have not been corrected for stream motion and thus subject the hypothesis of equipartition to a severe test. The Mount Wilson results for radial and space velocities include the K-term. For the late-type dwarfs, this is small, and negligible for the present discussion. Campbell, on the other hand, has freed his results from this term, which for the B stars is two-thirds of the mean radial velocity itself. If one prefers to regard the K-term as a real velocity, and not merely a systematic correction, its contribution to the energy can be found as indicated below.

It has been shown that the distribution of the space velocities for types F to M is not in accordance with Maxwell's law,[3] but agrees well with the assumption that the logarithms of the velocities follow a Gaussian distribution. Nevertheless, Campbell's theorem to the effect that the arithmetical mean space velocity equals twice the mean radial velocity, holds for the giants with close approximation.[4] We assume that a similar state of affairs exists for the B and A stars, and thus obtain for these types the arithmetical means of their space velocities. The square of the arithmetical mean space velocity could have been used directly for a test of equipartition; but to evaluate the influence of the K-term, considered as a velocity, it is simpler to use the mean-square space velocity.

---

[1] *Lick Observatory Bulletins*, **6**, 101, 1911; **7**, 19, 1912.

[2] Adams, Strömberg, and Joy, *Mt. Wilson Contr.*, No. 210; *Astrophysical Journal*, **54**, 9, 1921. These results are vital for the remainder of the discussion. Without them it could not have been undertaken.

[3] Kapteyn and Adams, *Mt. Wilson Comm.*, No. 1; *Proc. Nat. Acad. of Sciences*, **1**, 14, 1915. Adams, Strömberg, and Joy, *op. cit.*, p. 15.

[4] *Ibid.*, p. 13.

For a Gaussian distribution of the logarithms of the space velocities, the relation of the mean square velocity to the arithmetical and geometrical means is expressed by[1]

$$\left.\begin{aligned} \log \overline{v^2} &= 2 \log \bar{v} + \frac{1}{2h^2 \text{ Mod.}} = 2 \log \bar{v} + 0.148 \\ \log \overline{v^2} &= 2 \log \underline{v} + \frac{1}{h^2 \text{ Mod.}} = 2 \log \underline{v} + 0.296 \end{aligned}\right\} \qquad (12)$$

where h is the modulus of the distribution function. It is assumed that the value of h for types F to M given in *Contribution* No. 210 applies also to the B and A stars.

The mean radial velocities taken from Campbell's papers[2] are

B3, 6.2; B8.5, 6.7; A0, 10.3; A2, 11.4; A5, 12.6.

The corresponding mean square velocities were obtained by doubling the radial velocities, as indicated above, and substituting the results into the first of (12). For the later types the values of $\log \overline{v^2}$ were derived from the data for $\underline{v}$ given in *Contribution* No. 210. These were plotted—$\underline{v}$ against corresponding M—thus giving four curves, which refer to the approximate mean types F5, G5, K3, and Ma+. The mean absolute magnitudes of the dwarf stars of these types were then interpolated from Table IV and used as arguments to read from the curves values of $\underline{v}$ corresponding to the average dwarf of each of the four types. Graphical interpolation and an extrapolation to F0, followed by substitution into the second of (12), gave finally the required values of $\log \overline{v^2}$ for every

---

[1] The second equation is found by applying the mean value theorem to the frequency function

$$F(v) = \frac{h \text{ Mod.}}{\sqrt{\pi}} e^{-h^2 (\log v - \log \underline{v})^2}$$

The first results from the combination of the second with

$$\log \bar{v} = \log \underline{v} + \frac{1}{4h^2 \text{ Mod.}}$$

which is given by Adams, Strömberg, and Joy, *op. cit.*, p. 17.

[2] *Lick Observatory Bulletins*, 6, 127, 1911; 7, 28, 1912.

half-interval of spectral type from Fo to Ma. These mean-square velocities are not affected by any smoothing from type to type, since the interpolation card was drawn *through* the points derived from the four curves giving v the function of M.

The results, including those for log $\mathcal{M}\overline{v^2}$, are in the first six columns of Table IX. With the exceptions of the B stars, the

TABLE IX

THE ENERGY CONSTANT

Sp.	M	Log $\mathcal{M}$	Log $\overline{v^2}$	Log $\mathcal{M}\overline{v^2}$	Residual	Log θ^2	Log $\mathcal{M}\theta^2$	Residual
B3	−0.6	0.95	2.34	(3.29)	(+0.28)	1.74	(2.69)	(+0.07)
B8.5	+0.4	0.81	2.40	(3.21)	(+ .36)	1.62	(2.43)	(+ .33)
Ao	0.7	0.78	2.78	3.56	+ .01	2.00	2.78	− .02
A2	1.0	0.70	2.87	3.57	.00	2.10	2.80	− .04
A5	1.5	0.60	2.95	3.55	+ .02	2.19	2.79	− .03
Fo	2.4	0.40	3.11	3.51	+ .06	2.36	2.76	.00
F5	3.3	0.19	3.36	3.55	+ .02	2.56	2.75	+ .01
Go	4.4	9.99	3.62	3.61	− .04	2.76	2.75	+ .01
G5	5.2	9.88	3.78	3.66	− .09	2.84	2.72	+ .04
Ko	5.9	9.83	3.80	3.63	− .06	2.84	2.67	+ .09
K5	7.1	9.79	3.74	3.53	+ .04	2.92	2.71	+ .05
Ma	9.8	9.77	3.78	3.55	+0.02	3.06	2.83	−0.07
Means, average deviations				3.57	±0.036	......	2.76	±0.036

values of the energy show close accordance. For a range of 10 to 1 in the masses the average deviation in $\mathcal{M}\overline{v^2}$ is 9 per cent, and, by a moderate amount of smoothing, is easily reduced to 3 per cent. The large divergence for the B stars seems to be real. It cannot be supposed that the adopted values for their masses are in error by 50 per cent, nor does it seem permissible to assume that the velocities could by any chance be increased by the 2 or 3 km necessary to bring the energy up to the mean for the other types. It is more likely that the velocities are already too large, because of undetected spectroscopic binaries among the stars combined in the means.

The inclusion of the K-term as a velocity removes only a small part of the divergence. Thus, for any radial direction, the resultant mean-square velocity $\overline{r^2}$ would be

$$\overline{r^2}=\overline{v^2}+K^2-\overline{2vK\cos\alpha}=\overline{v^2}+K^2$$

where α is the inclination of the space velocities to the given line of sight. Extending this to all radial directions, we have for the entire group of B3 stars,

$$\overline{r^2}=(14.8)^2+(4.7)^2=241.1;\ \log \mathcal{M}\overline{v^2}=3.33,$$

an increase of only 0.04 in the logarithm of the energy.

The foregoing results depend upon the assumptions that the mean space velocities of the B and A stars may be found by doubling the mean radial velocities, and that the modulus h applies equally to all types. We may avoid these assumptions by restricting the test to the mobility in the line of sight. For this comparison the K-term has been included throughout. The mean radial velocities from Campbell's data thus become[1]

B3, 7.45; B8.5, 6.50; A0, 10.1; A2, 11.3; A5, 12.5 km/sec.

For the remaining types *Contribution* No. 210 was again used, the values being read from curves for radial velocity θ as a function of absolute magnitude as in the case of $\underline{v}$. The values of log $\mathcal{M}\theta^2$ (eighth column, Table IX) show about the same degree of accordance as those of log $\mathcal{M}\overline{v^2}$, the average deviations, without smoothing, again being 9 per cent. The inclusion of the K-term as a part of the radial velocity has brought the B3 stars into agreement with the mean for types A to Ma, and only the B8–B9 stars are now divergent.[2] But this improved agreement is not to be taken very seriously, and perhaps the most satisfactory point of view is that since the B stars are peculiar in many particulars, the abnormality shown by Table IX should not be looked upon as surprising, especially when it is remembered that they form a local aggregation[1] and that their masses are among the largest known.

---

[1] *Ibid.*, **6**, 108. The means for the B stars are those found by correcting Campbell's values V_1 by 4.7 (B0–B5) and 4.1 (B8–B9). For the A stars the mean of V_2, *Lick Observatory Bulletin*, **7**, 20, has been used without correction.

[2] Freundlich, *Physikalische Zeitschrift*, **20**, 561, 1919, has attempted to show that the K-term may be identified with the displacement of spectral lines toward the red required by the theory of relativity. This displacement may be involved, but results given later in this paper indicate that other factors must also play a part. See footnote p. 212.

There are suggestions of systematic divergencies in both sets of residuals, but by forming the means of the two series of values of the energy constant, these disappear, and the average deviation is reduced to 5 per cent.

Were the condition of equipartition exactly satisfied, we should have

$$\overline{v^2}=3\,\overline{\theta^2}\,.$$

For a Gaussian distribution of the radial velocities

$$\overline{\theta^2}=\frac{\pi}{2}\,\bar{\theta}^2$$

where $\bar{\theta}^2$ is the square of the arithmetical mean radial velocity used in Table IX. For unit mass, $\log\overline{v^2}=3.57$; and since $\log\pi/2=0.20$, $\log\overline{\theta^2}=2.96$. The mean-square velocities therefore appear to have a ratio of 4 to 1 instead of 3 to 1. It is known, however, that the radial velocities do not follow a Gaussian distribution closely.

Approaching the matter from another direction, we have for a random distribution in direction, irrespective of the form of the frequency function of the magnitudes of the velocities,

$$\bar{v}=2\,\bar{\theta}.$$

Substituting into the first of equations (12), we find the condition

$$\log\overline{v^2}=\log\theta^2+0.75$$

where θ^2 denotes the square of the arithmetical mean. The difference in the two members of this equation is 0.06 in the logarithm, or 11 per cent, a much better agreement than before. The remaining difference is doubtless to be attributed to the fact that the velocity distribution is not random; stream motion produces a preferential drift parallel to the galactic plane.

---

[1] This result follows directly from an analysis of star counts. Seares, *Publications of the Astronomical Society of the Pacific*, 30, 114, 115, 1918. Shapley in recent papers has accumulated much additional evidence: *Mt. Wilson Contr.*, Nos. 157, 161; *Astrophysical Journal*, 49, 311, 1918, and 50, 107, 1919; *Mt. Wilson Communications*, Nos. 54, 64; *Proceedings of the National Academy of Sciences*, 4, 224, 1918; 5, 434, 1919.

In spite of the known departures from Maxwell's law, there is, with the exception of the B stars, a surprisingly close approach to a state of equipartition. That the deviations are no larger is remarkable,[1] and suggests that for the stars considered (dwarfs) there is little difference between the different spectral types in the average contribution of stream motion to the total energy of translation. Since the unit of mass—that of the sun—is 1.9×10^{33} grams, and since the velocities are expressed in kilometers per second, the mean kinetic energy of translation is of the order of 3.5×10^{46} ergs.

9. DERIVATION OF MASS FROM THE ENERGY-CONSTANT

The constancy of the energy is apparently such as to justify an attempt to evaluate the masses of stars having luminosities and velocities different from those appearing in Table IX. Thus by reading from the curves referred to above the values of $\underset{\sim}{v}$ and θ corresponding to different values of M and combining them with the energy-constant, more or less hypothetical values of the corresponding masses can be obtained.

This procedure assumes that equipartition holds for the stars of high luminosity as well as the dwarfs, for which alone a direct test has been possible. The behavior of the B stars suggests caution in an extension of the principle to other giants; but since the translatory energy of the B's is of the same order as that found for the dwarfs, it is perhaps not too much to expect that the use of the energy constant will lead to masses for later-type giants which will also be of the right order of magnitude.

The results obtained in this manner are given in Table X. The values of log $\mathcal{M}$ are the means of the two values found with the aid of $\underset{\sim}{v}$ and θ from the two energy constants, log $\mathcal{M}\overline{v}^2$ and log $\mathcal{M}\theta^2$. To indicate the agreement between the masses derived with the aid of the two velocities, the differences log $\mathcal{M}_v -$ log $\mathcal{M}_\theta$ are also given in the table. In general these are reasonably small, although for the group of Ma stars the extreme values correspond to a two-to-one ratio in the masses. The data of Table X express, with more detail and precision, the correlation between mass and luminosity found by van Maanen.[1]

---

[1] In this connection see Jeans, *Problems of Cosmogony*, p. 238, 1919.

TABLE X

MASS AND LUMINOSITY

M	F5		G5		K3		Ma+	
	log $\mathcal{M}$	Diff.	log $\mathcal{M}$	Diff.	log $\mathcal{M}$	Diff.	log $\mathcal{M}$	Diff.
−3	......	....	0.74	−0.08	......	....	0.98	−0.36
−2	0.78	−0.02	.62	+ .02	......	....	.64	− .02
−1	.74	− .02	.51	+ .08	0.72	−0.10	.41	+ .16
0	.68	− .02	.38	+ .10	.45	+ .08	.23	+ .24
+1	.62	+ .02	.28	+ .14	.28	+ .14	0.08	+ .30
2	.51	.00	.17	+ .11	.17	+ .12	......	....
3	.30	− .02	0.06	+ .06	.07	+ .08	......	....
4	0.01	−0.04	9.96	− .02	0.01	+ .04	......	....
5	9.77	....	9.88	− .11	9.94	− .02	......	....
6	......	....	9.81	−0.21	9.89	− .04	......	....
7	......	....	......	....	9.84	− .06	......	....
8	......	....	......	....	9.81	−0.08	......	....
10	......	....	......	....	......	....	9.68	+0.14

The general relation of these results to spectral type and absolute magnitude is best seen by means of the diagram in Figure 2. This was prepared by plotting the data in Table X and reading from the resulting curves the values of M coresponding to integral values of the mass $\mathcal{M}$. These values of M were then plotted in the diagram of Figure 2, along with similar points on the dwarf branch, whose co-ordinates were derived from the second and last columns of Table IV. Through these points were drawn the full-line curves of the figure, which thus represent lines of equal mass.

The curves are highly irregular, the maximum near G0 followed by the minimum at K0–K5 being particularly noteworthy. Much of this disappears, however, when the ordinary visual absolute magnitude is replaced by the bolometric magnitude, which measures the total radiation and is therefore the quantity of physical significance. The reductions to bolometric magnitude (see following section) of interest here are

G0, −0.09; G5, −0.30; K0, −0.73; K5, −1.30; Ma, −1.60 mag.

---

[1] *Publications of the Astronomical Society of the Pacific*, **31**, 231, 1919.

The application of these corrections would practically remove the minima from the curves for all but the largest masses, and these

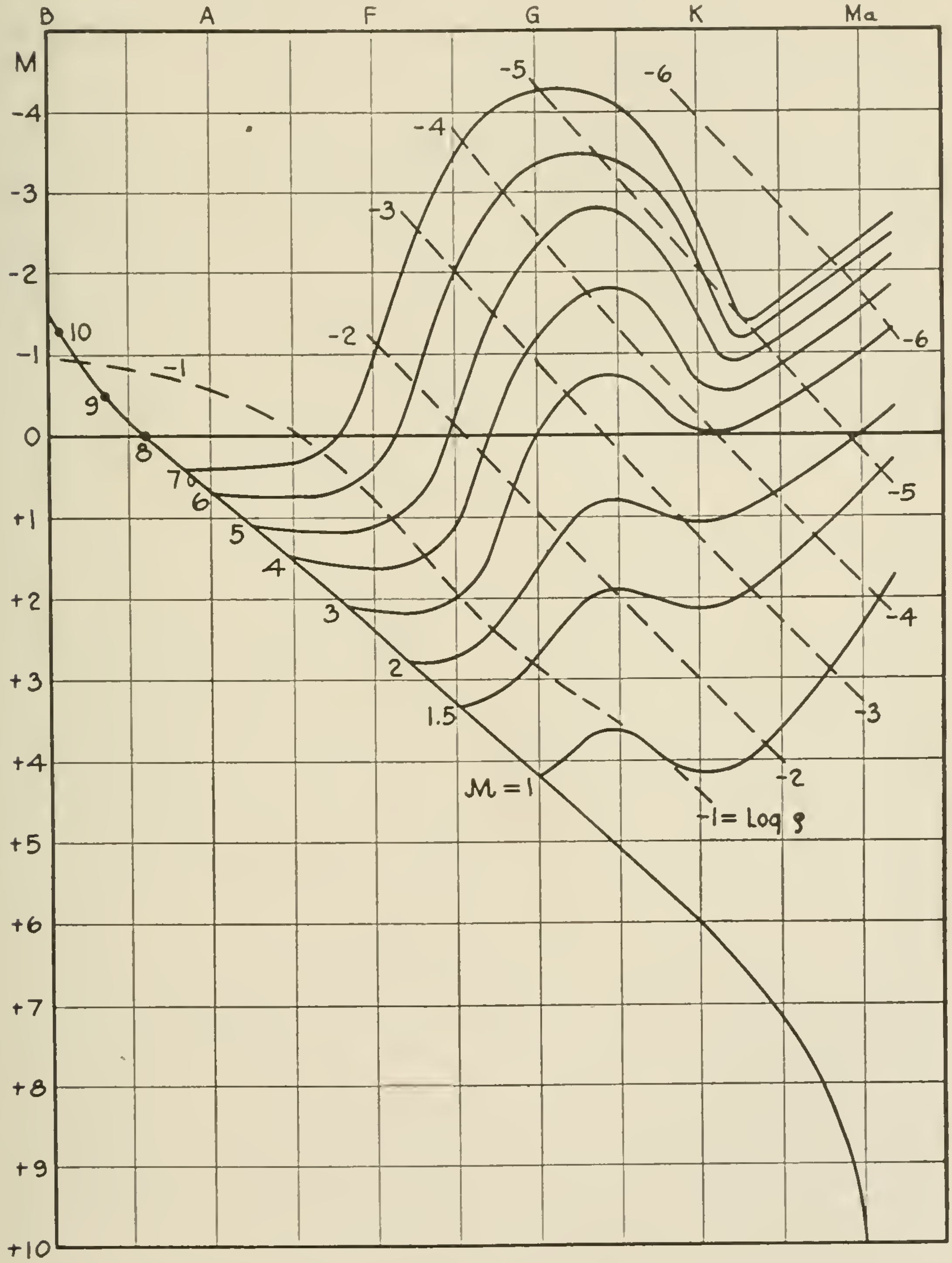

FIG. 2.—Distribution of mass (full-line) and mean density (broken curves) derived from the principle of equipartition. The full-line curve running downward to the right is the line of the maximum frequency of the dwarfs.

are relatively uncertain because they depend more or less upon extrapolations of the data in Table X.

To explain the derivation of the lines of equal density, which are also shown in Figure 2, it is necessary to consider the question of surface brightness.

10. SURFACE BRIGHTNESS

To derive values of surface brightness we may start from Stefan's law

$$E=\sigma T^4 \tag{13}$$

where E represents the total energy radiated per unit area of the surface of a star whose effective temperature is T. Let J be the integrated visual intensity, referred to the same unit of surface, and write $J=\alpha E$, whence

$$2.5 \log E=2.5 \log J-2.5 \log \alpha$$

and, by substitution into (13),

$$2.5 \log J-2.5 \log \alpha=2.5 \log \sigma+10 \log T.$$

Further, let M_B and j represent the total energy and surface brightness, respectively, expressed in magnitudes. The former is the bolometric absolute magnitude, while $M=-2.5 \log (J \times \text{Area})$ is the ordinary visual absolute magnitude. Since α is also the ratio of the visual energy to total energy received from the entire surface of the star,

$$-2.5 \log \alpha=M-M_B$$

and

$$j=M-M_B-10 \log T+\text{const.} \tag{14}$$

where the constant involves $\log \sigma$ and an additional constant depending on the zero point chosen for M_B. Eddington[1] has calculated values of the difference between the visual and bolometric absolute magnitudes $M-M_B$ for a range of temperatures including the normal classes of spectra. Through these values, which are based upon Nutting's measures of visual sensibility for the normal eye, j, by (14), becomes a simple function of T.

---

[1] *Monthly Notices*, 77, 605, 1917. Nutting's measures of visual sensibility, which are the basis of Eddington's calculation, are practically identical with the A.I.E. visibility-curve.

Results found by this equation may be checked by an equivalent formula derived by Hertzsprung in 1906. Starting from Planck's law and the visibility measurements of Langley, Abney, and others, he found[1]

$$j_H = +2.3\left(\frac{c}{T}\right)^{0.93} + \text{const.} \qquad (15)$$

in which c is the second constant in Planck's formula, for which the value adopted is 14300. Both (14) and (15) involve quadratures, and, starting as they do from entirely different observational data, independently discussed, provide an excellent numerical control. How close the agreement is may be seen from Table XI.

TABLE XI

SURFACE BRIGHTNESS AND TEMPERATURE

T	$M-M_B$	j	j_H	$j-j_H$
2540°	+2.59	+6.32	+6.32	0.00
3000	+1.71	+4.72	+4.68	+ 4
3600	+0.95	+3.17	+3.16	+ 1
4500	+0.35	+1.60	+1.58	+ 2
6000	0.00	0.00	0.00	0
7500	+0.02	−0.95	−0.93	− 2
9000	+0.12	−1.64	−1.62	− 2
10500	+0.31	−2.12	−2.09	− 3
12000	+0.53	−2.48	−2.45	−0.03

The values of $M-M_B$ have been taken directly from Eddington's table. The maximum difference between the results from the two formulae is only 0.04 mag., which is ample.

To connect these results with spectral type, Wilsing's spectral-photometric measures of the reciprocal temperature, c/T, of 199 stars[2] were plotted against their respective types. The ordinates (c/T) of the curve thus obtained are in the second column of Table XII. The corresponding effective temperature, T, and the surface brightness, j, calculated by the foregoing formulae and expressed in magnitudes ($\odot = 0.00$), are in the third and fourth columns, respectively.

---

[1] *Zeitschrift für wissenschaftliche Photographie*, **4**, 43, 1906.

[2] *Potsdam Publikationen*, No. 74, 1919.

With few exceptions, the stars in Wilsing's list are all giants whose mean absolute magnitudes, with sufficient approximation, may be assumed to be zero. To extend the results to other luminosities, use was made of the Mount Wilson color indices,[1] whose values are in the fifth and last columns of Table XII, those for the dwarfs corresponding to the mean absolute magnitudes in the column immediately preceding. The color indices were reduced to Schwarzschild's absolute system,[2] whose relation to effective temperature is known. This gave the relation between the Mount Wilson values and the temperature for both giants and dwarfs. Owing to various necessary assumptions the temperatures thus found for the giant stars differ slightly from the adopted values given in the first half of Table XII, and this systematic difference was made the basis for reducing the calculated temperatures for the dwarfs to the adopted system of Wilsing. The results, in

TABLE XII

SPECTRUM, EFFECTIVE TEMPERATURE, AND SURFACE BRIGHTNESS

Sp.	Giants, $M=0$				Dwarfs				
	c/T	T	j	MW CI	c/T	T	j	M	MW CI
B0	1.36	10500°	−2.28	−0.32	......	......	......	......	......
B5	1.43	10000	2.14	−0.17	......	......	......	......	......
A0	1.55	9230	1.89	0.00	......	......	......	......	......
A5	1.76	8110	1.45	+0.19	......	......	......	......	......
F0	2.04	7000	0.88	0.38	......	......	......	......	......
F5	2.35	6080	−0.26	0.62	2.35	6080	−0.26	+3.3	+0.62
G0	2.70	5300	+0.44	0.86	2.48	5770	0.00	4.4	0.72
G5	3.10	4610	1.24	1.15	2.60	5500	+0.25	5.2	0.83
K0	3.70	3860	2.41	1.48	2.93	4880	0.90	5.9	0.99
K5	4.37	3270	3.71	1.84	3.47	4120	1.96	7.1	1.26
Ma	4.65	3080	4.25	1.88	4.30	3330	+3.58	+9.8	+1.76
Mb	4.82	2960	4.58	+1.88	......	......	......	......	......
Mc	4.94	2890	+4.81	......	......	......	......	......	......

---

[1] These results, which have not hitherto been published, are still to be regarded as provisional. They take account of the important difference in color between giants and dwarfs, which cannot be disregarded in any discussion of the surface brightness of late-type stars. See *Mt. Wilson Comm.*, No. 59; *Proc. Nat. Acad. of Sciences*, 5, 232, 1919.

[2] *Göttingen Aktinometrie*, B, 29, 1912.

the sixth column of Table XII, were then used to compute the corresponding values of j as before.[1]

The difference in surface brightness between giants and dwarfs is large, and cannot be neglected. Unfortunately, the change in j with absolute magnitude is not well determined, for this must be inferred from the behavior of the color indices, and the data available at present do not extend to stars of the highest luminosity. This means that extrapolation will be necessary, and, in view of the consequent uncertainty, a simple linear relation of surface brightness to absolute magnitude has been used in the calculation of j for all values of M not appearing directly in Table XII.

The reliability of the foregoing results depends upon the possibility of representing the energy distribution in the spectra of stars of different types by means of the black-body radiation formula. It should be noted that it is not at all a question of agreement of the effective temperature, calculated from the radiation formula, with the true mean temperature of the radiating layers in the star's atmosphere. In general these will not agree. The stars are not perfect radiators; further, general and selective absorption deforms the energy-curve to such an extent that effective temperature cannot be an accurate measure of true temperature; but in the visible region the resultant curve seems to agree[2] approximately with a black-body curve, although not with the curve corresponding to the true mean temperature. That being the case, the surface brightness is immediately calculable by the foregoing formulae, provided the effective temperature corresponding to the deformed curve is employed for the computation; and it is of course just this temperature which is given by Wilsing's observations.

---

[1] The values of j in Table XII may be compared with Öpik, *Astrophysical Journal*, **44**, 296, 1916; Russell, *Publications of the Astronomical Society of the Pacific*, **32**, 307, 1920. Related questions are discussed by Wilsing, *Potsdam Publikationen*, No. 76, 1920; *Astronomische Nachrichten*, **214**, 185, 1921.

[2] See, for example, Wilsing, *Potsdam Publikationen*, No. 74, pp. 17, 18. The mean systematic deviations of the observed values of the energy at different points in the visual spectrum from Planck's formula are small. Further, Milne, *Monthly Notices*, **81**, 378, 1921, finds that the theoretical spectrum for non-selective absorption is practically identical with that corresponding to black-body radiation, the principal difference being a bodily displacement of the energy-curve, corresponding to a reduction of 3 per cent in the constant of Wien's displacement law.

The possibility of systematic error in the values of the temperature is more serious. Those for the B stars given in Table XII are almost certainly too small. The early-type stars in Wilsing's list are not numerous, and the dispersion in the values of c/T is large. In fact, the data would be almost equally well represented by assigning a temperature of 12,000° to B0, which would change j from -2.28 to -2.67. The value for B5 would also be slightly changed, but that for A0 can scarcely be modified without violence to the data.[1]

It will be noted that T for a G0 giant is nearly 500° lower than that for a dwarf of the same spectrum. Some question as to the reliability of Wilsing's measures has been felt because of the low value found for G0 stars as compared with the probable temperature of the sun. But the objects observed by him are giants; with proper allowance for the sun's absolute magnitude (4.85), the corresponding temperature from Wilsing's data would be about 5820°, which is not far from the values usually assigned, and indeed, agrees well with that derived by Abbot[2] from the solar constant (5860°).

A partial control of the values of j in Table XII is afforded by Pease's recent measures of the angular diameters of stars with the interferometer. In this connection, and for later use, it is convenient to insert at this point the following formulae, all easily derived, expressing relations between the various physical constants of a star: angular diameter (d), linear diameter (D), mass ($\mathcal{M}$), density (ρ), apparent (m) and absolute (M) magnitude, and surface brightness (j).

$$\log d = 0.2\,(j-m) - 2.061 \tag{16}$$

$$\log D = 0.2\,(j-m) - \log \pi - 0.030 \tag{17}$$

$$\log D = 0.2\,(j-M) + 0.970 \tag{18}$$

$$D = 107.4\,d/\pi \tag{19}$$

$$j = 5 \log d + m + 10.30 \tag{20}$$

$$\log \rho = \log \mathcal{M} - 3 \log R + 0.14 \tag{21}$$

$$\log \rho = \log \mathcal{M} + 0.6\,(M-j) - 2.77 \tag{22}$$

---

[1] See also Rosenberg, *Abhandlungen der Kaiserl. Leop.-Karol. deutschen Akademie der Naturforscher*, 150, No. 2, 1914.

[2] *Op. cit.*, p. 114.

These formulae give d in seconds of arc, D and $\mathcal{M}$ in terms of the solar diameter and mass, and j in magnitudes, the value for the sun being 0; the unit for ρ is the density of water. The numerical constants depend upon the following data for the sun: $D=865{,}000$ miles, $d=1920''$, distance from earth 92,930,000 miles, $m=-26.72$, $M=+4.85$. Equations (16) and (17) are the equivalent of formulae already given by Russell.[1]

Proceeding now to a comparison with the results of Pease's measures, we have the data in Table XIII. The "observed" values of j derived from the angular diameter by (20) are in the sixth line of the table. Immediately below are the calculated results interpolated from Table XII. It seems unlikely that the mean systematic difference for O−C will exceed one- or two-tenths of a magnitude. The effect of darkening at the limb has not been taken into account, either in the measures of d or in the calculation of j. Nor has the question of a possible differential effect from this source upon the observed and calculated values of j been considered, for it is evident that this cannot be large.

TABLE XIII

COMPARISON WITH MEASURED ANGULAR DIAMETERS*

	α Orionis	α Boötis	α Scorpii
Sp.	Ma	Ko	Map
m	+0.9	+0.2	+1.2
π	0.″020	0.″095	0.″0085
M	−2.6	+0.1	−4.2
d (Pease)	0.″047	0.″022	0.″040
Obs. j, equation (20)	+4.6	+2.2	+4.5
Cal. j, Table XII	+4.4	+2.4	+4.5
O−C	+0.2	−0.2	0.0
Obs. D, equation (19)	252	25	506
Cal. D, equation (18)	235	27	513
Approx. $\mathcal{M}$ (Fig. 3)	8	3	15
Approx. log ρ (Fig. 3)	−6.2	−3.8	−6.6

* Michelson and Pease, *Mt. Wilson Contr.*, No. 203; *Astrophysical Journal*, **53**, 249, 1921. Pease, *Publications Astronomical Society of the Pacific*, **33**, 171, 204, 1921. The parallax of α Scorpii assumes it to be a member of the Scorpius group. The other two parallaxes are weighted mean values.

It is of interest, further, to compare the values for the linear diameters calculated from the measured angular diameter by (19) with those derived from (17) or (18) with the aid of the adopted values of j. The results are in the third and fourth lines from the bottom of table. On the whole, Pease's measures afford an excellent confirmation of the surface brightness found for late-type stars of high luminosity, and at present there seems to be no observational evidence which would justify a modification of the values adopted.[1]

---

[1] *Publications of the Astronomical Society of the Pacific*, **32**, 307, 1920.

11. DISTRIBUTION OF DENSITY

The densities are now easily calculated by equation (22) with the aid of values of j from Table XII. The results for stars on the dwarf branch, including the B's, are in the fourth column of Table XIV, which also gives values for the mean linear diameters D found by (18).

TABLE XIV

LUMINOSITY, MASS, MEAN DENSITY, AND DIAMETER

(Units for $\mathcal{M}$ and D are values for sun; for ρ, that of water)

Sp.	Dwarf Branch				Giants, $M=0$			Giants, $\mathcal{M}=10$		
	M	$\mathcal{M}$	ρ	D	$\mathcal{M}$	ρ	D	M	ρ	D
B0	−1.60	10	0.04^5	6.8	.....	....	3.2	−1.2	0.08	6
B5	−0.20	8.3	0.20	3.8	8.2	0.26	3.5	−1.8	0.03	8
A0	+0.70	6.0	0.36	2.8	7.0	0.16	3.9	−2.4	0.008	12
A5	+1.50	4.0	0.40	2.4	5.6	0.071	4.8	−3.1	0.002	20
F0	+2.40	2.5	0.40	2.0	4.3	0.025	6.2	−3.6	0.0004	32
F5	+3.35	1.5	0.39	1.8	3.2	0.0078	8.3	−4.0	0.0001	52
G0	+4.35	1.0	0.68	1.26	2.6	0.0025	11.5	−3.9	0.00002	83
G5	+5.20	0.76	1.2	0.96	2.8	0.00087	17	−3.3	0.00001	102
K0	+6.00	0.68	1.3	0.89	3.0	0.00018	28	−2.3	0.00001	107
K5	+7.20	0.62	1.4	0.83	2.6	0.000026	51	−2.2	0.000002	182
Ma	+9.80	0.59	5.4	0.54	2.0	0.0000096	66	−3.0	0.0000006	288

For the determination of the equal-density lines (dotted) shown in Figure 2, values of M were read from each mass line in the diagram for every half-interval of spectrum. The use of (22) then gave the values of log ρ corresponding to each of these points in the sequence of spectral type. Plots of these results—log ρ against spectrum—then led to a series of curves, one for each integral value of the mass (also one for $\mathcal{M}=1.5$), from which were read spectral types corresponding to integral values of log ρ. The corresponding points were marked on the diagram and connected by the dotted lines shown in the figure.

---

[1] Mr. Pease has kindly placed at my disposal provisional results for three other stars. The observed and theoretical values of j and d, or D, are here also in excellent agreement, although the accidental deviations are larger than those shown in Table XIII.

Within the limits considered, and with the exception of that for $\log \rho = -1$, the curves of equal density are sensibly linear; the regularity of their spacing is remarkable. Including the line for $\log \rho = -1$ from A5 onward through the later types, the mean density corresponding to any given spectrum and absolute magnitude is represented by the formula

$$\left.\begin{array}{c} \log \rho = -1.22\, S + 0.57\, M + 1.11 \\ (S = 0 \text{ for B0, 1 for A0, etc.}) \end{array}\right\} \tag{23}$$

with a probable error of about 15 per cent, over a range in ρ extending from 0.1 to 0.000001.

The question now arises as to what means can be found for testing the validity of these results. Some control is obviously necessary, for with the exception of the masses and densities along the dwarf branch, the whole scheme of mass and density distribution depends upon the assumed applicability of the principle of equipartition. In this connection, the eclipsing variables, many of which are known to be of exceptionally low density, immediately suggest themselves as suitable for a test. The weak point, however, is that we do not know their absolute magnitudes, except in a very few cases. Any attempt to use hypothetical absolute magnitudes fails, because it involves an assumption for the mass, and this, as shown by (22), is equivalent to a direct assumption for the density.

Some general indications, however, can be obtained. With slight revisions of spectral classification, Shapley's data[1] for the densities of eclipsing variables give the following mean values:

Sp.	ρ	No. Stars
B6	0.12	15
A0+	0.20	48
F(dwarfs)	0.35	9

For these groups of B and A stars the values of $\log \rho$ are -0.9 and -0.7, respectively. From Figure 2 the corresponding values of M are seen to be -0.6 and $+0.2$. These are of the order to be expected, and are obviously possible values. The value $\rho=0.35$ for the F-type dwarfs agrees closely with that found here for F5, namely, 0.39. For the dwarfs the dispersion in absolute magnitude is so small that lack of knowledge of the luminosities gives rise to no appreciable error.

---

[1] *Contributions from Princeton University Observatory*, No. 3, p. 124, 1915.

These results are all satisfactory, as far as they go, but they do not reach that part of the diagram which is involved in the greatest doubt, namely the region of very high luminosity and exceptionally low density. On the other hand, if the validity of the mass and density distribution can once be established, the densities of the eclipsing variables should give a reliable determination of their distances. Fortunately, the uncertainty can be removed to a large extent with the aid of the Cepheid variables.

12. REVISION OF MASSES AND DENSITIES BY MEANS OF CEPHEID VARIABLES

There are still difficulties connected with the pulsation hypothesis as a means of explaining Cepheid variation, although there seems little doubt that, in some form or other, it must be used to account for the changes in brightness of these stars. That being the case, the mean density must vary inversely as the square of the period. Hence[1]

$$\log \rho = -2 \log P + \text{const.} \tag{24}$$

Further, the period-luminosity relation[2]

$$M = f\,(P) \tag{25}$$

---

[1] The exact form of the relation of density to period as applied to Cepheids is possibly open to some question. Emden, *Gaskugeln*, p. 451, 1907, finds for ellipsoidal oscillations of a polytropic gas sphere

$$P \propto (m\,\rho)^{-\frac{1}{2}}$$

where m is the order of the harmonic oscillation; the important vibration corresponds to $m=2$. Eddington, *Monthly Notices*, **79**, 2, 1918; 177, 1919, discusses pulsations which are symmetrical about the star's center and finds a result equivalent to (24), with the exception that the constant is replaced by a slowly varying function of the specific heats and the ratio of radiation-pressure to gravitation, the latter increasing with the mass. For a first approximation we may adopt (24).

[2] Shapley, *Mt. Wilson Contr.*, No. 151; *Astrophysical Journal*, **48**, 89, 1918.

determines the absolute magnitude. With M and the spectral type as arguments, log ρ and $\mathcal{M}$ can be interpolated from the mass-density diagram. Then,

a) The interpolated values of log ρ may be compared with those calculated by (24), the constant being adjusted to give the best representation of the densities of the entire group of stars. Since the range in ρ as determined by (24) is from about 0.1 to 0.00001, the control on the densities should be effective.

b) Having determined the constant in (24), we may write (22) in the form

$$\log \mathcal{M} = -2 \log P - 0.6\,(M-j) + \text{const.} \tag{26}$$

which expresses the mass of a Cepheid variable as a function of its period and surface brightness, for, by (25), M is a function of the period alone. The values of $\mathcal{M}$ interpolated from the diagram may be compared with those calculated by (26). This checks the distribution of mass.

c) Finally, with spectral type and log ρ calculated from (24), we may interpolate M from the diagram. The absolute magnitudes thus found may then be compared with the period-luminosity relation (25). This is not an independent test, but exhibits the results of (*a*) in a different form.

Because of the enormous range in the density, the application of these tests will mean little except in the case of stars of accurately determined spectra. This makes trouble at once, for the type of a Cepheid, in so far as determined from the hydrogen lines at least, varies with its brightness, as was first clearly shown by Pease's[1] observations of RS Boötis. Isolated determinations of spectrum based on the appearance of these lines are therefore unsuitable for the comparisons. Adams and Joy,[2] on the other hand, have shown that many spectral characteristics change little or not at all as the light of the star varies; their "estimated" spectral classes are practically independent of phase.

---

[1] *Publications of the Astronomical Society of the Pacific*, 26, 256, 1914.

[2] *Mt. Wilson Comm.*, No. 53; *Proceedings of the National Academy of Sciences*, 4, 129, 1918.

The list of spectroscopic parallaxes[1] includes twenty-nine Cepheids for which estimated types are available. One of these, RY Boötis, although usually classed as a Cepheid, does not show Cepheid spectral characteristics and has an absolute magnitude at variance with that derived from the period-luminosity relation. Further, three cluster-type Cepheids, SU Aurigae (8.7), SU Draconis (9.2), and SW Draconis (10.0), and the long-period Cepheid V Vulpeculae (8.6) are so faint that the types assigned are less certain than the others. The classification of faint stars, observed with low dispersion, is likely to be influenced to some extent by the hydrogen lines. The case of V Vulpeculae, moreover, is peculiar. The light-curve is irregular; and the period-luminosity relation leads to a value of M which not only differs widely from that derived from the spectrum, but falls outside the limits of the mass-density diagram. These five stars were therefore excluded,[2] leaving a total of twenty-four.

These data are supplemented by Shapley's[3] results for twenty Cepheids, based on systematic observations of spectral characteristics that do vary with the changes in light. The median value of the type, which was used for the discussion, is about 0.3 of a spectral interval earlier than the estimated spectrum.

This difference will lead to different values of the constants in the foregoing formulae, unless the value of M and the spectral type are referred to the same phase. Thus, the estimated type agrees with the hydrogen-line type at, or very near, the time of minimum brightness (estimated *minus* hydrogen-line type at minimum $= -0.1$ spectral interval). Hence for the comparisons, the minimum, and not the median M (the period-luminosity relation gives the latter), should be associated with the estimated spectra. The simplest procedure, however, is to use the median M and subtract 0.3 of an interval from the estimated spectra before making interpolations from the diagram. Sixteen stars are common to the two lists, but owing to the different methods of classification used, the duplicate observations have been treated as separate stars.

---

[1] *Mt. Wilson Contr.*, No. 199; *Astrophysical Journal*, **53**, 13, 1921.

[2] It was not noted until after the comparisons had been finished that, on the criterion of brightness, W Serpentis (9.0) should also have been excluded.

[3] *Mt. Wilson Contr.*, No. 124; *Astrophysical Journal*, **44**, 273, 1916. In general the means of the limiting values of the type as given by Shapley have been adopted. Deviations from this rule occur in a few cases where the distribution of the observations is such that the mean does not correspond to median brightness of the variable.

The results of the application of tests (*a*), (*b*), and (*c*) are summarized in Table XV, which gives the range in log ρ, log $\mathcal{M}$, and M over which the comparisons were made, and the average differences resulting therefrom. Thus, on the basis of estimated spectra, formula (24) represents the density distribution in Figure 2 over a range in log ρ from -1.1 to -4.8, with an average difference of ± 0.15. Similarly, the values of M interpolated from the diagram in the interval -0.3 to -4.7 agree with those from the period-luminosity relation within ± 0.30 mag. We conclude at once that the masses and densities derived with the aid of the principle of equipartition are of the right order of magnitude, at least as far as type G3, which is the latest occurring among the Cepheids used.

TABLE XV

REPRESENTATION OF MASSES AND DENSITIES
EQUATIONS (24) TO (26) AND FIGURE 2

TEST	RANGE	AVERAGE DIFFERENCE	
		Est. Sp.	H.L. Sp.
(*a*) log ρ......	-1.1 to -4.8	± 0.15	± 0.18
(*b*) log $\mathcal{M}$.....	0.46 to 1.28	0.15	0.16
(*c*) M........	-0.3 to -4.7	± 0.30	± 0.32

A classification of the differences in log ρ and log $\mathcal{M}$ according to M, which is also more or less a classification according to spectrum, revealed, however, the presence of systematic divergences. These run from about -0.18 (at $M = -0.7$, A8) to $+0.18$ (at $M = -3.8$, F8) in the logarithms of both quantities. The algebraic signs mean that the range of mass in Figure 2, for a given interval in M, is too small, that the masses of the most luminous Cepheids are larger, and those of less luminous stars smaller, than the values given by the diagram. The density lines, on the other hand, are too closely spaced.

These differences were made the basis of a readjustment of the lines of mass and density. The percentage divergence in ρ and $\mathcal{M}$

is the same, as it must be by (22), but since the scale for $\mathcal{M}$ is much larger than that for ρ (in passing from one curve to the next the mass changes by one unit while ρ changes tenfold), the adjustments were made in the mass-curves, the densities being computed by (22) as before. The masses and densities along the dwarf branch, of course, remain unchanged.

The result of several trials is the diagram shown in Figure 3. A repetition of tests (*a*), (*b*), and (*c*) gave the differences shown in the last six columns of Table XVI, the first column under each of the headings log ρ, log $\mathcal{M}$, and M referring to estimated spectra, the second to those based on the hydrogen lines. The average differences have been reduced to about two-thirds their original values, while the run in the differences has disappeared. Thus for four groups of eleven stars each, the mean systematic values are:

M	-1.0	-2.1	-2.7	-3.6
Sp	F0	F6	F7	F8
log ρ	-0.01	-0.03	$+0.02$	$+0.02$
log $\mathcal{M}$	-0.02	-0.01	-0.04	0.00

The comparison of the interpolated values of M with the period-luminosity relation is shown graphically in Figure 4.

In this connection it will be noted that values of M interpolated from the diagram with log ρ and the type as arguments are sensitive to uncertainties in the spectra. The relations are such that the average difference ±0.2 in M (Table XVI) corresponds to 0.1 of a spectral interval (see equation [23]). The normal uncertainty of classification therefore accounts for nearly all the deviation shown by individual stars in Figure 4.

The principal change in the diagram has been the depression of the mass-curves near G0 and the change in their curvature in the region of the early types. Since the data for the Cepheids do not extend beyond G3, the lines through types G to M have been left much as in the original diagram. As will be seen later, there is some evidence favoring the reality of the minimum near K0. If the reductions to bolometric magnitude given on page 194 be applied, the variation of mass with spectrum becomes fairly

TABLE XVI

Masses and Densities of Cepheid Variables

Star	Spectrum		P	Calculated				Calculated *minus* Fig. 3					
	Est.	H.L.		M	$\log \rho$	$\mathcal{M}$		$\log \rho$		$\log \mathcal{M}$		M	
α Ursae Minoris	F9	....	3.97	−1.8	−3.10	5.0		+0.01		+0.03		0.0	
TU Cassiopeiae	....	F4.5	2.14	−1.2	−2.56		5.5		+0.08		+0.11		−0.1
SU Cassiopeiae	F4	F1.5	1.95	−1.2	−2.48	3.0	2.9	−0.17	−0.09	−0.22	−0.24	+0.4	+0.3
SZ Tauri	F8p	F6	3.15	−1.6	−2.90	4.6	4.4	+0.01	+0.09	0.00	−0.01	0.0	−0.3
RX Aurigae	F9p	....	11.63	−3.4	−4.04	5.2		−0.18		−0.21		+0.3	
T Monocerotis	G1p	F8.5	27.01	−4.7	−4.76	13.8	13.2	0.00	+0.03	+0.06	+0.04	0.0	−0.1
RT Aurigae	F8p	F5	3.73	−1.8	−3.04	5.0	4.8	−0.03	−0.05	+0.02	−0.01	0.0	+0.1
W Geminorum	G0p	F6.5	7.92	−2.8	−3.70	5.8	5.5	+0.01	−0.06	−0.07	−0.09	0.0	+0.1
RS Boötis	....	A4	0.38	−0.3	−1.06		9.6		+0.18		+0.17		−0.2
ζ Geminorum	G0p	....	10.15	−3.2	−3.92	6.0		−0.06		−0.12		0.0	
X Sagittarii	F9p	F5	7.01	−2.6	−3.60	4.8	4.6	−0.14	−0.21	−0.12	−0.15	+0.3	+0.5
Y Ophiuchi	....	F9	17.11	−4.0	−4.36		14.4		+0.13		+0.16		−0.2
W Sagittarii	G0p	F6	7.60	−2.7	−3.66	5.5	5.2	0.00	−0.12	−0.07	−0.10	0.0	+0.3
Y Sagittarii	G2p	F9	5.77	−2.3	−3.42	9.6	9.1	+0.24	+0.27	+0.24	+0.22	−0.5	−0.5
U Sagittarii	G0p	....	6.74	−2.5	−3.56	6.0		0.00		0.00		0.0	
YZ Sagittarii	G1p	....	9.55	−3.1	−3.86	9.1		+0.05		+0.08		−0.2	
TT Aquilae	G2p	....	13.75	−3.6	−4.18	11.5		+0.13		+0.11		−0.3	
RR Lyrae	F0p	A5.5	0.57	−0.4	−1.42	6.6	6.3	+0.09	+0.02	+0.09	+0.03	−0.2	−0.1
U Aquilae	G0p	F9	7.02	−2.6	−3.60	5.5	5.2	+0.01	+0.19	−0.05	−0.07	0.0	−0.4
XZ Cygni	....	A3	0.47	−0.3	−1.24		5.5		−0.10		−0.08		+0.2
U Vulpeculae	G0p	F7	7.99	−2.8	−3.70	5.8	5.5	+0.01	−0.01	−0.07	−0.09	0.0	0.0
SU Cygni	F7p	F4	3.85	−1.8	−3.08	3.5	3.3	−0.17	−0.19	−0.16	−0.18	+0.3	+0.4
η Aquilae	F9p	F7	7.18	−2.6	−3.62	4.6	4.4	−0.11	−0.03	−0.14	−0.15	+0.3	+0.1
S Sagittae	G1p	F8.5	8.38	−2.9	−3.74	7.9	7.6	+0.12	+0.15	+0.06	+0.04	−0.2	−0.3
X Cygni	G3p	....	16.38	−3.9	−4.32	19.0		+0.24		+0.28		−0.5	
T Vulpeculae	F9	F5	4.44	−2.0	−3.20	5.2	5.0	+0.01	−0.11	+0.02	−0.02	0.0	+0.2
δ Cephei	G0	F6	5.37	−2.2	−3.36	6.3	6.0	+0.05	−0.07	+0.08	+0.05	−0.1	+0.1
W Serpentis	F9p	....	14.15	−3.7	−4.20	6.3		−0.19		−0.16		+0.4	
Average difference	....	....	....	....	....	....		$\pm0.08^{5}$	±0.11	±0.10	±0.10	±0.17	±0.22

regular, the course of the topmost line ($\mathcal{M}=10$) being indicated by the dotted curve in Figure 3.

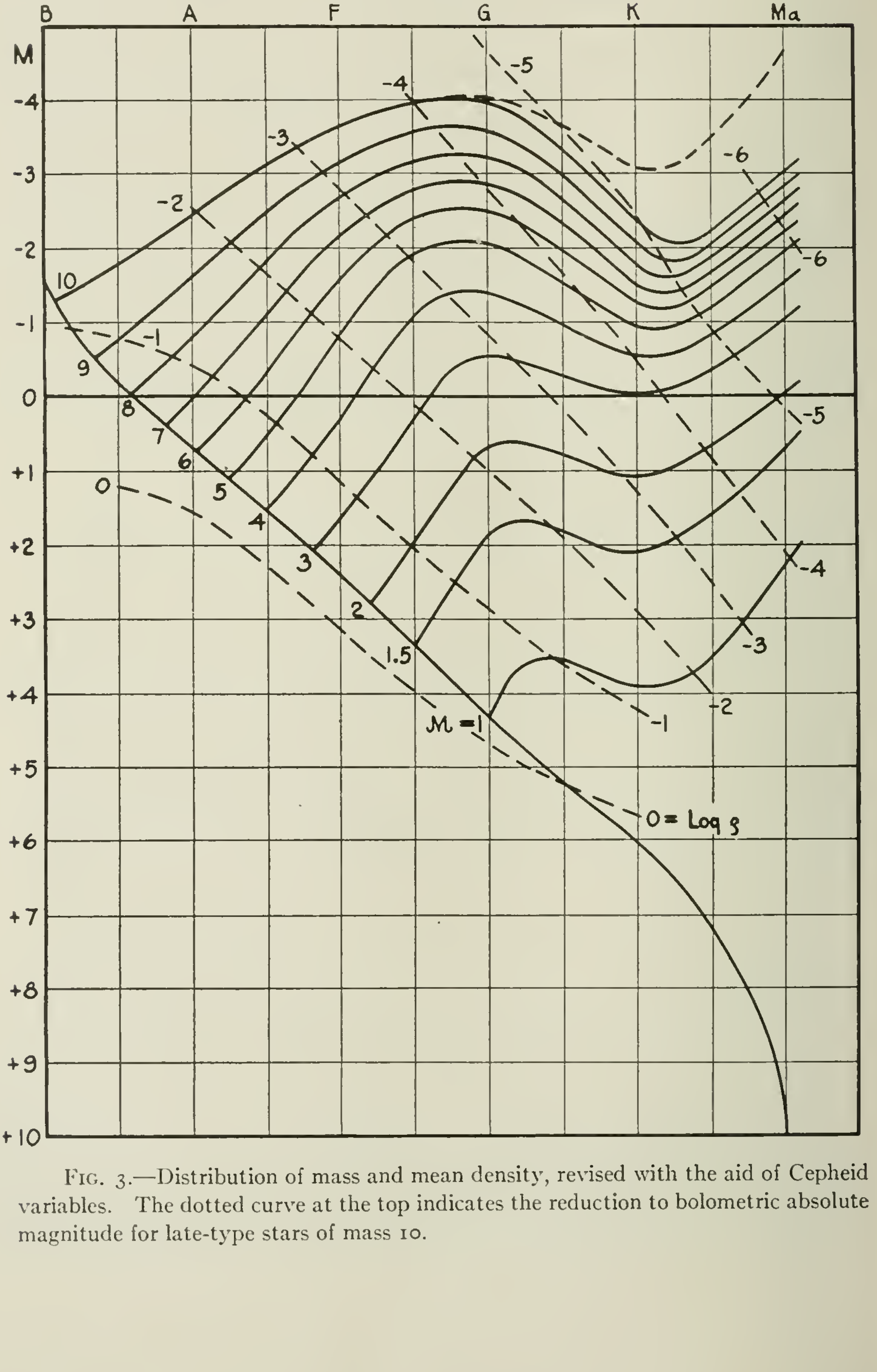

FIG. 3.—Distribution of mass and mean density, revised with the aid of Cepheid variables. The dotted curve at the top indicates the reduction to bolometric absolute magnitude for late-type stars of mass 10.

The curves of equal density are little changed. They still remain sensibly linear, but are no longer so closely parallel. Formula (23) has not wholly lost its applicability, for it still expresses approximately the relation of density to spectrum and absolute magnitude, though less accurately than before.

It will be noted that the densities along the dwarf branch are consistent with the values demanded by the density-distribution defined by the lines log $\rho = 0, -1, -2$, etc. In other words, if we interpolate, say, for the value log $\rho = -0.4$ ($\rho = 0.4$) along the line $\mathcal{M} = 6$, we find the point where it belongs, namely, on the dwarf branch. This detail is of some importance because it shows that the constants in the formulae for log ρ and log $\mathcal{M}$ have been correctly determined. The spacing of the lines is fixed by the periods of the variables; their position as a group, by the condition that they must be consistent with the densities adopted for the dwarfs, whose values are independent of any assumption as to equipartition.

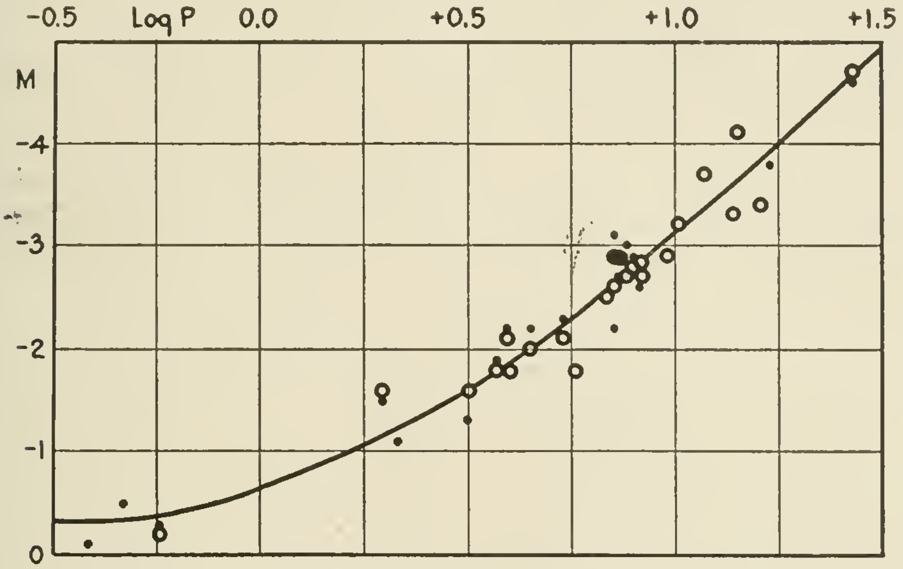

FIG. 4.—Absolute magnitudes of Cepheids interpolated from Fig. 3 with spectral type and log ρ from equation (24) as arguments. Circles, "estimated" spectra by Adams; points, hydrogen-line spectra by Shapley. The curve is Shapley's period-luminosity relation.

Presumably the diagram in Figure 3 is to be preferred to that in Figure 2. Certainly that is the case when Cepheid variables are concerned; and it seems likely that this holds also for the stars at large. The mass lines in Figure 2 pass *through* the points defined by the energy-constant and the velocities; no allowance for observational uncertainty by smoothing between the types was attempted; and with the exception of the terminal points on the dwarf branch everything preceding F5 is an extrapolation. On the other hand, an assumption of comparability is here involved, and it is perhaps worth remarking that if we reject the original diagram, we may thereby exclude relations between mass, density, luminosity, temperature, etc., which differentiate stars of constant light from Cepheid variables.

In view of the tentative character of the results, a detailed tabulation of the mass and density relations is unnecessary; Figure 3 will answer all practical purposes to which the results can be adapted. The data for the dwarf branch given in the first part of Table XIV, which are the most reliable, have already been referred to. To these have been added, by way of numerical illustration, results for the giants of zero absolute magnitude and for those whose masses are equal to 10.[1]

As a further illustration, the masses and densities corresponding to the spectra and absolute magnitudes of the individual stars measured by Pease with the interferometer have been given in the last lines of Table XIII. As a source of error, the values of M for these stars are probably as serious in respect to mass and density as the uncertainties of Figure 3 itself. Equation (22) shows that an error of 0.5 in M means an uncertainty factor of 2 in the density, whereas it seems unlikely that values from the diagram should be in error by so large an amount. In the case of an individual star, dispersion may of course enter, since the diagram gives mean values; but the probability of the occurrence of large deviations from the mean is small.

---

[1] Since the displacement of spectral lines required by relativity is proportional to $\mathcal{M}/R$ (R=radius of star) the results in Table XIV have a direct bearing on this question. The values of $\mathcal{M}/R$ do not run parallel to those of the K-term. Hence this term cannot be wholly identified with the relativity displacement, although the latter may of course be involved. As an illustration, the K-term for the B stars is about four times that for the A's. The ratio of the displacements on the other hand would be about 1.3. The most extreme deviation, however, is found by comparing the B's with the giant M stars. Their K-terms are of the same order of magnitude, whereas the red-displacement of the lines in M stars should be of the order of 0.01 that of the B's. See footnote No. 2, p. 191.

13. ON DISPERSION IN THE MASSES OF CEPHEIDS

From Shapley's work it appears that, for the variables in globular clusters at least, the deviations in M from the values determined by the period-luminosity relation are of the same order as the observational errors in the apparent magnitudes,[1] which of course must be used for any comparison. Practically, therefore, M is uniquely determined by P. Hence, by (26), the dispersion in the mass is related to that arising from such differences in j as may be associated with the same value of P, and it is an observational fact that the latter are small.

Direct evidence is also afforded by the comparison of the values of $\mathcal{M}$ for the Cepheids calculated by (26) with those interpolated from Figure 3. The average difference in log $\mathcal{M}$ is ± 0.10, corresponding to about 25 per cent in $\mathcal{M}$. But what part of this may be attributed to uncertainty in the spectrum?

With proper allowance for the systematic difference of 0.3 between the hydrogen line and estimated spectra, the internal agreement is such as to indicate an average uncertainty of 0.05 of an interval. Assume an adopted value of the type to be too late by this amount. From (26)

$$\text{Mod. } \frac{d\mathcal{M}}{\mathcal{M}} = +0.6\, dj. \tag{27}$$

For the region F0–G0, j increases about 0.07 for the assumed increase in the spectrum. Hence, the calculated $\mathcal{M}$ will be 10 per cent too large. On the other hand, we find from Figure 3, for F5, $M = -2.5$, as an average, that the same error in the spectrum leads to an interpolated $\mathcal{M}$ about 3 per cent too small. The resulting errors are in opposite directions; whence, in the difference, the uncertainty becomes 13 per cent.

This average percentage error, combined with the dispersion and the errors of interpolation, must equal the average deviation of 25 per cent from the mean masses of the diagram. Neglecting the interpolation errors, whose inclusion would make the dispersion still smaller, we find the probable dispersion $r(\mathcal{M})=19$ per cent. As far as the evidence goes, we should therefore expect one-half the Cepheids to have masses lying between 0.8 and 1.2 times the mean mass. Since the Cepheids are a very special class of objects, it would be too much to assume that this result holds for all classes of stars (see Section 7).

---

[1] *Mt. Wilson Contr.*, No. 151, p. 26; *Astrophysical Journal*, 48, 114, 1918.

14. MASSES AND DENSITIES OF CEPHEID VARIABLES

The calculated values of the masses and densities used for the comparisons with the diagram of Figure 3 have been collected in the sixth and seventh columns of Table XVI, while their deviations from the adopted distribution are in the following columns. The formulae used are:

$$\log \rho = -2 \log P - 1.90 \tag{29}$$

$$\log \mathcal{M} = -2 \log P - 0.6\,(M-j) + 0.87 \tag{30}$$

in which the constants are the means for the two sets of data, the individual values differing by only 0.02. In case the spectral type is the median value derived from the hydrogen lines, the median value of M, given directly by the period luminosity relation, is to be used. For estimated spectra, the minimum M is required, although it is simpler to subtract 0.3 from the estimated spectrum and use the median M.

The values of both density and mass depend upon the assumed constancy of the numerical term in (29), but this assumption apparently leads to results of the right order, although for stars of short period the percentage deviation may be considerable.

For individual stars the calculated values are probably to be preferred to those interpolated from Figure 3. This follows not merely because of the dispersion in mass, but also because the differences for stars having determinations based on both estimated and hydrogen-line spectra are almost always of the same sign. This indicates real deviations from the mean distribution, in addition to those arising from the unavoidable errors of spectral classification. In such cases the values from (29) and (30) are likely to be nearer the truth than those derived from the diagram.

The results in Table XVI, both calculated and interpolated, may be compared with the masses and densities derived by Eddington[1] for certain Cepheids on the basis of his theory of radiative equilibrium. The agreement shown by Table XVII is remarkable when it is considered that the two methods approach the problem from entirely different directions. There are a few cases of serious discordance, and some systematic divergence, but nothing so large as might have been expected. The agreement with (29) has been commented upon by Eddington himself.

TABLE XVII

COMPARISON WITH EDDINGTON'S RESULTS FOR CEPHEID VARIABLES

STAR	MASS			MEAN DENSITY		
	Eddington	Eq. (30)	Fig. 3	Eddington	Eq. (29)	Fig. 3
Y Ophiuchi	13.0	14.4	10	0.000080	0.000044	0.000032
ζ Geminorum	7.4	6.0	7.9	.00046	.00012	.00014
S Sagittae	6.1	7.8	6.9	.00019	.00018	.00013
W Sagittarii	5.5	5.4	6.5	.00041	.00022	.00025
η Aquilae	5.2	4.5	6.2	.00033	.00024	.00028
X Sagittarii	5.1	4.7	6.4	.00025	.00025	.00038
Y Sagittarii	4.3	9.4	5.5	.00027	.00038	.00021
δ Cephei	4.0	6.2	5.3	.00052	.00044	.00045
T Vulpeculae	3.6	5.1	5.1	.00072	.00063	.00071
SU Cygni	3.1	3.4	5.0	.00160	.00083	.0013
RT Aurigae	3.0	4.9	4.8	.00110	.00091	.0010
SZ Tauri	2.8	4.5	4.5	.0015	.0013	.0011
SU Cassiopeiae	2.3	3.0	5.0	.0028	.0033	.0045
RR Lyrae	1.7	6.4	5.6	0.015	0.038	0.033

The geometrical mean mass of the twenty-four Cepheids in Table XVI is 6.2, which happens to agree almost exactly with that derived from the principle of equipartition. This can scarcely be more than accidental, however, for the velocities of only fifteen of these stars are available.

---

[1] *Monthly Notices*, **79**, 5, 1918.

15. AVERAGE HEAT CONTENT AND CEPHEID VARIATION

On the basis of the theory of radiative equilibrium Eddington[1] finds for the central temperature of a star

$$T_c \propto \rho^{\frac{1}{3}} \mathcal{M}^{\frac{2}{3}} \beta m \tag{31}$$

where ρ is the mean density, β the ratio of radiation pressure to gas pressure, and m the atomic weight which is here assumed to be constant. The formula may also be written

$$T_c \propto \frac{\beta \mathcal{M}}{R} \tag{32}$$

R being the radius. $R = D/2$ is given by (18) or an equivalent expression; β is a function of $\mathcal{M}$, and $\mathcal{M}$ in turn appears in his formulae as a function of the luminosity alone, which can be obtained from (25). T_c can therefore be calculated for any star. For thirteen Cepheids with periods ranging from 2 to 17 days Eddington[2] finds that T_c/β is sensibly constant. There are accidental deviations, but no progressive change. Moreover, for two theoretical stars with periods of 4.5 and 30.8 days the values of T_c/β are practically identical. This suggests as a possible condition for Cepheid variation

$$\frac{\mathcal{M}}{R} = \text{const., or } \rho \mathcal{M}^2 = \text{const.} \tag{33}$$

Since $\mathcal{M}^2/R$ is proportional to the total heat-content of a star,[3] the physical significance of (33) is that the average heat-content per unit mass is a constant, or, in another form, that the gravitational potential at the surface of the star is constant for the Cepheids. Shapley[4] has discussed this condition from the standpoint of the relation of period to absolute magnitude and finds agreement with the observed period-luminosity relation (25). We may proceed somewhat differently by combining (24) and (26) in accordance with (33). This gives the theoretical period-luminosity relation

$$M = -5 \log P + j + \text{const.} \tag{34}$$

---

[1] *Monthly Notices*, **77**, 601, 1917.

[2] *Ibid.*, **79**, 5, 1918; 181, 1919.

[3] Jeans, *Problems in Cosmogony*, p. 191, 1919.

[4] *Mt. Wilson Contr.*, No. 190, p. 7; *Astrophysical Journal*, **52**, 79, 1920.

A comparison of the values of M from (34) for the twenty-eight stars in Table XVI with those from the observed relation, (25) above, gives results which are shown graphically in Figure 5. The agreement is not good, the divergence amounting to about a magnitude between $\log P = 0.25$ and 1.5, with even larger differences for the cluster-type Cepheids, which are not shown in the diagram.

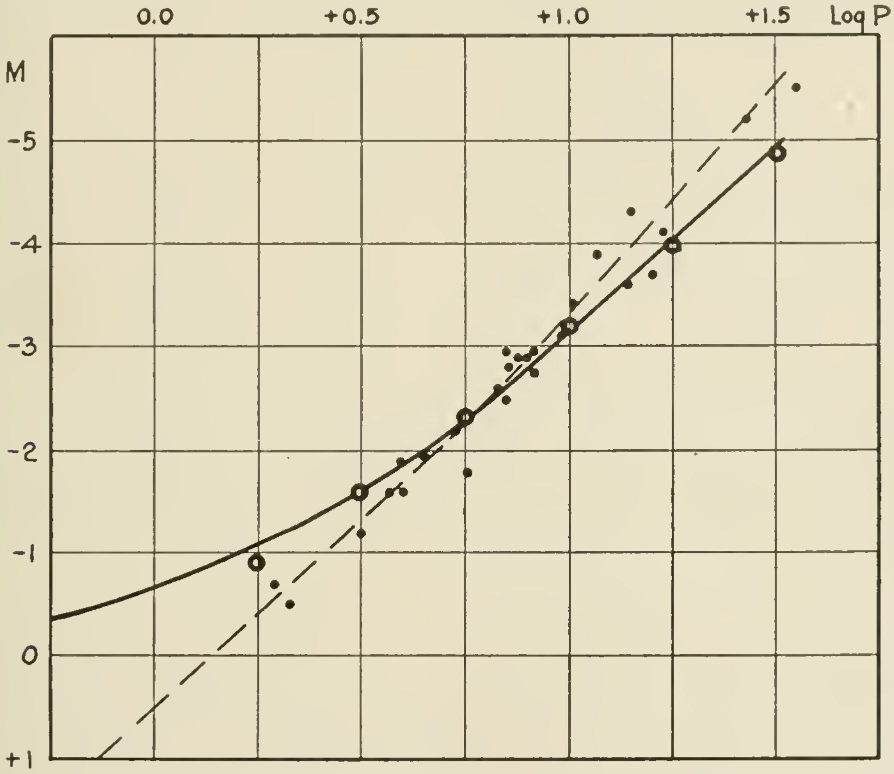

Fig. 5.—Absolute magnitudes of Cepheids based on the assumption of constant average heat content. The points are values for individual stars from equation (34). The circles, from equation (36), show the agreement with Shapley's period-luminosity relation when the term involving the specific heats in Eddington's expression for the density is included.

It will be noted that (33) is an empirical result which follows from an application to Cepheids of the period-luminosity relation (25) and the general theory of radiative equilibrium, but its derivation does not in any way involve the theory of Cepheid variation itself. If valid, it ought, however, in combination with the latter theory, to lead back to relation (25). But the comparison, as made, does not give complete agreement. Since the theory of Cepheids has entered only through (24), the difficulty presumably lies with that equation, which has been assumed to be applicable. If instead we use the corresponding relation derived by Eddington[1] himself, the difficulty disappears. For (24) we must substitute

$$\log \rho = -2 \log P - 2 \log (\gamma\alpha)^{\frac{1}{2}} + \text{const.} \tag{35}$$

where $(\gamma\alpha)^{\frac{1}{2}}$ is a function of β and of the ratio of the specific heats, and changes slowly with the mass. With this emendation, (34) becomes

$$M = -5 \log P + j - 5 \log (\gamma\alpha)^{\frac{1}{2}} + \text{const.} \tag{36}$$

The factor depending on the specific heats enters to the fifth power and thus becomes important. Its neglect in (34) causes the divergence shown by Figure 5.

The necessary corrections are easily calculated, however, with the aid of Table V of Eddington's paper. The values of $1-\beta$ required for the interpolation of $(\gamma\alpha)^{\frac{1}{2}}$ are given in *M.N.*, **77**, 602, 1917, under the heading "Molecular Weight 2," with the mass as argument. For $\mathcal{M}$ we may use the values in Table XVI, or more consistently with the present procedure, we may calculate $\mathcal{M}$ from

$$\log \mathcal{M} = -0.2\,(M - j) + \text{const.} \tag{37}$$

which follows at once from (18) and the condition $\mathcal{M} \propto R$ given by (33). The latter method was adopted, the constant in (37) being determined so that the mean $\mathcal{M}$ from (37) agrees with that from the diagram in Figure 3. We are interested only in the variation of $(\gamma\alpha)^{\frac{1}{2}}$, which is practically the same for all possible values of the ratio of specific heats. $\Gamma = 1\frac{4}{9}$ was used, however, since Eddington's results show that this agrees well with the data of observation. With the constant in (36) equal to 1.48, the values of $-5 \log (\gamma\alpha)^{\frac{1}{2}}$ are as shown in the third column of Table XVIII. The sums of the remaining terms on the right of (36) are given in the second column under the heading M_0. These are the co-ordinates of the dotted curve in Figure 5 and were read directly from a large-scale diagram. The calculated values of M from (36) (fourth column) when compared with those from (25) give the residuals in the last column of the table. For values of P between 3 and 30 days the agreement is very close. For $P<2$ days there is still a large divergence, but that is to be expected. For all but the cluster-type Cepheids, therefore, the theoretical relation (36) is practically the equivalent of the observed period-luminosity relation (25).

---

[1] *Monthly Notices*, **77**, 15, 1918.

TABLE XVIII

Theoretical and Observed Period-Luminosity Relation

Log P	M_0	$-5 \log (\gamma\alpha)^{\frac{1}{3}}$	M (36)	M (25)	O−C
0.25	−0.45	−0.45	−0.90	−1.08	−0.18
0.50	−1.30	−0.29	−1.59	−1.58	+0.01
0.75	−2.25	−0.08	−2.33	−2.26	+0.07
1.00	−3.34	+0.15	−3.19	−3.15	+0.04
1.25	−4.43	+0.45	−3.98	−4.05	−0.07
1.50	−5.54	+0.68	−4.86	−4.95	−0.09

Shapley's discussion referred to above starts with the assumption of constant heat-content and leads to a theoretical relation which agrees well with (25), but does not involve Eddington's theory of Cepheids because his comparison is based on equation (24) instead of (35). The close agreement found by Shapley is due partly to the fact that his final formula neglects $2.5 \log (\gamma\alpha)^{\frac{1}{3}}$ instead of $5 \log (\gamma\alpha)^{\frac{1}{3}}$, which by itself would lead to a divergence from (25) equal to one-half that shown in Figure 5, and partly to his readjustment of the mean atomic weight.

The matter is of interest from two or three points of view: First, because it shows the consistency of Eddington's theory of Cepheid variation with the general theory of radiative equilibrium, in that it is necessary to include the term depending on the specific heats in order to work back to the observed period-luminosity relation which was one of the premises; and second, because it exhibits the empirical result (33) in another form and possibly gives weight to the suggestion that constant average heat-content may be a determining circumstance in Cepheid variation.

The fact that the term which has been under discussion enters to so high a power subjects Eddington's theory of Cepheid variation to a severe test. Something of the sort is also true of the empirical condition (33). Assume for a moment that the relation $\mathcal{M} \propto R$ is not exact, and suppose that all the variations which occur are thrown into the mass. The maximum systematic deviation in log $\mathcal{M}$, by (18), (22), and (37), will then be equal to 0.4 of that shown by the differences in the last column of Table XVIII, which is well within the uncertainty of the comparison.

This close agreement justifies the mention of other relations which follow at once from the assumption of constant average heat-content, combined with the following equations of radiative equilibrium:[1]

$$\left.\begin{aligned} T_c^4 &\propto g(1-\beta) \propto \mathcal{M}^{\frac{1}{3}}\rho^{\frac{2}{3}}(1-\beta) \\ T_c &\propto \mathcal{M}^{\frac{2}{3}}\rho^{\frac{1}{3}}\beta \\ 1-\beta &\propto \mathcal{M}^2\beta^4 \end{aligned}\right\} \qquad (38)$$

where T_e and T_c are the effective and central temperatures, respectively, g the acceleration due to gravity, and $1-\beta$ the ratio of radiation pressure to gravitational attraction. Assuming $\mathcal{M} \propto R$ we find then

$$\left.\begin{aligned} &\mathcal{M}^2\rho = c_1;\ \mathcal{M}g = c_2;\ Rg \propto c_3;\ \rho \propto g^2 \\ &T_c \propto \beta;\ T_e \propto T_c\mathcal{M}^{\frac{1}{4}} \propto \mathcal{M}^{\frac{1}{4}}\beta \propto T_c\rho^{-\frac{1}{8}} \end{aligned}\right\} \qquad (39)$$

where c_1, c_2, and c_3 are constants. Further, with the aid of (35)

$$\mathcal{M} \propto (\gamma a)^{\frac{1}{2}}P;\ T_e \propto T_c(\gamma a)^{\frac{1}{8}}P^{\frac{1}{4}} \propto \beta(\gamma a)^{\frac{1}{8}}P^{\frac{1}{4}}. \qquad (40)$$

The relation $T_e \propto \mathcal{M}^{\frac{1}{4}}\beta$ is of special interest. Since β diminishes faster than $\mathcal{M}^{\frac{1}{4}}$ increases, T_e must decrease with increasing $\mathcal{M}$. The change for the range in $\mathcal{M}$ shown above corresponds to an increase of about one spectral interval, which agrees well with the observed range in spectral type. At the same time M decreases from -1.2 to -5.1.

The formulae of radiative equilibrium admit of no dispersion in the case of individual stars. This is also true of the relations (39) and (40) for the Cepheids. In the case of the masses and densities, we have already found reasons for believing that this is not strictly in accordance with the facts. Although the dispersion is small, it is in part undoubtedly real, for at present the theory necessarily neglects the modifications of gravitational acceleration produced by the rotation of the stars on their axes, which must influence the relation of radiation to other stellar characteristics.

---

[1] Eddington, *Monthly Notices*, 79, 180, 1919.

16. RELATION TO RUSSELL'S FREQUENCY DIAGRAM—REMARKS ON THE DISTRIBUTION OF MASS AND DENSITY

The justification for the discussion of Eddington's theory of Cepheids in this place is the light thrown upon the distribution of mass and density. Equations (35) and (37), for example, afford a basis for a further revision of the mass- and density-curves; but an additional approximation seems scarcely justified at present. Table XVII shows already a surprisingly good agreement between his results and those in Figure 3. Further modification would affect mainly the stars of masses 10 or larger, and these are not numerous. Moreover, Eddington himself has repeatedly emphasized the fact that his theory is but a first approximation, in that certain simplifying assumptions had to be introduced in order to make a beginning. Figure 3 is therefore allowed to stand as it is for the present, although the data in Table XIX are added to show, in a general way, what would result, for the Cepheids at least, from rigorous application of the theory. The values of M and the spectrum may be regarded as co-ordinates for the location of corresponding values of $\mathcal{M}$ in a diagram similar to Figure 3.

TABLE XIX

MASS, ABSOLUTE MAGNITUDE, AND SPECTRUM, EDDINGTON'S THEORY OF CEPHEIDS

$\mathcal{M}$	M	Sp.	$\mathcal{M}$	M	Sp.
2	−0.9	F1.0	10	−3.4	F8.0
3	−1.4	F4.0	12	−3.6	F8.4
4	−1.9	F5.2	15	−4.0	F9.0
6	−2.5	F6.5	20	−4.6	F9.3
8	−3.0	F7.5	25	−5.1	F9.6

The values of the masses are adjusted to give a mean value equal to that derived from Figure 3.

It is, of course, not to be supposed that the stars are uniformly distributed along the mass-curves of Figure 3. In general they cluster about certain lines of maximum frequency which, with one exception, bear little relation to the lines of equal mass. The most conspicuous of the frequency lines is that defined by the dwarfs, which continues through the A's and joins smoothly with the line of maximum frequency of the B stars. Along this line we have found a regular decrease in the average mass with increasing spectral type and absolute magnitude.

The number of A stars of very high luminosity seems to be relatively small.[1] If this is really the case, there must be a region of low frequency in the diagram between the most luminous B's and the very bright giants of the later types. Beyond F0 the giants fall into two groups, the Cepheids and pseudo-Cepheids, and a large group of G, K, and M stars whose absolute magnitudes lie mainly between $M=-0.5$ and $+2.5$. The Cepheids and pseudo-Cepheids attain very high luminosities and show a rather definite correlation line running approximately from $M=-0.4$, F4, to $M=-4$, G8, which in general cuts the mass lines obliquely. For the Cepheids alone, its course is determined by the intersections of the mass lines of Figure 3 with those defined by equation (37), which, empirically at least, is a condition of Cepheid variability.

The frequency line for the second and more numerous group of giants seems, on the other hand, to be definitely related to the distribution of mass. It has a clearly marked minimum at K0 and coincides approximately[2] with the mass line $\mathcal{M}=2$ as shown in Figure 3. The chief difference is a steeper descent from G0 to K0 and an even more pronounced minimum than is shown by the mass line. The coincidence is probably significant, for Eddington[3] finds on theoretical grounds that, among the giants, masses of this order of magnitude may be expected to have the highest frequency.

---

[1] The frequency diagram of Russell for the helium stars of Kapteyn and the stars in the list of spectroscopic parallaxes is illustrated in Annual Report, Mt. Wilson Observatory, *Year Book Carnegie Institution of Washington*, 1921.

[2] The position of this correlation line and of the line of maximum frequency for the G, K, and M giants is shown in Fig. 1. This figure also shows the course of the equal-mass line $\mathcal{M}=2$. The correlation of spectral type with absolute magnitude for the most luminous stars of our own immediate system is essentially that found by Shapley for the brightest stars in globular clusters; and it now appears from results not yet published that in some of the galactic clouds a similar correlation with apparent magnitude is to be found. It should be possible in such cases to estimate roughly the distances of the clouds. Provisional results indicate values of the order of 20,000 to 50,000 light years. See *Annual Report, loc. cit.*

[3] *Report of the British Association for the Advancement of Science*, 1920, p. 43.

These circumstances seem to afford justification for the peculiar course of the mass lines for the late-type giants, which otherwise must depend solely upon the applicability of the principle of equipartition.

The minimum itself, or what remains of it after the reduction of the visual absolute magnitudes to bolometric values in the manner indicated above, must not be taken too seriously, however, for the residual irregularity in the mass lines is little in excess of the small systematic uncertainties affecting the absolute magnitudes of the different spectral types.[1]

In this connection the result of page 183 for the masses of fourteen giant visual binaries may be recalled. Divided by 1.75 to reduce to the central component, the mean mass becomes 1.7 ± 0.9. For the same stars we find by interpolation from Figure 3, with spectral type and absolute magnitude as arguments, the mean value $\mathcal{M}=2.7\pm0.2$ The agreement is not good, but falls within the limits of uncertainty incident upon the small number of stars available for the comparison.

The decrease in mass along the dwarf branch from $\mathcal{M}=10$ at Bo to $\mathcal{M}=0.6$ at Ma raises a question of much interest, especially when it is recalled that the dispersion in mass is certainly small.[2] Practically, large masses are not to be found in our lists of dwarf stars. And yet the large-mass early-type stars are numerous. Why, therefore, do we not find more large masses among the dwarfs?

Several possibilities must be considered. Thus we might assume that the stars now on the dwarf branch (including the B's, as usual) began their development at much the same time, and that those of largest mass have only partially run their course and are now in the B stage. The assumption would seem less arbitrary could we suppose that all the stars began their evolutionary careers at the same time; but this apparently is not the case, for numerous objects with only moderate masses of 2 or 3 are still in an early stage of development. The most serious objection to this explanation, however, is that it takes no account of a peculiar kind of selection.

---

[1] Strömberg, *Mt. Wilson Contr.*, No. 220; *Astrophysical Journal*, **55**, 11, 1922.

[2] Russell has also discussed this correlation., *Observatory*, **37**, 173, 1914.

Let us therefore make the contrary assumption and suppose that stellar development has continued so long that all possible masses really occur among the dwarfs of late type. Among these, the large masses, say of the order of 10, will be of very low frequency as compared with the modal value for all types together. Kapteyn and van Rhijn place the maximum of the frequency-curve of absolute magnitudes at $M = +7.7$. The modal value of the mass therefore should be about 0.7, and since the dispersion is small, the large masses must be very infrequent.

Consider now only the stars in our lists of data. The dwarfs among these will all be included in a restricted region of space near the sun. The small masses will greatly predominate and the mean mass will be low. The giants, on the other hand, will be scattered through a large volume of space, and their average mass will be large, because only stars of large mass can attain high luminosity. The B's among them will form the collection at the upper end of the dwarf branch whose mean mass we have found to be 10. The total number of these in our catalogues will be considerable, because they represent those present in a large volume, whereas the large masses among the dwarfs will be absolutely as well as relatively infrequent, because we can see only those which are near us.

The stars of intermediate luminosity fill in the gap, and we must therefore expect to find a correlation of mass with absolute magnitude and spectral type very similar to that actually observed. The average mass decreases with advancing type; at the same time the number of stars of large mass in our catalogues decreases rapidly and the smaller masses appear in succession and in increasing numbers because they can attain the temperatures corresponding to the later spectral types.

One other possibility should also be borne in mind, namely, a decrease in mass through loss of energy by radiation. From the standpoint of relativity[1] any change dE in the total energy of a system implies a corresponding change of dE/c^2 in the inertial mass, where c is the velocity of light. A similar conclusion follows also on the basis of the Newtonian mechanics[1] from the phenomenon of radiation pressure, for, unless we attribute mass to radiation, there are certain cases, at least, in which neither the energy nor the motion of the center of gravity will be conserved. Since the principles of mechanics are inductions, we cannot be sure that they apply to physical phenomena with the degree of precision implied by assuming that mass actually changes with changes in the energy. But considerations of consistency are sufficient to give the matter importance, and it derives added interest from the fact that a decrease in mass has been invoked as a means of accounting for the enormous unknown supply of energy which is now generally recognized as an essential feature of stellar phenomena. The suggestion that the packing of electrons and the nuclei of hydrogen atoms to form nuclei of heavier elements, with an accompanying loss in mass which reappears in the form of great quantities of radiant energy, attaches itself naturally to the relation between mass and energy that harmonizes with fundamental mechanical principles, whether of Einstein or of Newton.

---

[1] Einstein, *Annalen der Physik*, **18**, 639, 1905.

Of these three factors which may affect the correlation of mass and spectral type, selection certainly enters in the manner indicated, but its quantitative evaluation is at present impossible. This leaves the operation of the other two factors entirely speculative. If, however, there is any appreciable change in the mass of the stars during their development, they will not follow the mass lines of Figure 3, but cut across them obliquely; and this leads to a peculiarity of these lines that immediately attracts attention.

The equal-mass lines do not meet the dwarf branch tangentially, as one might expect on the basis of a simple gravitational contraction with its accompanying changes of temperature, but intersect the frequency line at large angles. A comparison of Figures 2 and 3 shows that in this particular there is a large element of uncertainty; and yet the evidence seems to exclude the possibility of tangential intersections, unless we are prepared to abandon the principle of equipartition at the point where it seems to be best justified, namely, in the vicinity of the dwarf branch.

---

[1] *Ibid.*, **20**, 627, 1906. This result seems also to have been pointed out by others—Planck, for one, I believe—although I have been unable to locate the source.

The space-velocities of stars of any given type, say F5, show a definite correlation with absolute magnitude, the mean velocity increasing continuously as the brightness decreases. If equipartition holds for the stars of a given type which are near the frequency line of the dwarfs, as it does in the mean for the stars of different types scattered along the frequency line, there must be a continuous decrease in mass downward along the vertical lines of Figure 3. The data of Table X give a numerical expression to this relationship of mass to luminosity, which, quantitatively, should be most exact for values of M near the frequency line of the dwarfs. Now on this line, for spectral type F5, as an illustration, we find a mean mass of 1.5. Above this point in the diagram, that is, for more luminous stars, the masses are larger; below they are smaller. If the decrease in mass downward is really continuous, it follows at once, since the mass also decreases continuously along the dwarf frequency line, that curves connecting equal masses cannot meet the frequency line tangentially, but must intersect it at a considerable angle. In fact Figure 2 shows that the strict application of the principle of equipartition leads to angles in excess of 90°, counting as 0° the tangential junction required by gravitational contraction. The evolutionary path of any given star, however, when once it has joined the dwarf branch, must lie in the general direction of the frequency line.

The explanation of the contradiction lies in the peculiar selection which determines the decrease in mass along the dwarf branch. Consider for example two dwarf stars of Type F5, one a large mass which in its development has followed the dwarf branch downward from some earlier type, the other a star of mass so small that it has been unable to attain the high temperatures of the very early types and joins the dwarf branch at Type F5. The star of large mass will be the brighter of the two. Hence the path of the small star must intersect the line of maximum frequency at some point a little in advance of F5 in order that it may swing into position below the larger star. The path of the larger star, on the other hand, will lie above the frequency line. Similar reasoning applies to stars of intermediate mass and it is evident that the entire group of F5 dwarfs will show a correlation of mass with absolute magnitude similar to that found from the principle of equipartition. In their further evolution these stars will move as a group along paths approximately parallel to the line of maximum frequency. But these paths do not and cannot coincide with the equal mass lines of Figure 3, for when the group in question is at F5, there is at G0 another group, whose luminosities show a similar correlation with mass, but whose masses, because of selection, are systematically smaller than those at F5. If the points in the diagram corresponding to equal masses in these two simultaneously observed groups be connected, the lines of equal mass will cut the frequency line at high angles as shown in Figure 3. Hence there is no conflict between the mass-distribution shown by this diagram and the gravitational theory of stellar development. The only point is that in the vicinity of the dwarf branch the stars do not follow the equal mass lines.

17. IONIZATION AND MEAN ATOMIC WEIGHT

The final equations of Eddington's theory[1] are

$$L=\frac{4\pi c G \mathcal{M}}{k}(1-\beta) \tag{41}$$

$$1-\beta=0.0026\,\mathcal{M}^2\beta^4 m^4 \tag{42}$$

where c and G are constants. These formulae refer to the giant stage and assume that the mean atomic weight is independent of the temperature. Variations in m during the star's development would affect the relation between luminosity and spectral type. The absolute value of m fixes the relation between mass and radiation-pressure β, and hence determines the values of the mass which are most likely to occur.

It is unnecessary to repeat here Eddington's arguments in favor of a small value of m. In general these seem to be only strengthened by the results of recent investigations of ionization phenomena. Eggert,[2] for example, has considered the behavior of the iron atom when subjected to pressures and temperatures comparable with those at the center of a typical giant star and finds that 16 of the

---

[1] *Astrophysical Journal*, **48**, 208, 210, 1918.

[2] *Physikalische Zeitschrift*, **20**, 570, 1919.

26 electrons would be stripped from the atom, thus reducing the mean "atomic" weight to 3.3.

It is easy to extend this result to other parts of the star. Using the reaction isobar of Nernst and basing the calculation of the energy of dissociation on the dynamical relations of the Bohr atom, Eggert finds as the condition for the removal of 8 electrons from 99 per cent of the atoms[1]

$$2.68+0.4 \log P=\frac{-2\times 10^5}{T_i}+\log T_i \tag{43}$$

in which the pressure P is measured in atmospheres. For the separation of 16 electrons the corresponding condition is approximately the same as (43) except for the appearance of an additional factor of 10 in the first term on the right.

Equation (43) and its alternate may be used to calculate the values of T_i corresponding to the pressures at different points along the radius. The comparison of the ionization temperatures thus found with the corresponding stellar temperatures should then give some indication as to the variation in ionization throughout the star.

The total pressure P is given by the ordinary gas equation, divided by β, the factor arising from radiation-pressure.

$$P=\frac{p}{\beta}=\frac{\mathfrak{R}}{\beta m}\rho T \tag{44}$$

T and ρ may be found from Emden's[2] formulae, or we may use the values given by Eddington[3] for his typical star ($\mathcal{M}=1.5$, $\rho_m=0.002$), taking care to modify those for T, which contain the factor m, to make them conform with the degree of ionization expressed by (43) and its alternate. Since T contains both m

---

[1] Professor Paul Epstein of the California Institute of Technology calls my attention to an error in Eggert's expression for K (*op. cit.*, p. 573). A factor 8^8 has been omitted. It has little effect, however, on equation (43), the absolute term being increased from 2.32 to 2.68.

[2] *Gaskugeln*, p. 97, 1907. Eddington has called attention to the misprint in the formula for θ^3. The last factor in the denominator should be squared.

[3] *Astrophysical Journal*, 48, 213, 1918. Unless I am in error, Eddington's values for the temperature have been computed with $m=2$, whereas the text seems to imply that 2.8 has been used. If so, the tabular values should be increased by 40 per cent.

and β as factors, the total pressure P depends upon neither the value of the radiation-pressure nor the degree of ionization. T, however, depends upon both, and, moreover, β also depends upon m (see equation [42]).

For the removal of 8 and 16 electrons, respectively, the values of m become 6.2 and 3.3. Corresponding to these, for $\mathcal{M}=1.5$, $\beta=0.496$ and 0.766. With these data we find the values of P and T given in the second, third, and fifth columns of Table XX for various points along the radius. The unit for r is such that the distance from the center to the surface is 6.9. Substituting the values of P into Eggert's formula, we find the ionization temperatures given in the fourth and sixth columns of the table. These temperatures, required for the removal of 8 and 16 electrons, respectively, may be compared with the corresponding stellar temperatures. The latter, which change little with the assumed change in m, are approximately ten times the temperature required to separate 8 electrons from the nucleus, and of the same order as the ionization temperatures corresponding to the removal of 16 electrons. The decrease in pressure toward the surface compensates for the fall in temperature to such an extent that the ionization should be nearly constant throughout the star. It is only within a thin shell near the surface, which contains an insignificant fraction of the mass (see last column, Table XX), that m can rise much above the value 3.3.

TABLE XX

IONIZATION AND STELLAR TEMPERATURES, IRON IN EDDINGTON'S TYPICAL STAR

r	LOG P (ATM)	-8 ELECTRONS $m=6.2$		-16 ELECTRONS $m=3.3$		PERCENTAGE OF MASS OUTSIDE r
		T	T_i	T	T_i	
0	7.40	8.7×10^6	8.0×10^5	7.1×10^6	2.6×10^6	100
1	7.13	7.4	6.7	6.1	2.4	88
2	6.47	5.0	4.9	4.1	2.0	48
3	5.63	3.1	3.4	2.5	1.6	18
4	4.69	1.8	2.5	1.5	1.3	5
5	3.59	0.96	1.8	0.79	1.1	0.7
6	1.98	0.39	1.2	0.32	0.8	0.005

Radius of star$=6.9$, $\mathcal{M}=1.5$, $\rho_m=0.002$.

Eggert's formula is an extrapolation and involves assumptions which cannot at present be directly controlled; but its general indications are in close agreement with Eddington's conclusions. Even admitting the various underlying assumptions, the result applies only to a star consisting wholly of iron; but one can scarcely doubt that the mean values of m for all the elements actually present must be small and nearly constant for all points within the star except those close to the surface.

It seems worth while also to consider the relation of ionization to stellar temperature in giant stars of constant mass but differing spectral types, in order to gain some idea of the permanence of this relation as a star contracts under the action of gravitation.

Consider stars of Eddington's critical mass $\mathcal{M}=2$, which, as we have seen, are those occurring most frequently among the late-type giants. It will be sufficient to calculate the central temperatures and pressures, and in view of the preceding results it is clear that we may use $m=3.3$. The corresponding value of β is 0.70. Using Emden's formula as before (remembering that for the type of equilibrium considered $\rho_c=54.25\,\rho_m$), we find the results for T_c and P_c given in Table XXI. The values of M and $\log \rho_m$ in the second and third columns were read from the diagram of Figure 3. The ionization temperatures for the removal of 16 electrons are in the last column of the table.

TABLE XXI

CENTRAL TEMPERATURES AND PRESSURES, AND IONIZATION TEMPERATURES FOR IRON ($\mathcal{M}=2$, $m=3.3$)

Sp.	M	Log ρ_m	Log T_c	Log P_c (Atm)	T_c	T_i
Ma	0.0	−5.1	6.10	4.3	1.3×10^6	1.2×10^6
K5	+0.7	−4.1	6.43	5.6	2.7	1.5
K0	+1.1	−3.1	6.77	7.0	5.9	2.1
G5	+0.8	−2.7	6.90	7.5	7.9	2.6
G0	+0.7	−2.2	7.07	8.2	11.7	3.3
F5	+2.0	−1.0	7.47	9.8	29.5	7.0

These data represent the sequence of changes from an early stage of development, on the basis of Russell's theory, through to the dwarf stage, where the density is so large that Boyle's law is no longer accurately obeyed. The increases in T_c, ρ and P_c are approximately 20, 10,000, and 300,000 fold, respectively. In spite of these extraordinary changes, the ionization temperatures remain of the same general order as those at the center of the star throughout its development. Initially, the two temperatures are sensibly equal, and the gain in T_c over T_i is so slight that any further decrease in m must be small. The complete removal of the third sheath of electrons, for example, would give $m=2.2$.

Even for stars of the lowest density, such as Antares or Betelgeuse, conditions are very similar to those illustrated by the first line of Table XXI. Low density means relatively low central temperature and pressure, but this factor is compensated by the large masses which characterize the very luminous giants, so that the relation of ionization to stellar temperatures is much the same as for the objects already examined.

It may be remarked incidentally that the values of T_c in Table XXI throw some light upon the behavior of the effective radiating layers in stars of different types. The increase in T_c is approximately ten times that in the effective temperature. But for the type of equilibrium in question the temperature gradient is independent of the density, that is, the temperature increase for homologous points along the radius should be constant. The explanation must be that the thickness of the radiating layer in an Ma giant, because of the enormous difference in density, is very much greater than that for an F5 dwarf. As development progresses, radiation from the deeper and hotter strata is absorbed as a result of increasing density, and, in consequence, the increase in effective temperature is less rapid than would otherwise be the case.

On the basis of the preceding evidence we must expect a high degree of ionization at the earliest stages of stellar development with which we are familiar, and comparatively little decrease in the value of m as the development proceeds. The Bohr atom affords the only foundation we have for estimates such as have been made, and it is not certain that the results are of the right order of magnitude. One consequence of their acceptance, however, should not be overlooked, and that is the total amount of energy required for ionization. For the removal of 8 electrons this equals 1.8×10^7 calories per gram atom,[1] corresponding to an ionizing potential of about 800 volts. The mass of Eddington's typical star is approximately 2.9×10^{33} grams. The removal of 8 electrons from all the atoms in this mass would therefore require

$$U_0=\frac{2.9\times10^{33}\times1.8\times10^7\times4.2\times10^7}{56}=4\times10^{46}\text{ ergs},\tag{45}$$

while for the removal of the second sheath of 8 electrons a quantity of the order of ten times this amount, or

$$U_0=4\times10^{47}\text{ ergs}\tag{46}$$

would be necessary.

Now the total energy generated by gravitational contraction of the star from a state of infinite diffusion is[2]

$$\Omega=\frac{3(\gamma-1)}{5\gamma-6}\frac{G\mathcal{M}^2}{R}\tag{47}$$

where γ is the ratio of specific heats, G the gravitational constant, 6.66×10^{-8} cm³/grams sec.², and R the radius, 7×10^{11} cm; γ lies between the limits 4/3 and 5/3, whence the fractional coefficient on the right has the limiting values 3/2 and 6/7. At a maximum, therefore, which also corresponds to Eddington's model,

$$\Omega=\tfrac{3}{2}\cdot\tfrac{2}{3}\cdot\frac{10^{-7}\times9\times10^{66}}{7\times10^{11}}=1.3\times10^{48}\text{ ergs}.\tag{48}$$

Of this total the etherial energy alone,[3] namely,

$$(1-\beta)\Omega=0.234\,\Omega=3.0\times10^{47}\text{ ergs},\tag{49}$$

---

[1] Eggert, *loc. cit.*

[2] Emden, *Gaskugeln*, p. 125, 1907.

[3] Eddington, *Monthly Notices*, **79**, 23, 1918. Anderson, with whom I have had much stimulating discussion during the preparation of this paper, calls my attention to the fact that ionization cannot be produced by the collision of electrons with atoms without violating the Nernst formula of equilibrium, which is well established on thermodynamical grounds. This equation depends upon the pressure, whereas the hypothesis of ionization by collisions alone leads to a condition for equilibrium which is independent of pressure. If the effective energy is assumed to be partly radiant and partly kinetic, the pressure would enter, but not in the manner required by Nernst's equation. Since the internal kinetic energy of the atoms is not available, the radiant energy alone can be operative (as in the case of the photoelectric effect, for example). See also Milne, *Observatory*, **44**, 269, 1921.

seems to be available for ionization. This is of the same order as U_o, the energy of dissociation given in (46). Admitting, therefore, the validity of Bohr's theory and the applicability of the Nernst formula of equilibrium, the insufficiency of the gravitational theory presents itself in a new form. As an alternative, the question is perhaps raised as to whether the giant stars, even in their very earliest stages of development, are ever in a state other than one of high dissociation.

The calculation of the stellar temperatures in Tables XX and XXI neglects altogether the depletion of the available supply of energy by ionization. Were gravitation the only source, we could expect neither the temperatures nor the degree of ionization indicated by the discussion; but, instead, an equilibrium state which would be established for something less than the extremes of temperature and ionization shown by the tables.

18. COMPARISONS WITH EDDINGTON'S FORMULAE

The assumption concerning m which underlies equations (41) and (42) has been discussed in the preceding section. These formulae also assume that the outflow of energy across any surface of unit area is proportional to the gravitational acceleration at that point ($H \propto g$), and that the mass coefficient of absorption, k, is a constant. The energy assumption can also be stated in the form that the outflow throughout the star per unit of mass is constant. The source of the energy is not specified; it may be derived from gravitational contraction or any other source capable of providing an adequate supply. Assuming further that the transfer of energy is by radiation and not by convection, the conditions for equilibrium are found to be the same as those for adiabatic equilibrium with a ratio of specific heats equal to 4/3. It then follows through (41) and (42) that the bolometric magnitude of a star remains constant so long as it behaves as a perfect gas.[1]

A giant star in its development, however, presumably follows closely one of the equal-mass lines in the upper part of Figure 1, for the selection which enters along the dwarf branch has comparatively little influence on the average mass of the giants which come under observation. Observations indicate, therefore, that the absolute magnitude is not independent of the stage of development. The change is even larger than shown in Figure 3, for, as already stated, the visual absolute magnitudes must be corrected by the quantities given on page 194 to make them comparable with the bolometric magnitudes calculated by (41).

---

[1] As Jeans points out, *Monthly Notices*, **79**, 319, 1919, this general result follows at once, by simple considerations, from the assumption H/g=const. The nature of the dependence of radiation on mass and other characteristics is, however, another matter, less easily disposed of.

The question now arises as to the particulars in which the underlying assumptions must be modified in order to effect a closer agreement with observations. Such consideration as can be given here may be prefaced by the remark that Jeans,[1] starting from the assumptions of radiative conduction, gravitational contraction, and constant k and m, finds that the radiation of a star will remain constant as long as Boyle's law is obeyed. This is also the case if the star has sources of energy other than gravitational contraction, provided the rate of generation per unit mass is independent of the time. This is Eddington's result without his assumption that $H \propto g$; but the functional dependence of radiation upon the mass cannot be specified. Jeans also finds that H/g will be constant throughout the mass of gas only when the mass is so large that radiation-pressure predominates and β may be put equal to zero. For the ordinary run of stellar masses, however, H/g will not be constant within the star, but for a given point will be independent of the time, provided the only source of energy is gravitational.

Eddington[2] himself points out that H/g cannot be rigorously constant within the star, for, assuming gravitational contraction through a series of homologous states and a temperature- and pressure-distribution corresponding to adiabatic equilibrium with $\gamma = 4/3$, the outflow of energy per unit mass would increase about 70 per cent from the surface to the center.

In view of a probable variation of H/g of the order indicated, the original assumption gives close agreement with observations. The matter can be tested by comparing the calculated values of M corresponding to different values of $\mathcal{M}$ with that shown by Figure 3 for stars of the same spectral type. By proceeding in this manner we avoid disturbances arising from variations in k and m, since for stars of the same type these quantities should be less subject to change.

---

[1] *Loc. cit.*

[2] *Monthly Notices*, 77, 599, 1917.

The results are shown in Table XXII. This table gives the deviations of the observed values of M (Fig. 3) from those calculated by Eddington, which are in the second column of the table. Zero point corrections have been applied to the latter to make the mean O−C for each type equal to zero. There is a large progressive change for the F stars, but the agreement improves with advancing type and, with the exception of one difference, is practically perfect for the K and M stars. From this comparison it is clear that the error in the assumption $H/g=$const. is not very serious when we consider stars of a specified type.

TABLE XXII

Observed and Calculated (Eddington) Variation of Absolute Magnitude with Mass

$\mathcal{M}$	Cal. M	O−C				$\mathcal{M}$	Cal. M	O−C			
		Fo	Go	Ko	Ma			Fo	Go	Ko	Ma
1.5	−0.3	.....	+1.5	+0.7	+0.3	6	−2.9	+0.3	−0.3	−0.1	0.0
2	−0.9	.....	+0.9	+0.3	+0.2	7	−3.1	−0.1	−0.5	−0.1	0.0
3	−1.7	.....	+0.5	0.0	0.0	8	−3.3	−0.5	−0.6	−0.2	0.0
4	−2.2	+1.4	+0.1	0.0	0.0	9	−3.5	−0.7	−0.8	−0.3	0.0
5	−2.6	+0.7	−0.1	0.0	0.0	10	−3.7	−1.0	−0.9	−0.3	0.0

The lack of parallelism of the equal-mass lines with the axis $M=0$ is difficult to account for because the assumption of constancy for both k and m enters here, as well as that concerning the flow of energy. In general the luminosity for any given mass decreases with increasing temperature. For mass 4, as an illustration, the bolometric absolute magnitude increases from −3.1 at Ma to +0.3 at Fo. This is in the direction corresponding to decreasing values of m, and one might expect much of the change to be accounted for by increasing ionization. The evidence of section 17, however, is against any considerable variation in m. Even in the earliest visible stages of development we should not anticipate a value much in excess of 3.3, and unless there is a large amount of nuclear disintegration, which seems improbable, the value of m cannot fall below 2. It is easily shown that a decrease from $4\sqrt{2}$ to 2 would cause an increase in M of about one magnitude, which is only a third of the amount required. The admission of much larger initial values of m is insufficient to bridge the gap, for (42) shows that $1-\beta$, and hence the luminosity, are not much affected as m is increased.

The behavior of k is obscure. Although the conditions within the star which determine the degree of absorption must be analogous to those governing the absorption of X-rays, it should be borne in mind that the effective value of k is that corresponding to the outermost layers of the star where the temperature is very much lower than in the interior. Even near the surface the opacity is large, but we have no data as to its variations that are certainly applicable.

This leaves the larger part of the increase in the absolute magnitude unaccounted for, and it is not clear as to how the discrepancy is to be explained. If the contraction is homologous and the energy gravitational, or gravitational plus a source independent of the time, we should not expect variations in outflow with advancing development other than those caused by changes in k and in m.

As an explanation, changes in m that would be sufficient seem to be excluded; those of k are in doubt. There remain, however, the assumptions underlying the outflow of energy. The source of energy almost certainly is not wholly gravitational, and if not, with almost equal certainty, is not independent of the time. The outstanding questions therefore lead directly into the realm of atomic physics, and it seems more than ever likely that the problem of the stars will find its solution in the solution of the problem of the atom.

In conclusion, attention may be directed to the relation of mass to luminosity along the dwarf branch. Here Boyle's law is in general no longer obeyed. It will be noted, however, that the density increases slowly until the late types are reached, which suggests that the departure from the conditions of a perfect gas may affect the behavior of stars of different spectral types much alike, so that a formula giving the relation of luminosity to mass for the giants, with the exception of a constant, would also hold approximately for the dwarfs.

The matter is easily tested by calculating $\mathcal{M}$ from (41) for the values of L corresponding to the absolute magnitudes given in the second column of Table IV. Choosing the constant factor so that the mean of the values thus calculated agrees with the observed mean mass, we have the results in Table XXIII. With the exception of a spectral interval at either end of the series, where the deviations from the average density are large, the agreement is good.

TABLE XXIII

Values of Mass on Dwarf Branch

Sp.	Obs.	Cal.	Sp.	Obs.	Cal.
Bo	10	18	Go	1.0	1.0
B5	8.3	10.5	G5	0.76	0.76
Ao	6.0	6.6	Ko	0.68	0.62
A5	4.0	4.1	K5	0.62	0.48
Fo	2.5	2.5	Ma	0.59	0.26
F5	1.5	1.5			

I must express my grateful acknowledgments to Miss Joyner and Miss Richmond, of the Computing Division, for their efficient assistance in the extensive tabulations and calculations involved in the preceding discussion.

Mount Wilson Observatory
December 1921

ON THE CALCULATION OF MASSES FROM SPECTROSCOPIC PARALLAXES[1]

By HENRY NORRIS RUSSELL[2]

ABSTRACT

Calculation of masses of stars from spectroscopic parallaxes.—It appears probable that the line intensities upon which spectroscopic parallaxes are based are *functions of the temperature and density of the star's atmosphere.* If this were exactly true, all stars of the same surface brightness and density would have the same spectroscopic absolute magnitude, and *the masses, computed from the spectroscopic parallaxes, would come out the same for all the stars* of such a group (whatever the dispersion among their actual masses) and equal to the geometrical mean of the latter. To obtain a reliable measure of the dispersion in mass among binary stars, parallaxes must be determined in some other way.

Spectroscopic and dynamical parallaxes.—It follows that the spectroscopic parallaxes and the dynamical parallaxes (derived on the assumption that the mass of a binary system is equal to the mean value for stars of its spectral type and absolute magnitude) are *systematically equivalent to one another*, and really rest on the same physical relationships and assumptions.

Dispersion of mass among visual binaries (dwarf stars).—By an indirect method, depending on Strömberg's comparisons of spectroscopic and trigonometric parallaxes, Seares's conclusion that the dispersion is small is confirmed. The probable error of dispersion of log $\mathcal{M}$ appears to be less than ± 0.2, but cannot be exactly determined.

The very small values obtained by Seares in the preceding paper[3] for the dispersion in mass among dwarf stars suggest the following explanation.

It appears very probable, from physical considerations, that the spectral type of a star is determined by the temperature T of its outer atmosphere, while the characteristics associated with the absolute magnitude depend also, and mainly, upon the density of the atmosphere, ρ'. If M_s is the absolute magnitude, determined spectroscopically, we may then write

$$M_s = F(T, \rho'). \tag{1}$$

It is also probable that the surface brightness j depends almost entirely on the temperature, and that the density of the atmosphere above the visible surface is a function of the mean density ρ (though not necessarily proportional to it). We have then

---

[1] *Contributions from the Mount Wilson Observatory*, No. 227.

[2] Research Associate of the Mount Wilson Observatory.

[3] *Mt. Wilson Contr.*, No. 226.

$$M_s = f(j, \rho). \tag{2}$$

It may be that M_s depends to some degree on other variables, but it is probable that their influence is slight. The form of the function f cannot be predicted by theory, but can be found empirically when sufficient data regarding stellar masses and densities are available.

Assuming the relation for the moment to be exact, and introducing it into equation (22) of Seares's paper, we have

$$\log \mathcal{M}_s = \log \rho + 0.6j - 0.6f(j, \rho) + 2.77. \tag{3}$$

Hence $\mathcal{M}_s$ the mass corresponding to the spectroscopic parallax is itself a function of ρ and j alone. Like (22) this is a general result, holding good no matter how the mass is calculated, so long as the formula involves the absolute magnitude and our assumptions about the latter are correct.

Stated in words, this signifies: *If the spectroscopic absolute magnitude of a star depends only on its surface brightness and density, the masses computed from the spectroscopic parallaxes will be identical for all stars which have the same density and surface brightness, no matter how different their actual masses may be.*

In still other words, the spectroscopic parallax (on our assumptions) will be correct only in the case of stars having a certain average value of the mass. For larger or smaller masses there will be a systematic error in the absolute magnitudes, making the former too faint and the latter too bright, which will alter the spectroscopic parallax to just such a degree as to conceal entirely the real differences in mass.

If the spectroscopic calibration curves are adjusted so as to give a correct value for the mean absolute magnitude of the stars, the "spectroscopic mass" will be the geometrical mean of the individual masses, since, if j and ρ are constant, M varies proportionally to $\log \mathcal{M}$.

To determine the dispersion in mass among visual binaries, it is therefore necessary to have recourse in some way to parallaxes other than spectroscopic. One way of doing this is through Strömberg's[1] discussion of the errors of the spectroscopic parallaxes—which he has determined by comparison of individual spectroscopic and trigonometric parallaxes, allowing for the errors of the latter. Let the probable error thus found for log π be $\pm r$. Three sources contributory to this error may be distinguished: (1) the error just discussed, arising from differences between the masses of individual stars of the same surface brightness and density; (2) the error arising from other physical causes, on account of which the functional relation (2) is not exactly true; and (3) errors of observation. If we call the amounts of these, expressed as probable errors of log π, respectively, r_m, r_p, and r_e, we will have

$$r^2 = r_m^2 + r_p^2 + r_e^2 .$$

If, on the other hand, we compute individual masses as Seares has done, the error r_m will be without influence on these masses, while r_p and r_e will affect log $\mathcal{M}$ by 0.6 of their amounts, and there will be an additional source of error, due to the imperfections of the orbits and also to errors in the assumed ratio of the masses of the components, which we may call $\pm r_c$. If then r' is the probable error of distribution, which Seares calls $r(\Delta \log \mu)$, we have

$$\begin{aligned} r_m^2 + r_p^2 + r_e^2 = r^2 &= (0.36)^2 \\ 0.36(r_p^2 + r_e^2) + r_c^2 = r'^2 &= (0.22)^2 \\ r_m^2 &= 2.78\, r_c^2 - 0.004 . \end{aligned}$$

This would indicate that the actual dispersion in log $\mathcal{M}$ (which corresponds to the probable error $\pm 0.6\, r_m$) is very small—being substantially equal to the spurious dispersion which arises from errors in the orbital elements of the binaries.

The observed values of r and r' are, however, subject to some uncertainty, and it is possible that some other concealed correlation may still be making the agreement appear better than it should.

It is obvious, however, that a better way of determining the dispersion in mass among visual binaries of the same spectral type will be a direct comparison of "hypothetical" or dynamical parallaxes, computed with a mean value of the mass, with trigonometric parallaxes. In this case there seems to be no reason to fear a correlation of the sort discussed above.

---

[1] *Mt. Wilson Contr.*, No. 199, p. 15; *Astrophysical Journal*, 53, 13, 1921.

It may be noticed that the dynamical parallax of a binary, calculated on the assumption that the principal star has the mass $\mathcal{M}_s$ derived from spectroscopic parallaxes of stars of similar kind, and the spectroscopic parallax itself, must agree exactly in every case (barring the effects of errors of observation and the small uncertainty arising in the estimate of the ratio of the mass of the system to that of the brighter component), so that it may fairly be said that spectroscopic and dynamical parallaxes are systematically equivalent to one another, so long as the mass used in computing the dynamical parallaxes is taken as a function of both absolute magnitude and spectral type. The two then rest essentially on the same physical assumptions—though this is far from obvious at first sight. If this conclusion is correct, spectroscopic parallaxes are unfitted by their very nature to give us information about the differences in mass between systems which have similar spectra (with regard to the "absolute magnitude lines" as well as other characteristics).

When a direct determination of the dispersion in mass among visual binaries has been made—for example, from the trigonometric parallaxes—it will be possible to obtain a valuable control upon the theory which atttributes the spectroscopic phenomena in question to differences in density.

MOUNT WILSON OBSERVATORY
February 16, 1922

ON THE UPPER LIMIT OF DISTANCE TO WHICH THE ARRANGEMENT OF STARS IN SPACE CAN AT PRESENT BE DETERMINED WITH SOME CONFIDENCE[1]

By J. C. KAPTEYN[2] and P. J. VAN RHIJN

ABSTRACT

If both $\phi(M)$ and N_m, the luminosity-curve and the total numbers of stars for each apparent magnitude, were completely known, the star-density could be found for any distance from the sun. The paper deals with the question: What can be reached now that our knowledge of these quantities is limited?

The conclusion is that the incompleteness of our knowledge of $\phi(M)$ is of little importance, but that the contrary is true for N_m. Even if we assume the law of the densities, formula (2), to hold for all values of m, the constants cannot be determined with the accuracy needed for the derivation of the densities at considerable distances. The limits of distance for which the density can be determined within 25 or 40 per cent of its amount were finally found on the supposition that the values of N_m are known to $m=14$ and $m=20$, respectively, and are given in Table XII. With the limit $m=17$, visual, for which we may expect complete values of N_m in the near future, the densities should become pretty reliable for the whole of the domain within which the density exceeds 0.1 of that near the sun.

The conclusions of the present paper must be considered only provisional, mainly for the two following reasons: (*a*) The extinction of light in space has been assumed to be inappreciable; (*b*) No use has been made of a recent substantial improvement in the average parallaxes of the more distant stars.

A more definitive solution now being made at the Laboratory of Groningen will duly take into account these two points. The progress of such a solution being necessarily very slow, the present provisional treatment was undertaken mainly for the purpose of finding the most promising lines for conducting the further treatment of the sidereal problem.

The points which will be successively discussed are as follows:

I. If for any determined part of the sky we know *completely* (*a*) the luminosity-curve $y=\phi(M)$ and (*b*) N_m = the total number of stars of magnitude $m-1/2$ to $m+1/2$ *per ten thousand square degrees*, then we can find the star-density $\Delta(\rho)$ at any distance ρ.

---

[1] *Contributions from the Mount Wilson Observatory*, No. 229.

[2] Research Associate of the Mount Wilson Observatory.

The solution is contained in *Mount Wilson Contribution*, No. 188, formula (13). The difficulty of the problem lies exclusively in the required completeness.

II. Half of the difficulty may be safely ignored, for it can be shown that at present and for a long, long while to come we may certainly adopt the form

$$\phi(M)=\frac{H}{\sqrt{\pi}}\,e^{-H^2(M-M_0)^2}=e^{p+qM+rM^2} \tag{1}$$

as representing the luminosity-curve completely, that is, for all values of M from $-\infty$ to $+\infty$.

We will here adopt the values of the constants p, q, r, given in *Contribution* No. 188, modified in accordance with the changes in definitions to be explained presently.

III. There thus remains only the difficulty due to our incomplete knowledge of N_m. We will show what limitation is thereby introduced in the solution mentioned in I, and we will further try to show how the limits can be extended by future countings of the fainter magnitudes.

In this inquiry, proceeding from the simple to the more difficult, we will consider three cases:

a) We will *assume* that the formula

$$N_m=\frac{h}{\sqrt{\pi}}e^{-h^2(m-m_0)^2}=2e^{a+bm+cm^2} \tag{2}$$

holds not only for the magnitudes for which we have the necessary data but also for all fainter magnitudes.

b) We will drop the latter supposition, that is, in accordance with the results found thus far, we will adopt the error-curve (2) for the actually observed N_m, but will assume nothing about the fainter magnitudes which have as yet not been investigated.

c) We will consider the most general case, namely, that the actually observed values of N_m themselves are *not* distributed in an error-curve.

IV. Having thus found the limits within which a fairly reliable determination of the arrangement of stars in space can be made, we will introduce what we think must be considered a plausible supposition, by which these limits, at least for the lower galactic latitudes, can be somewhat farther extended.

Before entering on a discussion of these points it will be necessary to premise the following remarks:

a) Cluster observations by Shapley have fairly well proved the absence of any selective extinction of light in space, at least for distances like those considered in the present discussion. It does not follow that there is no appreciable general extinction of light, and the matter will be carefully considered in our definitive solution. Still, in view of Shapley's observations, we feel less hesitation in making the assumption of no appreciable extinction the basis of this provisional solution.

b) Up to the present, the luminosity-curve has expressed the number of stars of each magnitude contained in a specified volume of space in the neighborhood of the sun. It would certainly have been much more natural and convenient had it been given the form of a true frequency-curve, that is, one showing the fraction of all existing stars belonging to each absolute magnitude. This, of course, is not rigorously possible as long as our observations do not embrace all the stars, even the very faintest in existence. But since the luminosity-curve has been derived (in *Contribution* No. 188) over a range of more than twenty magnitudes and since its coincidence with a normal error-curve throughout this entire interval, which extends far beyond the maximum, is truly astonishing, it would seem very desirable to introduce the *assumption* that the best-fitting error-curve represents the luminosity-curve over its whole extent. In this way it becomes possible to define the luminosity function as a true frequency-curve.

Henceforth we will assume, therefore, that the luminosity-curve, over its whole extent, is perfectly representable by equation (1), which differs from formula (11) in *Contribution* No. 188, only in being divided by the factor $A=0.0451$, the number of stars per cubic parsec in the neighborhood of the sun. If later on it should appear that this assumption deviates sensibly from the truth, the final results will still be unaffected. The ordinates of the curve will have only to be multiplied by a certain factor, while the densities will be divided by that same factor.

c) The parsec is again taken as a unit of distance, and in accordance with this definition the absolute magnitude of a star will equal its apparent magnitude as seen from a distance of one parsec.

TABLE I*a*

LUMINOSITY-CURVE

(Equation [5])

M	$\phi(M)$	$\log\phi(M)$		
+10	0.00229	7.359		
			470	
+ 9	.00675	7.829		70
			400	
+ 8	.0169	8.229		68
			332	
+ 7	.0365	8.561		69
			263	
+ 6	.0667	8.824		69
			194	
+ 5	.104	9.018		70
			124	
+ 4	.139	9.142		68
			056	
+ 3	.158	9.198		69
			013	
+ 2	.153	9.185		69
			082	
+ 1	.127	9.103		70
			152	
0	.0893	8.951		68
			220	
− 1	.0538	8.731		70
			290	
− 2	.0276	8.441		67
			357	
− 3	.0121	8.084		70
			427	
− 4	.00456	7.657		70
			497	
− 5	.00145	7.160		68
			565	
− 6	.000394	6.595		69
			634	
− 7	.0000914	5.961		69
			703	
− 8	.0000181	5.258		70
			773	
− 9	.00000305	4.485		69
			842	
−10	0.00000044	3.643		

$M=m+5\log\pi$

d) Finally, the star-density $\Delta(\rho)$ now means the total number of stars from the brightest to the faintest in one cubic parsec.

Under these stipulations we have in (1), in accordance with *Contribution* No. 188,

$$H=0.2818, \qquad M_0=2.693 \tag{3}$$

$$p=-2.413^{1} \qquad q=+0.4278 \qquad r=-0.07944 \tag{4}$$

$$\log \phi(M)=-1.049+0.1858\,M-0.03450\,M^2 \tag{5}$$

$$M=m+5\log \pi=m-5\log \rho. \tag{6}$$

The numerical values of (5), that is, of the luminosity-curve according to the present definitions, have been tabulated in Table I*a*.

For convenience we give in Table III the values of the constants of *Contribution* No. 188, p. 13, changed to agree with our

TABLE I*b*

log Δ (ρ) (FORMULAE OF TABLE IV)

log ρ	Galactic Latitude				
	0°	30°	60°	90°	40°–90°
1.0	8.65−10	8.65−10	8.65−10	8.65−10	8.65−10
1.2	.65	.65	.65	.65	.65
1.4	.65	.65	.65	.65	.64
1.6	.65	.65	.65	.65	.61
1.8	.65	.65	.65	.65	.57
2.0	.65	.54	.50	.52	.49
2.2	.65	.46	.42	.45	.40
2.4	.65	.33	.25	.26	.25
2.6	.55	.16	.00	7.95	.03
2.8	.41	7.93	7.67	.51	7.73
3.0	.21	.64	.25	6.95	.32
3.2	7.97	.31	6.75	.27	6.85
3.4	.69	6.92	.15	5.46	.31
3.6	.35	.48	5.48	4.53	5.70
3.8	6.97	5.98	4.72	3.48	.01
4.0	.54	.44	3.88	2.30	4.24
4.2	.07	4.84	2.95	1.00	3.40
4.4	5.54	.19	1.93	....	2.48
4.6	4.97	3.49	0.84	....	1.49
4.8	2.35	2.73	....	....	0.42
5.0	3.68	1.92	....	....	....

---

[1] Differing from the corresponding value of p in *Contribution* No. 188, p. 15, by the amount $\frac{1}{\text{Mod.}}\log(0.0451)=3.099$.

TABLE II

Distribution in Distance. Fractions of Total Number of Stars (W, Equation [12])

log ρ	$m=8$	9	10	11	12	13	14	15	16	17	18	19	20
	Galactic Latitude = 0°												
$-\infty$ to 2.8	0.7779	0.6761	0.5596	0.4382	0.3224	0.2213	0.1409	0.0835	0.0458	0.0231	0.0107	0.0046	0.0018
2.8 to 3.0	.1223	.1590	.1886	.2037	.2002	.1804	.1478	.1107	.0753	.0470	.0268	.0138	.0065
3.0 to 3.2	.0640	.0972	.1344	.1689	.1950	.2048	.1961	.1708	.1366	.0994	.0658	.0400	.0220
3.2 to 3.4	.0256	.0456	.0734	.1085	.1456	.1781	.1994	.2040	.1900	.1610	.1252	.0886	.0570
3.4 to 3.6	.0080	.0164	.0309	.0531	.0833	.1197	.1568	.1864	.2026	.2016	.1825	.1505	.1131
3.6 to 3.8	.0018	.0046	.0100	.0202	.0370	.0617	.0942	.1316	.1670	.1931	.2041	.1975	1737
3.8 to 4.0	.0003	.0009	.0026	.0058	.0125	.0244	.0439	.0711	.1053	.1428	.1764	.1982	.2038
4.0 to 4.2	.0001	.0002	.0004	.0013	.0032	.0075	.0156	.0296	.0513	.0811	.1166	.1538	.1850
4.2 to 4.4	.0000	.0000	.0001	.0003	.0007	.0017	.0042	.0095	.0192	.0353	.0596	.0916	.1286
4.4 to 4.6	......	......	.0000	.0000	.0001	.0004	.0009	.0023	.0055	.0118	.0233	.0417	.0686
4.6 to 4.8	......	......	......	......	.0000	.0000	.0002	.0004	.0012	.0031	.0070	.0147	.0283
4.8 to 5.0	......	......	......	......	......	......	.0000	.0001	.0002	.0006	.0017	.0040	.0090
5.0 to 5.2	......	......	......	......	......	......	......	.0000	.0000	.0001	.0003	.0009	.0021
5.2 to 5.4	......	......	......	......	......	......	......	......	......	.0000	.0000	.0001	.0004
5.4 to 5.6	......	......	......	......	......	......	......	......	......	......	......	.0000	.0001
	Galactic Latitude 40°–90°												
$-\infty$ to 2.8	0.9190	0.8696	0.8015	0.7161	0.6168	0.5079	0.4001	0.2979	0.2097	0.1397	0.0873	0.0513	0.0281
2.8 to 3.0	.0569	.0860	.1213	.1585	.1920	.2168	.2263	.2207	.1991	.1671	.1298	.0944	.0633
3.0 to 3.2	.0188	.0330	.0545	.0830	.1178	.1551	.1894	.2145	.2267	.2220	.2017	.1706	.1337
3.2 to 3.4	.0044	.0093	.0177	.0317	.0520	.0802	.1143	.1517	.1863	.2131	.2262	.2226	.2042
3.4 to 3.6	.0008	.0018	.0042	.0087	.0168	.0300	.0499	.0774	.1113	.1480	.1837	.2111	.2252
3.6 to 3.8	.0001	.0003	.0007	.0017	.0039	.0081	.0157	.0285	.0480	.0743	.1078	.1446	.1806
3.8 to 4.0	.0000	.0000	.0001	.0003	.0006	.0016	.0036	.0076	.0149	.0271	.0457	.0717	.1045
4.0 to 4.2	......	......	.0000	.0000	.0001	.0003	.0006	.0015	.0034	.0071	.0141	.0256	.0437
4.2 to 4.4	......	......	......	......	.0000	.0000	.0001	.0002	.0005	.0014	.0031	.0067	.0133
4.4 to 4.6	......	......	......	......	......	......	.0000	.0000	.0001	.0002	.0005	.0012	.0029
4.6 to 4.8	......	......	......	......	......	......	......	......	.0000	.0000	.0001	.0002	.0004
4.8 to 5.0	......	......	......	......	......	......	......	......	......	......	.0000	.0000	.0001

modified definitions, that is, with (4) instead of with the values previously given for p, q, r.

The values in Table III lead to the formulae in Table IV. These have been tabulated in Table I*b*.

With these details premised we will now discuss the several points separately.

TABLE III

Parameter	Galactic Latitude				
	0°	30°	60°	90°	40°–90°
h	-8.929	-8.292	-12.320	-17.418	-10.984
k	$+5.705$	$+5.481$	$+9.320$	$+14.092$	$+8.120$
l	-1.366	-1.508	-2.441	-3.542	-2.171

TABLE IV

Gal. Lat.	Density and Distance
0°	$\log \Delta(\rho) = -3.878 + 2.478 \log \rho - 0.593 (\log \rho)^2$
30°	$= -3.602 + 2.381 \qquad -0.655$
60°	$= -5.351 + 4.048 \qquad -1.060$
90°	$= -7.565 + 6.120 \qquad -1.538$
40°–90°	$= -4.770 + 3.526 \qquad -0.943$

POINT I

As already mentioned, the solution of the problem involved in this case is contained in formula (13) of *Contribution* No. 188.[1] Modified in accordance with what precedes, this formula becomes:

$$N_m = 3.046 \int_0^\infty \rho^2 \Delta(\rho) \phi(m - 5 \log \rho) d\rho. \tag{7}$$

From this equation it is at once clear that given N_m and $\phi(M)$ for *all* values of m and M, we can find $\Delta(\rho)$, and this constitutes in reality the solution of our problem. The derivation involves the solution of the integral equation (7). For the case in which $\phi(M)$ has really the form (1) and N_m the form (2), Schwarzschild has given an elegant solution, which, quoted already in *Contribution* No. 188, but modified in accordance with our present definitions, is contained in the following formulae:

---

[1] For this formula, in a slightly different form, see *Astronomical Journal*, 24, 27 (No. 566), 1904.

$$\Delta(\rho) = e^{h + k \log \rho + l (\log \rho)^2} \tag{8}$$

$$\left.\begin{aligned}
l &= \frac{25cr}{r-c} \\
G^2 &= -l - 25r \\
R &= \frac{G^2(b-q)}{5r} \\
k &= 5q - R - \frac{3}{\mu} \\
h &= a - p + \frac{\log G}{\mu} - \frac{R^2}{4G^2} - 2.5203 \\
\frac{3}{\mu} &= \frac{3}{\text{Mod}} = 6.9078.
\end{aligned}\right\} \tag{9}$$

Admitting that (8), which for brevity we will call the Schwarzschild formula, holds for all distances from $\rho = 0$ to $\rho = \infty$, it is, of course, easy to determine all such quantities as those which follow (the area is always assumed to be 10,000 square degrees):

N_m = total number of stars of appt. mag. m
$(N_m)_0^\rho$ = the same within the distance ρ
N = total number of stars of all magnitudes together
N_ρ = the same within the distance ρ
$\boldsymbol{M}$ = median = distance within which lie one-half of all the stars
$W = (N_m)_0^\rho / N_m$
$Z = N_\rho / N$.

We find the formulae:

$$N_m = \frac{0.9696\pi\sqrt{\pi}}{\mu G} e^{G^2(\beta^2+\gamma)} = \frac{12.432}{G} e^{G^2(\beta^2+\gamma)} \tag{10}$$

$$(N_m)_0^\rho = W N_m \tag{11}$$

$$W = \frac{1}{\sqrt{\pi}} \int_{-\infty}^{G(\log \rho - \beta)} e^{-z^2} dz \tag{12}$$

$$2\beta G^2 = -R - 10rm \tag{13}$$

$$\gamma G^2 = h + p + qm + rm^2 \tag{14}$$

$$N=\frac{12.433}{\sqrt{-l}}\,e^{h-\frac{\left(k+\frac{3}{\mu}\right)^2}{4l}}\qquad\left(\frac{3}{\mu}=6.9078\right).\tag{15}$$

As a check on the computations of h, k, l, N we have, expressed in terms of a, b, c,

$$N=\frac{\sqrt{\pi}}{\sqrt{-c}}\,e^{a-\frac{b^2}{4c}}\tag{16}$$

$$\log \boldsymbol{M}=-\frac{k+\frac{3}{\mu}}{2l}\qquad\left(\frac{3}{\mu}=6.9078\right)\tag{17}$$

$$N_\rho=ZN\tag{18}$$

$$Z=\frac{1}{\sqrt{\pi}}\int_{-\infty}^{\sqrt{-l}(\log\rho-\log \boldsymbol{M})}e^{-z^2}dz.\tag{19}$$

Introducing the constants of Table III into (12), (13), and (14), we obtain

$$\left.\begin{array}{ll}\text{Gal. lat.}=0^\circ & \text{Gal. lat.}=40^\circ\text{ to }90^\circ\\ G=1.833 & G=2.039\\ \beta=1.560+0.1182m & \beta=1.550+0.0956m\end{array}\right\}\tag{20}$$

with the aid of which equation (12) gives at once an insight into the distribution in distance of the stars of each magnitude m. The results have been summarized for galactic latitudes 0° and for 40° to 90° in Table II. For the medians we find

$$\left.\begin{array}{lr}\text{Gal. lat. }0^\circ & \boldsymbol{M}=39{,}000\text{ parsecs}\\ 40^\circ\text{ to }90^\circ & 2{,}900\text{ parsecs}\end{array}\right\}\tag{21}$$

Since the Schwarzschild formula does not hold for the smaller distances, results for these have been omitted from the table.

But the supposition that we know $\phi(M)$ and N_m completely, that is, for all values of M and m, is far from being justified. In the present state of science this incompleteness of our knowledge is very serious in the case of N_m, but of little account in the case of $\phi(M)$. The latter part of this statement constitutes the second point.

POINT II

The practical sufficiency of our knowledge of the luminosity-curve is due to the fact, already alluded to, that it has now been found for so large a range of magnitudes, viz., from the very brightest down to about absolute magnitude $M=+9$.

According to (6) a star of apparent magnitude m will be of absolute magnitude $+9$, when its distance is such that

$$\log\rho=\frac{m-9}{5}.$$

If, therefore, we write the equation (7) in the form

$$\frac{N_m}{3.046}=\int_{\log\rho=-\infty}^{\log\rho=\frac{m-9}{5}}\rho^2\Delta(\rho)\phi(m-5\log\rho)d\rho+\int_{\log\rho=\frac{m-9}{5}}^{\log\rho=+\infty}\rho^2\Delta(\rho)\phi(m-5\log\rho)d\rho \qquad (22)$$

the difficulty introduced by incomplete knowledge of the luminosity-curve lies exclusively in the first integral, for the second includes only stars brighter than $M=+9$, for which $\phi(M)$ is known. The difficulty cannot, therefore, be very serious because the first integral involves only stars relatively near the sun. In fact, as will be explained below, the values of $\Delta(\rho)$ within the limits of the first integral may be considered as completely known and its divergence from (8), though considerable, still unimportant for the present question, by a method wholly independent of (7) for all apparent magnitudes to $m=23$ (corresponding to the limit 2.8 for $\log\rho$). It will undoubtedly be a long time before we can expect useful data for N_m beyond $m=23$.

This being so, it is easy to show that there is an overwhelming probability that the first integral in (22) is entirely negligible, at least to the limit $m=23$. We first determine the value of this integral, denoted by V_m, on the supposition that for $M>+9$, $\phi(M)$ is still represented by (1). It is evident that V_m represents the number of stars of apparent magnitude m, absolutely fainter than $M=+9$.

We easily find

$$\frac{V_m}{N_m}=\frac{1}{\sqrt{\pi}}\int_{-\infty}^{P} e^{-z^2}dz \tag{23}$$

$$P=\frac{9r-\frac{1}{2}(b-q)-cm}{\sqrt{c-r}}\,. \tag{24}$$

The constants p, q, r are given by (4); a, b, c in *Contribution* No. 188, p. 13.

Table V, computed by the aid of (23), shows that, if the luminosity-curve (1) were correct over its *whole* length, the stars fainter than absolute magnitude +9 would not contribute to the total number N_{23} in the Milky Way more than 1 star in 16,000, or to those in galactic latitudes 40° to 90° more than 1 star in 300. For N_{22}, N_{21}, etc., the contribution is much smaller still.

TABLE V

VALUES OF V_m/N_m

m	Gal. Lat. 0°	Gal. Lat. 40°-90°
18	0.00000050	0.0000113
19	.00000143	.0000414
20	.00000392	.000139
21	.0000104	.00043
22	.0000262	.00121
23	.0000634	.0032
24	.000148	.0076
27	.00143	.0635
30	0.0095	.267

Therefore, even if beyond $M=+9$, the error-curve (1) should begin to fail very seriously to represent the true frequencies of the absolute magnitudes, it will still lead to values of N_m which will be practically correct to magnitude 23 and probably to even much fainter stars.

Suppose for instance that the frequencies, which up to $M=+9$ are represented with such astonishing closeness by the error-curve (1), should, beyond this magnitude, suddenly become tenfold the frequencies furnished by (1); even then the representation would be quite satisfactory for all values of N_m to $m=23$. Of course the overwhelming probability is that matters are really much more favorable. For we must surely expect that even if the true curve begins to diverge from (1), it will not suddenly show tenfold values. We should rather expect a deviation which for $M=+10$ is still small and only gradually increases, perhaps to very considerable amounts, as we approach fainter and fainter stars. If so, the divergence in the representation of N_m will undoubtedly be still much smaller.[1]

The conclusion from what precedes can only be: as long as observations do not extend beyond $m=23$, formula (7), in which $\phi(M)$ is given by (1), must be considered as valid. Should they ever reach stars fainter than $m=23$, a direct extension of the luminosity-curve beyond $M=+9$ may seem desirable. It is easy to see how this could be accomplished. We should require, however, more extensive data on the very faint stars having very considerable proper motions.

POINT III

It now remains to be seen what result for $\Delta(\rho)$ can be deduced from formula (7) with the aid of our *incomplete* data for the values of N_m. First consider the case:

a) We *assume* the form (2) to hold for all magnitudes from the very brightest down to $m=\infty$, referring for less hypothetical considerations to III*b* and III*c*. The problem evidently is: given, $\phi(M)$ and N_m by the formulae (1) and (2) for all values of M and m; required, $\Delta(\rho)$ for all values of ρ.

The solution has been given above in equations (8) and (9). Although theoretically this solution leaves nothing to be desired, we find in most cases that, for moderately large values of ρ, it becomes practically illusory. The reason for this of course is that existing data do not furnish the values of the constants h, k, l, with sufficient precision.

---

[1] Perhaps this will not be granted, for of course it is not impossible, *mathematically*, that after $M=+9$, the frequencies instead of continuing to decrease, may begin to increase at such a tremendous rate that the preceding conclusion would no longer hold. Even this possibility must probably be denied. If after $M=+9$ the frequencies should increase at such a rate, the number of very faintly luminous stars near the sun, that is, apparently faint stars with very large proper motion would, I think, exceed what is reconcilable with the observations.

An example, which has a considerable interest of its own, will help to show the difficulty in its true light. As such, we will try to derive the arrangement in space of the stars in the star-cloud between β and γ Cygni. We choose this example because we happen to possess data for part of this region down to photographic magnitude 18.5 (=visual magnitude 17.33). The part in question is that covered by Selected Area (syst. plan) No. 64. The low limit of magnitude is reached by using unpublished results of the Mount Wilson photometric survey together with those in the Harvard Durchmusterung.[1] Simple countings gave the numbers in Tables VI and VII.

TABLE VI

HARVARD DURCHMUSTERUNG

HARV. PHOTOGRAPHIC MAG.		N'_m FOR 40′×40′	COMP. BY (25)	O−C
Limits	Mean			
8.00 to 8.99..........	8.5	1	2	−1
9.00 to 9.99..........	9.5	7	7	0
10.00 to 10.99..........	10.5	21	19	+2
11.00 to 11.99..........	11.5	42	49	−7
12.00 to 12.99..........	12.5	143	119	+24
13.00 to 13.99..........	13.5	227	269	−42
14.00 to +14.99..........	14.5	591	570	+21
Total...............	....	1032	....	....

TABLE VII

MOUNT WILSON PHOTOMETRIC SURVEY

M.W. PHOTOGRAPHIC MAG.		N'_m FOR 15′×15′	N'_m REDUCED TO 40′×40′
Limits	Mean		
12.5 to 13.5.................	13.0	20½	146
13.5 to 14.5.................	14.0	43½	309
14.5 to 15.5.................	15.0	97½	693
15.5 to 16.5.................	16.0	200½	1426
16.5 to 17.5.................	17.0	363½	2584
17.5 to 18.5.................	18.0	677½	4817
Total	....	1403	....

---

[1] *Harvard Annals* 101.

These tables do not contain even approximately all the stars in the two catalogues. The faintest stars measured on the Harvard plates are 15.75 (phot.), those on the Mount Wilson plates 18.86 (phot.). Stars fainter than 14.99 and 18.50, respectively, were excluded because we cannot be sure that the catalogues are absolutely complete below these limits.

We have first of all to reduce the magnitudes to the same scale and to the same area. The latter reduction has already been made in the last column of Table VII. To find the scale difference the observed numbers N'_m in Table VI were represented by an equation of the form of (2). The result may be written

$$\log N'_m = 2.074 + 0.370(m - 12.5) - 0.0145(m - 12.5)^2. \qquad (25)$$

The values computed by means of this formula are in the fourth column of Table VI; the fifth shows the residuals O−C, whose changes of sign are all that can be desired. With the aid of (25) the Harvard magnitudes were calculated for which the numbers N'_m become equal to the first three values of N'_m in Table VII, viz., 146, 309, 693. The results are 12.75, 13.68, and 14.78, whence we conclude:

	Mt. W.−Harv.
Harv. mag. 12.75 = Mt. W. mag. 13.0	$+0^{\mathrm{m}}.25$
Harv. mag. 13.68 = Mt. W. mag. 14.0	+0.32
Harv. mag. 14.78 = Mt. W. mag. 15.0	+0.22

There is no indication in the differences Mt.W.−Harv. of change with the magnitude, and we adopt

$$\text{mag. Mt. W.} - \text{mag. Harv.} = \text{Const.} = +0^{\mathrm{m}}.26. \qquad (26)$$

By means of (26) the values in Table VII can now be reduced to the scale of Table VI.

A further reduction from the photographic to the visual scale is necessary because the luminosity-curve defined by (1) and (4) gives the frequencies for the visual magnitudes. For this we have used the corrections given in *Groningen Publications*, No. 27, p. 42. The first five columns of Table VIII show the complete reduction.

TABLE VIII

N'_m FOR 40′×40′

PHOTOGRAPHIC SCALE		VIS. SCALE HARV.	AMPL.	m H.S.	N'_m AMPL. 1. MAG.	COMPUTED		O–C	
Harv.	Mt. W.					(27)	(28)	(27)	(28)
8.00 to 8.99	....	7.64 to 8.61	0.97	8.125	1	2	3	− 1	− 2
9.00 to 9.99	....	8.62 to 9.57	.95	9.095	7	7	8	0	− 1
10.00 to 10.99	....	9.58 to 10.52	.94	10.05	22	22	22	0	0
11.00 to 11.99	....	10.53 to 11.47	.94	11.00	44	55	54	− 11	−10
12.00 to 12.99	....	11.48 to 12.41	.93	11.945	154	134	127	+ 20	+27
13.00 to 13.99	....	12.42 to 13.34	.92	12.88	247	296	281	− 49	−34
14.00 to 14.99	....	13.35 to 14.28	.93	13.815	635	629	598	+ 6	+37
....	12.5 to 13.5	11.71 to 12.67	.93	12.175	157	163	155	− 6	+ 2
....	13.5 to 14.5	12.64 to 13.58	.94	13.11	329	358	340	− 29	−11
....	14.5 to 15.5	13.58 to 14.51	.93	14.045	745	748	716	− 3	+29
....	15.5 to 16.5	14.51 to 15.45	.94	14.98	1517	1475	1439	+ 42	+78
....	16.5 to 17.5	15.45 to 16.39	.94	15.92	2749	(2751)	2793	(− 2)	−44
....	17.5 to 18.5	16.39 to 17.33	0.94	16.86	5124	(4835)	5176	(+289)	−52

The fifth and sixth columns give the observational data fully reduced for the present discussion. The numbers in the cloud were first compared with the corresponding numbers for the average Milky Way. It turned out at once that these numbers are all but perfectly proportional, the cloud having about 2.39 times the number for the average Milky Way. This is shown by the seventh column of the table which gives the carefully interpolated values for the Milky Way according to *Groningen Publication*, No. 27, reduced to an area of $40' \times 40'$ and multiplied by 2.39. The agreement with the observed cloud numbers in the sixth column is as good as can be expected. The numbers in the Milky Way in *Groningen Publication*, No. 27, do not extend beyond magnitude 16. For these very faint magnitudes the table gives in parentheses the values furnished by

$$\log N'_m = -4.516 + 0.7242m - 0.0141m^2 \qquad (27)$$

which best fits the numbers of *Groningen Publication*, No. 27, reduced to $40' \times 40'$ and multiplied by 2.39.

On the assumption made in this paragraph, that the formula holds for *all* magnitudes, we conclude that at all distances the star-densities in the cloud are 2.39 times the corresponding densities in the average Milky Way.

Meanwhile we can represent the observed numbers quite as well by a formula somewhat different from (27); for instance, by

$$\log N'_m = -3.951 + 0.6334m - 0.0106m^2. \qquad (28)$$

The representation by this formula is also shown in Table VIII.

By means of the constants in (27) and (28) and those of the luminosity-curve (5), we can at once pass from the distribution of the values N_m to that of the densities by means of formulae (8) and (9). We thus obtain

	Solution (27)	Solution (28)	
h	-8.060	-3.488	
k	$+5.719$	$+2.678$	(29)
l	-1.375	-0.882	

The two solutions represent rather widely different arrangements in space. The best way of showing the difference in compact form will perhaps be to compute for both, by formulae (16) and (17),

N = total number of stars for a field of 40′×40′, and

M = median distance below which lie just half of all the stars.

Introducing the values (29), we find,

	Solution (27)	Solution (28)	
M	39,000 parsecs	272,000 parsecs	(30)
N_0^∞	579,000 stars	3,700,000 stars	

Identical data thus lead to two solutions for the arrangement in space of the stars in the cloud. In the second, judging by the median values, the star-distances are 7 times those of the first solution. The total numbers[1] are as 1 to 6.5.

Evidently, therefore, the data at present available do not lead to a reliable determination of the real structure of the cloud. The reason clearly lies in the fact that the data of Table VIII are insufficient for a good determination of the constants for N_m in equation (2), and it is readily understood that it is mainly the uncertainty in the position of the maximum to which the failure of the solution is due.

In the notation of (2), this maximum lies at the magnitude

$$m_0 = -\frac{b}{2c} \tag{31}$$

whence for

$$\left.\begin{array}{ll} \text{Solution (27)} & m_0 = 25.68 \\ \text{Solution (28)} & m_0 = 29.88 \end{array}\right\} \tag{32}$$

a difference of over 4 magnitudes!

We are thus led to consider the question as to how far the observed data must be extended in order to obtain a determination of $\Delta(\rho)$ which will satisfy moderate demands at least.

To answer this it will be necessary to determine: (*a*) how the precision of m_0 (prob. err. ρ_{m_0}) depends on the precision of the counts N_m; (*b*) how the precision of the median **M** depends on the precision of m_0.

---

[1] Since the total number of stars resulting from the two solutions differs enormously, it might seem worth trying to decide between them by measuring the total light of the cloud. To test the feasibility of such a plan I compared the values of the total light and found that the amounts involved in (27) and (28) are as 1.000 to 1.025. Practically, therefore, the idea is worthless, at least with the photometric means at present available.

As for (*a*): Consider first the somewhat easier question: What will be the accuracy of m_0 obtained from observed values of N_m for three, favorably chosen, equidistant magnitudes

$$m_1-\sigma; \qquad m_1; \qquad m_1+\sigma? \tag{33}$$

For brevity call this the simplified problem. Since a rough estimate is all that is wanted, assume that the probable error of log N_m for these three magnitudes is constant and equal to r. When this simplified problem has been solved it will be easy to estimate roughly the accuracy obtainable by the use of all values of N_m.

In the Appendix is derived the formula which shows the relation between the probable errors ρ_{m_0} and r, namely,

$$\rho_{m_0}=\pm\frac{r\sqrt{2}}{4\sigma^2 c\mu}\sqrt{12(m_0-m_1)^2+\sigma^2}\,. \tag{34}$$

The value of r is readily determined by means of the deviations of the observed log N_m from a close-fitting curve. In the case of the star-cloud the number of observed stars brighter than 12 is rather small. This being the case, consider only the Mount Wilson observations in Table VIII, which show a better agreement *inter se* than the Harvard values. For the best-fitting curve I used a third solution, intermediate between (27) and (28), for which the constants are:

$$\begin{array}{lll} a=-10.019 & h=-6.038 & \\ b=+1.570 & k=+4.289 & (\text{area}=40'\times 40') \\ c=-0.0294 & l=-1.165 & \\ m_0=26.73 & \text{Median } M=63{,}800 \text{ parsecs} & \end{array} \tag{35}$$

The value found for the probable error is $r=\pm 0.008$. Experience gained in other cases indicates that this value is accidentally low and that a better one would be

$$r=\pm 0.012. \tag{36}$$

For the fundamental magnitudes we choose the values (see Table VIII)

$$12.18, \qquad 14.52, \qquad 16.86, \tag{37}$$

then for the computation of ρ_{m_0} by (34)

$$\left.\begin{array}{ll} m_1 = 14.52 & \sigma = 2.34 \\ m_0 = 26.73 & c = -0.0294 \end{array}\right\} \qquad (38)$$

which lead to

$$\rho_{m_9} = \pm 2.6 \text{ mag.} \qquad (39)$$

Starting from solution (27) instead of (35), we find nearly the same result.

As for (*b*): We learn how the accuracy of the median M depends on that of m_0 by comparing the values of m_0 and M in the three solutions (27), (28), (35). Adding a fourth solution, we have altogether

$$\left.\begin{array}{cccc} m_0 & & \log M & \\ \hline 25.68 & & 4.592 & \\ & 1.05 & & 0.213 \\ 26.73 & & 4.805 & \\ & 1.05 & & 0.203 \\ 27.78 & & 5.008 & \\ & 2.10 & & 0.426 \\ 29.88 & & 5.434 & \end{array}\right\} \qquad (40)$$

Evidently log M changes very nearly proportionally to m_0. In fact

$$\log M = -0.544 + 0.2\, m_0. \qquad (41)$$

Therefore

$$\rho_{\log M} = 0.2\ \rho_{m_0}; \qquad (42)$$

consequently, adopting the values (39),

$$\rho_{\log M} = \pm 0.520 \text{ (simplified problem).} \qquad (43)$$

It is now easy to see what can be gained by future extension of the counts to fainter magnitudes.

Table IX shows how the probable errors of both m_0 and log M change with increase in the limiting magnitude. In accordance with what precedes, we adopted ±2.6 as the probable error of m_0 in the case of the limiting magnitude 17.5, i.e., for limiting $N_m = 17.0$. The remaining probable errors were then computed by formulae (34) and (42). The results are summarized in Table IX.

Hence, if we were able to photograph the stars to magnitude 20.5 (visual scale), the probable error of log M in the simplified problem would be diminished to 0.176, which, roughly speaking, is equivalent to a probable error of about 42 per cent in the numerical value of M. I believe the error would be further lowered to less than 30 per cent, if the calculation of m_0 were based on all the available data for N_m instead of merely on those for the three fundamental magnitudes used for the simplified problem.

From an absolute point of view this precision may not seem to be very satisfactory. Still if it can be reached—and at present this is hardly subject to doubt—an enormous step in advance will have been made, for it means that the median parallax will have been determined with a probable error of about $\pm 0''.00001$.

TABLE IX

Probable Error of m_0 and log M (Simplified Problem)

Limiting Magnitude	Fund. Mags.			m_1	σ	m_0 Sol. (35)	ρ_{m_0}	$\rho_{\log M}$
17.5	12.0	14.5	17.0	14.5	2.5	26.73	2.60	0.520
18.5	12.0	15.0	18.0	15.0	3.0		1.73	.346
19.5	12.0	15.5	19.0	15.5	3.5		1.21	.242
20.5	12.0	16.0	20.0	16.0	4.0		0.88	.176
21.5	12.0	16.5	21.0	16.5	4.5		0.66	.132
22.5	12.0	17.0	22.0	17.0	5.0		0.51	0.102

Moreover, the accuracy can be greatly increased by taking several fields instead of but one.

The preceding considerations on the structure of one small region may of course be applied without change to the investigation of larger parts of the sky, for instance, to the Selected Areas for different zones of galactic latitude. The only difference is that we will obtain a much greater accuracy.

From the data of *Groningen Publication*, No. 27, Table V, we have found the values of m_0 for different galactic latitudes (β) entered in the second column of Table X. The other quantities in the table were obtained in the manner already explained.

In this table the probable errors are given, in the simplified problem, as they would be found for a single region containing the same number of stars as that in the case treated above. In conformity with (39), ρ_{m_0} for $\beta = 0$ and lim. mag. 17.5 was put at ± 2.6. For the rest the computation was made with the aid of (34) and (42).

As was to be expected, the values of m_0 run somewhat irregularly. We therefore adopted the smoothed values of the third column, which, with the exception of that for $\beta = 20°$, represent the observations practically as well as those of the second column.

By using for each region all the material instead of the three values of N_m of the simplified problem, the probable error will be diminished. If further for each galactic latitude we take the greater part or all of the Selected Areas, the probable error will again be much reduced. Finally, a further important reduction can be made by taking into account the very extensive data for the brighter stars. In order to see more clearly what can be gained, some estimate must be made as to the effect of all these reducing causes. The matter certainly deserves careful study. We have not yet made such a study, but estimate provisionally that it should be easy to reduce the probable errors of Table X to one-third.[1]

TABLE X

PROBABLE ERROR IN SIMPLIFIED PROBLEM FOR A REGION 15′×15′

β	m_0	Adopted m_0	c	Lim. Mag. 17.5		Lim. Mag. 20.5	
				ρ_{m_0}	$\rho_{\log M}$	ρ_{m_0}	$\rho_{\log M}$
0°........	26.7	26.7	−0.0294	±2.6	±0.52	±0.88	±0.176
20........	27.2	25.6	− .0297	2.4	.48	.79	.158
40........	23.1	22.9	− .0333	1.6	.32	.51	.102
60........	19.1	19.9	− .0407	0.85	.17	.24	.048
80........	18.2	17.9	−0.0486	±0.45	±0.09	±0.11	±0.022

For clearness we may express roughly the accuracy corresponding to this assumption in percentages of the whole. The results for the median **M** are thus found to be as given in Table XI.

Granting the suppositions made in III*a*, and that we are in possession of data for N_m to magnitude 20.5, we conclude that we can obtain what may be considered a good insight into the distribution of the stars in all galactic latitudes. With data to 17.5 alone (Mount Wilson Survey) this can be said only for the regions of high galactic latitude. Below latitude 40° the solution becomes rapidly less reliable.

---

[1] The comparison of the values m_0 in the second column of Table X with the smoothed values in the third leads at once to a precision of about this amount, notwithstanding the fact that the data of *Groningen Publication*, No. 27, extend but little beyond magnitude 14.5 visual.

Remark.—Meanwhile we need an extension of star-counts for regions near the galactic pole quite as much and probably more than for the lower latitudes, for just these observations of N_m in the higher latitudes will lead to a judgment on the general validity or non-validity of the analytical form (2). This follows because of the lower value of m_0 (Table X). Suppose for instance that we obtain counts to apparent magnitude 20.5. In high latitudes the curve for N_m will then become known considerably beyond the maximum, that is, for a very considerable fraction of the whole, and a fraction very much greater than that covered in the lower latitudes. In case formula (2) is confirmed for this large part of the curve in the region of the galactic pole, we will use the same analytical form with much greater confidence for the lower latitudes also.

TABLE XI

PROBABLE ERROR OF MEDIAN *M* IN PERCENTAGE OF ITS AMOUNT

Gal. Lat.	Limiting Magnitude	
	17.5	20.5
0°..................	41	13
20..................	38	12
40..................	25	8
60..................	13	4
80..................	7	1.5

III*b*. We know by observation that as far as magnitude 14 the values of N_m are well represented by (2); for the stars fainter than 14 we know nothing of the sort.[1] What results will it be possible to obtain from this knowledge?

Schwarzschild's solution, which is based on the supposition that *all* values of N_m fall on the curve (2), led to formula (8) which, but for the observation errors, would yield a knowledge of $\Delta(\rho)$ for *all* distances. This solution is not now generally applicable and we must look for another. Such a solution, based on quite different principles, which I will call solution K, has already been given in *Groningen Publication*, No. 11, and has also been applied in *Contribution* No. 188. It has there been carried through for galactic latitude 40° to 90°, and shows the very gratifying fact, which we had no right to expect beforehand, that, but for small distances (where Schwarzschild's solution is confessedly wrong) it agrees wonderfully well with the Schwarzschild solution. With the exception referred to, therefore, solution (7) represents all the data, those of *Contribution* No. 88 as well as the values of N_m in a way that leaves hardly anything to be desired.

---

[1] We take the limit $m=14$ because it represents what at present is really well known. The reasoning, of course, holds for any other limit.

Therefore, notwithstanding what has just been said, the Schwarzschild solution (8) must still be considered the most plausible to be obtained with the aid of the data at present available. This must be owing to the fact that further values of N_m, particularly those for the most influential magnitudes 15, 16 . . . . , do not deviate very much from the curve (2). Still this does not prove that formula (8) gives even an approximate solution for $\Delta(\rho)$ at very great distances. We see, for instance, from Table II, that according to (8) there are, in high galactic latitudes, hardly any stars beyond $\log \rho = 4.2$. As a consequence thereof, suppose that between $\log \rho = 4.0$ and $\log \rho = 4.2$, the density is a hundred fold the value given by (8); the total numbers of stars N_{14} will be changed by about 1 per cent only. For the brighter magnitudes the change would be still smaller. Evidently, therefore, nothing can be concluded from our data about the densities at such great distances. They may or may not agree with formula (8); we have no means of judging. The matter would be different if we had good counts (N_m) for very much fainter stars. The question thus presents itself: To what distance can the densities computed by (8) be accepted with some confidence? Or to be more precise: To what distance can we trust the values of $\Delta(\rho)$, found by (8), to be correct within 25 and 40 per cent, respectively, of their values?

In considering this question we will *assume* that what was found in *Contribution* No. 188 for galactic latitudes 40° to 90° will also be found for other galactic latitudes, viz., complete agreement of solution K with solution (8). It seems to me very probable that such will turn out to be the case. As solution K is independent of the values of N_m for $m > 14$ we may thus accept formula (8) for $\log \rho \leqq 2.8$[1] (excepting of course the small distances).

The question under consideration comes to this: How much can we change the densities (8) for $\log \rho > 2.8$, without spoiling the representation of the values of N_m to $m = 14$? Suppose that, for galactic latitudes 40° to 90°, we multiply the densities for

$$\log \rho = 2.8 \text{ to } 3.0 \text{ by } F_1,$$
$$\log \rho = 3.0 \text{ to } 3.2 \text{ by } F_2, \text{ etc.}$$

Then the numbers in Table II (second part) for $\log \rho = 2.8$ to 3.0 will all be multiplied by F_1; those of the following line by F_2, etc.

The total number N_8 (see Table II) will thus be changed to

$$N_8(0.9190 + 0.0569F_1 + 0.0188F_2 + 0.0044F_3 + 0.0008F_4 + 0.0001F_5) \quad (44)$$

and, in order that the N_8 may still be represented, the sum must still equal N_8; or better, the expression in parentheses must equal 1.00. We also find similar expressions for magnitudes 9, 10, ... 14.

The question thus becomes: What is the smallest distance for which we can take for any one of the factors F, a value as high as 1.25 or as low as 0.75 (or, respectively, 1.40 and 0.60) without making it impossible to determine the remaining factors in such a way that the seven equations of condition are still bearably well satisfied. For "bearably well satisfied" we have used the condition that the range in the residuals should not exceed 10 per cent.

Suppose, therefore, having assumed the constant F for distance R to be 1.25, that we solve our equations of condition and obtain indeed a "bearable" set of residuals. Will this prove that for distance R a density deviating 25 per cent from (8) is admissible? By no means. For as a rule the values found for the other constants will be impossible or inadmissible because they lead to negative values of $\Delta(\rho)$ or to values running too wildly for the regularly increasing distances.

---

[1] In *Contribution* No. 188 this is the limit to which solution K extends.

In order to obtain an acceptable solution we must evidently introduce the condition that the values of F shall run smoothly for regularly increasing distances. This condition is pretty vague and introduces a certain degree of arbitrariness, but I think that there is really no serious objection to it. Moderate differences in the form of the curve will probably change the results little as long as we leave two or three constants indeterminate, to be found in a way best satisfying the conditions of the problem.

Before stating the form adopted for the factors F, consider the general course they must follow. From the value 1.00 for $\log \rho = 2.8$ they must either increase or decrease. Consider only the first case, because by satisfying this we more than satisfy the other. The initial increase cannot indefinitely continue because if all the factors are greater than 1.00, the total numbers N_m will all be increased. The values of N_m cannot well be represented, therefore, unless values of $F > 1.00$ are compensated by later factors < 1.00. The factors must therefore pass through a maximum, after which decrease sets in and they soon become 1.00. We assume that there is but one maximum. Consider now the various curves representing various hypotheses for the factors F. Take more curves for which the value of the maximum is respectively $F_{max} = 1.25$, $F_{max} = 1.30$, $F_{max} = 1.35$, ... and let R, R_1, R_2, ... be the values of the distance for which $F = 1.25$.

Then we think that generally

$$R < R_1 < R_2 \; . \; . \; . \; .$$

That is, the factor $F = 1.25$ will be reached sooner by that curve for which $F = 1.25$ is a maximum.[1]

Since we wish to find the smallest distance at which F can become equal to 1.25, we consider only the latter case, that is, find the minimum distance, R, at which F can reach 1.25 as a maximal value, without being led to an "unbearable" representation of N_m.

This being premised, we now give the mathematical form adopted for F:

---

[1] We have not tried to find the demonstration. We have been content to verify its truth further on by means of the data in Table X.

$$\left.\begin{array}{l} \text{A. For the case, maximum factor}=1.25 \\ \quad\text{Before the maximum, } F=0.96+0.29\,e^{-h^2x^2} \\ \quad\text{After the maximum, } F=1.25\,e^{-p^2x^2} \end{array}\right\} \qquad (45)$$

$$\left.\begin{array}{l} \text{B. For the case, maximum factor }=1.40 \\ \quad\text{Before the maximum, } F=0.96+0.44\,e^{-h^2x^2} \\ \quad\text{After the maximum, } F=1.40\,e^{-p^2x^2} \end{array}\right\} \qquad (46)$$

in both of which

$$x=\log\rho-\log R. \qquad (47)$$

There remain, therefore, the three constants R, h, p, to be determined in such a way that R corresponds to the smallest distance for which the values of N_m can be represented with residuals not exceeding 10 per cent. This form for the factors F gives perfect smoothness throughout. It is that which a priori seems most plausible. Beyond the maximum, $\Delta(\rho)$ is evidently again represented by a form like (8), which represented the densities for the smaller distances with such perfection.

It does not, however, start at $\log\rho=2.8$ with the initial value 1.00, as premised. The reason is that the small discontinuity thus introduced at $\log\rho=2.8$ is of no real importance, while the representation of N_m is appreciably better.

Substituting the expressions for F into (44) and equating the result to the successive values of N_m we obtained a number of equations of condition.

In solving them we generally began by assuming two values for R, for each of which these equations were solved for h and p in such a way that practically the best possible representation of N_m(to $m=14$) was obtained. The range of the residuals was then found for both cases. The value of R for which the range is 10 per cent could then usually be found by interpolation. If not, the computation was repeated for a third value of R. In this way were found all the values entered in Table XII.

In all cases, with the exception of the third for $m=14$, the range of the residuals in N_m is nearly 10 per cent. In the exceptional case it is only 6.5 per cent. In fact, in this case, the knowledge of N_m to $m=14$ takes us little beyond what was reached by solution *K*.

From Table XII we may be pretty sure, now that we know N_m with some precision to $m=14$, that in the Milky Way there will be in the densities as computed by (8), no error of 25 per cent up to $\log \rho = 3.1$ and no error of 40 per cent up to $\log \rho = 3.2$. As soon as we have reliable knowledge of N_m to $m=20$ these limits will rise to $\log \rho = 3.8$ and 4.0, respectively. We further learn from the table that by extending our knowledge of N_m from $m=14$ to $m=20$ we will extend the limits to which we can reliably determine the structure of the system:

$$\left.\begin{array}{ll}\text{In the Milky Way} & 5.6\text{ fold }(\log=0.75)\\ \text{In Gal. Lat. }40^\circ\text{ to }90^\circ & 3.5\text{ fold }(\log=0.55)\end{array}\right\}\qquad(48)$$

TABLE XII

LIMITS OF RELIABILITY OF $\Delta(\rho)$ BY (8)

GAL. LAT.	N_m KNOWN TO $m=14$				GAL. LAT.	N_m KNOWN TO $m=20$			
	F_{max}	log *R*	*h*	*p*		$F_{max.}$	log *R*	*h*	*p*
0°	1.25	3.1	7.0	1.66	0°	1.25	3.8	4.0	1.66
0.........	1.40	3.2	6.0	2.70	0..........	1.40	4.0	3.7	3.6
40 to 90...	1.25	2.9	......	2.20	40 to 90....	1.25	3.4	4.0	2.05
40 to 90...	1.40	2.9	......	3.0	40 to 90....	1.40	3.5	4.0	3.73

In the case of the Mount Wilson Survey, which will yield N_m to $m=17$, the gain will be about half this amount.

III*c*. If finally, having extended the counts N_m to some higher magnitude, we find that the values of N_m no longer fit an error-curve like (2), then evidently formula (8) will no longer hold for the densities. In this case we must fall back on formula (7). We will thus find different values for the densities $\Delta(\rho)$. We may certainly expect, however, that, as long as these values do not deviate very widely indeed from the densities furnished by such a formula as (8), our considerations on the limits of reliability will still practically hold. For the present, therefore, we may safely rest content with the results just obtained.

POINT IV. EXTENSION OF THE LIMITS OF TABLE XII

There is, we think, reason to assume that the limits shown in Table XII give rather too unfavorable an impression of the real reliability. The reason is that the deviation, having once reached 25 (or 40) per cent, will grow no further, or at least not much further before it begins to diminish. This it will continue to do until it becomes *zero* and begins to increase again and, possibly, go on increasing indefinitely (on the other side). That is to say, beyond the limits assigned in Table XII the deviation from (8) for a certain time will still be mostly very moderate or small. Still much more important than this is a fact which will appear in a further publication, by one of us, in which a formula is derived theoretically which in the last analysis is an expression of the differential quotient $d\Delta(\rho)/d\rho$ as a function of ρ and $\Delta(\rho)$. The integration of this differential equation, if the equation could be accepted as definitely proved, would give $\Delta(\rho)$ as a function of ρ for all distances. As it is, the equation is verified by observation as far as observation can fairly be relied on.

We thus have not only reliable values of $\Delta(\rho)$ up to the limits of Table XII, but also to these same limits, reliable values of $d\Delta(\rho)/d\rho$. This proves that we have a right to extend the use of the formula which yielded $\Delta(\rho)$ considerably beyond the limits of Table XII.

There is a third consideration which will enable us to extend the limits of Table XII with some probability of reliable results. In the publication just alluded to it will be shown that the equidensity surfaces are at least approximately similar ellipsoids. If we suppose that this form holds somewhat beyond the limits for which we have fair certainty, then the limits of Table XII will again be extended, at least for the lower galactic latitudes.

The three considerations (of which the second is the most important) together make us believe, that as soon as we have good data for N_m down to magnitude 17, which will be very shortly, we shall be able to find fairly reliable values of the $\Delta(\rho)$ for the entire region near the center for which $\Delta(\rho)$ exceeds one hundredth of density near sun, that is, for the whole of the space represented in Fig. 2, *Contribution* No. 188.

CONCLUDING REMARK

The conclusions arrived at in this paper may perhaps best be seen in their true bearing by comparing the limits within which we can find fairly reliable results for the structure of the stellar system by using different sets of data. Of course Table XIII claims no other merit than that of furnishing the means of a rough insight into what can be obtained at present or in the very near future.

TABLE XIII

LIMITS IN PARSECS WITHIN WHICH THE STRUCTURE OF THE STELLAR SYSTEM CAN BE FOUND

Method	Galactic Latitude		
	0°–20°	40°–90°	0°–90°
1. Direct parallax determination................	....	....	50
2. Parallactic motion, now well known, to $m=10$	320	240	300
3. The same, to $m=13$........................	(830)	(610)	(720)
4. Parallactic motion, stars to $m=10$ and $\mu=0''.01$	400	320	360
5. The same together with N_m (the latter to $m=14$)................................	1600	800	1200
6. The same, N_m to $m=17$	(4000)	(1600)	(2800)
7. Extension according to Point IV, N_m to $m=14$.	3000	1000	2000
8. The same, N_m to $m=17$....................	(8000)	1700	$\Delta=\Delta_0/100$

NOTES TO TABLE XIII

The limits in parentheses have not yet been reached but may be attained in two or three years.

1. The magnificent results lately obtained in direct parallax determinations by means of long-focus instruments show probable errors of the order of $0''.01$. Even if there were demonstrably no systematic errors left, a probable error of $0''.01$ would imply that we cannot derive from them the structure of the system beyond the limit of the table. Since the absence of systematic error cannot be claimed, the limit of the table is probably rather high.

2, 4. The table gives simply the mean distances corresponding to the mean parallaxes in *Groningen Publication*, No. 29, and in a paper not yet published.

3. Simple repetition of the parallax plates obtained at the Mount Wilson Observatory some five or more years after their first exposure, would give excellent values for the parallactic motion of the stars of magnitude 13. Similar repetition of the parallax work done in America on Boss stars by other observatories with long-focus instruments would also contribute to an important degree.

5, 6. From Table XII of the present paper.

7, 8. According to Point IV of present paper. In the last column of No. 8, $\Delta=\Delta_0/100$ means that for all latitudes the densities are fairly reliable for the whole of the space where the density is greater than 0.01 of that near the sun (compare Fig. 2, *Contribution* No. 188).

All the results will be greatly strengthened as soon as we know N_m to $m=20$. At the same time this will enable us to make good estimates for still greater distances.

APPENDIX

POINT III*a*. ON THE SIMPLIFIED PROBLEM

Given, r = probable error of each of the quantities $\log N_1$, $\log N_2$, $\log N_3$, required, ρ_{m_0} = probable error of the constant m_0.

By formulae (31) and (2) of the text

$$\log N_m = \mu a - 2\mu m_0 cm + \mu cm^2 \qquad (\mu = \text{mod.}). \tag{a}$$

Hence

$$\left.\begin{aligned} \log N_1 &= \mu a - 2\mu m_0 c(m_1-\sigma) + \mu c(m_1-\sigma)^2 \\ \log N_2 &= \mu a - 2\mu m_0 cm_1 + \mu cm_1^2 \\ \log N_3 &= \mu a - 2\mu m_0 c(m_1+\sigma) + \mu c(m_1+\sigma)^2 \end{aligned}\right\} \tag{b}$$

from which for m_0

$$m_0 - m_1 = \frac{(H+1)\sigma}{2(H-1)} \tag{c}$$

in which

$$H = \frac{\log N_2 - \log N_1}{\log N_3 - \log N_2}. \tag{d}$$

Consequently

$$\rho_{m_0} = \frac{\sigma}{(H-1)^2}\rho_H \tag{e}$$

in which the probable error ρ_H must be found from (d). Since we assume

$$\text{Probable errors of } N_1,\ N_2, \text{ and } N_3 \text{ each} = r, \tag{f}$$

we obtain as in the text

$$\rho_{m_0} = \pm\frac{r\sqrt{2}}{4\sigma^2 c\mu}\sqrt{12(m_0-m_1)^2+\sigma^2}\,. \tag{g}$$

LEIDEN, HOLLAND
August 1921

COMPARISON STARS FOR NOVA PERSEI, No. 2
A CORRECTION

Father Hagen has called my attention to an error in the identification of one of the comparison stars for Nova Persei, No. 2, whose magnitudes are given in *Mt. Wilson Contr.*, No. 192; *Astrophysical Journal*, **52**, 183, 1920. The star in question is No. 57 of his sequence. An uncertainty in the position and brightness was noted during the measurement of the photographs, but was overlooked when the MS was prepared several months later.

The confusion arose from the fact that the declination coordinates of stars 57 and 62 ($+12'.6$ and $+11'.5$, respectively) are interchanged in the Chart and Catalogue of Father Hagen. The star actually observed here is close to the catalogue position of No. 57, but is much fainter than that object. Neither No. 57 nor 62 has been measured on the Mount Wilson photographs; No. 57, in fact, is just outside the limit of distance from the center of the plate usually adopted. The visual magnitudes on the Mount Wilson scale are readily found, however, by reducing Father Hagen's values to that system. The results are

No. 57 $12\overset{\mathrm{M}}{.}7$; No. 62 $12\overset{\mathrm{M}}{.}8$

F. H. SEARES

THE
ASTROPHYSICAL JOURNAL
AN INTERNATIONAL REVIEW OF SPECTROSCOPY
AND ASTRONOMICAL PHYSICS

VOLUME LV MAY 1922 NUMBER 4

THE QUANTUM THEORY OF BAND SPECTRA AND ITS APPLICATION TO THE DETERMINATION OF TEMPERATURE

By RAYMOND T. BIRGE

ABSTRACT

Structure and theory of spectrum bands.—(1) *A summary of recent work* by Fortrat, Heurlinger, Kratzer, and others is given. It is now known that bands in the visible have the same structure as infra-red bands, each starting from a line of zero intensity and increasing in intensity symmetrically in both directions to maxima, the separation of the lines in one branch meanwhile decreasing until it becomes zero and then negative, the branch reaching a head. It is shown that Kemble's formula, $m^2_{\text{max}}=0.699T/\Delta\nu_0$, for the number of the line of maximum intensity, m_{max}, as a function of absolute temperature and limiting separation of successive lines for $m=+1$, a formula based on the statistical distribution of angular velocity given by the quantum theory, may be expected to give fairly accurate values of T though it neglects some factors. (2) *Evidence* is presented to show *that Kemble's formula holds* not only for infra-red bands but also for the CN band λ 3883.

Cyanogen band λ 3883.—(1) *Position of maximum intensity as function of temperature.* From a study of spectrograms made by Strutt and Fowler and by King, m_{max} is found to vary from 9 ± 2 for light from a discharge tube containing active nitrogen at about 100°C, to 23 ± 2 for light from a furnace at 2500° to 2700°C, while the values corresponding to these temperatures as computed from Kemble's formula are 8.4, 22.9, and 23.7 respectively. This agreement justifies us in using the formula to determine the approximate temperature in the case of arcs, the sun, and similar sources which emit or absorb these bands. (2) *The intensity distribution in the A series from a 13-ampere arc* is symmetrical and corresponds to the empirical formula $\log I=1.5\log m-c_2m^{1.5}+\text{const.}$ (3) *The relative intensity of the A, B, C, and D series* seems to be *independent of the temperature.*

Spectroscopic determination of temperature, using CN bands.—From the position of maximum intensity on spectrograms made by the author, the *temperature of a 13-ampere arc* was computed to be 4500°C ± 300, while from King's spectrograms *the temperature of a 4-ampere arc* comes out 3900°C ± 300. By comparing solar spectrograms taken by St. John with the arc spectrograms the *temperature of the reversing layer of the sun* comes out 4000°C ± 500.

INTRODUCTION

King[1] has recently obtained spectrograms of the λ 3883 CN band[2] in the electric furnace, at temperatures of 2300° C., 2500° C., and 2700° C. It seemed to the author that these spectrograms furnished valuable material for the quantitative testing of a number of points in connection with the quantum theory of band spectra, and Dr. King has kindly loaned for this purpose all his original plates. He furnished also an absorption spectrogram of the λ 3883 band, taken in the furnace with the plug at about 3500° C. All of these plates were taken in the third order of the 30-foot plane grating of the Pasadena laboratory, and have a dispersion of 1.73 mm per A. The author is indebted also to Dr. St. John, of the Mount Wilson Observatory, for a solar spectrogram of this band, having a dispersion of 1.76 mm per A. I have, in addition, a series of spectrograms of the λ 3883 band, as emitted by the carbon arc, taken in the third order of the 21-foot concave grating of the University of Wisconsin (dispersion 1.13 mm per A). Enlargements, of varying intensity, were made of all of these plates, on a uniform scale of 1.05 cm per A (the scale of King's published enlargement). These and numerous direct contact prints have furnished the chief material for a study of the intensity relations in this band. Additional quantitative wave-length measurements were made from the original negatives, using the eight-inch Gaertner comparator for which the author is indebted to the Rumford Committee of the American Academy of Sciences. Two preliminary reports on this work have been made to the American Physical Society.[3] The present paper is concerned mainly with the results submitted in the later report.

The recent important development of the quantum theory of band spectra, as applied particularly to diatomic molecules, was initiated independently by Heurlinger[4] and by Lenz.[5] Further developments, of use in the present investigation, have been made by Heurlinger[1] and by Kratzer.[2] In the case of ordinary bands, such as the λ 3883 band, the empirical formulation of the experimental material is due chiefly to Heurlinger,[3] who elaborated an idea first suggested by Fortrat.[4] The results are briefly as follows.

---

[1] *Astrophysical Journal*, **53**, 161, 1921.

[2] Theoretical considerations indicate that this band is due to nitrogen, but its origin is still a matter of dispute (see Barratt, *Proceedings Royal Society* [A], **98**, 40, 1920, and Holst and Oosterhuis, *K. Akad. Amsterdam, Proc.*, **23**, 5, 727–728, 1921).

[3] Berkeley, August, 1921 (Abstract, *Physical Review*, **18**, 319, 1921) and Toronto, December, 1921.

[4] *Physikalische Zeitschrift*, **20**, 188, 1919.

[5] *Verhandlungen der deutschen physikalischen Gesellschaft*, **21**, 632, 1919.

There is no essential difference in the structure of near infra-red bands, such as the halogen acid bands investigated by Imes[5] and by Colby and Meyer,[6] and many ordinary bands in the visible and ultra-violet, such as the λ 3883 CN band, investigated in great detail by Uhler and Patterson,[7] Birge,[8] Heurlinger,[9] Bachem,[10] and many previous workers. Each true "band" consists of one "series" having two similar branches. The common origin of these two branches is a line of zero intensity, and is labeled $m=0$. From this point the positive branch (Heurlinger's "*P*" branch) runs toward the longer wave-lengths and successive lines are designated $m=+1$, $+2$, etc. The negative branch (Heurlinger's "*R*" branch) runs in the opposite direction and the lines are designated $m=-1$, -2, etc. Successive lines are not equally spaced but crowd closer together in one direction, until the series presently reaches a turning-point, where the separation of successive lines has become zero, and then turns back on itself. This turning point is what has always been known as the "head" of a band. Either the positive or the negative branch may thus invert. In the former case, illustrated by the λ 3883 CN band, the band is said to be degraded toward the violet, while in the latter case, illustrated by the halogen acid infra-red bands, the band is said to be degraded toward the red.

The two types of bands, ultra-violet and infra-red, do not appear similar in structure, due mainly to the fact that the infra-red bands have not been followed to the "head" because of the rapid decrease in intensity of the lines. But this in turn is due merely to the low temperature of the absorbing molecules, in the experimental conditions employed. Theoretically, each line of a band series corresponds to a different change of molecular rotation. The entire series corresponds to the same change of atomic vibratory motion for the near infra-red bands, or to a simultaneous change in atomic vibratory and electronic rotatory motion, in the case of visible and ultra-violet bands. The exact relation between the labeling of the lines (value of m) and the number of quantum units of angular momentum was in doubt until the work of Kratzer (*loc. cit.*). His conclusions, which seem to the author to be entirely valid, are that the missing line ($m=0$) indicates, in emission, the transition from one to zero units of angular momentum ($1 \rightarrow 0$). In absorption it indicates the reverse transition $0 \rightarrow 1$. The positive branch always indicates, in emission, an increase in momentum, while the negative indicates a decrease. The relations are reversed in the case of absorption. The value of m, for any line, thus indicates in the case of absorption, the initial number of units of angular momentum possessed by the molecule, while in the case of emission it indicates the final number. Thus in emission $m=+60$ indicates the transition $59 \rightarrow 60$, $m=-59$ indicates the transition $60 \rightarrow 59$.

---

[1] *Zeitschrift für Physik*, **1**, 82, 1920.

[2] *Ibid.*, **3**, 289, 1920.

[3] Dissertation, Lund, 1918.

[4] Thesis, Paris, 1914.

[5] *Astrophysical Journal*, **50**, 251, 1919.

[6] *Ibid*, **53**, 300, 1921.

[7] *Ibid.*, **42**, 434, 1915.

[8] *Ibid.*, **46**, 85, 1917; *Physical Review*, **11**, 136, 1918.

[9] Dissertation, Lund, 1918.

[10] *Zeitschrift für Physik*, **3**, 372, 1920.

In the case of all visible and ultra-violet bands, it has been customary to consider a series as starting at the point for which $\Delta\nu=0$, where a strong head generally appears, and the lines are numbered from this point. The numbers thus obtained will be indicated, in the present article, by m', and in the case of the λ 3883 band, the actual numbers for the A series are those used by Uhler and Patterson (*loc. cit.*). The idea that a series has two branches, centering at a point other than the "head" of the band, is due to Fortrat (*loc. cit.*) who found that the lines showing irregularities of position (the "perturbations") could thus be arranged in pairs at $\pm m$. Heurlinger found that by taking for this new origin the point of minimum intensity, similar perturbations occurred for the lines[1] $+m$ and $-(m-1)$. The reason for this discrepancy of one unit does not seem to have been explained, but the explanation follows immediately from Kratzer's hypothesis and is an important verification of the truth of this hypothesis. Thus the lines +60 and −59 show the same perturbation, and as previously noted these two lines indicate transitions between the same two rotational energy states (59 and 60) but in opposite directions. There is evidently an irregularity in this transition which affects the emitted and absorbed frequency. The experimental material at hand has furnished new data on the quantitative relations, in the case of perturbations, but this matter is reserved for a separate article. Suffice it to say here that Bachem's results (*loc. cit.*) for the perturbations, from magnetic effects, are independently confirmed by King's furnace plates, while the similarity of corresponding perturbations is even greater than has been supposed.

---

[1] Heurlinger in his dissertation had not yet theoretically interpreted the two branches. He seems to have adopted the policy of calling the branch which returned on itself the negative branch, and gave the lines of this branch negative values of m. This is theoretically correct for all bands degraded to the red, but is incorrect for all

Heurlinger found that by taking the origin of a band series at the point of minimum intensity, the two "branches" of the series show qualitatively a similar intensity-curve. Each branch begins at zero intensity, rises to a maximum, and then decreases. Heurlinger also called attention to the fact that the intensity distribution in at least one branch changed with physical conditions and could be interpreted as a change due to temperature. In the case of near infra-red bands, each branch changes with temperature, the point of maximum intensity moving toward the higher m's, as the temperature increases. The main purpose of the present investigation has been to make a quantitative study of this matter for the λ 3883 band.

The theoretical material on this point is as follows. The intensity[1] of an absorption line (in band spectra) depends on three factors, i.e.,

$$I=(E_{m'}-E_m)B_{m'}^{m}\,a_m \tag{1}$$

---

bands degraded to the violet. In agreement with most other investigators such as Bachem (*loc. cit.*) the author in his August, 1921, report used the original Heurlinger nomenclature for the λ 3883 band. But in the present paper the theoretically correct nomenclature is used, thus reversing the sign of m, and the designation of the two branches. In the old nomenclature, the rule for equal perturbations reads $+m$ and $-(m+1)$.

[1] Heurlinger, *Zeitschrift für Physik*, 1, 82, 1920.

where the transition is from m to m' units of angular momentum. The first factor (energy change) is proportional to the emitted frequency and changes by only 6 per cent during the course of the longest (A) series of the λ 3883 band. The second factor gives the probability of a transition from m to m', under the influence of absorbed radiation of the proper frequency. Little is known concerning this factor except that, from experimental data, it changes rather slowly in value with m, if m is not too small. It is also probable that

$$B^m_{m+1} = B^m_{m-1}.$$

The third factor, a_m, gives the number of molecules, at any instant, possessing m units of angular momentum. A statistical distribution of angular momentum is to be expected, on either classical or quantum theory, and such a distribution was computed first by Kemble,[1] who applied it to the 4.7 μ CO infra-red band, on the assumption that the intensity depended on this one factor alone. Kemble, as a matter of fact, worked out the distribution of angular velocity, and accordingly the results hold for angular momentum only in case $J =$ constant, where J refers to the initial moment of inertia, in the case of absorption. This does not exclude a possible change in the moment of inertia (from J to J') during the transition, due presumably to the change in vibration and electronic configuration. What is required is that J and J' be independent of the amount of molecular rotational energy. If $J = J'$ the lines of a series would have constant frequency difference. If J = constant, and $J' =$ another constant, then Deslandres' parabolic law should be true.[2] But Deslandres' formula is probably not accurately true for any known band,[3] including infra-red bands, and this indicates that J (and presumably J') both vary slowly with m. No attempt has yet been made to interpret the variation quantitatively in terms of J and J'.

Thus Kemble's formula is not a true expression for a_m, but probably approximates it very closely. The value of m corresponding to the line of maximum intensity is given, in Kemble's formula, by

---

[1] *Physical Review* (2), **8**, 689, 1916.

[2] See Sommerfeld's *Atombau* (second edition), pp. 550–566, for a summary of the work underlying these conclusions.

[3] Birge, *Physical Review* (2), **13**, 360, 1919.

$$m_{\max}=\frac{2\pi}{h}\sqrt{kJT}\,. \qquad (2)$$

where h = Planck's constant (6.55×10^{-27} erg-sec.), k = gas constant per molecule (1.372×10^{-16} erg/degree) and T = absolute temperature. If J is constant, its value can be accurately obtained from the limiting separation of successive lines ($\Delta\nu$) for $m=+1$, in which case

$$\Delta\nu_0=h/4\pi^2J.$$[1]

Hence it is possible to compute the temperature of the absorbing molecules, from the value of m for the line of maximum intensity, in either branch of a band series. Heurlinger (dissertation, p. 65) obtained this result, but considered that from experimental evidence only qualitative values of temperature were to be expected, in the case of ordinary band spectra. It will, however, be shown in this article that from recent experimental evidence the various approximations made must have relatively little effect, so that a close estimate of temperature is possible. Since in the case of discontinuous emission and absorption by vapors, no other method of quantitative temperature determination is as yet known, any results, even if approximate, should be of value in both terrestrial and astronomical work.

A formula similar to (1) applies to the case of emission, but the explanation of the expected value of the various factors is more involved. It therefore seems simpler to use the fact of the known similarity of absorption and emission spectra, and to express all results, for either emission or absorption, in terms of the absorption formula.

---

[1] In Sommerfeld's *Atombau* (p. 555, 2d edition) J' denotes the true moment of inertia (i.e., that corresponding to the initial state in the case of absorption, or to the final state in the case of emission). Sommerfeld's equations then indicate that J' is to be obtained from the limiting $\Delta\nu$ for $m=0$. But, as used by Sommerfeld, m refers to the initial amount of angular momentum, in the case of emission, and as Kratzer has shown, the line $m=0$ is then not the missing line, but the first line of the positive branch. Hence the true moment of inertia (designated J in this article) is to be obtained directly from the value of $\Delta\nu$ corresponding to the first line to the red of the missing line (designated here as $m=+1$) while the value of $\Delta\nu$ corresponding to the missing line itself gives J', the moment of inertia of the molecule in an "energized" condition. Kratzer himself used an analytic method for obtaining the correct value of $\Delta\nu$, for the halogen acids, but an equally accurate value can be obtained readily from a simple graph of $\Delta\nu$ and m, using the value of $\Delta\nu$ corresponding to $m=+1$.

EXPERIMENTAL DATA AND RESULTS

The λ 3883 CN band consists actually of five overlapping bands, each formed by one complete series. The positive branches of each of the five series (called the A, B, C, D, and E series) return on themselves, and thus cause the five heads of this band. Each series is a doublet series, with variable doublet separation (Δn), but corresponding terms ($\pm m$) in the two branches have the same value of Δn, another criterion for the division into branches. The value of Δn is zero for $m=0$. From here Δn increases to about 0.037 A at $m=-28$ (the first resolvable doublet) and to a maximum of about 0.075 A at $m=-75$. It then diminishes toward zero, the last resolvable doublet being $m=-126$. It is probable that the entire $\Delta n:m$ curve is symmetrical with respect to $m=75$, and can be considered as practically linear in the region of the unresolved doublets. This latter assumption was checked by the measured width of the unresolved doublets, after correcting for variation due to intensity.

Because of the blending of lines of the various series, the strong A series presents the best material for study. It has, however, been possible to secure enough data on the other series to indicate quite definitely that the results herein presented for the A series apply to each of the other series. The A series has its origin ($m=0$) at λ 3875.198, this being the theoretical position of the missing line ($m'=-28$) of the A_1 "singlet" series.[1] The positive branch proceeds toward the λ 3883 head as a series of apparently single (A_1) lines, but returns as a series of doublets (A_2). Actually, as noted, the A_1 lines are increasing in width and from analogy with the negative branch, the first resolvable doublet should be just at the λ 3883 head ($m=+28$). It is this apparent discrepancy in the two portions of the positive branch which so long hindered a true realization of the facts. The details concerning this and other matters connected with the frequency relations in the λ 3883 band are reserved for a separate paper.

---

[1] If, beginning at the λ 3883 head, the lines of the A_1 series are labeled by negative values of m', while the adjoining A_2 doublet to the red is given by an equal positive value, then $m=m'+28$, always. The missing B_1 line is $m'=-29$. Hence the transformation for the B series is $m=m'+29$, while for the C series it is $m=m'+30$.

A quantitative curve of the intensity distribution of the negative branch of the A series (consisting entirely of A_1 lines) has been obtained from the series of exposures (all on the same plate) taken with a 13 ampere 170 volt carbon arc at the University of Wisconsin. The usable exposures vary from 40 minutes to 15 seconds in length. The results were obtained by finding lines of equal photographic blackening, assuming the "Reciprocity Law" (It = constant, for equal blackening). This law is known to be only approximate, and in even the modified Schwarzschild formula IT^p = constant, it appears that p can have a considerable range of values, depending on many different circumstances.[1] However, under the conditions employed by the author, it is believed that the error over the entire intensity-curve will be less than possibly 50 per cent, while for the restricted portion of the curve which is of chief value, the error should be quite negligible.

It was found that by using on the prints only lines of rather low intensity, the error of a single comparison was about 10 per cent, and this could be greatly reduced by averaging many independent comparisons. The prints were cut up, and the lines to be compared brought into actual contact. One of the inherent difficulties is due to the fact that resolved doublets have frequently to be compared with unresolved doublets. This was partly overcome by making prints on medium contrast (Azo) paper, so that none of the doublets were resolved. On maximum contrast Azo (used for both prints and enlargements) the definition is equal to that on the original negatives, while with proper exposure, the intensity variations are far more evident to the eye.

In this work it is essential that there be used only lines quite free from all other lines. While it is frequently evident that lines are "blends," it is not so evident in many other cases, and certain knowledge on this point results only from a complete analysis of all of the series of the band, i.e., a computation of the "theoretical" position of every line of every series. The author, as a result of his work on this band (*loc. cit.*) has such data for all of the stronger series, and the only series or portions of series still not analyzed are of such low intensity that they can scarcely produce any appreciable error. This data, most of which is still unpublished, has been of invaluable aid in this entire investigation. A very few theoretically "free" lines show irregular intensity, but in most cases this is evidently due to the effect of extraneous lines (line spectrum of carbon?) of which there are quite a number scattered throughout the band.

---

[1] See Odencrants, *Zeitschrift für wissenschaftliche Photographie*, **16**, 111, 125, 189, 1916, for complete review of work to date, and Helmick, *Physical Review*, **17**, 135, 1921, for the latest results.

The variation of intensity throughout the observed A series lines is about seven hundred fold. The Kemble formula does not fit the intensity-curve obtained. Thus if the theoretical and experimental curves are made to coincide at the point of maximum intensity ($m=-30.4$) the experimental value at the last known line at $m=-137$ (4.5 times 30.4) is 5.5 times too large, and this evidently exceeds the possible experimental errors. As far as the chance experimental errors of the blackening comparisons are concerned, it is believed that the curve is accurate to about 10 per cent, except for very small values of m (0–5) where the error may be much greater. Other possible sources of error are (1) change of sensitiveness with wave-length of the plate, (2) uneven illumination of the printing paper, (3) uneven development of the plate or paper. It is thought that none of these causes separately would produce errors much in excess of 10 per cent. It is therefore believed that the foregoing discrepancy is due to the various approximations inherent in the use of the Kemble formula for the distribution of intensity, i.e., the neglect of the first two factors in equation (1), and the assumption of constant J.

It is convenient to have a purely empirical equation for the experimental curve, and such an expression is found to be

$$I=c_1m^{\frac{3}{2}}e^{-c_2m^{\frac{3}{2}}}. \tag{3}$$

The corresponding Kemble formula is

$$I=c_1me^{-c_2m^2} \tag{4}$$

Equation (3) fits the experimental curve to within about 10 per cent from $m=5$ to 137, taking $m_{\text{max.}}=30.4$.

The only previous quantitative work on the distribution of intensity in this band is that of Haferkamp,[1] where, however, only the region λ 3883 to λ 3865 was studied. The quantitative portion of this work was based purely on the equality of the three lines of certain A_1A_2 triplets. At these points ($m'=15$ and 35, according to Haferkamp) the A_1 and A_2 series are taken to be of equal intensity. Actually, however, since the A_1 line is an unresolved doublet, the A_2 term is twice as strong as the A_1. In addition Haferkamp finds an irregularity at $m=-4$. This results from his misinterpretation of the A_2 perturbation at that point. The lines comprising the perturbations are, I believe, regular as regards intensity, and irregular only as regards position. The net result is that Haferkamp's intensity-curves are more or less irregular, and are not symmetrical for the two branches, a fact which has caused a real difficulty in the application of theory.[2]

Now while it is not possible to obtain directly a complete intensity-curve for the positive branch of the A series, enough intensity comparisons of the lines of the two branches can be made to make possible the conclusion that within the rather narrow limits of experimental error the distribution of intensity in the two branches is probably exactly the same. This result seems to the author of considerable importance, for it shows that these CN bands are entirely similar to the infra-red bands in intensity distribution, and thus furnishes a foundation for the use of the quantum theory of band spectra in the quantitative determination of temperature. But while the two branches seem to have intensity-curves of the same shape, the actual intensity of the positive branch averages some 10 to 20 per cent greater than that of the negative. The difference appears to be independent of the wave-length separation of the two lines compared (amounting to 3 to 85 A), and so can scarcely be due to a possible change with wave-length of the sensitiveness of the photographic plate.

[1] *Zeitschrift für wissenschaftliche Photographie*, **9**, 19, 1910.

[2] See Eucken, *Jahrbuch d. Radioaktivität und Elektronik*, **16**, 397, 1920.

Equation (1) indicates why the distribution of intensity in the two branches should be at least very closely the same. For in the case of absorption each pair of corresponding lines ($\pm m$), have the same a_m term; theory indicates that the middle factor should have the same value for the lines of a pair (i.e., the transitions $m \rightarrow m-1$ and $m \rightarrow m+1$ are equally probable for absorption); and the first factor differs at the most by 2 per cent (85 A) for the two lines of a pair.

While the experimental results thus indicate that Kemble's formula is only approximate, as applied to the complete intensity distribution in the λ 3883 band, it seems to the author probable from theoretical considerations that equation (2) giving the m_{max} should be more nearly correct. Let us first see if this equation checks in the case of infra-red bands. E. v. Bahr,[1] using the classical theory, showed that between 17° and 1430° C. the frequency separation of the maxima of the two branches was directly proportional to $\sqrt{T}$, as predicted. On quantum theory it is not the frequency separation, but the separation in terms of number of lines that should vary with $\sqrt{T}$, i.e., $m_{\text{max}}=k\sqrt{T}$. If the lines were equally spaced, as they are approximately, the two viewpoints would coincide. In the work quoted the results to be expected by the two theories differ by less than the experimental error, so that the quantum theory is equally well substantiated.

The best infra-red data is that by Colby and Meyer (*loc. cit.*) for the fundamental HCl band, at room temperature, and at a temperature described as "the tube was heated to a glow which could just be seen in a darkened room." I take this to be about 500° C. It is convenient to express formula (2) in terms of the limiting $\Delta\nu$ for $m=+1$. ($\Delta\nu_0=h/4\pi^2 J$.) One thus obtains

$$T=1.431\,\Delta\nu_0 m_{\text{max}}^2 \tag{5},$$

where $\Delta\nu_0$ is expressed in frequency units. Using the accurate value of $\Delta\nu_0$ (21.30) computed by Kratzer[2] (*loc. cit.*), for $T=300°$ absolute $m_{\text{max}}=3.13$, for 773°, $m_{\text{max}}=5.03$. Colby and Meyer's curves (*op. cit.*, p. 301) indicate that these values are correct, as nearly as can be ascertained.

---

[1] *Verhandlungen der deutschen physikalischen Gesellschaft*, **15**, 731, 1913.

[2] This value is from Imes's data. Colby and Meyer's data yield the same value, from the $\Delta\nu{:}m$ graph.

Let us turn again to the λ 3883 band. The outstanding feature of King's furnace spectrograms is the redistribution of intensity in each branch of the various series, as compared to the arc exposures.[1] Due presumably to the lower temperature of the furnace, the $m_{\max}$ has a smaller value, and starting at $m=0$ each branch increases very rapidly in intensity. There is a correspondingly rapid falling off of intensity for the larger values of m. Thus in my 13 ampere arc the lines $m=4$ and 83 are approximately equal, while in the 2700° furnace the equality is between $m=4$ and 52. In the 13 ampere arc $m=52$ is 4.5 times as strong as $m=83$. But again theory is verified by the fact that the redistribution of energy is the same for each branch. Thus self-reversal starts in the 2700° furnace at $m=61$ and $1\frac{1}{2}$, in each branch; and in the 2500° spectra at 51 and 3, in each branch, as nearly as can be judged. A direct comparison of $m=\pm 1$, ± 2, and ± 3 seems to indicate a small difference in absolute intensity of the two branches, but probably not as great as that in the case of the arc spectra. The ± 61 and ± 51 equalities would indicate no difference, but this criterion is not a very sensitive one.

The experimental difficulties in determining intensities are much greater, in the case of the furnace spectra, due to the self-reversal of the stronger lines. It has, however, been possible to obtain $m_{\max}$ directly by measurements of the width (a) of the self-reversed portion of the lines, since this width varies rapidly with intensity. King's furnace plates contain an arc comparison (arc of about 4 amperes, 170 volts). The width (e) of the emission line was subtracted from a. This eliminates the variation in a due to changing doublet separation. (In the region used the doublets are still unresolved.) The (a–e) computed was then corrected for the variation in e due to intensity, the amount of this correction being determined by a separate study of the width of single arc emission lines. The resulting corrected values of (a–e) gave a fairly smooth symmetrical curve, with a definite maximum. In the case of arc spectra, a direct determination (method 1) of $m_{\max}$

---

[1] See King, *op. cit.*, Plate XX.

is possible, as well as an indirect method (method 2) from pairs of lines of observed equal intensity, using formula (3). The direct comparison is of course virtually the comparison of pairs of lines of equal intensity, but close to $m_{\max}$ so that the arithmetic mean may be used.

One of the first facts noted in this investigation was that King's 4 ampere arc did not show the same intensity distribution as my 13 ampere arc. Thus consider the A_1A_2 "triplet" $m'=33$ (the first to the red of the second head). In the 4 ampere arc all three lines are of practically equal intensity, as shown on King's published enlargement. In the 13 ampere arc the A_1 line is decidedly weaker than the two A_2 lines. As far as can be ascertained, equation (3) applies equally well to the 4 ampere arc. Nothing can be said as to the furnace spectra, since the data are too fragmentary. Likewise no quantative results seem possible, for the 2300° C. furnace plate, due to the weakness of the lines.

The experimental values of $m_{\max}$ are as follows:[1]

		Method 1	Method 2
13 amp. arc, $m_{\max}$	=	30 ± 1	30.4
4 amp. arc, $m_{\max}$	=	28 ± 1	28.2
2700° furnace $m_{\max}$	=	23 ± 2	
2500° furnace $m_{\max}$	=	23 ± 2	

Further material on this band is furnished by its appearance in active nitrogen.[2] Although the published photograph is one with rather small dispersion, I estimate $m_{\max}$ at 9 ± 2. The A series at this point is however contaminated by the B series, and a more accurate value is obtainable from the λ 4216 band, since here the A series is not thus contaminated. It has, moreover, practically the same $\Delta\nu_0$ and therefore its $m_{\max}$ should be the same. The result is $8 \pm 1\frac{1}{2}$. The peculiar appearance of these bands, in active nitrogen, is in fact due solely to the radical redistribution of intensity in each branch of the various series. Thus in the neighborhood of $m=0$, the usual appearance of the band, under low dispersion, is due almost solely to the A_2 lines, the A_1 lines being very faint. But in active nitrogen, the A_2 series is practically missing, due to the rapid decrease in intensity for higher values of m. These photographs also indicate most beautifully the similar redistribution in the other series of the CN bands. The relative intensity of the A, B, C, and D series, in active nitrogen and in King's furnace plates, seems to be changed but little, if at all.

---

[1] Since unconscious bias can easily enter into such determinations, it seems only fair to state that all of the quantitative results here presented were obtained before their quantitative theoretical significance was fully realized, and no change of any kind in the data has since been made. The value of 22 given for the furnace spectra in the August report was a preliminary one, based on a few uncorrected (*a–e*) readings.

[2] Strutt and Fowler, *Proceedings Royal Society* (A), 86, 1911. Plate opposite p. 117.

The value of $\Delta\nu_0$ for the A series of the λ 3883 band[1] is 3.704. Putting this value in equation (5) we have

$$T=5.30\, m_{\max}^2 . \tag{6}$$

From

$$m_{\max}=8\pm 1\tfrac{1}{2},\quad T=70^\circ\ \text{C.}\pm 150^\circ .$$

Strutt considers the temperature in active nitrogen about 100° C. E. P. Lewis thinks this estimate too high. The temperature must be above room temperature but probably very little above. Using the reverse process for the furnace spectrograms, we have

$$T=2700^\circ\ \text{C. gives } m_{\max}=23.7$$
$$T=2500^\circ\ \text{C. gives } m_{\max}=22.9$$

The experimental values were 23 ± 2 in each case. It therefor seems to the author that there is fairly conclusive evidence to the effect that over a considerable range of temperature, formula (2) is capable of giving quantitative results. This formula admittedly involves a number of real approximations, but the errors thus introduced seem to be smaller than the necessary experimental errors involved in determining $m_{\max}$.

It further seems that formula (2) should yield at least very approximate results in the case of higher unknown temperatures, in the case both of absorption and of emission spectra. It will be noted that in the previous data, the HCl band is in absorption, the active nitrogen in emission, and the furnace spectra mostly self-reversed and so a combination of emission and absorption. In postulating a similar intensity distribution for emission and absorption spectra at the same temperature, all that is assumed is that two lines of equal intensity in absorption will be of equal intensity in emission, and that the line having the greatest absorption coefficient will also show the greatest emitted intensity. The actual photometric curve of an absorption spectrum will of course depend on the depth and density of the absorbing layer. The same statement is true, to a lesser degree, for emission, as is indicated by the phenomena of self-reversal.

---

[1] Heurlinger's value of c_1 $(=\Delta\nu$ for $m=0)$ is 3.84. The value of $\Delta\nu$ for $m=+1$ is obtained from $c_1-2c_2=3.84-2\times 0.068$.

King's absorption plate of the λ 3883 band yields information on this subject. The plate was taken with the plug at 3500° C., and Dr. King estimates the effective temperature of the vapor as in the neighborhood of 3000° C. An accurate comparison of this plate with the furnace spectrograms is difficult, due as usual to the self-reversal in the latter, but the results are as follows. The absorption intensity relations are definitely different from those of the 2500° C. furnace plate, and as nearly as can be ascertained, the same as those of the 2700° C. plate. The difference, if any, is such as to indicate a higher temperature. I, therefore, estimate its temperature as 2700–2900° C. From the known plug temperature, this value cannot be very greatly in error.

Formula (2) can now be applied in two cases to the determination of unknown temperatures, (1) the CN vapors of the electric arc, (2) the CN vapors in the sun's reversing layer.

From the data for m_{max} already given (method 1), we have for the 13 ampere arc $T=4500°\ \text{C}\pm 300°$, and for the 4 ampere arc $T=3900°\ \text{C}\pm 300°$. It is known that the hottest portion of the arc crater is about 4000° C., but it seems very probable that the vapors are still hotter, since it is the impact of the electrons and ions of these vapors which causes the crater temperature.[1] The author is aware that there is considerable uncertainty as to just what is meant by "temperature" in a case like this, where there is no thermal equilibrium. The same problem enters into many questions concerning solar and stellar temperature. The term "effective temperature" is therefore used, leaving open the question of its relation to temperature, as measured by more ordinary methods.

---

[1] See Marx, *Handbuch der Radiologie*, 4, 378–390, for summary of work on this subject.

In the case of the solar spectrum of the λ 3883 band, it is impossible to obtain directly the value of m_{max}. The only available criterion is a comparison of relative intensities of adjacent lines in the solar and in the arc spectrograms. The best lines for this purpose are the "triplet" groups in the neighborhood of $m=0$. For the A_1 lines quickly rise in intensity, going in each direction from this point, and presently equal in intensity the adjacent A_2 lines. The point where this equality occurs varies with the temperature. The available data are even more fragmentary than is indicated in Rowland's table,[1] for a detailed comparison of intensities, using enlargements of St. John's solar plate, indicates that many CN lines marked as free by Rowland are actually blends.[2] The only really available triplet groups seem to be those for which $m'=16$, 18, 19, and 26. Of these $m'=19$ (λ 3879.851, λ 3879.796, and λ 3879.716, on Rowland's scale) furnishes the most sensitive criterion. For this group, the furnace spectra and King's absorption plate show A_1 much stronger than the two A_2 lines. King's 4 ampere arc shows the three lines equal. In my 13 ampere arc A_1 is slightly weaker than A_2. In the sun the three lines seem equal. If there is any difference, A_1 is the stronger. Hence the solar temperature is in the neighborhood of the effective temperature of the 4 ampere arc (4000° C.). A study has been made also of a large number of "free" solar CN lines, and the results are in at least qualitative agreement with this conclusion. A quantitative study does not seem possible.

Grebe and Bachem's micro-photometric curves[3] yield similar results.[4] It should be noted, in this connection, that the curves on page 419 are mislabeled. The actual A_1 lines marked by dots in both arc and sun are $m'=25$, 23, and 18, and not 26, 24, and 19 as the printed wave-lengths indicate. In these curves the red is to the right, except in the solar λ 3879.716 curve. The scale is 2 cm = 1 A.

---

[1] *Astrophysical Journal*, **1**, 29, 1895.

[2] My first estimate of solar temperature (4700° C.) was partly due to the accidental use of such lines.

[3] *Zeitschrift für Physik*, **2**, 419, 1920.

[4] Grebe and Bachem's λ 3873.504 curves seem to furnish the best material for this test. But this triplet group ($m'=31$) is not usable in the sun, and the published "solar" curve has seemingly no relation to the actual solar spectrum at this point.

The results show that Grebe and Bachem's arc is about the same temperature as my 13 ampere arc, while their solar curves indicate a lower temperature than their arc, but possibly not as low as that of the 4 ampere arc. This temperature of about 4000° C., according to Dr. St. John,[1] is lower than anticipated, but I feel that it is probably correct to about 500° C.

The only other method for such determinations is that of Saha[2] but this method requires a knowledge of the pressure, so that the temperature determinations may be in error by large amounts. It would seem as though the present method, with increasing theoretical knowledge, should be capable of fairly accurate quantitative results. Meanwhile many possible investigations immediately suggest themselves, such as a determination of the relative temperature in sun-spots and in other portions of the solar atmosphere, and the variation of effective arc temperatures with varying physical conditions. In this connection it is to be remembered that in addition to the CN bands, others such as the λ 5165 Swan band[3] are already known to exhibit similar variations with temperature, and may therefore be used in such work.

Physical Laboratory
University of California
January 1922

---

[1] Personal communication.

[2] *Zeitschrift für Physik*, **6**, 40, 1921, and contained references.

[3] See King (*loc. cit.*); Konen, *Das Leuchten der Gase und Dampfe*, p. 317; and Heurlinger, Dissertation, pp. 46–55.

THE ARC SPECTRA OF GALLIUM AND INDIUM

By H. S. UHLER and J. W. TANCH

ABSTRACT

Arc spectra of gallium and indium, λ 4511 to λ 2170.—To identify the lines, spectrograms obtained with the pure elements and with various compounds and mixtures were compared; these were made with a short focus concave grating spectrograph and with a large quartz prism spectrograph. *For the accurate determination of the wave-lengths,* spectrograms were made with a 21-foot concave grating, special precautions being taken to minimize pole effects, to avoid mechanical displacements and to obtain the lines sharp and separated from close lines of other elements. The wave-lengths for air, accurate in most cases to a few thousandths of an angstrom, and the vacuum wave-numbers are given for 23 gallium lines and for 34 indium lines. All the gallium lines and 28 of the indium lines were found to belong to the *two subordinate series,* for each of which from 5 to 8 terms were identified. Preliminary values of the *constants of the Ritz-Paschen formula* for these series were calculated for both elements, but the agreement between observed and calculated wave-numbers is not satisfactory. The Mogendorff-Hicks formula was tested for gallium with even worse results. Four indium lines, previously supposed to be single, were resolved into from three to six components each.

Absorption spectrum of indium in a furnace.—Specially designed furnaces were used but only λλ 4511 and 4102 were obtained.

INTRODUCTION

The present paper largely fulfils the promise made in the following quotation: "As soon as possible the wave-lengths of the gallium lines will be accurately determined by means of a 21-foot grating so that the constants of the series formula may be calculated independently of the analogous data of aluminium, thallium, indium, etc."[1]

The necessity for the investigation is sufficiently stated by H. Kayser[2] in the sentence: "Alles in Allem ist das Spectrum des Ga noch so gut wie unbekannt." The data for indium given in the fifth and sixth volumes of the same classic show that spectroscopic work on this element is also highly desirable.

The bibliography of the subject may be dispensed with by merely referring to Kayser's *Handbuch* and to a more recent paper by F. Paschen and K. Meissner.[3]

---

[1] Philip E. Browning and Horace S. Uhler, *American Journal of Science,* **41**, 351, 1916; see also, *ibid.,* **42**, 389, 1916.

[2] *Handbuch der Spectroscopie,* **5**, 461, 1910.

[3] *Annalen der Physik,* **43**, 1223, 1914.

The experimental work was begun before the year 1916 and it was closed in August 1919, but the attempted calculations and preparation for publication were inordinately delayed, first by the war and later by the temporary incapacity of the senior author.

The investigation involved two problems, the first of which consisted in vaporizing carefully purified metals in the arc in order to identify all of the lines radiated respectively by gallium and by indium, and to obtain the approximate wave-lengths of these lines. The second problem involved a more detailed study of the discrete lines and the more accurate determination of the wave-lengths of all the lines, except the very faintest ones.

APPARATUS, MATERIAL, AND METHOD

For the identification of the lines most of the spectrograms were obtained with two instruments: (*a*) a grating spectrograph[1] of one meter radius of curvature designed by the senior author, and (*b*) a large quartz prism spectrograph of the Littrow type made by A. Hilger and owned by the American Brass Company in Waterbury, Connecticut. Most of the films used in the grating apparatus were made either by the Wratten & Wainwright Company or to special order—through the courtesy of Dr. C. E. K. Mees—by the Eastman Company. The plates employed in the prism spectrograph were Wratten and Wainwright backed, red-sensitive plates and also special Schumann plates made and presented by Dr. I. C. Gardner. Unfortunately the plates last mentioned did not bring out any more lines in the ultra-violet than were recorded on the Wratten plates. Since the Schumann plates were of excellent quality, the negative result obtained with them indicated that the lines of high order were not radiated with observable intensity under the experimental conditions of the arcs. The metals were prepared and purified by the senior author, and they were vaporized upon positive electrodes either of Acheson graphite or of copper. This part of the work should be thoroughly reliable, as a large number of spectrograms were also taken with the materials which Browning obtained while studying the chemical separation of gallium and indium.

---

[1] *American Journal of Science*, 41, 353, 1916.

For the more accurate determination of the character and wave-lengths of the stronger lines the large grating spectrograph of the Sloane Laboratory was used. The grating was ruled by J. A. Anderson; it has a radius of curvature of about 640 cm (21 ft.) with 590 lines per mm (15,000 per inch). The mounting is according to Rowland's plan and it is characterized by great rigidity. The foundation upon which the whole apparatus rests is of solid masonry and it is situated in the sub-basement of the building. The grating-room was specially designed to maintain constant temperature, a condition that is admirably fulfilled. The spectral lines between λ 4511 and λ 2932 were obtained by using both the second and the third orders, while the range between λ 2932 and λ 2300 was obtained only in the second order. The linear dispersions in the second and third orders are about 1.32 A per mm and 0.87 A per mm, respectively. The grating was very carefully tested to ascertain whether it would admit of the use of the "method of coincidences." This test was necessary because the ultra-violet lines of the third order were determined by interpolation between the standard iron lines of the second order. It was found that the grating fulfilled the requirements well within the limits of experimental error. This result was not unexpected, since it is in full accord with the investigation of Miss J. T. Howell.[1]

In several cases (e.g., Ga λ 2874) the lines under investigation sensibly coincided with iron lines and hence necessitated the use of a semaphore. The base upon which this screen was mounted was screwed to the rigid foundation of the spectrograph, very close to the incidence side of the camera. In order to avoid displacing the plate during exposure, the semaphore was raised or lowered by means of cords passing through the partition between the arc-room and the grating-room.

The plates used with the large grating were Cramer Isochromatic Instantaneous and Seed 26 and 30. Jewell's simple hydrochinone developer was invariably used with these plates.

In order to minimize the pole effect of the iron arc and to comply with the then recognized regulations for international standards, a modified form of the Pfund arc was employed.[2] This arc had a length between 8 mm and 12 mm with a direct current of 5 amperes or less fed by 110 volt mains. Under these conditions it burned steadily as long as desired without restriking. A length of about 1.25 mm at the central portion of the arc was used as the source of illumination of the slit, the light from the remaining portions being screened off by a metal diaphragm which was perforated by a rectangular hole 1.25 mm high and much wider horizontally. This diaphragm was placed about 7 mm from the flame and it was rigidly attached to the base of the lamp. The upper, or negative, electrode was a rod of common carbon, while the positive electrode consisted of pure electrolytic iron kindly supplied by the United States Bureau of Standards. All the other specimens of iron tested contained manganese as an impurity, several of the lines of which nearly coincided with certain gallium and indium lines.

---

[1] *Astrophysical Journal*, **39**, 230, 1914.

[2] *Ibid.*, **42**, 231, 1915, and **46**, 150, 1917.

The secondary interferometer standards published by the Bureau of Standards[1] were used for the region between λ 4528 and λ 3233, while for wave-lengths shorter than λ 3233 the earlier data given by Fabry and Buisson were employed.

The original source of the gallium and indium was a leady residue which contained these metals as impurities to the amount of about 0.5 per cent and 2.0 per cent, respectively. This material was usually shaved into small fragments with an ice-plane and then tamped into a deep hole that had been drilled in the axis of a rod of Acheson graphite. When the lines radiated from the positive electrode thus formed were too widely reversed, the leady residue was diluted by stirring little pieces of it in ordinary liquefied lead. After the mixture or solution became homogeneous it was poured into cored carbon or graphite rods. In cases where the lines under investigation were obscured by lead lines, indium hydroxide or indium oxide, containing gallium as an impurity, was used in the cores. In other cases, lead oxide, reduced from lead nitrate which had been obtained as a by-product in the chemical work, was used to advantage. The upper electrode was invariably a rod of common carbon.

The exposure time was usually 5 min. or 10 min., but sometimes an hour or more. In some cases, half the exposure to the iron arc was given, then the full exposure to the material in question, and, finally, the second half of the iron exposure. Check plates were always taken with the iron lines impressed simultaneously with the lines of the rare elements.

---

[1] *Bulletin No. 274*, 1916.

RESULTS

Gallium. Experimental.—The numerical data are collected in Table I. The numbers in the first column are merely for reference. The series notation in the second column should be obvious. The third column contains the wave-lengths in air given by Exner and Haschek. The next column presents the new wave-lengths in air obtained by the present authors. The reduction from the fourth column (15° C.) to the fifth (*vacuo*) was based on the formula given on page 722 of *Bulletin No. 327* of the United States Bureau of Standards.

TABLE I

No.	Series	λ in Air		Wave-Number $\nu_0=\lambda_0^{-1}\times 10^8$	$\Delta\nu_0$	Int.
		E. and H.	U. and T.			
1	S_1 (2)	4172.06	4172.048	23962.31	826.30	10
2	S_2 (2)	4033.03	4032.975	24788.61	....	10
3	D_1' (3)	2944.18	2944.175	33955.47	826.16	6
4	D_1 (3)	2943.66	2943.639	33961.66	....	6
5	D_2 (3)	2874.24	2874.240	34781.63	....	6
6	S_1 (3)	2719.66	2719.664	36758.39	826.23	3
7	S_2 (3)	2659.84	2659.873	37584.62	....	3
8	D_1' (4)	....	2500.714	39976.53	826.14	3
9	D_1 (4)	2500.18	2500.187	39984.96	....	7
10	D_2 (4)	2450.10	2450.078	40802.67	....	6
11	S_1 (4)	....	2418.699	41331.96	825.67	2
12	S_2 (4)	....	2371.325	42157.63	....	2
13	D_1' (5)	....	2338.596	42747.57	827.12	1
14	D_1 (5)	....	2338.293	42752.47	....	2
15	S_1 (5)	....	2297.869	43505.12	826.15	1
16	D_2 (5)	....	2294.202	43574.69	....	1
17	${}_1D_1'$ (6)	....	2259.227	44249.16	826.24	1
18	S_2 (5)	....	2255.034	44331.27	....	1
19	S_1 (6)	....	2236.103	44706.68	823.30	1
20	D_2 (6)	....	2218.039	45075.40	....	1
21	${}_1D_1'$ (7)	....	2211.753	45198.83	828.	1
22	S_2 (6)	....	2195.665	45529.98	....	1
23	D_2 (7)	....	2171.9	46027.	....	1

The differences $\Delta\nu_0$ are printed in the same horizontal line as the other data for the less refrangible of the two components involved. This scheme avoids overlapping of braces and confusion where the subordinate series get out of step.

As is often the case, the column of intensities means but little more than is contained in the following verbal statements. The less refrangible component of each doublet is somewhat stronger than the more refrangible one. The satellites are very much weaker than either of the main components of the same doublet. In any one series the intensities of the lines decrease very rapidly as the order (m) of the line increases. When approximately pure gallium is burned in air all of the lines are widely reversed. For all the strong lines the reversal was suppressed when the metal was caused to radiate as a minute impurity in some mixture. The wave-lengths obtained with the very fine unreversed lines agreed, within the limits of experimental error, with the wave-lengths observed by setting upon the axis of the widely reversed lines.

The lines numbered 1 and 5 received special attention because of their closeness respectively to the iron lines at λ 4172.128 and λ 2874.176. Lines 1 to 5 inclusive were measured on third-order plates, while all of the lines were determined in the second order. When a line was measured in both orders, the difference between the results for each individual line was never greater than 0.004 A, and usually less. Each line was always measured four times in one direction, then the plate was reversed and the line measured four times in the other direction.

Theoretical.—In attempting to represent the series lines of gallium by an empirical equation we began by using the Ritz formula in the following form

$$\nu_m = A - \frac{N}{[m+a+b(A-\nu_m)]^2}, \qquad (1)$$

because it has been so advantageously employed by Paschen and others. In terms of the frequences ν_m, ν_n, ν_r of any three lines of the same single series the above formula easily leads to the condition

$$(\nu_r-\nu_n)\sqrt{\frac{N}{A-\nu_m}}+(\nu_m-\nu_r)\sqrt{\frac{N}{A-\nu_n}}+(\nu_n-\nu_m)\sqrt{\frac{N}{A-\nu_r}} \\ +(r-n)\nu_m+(m-r)\nu_n+(n-m)\nu_r=0, \qquad (2)$$

from which A may be determined by the method of "trial and error." An inspection of formula (2) shows that A is not at all dependent upon the numerical value given to m, say. This follows from the fact that m, n, and r enter equation (2) only as binomial differences. For this reason, and quite regardless of the theoretical considerations of Bohr, Sommerfeld, and others, we have chosen to define m for the first line of a given series as the smallest positive multiple of 1/2 that will make a numerically less than 1/2. When A has been determined from relation (2), formula (1) only gives the value of $m+a$ as a sum, but not of m and a separately. These remarks account for the numbers in the parentheses of the column headed "Series" in Table I.

Using R. T. Birge's latest value $N=109677.7$, Dr. E. Klein and the senior author obtained the following data from the wave-numbers of the first three lines of each single series of gallium. For the satellites of the first subordinate series $m=3$, $A'=47491.90$, $a'=-0.2126354$, $b'=+4.366673\times10^{-6}$, and $\lambda_\infty=2105.622$. For the most refrangible components of this series $m=3$, $A=48320.76$, $a=-0.2138487$, $b=+4.434379\times10^{-6}$, and $\lambda_\infty=2069.504$. For the companion of the satellite of the same series $m=3$, $A=47489.91$, $a=-0.2076978$, $b=+4.067868\times10^{-6}$, and $\lambda_\infty=2105.710$. For the least refrangible components of the second subordinate series $m=2$, $A=47553.53$, $a=+0.2138570$, $b=-2.445062\times10^{-6}$, and $\lambda_\infty=2102.893$. Finally, for the most refrangible components of the second subordinate series $m=2$, $A=48378.55$, $a=+0.2141350$, $b=-2.454515\times10^{-6}$, and $\lambda_\infty=2067.032$. These results are unsatisfactory, for the convergence wave-numbers of the least refrangible components of the two subordinate series differ by 61.63 or 2.73 A. The most refrangible components failed to converge to the same place by about the same amount, namely 57.79 or 2.47 A. Formula (1) was considered disproportionately complicated to apply the method of least squares to all of the lines of a single series. However, this method was applied to the Mogendorff-Hicks formula

$$\nu_m=A-\frac{N}{(m+a+b/m)^2}\,. \tag{3}$$

The equation analogous to relation (2), as derived from equation (3), shows that the value of A depends upon the number assigned to m. By actual trial it was found that the convergence wave-numbers for the subordinate series did not agree even as well as when formula (1) was employed. For the least refrangible components of the second subordinate series, the values of the constants in equation (3) were found, by the method of least squares, to be: $A = 47555.879$, $a = 1.2183276$, $b = -0.06226206$, and $\lambda_\infty = 2102.789$. m was chosen equal to unity for the first line. For the wave-numbers the differences "observed" minus "calculated" were $+0.041$, -0.552, $+0.824$, $+1.063$, and -1.375 or, in terms of the angstrom, -0.007, $+0.041$, -0.051, -0.056, and $+0.069$, respectively. These numbers are written in the order of decreasing wave-length of the lines. The conclusion reached by us is that the number of lines is too small and the perturbations of the lines with respect to a non-inflectional curve are too large to justify pursuing the series constants further.

No attempt was made to determine the wave-lengths of the red and green lines of the principal series of gallium for the following reasons. These lines appeared only on the spectrograms taken with the meter grating and with the large quartz spectrograph when nearly pure metallic gallium was used. They were not recorded with the oxide (which forms very promptly in the arc in air) or with the leady residue, or with any of the compounds or mixtures which contained gallium as an impurity. Whenever obtained, these lines were extremely broad and unsymmetrical. Consequently it was not feasible to make exposures with such valuable material with the large grating as mounted. Moreover, the investigation of the red region was in full sway at the Bureau of Standards, where all of the conditions are most favorable for obtaining the wave-lengths in question. The only earlier, fairly accurate, measurements of the principal series doublets seem to be those of Exner and Haschek which are quoted by Paschen and Meissner.[1]

Indium. Experimental.—Most of the investigations of the radiations of indium have been confined to the spark spectrum, with which we are not directly concerned in the present paper. The lines of the principal series have been very carefully determined by Paschen and Meissner.[2] The results of our study of the arc spectrum in air are given in Table II, the notation being the same as in the preceding table for gallium. Lines 1 to 22 inclusive were obtained with the large grating, while the remaining ones were recorded only with quartz spectrographs. Line number 10 was close to the iron lines at λ 2753.668 and λ 2754.034, and line number 19 to the iron line at λ 2399.339, hence the semaphore screen was used in photographing these indium lines. Special interest attaches to the four lines numbered 6, 8, 9, and 22, respectively. These lines are not single, but are made up of groups of fine components the number of which is indicated by the subscript following the representative wave-

---

[1] *Annalen der Physik*, 43, 1223, 1914.

[2] *Ibid.*

TABLE II

No.	Series	λ in Air		Wave-Number $\nu_0=\frac{10^8}{\lambda_0}$ cm^{-1}	Δν	Int.
		E. and H.	U. and T.			
1	S_1 (2.5)	4511.38	4511.310	22160.05	2212.83	10
2	S_2 (2.5)	4101.80	4101.764	24372.88	...	10
3	D_1' (3)	3258.54	3258.565	30679.34	2212.85	4
4	D_1 (3)	3256.08	3256.089	30703.17	...	8
5	D_2 (3)	3039.34	3039.356	32892.19	...	8
6	...	2957.02	2957.012$_4$	33808.33	2212.51	6
7	S_1 (3.5)	2932.64	2932.633	34089.03	2212.49	5
8	...	2836.90	2836.911$_6$	35239.04	...	8
9	...	2775.36	2775.355$_3$	36020.84	...	4
10	S_2 (3.5)	2753.89	2753.889	36301.52	...	4
11	D_1' (4)	2713.91	2713.932	36835.87	2212.53	3
12	D_1 (4)	2710.28	2710.264	36885.49	...	5
13	S_1 (4.5)	2601.81	2601.756	38424.13	2212.73	2
14	D_2 (4)	2560.15	2560.157	39048.40	...	4
15	D_1' (5)	...	2522.854	39625.34	2212.90	3
16	D_1 (5)	2521.32	2521.371	39649.04	...	6
17	S_1 (5.5)	2468.12	2468.012	40506.23	2212.21	5
18	S_2 (4.5)	2460.16	2460.079	40636.86	...	3
19	S_1 (6.5)	...	2399.189	41668.05	2211.9	3
20	D_2 (5)	...	2389.543	41838.24	...	3
21	S_2 (5.5)	2340.27	2340.191	42718.44	...	3
22	...	2306.09	2306.073$_3$	43350.39	...	4
23	S_2 (6.5)	...	2278.3	43879.9	...	2
24	S_2 (7.5)	...	2240.9	44611.9	...	1
25	D_2 (8)	...	2229.8	44833.5	...	1
26	S_2 (8.5)	...	2219.4	45044.9	...	1
27	D_2 (9)	...	2210.9	45236.3	...	1
28	S_2 (9.5)	...	2202.5	45389.2	...	1
29	D_2 (10)	...	2198.2	45477.9	...	1
30	S_2 (10.5)	...	2192.0	45606.0	...	1
31	D_2 (11)	...	2189.0	45669.7	...	1
32	D_2 (12)	...	2181.7	45822.9	...	1
33	...	...	2177.7	45906.6	...	1
34	...	...	2171.0	46039.0	...	1

length given in Table II. Lines 6, 8, and 9 were not obtained by Kayser and Runge,[1] but they are recorded by Exner and Haschek[1] as *single* lines with the respective characterizations 2 *R*, 3 *R*, and 1. Line number 22 is also given as single by both pairs of authors. To minimize the possibility of drawing erroneous conclusions we made a special study of these four lines and found that (*a*) each group displayed the same characteristics whether the exposure had been long or short, the lines faint or intense, (*b*) the character of the lines was independent of the material containing the indium—whether it had been the leady residue or its products, indium oxide or hydroxide, or lead oxide, and (*c*) the lines invariably appeared when indium was present in the arc. Line number 8 suggested a small portion of a band spectrum. It could not be interpreted as a triplet, each of whose components was reversed, because all of the six components were sharp and symmetrical with no suggestion of winglike structure. The four lines are probably "combination lines," since they do not fit into the series directly. The difference in wave-number for lines 6 and 9 (when treated as unresolved) is 2212.51, which is the characteristic value for the series lines of indium. The wave-lengths of the resolved components are given in Table III.

TABLE III

Reference No.	λ	Reference No.	λ
6	2957.094	9	2775.408
	2957.047		2775.355
	2956.994		2775.292
	2956.735		
8	2837.039	22	2306.147
	2836.998		2306.082
	2836.957		2306.029
	2836.910		
	2836.856		
	2836.793		

In Table II the lines numbered 24 to 34 were always accompanied by so much intermediate radiation as to make them appear as absorption lines in a continuous background, rather than as ordinary emission lines with reversed axes. Nevertheless the serious attempts made by Dr. E. Klein and the senior author to obtain the absorption spectrum of indium vapor, when heated in specially designed furnaces, failed to give anything more than the two strongest lines numbered 1 and 2.

---

[1] Kayser's *Handbuch*, 5, 584.

Theoretical.—The time-consuming difficulties which presented themselves when the attempt was made to determine the various constants for gallium have caused us to defer a similar numerical investigation for indium until some later occasion. Moreover, as stated earlier, the presentation in published form of the experimental data has already been delayed far too long. Accordingly the following tentative constants must suffice.

Taking $m=2.5, 3.5, \ldots\ldots$ for the first three components of the second subordinate series it was found that, for formula (1),

$$\begin{aligned}A_1&=44449.3\\A_2&=46662.0\\a_1=a_2&=-0.215623\\b_1=b_2&=-2.96938\times10^{-6}.\end{aligned}$$

Assuming the same values for A_1 and A_2, and letting $m=3, 4, \ldots\ldots$ the remaining parameters for the satellite and the most refrangible component of the first subordinate series have the approximate values

$$\begin{aligned}a_1=a_2&=-0.237740\\b_1=b_2&=4.35554\times10^{-6}.\end{aligned}$$

In conclusion the authors desire to make public acknowledgment of their debt of gratitude to Dr. I. C. Gardner for his Schumann plates, to Mr. W. H. Bassett, technical assistant and metallurgist of the American Brass Company, for placing at the disposal of the senior author all of the spectroscopic facilities of the research laboratory, and to Mr. C. H. Davis for his untiring and invaluable aid in obtaining the spectrograms with the large quartz prism apparatus.

SLOANE LABORATORY
YALE UNIVERSITY
September 1921

FIRST ATTEMPT AT A THEORY OF THE ARRANGEMENT AND MOTION OF THE SIDEREAL SYSTEM[1]

By J. C. Kapteyn[2]

ABSTRACT

First attempt at a general theory of the distribution of masses, forces, and velocities in the stellar system.—(1) *Distribution of stars.* Observations are fairly well represented, at least up to galactic lat. 70°, if we *assume that the equidensity surfaces are similar ellipsoids of revolution,* with axial ratio 5.1, and this enables us to compute quite readily (2) *the gravitational acceleration at various points due to such a system,* by summing up the effects of each of ten ellipsoidal shells, in terms of the acceleration due to the average star at a distance of a parsec. The *total number of stars* is taken as 47.4×10^9. (3) *Random and rotational velocities.* The nature of the equidensity surfaces is such that the stellar system cannot be in a steady state unless there is a general rotational motion around the galactic polar axis, in addition to a random motion analogous to the thermal agitation of a gas. In the neighborhood of the axis, however, there is no rotation, and the behavior is assumed to be like that of a gas at uniform temperature, but with a gravitational acceleration ($G\eta$) decreasing with the distance ρ. Therefore the density Δ is assumed to obey the barometric law: $G\eta=-\bar{u}^2(\delta\Delta/\delta\rho)/\Delta$; and taking the mean random velocity $\bar{u}$ as 10.3 km/sec., the author finds that (4) *the mean mass of the stars* decreases from 2.2 (sun = 1) for shell II to 1.4 for shell X (the outer shell), the average being close to 1.6, which is the value independently found for the average mass of both components of visual binaries. In the galactic plane the resultant acceleration—gravitational minus centrifugal—is again put equal to $-\bar{u}^2(\delta\Delta/\delta\rho)/\Delta$, $\bar{u}$ is taken to be constant and the average mass is assumed to decrease from shell to shell as in the direction of the pole. The angular velocities then come out such as to make the linear rotational velocities about constant and equal to 19.5 km/sec. beyond the third shell. If now we suppose that part of the stars are rotating one way and part the other, the relative velocity being 39 km/sec., we have a quantitative explanation of the phenomenon of star-streaming, where the relative velocity is also in the plane of the Milky Way and about 40 km/sec. It is incidentally suggested that when the theory is perfected it may be possible to determine *the amount of dark matter* from its gravitational effect. (5) The *chief defects of the theory* are: That the equidensity surfaces assumed do not agree with the actual surfaces, which tend to become spherical for the shorter distances; that the *position of the center of the system* is not the sun, as assumed, but is probably located at a point some 650 parsecs away in the direction galactic long. 77°, lat. −3°; that the average mass of the stars was assumed to be the same in all shells in deriving the formula for the variation of $G\eta$ with ρ on the basis of which the variation of average mass from shell to shell and the constancy of the rotational velocity were derived—hence either the assumption or the conclusions are wrong; and that no distinction has been made between stars of different types.

1. *Equidensity surfaces supposed to be similar ellipsoids.*—In *Mount Wilson Contribution* No. 188[3] a provisional derivation was given of the star-density in the stellar system. The question was there raised whether the inflection appearing near the pole in the

---

[1] *Contributions from the Mount Wilson Observatory,* No. 230.

[2] Research Associate of the Mount Wilson Observatory.

[3] *Astrophysical Journal,* 52, 23, 1920.

equidensity surfaces for small densities is real or not. I have since found that these inflections can be avoided without doing very serious violence to the results of observation. If this is done, the equidensity surfaces become approximately ellipsoids, and not only that, but the data can be represented without exceeding the possible limits of observation error, by assuming the equidensity surfaces to be *concentric, similar revolution ellipsoids, similarly situated.*

2. *Elements of the ellipsoids.*—Taking as unit of star-density that in the neighborhood of the sun, the adopted axes of the ellipsoids, which will be referred to as ellipsoids I, II, ... X and which

TABLE I

EQUIDENSITY ELLIPSOIDS

Ellipsoid	Log Δ	*A*	*B*	*B/A*
		parsecs	parsecs	
I	9.80−10	118	602	5.102
II	9.60	198	1010	5.102
III	9.40	296	1510	5.102
IV	9.20	413	2106	5.102
V	9.00	553	2820	5.102
VI	8.80	717	3656	5.102
VII	8.60	902	4600	5.102
VIII	8.40	1114	5675	5.102
IX	8.20	1365	6960	5.102
X	8.00	1660	8465	5.102

correspond to the values (Δ being the density) $\log \Delta + 10 = 9.8, 9.6,$ . . . . 8.0, are as shown in Table I. The *A*-axis is directed toward the galactic Pole, the *B*-axis lies in the plane of the Milky Way.

For the Milky Way and for the direction toward the Pole this table yields densities which are fairly well represented, for $\rho > 150$ parsecs, by the formulae,

$$\log \Delta = -2.135 + 2.368 \log \rho - 0.593 (\log \rho)^2 \quad \text{(M.W.)}, \qquad (1)$$

$$\log \Delta = -5.356 + 4.890 \log \rho - 1.200 (\log \rho)^2 \quad \text{(Pole)}, \qquad (1a)$$

A section of the equidensity-ellipsoids through the sun (which has been assumed to be the center of the system) at right angles to the plane of the Milky Way is shown in Figure 1.

The agreement of the densities furnished by Table I with those of *Contribution* No. 188 is fairly good for all galactic latitudes up to 65° or 70°. For still higher latitudes it may perhaps still be called tolerable. At least the deviations hardly exceed what would be produced by an error of 0.1 mag. in the photometric scale for these regions.

In the present paper I have substituted these ellipsoids for the surfaces derived directly from observation in *Contribution* No. 188, *not* because I think they are nearer the truth, but simply because they are so enormously more convenient for further computation.

My aim in the present paper is simply to get hold of some approximate information about the real structure and motion of the system, and quantitative accuracy has been considered of secondary importance as long as we may hope that the main features are not affected. I trust that this hope will not be disappointed, notwithstanding the many defects—defects that will be duly pointed out—which still attach to the present treatment.

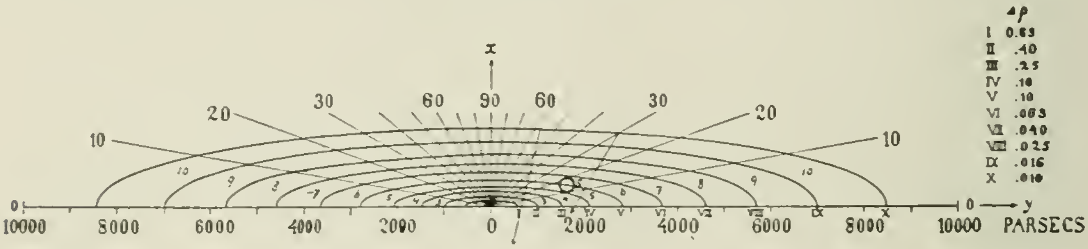

FIG. 1

3. *Advantage of the adoption of the ellipsoids.*—The form of the equidensity surfaces thus adopted has the advantage that it calls attention to the possibility of determining with some precision the gravitational attraction of the *whole* of the stellar system on any point inside ellipsoid X, while at the same time it renders the computation of that attraction a relatively easy matter.

In another paper[1] van Rhijn and I have tried to show that, as soon as we possess good counts of stars for each interval of magnitude down to apparent magnitude 17 (visual), we shall know with some tolerable approximation the density of the whole region covered by Figure 1, that is, of the whole extent of the stellar system for which the density exceeds one-hundredth of that in the neighborhood of the sun.

---

[1] *Mt. Wilson Contr.*, No. 229; *Astrophysical Journal*, 55, 242, 1922.

In the near future such counts will be available. They will be furnished by the Mount Wilson "Catalogue of the Selected Areas" (from $\delta = -15°$ to $\delta = +90°$), the discussion of which is in the hands of Seares. A few provisional counts make it probable that this work will in the main confirm the elements used for Table I and Figure 1. I will assume, therefore, that even now the densities are sufficiently well known for the whole of ellipsoid X.

The advantage just alluded to is a consequence of the well-known property that the attraction of an ellipsoidal shell of constant density, bounded by two similar and similarly situated ellipsoids, on an internal point is *zero*. For it is evident by this property that, if in all that part of the system which lies outside ellipsoid X—for which part accurate data are still wanting—the arrangement in similar ellipsoids also holds, the attraction of this outside domain on a point inside ellipsoid X would be *zero*. And as the distribution of density inside ellipsoid X is known, the possibility of computing the attraction of the total system on a point inside of X becomes evident. If on the contrary the same arrangement does not hold outside ellipsoid X, it still seems highly probable a priori that any change in the form of the equidensity surfaces must be gradual, that is, the equidensity surfaces in the neighborhood of X will diverge little from similar ellipsoids, and the greater changes will begin to appear only at more considerable distances. For the consecutive shells, therefore, the attraction on an internal point will begin by being very small, both on account of the near approach to similarity of these shells and their small density and greater distance from the attracted point. For more distant shells the first circumstance will probably diminish in importance with increasing distance, while, on the contrary, the second becomes more and more important. On the whole, therefore, the attraction of all of that part of the system which lies outside X will be small, and its neglect will presumably not prevent us from obtaining fairly exact ideas about the total forces.

4. *Computation of the gravitational forces.*—In ellipsoid I, which for brevity I will call shell 1, and in each of the shells 2, 3, ... 10, between the surfaces of ellipsoids I, II, ... X, the density varies between limiting values which are in the ratio of 1 to 1.585.

In what follows I will assume for each shell a constant average density.

The computation of the gravitational forces has been carried through for:

(1) 10 points in galactic latitude 0° lying in the surfaces of ellipsoids I, II, ... X; these points have been designated by I, 0°; II, 0°; . . . . X, 0°.

(2) 5 points in galactic latitude 30°, situated on the surfaces II, IV, VI, VIII, X; denoted by II, 30°; IV, 30°; . . . . X, 30°.

(3) Similarly for the 5 points II, 57°.1; IV, 57°.1; . . . . X, 57°.1. (57°.1 = average latitude between 40° and 90°.)

(4) The 10 points I, 90°; II, 90°; . . . . X, 90°.

As a unit of attraction I have used the attraction on each other of two stars of average mass separated by a distance of 1 parsec.

I first computed the attraction of the full ellipsoids I, II, ... X on the points specified above, on the supposition that they are of a constant density such that every cubic parsec contains a single star. The formulae for this computation are given in the Appendix.

The attraction of the full ellipsoids having been found, simple subtraction gives the attraction of the separate shells 1, 2, ... 10, all supposed to have the density corresponding to one star per cubic parsec. The actual attraction of the shells was obtained by multiplying these results by the number of stars per cubic parsec contained in each shell. For the average densities, expressed in terms of the density in the neighborhood of the sun, I adopted the values corresponding to the logarithms 9.9, 9.7, 9.5, ... 8.1, each minus 10, multiplied by 0.0451, which according to *Contribution* No. 188 (12) is the number of stars per cubic parsec near the sun; this gives the numbers in Table II.

TABLE II

AVERAGE NUMBER OF STARS PER CUBIC PARSEC

Shell	No. Stars	Shell	No. Stars
1	0.0358	6	0.00358
2	.0226	7	.00226
3	.0143	8	.00143
4	.00900	9	.000900
5	0.00568	10	0.000568

Having found the separate attractions, the components of the total attractions parallel to the axes can at once be determined by noting that the attraction of any shell on an internal point is *zero*, and further, by neglecting the attraction of that part of the system outside of ellipsoid X on a point inside this ellipsoid. Instead of the components I have entered in Table III the total forces G and the angles that these forces make with the X-axis. These are of course found by the formulae

$$X = G \cos \phi \qquad Y = G \sin \phi. \tag{2}$$

In addition, I have given the values of $\phi - \psi$, ψ being the angle which the normal to the ellipsoid through the attracted point makes with the X-axis; ψ is determined by

$$\tan \psi = \frac{A^2}{B^2} \frac{\beta}{\alpha} \tag{2a}$$

The angle $\phi - \psi$ is of course the inclination of the direction of the force to the normal.

The interpretation of this table—of the first entry, for example—is: Attraction of the whole stellar system on a body in the point I, 0° is a force equal to the attraction of 33.19 stars of average mass at the distance of 1 parsec from that same body. This force makes an angle of 90° with the X-axis, and an angle of 0° with the normal to the equidensity ellipsoid through the attracted point.

5. *Analytical representation of G for galactic latitudes* 0° *and* 90°.—In trying to represent the force G by an analytical formula, I started from the consideration that, as the density is constant near the center, the attraction must be nearly proportional to the distance ρ for very small values of ρ; further, that for distances very great as compared with the dimensions of the stellar system, the attraction must be practically the same as it would be were the mass of the whole system concentrated in the center. For these latter distances, therefore, G must be proportional to $1/\rho^2$.

The following easily managed formula satisfies both conditions:

$$G = \frac{A\rho}{1 + B\rho + C\rho^2 + D\rho^3}. \tag{3}$$

TABLE III

TOTAL ATTRACTIONS OF THE WHOLE SYSTEM

ATTR. POINT	LOG Δ	CO-ORDINATES ATTR. POINT		G	ϕ	$\phi-\psi$	ATTR. POINT	LOG Δ	CO-ORDINATES ATTR. POINT		G	ϕ	$\phi-\psi$
		α	β						α	β			
		parsecs	parsecs						parsecs	parsecs			
I, 0°......	9.80−10	0	602	33.19	90°	0°	I, 90°.....	9.80−10	118	0	40.06	0°	0°
II, 0	9.60	0	1010	37.76	90	0	II, 90	9.60	198	0	54.26	0	0
III, 0	9.40	0	1510	37.95	90	0	III, 90	9.40	296	0	62.45	0	0
IV, 0	9.20	0	2106	35.71	90	0	IV, 90	9.20	413	0	65.95	0	0
V, 0	9.00	0	2820	32.09	90	0	V, 90	9.00	553	0	66.12	0	0
VI, 0	8.80	0	3657	27.71	90	0	VI, 90	8.80	717	0	64.00	0	0
VII, 0	8.60	0	4600	23.67	90	0	VII, 90	8.60	902	0	60.63	0	0
VIII, 0	8.40	0	5675	20.12	90	0	VIII, 90	8.40	1114	0	56.41	0	0
IX, 0	8.20	0	6960	16.59	90	0	IX, 90	8.20	1365	0	51.56	0	0
X, 0	8.00	0	8465	13.53	90	0	X, 90	8.00	1660	0	46.52	0	0
II, 30°.....	9.60	187	325	52.34	18° 6′	14°18′	II, 57°.1....	9.60	196	127	53.99	6°54′	5°29′
IV, 30	9.20	391	677	59.26	22 6	18 18	IV, 57.1....	9.20	410	265	64.86	8 49	7 24
VI, 30	8.80	679	1176	53.97	25 8	21 20	VI, 57.1....	8.80	711	460	62.10	10 33	9 8
VIII, 30	8.40	1055	1827	44.64	28 2	24 14	VIII, 57.1....	8.40	1105	715	53.91	12 5	10 40
X, 30	8.00	1572	2723	34.46	30 54	27 6	X, 57.1....	8.00	1647	1066	43.85	13 42	12 17

In this formula A/D evidently equals the total number of stars, N, in the stellar system.

A rough estimate of this number can be made by assuming that formula (15) of *Contribution* No. 188, viz.,

$$N_m = e^{a+bm+cm^2}, \tag{4}$$

is true for all values of m. Integration over m gives

$$N = \frac{\sqrt{\pi}}{\sqrt{-c}} e^{a - \frac{b^2}{4c}}. \tag{5}$$

For the values of a, b, c best satisfying the numbers in *Groningen Publications*, No. 27, Table V, which gives number of stars per square degree, I find the following:

Gal. Lat.	a	b	c	Number of Square Degrees
0° to ±20°	−10.564	+1.5985	−0.0276	14110
±20 to ±40	−10.539	+1.5468	−0.0288	12420
±40 to ±90	−10.815	+1.6592	−0.0414	14730

With these data, computing the total number of stars for each of the three zones, I obtained

Gal. Lat.	No. Stars
0° to ±20°	43.8×10^9
±20 to ±40	3.6×10^9
±40 to ±90	0.043×10^9

whence

$$\frac{A}{D} = N = 47.4 \times 10^9. \tag{6}$$

The remaining constants were so determined that (3) represents the values of G in Table III. I thus found

$$\left.\begin{array}{ll} \text{Gal. Lat.}=0^\circ & \text{Gal. Lat.}=90^\circ \\ A=0.110 & A=0.376 \\ B=1.30\times10^{-3} & B=1.83\times10^{-3} \\ C=0.657\times10^{-6} & C=3.40\times10^{-6} \\ D=2.32\times10^{-12} & D=7.93\times10^{-12} \end{array}\right\} \tag{7}$$

The representation of the tabular values is as follows:

ρ	Gal. Lat. =0°			ρ	Gal. Lat. =90°		
	G. Tab.	G. Form.	Tab. − Form		G. Tab.	G. Form.	Tab. − Form
500	30.0	30.2	−0.2	200	54.3	50.1	+4.2
1000	37.8	37.0	+0.8	500	66.2	68.0	−1.8
2000	36.0	35.0	+1.0	1000	58.5	60.3	−1.8
3000	31.7	30.2	+1.5	1500	49.1	49.4	−0.3
4000	26.0	26.0	0.0				
6000	19.0	19.9	−0.9				
8000	14.0	16.0	−2.0				

The agreement is not very good, but seems sufficient for our present purpose.

6. *Application of kinetic theory of gases.*—The results thus far obtained rest, it is true, on provisional data, which even now might be materially improved; they further depend on the supposition, not yet fully demonstrated, that, within the distances here considered, there is no appreciable extinction of light in space, but they are, nevertheless, I think, the legitimate outcome of our data.

For what follows I will now introduce some considerations borrowed from the kinetic theory of gases, the applicability of which to the stellar system might be considered doubtful. At all events I do not pretend to have demonstrated this applicability. The results which will be derived cannot lay claim to be demonstrably correct, but they seem to me to be so remarkable that, after a good deal of hesitation, I have resolved to publish them, in the hope that others, better versed in these matters, may furnish us with a more rigorous solution of the problem involved.

Even though it has been shown, in the main by unpublished investigations, that the peculiar motions[1] of the stars with some crude approximation are Maxwellian, the stellar system cannot be treated as a gas at rest; first, because of the existence of stream-motion; second, because of the form of the equidensity surfaces, which is certainly different from that of the equipotential surfaces of the gravitational force.

---

[1] Peculiar velocity is defined as the motion corrected for both the solar and stream-motion. The radial and transverse velocities agree in showing a certain excess of very large motions over the Maxwellian distribution. They are both represented satisfactorily by the sum of *two* Maxwellian distributions. A thorough separate treatment of all the spectral classes is still a great desideratum.

That they are different is proved by the fact, among others, that in general the forces are not normal to these surfaces. This is evident enough without further explanation. Moreover, it is clearly brought out by Table III, where the angle with the normal reaches values of more than 27°. Further it is well known that in a gas at rest under its own attraction, the equidensity surfaces are spherical.

The system cannot therefore be in a steady state unless it has a systematic motion. Since the discovery of the star-streams it is clear that such a motion really exists and that it is parallel to the plane of the Milky Way.

It seems rational, therefore, to assume that the system has a sort of rotational motion round the X-axis (see Fig. 1) which is directed toward the pole of the galaxy. The form of the equidensity surfaces found directly in *Contribution* No. 188 as well as that now adopted, strongly indicates some such motion.

This being assumed, the stars along the axis will still have no other motion than their peculiar motions, which, as was just mentioned, are Maxwellian, at least with some approximation. I venture to assume, therefore, that the stars in the immediate neighborhood of this axis are arranged as the molecules of a gas in a quiescent atmosphere.

If:

Δ be the star-density (number of stars per cubic parsec);
u one of the components of the peculiar velocity;
η the acceleration produced by the attraction of a star of average mass at a distance of one parsec, then on the above assumption

$$\overline{u^2}\frac{\delta\Delta}{\Delta} = -G\eta\delta\rho, \tag{8}$$

$\overline{u^2}$ being the average value of u^2.

The formula is analogous to that used for barometric determinations of altitude in an atmosphere of constant temperature throughout. On the other hand, we have found empirically formulae such as (1) and (1*a*) (see also *Contribution* No. 188, p. 13 [21]); in other words,

$$\log \Delta = -P + Q \log \rho - R(\log \rho)^3 \quad (\rho > \rho_0), \tag{9}$$

from which, by differentiation

$$\frac{\delta\Delta}{\Delta} = \frac{Q - 2R \log \rho}{\rho} \delta\rho. \tag{10}$$

Comparing the two expressions, (8) and (10), for $\delta\Delta/\Delta$

$$G\eta = -\overline{u^2}\left[\frac{Q - 2R \log \rho}{\rho}\right] \quad (\rho > \rho_0). \tag{11}$$

As the motions are supposed to be Maxwellian, the well-known formula used in the theory of least squares gives

$$\overline{u^2} = \frac{\pi}{2}(\overline{u})^2. \tag{12}$$

From observations of the radial velocities at the Lick Observatory, where no choice has been made on the basis of proper motion (*Lick Observatory Bulletin*, **6**, 126), I derived the value[1]

$$\overline{u} = 10.3 \text{ km/sec}. \tag{13}$$

or since

$$\begin{aligned} 1 \text{ kilometer} &= 3.25 \times 10^{-14} \text{ parsecs} \\ 1 \text{ parsec} &= 3.08 \times 10^{13} \text{ kilometers} \end{aligned} \tag{14}$$

I find, in the units parsec and second, here adopted,

$$\overline{u} = 3.35 \times 10^{-13} \tag{15}$$

$$\overline{u^2} = 1.763 \times 10^{-25} \tag{16}$$

so that (11) becomes

$$G\eta = -1.763 \times 10^{-25} \frac{Q - 2R \log \rho}{\rho} \quad (\rho > \rho_0) \tag{17}$$

Finally, for galactic latitude 90°, we obtain from equation (1*a*) the values:

$$Q = +4.890 \quad R = +1.200 \tag{18}$$

$$\eta = \frac{(-8.620 + 4.229 \log \rho) \times 10^{-25}}{G\rho} \quad (\rho > 150). \tag{19}$$

---

[1] There is a mistake in the derivation of this value. The true value is certainly somewhat lower. From considerations given below I have not deemed it necessary for the present paper to repeat the computations with an improved value of $\overline{u}$.

For small values of ρ, formula (9) does not hold. According to *Contribution* No. 188, and particularly according to *Contribution* No. 229, it represents the observations excellently for values of ρ well beyond the maximum (which in the present case lies near $\rho = 110$ parsecs). For values of ρ below the maximum the density is nearly constant. The differential-quotient $\delta\Delta/\delta\rho$ thus becomes very small and $\delta\Delta/\Delta\delta\rho$ very unreliable. In the present case it will probably be well not to rely on the formula below, say, 150 parsecs. This limit was adopted in (19).

I have computed the values of η from (19) both on the supposition that G has the values found directly in Table III and that it has the values yielded by formula (3). The former were adopted (Table IV).

TABLE IV

VALUES OF η AND $\overline{m}$

Point	ρ	η Form. (3)	η Adopted	$\overline{m}$ (Sun = 1)
	parsecs			
II, 90°	198	11.1×10^{-30}	10.2×10^{-30}	2.2
IV, 90	413	$8.9 \quad 10^{-30}$	$9.0 \quad 10^{-30}$	2.0
VI, 90	717	$7.3 \quad 10^{-30}$	$7.5 \quad 10^{-30}$	1.7
VIII, 90	1114	$6.6 \quad 10^{-30}$	$6.8 \quad 10^{-30}$	1.5
X, 90	1660	$6.5 \quad 10^{-30}$	$6.5 \quad 10^{-30}$	1.4

The quantity η is, as stated above, the acceleration per second, in parsecs, produced by the attraction of a star of average mass on a body at a distance of one parsec. The acceleration which the sun would produce, expressed in the same units, is

$$\text{Acceleration by sun} = 4.53 \times 10^{-30}. \tag{20}$$

This enables us to find the average mass $\overline{m}$ of a star expressed in the mass of the sun as a unit. The values of $\overline{m}$ thus found have been inserted in the last column of Table IV.

These values agree surprisingly well with what has been found by totally different considerations. In a recent paper[1] Jackson and Furner find for visual binary stars, as the best average

$$\frac{1}{\sqrt{m_1 + m_2}} = 0.855.$$

---

[1] *Monthly Notices*, 81, 4, 1920.

Consequently $m_1+m_2=1.60$, which agrees with Table IV if we suppose that the combined mass of the two components and not that of a single component is comparable with the mass of a single star, and especially if we further consider that there are theoretical grounds for expecting that the average mass will decrease for increasing distance.[1]

Remark. Dark matter. It is important to note that what has here been determined is the total mass within a definite volume, divided by the number of luminous stars. I will call this mass the average effective mass of the stars. It has been possible to include the luminous stars completely owing to the assumption that at present we know the luminosity-curve over so large a part of its course that further extrapolation seems allowable.

Now suppose that in a volume of space containing l luminous stars there be dark matter with an aggregate mass equal to Kl average luminous stars; then, evidently the effective mass equals $(l+K)\times$average mass of a luminous star.

We therefore have the means of estimating the mass of dark matter in the universe. As matters stand at present it appears at once that this mass cannot be excessive. If it were otherwise, the average mass as derived from binary stars would have been very much lower than what has been found for the effective mass.

7. *Angular velocities* (ω) *in the plane of the galaxy.*—Ignoring for an instant the fact that the stars in the Milky Way cannot be systematically at rest and treating the stars near this plane in the same way as those near the axis, I am led by a formula analogous to (17) to values of η which are not quite half those given in Table IV. I suppose that the difference must be wholly due to the centrifugal force induced by the rotational motions. In fact, I assume that the average mass is the same throughout the whole system, at least for points on the same equidensity surface.

If, therefore, ρ and ρ' represent the distances from the center, of two points on the same equidensity surface, the first in the direction of the Pole, the second in the Milky Way, for which points the total attractive forces of the system are respectively G and G', formula (11) gives

---

[1] Jeans, *Problems of Cosmogony and Stellar Dynamics* (1919), p. 239.

$$\text{For the Pole} \qquad G\eta = -\overline{u^2}\,\frac{Q-2R\log\rho}{\rho}, \tag{21}$$

$$\text{For the Milky Way} \quad G'\eta-\rho'\omega^2 = -\overline{u^2}\,\frac{Q'-2R'\log\rho'}{\rho'}, \tag{22}$$

where ω represents the angular velocity for the point in the Milky Way, and Q' and R' the constants of equation (9) for that same plane. The two equations determine η and ω. The equation for the latter is

$$\omega^2 = \frac{G'}{\rho'}\cdot\overline{u^2}\left[\frac{Q'-2R'\log\rho'}{G'\rho'}-\frac{Q-2R\log\rho}{G\rho}\right], \tag{23}$$

in which, for $\overline{u^2}$ see (16); for G' and G see Table V; and for Q and R see (18), and where finally, by comparing (9) and (1),

$$Q'=2.368 \text{ and } R'=0.593 \tag{24}$$

The maximum of Δ according to formula (9) lies, for the Milky Way at about $\rho=100$, for the direction toward the Pole at $\rho=110$. As has been mentioned, the formula ceases to be correct below these values. I assume, as before, that the limit of validity is $\rho=150$.

8. *Angular velocity for stars not in the galaxy.*—For the regions not in galactic latitudes 0° or 90° I determine the angular velocity by the condition that the resultant of the attractive and centrifugal forces must be at right angles to the equidensity surfaces.

In order that the system may be in the steady state, I assume that the equidensity surfaces are at the same time equipotential surfaces for the resultant of the attractive and centrifugal forces. The above condition is implied in this assumption.

Since

$$X \text{ component of resultant acceleration} = -X\eta,$$
$$Y \text{ component of resultant acceleration} = -Y\eta+\beta\omega^2,$$

and since ψ is the angle between the normal and the X-axis, the equation for ω is

$$\beta\omega^2 - X\eta = -X\eta\tan\psi,$$

which becomes slightly more convenient by writing

$$X = G \cos \phi \qquad Y = G \sin \phi .$$

Whence

$$\omega^2 = \frac{G\eta}{\beta} \frac{\sin(\phi - \psi)}{\cos \psi} . \tag{25}$$

For the points in Table V, $\phi - \psi$ and ψ were taken from Table III. The computation was made with the aid of formulae (23) and (25).

TABLE V

VALUES OF ω^2

Point	ω^2	Point	ω^2	Point	ω^2
II, 0°.	0.1757×10^{-30}	II, 30°..	0.4066×10^{-30}	II, 57°.1..	0.4132×10^{-30}
IV, 0 .	.0902 10^{-30}	IV, 30 ..	.2477 10^{-30}	IV, 57.1..	.2835 10
VI, 0 .	.03175 10^{-30}	VI, 30 ..	.1255 10^{-30}	VI, 57.1..	.1606 10
VIII, 0 .	.01237 10^{-30}	VIII, 30 ..	.0683 10^{-30}	VIII, 57.1..	.0949 10
X, 0 .	.00510 10^{-30}	X, 30 ..	.0376 10^{-30}	X, 57.1..	.0568 10

For these same points I have furthermore computed the linear velocities in kilometers per second. They are in Table VI.

TABLE VI

LINEAR VELOCITIES

Point	β	$\beta\omega$	Point	a	β	$\beta\omega$	Point	a	β	$\beta\omega$
		km/sec.				km/sec.				km/sec.
II, 0°..	1010	13.0	II, 30°.	187	325	6.4	II, 57°.1	196	127	2.5
IV, 0 ..	2106	19.5	IV, 30.	391	677	10.4	IV, 57.1	410	265	4.4
VI, 0 ..	3657	20.1	VI, 30.	679	1176	12.8 (13.1)	VI, 57.1	711	460	5.7 (6.3)
VIII, 0 ..	5675	19.4	VIII, 30.	1055	1827	14.7 (15.7)	VIII, 57.1	1105	715	6.8 (9.1)
X, 0 ..	8465	18.6	X, 30.	1572	2733	16.3 (17.9)	X, 57.1	1647	1066	7.8 (11.1)

9. *Explanation of star-streaming.*—According to these numbers the angular velocity is not the same for the same distance β from the axis at different distances a from the plane of the Milky Way. Further on I will explain why the present solution must necessarily be a very crude one. For this reason I am not prepared to maintain the reality of this difference. On the contrary it seems very possible that a more definite solution will finally lead to the conclusion that all the points on a cylinder around the axis of the system move with the same velocity. In fact, if we base our solution on the equidensity surfaces as really derived from the observations,[1] instead

---

[1] *Mt. Wilson Contr.*, No. 188; *Astrophysical Journal*, 52, 23, 1920.

of assuming similar ellipsoids, we approach at once much closer to this state of affairs. The numbers in parentheses in Table VI give rough estimates of $\beta\omega$ based on this supposition. In the absence of a more definite solution I will confine myself mainly to points in the plane of the Milky Way, the motions of which, except for small values of β, seem to be somewhat better determined.

The most striking feature brought out by these numbers is undoubtedly the fact that at distances from the axis exceeding 2000 parsecs the linear velocity of the stars is nearly constant, the average being 19.5 km/sec.; that is, the great bulk of the stars must have a motion of 19.5 km in a direction parallel to the plane of the Milky Way. Observation has already proved that there really exists a systematic motion of the stars, that it is exactly parallel to the plane of the Milky Way, and that the motion takes place in two exactly opposite directions, the two streams having a relative velocity of about

$$40 \text{ km/per sec.} \tag{26}$$

Since in the preceding theory the motion is introduced simply to explain certain centrifugal forces, it is at once evident that it supposes nothing about the direction in which the motion takes place. Nothing prevents us from assuming that part of the stars circulate one way, while the rest move in the opposite direction. The relative motion of the two groups will then evidently be

$$2\times 19.5 = 39 \text{ km/sec.} \tag{27}$$

The motion to which our theory leads, besides being in the same plane, has therefore practically the exact value which is known from observation to exist. In fact we are led in the most direct and natural way to a complete explanation of the phenomenon of star-streaming. The circumstance that observation led us to assume two rectilinear streams, whereas we here find the motion to be circular, is probably unimportant. It is of course infinitely probable that the sun must be at a certain distance from the center of the system. If we suppose it to be at the point S (see Fig. 1) then the star-streams are derived from the observed motions of stars within a volume whose dimensions are of the order of those of the sphere around S shown in the figure. As long as the radius of this sphere is small in comparison with the distance of S from the center, the curvature of the stream-lines must be inappreciable.

When we consider that the value (27) has been obtained by a study of the arrangement of stars in space, in which the proper motions play no other part than that of a criterion of distance, while the value (26) has been obtained by a study of the motions themselves, both radial and transverse, the close agreement of the two results seems very significant. It becomes more so through the fact that both theories yield a motion exactly parallel to the plane of the Milky Way. Further, if we take into account the fact that the present theory leads to a value for the average mass of the stars which is in close accordance with what has also been found from utterly different investigations, and if we add a final point, namely, the natural explanation of the different arrangement of the stars of different spectral types, we are led irresistibly to the following conclusion:

The theory here propounded, though it may require considerable modification on account of its defectiveness both as to observational basis and mathematical treatment is probably correct in its main features.

The last point mentioned, which is open to quantitative verification, requires further investigation, but even now promises to be no less significant than the others. It is referred to again in section 14 below.

10. *Accelerations including centrifugal effect.*—If with the aid of Table V we now add the acceleration due to the centrifugal forces to that produced by the attractive force, the resultant will be in the direction of the normal. We find the results in Table VII.

TABLE VII

ACCELERATION, INCLUDING EFFECT OF CENTRIFUGAL FORCE

Point	$G\eta$	Point	$G\eta$	Point	$G\eta$	Point	$G\eta$	$G_{\text{Pole}}/G_{\text{MW}}$
II, 0°..	208×10^{-30}	II, 30°..	508×10^{-30}	II, 57°.1.	547×10^{-30}	II, 90°..	553×10^{-30}	2.7
IV, 0 ..	131 10^{-30}	IV, 30 ..	495 10^{-30}	IV, 57.1.	577 10^{-30}	IV, 90 ..	593 10^{-30}	4.5
VI, 0 ..	90 10^{-30}	VI, 30 ..	367 10^{-30}	VI, 57.1.	458 10^{-30}	VI, 90 ..	480 10^{-30}	5.3
VIII, 0 ..	65 10^{-30}	VIII, 30 ..	268 10^{-30}	VIII, 57.1.	359 10^{-30}	VIII, 90 ..	384 10^{-30}	5.9
X, 0 ..	48 10^{-30}	X, 30 ..	193 10^{-30}	X,57.1.	277 10^{-30}	X, 90 ..	302 10^{-30}	6.3
ψ	90°		3°49′		1°25′		0°	

11*a*. *Velocity of escape*.—Assuming formula (3) to be valid for all distances, I find for the velocity of escape of a star near the center of the system

$$\left.\begin{array}{ll}\text{In the Milky Way} & 104 \text{ km/sec.}\\ \text{In the direction of Pole} & 98 \text{ km/sec.}\end{array}\right\} \qquad (28)$$

As a matter of convenience I used for this computation the constant value

$$\eta = 7.5 \times 10^{-30} \qquad (29)$$

11*b*. *Velocity compared with circular velocity*.—The velocity of a star which moves in the plane of the Milky Way in a circular orbit is determined by the formula

$$V_c^2 = G\eta\beta. \qquad (30)$$

If for the point II, 0° we take $\eta = 10.2 \times 10^{-30}$, and for the others the value (29), we obtain the results in Table VIII. The linear velocities $\beta\omega$ are thus seen to be well below the critical velocity V_c.

TABLE VIII

LINEAR AND CIRCULAR VELOCITIES IN PLANE OF MILKY WAY

Point	β	G	$\beta\omega$ Table VI	V_c
			km/sec.	km/sec.
II, 0°	1010	37.76	13.0	19.2
IV, 0	2106	35.71	19.5	23.1
VI, 0	3656	27.71	20.1	26.8
VIII, 0	5675	20.12	19.4	28.5
X, 0	8465	13.53	18.6	28.5

12. *Defects of solution*.—The way in which the values ω have been determined has made the resultant of gravitational and centrifugal forces perpendicular to the equidensity surfaces. In order that the surfaces may be really equipotential there is, however, a second condition to be satisfied, viz., that for points on the same surface the total force shall be inversely as the distance of two consecutive surfaces. This condition is *not* satisfied. The difference is shown, in its most extreme form, in the last column of Table VII, which, for the points in the Milky Way and in the direction of the Pole, situated on the same ellipsoid, shows the quotient

$$\frac{\text{Force at Pole}}{\text{Force in Milky Way (including centrifugal force)}}\cdot \qquad (31)$$

If the equidensity surfaces were really accurately represented by concentric similar ellipsoids, similarly situated, as assumed thus far, this quotient in every case would be 5.1. In reality this is far from being so.

There are certain facts indicating that actually the equidensity surfaces cannot be similar ellipsoids as hitherto supposed in this article. It is a well-known fact[1] that the stars of large proper motion show no concentration toward the Milky Way, but are distributed over the various galactic latitudes with very approximate uniformity. The meaning of this can hardly be other than that the equidensity surfaces for the smaller distances are spherical. The equipotential surfaces of the gravitational and centrifugal forces, in order to coincide with the equidensity surfaces, therefore must also be spherical for vanishing distances; hence the quotient (31) must approach 1.00. Now this is just what the values of the quotient given in Table VII do. The change in these values is therefore an encouragement toward an attempt at an improved theory rather than otherwise.

13. *Position of the sun relative to the center of the system.*—Before such an attempt can be made with any hope of success it will be necessary, however, to free the data from several imperfections. Foremost among these is the imperfection in the adopted position of the sun. The data used in what precedes rest on the assumption that the sun is at the center. It seems infinitely improbable that this should be the case. Our theory, crude though it necessarily must be, paves the way for overcoming this difficulty:

First, as seen from the sun, the center of the system must lie in a plane at right angles to the true stream-motion. Adopting for the vertex of the relative motion of the two streams $\alpha = 6^h 17^m$, $\delta = +11^\circ 9$, or gal. long. $= 167^\circ$, gal. lat. $= 0^\circ$, we find that the center, as seen from the sun, must lie in gal. long. 77° or 257°.

Second, nearly all astronomers who have dealt with the question, though from a very different point of view, agree in assuming for the center a *southerly* galactic latitude.[2]

---

[1] See for instance in *Verslag. Kon. Ak. v. Wetensch.*, Amsterdam, April, 1893, p. 137 (128).

[2] For instance, Struve, *Etudes d'Astronomie Stellaire*, pp. 61–62; Kapteyn, *Kon. Ak. Amsterd.*, April, 1893, p. 137; Hertzsprung, *Astronomische Nachrichten*, **196**, 207, 1914.

Third, Hertzsprung[1] from Cepheid variables finds the sun to be 38 parsecs north of the central plane of the Milky Way.

Fourth, the most difficult question probably will be that of the distance of the sun from the center. Still I think we can indicate a method which promises well.

For a first approximation, I start from the supposition, for want of a better one, that, even for the smaller distances, the *true* densities are as found in *Contribution* No. 188, which were derived on the basis of the erroneous assumption that the sun is the center. Further, for the moment, I will neglect the distance of the sun from the central plane of the Milky Way, which seems to be small.

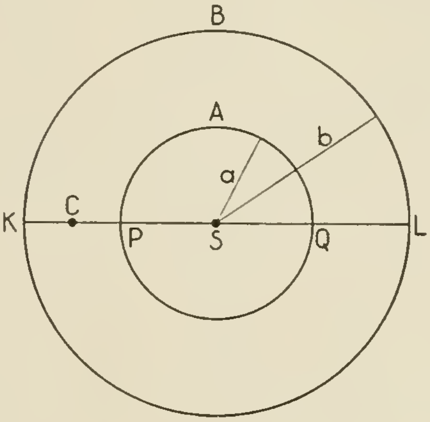

FIG. 2

In Figure 2, S represents the sun, C the center, and $CS=y$, the required distance. Let Δ_ρ represent the true star density at the distance ρ from the center. Now that we give up the erroneous supposition made in *Contribution* No. 188 and the present paper, we must consider the meaning of the densities given in Table VI of *Contribution* No. 188. What this table gives for a specified value of a (see Fig. 2) is in fact Δ', the average of the true densities at all points along the circumference PAQ around S with the radius a. This average will probably be not very different from the mean of the true densities at the points P and Q, and for the present, since our aim is only to arrive at a rough approximation, we will assume that it is exactly the case. Therefore, Δ being the true density,

$$\left.\begin{aligned}\Delta'_a&=\tfrac{1}{2}(\Delta_{y-a}+\Delta_{y+a})\text{ if }y<a\\ \Delta'_b&=\tfrac{1}{2}(\Delta_{b-y}+\Delta_{b+y})\text{ if }y>b\end{aligned}\right\}\qquad(32)$$

---

[1] *Ibid.*, p. 208.

If now, as a first approximation, we take as the true densities those obtained by formula (1) and assume in succession $y=1500$, 1000, and 500 parsecs, we find values of Δ' corresponding to different values of a as given in Table IX.

Such a table then, or something like it, would have been obtained, instead of Table VI (lat. = 0°) of *Contribution* No. 188, if the center were actually at a distance y from the sun. Thus, if y were indeed 1500 parsecs, the considerations of *Contribution* No. 188 would have led to densities which, from distance *zero* up to distance somewhere near 1500 parsecs, would have increased. For $y=1000$ we should still have found an initial increase, and even for $y=500$ the same would have held. In this last case, however, the increase would have been so small that it might well have been overlooked owing to the errors of observation. Since in reality the observations lead to a regular decrease of the density throughout, I think we must conclude that y cannot have as high a value as 1500 or even 1000 parsecs. As an upper limit, we may take

$$y<700 \text{ parsecs.} \tag{33}$$

TABLE IX

VALUES OF Δ'

a (Parsecs)	y in Parsecs		
	1500	1000	500
0	0.25	0.40	0.73
250	.26	.45	.865
500	.29	.49	.70
1000	.43	.59	.49
1500	.55	.43	.29
2000	.30	.245	.19
3000	.145	.115	.10
4000	.079	.062	.055
5000	0.044	0.039	0.035

We can also find a *lower* limit from the condition that the relative velocity of the two star-streams must not deviate greatly from the value of 40 km/sec. derived from observation.

In the neighborhood of the sun the linear rotatory motion of the system, that is, one-half the relative velocity of the star-streams, is $y\omega$.

If this velocity exceeded the circular velocity of a star at distance y from the center moving under the attraction of the whole system, the system certainly would not be in a steady state. Hence, on the assumption of a steady state,

$$y\omega < V_c, \tag{34}$$

or by formula (30)

$$y\omega < \sqrt{G\eta y}\,. \tag{35}$$

Assuming that inside ellipsoid II η, has everywhere the constant value 10.2×10^{-30}, we thus find, expressing results in kilometers, for

$y = 1000$ parsecs	$y\omega < 19.1$ km/sec.
700 parsecs	< 18.2 km/sec.
500 parsecs	< 16.5 km/sec.

If, therefore, we admit that $2y\omega$, the relative stream-velocity, cannot well be below 35 km/sec., we obtain as a lower limit

$$y > 600 \text{ parsecs} \tag{36}$$

The two limits (33) and (36) yield, as a first approximation,

$$y = 650 \text{ parsecs} \tag{37}$$

All these results agree fairly well in locating the center, as seen from the sun, at

$$\left.\begin{array}{lll} \text{Gal. long. } 77^\circ & \text{or} & \alpha = 23^{\text{h}}10^{\text{m}} \\ \text{Gal. lat. } -3^\circ & & \delta = +57^\circ \\ \multicolumn{3}{l}{\text{Distance projected on galactic plane } = 650 \text{ parsecs}} \\ \multicolumn{3}{l}{\text{Distance projected at right angles to that plane } = 38 \text{ parsecs}} \end{array}\right\} \tag{38}$$

The principal remaining uncertainty is perhaps that for the galactic longitude, which instead of 77° might be 257°. Personally I am strongly in favor of adopting the former value, which is in good accordance with the investigations of Herschel, Struve, and myself already quoted. My own result[1] was

$$\alpha = 0^h, \quad \delta = +42^\circ.$$

The determination (38) lays claim to no accuracy. To improve it, it will be necessary to carry through a second, and perhaps a third and fourth, approximation, for the determination of the lower limit of y; besides, I think we may still improve or corroborate the values of the distance of the sun from the galactic plane.[1] Altogether, the location of the center would seem to be a laborious problem rather than one of great difficulty.

---

[1] *Verslag. Kon. Akad. Amsterdam*, January, 1893, p. 129.

There is, moreover, the possibility of a direct determination. Given sufficient data on numbers of stars and proper motions for the regions around galactic latitude 0° and longitudes 77° and 257°, there would be no difficulty in deriving separately the star-densities at different distances from the sun in these regions. If there is truth in the above theory, these densities must *increase* with the distance up to distance y, in the direction *toward* the center, whereas in the opposite direction they must decrease with increasing distance. The two solutions together must yield a rather crucial test of the whole theory.

14. *Further defects. Separate treatment of the different spectral types.*—There are several further defects in the solution of the present paper. I will enumerate those that occur to me:

a) In the investigation on which the present paper is based the average parallax, as a function of magnitude and proper motion, has been taken from *Groningen Publication*, No. 8. At the present moment we have already available, though not yet published, much improved values, especially for the very small proper motions.

b) The value of $\overline{u^2}$ is not the very best that could have been obtained.

c) The values of G in Table III have been computed on the supposition that the average mass of a star is independent of the distance, whereas later, in section 8, it was found that this is not the case.

d) In this same computation for G, it was further assumed that the attraction of the whole of the system outside ellipsoid X on an internal point is zero. Though reasons were given for admitting that this attraction is small, it may not be negligible. Since according to what precedes it is highly improbable that the equidensity surfaces within X, as well as without, are really similar ellipsoids, the whole computation for G will have to be revised in a more definitive treatment.

---

[1] Furthermore the distance of the center from the sun, as here found, is so small that, if special attention is given to the matter, it may not be hopeless to get evidence of the curvature of the stream-lines, particularly for the rather distant stars (faint stars having small proper motion).

e) The present solution is for all the stars together, that is, for a very heterogeneous collection of stars.

Only the last point is of fundamental importance, and I will devote a few lines to it. Just as in the higher, very attenuated parts of an atmosphere, where the molecular encounters become relatively rare and the different gases are, as it were, sorted out, so among the stars we must expect that the different spectral classes will show different arrangements in space, owing to the different values of $\overline{u^2}$ and η (mass) peculiar to these classes. The two cases are not identical, owing to the stream-motion in the stellar system, which is not supposed to exist in the atmosphere. Still there must be analogy. So, to take an extreme example, if there exists a class of stars for which $\overline{u^2}$ is zero, these stars, according to the present theory, would be confined exclusively to the central plane of the galaxy. For evidently a star not in that plane could not have pure stream-motion; that is, it could not move in a perfect circle around the axis and perpendicular to it, because the attractive force of the system on such a point does not lie in that plane. Therefore it would necessarily have a peculiar motion.

This simple consideration makes us understand at once the otherwise astonishing fact that the Wolf-Rayet stars lie with such close approximation in the central plane of the Milky Way. In the present theory this means simply that they can have no other than pure stream-motion (possibly with some peculiar motion *in* the plane of the Milky Way[1]). We thus realize that for the several classes of spectra there must be a very intimate connection between the values of $\overline{u^2}$ and η on the one hand, and the well-known differences in concentration toward the galaxy on the other.

Such considerations show that for the totality "all stars together" the value of $\overline{u^2}$ will doubtless change with the position in space and in particular with the distance of the stars from the plane of the Milky Way. The present investigation, therefore, suffers from the defect that this circumstance was neglected, $\overline{u^2}$ having been taken the same for the whole of the system. I think that this shows sufficiently the absolute necessity of treating the different spectral classes separately.

---

[1] It is noteworthy that, provided the peculiar motion *in* the Milky Way is also *zero* (as it must be when the Maxwellian distribution holds for this limiting case), the parallax of these stars becomes a pure function of the linear velocity, that is, of the quotient, radial velocity divided by sin λ, λ being the angular distance, star-apex.

For such a treatment the necessary data are not yet available, or at least not available in a satisfactory form. Fortunately, however, there exist at present instruments capable of dealing successfully with difficulties which, not so long ago, would have been insurmountable. With their aid we may hope to obtain material for several spectral classes separately, little or not at all inferior to what has already been obtained for the stars as a whole. I think that the determination of the spectral class for some 1000 stars of magnitudes 11 to 12, well distributed over the sky and for which the proper motion is either already sufficiently well known, or may be determined by taking a few additional photographic plates, will go far toward supplying us with what is so urgently wanted.

APPENDIX

Formulae for the computation of the attraction of a homogeneous revolution ellipsoid, of unit density (1 star per cubic parsec), on an exterior point.

Take the axis of revolution as X-axis and let the xy-plane contain the attracted point whose co-ordinates are α and β. Let A and B be the axes of the ellipsoid, the first coinciding with the axis of revolution, and let X and Y represent the components of the required attraction, Z being zero. Then from the well-known formulae,[1] if we put

$$\lambda^2=\left(\frac{B}{A}\right)^2-1 \qquad (h)$$

$$K=\frac{2K}{\lambda^3}\left(\frac{B}{A}\right)^2 \qquad (k)$$

$$p=\lambda\frac{A}{A'}, \qquad (l)$$

---

[1] I have used the formulae as given by Duhamel, *Cours de mécanique*, V, 1, pp. 321 and 318.

where, if $\alpha=0$, A' is obtained from

$$A'=\sqrt{\beta^2-A^2\lambda^2} \tag{m}$$

and if $\beta=0$, from

$$A'=\alpha. \tag{n}$$

For other values of α and β we may write

$$E^2=\frac{\lambda^2}{2}-\frac{\alpha^2+\beta^2}{2A^2} \tag{o}$$

$$\eta=\lambda\frac{\alpha}{A} \tag{p}$$

$$\left(\frac{A'}{A}\right)^2=-E+\sqrt{E^2+\eta^2} \tag{q}$$

With these auxiliary quantities we find

$$X=-\alpha K\phi\ (p), \tag{r}$$

$$Y=-\beta K\omega\ (p), \tag{s}$$

in which $\phi(p)$ and $\omega(p)$, or rather their logarithms, have been tabulated in Table X by means of the formulae

$$\phi(p)=2[p-\text{arc tan } p] \tag{t}$$

$$\omega(p)=\text{arc tan } p-\frac{p}{1+p^2} \tag{u}$$

TABLE X

Values of Log ϕ (p) and Log ω (p) According to Formulae (t) and (u)

p	Log ϕ	Log ω	p	Log ϕ	Log ω	p	Log ϕ	Log ω
0.000	$-\infty$	$-\infty$	0.05	5.920^{-10}	5.920^{-10}	0.5	8.861^{-10}	8.804^{-10}
1	0.824^{-10}	0.824^{-10}	6	6.157	6.156	0.6	9.076	8.997
2	1.727	1.727	7	6.358	6.357	0.7	9.252	9.149
3	2.255	2.255	8	6.531	6.530	0.8	9.399	9.272
4	2.630	2.630	9	6.685	6.682	0.9	9.524	9.372
5	2.921	2.921	10	6.821	6.819	1.0	9.633	9.455
6	3.158	3.158	11	6.945	6.942	1.1	9.728	9.525
7	3.359	3.359	12	7.058	7.054	1.2	9.812	9.585
8	3.533	3.533	13	7.161	7.157	1.3	9.886	9.635
9	3.687	3.687	14	7.257	7.252	1.4	9.954	9.679
10	3.824	3.824	15	7.346	7.341	1.5	0.015	9.717
11	3.948	3.948	16	7.430	7.423	1.6	0.070	9.750
12	4.061	4.061	17	7.508	7.500	1.7	0.121	9.780
13	4.166	4.166	18	7.581	7.573	1.8	0.168	9.806
14	4.262	4.262	19	7.651	7.642	1.9	0.211	9.828
15	4.352	4.352	20	7.717	7.707	2.0	0.252	9.850
16	4.436	4.436	21	7.779	7.768	2.1	0.289	9.869
17	4.515	4.515	22	7.839	7.827	2.2	0.325	9.885
18	4.590	4.590	23	7.896	7.882	2.3	0.358	9.900
19	4.660	4.660	24	7.950	7.935	2.4	0.389	9.914
20	4.727	4.727	25	8.002	7.986	2.5	0.418	9.927
21	4.790	4.790	26	8.052	8.035	2.6	0.446	9.939
22	4.851	4.851	27	8.100	8.081	2.7	0.472	9.950
23	4.909	4.909	28	8.146	8.126	2.8	0.497	9.960
24	4.964	4.964	29	8.190	8.169	2.9	0.521	9.969
25	5.018	5.017	30	8.233	8.210	3.0	0.544	9.977
26	5.069	5.068	31	8.274	8.250	3.1	0.566	9.985
27	5.118	5.118	32	8.314	8.288	3.2	0.587	9.993
28	5.165	5.165	33	8.352	8.325	3.3	0.607	0.000
29	5.211	5.211	34	8.390	8.361	3.4	0.626	0.006
30	5.255	5.255	35	8.426	8.396	3.5	0.645	0.012
31	5.298	5.297	36	8.461	8.429	3.6	0.663	0.018
32	5.339	5.339	37	8.495	8.461	3.7	0.680	0.023
33	5.379	5.379	38	8.528	8.493	3.8	0.697	0.028
34	5.418	5.418	39	8.560	8.523	3.9	0.713	0.033
35	5.456	5.455	40	8.591	8.552	4.0	0.728	0.038
36	5.492	5.492	41	8.621	8.581	4.1	0.743	0.042
37	5.528	5.528	42	8.651	8.609	4.2	0.758	0.046
38	5.563	5.563	43	8.680	8.635	4.3	0.772	0.050
39	5.597	5.596	44	8.707	8.662	4.4	0.786	0.054
40	5.630	5.629	45	8.735	8.687	4.5	0.799	0.057
41	5.662	5.661	46	8.761	8.712	4.6	0.812	0.060
42	5.693	5.693	47	8.787	8.736	4.7	0.825	0.064
43	5.724	5.723	48	8.813	8.759	4.8	0.837	0.067
44	5.754	5.753	49	8.837	8.782	4.9	0.849	0.070
45	5.783	5.782	0.50	8.861	8.804	5.0	0.861	0.072
46	5.812	5.811						
47	5.840	5.839						
48	5.867	5.866						
49	5.894	5.893						
0.050	5.920	5.920						

Leiden
September 1921

A CONTINUOUS SPECTRUM FROM MERCURY VAPOR

BY C. D. CHILD

ABSTRACT

Continuous spectrum of *mercury, red to ultra-violet.*—(1) *Conditions for emission in discharge tube.* A continuous spectrum identical with the fluorescence spectrum is emitted in addition to the ordinary line spectrum only when (*a*) the temperature of the vapor is above 120° C. and below 300° to 400°, depending on the pressure, when (*b*) the pressure is above 1 mm. when (*c*) the current-density is low, of the order of 10^{4} amp/cm² or less and (*d*) when very little air or other contaminating gas is present. An influence machine or transformer is better as a source of current than an induction coil, especially one with condensers. Ionization of the vapor is not necessary for the emission of this spectrum since it was obtained with only 7 volts between the Wehnelt cathode and surrounding cylinder. (2) *In explanation* it is suggested that *the carriers of the spectrum* are molecules consisting of two or more atoms, which emit the fluorescence spectrum as a result of excitation by ultra-violet radiation λ 2536 emitted by atoms struck by electrons with energies corresponding to 4.9 volts or more.

Continuous spectrum of sodium.—Preliminary observations on heated sodium vapor in a discharge tube indicated that a continuous spectrum was present but much fainter than the line spectrum.

Ionization potential for mercury.—Some observations on the current from a heated filament to a concentric electrode as a function of voltage seem to show that the ionization potential *varies with the temperature*, reaching a minimum for about 140°, when it was 3 volts less than for 50°.

Change in chemical behavior of mercury vapor at about 120°C.—Above that temperature it *reacts with air* to form a dark compound, but not below. This reaction is associated with the appearance of the continuous spectrum.

The writer has recently observed that under certain conditions the electric discharge through mercury vapor produces a glow that is distinctly green. This shows the well-known line spectrum of mercury and also one that is apparently continuous from the red into the blue, being most prominent to the eye in the green. A brief mention was made by Warburg[1] in 1890, that he had observed a continuous spectrum when studying the electric discharge through mercury vapor. This was verified by Wiedemann and Schmidt,[2] Kalähne,[3] and Kowalski.[4] A continuous spectrum was also found by Hartley[5] when mercury vapor is excited to fluorescence by ultra-violet radiation, and was further studied by Wood[6] and others. However, no extended study has been made of this spectrum when excited by an electric discharge, and the investigation described in the following paragraphs was, therefore, undertaken.

---

[1] *Wiedemann's Annalen*, **40**, 14, 1890.

[2] *Ibid.*, **57**, 457, 1896.

[3] *Ibid.*, **65**, 826, 1898.

[4] *Physikalische Zeitschrift*, **15**, 249, 1914.

[5] *Proceedings Royal Society*, A, **76**, 428, 1905.

[6] *Philosophical Magazine* (6), **18**, 240, 1909, and (6), **23**, 689, 1912.

Conditions necessary for obtaining the continuous spectrum. Small current-density.—There are three conditions necessary for obtaining the continuous spectrum by an electric discharge with any considerable brightness; the first being that the current-density must be small. As the current-density is increased the line spectrum becomes more prominent and the continuous spectrum less so. Contracting the tube as in the Plücker tube has the same effect as increasing the current.

The best source of current for showing this spectrum is the Wimshurst or Toepler-Holtz machine. With the current from such a machine it is often impossible to detect any lines even when the continuous spectrum is very bright. A step-up transformer may also be used to advantage. An induction coil is not so satisfactory. It is possible to obtain the continuous spectrum with the discharge from a hot wire covered with calcium oxide, if the current is sufficiently small. Putting condensers in parallel with the induction coil has the same effect as increasing the current. In most of the experiments described in this paper the discharge was obtained from a transformer, the current being approximately 5×10^{-5} amperes per square centimeter.

Temperature and density necessary for the continuous spectrum.—The second condition necessary for obtaining the continuous spectrum is that the temperature must be above 120° C. and below a higher temperature which depends on the density of the vapor. Kowalski found that mercury vapor excited by an electrodeless discharge gave a white glow at room temperature and a green glow when heated to 140° C. This is approximately the same temperature as that which was found necessary to produce the continuous spectrum.

A third condition necessary for the continuous spectrum is that the vapor have a density approximately that of saturated vapor at 120° C. This may be shown by maintaining the lower part of a tube containing a small amount of liquid mercury at a temperature below 120° C., while the upper part is kept above that temperature. The vapor in such a tube is less dense than that required and does not show the continuous spectrum. This will be discussed more fully in a following paragraph.

Even when the density of the vapor is kept constant the continuous spectrum becomes less prominent, if the temperature is raised too high. This was shown by a tube 25 cm long which was heated while being exhausted until all but a few minute drops of the liquid mercury were vaporized. It was then sealed off from the pump and further heated until the mercury was completely vaporized. This showed the continuous spectrum with scarcely a trace of the line spectrum. If it was further heated until the glass became slightly conducting the glow became distinctly blue with the discharge concentrated in a line in the center of the tube. The line spectrum was then prominent with but little of the continuous spectrum.

An experiment by Wood[1] showed that the same effect occurs at a higher temperature when the continuous spectrum is excited by ultra-violet light. In his experiment a quartz tube containing a very small drop of mercury was exhausted and sealed off from the pump and heated until the mercury was completely vaporized and the tube became red hot. It was found that after the mercury had all vaporized the fluorescence diminished in intensity and finally disappeared.

It is difficult to determine the exact temperature and density necessary to produce the continuous spectrum not only because any change in the spectrum due to heating the tube occurs gradually, but also because any trace of gas other than mercury hinders the production of the continuous spectrum. When a tube is sealed off from the pump and used for a time such gases are apt to occur. Lastly it is difficult to distinguish between effects due to temperature and those due to density, since it is impossible to increase the density of the vapor without increasing the temperature.

However, the arrangement shown in Figure 1 gives results of some value.

---

[1] *Philosophical Magazine* (6), 18, 246, 1909.

The tube *T* was connected to the pump by a trap *d*. Observations were made with this open and with it closed. The upper parts of *T* and *c* were surrounded with an asbestos jacket which was heated by a ring burner. The lower part, including *d*, was immersed in an oil bath which was kept at a lower temperature. When the trap at *d* was open the tendency for the mercury to distil into the pump was hindered by placing a capillary tube 20 cm long and 1.25 mm in diameter at *c*.

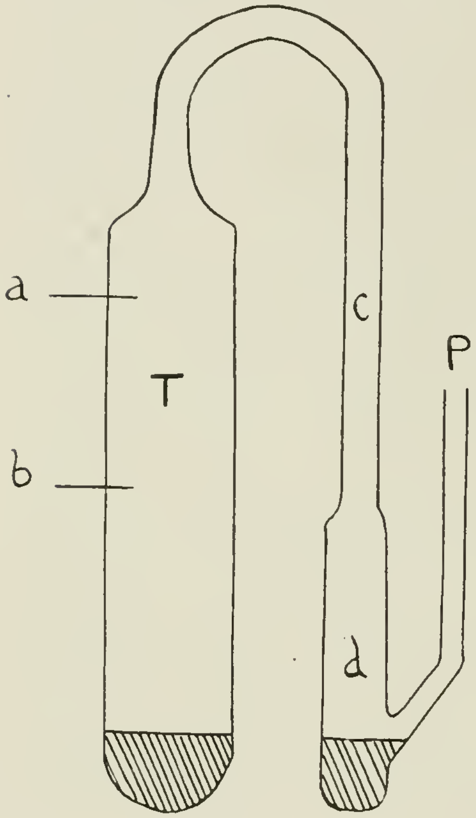

Fig. 1

The trap at *d* could be closed by distilling mercury over from the tube until the opening to *P* was closed. Both with the trap open and with it closed the tube was heated for some time before observations were taken.

It was found that both the upper and the lower parts of the tube must be at least at 130° C. in order to show the continuous spectrum prominently. Heating the upper alone was not sufficient even when the lower was but a few degrees below the required temperature. This again shows that it is not only necessary to have a required temperature but also a certain density of the vapor.

The lower part of the tube was then maintained at various temperatures above 130° C. and the upper part was heated until the continuous spectrum approximately disappeared. In this case the density of the vapor did not remain constant but diminished as the temperature of the upper part was raised. The results of such observations taken with the trap open are given in Table I but approximately the same results were obtained with the trap closed. Column 1 gives the temperature of the bath surrounding the bottom of the tube, and Column 2 gives the approximate temperature of the air inside the jacket above which the vapor ceases to give the continuous spectrum. Above 400° C. the glass became somewhat conducting, so that no higher temperature could be taken with the apparatus at hand.

TABLE I

Column 1	Column 2
132	310
140	335
150	375
160	410
167	440

As has been stated, the values given in the second column are rough approximations, but they are sufficiently accurate to prove that the temperature at which the continuous spectrum disappears depends on the density of the vapor in the tube. This is what might be expected if the continuous spectrum depends on the presence of molecules in the vapor. According to the mass law, if both atoms and molecules are present, the greater the density of the vapor the greater the relative number of molecules at a given temperature, and the higher the temperature needed to break up all of the molecules into atoms.

If both the vapor and the liquid mercury are heated above 200° C. the discharge becomes concentrated at the center of the tube. At 280° C. with a pressure of 15 cm the discharge is almost a line, which is very bright and shows the line spectrum much more prominently than the continuous spectrum.

Effect of vaporization and condensation.—It is easier to obtain the continuous spectrum where vaporization and condensation are taking place, as may be shown by heating a tube at some part where a few drops of mercury have condensed. If a discharge is passed through the tube, the continuous spectrum is much more prominent in the region where the vaporization occurs than elsewhere.

However, neither vaporization nor condensation is essential for the production of the continuous spectrum. This was shown in the experiment already described where a tube was heated until the mercury was completely vaporized. When there was neither vaporization nor condensation, there was still the continuous spectrum with scarcely a trace of the line spectrum.

There is, however, no question but that condensation aids in showing the continuous spectrum and also that it is the condensation rather than the vaporization that is helpful. It is somewhat difficult to prove this since newly formed vapor ordinarily expands as soon as it leaves the surface of the hot mercury and in doing so may condense enough to show the continuous spectrum. However, that the preceding statement is correct was shown by the tube illustrated in Figure 2. The electrode *a* extended into the liquid mercury. This was heated and the part of the tube at the left of *c* was kept as hot as possible. The part at the right was allowed to remain comparatively cool. The connection to the pump was left open, so that only a part of the vapor passed into the tube. Under these conditions the glow over the liquid mercury and as far as *c* was white, while that at the right of *c* was green. By having a current slightly greater than the minimum it is possible to obtain a discharge which shows no continuous spectrum at the left of *c* while it shows it very prominently at the right.

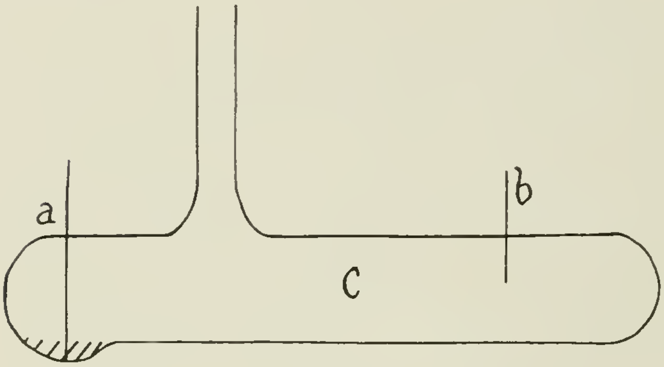

Fig. 2

Effect of other gases on the mercury vapor.—Wood[1] found that mercury would not fluoresce when mixed with other gases. The same has been found true when the continuous spectrum is produced by an electric discharge. As has been stated, a very slight amount of air changes very greatly the upper temperature at which the continuous spectrum disappeared. Again, with 2 or 3 mm of air and a small amount of mercury vapor it is impossible to obtain a continuous spectrum at any temperature. Thus in the preceding experiment, with the bath at the bottom of the tube at 140° C. and 3 mm of air present, no continuous spectrum could be obtained, whatever the temperature of the upper part of the tube. When the upper part was at 230° C. only the line λ 5461 could be detected. A somewhat similar phenomenon has been observed by Robertson[1] when exciting mercury vapor by electrodeless discharge.

---

[1] *Astrophysical Journal*, 26, 43, 1907; *Philosophical Magazine* (6), 18, 244, 1909, and (6), 21, 314, 1911.

Continuous spectrum not affected by the kind of electrode, kind of glass, nor purity of mercury.—The continuous spectrum is not affected by the shape of the tube nor that of the electrode, providing the current-density is not increased. It is shown equally well with platinum, iron, or mercury electrodes and in tubes made of soda, lead, or Pyrex glass. It showed equally well with mercury that had been distilled three times and with mercury containing zinc, lead, cadmium, or sodium as impurities.

Mercury was also purified by distilling it in a stream of air. It is claimed by Hulett and Minchin[2] that mercury so distilled has less than one part of zinc to 10^{10} parts of mercury and that other oxidizable metals are removed to an equal extent. Mercury thus purified showed the same spectrum as other mercury.

Differences between normal mercury vapor and that giving the continuous spectrum. Ionization of the gas not necessary for radiation.—In a number of ways the vapor which is in a condition to give the continuous spectrum behaves differently from mercury vapor at room temperature. First it may be made to give visible radiation without being ionized. This might be expected from the fact that it fluoresces under the influence of ultra-violet radiation without becoming ionized, as has been shown by Wood.[3] That such radiation may also be produced by an electric discharge without ionizing the vapor is shown by the following experiment. Current from a hot wire covered with calcium oxide was passed to a surrounding cylinder. When the mercury at the bottom of the tube was heated so as to send a stream of hot vapor through the cylinder the region above the cylinder showed a faint glow which gave the continuous spectrum even when the voltage between the wire and the cylinder was much below that needed to produce ionization.

---

[1] *Science*, **52**, 386, 1920.

[2] *Physical Review*, **21**, 388, 1905.

[3] *Philosophical Magazine* (6), **23**, 713, 1912.

In the experiment as performed the wire was 4 cm long and 2 mm in diameter. The surrounding cylinder was of iron, 5 cm long and 2 cm in diameter. At approximately 7 volts there was a faint glow above the cylinder, which grew somewhat brighter as the voltage was raised, but there was no large increase in the current until a difference of potential of 12 volts was applied, when the current suddenly increased and the region between the wire and the cylinder became luminous. The change above 12 volts was no doubt due to the beginning of ionization of the vapor. This would, therefore, seem to justify the conclusion that the continuous spectrum may be produced without ionizing the vapor.

A lower ionization potential.—Again the ionization potential of the vapor giving the continuous spectrum appears to be lower than that of normal mercury vapor. This was shown by examining at different temperatures the voltage at which there occurs a large increase in the current passing from a hot wire to a surrounding cylinder without any corresponding increase in the voltage. The same tube was used for this purpose as in the preceding experiment where the discharge from a hot wire was examined. The air was pumped out by a diffusion pump until no reading could be made on a McLeod gauge that read down to .0002 mm. The tube was then heated for some time so as to drive off any residual air, the tube becoming filled with mercury vapor from mercury kept in the bottom of the tube. The current through the platinum wire was kept at 4.5 amperes.

At approximately 50° C. the critical voltage was 16 volts. When the tube was heated until the continuous spectrum appeared the critical voltage was approximately 13 volts. On further heating until the mercury at the bottom was freely boiling the critical voltage increased to 18 volts. On allowing the tube to cool this voltage again decreased to 13 volts and then increased to 16 volts.

Data taken with different temperatures of the wire and with different sizes of wire all showed a minimum critical voltage when the tube was barely hot enough to show the continuous spectrum.

A check upon this is given by the fact that when a current is sent through a tube from a Wimshurst machine, the potential difference between the electrodes is smallest when the temperature is such that the continuous spectrum begins to appear. This was shown by rough measurements taken with an electroscope.

The high voltage required when the temperature was high was no doubt due to the large density of the mercury vapor. Although impact between electrons and atoms of mercury at low voltage is elastic, a small amount of energy is lost to the electron at each impact, so that with large density much of the energy is lost and a high voltage is necessary to produce ionization.

The decrease in voltage occurring when the temperature is such that the continuous spectrum is barely visible must, of course, be explained in some other way. It might be thought that at the lower temperatures there was some impurity in the gas which caused the critical voltage to be high. This does not, however, seem probable, first, because the amount of gas other than mercury vapor which was left in the tube was very small, its pressure being less than .0002 mm. Secondly, even this small amount would be swept out by the flow of mercury vapor into the cooler parts of the apparatus.

Again the lower critical value occurring when the continuous spectrum appeared might be explained on the ground that the platinum wire became hotter as the tube was heated and that the apparent critical voltage became lower because of the higher velocity of the emitted electrons. However, the resistance of the wire was measured by a Wheatstone bridge arrangement and it was found that when the tube was heated and the current through the wire was kept constant, the resistance of the wire became slightly less, indicating that the temperature of the wire decreased instead of increasing. This, no doubt, was due to the cooling effect of the mercury vapor about the wire. As the temperature of the tube is raised the density of the vapor increases and the denser vapor is able to conduct more heat from the wire, so that its temperature is lower, although the temperature of the surrounding tube is higher.

It, therefore, seems necessary to accept the view that the lower critical voltage is due to the fact that the ionization potential of the mercury vapor is less when the vapor is in a condition to give the continuous spectrum than when it is at room temperature. Whether this lowering is due directly to a change in the condition of the molecules which makes them more easily ionized, or to some ability which they acquire of absorbing radiation, cannot at present be stated. A more direct method of measuring the ionization potential is desirable in order to give us further knowledge of this subject.

Hot vapor active chemically.—During these experiments it was noticed that if any appreciable amount of air was left in the tube and the temperature raised sufficiently high to produce the continuous spectrum, a dark compound was formed which stuck to the sides of the glass. The substance was not formed when the discharge was passed through a tube at room temperature. By using a tube that was hotter at the bottom than at the top it was possible to observe the boundary between the region showing the continuous spectrum and that showing the line spectrum and it was found that this was also the boundary between the glass covered with the deposit and the clean glass.

Continuance of the glow.—When this discharge showed the continuous spectrum there was usually a green glow for several centimeters above the upper electrode. This could be explained as due to carriers of the continuous spectrum continuing to radiate for an appreciable time after they were excited. This continuance of the glow was examined by two different methods. One of those used has been described in a preceding article.[1] The discharge was passed from the secondary of a transformer and the time at which the current ceased was compared with the time at which the light ceased to be visible. This method indicated a continuance of the light for .002 seconds after the current ceased.

There is, however, an objection to this method owing to the possibility of the glass's becoming charged at the time the discharge passes and producing a luminous discharge after the current proper has ceased. The following arrangement obviates this difficulty to a large extent. The tube which has already been described in showing the discharge from a hot wire to a cylinder surrounding it was used. The current between the wire and the cylinder was made and broken by a wheel attached to the synchronous motor used in the preceding experiment. The difference in time between the breaking of the current and the time when the light ceased to be visible was apparently .008 seconds.

---

[1] *Physical Review* (2), **9**, 1, 1917.

Since the voltage here was not more than 30 volts and the wire was so nearly surrounded by the cylinder, it seems as if the glass could not have been charged to a sufficient amount to produce any light. On the other hand the fact that the light was here observed to continue for a period longer than that found with a spark discharge which is known to be somewhat untrustworthy makes it desirable to study this phenomenon further.

Character of the spectrum.—As far as could be determined by observations with the eye and by some rather crude photographs of the spectrum the continuous spectrum here studied is the same as that given by Wood[1] but the writer has neither the apparatus nor the experience to warrant further work with this. Wood's work has shown that this spectrum is continuous from the yellow into the ultra-violet at about the wave-length λ 3000 with a minimum at λ 3600. When the glow is produced by electric means and the conditions are at their best the red is also visible.

Again we might expect the relative intensity of different parts of the spectrum to vary as the conditions of the experiment varied. Such a variation was found by Wood[2] in the case of iodine vapor when its density was changed. A difference of this sort would indeed be expected if the molecules giving the spectrum differ in size or are subject to any change which progresses as the temperature is varied.

However, there does not appear to be any such variation in the continuous spectrum from mercury vapor, as is shown by the following experiments. A discharge was passed from the bottom of a tube containing boiling mercury to an electrode 24 cm above it. It is probable that if the molecules change either in size or in condition, they do so in passing from the hot liquid to the cooler region above. However, no difference could be observed in the character of the spectrum coming from different parts of the tube. Neither did changing the intensity of the light produce any change in the relative brightness of different parts of the spectrum.

---

[1] *Philosophical Magazine* (6), **18**, 240, 1909. Plate 7, Fig. 6.

[2] *Ibid.* (6), **27**, 531, 1914.

Again the color of the discharge through tubes differing in temperature and in density of vapor is the same as long as only the continuous spectrum appears. For example one tube was heated to approximately 140° C. and second to 220° C. The pressure of the vapor in the first case was 2 mm and in the second was 3 cm. When the two tubes were placed side by side and the same current sent through them no difference in color could be detected. At higher temperatures the discharge becomes concentrated in the center of the tube and the line spectrum becomes noticeable. In that case a difference of color is, of course, noticeable.

Moreover, Wood and others who have examined the fluorescence of mercury vapor when at atmospheric pressure mention the color as being green, which is the same as that given by the vapor at low pressure.

The evidence obtained from the spectrum would, therefore, indicate that the oscillating system which gives the continuous spectrum is distinctly different from that which gives the line spectrum, that the light always comes from the same oscillating system rather than from a number of different ones and that it is not affected by the frequency of the impacts between the molecules.

The carriers of the continuous spectrum.—In attempting to determine the carriers of the continuous spectrum two explanations have been considered. One is that the same vibrating system gives both the line and the continuous spectrum, the vibrations being modified when the vapor is dense by the greater number of impacts. There are two objections to this view. First, experiment shows that when the density is kept constant and the temperature of the vapor is raised the ability of the vapor to give the continuous spectrum is impaired, if not destroyed. But under these conditions there is an increase in the number and intensity of impacts per second and if the continuous spectrum is due to impacts between atoms, one would expect the continuous spectrum to become more conspicuous instead of less so.

Secondly, there are impacts at 120° C. as well as at 140° C. They are indeed more than twice as frequent in the latter case and somewhat more intense, but if the impacts affect the oscillations at one temperature, one would expect some effect at the other and yet at the lower temperature there is usually no indication of the continuous spectrum, while at the higher one it almost entirely displaces the line spectrum. Moreover, the usual change in the spectrum to be produced by increasing the density is a broadening of the lines and not a complete change of the spectrum.

It seems to the writer that a more probable explanation is that the carriers of the continuous spectrum are molecules of mercury while the atoms are the carriers of the line spectrum. The determination of the specific gravity of mercury vapor indicates that it is monatomic, but these determinations are not sufficiently accurate to make the presence of the molecules seem improbable even when the temperature is high, and it is difficult to believe that a monatomic vapor can give two such radically different spectra and behave in other ways as differently as this vapor does.

Such an assumption would explain the fact that with high temperatures or with large currents such as occur with the mercury arc the continuous spectrum does not appear, for in such cases the molecules are no doubt split up into atoms which give only the line spectrum.

This, however, does not explain the large change in the spectrum which occurs at 130° C. We are, therefore, compelled to make the further assumption that the molecules are more easily excited at high temperatures than at low. Such an assumption is not unreasonable. While energy is probably not absorbed by the internal structure of isolated atoms when the gas is heated, it probably is absorbed by molecules of two or more atoms. If so, such molecules may be more easily ionized and excited to radiate at higher temperatures. According to such an assumption, at room temperatures the atoms are the more easily excited and only the line spectrum appears, while at the higher temperatures the molecules are more easily excited and we have also the continuous spectrum. The facts can, therefore, be explained on the following assumptions: *First, the carrier of the continuous spectrum are molecules consisting of two or more atoms, and secondly, these molecules are more easily excited at high temperatures than at low.*

Manner of excitation.—There are at least two ways in which the vibrations giving the continuous spectrum may be excited; the molecules may be agitated by impacts of electrons on the molecules, or by the absorption of ultra-violet radiation. The impact of electrons on the atoms of mercury no doubt produces radiation of wave-length λ 2536 and in a similar way the impact on molecules may produce the continuous spectrum, but since this spectrum is certainly produced by ultra-violet radiation, as was shown by Wood, and since radiation of wave-length λ 2536 is produced by the impact of electrons on atoms as has been shown by Franck and Hertz, it seems to the writer more probable that there is first a production of the radiation of wave-length λ 2536 and that this under proper conditions causes fluorescence of the vapor which gives out the continuous spectrum.

When an electron which has passed through a difference of potential of 4.9 volts, hits a mercury atom, it gives up its energy to the atom and the atom radiates this energy as ultra-violet light. When the gas is as dense as in the cases here studied the greater part of the energy goes primarily into such radiation, for with such densities the electrons will in almost every case hit an atom after it has passed through 4.9 volts and before it has passed through 10.4 volts, which is the voltage necessary to produce ionization.

An atom which has thus been partially ionized may be hit by a second electron before it radiates its energy and complete ionization may occur, as has been pointed out by Van der Biji[1] and Compton.[2] The recombination resulting from such ionization produces the line spectrum of mercury. With larger currents the chance of an atom being hit a second time before it has radiated its energy is, of course, greater than with small currents, so that entirely aside from the increase in temperature caused by the large current the line spectrum is more apt to be prominent when the current is large.

On the other hand, if the partially ionized atom is not quickly hit, it will radiate its energy. This may pass to a second atom and partially ionize it, which in turn may give out this same kind of radiation. This last is the kind of fluorescence which is known as resonance radiation.[1]

---

[1] *Physical Review* (2), 10, 546, 1917.

[2] *Ibid.* (2), 15, 476, 1920.

If there are no molecules present, or if they are not in a condition to absorb this energy, as they apparently are not at room temperature, then all of the energy of this radiation will either aid in ionizing atoms or will be radiated from the gas as wave-length λ 2536. If, however, there are molecules of two or more atoms present which are in a condition to absorb the energy of this radiation, they fluoresce, emitting a radiation which gives the continuous spectrum.

The manner of excitation of the continuous spectrum is then conceived to be as follows: The electrons partially ionize some of the atoms. These radiate energy of wave-length λ 2536. If this radiation falls on molecules which are capable of absorbing it, the vapor fluoresces, giving out the radiation which gives the continuous spectrum.

The experiment which has been described showing that it is possible to produce the continuous spectrum without ionization confirms this explanation.

The fact that the line spectrum appears at the cathode even when the continuous spectrum appears in the positive column may be explained by assuming that in the cathode drop where the electric force is large the electrons attain sufficient velocity to completely ionize the atoms upon impact, and the resulting recombination of the positive ions with the electrons gives the line spectrum.

The condensed discharge.—As has been stated the discharge from an induction coil does not give as prominent a continuous spectrum as that from a Wimshurst machine. This is especially true, if condensers are in parallel with the tube. A tube so heated that the discharge from a Wimshurst machine will show only the continuous spectrum will scarcely show anything but the line spectrum with the spark from an induction coil.

There are two respects in which the condensed discharge differs from the uncondensed. The maximum current is greater with the condensed discharge, and the voltage when the spark commences is higher due to the fact that the ions have nearly all recombined since the preceding discharge. The following experiment indicates that it is the large current rather than the high voltage which causes the difference. The current from a Wimshurst machine was passed between *a* and *b* in Figure 3 when the tube was so heated as to give the continuous spectrum. A spark from an induction coil having capacity in parallel with the tube was then passed between *c* and *d*. This was found to show the line spectrum as plainly between *a* and *b* as in the other parts of the tube. The voltage between *a* and *b* could not in this case have been greater with the spark since the glow discharge would keep the gas in this region conducting while the current from the induction coil was interrupted.

---

[1] *Philosophical Magazine* (6), 23, 699, 1912.

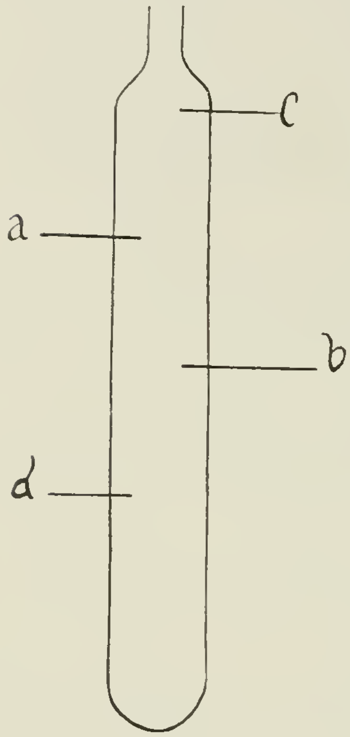

FIG. 3

Continuous spectrum from other gases.—If this explanation is correct, it would be reasonable to expect a continuous spectrum from other gases, or at least with other monatomic gases when near the point of condensation. Some observations were made on the discharge through sodium vapor when heated. There appeared to be a continuous spectrum present but it was much fainter than the line spectrum, so that no very definite description of it can be given. It is probable that it was the fluorescent spectrum of sodium vapor which has been described by Wiedemann and Schmidt[1] and others.

I desire to express my appreciation of the assistance which has been given me in the preceding work by Mr. B. K. Northrup, of Cornell University, and Professor A. E. Wood, of Colgate University.

COLGATE UNIVERSITY
September 1921

---

[1] *Annalen d. Physik*, 56, 18, 1895.

FORMATION AND LIFE OF METASTABLE HELIUM

By FABIAN M. KANNENSTINE

ABSTRACT

Current-potential curves for alternating and intermittent arcs in pure helium between a Wehnelt cathode and nickel anode were obtained by use of a Braun-tube oscillograph, for pressures of from 0.06 to 2 mm. With alternating voltages, the striking potential for each half-cycle was 29 volts or more for frequencies of 200 or less, but for frequencies of 220 cycles and above, the current started at about 5 volts and soon reached a saturation value until about 25 volts caused a further increase. In all cases the breaking potential was about 5 volts. To form the intermittent arc, the voltage was periodically dropped from 36 to some lower predetermined value. If this lower potential was less than 4.6 volts, the arc was suddenly extinguished; if between 4.6 and 23.7 volts, the arc died out gradually; and if it was 25.3 volts or above, the arc was maintained. All the foregoing values include a correction of 1.1 volts added to the actual readings to bring them in agreement with accepted results.

Evidence as to the life of metastable helium.—To explain various experimental results, it has been suggested that atoms of helium, partially ionized by electronic collisions of 20.8 volts or more and hence capable of complete ionization by further impacts of 4.8 volts or more, remain in this metastable condition for an appreciable time. The foregoing results not only confirm this suggestion but also show that under the circumstances of this experiment the metastable form persists for about 0.0024 second.

INTRODUCTION

Experiments with electron impacts in helium have led to a value for the minimum ionizing potential of 25.3 volts and to two radiating potentials, one at 20.5 volts[1] and another at 21.3 volts.[2] Franck and Reiche[3] and Franck and Knipping[2] conclude that the partially ionized state formed when the atom has been excited by the impact of 20.5 volt electrons is a "metastable" state, which may persist for some time and may be even permanently stable in absolutely pure helium. This conclusion is drawn from the fact that the radiation usually observed with electron impacts at this voltage disappeared when the helium was very pure, indicating that the displaced electrons do not return to the normal state. In slightly impure helium they also observed that the radiation, as measured by its photo-electric effect, appeared to continue for a brief time after the exciting electron impacts ceased.

---

[1] F. Horton and A. C. Davies, *Philosophical Magazine*, **42**, 746, 1921; J. Franck and P. Knipping, *Physikalische Zeitschrift*, **20**, 481, 1919; K. T. Compton, *Philosophical Magazine*, **40**, 553, 1920; F. S. Goucher, *Proceedings Physical Society of London*, **33**, 13, 1920.

[2] J. Franck and P. Knipping, *loc. cit. Zeitschrift für Physik*, **1**, 320, 1920. F. Horton and A. C. Davies, *loc. cit.*

[3] *Zeitschrift für Physik*, **1**, 54, 1920.

Experiments by Paschen,[1] which show that in pure excited helium resonance radiation may be caused by the infra-red line 10830 A, also support the conception of a metastable state. All the energy of this wave-length absorbed by the excited atoms was found to be re-emitted as radiation of this same wave-length. In terms of Bohr's model this means that the radiation is absorbed by atoms which have already absorbed the energy corresponding to the radiating potential 20.5 volts, and that the displaced electrons return to this partially ionized state only, and not to the normal state.

The semi-stable existence of partially ionized helium atoms is also useful in explaining the phenomena in low-voltage arcs in helium, especially the striking of the arc at 20.5 volts with dense electron currents.[2] The phenomena of successive impacts as discussed by Compton[3] are of much more importance when the partially ionized atoms have a relatively long life. The metastable helium should be completely ionized by electrons with a speed corresponding to a potential of $25.3 - 20.5 = 4.8$ volts. If we assume that the metastable state may be produced by the arc radiations,[4] then an arc might be maintained with dense enough electron currents down to 4.8 volts. It is of interest that in this way Compton, Olmstead, and Lillie have maintained an arc with potentials as low as 8 volts between the electrodes. Horton and Davies[5] report an unsuccessful attempt to observe the ionization of abnormal helium atoms by bombardment with electrons of 4.8 volts.

In this paper experiments with helium arcs are described which show that helium may exist temporarily in a metastable form, and that arcs may be maintained in it with 3.5 volts. An approximate determination of its life is also reported.

[1] *Annalen der Physik*, **45**, 625, 1914.

[2] K. T. Compton, E. G. Lillie, P. S. Olmstead, *Physical Review*, **16**, 282, 1920.

[3] *Physical Review*, **15**, 476, 1920.

[4] O. W. Richardson and C. B. Bazzoni, *Nature* **98**, 5, 1916; F. Horton and A. C. Davies, *op. cit.*, **42**, 752, 1921.

[5] *Ibid.*, **42**, 763, 1921.

ARCS WITH LOW-FREQUENCY VOLTAGES

The arcs were formed between a Wehnelt cathode and nickel anode in a pyrex tube containing carefully purified helium. The helium was purified by passing over heated copper oxide and charcoal immersed in liquid air. Before passing into the experimental tube the helium passed through two additional charcoal tubes and a liquid-air trap. The tube and liquid-air trap were baked out at 450° C. for several days before the helium was admitted.

In the first experiments the helium was excited by an alternating e.m.f. An electromagnetic oscillograph was used to obtain curves showing the variation of current and voltage with time. From such curves the current-voltage curve may be obtained.

A decided dissymmetry in the growth and decay of the arc current could be observed, and also an apparent continuation of the arc current down to very low voltages. To obtain greater sensitiveness and to avoid the possible distortion from the inertia of the oscillograph elements, a sensitive Braun tube oscillograph was used in most of the later experiments. The electrostatic deflecting plates of the Braun tube were connected across the anode and cathode of the helium tube, while the arc current passed through the electromagnetic deflecting coils. The electrostatic and electromagnetic deflections were at right angles, so that the figure on the screen of the Braun tube was a graph in rectangular co-ordinates of the impressed e.m.f. and the arc current. The deflecting coils were so adjusted that the thermionic current alone did not produce any observable deflection.

Figure 1 shows the kind of curve obtained with a 60-cycle e.m.f. in helium at a pressure of 2 mm. It is seen that at a certain voltage the arc strikes, and as the voltage increases the current increases also. When the voltage decreases the current decreases at the same time, but continues with considerable magnitude until the voltage reaches a value of about 4 volts, when the current ceases to flow. Careful observation showed a sudden drop to zero at this lower voltage. This continuation of the arc to very low potentials may be attributed to the persistence of a metastable form of helium in which an arc may be maintained down to about 4 volts. Two other breaks in the down curve may be observed just below the striking potential of the helium itself. These breaks will be referred to later.

This type of curve was observed with 60 cycles at pressures down to 0.06 mm. Down to 1 mm pressure the striking potential was about 28 volts, and at the dying-out potential of about 4 volts a very decided drop of the arc current to zero was observed. As the pressure was decreased below 1 mm the striking potential increased and the dying-out potential became less certain, i.e., the drop to zero current was not so sudden as at higher pressures. At 0.06 mm the striking potential had increased to about 40 volts and the dying-out potential to about 20 volts. Figure 2 shows the type of curve obtained at 0.06 mm pressure. At all these pressures the filament temperature was approximately constant. The mean arc current varied from 25 milliamperes at 2 mm pressure to 10 milliamperes at 0.06 mm pressure.

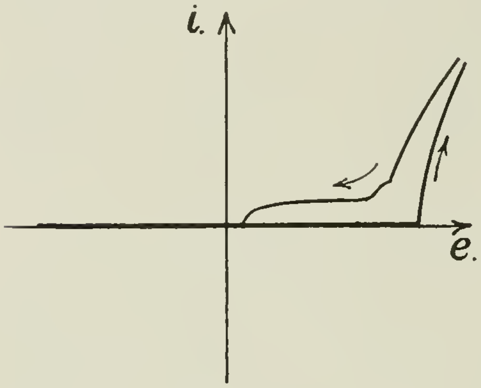

Fig. 1

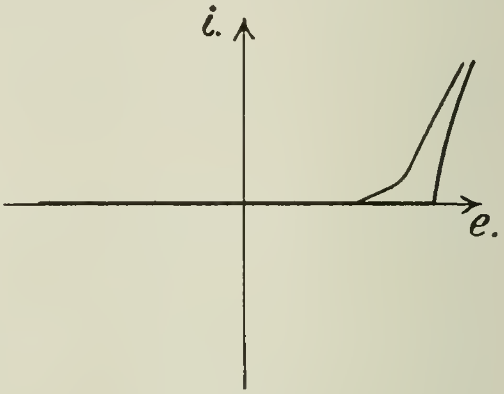

Fig. 2

If any impurities are present one would expect their effect to be more marked at lower pressures. Franck and Knipping have assumed that metastable helium will not return to normal helium except in the presence of impurities, so that with larger amounts of impurities we might expect the metastable helium to be destroyed in a shorter time. This is probably the interpretation of the gradual dying out of the arc before the voltage had dropped to 4 volts, as was observed when the pressure was very low. Experiments were made directly with the method discussed in the next section to see if the life was affected by impurities obtained by removing the liquid air from the charcoal for a short time till the helium had become very impure. The experiments indicated that while the impurities suppressed the amount of the metastable helium, the part remaining had the same life as that formed in the pure helium. The increase in the striking potential as the pressure was reduced is more difficult to interpret and is probably connected with the mechanism of the arc formation.

ARCS WITH HIGH-FREQUENCY VOLTAGES

With a sufficiently high frequency the e.m.f. should pass from +4 volts to its negative maximum and back to +4 volts before the metastable helium has disappeared, and upon reaching 4 volts the arc should strike, due to the ionization of the metastable helium still present.

Accordingly various frequencies from 60 to 10,000 cycles were impressed on the arc. An audion oscillator was used as a source for these frequencies. The author wishes to acknowledge his indebtedness to Dr. J. P. Minton and Mr. V. O. Knudsen for the use of their oscillators in this work. The alternating e.m.f. impressed on the arc was obtained from the secondary of an iron core transformer having its primary winding in the plate circuit of the oscillator.

Figure 3 shows the type of figure observed above 220 cycles per second at 2 mm pressure. The arc struck at about 4 volts, and the current rapidly attained a saturation value at which the arc current continued until the voltage had reached about 25 volts, when a second sudden increase was obtained. The decreasing part of the curve was above the increasing part but fell to zero at the lower striking voltage.

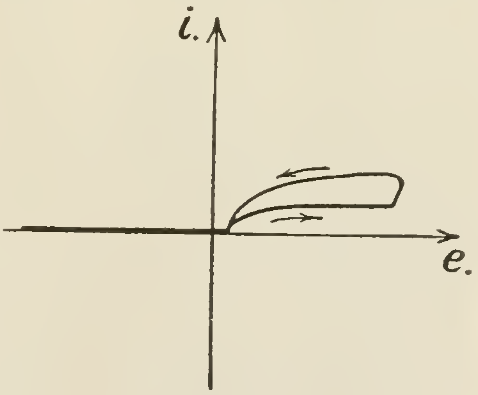

FIG. 3

With 200 cycles no appreciable arc formation at the lower voltage could be observed, indicating that the metastable helium practically disappeared in less than approximately $\frac{1}{400}$ of a second. The striking of the arc at about 4 volts with 220 cycles indicates that enough of the metastable helium was left after approximately $\frac{1}{440}$ of a second to give an observable indication of ionization.

All the figures above 220 cycles were similar, except that as the frequency was increased the striking at about 4 volts became more and more marked.

In using the oscillator as a source of alternating e.m.f. smooth curves were not always obtained. As the mean arc current was increased, by raising the electron emission, certain parts of the curve became wavy. This was particularly noticeable on the striking of the arc at about 25 volts. Instead of the arc current increasing as in Figure 1, it increased in a wavy form, indicating that the impressed voltage rose and fell during this striking period. This is provisionally attributed to self-induction in parts of the circuit or to the presence of iron in the oscillating circuit.

ARCS WITH INTERMITTENT CONSTANT VOLTAGES

In another series of experiments intermittent constant voltages from a battery were impressed between the hot cathode, *C*, and the anode, *A* (see Fig. 4). When the mercury interrupter, *H*, was open the voltage impressed on the electrodes was about 35 volts, and when the interrupter shorted the section *BD*, the voltage dropped to a value dependent upon the position of the slider *B*. In this way it was possible to impress a voltage of about 35 volts and suddenly change this voltage to a lower value. The arc current was passed through the deflecting coils, *M*, of the Braun tube. The spot was examined directly and also with a rotating mirror. Since it was rather difficult to observe the spot in the rotating mirror the following arrangement was also used. A uniform time deflection was obtained by connecting the deflecting plates to a potentiometer with a rotating contact, which was mounted on the shaft of the mercury interrupter. The electrostatic deflection was therefore proportional to the time and the

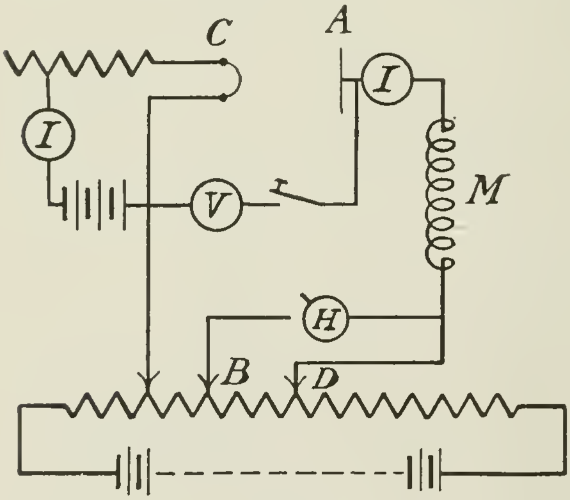

Fig. 4

magnetic deflection proportional to the current through the arc. These two deflections were at right angles. Furthermore, since the rotating contact was mounted on the interrupter shaft, the figure produced was stationary and could be carefully examined as the slider *B* was moved.

With the lower voltage below 3.5 volts and without the time deflection two spots appeared on the Braun tube screen, the upper one corresponding to the current for 35-volt excitation and the lower one for zero current. Using the time deflection, it was seen that the arc was extinguished in a time too short to be so observed, as shown at the right of Figure 5. Only a very faint vertical line appeared, since the spot moved very rapidly from the upper to the lower positions.

As the lower voltage was increased to 3.5 volts the lower line suddenly became curved as shown in Figure 6, indicating a gradual decrease of the current to zero value. This sudden curving of the lower line at 3.5 volts may be attributed to the presence of metastable helium produced during the 35-volt excitation. That is, the voltage dropped from 35 volts to 3.5 volts in a time short compared with the life of the metastable helium, and the arc was maintained by 3.5 volts as long as the metastable helium was present.

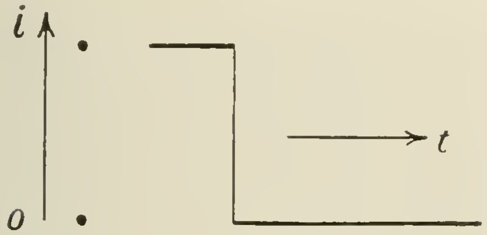

FIG. 5

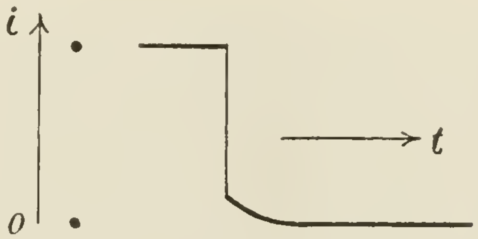

FIG. 6

The dying out of the arc continued to have the same appearance until the lower voltage had been increased to 22.6 volts, when a third spot appeared slightly above that for zero current as in Figure 7. Using the time deflection, it was seen that the arc was maintained for a brief time with this voltage before dying out.

A slight further increase of the lower voltage to 23.6 volts brought out still another spot, as in Figure 8, and the time deflection showed a dying out of the current in two stages as shown. The voltages for these two breaks in the decrease correspond to the voltages for the two breaks observed in the down curve of the alternating e.m.f. figure already described. This decrease in two stages may be connected with the fact of the existence of two radiating potentials of helium 0.8 volts apart corresponding to the first coplanor orbit (helium) and the first crossed orbit (parhelium) on Franck and Knipping's interpretation.

With a slightly increased lower voltage of 24.2 volts the arc was maintained. The two lower spots of Figure 8 disappeared, and the arc current jumped between the two values indicated by the two upper spots.

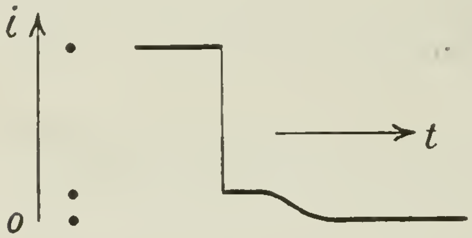

FIG. 7

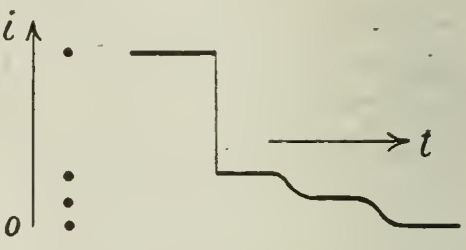

FIG. 8

These phenomena were qualitatively the same at pressures ranging from 2 mm down to 0.06 mm. The above exact determinations were all made visually with the Braun tube oscillograph, but for the purpose of illustration photographs made with the electromagnetic oscillograph show qualitatively the same phenomena, although with less sharpness in the details. Plate VI shows the various changes which occur as the lower voltage is increased from zero to 24.2 volts. These oscillograms were obtained by passing the arc current through an element of the electromagnetic oscillograph and photographing the curve while the mercury interrupter was operating. In *a* the lower voltage was below 3.5 volts, and it is seen that the arc current drops to zero in a very short time. The curving of the lower current line when the lower voltage reaches 3.5 volts is shown in *b*. The brief maintenance of the arc at a lower voltage of 22.6 volts is shown in *c*, and the decrease in two stages at a lower voltage of 23.6 is shown in *d*. The maintenance of the arc at 24.2 volts is shown in *e*.

A number of readings were taken of these voltages, and then the cathode current was reversed in order to eliminate the drop in voltage along the cathode, and another set of readings taken. The

PLATE VI

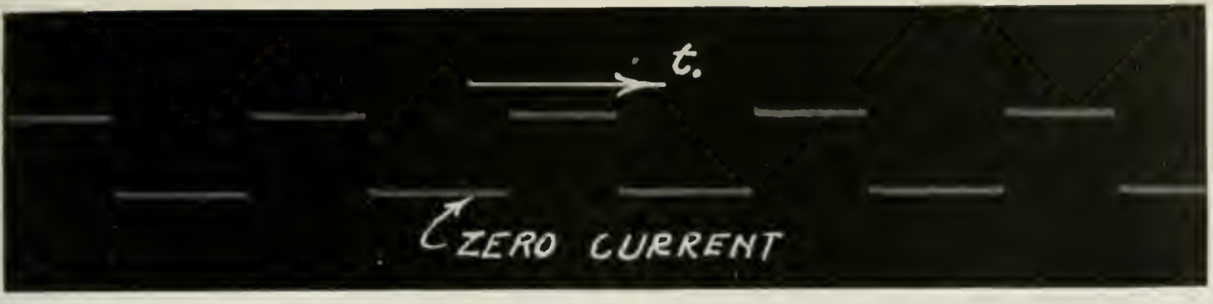

a

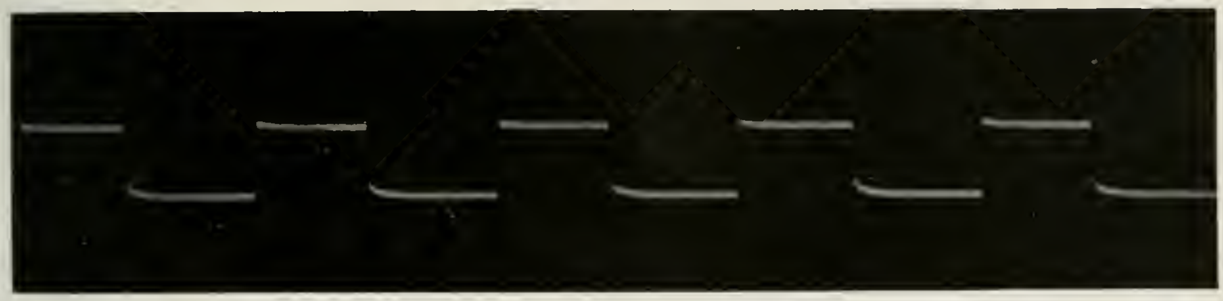

b

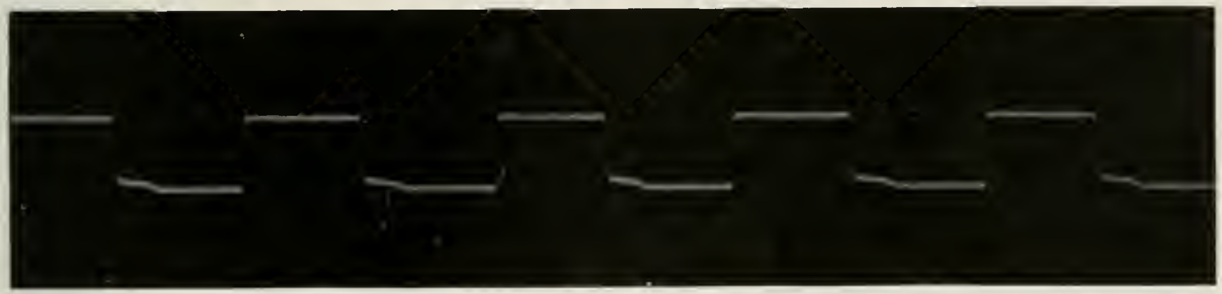

c

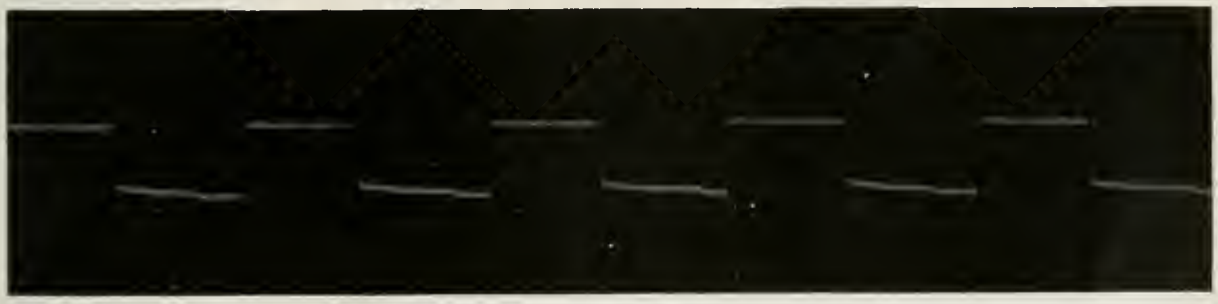

d

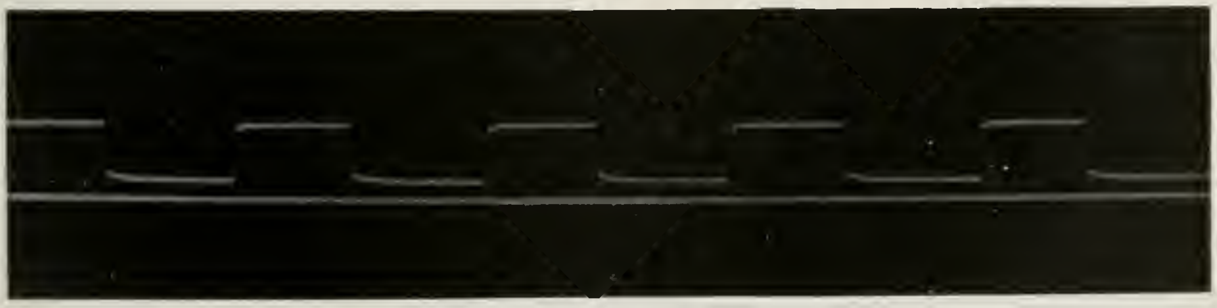

e

above values are the mean of all these values and thus are the potentials correct to approximately 0.1 volt between the anode and the center of the cathode. Corrections are necessary to allow for the initial velocity of emission of the electrons, the contact difference of potential, and the fact that some of the electrons are emitted from a more negative part of the filament than the center. As the drop of potential from the center to one end was 0.9 volt, this last correction may amount to about 0.4 volt. The other two corrections may easily amount to one volt or more according to a recent theory of K. T. Compton[1] in explanation of the results obtained by Hebb[2] on the arcing voltage in mercury vapor. It is thus permissible to apply a correction of 1.1 volts to the observed values given to make the upper voltage required to maintain the arc, 24.2, agree with the observed value of the ionization potential in helium, viz., 25.3 volts. This correction applied to the lowest potential observed for striking or maintaining the arc, 3.5 volts, gives a value of 4.6 volts in agreement within experimental error, with the theoretical ionization potential for metastable helium. Or, avoiding the question of corrections entirely, we may say that the difference between the two voltages observed, the lowest potential required to maintain an arc in helium with low electron density, and the minimum potential to maintain an arc in metastable helium is $24.2-3.5=20.7$ volts, and this value is within experimental error the minimum potential required to produce the metastable form of helium.

The author wishes to express his thanks to Professor H. G. Gale for his kind encouragement and advice during the progress of this work, and to Professor A. J. Dempster, who proposed the investigation of this particular phase of helium arcs, and without whose suggestions and assistance this work would not have been possible.

RYERSON PHYSICAL LABORATORY
April 1922

---

[1] American Physical Society Meeting, Washington, April 22, 1922.

[2] *Physical Review*, 16, 375, 1920.

NOTES ON IONIZATION IN THE SOLAR ATMOSPHERE[1]

By HENRY NORRIS RUSSELL[2]

ABSTRACT

Ionization in the solar atmosphere.—The absorption of photospheric radiation by atoms in the sun's atmosphere tends to increase the degree of ionization, both directly, by shifting an electron into a position from which its removal is easier, and indirectly, when enhanced lines are absorbed, by getting the ionized atoms into states in which they are probably less likely to combine with electrons. Both these influences operate strongly in the case of barium and weakly, if at all, for sodium. This probably explains why barium is much more highly ionized in the sun than sodium, although their ionization potentials are the same. The case of lithium, which is also ionized to an abnormally high degree, cannot be explained in this way. The greater width of the lines, due to the thermal agitation of so light an atom, may help to solve the problem.

Barium.—The lines of this element which are present, or doubtful, in the solar spectrum are tabulated. All the strong lines arise from the ionized atom. A few faint lines of the neutral atom are probably present.

Rubidium.—Three enhanced lines of this metal are present, though faint, in the normal solar spectrum.

Manganese.—The ionization potential 7.6 volts agrees well with the value predicted from the behavior of its lines in the solar spectrum.

The following remarks may be regarded as extensions of the writer's recent paper, "The Theory of Ionization and the Sun-Spot Spectrum."[3] The ideas on which they are based grew largely out of conversations between the writer and Professors K. T. Compton, of Princeton, and F. A. Saunders, of Harvard, to both of whom he desires to acknowledge his indebtedness.

1. *Barium.*—The spectroscopic behavior of this element indicates that it is ionized to a much higher degree in the solar atmosphere, and even in the spots, than would be expected from its ionization potential, which is substantially identical with that of sodium.

The statement in the previous paper, that none of the lines of the neutral barium atom appear in the solar spectrum, is incorrect, for the second line of the principal series at λ 3071 is faintly present, although the first (at λ 5535) is absent or excessively faint, and

---

[1] *Contributions from the Mount Wilson Observatory*, No. 236.

[2] Research Associate of the Mount Wilson Observatory.

[3] *Mt. Wilson Contr.*, No. 225; *Astrophysical Journal*, 55, 119, 1922.

King[1] records that a number of lines belonging to the fundamental series of triplets,[2] which are very diffuse in the arc, but sharp in the vacuum furnace, are present in the sun, though very faint. Table I gives a list of all those barium lines which can be identified with tolerable certainty in the solar spectrum. The first three columns

TABLE I

LINES OF BARIUM IN THE SOLAR SPECTRUM

ARC SPECTRUM (KING)			SOLAR SPECTRUM (ROWLAND)				
I. A.	Int.	Class	λ	Origin	Int.	Δλ	Notes
3071.592.......	100 R	III	1.662	Ba	00	−0.044	(1)
3891.788.......	50	V	1.918	....	0	− .012	(2)
3995.633.......	30	III	5.769	Ba?	000	− .010	(3)
4130.683.......	80	V	0.804	Ba	2	− .036	(2)
4166.027.......	20	V	6.161	Ba	0	− .018	(2)
4524.946.......	35	V	5.110	....	0	− .004	(4)
4554.038.......	1000 R	II	4.211	Ba	8	+ .003	(5)
4636.333.......	15 N	IV	6.501	....	0	− .007	....
4934.099.......	700 R	II	4.214 4.277	Ba	3 4	− .027	(5)
5267.013.......	20	IV?	7.203	....	000	+ .005	....
5853.699.......	200	III	3.902	Ba?	5	− .009	....
6141.760.......	600 R	III	1.938	Fe, Ba	7	− .032	....
6496.902.......	600 R	III	7.128	Fe	4	+0.013	(6)
	Doubtful Lines						
3993.395.......	80	II	3.616	Ba?	00 N	+0.065	(3)
4132.444.......	20	I	2.560	Ba?	0	− .041	....
4283.111.......	100	II	3.414	Ba?	00 N	+ .141	....
4350.375.......	80	II	0.550	Ba?	00 N	+ .012	....
4505.936.......	40	II	6.259	Ba?	00 N	+ .156	....
4573.881.......	40	II	3.960	Ba?	000	− .091	....
4899.970.......	35	IV?	0.095	Ti, La	2	(− .055)	(4) (7)
6019.505.......	100	II	9.596	Ba?	000	− .127	....
6110.808.......	300 R	II	1.005	....	0000	+ .064	....
6595.351.......	125	I	5.590	....	0000	+0.010	....

NOTES

1. Second member of the principal series of neutral atom 1s–3p.
2. Second member of diffuse series of enhanced lines 2P–4D.
3. Part of first member of fundamental series of neutral atom 3d–4f.
4. First pair of sharp series of enhanced lines 2P–3S.
5. First pair of principal series of enhanced lines 1S–2P.
6. Rowland gives this as an iron line: but the line in question is at 6496.462 (I.A.) according to Burns. The solar line is probably due to barium.
7. The barium line, if present, is masked.

---

[1] *Mt. Wilson Contr.*, No. 150; *Astrophysical Journal*, 48, 13–34, 1918.

[2] Saunders, *Astrophysical Journal*, **51**, 25, 1920.

give the wave-length in I.A. from the measures of King or Schmitz, the intensity in the arc, and the temperature class; the next three, Rowland's wave-length, origin, and intensity; and the next, the difference Δλ between Rowland's wave-length and the laboratory value after the application of St. John's value of the systematic correction.

All the high-temperature lines of King's classes IV and V, which are of intensity greater than 20 in the arc, appear in the solar spectrum, while numerous very strong low-temperature lines of classes I and II and intensities from 200 to 1000, are entirely absent. Most of the lines which are certainly present are well-known enhanced lines. The strong lines at 5853, 6141, and 6496 constitute, according to Saunders,[1] the first member of the diffuse series of enhanced lines, and are analogous to λλ 8662, 8542, 8498 of calcium, but reversed in order of wave-length. They are unaffected in the spot spectrum. The enhanced lines of the sharp series appear to be faintly present, and not absent, as stated earlier.

It appears, therefore, that neutral atoms of barium are probably present in the solar atmosphere, in a proportion which, though very small, is not insensible, as was stated in the preceding paper. The conclusion that barium is very highly ionized in the reversing layer, and even in spots, is confirmed by the re-examination of the data.

The conspicuous difference between its behavior and that of sodium remains to be explained. The solution of the puzzle probably lies in the fact that two ionizing agencies are certainly at work in the solar atmosphere—the temperature of the medium, and the radiation poured through it from the hotter photosphere below. Only the first is taken into consideration in the equations of Nernst and the theory of Saha, and, if it alone were active, there would be very strong reason to expect that the percentage of ionized atoms would be the same for the two elements. It is easy to see, however, that the second must create a difference of the sort which is observed.

Consider a barium atom which has just become ionized. Its first (or most easily removable) outer electron is lost; the second will be in the normal state of least energy content, denoted by 1S. In this condition it will immediately recombine with an electron which meets it under suitable conditions. But, if photospheric radiation ($\lambda\lambda$ 4934, 4554) falls upon it, it will absorb energy and the second electron will be lifted into one of the pair of positions 2P. If, after this, the charged atom meets a free electron, it is not so certain what will happen. It may be that it cannot recombine at all unless the second electron is in the normal position. If it can do so, the energy corresponding to the shifting of the second electron and the binding of the first one would have to be radiated. If this was done in a single quantum, the frequency would correspond to a "combination" between terms of the series of ordinary and enhanced lines, and such combinations have never been observed. Leaving aside the more delicate question whether the atom could emit two quanta at once from different electrons, it appears probable in any event that the $Ba+$ atom with its second electron in the 2P state would be *less likely* to recombine than one in the 1S state. Moreover, it will be decidedly easier to ionize a second time, for the energy required to remove the second electron is less (7.15 volts instead of 9.86, after absorption of λ 4554). There is also the probability to be considered that the absorption of a second quantum of radiation may raise the second electron to the state 3D, to which the considerations just urged will apply with even greater force.

---

[1] Unpublished.

The absorption of photospheric radiation by the ionized atoms of barium must therefore discourage recombination and encourage further ionization. Similar absorption by the neutral atoms will assist their ionization, so that, on the whole, the radiation must have a powerful ionizing influence.

For sodium, this influence must be very much smaller, and that for two reasons. In the first place, the enhanced lines of sodium, or at least the fundamental ones, lie in the extreme ultra-violet, beyond λ 377,[1] where the radiation of the photosphere is probably insensible, so that the sodium atom, once ionized, is not further disturbed by sunlight. Secondly, the principal lines of the neutral atom (the D lines) are very strong in the solar spectrum, with wings which indicate that they are absorbed to a great depth. Sodium atoms in the outer parts of the solar atmosphere are therefore exposed to a much enfeebled radiation of just those wavelengths which would be effective in aiding ionization.

---

[1] Millikan, *Proceedings of the National Academy of Sciences*, 7, 290, 1921.

For the corresponding lines of barium, on the contrary, the absorption is exceedingly small, and neutral atoms in the upper atmosphere are exposed to the full influence of the radiation.

When all these factors are considered, it is no longer surprising that barium is more highly ionized than sodium, in spite of the equality of their ionization potentials.

Whether the influence of radiation is competent to produce as great an effect as that which is observed can be determined only when a quantitative theory of its action has been developed. It may be noticed, however, that the 3D–2P lines of $Ba+$ are almost as strong in the solar spectrum as the pair 1S–2P, which indicates that a large fraction of all the singly ionized barium atoms in the reversing layer are in the states of "abnormally" large energy content.

The principle here sketched is evidently generally applicable. An element which has strong enhanced lines in the region where the continuous spectrum of the sun (or, for that matter, of any star) is strong, will behave as if it was relatively easier to ionize than one which does not possess such lines. The behavior of strontium, which resembles barium, but is less conspicuously "anomalous," is thus explained.

Most of the elements which are prominent in the solar spectrum possess such enhanced lines, with the exception of the alkali metals. The spectroscopic method suggested in the former paper should, therefore, give relatively high values for the ionization potentials of these metals, while it is probable that the errors for the other elements will be smaller. The alkaline earths, whose enhanced lines are very favorably situated, will probably come out with ionization potentials too low.

2. *Manganese*.—Saha[1] quotes the value 7.6 volts for the ionization potential, derived from unpublished studies by Catalan upon the series in its spectrum. This agrees satisfactorily with the spectroscopic evidence which puts its ionization potential rather more than halfway from *Ca* (6.1) to *Zn* (9.4).

---

[1] *Nature*, 107, 683, 1921.

3. *Rubidium.*—Saunders[1] notes that the strongest of the enhanced lines given by Kayser[2] appear to be present, though faint, in the solar spectrum—the wave-lengths on Rowland's scale being given in Table II.

TABLE II

Enhanced Lines of Rubidium

Spark (Exner and Haschek)		Sun (Rowland)	
λ	Int.	λ	Int.
3940.62	20	Absent	....
4104.49	10	4104.459	00
4244.50	30	4244.500	00
4294.08	10	4294.077	000

The evidence for the presence of this metal in the sun is therefore strengthened. The principal enhanced lines lie probably in the far ultra-violet.

None of the stronger enhanced lines of the other alkali metals, as given in Kayser's *Handbuch*, appear to be present in Rowland's tables.

4. *Lithium.*—The absence of lithium lines from the solar spectrum, and their faintness in spots, still presents much difficulty. Lithium behaves almost exactly like rubidium, though its ionization potential is 5.37 volts, and that of the latter 4.16.

We cannot invoke any absorption of enhanced lines here, for none have even been discovered.[3] Compton suggests[4] that one factor in the problem is the small atomic weight. This will cause the mean atomic velocity of temperature agitation to be greater than for other elements (about three and one-half times that for rubidium), and so broaden out all its lines, so that the atoms are able to take hold (so to speak) of a correspondingly greater range of wave-length in the photospheric radiation, and use it in assisting their ionization.

What other factors may enter remains for future discovery.

Mt. Wilson Observatory
February 22, 1922

---

[1] Not previously published.

[2] *Handbuch der Spectroskopie*, 6, 350.

[3] Millikan, *op. cit.*, p. 292.

[4] Unpublished.

NOTICE TO CONTRIBUTORS

There is occasionally published in the *Astrophysical Journal* a Standing Notice (for instance, on pages 179–80 of the number for September 1917). This is principally intended to guide contributors regarding the manuscript, illustrations, and reprints. This notice contains the following paragraph:

> Where unusual expense is involved in the publication of an article, on account of length, tabular matter, or illustrations, arrangements are made whereby the expense is shared by the author or by the institution which he represents, according to a uniform system.

The present sheet has been printed for amplifying further that paragraph.

The "uniform system" according to which "arrangements are made" is as follows: The cost of composition in excess of $50, and of stock, presswork, and binding of pages in excess of 40 pages, for any one article shall be paid by the author or by the institution which he represents at the current rates of the University of Chicago Press. When four articles from one institution or author have appeared in any one volume, on which the cost of composition has amounted to $50 each, or when the total cost of composition incurred by the *Astrophysical Journal* on articles for one institution has reached the sum of $200, the entire cost of the composition, stock, presswork, and binding of any additional articles appearing in that volume shall be paid by the author or by the institution which he represents.

As to illustrations, the arrangement cannot be quite as specific, but it may be generally assumed that not more than three half-tone inserts can be allowed without payment by the author. The cost of paper, presswork, and binding for each full-page insert is about $8.00, aside from the cost of the half-tone itself. In the matter of zinc etchings, considerable latitude has to be allowed, as in many cases diagrams take the place of more expensive tables. It may be assumed, however, that it will seldom be possible for the *Journal* to bear an expense of over $25 for diagrams and text illustrations in any one article.

Contributors should notice that since January, 1917, it has been impossible to supply any free reprints of articles.

Reprints of articles, with or without covers, will be supplied to authors at cost. No reprints can be furnished unless a request for them is received before the *Journal* goes to press.

Every article in the *Astrophysical Journal*, however short, is to be preceded by an abstract prepared by the author and submitted by him with the manuscript. The abstract is intended to serve as an aid to the reader by furnishing an index and brief summary or preliminary survey of the contents of the article; it should also be suitable for reprinting in an abstract journal so as to make a reabstracting of the article unnecessary. For details concerning the preparation of abstracts, see page 231 in the April, 1920, number of the *Journal*.

THE EDITORS

THE
ASTROPHYSICAL JOURNAL
AN INTERNATIONAL REVIEW OF SPECTROSCOPY
AND ASTRONOMICAL PHYSICS

VOLUME LV JUNE 1922 NUMBER 5

PARTIAL EXPLANATION, BY WAVE-LENGTHS, OF THE K-TERM IN THE B-TYPES

By SEBASTIAN ALBRECHT

ABSTRACT

K-term of the radial velocity of Class B stars.—Whether the K-term is due to an expanding universe, to causes within the stars or to the Einstein effect, it is of importance to determine *the part due to the use of inaccurate normal wave-lengths* in the reductions. For most of the lines upon which the B-type velocities are based, such as those of Si and He, sufficiently accurate wave-lengths are not available; but in the case of twenty O and N lines, new wave-lengths by Clark are found to be systematically 0.063 A longer than the adopted normals. A discussion of the available portions of the data on which the K-term is based, indicates that the new wave-lengths for this one group of lines alone would reduce the K-term, which is about 4 km, by about 0.3 km for the entire B class and by about 0.8 km for classes B0–B2.

Test of the relative accuracy of groups of wave-length normals.—Since the spectra of different classes of stars are radically different, it is *suggested* that a comparison of the mean wave-lengths for the lines which these classes have in common might give evidence as to the relative accuracy of the principal group of normals involved in each case. For instance the wave-lengths of types B0–B2 are based more on O, N, and Si lines than those of types B3–B5 and they are systematically 0.015 A shorter.

In 1911 Campbell[1] found that, after the radial component of the sun's motion in space had been deducted from the radial velocity of each star, the remaining portions of the radial velocities were not at random but in every part of the sky showed a systematic average residual directed away from the observer. This residual, which has become known as the K-term, appeared to be essentially the same for all limited areas of the sky, but to differ according to the spectral class of the star. Interpreted as a phenomenon of stellar motion, it means that the universe, represented by the stars employed by Campbell, is an expanding one, the rate of expansion depending upon the spectral class. Thus the stars of types B and M are systematically moving away in all directions from the position occupied at any instant by the solar system with a speed of about 4 km per second. The A and K types are moving outward with speeds of about 1 and 2 km per second respectively, while the F and G types show a K-term which is essentially zero.

---

[1] *Lick Observatory Bulletins*, 6, 107 and 127, 1911.

However, the K-term could be produced, as was also pointed out by Campbell, by the use of wave-lengths which are on the average too low. Thus if it could be assumed that the wave-lengths which were employed in the reductions for radial velocity for the B types were too small by about 0.06 A, then the entire K-term for these types would disappear. Campbell was inclined toward the view that such changes in the wave-lengths may be due to causes within the stars, such as high pressures, absorption through a wide range of depth in the stellar atmospheres and, with particular reference to helium, conditions in the stars such as to augment considerably the red components of lines which occur in close pairs. Freundlich[1] suggested that, due to the Einstein effect, all stellar lines are displaced toward the longer wave-lengths relatively to terrestrial comparison spectra. Such displacements, which would merge with displacements due to radial velocity and reappear in the K-term, would differ for stars of the different spectral classes due to mean differences in their masses. Although these factors must not be disregarded, nevertheless the laboratory values themselves require close scrutiny.

At about the same time that the K-term was found, attention was called by the writer to the unsatisfactory state of our knowledge in regard to the laboratory values of the wave-lengths upon which the radial velocities for the B-type depend.[2] This is especially true for the three prominent and important silicon lines λ 4552, λ 4567, and λ 4574, for which the two most accurate laboratory determinations differ by an average of 0.09 tenth meters, corresponding to a systematic difference of 6.0 km in the radial velocities derived from them. There has been only one response, I believe, in the ten years which have elapsed, to the appeal which was made for additional laboratory determinations. Mr. Clark,[1] under the direction of Professor Fowler, has redetermined the wave-lengths for the oxygen and nitrogen lines. The effect of the new wave-lengths upon the radial velocities and the K-term can be approximated.

---

[1] *Astronomische Nachrichten*, **202**, 17, 1915.

[2] *Publications of the Astronomical and Astrophysical Society of America*, **2**, 71, 1911.

TABLE I

λ Clark (Rowland System)	λ Normal (F. and A.)	λ Clark − λ Normal	Change in Radial Velocity	Element
		A	km	
4317.327	.272	+0.055	−3.8	O
19.814	.762	+ .052	−3.6	O
45.738	.677	+ .061	−4.2	O
48.246	.134	+ .112	−7.7	N
49.602	.541	+ .061	−4.2	O
51.443	.495	− .052	+3.6	O
67.074	.012	+ .062	−4.3	O
4415.057	.076	− .019	+1.3	O
17.143	.121	+ .022	−1.5	O
4447.205	.163	+ .042	−2.8	N, O
4591.158	.066	+ .092	−6.0	O
96.365	.291	+ .074	−4.8	O
4621.582	.548	+ .034	−2.2	N
30.729	.703	+ .026	−1.7	N
39.043	.937	+ .106	−6.9	O
42.006	.886	+ .120	−7.8	O
49.327	.250	+ .077	−5.0	O
51.032	.925	+ .107	−6.9	N, O
61.829	.728	+ .101	−6.5	O
4676.426	.291	+ .135	−8.7	O
Means (20 lines)		+0.063	−4.2	

Table I, which is self-explanatory, contains such of the oxygen and nitrogen lines as were included in the reductions for radial velocity. For the 20 lines listed the wave-lengths by Clark are on the average higher by 0.063 A, which corresponds to a change of −4.2 km in the radial velocities derived from them.

The details of the radial velocities from which Campbell derived the K-term have not been published, so that it is not possible to determine the exact part played by any particular group of lines in the reduction of his 225 B-type stars. However, this can be very roughly approximated with the aid of two partial sets of data for which such details are available, namely, the measures of 20 Orion-type stars by Frost and Adams[1] and the B-type stars contained in Volume IX of the *Publications of the Lick Observatory*. For these data the changes in the radial velocities produced by the substitution of the wave-lengths of Clark in place of the normal wave-lengths which were employed are summarized in Tables II and III. Tables IV and V show, for the smaller subdivisions of Class B, the relative representation of the different groups of lines in the measures. As far as can be judged from Tables II to VI the inference seems to follow that the new wave-lengths of Clark for oxygen and nitrogen will reduce the K-term for the entire Class B by about 0.3 km, and for B0–B2 by about 0.7 or 0.8 km.

---

[1] *Astrophysical Journal*, 40, 332, 1914.

TABLE II

CHANGES IN RADIAL VELOCITY PRODUCED BY WAVE-LENGTHS OF CLARK. MEASURES BY FROST AND ADAMS

Star	Type	Change for O and N Lines		Change for Star		Relative Representation of the O and N Lines in the Measures (in per cent)
		km	Plates	km	Plates	
ε Orionis	B0	−6.9	1	−0.1	7	22
ζ Orionis	B0	−1.5	3	−0.2	7	13
κ Orionis	B0	−1.4	7	−0.2	10	15
ζ Persei	B1	−2.5	7	−0.7	7	31
β Can. Maj.	B1	−2.2	5	−1.0	5	42
ε Can. Maj.	B1	−2.2	4	−0.7	4	33
γ Pegasi	B2	−0.4	12	−0.2	12	22
ζ Pegasi	B2	−0.5	3	−0.1	6	8
γ Orionis	B2	−2.9	6	−0.4	10	9
102 Herculis	B2	−0.1	2	0.0	5	6
ι Herculis	B3	+1.3	1	0.0	6	1
η Lyrae	B3	−1.5	1	0.0	6	2
ζ Draconis	B5	−1.5	2	−0.1	6	5
ε Delphini	B5	−0.1	2	0.0	4	8
β Orionis	B8p	−1.5	1	0.0	24	0

It does not seem unlikely that additional portions of the K-term may have their origin in the normal wave-lengths of other groups of lines. In this connection it may not be amiss to recall

---

[1] *Publications of the Yerkes Observatory*, 2, 143, 1904.

TABLE III

CHANGES IN RADIAL VELOCITY PRODUCED BY WAVE-LENGTHS OF CLARK MEASURES IN *Publications of Lick Observatory*, 9

Star	Type	Change for O and N Lines	Change for Star	Relative Representation of the O and N Lines in the Measures	Measured by
		km	km	Percentage	
τ Scorpii.	B0	−2.0	−0.9	44	A
		−2.0	−1.2	56	P
β Crucis.	B1	−1.7	−0.8	45	A
		−1.9	−1.0	53	P
α Pyxidis.	B2	−2.1	−1.0	46	A
α Lupi.	B2	−1.8	−1.1	60	A
		−1.9	−1.0	52	P
α Pavonis.	B3	−1.6	−0.3	15	A

A = S. Albrecht P = H. K. Palmer

TABLE IV

FROM MEASURES BY FROST AND ADAMS

Type	No. of Stars	Hγ	Mg	He	Si	O and N	Metals
		Percentage	Percentage	Percentage	Percentage	Percentage	Percentage
B0.	3	15	4	58	10	11	0
B1.	3	3	3	23	33	36	1
B2.	4	5	14	42	26	11	1
B3.	2	2	30	54	12	1	0
B5.	5	12	35	47	4	2	1
B8.	2	8	29	28	1	0	35
B0–B8.	19	8	19	43	14	11	5

TABLE V

FROM *Publications of the Lick Observatory*, 9

Type	No. of Stars	Hγ	Mg	He	O and N	C	Metals
B0.	1	5	6	16	50	5	18
B1.	1	15	5	32	33	10	5
B2.	6	33	4	39	13	9	3
B3.	9	30	14	42	1	12	1
B5.	2	0	32	68	0	0	0
B8.	2	64	14	14	0	6	*
B0–B9.	21	29	12	39	8	9	2

* A number of unidentified lines were not included in the percentages for B8.

that systematic differences between Lick and Bonn radial velocities[1] for types F–M, of the same order of magnitude as the K-term for these types, have been found to be due to differences in the normal wave-lengths which were employed in the reductions. The normal wave-lengths for the lines in Class B are perhaps not as accurately known as those for types F–M. I wish again to urge the desirability of additional laboratory study of the other groups of lines which occur in Class B stars, and especially those of silicon and helium. In view of the importance of the problem and the apparent difficulties with the laboratory spectra, a certain amount of duplication would not be wasted effort.

TABLE VI

DATA FROM WHICH THE K-TERM WAS DETERMINED

Type	No. of Stars	Part of Total Number (in per cent)	
B0	13	6	24
B1	17	7	
B2	25	11	
B3	72	32	56
B4	2	1	
B5	51	22	
B8	22	10	20
B9	21	10	
A0*	2	1	
B–A	225	100	

* Two of Campbell's stars seem to have been reclassified as A0 at Harvard.

If Tables IV and V may be regarded as approximately representative for the B types, they may also serve as a basis for a somewhat coarser grouping of the subdivisions of Class B for certain statistical purposes. B. Boss pointed out that the proper motions of stars of Classes B8–B9 more nearly resemble those of A type than those of early B type, and that therefore the B8–B9 stars should be grouped with early A types rather than with early B types. These results were confirmed by Campbell, and my Table IV is also in accord with this conclusion, the abruptly large representation of the metallic lines being the principal distinguishing characteristic. Additional subdivisions indicated are B0–B2 and B3–B5.. In the former silicon and oxygen are strongly represented in the measures and magnesium only slightly, while in the latter the reverse is true.

---

[1] *Astrophysical Journal*, 40, 475, 1914.

The low values of the normal wave-lengths for the oxygen and nitrogen lines contribute toward the progression in K which is indicated within the B types. Campbell's 225 stars are probably inadequate, under present limitations, for accurate solutions for subdivisions B0–B2, B3–B5, and B8–B9. Campbell (*op. cit.*, p. 123) finds K = +4.7 km per second for stars of Class B0–B5 and only +4.1 km for the entire class B0–B9. His Class B0–B5 comprises 80 per cent (see Table VI) and his Class B8–B9 only 20 per cent of his list. Campbell also finds K = +1.62 km for 222 stars of Classes B8–A9 and K = +0.95 km for 177 stars of Classes A0–A9 alone. On the basis of proportionality the former results would give approximately K = +2 km, while the latter results would give K = +4 km for classes B8–B9. Perhaps a K-term of about +3 km for B8–B9 will fairly well represent the actual facts for the data concerned. In view of the strong representation of the oxygen and nitrogen lines in B0–B2 and their practical absence in the measures of stars B3–B5, K is probably greater in the former than in the latter subdivisions.

The observed wave-lengths for the stellar lines are capable of contributing, so to speak, circumstantial evidence toward the relative correctness of the adopted normal wave-lengths for different groups of lines. A general discussion of this nature will be more worth while after the laboratory has contributed more nearly its full share toward this problem. For the present I shall be content with merely indicating how low values of the normal wave-lengths for the oxygen and nitrogen lines will impress a corresponding effect upon the observed stellar wave-lengths. The subdivisions B0–B2 and B3–B5 are suitable for this purpose, because the oxygen and nitrogen lines are strongly represented in the former and nearly absent in the latter. If the normal wave-lengths for the oxygen and nitrogen lines, constituting nearly 20 per cent of the lines actually employed in B0–B2, averaged 0.056 A too low, the radial velocities for these lines will average 3.7 km too high, making the mean radial velocities for the stars about 0.74 km too high. In the residuals of velocity the oxygen and nitrogen lines will show up as 2.96 km too high, and the remaining 80 per cent of the lines as 0.74 km too low. Thus the observed wave-lengths for the oxygen and nitrogen lines will be brought up four-fifths of the way toward where they should be, while the other 80 per cent of the lines will have their observed wave-lengths lowered from where they should be by an amount equal to one-fifth of the average error in the adopted normal wave-lengths for oxygen and nitrogen. Thus all the observed wave-lengths on the plates will finally be 0.011 A too low. Therefore, considering only the effects due to the oxygen and nitrogen lines, all the observed wave-lengths in classes B0–B2 should, on the average, be 0.011 A lower than in classes B3–B5. Table VII may be of interest in this connection, even though the wave-lengths given are not strictly definitive and the effects of errors in the normal wave-lengths of other groups of lines are also involved. The subscripts represent provisionally adopted weights, based partly upon the number of plates and partly upon the number of stars. Of the seventeen comparisons listed, fourteen give the wave-length smaller in B0–B2 than in B3–B5 and only two give it as larger. The mean difference in wave-length is 0.015 A, not all of which is necessarily due to the oxygen and nitrogen lines.

TABLE VII

OBSERVED WAVE-LENGTHS IN CLASSES B0–B2 AND B3–B5

LINE	NOR. MILLS λ 4500 CENTRAL		FROST AND ADAMS λ 4500 CENTRAL		SO. MILLS λ 4340 CENTRAL		β CAN. MAJ. λ 4500 CENTRAL
	B0–B2	B3–B5	B0–B2	B3–B5	B0–B2	B3–B5	B1
4267.3 C	....	....	....	....	0.260_{14}	0.278_{18}	....
4340.6 Hγ	0.618_{30}	$.643_{16}$	0.622_{30}	0.642_{16}	$.625_{15}$	$.632_{18}$	$.609_{29}$
4388.1 He	$.073_{43}$	$.109_{6}$	$.094_{37}$	$.099_{19}$	$.109_{15}$	$.109_{18}$	$.082_{33}$
4437.7 He	....	....	$.713_{26}$	$.726_{13}$	$.727_{12}$	$.725_{15}$	$.721_{22}$
4471.6 He	$.664_{46}$	$.685_{14}$	$.668_{39}$	$.689_{22}$	$.684_{15}$	$.707_{18}$	$.672_{34}$
4481.4 Mg	$.365_{42}$	$.375_{13}$	$.376_{33}$	$.397_{22}$	$.368_{15}$	$.376_{18}$	$.362_{34}$
4552.7 Si	$.752_{47}$	$.798_{8}$	$.769_{34}$	$.752_{8}$	....	....	$.753_{34}$

The results in Tables II–V are probably fairly representative for the dispersion of three prisms. For several reasons, among them the broad character of the spectrum lines in many B-type stars, a considerable number of the radial velocities are based on the lower dispersions of one and two prisms. The effects of systematic differences between results obtained with dispersions of one, two, and three prisms will also have to be evaluated. The details required for this purpose have not been published. However, unless my memory is in error on this point, the radial velocities obtained with the lower dispersions showed a systematic tendency toward larger positive values than those obtained with three prisms. Any uneliminated portions of such systematic differences will directly contribute toward the K-term.

This work is a portion of that accomplished under a grant of $200 from the American Association for the Advancement of Science.

Dudley Observatory
Albany, New York
January 1922

EFFECTIVE WAVE-LENGTHS OF 129 STARS WITHIN 0°5 OF THE NORTH POLE AND OF THE Σ COMPANION OF POLARIS[1]

By EJNAR HERTZSPRUNG

ABSTRACT

Effective wave-lengths, color indices, and magnitudes of 129 stars within 0°5 of the North Pole.—The results of measurements of about 500 images on 12 plates (Lumière Σ) taken in 1912 with the 60-inch reflector and a grating whose constant was 6 mm, are given in Table II. In determining the effective wave-length λ_{eff}, corrections were made (1) for diameters differing from the normal diameter 0.10 mm and (2) to reduce to zenith transmission. For each star the effective color index I_λ was obtained from λ_{eff} by use of the formula: $I_\lambda = 0.005(\lambda_{\mathrm{eff}} - 4216\ \mathrm{A}) = 19.721(\lambda_{\mathrm{eff}} - 1.069\ \mathrm{mm})$. The star, *Harvard Annals*, 48, No. 85, is probably wrongly included in the series of red stars of the North Polar Sequence. For the *Σ companion to Polaris*, I_λ was found equal to $+0.11 \pm 0.07$, which corresponds to a spectrum of type A0 to A5.

Relation between effective color-index and the color-index of Seares.—For 76 stars both I_λ and I_{MW} (the difference between photovisual and photographic magnitudes) were available for comparison. It was found that $I_\lambda = (0.90 \pm 0.05) I_{MW} - (0.10 \pm 0.05)$, a very satisfactory result.

Relation between photographic magnitude and diameter of image was found to be: $m = \mathrm{Const.} - 34d + 35d^2$, for d between 0.05 and 0.30 mm.

During my stay at Mount Wilson in 1912 the plates of the North Polar region listed in Table I were taken with the 60-inch reflector for the determination of effective wave-lengths.[2] Lumière Σ plates were used. The focal length of the instrument is 7606 mm and the grating constant was exactly 6 mm.

The co-ordinates of the center of the field are given in the system of *Harvard Annals*, **48**, 21, Table VI, sixteenth and seventeenth columns. The efficiency of each plate is indicated by the photographic magnitude of stars whose central image has a diameter of one-tenth of a millimeter. The total number of images measured is somewhat greater than that used in the present note because some stars showing only very faint images were finally rejected. The effective wave-lengths of hazy images were given half-weight. The mean weight-factor of a plate, which is given in the last column of Table I, may therefore be taken as a measure of the mean quality of the images. The quality 0.50 thus means that all images of the plate were given half-weight.

---

[1] *Contributions from the Mount Wilson Observatory*, No. 231.

[2] Compare *Mt. Wilson Contr.*, Nos. 100, 101; *Astrophysical Journal*, **42**, 92, 111, 1915.

TABLE I

PHOTOGRAPHS OF THE NORTH POLE

Plate No.	Date 1912	Aperture (inches)	Sidereal Time at Middle of Exposure	Exposure Time (min.)	Co-ordinates of Center of Field		Efficiency of Plate	Number of Images Measured	Quality of Images
					x	y			
4.....	July 19	60	$20^{h}\ 5^{m}$	60	$-480''$	$+70''$	$14^{m}8$	32	0.64
5.....	....	40	22 23	95	-520	$+30$	14.6	108	.70
6.....	....	40	23 26	9.5	-510	$+50$	12.0	15	.83
10.....	July 20	40	21 1	9.5 3	-180 -350	$+50$	11.9 10.9	29	.83
11.....	....	40	22 36	95	-190	$+50$	14.6	112	.69
14.....	July 21	40	18 16	31.3	$+10$	$+140$	13.3	44	.50
15.....	....	40	19 15	30	-40	$+90$	13.7	34	.56
16.....	....	40	19 53	10.5 1, 0.3	$-60, +20$ $+120, +190$	$+60$	12.7, 11.7 10.7, 9.7	27	.52
17.....	....	60	21 48	60	-200	$+30$	14.9	23	.50
204.....	September 14	40	21 7	6	-120	-10	11.6	14	.79
205.....	....	40	21 43	60	-80	-50	13.8	44	.56
206.....	....	40	22 29	19	-60	-70	12.7	29	0.83

The diameter of the field measured was 1150″ when the full aperture was used, and 2500″ when the mirror was diaphragmed down to 40 inches. The plates were measured and reduced at Potsdam. At the same time a series of plates of the Pleiades has been discussed, which afford 9972 effective wave-lengths. This last material has been used for a more thorough determination of the variation of the effective wave-length with the intensity of the image. The effective wave-lengths were measured in millimeters by moving the plateholder with a micrometer screw and reading to $\frac{1}{2}\ \mu$. The diameter of the central image of the star was taken as a measure of the intensity of the spectra of first order. As normal strength that shown when the diameter of the central image is 0.1 mm or 100 μ was chosen. For other diameters of the central image the following corrections to the normal diameter were found:

Diameter of central image $d=$	0.05	0.06	0.07	0.08	0.09	0.10 mm	0.11	0.12	0.13	0.14	0.15	0.16	0.17	0.18	0.19–0.24 mm
Correction to $d=0.10$ mm	$+13$	$+10$	$+7$	$+4$	$+2$	$+0\ \mu$	-2	-3	-4	-5	-6	-6	-7	-7	-7μ

No conspicuous difference in the corrections for stars of different effective wave-lengths was noted.

These corrections were also used in reducing the effective wave-lengths given in the present note. The correction required to reduce the effective wave-lengths to the zenith owing to selective extinction of light in the earth's atmosphere amounts to -23 A or $-6\ \mu$ for the North Polar region as seen from Mount Wilson.

To convert the effective wave-lengths expressed in millimeters into Angstrom units they must be multiplied by 3944.2. It will be more convenient for comparison with determinations of the difference between photographic and visual magnitudes, however, to transform the effective wave-length measured in mm directly into the equivalent values of color index.

I have found that a difference of 1^{M} in the color index in the system of I_H of the Göttingen Actinometry, Part B, corresponds nearly to a difference of 200 A in the effective wave-length. By adopting this and comparing the color indices I_H of stars occurring in the Göttingen Actinometry with their effective wave-lengths on other plates taken with the 60-inch reflector it was found that $I_H=0$ corresponds to an effective wave-length of 1.069 mm or 4216 A. · Hence, indicating the color index calculated from the effective wave-length by I_λ, we have

$$I_\lambda = \tfrac{1}{200}(\lambda_{\text{eff}} - 4216\text{ A}) = 19.721(\lambda_{\text{eff}} - 1.069\text{ mm})$$

The accuracy of the effective wave-length varies with the intensity of the image. Different weights were therefore assigned to the effective wave-lengths, according to the diameter of the central image. These weights were decreased for images which were not of normal strength, because of the uncertainty of the reduction of the effective wave-length to $d=0.10$ mm, which may vary with the quality of the image. The following weights of I_λ were finally adopted for different values of the diameter d of the central image.

$d=$	0.05	0.06	0.07	0.08	0.09	0.10	0.11	0.12	0.13 mm
$1/\lambda_2(I_\lambda)=1/(\text{m.e.})^2$	2	4	8	18	28	38	48	56	58

$d=$	0.14	0.15	0.16	0.17	0.18	0.19	0.20	0.21	0.22	0.23	0.24 mm
$1/\lambda_2(I_\lambda)=1/(\text{m.e.})^2$	52	44	36	28	22	16	12	8	6	4	2

For example, for $d=0.19$ mm, the adopted weight is 16, corresponding to a mean error in the color index I_λ of $\pm\sqrt{1/16}=\pm 0.25$. As stated above, for bad (hazy) images these weights were divided by 2. In fact the North Polar plates here employed are perhaps the poorest I took at Mount Wilson.

The results are given in Table II. The first column contains the number of the star taken from the *Harvard Annals*, **48**, 21, Table VI, and the second, the number of the North Polar sequence. The third column gives the photographic magnitude as derived from my estimates of the diameter of the central image. These magnitudes, according to which the stars have been arranged in the table, are only approximate. No correction for distance from the center of the field has been applied. The scale of Seares[1] was taken as a standard. The following relation between magnitude and diameter d of the central image was found.

$d=$				0.04	0.05	0.06	0.07	0.08	0.09 mm
$m+$plate constant$=$				16.0	15.9	15.8	15.5	15.2	14.8
0.10	0.11	0.12	0.13	0.14	0.15	0.16	0.17	0.18	0.19 mm
14.6	14.3	14.0	13.8	13.6	13.3	13.1	12.9	12.7	12.5
0.20	0.21	0.22	0.23	0.24	0.25	0.26	0.27	0.28	0.29 mm
12.2	12.0	11.9	11.6	11.5	11.4	11.2	11.0	10.9	10.7

The fourth column contains the color index I_λ as derived from the effective wave-length, and the fifth column, its weight, i.e., the reciprocal square of the mean error. The sum of the weights of I_λ for all 129 stars is 10,281. The sixth column gives the number of images used, respectively, for the estimation of magnitude and for the determination of effective wage-length.

Of special interest is a comparison of I_λ with the color index of Seares[2], which is defined as the difference between the photographic and the photovisual magnitude

$$I_{MW}=m_{Pg}-m_{Pv}.$$

This comparison has been made in the following way. In Table II there are 77 stars for which both I_λ and I_{MW} have been deter-

---

[1] *Mount Wilson Contr.*, No. 97, Table IX; *Astrophysical Journal*, **41**, 206, 1915.

[2] *Loc. cit.*

TABLE II

COLORS OF THE NORTH POLAR STARS

No.		m_{Pg}	I_λ	$p(I_\lambda)$	n_m, n_λ
H.A. 48	N.P.S.				
420	10	9.48	+ .03	66	8,5
356		10.37	− .03	30	3,2
101	13	10.59	+ .21	173	7,6
386	14	10.89	+ .35	240	12,10
184	7*r*	11.03	+ .93	293	12,10
350		11.09	+ .22	252	13,11
195	8*r*	11.10	+ .83	24	2,2
227	5*s*	11.23	+ .90	300	14,12
197	15	11.26	+ .17	271	12,11
419		11.40	+ .40	44	3,3
309		11.44	+ .27	144	8,7
75	6*s*	11.46	+ .65	255	12,11
62		11.57	+ .70	71	3,3
408	16	11.63	+ .15	209	9,8
282	17	11.85	+ .61	76	4,4
430		12.13	+ .71	57	3,3
67	9*r*	12.2	+1.28	6	1,1
320	18	12.32	+ .21	183	12,10
85	10*r*	12.62	+ .30	174	9,9
225	7*s*	12.66	+ .39	206	14,11
268	19	12.75	+ .25	194	10,9
494		12.83	+ .66	107	6,5
57		12.93	+ .43	124	9,8
302	20	12.94	+ .23	179	10,9
362		13.05	+ .54	158	8,7
219	11*r*	13.20	+1.11	201	10,9
427		13.24	+ .96	91	7,5
262		13.4	+ .56	32	2,2
234	23	13.44	+ .35	190	8,8
479		13.44	+ .51	88	5,5
489		13.45	+ .14	98	4,4
451		13.48	+ .45	83	5.5
292	22	13.52	+ .44	144	6,6
174		13.54	+ .52	105	5,5
248	21	13.57	+ .79	144	6,6
389		13.70	+ .60	116	5,5
151		13.79	+1.01	194	7,7
103		13.8	+ .81	58	1,1
436		13.82	+ .39	59	4,4
172		13.84	+1.21	144	5,4

TABLE II—*Continued*

No.		m_{pg}	I_λ	$p(I_\lambda)$	n_m, n_λ
H.A. 48	N.P.S.				
426	....	13.90	+ .32	95	4,4
25	....	14.0	+1.00	56	1,1
34	....	14.0	+ .05	28	1,1
300	12*r*	14.00	+1.17	149	5,5
279	24	14.04	+ .36	116	5,5
345	....	14.08	+1.50	141	5,5
90	....	14.12	+1.23	129	5,4
127	....	14.13	+ .66	168	6,4
243	....	14.15	+ .32	52	2,2
378	....	14.15	+1.07	116	4,3
146	....	14.17	+ .55	108	3,3
28	....	14.3	+ .15	24	1,1
33	....	14.3	+ .89	24	1,1
329	....	14.3	+ .88	115	4,4
134	....	14.33	+ .41	141	6,6
263	25	14.35	+ .30	117	6,6
319	....	14.38	+ .62	26	4,2
424	....	14.4	+ .39	48	2,1
131	....	14.43	+ .72	62	3,2
281	....	14.45	+ .38	80	4,4
332	....	14.45	+ .56	76	4,3
403	....	14.45	+ .22	67	2,2
142	....	14.47	+ .57	86	3,2
152	....	14.48	+ .67	162	6,4
176	....	14.48	+ .36	140	6,5
230	....	14.53	+ .78	90	3,3
401	....	14.53	+ .96	67	3,2
256	....	14.55	+ .75	142	4,4
191	8*s*	14.56	+ .66	148	5,4
13	....	14.6	+1.12	19	1,1
14	....	14.6	+1.08	38	1,1
327	....	14.6	+ .68	76	2,2
437	....	14.6	+1.10	19	1,1
439	....	14.6	+ .88	38	1,1
459	....	14.6	+1.30	19	1,1
480	....	14.6	+ .63	19	1,1
391	....	14.64	+ .52	64	5,3
265	9*s*	14.68	+ .86	128	4,4
154	....	14.7	+ .18	33	2,2
288	26	14.73	+ .85	66	3,3
60	....	14.8	+ .83	28	1,1
86	....	14.8	+ .38	28	2,2
105	....	14.8	+ .58	66	3,3
107	....	14.8	+1.36	28	2,2
111	....	14.8	+ .49	42	2,2

TABLE II—*Continued*

No.		m_{Pg}	I_λ	$p(I_\lambda)$	n_m, n_λ
H.A. 48	N.P.S.				
125		14.8	+ .57	61	3,3
175		14.8	+ .31	42	2,2
333		14.8	+1.06	28	1,1
336		14.8	+1.05	28	2,2
338		14.8	+ .83	42	2,2
342		14.8	+ .19	28	2,2
348		14.8	− .41	14	1,1
226		14.85	+ .51	94	4,4
74		14.9	+ .90	28	2,2
324	27	14.97	+ .80	56	3,3
192		14.98	+ .37	56	4,4
88		15.0	+ .66	23	2,2
130		15.0	+ .65	51	3,3
140		15.0	+1.06	65	3,3
283		15.0	+1.28	23	2,2
311		15.0	+ .14	37	2,2
159		15.08	+ .43	65	4,4
158		15.12	+ .63	55	4,4
190	28	15.15	+ .75	50	4,4
334		15.15	+ .80	18	2,2
132		15.2	+1.25	18	1,1
306		15.2	+ .53	18	2,2
341		15.2	+ .91	27	2,2
323	10*s*	15.2	+ .56	36	3,3
196		15.30	+ .65	36	4,4
139		15.35	+1.72	13	2,2
193		15.35	− .04	17	2,2
277		15.35	+ .62	13	2,2
254	11*s*	15.38	+ .65	35	4,4
215		15.40	+1.50	44	4,4
126		15.43	+1.04	8	3,2
165		15.45	+ .43	13	2,2
163		15.5	+ .76	4	1,1
201		15.5	+ .19	11	2,2
205		15.5	+ .76	8	1,1
218		15.5	+1.12	12	2,2
358		15.5	+1.09	9	2,1
339	13*s*	15.6	+ .81	6	3,2
365	12*s*	15.65	+ .94	10	2,2
295		15.7	+ .28	4	2,1
164		15.90	+1.25	2	4,1
368		15.9	+1.28	2	1,1
212	29	15.95	+ .21	2	2,1
186		16.1	+ .57	2	1,1

mined. Of these the star 439, for which the photographic magnitude of Seares and consequently I_{MW} is uncertain, was omitted. Among the other 76 stars there are 40 for which the weight of I_λ is less than 90. These and the star 101 have been combined into means of 2 or more stars as follows: 420 and 101 (combined weight of I_λ 239); 195 and 282 (100), 319, 424, and 403 (141); 142 and 401 (153); 391 and 154 (97); 288 and 125 (127); 336, 338, and 342 (98); 324 and 130 (107); 283, 311, and 159 (125); 158 and 190 (105); 334, 341, 323, and 139 (94); 254, 215, 126, 163, 205, 218, 358, 339, 365, 295, 164, 368, 212, and 186 (148). Thus 35 single and 12 combined objects were available. These 47 objects are given in Table III, arranged according to the photographic magnitudes of Table II. The first column of Table III contains the mean of the photovisual and photographic magnitudes of Seares, m_m, which is independent of their difference I_{MW}. The material

TABLE III

m_m	I_{MW}	I_λ	I_λ O−C
10.08	+ .13	+ .16	+ 9
10.76	+ .44	+ .35	+ 2
10.42	+1.04	+ .93	+ 5
10.82	+ .37	+ .22	− 5
10.58	+1.03	+ .90	+ 3
11.06	+ .33	+ .17	− 6
11.06	+ .65	+ .65	+13
11.42	+ .39	+ .15	−13
11.42	+ .69	+ .66	+11
12.08	+ .38	+ .21	− 5
12.36	+ .51	+ .39	+ 2
12.48	+ .41	+ .25	− 3
12.76	+ .51	+ .23	−14
12.72	+ .82	+ .54	−11
12.64	+1.16	+1.11	+16
12.67	+1.20	+ .96	− 3
13.35	+ .50	+ .35	0
13.12	+ .63	+ .44	− 3
12.90	+ .85	+ .79	+12
13.20	+ .74	+ .60	+ 3
13.15	+1.14	+1.01	+ 8
13.04	+1.61	+1.21	−14
13.58	+ .50	+ .32	− 3
13.15	+1.38	+1.17	+ 3
13.63	+ .60	+ .36	− 7
12.90	+1.78	+1.50	0
13.83	+1.04	+ .66	−17
13.44	+1.40	+1.07	− 8
14.04	+ .96	+ .55	−20
13.83	+ .98	+ .88	+11
13.98	+ .89	+ .41	−28
13.84	+ .48	+ .30	− 3
14.09	+ .82	+ .35	−28
14.16	+ .80	+ .67	+ 6
14.12	+ .90	+ .74	+ 4
14.26	+ .81	+ .75	+14
14.14	+ .71	+ .66	+13
14.38	+ .72	+ .40	−13
14.30	+ .90	+ .86	+17
14.45	+ .84	+ .72	+ 8
14.38	+ .89	+ .71	+ 3
14.58	+ .70	+ .51	0
14.68	+ .81	+ .73	+12
14.68	+ .81	+ .50	−11
14.87	+ .62	+ .69	+26
14.74	+1.00	+ .87	+ 9
14.86	+1.21	+1.02	+ 6

of Table III was treated according to least squares with the following result:

$$I_\lambda - 0.632 = \underset{\pm 0.054}{0.895}(I_{MW} - 0.810) - \underset{\pm 0.014}{0.015}(m_m - 13.128) \quad \text{(m.e.)}$$

or written in another way

$$I_\lambda - 0.632 = 0.888(m_{Pg} - 13.533) - 0.902(m_{Pv} - 12.723).$$

The differences O−C between the observed and calculated values of I_λ are given in the last column of Table III. These differences do not show any distinct run, the number of changes in sign being 25, where we should expect 23±3.4 (m.e.). The linear formulae therefore represent the observations sufficiently well.

From the first of these formulae it is seen that there is no sensible magnitude equation between I_λ and I_{MW}, as the coefficient of m_m practically does not exceed its mean error. This result is perhaps the most satisfactory one of the present note. As described above, special care was taken to avoid a magnitude error in the values of I_λ. Although an error of this kind does not appear in the differences $m_{Pg} - m_{Pv}$ this does not prove that the scales for m_{Pg} and m_{Pv} are necessarily correct; but they must be parallel.

To say the least the values of I_λ do not indicate any such inequality between the two scales of Seares.

To $m_m = 13.128$ and $I_\lambda = 0$ corresponds $I_{MW} = +0.10 \pm 0.05$ (m.e.), although we have both intended to reduce our scale of color index to the same zero point. As the small disagreement found is only about twice its mean error its reality is not beyond question.

The mean square of the difference O−C in Table III is $0.0141 = (\pm 0.12)^2$. As this square is the sum of the squares of the mean errors of I_λ and I_{MW} the accuracy indicated is about what could be expected.

Considering the individual stars, it may be observed that the star 85, for which $I_\lambda = +0.30 \pm 0.08$ (m.e.), seems to be wrongly included with the *r* series (No. 10*r*), as it does not appear to be of deep color. My photographic magnitude 12.62 gives in connection with the photovisual magnitude 12.03 of Seares: $I_{MW} = +0.41$, corresponding to $I_\lambda = +0.29$, thus confirming the value found directly.

On September 14, 1912, a plate (No. 207) was taken with several exposures of the Pole star in order to determine the effective wave-length of its Σ companion 18″3 distant. From six images was found $I_\lambda = +0.11$ with weight 188, or a mean error of ±0.073. This value of I_λ corresponds to a spectrum of A0 to A5 of the Harvard classification. Recently F. C. Leonard (*Publ. Astr. Soc. of the Pacific*, **33**, 215, 1921) has found the spectrum of the companion to be of class F0.

Leiden
November 12, 1921

ELECTRIC FURNACE EXPERIMENTS INVOLVING IONIZATION PHENOMENA[1]

By ARTHUR S. KING

ABSTRACT

Furnace temperature required to obtain the subordinate series lines of the alkali metals in absorption.—With the central plug at about 2600°C, the stronger lines of both the first and second subordinate series of K, Cs, and Rb were readily obtained, while for Na, less than 2350° was required. The lines observed for each metal are listed. The temperature of the absorbing vapor may be taken as about 400° less than that of the plug.

Furnace absorption spectrum of iron vapor above 2800°C.—Using lower temperatures, no absorption lines had previously been obtained longer than λ 5507, but with a plug temperature above 3200°, practically all the high temperature emission lines were obtained in absorption, up to the end of the range photographed, λ 6700.

Furnace spectra of Ca, Sr, and Ba vapors mixed with more easily ionized elements, K and Cs.—*Flame lines* are not affected, but the *intensity of enhanced lines* was found to be decreased for both absorption and emission spectra, when the easily ionized vapor of K (4.3 volts) or of Cs (3.8 volts) was added, the effect being very marked for Ca (6.1 volts), somewhat less for Sr (reduction to one-third) and small for Ba (5.2 volts), while adding Na (5.2 volts) to Ba vapor produced no change. Evidently the *quenching effect* depends upon the relative ease of ionization of the two vapors. Temperatures of 1800–1830° were used.

Furnace temperatures required to obtain certain flame lines in absorption and in emission.—The lines λ 4227 (*calcium*), λ 4607 (*strontium*), and λ 5535 (*barium*) were obtained in absorption (tungsten lamp source) but not in emission (exposure 2 hours) at temperatures of 1275°, 1200°, and 1400°C respectively. This lag of emission over absorption may be partly due to the wideness of the lines, and is not noticeable for sharp *iron* lines.

Relation of furnace observations to Saha's theory of spectra.—The foregoing results verify Saha's predictions that the subordinate series of the alkalies could be obtained in absorption if sufficiently hot vapor were used, and that a gas too cool to emit light should still be able to absorb the lines of the principal series; and the results with mixed gases are such as would be expected if flame and enhanced lines are associated with neutral and ionized atoms respectively, as Saha assumes.

This paper gives the results of some experiments which bear on certain features of the theory recently advanced in a series of papers by M. N. Saha,[2] concerning the part which ionization may have in the production of certain types of spectral lines. The points tested are (1) the possibility of obtaining in absorption the lines of the subordinate series of the alkali metals, and in general, the conditions necessary for any type of lines to appear in absorption, (2) the effect, on lines presumed to be due to the ionized atom, of mixtures with elements having lower ionization potentials, and (3) whether, under given conditions of the metallic vapor, a line appears in absorption at a lower temperature than it can be obtained in emission.

---

[1] *Contributions from the Mount Wilson Observatory*, No. 233.

[2] *Philosophical Magazine*, **40**, 472, 809, 1920; **41**, 267, 1921; *Proceedings of the Royal Society*, A, **99**, 135, 1921

The tube-resistance furnace offers special possibilities for an investigation of this sort by reason of the close control of the temperature and pressure. Absorption spectra also are readily obtained, either by the use of a diaphragm within the tube or by passing white light through the tube from an external source.

The special means of excitation employed will be described under each heading. The furnace chamber was usually pumped out to about 8 mm of mercury. The spectrograms were all made with the bright first order of a 15-foot concave grating, giving a scale of 3.7 A per mm.

I. ABSORPTION SPECTRA OF SODIUM, POTASSIUM, CAESIUM, AND RUBIDIUM

In his discussion of absorption spectra,[1] Saha notes that for these elements only the lines of the principal series have been obtained in absorption, the experiments with sodium having been by Wood[2] and those with potassium, caesium, and rubidium by Bevan.[3] Saha's explanation of the failure of the subordinate series to appear is that the temperature of the absorbing vapor was not high enough. In view of the writer's recent study[4] of the production in absorption of lines belonging to various temperature classes, this explanation seemed reasonable. The subordinate series of lines certainly require, in emission spectra, a stronger excitation than the lines of the principal series, and they should appear in absorption when the temperature is high enough to furnish a fairly large number of atoms capable of emitting the subordinate series lines. However, it was worth while to test this in the specific case of the alkali metals.

Sodium.—A trial of the furnace with sodium, operated as usual to give emission spectra, yielded at 2250° C and without prolonged exposure the pair λλ 5683–88 of the first subordinate series, and two pairs, λλ 5149–54 and 6155–61 of the second subordinate series, in addition to the widely reversed D lines. This showed that the production of the required atomic orbits was well within the range of the furnace.

---

[1] *Philosophical Magazine*, **41**, 267, 1921.

[2] *Astrophysical Journal*, **29**, 97, 1909.

[3] *Proceedings of the Royal Society*, A, **83**, 421, 1910; **85**, 54, 1911.

[4] *Mt. Wilson Contr.*, No. 174; *Astrophysical Journal*, **51**, 13, 1920.

In order to obtain the absorption spectrum, a plug of graphite was placed near the middle of the furnace tube. The spectrograph was set to give, in addition to the pairs above mentioned, those at λλ 4979–83, 4748–52, 4665–68, the plate thus including three members each of the first and second subordinate series. A plug temperature of 2650°–2700° gave distinctly in absorption all six pairs. A temperature of 2350°, however, sufficed to show the three pairs of the first or diffuse series and the strongest pair of the second or sharp series at λλ 6155–61. The absence of the weaker sharp pairs was probably due to their extreme narrowness at low temperature in a vacuum source, so that the absorption lines were below the limit of photographic resolution. Aside from this feature, the sharp and diffuse series appeared in absorption with equal ease.

The temperature of the absorbing vapor was necessarily much below that of the plug, about 400° lower, according to the experiments previously reported,[1] which have since been confirmed so often that this value may be considered a constant of the special experimental arrangement employed. This means that near the end of the heated portion of the tube there is a layer of vapor sufficiently cooler than the plug to absorb radiation from the latter. The present experiments thus indicate that sodium vapor at 2000° C or higher, with a sufficiently hot background, will absorb the lines of the two subordinate series.

Potassium.—A trial with a plug temperature of 2700° gave in absorption the stronger lines of the subordinate series groups near λλ 5800 and 5340. These consist in each case of one pair belonging to the first and one to the second series.

Caesium.—The absorption spectrum with caesium chloride in the furnace was photographed from λ 5400 to λ 7000. All but the faintest of the arc lines in this region were obtained in absorption for a plug temperature of 2600°. The absorption spectrum showed nine lines of the first subordinate series and five weaker ones which Saunders,[1] by reason of the constant differences occurring among them, considers to belong to the second subordinate series. The two groups are as follows:

---

[1] *Loc. cit.*

I		II
5466	6011	5746
5503	6213	5839
5635	6724	6034
5664	6974	6355
5845		6587

Three lines, given by Saunders as λλ 5847.8, 6217.6, 6983.8, and classed by him as satellites of adjacent strong lines, are visible also in the absorption spectrum. In the arc the lines which presumably belong to the second series are very unsymmetrical toward the red, while the absorption furnace in vacuum gives for each of these a narrow line at the extreme violet side of the position of the arc line. Dissymmetries occurring among the lines of the first series are also eliminated by the furnace. When the furnace spectrum is more completely photographed, with proper standards, a revision of the wave-lengths can be made and the character of the second series definitely settled.

Rubidium.—For this element also, there was no difficulty in obtaining in absorption nearly all of the lines given by the arc. In the range λ 5100 to λ 6400, the following lines of the first and second subordinate series showed as absorption lines, only the fainter members of the second series being absent:

I		II
5151	5648	5654
5196	5724	6071
5260	6207	6160
5363	6299	
5432		

While not bearing so directly upon the ionization theory as the foregoing, a series of experiments with the iron spectrum in absorption may be mentioned. In the previous investigation,[2] when the furnace was heated in vacuum with the plug at about 2600° C, no iron lines were obtained in absorption to the red of λ 5507, an effect probably due, as was explained then, to the high-temperature character of the iron lines in the yellow and red. Later experiments have extended this limit. The furnace, operated at atmospheric pressure, had its tube thinned in the central region to permit very high temperatures of the plug and to give a strong gradient in the portion of the tube containing the iron vapor. Plug temperatures above 3200° C, the highest reading of the pyrometer employed, were thus obtained. The spectrum was photographed to λ 6700, and gave in absorption practically all of the lines shown in emission by the furnace at high temperature.

---

[1] *Astrophysical Journal*, 20, 188, 1904.

[2] *Loc. cit.*

The conclusion from these results is that a sufficiently high temperature of the absorbing vapor, and proportionately higher temperature of the incandescent background, give in absorption all lines which the furnace can emit, and experience has shown these to include probably all lines not requiring conditions similar to those of the spark discharge.

This condition, which is an obvious consequence of the difference in excitation required to produce different groups of lines in the same spectrum, is enunciated by Saha to the effect that in order to reverse a given set of lines, it is not sufficient to send a beam of white light through a cooler layer of the vapor, but that "in the atoms present, there should be a fairly large number with orbits corresponding to the first term of the pulse of radiation to be absorbed. Thus in order that lines (*2p–md*) may be absorbed (as those of the subordinate series of the alkalis), we must have a sufficient number of atoms with (*2p*) orbits."[1]

2. EFFECT OF MIXTURES OF ELEMENTS HAVING DIFFERENT IONIZATION POTENTIALS

In the writer's studies of electric furnace spectra, it has been noted repeatedly that a mixture of substances may be vaporized without any suppression of the spectrum of one by reason of the presence of the others. In contrast with the arc containing such a mixture, each vapor appears to give its spectrum as if it were alone.

---

[1] *Op. cit.*, p. 277

No evidence against this view has been found as regards the great majority of the lines emitted by the furnace. These lines, according to the modern view, are emitted by various electron orbits of the "normal atom," that is, an atom which is not ionized through the removal of one or more electrons. The furnace is capable, however, of emitting, in general rather faintly, some of the enhanced lines, which are regarded as due to the ionized atom. For these lines, the degree of ionization is a determining factor, and this may be affected by conditions other than the temperature and pressure which are controlled in the furnace.

The calcium spectrum contains various series emitted by the normal atom, and also the enhanced lines H and K arising from the ionized atom. Designating the normal atom by Ca and the ionized atom and its lost electron by Ca^+ and e, respectively, Saha[1] states, "At a given temperature and concentration, a definite equilibrium will be established between the proportions of Ca, Ca^+, and e, as represented by the van't Hoff formula of reversible chemical action, $Ca \rightarrow Ca^+ + e$."

If then we add a large supply of electrons from some substance which becomes ionized more readily than calcium, fewer electrons from the calcium can exist in the free state, and the proportion of Ca^+ atoms becomes less, with a corresponding weakening of the H and K lines, relative to the lines of the normal atom. Since the ionizing potential of an element may be taken as the measure of its ionization under a given stimulus, a mixture of calcium with an element having a lower ionization, such as potassium, caesium, or rubidium, should alter the calcium ionization to an appreciable extent. A fairly crucial test of the basic assumptions of Saha's theory should thus be possible, and Dr. H. N. Russell has suggested to the writer that the control of conditions in the electric furnace affords an excellent means of applying the test. The following experiments were accordingly carried out for the spectra of calcium, strontium, and barium.

Calcium.—A temperature of about 1800° C was selected, which gives the H and K lines distinctly, and yet with intensities low enough to register easily any disturbance in the vapor producing them. The first experiments were with absorption spectra, which permit short exposures, during which there would be little change in the vapor within the tube. Instead of using a plugged tube, white light from a strong tungsten projection lamp was sent through the tube of the vacuum furnace. As the filament of the lamp was many hundred degrees hotter than the furnace tube, it could safely be assumed that the vapor in the highly heated portion produced the absorption, instead of that near the end as was evidently the case when a plug was used. The first mixture tried was calcium and potassium, whose ionization potentials are 6.08 and 4.32 volts, respectively. The absorption spectrum was first photographed with metallic calcium alone in the tube. The furnace was then recharged with a mixture of calcium and potassium chloride, and a second exposure made under the same conditions as the first. The quenching effect on the H and K lines was very distinct. With calcium alone, H and K appeared as absorption lines of moderate strength, comparable with some of the lines in the group of six near λ 4300 and in the series triplet λλ 4425–55. When calcium and potassium were vaporized together, scarcely a trace of H and K was to be seen, while the comparison lines due to the normal atom were practically unchanged. The nearly equal width of the strong flame line λ 4227 in the two exposures indicated that the density of calcium vapor was nearly the same in both cases. The experiment was repeated, the tube being wiped out before charging with the calcium alone, but the potassium was not entirely removed, as was shown by the presence of the violet potassium pair. H and K were thus somewhat weakened in the first exposure, but much more affected in the second with a large supply of potassium.

---

[1] *Proceedings of the Royal Society*, A, **99**, 139, 1921.

The comparison was repeated with a new tube and metallic potassium, instead of the chloride, for the second exposure. This eliminated a band structure in the H and K region which may have had some effect in the previous experiment. H and K were again much weakened with reference to the other calcium lines, though the narrower potassium lines showed that the metal did not give as effective a mass of vapor in the tube as was obtained with the chloride.

Experiments with emission spectra were next made, first with potassium chloride and then with caesium chloride, which were compared with calcium alone. The exposures were much longer, with resulting variations in the supply of vapor during the runs, but the effects observed for absorption were repeated, H and K being distinctly reduced in intensity when a mixture was used. As was to be expected, the effect of caesium, with an ionization potential of 3.81, appeared greater than that of potassium, but the effective quantities of the two may have been different, and at present it is desired to lay stress only on the general effect of a substance with lower ionizing potential.

Strontium.—The experiments with strontium were made first for the absorption spectrum with the chloride in the tube, at a temperature of 1860° C, then with a mixture of strontium chloride and potassium chloride. The enhanced lines λλ 4078 and 4216 were compared with the flame line λ 4607 and a group of strong furnace lines from λ 4722 to λ 4876, presumably due to the normal atom. As with calcium, the enhanced lines showed a decided effect from the mixture of potassium. λ 4078 was disturbed by a band spectrum, but λ 4216 was favorable for comparison, and relatively to the other lines, showed a reduction to not more than one-third of its former intensity. A repetition of the experiment, this time for the emission spectrum at 1830°, permitted both λ 4078 and λ 4216 to be observed. They were found to be weakened by the addition of potassium to approximately the same degree as in absorption. This tube was afterward used for the experiment with calcium alone and calcium with caesium in emission, mentioned in the preceding section. The stronger strontium lines persisted and the enhanced pair was much reduced by the addition of caesium.

Barium.—A series of experiments was made for the absorption spectrum of barium at λ 1830° C, using both barium chloride alone and also mixtures of either potassium chloride or caesium chloride. The enhanced lines λλ 4554 and 4934 were compared with λ 5535 and the strong furnace lines from λ 5778 to λ 6063. The effect on the enhanced lines was much smaller than with the corresponding lines of calcium and strontium, but a perceptible relative weakening of the enhanced pair followed the addition of both of the substances with lower ionizing potentials.

The ionization potential of barium is lower than that of strontium or calcium, being in fact halfway between potassium and calcium. This and the fact that the region occupied by the barium lines is not so favorable for the observation of absorption effects as the portion farther to the violet may be responsible in some measure for the smaller influence in the case of barium. A mixture with sodium vapor, whose ionization potential is almost exactly the same as that of barium, was tried and no effect whatever could be detected.

3. TEMPERATURES REQUIRED FOR THE INITIAL APPEARANCE OF A GIVEN LINE IN ABSORPTION AND IN EMISSION

It is desirable to extend the observations on this point much farther than has yet been possible, but the tests made on lines of a favorable type have given definite results, which will be reported here.

In his discussion of the radiation of the characteristic lines of the neutral atom,[1] Saha reasons that a mass of gas too cool to emit any light should still be able to absorb lines of the principal series. Further heating causes the atoms to progress toward ionization, and radiation will follow as a result of the mutual interchange of orbits. When the gas can emit the principal series rather strongly, it should absorb the lines of the subordinate series, a still higher temperature producing the latter series in emission.

The tests thus far made have been concerned with the question whether there is a temperature at which the principal series Ca λ 4227, Sr λ 4607, and Ba λ 5535 will appear in absorption and not in emission. The higher critical stage at which these lines are emitted and at which the subordinate series may show only in absorption has not yet been looked for.

The experimental arrangement provided a transition from absorption to emission conditions by simply turning off a 900-watt tungsten lamp, whose light was directed through the tube during the absorption exposure.

The exposures required for the absorption and the emission spectrograms were very different. For absorption one-half to one minute was sufficient to produce a continuous ground of the proper strength to show any absorption which was present. For the emission spectrum, it was a question of registering a very faint image, and a period of two hours was considered a fair time, in view of the power of the spectrograph, to show anything which the vapor could emit. Absorption spectra were photographed at the beginning and end of the emission run.

---

[1] *Proceedings of the Royal Society*, A, **99**, 140, 1921.

At 1275° C, λ 4227 of calcium appeared in absorption, 0.5 A in width, persisting as a well-defined absorption line at the close of a two-hour exposure for the emission spectrum, but the line failed to show in emission. At the same temperature, a very faint trace of λ 4607 of strontium could be seen as an emission line, but nothing whatever appeared in emission at 1200°, though at the latter temperature the absorption line λ 4607 was strong at the beginning and end of the period.

The barium line λ 5535 could be seen very faintly in emission at 1500°; but with the temperature held close to 1400°, at no time rising above 1440°, the line entirely disappeared. The absorption line was still strong at 1400°.

Some inherent difficulties must be recognized in tests of this sort. Lines such as the three just considered have, when plenty of the material is present, low photographic density and a considerable width, which features should make them appear in absorption under minimum excitation. The same characteristics retard their development through the threshold condition in emission. Lines which tend, when faint, to become very narrow, as is the case with the great bulk of furnace lines, hold up relatively better in emission than in absorption as the temperature becomes lower; since in absorption the very narrow line may disappear too soon by reason of failure of the spectrograph to produce the resolution of the continuous spectrum which enables an absorption line to be perceived. This fact, which with the narrow lines of the vacuum furnace would make the emission line in its early stages easier to see than the absorption line, may account for the fact that in the iron spectrum, emission and absorption spectra for the same temperature of the furnace are very nearly duplicates. While the series for iron are not known, the lines fall into definite temperature classes,[1] and the initial appearance of a line of certain type may be watched. An iron line in this sensitive state and with proportional exposures, shows as readily in emission at a given temperature as in absorption. This was tested through a range extending from the ultra-violet into the red. From the green into the red, it is somewhat easier, at a certain temperature, to be sure of the presence of a faint iron line in emission than in absorption. We may therefore say that the evidence thus far does not always favor the absorption method as a means of producing more numerous lines than are shown under equal excitation in emission, though the earlier appearance in absorption of principal series lines appears to take place in the spectra of calcium, strontium, and barium.

MOUNT WILSON OBSERVATORY
January 1922

---

[1] *Mt. Wilson Contr.*, No. 66; *Astrophysical Journal*, **37**, 239, 1913.

CARBON DIOXIDE ABSORPTION IN THE NEAR INFRA-RED

By E. F. BARKER

ABSTRACT

Infra-red absorption bands of CO_2 at 2.7 and 4.3 μ.—*New absorption curves* have been obtained, using a special prism-grating double spectrometer of higher resolution (Figs. 1–3). The 2.7 μ region, heretofore considered to be a doublet, proves to be a pair of *doublets*, with centers at approximately 2.694 μ and 2.767 μ. The 4.3 μ band appears as a single doublet with center at 4.253 μ. The frequency difference between maxima is nearly the same for each of the three doublets, and equal to 4.5×10^{11}. Complete resolution of the band series was not effected, even though the slit included only 12 A for the 2.7 μ region, but there is evidently a complicated structure, with a "head" in each case on the side of shorter wave-lengths. The existence of this head for the 4.3 μ band is also indicated by a *comparison with the emission spectrum* from a bunsen flame, and the difference in wave-length of the maxima of emission and absorption is explained as a temperature effect similar to that observed with other doublets.

Molecular structure of CO_2.—If a linear configuration of the three atoms is assumed, the *moment of inertia* of the molecule, computed from the doublet frequency difference, comes out 50×10^{-40}. This gives the distance from the central C atom to each O atom as 0.97×10^{-8} cm. Since the linear molecule could have only three modes of vibration, it is suggested that the two doublets at 2.7 μ may correspond to two successive changes in stationary state for the same vibration.

Echelette gratings, used in the research, were ruled with 3000, 1000, and 500 lines per inch, on surfaces of aluminum.

In the prismatic spectrum of carbon dioxide three infra-red absorption bands have been observed,[1] at approximately 2.7 μ, 4.3 μ, and 14.7 μ. The first region shows two absorption maxima with no indication of fine structure, but, from its behavior when the gas is subjected to various temperatures and pressures, von Bahr concluded that it is not a simple doublet. The region at 4.3 μ is narrow and for it no structure was observed. Using small echelette gratings, Trowbridge and Wood[2] found several maxima and minima in the emission spectrum from a bunsen flame between 4 μ and 4.5 μ, but they apparently did not take into account the reversal effect due to atmospheric absorption. These two regions have now been re-examined with the maximum available dispersion, using a prism-grating spectrometer designed for the purpose.

---

[1] Von Bahr, *D. Phys. Ges.*, **15**, 710 and 1150, 1913; Burmeister, *D. Phys. Ges.*, **15**, 589, 1913.

[2] *Philosophical Magazine*, **20**, 898, 1910.

The arrangement of the optical system is shown in Figure 1. The prism is of rock salt, with an angle of 38° and faces about 7×10 cm. It separates the incident beam into a spectrum which is focused at the plane of a slit forming the source for the grating spectrometer; thus a narrow spectral region is presented to the grating for analysis, and overlapping of spectra is avoided. The detecting system is a silver-bismuth thermopile actuating a high sensitivity galvanometer of the Paschen type. An absorption cell with windows of thin glass or mica is placed immediately behind the first slit, and may be moved into and out of the optical path.

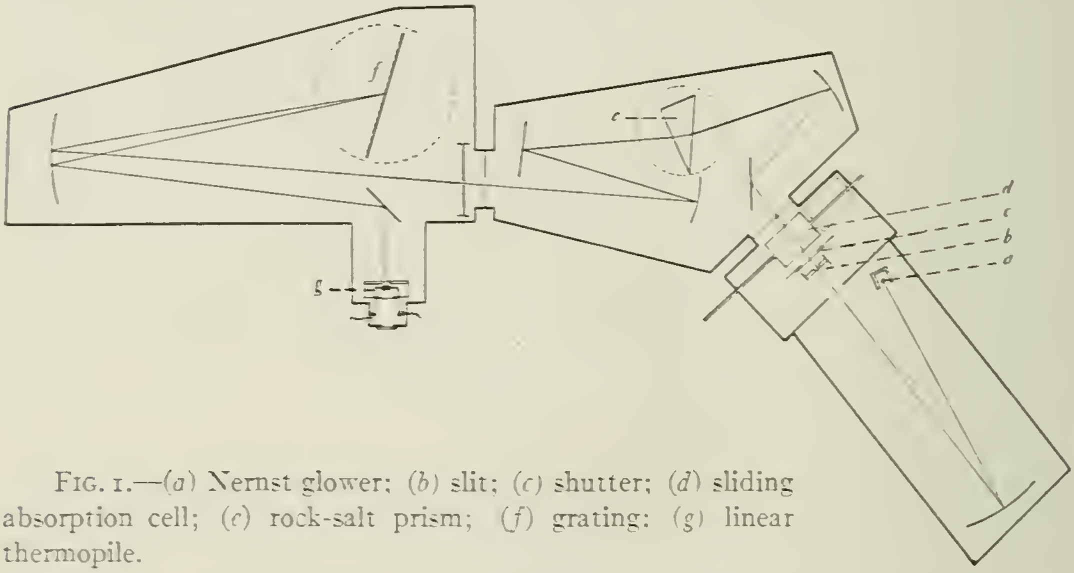

FIG. 1.—(*a*) Nernst glower; (*b*) slit; (*c*) shutter; (*d*) sliding absorption cell; (*e*) rock-salt prism; (*f*) grating; (*g*) linear thermopile.

The whole optical system is inclosed in a heavy metal case supplied with valves so that it may be thoroughly washed, dried, or even evacuated, as desired.

The region of 2.7 μ is accessible with a grating having approximately 15,000 lines per inch, and has also been examined in the first and second orders of a 5000-line grating. For the 4.3 μ band the latter grating failed to give spectra of measurable intensity and it has been necessary to prepare a number of coarser ones having approximately 3000, 1000, and 500 lines per inch. These have been ruled in the echelette form on 5″×7″ aluminium surfaces, and this department is indebted to the department of physics of Johns Hopkins University for the use of one of the Rowland ruling machines.

Observations.—Three absorption curves for the 2.7 μ band have been mapped with different dispersions, corresponding to approximately 55, 25, and 12 angstrom units, included by the half-millimeter slit. The absorption cell was five centimeters in length with glass windows about 0.25 mm thick. These extended beyond the cell so as to be traversed by the radiation even when the cell itself was removed from the optical path. Mica windows were used for greater wave-lengths, with a similar arrangement for compensation, but were avoided here on account of the absorption band of mica near 2.7 μ. The observations consisted in noting ten or twelve galvanometer deflections for a given setting of the grating, with the cell in and out alternately, from which the mean relative decrease in deflection due to the CO_2 absorption was computed. The interval between successive grating positions was somewhat less than the slit width.

The three different dispersions all show this absorption region to consist of a pair of doublets, so that we have, not a single typical band, but two, lying close together, with centers at approximately 2.69 μ and 2.76 μ. The use of different gratings, and the method of observing alternately with and without the absorption cell, completely eliminate the possibility of attributing this result to peculiarities of the ruled surface.

The curves of Figure 2 show the percentages of absorption obtained in the second-order spectrum of the 5000-line grating and the first-order spectrum of the 15,000-line grating. The existence of a complicated structure in these bands is very evident, but the available resolution is not sufficient to separate the individual members of the series. When using the 15,000-line grating the angle between the normal and the incident beam was 54°, so that obviously little is to be hoped for from finer gratings. The half-millimeter slit might be narrowed somewhat if a more intense source or a more sensitive detecting device were available.

The absorption band at 4.3 μ is narrow and intense, and may be observed as an atmospheric absorption even after long-continued washing of the spectrometer with CO_2—free air. That it is actually attributable to carbon dioxide is, however, established by the measurements with a 3 cm cell containing pure, dry CO_2, which absorbs more than 90 per cent of the incident energy throughout a considerable range of frequencies. With both the 1000-line and the 3000-line gratings the band appears as a distinct doublet, though there is little indication of the serrated structure which might be anticipated with higher dispersion. Figure 3A shows the atmospheric absorption obtained in the second-order spectrum from the 1000-line grating, the slit including 150 angstrom units. Figure 3B indicates the method employed to compute the percentage absorption, and Figure 3C is the absorption curve obtained in the first order of the 3000-line grating. The effect of introducing the absorption cell is shown in each. The dotted line of Figure 3B indicates the probable course of the energy curve for zero absorption, which could only be observed at the limits of the band. Its inclination to the horizontal is partly due to the falling off of energy as wave-lengths increase, and partly to the chosen prism setting.

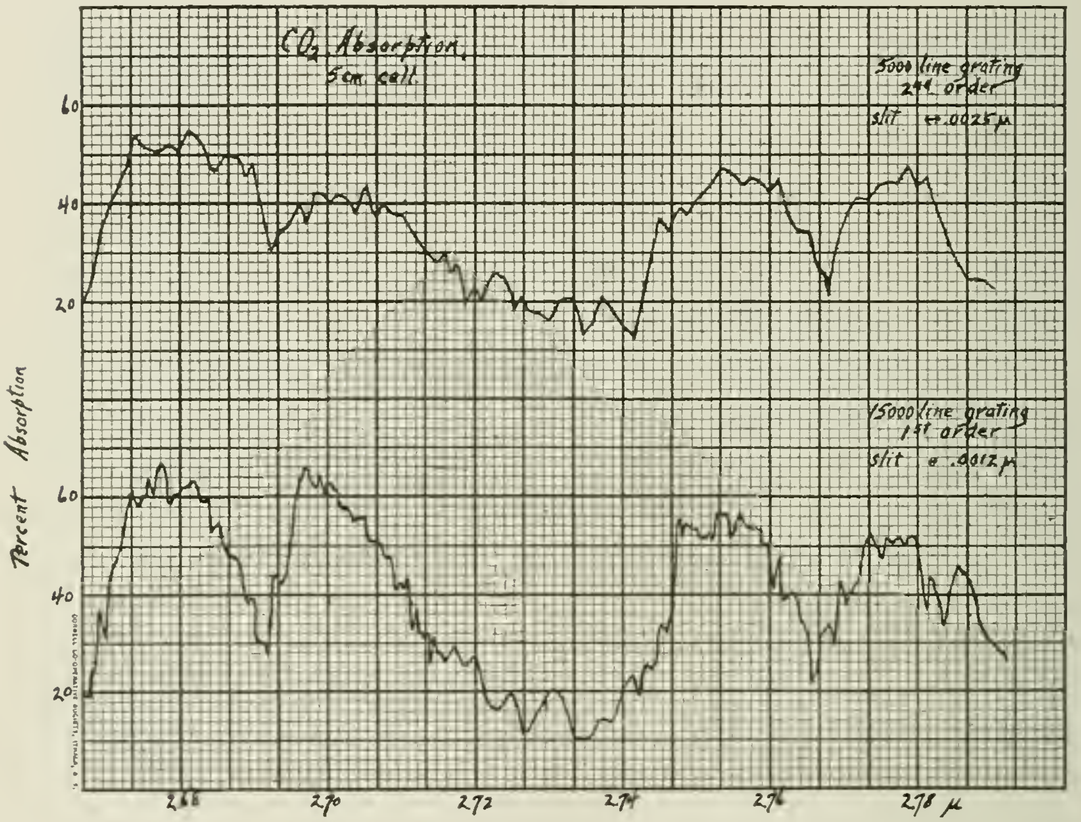

FIG. 2

The correction for slit width and slope of the energy curve[1] very slightly accentuates the doublet form, but does not displace the center nor the maxima appreciably.

The great intensity of the atmospheric absorption at 4.3 μ would seem to indicate that the emission band from a bunsen flame should be rapidly absorbed, though experimentally energy of approximately this wave-length is easily obtained through thick layers of air. The explanation is immediately obvious from Figure 4, which shows on the same scale the absorption of cold atmospheric CO_2 and the emission from the hot flame. As has been observed for other doublets, the widening due to increased temperature occurs almost entirely on the side of longer wave-lengths. From these curves it is evident that the doublet form would not be expected in the emission band unless precautions are taken to effectively eliminate absorption by cooler layers of CO_2—except, of course,

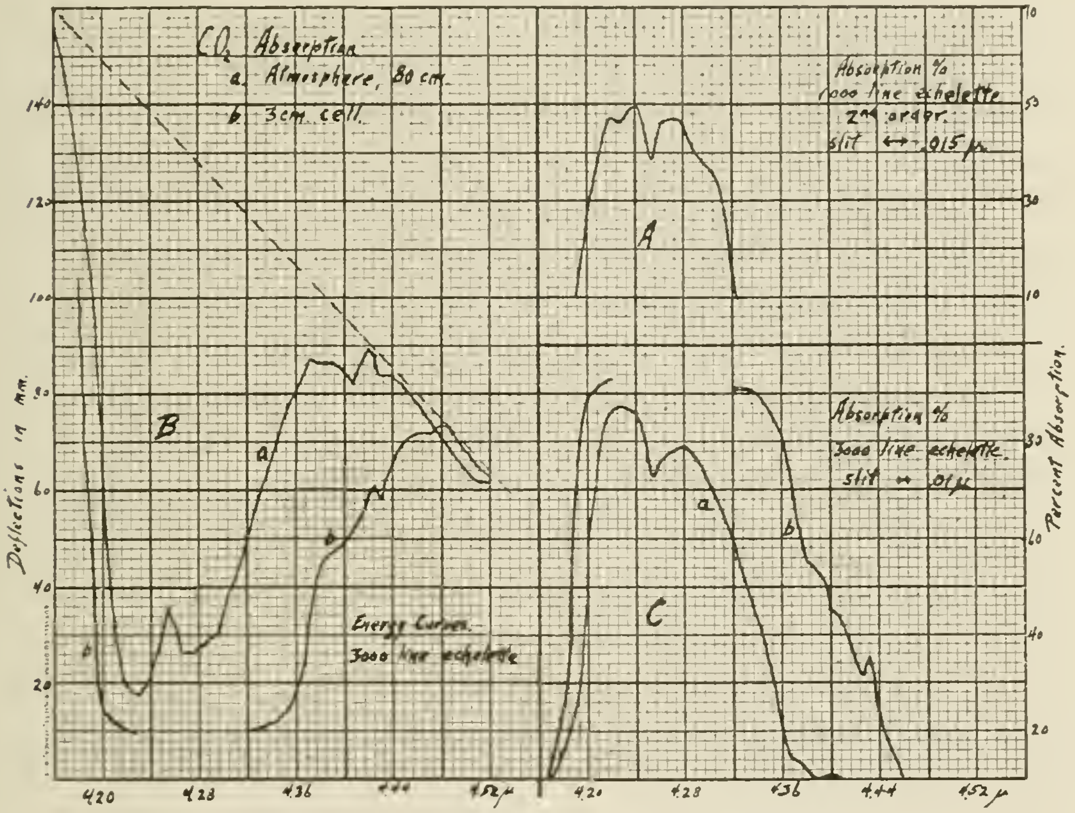

FIG. 3

---

[1] Paschen, *Annalen der Physik*, 60, 712, 1897.

that the "reversal" reveals an inverted doublet produced by absorption, leaving three apparent maxima in the energy curve as observed. Of these, the weakest, corresponding to the central notch in the absorption curve, occurs at 4.25 μ, while the positions of the others, which we observe at approximately 4.2 μ and 4.4 μ, depend upon the mass of gas in the cooler absorbing layers between the flame and the thermopile. Trowbridge and Wood (*loc. cit.*) observed maxima at 4.2 μ, 4.4 μ, and 4.5 μ with one grating, and at 4.32 μ and 4.43 μ with another. The dotted line in Figure 4 shows approximately what the energy curve would have been had no absorption occurred.

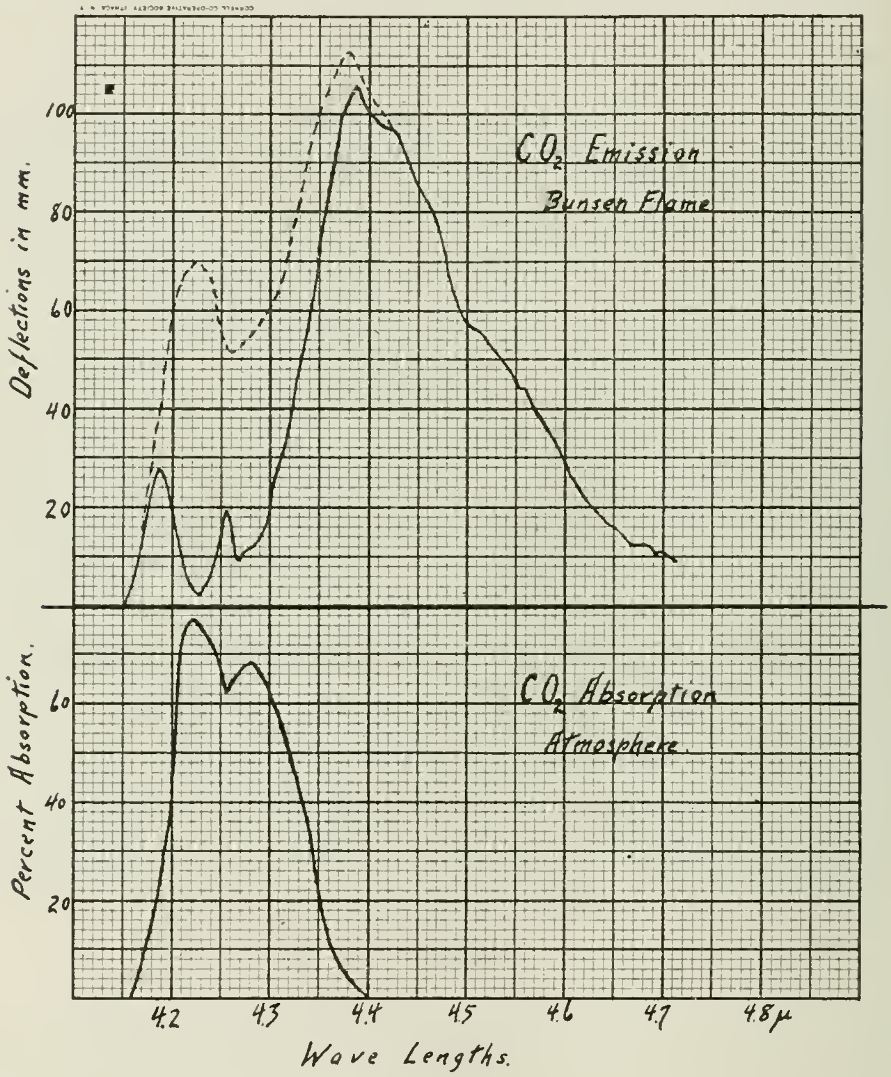

Fig. 4

Although from the measurements here presented it is not possible to isolate the various band series, several interesting conclusions may nevertheless be drawn. In the doublet of Figure 3 and both those of Figure 2 the side toward shorter wave-lengths is steep while the bands appear broadened toward longer wave-lengths; also the higher frequency maximum is the more intense. This suggests band series similar to those of the halogen acids[1] in which the individual members are crowded on the side of shorter wave-lengths and separated by increasing intervals on the other side. For the 4.3 μ band it would appear that our measurements approach very close to the head of the series, since increases in the mass of the absorbing gas and in the temperature (Figures 3C and 4) build up the absorption almost entirely on one side.

A simple band series like that of HCl would be expected only if the CO_2 molecule were linear, as in Langmuir's model, with a single effective moment of inertia. The spacing of members near the middle of the band would then be about $h/4\pi^2 I$. A fair approximation to the value of I may be obtained from the frequency differences of the two maxima in the various doublets. Calling this interval $2\nu_m$, we have, since ν_m is the most probable frequency of rotation,

$$I = \frac{RT}{4\pi^2 N \nu_m^2} = \frac{1.11 \times 10^{-15}}{\nu_m^2} .$$

Table I shows the values of ν_m taken from Figures 2 and 3, with corresponding values of I.

TABLE I

Band Center	Maxima	$\Delta\lambda$	ν_m	I
2.694	2.677, 2.698	.021	4.35×10^{11}	53.4×10^{-40}
2.767	2.753, 2.776	.023	4.52	49.5
4.253	4.225, 4.280	.055	4.56	48.6
Mean	....	....	....	50.5

For a symmetrical linear molecule with moment of inertia equal to 50.5×10^{-40}, each O atom would lie at a distance of 0.975×10^{-8} cm from the central C atom, a not improbable dimension.

---

[1] Imes, *Astrophysical Journal*, **50**, 251, 1919, and Colby and Meyer, *Astrophysical Journal*, **53**, 300, 1921.

This value of I is, however, much larger than that derived from the thermal constants of the gas, assuming three principal moments of inertia, A, B, and C. Thus Schames[1] computes for carbon dioxide

$$\sqrt[3]{ABC} = 5.80 \times 10^{-40}.$$

Bjerrum[2] has discussed the triangular CO_2 molecule, deriving three possible vibration frequencies. From the laws of motion for the linear form it is easily shown that there are two degrees of freedom for vibration along the axis, to which we may add one vibration frequency for motion of the atoms at right angle to the axis. Thus either assumption apparently predicts three fundamental vibration spectra. Our analysis, however, reveals four bands, none of which may be considered as a so-called harmonic. The close proximity of the two bands near 2.7 μ suggests as a possible explanation that these may both be "fundamentals" of the same vibration, one corresponding to the vibrational transition from state 0 to state 1, the other to the transition from state 1 to state 2. Such a double fundamental would be expected if the motion is not simple harmonic, and has been predicted for HCl at 3.4 μ with a frequency difference for the two bands about the same as observed here.[3] This explanation would, however, involve the probable existence of a harmonic which has never been observed at about 1.4 μ, a region in which water vapor has an intense absorption band. The almost equal intensities of the two series of Figure 2 would indicate a number of molecules in the first state of vibration almost equal to the number in the zero state at ordinary temperatures. The ultimate decision as to whether or not the arrangement of atoms in the carbon dioxide molecule is linear or triangular must await an analysis of the bands with sufficiently high resolution to reveal the series of which they are constituted.

This investigation has been carried on at the Physical Laboratory of the University of Michigan under a Research Fellowship of the National Research Council.

UNIVERSITY OF MICHIGAN
January 1922

---

[1] *Physikalische Zeitschrift*, **21**, 38, 1920.

[2] *D. Phys. Ges.*, **16**, 737, 1914.

[3] Kratzer, *Zeitschrift für Physik*, **3**, 289, 1920.

THE BROADENING OF THE BALMER LINES OF HYDROGEN WITH PRESSURE

By E. O. HULBURT

ABSTRACT

Photographic width of the Balmer lines of hydrogen for pressures up to 135 mm.—There is some question as to whether among the possible causes of the widening of lines with pressure, the decrease of mean free path is important. A theoretical calculation of the width to be expected for hydrogen lines if the length of the train of waves emitted is limited by the time between molecular collisions, gives for a temperature of 600° C. and a pressure of 100 mm a width of about 0.04 A, between wave-lengths where the intensity is one-tenth of that at the middle. Experimentally, however, it was found that a pressure of about 100 mm gave photographic images 80 A wide. Purified hydrogen in a capillary discharge tube was excited by condensed discharges and a series of spectrograms were taken for pressures from 0.2 to 135 mm. The exposure time was 30 minutes in each case and the discharge was regulated so that the intensity of the central portion of $H\beta$ was practically the same for all pressures. As shown by Figure 2, $H\beta$, $H\gamma$, and $H\delta$ behave very much alike. The fact that the actual width is much greater than that computed theoretically indicates that the widening of spectrum lines is probably due to some other cause, perhaps electrical fields.

Introductory.—The former Lord Rayleigh has summarized the causes which interfere with the absolute homogeneity of spectrum lines under five headings:[1] (1) The translatory motion of the radiating particles in the line of sight operating in accordance with Doppler's principle. (2) A possible effect of the rotation of the particles. (3) Disturbance depending on collision with other particles either of the same or of another kind. (4) Gradual dying down of the luminous vibrations as energy is radiated away. (5) Complications arising from the multiplicity of sources in the line of sight. To which is added a sixth cause proposed and investigated by Merton.[2] (6) The effect of an electric field on the radiating particle. The electric field may be that imposed on the electrodes of the tube or may be the field of neighboring atoms as suggested by Stark,[3] or a superposition of the two.

The researches of Fabry and Buisson[4] and Michelson[5] have demonstrated that for pressures of the luminous gas below one millimeter of mercury (1) is probably the only cause of broadening of the spectrum line. This cause is, however, impotent to explain the tremendously greater broadening produced in certain lines by the use of either greater pressures or condensed discharges, and therefore recourse must be had to the other causes mentioned. Of these the effects of (2) and (4) must perforce be omitted from discussion, for our present knowledge of atomic constitution and the nature of radiation is insufficient for a successful consideration of the effect of rotation of the luminous particle and of the damping of the vibration as the energy is radiated away. We also neglect (5), for this merely aggravates the effects of the other causes. There remain (3) and (6). From their recent work on the energy distribution in the broadened lines of hydrogen, helium, and lithium by high pressures stimulated by condensed discharges, Merton and Nicholson[1] concluded that cause (6) was all important in producing the broadening and that (2) played no part whatsoever. Their observations were concerned with the *form* of the broadened line and did not touch upon the *magnitude* of the broadening. In view of the novelty of this conclusion it seemed of interest to determine the magnitude of the broadening. The present work was carried out to this end and the photographic widths of Hβ, Hγ, and Hδ of the Balmer series of hydrogen were measured for pressures from 0.2 to 135 mm of mercury. The broadening which might be expected from cause (3) under the conditions of the present experiment was then calculated and was found to be considerably less than the observed broadening. This evidence thus supported the conclusions of Nicholson and Merton in that it threw doubt on the validity of (3) as a cause of the widening.

---

[1] *Philosophical Magazine*, **29**, 274, 1915.

[2] *Proceedings of Royal Society*, **92**, 322, 1915.

[3] *Elektrische Spectralanalyse chemischer Atome*, 1914.

[4] *Journal de Physique*, **2**, 442, 1912.

[5] *Astrophysical Journal*, **2**, 251, 1895.

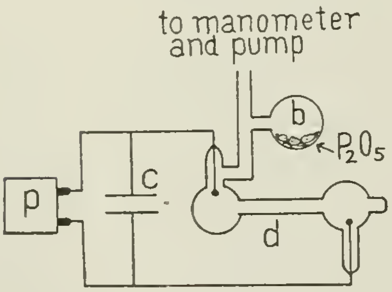

Fig. 1

Experimental.—Hydrogen, prepared from hydrochloric acid and zinc and purified through sodium hydroxide solution and concentrated sulphuric acid, was passed into the end-on discharge tube *d*, Figure 1, made of glass with aluminum electrodes arranged out of line with the

---

[1] *Philosophical Transactions*, Vol. 216, 459, 1916.

4[illegible]

PLATE VII

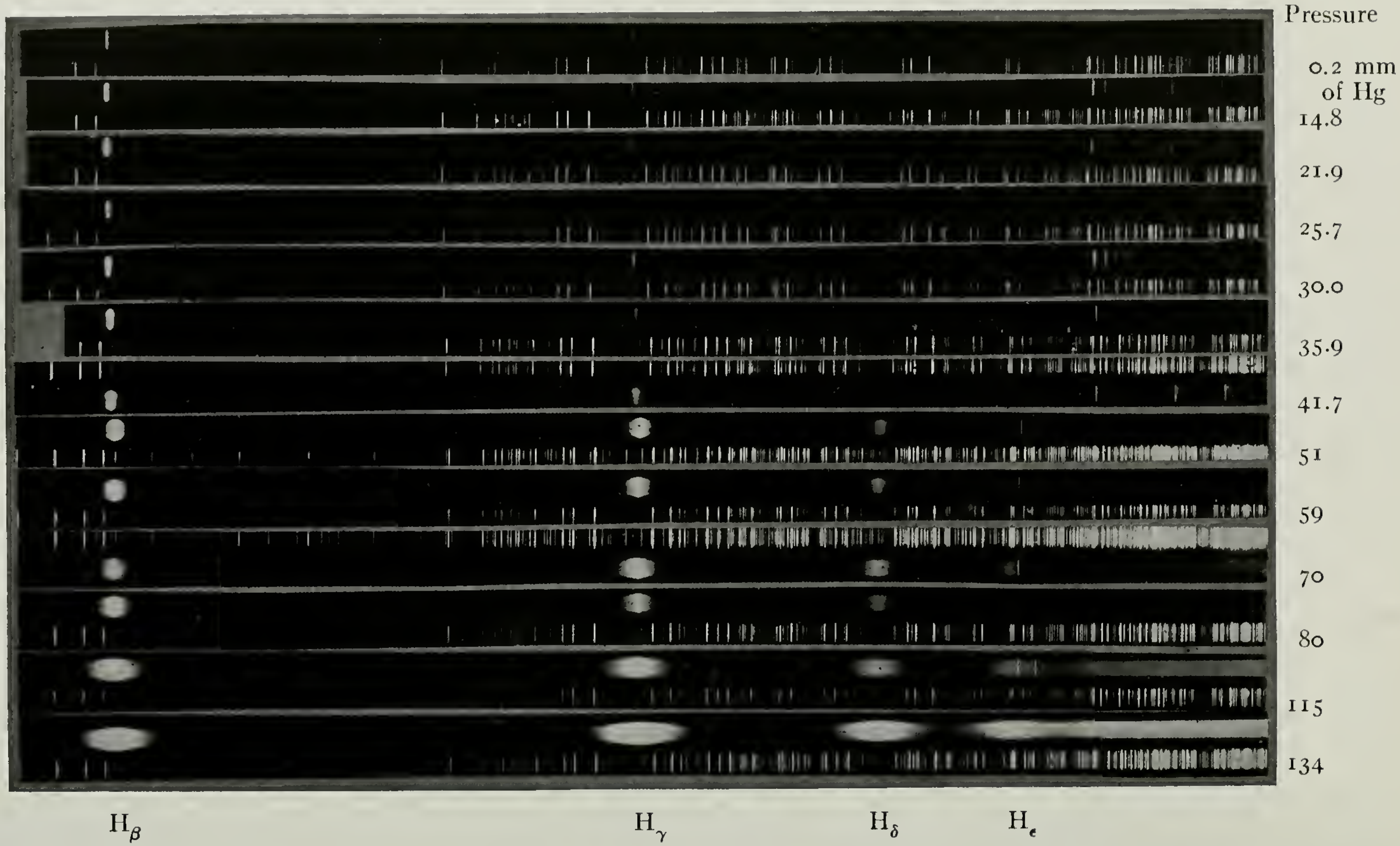
Pressure
0.2 mm of Hg
14.8
21.9
25.7
30.0
35.9
41.7
51
59
70
80
115
134
H_β
H_γ
H_δ
H_ϵ

capillary. The capillary was 10 cm long and 5 mm in diameter. A bulb *b* with phosphorous pentoxide was sealed to the tube. The tube was connected by glass tubing about a meter in length to a bulb of perhaps 200 c.c. capacity and a mercury manometer. The total capacity of the discharge tube and glass system, perhaps 300 c.c., was filled with hydrogen at various pressures and no change in pressure was observed when the discharge was run continuously for an hour. The condenser *c*, Figure 1, of capacity of about 0.01 μ F, which discharged through the tube, was charged by the 25,000 volt transformer *p*. The spectra were photographed in the first order of a concave grating of 2 meters radius of curvature and ruled 14,435 lines to the inch, the dispersion being about 8.8 A per mm.

Spectra of hydrogen were taken for a series of pressures from 0.2 to 135 mm. These are shown in Plate VII with the iron arc comparison spectrum. The tube was maintained rigidly in position throughout the series and the time of exposure was 30 minutes for each spectrogram. In order to obtain conditions for the various pressures that might be compared the procedure was as follows: A glass prism spectroscope was trained on the hydrogen tube so that Hβ could be observed visually at the same time that the spectrum was being photographed. A small region at the center of the line was isolated by the second slit of the prism-spectroscope and observed by a low-power eyepiece. A comparison line was reflected into the field of view of the eyepiece obtained by illuminating a portion of the first slit with the light from a tungsten lamp filtered through a greenish-blue filter. The intensity of the comparison line was maintained constant, and by adjusting the power consumed in the hydrogen tube the intensity of the central portion of Hβ was kept approximately constant for each pressure. It is worthy of remark that the condensed discharge through the hydrogen tube was at all times an oscillatory one, the frequency as measured by a wave-meter being 0.28×10^6 alternations a second. For this reason the electrical power consumed in the tube could not be determined in a simple manner by electrical methods.

The widths in angstrom units of Hβ, Hγ, and Hδ were measured from the photographs of Plate VII, and were plotted in Figure 2 as ordinates against pressures in mm of mercury as abscissae. The measurement of the width was made simply by judging the points on the edges of the lines on the plates where the blackening became slight and measuring between these points. This was manifestly inaccurate but was deemed sufficiently precise for the purpose in hand. The last two points on each of the curves were too high, for at these two highest pressures it was not possible to reduce the intensity of the center of Hβ to the intensity used at the lower pressures and still maintain sufficient voltage to render the gas luminous.

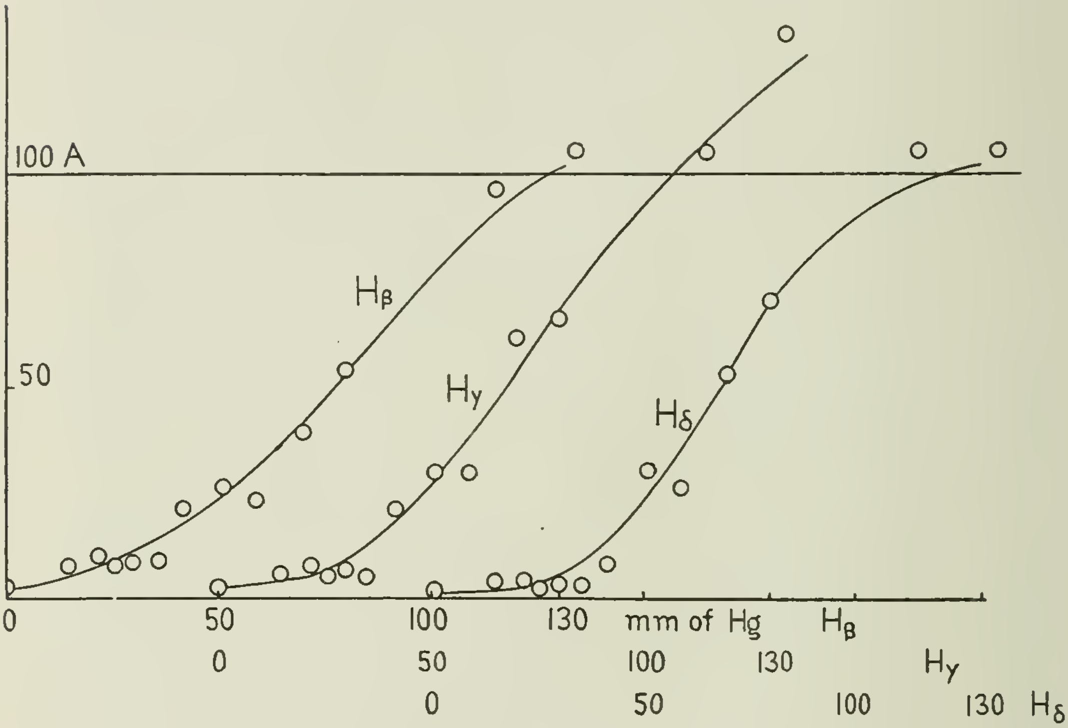

Fig. 2

Theoretical.—The third cause of widening mentioned in the introduction is the disturbance of the free vibration of the radiating particle due to encounters with other bodies. The simplest supposition open to us is that an entirely fresh start is made at each collision, so that we have to deal with a series of regular vibrations of finite length. The problem thus arising has been treated by Godfrey[1] and Schönrock.[2] The Fourier analysis of the limited train of waves of length r gives for the intensity of various parts of the spectrum line

---

[1] *Philosophical Transactions*, **195**, 329, 1899.

[2] *Annalen der Physik*, **22**, 209, 1907.

$$I = I_0 \frac{\sin^2 \pi r \left(\frac{1}{\lambda_0} - \frac{1}{\lambda} \right)}{\left(\frac{1}{\lambda_0} - \frac{1}{\lambda} \right)^2} \tag{1}$$

where I_0 and λ_0 are the intensity and wave-length respectively of the center of the spectrum line and I and λ are the respective quantities in any part of the line. r is the length of the train of waves in cms. λ_0 is the wave-length which would be dominant if r were infinitely long.

We calculate r from the Kinetic Theory of Gases,[1] to be

$$r = \frac{c}{4\,\nu\sigma^2} \sqrt{\frac{m}{\pi \mathrm{RT}}} \tag{2}$$

where ν is the number of molecules per unit volume at the pressure and temperature in question, σ is the diameter of the sphere of molecular action from the Kinetic Theory standpoint, m is the mass of the molecule, c is the velocity of light *in vacuo* and R is the gas constant.

Substituting (2) in (1) gives

$$I = I_0 \frac{\sin^2 \frac{\pi c}{4\,\nu\sigma^2} \sqrt{\frac{m}{\pi \mathrm{RT}}} \left(\frac{1}{\lambda_0} - \frac{1}{\lambda} \right)}{\left(\frac{1}{\lambda_0} - \frac{1}{\lambda} \right)^2} \tag{3}$$

Formulae (2) and (3) assume slightly different forms depending on the methods used in averaging the velocities of the gas particles. These have been discussed by Tait,[2] Rayleigh,[3] and Godfrey,[4] and it seems that the various methods yield expressions which differ from (2) and (3) by not more than 10 per cent. This difference is small enough to be ignored in the present case.

---

[1] Jeans, *Dynamical Theory of Gases*, p. 32.

[2] *Transactions Royal Society of Edinburgh*, **33**, 74, 1886.

[3] *Proceedings Royal Society, A*, **76**, 440, 1905.

[4] *Loc. cit.*

Comparison of theory and experiment.—By giving values to ν corresponding to the various pressures I was determined by means of (3) as a function of λ for each pressure, and from this the width of the spectrum line was calculated for each pressure. At a temperature 0° C. and 760 mm pressure ν was taken to be 4×10^{19}. The diameter of a hydrogen molecule was 2×10^{-8} cm. We assume that the gas was always at the temperature 600° C. $c=3\times10^{10}$, $R=9.3\times10^{-17}$, and $m=2.25\times10^{-24}$ grams. Introducing these values into (3) leads to

$$I=I_0\frac{\sin^2\frac{10634}{p}\left(\frac{1}{\lambda_0}-\frac{1}{\lambda}\right)}{\left(\frac{1}{\lambda_0}-\frac{1}{\lambda}\right)^2}, \qquad (4)$$

where p is the pressure of the hydrogen in mm of mercury. When I was computed from (5) for pressures within the range of the present measurements, curves of the type shown in Figure 3 were obtained. The width of the line increased with increase of pressure but was very narrow in all cases. For example, Figure 3 gives a curve for $\lambda_0=5000$ A and $p=100$ mm of mercury, and the width of the line represented by the curve is less than 0.04 A. In short, the broadening with pressure to be expected from the collision theory, or cause (3), is smaller by a different order of magnitude than that observed in the Balmer lines of hydrogen. In order to make the calculation agree approximately with the experimental measurements as far as the actual magnitude of the broadening is concerned, the number of equation (5) should be about 75 instead of 10634. The calculation was made on the basis

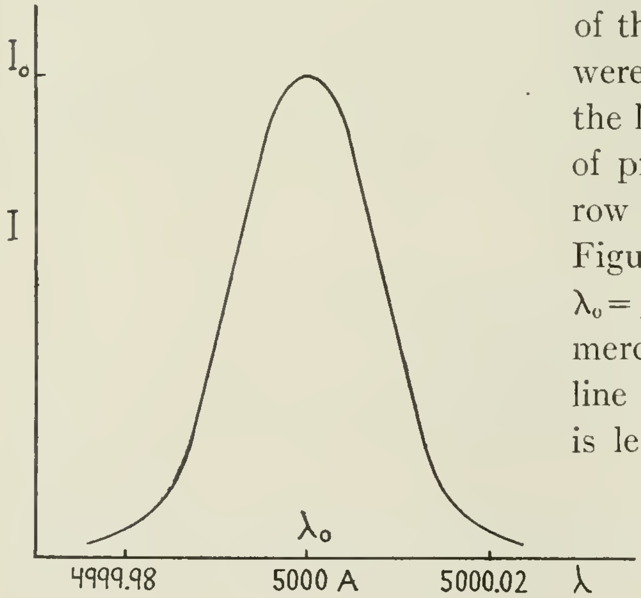

Fig. 3

of molecular hydrogen. Many researches, however, point to the fact that a disruptive discharge breaks the hydrogen molecule into its component atoms. If, then, we use values referring to the atoms, that is, employ a value for ν twice as great and for σ and m one-half as great as the molecular values previously substituted in (3), we find the number of equation (4) to be larger by the square root of two. This would make the calculated width of the line still smaller.

Discussion.—The discrepancy between theory and experiment is probably not to be found in experimental errors, approximate though the measurements were, or in a wrong assumption of the temperature of the gas. The discrepancy should rather be attributed to more fundamental errors of assumption, and in the light of the present experiment and the experiments of Merton and Nicholson (*loc. cit.*) we are ready to abandon cause (3) as inadequate and to turn to cause (6) as a possible explanation, as suggested by Merton (*loc. cit.*).

If the principal cause of the widening be attributed to the influence of an electric field on the radiating particle we may well inquire whether the electric field is the one imposed on the tube or is due to neighboring particles. Careful experiment on the separate influences of pressure and intensity of the discharge on the broadening combined with the known data of the Stark effect might differentiate between the two actions if they both exist. If the broadening is due to the electric field of neighboring particles we again return to the idea of collision. The effect of the collision upon the radiating particle, however, would be not merely a disturbance of the radiating centers by a mechanical shock but a profound momentary influence of an intense electric field.

State University of Iowa
Iowa City, Iowa
April 1922

AN ESTIMATE OF THE DISTANCE OF THE ANDROMEDA NEBULA

By E. OEPIK

ABSTRACT

Andromeda Nebula.—Assuming the centripetal acceleration at a distance r from the center is equal to the gravitational acceleration due to the mass inside the sphere of radius r, an expression is derived for the *absolute distance* in terms of the linear speed v_0 at an angular distance ρ from the center, the apparent luminosity i, and E, the energy radiated per unit mass. From observations, v_0 comes out 157 km/sec. for $\rho = 150''$; and giving i a value corresponding to magnitude 6.1, and assuming E the same as for our Galaxy, the distance is computed to be 450,000 parsecs. This result is in agreement with that obtained by several independent methods. If it is correct, the *mass* within 150″ of the center is about 4.5×10^9 times the sun's mass, and the nebula is a stellar universe comparable with our Galaxy. *The ratio of the axes of the central ellipsoid*, whose shape is supposed to be due to rotation, was determined from photographs to be about 0.79.

Various estimates of the distance of the Andromeda Nebula have been made hitherto by H. Shapley,[1] H. D. Curtis,[2] K. Lundmark,[3] Luplau-Janssen and Haarh[4] and others; these estimates, based on the hypothesis that the Nebula consists of stellar matter similar to the matter of our Galaxy, lead to a distance of about 10^5 to 10^6 parsecs. Here we shall propose a method based on observed rotational movement, a method which may be applied to any nebula or cosmic system provided sufficient data are available. The principle is the same as that used by Campbell and Moore[5] to estimate the minimum mass of a planetary nebula.

Let v_0 be the velocity of motion along a circular orbit at a given point of the nebula, r, the distance from the center in astronomical units, M, the mass of the nebula within the radius $r(\odot = 1)$, w, the orbital velocity of the earth; then

$$\left(\frac{v_0}{w}\right)^2 = \frac{M}{r}. \qquad (1)$$

---

[1] *Publications of the Astronomical Society of the Pacific*, **29**, 216, 1917.

[2] *Ibid.*, **29**, 206, 1917.

[3] *Astronomische Nachrichten*, **209**, 378, 1919.

[4] *Ibid.*, **215**, 285, 1922.

[5] *Lick Observatory Bulletin*, **9**, 4, 1916.

Let the integrated absolute luminosity ($\odot = 1$) of the nebula within the radius r be I and the apparent luminosity $i(\odot = 1)$; then

$$\frac{i}{I} = \frac{1}{D^2}, \tag{2}$$

D being the distance in astronomical units. Let ρ be the angular distance from the center of the nebula, so that $r = D \sin \rho$, and let $E = \frac{I}{M}$; then, combining (1) and (2), we obtain

$$D = \frac{E \sin \rho}{i} \left(\frac{v_0}{w} \right)^2; \tag{3}$$

ρ, i, and w are known from observation; for v_0 an inferior limit is given by the relation $v_0 > \frac{v'}{\sqrt{2}}$, v' being the velocity of rotation or, more generally, of any internal movement, observed spectroscopically. Thus the estimation of the distance depends chiefly upon the quantity E, representing the average loss of energy per unit mass; this quantity plays an important part in Eddington's theory of the radiative equilibrium of stars.

If there exists absorption of light in space, and if ω is the fraction of light transmitted, and D' is the true distance, then the equations will be modified as follows:

$$\frac{i}{I} = \frac{\omega}{D'^2}; \tag{2'}$$

$$r = D' \sin \rho,$$

whence

$$D' = \frac{\omega E \sin \rho}{i} \left(\frac{v_0}{w} \right)^2 \tag{3'}$$

or

$$D' = \omega D, \tag{4}$$

D representing the distance computed without absorption.

Hitherto no assumptions as to the minute structure of the nebula have been made; if we postulate the existence of stars of a given absolute luminosity, and if α is their apparent luminosity computed without absorption, α', the same quantity corresponding to the absorption factor ω and distance D', then it is easy to obtain

$$\alpha' = \frac{\alpha}{\omega}. \tag{5}$$

Thus increased absorption diminishes the hypothetical distance but increases the apparent brightness of individual stars; this circumstance furnishes an upper limit of the hypothetical absorption, above which the individual stars of the nebula should become visible. Observational evidence indicates that if the Andromeda Nebula is a stellar universe with a luminosity-curve similar to that of our own stellar system, then ω cannot differ sensibly from unity.

For the Andromeda Nebula the following data may be used. F. G. Pease[1] has found a rotational velocity $v' = 72$ km/sec. at a distance of $\rho = 150''$ for which $\sin \rho = 0.000728$. To estimate the probable value of the circular velocity v_0, we shall suppose that the ellipsoidal shape of the inner parts of the nebula is a result of rotation. If a and b are the axes of the ellipsoid of revolution, $a > b$, $k = 1 - \frac{b}{a}$, then for small values of k and for a rotating nonhomogeneous gaseous mass condensed at the center we have approximately

$$k = \left(\frac{v}{v_0}\right)^2, \tag{6}$$

v being the equatorial velocity of rotation. To obtain k, a plate taken with the 6-inch Petzval camera of the Dorpat Observatory, exposure 90 minutes, has been measured on a Hartmann microphotometer. Curves of equal density were constructed and the ratio of axes of these curves is given in the following table:

---

[1] *Proceedings of the National Academy of Sciences*, 4, 21–24, 1918.

Density of Negative	Millimeters		$b:a$
	$2a$	$2b$	
5.00	0.87	0.69	0.79
4.60	1.12	0.88	0.79
4.30	1.40	1.02	0.73

Scale of the photograph: 1 mm = 261″.

These data give for $a = 150''$ the ratio $\frac{b}{a} = 0.79$ and $k = 0.21$. The angle between the line of sight and the equatorial plane of the nebula being small (about 8°) and the central condensation strong, we may assume that the values found represent the true ratio of axes of the ellipsoidal surfaces of equal density of the stellar or nebular matter within the nebula. Applying formula (6) with $k = 0.21$ and $v = v' = 72$, we obtain $v_0 = 157$ km/sec. This value must be regarded as an inferior limit, for in a stellar universe rotations in opposite directions may occur, and the spectroscopic velocity, representing the algebraic mean of all velocities, will be less than the mean absolute velocity.

As for E, we shall assume it equal to the corresponding value for our Galaxy. According to data given by Kapteyn and Van Rhijn,[1] 1000 cubic parsecs contain 44.7 luminous stars brighter than absolute magnitude 9.8, whose total luminous emission equals 55.5 stars of absolute magnitude zero[2] (nearly $= \odot$); J. H. Jeans[3] found that the observed motions of stars of our universe together with the distribution of density given by Kapteyn indicate that every luminous star counted by Kapteyn must correspond to an average mass equal to $3.2(\odot = 1)$; thus we obtain $E = \frac{55.5}{3.2 \times 44.7} = 0.38(\odot = 1)$ for our Galaxy.

The stellar magnitude of the Andromeda Nebula we shall assume $= 5.0$; the stellar magnitude of the sun $= -26.6$ (corresponding to absolute magnitude zero). From a paper by Reynolds,[4]

[1] *Mt. Wilson Contr.*, No. 188; *Astrophysical Journal*, **52**, 23, 1920.

[2] F. H. Seares, *Mt. Wilson Contr.*, No. 191; *Astrophysical Journal*, **52**, 167, 1920.

[3] *Monthly Notices*, **82**, 133, 1922.

[4] *Ibid.*, **74**, 132, 1914.

by a slight extrapolation, it has been found that the light of the nebula within 150″ from the center equals three-eighths of its total light; that corresponds to stellar magnitude 6.1. From these data we obtain $i=2.512^{-32.7}$.

Substituting the data found above into equation (3), we find $D=9.10^{10}$ astron. units or 450,000 parsecs. From equation (1) we obtain $M=1.8\times 10^9(\odot=1)$ within 150″ distance from the center. For a stellar system the mass within a given volume may be assumed proportional to the total luminous emission; thus the total mass of the Andromeda Nebula must be eight-thirds times greater or 4.5×10^9 times our sun's mass. This would correspond to about 1500 million of stars brighter than 1/10,000 of our sun, if the luminosity-curve and distribution of mass in the nebula were the same as in the regions of space surrounding us.

The order of the distance found above is in agreement with other estimates of the distance of the Andromeda Nebula; the coincidence of results obtained by several independent methods increases the probability that this nebula is a stellar universe, comparable with our Galaxy. It may be added that in our computation this statement did not enter as an initial hypothesis. The only assumption concerning the constancy of the energy-production E may be true for any great aggregation of mass, without regard to the structure of the system; if we suppose that the energy of celestial bodies has its source in some processes like radioactivity, then our assumption would mean that the percentage of radioactive matter in the system of the Andromeda Nebula and in the Galactic system are equal.

TARTU (DORPAT)
April 7, 1922

NOTE ON THE THICKNESS OF AIR REQUIRED TO PRODUCE THE ATMOSPHERIC ABSORPTION BANDS, A, *a*, AND B[1]

By ARTHUR S. KING

ABSTRACT

Thickness of air required to give the absorption bands A, a, and B.—On a plate stained with dicyanin, the A and B bands were obtained when the light from a tungsten lamp traversed minimum thicknesses of only 7 and 40 meters respectively; and though the air was hot and dry, the water band *a* at λ 7200 was obtained with absorption of 9.5 meters. To give the bands A and B visually respectively twelve and five times greater thicknesses of air are required.

In the course of experiments on absorption spectra in which the light from a 900-watt tungsten lamp passed through a heated graphite tube and thence to a 15-foot concave grating spectrograph, it was noted that the A band at λ 7600 frequently appeared on the spectrograms. This band is ascribed to the absorption of oxygen in the atmosphere. A test with the furnace cold showed that the absorption was due to the air at room temperature. The distance traversed by the beam through the air in the laboratory and in the spectrograph was about 12 meters. As this air-path is much shorter than that usually regarded as necessary to produce this band, other distances were tried in order to find, if possible, the minimum thickness required to give A, and also under what conditions the companion band B near λ 6900 could be obtained.

Placing the lamp as near the slit as could be conveniently arranged gave an air-path of 9.5 meters. The A band was still fairly strong and evidently would appear with a path considerably shorter. A surprising feature was that the water-vapor band a at λ 7200 could be detected at this distance. It was just at the limit of visibility on spectrograms having a favorable density of the continuous ground. As a part of the air-path was in the spectrograph pit, a determination of the humidity was not attempted; but the experiments were made on a particularly dry day, a hot wind blowing from the Mojave desert, so that the water-content of the air, both in the laboratory and in the ventilated pit, must have been very low.

---

[1] *Contributions from the Mount Wilson Observatory*, No. 232.

Changing the air-path to 19 meters strengthened both A and *a*, but B was still invisible. The light was then passed the length of the laboratory to a plane mirror and back to the spectrograph, a distance of 39.4 meters. B now appeared, extremely faint, but the structure of both branches of the band could nevertheless be made out. Both A and *a* were strongly developed.

To find how small a layer of air would give A, it was necessary to use a shorter-focus spectrograph, and a 1-meter concave grating was tried. This involved a greatly reduced scale and, as the component lines of the atmospheric bands produced in this way are very fine, the matter of photographic resolution became important. Finally, by using a fine-grained film stained with dicyanin, the A band was detected with an air-path of seven meters.

These minimum distances of seven meters for A and approximately forty meters for B are much shorter than those given by Liveing and Dewar,[1] who extended the earlier observations of Egoroff and Janssen. Their tests, however, were visual, and the red-sensitive plate is certainly far more effective for the observations of A; while in the B region the plate probably still has an advantage over the eye in the detection of faint objects, on account of the possibility of adjusting contrast and the strength of the continuous ground.

Liveing and Dewar found that 7 atmospheres pressure in a steel tube 18 meters long rendered A visible, while 18 atmospheres were required to show B. The same tube filled with pure oxygen at atmospheric pressure showed A, while two atmospheres of oxygen were needed for B to appear. From this observation, A should be discernible through 90 meters of air. Egoroff[2] observed it through 80 meters of air, or nearly twelve times the amount found necessary in the writer's experiments by the photographic method.

Mt. Wilson Observatory
November 1921

---

[1] *Proceedings of the Royal Society*, 46, 222, 1889.

[2] *Comptes Rendus*, 101, 1143, 1885.

SPECTROPHOTOMETRIC METHODS FOR DETERMINING STELLAR LUMINOSITY. A CORRECTION

Corrected parallax for Messier 11.—In the *Publications of the Astronomical Society of the Pacific*, **34**, 115, 1922, Dr. K. Lundmark has corrected an unfortunate error in my paper, *Mt. Wilson Contr.*, No. 228; *Astrophysical Journal*, **55**, 85, 1922. For the cluster Messier 11 I found the modulus $M-m=-12$, which corresponds to the parallax 0".00040 and the distance 2500 parsecs or 8000 light-years (erroneously given 0".00025, 4000 parsecs, and 13,000 light-years).

Bertil Lindblad

INDEX TO VOLUME LV

SUBJECTS

PAGE

Absorption Bands A, a, and B, Production of. *Arthur S. King* . . . 411

Absorption, Carbon Dioxide, in Near Infra-Red. *E. F. Barker* . . . 391

Andromeda Nebula, Distance of the. *E. Oepik* 406

Arc, Low Voltage, Enhanced Spectra of Sodium and Potassium in. *Paul D. Foote, W. F. Meggers,* and *F. L. Mohler* 145

B-Types, K-Term in, Partial Explanation of, by Wave-Lengths. *Sebastian Albrecht* 361

Balmer Lines of Hydrogen, Broadening of, with Pressure. *E. O. Hulburt* 399

Bands, A, *a*, and B, Production of Absorption. *Arthur S. King* . . . 411

Binaries 1 Hydrae and 75 Cancri, The Orbits of the Spectroscopic. *R. F. Sanford* 30

75 Cancri, Orbit of Spectroscopic Binary. *R. F. Sanford* 30

Carbon Dioxide Absorption in Near Infra-Red. *E. F. Barker* . . . 391

Color-Transparency of Ray-Filters in Use at Yerkes Observatory. *Ernest C. Bryant* 1

Corona, Spectrum of. Eclipse of June 8, 1918. *V. M. Slipher* . . . 73

Correction. Comparison Stars for Nova Persei, No. 2. *Frederick H. Seares* 272

Correction to "Spectrometric Methods for Determining Stellar Luminosity." *Bertil Lindblad* 413

Distance, Upper Limit of, to Which Arrangment of Stars in Space Can Be Determined. *J. C. Kapteyn* and *P. J. Van Rhijn* 242

Eclipse of June 8, 1918, Spectrum of Corona at. *V. M. Slipher* . . 73

Electric Furnace Experiments Involving Ionization Phenomena. *Arthur S. King* 380

Filters, Ray-, in Use at Yerkes Observatory, Color-Transparency of. *Ernest C. Bryant* 1

Gallium, Arc Spectra of. *H. S. Uhler* and *J. W. Tanch* 291

Helium, Formation and Life of Metastable. *Fabian M. Kannenstine*. 345

1 Hydrae, Orbit of Spectroscopic Binary. *R. F. Sanford* 30

Hydrogen, Broadening of Balmer Lines of, with Pressure. *E. O. Hulburt* 399

Index 414

Indium, The Arc Spectra of. *H. S. Uhler* and *J. W. Tanch* 291

Infra-Red, Carbon Dioxide Absorption in Near. *E. F. Barker* . . . 391

Interferometer Measurements, Wave-Length in Astronomical. *J. A. Anderson* 48

PAGE

Ionization Phenomena, Electric Furnace Experiments Involving. *Arthur S. King* 380
Ionization in Solar Atmosphere. *Henry Norris Russell* 354
Ionization, Theory of, and Sun-Spot Spectrum. *Henry Norris Russell* . 119
K-Term in B-Types, Partial Explanation of, by Wave-Lengths. *Sebastian Albrecht* 361
Lowell Observatory, Spectrum of Corona of June 8, 1918, as Observed by Expedition from. *V. M. Slipher* 73
Luminosity, Stellar, Spectrophotometric Methods for Determining. *Bertil Lindblad.* (*See also* Correction, p. 413) 85
Masses, Calculation of, from Spectroscopic Parallaxes. *Henry Norris Russell* 238
Mercury Vapor, A Continuous Spectrum from. *C. D. Child* . . . 329
Metals, Vacuum-Spark Spectra of the. *Edna Carter* 162
Orbits of Spectroscopic Binaries ι Hydrae and 75 Cancri. *R. F. Sanford* . 30
Nebula, Distance of the Andromeda. *E. Oepik* 406
Nova Persei, A Correction to Comparison Stars for. *Frederick H. Seares* 272
Parallaxes, Calculation of Masses from Spectroscopic. *Henry Norris Russell* 238
Parallaxes, Systematic Corrections to Spectroscopic and Trigonometric. *Gustaf Strömberg*. 11
Persei, Nova, A Correction to Comparion Stars for. *Frederick H. Seares* 272
Polaris, Effective Wave-Lengths of the Σ Companion of. *Ejnar Hertzsprung*. 370
Pole, Effective Wave-Lengths of 129 Stars within 0°5 of North, and of Σ Companion of Polaris. *Ejnar Hertzsprung* 370
Potassium in Low Voltage Arc, Enhanced Spectra of. *Paul D. Foote, W. F. Meggers,* and *F. L. Mohler*. 145
Pressure, Broadening of the Balmer Lines of Hydrogen with. *E. O. Hulburt*. 399
Procyon, On the System of. *Joseph Lunt* 71
Quantum Theory of Band Spectra and Its Application to Determination of Temperature. *Raymond T. Birge* 273
Radiation, Stellar. *W. W. Coblentz* 20
Sidereal System, First Attempt at a Theory of Arrangement and Motion of. *J. C. Kapteyn* 302
Sodium in Low Voltage Arc, Enhanced Spectra of. *Paul D. Foote, W. F. Meggers,* and *F. L. Mohler* 145
Solar Atmosphere, Ionization in. *Henry Norris Russell* 354
Solar Constant, Sun-Spots, and Solar Activity. *Anders Ångström* . . 24
Spectra, Arc, of Gallium. *H. S. Uhler* and *J. W. Tanch*. 291
Spectra, Band, Quantum Theory of, and Its Application to Determination of Temperature. *Raymond T. Birge* 273

PAGE

Spectra, Enhanced, of Sodium and Potassium in Low Voltage Arc. *Paul D. Foote*, *W. F. Meggers*, and *F. L. Mohler* 145
Spectra of the Metals, Vacuum-Spark. *Edna Carter*. 162
Spectrophotometric Methods for Determining Stellar Luminosity. *Bertil Lindblad*. (*See also* Correction, p. 413) 85
Spectrum of Corona at Eclipse of June 8, 1918. *V. M. Slipher* . . 73
Spectrum from Mercury Vapor, A Continuous. *C. D. Child* . . . 329
Spectrum, Sun-Spot, Theory of Ionization and. *Henry Norris Russell* . 119
Stars, Effective Wave-Lengths of 129, within 0°5 of North Pole. *Ejnar Hertzsprung*. 370
Stars, Masses and Densities of. *Frederick H. Seares* 165
Stars, Upper Limit of Distance to Which Their Arrangement in Space Can Be Determined. *J. C. Kapteyn* and *P. J. Van Rhijn* . . 242
Stellar Radiation, New Measurements of. *W. W. Coblentz* . . . 20
Sun-Spots, Solar Constant, and Solar Activity. *Anders Ångström* . . 24
Sun-Spot Spectrum, Theory of Ionization and. *Henry Norris Russell* . 119
System, Arrangement and Motion of Sidereal. *J. C. Kapteyn* . . 302
Temperature, Quantum Theory of Band Spectra and Its Application to Determination of. *Raymond T. Birge* 273
Wave-Length in Astronomical Interferometer Measurements. *J. A. Anderson* 48
Wave-Length of Atmospheric and Solar Lines, Investigation of Constancy in. *Charles E. St. John* and *Harold D. Babcock* 36
Wave-Lengths, Effective, of 129 Stars within 0°5 of the North Pole and of the Σ Companion of Polaris. *Ejnar Hertzsprung* 370
Wave-Lengths, Partial Explanation by, of K-Term in B-Types. *Sebastian Albrecht* 361
Yerkes Observatory, Color-Transparency of Ray-Filters in Use at. *Ernest C. Bryant* 1

INDEX TO VOLUME LV

AUTHORS

PAGE

Albrecht, Sebastian. Partial Explanation, by Wave-Lengths, of the K-Term in the B-Types . . . 361

Anderson, J. A. The Wave-Length in Astronomical Interferometer Measurements . . . 48

Ångström, Anders. Sun-Spots, Solar Constant, and Solar Activity .. 24

Babcock, Harold D., and Charles E. St. John. An investigation of the Constancy in Wave-Length of the Atmospheric and Solar Lines . . . 36

Barker, E. F. Carbon Dioxide Absorption in the Near Infra-Red . 391

Birge, Raymond T. The Quantum Theory of Band Spectra and Its Application to the Determination of Temperature . . . 273

Bryant, Ernest C. Color-Transparency of Ray-Filters in Use at Yerkes Observatory . . . 1

Carter, Edna. The Vacuum-Spark Spectra of the Metals . . . 162

Child, C. D. A Continuous Spectrum From Mercury Vapor. . . 329

Coblentz, W. W. New Measurements of Stellar Radiation . . . 20

Foote, Paul D., W. F. Meggers, and F. L. Mohler. The Excitation of the Enhanced Spectra of Sodium and Potassium in a Low Voltage Arc . . . 145

Hertzsprung, Ejnar. Effective Wave-Lengths of 129 Stars within 0°5 of the North Pole and of the Σ Companion of Polaris . . . 370

Hulburt, E. O. The Broadening of the Balmer Lines of Hydrogen with Pressure . . . 399

Kannenstine, Fabian M. Formation and Life of Metastable Helium . 345

Kapteyn, J. C., and P. J. Van Rhijn. On the Upper Limit of Distance to Which the Arrangement of Stars in Space Can at Present Be Determined with Some Confidence. . . . 242

First Attempt at a Theory of Arrangement and Motion of the Sidereal System. . . . 302

King, Arthur S. Electric Furnace Experiments Involving Ionization Phenomena. . . . 380

Note on the Thickness of Air Required to Produce the Atmospheric Absorption Bands A, *a*, and B . . . 411

Lindblad, Bertil. Spectrophotometric Methods for Determining Stellar Luminosity. (*See also* Correction, p. 413) . . . 85

Lunt, Joseph. On the System of Procyon . . . 71

PAGE

Meggers, W. F., Paul D. Foote, and F. L. Mohler. The Excitation of the Enhanced Spectra of Sodium and Potassium in a Low Voltage Arc 145

Mohler, F. L., Paul D. Foote, and W. F. Meggers. The Excitation of the Enhanced Spectra of Sodium and Potassium in a Low Voltage Arc 145

Oepik, E. The Distance of the Andromeda Nebula 406

Russell, Henry Norris. The Theory of Ionization and the Sun-Spot Spectrum 119

On the Calculation of Masses from Spectroscopic Parallaxes . . 238

Notes on Ionization in the Solar Atmosphere 354

St. John, Charles E., and Harold D. Babcock. An Investigation of the Constancy in Wave-Length of the Atmospheric and Solar Lines . 36

Sanford, R. F. The Orbits of the Spectroscopic Binaries ι Hydrae and 75 Cancri 30

Seares, Frederick H. The Masses and Densities of the Stars . . 165

Comparison Stars for Nova Persei, No. 2—A Correction . . . 272

Slipher, V. M. The Spectrum of the Corona as Observed by the Expedition from the Lowell Observatory at the Total Eclipse of June 8, 1918 73

Strömberg, Gustaf. Systematic Corrections to Spectroscopic and Trigonometric Parallaxes 11

Tanch, J. W., and H. S. Uhler. The Arc Spectra of Gallium and Indium. 291

Uhler, H. S., and J. W. Tanch. The Arc Spectra of Gallium and Indium. 291

Van Rhijn, P. J., and J. C. Kapteyn. On the Upper Limit of Distance to Which the Arrangement of Stars in Space Can at Present Be Determined with Some Confidence. 242

THE ASTROPHYSICAL JOURNAL

THE UNIVERSITY OF CHICAGO PRESS
CHICAGO, ILLINOIS

THE CAMBRIDGE UNIVERSITY PRESS
LONDON

THE MARUZEN-KABUSHIKI-KAISHA
TOKYO, OSAKA, KYOTO, FUKUOKA, SENDAI

THE MISSION BOOK COMPANY
SHANGHAI

THE

ASTROPHYSICAL JOURNAL

An International Review of Spectroscopy and
Astronomical Physics

EDITORS

George E. Hale
Mount Wilson Observatory of the Carnegie
Institution of Washington

Edwin B. Frost
Yerkes Observatory of the
University of Chicago

Henry G. Gale
Ryerson Physical Laboratory of the
University of Chicago

COLLABORATORS

Joseph S. Ames, *Johns Hopkins University;* Aristarch Belopolsky, *Observatoire de Poulkova;* William W. Campbell, *Lick Observatory;* Henry Crew, *Northwestern University;* Charles Fabry, *Université de Paris;* Alfred Fowler, *Imperial College, London;* Charles S. Hastings, *Yale University;* Heinrich Kayser, *Universität Bonn;* Albert A. Michelson, *University of Chicago;* Hugh F. Newall, *Cambridge University;* Ernest F. Nichols, *Nela Laboratory, Cleveland;* Alfred Perot, *Paris;* Carl Runge, *Universität Göttingen;* Henry N. Russell, *Princeton University;* Sir Arthur Schuster, *Twyford;* Frank Schlesinger, *Yale Observatory*

VOLUME LVI

JULY–DECEMBER, 1922

THE UNIVERSITY OF CHICAGO PRESS
CHICAGO, ILLINOIS

Published
July, September, October, November, December, 1922

Composed and Printed By
The University of Chicago Press
Chicago, Illinois, U.S.A.

CONTENTS

NUMBER I

PAGE
The Voltage-Current Relation in Central Anode Photo-Electric Cells. Herbert E. Ives and Thornton C. Fry 1
The Width of Certain Lines of the Spectrum of Helium as a Function of Pressure in the Source. Lloyd W. Taylor 16
On Einstein's Aberration Experiment. C. V. Raman 29
The Quantum Theory of the Spectrum of Hydrogen. H. A. Wilson 34
Interferometer Observations of Double Stars. Paul W. Merrill . 40
A Determination of the Wave-Lengths of 118 Titanium Lines by Means of the Interferometer. Frederick L. Brown . . . 53
Minor Contributions and Notes: Majorana's Theory of Gravitation. A. S. Eddington 71

NUMBER II

Revision of the Series in the Spectrum of Strontium. F. A. Saunders 73
Further Evidences on the Brightness of the Stars of the North Polar Sequence. Frederick H. Seares and Milton L. Humason . 84
Revised Magnitudes for Stars near the North Pole. Frederick H. Seares 97
On the Spectrum of Neutral Helium. Ludwik Silberstein . . . 119
The Variable Double Star X Ophiuchi. C. H. Gingrich . . . 132
Parallaxes of Stars in the Region of B.D.+31°643. C. H. Gingrich 139

NUMBER III

J. C. Kapteyn, 1851–1922. A. van Maanen 145
Visible and Infra-Red Radiation of Hydrogen. Frederick Sumner Brackett 154
A General Study of Diffuse Galactic Nebulae. Edwin Hubble . 162
Investigations on Proper Motion, Seventh Paper. Adriaan van Maanen. 200
Investigations on Proper Motion, Eighth Paper. Adriaan van Maanen. 208
Corrigenda 216

NUMBER IV

PAGE

THE CEPHEID VARIABLE η AQUILAE. Charles Clayton Wylie 217

THE ECLIPSING BINARY σ AQUILAE. Charles Clayton Wylie 232

A SPECTROSCOPIC METHOD OF DETERMINING THE ABSOLUTE MAGNITUDES OF A-TYPE STARS AND THE PARALLAXES OF 544 STARS. Walter S. Adams and Alfred H. Joy 242

THE DISTRIBUTION OF THE VELOCITIES OF STARS OF SPECTRAL TYPES F TO M. Gustaf Strömberg 265

THE APPLICATION OF VACUUM THERMOCOUPLES TO PROBLEMS IN ASTROPHYSICS. Edison Pettit and Seth B. Nicholson 295

THE ELECTRIC FURNACE SPECTRUM OF IRON IN THE ULTRA-VIOLET, WITH SUPPLEMENTARY DATA FOR THE BLUE AND VIOLET. Arthur S. King 318

CHANGES IN THE SPECTROGRAPHIC ELEMENTS OF Y SAGITTARII. John C. Duncan. 340

PREPARATION OF ABSTRACTS 344

NUMBER V

ASTRONOMICAL PHOTOGRAPHIC PHOTOMETRY AND THE PURKINJE EFFECT. II. F. E. Ross 345

THE SPARK SPECTRUM OF GALLIUM IN AIR AND IN HYDROGEN. Elias Klein 373

THE ABSENCE OF OXYGEN AND WATER-VAPOR LINES IN THE SPECTRUM OF VENUS. Charles E. St. John and Seth B. Nicholson 380

THE SOURCE OF LUMINOSITY IN GALACTIC NEBULAE. Edwin Hubble . 400

ORBIT OF THE ECLIPSING BINARY TW ANDROMEDAE. Martha Betz Shapley. 439

ORBITS OF THE SPECTROSCOPIC BINARIES LALANDE 13792 AND AOE 12584. R. F. Sanford 446

STELLAR SPECTRA OF CLASS S. Paul W. Merrill 457

THE BEHAVIOR OF SPECTRAL LINES AT THE POSITIVE POLE OF THE METALLIC ARC. Paul W. Merrill 475

GEOMETRICAL PROOF FOR THE WADSWORTH CONSTANT DEVIATION SYSTEM. R. C. Gibbs and J. R. Collins 483

REVIEWS: *The Telescope*, Louis Bell (A. S. Y.), 486; *Geschichte und Literatur der veränderlichen Sterne*, G. Müller and E. Hartwig (J. A. Parkhurst), 488.

INDEX 489

THE
ASTROPHYSICAL JOURNAL
AN INTERNATIONAL REVIEW OF SPECTROSCOPY
AND ASTRONOMICAL PHYSICS

VOLUME LVI JULY 1922 NUMBER 1

THE VOLTAGE-CURRENT RELATION IN CENTRAL ANODE PHOTO-ELECTRIC CELLS

By HERBERT E. IVES and THORNTON C. FRY

ABSTRACT

Current-voltage relation in a central-anode vacuum photo-electric cell as a function of the frequency of the exciting radiation.—In the case of some potassium cells it was observed that the higher the frequency of the light the higher the voltage required for saturation. The *mathematical theory* was then developed for the case of a spherical anode of radius b at the center of a spherical cathode of radius a. Electrons emitted from a photo-sensitive spot on the cathode describe elliptic orbits determined in each case by the initial direction and velocity and by the electric field. If the maximum velocity of emission of the electrons for radiation of frequency ν is v_m, where $\frac{1}{2}mv_m^2=h(\nu-\nu_0)$, the minimum difference of potential for saturation comes out $V_s=h(\nu-\nu_0)(a^2-b^2)/cb^2$. Assuming that the distribution as to direction follows the cosine law and that the distribution as to energy follows a parabolic law with a maximum at half the limit set by the quantum relation $\frac{1}{2}mv_m^2=h(\nu-\nu_0)$, then the fraction of saturation for any voltage below V_s is $1-\{(a^2-b^2)/a^2\}\{1-V/V_s\}^3$. For an assumed case of $a/b=15$ and $\nu_0=5\times10^{14}$, (6000 A), V_s comes out 40 and 160 volts for radiation of wave-length 5500 A and 4500 A respectively. These differences agree as to order of magnitude with some *experimental observations* shown in Figure 7. This effect should evidently be taken into consideration whenever such cells are used to compare the intensities of radiations of different spectral distributions.

1. *Introduction.*—The type of photo-electric cell most commonly used at the present time consists of a cathode in the form of a spherical shell of sensitive material (e.g., potassium on the inside of a glass bulb) together with a centrally placed anode in the form of a loop or grid. This construction is the exact opposite of that which would be chosen if we desired to reach the saturation current at low voltages. Probably this is not a serious disadvantage in the

majority of uses to which photo-electric cells are put, particularly as most of the cells employed for light-measuring purposes are of the gas-filled type operating on high voltages in order to get the advantage of ionization by collision. What may be a serious matter, however, is the fact that the rate at which saturation is approached depends upon the wave-length of the incident light.

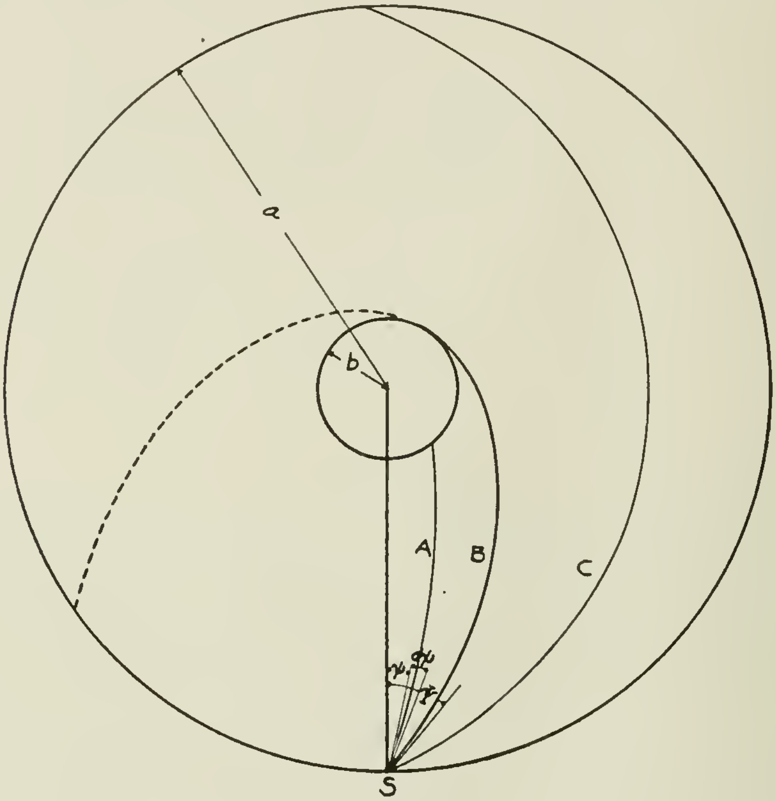

FIG. 1.—Diagrammatic central anode photo-electric cell

In other words, *the voltage current relation is different for light of different colors.*

This effect was discovered in the course of some experiments conducted with other objects in view upon a series of potassium photo-electric cells. In every cell measured it was found that the rate at which the current rose toward saturation with increasing voltage was less the greater the frequency of the light used. This phenomenon appears not to have been noticed or discussed before, although we shall find in the study which follows that it is a necessary consequence of well-recognized laws of photo-electric emission.

2. *General theoretical considerations.*—For the purposes of a theoretical study we shall assume a photo-electric cell (Fig. 1) consisting of a spherical target of radius *b*, at the center of a spherical shell of conducting material, the radius of which is *a*. On the surface of the shell we assume a small spot of photo-sensitive material *S*. The bulb is assumed to have a window of negligible size through which the sensitive spot may be illuminated. The central sphere is to be connected to the positive side and the shell to the negative side of a battery the voltage of which can be varied at will.

If an electron is emitted from *S* it will traverse a path of some form or other under the action of the electrical field which exists between the two electrodes and ultimately will either collide with the target, and thus contribute to the current observed, as in the case of curve *A* (Fig. 1), or else it will collide with the spherical shell as in curve *C*, and thus be returned to the original circuit. The problem of determining the voltage-current characteristic of the tube is therefore identical with that of determining what proportion of the total number of electrons emitted traverse paths of such a shape as to bring them into collision with the central target.

The path traveled by an electron is completely determined by two initial properties. The one of these is the velocity with which the electron is emitted; the other is its initial direction relative to the radius of the sphere. If every electron possessed the same initial velocity and was shot off at the same angle with the radius as every other electron, all would describe similar paths, and therefore either all or none would be caught by the target. Under these circumstances no current whatever would flow until the potential difference between the electrodes reached a certain critical value, at which value the saturation current would suddenly come into being and would continue unchanged for all higher voltages.

It is obvious, therefore, that the current-voltage relation which we seek depends in a very vital way upon the distribution of initial velocities and initial directions among the electrons, and it is our problem to show the effect of each of these factors.

3. *The voltage-current relation when all electrons have the same initial velocity but not the same initial direction.*—Referring again

to Figure 1 we notice that, whatever the exact form of the electron's path, there must be a certain limiting angle Ψ possessing the property that all the electrons of the same initial velocity whose initial directions lie within a cone of central angle 2Ψ about the radius as an axis contribute to the observed photo-electric current, while those which have initial directions lying outside this cone do not. If we denote by n_0 the number of electrons emitted and adopt the symbol $\phi(\psi)d\psi$ to represent the fraction having initial directions which lie between cones of central angles 2ψ and $2(\psi+d\psi)$ about the radius as an axis, it is evident that the number reaching the anode is given by the formula

$$n=n_0\int_0^{\Psi}\phi(\psi)d\psi. \tag{1}$$

Since the limiting angle Ψ is a function of the potential difference between anode and cathode, it follows that the ratio $\frac{n}{n_0}$ is defined by (1) as a function of the voltage. Since this ratio is equal to the current if the saturation current is taken as the unit, we shall hereafter for simplicity speak of $\frac{n}{n_0}$ as "current." With this understanding, (1) is the equation of the voltage-current distribution for the case in which all electrons have like initial velocities. However, before it can be of any service to us, we must know both the relationship between Ψ and the potential difference V, and the nature of the distribution function $\phi(\psi)$.

Since the force between the two spheres is central and inversely proportional to the square of the distance from their common center, it follows that the path of an electron emitted from the shell is an ellipse having the center of the spheres as one of its foci. The curves A, B, and C of Figure 1 are drawn as such ellipses. If r and θ are polar co-ordinates referred to the focus of this ellipse as origin and its major axis as axis of co-ordinates, the equation of this ellipse is

$$r=\frac{v^2a^2\sin^2\psi}{\mu+\sqrt{\mu^2+(v^4a^2-2\mu v^2a)\sin^2\psi}\cos\theta}. \tag{2}$$

In this equation v and ψ are the initial velocity and direction, and

$$\mu = \frac{\frac{e}{m}V}{\frac{1}{b}-\frac{1}{a}}\,.$$

Once we know this equation for the trajectory, it is a simple matter to find the relation between V and Ψ. All that is necessary is to build up the condition that the least value of r as given by (2) shall be the radius b of the anode. It is obvious that this least value of r corresponds to $\theta=0$. Hence, setting $\theta=0$ and $r=b$ in (2) and solving for Ψ, we obtain the solution

$$\sin^2\Psi=\frac{b^2}{a^2}\left[1+\frac{2eV}{mv^2}\right]. \tag{3}$$

It should be noticed that the value of Ψ defined by (3) varies with both V and v. As the voltage is increased the sine of Ψ increases (and therefore Ψ itself increases) until the voltage becomes

$$V=\frac{mv^2(a^2-b^2)}{2eb^2}\,.$$

For this voltage $\Psi=\frac{\pi}{2}$, i.e., all electrons which leave the cathode are caught by the anode regardless of their initial directions. For higher potential differences it is obvious from physical considerations that the current must remain unchanged, a statement which may be translated into mathematical terms by saying that for all larger values of V the upper limit of integration in (1) shall be $\frac{\pi}{2}$.

We have thus established the relationship existing between Ψ and the potential difference V. This is one of the two facts which we have already said must be available before (1) can be computed. The other is the nature of the distribution function $\phi(\psi)$. With regard to this latter it seems quite reasonable to assume that the number of electrons emitted in unit solid angle in the direction ψ is proportional to $\cos\psi$, so that the fraction emitted between cones of central angles 2ψ and $2(\psi+d\psi)$ is

$$\phi(\psi)d\psi=2\sin\psi\cos\psi\,d\psi\,. \tag{4}$$

Introducing this formula into (1) and integrating between the limits 0 and Ψ we find that the current $\frac{n}{n_0}$ is either

$$\frac{n}{n_0} = \sin^2 \Psi = \frac{b^2}{a^2}\left[1 + \frac{2eV}{mv^2}\right] \tag{5}$$

or

$$\frac{n}{n_0} = 1 ,$$

according as V is less than or greater than the critical voltage at which saturation first occurs. The voltage-current relation therefore takes the form shown in Figure 2. When both cathode and anode are at the same potential the current is $\frac{b^2}{a^2}$ times the saturation current, and it increases linearly with the voltage until the critical potential $\overline{V}$ is reached, continuing unchanged for all higher voltages.

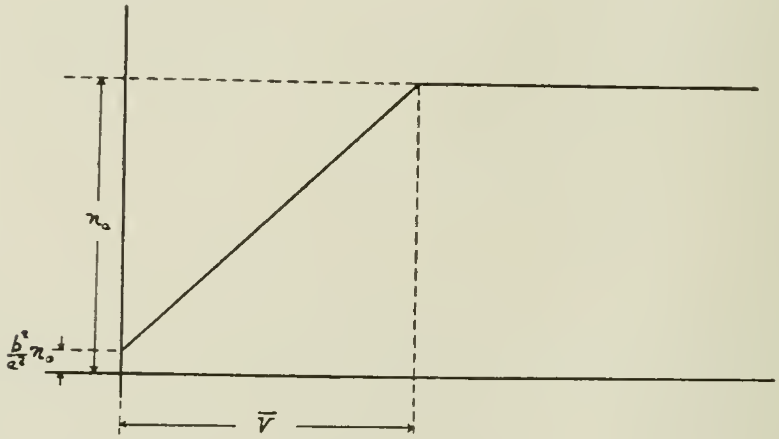

FIG. 2.—Voltage-current relation where electrons are emitted in all directions at a single velocity.

All of this is on the assumption that all electrons are emitted with the same initial velocity. Our next problem will be that of determining what conditions exist when this is not true.

4. *The voltage-current relation when both initial direction and initial velocity are different for different electrons.*—Let us assume that all the electrons shot off from the cathode are grouped into classes, the individual members of which have approximately the same velocity. Let us call the total number shot off n_0 and denote

by $f(v)dv$ the proportion of these which have velocities between v and $v+dv$. Each of these classes will have its own current-voltage curve similar to the one shown in Figure 2, but the curves for different classes will differ from one another in two important respects: (*a*) Since the number of electrons is not the same for all classes, the horizontal portion of the curve will not be at the same height in every case. (*b*) Since $\overline{V}$ varies with the initial velocity v, the voltage at which the break in the curve occurs will differ from one class to another. For this reason a set of voltage-current curves for the separate classes would present somewhat the appearance shown in Figure 3, where the larger subscripts indicate the larger values of v. Each of these curves represents a fraction of the total current observed. The complete current for any voltage may obviously be obtained by taking the sum of all the ordinates corresponding to that voltage. Since these different ordinates correspond to different values of v this sum must of necessity take the form of an integral with respect to v. It only remains to determine the nature of the integral.

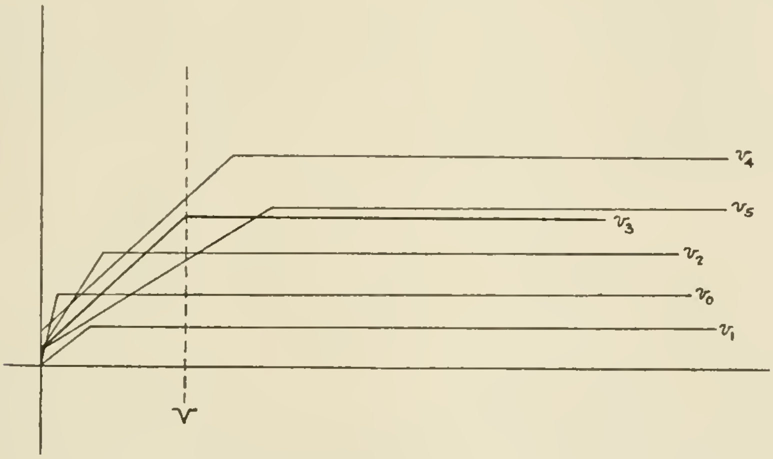

FIG. 3.—Current increments due to groups of electrons emitted in all directions at different velocities.

Consider the ordinates for the value of V shown in Figure 3. For the three lowest values of v, which have been called v_0, v_1, and v_2, respectively, this voltage is sufficiently high to produce the saturation current. The ordinate is therefore

$$n_0 f(v) \tag{6}$$

in each case.

For the curves v_4 and v_5 the voltage V is not large enough to produce the saturation current, and therefore the ordinate instead of being equal to $n_0 f(v)$ is smaller than this by a factor determinable from the equation of the sloping portion of the curve. Referring to equation (5) we find that under these circumstances the ordinate is

$$n_0 f(v)\frac{b^2}{a^2}\left[1+\frac{2eV}{mv^2}\right]. \tag{7}$$

For the particular velocity v_3, the break comes exactly at the voltage V, so that for this one velocity either (6) or (7) is a legitimate formula.

Since the formula for our ordinates is different according as v is less than or greater than v_3 we cannot express their sum by means of one integral, but must break up the sum into two integrals taken over appropriate ranges. The result is:

$$\frac{n}{n_0}=\int_0^{v_3} f(v)dv+\int_{v_3}^{\infty} f(v)\frac{b^2}{a^2}\left[1+\frac{2eV}{mv^2}\right]dv. \tag{8}$$

Before this formula can actually be evaluated we must know two things: (1) the relation between v_3 and the potential V, and (2) the nature of the velocity distribution function $f(v)$. The first of these is the velocity for which the critical voltage $\overline{V}$ is the particular value of V with which we are dealing. It follows immediately from the definition of $\overline{V}$ that it is

$$v_3=\sqrt{\frac{2eb^2V}{m(a^2-b^2)}}. \tag{9}$$

The distribution of the electrons according to velocity must be obtained from the field of experimental photo-electricity. A satisfactory theoretical formula has not as yet been found for this, so that we must adopt an empirical one. As a guide to a choice of such a formula we note the experimental findings that

a) There are no electrons having energies greater than $h(\nu-\nu_0)$ where h is the quantum constant, ν is the frequency of the incident light, and ν_0 is the frequency of the longest radiation which is capable of causing emission.

b) The number of electrons having *energies* between 0 and $h(\nu-\nu_0)$ may be represented approximately by a curve which is symmetrical about the mean value of the energy.

For purposes of calculation we have assumed this curve of energies, symbolized by α, to be a parabola cutting the energy axis at 0 and $\alpha_m=h(\nu-\nu_0)$, (Fig. 4), and symmetrical about the mean energy $\frac{\alpha_m}{2}$. The equation of this parabola is

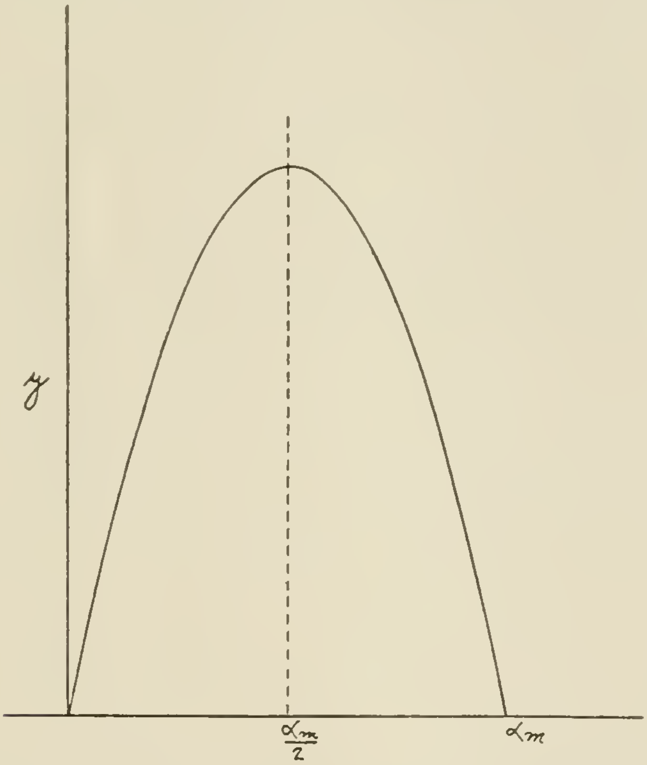

Fig. 4.—Assumed distribution of electrons according to energy of emission

$$y=n_0\left[1-\left\{1-\frac{2\alpha}{\alpha_m}\right\}^2\right], \tag{10}$$

and therefore $y\,d\alpha$ represents the number of particles having energies between α and $\alpha+d\alpha$.

Since energy is proportional to the square of velocity it follows that $\frac{\alpha}{\alpha_m}=\frac{v^2}{v_m^2}$, where v_m is the largest velocity of emission which any of the electrons can have. Substituting this value in (10) we obtain as the number of electrons with velocities between v and $v+dv$ the function

$$n_0 f(v)dv = 4n_0\left[\frac{v^2}{v_m^2}-\frac{v^4}{v_m^4}\right]d\alpha = \frac{8n_0\alpha_m}{v_m^2}\left[\frac{v^2}{v_m^2}-\frac{v^4}{v_m^4}\right]v\,dv\,. \qquad (11)$$

We have now determined both of the quantities necessary to enable us to integrate (8). Carrying out these integrations we find that

$$\frac{n}{n_0}=\frac{b^2}{a^2}+\frac{a^2-b^2}{a^2}\left[3-3\frac{v_3^2}{v_m^2}+\frac{v_3^4}{v_m^4}\right]\frac{v_3^2}{v_m^2}=1-\frac{a^2-b^2}{a^2}\left[1-\frac{v_3^2}{v_m^2}\right]^3. \qquad (12)$$

This is the equation of the current-voltage curve. It shows that the current increases steadily with v_3 (which, as is easily seen from equation [9], means that the current increases steadily with voltage) until, when the value $v_3=v_m$ is reached, saturation occurs. For larger voltages it is obvious from physical conditions that the current no longer increases and that therefore $\frac{n}{n_0}=1$. The potential at which saturation occurs is easily found by equating v_3 to v_m. Since

$$\alpha_m=\frac{mv_m^2}{2}=h(\nu-\nu_0)$$

and

$$v_3^2=\frac{2eb^2V}{m(a^2-b^2)}$$

it is

$$V_s=\frac{h(\nu-\nu_0)(a^2-b^2)}{eb^2}.$$

Also, since

$$\frac{v_3^2}{v_m^2}=\frac{V}{V_s},$$

(12) reduces to the simple form

$$\frac{n}{n_0}=1-\frac{a^2-b^2}{a^2}\left[1-\frac{V}{V_s}\right]^3. \qquad (13)$$

Computations have been made from formula (13) for $\frac{b}{a}=\frac{1}{15}$, and for radiations of which the frequencies and wave-lengths are

$\nu_0 = 500.0 \cdot 10^{12}$ $(\lambda_0 = 6000 \text{ A})$
$\nu_1 = 545.5 \cdot 10^{12}$ $(\lambda_1 = 5500 \text{ A})$
$\nu_2 = 666.7 \cdot 10^{12}$ $(\lambda_2 = 4500 \text{ A})$

The results of these computations are shown in Figure 5. The curves show that if the assumptions which we have made are correct we may expect the current to rise to complete saturation only at fairly high voltages—40 in the case of illumination by a wave-length only 500 A from the limiting wave-length, 160 for a wave-length 1500 A from the same limit. If these computations are correct they mean that, in the design of cell considered, an initial difference of velocities corresponding to only half a volt results in diverting electrons from the anode which can only be recovered by an applied field of over a hundred volts. The ratio between photo-electric currents produced by two different wave-lengths may vary by a factor of as much as two, depending on whether or not the complete saturation voltage is used.

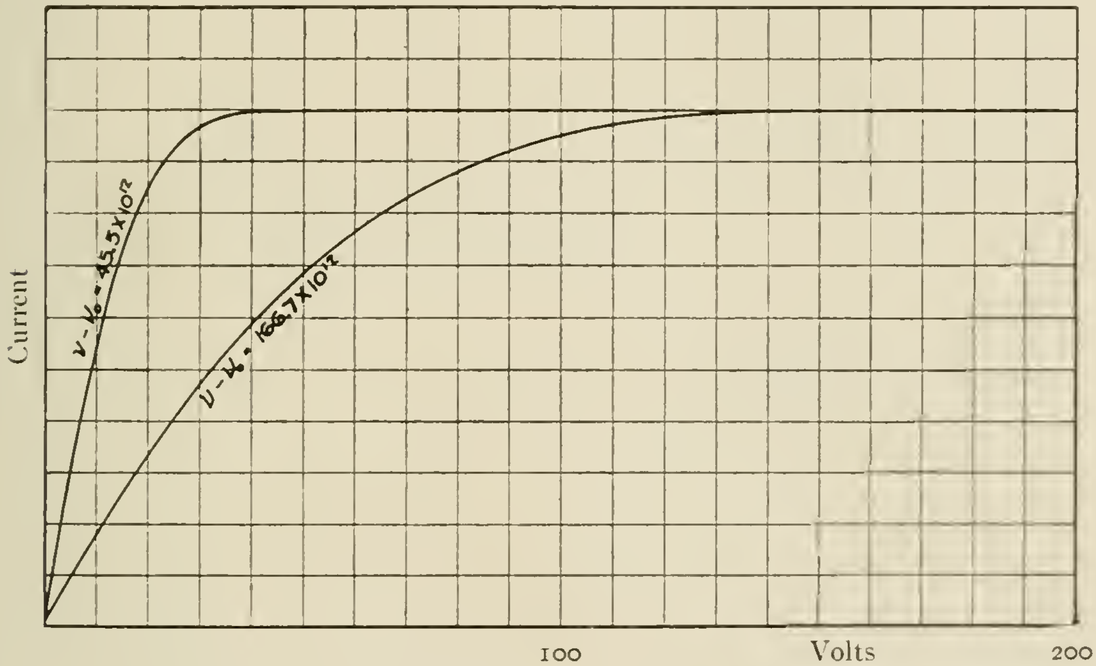

Fig. 5.—Computed voltage-current curves for two different wave-lengths of exciting radiation.

5. *Experimental confirmation.*—The curves of Figure 5 are not greatly different from those obtained with the central grid potassium

cells in which the effect was first observed. However, in order to approximate more closely to the conditions assumed in the computations, a special cell was built. This is shown diagrammatically with its dimensions in Figure 6. The outer shell was of glass and was silvered on the inside except for a small window *W*. The anode A was a brass ball ($b = \frac{1}{15} a$ as in the computed case) carried on a slender wire leading out through the stem, to which

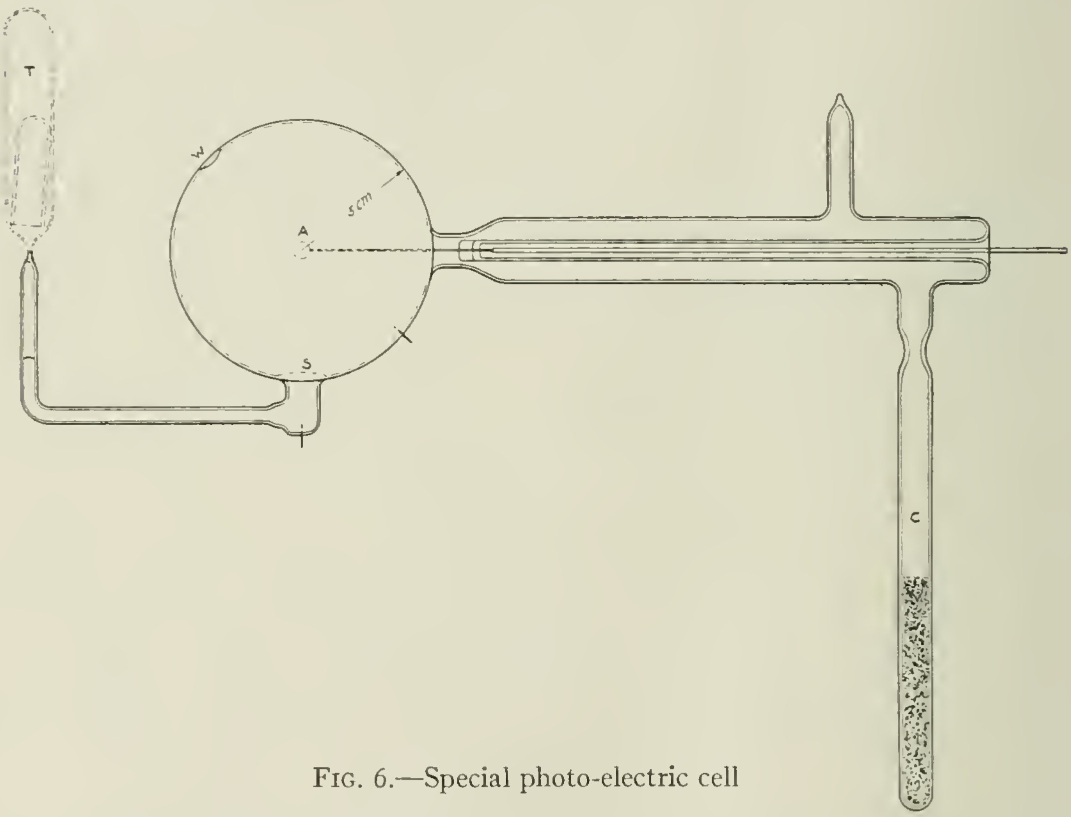

Fig. 6.—Special photo-electric cell

was connected a charcoal tube *C*. In preparing the cell, the whole structure was first thoroughly baked out on the pump at 350° C. Then a pyrex glass tube of vacuum-distilled potassium was introduced into the side tube *T*. Finally after long pumping and roasting of the charcoal in *C*, the potassium was melted and ran into the bulb through the connecting tube, forming a pool at *S*.

This cell was investigated for its voltage-current relation by illuminating the potassium with an incandescent lamp, the light from which passed through colored glasses. Currents were measured by a wall galvanometer. It was found that it was sensitive to the whole visible spectrum, so that the limiting wave-length must lie in the infra-red. In this respect it differs from the cell assumed in the theoretical study ($\lambda_0 = 6000$), but inspection of the theoretical development shows that the actual limiting wave-length is of no special consequence, since the computations depend only upon the amount by which the wave-length of the incident light differs from this limiting wave-length.

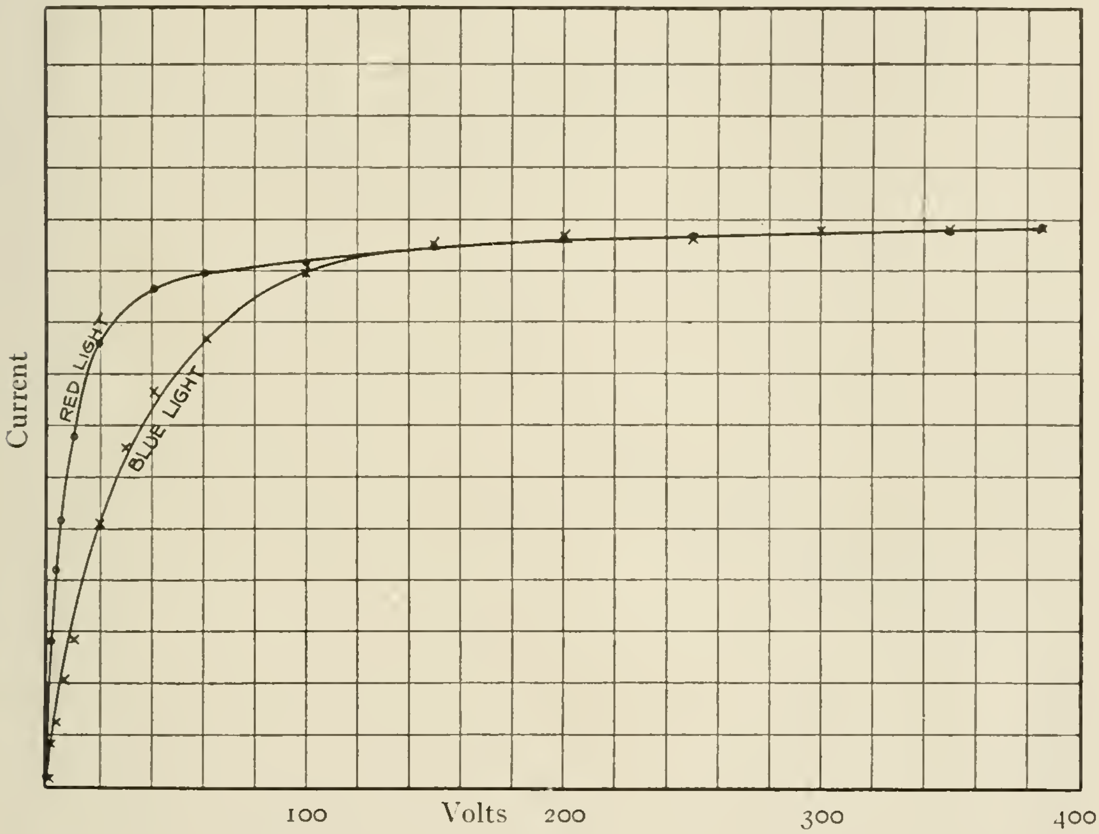

FIG. 7.—Observed voltage-current relation for red and blue light

Figure 7 shows two voltage-current curves; one taken with a monochromatic red glass, the other with a fairly monochromatic blue glass, the illumination being so adjusted that the currents at 400 volts were equal in both cases. Comparison of these curves with those of Figure 5 shows that the predictions of the theory are substantially correct. The rather close similarity in shape of the predicted and experimental curves may be taken to show that the various assumptions as to the distribution of emission with respect to direction and velocity are not seriously incorrect. However, the experimental red-blue curves lie closer together than is to be expected from the theory, since they are separated by somewhat less than the amount computed for a yellow-blue frequency difference. This quantitative discrepancy is probably to be ascribed to some effect of residual gas, and is being investigated further.

6. *Discussion.*—Two fields suggest themselves in which this effect may influence the interpretation of measurements made with the photo-electric cell. One is in the determination of spectral distribution of response in connection with theories of the photo-electric effect. Unless a potential difference of several hundred volts is used (where the frequencies utilized cover a range as great as the visible spectrum), the resultant curves connecting wave-length and response will be distorted. A second field is in the use of photo-electric cells for investigating color relations, such as the color indices of stars. For any such application the cell must obviously be calibrated and used at one definite voltage,

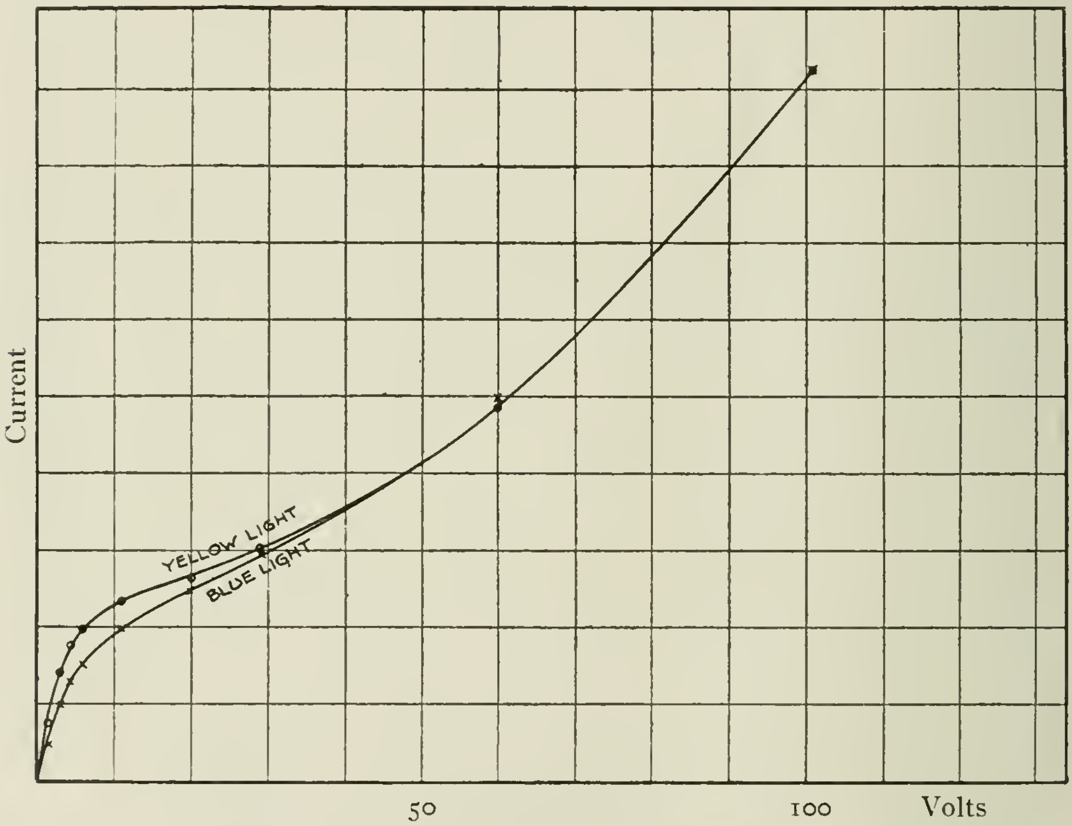

FIG. 8.—Observed voltage-current relation for yellow and blue light, in gas-filled cell.

unless the voltage employed produces complete saturation. In this connection a pertinent question is whether these differences in the current relation are present in a gas-filled cell. The answer is that in general they are, as is shown by Figure 8, presenting data obtained with a gas-filled cell with a grid anode closely similar to those which have been used in stellar photometry. However, owing to other factors which may be discussed in a future communication, the presence of the gas frequently acts in such a way as to diminish the effect here described.

Research Laboratories of the American
Telephone and Telegraph Co., and the
Western Electric Company, Inc.
March 14, 1922

THE WIDTH OF CERTAIN LINES OF THE SPECTRUM OF HELIUM AS A FUNCTION OF PRESSURE IN THE SOURCE

By LLOYD W. TAYLOR

ABSTRACT

Visibility-curve photometer for measuring the width of spectrum lines.—In the visibility-curve method, the difference of path of the two beams of light in a Michelson interferometer is increased until the visibility of the circular fringes drops to half its maximum value. To enable the visibility as a function of path difference to be determined more accurately, a comparison system of circular fringes of known and variable visibility was provided by means of a concave plate of doubly refracting crystal (selenite) placed in a beam of monochromatic plane-polarized light and viewed through a nicol prism. The two systems of fringes appeared side by side, and readings were taken by rotating the crystal plate about its axis of symmetry until both systems were equally visible. In this way line widths of from 0.03 to 0.12 A were measured within a few per cent.

Widths of three helium lines as a function of pressure.—Pure helium was excited in an ordinary Plücker tube by means of a transformer. *The effect of varying the power input* was found to be small, in fact multiplying the power by $4\frac{1}{2}$ increased the width only 12 per cent. Also a change of capillary diameter from 1 mm to 2 mm did not affect the results. Using a constant power of about 9 watts, the widths of the *lines* λλ *6678, 5876, and 5016* were measured to pressures of 12, 35, and 22 cm respectively. Contrary to expectation, the widths do not increase quite linearly with the pressure but approximately according to the formulae: $2W(6678)=.045+.0088p-.0002p^2$; $2W(5876, \text{ main component})=.040+.0034p-.00012p^2$; $2W(5016)=.030+.0045p-.0001p^2$; where p is in centimeters of mercury and $2W$ is in Angstroms.

INTRODUCTION

That the spectral lines into which the radiation emitted by incandescent gases or vapors may be resolved possess finite and measurable widths constitutes one of the most elementary considerations in the field of spectroscopy. It is almost equally well known that the width of any one of these lines is not constant, but varies with changing conditions. One of the factors thus affecting the width of spectral lines is the pressure which exists in the source.

The present investigation was undertaken for the purpose of discovering the relation which exists between pressure and width in some of the more prominent lines of the spectrum of helium. Three of these lines (λλ 5016, 5876, and 6678 respectively) have been studied. A preliminary report on one of them (λ 5876) was read before the American Physical Society on November 27, 1921.[1] The present article extends the somewhat limited conclusions that it was possible to make at that time concerning that line and makes a similar report on the other two named.

HISTORY

The first observation on record concerning the effect of pressure on spectral line width is that of Ångström[2] in 1853. Among other early observers may be mentioned Wüllner[3] and Frankland.[4] In 1889 Rayleigh[5] investigated theoretically molecular velocities in the line of sight (the Doppler effect) as a possible cause of the width of spectral lines. This is of course a temperature phenomenon. In two subsequent contributions, Michelson[6] extended Rayleigh's theory to include pressure effect, and at the same time published the first comprehensive experimental data. His observations on the pressure effect were made on the α line of hydrogen at pressures up to 9 cm of mercury, and on prominent lines in the spectra of a number of metallic vapors. His theory indicated linear increase of width with pressure, and his observations indicated that the theory furnished "a very good first approximation to the truth," since he had observed that in all cases investigated "when the pressure is increased, the width increases in a nearly linear proportion."

Rather steady contributions to this field were made during the twenty years subsequent to this work. All of this, as well as the earlier work, has been summarized by Stark,[7] who in a comprehensive publication outlines the status of our present knowledge of the width of spectral lines, and the factors affecting it. The results of several contributions, both theoretical and experimental, have been published since then. It is probable, however, unless some revolutionary discovery should be made, that Stark's publication will constitute the chief reference for some time to come concerning the facts and theories of the width of spectral lines.

---

[1] Taylor, *Physical Review*, **19**, 255, 1921.

[2] Ångström, *Annalen der Physik*, **94**, 141, 1855.

[3] Wüllner, *Annalen der Physik*, **137**, 339, 1869.

[4] Frankland, *Proceedings Royal Society*, **17**, 288, 1869.

[5] Rayleigh, *Nature*, **8**, 474, 1873.

[6] Michelson, *Philosophical Magazine*, **34**, 280, 1892; *Astrophysical Journal*, **2**, 251, 1895.

[7] Stark, *Jahrbuch der Radioaktivität*, **12**, 349, 1915.

PRELIMINARY CONSIDERATIONS

There are a number of factors known to influence the width of spectral lines. These may be classified in different ways, depending on the point of view. It will be convenient for our purpose to divide them into three groups: temperature, pressure, and electrical effects respectively. A number of experimental studies have been made recently on these factors, among which should be mentioned Buisson and Fabry[1] on temperature effect in some of the rare gases, Rossi[2] on the effect of high pressure in the hydrogen arc, and Merton[3] on electrical effects in helium. In general, there is less experimental material on the effect of pressure than on either of the other two. It is hoped that the present investigation may make a step toward supplying this deficiency.

There were several considerations pointing toward the advisability of using helium as the gas to be studied. One was the fact that under discharge-tube conditions its visible spectrum consists of a relatively few quite brilliant lines, sufficiently separated so that the present method of investigation was readily applicable. The second consideration was the familiar fact that helium will maintain the vacuum-tube type of discharge up to higher pressures than will any other gas.

Another consideration was its low atomic weight. There is considerable evidence to show that, other conditions being fixed, the width of a line is inversely proportional to the atomic or molecular weight of the gas constituting the source. There is some advantage therefore, particularly in the earlier stages of an experimental study, in choosing a gas of low atomic weight. And finally, its chemical inertness and the supposedly simple structure of its atom furnish every reason for accumulating all the data concerning its physical properties that can in any way be made available.

---

[1] Buisson and Fabry, *Journal de physique*, **2**, 442, 1912; *Comptes rendus*, **154**, 1349, 1912.

[2] Rossi, *Astrophysical Journal*, **34**, 299, 1911.

[3] Merton, *Proceedings Royal Society*, *A***95**, 30, 1918.

METHOD

In carrying out the experiment, the interference method known as that of visibility-curves has been chosen,[1] and the half-width of the lines as defined by the fall of visibility to one-half its maximum with increasing difference of optical path has been measured for different pressures. Two other methods were available: (1) direct measurement of width in a high-order spectrum such as that given by an echelon grating and (2) the interference method involving observation of the point at which the fringes in a Fabry-Perot interferometer cease to be visible with increasing distance between the mirrors. It is believed, however, that the visibility-curve method avoids the blunders which would be inevitable in the direct measurement of a length so small as that involved in the width of spectral lines, and also the high element of personal equation which is necessarily involved in any limit-of-perception method. The visibility method possesses the significant advantage that any maladjustment of the apparatus, or any shortcomings of the observer become immediately apparent, and the observer is furnished definite grounds for rejecting his observation.

The manipulative problem involved in the investigation was twofold: (1) the purification and control of pressure of the helium and (2) the taking of visibility data.

It is not considered necessary to enter into any detailed description of the purification system. The familiar method of passing the gas over hot copper oxide to remove hydrogen, and of absorbing other impurities by charcoal in liquid air, was used. A spectroscopic trace of neon existed in the purified gas at the higher pressures, and sufficient hydrogen to become just visible under a disruptive discharge, but not otherwise. The helium used as a source of supply came from the natural-gas fields of the Southwest, and was initially about 97 per cent pure. A Toepler pump was used for the double purpose of circulating the gas over the battery of purification tubes and of controlling the pressure of the purified helium in the discharge tube.

The optical part of the apparatus is shown in Figure 1. Light from a discharge tube is passed through a condensing lens into a

---

[1] Rayleigh, *Philosophical Magazine*, **27**, 298, 1889.

Michelson interferometer, which is adjusted for circular fringes. The emergent light is focused on to the slit of a prism spectrometer. On the images of the slit (whose aperture is maintained as wide as circumstances will permit) are seen the circular fringes from the interferometer. The line to be investigated is brought into the field of view of the telescope, and the visibility of the fringes measured, over as great a difference of path as they can be seen.

Direct estimation of the visibility of a set of interference fringes, except by an eye which has been exceedingly carefully trained, is a process whose precision is very questionable. It has accordingly been deemed advisable for the present investigation to construct what might appropriately be termed a "visibility photometer." It is well known that if a concave plate of doubly refracting crystal be placed in a beam of monochromatic, plane-polarized light and viewed through a nicol prism, a system of concentric rings will be seen, similar in appearance to the circular fringes just described. The "visibility" of these rings can be altered at will by rotating the crystal plate about its axis of symmetry, and is a relatively simple function of the angle between the optic axis of the crystal and the plane of polarization of the incident light. If such a system be projected into the field of view of the observing telescope, the observer sees side by side the

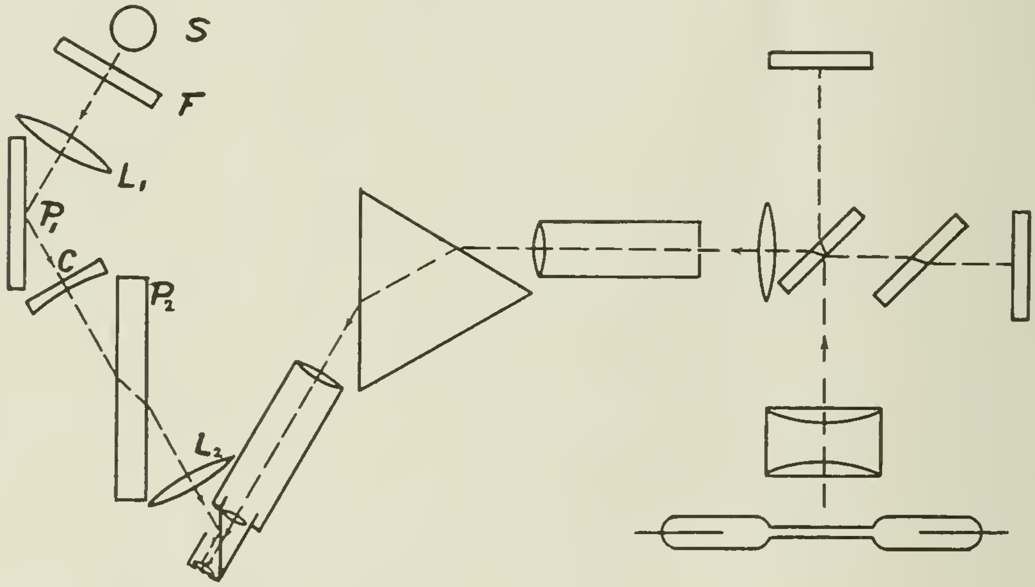

FIG. 1

two systems of circular fringes; one from the interferometer, having an unknown visibility, and the other from the comparison source, having a known and controllable visibility. If now the comparison fringes be caused to match the interferometer fringes and the orientation of the crystal noted, we have a direct measurement of visibility, possessing the degree of precision characteristic of any photometer measurement.

The application of this method is indicated in Figure 1. Light from an incandescent electric lamp *S*, screened by a filter *F* to a close color match with the line under observation, was reflected at the polarizing angle from a glass plate P_1, passed through the crystal *C*, and projected into the field of view of the telescope as shown. The second reflecting plate, which was mounted in the eyepiece, served as the analyzer. Collimating and telescopic lenses L_1 and L_2, and a glass-plate pile P_2, for initially matching the maximum visibility of the comparison system with that of the interferometer system, completed the equipment.

The source of illumination for the spectral lines studied was a Plücker tube of conventional type. Several different tubes were used in the course of the investigation. The only difference in their construction which could be of any conceivable importance in affecting line width was the size of the capillary portion. This was of 2 mm diameter in case of the study on λ 5876, and 1 mm in the case of the other two. Since there is a little evidence[1] that current density affects line width, several readings were taken on λ 5876 with a 1-mm tube as a source, other conditions being maintained the same as in earlier readings on the 2-mm tube. Line widths were found the same within the limits of experimental error.

The tube was excited from the secondary of a transformer energized by a 60-cycle alternating current. The potential difference necessary to excite a sufficient degree of luminescence varied from 400 to 1300 volts, and the average power consumption was in the neighborhood of 9 watts. This was sufficient to cause the tube to become almost dangerously hot, but was found necessary in order to give lines sufficiently strong for study at the higher pressures.

---

[1] Rossi, *Astrophysical Journal*, 40, 232, 1914.

Since it is known that line width depends upon temperature and electrical conditions (e.g., upon capacity and induction in the circuit) as well as upon pressure it was necessary to take precautions to maintain both of these conditions constant through the course of the investigation. Constancy of electrical conditions, aside from current and potential-difference, was easily maintained by measures so elementary that they do not need to be recounted. Preliminary experiments on temperature influence indicated that the conditions which must be satisfied in order to insure that the effect of temperature changes was negligible in comparison with the effect of pressure were not particularly exacting. The evidence was conclusive that temperature of a sufficient degree of constancy could be maintained by maintaining in the tube a constant power consumption. Hence the current was modified in inverse proportion to the potential-difference found necessary to drive a discharge through the tube at different pressures, and the assumption was made that constant power consumption satisfied sufficiently the condition of constant temperature. Needless to say, sufficient time was always allowed for the tube to reach a state of radiation equilibrium with its surroundings before any readings were taken.

For the purpose of determining roughly the effect of large changes in power consumption, visibility-curves have been run under different power consumptions. It was found that it was necessary to alter it through 100 per cent before the resulting change in width became at all measurable. With the consumption raised to four and one-half times its initial value, the increase in half-width of the lines became of the order of 12 per cent. Since during the course of this investigation the power consumption underwent a maximum variation of less than 20 per cent, it was considered that we were well within the limits of precision imposed by constant temperature.

Half-widths (W) were calculated from observations of the difference of path (Δ) necessary to cause a fall of visibility to half its maximum, in accordance with the familiar relation

$$W = \frac{.22}{\Delta} \lambda^2 .$$

As is well known, this relation is derived on the assumption that the distribution of intensity within the line follows an exponential law of the form

$$f(x)=e^{-k^2x^2},$$

where $f(x)$ represents intensity, x represents the distance on either side of the central maximum, and k is a constant. The "half-width," W, corresponds to a value $f(x)=1/2$, and is hence the distance from the *central maximum* to the point of half-intensity on either side. It is quite possible to adopt any other measure of the line width, provided that this be sufficiently defined. The one here given is, however, the convention which meets with general acceptance.

RESULTS

The results of the present investigation are summarized in Tables I, II, III, and IV, and are presented in graphical form in Figures 2, 3, 4, and 5. Each plotted ordinate on these curves represents the mean half-width as determined from measurements on from four to twelve visibility-curves taken on that line at that pressure.[1] This is not, of course, a sufficient number of observations to warrant any conclusion as to the "probable error." Aside from completeness in description of apparatus and procedure, the best criterion for the magnitude of the experimental error would probably be given by a publication of all of the visibility-curves

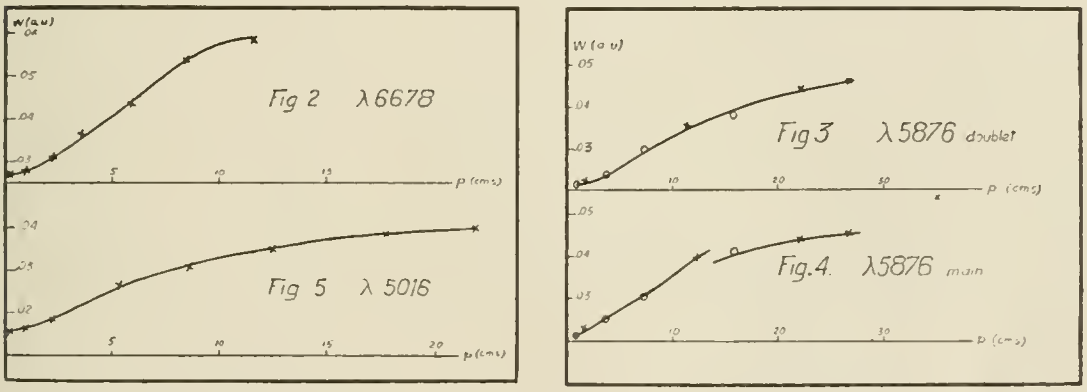

FIGS. 2, 3, 4, 5

---

[1] The conditions surrounding the highest-pressure readings on λ 5876 could not be duplicated, and since only one reading was possible, the degree of precision of the measurement of width at that pressure may be questioned. The reading is submitted, however, for what it is worth.

taken. Since this is scarcely feasible, the following data concerning deviations of values of the half-width from the mean value are given. It is to be noted that the closeness of agreement between different readings on the same line under the same conditions depends, in this type of investigation, mainly on the sensitivity of the eye to photometric matches of intensity, and that this depends largely on color. There is consequently some justification in grouping deviations from mean values of half-width separately for each line.

		λ 6678	λ 5876	λ 5016
Per cent of deviation from mean	maximum.......	3.9	6.8	5.4
	mean...........	1.7	3.0	2.2

TABLE I

$6678\ (1P)-(mD)$

Pressure (cm)	Δ (mm)	*W* (a.u.)
11.8........	16.8	.0584
8.4........	18.2	.0539
5.9........	22.5	.0436
3.5........	26.6	.0369
2.2........	31.5	.0312
0.9........	35.2	.0279
0.2........	36.4	.0220

TABLE II

$5876\ (1p)-(md)$

Pressure (cm)	Δ (mm)	*W* (a.u.)
35.3.......	14.0	.0543
26.9.......	16.3	.0460
22.3.......	17.2	.0442
15.8.......	20.0	.0380
11.3.......	21.5	.0354
7.3.......	25.5	.0298
3.6.......	32.1	.0237
1.6.......	34.0	.0224
0.8.......	35.9	.0212

TABLE III

5876 (Main)

Pressure (cm)	Δ (mm)	*W* (a.u.)
35.3........	14.0	.0543
26.9........	16.3	.0460
22.3........	17.2	.0442
15.8........	18.4	.0413
11.3........	19.0	.0400
7.3........	24.9	.0305
3.6........	30.0	.0253
1.6........	32.6	.0233
0.8........	35.7	.0213

TABLE IV

$5016\ (1S)-(mP)$

Pressure (cm)	Δ (mm)	*W* (a.u.)
22.0.......	13.8	.0401
17.8.......	14.2	.0389
12.5.......	15.7	.0352
8.6.......	18.0	.0308
5.3.......	20.6	.0269
2.2.......	30.7	.0181
0.9.......	33.8	.0164
0.2.......	35.4	.0157

There will be found in Figures 6–35 one visibility-curve for each line at each pressure. Each of these curves is the graphical "average" of all visibility-curves taken on that line at that pressure. As will be noted, the visibility-curves for λ 5876 represent a double source. In this case, the half-width is by common convention defined by the fall of the *envelope* of the visibility-curve to

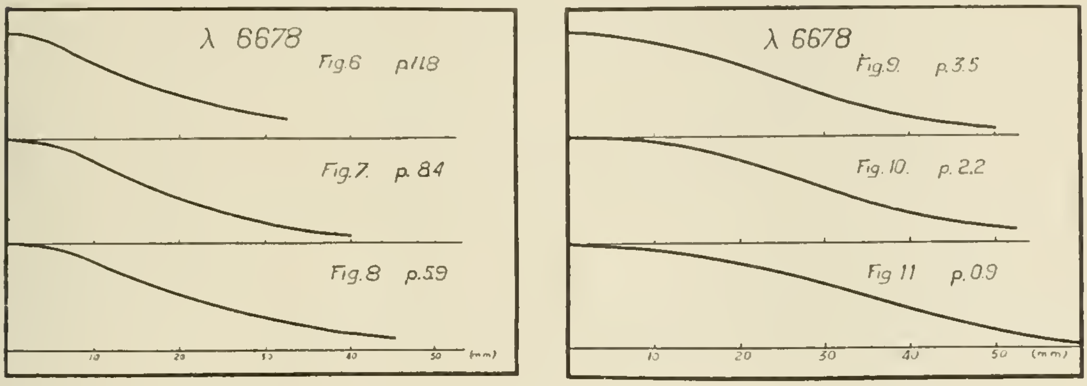

Figs. 6, 7, 8, 9, 10, 11

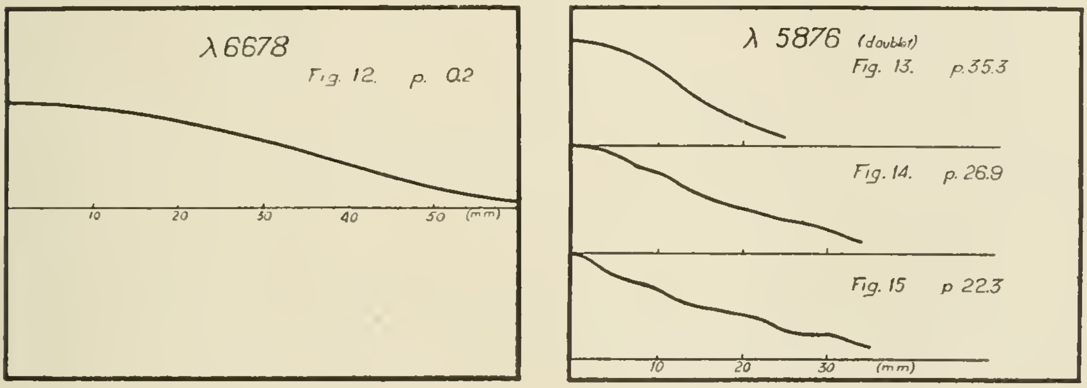

Figs. 12, 13, 14, 15

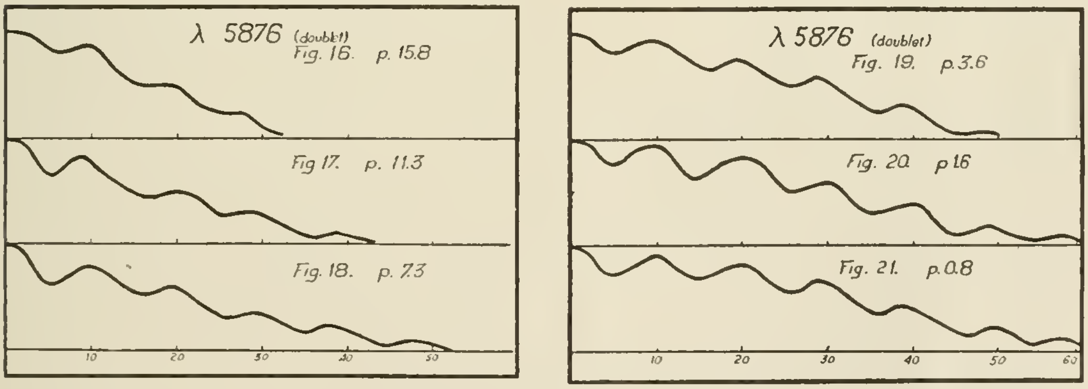

Figs. 16, 17, 18, 19, 20, 21

the ordinate representing half-visibility. The curves of Figures 22–27 do not constitute an independent set of readings, but are analyzed out of the curves of Figures 16–21 by methods which are immaterial here.[1] The minor components of λ 5876 are too faint to allow of any conclusive inference concerning its half-width.

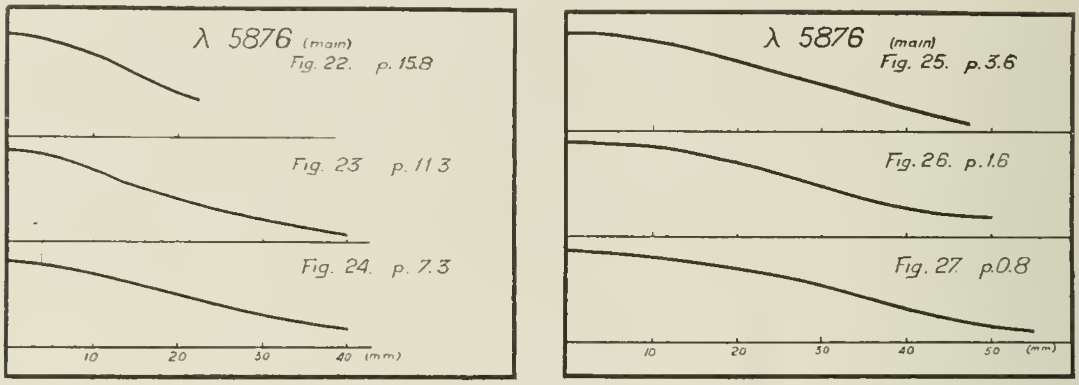

FIGS. 22, 23, 24, 25, 26, 27

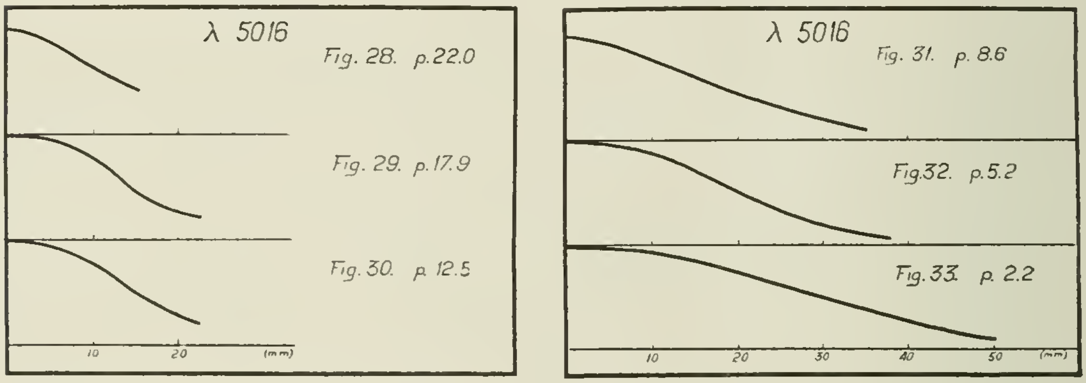

FIGS. 28, 29, 30, 31, 32, 33

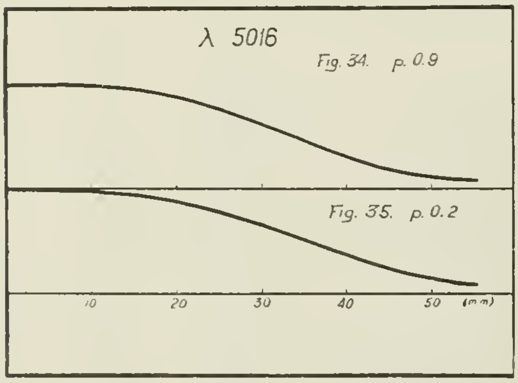

FIGS. 34–35

With increasing pressures, the intensity of the lines becomes continually lower. The point at which the intensity of any line became so low that accurate judgment of visibilities became impossible, determined the upper limit of pressure at which readings could be taken.

---

[1] With increasing pressure, the visibility-curve for the λ 5876 changed its character, possessing less the features of a doublet and more nearly those of a single source as the components merge into one another with increasing width. Above a pressure of 15.8 cm it became impossible to analyze out the visibility-curve for the main component, and from this point on no distinction was made between the width of the doublet and that of the mean component. This causes a discontinuity in the pressure-width curve (Fig. 4).

As will be noticed, the order in which this limit was reached with increasing pressure was λλ 6678, 5016, and 5876 respectively.

It will be noted that Figures 2–5 show that half-width is an increasing function of pressure, but *not* a linear function. The deviation from linearity is sufficiently small so that one could proceed over considerable ranges of pressure in properly chosen portions of the curves without any very startling deviation from a linear variation of half-width. In fact, on the occasion of the author's preliminary report, referred to above, at a time when the only information available was given by the four points designated with circles, the conclusion was drawn that "the half-width of the line is found to increase at a rate which is very nearly linear," and the statement was made that an attempt was under way to "materially extend the upper limit of pressure, in order to discover whether, at higher pressures, there may exist any notable deviation from this law."

Such a deviation seems to exist, under the conditions of this experiment. It is not of any very great magnitude, but it is too consistent, and too far outside of what may be considered the limits of experimental error, to be ignored. All available information on the theory of pressure-broadening, with one exception,[1] indicates a linear broadening with increase of pressure, a prediction which up to the present seems to have been confirmed by experiment. The discrepancy between these considerations and the observations submitted herewith has been the occasion for an exceedingly careful scrutiny of the work performed. Failure to find any circumstances outside of a real pressure-effect which might form a cause, has rendered advisable a rather minute description of the conditions under which the experiment was performed.

It should perhaps be remarked that the method used in this investigation does not permit the detection of any lack of symmetry in the broadening of the lines with increasing pressure. There is considerable evidence to show that, at least at the pressures used, no such asymmetry is to be expected. If it should occur, it would probably manifest itself in an apparent change of wave-length with changing pressure. An investigation is at present under way in this laboratory for the purpose of detecting whether any such "pressure-shift" is to be observed.

---

[1] Gianfranceschi, *Il Nuovo Cimento*, 18, 57, 1919.

SUMMARY

The widths of three of the prominent lines in the spectrum of helium have been measured for different pressures in the source. "Half-widths" have been found to increase with increasing pressures, at rates which exhibit consistent deviations from the linear one called for by the theory.

The method used was that of visibility-curve analysis.

The writer takes pleasure in acknowledging his indebtedness to Professor H. G. Gale, who suggested both the problem and the method, and who has maintained a constant interest throughout the course of the investigation; to Professor A. A. Michelson for the use of the interferometer and concave selenite plate which he himself had used in previous investigations; and to Mr. F. M. Kannenstine for valuable suggestions concerning the purification of the helium.

Ryerson Physical Laboratory
University of Chicago
March 10, 1922

ON EINSTEIN'S ABERRATION EXPERIMENT

By C. V. RAMAN

ABSTRACT

Aberration experiment proposed by Einstein to decide between the theories of light.—According to Einstein, if light from swift canal rays were focused on a slit and the transmitted rays were made parallel and were then focused on cross hairs, the image of the slit would be shifted when a plane-parallel layer of a dispersing medium such as CS_2 is placed in the path of the parallel rays, because, due to the motion of the canal rays, the light rays on one side of the beam would have a shorter wave-length than those on the other side and hence, if the ordinary wave theory is correct, the wave front should be rotated. It is here shown, however, that this conclusion is based on a misconception of the behavior of such wave fronts; that the position of the final image is independent of the relative wave-lengths of the different light rays; and that, therefore, no shift is to be expected either according to the wave theory or according to any other theory of light. Hence the experiment cannot help discriminate between the rival theories.

In a recently published communication[1] Einstein has suggested an experiment which according to him furnishes a method for deciding between the two alternative hypotheses regarding the nature of the elementary process of light-emission now holding the field, viz., the classical or undulatory theory in which light-waves are regarded as given out continuously from the luminous atom, and the quantum theory in which light is emitted as the result of an explosive act involving a definite energy-change in the atom and uniquely determining its frequency. It is proposed here briefly to summarize Einstein's paper and then to examine his arguments. It will be shown that his discussion of the phenomena to be expected is at fault and that in reality no effect is indicated by either theory and hence the proposed experiment will not serve to differentiate between them.

The proposed experiment is based upon J. Stark's well-known observation that the light emitted by the luminous atoms in the *Kanalstrahlen* exhibits the Doppler effect, the magnitude of the shift of wave-length depending on the angle between the line of movement of the atoms and the direction of observation. Einstein points out that according to the classical or undulatory theory, light is emitted from the atom simultaneously in different directions with different frequencies, and proposes to test whether this is actually the case in the following way:

---

[1] *Sitzung. Preuss., Akad. Wiss.*, 1921, p. 882.

In Figure 1, K represents a stream of canal rays, L_1 is a lens which focuses an image of the same on a slit S contained in an opaque screen. The light passing through the slit falls on a collimating lens L_2, which renders the beam parallel. The collimated beam then falls upon the object-glass of a telescope focused for infinity (not shown in the figure). An image of the slit S will then be seen in the field of view. Einstein puts forward the proposition that if now a plane-parallel layer of a dispersing medium, e.g., carbon disulphide, be put in between the lens L_2 and the observing telescope, a displacement of the image of the slit is indicated by the principles of the wave theory, the deviation angle α being given by the formula:

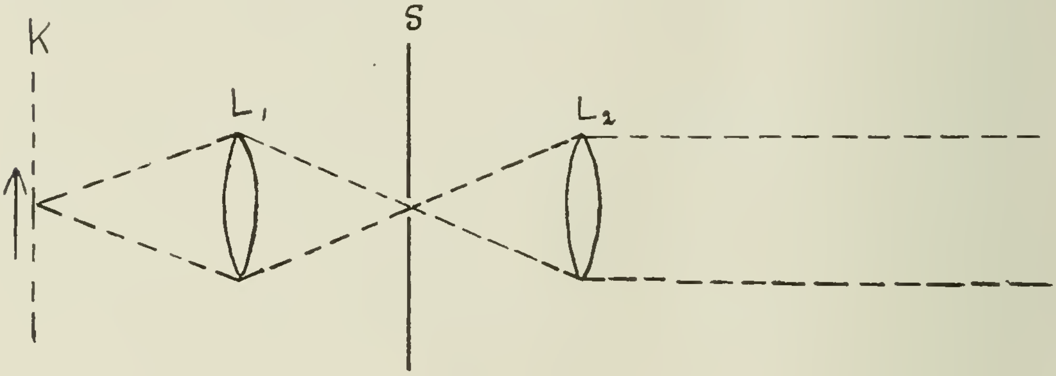

FIG. 1

$$\alpha = \frac{l}{\Delta} \cdot \frac{v}{c} \cdot \frac{dn}{\left(\frac{d\nu}{\nu}\right)} \tag{1}$$

where $\frac{v}{c}$ is the ratio of the velocity of the atoms in the *Kanalstrahlen* to the velocity of light, l is the thickness and n the refractive index of the dispersing medium, Δ is the distance SL_2; KL_1 and L_1S are assumed to be equal and ν is the frequency of the light.

We now proceed to indicate the argument on which Einstein bases his derivation of formula (1) which is briefly as follows: The surfaces of constant phase in the light from a luminous atom on emergence from the lens L_2 are obviously plane. But since the light falling upon the upper and lower edges of the lens system is according to the Doppler principle of different wave-lengths, the wave fronts after emergence from L_2 are not exactly parallel to each other but are slightly inclined in the manner of the leaves of a fan. If no dispersing medium be interposed, the wave fronts after passing through the object-glass of the observing telescope reach foci, which are not coincident but form an image of the slit of finite width in the same position as when the luminous atoms emitting the waves are at rest. If, however, between the lens L_2 and the observing telescope a plane layer of a dispersing medium be interposed, the conditions are altered. The upper and lower portions of the wave fronts correspond to different frequencies and therefore move forward with different velocities and hence the wave fronts swing round to a greater and greater extent proportionately with the length of the medium traversed. Einstein then supposes that as the result of this swinging round of the wave fronts, the image of the slit in the observing telescope should suffer a corresponding deflection the magnitude of which is given by formula (1).

The error in Einstein's reasoning enters at the last stage, that is, in his assuming that the swinging round of the wave fronts involves a deflection of the image of the slit in the focal plane of the observing telescope. Referring to Figure 1, we see that as a luminous atom moves along the stream of *Kanalstrahlen*, the waves emitted by it enter the slit S only for a limited period of time depending on its width, that is, the disturbance passing through it forms a wave-group of limited extension. It is perfectly true, as pointed out by Einstein, that when the disturbance enters a dispersing medium, the wave fronts in it swing round steadily as they pass through it. But the position of the image of the slit is determined not by the inclination of any particular wave front to the axis of the optical system, but by the normal to the wave group considered as a whole. It is easily shown that the latter remains fixed and does not turn round. The problem is exactly similar to that which arises in connection with Michelson's determination of the velocity of light in dispersive media by the revolving mirror method, and was very clearly dealt with by Willard Gibbs.[1] The group velocity is given by the relation

$$U = V - \lambda \frac{dV}{d\lambda}; \qquad (2)$$

the individual wave planes in the group rotate with an angular velocity

$$\frac{dV}{d\lambda} \cdot \beta$$

where β is the angle between successive wave planes; they also move forward through the group with a velocity $(V-U)$, and in the interval of time

$$\frac{\lambda}{(V-U)}$$

in which each wave plane moves into the position of the next in the group, it rotates through an angle

$$\beta \cdot \frac{dV}{d\lambda} \cdot \frac{\lambda}{(V-U)}$$

which by relation (2) is exactly β. Hence the second wave plane in passing a point moving with the group has exactly the same position which the first one had. Hence as the wave planes move out of the group and disappear and are followed by fresh ones, the inclination of the wave normal to the group considered as a whole remains fixed. In other words, after emerging from the layer of dispersing medium, the group would come to a focus in precisely the same position as when no dispersing medium is introduced.

The matter may also be viewed from another standpoint. Referring to Figure 1, it is clear that what is observed in the field of view of the telescope are not the moving luminous atoms but the fixed slit illuminated by the finite width of the pencil of canal rays. An appropriate method of treating the problem is therefore to regard the slit as a secondary source of light in accordance with the Fresnel-Huyghens principle. If the slit S be very narrow it may be simply regarded as a source of cylindrical waves which diverge from it in all directions, and in the disturbance reaching the lens L_2, all differences in the frequencies at different points would cease to exist and the image of the slit would be formed in the focal plane of the observing telescope according to the ordinary laws of geometrical optics. No difference would therefore be made by the interposition of a plane-parallel layer of dispersing medium. If the slit S be wider, we may conceive it to be divided up into a large number of very small elements, the image of each of which is formed in a fixed position in the same way as in the case of a very narrow slit, and precisely identical results are reached.

---

[1] *Nature*, April 1886, p. 582, and *Scientific Papers*, 1, 253.

That no displacement of the image in the slit in the observing telescope can occur on the introduction of a dispersing layer can also be shown on purely kinematical reasoning independent of any theory or hypothesis regarding the nature of light. To do this, we have merely to replace the stream of canal rays at K by a stationary source which emits light of different color in different directions, e.g., a small dispersing prism from which a spectrum diverges and falls upon the lens L_1 and which after being focused at the slit S and passing through the lens L_2 is viewed through the observing telescope. It is clear that the introduction of a dispersing layer bounded by parallel faces will not influence the observed position of the source in the field of view.

CALCUTTA
March 20, 1922

THE QUANTUM THEORY OF THE SPECTRUM OF HYDROGEN

By H. A. WILSON

ABSTRACT

Energy of an electron moving near a positive nucleus.—It is shown that, at least when the speed of the electron is small, an appreciable fraction of the mutual energy of the two charges lies near the electron and therefore may be expected to move with the electron and modify its motion as determined by the quantum equation. Hence the *influence of the field of the nucleus* is probably not negligible, as is ordinarily supposed.

Quantum theory of the doublets of hydrogen and of ionized helium.—Assuming a fraction ($f/2$) of the mutual energy of electron and nucleus moves with the electron, equations are derived for the energy in different orbits, which give Sommerfeld's expression for the separation of the doublets but multiplied by the factor $(1-f)$. Comparison of the observed separation of the hydrogen doublets (0.30) with that computed by Sommerfeld (0.365) indicates that f is about 0.2; that is, about one-tenth of the mutual energy may be moving with the electron. In the case of ionized helium, the agreement between calculation and observation indicates that f must be quite small.

In the quantum theory of the spectrum of atomic hydrogen, as developed by Bohr and Sommerfeld, it is assumed that the energy of an electron moving with a velocity v is equal to $m(1-\beta^2)^{-\frac{1}{2}}$ where m denotes its energy when at rest and $\beta=v/c$ where c denotes the velocity of light.

This expression for the energy of a moving electron follows from the electromagnetic theory of the motion of electrical systems and can also be deduced from the special theory of relativity. It is obtained in the case of an electron moving with uniform velocity in a straight line when no other charged bodies are present.

In the hydrogen atom the electron is supposed to be describing an orbit round the positive nucleus so that it is not clear that its energy can be taken equal to $m(1-\beta^2)^{-\frac{1}{2}}$ as though it were moving uniformly along a straight line.

Let the electron be a hollow sphere of electricity of amount e and radius a and let the positive nucleus be another one of amount E and radius b and let the distance between their centers be r. The electrostatic energy of the electron and nucleus when they are at rest is then

$$\frac{1}{2}\frac{e^2}{a}+\frac{1}{2}\frac{E^2}{b}+\frac{eE}{r}$$

the total energy is

$$\tfrac{2}{3}\frac{e^2}{a}+\tfrac{2}{3}\frac{E^2}{b}+\frac{eE}{r}$$

because the electron and nucleus must be supposed to contain internal energies $\frac{1}{6}e^2/a$ and $\frac{1}{6}E^2/b$ respectively.

If the electron and nucleus are supposed to be both moving with uniform velocity v in the same direction the total energy will be

$$\left(\tfrac{2}{3}\frac{e^2}{a}+\tfrac{2}{3}\frac{E^2}{b}+\frac{eE}{r}\right)(1-\beta^2)^{-\frac{1}{2}}$$

in accordance with the general principle that the energy of a system moving with uniform velocity in a straight line is equal to its energy when at rest multiplied by $(1-\beta^2)^{-\frac{1}{2}}$.

The energy $m(1-\beta^2)^{-\frac{1}{2}}$ of the electron, where $m=\frac{2}{3}e^2/a$, is located very near to its center because the energy density varies inversely as the fourth power of the distance, so that it is clear that this energy can be regarded as moving with the electron.

The energy $eEr^{-1}(1-\beta^2)^{-\frac{1}{2}}$ is distributed symmetrically about the nucleus and electron, when they are moving slowly, but is not concentrated near to them so that it is not clear that it can be regarded as associated with either of them although when both have the same velocity it certainly moves along with them.

If the nucleus is supposed fixed and the electron moving near it, then the energy $m(1-\beta^2)^{-\frac{1}{2}}$ is regarded as moving with the electron and the energy $2l(1-\beta^2)^{-\frac{1}{2}}$, where $l=eE/2r$, is usually regarded as remaining at rest. This makes the total energy equal to

$$m(1-\beta^2)^{-\frac{1}{2}}+2l+\tfrac{2}{3}\frac{E^2}{b},$$

so that if $\mathfrak{E}$ denotes the lost energy, or the difference between the energy when the electron and nucleus are at rest at a great distance apart and the energy in the orbit the electron is describing, then

$$\mathfrak{E}=m-m(1-\beta^2)^{-\frac{1}{2}}-2l,$$

which is the energy equation used in the quantum theory.

This equation is obtained by supposing that the mutual energy $2l$ remains at rest when the electron moves, which is evidently only approximately true, for when the velocity is small the energy $2l$ is symmetrically distributed about the two charges e and E so that its center of mass is halfway between them and so has a velocity equal to one-half that of the electron.

The distribution of the mutual energy $2l$ about the charges can be easily calculated when their velocities are small, since it is then approximately the same as when they are at rest.

Let A be the electron and B the nucleus. At any point P the electrostatic energy density, if $AP=s$ and $BP=t$, is

$$\frac{1}{8\pi}\left(\frac{e^2}{s^4}+\frac{E^2}{t^4}+\frac{2eE\cos\theta}{s^2t^2}\right),$$

where θ denotes the angle APB.

Let $\widehat{PAB}=\alpha$ and $\widehat{PBA}=\beta$ and consider the mutual energy in the ring-shaped element of volume between α and $\alpha+d\alpha$ and β and $\beta+d\beta$ formed by supposing the lines bounding $d\alpha$ and $d\beta$ to revolve round AB as axis. This element of volume is equal to

$$\frac{2\pi s^2t^2\,d\alpha\,d\beta}{r}$$

so that the mutual energy in it is

$$-\frac{eE\cos(\alpha+\beta)d\alpha d\beta}{2r}$$

since $\cos\theta=-\cos(\alpha+\beta)$.

Thus the mutual energy is equal to

$$-\frac{eE}{2r}\int\int\cos(\alpha+\beta)d\alpha d\beta$$

which gives eE/r for the total mutual energy, as it should.

By means of this integral it is easy to calculate the mutual energy in any part of the space surrounding the electron and the nucleus.

The mutual energy outside a sphere described on r or AB as diameter is 1.2854 Ee/r and that inside this sphere is -0.2854 Ee/r. The mutual energy inside any sphere described with center at either A or B and radius less than AB is zero. Hence the mutual energy between a sphere with center A and radius AB and one described on AB as diameter is equal to $+0.2854\ Ee/r$.

Thus it is clear that an appreciable fraction of the mutual energy is near to the electron and so might be expected to move with it and modify its motion.

To obtain information about the effect of the motion of the mutual energy with the electron, let us suppose that a fraction f of one-half of it can be regarded as moving with the electron and the rest as remaining at rest with the nucleus. Thus if $f=1$ half the mutual energy moves with the electron and half remains at rest.

The energy equation then becomes

$$\mathfrak{E}=m-\frac{m+fl}{\sqrt{1-\beta^2}}-(2-f)l. \tag{1}$$

If p denotes the angular momentum of the electron about the nucleus, we have then

$$p=\frac{m+fl}{c^2\sqrt{1-\beta^2}}r^2\dot{\theta} \tag{2}$$

where θ now denotes the angle between the radius vector r and a fixed radius in the plane of the orbit.

On working out the equation of the orbit from (1) and (2) in the usual way[1] we get writing u for r^{-1}

$$\left(\frac{du}{d\theta}\right)^2+u^2=\frac{-(2m-\mathfrak{E}-2l+2fl)(\mathfrak{E}+2l)}{p^2c^2} \tag{3}$$

$$\frac{d^2u}{d\theta^2}+u=-\frac{Ee}{p^2c^2}\left(m-\mathfrak{E}+f\frac{\mathfrak{E}}{2}-Eeu(1-f)\right) \tag{4}$$

and

$$u=C(1+\epsilon\cos\gamma\theta) \tag{5}$$

where ϵ denotes the eccentricity,

$$\gamma^2=1-\frac{E^2e^2}{p^2c^2}(1-f)$$

and

$$C=-\frac{Ee}{p^2c^2\gamma^2}\left\{m-\mathfrak{E}\left(1-\frac{f}{2}\right)\right\}.$$

Let $p_0=-Ee/C$ so that $\gamma^2=1-p_0^2(1-f)/p^2$.

---

[1] See for example Silberstein's *Report on the Quantum Theory of Spectra.*

Now putting the value of u given by (5) in (3) we get

$$\mathfrak{E} = m\left\{\frac{1-\alpha+\dfrac{\alpha f}{2}-\sqrt{1-\alpha+\alpha f}}{1-\alpha+\alpha f-\dfrac{\alpha f^2}{4}}\right\}$$

where

$$\alpha = \frac{p_0^2(1-\epsilon^2).}{p_0^2(1-f)-p^2}\,.$$

We now apply the fundamental equation of the quantum theory $\int pdq = nh$ and obtain

$$p = \frac{n_1 h}{2\pi}$$

and

$$n_2 h = -p\int_0^{2\pi/\gamma}\frac{d}{d\theta}\left(\frac{1}{r}\right)\frac{dr}{d\theta}\,d\theta$$

which gives

$$n_2 h = 2\pi p\gamma\left(\frac{1}{\sqrt{1-\epsilon^2}}-1\right).$$

Hence

$$\alpha = \frac{-4\pi^2 p_0^2/h^2}{\left(n_2+\sqrt{n_1^2-4\pi^2 p_0^2(1-f)/h^2}\right)^2}\,.$$

Since α is small we may expand $\mathfrak{E}$ in a series of powers of α, so that, neglecting powers of α above α^2, we get

$$\mathfrak{E} = m\left\{-\frac{\alpha}{2}-\alpha^2\left(\frac{3}{8}-\frac{f}{4}\right)\right\}$$

which gives on substituting the value of α and putting $k = 4\pi^2 p_0^2/h^2$ and $n = n_1+n_2$

$$\mathfrak{E} = \frac{mk}{2}\left\{\frac{1}{n^2}+\frac{k}{n^4}\left(\frac{n_2}{n_1}(1-f)+\frac{1}{4}-\frac{f}{2}\right)\right\}.$$

Hence the frequencies of the spectral lines emitted will be given by

$$h\nu = \frac{mk}{2}\left\{\frac{1}{n^2}-\frac{1}{n'^2}+\frac{k}{n^4}\left(\frac{n_2}{n_1}(1-f)+\frac{1}{4}-\frac{f}{2}\right)-\frac{k}{n'^4}\left(\frac{n'_2}{n'_1}(1-f)+\frac{1}{4}-\frac{f}{2}\right)\right\}$$

where

$$n' = n'_1+n'_2\,.$$

If $f=0$, this agrees with Sommerfeld's theory as it should, and if $f=1$, the frequency ν depends on n and n' only, so that we get single lines without any fine structure at all.

For the Balmer series $n=2$ and $n'=3, 4, 5$, etc. Each line is a doublet the separation of which is got by putting $n_2=0$, $n_1=2$ and $n_1=1$, $n_2=1$ so that the separation is

$$\frac{mk^2(1-f)}{32h}.$$

If $f=0$, this is equal to 0.365 (cm^{-1}). The separation of the doublets has been measured by a number of physicists[1] and in the case of H_α the mean of ten determinations is about 0.30 (cm^{-1}). This gives

$$1-f=\frac{0.30}{0.365}$$

so that

$$f=0.18.$$

For H_β the mean of five determinations of the separation is also 0.30 (cm^{-1}); for H_γ there are only two results, 0.31, and 0.33, and for H_δ also two, 0.26 and 0.29. Thus these results seem to indicate that f may be about 0.2 for the orbits corresponding to $n=2$ of the hydrogen atom.

In the case of ionized helium the agreement between Sommerfeld's calculations of the fine structure and Paschen's observations indicates that f must be quite small.

Rice Institute
Houston, Texas
May 10, 1922

---

[1] For a list of all observations see J. C. McLennan, *Proc. Roy. Soc.*, A, 100, 217, 1921.

INTERFEROMETER OBSERVATIONS OF DOUBLE STARS[1]

By PAUL W. MERRILL

ABSTRACT

Interferometer observations of double stars.—(1) *Revised elements of the orbit of Capella* were obtained by combining the previously reported measurements of Anderson, slightly corrected, with observations made on ten nights from October, 1920, to April, 1921, using the rotating interferometer attached to the 100-inch telescope. The chief results are: $P=104.022$ days; $a=0''.05360$; $a_1+a_2=126.63\times10^6$ km; $\pi=0''.0632$; $m_1=4.2\odot$; $m_2=3.3\odot$. The average residuals are 1° for position angle and $0''.0007$ for separation. (2) κ *Ursae Majoris* was independently discovered as a double and was measured on five nights, March 1 to April 30, 1921. The separation decreased from $0''.0836$ to $0''.0772$, but the position angle changed only 2°. One component is brighter by perhaps half a magnitude. (3) ν^2 *Boötis* was found to be difficult to measure as the fringes behaved abnormally, so only a rough measurement was possible. The system may be complex. (4) *Search for new measurable double stars.* Some spectroscopic binaries, stars with composite spectra, variable stars, and some bright stars taken at random—in all 85 stars, of varying magnitude down to 5.7 (Table IV)—were examined for duplicity, but with the exception of six doubtful cases, δ Cancri, 10 Leonis Minoris, o Leonis, ϵ and f Ursae Majoris, and υ Sagittarii, no changes in fringe visibility with position angle of the interferometer were observed.

Tests by Michelson at the Yerkes and Mount Wilson observatories[2] showed that even in poor seeing interference fringes can be observed in star images with slit separations ranging from 40 to nearly 100 inches. Following these results in an attempt to make the interference method sufficiently accurate and convenient to justify its extended use in the measurement of double-stars, Mr. Anderson devised a new type of stellar interferometer with which settings are made by rotating a pair of fixed slits. This instrument he applied with great success to the determination of the relative positions of the components of Capella.[3] His measures of distance, on five nights, ranged from $0''.0418$ to $0''.0505$, while the position angles were shown to be decreasing at a rate in keeping with a revolution period of 104 days. A double-star orbit was computed by him, using the spectroscopic elements previously determined at the Lick Observatory.

---

[1] *Contributions from the Mount Wilson Observatory*, No. 240.

[2] *Mt. Wilson Contr.*, No. 184; *Astrophysical Journal*, **51**, 257, 1920.

[3] *Mt. Wilson Contr.*, No. 185; *Astrophysical Journal*, **51**, 263, 1920.

It is interesting to note that in 1900 J. Miller Barr called attention to the desirability of attempting the observation of Capella as a double star by interferometer methods.[1]

The present paper is a record of further applications of the rotating type of interferometer to known double stars, and to a search for new doubles of small angular separation. The 100-inch Hooker telescope was used in all the observations, and practically the same procedure as that described by Anderson was followed throughout.

The constants of the interferometer were re-determined independently. The factor which is used to reduce the actual separation of the slits to their corresponding separation in the Gauss plane was found by dividing the equivalent focal length of the telescope, 1606 inches, by 28.00 inches, the distance of the slits from the focus. The value thus obtained, 57.34, was checked by a direct determination. At the upper end of the telescope tube, on the struts supporting the secondary mirror, were placed two rectangular pieces of wood of the same shape as the slits, but with dimensions slightly smaller than those of the slits as projected in the Gauss plane. Thus, when the telescope was directed to a bright star, by removing the eye-piece and placing the eye at the focus, the blocks could be centered in the slits, leaving lines of light at the edges. The separation of the blocks, divided by the separation of the slits, gives the factor desired. This experiment yielded the value 57.2, which was thought to be a trifle small. The factor adopted for all the reductions was 57.3, which falls within the limits of uncertainty of both determinations.

CAPELLA

R.A. 1900 = $5^h9^m.3$; Dec. 1900 = $+45°54'$; Mag. 0.2; Class G0.

Additional interference measures of Capella have been made by the writer on ten nights, and a revised orbit has been calculated.

As the series of observations was made during the winter months poor seeing was frequently experienced. Although the observing routine could usually be carried through in the regular way, on a few occasions the conditions became so bad that reliable settings could be made only by watching patiently and utilizing the best moments. The nights on which bad seeing prevents interferometer observations of Capella are quite rare. This is not true to the same extent of fainter stars.

---

[1] *Astrophysical Journal*, 11, 248, 1900.

The new measures of Capella appear in Table I, in which the third column, with the heading Slits, gives the separation (in the Gauss plane) of the slits; the fourth column, η, contains the

TABLE I

Observations of Capella

Date	P.S.T.	Slits	η	θ	ρ	
1920 Oct. 5....	16^h15^m	174.2 cm	46°.65	253°.9	474	
Nov. 3....	13 20	142.8	24.75	164.8	437	
	14 05	173.3	41.90	164.6	440	
	14 39	203.6	50.80	163.8	441	
1921 Jan. 14....	7 36	142.2	30.12	263.5	461	
	8 31	172.6	45.25	262.9	467	
	9 08	202.9	52.65	262.2	461	
	10 25	202.9	51.78	261.2	452	Weight ½
Jan. 31....	7 07	142.2	43.45	213.7	550	
	7 19	172.6	52.40	214.0	539	
	7 29	202.9	58.82	214.8	540	
	7 46	123.9	33.32	212.8	548	
Feb. 2....	7 18	172.6	52.67	209.8	542	
	7 52	142.2	43.30	208.6	548	
	8 55	202.9	58.07	207.9	529	Weight ½
Mar. 1....	6 52	172.6	36.95	106.0	411	
	7 10	202.9	47.00	105.6	410	
	7 23	232.8	53.25	106.2	407	
Mar. 2....	6 44	202.9	48.32	101.2	421	
	6 52	172.6	39.22	102.4	424	
	7 04	232.8	54.35	101.4	418	
Mar. 3....	6 52	172.6	39.27	98.1	425	
	7 08	202.9	48.10	97.8	419	
	7 23	232.8	54.05	98.4	415	
Mar. 31....	7 07	172.6	51.00	15.0	522	
	7 23	202.9	56.60	14.2	508	
	7 38	142.2	38.87	14.3	512	
Apr. 1....	7 16	142.2	37.50	11.4	503	
	7 35	172.6	48.65	11.4	498	
	7 55	202.9	56.32	11.7	504	

angle of projection for minimum fringe visibility;[1] the fifth column, θ, the position angle of the components; and the sixth column, ρ, their separation in units of one ten-thousandth of a second of arc, i.e., $474 = 0''.0474$. The effective wave-length was taken to be 5500 A.

In Table II are collected the mean values for each night. The weights assigned depend principally on the number of complete individual observations. The total number of settings was increased during poor seeing in an attempt to give approximately standard accuracy to each complete observation. Since the factor 57.3 is somewhat smaller than that used by Anderson in the first observations, it was decided by mutual agreement between him and the writer that it would be better to change the original reductions. Hence the first five values of ρ in Table II are larger by 2.4 per cent than the corresponding figures in *Contribution* No. 185.

TABLE II

MEAN CO-ORDINATES OF COMPONENTS OF CAPELLA

G.M.T.	θ	O−C	ρ	O−C	Weight	
(1) 1919 Dec. 30.65	....	....	428	+ 3	⅓	Anderson
(2) 1920 Feb. 13.63	5.0	+2.2	469	− 7	⅔	Anderson
(3) Feb. 14.65	1.0	+1.6	462	− 6	1	Anderson
(4) Feb. 15.66	356.4	+0.5	454	− 6	1	Anderson
(5) Mar. 15.63	242.0	+1.9	517	+10	⅔	Anderson
(6) Apr. 23.63	107.0	+0.4	....	....	⅓	Anderson
(7) Oct. 6.01	253.9	+2.6	474	− 7	⅓	....
(8) Nov. 3.92	164.4	−1.6	439	− 4	1	....
(9) 1921 Jan. 14.70	262.6	−0.1	461	+ 5	1	....
(10) Jan. 31.64	213.8	+0.6	544	+11	1	....
(11) Feb. 2.66	208.9	+1.1	542	+14	1	....
(12) Mar. 1.63	105.9	−0.9	409	−11	1	....
(13) Mar. 2.62	101.6	−1.1	421	− 5	1	....
(14) Mar. 3.63	98.1	−0.4	420	−12	1	....
(15) Mar. 31.64	14.5	−1.0	514	+ 7	1	....
(16) Apr. 1.65	11.5	−1.0	502	+ 2	1	....

The orbital elements deduced by Anderson gave a fair representation of the additional observations but it was found possible to make some slight improvements.

---

[1] The out-of-step appearance of the fringes shown in Anderson's laboratory experiments (see illustration in *Mt. Wilson Contr.*, No. 185) was not observable. Accordingly the sensitive method of fringe bisection could not be used, but settings were made for the minima of visibility.

By comparing recent spectroscopic observations at Mount Wilson with those made at the Lick Observatory in 1900 Sanford[1] has found that the original figures for the period, 104.022 days, are very nearly correct. Accordingly this value has been used throughout the present computations.

Preliminary trials showed that the eccentricity is probably smaller than 0.016 as given by Reese. Hence it did not seem necessary to vary both T and ω. The date 2422596.79 was chosen for T by trial and retained thereafter. This corresponds to a periastron time 0.8 days later than that adopted by Anderson. Corrections to a and to Ω were then found by direct algebraic processes. Finally a least-squares solution was carried through for the elements ω, i, and e. This yielded very small corrections to the preliminary values.

The adopted elements follow:

$T=$ J.D. 2422596.79
$P=104.022$ days, angles decreasing.
$\omega=114^{\circ}.30$
$i=-41^{\circ}.08$
$\Omega=38^{\circ}.70$
$e=0.0086$
$a=0''.05360$

To these may be added the following quantities found by combining the foregoing elements with the spectroscopic results:

$a_1+a_2=126{,}630{,}000$ km $m_1=4.2\odot$
$\pi=0''.0632$ $m_2=3.3\odot$

The residuals from these elements are given in Table II. They are considerably larger than one might expect from the degree of accordance of the individual observations as shown by Table I. Moreover, observations made on successive nights exhibit a tendency toward similar residuals. This would seem to mean either that there are systematic errors in the observations, or that the best orbital elements have not been found, or that the orbit is not a true ellipse, or that there is present a combination of two or three of these causes.

---

[1] *Publications Astronomical Society of the Pacific*, 34, 178, 1922.

As to systematic errors it must be admitted there are possibilities of slight effects. For instance, no ready direct method was found of checking the position angle circle of the interferometer when attached to the telescope, so that the actual position angles of the slits may conceivably have differed by small amounts from the angles as read from the circle. Again, the condition of the telescope mirrors, the position of the struts supporting the secondary mirror, the settings of the compensator, the exact location of the focus, the condition and position of the observer's eyes, may have been responsible for small systematic errors. For the most refined results in an extensive investigation all these factors should receive attention.

In regard to the orbital elements it may be that a different set of values would give smaller residuals. Indeed it has been found by taking $T = 2422563.76$, $\omega = 0^\circ\!.0$, $e = 0.01$, that the residuals in ρ are considerably reduced while the θ residuals are somewhat increased. With a circular orbit the representation is also very good. This indicates that as far as the interferometer observations are concerned the eccentricity and the time of periastron are practically indeterminate. As compared with the spectroscopic orbit this condition doubtless arises from the flexibility of the double star orbit due to the inclusion of the element representing the inclination of the orbit plane. By varying the orbital elements *arbitrarily* a better set of residuals than those in Table II could probably be found, but in view of the spectroscopic data there would apparently be no physical justification for such procedure and it has been thought better to retain the elements given on page 44 until future observations shed more light upon the situation.

One curious feature appears with several different trial sets of orbital elements, namely, that the early observations persist in giving positive residuals for θ (O − C). This may be due either to a systematic difference between Anderson's observations and the writer's, or to perturbations causing the position angle of the real node to decrease with time at the rate of about $2^\circ\!.4$ per year, or about $0^\circ\!.6$ in one orbital revolution. The physical interpretation and probability of such a perturbation may be a matter of interest to mathematical astronomers.

If, from the orbit adopted in this paper, we compute the position angles corresponding to the Greenwich observations[1] in 1900 (mean places), we find a fairly consistent set of residuals averaging $+18^{\circ}$. Compared with the interferometer observations, this residual would be removed by a motion of the node of $0\overset{\circ}{.}9$ per year in the same direction as that suggested by the residuals of the interference measures themselves.

Capella presents one of the very small number of cases in which a comparison of the visual and spectroscopic data leads to an accurate value of the parallax. The value found in the present investigation, $0\overset{''}{.}063$, agrees well with the mean trigonometric determination, $0\overset{''}{.}067$, and the spectroscopic value,[2] $0\overset{''}{.}076$.

κ URSAE MAJORIS

R.A. $1900=8^{\mathrm{h}}56\overset{\mathrm{m}}{.}8$, Dec. $1900=+47^{\circ}33'$; Mag. 3.7; Class A0.

On the night of March 1, 1921, Mr. Anderson and the writer were engaged in making some tests in connection with the stellar interferometer attached to the Hooker telescope, of a special apparatus[3] devised by the former to produce an artificial double star of known separation by means of which the constants used in the regular reductions might be checked. It consisted of a quartz plate two and a half millimeters thick, cut at 45° to the optic axis, which, when mounted in the converging beam, transformed a single star into a double star having a separation of 12 microns, which corresponds to $0\overset{''}{.}06$ at the Cassegrain focus of the Hooker telescope. When the telescope was pointed toward κ Ursae Majoris and the observations were begun, anomalous results were obtained. Instead of the usual *four* minima in a complete revolution, a larger number appeared. We recognized that the behavior corresponded to that of a quadruple star and surmised that the star would be measurable as a double without the quartz plate. Proceeding at once to verify this by removing the quartz plate and making settings in the ordinary manner, we determined the position angle and separation to be $251\overset{\circ}{.}9$ and $0\overset{''}{.}0836$. It was not

[1] *Monthly Notices, Royal Astronomical Society*, **61**, 72, 1901.

[2] *Mt. Wilson Contr.*, No. 199; *Astrophysical Journal*, **53**, 34, 1921.

[3] *Mt. Wilson Contr.*, No. 222; *Astrophysical Journal*, **55**, 48, 1922.

until a few days later that we learned that this star is a known double, A 1585, discovered by Aitken[1] in 1907 when its separation was about twice as great. This incident illustrates the fact that a close quadruple star can readily be detected by the interference method.

Subsequent interferometer measures made during March and April 1921 showed that the separation was decreasing at the rate of 0″.003 per month, and the position angle by about one degree per month.

TABLE III

MEASURES OF κ URSAE MAJORIS

Date	Position Angle	Distance	
1907.83	283°.2	0″.21	Aitken, micrometer
1909.33	281.4	0.25	Aitken, micrometer
1919.29	264.9	0.15	Aitken, micrometer
1921 Mar. 1	251.9	0.0836	. . . .
Mar. 2	252.5	0.0833	. . . .
Mar. 31	251.3	0.0801	. . . .
Apr. 1	250.7	0.0796	. . . .
Apr. 30	250.2	0.0772	. . . .

In good seeing the fringes are quite distinct even at minimum visibility, showing that the components are not equal. The magnitude difference is perhaps two or three times as great as in Capella, but probably does not much exceed one-half of a magnitude.

ν^2 BOÖTIS

R.A. 1900 = $15^h28^m.2$; Dec. 1900 = +41°14′; Mag. 5.0; Class A2.

At the suggestion of Dr. Aitken the double star ν^2 Boötis, A 1634,[2] was placed upon the observing list. This close double of separation 0″.1 or less had been found to be a difficult object to resolve with the Lick 36-inch refractor. His observations[3] indicate that the position angle has decreased from 237° in 1907 to about 213° in 1920.

Examination of this star with the interferometer showed that the visibility changed as the slits were rotated, but observations on different nights, and with different slit separations, did not yield the consistent results obtained with Capella and κ Ursae Majoris, and to be expected of any double star. The observations were rather difficult on account of the faintness of the image. The regular sized slits were employed although it might have been an advantage to use larger ones.

---

[1] *Lick Observatory Bulletin*, 4, 168, 1908.

[2] *Ibid.*

[3] Kindly communicated by letter.

On the night of June 18, 1921, immediately following rather unsuccessful attempts at measurement, this note was written:

> Seeing and visibility are good but settings on ν^2 Boötis seem almost impossible. Fringes are certainly visible in all position angles at 108.9, 142.2, 172.6, and 202.9 cm (slit separation). It is a question of *small* differences in visibility; these differences seem smaller tonight than previously. One must guard against the physiological factor that fringes appear more distinct when parallel to the line joining the eyes. This may cause some of the above readings to be illusory. However, I believe there are real variations in visibility. Perhaps the star is triple or complex. Sometimes there appear to be regions 20° to 30° wide of low visibility. There appear to be "shoulders" in the visibility curve; i.e., the visibility drops off on rotating 5°–10° but does not return at once on rotating further. Star is a puzzle so far. Perhaps a wide double with one star a close pair.

Mr. Humason also examined this star on the same evening, June 18, 1921, and thought the variations in visibility to be real.

If we assume the object to be a double star the most probable result deduced from all the settings appears to be $\theta = 192°$, $\rho = 0''.061$. This depends very largely on observations with a slit separation of 142.2 cm. The mean epoch was May 1921.

EXAMINATION OF STARS FOR DUPLICITY

A number of stars have been tested for evidences of duplicity by looking for variations in the visibility of the fringes as the slits were rotated. Slit separations up to 200 cm (80 inches) were used in nearly all cases. The stars in Table IV exhibited no appreciable variation of fringe visibility with position angle of the slits. If these stars are double, their components could not have been as much as $0''.03$ apart on the date of observation, provided their magnitudes are nearly equal. If the difference in magnitude is greater than 0.5, changes in visibility might escape detection unless the circumstances were especially favorable. The stars examined include spectroscopic binaries, stars with composite spectra, variable stars, and some bright stars taken at random.

TABLE IV

Stars Apparently Single

Star	Mag.	R.A. 1900	Star	Mag.	R.A. 1900
β Persei	var.	3^h $1^m.7$	*d* Boötis	4.8	14^h $5^m.8$
ζ Tauri	3.0	5 31.7	α Boötis	0.2	14 11.1
51 Aurigae	5.7	6 31.7	A Boötis	4.8	14 13.8
ψ^5 Aurigae	5.3	6 39.5	θ Boötis	4.1	14 21.8
α Geminorum	2.0, 2.8	7 28.2	ρ Boötis	3.8	14 27.5
β Geminorum	1.2	7 39.2	ε Boötis	2.7, 5.1	14 40.6
40 Lyncis	3.3	9 15.0	109 Virginis	3.8	14.41.2
θ Urs. Maj.	3.3	9 26.2	β Boötis	3.6	14 58.2
ε Leonis	3.1	9 40.2	δ Boötis	3.5	15 11.5
η Leonis	3.6	10 1.9	ι Draconis	3.5	15 22.7
α Leonis	1.3	10 3.0	β Cor. Bor.	3.7	15 23.7
λ Urs. Maj.	3.5	10 11.1	ν Boötis	5.2	15 27.3
ζ Leonis	3.6	10 11.1	α Cor. Bor.	2.3	15 30.5
μ Urs. Maj.	3.2	10 16.4	κ Serpentis	4.3	15 44.2
ρ Leonis	3.8	10 27.5	α Scorpii	1.2	16 23.3
46 Leo. Min.	3.9	10 47.7	β Herculis	2.8	16 25.9
ψ Urs. Maj.	3.2	11 4.0	α Herculis	3.5, 5.4	17 10.1
δ Leonis	2.6	11 8.8	δ Herculis	3.2	17 10.9
ξ Urs. Maj.	4.4, 4.9	11 12.9	π Herculis	3.4	17 11.6
ν Urs. Maj.	3.7	11 13.1	ο Herculis	3.8	18 3.6
χ Urs. Maj.	3.8	11 40.8	*d* Serpentis	5.3	18 22.1
93 Leonis	4.5	11 42.8	α Lyrae	0.1	18 33.6
β Leonis	2.2	11 44.0	β Lyrae	Var.	18 46.4
β Virginis	3.8	11 45.5	113 Herculis	4.6	18 50.5
γ Urs. Maj.	2.5	11 48.6	β Cygni	3.2, 5.4	19 26.7
δ Urs. Maj.	3.4	12 10.5	δ Sagittae	3.8	19 42.9
γ Corvi	2.8	12 10.7	η Aquilae	Var.	19 47.4
η Virginis	4.0	12 14.8	31 Cygni	4.0	20 10.5
δ Corvi	3.1	12 24.7	32 Cygni	4.2	20 12.3
8 Can. Ven.	4.3	12 29.0	β Capricorni	3.2	20 15.4
δ Virginis	3.7	12 50.6	47 Cygni	4.8	20 30.0
43 Com. Ber.	4.3	13 7.2	α Equulei	4.1	21 10.8
20 Can. Ven.	4.7	13 13.1	14 Pegasi	5.0	21 45.4
ζ Urs. Maj.	2.4, 4.0	13 19.9	δ Cephei	Var.	22 25.4
17 Can. Ven.	5.0	13 30.3	η Pegasi	3.1	22 38.3
τ Boötis	4.5	13 42.5	ο Androm.	3.6	22 57.3
η Boötis	2.8	13 49.9			

NOTES

$7^h 28^m.2$,	α Geminorum, both components, 2.0, 2.8.
11 12.9,	ξ Urs. Maj., both components, 4.4, 4.9.
13 19.9,	ζ Urs. Maj., both components, 2.4, 4.0.
14 40.6,	ε Boötis, both components, 2.7, 5.1.
17 10.1,	α Herculis, both components, 3.5, 5.4.
18 22.1,	*d* Serpentis, brighter component, 5.3.
19 26.9,	β Cygni, both components, 3.2, 5.4.

Although the dates of observation, slit separations employed, the seeing, and notes on any apparent peculiarities were, of course, recorded in the observing book and will be made available to anyone interested in a particular star, these details do not seem worth publishing. For the most part the dates of observation lie between February 1 and June 17, 1921. Several stars observed by Anderson about a year earlier are included in Table IV. On a few nights Mr. Humason alternated with the writer in the examination of stars for duplicity.

Variations in visibility for *f* Ursae Majoris (R.A. 1900 = $9^h 1^m.9$; Dec. 1900 = $+52°0'$; Mag. 4.5; Class A3p) were suspected on the night of April 30, 1921, but a complete set of minima as for a double star was not obtained and the variations were not definitely confirmed.

The following stars were also suspected of changes in visibility, but the reality of the changes is doubtful. They do, however, deserve careful re-examination, which it is hoped other observers will give them, as the double star work at the Mount Wilson Observatory has been discontinued.

	Mag.	R.A. 1900
δ Cancri	4.2	$8^h 39^m.0$
10 Leo. Minor	4.6	9 28.1
o Leonis	3.8	9 35.8
ε Urs. Maj.	1.7	12 49.6
υ Sagittarii	4.6	19 16.0

In searching for doubles with the interferometer, poor and, in particular, variable seeing is a great disadvantage and renders conclusions uncertain. To illustrate this the following quotations from the observing record may be of interest.

γ Boötis R.A. 1900 = $14^h 28^m.1$; Dec. 1900 = $+38°45'$; Mag. 3.0; Class F.
1921 April 1 Seeing fair. "Several times suspected slight variations but cannot make any settings. Probably single."
June 16 Seeing poor. "Visibility very low on account of poor seeing. Fringes seen only by rare glimpses."
June 18 Seeing fair. "Round."

γ Lyrae	R.A. 1900 = $18^{h}55^{m}.2$; Dec. 1900 = +32°33′; Mag. 3.3; Class A.
1921 April 30	Seeing good but rather irregular. "Suspect slight variation but may not be real."
June 14	Seeing poor and variable. "Followed around at 142 cm with some suspicion as to variability (doubtless due to variable seeing). Followed partly around at 173 cm but seeing turned very poor and fringes disappeared."
June 17	Seeing poor. "About equally distinct in all position angles at 142 cm and 197 cm. Fairly well seen by waiting for best moments."

While complete disappearance of the fringes, as for a close double of equal components, would be noticed in any except the very worst seeing, small variations in visibility cannot be recognized with certainty in poor and irregular seeing. Thus the suspected doubles noted in preceding paragraphs may be spurious, while some of the stars in Table IV may prove to have small variations in visibility, due to unequal components, which were overlooked by the writer. The brighter the star the less the difficulty caused by the seeing.

GENERAL REMARKS

In the Mount Wilson interferometer the slits are separated by turning a divided head, the readings of which are calibrated in terms of the actual slit separation. For systematic double star observations it would probably be better to replace this design by a metal plate containing pairs of slits at several fixed separations so arranged that any pair could be easily moved to the center of the field, the others remaining covered. Time would be saved in observing and the possibility of errors in setting and reading the separations greatly reduced. The separations, moreover, would not be subject to change with time or with readjustment of the instrument, unless the distance of the plate from the focus were changed.

The accuracy of the results obtained by Anderson's method of rotating the apertures and the convenience with which it can be applied are so great as to make it probable that this method will become very important in the future of double star astronomy. The range in the separations and magnitude differences of the double stars to which it can be successfully applied is, of course, small, but the interferometer results would supplement the ordinary micrometer measures in a most desirable way, making it possible to follow some very close and especially interesting pairs with highly satisfactory precision. The new pairs discovered by the interferometer will not be numerous as compared to those now known through direct observations, but they are likely to be of very great individual importance.

The present investigation has been greatly facilitated by Mr. Anderson's kindness in placing his experience with the stellar interferometer in so far as possible at the disposal of the writer, and by considerable assistance in securing and recording the observations. This kindness is gratefully acknowledged, as well as that of Mr. Humason in aiding with the observations on several nights.

Mount Wilson Observatory
April 1922

A DETERMINATION OF THE WAVE-LENGTHS OF 118 TITANIUM LINES BY MEANS OF THE INTERFEROMETER

By FREDERICK L. BROWN

ABSTRACT

Interferometer measurements of the wave-lengths of 118 titanium lines from a vacuum arc, λλ 4263 to 6261 A.—Because of the importance of the titanium spectrum in astrophysics, a more accurate determination of the wave-lengths was undertaken, using a Fabry-Perot interferometer in connection with a Hilger constant deviation spectrograph. The sources of light were two water-cooled vacuum arcs, one for the titanium and the other for the cadmium lines. In order that both spectra might be photographed simultaneously an image of the Ti arc was formed, by means of a concave mirror, at the center of the Cd arc, thus making the paths through the optical system the same for both. Two etalon separators, 9.81 and 4.99 mm thick, were used to enable the phase correction to be determined from a comparison of the uncorrected wave-lengths obtained with the two separators, five plates being made with each. In reducing the measurements, Kilby's wave-lengths were used as a point of departure and the Cd line 6438.4696 as standard. Temperature and pressure-corrections were negligible. The results from the various plates agree on the average within 0.002 or 0.003 A.

Interferometer measurements of the wave-lengths of 25 iron lines and two manganese lines from a vacuum arc are also included. Making allowance for the pressure-shift as given by Gale and Adams, the mean deviation from the results of Burns, Meggers, and Merrill for the iron lines is ±0.003 A. For the Mn lines λλ 4783 and 4823, the deviation from the measurements of Goos is −0.020 A, perhaps a pressure-effect.

INTRODUCTION

The measurement of some of the principal lines in the spectrum of titanium with the interferometer was undertaken in order to supplement the data already available on this important element.

The first measures of titanium lines were made by Thalén at Upsala in 1868.[1] Later, Hasselberg,[2] also Exner and Haschek[3] measured a large number of lines in both arc and spark. Kilby,[4] at Johns Hopkins in 1909, measured several hundred lines between λ 2800 and λ 6300 with a Rowland grating, interpolating between the iron standards. The effect of pressure-shift has been examined by Humphreys, Haschek, Gale, and Adams;[1] induction and capacity shifts have been studied by Kent and Middlekauf;[2] the Zeeman effect and electric furnace spectra, by A. S. King;[3] E. J. Evans[4] has extended the measures of wave-lengths down to λ 7364; Kiess and Meggers[5] down to λ 9743; and various other observers have studied the several phases of the arc and spark spectra of this metal;[6] there has, however, so far as the author is aware, been no previous measurement of the spectrum of titanium with the interferometer.

---

[1] Thalén, *Nova Acta Reg. Soc. Sc. Upsala*, Ser. III, **6**, 1868.

[2] Hasselberg, *Astrophysical Journal*, **4**, 116–134 and 212–233, 1896.

[3] Exner and Haschek, *Die Spektren der Elemente bei Normalen Druck*, 1911.

[4] Kilby, *Astrophysical Journal*, **30**, 243–266, 1909.

The value of titanium as a comparison spectrum was first pointed out by Frost[7] who found it especially good for solar and stellar work on account of the wealth of bright sharp lines in the region λ 4200 to λ 5200. Furthermore, Jewell,[8] studying the chromosphere, has found it of service as a comparison spectrum in the violet and ultra-violet region.

THEORY

The contest between the grating and the interferometer as the fundamental method for wave-length determination was decided in favor of the latter through the masterly work of Michelson.[9] In the hands of Fabry and Perot the interferometer developed into an instrument of precision and of great experimental possibilities. Used in connection with even a moderate dispersion piece this device makes possible the accurate measurement of a large number of lines on a single photograph.

---

[1] Humphreys, *Astrophysical Journal*, **6**, 169–232, 1897; Haschek, *ibid.*, **14**, 181–201, 1901; Gale and Adams, *ibid.*, **35**, 10–47, 1912, and **37**, 391–394, 1913.

[2] Kent, *ibid.*, **17**, 286–299, 1903; **22**, 182–198, 1905; **27**, 70–77, 1908; Middlekauf, *ibid.*, **21**, 116–150, 1905.

[3] King, *ibid.*, **28**, 300–314, **29**, 76–83, 1908; **30**, 1–13, 1909; **31**, 433–458, 1910; **34**, 225–250, 1911, etc.

[4] Evans, *ibid.*, **29**, 160–163, 1909.

[5] Kiess and Meggers, *Sci. Papers, Bureau of Standards*, No. 372, 1920.

[6] Kayser, *Handbuch der Spectroscopie*, **6**, 655–708, 1912.

[7] Frost, *Astrophysical Journal*, **10**, 207–208, 1899.

[8] Jewell, *ibid.*, **11**, 243–244, 1900.

[9] Michelson and Benoit, *Travaux et Memoirs du Bureau Intern. des Poids et Mesures*, **11**, 1895.

The theory[1] of the instrument is so well known that it need not here be given. The laboratory equation without corrections of any kind as given by Pfund[2] is:

$$\lambda = \frac{\lambda_s P_s}{P}\left(1 + \frac{D_s^2}{8R_s^2} - \frac{D^2}{8R^2}\right)$$

where λ is the wave-length to be determined; P is the order of interference (approximately $\frac{2e}{\lambda}$, where e is the distance between the etalon plates) for the bright ring measured; D is the linear diameter of this ring; R is the effective focal length of the optical train for light of wave-length λ; and λ_s, P_s, D_s, and R_s are the corresponding quantities for a bright ring of the system formed by the standard red cadmium line.

To this computed value of λ two principal corrections must be applied, one for phase, the other to reduce the computed wave-lengths to standard conditions of pressure and temperature. The wave-length of the red cadmium ray which has been adopted as the primary standard by the International Solar Union[3] is 6438.4696 A, the etalon space being filled with dry air at 760 mm of mercury and 15° C., and the radiation produced in vacuum.

DESCRIPTION OF APPARATUS

1. *Source.*—The sources of radiation in the present experiment are two water-cooled vacuum arcs. They consist of two concentric cylindrical brass vessels so arranged as to give a fairly large chamber for the arc; the space between the walls of the vessels form a water jacket. The accompanying diagram (Fig. 1) shows a vertical section with the electrodes in place.

The heavy cone-shaped top C fits snugly against the upper ring D in such fashion as to render the joint air tight and allow the main chamber to be exhausted through a side tube.

---

[1] Fabry and Perot, *Astrophysical Journal*, **15**, 73–96 and 261–273, 1901.

[2] Pfund, *ibid.*, **28**, 197–211, 1908.

[3] *Transactions of the International Union for Co-operation in Solar Research*, **2**, 109–137, 1907.

The electrodes are held in place by two insulating frames, *HH*, which slide up and down a pair of guides and are operated by means of a right- and left-handed screw *JJ* so as to be brought together and then separated to any desired distance after the arc has started. The current is introduced at the terminals *KK*, which are connected to the electrodes by stranded copper wire incased in short lengths of clay pipe-stem. It is evident from the diagram that the entire system of electrodes, clamps, etc., can be removed by lifting off the top.

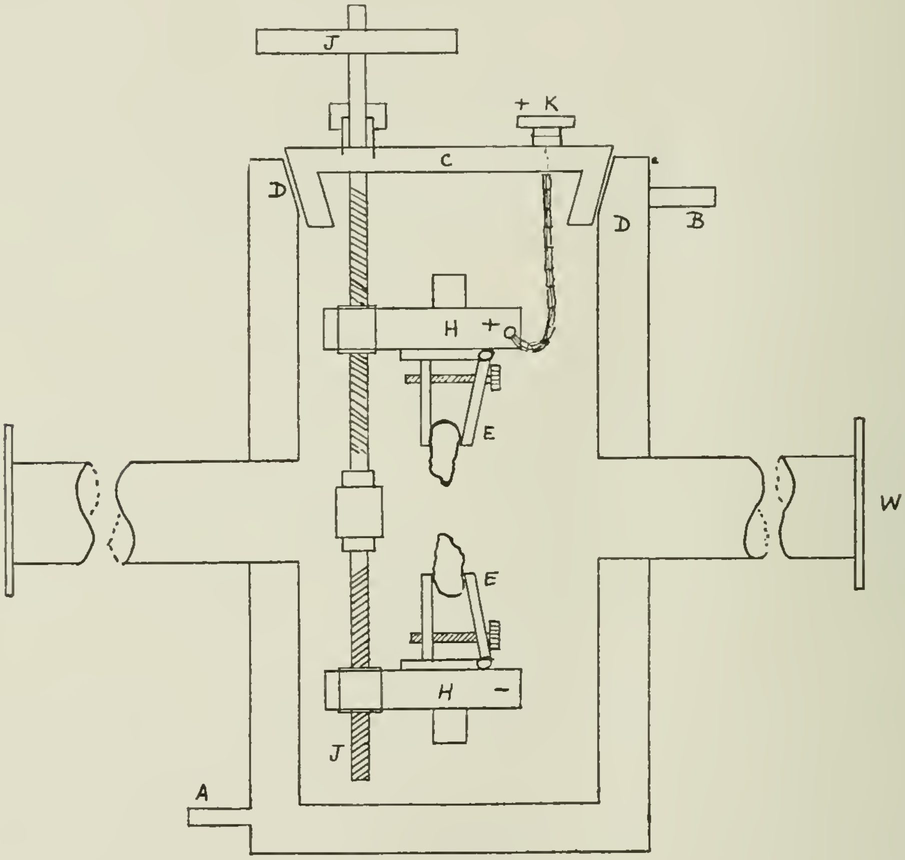

FIG. 1

The water for cooling the chamber enters the outer can at the bottom through *A* and leaves at the top through *B*. The arc is adjusted so that the light from it passes directly out of the windows *WW*. The long tubes keep the glass from becoming soiled and spattered by the arc.

A vacuum of five or six millimeters of mercury could be maintained very easily. The arcs worked best with a pressure of about

10 mm for Cd and about 40 mm for Ti. Under these conditions the light is steadier and brighter than under a pressure of only one or two millimeters. They were supplied with direct current from a 220-volt generator, the titanium arc using from 5 to 7 amperes while the cadmium arc took from 0.5 to 2.0 amperes.

The electrodes for the Cd arc were carbon, the lower one being bored out and filled with metallic cadmium. The electrodes for the titanium arc were small wedge-shaped pieces of metallic titanium clamped in iron jaws. The arc was usually quite steady, but would occasionally jump to the iron clamps thereby introducing the iron impurity lines measured on some of the plates. The greatest difficulty with the cadmium arc arose from the easy volatilization of the metal and its condensation on the electrodes and their insulating supports, thus producing short circuits from time to time that required the removal and thorough cleaning of the entire apparatus. The cadmium often had to be replenished two or three times during a single exposure.

The vacuum vessels were mounted on sliding ways so that by means of adjusting screws the light could be kept accurately centered on the diaphragm of the etalon even when the arc moved from one point of the electrode to another.

I am glad to remark here that the design of this arc is due to Professor Henry Crew and Dr. George V. McCauley,[1] and that the apparatus was made with great accuracy by Mr. F. Küng, the mechanician of the department.

2. *Interferometer and optical train.*—The interferometer was made by Hilger for use with his spectrograph. The plates were cleaned and resilvered by a modified form of the process described by Wood.[2] The deposit was good over the central area, the only portion used, and gave clear sharp rings. The same portions of the mirrors were used throughout the experiment.

The original interferometer has a quartz etalon of 9.81 mm separation, in addition to which a second one, of 4.99 mm separation, was also made in order to determine the phase correction. A diagram of the optical train is given in Figure 2.

---

[1] Crew and McCauley, *Astrophysical Journal*, **39**, 29–38, 1914.

[2] Wood, *Physical Optics*, 2d edition, p. 281.

The light from the titanium arc, *A*, is brought to a focus at the center of the cadmium arc, *C*, by the concave mirror, *B*. From here on the two pencils, one from each source, travel the same path.

The lens, *D*, collects and focuses the rays on the diaphragm, *E*, in front of the etalon *F*. At *G*, there is placed an achromatic lens which projects the ring system on the slit-plate of the spectrograph, of which *H* is the collimator, *I*, the prism and *J*, the camera.

The special and most important feature of the arrangement is the use of the concave mirror, *B*, which enables one to use both arcs simultaneously. In this way the optical system for both Cd and Ti is identical from the crater of the Cd arc to the plate. No changes being required, the chances of shift of the rings on the plate due to alternate exposures is entirely eliminated. This important suggestion was made by Professor Crew who had used a similar arrangement for work with a large grating.

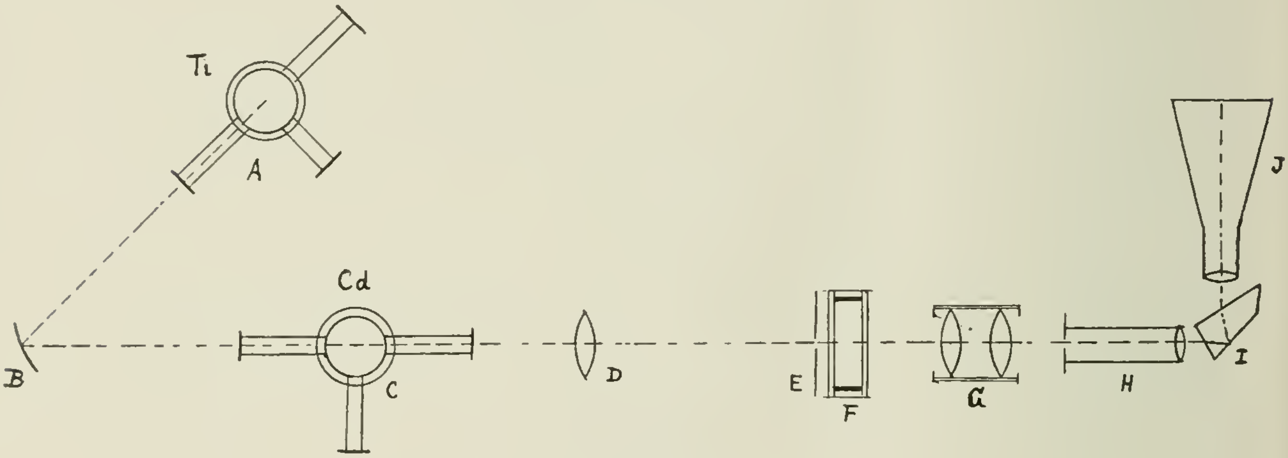

FIG. 2

3. *The spectrograph* is one of the constant-deviation prism type made by Hilger. The collimator and camera lenses are very good, and the adjustments on the camera make it possible to secure good definition over the entire range of the plates.

There are two disadvantages in the use of a prism for this work, namely, its low dispersion in the orange-red region and the absorption of the short wave-lengths. However, titanium is richest in lines shorter than 5200, and the use of glass plates in the interferometer and glass lenses in the rest of the optical train cuts out almost as much of the ultra-violet as does the prism.

METHOD OF EXPERIMENT

The adjustment of the optical train was carried out in the usual manner, care being taken to make certain that the image of the titanium arc, *A*, formed by the concave mirror, *B*, coincided with the center of the cadmium arc, *C*, and that the light from both sources followed the same path through the optical train. The diaphragm, *E*, not only delimits the portion of the mirrors used, thereby sharpening the rings, but also cuts off light from the poles of the arc and allows only that from the center to reach the plates of the etalon.

The photographic plates used were Wratten and Wainwright panchromatic, $3\frac{1}{4}\times4\frac{1}{4}$ inches; to make them more sensitive to the red and faster over the entire range, they were bathed in ammonia and dried in an air-current shortly before exposure.[1] The camera gave a spectrum whose width was about three-fourths of an inch.

When the adjustment of the instrument and good condition of the arcs had been assured, the exposure was begun and the arcs kept running for some three hours. Stopcocks in the vacuum pump line allowed one arc to be opened to the air and its electrodes replaced without disturbing the other one. In this way the exposure was continuous, and during the major portion of the time both sources were in simultaneous operation.

On a great many plates a direct exposure, i.e., a photograph without the etalon was put on the plate, either above or below the ring system which was, of course, in the middle. These direct exposures required only a few seconds and were added after the interference fringes had been photographed. They gave a convenient comparison spectrum in case of question of identification of lines. The width of the lines on the photographic plates varied from 0.10 to 0.15 mm for the interference fringes; for the direct exposures it was of course much narrower.

The list of plates used in the final computation is given in Table I. It will be noticed that some were taken in July and August 1920, and some in February 1921. The set of plates made with the 4.99 mm etalon in the summer of 1920 looked beautiful and gave promise of good results, but something must have been out of adjustment and escaped detection, for the wavelengths computed from them proved to be inconsistent among themselves as well as at variance with the values given by the 9.81 mm etalon. Consequently the separator of the short etalon was reground and the entire apparatus readjusted. Two additional plates with the long etalon were also made as a check and one of these (No. 98) was measured and completely reduced. The new set of plates are in good agreement and there is no question but that the difficulty, still unknown, that vitiated the first set was entirely removed.

---

[1] Burka, *Journal of the Franklin Institute*, **189**, 25–46, 1920.

TABLE I

Plates Measured

Pate Number	Date	Time of Day	Source	Exposure Length	Current Amps.	Room Temperature	Atmospheric Pressure
B 63...	1920 July 30	9:00–12:00	Cd Ti	3 hrs. 3	1–2 6–7	24°5 C.	745 mm
B 64...	July 30	2:30– 5:30	Cd Ti	3 3	1–2 6–7	24.5	744
B 75...	Aug. 7	9:00–12:00	Cd Ti	2+ 3	1–2 5–7	25.0	746
B 76...	Aug. 7	1:30– 5:00	Cd Ti	2:15 3	1–2 5–7	25.0	745
B 88...	1921 Feb. 5	3:00– 6:00	Cd Ti	1:30 2+	1 5–7	20.0	742
B 89...	Feb. 8	3:00– 5:00	Cd Ti	1+ 2−	1 5–7	20.0	745
B 90...	Feb. 10	2:00– 5:30	Cd Ti	2+ 3+	1–7 5–7	21.0	742
B 91...	Feb. 12	2:30– 5:30	Cd Ti	2+ 3−	0.5–1 5–7	22.0	745
B 93...	Feb. 17	2:30– 4:30	Cd Ti	1:30 2	0.5–1 5–7	20.5	754
B 98...	Feb. 19	2:30– 5:30	Cd Ti	1 2:30	0.5–1 5–7	20.5	757

9.81 mm etalon used for plates Nos. 63, 64, 75, 76, 98.

4.99 mm etalon used for plates Nos. 88, 89, 90, 91, 93.

MEASUREMENT OF THE PLATES

The plates were all measured at the Dearborn Observatory on a Gaertner engine designed for stellar parallax plates. Through the kindness of Professor Philip Fox, this instrument was made available and greatly facilitated the work, since it has two mutually perpendicular screws. These make it possible to measure all the rings on all lines without touching the plate, and since the dispersion is not large, it makes identification of the ring systems a simple matter. The machine is equipped with half-millimeter screws which enable one to read settings directly to 0.001 mm.

The plate was placed on the machine so that the spectral lines were perpendicular to the horizontal screw, and the position of each good line was located by means of this screw. This position was necessary to identify the line. Then by use of the other screw the diameters of the different rings in each line were measured.

In general, three settings were made on each ring, the mean being used in subsequent computation. For the fine sharp rings of the red cadmium and other similar lines, the settings on any one ring are almost identical, while, for very wide, hazy, or overexposed ring systems, they differ by as much as three or four hundredths of a millimeter. For the ordinary line, the two inner rings were measured except when the innermost ring was too small, or too hazy, in which case, the second and third were chosen. However, for the four cadmium lines and for ten titanium lines scattered through the spectrum, the innermost three or four rings and also the outermost three or four rings were measured. These fourteen special lines were used in the computation of R, the effective focal length of the optical train. As a further precaution and check, these special lines were generally measured twice, once before the general lines were measured and again afterward. The different values of the ring diameters gave an idea of the setting error and made it clear that for many rings it is not possible to repeat the measures closer than 0.01 mm; for sharp rings the deviation is less than half this amount. Throughout the computation all figures are retained to 0.001 mm to prevent errors from accumulating. On some of the plates a few iron impurity lines show; on another two manganese lines were strong enough to permit measurement.

The intensity and quality of each ring system was judged and recorded at the time of measurement. The author used 0 to 20 for intensity gradings, but in the final table the means of his values have been reduced to a scale of 0 to 10 to agree with general usage. The quality was denoted as poor (p), fair(f), good (g), very good, (vg), and the two intermediate ones (fp) and (fg).

Frequently it was not possible to measure an entire plate at one sitting and since the instrument was in constant use, the plate had to be removed between times; but this introduced no error into the results, for each line has its own independent ring system, and only diameters which are the differences of settings made at the same time are used in the computation.

REDUCTION OF MEASURES

The computation was carried out in much the same manner as that described by Pfund[1] so need not be given in detail here. Kilby's wave-lengths[2] for the titanium lines were used as a point of departure. The exact order of interference was determined by the method of Lord Rayleigh,[3] using the best available wave-lengths of the four cadmium lines. Then by use of the laboratory equation given earlier in this paper, the uncorrected wave-length of each line on each plate was computed.

CORRECTIONS

1. *Phase change.*—The next question is the correction to be applied for change of phase. If one assumes, according to the general view, that change of phase is produced by waves of different length penetrating the silver film to different depths, then it is clear that one has a different etalon distance for each different line on the spectrum.

The wave-lengths computed above were of course based on the assumption that the etalon distance was the same for all, namely, its effective distance for the standard Cd ray. If, however, it has a different value for the blue ray, then the order of interference should be corrected for this difference in path, but this amounts to a correction to λ. Furthermore, since the depth of penetration of the rays is independent of the etalon distance, its relative value will be large for a short etalon and almost negligible for a very long one. For the case in hand it will be nearly twice as great for the 4.99 mm as for the 9.81 mm etalon. In fact the ratio of the two distances is 1.92+ and since the correction will be small in any case we may without appreciable error call this ratio exactly two. For the standard ray we may assume that the phase change is zero in both cases. Consequently the uncorrected values of λ given by the short etalon should be just twice as far from the correct value as those given by the long one; or what amounts to the same thing, *the difference between the uncorrected values given by the two etalons is equal to the phase correction which must be applied to the longer etalon values; and is half of what must be applied to the short etalon values.*

---

[1] Pfund, *Astrophysical Journal*, 28, 197–211, 1908.

[2] Kilby, *ibid.*, 30, 243–266, 1909.

[3] Rayleigh, *Philosophical Magazine*, 11, 685–703, 1906.

For if

$$\lambda=\lambda'+d$$

for the long etalon and,

$$\lambda=\lambda''+2d$$

for the short etalon, then subtracting,

$$0=\lambda''-\lambda'+d \text{ or } d=\lambda'-\lambda''$$

where λ is the correct value; λ' and λ'' are the approximate values given by the long and short etalon respectively and d is the phase correction to be applied to the long etalon values. From this it is evident that we can calculate the phase correction as soon as pairs of uncorrected wave-lengths from the two etalons are known.

The values of this correction obtained from the fourteen special lines were plotted against wave-lengths. Then for additional information the values of the correction for all other lines appearing on all ten plates were grouped by zones of wave-length and the mean correction for each zone plotted. Through this double set of points a single curve was drawn and the phase correction given by this curve was applied to the uncorrected values of the wave-lengths.

A glance at the curve will show that the points are scattered principally over the range from 0.0040 to 0.0060 A, between λ 4200 and λ 5400 and it was felt that the straight line $Y = 0.0050$ represented as well as any curve this portion of the graph. From λ 5400 to λ 6400 there is a serious lack of data that makes the shape of the curve in this region a mere guess. Certain it is that it must be zero at λ 6438 and the two values near λ 5900 give the only other information.

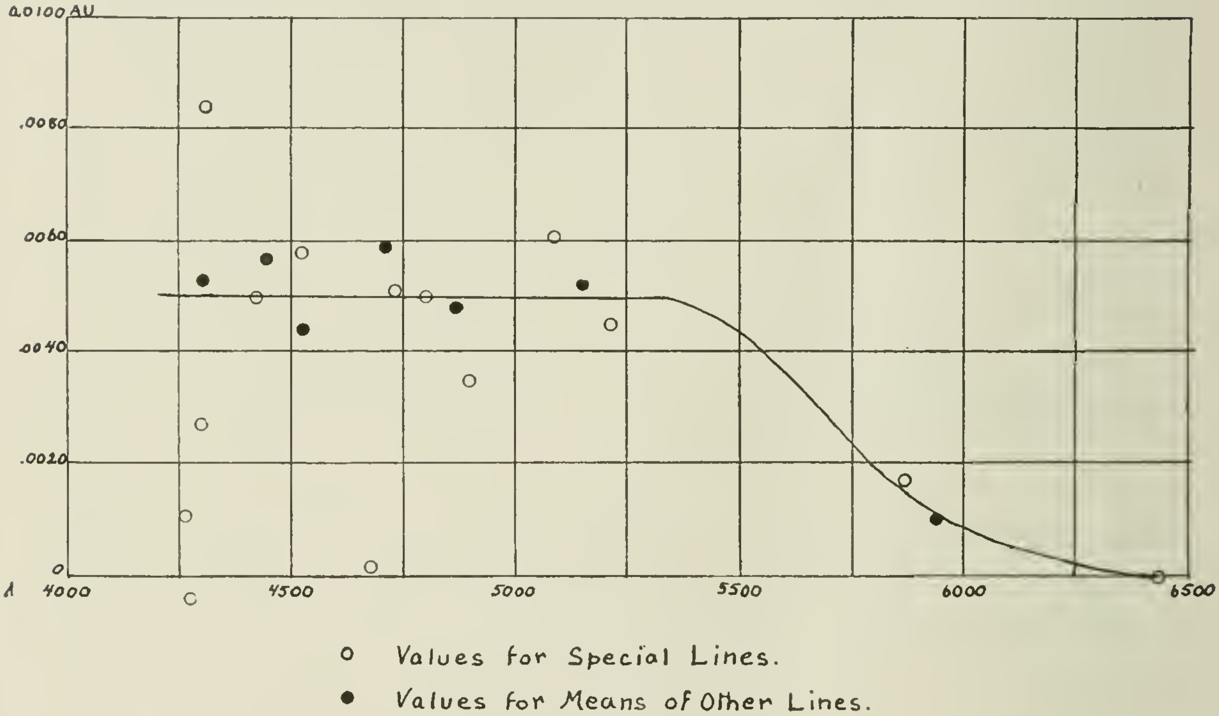

FIG. 3.—Phase change curve

In drawing the curve the values of λ 4263 and λ 4274 are left out of consideration because these lines do not appear on all the plates and are difficult to measure on many of the plates where they do show. Likewise, the values of Cd 4678 are discarded, for the line is known to be complex and it is so close to the stronger line Ti 4681 that it is very hard to measure.

2. Still another correction must be applied in order to reduce the wave-lengths to standard conditions of pressure and temperature (760 mm of mercury and 15° C.) for the air in the etalon space. The maximum value of this correction is of the order of 0.001 A and it was felt that in view of the small relative size of

this error compared to the accidental setting error, and the amount of labor required to compute it for all lines on all plates, it might be omitted without causing appreciable error in the final results.

3. In the case of the standard iron lines measured, a different kind of correction must be considered, before comparing the values in this table·with the International Standards. These standards are obtained from a Pfund arc operated in air at a pressure of one atmosphere; while the source used in this work was in a vacuum. One would expect a pressure-shift. This will be spoken of later.

DISCUSSION OF RESULTS

A comparison of the computed values of the wave-length for any one line given by the short etalon plates shows them to be less in accord among themselves than the values given by the long etalon plates, as indeed one would naturally expect, since the order of interference is greater for the long etalon than for the short. Consequently the values from the short etalon have been given a weight of 2, while those from the long etalon have been given a weight of 3, in computing the mean value. The final wave-length for any line given in Table II is found by correcting each plate value for phase change and taking the weighted mean of these corrected values.

Table II gives the final values for all the lines measured and is arranged as follows: Column 1 gives the weighted mean of the plate values computed in this work. Column 2 gives the wave-length according to Kilby[1] for the titanium lines, and according to Burns, Meggers, and Merrill[2] for the iron lines, and according to Goos[3] for the manganese lines and a few iron lines not given in the Bureau publication. Column 3 gives the average deviation of the individual measures from the mean. Column 4 gives the number of plates on which the line was measured. Column 5 gives the mean value of the intensity on a basis of 10. Column 6 gives the mean value of the quality of the line. Column 7 shows the difference between the values in the first two columns taken in the sense

---

[1] Kilby, *Astrophysical Journal*, **30**, 243–266, 1909.

[2] Burns, Meggers, and Merrill, *Sci. Papers, Bureau of Standards*, No. 274, 1916.

[3] Goos, *Astrophysical Journal*, **35**, 221–232, 1912; **37**, 48–59, 1913.

TABLE II

Brown Wave-Length in I.A.	Kilby Wave-Length in I.A.	Mean Deviation	No. Plates Measured	Intensity	Quality of Lines	Diff. λ Kilby — Brown	Pressure-Shift per Atm.	Notes
Fe 4250.794...	.791	....	1	1	fp	−.003	+.003	
Fe 4260.474...	.489	.000	2	2	f	+.015	+.006	
4263.134...	.142	.003	5	3	fg	+.008	+.003	(1)
Fe 4271.760...	.764	.003	5	3	fg	+.004	+.003	
4274.585...	.600	.002	4	3	g	+.015	....	(1)
4282.696...	.715	.000	2	2	g	+.019	+.003	
4286.006...	.012	.002	8	3	fg	+.006	+.003	
4287.406...	.412	.004	2	2	f	+.006	+.003	
4289.072...	.080	.001	4	3	f	+.008	+.003	
4290.932...	.936	.002	8	3	fg	+.004	....	
4294.103...	.102	....	1	1	fp	−.001	+.004	
4295.751...	.755	.002	8	3	fg	+.004	+.003	
4298.666...	.666	.002	10	4	fg	.000	+.003	(1)
4305.910...	.907	.001	9	8	fg	−.003	+.003	
Fe 4307.899...	.910	.002	5	3	fg	+.011	+.003	
4314.800...	.800	.002	10	5	g	.000	+.002	(1)
4318.630...	.635	.002	5	2	fg	+.005	....	
4321.652...	.659	.002	2	3	g	+.007	....	
Fe 4325.762...	.770	.003	4	5	fg	+.008	+.003	
4337.915...	.915	.004	2	2	fg	.000	+.002	
Fe 4383.544...	.548	.002	6	8	vg	+.004	+.003	
4395.036...	.037	.003	3	3	fg	+.001	+.003	
4404.276...	.273	.003	5	4	g	−.003	+.003	
Fe 4404.749...	.752	.002	4	7	g	+.003	+.003	
Fe 4415.124...	.127	.004	3	4	g	+.003	+.002	
4417.275...	.278	.003	4	4	g	+.003	+.003	
4427.098...	.102	.001	10	7	g	+.004	+.002	(1)
4440.345...	.343	....	1	3	vg	−.002	+.004	
4443.799...	.801	.003	4	4	fg	+.002	+.003	
4449.143...	.127	.003	10	7	g	−.016	+.004	
4450.893...	.902	.005	2	3	fg	+.009	+.004	
4453,308...	.323	.003	3	5	g	+.015	+.005	
4455.319...	.324	.005	2	3	fg	+.005	+.005	
4457.427...	.427	.002	10	7	g	.000	+.005	
4465.807...	.803	.002	8	3	g	−.004	+.003	
4468.493...	.493	.001	5	4	fg	.000	+.006	
4471.239...	.235	.002	8	3	g	−.004	+.003	
4481.259...	.267	.002	7	5	fg	+.008	+.003	
4489.089...	.096	.002	9	5	g	+.007	+.004	
4496.146...	.150	.003	9	4	g	+.004	....	
4501.269...	.271	.002	9	3	g	+.002	+.006	
4512.734...	.736	.002	10	7	g	+.002	+.004	
4518.024...	.026	.002	10	8	g	+.002	+.004	
4522.797...	.803	.002	10	7	g	+.006	+.004	(11)
4527.305...	.315	.002	10	7	g	+.010	+.004	(1)
4544.689...	.700	.002	10	7	vg	+.011	+.004	
4548.767...	.772	.002	7	9	g	+.005	+.004	
4552.454...	.400	.002	10	7	g	....	+.004	(12)
4555.485...	.498	.002	10	7	vg	+.013	+.004	
4563.757...	.765	.003	9	3	fg	+.008	+.004	
4571.970...	.981	.002	10	6	g	+.011	+.006	
4617.270...	.268	.002	10	8	vg	−.002	+.004	

TABLE II—*Continued*

Brown Wave-Length in I.A.	Kilby Wave-Length in I.A.	Mean Deviation	No. Plates Measured	Intensity	Quality of Lines	Diff. λ Kilby − Brown	Pressure-Shift per Atm.	Notes
4623.098...	.098	.002	10	6	vg	.000	+.003	
4629.337...	.335	.002	10	4	g	−.002	+.005	
4645.194...	.188	.001	2	4	g	−.006	+.005	
4650.016...	.017	.003	2	3	fg	+.001	+.005	
4656.468...	.474	.002	5	7	g	+.006	+.002	
4667.585...	.589	.001	5	7	g	+.004	+.003	
Cd 4678.155...	.152	.003	10	6	g	−.003	....	(1), (2)
4681.909...	.914	.003	10	8	g	+.005	+.002	(1)
4691.334...	.341	.003	10	4	g	+.007	+.005	
4698.763...	.790	.002	9	3	g	+.027	+.005	
4710.187...	.194	.002	10	3	g	+.007	+.005	
4722.603...	.621	.001	4	3	g	+.018	+.005	(3)
4723.171...	.179	.001	4	3	g	+.008	+.005	(3)
4742.790...	.801	.003	10	5	vg	+.011	+.005	
4778.263...	.271	....	1	2	g	+.008	+.006	
Mn 4783.415...	.437	....	1	1	fg	+.022	....	
4792.484...	.499	.002	4	2	fg	+.015	....	
Cd 4799.915...	.911	.002	10	9	g	−.004	....	(1), (4)
4805.418...	.434	.003	9	3	fg	+.016	+.009	
4820.412...	.420	.002	10	4	vg	+.008	+.004	
Mn 4823.507...	.526	....	1	3	vg	+.019	....	
4840.874...	.878	.002	10	7	vg	+.004	+.001	
4856.012...	.013	.003	10	6	vg	+.001	+.004	
4868.261...	.286	.003	6	3	fg	+.025	+.003	
4870.129...	.141	.003	7	5	fg	+.012	+.004	
4885.082...	.093	.002	10	7	vg	+.011	+.003	
Fe 4890.773...	.771	.001	3	3	g	−.002	+.009	(5)
Fe 4891.490...	.510	.001	3	3	g	+.020	+.007	(5)
4899.911...	.925	.003	10	7	vg	+.014	+.002	(1)
4913.617...	.625	.002	10	6	vg	+.008	+.003	
Fe 4920.509...	.521	....	1	....	....	+.012	+.001	
4928.339...	.357	.003	9	3	fg	+.018	+.004	
4938.291...	.306	....	1	3	g	+.015	....	
Fe 4957.594...	.612	.001	5	4	g	+.018	+.011	
4981.734...	.746	.002	9	10	g	+.012	+.003	
4991.065...	.077	.002	9	9	g	+.012	+.004	
4999.502...	.512	.002	9	9	g	+.010	+.004	
5007.211...	.218	.003	9	9	g	+.007	+.003	
5014.283...	.262	.002	3	7	g	−.021	+.003	
5016.165...	.174	.005	3	3	f	+.009	+.003	
5020.023...	.045	.002	3	4	g	+.022	+.005	
5022.864...	.872	.006	3	5	f	+.008	+.004	
5024.831...	.853	.002	3	4	fg	+.022	+.003	(6)
5025.589...	.580	.002	3	4	fg	−.009	....	(6)
5039.953...	.962	.003	5	6	fg	+.009	....	
5064.656...	.659	.003	10	7	vg	+.003	+.002	
5071.475...	.490	....	1	5	fg	+.015	+.010	
Cd 5085.823...	.822	.002	10	8	vg	−.001	....	(1), (7)
5113.444...	.441	.003	7	3	g	−.003	+.004	
5120.419...	.429	.003	10	3	g	+.010	+.001	
5145.463...	.470	.002	4	3	fg	+.007	+.004	
5147.487...	.476	....	1	4	vg	−.009	+.002	

TABLE II—*Continued*

Brown Wave-Length in I.A.	Kilby Wave-Length in I.A.	Mean Deviation	No. Plates Measured	Intensity	Quality of Lines	Diff. λ Kilby—Brown	Pressure-Shift per Atm.	Notes
5152.185...	.184	.003	4	3	fg	—.001	+.002	
Fe 5167.491...	.495	.003	2	3	g	+.004	....	
5173.744...	.744	.002	10	7	vg	.000	+.003	
5192.970...	.978	.002	10	7	vg	+.008	+.002	
5210.386...	.394	.001	10	8	vg	+.008	+.002	(1)
5224.304...	.323	....	1	....	....	+.019	....	(13)
5224.946...	.960	....	1	....	....	+.014	....	(13)
Fe 5232.940...	.957	....	1	2	fg	+.017	+.014	
5255.811...	.824	.002	4	3	g	+.013	+.036	
5265.971...	.968	.003	6	3	g	—.003	+.021	
Fe 5269.536...	.532	.003	5	5	vg	—.004	+.003	(8)
Fe 5270.372...	.360	.003	5	5	vg	—.012	....	(8)
5283.441...	.448	.002	3	3	g	+.007	....	
Fe 5324.180...	.195	.002	2	1	f	+.015	+.015	
Fe 5328.040...	.044	.003	4	3	g	+.004	+.004	
Fe 5371.494...	.497	....	1	4	vg	+.003	+.004	
Fe 5397.135...	.132	....	1	3	g	—.003	+.004	
Fe 5405.776...	.781	....	1	3	g	+.005	+.003	
5409.614...	.625	....	1	2	g	+.011	+.002	
Fe 5429.700...	.701	....	1	3	g	+.001	+.004	
Fe 5446.916...	.920	....	1	3	g	+.004	+.004	
Fe 5455.613...	.614	....	1	1	fp	+.001	+.004	
5477.697...	.732	....	1	5	f	+.035	....	
5512.526...	.538	.002	5	7	g	+.012	+.006	(9)
5514.350...	.364	.002	5	7	g	+.014	+.006	(9)
5514.536...	.541	.003	5	5	g	+.005	+.007	(9)
5565.477...	.507	.002	4	3	g	+.030	+.006	
Fe 5615.643...	.661	....	1	3	g	+.018	+.016	
5644.136...	.181	.004	10	4	g	+.045	+.004	
5662.155...	.211	.003	6	3	fg	+.056	+.029	
5675.413...	.474	.003	3	2	fg	+.061	+.031	
5804.264...	.388	....	1	2	fg	....	....	(14)
5866.451...	.508	.002	10	5	g	+.057	+.004	(1)
5899.292...	.338	.002	8	4	g	+.046	+.004	
5922.109...	.160	.001	2	2	fg	+.051	+.006	
5953.160...	.205	.004	10	3	g	+.045	+.003	
5965.825...	.862	.003	10	3	g	+.037	+.005	
5978.541...	.582	.004	10	3	fg	+.041	+.002	
6085.224...	.247	....	1	4	g	+.023	+.003	
6091.172...	.188	.003	2	3	g	+.016	+.006	
6126.213...	.239	.002	3	3	g	+.026	+.002	
6258.099...	.110	.004	4	5	g	+.011	+.009	(10)
6258.700...	.708	.006	3	6	g	+.008	+.008	(10)
6261.097...	.096	.004	3	5	f	—.001	+.009	(10)

NOTES

Fe values in second column are taken from the values of Burns, Meggers, and Merrill.

The wave-lengths of the Mn lines and of a few Fe lines not given in foregoing reference are taken from Goos.

(1) Special line. Mean of all values.

(2) Meggers' value, 4678.1504.

(3) Close double. These two lines show only one ring system. Measured on long etalon only.

(4) Meggers' value, 4799.9139.

(5) Close double. Only one ring system. Measured on short etalon plates only.

(6) Close double. These two lines show only one ring system. Measured on short etalon plates only.

(7) Meggers' value, 5085.8230.

(8) Close double. Only one ring system. Measured on short etalon plates only.

(9) and (10) These three lines show only one ring system on the long etalon plates. On the short etalon plates they are distinct. Values given here are from short etalon only.

(11) Misprint in Kilby, given as 4522.303, corrected from Kayser's *Handbuch.*

(12) Error in Kilby corrected from Kayser's *Handbuch.*

(13) Two distinct systems of rings on short etalon plate B 90.

(14) Evidently a typographical error in Kilby.

Kilby minus Brown. Column 8 contains the pressure-shift per atmosphere as given by Gale and Adams[1] for Fe and Ti. Column 9 refers to notes at the end of the table.

An examination of column 3 shows that the mean deviation for most of the lines is 0.002 or 0.003 A; dividing this by the square root of the number of plates measured we have an approximate value for the probable error. For the large majority of the lines this is of the order of 0.001 A. From these considerations it is evident that the values in the table compare favorably with other determinations of wave-length by interference methods.[2]

The table includes four pairs of very close lines, each pair showing a single ring system. Three of the pairs showed only on the short etalon plates; one was measured on the long etalon plates only. As it was impossible to decide which one if only one of the two lines was responsible for the ring system, the values as determined for both lines of each pair are given in the table. They are probably interesting rather than valuable. There also appear in the table two sets of triplets in the orange-red region. Here the prism has low dispersion and on the long etalon plates only a single, wide ring system appears for each set of triplets. In both cases, however, the short etalon plates show a ring system for each line. The values given in the table are therefore taken from the short etalon plates only.

---

[1] Gale and Adams, *Astrophysical Journal*, **35**, 10–47, 1912.

[2] Fabry and Buisson, *Journal de Physique*, August, 1913; *Transactions, Solar Union*, **3**, 139–140, 1910; **4**, 46–48, 1913.

The differences of wave-length between Kilby's values and mine are for the most part small and these small differences may well be due to pressure-shift. It is assumed that Kilby's arc was operated at atmospheric pressure since he mentions no vacuum. In the orange and red regions, however, the differences are sometimes as much as 0.050 A, but no explanation can be given by the present author as his own values agree among themselves within a few thousandths of an angstrom.

The differences shown in column 7 for the iron lines are some large, some small, but whether large or small most of them agree in sign and magnitude with the pressure-shift given by Gale and Adams and are to be expected from the fact that my arc was worked in vacuum. In so far as they do not agree they point out more clearly the need of further work on the iron arc in vacuo.[1]

The two manganese lines show large differences but here again pressure-shift is probably the cause. Humphreys,[2] grouping all iron lines together and all manganese lines together, finds that on the average the iron lines are shifted 0.025 A by a change of pressure of 12 atmospheres while the manganese lines are shifted 0.033 A by the same change in pressure.

In the case of cadmium, two of the three lines agree well with the latest values of Meggers.[3] The other, λ 4678, differs by 0.005 A. However, the means of the values given by the long and the short etalon differ by this amount and as pointed out in the discussion of the correction for phase the line is known to be complex and is very hard to measure especially on the short etalon plates.

In conclusion the author wishes to express his sincere thanks to Professor Crew and to Professor Fox for their constant interest and many helpful suggestions throughout the course of this work.

NORTHWESTERN UNIVERSITY
April 1922

---

[1] St. John and Babcock, *Astrophysical Journal*, **53**, 260–299, 1921.

[2] Humphreys, *ibid.*, **6**, 169–232, 1897.

[3] These values are not yet published but were made available through the kindness of the author.

MINOR CONTRIBUTIONS AND NOTES

MAJORANA'S THEORY OF GRAVITATION

ABSTRACT

Consequences of Majorana's gravitational results.—The more obvious objections to these results are removed if account is taken of the relativity of the gravitational field and we suppose that the *absorbing effect* is zero for a freely falling body. In fact a confirmation of these results would give a direct demonstration of the *principle of equivalence.* Nevertheless, other very formidable difficulties arise if we attempt to construct a complete theory on this basis. If the results are correct it should be possible to construct a *perpetual-motion machine.*

With reference to Professor Russell's paper on "Majorana's Theory of Gravitation" (*Astrophysical Journal*, 54, 334), it may not be out of place to consider from a different point of view what theoretical deductions would have to be drawn if the provisional experimental results were confirmed. Russell's results take a different aspect, if account is taken of the relativity of the gravitational field. Clearly a body can only be expected to absorb the gravitational field which is relative to itself, and not the field which is relative to something else. If the body of a man absorbs $1/K$ of the field passing through him, the absorption by "the man in the lift" will be $1/K$ of the enhanced or reduced field which he experiences in the lift, and not $1/K$ of the ordinary G. Now the particles of a planet are all falling freely, so that (except for the minute tide-raising force) the sun's field *relative to them* is zero, and no absorption takes place because there is nothing to absorb; the rear part of the planet is not screened by the front part. In brief, the mercury in Majorana's experiment absorbs because it is not allowed to fall; the planet does not absorb because it is allowed to fall. It is scarcely too much to say that a confirmation of Majorana's result, coupled with the absence of such an effect for the planets as shown by Russell, would give a direct demonstration of the principle of equivalence.

Since the outer parts of the sun and planets are not allowed to fall relatively to the inner parts, the effective mass as measured by the gravitation-exerting power on surrounding objects would be less than the "true" mass, quite in accordance with Majorana's and Russell's formulae.

While the more obvious objections to Majorana's results are removed by this consideration, it seems that other very formidable difficulties arise if we attempt to construct a complete theory on this basis; so that, although confirming the principle of equivalence, Majorana's absorption would be far from acceptable to gravitational theory as a whole. It may be remarked that since the supposed absorption must be coupled with the condition that the body is not allowed to fall, it may be attributed to the cause which prevents a fall. That is to say, the stresses (which hold up the body) exert a gravitational field, which, superposed on the ordinary attraction of the masses, modify the gradient of the field in a way which is interpreted as absorption. Einstein's theory admits that stresses as well as masses exert gravitation, and a very minute absorption by a supported body would, I think, be consistent with his theory; but his results, based on the conservation of energy and momentum, are of a far smaller order of magnitude than Majorana's. This is not surprising since, if Majorana's theory is correct, it should be easy to construct a perpetual-motion machine.

A. S. EDDINGTON

THE
ASTROPHYSICAL JOURNAL
AN INTERNATIONAL REVIEW OF SPECTROSCOPY
AND ASTRONOMICAL PHYSICS

VOLUME LVI SEPTEMBER 1922 NUMBER 2

REVISION OF THE SERIES IN THE SPECTRUM OF STRONTIUM

By F. A. SAUNDERS

ABSTRACT

Series of triplets and singlets in the spectrum of strontium.—These series belong to the neutral atom of Sr. Their remarkable similarity to the corresponding series of Ca, which have previously been critically studied, was of great assistance in working out the structure. The present study is based on measurements of spectrograms, from ultra-violet to infra-red, taken by Randall, King, and the author, of light from a great variety of sources, including sparks, arc in air and in vacuo, tube-resistance furnace and red-hot quartz discharge tube containing very pure Sr vapor. Revised *wave-lengths* are given for most of the 180 lines from 0.22 to 3.06 μ, including some *seventy new lines.* The limits of all the series have been more accurately found, and the various "terms" have been calculated. Details are given, with tables, of four type series of triplets and four of singlets, four combination series in the triplet system, three in the singlet system, and five inter-system combination series. Of the *twenty series* here mentioned, some are very faint and are represented by one term only, and about half are believed to be new. Evidence is also presented of the existence of *new types of singlet series* corresponding to formulae $(1P)-(mX)$, $(1p)-(mX)$, $(1P)-(mY)$, etc. The terms are all large, so that the series cannot be of the sort suggested by Sommerfeld.

New type of series of singlets in the spectrum of calcium.—Three singlet lines are found to correspond accurately to $(1P)-(mX)$, $(1p_1)-(mX)$ and $(1p_2)-(mX)$ where (mX) is 8584.8. This points to the existence of series similar to those last mentioned for Sr.

The spectra of Ba and Ca have recently[1] been critically examined in the attempt, only partially successful, to arrange all of their lines into series. The present article is to give an account of similar results for Sr. As before, attention is here directed to the spectrum of the normal atom only, excluding those series (pairs), which are due to the atom (Sr^+) in an ionized condition. These will, it is hoped, be the subject of a later communication.

---

[1] *Astrophysical Journal*, **51**, 23, 1920, and **52**, 265, 1920.

The spectrum, thus restricted, consists of series of triplets and of singlets, and these form two systems. Each system contains at least four types of series, with combination series formed from these; and there are combinations also formed between the two systems. The amazing similarity between the spectra of Ca and of Sr, extending as it does down to the minutest details, makes it easy to deduce the structure of one from that of the other. Rydberg[1] has indeed laid the two down in parallel columns, and the new data admit of like treatment.

The observations upon which the present work is based comprise photographs taken with grating and with prism instruments of a great variety of sources. Of the greatest value in this connection have been some of the admirable oven spectra taken by Dr. A. S. King, and kindly sent to me for study. These were spectra of a mixture of Sr and Ba, and on this account the weaker Sr lines did not appear, but the plates were very useful on account of their high dispersion (up to 1.86 A per mm) and their sharpness. Many close doubles were thus separated. The use of the oven under reduced pressure also made it possible to obtain as sharp fine lines certain Sr lines which are usually (e.g., arc in air) very much broadened. To supplement these plates, I took others, using as source a red-hot quartz tube, well exhausted, and supplied with metallic Sr, through whose vapor a discharge from a small 10,000-volt transformer was passed. The metal I owe to the kindness of Dr. B. L. Glascock,[2] who prepared it with great care, so that it is almost entirely free from impurities, and contains, in particular, almost no Ca. The spectrum of this source is in striking contrast to the ordinary Sr spectrum, through the absence of the usual oxide bands, and the sharpness of all the lines. The oven, moreover, encourages certain lines, of King's temperature Classes I and II, which I find to belong to the singlet system of series, and on this account very many new ones were observed. For work in the visible part of the spectrum I am indebted to the Rumford Fund Committee for a grant which enabled me to construct a large Littrow form of glass spectrograph, which gives excellent spectra, on a fairly large scale (10 inches for the visible spectrum) and makes it possible to carry the search for faint lines down into the beginning of the infra-red. I am also indebted to Dr. Meggers, of the Bureau of Standards, for a small quantity of dicyanin for this purpose.

---

[1] *Wied. Ann.*, 52, 119, 1894.

[2] See *Journal of the American Chemical Society*, 32, 1222, 1910.

Other sources also have been used, such as the arc in air and in vacuo and the spark under a variety of conditions. Professor H. M. Randall's recent study of the arc spectrum of Sr (unpublished), concerning the progress of which he has kindly kept me informed by letter, has been of great service. The correct arrangement of lines in series is that which leads accurately to combination lines, which frequently lie in the infra-red; and it has been possible to settle many doubtful points only through such tests. Advantage has also been taken of the observations of Hampe,[1] Lorenser,[2] C. F. Meyer,[3] and Meggers.[4]

The results are presented, as before, with the same notation, under the headings of the individual series. All wave-lengths are on the international system. The numeration (values of m) chosen in my tables differs from that used by Fowler in his *Report on Series in Line Spectra* (1922) only in respect to the fundamental series in both singlet and triplet systems. My values of m for these series must be increased by 2 to bring them into agreement with those of Fowler.

THE TRIPLET SYSTEM

Principal series of triplets: $(1s)-(mp)$.—The first member of this series is shared with the sharp series of triplets; its lines are λλ 7070.28, 6878.12, 6791.06. The corresponding terms $(1p)$ are 31026.8, 31421.1, 31608.0. The second triplet was found by Randall, but its place was predicted through the combination series $(1d)-(mp)$, given below. The predicted wave-lengths are λλ 20259; 20698; 20762;[1] and those observed by Randall λλ 20263; 20705; 20767. The third triplet can be calculated in the same manner and should be at λλ 9595; 9624; 9637. Randall has observed one line at λ 9597. The fourth triplet has not been positively identified; its strongest line should be near λ 7873, but it is probably extremely faint.

---

[1] *Zeitschrift. wiss. Phot.*, 13, 348, 1914.

[2] Tübingen dissertation, 1913.

[3] *Astrophysical Journal*, 45, 93, 1917.

[4] *Scientific Papers of Bureau of Standards*, No. 312, 1918.

Sharp series of triplets: $(1p)-(ms)$.—Table I gives the wave-lengths of the lines of this series, together with the wave-number differences within each triplet, which should remain constant. The "terms" are also given. The last four lines are believed to be new. The series is of medium strength, well developed in arc and in oven spectra.

TABLE I

Sharp Series of Triplets. $(1p)-(ms)$				Limits 31026.8; 31421.1; 31608.0		
λ I.A.	$\Delta\nu_1$	λ I.A.	$\Delta\nu_2$	λ I.A.	Terms	m
7070.28	395.0	6878.12	186.2	6791.06	16886.8	1
4438.03	394.0	4361.74	186.8	4326.47	8500.9	2
3865.46	395.5	3807.24	186.8	3780.35	5163.2	3
3628.33	393.7	3577.20	188.9	3553.19	3473.4	4
3504.04	391.9	3456.56	187.6	3434.28	2498.0	5
3430.16	394.1	3384.39	....	....	1882.0	6
3382.10	394.6	3337.65	....	....	1467.7	7

Diffuse series of triplets: $(1p)-(md)$.—This is the most obvious series in the spectrum of Sr, and contains some very strong lines. Of the lines given in Table II some fifteen are believed to be new, and most of the lines have been redetermined on plates taken from vacuum sources, where the lines lose their characteristic diffuseness and become accurately measurable. The complexity of the triplets is thus disclosed, and there appears a trace of the same abnormality in the spacing of these complexities as was noted in the corresponding series in Ca, though the observations are here less complete. The "curve of residuals" also takes a form somewhat like that for Ca and given in Figure 1 of the Ca article referred to above.[2]

---

[1] See footnote on p. 78.

[2] *Astrophysical Journal*, **52**, 265, 1920.

TABLE II

Diffuse Series of Triplets. (1p) − (md)				Limits Same as in Sharp Series		
λ I.A.	$\Delta\nu_1$	λ I.A.	$\Delta\nu_2$	λ I.A.	Terms	m
30665	394.7	27355.3	187.1	26023.6	27606.0	1
30109.7	394.3	26914.5			27706.4	
29225.0					27766.0	
4971.65	394.2	4876.06	186.7	4832.08	10880.5	2
4967.93	394.0	4872.51			10903.3	
4962.31					10918.3	
4033.19	394.2	3970.05	186.9	3940.81	6222.2	3
4032.39	394.3	3969.27			6234.5	
4030.39					6239.4	
		3653.93	186.9	3629.14	4051.0	4
3706.74	395.0	3653.26			4056.5	
3705.98					4061.1	
		3500.11	186.8	3477.37	2850.6	5
3548.65	394.2	3499.69			2855.1	
3548.09					2858.7	
				3390.67	2116.4	6
3458.47	394.2	3411.94			2120.5	
3457.98					2123.7	
				3336.13	1634.0	7
		3356.69			1638.4	
3401.22					1641.7	
					1300.3	8
3363.84	395.0	3319.72			1307.0	
3363.04						
					1060.5	9
3336.58	392.7	3293.42			1065.4	
3336.13						
3316.32					881.5	10
"Covered" by other strong lines						11
3289.74					638.0	12
3280.54					552.8	13

Fundamental series of triplets: (1d) − (mf).—This series was first found by Fowler. It has been remeasured and several close pairs resolved in it. From λ 3852 on, all the lines are new. Its triplets are complex, like those of the corresponding Ba series, but very close.

TABLE III

FUNDAMENTAL SERIES OF TRIPLETS. $(1d)-(mf)$				LIMITS 27606.0; 27706.6.1; 27766.0		
λ I.A.	$\Delta\nu_1$	λ I.A.	$\Delta\nu_2$	λ I.A.	Terms	m
4893.12	100.3	4869.19	59.7	4855.08	7170.2	1
4892.69	100.5	4868.74	....	....	7172.9	....
4892.03	....	....	....	....	7174.6	....
....	....	4319.12	58.7	4308.07	4558.7	2
4337.89	100.6	4319.03	....	....	4559.6	....
4337.70	....	....	....	....	4560.4	....
4087.46	99.5	4070.88	59.2	4060.92	3147.6	3
3950.65	100.1	3935.10	59.7	3925.86	2301.1	4
3866.98	99.8	3852.11	60.1	3843.12	1753.5	5
3811.94	99.6	3797.50	59.5	3788.94	1380.5	6
3773.76	99.6	3759.62	59.3	3751.26	1115.3	7
3746.13	99.7	3732.19	60.4	3723.80	919.7	8
3725.24	....	....	....	....	769.6	9
3708.87	....	....	....	....	651.2	10

COMBINATION SERIES IN THE TRIPLET SYSTEM

Series $(1d)-(mp)$.—If we subtract the three terms $(2p)$, which are 11952.2, 12056.9, and 12071.5 (or 12098.2 ?[1]) from the three terms $(1d)$ given above, we obtain nine wave-numbers of which six give real lines in a group in the red, first completely observed by Lorenser. This group is the second member of this series, the first being the first of the diffuse series triplets, taken with negative sign i.e., $-(1p)+(1d)$. The third member of this series is composed of a group of six lines at λλ 4729.52; 4713.96; 4707.10; 4703.93;

[1] There is a curious difficulty here. The term 12071.5 corresponds to a line, λ 6369.91, in the group $(1d)-(2p)$, which has the right intensity, but is, by analogy with Ca, too close to the next group line, λ 6363.88. The corresponding $(1s)-(2p)$ line is λ 20767, which appears (Randall) to have the correct intensity. If, however, we were to consider λ 6380.72 as the true line in the $(1d)-(2p)$ group, we should also find a $(1s-2p)$ line at λ 20882 in the right position and of a tolerable intensity; but a new objection arises from the fact that λ 6380.72 appears to belong also to another group of lines, whose series significance is not yet clear, and observations on the Zeeman effect (Paschen; unpublished) indicate that this classification is correct. Hence, since analogy is a less trustworthy guide, I have discarded this second alternative.

4700.75; 4693.89; which yield terms ($3p$) as follows: 6467.8; 6498.7; 6513.1. By means of these the third triplet of the principal series was calculated. The fourth member of the series may begin with a line at λ 4269.20, but, if so, others of this group are too faint to have been observed.

Series $(2d)-(mf)$.—This series is represented by a triplet in the infra-red at λλ 26947; 26806; 26714, given by the combination $(2d)-(1f)$. The next member does not appear, doubtless on account of faintness.

Series $(2p)-(md)$.—This series is also represented by a triplet in the infra-red at λλ 17446; 17170; 17137, given by the combination $(2p)-(3d)$. The next member is not found.

Series $(2p_1)-(ms)$.—One line, λ 28964, appears to be the combination $(2p_1)-(2s)$. No others have been found. This combination was not found in Ca. The region in which it lies in Ba has not yet been investigated. It is probably real.

THE SINGLET SYSTEM

Principal series of singlets: $(1S)-(mP)$.—This series is the one formerly called $SL1$.[1] Its later lines have been measured, and the limit much more accurately obtained. Table IV gives numerical data of this series. The terms there given are averages obtained from this series and the combination series $(1D)-(mP)$ given below (p. 82).

TABLE IV

SYSTEM OF SINGLET SERIES

	PRINCIPAL $(1S)-(mP)$		SHARP $(1P)-(mS)$		DIFFUSE $(1P)-(mD)$		FUNDAMENTAL $(1D)-(mF)$	
m	λ I.A.	Terms	λ I.A.	Terms	λ I.A.	Terms	λ I.A.	Terms
1....	4607.34	24227.1	−4607.34	45925.6	−(6.45μ)	25776.3	5156.07	6387.0
2....	2931.88	11827.5	11242.3	15334.5	7621.54	11110.0	4678.35	4406.9
3....	2569.50	7019.0	5970.10	7481.6	5543.42	6192.4	4406.05	3086.8
4....	2428.11	4753.5	5165.45	4873.1	4965.54	4093.7	4252.97	2269.9
5....	2354.32	3463.4	4783.93	3329.6	4688.59	2904.7	4158.49	1735.8
6....	2307.39	2598.8	4582.91	2412.8	4527.29	2145.0	4096.14	1370.0
7....	2275.29	1989.2	4463.31	1828.3	....	....	4052.47	1106.9
8....	2253.32	1559.8	....	....	....	....	4021.02	913.9
9....	2237.65	1251.0	....	....	....	....	3997.16	765.6
10....	2226.38	1022.0	....	....	....	....	3978.47	648.1

---

[1] *Astrophysical Journal*, 32, 153, 1910.

Sharp series of singlets: $(1P)-(mS)$.—There is the same difficulty in discovering this series as arose in the case of Ca, and the arrangement given in Table IV must be regarded as tentative, especially as regards the last three lines. λ 4783.93 appears on one of my plates as a wing on the strong line λ 4784.39, from which it is not clearly resolved; and there is some question whether a faint line at λ 4585.92 should not be put in place of λ 4582.91. The last four lines given in the table are new, and indicate to what an extent the oven brings out the lines of these rather retiring series.

Diffuse series of singlets: $(1P)-(mD)$.—In harmony with the arrangement already adopted in Ba and Ca, the term 25776.3, which occurs as the limit of the two series formerly called $SL2$ and $SL3$, is considered to be $1D$, the first term of the diffuse series. The second line in this series should lie at the edge of the infra-red, and the choice shown in Table IV must be regarded as somewhat uncertain. There are several good lines in this neighborhood, and a selection among them is difficult. Lacking Stark-effect observations to guide us, we must turn to combinations which would result in consequence of our choice. A number of such combinations occur, but in no case is their arrangement precisely similar to the case of Ca. The choice for the second line of the series seems to lie between λ 7621.54 and λ 7673.11, both of which give interesting combinations. As far as the combinations go, λ 7673.11 is more like the Ca line selected for this place (λ 7326.10), but it fits less well into the "curve of residuals" for the series. It is not now possible to make a final decision on this point. The rest of the series, however, seems fairly certain, and the form of the curve of residuals is exactly like the one for the same series in Ca.

Fundamental series of singlets: $(1D)-(mF)$.—This is the series formerly known as $SL3$. Its lines, given in Table IV, are remeasured with much greater precision, and six new ones have been added. Its terms are, as usual with this type, not far from those of the series in hydrogen.

Indications of new types of singlet series.—Both Ca and Sr show a few strong lines which do not fit into the conventional series scheme, as above outlined, and yet which show, through their

Zeeman effect and their temperature classification, so far as known, that they belong to the singlet system. Sommerfeld has suggested, following an indication given earlier by Paschen, that there are more than four types of series; and the new types should approach more and more nearly to the hydrogen type. Apparently their terms can never be large, and must be less, in fact, than those of the fundamental series. Any indications, therefore, of the existence of new types of series whose terms are *not* small enough to harmonize with Sommerfeld's suggestion, would be of considerable interest, as tending to show that these spectra contain greater complexities than the present atomic model suggests. Such terms we may call (mX), (mY), etc., without attempting to specify what sort of series they may belong to.

If $(mX)=8964.5$, I find that $(1P)-(mX)$ leads exactly to λ 6550.25 (calculated $\nu=15262.6$; observed, 15262.4); $(1p_1)-(mX)$ leads to λ 4531.32 (calculated $\nu=22062.3$; observed, 22062.4); $(1p_2)-(mX)$ leads to λ 4451.80 (calculated $\nu=22456.6$; observed, 22456.3); $(1p_3)-mX)$ leads to λ 4414.87 (calculated $\nu=22643.5$; observed, 22644.5, but some doubt as to whether this is a true Sr line). The corresponding term in Ca is 8584.8, and $(1P)-(mX)$, $(1p_1)-(mX)$, $(1p_2)-(mX)$ there lead to observed lines at λλ 5857.48; 3935.36; and 3918.90, respectively, with great accuracy. I cannot find a second term for this series.

If $(mY)=11198.2$, then $(1P)-(mY)$ leads to λ 7673.11 (calculated $\nu=13028.9$; observed, same), and $(1p_2)-(mY)$ to λ 5041.85 (calculated $\nu=19828.6$; observed, 19828.5).

If $(mZ)=8765.2$, then $(1P)-(mZ)$ leads to λ 6465.79 (calculated $\nu=15461.9$; observed, 15461.8); $(1p_1)-(mZ)$ leads to λ 4491.01, a faint oven line (calculated $\nu=22261.6$; observed, 22260.5, perhaps an accidental agreement) and $(1p_2)-(mZ)$ leads to λ 4412.62 (calculated $\nu=22655.9$; observed, 22656.0).

Several of the lines involved in these combinations are new and fairly strong in the oven spectra.

All of these terms are large, and it seems unavoidable to conclude that if they belong to new types of series, as one would expect from the existence of the foregoing combinations, such series cannot be of the sort contemplated by Sommerfeld.

COMBINATION SERIES IN THE SINGLET SERIES

Series $(1D)-(mP)$.—This is the series formerly called $SL2$. Its lines have been remeasured, and three new ones found. The revised wave-lengths run as follows: λλ 7167.29; 5329.82; 4755.57; 4480.54; 4313.18; 4202.81; 4128.24; 4076.32; 4038.53. The corresponding terms have been given in Table IV on page 79. This is the strongest of the combination series of the singlet system, and is very well brought out in oven spectra.

Series $(1S)-(mD)$.—This is a faint series, whose existence seems certain, in spite of rather defective observations. The first line occurs at λ 4961.50 and was found by Dr. King precisely in its predicted position, on one of his high dispersion plates, and clearly separated from its strong neighbor λ 4962.31 of the diffuse triplet series. The second member should appear at λ 2871.43. A faint, diffuse line appears in the arc in air near λ 2871.00 which is probably the line in question. The third member has not been found, but a faint line at λ 2389.3 may be the fourth member of the series.

Series $(2S)-(mP)$.—One line of this series seems to have been found by Randall, namely $(2S)-(2P)$; calculated λ 28505; observed, 28516. The agreement is not very satisfactory.

INTER-SYSTEM COMBINATION SERIES

Series $(1S)-(mp_2)$.—This series is well known, on account of the importance of its first line in connection with radiation potentials. This line is at λ 6892.60, as was first pointed out by Lorenser. The second was found in oven spectra at precisely the calculated place, λ 2951.71. The third line is too faint to be visible on any of my photographs.

Series $(2S)-(mp_2)$.—The first line of this series may be the line observed by Randall at λ 30482, though the calculated position is 12 A lower.

Series $(1D)-(mp)$.—One triplet of this series occurs, $(1D)-(2p)$ or at least two of its lines, at λλ 7232.24 and 7287.44, reasonably near their calculated positions. The third line $(1D)-(2p_3)$ should coincide with λ 7309.46, which is too strong, relative to the others, to be formed from this combination. Perhaps there are two lines, not resolved, at this place.

Series $(1p)-(mS)$.—Since $(1p)$ has three values, this combination calls for three series, of which only one appears, namely $(1p_2)-(mS)$ and that very imperfectly. The combination $(1p_2)-(3S)$ leads to λ 4175.84, a faint line in oven spectra, with an accuracy of about 0.1 A.

Series $(1p)-(mD)$.—Lines occur at $(1p_2)-(3D)$ and $(1p_2)-(4D)$, λλ 3962.61 and 3658.23, both new oven lines, the first rather strong. The agreement with calculation is satisfactory, the differences being less than 0.1 A. No other line of the series could be found. Another line, λ 4025.52, of the same character, seems to be $(1p_1)-(3D)$, and possibly the combination $(1p_1)-(4D)$ also occurs, at λ 3711.90, which is a faint oven line. It seems likely, therefore, that both series $(1p_1)-(mD)$ and $(1p_2)-(mD)$ occur. If $(1p_3)-(mD)$ occurs, it must be much fainter than the others.

Jefferson Physical Laboratory
Harvard University
July 1922

FURTHER EVIDENCE ON THE BRIGHTNESS OF THE STARS OF THE NORTH POLAR SEQUENCE[1]

By FREDERICK H. SEARES and MILTON L. HUMASON

ABSTRACT

Mount Wilson photographic and photo-visual scales of magnitude.—These scales were based wholly on plates made with the 60-inch reflector and as there was some question as to photographic magnitudes brighter than the tenth, and photo-visual magnitudes fainter than the eighth, *additional data* have recently been secured with the 10-inch Cooke refractor. Exposures both with and without a wire screen which absorbs 3.02 magnitudes were made on 54 plates. Taking the photographic magnitude of each star to be $0\overset{\mathrm{M}}{.}19\,C$ less for the 10-inch than for the 60-inch, where C is the color-index, and the photo-visual magnitude to be the same for both, the investigation reveals no appreciable error in the photographic scale and shows it to be homogeneous from the fourth to the fourteenth magnitude; and the slight correction of $+0\overset{\mathrm{M}}{.}05$ indicated for the photo-visual scale near the ninth magnitude is not confirmed by more reliable exposure-ratio results to be reported elsewhere. The original scales are therefore retained.

Revised magnitudes of stars of the Polar Sequence.—The plates also enable corrections to be given to the photographic magnitudes of 45 stars and to the photo-visual magnitudes of 28 stars. These average $\pm 0\overset{\mathrm{M}}{.}03$ and $\pm 0\overset{\mathrm{M}}{.}04$, respectively, for the two scales. The larger photographic corrections are in substantial agreement with those recently found at Greenwich by Jones.

The following pages summarize a recent investigation of the brightness of stars near the North Pole, undertaken in connection with the work of the International Commission on Stellar Magnitudes. Certain results of the earlier investigation[2] had not yet been fully confirmed by observations made elsewhere,[3] and, as the original measures had been wholly with the 60-inch reflector, it seemed desirable that additional data be secured with an entirely different instrument.

The question at issue related mainly to the photographic magnitudes of stars brighter than the tenth magnitude. From the tenth to the fifteenth or sixteenth magnitudes there was evidence that the scale had been well determined; but between the sixth and tenth magnitudes there remained an unexplained difference of a quarter of a magnitude between the Harvard and Mount Wilson results.

---

[1] *Contributions from the Mount Wilson Observatory*, No. 234.

[2] *Mt. Wilson Contr.*, No. 97; *Astrophysical Journal*, **41**, 206, 1915.

[3] Besides short series of measures by Parkhurst and Schwarzschild, King's results, *Harvard Annals*, **76**, No. 10, were in agreement with Mount Wilson. Jones's observations, *Monthly Notices*, **82**, 21, 1921, which are also in excellent agreement, appeared after the present investigation was begun.

Visual magnitudes of the stars of the Polar Sequence have been measured at the Harvard Observatory to the thirteenth magnitude. Besides these and the Mount Wilson photo-visual results published simultaneously with the photographic magnitudes in *Mt. Wilson Contribution* No. 97, there is no evidence bearing on the visual or photo-visual scale of the stars in the polar region fainter than the eighth magnitude. Further investigation of this scale was therefore also desirable.

The instrument used for the present investigation was the 10-inch Cooke refractor of 45 inches focal length, which represents a radical change in conditions as compared with the 60-inch reflector. Its relatively small aperture implies an entirely different relation between diffraction pattern and resulting photographic image of a star; its small focal length means minimized influence of atmospheric tremor; its large field results in small corrections for distance error (for a compact group of stars at least); while its large color equation presents an extreme example of the difference in the color-sensibility that may affect the instrumental equipment.

The reduced-intensity exposures were made with a wire screen absorbing about three magnitudes, placed in front of the objective. As usual, equal multiple exposures, arranged in a symmetrical sequence (for example: full aperture, screen, screen, full aperture), were made on each plate, the exposures for different plates ranging from 1 to 32 minutes in order that stars of widely differing brightness might be accurately measured.

The longer exposures for photographic brightness extend several magnitudes below the questionable portion of the scale. This greatly simplified the reductions; for since the photographic scale below the tenth magnitude may be accepted as reliable, the magnitudes in this region could be used to determine the absorption produced by the screen. Moreover, as will appear shortly, a series of photographs covering a wide range in exposure time affords a simple means of testing the homogeneity of the scale without actually calculating the magnitudes of individual stars. This calculation is eventually necessary, but it is convenient to see in advance if a divergence in scale is to be expected.

The photographs were taken and measured by Humason. For much of the calculation connected with their reduction we are greatly indebted to Miss Joyner. For the determination of the photographic scale 43 plates were available. The investigation of the photo-visual scale, which depends on only 11 plates, could be much abbreviated, since the results are supplemented by independent evidence obtained by combining the adopted photographic magnitudes with values of the color-indices derived by the method of exposure ratios. To restrict the labor as much as possible, only stars of the Polar Sequence were measured. Corrections for distance from the center of the plate were neglected, since the distances themselves are small. Only a few of the brighter stars are more than a degree or two from the Pole, and these were brought to the center of the plate by shifting the telescope before making the screen exposures.

The measurement of each photograph yielded two series of scale readings, one for full-aperture and one for screen exposure. These were first used to determine the screen constant and to test for homogeneity the scales of *Contribution* No. 97.

Since these scales refer to the color-system of the reflector, the individual magnitudes must be reduced to the system of the 10-inch refractor before they can be used with the latter instrument or compared with results obtained with it. The differences in the color-sensibility of different telescopes (together with the photographic plate) are of the same order as those in the visual color-perception of different observers. In careful work these instrumental peculiarities cannot be neglected, but in practice the data necessary for reduction to a normal system of color are usually lacking. It is not difficult to determine the relative color-equation of two instruments, but the second essential—the color of the star whose brightness is to be determined—is generally unknown, and the comparison of results obtained with different instruments then means little unless the relative color equations are small. In the present case, however, the colors of the stars are known.

The chief instrumental source of the color-equation lies in the violet and ultra-violet absorption occurring in the optical system. Since light of these colors plays little part in forming a photo-visual image, the relative color-equations for photo-visual magnitudes are much smaller than those for photographic, as long as the same brand of plate and the same filter are used. In the present instance we adopt provisionally for the reduction to the system of the 10-inch refractor[1]

$$m_{10}=m_{60}-0.19\ C \quad \text{(Photographic)} \qquad (1)$$

$$m_{10}=m_{60} \quad \text{(Photo-visual)} \qquad (2)$$

where m_{60} and C are magnitudes and color-indices given in *Contribution* No. 97. The resulting values of m_{10} are in the second column of Tables III and VI.

These magnitudes were plotted against the two series of scale readings (full-aperture and screen images, respectively) derived from each plate. In the ideal case of perfectly accurate magnitudes and no errors of observation, the plotted points would define two parallel curves, whose separations, measured parallel to the magnitude (ordinate) axis, would be equal to the value of the screen constant. Actually the behavior of the curves indicates the degree of homogeneity in the given scale. In the present case the photographic scale below the tenth magnitude is known to be substantially correct, and we should expect the curves in this region to be sensibly parallel. The screen constant is determined from this portion of the data.

Detailed results for the differences in the ordinates of the curves are given for individual plates in Tables I and II, omitting only those whose screen exposures show but one or two stars each. The first column indicates the ordinate (magnitude) of the full-aperture curve from which the distance between the curves was measured. The values of the separation for every half-magnitude are shown in the body of the tables in the form of deviations from an even three magnitudes. Thus the first value in Table I for plate 517, exposure 32 *m*, indicates a separation of 3.10 mag., measured

---

[1] Seares and Hubble, *Mt. Wilson Contr.*, No. 187; *Astrophysical Journal*, 52, 8, 1920.

TABLE I

SCREEN CONSTANT, PHOTOGRAPHIC DATA

Mag.	32^m		16^m		8^m					$4m$					2^m		
	517	525	508	509	479	493	494	495	496	478	489	490	491	492	477	485	486
9.0	....	....	....	....	+ 8	....	....	....	....	0	+2	−30	0	−15	0	−7	+8
9.5	....	....	+10	−5	+10	+23	+11	+20	+10	− 2	0	−18	0	− 8	−7	−4	+5
10.0	....	....	+ 6	−5	+10	+20	+10	+13	+ 7	+ 5	+2	− 8	−3	− 3	−4	−3	+2
10.5	....	....	+ 2	−5	+ 9	+16	+11	+ 8	+ 4	+12	+4	+ 3	0	0	−5	0	−3
11.0	....	+ 8	− 1	−6	+10	+14	+14	+ 5	+ 1	+18	+4	+ 4	0	+ 3	−4	+5	−2
11.5	+10	+ 1	− 5	−5	+10	+17	+20	+ 4	+ 6	+18	+2	+ 3	+6	+ 8	−1	0	−2
12.0	+ 4	− 7	− 5	−5	+10	+20	+20	+10	+10	+20	+5	0	+9	+13	+2	−4	−4
12.5	0	−16	−10	−1	+ 6	+17	+20	+14	+10	+16	+6	− 4	+4	+14	+8	−5	−1
13.0	− 2	−17	− 9	−2	0	+10	+21	+16	+10	+ 4	+4	− 4	+3	+ 9	....	−4	−1
13.5	− 6	−16	− 9	−4	0	+10	+ 4	+ 8	0	....	+3	+ 2	0	+ 2	....	....	....
14.0	+ 5	− 8	− 4	−7	− 2	+10	+11	0	− 2	....	....	....	....	....	....	....	....
14.5	+15	− 4	0	−5	....	....	....	....	....	....	....	....	....	....	....	....	....
15.0	+20	− 2	....	....	....	....	....	....	....	....	....	....	....	....	....	....	....
Mean	+ 6	− 7	− 2	−5	+ 7	+16	+14	+10	+ 6	+10	+3	− 5	+2	+ 2	−1	−2	0
S.C.	− 4	+ 9	+ 4	+7	− 5	−14	−12	− 8	− 4	− 8	−1	+ 7	0	0	+3	+4	+2

Mag.	2^m		1^m										No.	Mean(1)	Mean(2)
	487	488	476	481	482	483	484	510	511	512	513	514			
9.0	+ 4	0	0	+15	−18	−5	−12	+14	+22	− 2	+5	+15	21	3.00	3.00
9.5	+ 3	0	+6	+11	− 9	−2	− 7	+14	+10	− 3	+7	+13	27	3.03	3.02
10.0	+ 4	+ 1	+6	+ 7	0	0	− 2	+ 9	− 2	+ 2	+7	+18	27	3.04	3.02
10.5	+ 5	0	+6	+ 4	+ 1	+3	+ 2	+ 2	−11	− 2	+9	+20	27	3.04	3.02
11.0	+ 8	− 2	+4	0	0	+2	+ 2	+ 2	−11	− 9	+4	+22	28	3.03	3.02
11.5	+10	− 1	−4	− 5	0	0	+ 2	+ 5	−13	−20	+2	+20	29	3.03	3.02
12.0	+13	+ 4	...	....	− 2	0	+ 2	+ 4	−12	−23	−4	+22	27	3.04	3.03
12.5	+15	+10	...	....	....	+6	+ 2	....	....	....	....	....	21	3.05	3.04
13.0	+20	+15	...	....	....	...	....	....	....	....	....	....	18	3.04	3.02
13.5	....	....	...	....	....	...	....	....	....	....	....	....	13	3.00	2.98
14.0	....	....	...	....	....	...	....	....	....	....	....	....	9	3.00	2.97
14.5	....	....	...	....	....	...	....	....	....	....	....	....	4	3.02	3.05
15.0	....	....	...	....	....	...	....	....	....	....	....	....	2	3.09	3.12
Mean	+ 9	+ 3	+3	+ 5	− 4	0	− 1	+ 7	− 2	− 8	+4	+19	253	3.03	3.02
S.C.	− 7	− 1	−1	− 3	+ 6	+2	+ 3	− 5	+ 4	+10	−2	−17	....	....	....

TABLE II

SCREEN CONSTANT, PHOTO-VISUAL DATA

Mag.	32^m			16^m				8^m				No.	Mean (1)	Mean (2)
	526	527	543	539	540	541	542	535	536	537	538			
9.0	+5	−11	− 6	+6	− 5	0	+4	− 4	−14	+1	+ 2	11	2.98	2.98
9.5	+6	−15	− 6	+4	0	+2	+6	− 2	− 4	0	+ 4	11	3.00	2.99
10.0	+5	−14	− 9	+2	+ 7	+9	+4	+ 5	+ 7	0	+ 6	11	3.02	3.02
10.5	+5	−10	−14	+3	+10	+8	+4	+15	+13	+5	+10	11	3.04	3.04
11.0	+4	− 5	−14	−1	+14	0	+8	+23	+20	+6	+ 7	11	3.06	3.05
11.5	+2	− 1	−10	−6	+ 8	−6	+8	....	....	...	....	7	2.99	3.00
12.0	+2	0	0	...	....	...	...	....	....	...	....	3	3.01	3.06
12.5	+4	+ 2	+ 7	...	....	...	...	....	....	...	....	3	3.04	3.09
Mean	+4	− 7	− 6	+1	+ 6	+2	+6	+ 7	+ 4	+2	+ 6	68	3.02	3.02
S.C.	−2	+ 9	+ 8	+1	− 4	0	−4	− 5	− 2	0	− 4	....	....	....

from the point on the full-aperture curve whose ordinate is magnitude 11.5. For plate 508, on the other hand, the separation for the same ordinate is 2.95 mag.

Restricting our attention for the moment to the photographic scale (Table I), we note that the two values just given depend upon stars whose mean magnitudes are 11.5 and 8.5, respectively, those of the latter value having been reduced to an apparent brightness of 11.5 by the use of the screen. Were the magnitudes of these stars as given in *Contribution* No. 97 certainly dependable, the numbers 3.10 and 2.95 could be accepted at once as approximations for the screen constant. But since we assume the scale to be known only for stars fainter than magnitude 10, it follows that only values of the separation of the curves for ordinates 13.0 and fainter are available for the calculation of the constant.

We note, however, that the means of the quantities in each line of Table I, which are given in the last column but one under the heading "Mean (1)," are very nearly constant. There is no evidence of a progressive change, and this shows at once that the photographic scale of *Contribution* No. 97 is sensibly homogeneous, for, no matter what portion of this scale between the sixth and fifteenth magnitudes is used, we find appreciably the same value of the screen constant. Assuming the scale to be correct from the tenth magnitude downward, that between the sixth and tenth magnitudes must also be substantially correct. In the mean, the photographic data in Table I give the following result:

$$\left.\begin{array}{l}\text{Stars between mags. 6 and 10, } \Delta m = 3.03 \text{ (207 values)} \\ \text{Stars between mags. 10 and 15, } \Delta m = 3.02 \text{ (46 values)}\end{array}\right\} \qquad (3)$$

The value 3.02 mag. is therefore adopted for the screen constant. There is so little progressive change in the values of Mean (1) that the treatment of the photographic data reduces itself to a simple combination, arranged to diminish as much as possible the accidental errors in the individual magnitudes.

The agreement in the values of Mean (1) for the photo-visual results shown in Table II is nearly as satisfactory. The irregularities are a little larger and there seems to be a small progressive change, but the number of plates included in each mean is much smaller than in Table I. From all the data in Table II,

Stars between mags. 6 and 12.5, $\Delta m = 3.02$ (68 values) (4)

which is the same as the adopted constant found from the photographic data. We conclude, therefore, that the photo-visual scale is very nearly, if not quite, homogeneous; moreover, (4) shows that in the mean it is consistent with the photographic scale, and hence should be substantially correct. We shall examine the small progressive change in the values of Mean (1), Table II, in a later paragraph.

The individual values of Δm in both Tables I and II show the influence of appreciable systematic errors which are peculiar to a plate. The means for the separate plates shown at the bottom of the tables range from 2.92 to 3.19 (plates 512 and 514) and 2.93 to 3.07 (plates 527 and 535), respectively, with an average deviation of ±0.05 mag. This is only to be expected from observations which depend upon multiple exposures. Fluctuations in atmospheric conditions, the absorption of water vapor by the photographic film, and a variety of other factors combine to produce an effective value of the screen constant for each plate which differs more or less from the true value. The disturbance can be rendered accidental by increasing the number of plates, as in the present investigation, where its influence upon the adopted constant is very small.

The effect upon the magnitudes of individual stars will be more serious, however, unless special precautions are taken, for some of the stars appear on a few plates only. The difficulty can be avoided by reducing each plate with its effective constant; but we must first see whether this will modify the scale. This may be determined by applying to each value of Δm in each column the corresponding systematic correction in the last lines of Tables I and II, the corrections being the difference between 3.02 and the mean Δm for the plate in question. The horizontal means of the results thus found are given under the heading "Mean (2)," and represent what would have appeared under Mean (1), had the effective Δm for each plate been equal to 3.02. The revised values are sensibly the same as those of Mean (1), which shows that the scale will not be altered by reducing the individual plates with their effective constants. By so proceeding the errors in the individual magnitudes are appreciably diminished.

Since Table I gives no evidence of appreciable error in the photographic scale of *Contribution* No. 97, the determination of the magnitudes is a simple matter. It is only necessary to read from the full-aperture curves referred to above, with scale reading as argument, the magnitude of each star, and subtract from those interpolated with readings of images obtained with the screen, the values of the effective constant. Since the effective constant cannot be determined when only one or two screen images appear, several photographs of bright stars were reduced with the mean constant 3.02 mag.

Each of the magnitudes thus found yields a correction to the corresponding magnitude given in *Contribution* No. 97. The results are summarized in Table III, which shows the mean correction derived from each group of plates, classified according to exposure time. The second column of the table gives the magnitude from *Contribution* No. 97, reduced to the color-system of the 10-inch refractor. The headings of the six following columns indicate the exposure and the number of plates in each group. The corrections in the body of the table are given separately for full-aperture (left-hand series) and screen exposures. The number of values included in each mean correction is usually the same as the number of plates in the group, except in the case of the 1-minute plates. For these the number varies from 1 to 24, with an average of 9. Individual corrections in excess of 0.3 mag., 4 in a total of 954, were rejected. The weighted means from all the data and the total numbers of values appear in the last two columns.

The corrections for stars 1, 4, 3*s*, and 1*r*, and for the faintest stars in the list are of relatively low weight. The largest among the corrections of high weight is −0.08 mag. The average deviation of a single magnitude is ±0.070 mag. The simple mean of the corrections based on five or more determinations is ±0.028 mag. The probable reality of the larger corrections is indicated by the agreement shown in Table IV with similar corrections found by

Jones,[1] the quantities in parentheses being the approximate relative weights within the respective series. There are only two cases of an actual difference in algebraic sign, which shows a close accordance between the recent Greenwich investigation and that reported here.

TABLE III

CORRECTIONS TO PHOTOGRAPHIC MAGNITUDES

Star	Pg. m_{10}	Exposure and Number of Plates						No.	Mean Corrn.
		32^m, 2	16^m, 2	8^m, 5	4^m, 5	2^m, 5	1^m, 24		
1	4.39	....	....	....	....	....	+ 7	4	+ 7
4	5.90	....	....	....	....	....	+14	4	+14
2s	6.43	....	....	+ 9	− 4	+ 4	− 2	25	+ 1
5	6.45	....	....	+ 6	−11	− 5	−10	20	− 5
3s	6.58	....	....	....	....	....	− 6	5	− 6
1r	6.32	....	....	....	....	....	+ 9	6	+ 9
6	7.10	....	+ 4	− 5	+ 1	+ 2	+14, 0	26	+ 2
7	7.43	....	− 8	− 5	+ 3	− 4	+ 8, + 4	36	+ 2
2r	7.64	....	+ 5	+ 3	+ 1	− 5	− 9, + 6	31	− 1
8	8.28	− 5	+10	+ 2	+10	0	+ 2, 0	34	+ 3
3r	8.69	0	+ 4	+ 5	+ 7	− 4	− 6, − 1	38	0
9	8.87	+10	+ 2	+ 3	+10, +14	+ 5, +10	+ 3, − 2	54	+ 5
10	9.11	+ 1	+ 8	0, +11	− 7, +10	− 4, + 6	− 2, − 4	57	+ 1
4r	9.04	− 6	−11	+11, − 5	+ 1	+ 3, + 2	+ 1, − 3	35	− 1
11	9.69	0	+ 9, − 6	+ 1, +10	− 3, − 1	+ 3, − 8	− 4	49	− 1
12	10.03	−14	+ 1, −10	− 5, 0	− 8, − 8	− 3	− 2	46	− 4
5r	9.85	−20	+ 8	0	+ 7, + 2	− 1, − 6	+ 3	30	+ 1
4s	10.17	−16	−10	+ 1, + 9	+ 5, 0	+ 3	+ 2	38	+ 1
13	10.50	−19	− 1, − 6	− 2, −10	− 1	+ 2	+ 7	35	− 1
6r	10.22	− 4	+ 2	+ 4, + 2	− 2, + 1	+ 2	− 1	38	0
14	10.90	− 4, − 8	−10, + 8	− 4, −22	− 3	−10	−11	37	− 8
7r	10.74	+12, + 7	+ 4, − 3	+ 7, − 3	− 1	+ 1	− 1	35	+ 1
5s	10.89	− 3	....	....	....	+12	−12	14	− 4
15	11.16	− 3, + 8	+ 6, + 2	+ 7	+ 8	+ 5	+ 8	33	+ 6
6s	11.26	−2	− 9	+ 1	+ 4	− 4	0	24	− 1
8r	11.25	+ 2, + 6	0, − 4	+ 5	+ 6	− 4	0	29	+ 2
16	11.55	− 9, 0	+ 1	0	− 2	− 3	0	22	− 2
17	11.76	0, +19	+ 5	+ 1	+ 2	+ 6	+ 1	29	+ 3
18	12.20	+11, +11	+ 9	0	− 4	+ 2	− 7	23	+ 1
19	12.61	0	+ 2	+ 1	− 1	− 2	....	18	0
20	12.92	+ 2	+ 4	− 4	0	− 9	....	16	− 2
21	13.17	− 3	− 2	− 1	+ 4	....	....	11	0
11r	13.00	....	− 4	+10	+11	....	....	7	+ 6
22	13.32	+18	− 4	+ 7	....	....	....	8	+ 7
23	13.50	+ 6	+12	+ 6	....	....	....	8	+ 7
12r	13.58	+ 2	....	....	....	....	....	2	+ 2
24	13.82	+ 7	− 2	− 1	....	....	....	7	0
25	13.99	+ 4	+ 5	....	....	....	....	4	+ 4
8s	14.36	−10	....	....	....	....	....	2	−10
26	14.47	−13	− 3	....	....	....	....	3	−10
9s	14.58	−16	....	....	....	....	....	2	−16
27	14.80	− 6	....	....	....	....	....	2	− 6
10s	15.14	+16	....	....	....	....	....	2	+16
11s	15.13	− 2	....	....	....	....	....	2	− 2

---

[1] *Loc. cit.*

For the seven red stars of high weight, 2*r* to 8*r* inclusive, there are two zero differences, four of 0.01 mag., and one of 0.02 mag. This confirms the reality of the large color equation of the 10-inch refractor for photographic magnitudes, and shows that the adopted coefficient in equation (1) is sensibly correct.

TABLE IV

COMPARISON WITH CORRECTIONS FOUND BY JONES

Star	Table III	Jones	Star	Table III	Jones
1*r*.........	+9(6)	+11(11)	5.........	−5(20)	+1(26)
14..........	−8(37)	−10(109)	12.........	−4(46)	0(113)
15..........	+6(33)	+ 5(96)	5*s*........	−4(14)	−6(108)
11*r*.........	+6(7)	+ 7(8)	8.........	+3(34)	+3(39)
3*s*.........	−6(5)	+ 1(9)	17.........	+3(29)	+2(56)
9..........	+5(54)	+10(33)	....	......	....

The corrections in the last column of Table III may be combined with the magnitudes in the second column to form weighted mean values referred to the system of the 10-inch refractor, or with the photographic magnitudes of *Contribution* No. 97, to obtain a revised system for the 60-inch reflector. Other data are available, however; and the final results, based on all the material which has been accumulated, are given in the following *Contribution* No. 235.

Turning now to the photo-visual magnitudes, consider first the small progressive change in the screen constant indicated by the last two columns of Table II. This suggests that the photo-visual scale requires a slight readjustment. The smoothed values of the constant are given in the second column of Table V, and it is readily seen that each of these would become equal to the adopted mean, were the original scale modified by the quantities shown in the third column of the table. Thus, since the first value of Δm depends upon the difference in brightness of stars whose mean magnitudes are 6.0 and 9.0, respectively, corrections of 0.00 and +0.05 at these two points of the scale would increase the observed value from 2.97 to 3.02. Again, the last value of Δm depends upon stars of mean magnitude 9.5 and 12.5. Corrections of +0.04 and +0.01, respectively, give the required reduction of 0.03 from 3.05 to the adopted mean. The maximum correction is +0.05 mag. in the vicinity of magnitude 9.

These results, however, scarcely justify a change in the original scale, for the divergence in question arises almost wholly from two of the eleven plates, Nos. 535 and 536, both of which show large differences in gradation between the full-aperture and the screen exposures (see Table II). There is, moreover, additional evidence. The colors of the stars near the Pole have been extensively observed by the method of exposure ratios, and since we now have reason to believe that the photographic scale for the brighter stars is reliable, it is clear that the photo-visual scale may be independently established by combining photographic magnitudes with color-indices derived from the exposure ratios. This material is discussed in *Contribution* No. 235, but the results are summarized in the last four columns of Table V, the significant quantities appearing under the heading "Corrn. (2)."

TABLE V

SCALE CORRECTIONS

Pv. Mag.	Δm	Scale Corrn. (1)	Pv. Mag.	Scale Corrn. (2)	No. Stars	Rel. Weight
6.0		0	3.0	−3	2	3
6.5		+2	5.4	+3	4	4
7.0		+3	6.5	0	5	3
7.5		+4	8.0	−7	5	4
8.0		+4	9.5	−9	6	10
8.5		+5	10.4	−1	5	22
9.0	2.97	+5	11.1	−1	5	14
9.5	3.00	+4	12.4	+3	14	38
10.0	3.02	+3	13.5	+3	22	22
10.5	3.03	+3	14.3	+1	28	17
11.0	3.04	+2	15.4	−1	40	10
11.5	3.05	+2	16.2	+3	31	7
12.0	3.05	+2	16.9	−2	49	6
12.5	3.05	+1				

With the exception of the values for 8.0 and 9.5 it will be noted that these corrections are small and in general accidental in character. Further, the two large corrections are opposite in sign to the values of Corrn. (1). In view of these results, which are of good weight, it appears that Corrn. (1) is of the order of the uncertainty affecting its determination, and may be disregarded. Nor does Corrn. (2) itself afford any certain basis for a change in the opposite direction. The exposure-ratio observations in these two groups are not well distributed, and most of the difference can be traced to three or four stars. A small systematic effect is certainly present, but as between the two series of magnitudes and the exposure ratios, its source cannot be located. The photo-visual scale of *Contribution* No. 97, as well as the photographic, is therefore adopted unchanged.

The problem of photo-visual magnitudes, provisionally at least, is therefore also one of diminishing the accidental errors of the original values in *Contribution* No. 97. Proceeding as for the photographic data, we find the results given in Table VI.

TABLE VI

Photo-visual Magnitudes of Polar Sequence Stars

Star	Pv. Mag. *Cont.* 97	Sums of Deviations +, −	No.	Corrn.	Star	Pv. Mag. *Cont.* 97	Sums of Deviations +, −	No.	Corrn.
2*s*	6.33	5,76	11	$-0^{\mathrm{M}}.06$	4*s*	9.83	35, 27	11	$+0^{\mathrm{M}}.01$
2*r*	6.35	8,73	11	− 6	7*r*	9.90	0,114	11	− 10
5	6.47	9,38	11	− 3	13	10.37	29, 17	11	+ 1
6	7.05	32,18	11	+ 1	8*r*	10.44	55, 11	11	+ 4
7	7.52	80, 7	10	+ 7	14	10.54	50, 0	11	+ 5
3*r*	7.56	36,12	11	+ 2	6*s*	10.73	0, 17	2	− 8
8	8.13	24,34	7	− 1	15	10.89	17, 30	11	− 1
4*r*	8.26	23,12	6	+ 2	16	11.23	24, 7	7	+ 2
5*r*	8.65	0,31	3	− 10	17	11.28	39, 0	7	+ 6
9	8.81	54,11	7	+ 6	18	11.89	11, 2	3	+ 3
10	9.07	19,46	12	− 2	11*r*	12.06	8, 0	2	+ 4
6*r*	9.21	81,22	13	+ 5	19	12.28	0, 39	3	− 13
11	9.53	69, 8	13	+ 5	21	12.48	16, 0	2	+ 8
12	9.80	7,82	11	−0.07	20	12.51	0, 30	2	−0.15

The magnitudes in the second column are taken directly from *Contribution* No. 97. The third column contains the sums of the positive and negative deviations for the 11 plates; the fourth column, the total number of values; and the fifth, the mean corrections to the magnitudes in the second column. Thus the first correction is $(+5-76)/11=-6$.

Neglecting three rejected corrections which exceed 0.3 mag., we find for the mean of the 231 remaining deviations ±0.065. The weighted algebraic mean of the final corrections for the red stars is less than 0.01 mag. This shows that for photo-visual magnitudes the color-systems of the 10-inch refractor and the reflector are identical, and justifies the assumption expressed by equation (2).

As in the case of Table III, the corrections may be combined with the original magnitudes to form revised values. Those finally adopted, like the photographic results, also depend on data drawn from other sources and are given in *Contribution* No. 235.

In résumé, the investigation with the 10-inch refractor reveals no appreciable error in the photographic scale of *Contribution* No. 97 between the fourth and fourteenth magnitudes. The photovisual scale has been examined between magnitudes 6.3 and 12.5. A maximum correction of +0.05 mag. near the ninth magnitude is suggested, but independent data of higher weight do not confirm this result. The original scale is therefore adopted. The corrections to the magnitudes of *Contribution* No. 97 for accidental error (5 or more values) average ±0.03 and ±0.04 mag., respectively, for the two scales. The larger corrections for the photographic scale are in substantial agreement with those recently found at Greenwich by Jones.

MOUNT WILSON OBSERVATORY
February 1922

REVISED MAGNITUDES FOR STARS NEAR THE NORTH POLE[1]

By FREDERICK H. SEARES

ABSTRACT

Revised magnitudes and color-indices for stars near the North Pole.—Numerous comparisons with the polar standards have incidentally given extensive material for determining the errors affecting the standards themselves. The results for 55 stars (Table I) lead to revised magnitudes which are averaged with previously reported results obtained with the 60-inch reflector and the 10-inch Cooke refractor to give the adopted values listed in Table VIII. This table also gives the corresponding color indices from magnitudes and from exposure-ratios for these and 37 other polar stars, all based on the color system of the 60-inch reflector and the accessory equipment.

Exposure-ratio method of determining color-indices has been previously described. A discussion of the results of 177 exposures including stars of photo-visual magnitude ranging from 2 to 17.3, indicates that the average deviation of a single determination is ±0.12 magnitude, about half of which is due to the mean systematic error of the plate, and that in general the *probable error* is about 30 per cent less than in the case of a color-index derived by combining a photographic and a photo-visual magnitude. *Normal points for the calibration curve*, color-index as a function of log E, determined by observations on 216 stars, are given in Table IV and the adopted values in Table V.

Differential error between photo-visual and photographic scales of magnitude.—Although the exposure-ratio color scale is calibrated by measurements on stars of known color index, systematic errors in the two magnitude scales upon which the color scale depends were eliminated by using stars with a wide range of magnitude. Hence the exposure-ratio scale is independent of the magnitude scales and may be used to test the differential error between them. The data (Table VII) show agreement to within $\pm 0^{\mathrm{M}}.03$ from photo-visual magnitude 3 to 17, except for a few stars near magnitude 9 for which the mean difference is $0^{\mathrm{M}}.09$.

The following pages bring together the results of several investigations bearing upon the magnitudes of stars near the North Pole. The basic determination of both photographic and photo-visual scales is that of *Mt. Wilson Contribution* No. 97,[2] which depends entirely upon observations with the 60-inch reflector. These results refer to the color-system of that instrument as used with the photographic plates[3] and a certain yellow filter habitually employed in photometric work at Mount Wilson.

To diminish the effect of accidental errors, the individual magnitudes of about fifty of the stars in *Contribution* No. 97 have been combined with a large amount of material obtained incidentally in connection with an entirely different investigation.

---

[1] *Contributions from the Mount Wilson Observatory*, No. 235.

[2] *Astrophysical Journal*, 41, 206, 1915.

[3] Seed's Gilt Edge, 27's and 30's, and Cramer's Instantaneous Isochromatic.

The revised magnitudes are on the scale and color-system of *Contribution* No. 97.

At various times during the last six years numerous measures of the colors of stars near the Pole have been made by the method of exposure ratios. The method must be calibrated upon stars of known color-index, but this can be accomplished in such a manner that systematic errors in the magnitude scales upon which the colors themselves depend do not enter into the calibration curve. Colors found from exposure ratios are thus essentially independent of the scale, and may therefore be used to test for differential error between photographic and photo-visual scales, since in the mean there should be no difference between the colors found by the two methods. A discussion of these data shows excellent agreement to the seventeenth photo-visual magnitude, except for a few stars near the ninth magnitude for which the mean difference is 0.09 mag.

Observations made at Greenwich, Harvard, and Potsdam confirm the substantial accuracy of the photographic scale of *Contribution* No. 97 to the sixteenth photographic magnitude.

A recent investigation made at Mount Wilson[1] with the 10-inch Cooke refractor affords further evidence on both the scales. The photographic scale is again confirmed. The photo-visual results are less reliable, but, considered in connection with the measures of colors, show that the scale of *Contribution* No. 97 must also be close to the truth.

These several investigations are combined to form a system of magnitudes embodying all the data bearing on standard polar stars thus far collected at Mount Wilson. The final results, which are on the color-system of the reflector and the accessory equipment mentioned above, represent the contribution of this observatory to the report of the International Commission on Stellar Magnitudes for 1922.

I. REVISION TO DIMINISH ACCIDENTAL ERROR

In determining the magnitudes of faint stars in the Selected Areas[2] it has been necessary to make a large number of comparisons, both photographic and photo-visual, with the polar standards of *Contribution* No. 97. Since the comparisons were intended only to establish the zero point of the magnitudes in the Selected Areas, and not the scale, the exposures were short, 2^m and 3^m, respectively. They afford, nevertheless, extensive material for the reduction of the accidental errors affecting the polar standards themselves.

---

[1] Seares and Humason, *Mt. Wilson Contr.*, No. 234. *Astrophysical Journal*, **56**, 84, 1922.

[2] See recent "Annual Reports of the Director of the Mount Wilson Observatory," *Year Book of the Carnegie Institution of Washington.*

We are here concerned only with exposures on the Pole of which there are two on each plate. As a part of the reduction, the scale readings for these had been plotted against the adopted standards in the usual manner. The deviations of individual stars from the smooth curves defined by the plotted points represent the combined influence of the accidental errors in the standards and the errors affecting individual plates. In the mean the latter are accidental, whereas the former enter systematically into the observed deviations from the curves and should be brought to light by forming the algebraic mean of a large number of such deviations.

Table I summarizes the results of this revision. The second, third, and fourth columns contain the mean systematic deviation for each star, obtained as just explained, and the number of values upon which each mean depends. The deviations are the corrections required by the magnitudes in *Contribution* No. 97 to bring them into agreement with the results of the polar comparisons. The fifth and sixth columns give the revised magnitudes. These are means of the values in *Contribution* No. 97 and those derived from the polar comparison plates, formed with weights equal to the respective numbers involved. The last two columns give the revised color-indices and the total numbers of individual observations for each star.

A few corrections are large and indicate cases of more or less serious discordance. Most of these are the result of low weight in one determination or the other.[1] For example, the photographic magnitude of star 439 given in *Contribution* No. 97 is clearly in error by a large amount and is rejected outright. Again, star 358 shows a difference of 0.47 mag. in the photo-visual magnitudes. Here both determinations are uncertain, and the adopted mean is

---

[1] Note that the numbers of values included in the means in *Contribution* No. 97 are equal to the differences in corresponding quantities in the fourth and last columns of Table I.

TABLE I

Magnitudes and Colors Derived with 60-Inch Reflector

Star	N.P.C.—*Contr.* 97			Revised Mags. and C.I.			
	Pg.	Pv.	No.	Pg.	Pv.	C.I.	No.
14.......	+5	+3	37, 9	11.00	10.55	0.45	94,27
16.......	−8	−4	21,13	11.59	11.21	0.38	64,29
19.......	+5	−5	57,54	12.71	12.24	0.47	135,66
20.......	−7	+2	69,60	12.99	12.53	0.46	155,72
22.......	+15	+6	27,25	13.47	12.84	0.63	72,36
23.......	−2	−12	69,58	13.59	13.00	0.59	149,70
24.......	+1	−3	44,34	13.93	13.31	0.62	115,46
25.......	+5	−2	50,44	14.10	13.58	0.52	128,56
26.......	−4	−4	66,44	14.62	13.69	0.93	140,56
27.......	−10	−12	62,12	14.86	14.25	0.61	123,19
28.......	0	+4	28, 1	15.27	14.54	0.73	68, 8
31.......	0	....	17,..	16.41	15.62	0.79	62, 6
5s.......	+5	0	36, 3	11.11	10.06	1.05	96,31
7s.......	+10	−8	44,45	12.65	12.04	0.61	114,57
8s.......	+10	−3	29,10	14.53	13.77	0.76	79,22
9s.......	−1	−14	68,41	14.74	13.74	1.00	134,53
10s.......	−1	+25	22, 1	15.29	14.52	0.77	67, 8
11s.......	−2	+1	52, 8	15.30	14.35	0.95	115,18
12s.......	+2	−9	39, 2	15.34	14.67	0.67	100, 9
13s.......	−5	....	22,..	15.52	14.54	0.98	65, 3
14s.......	+3	−15	26, 1	16.00	15.05	0.95	73, 8
15s.......	−3	....	5,..	16.57	15.71	0.86	46, 5
16s.......	+4	....	1,..	16.86	15.50	1.36	37, 4
11r.......	+1	+1	43,41	13.22	12.07	1.15	122,53
12r.......	−8	+1	69,59	13.81	12.47	1.34	151,71
125.......	−30	....	1,..	15.02	14.37	0.65	3, 5
127.......	−4	....	2,..	14.34	13.31	1.03	8,11
130.......	−21	....	1,..	15.19	14.21	0.98	3, 9
134.......	−17	....	1,..	14.41	13.54	0.87	7,10
151.......	−2	+18	3, 9	13.72	12.66	1.06	32,20
152.......	+12	−3	3, 1	14.58	13.76	0.82	24,13
158.......	0	....	1,..	15.10	14.57	0.53	17, 5
176.......	+14	−13	5, 4	14.35	13.78	0.57	41,16
226.......	−8	−21	25, 4	14.90	14.15	0.75	71,11
256.......	−4	−4	28, 8	14.66	13.84	0.82	78,19
277.......	+6	−15	49, 4	15.33	14.56	0.77	111,11
311.......	+4	−5	42, 6	15.02	14.34	0.68	95,13
319.......	+9	+7	14,25	14.46	13.61	0.85	54,28
329.......	+10	+19	14,27	14.35	13.51	0.84	52,30
334.......	−1	+3	51,14	15.20	14.44	0.76	121,21
338.......	+8	+6	5,10	14.73	13.84	0.89	33,13
341.......	−6	+12	8,15	15.15	14.02	1.13	34,18
345.......	−1	+5	36,35	13.79	12.05	1.74	94,46
350.......	+3	+14	26,11	11.02	10.71	0.31	72,23
358.......	+9	+47	9, 2	15.24	14.34	0.90	35, 4

TABLE I—*Continued*

Star	N.P.C.—*Contr.* 97			Revised Mags. and C.I.			
	Pg.	Pv.	No.	Pg.	Pv.	C.I.	No.
362	−12	− 5	67,61	13.08	12.27	0.81	153,73
378	− 2	+ 8	64,54	14.13	12.81	1.32	118,59
389	+ 8	+ 8	48,43	13.61	12.90	0.71	91,51
391	− 2	− 2	46,32	14.62	13.83	0.79	84,38
401	− 8	+10	25,33	14.50	13.70	0.80	61,36
403	− 4	+ 9	27,34	14.49	13.83	0.66	68,37
424	+ 2	+15	20,26	14.52	13.77	0.75	49,29
426	+ 7	+ 6	12,14	13.85	13.38	0.47	40,17
427	− 1	− 2	23,41	13.27	12.05	1.22	56,46
439	−51	....	21,..	14.78	13.49	1.29	21, 3

of little value. Occasionally, a difference is large although numerous observations enter into each of the values combined to form the revision. Star 22 is an example, with a difference of 0.15 mag. The most plausible explanation is a small error in the distance correction. The star is at the edge of the useful field; the exposures for the polar comparison plates were always the same, while those for the original investigation were varied. Errors in distance correction tend to neutralize each other in the latter case because the photographic image varies in size from plate to plate, whereas there is no compensation in magnitudes derived from the comparison photographs. On this account the value from the polar comparisons has been given half weight. In general, however, the differences are as satisfactory as can be expected from results derived with a reflector of focal ratio.

It should be noted that the revision concerns only the accidental errors affecting the original magnitudes. The reliability of the scales is a separate question, discussed partly in *Contribution* No. 234 and partly in the following sections of this paper.

2. COLORS OF POLAR STARS FROM EXPOSURE RATIOS

The method of exposure ratios for measuring a star's color has been described briefly in previous communications.[1] The term

---

[1] *Mt. Wilson Comm.*, Nos. 33, 38, 59; *Proc. Nat. Acad. Sci.*, **2**, 521, 1916; **3**, 29, 1917; **5**, 232, 1919. The second of these contains provisional results of the investigation discussed in this section.

"exposure ratio" is used to designate the logarithmic ratio of exposure times (symbol, log *E*) which produce blue and yellow images of the same size. This quantity can obviously be used as a measure of color.

Experience shows that for a given star the values of log *E* from plates of the same emulsion are nearly constant. The systematic differences in the means from groups of 5 or 6 plates each are usually negligible. Observations are now generally arranged in such a way as to check, if not actually determine, the zero point for each plate, but in the beginning a direct control, beyond that of accordance with other plates, was not ordinarily applied, the errors being minimized by multiplying the number of plates. In the case of bright stars, which must be observed individually, it is now customary to photograph several objects on the same plate, which greatly facilitates the reduction to a homogeneous system. In so far as possible, the same emulsion was used in all the earlier measures. When a change became necessary, the constant for reduction to a uniform system was carefully determined.

To translate values of log *E* into color-indices, which is an important step in giving them physical meaning, stars of known color-index must be measured. Inasmuch as the stars in the polar region are the basis of the Mount Wilson photometric system, they have been extensively observed for this purpose. The resulting data give not only the desired relation between color-index and log *E*, but also an independent determination of the colors of the individual stars. The exposures for the yellow images range from 8^s to 64^m, and results are now available for an interval of about 16 magnitudes, the lower limit being approximately 17 of the photo-visual scale. The details of interest in the present connection are as follows:

Series a.—About 150 plates; yellow exposures mostly 16^s and 32^s, on stars brighter than the eleventh magnitude, observed with images of standard size. A few plates of longer exposure extend the series to the thirteenth photo-visual magnitude.

Series b.—Nine plates with yellow exposures of 128^s. The faintest stars observed are of about the fourteenth magnitude.

Series c.—Three plates with yellow exposures of 8^m, three of 10^m, and two of 30^m. The limiting magnitudes range from 15.5 to 16.9.

Series d.—Nine plates with yellow exposures ranging from 8^s to 5^m. Only 17 stars between 9.0 and 12.5 were included, however, because the longer exposures were made with reduced apertures. This group of plates, along with several others included in the various series, was made under unusual conditions to test various details of the method which are of no interest in the present connection.

Series e.—Four plates, each including 10 to 15 stars brighter than the tenth magnitude, observed individually with yellow exposures of 8^s to 32^s and a standard size of image. In addition, observations with yellow exposures of from 32^s to 128^s were made at the beginning and end, to include stars between magnitudes 10.0 and 12.5. The results supplement and strengthen those of series *a*.

Series f.—Two plates with yellow exposures of 64^m each. The limiting magnitude is 17.3 photo-visual.

Lack of space prevents a detailed presentation of the reduction of these data, which has involved much time and several revisions as the results have accumulated. The discussion is therefore limited to a general statement of procedure, with extracts from the reduction sheets showing the accordance attained, supplemented by a collection of results, made particularly from the standpoint of their bearing on the magnitude scales.

The earlier observations were restricted to stars brighter than the eleventh photo-visual magnitude, because of the ease with which certain systematic errors could thereby be eliminated. It is well known that a photographic image produced by yellow light usually grows at a different rate from one produced by blue light; the value of log E therefore depends to some extent upon the size of the images from which it is derived. Differences in photographic gradation for light of different wave-lengths seem to depend upon a number of factors. In practice these are hard to control, and the most satisfactory results are obtained when the observations are arranged in such a way as to eliminate the disturbance or to permit its determination for each plate.

In the case of the preliminary measures this was accomplished by reducing all the stars to a standard intensity with the aid of screens and diaphragms and by using an essentially constant series of exposures throughout. Those for the yellow images were 16 and 32 seconds, although a few photographs with exposures ranging from 1 to 4 minutes were subsequently added. The latter gave results for bright stars already observed with short exposures, as well as for fainter stars, the overlap being sufficient to determine the zero-point and the correction to be applied for gradation. In practice the two corrections were combined. The differences in log E for stars within the overlapping region, when arranged in order of photo-visual magnitude, define a curve which could be extrapolated for an interval of one or two magnitudes without danger of serious error.

The discussion of the data of series *a* carried the results to the thirteenth magnitude. To extend them to still fainter stars, the procedure just described was applied in succession to the plates of series *b*, *c*, and *f* in the order of increasing exposure time. Series *d* and *e*, which control and strengthen the results of series *a*, were inserted and reduced in the order indicated by the series notation. The adopted values of C_e, the color-index derived from log E, and the number of determinations upon which each depends are given in the eighteenth and nineteenth columns of Table VIII, although results for a few stars, mostly of low weight, not included in the final collection of data, appear in Table VI.

The plates of series *f* show many faint stars for which individual results are not printed, although the means for groups of these stars appear in some of the statistical comparisons (see Table IV, for example).

The question as to how much the values of log E for faint stars have been affected by errors incident upon the extrapolation of the correction curve for gradation is important. The results for a single plate are systematically in error by small amounts at least; but for a series of plates these errors become accidental. An examination of the residuals for series *c*, in the interval 14.1 to 15.7, shows that the effect on the mean must be small. Although some of the plates of series *b* contribute results for two or three stars falling within the interval mentioned, the gradation curves for series *c* are in fact extrapolations from 13.7. The systematic deviations of individual plates from the mean, expressed in hundredths of a magnitude, are

Systematic deviation	− 9	− 1	− 8	+ 6	+ 8	+ 4	−5	+10
No. of stars	13	13	20	11	19	16	5	4

The average is ±0.064 mag., whence the probable value of the systematic error in the mean color-indices derived from log *E* for stars in this interval is of the order of ±0.02 mag. This could have been depressed to a still lower value by adding more plates, but the precision is sufficient for the present purpose.

As a further indication of accordance, it may be added that from the same data the average deviation for a single value of log *E*, including systematic errors, corresponds to ±0.118 mag. For stars in the interval between the tenth and thirteenth magnitudes, on the other hand, the agreement is as shown in Table II, which compares the mean results for each star as derived from series *a* to *e*. The table gives the deviations in log *E* in units of the third decimal and the number of values upon which each difference depends. There is here little evidence of residual systematic error; and since 0.010 in log *E* is equivalent, on the average, to 0.028 mag., the accidental deviations are also satisfactory. The combined effect of both types of error is indicated by the average of the 43 deviations based on 7, 8, or 9 observations each, whose value is ±0.013 in log *E*, or ±0.036 mag.

Finally, an examination of some of the bright stars in series *a*, which were observed individually with a standard size of image, throws light upon the fluctuations in the relative blue and yellow sensitiveness of different plates. Since for these stars no attempt was made to determine the zero-point correction for individual plates, the average deviations include the full effect of this error, combined with the accidental error of estimating the value of log *E*. Further, the mean log *E* usually depends upon two or even three different emulsions. The results have been referred to a standard emulsion, but the reduction constants are affected by an uncertainty which also enters into the average deviations.

The results for 15 of these stars which have been extensively observed are shown in Table III. The second and third columns give the number of plates and of emulsions used. In every case the observations extend over a period of more than a year, and many of the later measures were made with the original emulsion with which the observations were begun. There are small systematic differences affecting groups of plates of nearly the same date, but little evidence of actual changes in the color-properties of an emulsion with increasing age. The average deviations for a single plate in the fourth column show considerable fluctuation; their mean is ±0.106 mag. From other evidence it seems likely that this error is to be about equally divided between the neglected plate constants and the uncertainty in estimating the value of log *E*.

TABLE II

DEVIATIONS IN LOG *E* FOR DIFFERENT SERIES

Unit=0.001 in log *E;* No. of Values in Parentheses

STAR	PV. MAG.	SERIES				
		a	*b*	*c*	*d*	*e*
7r	9.90	− 5 (31)	−11 (9)	+25 (3)	+ 6 (9)	+30 (8)
5s	10.06	0 (35)	+ 5 (9)	0 (4)	− 2 (9)	+15 (7)
13	10.37	− 1 (14)	+18 (3)	....	....	....
8r	10.44	− 1 (15)	+10 (6)	+ 7 (5)	....	....
14	10.55	+ 6 (24)	+23 (9)	− 5 (7)	+16 (9)	−59 (6)
350	10.71	− 8 (24)	− 5 (7)	+11 (3)	+16 (9)	+26 (6)
6s	10.73	+10 (12)	+21 (8)	− 6 (6)	−23 (7)	....
15	10.89	+ 5 (15)	+23 (6)	−12 (6)	− 9 (9)	....
16	11.21	−32 (3)	− 1 (8)	+ 6 (8)	− 4 (9)	....
17	11.28	−28 (6)	− 3 (9)	+53 (6)	....	....
18	11.89	−16 (4)	− 1 (9)	+25 (8)	....	....
345	12.05	− 1 (11)	−10 (7)	−36 (2)	+52 (3)	+ 24 (4)
11r	12.07	− 3 (15)	+17 (9)	− 6 (8)	+17 (5)	− 9 (4)
427	12.05	−63 (1)	+ 6 (8)	+19 (8)	− 5 (5)	....
7s	12.04	+ 5 (18)	+11 (9)	+14 (7)	−30 (6)	+ 2 (6)
172	12.24	....	+42 (1)	+28 (2)	....	....
19	12.24	+20 (9)	− 9 (9)	− 9 (8)	+13 (5)	+ 7 (4)
362	12.27	+ 7 (19)	0 (9)	−27 (8)	+ 6 (5)	+43 (4)
12r	12.47	....	+22 (9)	−10 (8)	....	....
21	12.48	....	− 4 (6)	+13 (8)	....	....
20	12.53	+21 (18)	−23 (8)	−17 (8)	+42 (5)	−37 (4)
151	12.66	....	+37 (3)	− 9 (8)	....	....
378	12.81	+19 (16)	− 8 (6)	−24 (8)	....	....
22	12.85	....	0 (5)	+ 8 (8)	....	....
389	12.90	....	− 8 (7)	+18 (8)	....	....
23	13.00	+17 (13)	+ 8 (6)	−25 (8)	....	....

As mentioned above, it is now customary to determine the plate constant by comparison with standard fields, either directly or indirectly, which increases the precision appreciably. The results just discussed show, however, that even when the variations in color-sensitiveness from plate to plate are neglected, the exposure ratios lead to values of the color which are at least comparable in accuracy with those found by other methods of direct color-measurement. The errors given above are of the same order, for example, as those affecting individual magnitudes in the general run of photometric work. The uncertainty of a color-index derived by combining a photographic and a photo-visual magnitude should therefore be greater than that of a value from log E in the ratio of about 1.4 to 1. This is a fair statement of the advantage of the method of exposure ratios from the standpoint of precision.

TABLE III

Average Deviation in Color Index. Bright Stars

Star	No. Obs.	No. Em.	A.D.	Star	No. Obs.	No. Em.	A.D.
			mag.				mag.
10........	23	2	±0.135	7s.......	16	2	±0.124
13........	14	1	.092	1r.......	13	1	.119
14........	24	2	.084	3r.......	9	2	.093
15........	15	2	.097	7r.......	31	2	.099
20........	18	2	.105	8r.......	15	1	.072
1s.......	39	3	.097	10r.......	8	1	.138
5s.......	35	2	.111	11r.......	15	2	±0.155
6s.......	12	1	±0.062				

The calibration curve for the transformation of log E into color-index has been revised several times. The first approximation, which differs little from the adopted relation, was obtained from series *a* by first arranging the mean values of log E for each star in the order of increasing color-index as given in *Contribution* No. 97 and then forming the means of log E and of color-index for groups of stars within narrow limits of color. Accidental irregularities were eliminated by plotting the results and drawing a smooth curve. This curve represents the relation by means of which values of log E may be expressed in the customary form as color-indices.

Since most of the groups include stars scattered over a wide range in brightness, the errors in the photographic and photo-visual scales, which of course appear in the color-indices, are almost completely neutralized. In the present case, in which the scale errors are known to be small, their effect upon the mean relation between color-index and log *E* is negligible. Values of the color calculated from log *E* should therefore be free from errors in the scales, and when compared with the original color-indices arranged in order of increasing magnitude must bring to light any differential error in the scales themselves.

TABLE IV

NORMAL POINTS FOR RELATION BETWEEN COLOR-INDEX AND LOG *E*

C_m	log *E*	*v*	Pv. Interval	No. Stars
mag.		mag.		
0.04	9.040	+0.03	5.3– 8.8	8
0.26	.109	− 1	5.6–10.6	8
0.43	.186	+ 2	2.1–12.5	8
0.58	.229	− 1	11.3–15.2	10
0.67	.268	0	10.7–16.9	15
0.71	.319*	+ 10	15.5–16.8	15
0.81	.299	− 5	12.5–15.6	22
0.88	.367*	+ 7	15.5–17.0	15
0.99	.389	+ 2	8.3–16.3	18
0.99	.365*	− 4	14.8–17.0	15
1.06	.412*	+ 2	15.2–17.0	15
1.15	.410*	− 7	15.5–17.0	15
1.19	.444	− 1	9.2–16.0	17
1.23	.464*	+ 1	15.6–17.3	15
1.34	.485*	− 3	15.1–17.3	15
1.59	9.546	−0.08	5.1–12.0	5
Sum				216

* Supplementary faint stars from series *f*.

To obtain the last approximation for the reduction curve, the method just described was applied to the data from all the series as summarized in Tables VI and VIII, including the slight revisions of color-index given in Table I. The results are shown in Tables IV and V. The former gives the normal points and their representation by the adopted curve in Table V. Table IV also gives seven supplementary points based upon 105 faint stars between photovisual magnitudes 14.8 and 17.3, which appear only on the two plates of long exposure in series *f*. Although of much lower weight, these points show substantially the same change in log *E* with color-index as the brighter stars. The average deviations of the two series of normal points in Table IV from the adopted curve are

±0.026 and ±0.049 mag., respectively. The average for the points in the first approximation, referred to the *final* curve, is ±0.028 mag. This approximation, it will be recalled, was based exclusively upon series *a*, which includes only stars brighter than the thirteenth magnitude. The large residual of −0.08 for the last point in Table IV arises mainly from the star 345, magnitude 12.05, which, in view of the numerous measures, is seriously discordant. (See Table VIII, last column.) No explanation suggests itself, except possibly systematic error in the estimates caused by the proximity of the brighter object, No. 350, magnitude 10.71.

TABLE V

Color-Index and Logarithm of Exposure Ratio

C.I.	log *E*	Diff. for 0.01 in log *E*	C.I.	log *E*	Diff. for 0.01 in log *E*
mag.		mag.	mag.		mag.
−0.2	8.940	0.026	0.8	9.315	0.028
0.0	9.015	.027	1.0	9.385	.030
+0.2	9.090	.027	1.2	9.450	.031
0.4	9.165	.027	1.4	9.513	.033
0.6	9.240	.027	1.6	9.573	.034
0.8	9.315	0.028	1.8	9.632	0.035

The absence of blue stars from the fainter objects is noteworthy, and confirmatory of earlier results. Among the supplementary stars from series *f* there is none with a color-index less than 0.6 mag.

From the ordinates of the adopted relation between color-index and log *E* given in Table V, it appears that the curve is nearly linear. The zero-point for log *E* is of course arbitrary. For comparison with the provisional relation between log *E* and spectral type given in Figure 1, *Mt. Wilson Communications*, No. 59,[1] a correction of −0.07 must be applied to the values of log *E* in Table V. This comparison leads to a result of importance, namely, the relation of the color-indices of the Mount Wilson photometric system to spectral type. Provisional values of the equivalents are listed in Table XII, *Contribution* No. 226. Detailed results and revised equivalents will be given in a later paper.

The data of Table V were used to calculate the color-indices for individual stars whose values, C_c, appear in Tables VI and

---

[1] *Proc. Nat. Acad. Sci.*, 5, 232, 1919.

VIII. Subtracted from the values of C_m found by comparing photographic and photo-visual magnitudes, these lead to the differences in the last column of the tables. These differences should be judged in connection with the number of separate determinations of the photographic and photo-visual magnitudes (sixteenth column, Table VIII) which enter into the observed color-indices, and of C_e (nineteenth column). Well-observed stars usually show a satisfactory agreement, although there are some unexpectedly large values. The case of No. 345 (12.05) has already been mentioned. No. 427 (also 12.05) should also show better agreement than it does. A similar difference for No. 172 (12.24), on the other hand, is not at all surprising, and this is also true of the four differences approximating 0.4 mag., all but one in Table VI. These latter results might have been rejected at once because of uncertainty, but they have been retained to show that

TABLE VI

OBSERVATIONS OF COLOR

(Stars not included in Table VIII, mostly of low weight)

No. H.A. 48	*Contr.* 97			EXPOSURE RATIOS		$C_m - C_e$
	Pg.	C_m	No.	C_e	No.	
126	15.58	0.93	2, 4	1.08	3	−15
139	15.30	1.34	2, 7	1.20	4	+14
142	14.60	0.89	2, 11	0.72	5	+17
143	16.35	0.84	7, 2	0.68	7	+16
146	14.52	0.96	2, 10	0.62	5	+34
154	14.95	0.59	8, 9	0.48	5	+11
159	15.20	0.70	16, 4	0.79	3	− 9
163	15.13	1.20	1, 3	0.82	3	+38
164	16.02	0.99	18, 5	0.86	3	+13
172	13.85	1.61	2, 1	1.38	4	+23
202	16.12	0.71	27, 4	0.78	3	− 7
205	15.97	0.89	11, 4	0.78	3	+11
214	15.39	0.73	9, 7	0.48	3	+25
215	15.47	1.78	10, 3	1.34	3	+44
218	15.47	1.36	17, 8	1.38	10	− 2
258	16.07	0.85	6, 4	0.64	3	+21
283	14.87	1.37	28, 3	1.24	4	+13
295	15.57	0.64	32, 5	0.66	8	− 2
301	16.23	0.66	26, 2	0.74	3	− 8
336	14.92	0.95	26, 5	0.77	5	+18
342	14.86	0.77	26, 3	0.64	5	+13
368	15.78	1.30	2, 3	1.21	3	+ 9

the values already published in *Contribution* No. 97 are open to suspicion. Superficially, one would expect a smaller difference for star 2 (5.28); its case is exceptional in that the values of log E for series a and e are discordant by about 0.4 mag., owing probably to an unfavorable combination of neglected plate constants. The persistent negative sign shown by the Polar Sequence stars near the fifteenth magnitude disappears when the differences for the *H.A.* 48 stars of the same brightness, in the latter part of Table VIII, are also taken into account. The systematic difference near the ninth magnitude is discussed in the following section.

TABLE VII

COMPARISON OF COLOR-INDICES FROM MAGNITUDES AND FROM EXPOSURE RATIOS

Pv. Mag.	Series a			Series a–f		
	$C_m - C_e$	No. Stars	No. log E	$C_m - C_e$	No. Stars	No. log E
	mag.			mag.		
3.0	+0.02	2	42	−0.03	2	46
5.4	+ 3	4	21	+ 3	4	36
6.5	0	5	14	0	5	34
8.0	− 5	5	25	− 7	5	39
9.5	− 8	6	65	− 9	6	103
10.4	− 1	5	112	− 1	5	217
11.1	+ 1	6	51	− 1	5	143
12.4	+0.04	8	109	+ 3	14	379
13.5	....	....	....	+ 3	22	216
14.3	....	....	....	+ 1	28	167
15.4	....	....	....	− 1	40	105
16.2	....	....	....	+ 3	31	68
16.9	....	....	....	−0.02	49	59
Sums...	....	41	439	....	216	1,612

3. CORRECTIONS TO PHOTO-VISUAL SCALE

It should be repeated that the two methods of deriving color-indices are independent, and that the values obtained from log E are essentially free from differential errors in the magnitude scales, as may be seen from the limits of brightness for the stars included in the normal points of Table IV (fourth column). The values of the differences $C_m - C_e$, when combined into means for groups of stars within narrow limits of magnitude, should therefore indicate the relative error in the scales. Since the photographic scale may

TABLE VIII

MEAN MAGNITUDES AND COLOR-INDICES

STAR	PHOTOGRAPHIC						PHOTO-VISUAL						ADOPTED MAGNITUDE			COLOR-INDEX			
	Contr. 97		10-Inch		N.P.C.		*Contr.* 97		10-Inch		N.P.C.		Pg.	Pv.	No.	C_m	C_e	No.	C_m-C_e
	Mag.	No.	Diff.	No.	Diff.	No.	Mag.	No.	Diff.	No.	Diff.	No.							
(1)	(2)	(3)	(4)	(5)	(6)	(7)	(8)	(9)	(10)	(11)	(12)	(13)	(14)	(15)	(16)	(17)	(18)	(19)	(20)
1s.....	2.54	40	.....	....	....	....	2.08	23	.....	....	....	....	2.54	2.08	40,23	+0.46	+0.51	39	− 5
1......	4.39	20	+ 7	4	....	....	4.37	9	.....	....	....	....	4.40	4.37	24, 9	0.03	−0.01	7	+ 4
2......	5.30	15	.....	....	....	....	5.28	11	.....	....	....	....	5.30	5.28	15,11	0.02	−0.18	7	+20
3......	5.83	22	.....	....	....	....	5.56	11	.....	....	....	....	5.83	5.56	22,11	0.27	+0.14	6	+13
4......	5.91	23	+14	4	....	....	5.84	9	.....	....	....	....	5.93	5.84	27, 9	+0.09	0.21	6	−12
5......	6.45	25	− 5	20	....	....	6.47	10	− 3	11	....	....	6.43	6.45	45,21	−0.02	0.02	8	− 4
2s.....	6.45	33	+ 1	25	....	....	6.33	10	− 6	11	....	....	6.45	6.30	58,21	+0.15	0.18	7	− 3
1r.....	6.61	27	+ 9	6	....	....	5.09	10	.....	....	....	....	6.63	5.09	33,10	1.54	1.54	17	0
3s.....	6.64	22	− 6	5	....	....	6.35	10	.....	....	....	....	6.63	6.35	27,10	0.28	0.23	4	+ 5
6......	7.11	16	+ 2	26	....	....	7.05	10	+ 1	11	....	....	7.12	7.06	42,21	+0.06	+0.05	7	+ 1
7......	7.41	26	+ 2	36	....	....	7.52	12	+ 7	10	....	....	7.42	7.55	62,22	−0.13	−0.16	7	+ 3
2r.....	7.94	22	− 1	31	....	....	6.35	12	− 6	11	....	....	7.93	6.32	53,23	+1.61	+1.55	8	+ 6
8......	8.32	36	+ 3	34	....	....	8.13	14	− 1	7	....	....	8.33	8.13	70,21	0.20	0.31	8	−11
9......	8.88	26	+ 5	54	....	....	8.81	12	+ 6	7	....	....	8.91	8.83	80,19	0.08	0.24	4	−16
3r.....	8.96	19	0	38	....	....	7.56	11	+ 2	11	....	....	8.96	7.57	57,22	1.39	1.43	13	− 4
10.....	9.12	21	+ 1	57	....	....	9.07	12	− 2	12	....	....	9.13	9.06	78,24	0.07	0.19	24	−12
4r.....	9.22	20	− 1	35	....	....	8.26	9	+ 2	6	....	....	9.21	8.27	55,15	0.94	1.10	7	−16
11.....	9.73	28	− 1	49	....	....	9.53	10	+ 5	13	....	....	9.72	9.56	77,23	0.16	0.26	3	−10
12.....	10.09	25	− 4	46	....	....	9.80	12	− 7	11	....	....	10.06	9.77	71,23	0.29	0.31	5	− 2
5r.....	10.13	24	+ 1	30	....	....	8.65	12	−10	3	....	....	10.14	8.63	54,15	1.51	....	....	.....
4s.....	10.25	19	+ 1	38	....	....	9.83	11	+ 1	11	....	....	10.26	9.83	57,22	0.43	0.52	2	− 9
6r.....	10.46	26	0	38	....	....	9.21	12	+ 5	13	....	....	10.46	9.24	64,25	1.22	1.24	7	− 2
13.....	10.53	19	− 1	35	....	....	10.37	16	+ 1	11	....	....	10.52	10.37	54,27	0.15	0.29	17	−14
7r.....	10.94	34	+ 1	35	....	....	9.90	28	−10	11	....	....	10.95	9.87	69,39	1.08	1.13	62	− 5
14.....	10.98	57	− 8	37	+ 5	37	10.54	18	+ 5	11	+ 3	9	10.97	10.56	131,38	0.41	0.48	57	− 7

5s.....	11.09	60	− 4	14	+ 5	36	10.06	28	.....	....	0	3	11.10	10.06	110,31	+1.04	+1.10	66	− 6
15.....	11.22	30	+ 6	33	....	....	10.89	10	− 1	11	....	....	11.25	10.88	63,21	0.37	0.37	37	0
6s.....	11.38	9	− 1	24	....	....	10.73	13	− 8	2	....	....	11.37	10.72	33,15	0.65	0.71	34	− 6
8r.....	11.44	32	+ 2	29	....	....	10.44	17	+ 4	11	....	....	11.45	10.46	61,28	0.99	0.97	26	+ 2
16.....	11.62	43	− 2	22	− 8	21	11.23	16	+ 2	7	− 4	13	11.60	11.22	86,36	0.38	0.35	30	+ 3
17.....	11.87	43	+ 3	29	....	....	11.28	13	+ 6	7	....	....	11.88	11.30	72,20	0.58	0.50	21	+ 8
18.....	12.27	49	+ 1	23	....	....	11.89	14	+ 3	3	....	....	12.27	11.90	72,17	0.37	0.40	21	− 3
10r.....	....	....	.....	....	....	....	12.03	5	.....	....	....	....	....	12.03	5	....	....	....	.....
7s.....	12.61	70	.....	....	+10	44	12.10	12	.....	....	− 8	45	12.65	12.04	114,57	0.61	0.56	48	+ 5
19.....	12.69	78	0	18	+ 5	57	12.28	12	−13	3	− 5	54	12.71	12.24	153,69	0.47	0.44	37	+ 3
20.....	13.02	86	− 2	16	− 7	69	12.51	12	−15	2	+ 2	60	12.99	12.52	171,74	0.47	0.54	45	− 7
11r.....	13.22	79	+ 6	7	+ 1	43	12.06	12	+ 4	2	+ 1	41	13.23	12.07	129,55	1.16	1.10	43	+ 6
21.....	13.33	37	0	11	....	....	12.48	12	+ 8	2	....	....	13.33	12.49	48,14	0.84	0.69	16	+15
22.....	13.44	45	+ 7	8	+15	27	12.81	11	.....	....	+ 6	25	13.48	12.84	80,36	0.64	0.58	15	+ 6
23.....	13.60	80	+ 7	8	− 2	69	13.10	12	.....	....	−12	58	13.59	13.00	157,70	0.59	0.53	29	+ 6
12r.....	13.84	82	+ 2	2	− 8	69	12.46	12	.....	....	+ 1	59	13.80	12.47	153,71	1.33	1.30	19	+ 3
24.....	13.93	71	0	7	+ 1	44	13.33	12	.....	....	− 3	34	13.93	13.31	122,46	0.62	0.64	13	− 2
25.....	14.08	78	+ 4	4	+ 5	50	13.60	12	.....	....	− 2	44	14.10	13.58	132,56	0.52	0.62	14	−10
8s.....	14.49	50	−10	2	+10	29	13.78	12	.....	....	− 3	10	14.52	13.77	81,22	0.75	0.85	12	−10
26......	14.64	74	−10	3	− 4	66	13.72	12	.....	....	− 4	44	14.62	13.69	143,56	0.93	1.06	13	−13
9s.....	14.75	66	−16	2	− 1	68	13.85	12	.....	....	−14	41	14.74	13.74	136,53	1.00	1.08	12	− 8
27.....	14.91	61	− 6	2	−10	62	14.33	7	.....	....	−12	12	14.86	14.25	125,19	0.61	0.69	10	− 8
28.....	15.27	40	.....	....	0	28	14.54	7	.....	....	+ 4	1	15.27	14.54	68, 8	0.73	0.92	5	−19
10s.....	15.29	45	+16	2	− 1	22	14.49	7	.....	....	+25	1	15.29	14.52	69, 8	0.77	0.92	7	−13
11s.....	15.31	63	− 2	2	− 2	52	14.35	10	.....	....	+ 1	8	15.30	14.35	117,18	0.95	0.97	10	− 2
12s.....	15.33	61	.....	....	+ 2	39	14.69	7	.....	....	− 9	2	15.34	14.67	100, 9	0.67	0.76	7	− 9
13s.....	15.54	43	.....	....	− 5	22	14.54	3	.....	....	....	....	15.52	14.54	65, 3	0.98	1.10	8	−12
29.....	15.82	40	.....	....	....	....	15.21	6	.....	....	....	....	15.82	15.21	40, 6	0.61	0.75	5	−14
14s.....	15.99	47	.....	....	+ 3	26	15.07	7	.....	....	−15	1	16.00	15.05	73, 8	0.95	1.21	7	−26
30.....	16.18	34	.....	....	....	....	15.44	5	.....	....	....	....	16.18	15.44	34, 5	0.74	0.74	5	0

TABLE VIII—*Continued*

STAR	PHOTOGRAPHIC						PHOTO-VISUAL						ADOPTED MAGNITUDE			COLOR-INDEX			
	Contr. 97		10-Inch		N.P.C.		*Contr.* 97		10-Inch		N.P.C.		Pg.	Pv.	No.	C_m	C_e	No.	C_m-C_e
	Mag.	No.	Diff.	No.	Diff.	No.	Mag.	No.	Diff.	No.	Diff.	No.							
(1)	(2)	(3)	(4)	(5)	(6)	(7)	(8)	(9)	(10)	(11)	(12)	(13)	(14)	(15)	(16)	(17)	(18)	(19)	(20)
31	16.41	45	....	....	0	17	15.62	6	....	....	....	....	16.41	15.62	62, 6	+0.79	+0.78	5	+ 1
15s	16.57	41	....	....	− 3	5	15.71	5	....	....	....	....	16.57	15.71	46, 5	0.86	0.74	4	+12
32	16.76	33	....	....	....	....	15.58	3	....	....	....	....	16.76	15.58	33, 3	1.18	1.44	4	−26
16s	16.86	36	....	....	+ 4	1	15.50	4	....	....	....	....	16.86	15.50	37, 4	1.36	1.45	4	− 9
33	17.06	32	....	....	....	....	15.97	3	....	....	....	....	17.06	15.97	32, 3	1.09	1.11	3	− 2
34	17.24	24	....	....	....	....	16.29	2	....	....	....	....	17.24	16.29	24, 2	0.95	1.10	3	−15
35	17.63	20	....	....	....	....	16.94	2	....	....	....	....	17.63	16.94	20, 2	0.69	0.80	3	−11
125	15.12	2	....	....	−30	1	14.37	5	....	....	....	....	15.02	14.37	3, 5	0.65	0.65	5	0
127	14.35	6	....	....	− 4	2	13.31	11	....	....	....	....	14.34	13.31	8,11	1.03	0.89	12	+14
130	15.26	2	....	....	−21	1	14.21	9	....	....	....	....	15.19	14.21	3, 9	0.98	0.60	3	+38
134	14.43	6	....	....	−17	1	13.54	10	....	....	....	....	14.41	13.54	7,10	0.87	....	....	....
151	13.72	29	....	....	− 2	3	12.58	11	....	....	+18	9	13.72	12.66	32,20	1.06	1.14	13	− 8
152	14.56	21	....	....	+12	3	13.76	12	....	....	− 3	1	14.58	13.76	24,13	0.82	0.68	12	+14
158	15.10	16	....	....	0	1	14.57	5	....	....	....	....	15.10	14.57	17, 5	0.53	0.64	3	−11
176	14.33	36	....	....	+14	5	13.81	12	....	....	−13	4	14.35	13.78	41,16	0.57	0.59	6	− 2
226	14.93	46	....	....	− 8	25	14.23	7	....	....	−21	4	14.90	14.15	71,11	0.75	0.82	8	− 7
256	14.67	50	....	....	− 4	28	13.86	11	....	....	− 4	8	14.66	13.84	78,19	0.82	0.92	10	−10
277	15.30	62	....	....	+ 6	49	14.61	7	....	....	−15	4	15.33	14.56	111,11	0.77	0.72	9	+ 5
311	15.00	53	....	....	+ 4	42	14.36	7	....	....	− 5	6	15.02	14.34	95,13	0.68	0.56	10	+12
319	14.44	40	....	....	+ 9	14	13.55	3	....	....	+ 7	25	14.46	13.61	54,28	0.85	0.73	10	+12
329	14.32	38	....	....	+10	14	13.34	3	....	....	+19	27	14.35	13.51	52,30	0.84	0.76	11	+ 8
334	15.20	70	....	....	− 1	51	14.42	7	....	....	+ 3	14	15.20	14.44	121,21	0.76	0.86	9	−10
338	14.72	28	....	....	+ 8	5	13.79	3	....	....	+ 6	10	14.73	13.84	33,13	0.89	0.82	8	+ 7
341	15.16	26	....	....	− 6	8	13.92	3	....	....	+12	15	15.15	14.02	34,18	1.13	1.06	8	+ 7
345	13.79	58	....	....	− 1	36	12.01	11	....	....	+ 5	35	13.79	12.05	94,46	1.74	1.50	29	+24

350.....	11.01	46	.....	....	+ 3	26	10.64	12	.....	....	+14	11	11.02	10.71	72,23	+0.31	+0.24	51	+ 7
358.....	15.22	26	.....	....	+ 9	9	14.11	2	.....	....	+47	2	15.24	14.34	35, 4	0.90	0.81	7	+ 9
362.....	13.13	86	.....	....	−12	67	12.31	12	.....	....	− 5	61	13.08	12.27	153,73	0.81	0.82	47	− 1
378.....	14.14	54	.....	....	− 2	64	12.74	5	.....	....	+ 8	54	14.13	12.81	118,59	1.32	1.33	32	− 1
389.....	13.57	43	.....	....	+ 8	48	12.83	8	.....	....	+ 8	43	13.61	12.90	91,51	0.71	0.62	17	+ 9
391.....	14.63	38	.....	....	− 2	46	13.85	6	.....	....	− 2	32	14.62	13.83	84,38	0.79	0.75	11	+ 4
401.....	14.53	36	.....	....	− 8	25	13.61	3	.....	....	+10	33	14.50	13.70	61,36	0.80	0.77	10	+ 3
403.....	14.51	41	.....	....	− 4	27	13.75	3	.....	....	+ 9	34	14.49	13.83	68,37	0.66	0.72	9	− 6
424.....	14.51	29	.....	....	+ 2	20	13.64	3	.....	....	+15	26	14.52	13.77	49,29	0.75	0.58	10	+17
426.....	13.83	28	.....	....	+ 7	12	13.33	3	.....	....	+ 6	14	13.85	13.38	40,17	0.47	0.55	10	− 8
427.....	13.27	33	.....	....	− 1	23	12.07	5	.....	....	−2	41	13.27	12.05	56,46	1.22	1.05	24	+17
439.....	(15.29)	1	.....	....	−51	21	13.49	3	.....	....	....	....	14.78	13.49	21, 3	1.29	1.39	10	−10

be accepted as substantially correct, it follows that the means may be regarded as corrections to the original photo-visual scale of *Contribution* No. 97.

Table VII shows the results found in this manner, both provisionally from series *a* and finally from the data in Tables VI and VIII supplemented by the faint stars appearing in series *f* alone. The means depend upon weights approximately proportional to the number of values of log E, unless C_m is much less reliable than usual. Technically, this is not the best method of procedure, but practically the final differences are little affected by the system of weighting or the grouping. It is noteworthy that the provisional corrections to the photo-visual scale given in the second column of Table VII, as far as they go, are in close agreement with those in the fifth column based upon much more extensive data.

With the exception of differences of -0.07 and -0.09 at magnitudes 8.0 and 9.5, the corrections are insignificant, and show that within very small limits of error the photographic and photo-visual scales of *Contribution* No. 97 are mutually consistent as far as the seventeenth photo-visual magnitude (about 18 photographic). The two discordant points indicate a small local systematic error, but its source cannot certainly be located.

The investigation with the 10-inch refractor[1] makes a negative correction to the photo-visual scale rather improbable. At the same time, the exposure-ratio observations are not very uniformly distributed, and some of them may be systematically affected by neglected plate constants. For the present it seems best to let the magnitude scales stand as they are, and to regard the results from exposure ratios as a check which establishes the mutual consistency of the scales within a few hundredths of a magnitude.

4. COLLECTION OF RESULTS. ADOPTED MAGNITUDES

The various results on the magnitudes and colors of stars near the Pole can now be brought together and combined into means. These results include: (*a*) the original determination in Table IX of *Contribution* No. 97, made with the 60-inch reflector; (*b*) the determination with the 10-inch Cooke refractor, in Tables III and VI of *Contribution* No. 234; (*c*) the revision for the reduction of accidental error, discussed in section 1 above; and (*d*) the values of the color-indices found from exposure ratios.

---

[1] *Loc. cit.*

Assuming the photographic scale of (*a*) to be correct between magnitudes 10 and 15, (*b*) confirms the photographic scale of (*c*) between magnitudes 6 and 14, and the photo-visual scale between 6 and 12; (*d*) shows that the two scales are mutually consistent to the seventeenth photo-visual magnitude, with a maximum difference of 0.09 mag. at the ninth magnitude.

The essential details of the combination of these results are in Table VIII. The stars of the Polar Sequence, arranged in order of photographic magnitude, are given as far as Nos. 35 and 16*s*, where the revisions cease. The latter part of the table includes 30 additional stars in order of the *H.A.* 48 number.

The data in the first three and the eighth and ninth columns are copied directly from Table IX, *Contribution* No. 97. The results from (*b*) are in the fourth and fifth, and tenth and eleventh columns, and have been transcribed directly from the last two columns of Tables III and VI, respectively, of *Contribution* No. 234. Those from (*c*) are in the sixth and seventh, and twelfth and thirteenth columns, and have been taken from Table I above. The algebraic signs are such that when the differences are added algebraically to the magnitudes of *Contribution* No. 97 they give the results of the various revisions.

The final magnitudes are in the fourteenth and fifteenth columns. These are the means of the results in columns two to seven, and eight to thirteen, respectively, weighted according to numbers of values involved in each, excepting that the polar-comparison values for star 22 have received half the usual weight. Resulting color-indices, C_m, and the total numbers of observations are in the sixteenth and seventeenth columns. The results from exposure ratios in the eighteenth and nineteenth columns have already been discussed.

With the exception of the stars in Table IX of *Contribution* No. 97 not included in the revision, which stand as they are, Table VIII above summarizes all of the work done at Mount Wilson on the magnitudes and colors of stars near the Pole. The table itself gives little indication of the labor which lies behind it, the great burden of which in the measurement and reduction of the plates has fallen upon Miss Richmond and Miss Joyner of the Computing Division. I am deeply indebted to them for their part in an investigation which could not have been completed without generous assistance.

Mount Wilson Observatory
March 1922

ON THE SPECTRUM OF NEUTRAL HELIUM[1]

By LUDWIK SILBERSTEIN

ABSTRACT

Quantum theory of spectrum lines of neutral helium.—No attempt has hitherto been made to account for any of these lines because, since the neutral atom has two electrons besides the nucleus, the theoretical explanation is generally supposed to depend on the solution of the problem of three bodies. But while we do not possess a general solution of this problem, particular solutions are known and it is of interest to see what results they give. For the case of permanent collinearity of the three bodies, we get a spectral formula of the Balmer type, $\nu=(49N/8)\ (1/n^2-1/m^2)$, but this represents none of the observed lines. If, however, we assume that the mutual perturbation of the electrons is negligible, the formula comes out $\nu=4N[1/n_1^2-1/m_1^2+1/n_2^2-1/m_2^2]$; and if the proper integral values are taken, up to 9 for the n's and up to 32 for the m's, this formula gives 84 out of the 111 observed lines, in general within a fraction of an angstrom. Although the resulting classification does not correspond to the usual series arrangement, the success of the formula suggests that the *force between intra-atomic electrons* may be much less than that given by the Coulomb law.

It is but too well known that, up to the present, the quantum theory of spectrum emission has proved utterly unable to deal satisfactorily with any spectra but those of atomic hydrogen and, what essentially is the same thing, of ionized helium. It being generally admitted that the neutral helium atom consists of a nucleus and two electrons, the notoriously prohibitive nature of the general problem of three bodies was invoked by the leading spectroscopists as a sufficient excuse for not as much as attempting to account theoretically for a single one out of the hundred and odd lines observed in the emission spectrum of that element.[2] The more so, of course, in the case of atoms containing three or more electrons. But though it be true that we are as far as ever from possessing a general solution of that famous problem (not Sundman's, of course) in anything like a practicable form for the purpose in hand, yet some particular solutions are known, simple enough to be treated at once by the quantitizing method of modern spectroscopy, and it has seemed worth while to try the possibilities in this direction and thus, perhaps, to break the spell which has hitherto paralyzed all desire of attacking the non-hydrogenic spectra.

---

[1] *Communication No. 156* from the Research Laboratory of the Eastman Kodak Company.

[2] Thus, e.g., Sommerfeld, passing from hydrogen to neutral helium, appeals to Goethe's Faust ("Hier stock ich schon, wer hilft mir weiter fort?") and concludes the section by consoling himself with the fact that "so also were the astronomers, in spite of centuries of attempts, unable to solve satisfactorily the three-body problem." *Atombau und Spektrallinien.*

At first the writer thought of applying the well-known particular solution of the problem of three bodies given by Lagrange as long ago as 1772. But the corresponding spectrum formula, which is easily deduced, proved impotent to cover as much as a single observed line of neutral helium. In fact, what of Lagrange's solution remains for the purpose in hand is the case of permanent *collinearity* of the three bodies, the two electrons describing (apart from relativistic refinements) equal and coplanar ellipses around the nucleus as one of the foci, with overlapping major axes and the other foci situated on opposite sides of the nucleus.[1] Each electron is then easily seen to move as if it had only the charge $-\frac{7}{8}e$ (instead of $-e$) and as if the other electron were absent. The total energy of the system is found at once to be, with a as major semi-axis,

$$E=-\frac{7e^2}{4a}=-\frac{49}{8}\frac{2\pi^2m_0e^4}{h^2(n'+n'')^2},$$

where n' and n'' are the azimuthal and the radial quantum numbers defining any stationary state, and the remaining symbols have their usual meaning. Writing $n=n'+n''$ for the total quantum number and introducing the Rydberg constant, $N=2\pi^2m_0e^4/ch^3$, we have

$$E=-\frac{49}{32}\cdot\frac{4Nhc}{n^2}.$$

Bohr's older model of the passive (non-emitting) He atom corresponds to the case $n=n'=1\,(n''=0)$, when both electrons describe the same circle; it gives $E=-\frac{49}{8}Nhc$, whence also the familiar (and somewhat too large) ionization potential, which need not detain us here. By the last energy formula, with n for the final and m for the initial quantum number, we have the spectrum formula

$$\nu=\frac{49}{8}N\left(\frac{1}{n^2}-\frac{1}{m^2}\right),$$

---

[1] This is but a special case of any number of equal ellipses distributed symmetrically around the nucleus, as used by Landé and others for a coarse representation of the higher atoms for X-ray purposes.

which is of the simple Balmer type, each frequency ν being merely that of ionized helium magnified $\frac{49}{32}$ times. Since in the present case there is no wobbling of the nucleus, we have to take, instead of the usual He value, $N=N_{\infty}$, i.e., about 109737 cm^{-1}. Ultimately, therefore, the spectrum formula corresponding to the class of *collinear* solutions becomes

$$\nu=672139\left(\frac{1}{n^2}-\frac{1}{m^2}\right).$$

Now, if one may judge from a week's personal experience spent over a multitude of trials, this formula does not cover any of the observed helium lines, at least as tabulated in Fowler's last *Report.*[1] The nearest "hit" was $n=4, m=7$, giving $\lambda_{\text{air}}=3535$, but even this was full two angstroms below the nearest observed line which is at about $\lambda=3537$. Of course, one felt from the outset that by such an extremely narrow class of solutions, as are the collinear ones, one could not reasonably expect to cover more than a very small part of all the observed lines, perhaps one or two only. But the formula refused to yield a single one.

In fine, the collinear solutions, though rigorous, do not represent any of the observed lines of neutral helium.[2]

Such being the case, the idea occurred to me that one might perhaps be more successful with some broader, though only approximate, solutions of the three-body problem, and as such the most simple, nay trivial, class of motions suggested itself, namely those in which *the mutual perturbation of the two electrons is practically nil or negligible.* At first the idea seemed almost repugnant, through its very banality, but on trial it proved surprisingly useful, as will appear hereafter.

As a matter of fact, we have no good evidence that the electrons, especially as trabants of the nucleus within the atom, do act upon each other at all, and some bold modern physicist, encouraged by the recognized prohibition to radiate, might deny the electrons the right to interact while they are busy obeying the orders of the central body driving them around on stationary orbits. But it is safer to put the restriction as above, i.e., as an approximate assumption. Whether at all and how often such cases of practically negligible mutual perturbation actually occur within the atom of helium (and similarly in other atoms), cannot be decided beforehand, but only by experience. If the corresponding spectrum formula works and covers some of the observed lines, it can be reasonably inferred that such comparative independence of the electrons does occur, statistically, in a good number of individual atoms. If no lines are covered, the conclusion will be that such a state of things does not occur at all or only very sporadically.

---

[1] A. Fowler, *Report on Series in Line Spectra*, Phys. Soc. London, 1922, pp. 93–94. I have taken account also of some special papers quoted by Fowler.

[2] This result throws even, in the writer's opinion, a flood of doubt upon the admissibility of Bohr's older model of the passive He atom, which belongs to the same class of solutions, as already mentioned.

The spectrum formula corresponding to this class of motions can be written down at once. If n_1, n_2 (and similarly m_1, m_2) be the total quantum numbers of the first and the second electrons, the total energy of the system in any stationary state is simply the sum of

$$E_1=-\frac{4Nhc}{n_1^2} \quad \text{and} \quad E_2=-\frac{4Nhc}{n_2^2}.$$

The required formula is, therefore,

$$\nu=4N\left[\frac{1}{n_1^2}+\frac{1}{n_2^2}-\frac{1}{m_1^2}-\frac{1}{m_2^2}\right], \tag{1}$$

where n_1, etc., are four independent integers, fixing the final and the initial state, or, introducing a conveniently short symbol for the bracketed expression,

$$\nu=4N\left(\frac{m_1,\ m_2}{n_1,\ n_2}\right). \tag{1a}$$

We shall also speak of the spectrum line having this frequency as "the line m_1, m_2/n_1, n_2." This formula amounts, obviously, to putting

$$\nu=\nu_1+\nu_2, \tag{2}$$

where ν_1,ν_2 are, apart from a possible slight difference of N, the frequencies of any two lines of ionized helium, observed or only theoretical. This would then be a new kind of the combination principle: the sum of frequencies belonging to one atomic system (ionized helium) giving the frequency for *another system* (neutral helium).

As to the value of N, it is certainly not rigorous to take that found experimentally for ionized helium or that (but slightly different) used by empirical spectroscopists for neutral helium. To be accurate, somewhat different values of N should be used for different lines, according to the nature and the mutual configuration of the two pairs of orbits (influencing the amount of wobbling of the nucleus), and these being unknown, one would have to adopt some statistically computed compromise value. But such niceties may be postponed to a future opportunity, and since for the present it will be enough to write all wave-lengths to four or five figures, we shall, without much ado, adopt in formula (1) the value $N=109723.2$ used for He^+ in Fowler's *Report*, the more so as in using the form (2) it will be convenient to take directly ν_1 and ν_2 as given by Fowler (p. 95) for the observed frequencies of ionized helium. Thus we shall have ultimately, in cm.$^{-1}$,

$$\nu=438893\left(\frac{m_1,\ m_2}{n_1,\ n_2}\right). \tag{3}$$

In what follows λ_0 will be written for the wave-length in vacuo, the reciprocal of ν, and λ for λ_{air}. All observed values will be quoted from Fowler's *Report*, where the wave-lengths are in I.A. For the present no other material, scattered in special papers (and doubtful as to the origin of the lines), will be taken into account.

Passing now to try out the formula (3) or (2), let us notice that any line of the type $m_1,\ m_2/n,\ n$ will be an additive combination of two members of one and the same series of ionized helium. But we shall have also interesting cases of $n_1 \neq n_2$, when the addends belong to different He^+ series, not necessarily both observed, and yet give rise to an observed He line.

Lines of the type $m_1,\ m_2/2,\ 2$, i.e., derivable from the Lyman series of He^+, need not detain us here, since they all fall between 698 and 498, a region thus far not sufficiently explored.

For the same reason, though to a lesser extent, we may omit for the present the He lines derivable from Fowler's or the principal series of He$^+$, these lines, of the type $m_1, m_2/3, 3$, stretching all beyond 1903 A into the ultra-violet.

Let us, therefore, pass at once to lines of the type

$$\frac{m_1,\ m_2}{4,\ 4}$$

i.e., derivable from the Pickering series. We can now use directly the formula (2) adding up pairs of Pickering frequencies. Thus, and writing (5), (6), etc., for the values of m_1 or m_2, we find the following interesting results:

$$\frac{5,\ 14}{4,\ 4} \qquad \begin{array}{ll} (5) & 9875.1 \\ (14) & 25191.8 \\ \hline \end{array}$$

$$\nu = 35{,}067;\ \therefore\ \lambda_0 = \begin{array}{r} 2851.7 \\ -0.8 \\ \hline \end{array}$$

$$\lambda = 2850.9;$$

the nearest line observed (Fowler, p. 94) has $\lambda = 2851$, and is tabulated among the combination lines of neutral helium;

$$\frac{5,\ 20}{4,\ 4} \qquad \begin{array}{ll} (5) & 9875.1 \\ (20) & 26333.6 \\ \hline \end{array}$$

$$\nu = 36{,}209;\ \lambda = 2761.8 - 0.8 = 2761.0,$$

nearest line observed for He (*loc. cit.*) $\lambda = 2761$;

$$\frac{5,\ 25}{4,\ 4} \qquad \begin{array}{ll} (5) & 9875.1 \\ (25) & 26728.7 \\ \hline \end{array}$$

$$\nu = 36{,}604;\ \lambda = 2732.0 - 0.8 = 2731.2,$$

nearest line observed for He (*loc. cit.*) $\lambda = 2732$.

These three agreements are remarkably close. The next but one theoretical line is

$$\nu = 4N\left(\frac{5, 18}{3,\ 8}\right) = 36{,}713.3;\ \lambda = 2723.8 - 0.8 = 2723.0,$$

the nearest He line (*loc. cit.*), observed by Merton, being λ 2722.

Notice that we could take also $m_1 = m_2$, which would mean simply doubling the frequency of a Pickering-series member, i.e.

taking $\nu_1 = \nu_2$. But none of these theoretical lines $m, m/4, 4$ fits an observed He line, even the nearest hit $(5, 5/4, 4)$ with $\nu = 19{,}750$ being too distant from the observed He line $\nu = 19{,}931$.

We will thus content ourselves with the three or four good results derived from the Pickering series alone, and pass on to consider a few lines of the type

$$\frac{m_1,\ m_2}{5,\ 4},$$

i.e., combinations of the members of the Pickering series with those of a purely theoretical He$^+$ series $\nu_i = 4N(1/5^2 - 1/m_i^2)$, never observed. Notwithstanding the latter circumstance, neutral helium shows at least three lines agreeing admirably with the theoretical lines of this type. In fact, we have, always by formula (3),

$$\left(\frac{6,\ 9}{5,\ 4}\right) = 0.0623765,\ \nu = 27{,}377,\ \lambda = 3652.8 - 1.0 = 3651.8,$$

the nearest observed He line being 3652.0, tabulated in the sharp doublet series. Next,

$$\left(\frac{6,\ 17}{5,\ 4}\right) = 0.0712620,\ \nu = 31{,}276,\ \lambda = 3197.3 - 0.9 = 3196.4,$$

the nearest observed He line being 3196.7 (principal, $1S - mP$, *loc. cit.*), and finally,

$$\left(\frac{6,\ 19}{5,\ 4}\right) = 0.0719521,\ \nu = 31{,}579,\ \lambda = 3166.6 - 0.9 = 3165.7,$$

which covers the observed He line 3166 (combin., *loc. cit.*). [See also the combination $(4.15/3.6)$ in the table below.]

To close this preliminary report on well-fitting lines it may be well to quote at least two examples in which both of the addends (ν_1 and ν_2) are purely theoretical. The first of these is

$$\left(\frac{6,\ 28}{5,\ 5}\right) = 0.0509467,\ \nu = 22{,}360,\ \lambda = 4472.25 - 1.25 = 4471.00,$$

with the nearest observed He line at $\lambda = 4471.48$ (diffuse doublet series, *loc. cit.*, p. 93), and the second, which has seemed interesting as it concerns an infra-red line,

$$\left(\frac{10,\ 15}{7,\ 14}\right)=0.0110658, \quad \nu=4856.7,$$

which agrees fairly well with the observed He line (sharp, $1P-mS$) at $\nu=4857.3$.

Whether these nine or ten lines of neutral helium can also be covered by some other pairs of initial and final states of the system, in which the interaction of the electrons *is* taken into account, must for the present remain an open question. For no such solutions are known or likely to be forthcoming soon. In the meantime one would be justified to conclude from these results that there is a good deal of mutual independence of the two electrons within the radiating helium atom, which is particulary surprising in the case of such small orbits (of both) as those corresponding to the quantum number 4. A quantitative estimate of the perturbations to be expected on the ordinary repulsion law between the electrons, together with possible conclusions concerning those theoretical lines that do deviate from the observed ones by a few angstroms, will occupy our attention in a future publication.

In much the same way one could try to cover some lines of lithium (without awaiting, of course, an amputation of two of its three limbs or electrons) by three pairs of terms, i.e., by the formula $\nu=9N(m_1,\ m_2,\ m_3/n_1,\ n_2,\ n_3)$, and some spectrum lines of the higher atoms by four, five and more pairs of terms. But the larger the number of electrons, the less likely are the states of their comparative independence. Moreover, the larger the number of independent term pairs, the less convincing will be even a thorough fitting, so that it does not seem worth while to push the procedure much beyond lithium. At any rate the case of neutral helium has seemed the most interesting one, and an analogous treatment of lithium is now in progress.

ROCHESTER, N.Y.
July 4, 1922

ADDENDUM

Since the foregoing was sent to the Editors of the *Astrophysical Journal*, I have subjected all the observed spectrum lines of neutral helium to a kind of arithmetical sieve which enabled me to sweep the field with comparative ease. The result was, much to my own surprise, that practically the whole spectrum of helium is covered by the proposed formula

$$\nu = 4N\left(\frac{m_1 \cdot m_2}{n_1 \cdot n_2}\right),$$

in the majority of cases within a fraction of an angstrom, the same value N, namely 109723.2,[1] being used throughout.

The numerical results, ordered for the present according to the total quantum numbers defining *the final state* $(n_1 \cdot n_2)$, are given in the following tables, with the calculated and the observed wave-number ν in the second, and the excess $\delta\lambda$ of the calculated over the observed wave-length, in angstroms, in the third column. The last column gives the empirical qualifications of the observed lines, with the abbreviations

P = principal, S = sharp, D = diffuse, F = fundamental, d = doublet system, s = singlet system, C = "combination,"

and with the intensities, where available, expressed by the bracketed numbers. The whole observed material is taken from Fowler's *Report*, already quoted, with the only addition of ν 21866 (λ 4572), observed by Stark in a strong electric field,[2] thus making a total of 111 observed lines. The initial and final orbit numbers are given in the first column. Spectrum lines of the type (m/n) can manifestly be interpreted as corresponding either to a jump of one electron from m to n, while the other electron remains on any stationary orbit, or else as corresponding to a jump of one electron from m to any integer x, and of the other electron from x to n,

$$\left(\frac{m}{n}\right) = \left(\frac{m \cdot x}{n \cdot x}\right) = \left(\frac{m \cdot x}{x \cdot n}\right).$$

Such, for instance, is the line (6/3), written $(6 \cdot n/3 \cdot n)$, and similarly for the remaining five lines of this type. They are interesting inasmuch as they might also be produced by ionized helium, as far as mere arithmetic goes. All other lines are of the irreducible type $m_1 \cdot m_2/n_1 \cdot n_2$. That the classification according to n_1, n_2 lacerates the usual empirical classification (principal, sharp, etc.) may be regrettable but need not detain us here. Moreover, now and then,

---

[1] This was fixed provisionally and may still be slightly retouched, but not until one comes to consider the relativistic refinements and the dynamics ot the wobbling of the nucleus.

[2] *Annalen der Physik.*, 56, 577, 1918.

TABLE I

$\frac{m_1 \cdot m_2}{n_1 \cdot n_2}$	ν calc. ν obs.	δλ		$\frac{m_1 \cdot m_2}{n_1 \cdot n_2}$	ν calc. ν obs.	δλ	
$\frac{13.n}{4.n}$	24,834 24,830	−0.6	D.d. (5)	$\frac{8.15}{4.5}$	36,178 36,171	−0.5	P.d. (2)
$\frac{18.n}{4.n}$	26,076 26,078	+0.4	D.s. (1)	$\frac{5.14}{4.6}$	19,827 19,82$_4$	−0.$_9$	C.s.
$\frac{22.n}{4.n}$	26,524 26,526	+0.3	D.s. (1)	$\frac{5.16}{4.6}$	20,352 20,358	+1.5	C.s.
$\frac{26.n}{4.n}$	26,781.5 26,781.6	+0.01	S.d. (1)	$\frac{7.15}{4.6}$	28,715 28,716	+0.1	S.d.
$\frac{30.n}{4.n}$	26,943 26,938	−0.7	C.d.	$\frac{11.15}{4.6}$	34,045 34,05$_0$	+0.$_5$	C.d.
$\frac{4.9}{3.5}$	33,472 33,48$_0$	+0.$_6$	C.d.	$\frac{11.26}{4.6}$	35,346 35,337	−0.7	P.d. (4)
$\frac{4.18}{3.5}$	37,536 37,537.5	+0.1	P.d. (1)	$\frac{12.28}{4.6}$	36,015 36,00$_0$	−1.$_2$	C.d.
$\frac{4.20}{3.5}$	37,794 37,798	+0.3	P.d.	$\frac{16.23}{4.6}$	37,078 37,079	+0.1	P.d. (1)
$\frac{4.15}{3.6}$	31,576 31,57$_6$	0.$_0$	C.d.	$\frac{17.24}{4.6}$	37,341.6 37,342.7	+0.1	P.d. (1)
$\frac{4.14}{3.7}$	28,053 28,058	+0.7	S.d. (1)	$\frac{20.23}{4.6}$	37,695 37,683	−0.9	P.d.
$\frac{4.16}{3.7}$	28,577 28,574	−0.4	D.d. (1)	$\frac{6.10}{4.7}$	19,807 19,805	−0.5	S.s. (2)
$\frac{5.18}{3.8}$	36,713 36,711	−0.15	P.d. (1)	$\frac{8.19}{4.7}$	28,314 28,316.5	−0.3	D.d. (1)
$\frac{4.25}{3.8}$	27,490.6 27,489.3	−0.2	C.d.	$\frac{8.25}{4.7}$	28.827.9 28,82$_7$.	0.$_0$	C.s.
$\frac{4.19}{3.8}$	26,977.0 26,982.4	+0.7	D.d. (3)	$\frac{8.26}{4.7}$	28,881 28,883	+0.3	D.d. (1)
$\frac{5.14}{4.4}$	35,067 35,06$_4$	−0.$_2$	C.d.	$\frac{8.27}{4.7}$	28,928 28,921	−0.8	D.d. (1)
$\frac{5.20}{4.4}$	36,208.7 36,20$_8$	0.$_0$	C.d.	$\frac{8.28}{4.7}$	28,970 28,97$_7$	+0.$_8$	C.s.
$\frac{5.25}{4.4}$	36,603 36,59$_2$	−0.$_8$	C.d.	$\frac{9.14}{4.7}$	28,730 28,736	+0.6	D.d. (1)
$\frac{6.9}{4.5}$	27,377 27,374	−0.35	S.d. (1)	$\frac{9.26}{4.7}$	30,320 30,324	+0.4	P.s. (1)
$\frac{6.17}{4.5}$	31,276 31,274	−0.3	P.s. (1)	$\frac{15.30}{4.7}$	33,950 33,945	−0.4	P.d. (6)
				$\frac{28.32}{4.7}$	35,399 35,40$_1$	+0.$_1$	C.d.

TABLE I—*Continued*

$\frac{m_1\cdot m_2}{n_1\cdot n_2}$	ν calc. ν obs.	$\delta\lambda$		$\frac{m_1\cdot m_2}{n_1\cdot n_2}$	ν calc. ν obs.	$\delta\lambda$	
$\frac{7.18}{4.8}$	23,977 23,980	+0.5	S.s. (1)	$\frac{6.16}{5.5}$	21,205.5 21,210.8	+1.2	S.d. (1), (3)
$\frac{9.12}{4.8}$	25,822.5 25,820.5	−0.3	D.s. (1)	$\frac{6.28}{5.5}$	22,360.1 22,357.7	−0.5	D.d. (6)
$\frac{9.18}{4.8}$	27,516 27,508	−0.9	D.d. (2)	$\frac{7.11}{5.5}$	22,527.4 22,518.6	+0.3	S.s. (1)
$\frac{9.20}{4.8}$	27,773 27,775	+0.2	S.d. (1)	$\frac{7.19}{5.5}$	24,938.6 24,935.2	−0.5	D.s. (1)
$\frac{9.21}{4.8}$	27,874.9 27,874.1	−0.1	C.d.	$\frac{7.21}{5.5}$	25,159 25,157	−0.3	C.s.
$\frac{9.27}{4.8}$	28,268 28,266	−0.3	S.d. (1)	$\frac{7.25}{5.5}$	25,452 25,460	+1.3	D.s. (1)
$\frac{10.11}{4.8}$	26,272 26,269	−0.6	D.s. (1)	$\frac{8.24}{5.6}$	22,128 22,125	−0.5	C.d.
$\frac{10.14}{4.8}$	27,661 27,665	+0.6	P.s. (3)	$\frac{10.20}{5.6}$	24,261.1 24,260.3	−0.16	S.d. (3)
$\frac{10.18}{4.8}$	28,545.0 28,544.4	−0.07	S.d. (1)	$\frac{11.22}{5.6}$	25,213 25,215	+0.3	P.s. (4)
$\frac{10.20}{4.8}$	28,802 28,795	−0.8	D.d. (1)	$\frac{12.27}{5.6}$	26,098 26,103	+0.85	C.d.
$\frac{11.14}{4.8}$	28,422.3 28,422.6	+0.04	S.d. (1)	$\frac{13.20}{5.6}$	26,053 26,047	−0.9	S.s. (1)
$\frac{12.13}{4.8}$	28,644 28,640	−0.5	S.d. (1)	$\frac{13.22}{5.6}$	26,244 26,247	+0.3	C.s.
$\frac{12.14}{4.8}$	29,001 28,997	−0.5	P.s. (2)	$\frac{13.24}{5.6}$	26,388.4 26,395.2	+1.0	S.s. (1)
$\frac{13.28}{4.8}$	31,132 31,129	−0.3	P.s. (1)	$\frac{14.20}{5.6}$	26,411 26,413	+0.3	D.s. (1)
$\frac{14.14}{4.8}$	29,810 29,802	−0.9	P.s. (1)	$\frac{14.21}{5.6}$	26,513.0 26,513.7	+0.1	S.s. (1)
$\frac{14.18}{4.8}$	30,695 30,687	−1.4	P.s. (1)	$\frac{15.15}{5.6}$	25,846.0 25,848.9	+0.4	S.d. (1), (2)
$\frac{16.20}{4.8}$	31,476.9 31,472.4	−0.45	P.s. (1)	$\frac{18.24}{5.6}$	27,630.6 27,632	+0.2	C.s.
$\frac{16.19}{4.8}$	31,358 31,361	+0.3	P.d. (8)	$\frac{20.25}{5.7}$	24,713 24,710	−0.6	C.d.
$\frac{11.24}{4.9}$	28,460.0 28,461.6	+0.20	D.d. (1)	$\frac{22.24}{5.7}$	24,843.9 24,843.96	+0.01	S.s. (1)

TABLE I—*Continued*

$\frac{m_1 \cdot m_2}{n_1 \cdot n_2}$	ν calc. ν obs.	δλ		$\frac{m_1 \cdot m_2}{n_1 \cdot n_2}$	ν calc. ν obs.	δλ	
$\frac{14.14}{5.8}$	19,935 19,932	−0.9	P.s. (6)	$\frac{9.24}{6.7}$	14,968 14,970	+0.9	D.s. (6)
$\frac{16.23}{5.8}$	21,869 21,866	−0.7	C.*	$\frac{10.15}{7.14}$	4856.7 4857.3	δν −0.6	P.s. (20) also S.s.
$\frac{22.25}{5.8}$	22,804 22,802	−0.6	C.s.				
$\frac{9.15}{6.6}$	17,014.0 17,014.3	+0.1	D.d. (1), (10)	$\frac{23.11}{8.9}$	7819.2 7819.9	δν −0.7	F.d. (1)

* Line λ 4572 observed by Stark in an electric field of 28500 volt/cm. Not contained in Fowler's *Report.*

a good portion of an empirical series, such as "P.s." at $n_1 \cdot n_2 = 4.8$, reasserts itself.

These are, thus far, 84 different observed lines of helium. Of the 27 observed lines thus left unaccounted for the infra-red ones could not, up to the present, be covered within less than $\delta\nu = \pm 10$, without exceeding $n = 9$ for the final orbits. Of the remaining lines I have thus far succeeded in covering a few more within less than 2 angstroms, while fourteen show a difference of 2 to 3, and one of about 5 angstroms. The corresponding numerical details may be omitted for the present.

Thus, to say the least, over eighty out of the 111 observed lines of He are well represented by the aforesaid formula whose structure is such as if *the two electrons did not influence each other at all,* each being acted upon only by the nucleus.

At first one might, perhaps, expect this formula to represent *only* such lines as correspond to a passage from an initial to a final state in both of which the two electrons are on the whole so distant from each other that their initial energy required by the Coulomb law,

$$\Phi = e^2/r_{12}\,,$$

is negligibly small. If this were so, then the well-fitting cases would be simply as many approximate solutions of the three-bodies problem in its sanctioned form (Coulomb's law for each pair), and there would be nothing very surprising in those coincidences. But this is by no means the case. On the contrary, the energy neglected, or rather deliberately disregarded by the writer, in all these cases would amount, in terms of ν, to several thousand units,[1] and the amounts neglected in the initial and the final states by no means compensate each other—and even if they did, the considerable force of interaction would in each case have modified thoroughly the orbits themselves, spoiling the fitting altogether. If there is at all any repulsion between the two electrons, then, to make it compatible with the eighty results obtained, it can scarcely amount to more than one-ten-thousandth of the Coulomb force. To say the least, we are entitled to strongly suspect the validity of anything like the usual repulsion law between the electrons within an atomic system. Evidence of the same kind is afforded by the spectrum of lithium for which the writer has recently found several remarkably close coincidences with

$$\nu=9N\left(\frac{m_1\cdot m_2\cdot m_3}{n_1\cdot n_2\cdot n_3}\right),$$

to be described at an early opportunity. As a matter of fact, there is (apart from a few slightly defective computations of ionization potentials) no experimental evidence for the Coulomb repulsion between intra-atomic electrons, anyhow. On the other hand its denial gave us a huge majority of the spectrum lines of helium, not a single one of which has been accounted for by models based on such a repulsion nor, in fact, in any other way.

In conclusion it may be well, in anticipation of possible objections, to notice that the results obtained can by no means be explained away as so many chance coincidences. In fact, a laborious computation of *all* the theoretical lines of the aforesaid type with the restriction to $n \leq 8$ and $m \leq 20$, which need not be reproduced here, has shown that the probability of only twenty of our tabulated lines (in the interval $\nu = 22{,}000$ to $38{,}000$) hitting the observed lines within the actual $\delta\nu$ by mere chance is less than 10^{-17}. And if some, at least, of the remaining sixty items are taken into account, the odds against a chance hit will be found to be enormous.

August 2, 1922

---

[1] E.g., for states such as (4.4) it amounts as a simple computation will show, to more than 13,500 waves (units of ν).

THE VARIABLE DOUBLE STAR X OPHIUCHI[1]

By C. H. GINGRICH

ABSTRACT

Variable double star X Ophiuchi.—From direct measurements by Hussey and later by Van Biesbroeck it is known that the two components of this interesting system are about 0".22 apart and were in a nearly north and south line in 1921, and that the north component is variable. During 1921 van Maanen made 16 plates to determine the parallax, which came out 0".000±0".007. These plates have since been measured in declination to see whether any *displacement of the combined image* due to the variation in relative brightness of the components could be detected. With reference to exposures made near a maximum of the combined light, a mean displacement of about 0".15 to the south was found for a group of eight exposures made about midway between maximum and minimum. This result is in agreement with the previous conclusions mentioned above. On the plates measured there was no evidence of elongation of the image.

This interesting and rather exceptional object, whose position for 1900 is $\alpha = 18^h 33^m 24^s$, $\delta = +8°44'$, was noted as variable first by Espin in 1886. It is included in the list of variable stars in *Harvard Annals*, **55**, 22, as star 183308, and is there assigned a range in magnitude from 6.5 to 9.0 in a period of 335 days. Its spectral classification is Md. Subsequent study of the variability of this star by Mr. Leon Campbell of the Harvard College Observatory based upon mean light curves extending over the interval from the year 1904 to the year 1921 indicates that the range is from magnitude 6.7 to 8.8 in a period of 337 days; $M-m=$ 189 days, $m-M=148$ days.

Hussey in 1900 discovered that this object is a double star, the components being separated by 0".22 in position angle 195°.2. It appears as Hu 198 in the list of double stars published by him in the *Astronomical Journal*, **21**, 35 (No. 485), 1900.

Merrill, without realizing that the star was double, noticed that the spectrum of this object changed to such an extent from time to time as to suggest that there were two sources of light, and that at certain times the one predominated and at other times the other. Through correspondence with Van Biesbroeck, of the Yerkes Observatory, it was learned that in his program of remeasuring all the double stars discovered by Hussey his attention had been attracted to this object by its deep orange color, and that he was measuring the pair and observing the light variation for the purpose of determining which of the components was responsible for the variation of the pair or whether both components were variable. The mean results of six measures which he made in 1920 are

---

[1] *Contributions from the Mount Wilson Observatory*, No. 238.

$$1920.668 \quad 171^{\circ}\!.1 \quad 0''\!.218.$$

Later Van Biesbroeck furnished a light curve of the pair from estimates of magnitude extending from July, 1920, to October, 1921, covering more than one period of the variable, and showing the date of a maximum to be 1921, May 5. He also deduced the conclusion from estimates of relative brightness of the two components that the "north preceding star is the variable one."

In May, 1921, van Maanen completed a series of plates for determining the relative parallax of this object, and from them deduced the following result:

$$\pi = 0''\!.000 \pm 0''\!.007, \quad \mu_a = 0''\!.000 \pm 0''\!.020.$$

Van Maanen and Merrill suggested that, since the image is undoubtedly displaced because of the relative change in brightness of the components, it would be desirable to measure the plates of the parallax series in order to discover the amount and direction of this displacement and thereby obtain an independent determination of the distance between the two, and also an indication as to which was varying.

Since the plates were taken within the period during which Van Biesbroeck made his measures, which show the stars to be nearly in a north and south line, it was immediately clear that the displacement due to variation in magnitude would be almost entirely in declination. Consequently the plates were arranged for measurement with the stereocomparator in the same pairs that van Maanen had used for the parallax measures, but were measured in declination instead of in right ascension as he had done. As the plates had been taken for maximum parallax displacement in right ascension they were of necessity extremely unfavorable to parallax determination in declination, but, as van Maanen had already shown the relative parallax to be very small, this feature was of no special importance for the present purpose.

It should perhaps be stated that on the plates measured there was no evidence of elongation of the image and that consequently the settings were made so as to bisect the image resulting from the combined light of the pair.

I used the light curve derived by Van Biesbroeck for obtaining the magnitude of the pair at the times when the several plates were taken and assumed the magnitude at minimum to be the magnitude of the invariable component, and by use of the formula

$$\log b_n = \log b_m - 4/10\ (n-m)$$

given in Young's *General Astronomy*, page 509, constructed the following table of values:

TABLE I

Plate No.	Date	Combined Mag.	Ratio of Light Intensity		Mag. Var.
			Var. / Inv.	Inv. / Comb.	
2675	1920, May 15	7.1	2.98	0.25	7.4
2699	25	7.0	3.37	.23	7.3
2802	Aug. 7	8.0	0.74	.58	8.9
2814	8	8.0	0.74	.58	8.9
2819	20	8.2	0.45	.69	9.5
2831	21	8.2	0.45	.69	9.5
2846	22	8.2	0.45	.69	9.5
3083	1921, Apr. 13	7.2	2.63	.28	7.6
3100	May 1	7.0	3.37	.23	7.3
3112	13	7.0	3.37	0.23	7.3

By using data determined by Campbell and by Van Biesbroeck it was found that the star was at maximum brightness on 1920, June 2, and 1921, May 5, and at minimum brightness on 1919, November 25; 1920, October 28; and 1921, September 30. The mean date of the first two plates, May 20, is only thirteen days before the maximum of June 2, and the mean date of the last three, April 29, is only seven days before the maximum of May 5.

The mean date of the remaining five plates, August 18, is seventy-one days before the minimum of October 28.

In the reductions of the measures the factors in the next to the last column in Table I were taken to represent the proportionate displacement of the image from the position of the variable star toward the position of the invariable one. It is probable that the displacement of the image of the combined light due to variation in one of the components does not take place rigorously according to the law implied in this method. However, in the absence of accurate knowledge at this point this assumption is the best which can be made as a working hypothesis.

At first that part of Van Biesbroeck's measured distance between the stars, namely $0''.218$, indicated by the assumption just referred to, was applied to the measured quantities in a direction consistent with the conclusion that the north star is the variable one, and the residual quantities were used for determining parallax and proper motion in declination. However, because of the small parallax factors already referred to and because of the short interval of time involved, the probable errors of these determinations were so large as to make the values entirely unreliable and practically meaningless. Next an equation was formed for each pair of plates with the distance between the stars, as well as the parallax and proper motion, left as unknown. The same factors as before were used as coefficients of the unknown distance δ. A least-squares solution of these equations led to the following results:

$$\pi = -0''.088 \pm 0''.092;\ \mu_\delta = -0''.037 \pm 0''.022;\ \delta = 0''.348 \pm 0''.025.$$

Inasmuch as this computed distance differs considerably from the distance measured directly, corrections based upon the computed distance were applied to the plate measures as before and a new determination of the parallax and proper motion made. The results were

$$\pi = -0''.012 \pm 0''.102;\ \mu_\delta = -0''.030 \pm 0''.015.$$

These values of π and μ_δ are at least possible, but the probable errors make it unsafe to attach very much weight to them, especially in the case of the parallax value.

It was then decided to remeasure the plates by comparing each available exposure with a given exposure chosen as the standard, in order to detect the displacement from this standard position. The exposure on the plate numbered 3100 was chosen as standard because the date of the exposure, 1921, May 1, so nearly coincided with the date of the observed maximum, 1921, May 5. In all, fifteen exposures were compared with this standard, and equations formed, coefficients for π, μ_δ and δ (distance) determined by the same method as before being used. The following results were obtained:

$$\pi = +0''.002 \pm 0''.063; \quad \mu_\delta = -0''.001 \pm 0''.012; \quad \delta = -0''.385 \pm 0''.024.$$

The value of the parallax agrees well with that obtained by van Maanen by measuring these plates in right ascension, as already stated. Even though the time interval is short the probable error of the determined proper motion is small, and hence the value of μ_δ may be relied upon with some degree of confidence.

As for the value of the distance, the sign shows the displacement to be to the south of the standard position, and, since the standard exposure was made at a period of maximum, a time when the variable star was dominant, this fact furnishes independent confirmation of the conclusion by Van Biesbroeck that the north star is the variable one. The numerical value requires further consideration. The displacements obtained from the several plates are shown in Table II.

TABLE II

Plate Nos.	Displacement	Plate Nos.	Displacement
2675_1–3100	−0″.015	2831_1–3100	−0″.154
2675_2–3100	− .035	2831_2–3100	− .194
2699_1–3100	+ .039	2846_1–3100	− .165
2699_2–3100	+ .003	2846_2–3100	− .167
2802_1–3100	− .126	3083_1–3100	− .035
2802_2–3100	− .115	3083_2–3100	− .002
2814_1–3100	− .168	3100–3100	.000
2819_1–3100	−0 .190	3112–3100	−0 .018

It has been shown that the relative parallax and proper motion of this object are very small, and their effect in displacing the image is therefore negligible. Hence the measured displacements may be considered as due to the relative change in magnitude alone. The mean displacement of the first four and the last four exposures, all of which were made very near to a period of maximum brightness, is $-0''.008$; the mean displacement of the remaining eight exposures, which were made within an interval of fifteen days, although seventy-one days before minimum, is $-0''.160$. There is therefore a measured displacement of $-0''.152$ in the interval from near maximum to seventy-one days before minimum. As the time during which this displacement took place is only one-half the interval from maximum to minimum, one might be led to conclude that a displacement of twice this amount would result from plates taken at minimum. As the distance between the stars obviously cannot be less than the measured displacement, this conclusion would indicate a distance fairly accordant with the computed value obtained above. Table I, however, would contradict such a conclusion in that it shows that on the mean date, August 18, of the second group of plates the invariable contributes more than twice as much light as the variable, instead of only an equal amount, as would seem to be required if the resultant image is to have a position midway between the extremes.

It seems, therefore, impossible to reach a definite conclusion because of uncertainty in two respects: first, the exact magnitude of the invariable star upon which depend the relative amounts of light contributed by the two components at the times of the exposures and, second, the effect of variable intensities upon the position of the resulting image. Both of these difficulties would vanish in a case in which we knew that the variable was entirely ineffective at minimum and completely dominated the formation of the image at maximum, and if we had one series of plates at maximum and another at minimum. The latter condition is not fulfilled in this instance, and it is probable that the former is not. The assumption of 8.6 as the magnitude of the invariable leads, as is seen in Table I, to the conclusion that the invariable star is responsible for one-fourth of the total light at maximum and for all of the light at minimum. It does not seem likely that the variable becomes so faint at minimum as to be entirely without any effect in the formation of the image at that time. Even though it may contribute a part of the light, it may, however, be such a small percentage as to be ineffective in displacing the measured center of gravity. In that case the computed value for the distance between the stars, 0."385, would be too large. On the other hand the measured displacement, 0."152, although apparently more than half the distance between the stars, is somewhat smaller than the distance. The true value for the distance would therefore lie between these two limits. A number of suppositions might be made which would lead from the foregoing conclusion to a value almost identical with the value obtained by Van Biesbroeck from direct measurement. We may therefore say, in conclusion, that this investigation shows without any doubt that the north star is the variable one, and if it does not confirm the value for the distance between the stars it most certainly does not contradict it. The writer expects to continue the study of this pair by securing plates at maximum and at minimum.

The suggestions by Mr. van Maanen and Mr. Merrill during this work were of great help and were thoroughly appreciated by the writer. Valuable assistance was rendered also by Mrs. Marsh, of the Computing Division, who checked the computations in the early part of the study.

MOUNT WILSON OBSERVATORY
May 1922

PARALLAXES OF STARS IN THE REGION OF B.D.+31°643[1]

By C. H. GINGRICH

ABSTRACT

Diffuse, irregular nebula, and stars around B.D.+31°643.—A photograph made by Hubble with the 100-inch reflector is reproduced. From a series of plates taken by van Maanen with the 60-inch reflector, the *parallaxes and proper motions of 20 stars* with reference to six or seven among them which appear not to be related to the nebula, were determined. Five of these have *color-indices* from 0.74 to 0.95 in excess of normal and seem to be involved in the nebula. The mean of the parallaxes of these five stars is 0".0095±0".006. This is therefore taken to be the *parallax of the nebula*, equivalent to a distance of 350 light years from the sun.

The star B.D.+31°643 is of special interest because it is apparently imbedded in the densest part of a diffuse, irregularly shaped nebula extending over the region surrounding this star. The photograph of this region published herewith is reproduced from a negative made by Mr. Hubble with the 100-inch Hooker telescope, November 9, 1920, and kindly loaned to me for this purpose. The exposure time of this negative was 180 minutes.

A series of plates of this same region, taken by Mr. van Maanen with the 60-inch reflector as a part of his regular parallax program, was begun in December, 1919, and finished in January, 1922. The stars which appear on the parallax plates are numbered on the photograph (Plate I), except the brightest star, whose image was too large for measurement. The one designated as π is the star B.D.+31°643. Mr. van Maanen gave me these plates to measure in order to find out whether, on the basis of the parallaxes, the stars could be classified in two groups, the one containing those stars which belong to the nebula and the other those which do not.

Another basis for a separation into such groups had already been suggested by Mr. Hubble, namely, a comparison of color-index with spectral type. He had noticed that in the case of certain of the stars the color-index was larger than would be accounted for by the spectral type, which led him to the conclusion that the excessive redness was due to the absorption of the blue light by surrounding nebulous matter.

---

[1] *Contributions from the Mount Wilson Observatory*, No. 239.

In Table I the first column gives the numbers assigned to the stars on the parallax plates and corresponding to the numbering on Plate I; the second and third columns give, respectively, the distances of the various stars from the central star in right ascension and declination, in minutes of arc; the next five columns were supplied by Mr. Seares and Mr. Hubble from material now being prepared for publication by them; the last two columns give the final mean values of parallax and proper motion in right ascension, expressed in thousandths of a second of arc. These last quantities will be explained more fully later.

TABLE I

No.	x	y	Photo. Mag.	Spectrum	Observed Color-Index	Normal Color-Index	Color-Excess	π (Mean)	μ_a (Mean)
π.....	0′.0	0′.0	9.07	B6	+0.65	−0.14	0.79	− 8	− 14
1.....	−14.8	+7.7	....	.....	....	....	....	+ 67	− 56
2.....	− 9.0	+3.3	....	.....	....	....	....	− 17	− 34
3.....	− 7.6	0.0	11.81	.....	+ .59	....	....	+ 13	+ 25
4.....	− 5.5	−2.5	10.19	B8	+ .42	− .07	.49	+ 31	− 10
5.....	− 5.2	−2.7	10.31	B8	+ .48	− .07	.55	+ 28	− 15
6.....	− 3.2	−0.3	12.32	A2	+ .71	+ .07	.64	+ 8	+ 4
7.....	− 2.7	−2.2	12.08	F2	+ .65	+ .48	.17	+ 2	+ 10
8.....	− 2.2	+1.2	14.6±	.....	....	....	....	− 14	− 5
9.....	− 2.1	+0.4	12.14	A1	+ .82	+ .03	.79	+ 28	+ 22
10.....	− 0.7	+0.1	12.32	B9	+ .71	− .03	.74	+ 5	− 5
11.....	− 0.5	−3.4	11.42	B9	+ .92	− .03	.95	− 5	− 9
12.....	+ 0.3	+0.3	10.80	B9	+ .80	− .03	.83	+ 32	+ 75
13.....	+ 0.7	−3.0	14.5±	.....	....	....	....	− 44	− 85
14.....	+ 2.9	+5.8	14.8±	.....	....	....	....	+ 24	+115
15.....	+ 3.2	+7.1	14.3±	.....	....	....	....	+ 50	+ 75
16.....	+ 3.4	+9.5	11.99	A0	+ .96	.00	.96	+100	+210
17.....	+ 7.1	+0.7	14.0±	.....	....	....	....	0	+ 15
18.....	+ 7.1	−9.2	14.22	.....	+1.02	....	....	− 36	−162
19.....	+11.1	+7.5	9.40	K0	+1.53	+1.48	0.05	+ 34	+ 29

The plates were arranged in pairs and measured with the new stereocomparator of the Mount Wilson Observatory according to the method developed by van Maanen and fully described by him in *Mount Wilson Contribution* No. 111. For comparison stars those were chosen which, according to the color-index cri-

PLATE I

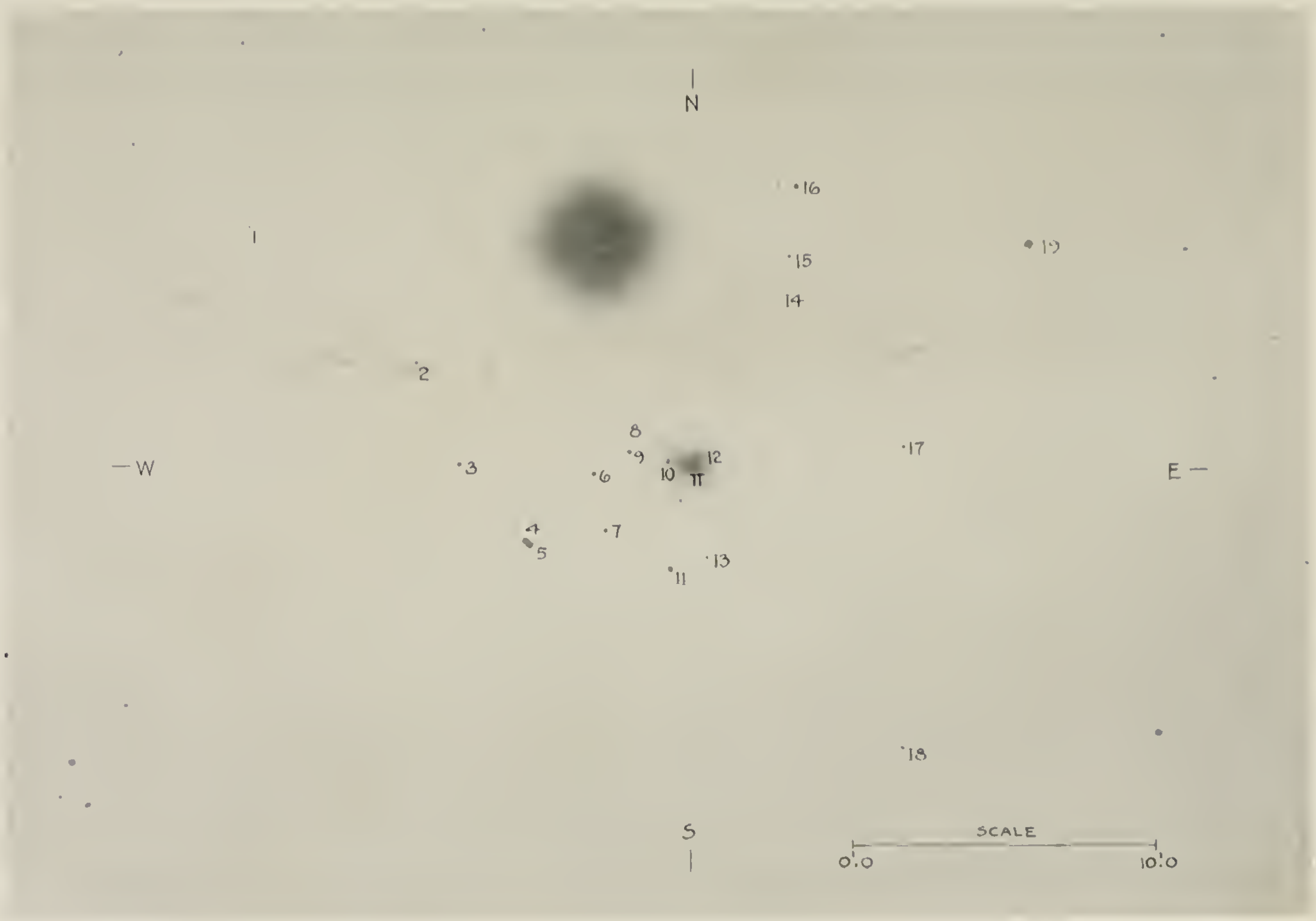

Region of B.D. +31°643 Photographed by Hubble with the 100-Inch Hooker Reflector, November 9, 1920

terion, had no connection with the nebula. As was to be expected, this selection resulted in having as comparison stars those situated at some distance from the nebula and consequently located at considerable distances from the center of the plate. It was accordingly advisable to use quadratic terms in the reductions. However, as the exclusion of the stars which may be connected with the nebula left only seven stars available for that purpose, the six plate constants could not be determined with great accuracy. Two other solutions were therefore made, omitting the quadratic terms. The number of comparison stars in the first solution was seven and in the later ones six and four, omitting those so far from the center as to show unsymmetrical images on some of the plates.

The fact that the number of comparison stars available was small is probably not a matter of mere accident. On the parallax plates certain regions are easily noticeable in which no stars appear. It therefore seems likely that the nebula so conspicuous in certain parts of the field extends faintly over perhaps the entire region of the parallax plates with the result that the light of the fainter stars is absorbed or scattered by it. This conclusion is confirmed on the basis of the total number of stars on the parallax plates. According to *Groningen Publications* No. 27, the total number of stars would indicate that the faintest stars appearing are of magnitude 12.3 approximately, whereas as a rule stars as faint as magnitude 13.7 appear on the plates. In other words we should normally expect to find more than three times as many stars on plates at the galactic latitude of this field as are actually found on these.

Moreover, as will be seen in Table II, no definite classification of the stars into nebulous and non-nebulous is possible on the basis of the parallaxes found.

The values of parallax and proper motion in right ascension for each of the stars from each of the three reductions are shown in Table II. The first values resulted from a solution including quadratic terms and using stars 1, 2, 3, 7, 17, 18, 19 as comparison stars; the second, not including quadratic terms and employing stars 2, 3, 7, 17, 18, 19 as comparison stars; the third is like the second except that only four comparison stars were used, 2, 3, 7, 17. The results are expressed in thousandths of a second of arc.

In order to determine the weights to be assigned to each of these sets of values the arithmetical means of the three were formed and the deviations from the means noted. These deviations indicated that weights 1, 1, 2 should be used. Adopting these weights the mean values of π and μ_a given in the last two columns of Table I were obtained. The mean probable error of all the parallaxes is ±0.″013 and of all the proper motions is ±0.″019. These values are unusually large because stars 1, 16, 18, and 11 are more than 10′ from the center, the limit usually set for parallax determinations, and hence not well suited for measurement. Excluding these stars from the computation, we find the mean probable error of the remainder of the parallaxes to be ±0.″009, and of the proper motions ±0.010.

TABLE II

SUMMARY OF π AND μ_a

	π_1	*p.e.*	μ_{a1}	*p.e.*	π_2	*p.e.*	μ_{a2}	*p.e.*	π_3	*p.e.*	μ_{a3}	*p.e.*
π..........	+ 36	8	− 2	12	− 22	7	+ 5	10	− 23	6	− 30	9
1..........	+ 11	3	+ 12	4	+ 57	31	−192	45	+100	19	− 21	28
2..........	− 24	5	− 30	8	− 25	11	− 75	16	− 10	3	− 16	4
3..........	− 7	3	+ 4	4	+ 24	7	+ 41	10	+ 18	5	+ 28	7
4..........	+ 26	9	− 18	14	+ 47	11	+ 38	16	+ 25	10	− 31	15
5..........	+ 25	2	− 20	3	+ 45	8	+ 37	12	+ 21	5	− 39	7
6..........	+ 40	9	+ 12	14	+ 2	11	+ 22	16	− 4	8	− 9	12
7..........	+ 26	5	+ 20	8	+ 7	9	+ 54	13	− 12	4	− 17	6
8..........	+ 33	11	+ 8	17	− 34	5	− 7	7	− 27	5	− 10	7
9..........	+ 70	11	+ 32	16	+ 13	8	+ 32	12	+ 14	6	+ 11	9
10..........	+ 50	21	+ 7	30	− 10	18	+ 12	26	− 10	20	− 19	29
11..........	+ 27	13	+ 17	19	+ 1	13	+ 51	19	− 24	8	− 52	12
12..........	+ 78	18	+ 88	26	+ 15	9	+ 91	13	+ 17	10	+ 61	15
13..........	− 10	11	− 58	16	− 40	10	− 31	15	− 64	12	−126	18
14..........	+107	33	+159	48	− 31	8	+ 51	12	+ 10	18	+125	26
15..........	+148	32	+138	46	− 16	8	− 13	12	+ 35	18	+ 88	26
16..........	+229	48	+319	71	+ 12	13	+ 75	19	+ 80	24	+224	35
17..........	− 1	1	+ 1	2	− 6	8	+ 48	12	+ 4	1	+ 5	1
18..........	− 5	1	− 5	2	− 6	7	− 51	10	− 66	45	−297	66
19..........	0	1	− 1	1	+ 5	4	− 18	6	+ 66	21	+ 68	31

A direct examination of the original negative from which the accompanying plate has been made would indicate that the stars numbered 1, 2, 3, 7, 14, 15, 17, 18, and 19 are not connected with the nebula; that those numbered 8, 13 are probably involved in it; and that those numbered π, 9, 10, 11, 12, 16 are apparently enmeshed in it. There is no nebulosity visible about the stars 4, 5, 6, but their color-indices are such as to lead one to suspect the presence of nebulous matter.

Selecting from Table I those stars which to all appearances are imbedded in the nebula, omitting the one numbered 16 because of uncertainty due to its distance from the center of the plate and from the other stars of the group, we have for the five stars, π, 9, 10, 11, 12, a mean relative parallax of $+0\overset{''}{.}0104$. Two other stars, those numbered 3 and 6, have about the same parallax as the mean just found. The latter, as already stated, should probably be included among the five because of the evidence furnished by its color-index; as for the former, no evidence of connection with the nebula or with the group is indicated other than that of its parallax.

We are therefore led to the conclusion that the mean relative parallax of the five stars and hence the parallax of the nebula of which they almost certainly form a part is $+0\overset{''}{.}0104$. By applying to this the correction of $-0\overset{''}{.}0009$ derived by van Maanen[1] to reduce it to absolute parallax we find as the absolute parallax of the nebula $+0\overset{''}{.}0095$. This value of the parallax indicates a distance from the sun of about 350 light-years.

The very bright star in the photograph is *o* Persei. Two determinations of the parallax of this star have been made: one at the Sproul Observatory, $+0\overset{''}{.}035$; the other at the Allegheny Observatory, $+0\overset{''}{.}003$. The mean of these shows a value not greatly at variance with the parallax found for the nebula.

The double star 4 and 5 is listed as number 1832 in Burnham's *General Catalogue* and is there assigned a separation of $11\overset{''}{.}14$ in position angle $128\overset{\circ}{.}6$. Measures extending from the year 1868 to the year 1903 show no change in either of these quantities.

The central star B.D.+31°643, designated on the plates used as π, is also a double star. It is numbered 1836 in Burnham's *General Catalogue* and consists of two stars of nearly the same brightness and only $0\overset{''}{.}45$ apart in 1880. Measures from the year 1891 to the year 1893 indicate a slight progressive increase in the distance. On the scale of our plates the two components combine to form a single symmetrical image.

---

[1] *Mt. Wilson Contr.*, No. 237.

This investigation would have been entirely impossible at this time had it not been for the series of plates taken by Mr. van Maanen, and in a sense therefore these results are due to him. Furthermore, his large experience in parallax work was heavily drawn upon throughout this work, and numerous constructive suggestions were cheerfully made by him.

The writer wishes also to express his hearty appreciation of the willing and generous co-operation of Mr. Seares and Mr. Hubble in the ways already indicated.

Mount Wilson Observatory
April 1922

J. C. KAPTEYN

Photograph taken by F. Ellerman in 1914, during Kapteyn's last visit to Mount Wilson.

THE
ASTROPHYSICAL JOURNAL
AN INTERNATIONAL REVIEW OF SPECTROSCOPY
AND ASTRONOMICAL PHYSICS

VOLUME LVI OCTOBER 1922 NUMBER 3

J. C. KAPTEYN, 1851–1922

By A. VAN MAANEN

In Amsterdam, on June 18, Jacobus Cornelius Kapteyn, since 1921 retired professor of astronomy and director of the Astronomical Laboratory at Groningen, died at the age of seventy-one years. In him astronomy loses one of its foremost pioneers.

Kapteyn was born January 19, 1851, at Barneveld, a small village where his father had a well-known boarding school. Of the fifteen children of this family several became leaders in the scientific world in Holland. From 1869 to 1875 Kapteyn was a student at the University of Utrecht, where his principal teachers were Buys Ballot and Grinwis, so that it is no wonder that his doctoral thesis was in physics: "Onderzoek der Trillende Platte Vliezen." Just at this time, however, the position of observer at the Leiden Observatory was vacant, and Kapteyn applied for and obtained the position. By this accidental circumstance astronomy secured the privilege of counting Kapteyn as one of its workers and before long as one of its foremost leaders. His ability was soon recognized, and at the age of twenty-seven, which for Holland is extremely young, he was appointed full professor in astronomy at the University of Groningen. On entering office, February 20, 1878, his opening address had as subject: "The Parallax of the Fixed Stars."

The problem of the stellar distances was naturally of first importance to him, whose ideal was to throw some light on the structure of the universe. We do not know when this idea began to ripen in Kapteyn's mind, but it probably dates from the time that he decided to devote his life to astronomy. And no better man could be found to push astronomy ahead along these lines, because Kapteyn had two qualities which were needed for such investigations: he could grasp a great problem and at the same time both could and was willing to devote much time to essential details. These two qualities show up through all his life and we see him, never losing view of the greatest of astronomical problems, the structure of the universe, and at the same time working with painstaking assiduity to develop and improve the methods of securing the necessary data. Of this part of his work no better example can be given than the succession of new methods that he developed to obtain stellar distances. In 1882 the parallaxes of only thirty-four stars were known, the best results being due to heliometer observations, especially by Gill and Elkin at the Cape of Good Hope.

When Kapteyn came to Groningen his appointment was to the professorship in astronomy, calculus of probabilities, and theoretical mechanics, but he found no observatory at his disposal. Good mathematician as Kapteyn was, his heart was drawn more toward the practical side of his science, and during the first years in Groningen he tried hard to secure funds for an observatory, with a six-inch heliometer as its principal instrument. In the beginning his efforts seemed to promise success, and ground for the observatory was bought a little outside of the city, but funds for the erection of the buildings were not forthcoming until many years later, by which time Kapteyn in his unique astronomical laboratory had founded an establishment which satisfied, better than an observatory could have done, the needs of this wonderful combination of the practical and the theoretical astronomer.

Lack of an opportunity for observational work was, however, keenly felt by Kapteyn during the early years of his professorship, and he requested Professor H. G. van de Sande Bakhuyzen to let him use the meridian circle of the Leiden Observatory during his vacations. The request was granted and Kapteyn planned a careful program for the observation of stellar parallaxes; he introduced the differential method of observations in right-ascension, thus deriving parallaxes for fifteen stars, which in accuracy competed with those yielded by the heliometer, while the observations required less time. His thorough discussion of the method and of these observations in Volume VII of the *Annals of the Leiden Observatory* is one of the many contributions from his hand which will be recorded among the classics of astronomy.

But it was clear that for a solution of his great problem parallaxes must be determined more rapidly. In 1889, at the conference of the Carte du Ciel, Kapteyn outlined an ingenious scheme for measuring the parallaxes of a large number of stars by means of photography. The plan is extremely simple in theory: on the same plate three exposures are made at the epoch of maximum parallactic displacement; half a year later, at the minimum, six other exposures are made on the same plate, and three again at the following maximum; after development the plate shows twelve images of each star which in practice are arranged as follows:

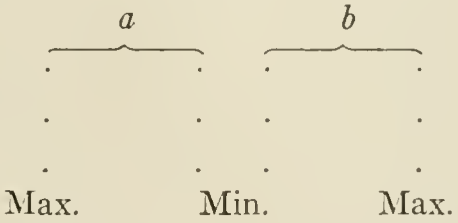

FIG. 1.—Arrangement of exposures for the determination of stellar parallaxes according to Kapteyn's plan.

The distances a and b are then measured and reduced by a simple process; and yield, with respect to the mean parallax of all the stars measured, the parallax of every star visible on the plates. The method was put into practice by Kapteyn and Donner and the first results were published in 1900 as Number 1 of the *Publications of the Astronomical Laboratory at Groningen*, a remarkable series of publications which has contributed much to the development of astronomy in the last twenty years.

While similar results for different fields, mostly in collaboration with De Sitter, appear in the *Groningen Publications*, we soon perceive a change in his policy of attack on the general problem. The change from parallaxes to proper motion, however, is more apparent than real, and is founded on the practical fact, that by using the proper motions we can base the parallaxes on the ever increasing base line of the sun's motion through space, and on the theoretical fact, that for the structure of the universe it is not at all necessary to know the distances of individual stars, but the mean distances of groups of stars for different magnitude, spectral type, and galactic latitude. The problem has two requirements: an accurate determination of the sun's motion through space and a knowledge of the distribution of proper motion for an increasingly great number of fainter and fainter stars. Along both lines the *Groningen Publications* reveal how much Kapteyn advanced our knowledge. And it is in just such work as this that Kapteyn's double aptitude for recognizing great problems and at the same time perceiving the practical difficulties, was of the greatest usefulness. Kapteyn would work out a new method which, with the proper material, would give the desired results; but he would at the same time also apply his method to the material available, even when it was scanty and likely to yield only defective results. This, however, had the advantage of showing at once where the method itself could be improved and what data would be most needed. We see him follow this means of attack in all his problems, by successive steps coming ever closer to the laws governing the structure of the universe.

Incidentally the investigations on proper motion led Kapteyn to his discovery of the two star streams, which, rightly, was recently selected by Eddington as one of the five greatest astronomical events of the last hundred years, a discovery which has revolutionized our ideas of the structure of the universe. In deriving the solar motion Kapteyn was struck by the divergency of the results of former investigators. In these researches it was usually assumed that the *motus peculiaris* of the stars was at random, a natural hypothesis, since with the enormous distances of the stars from one another it was difficult to see why there should be any relation between the individual motions of different stars. Yet stars moving together in pairs or even in large groups were known. As early as 1896, however, Kapteyn had noticed that the distribution of motion was not at random, but it was not until 1904 that he showed that there is a fundamental peculiarity in these motions and that they are not moving even approximately in a haphazard way. Instead of moving in all directions, as a random distribution would require, the stars tend to move in two preferential directions. That this tendency was so long overlooked by those who were working on a determination of the solar motion is principally due to the fact that they used the mean motions of all the stars in certain parts of the sky. Kapteyn, however, went to work in a different way, plotting the proper motions for limited regions of the sky. If for convenience' sake we assume all the stars in a certain region to be located in the same point *S* of the sphere, then with a random distribution of the *motus peculiaris* alone, we find about the same number and about the same total motion in each direction. A motion of the observer, such as we have as a result of the sun's motion through space, will add to each star a parallactic motion in the direction of the antapex. While this of course will disturb the symmetry of the motions around the point *S*, we still will have bilateral symmetry, the line of symmetry evidently passing through the point *S* and the apex. This evident condition of bilateral symmetry would probably furnish the best means of determining the apex, as these lines of symmetry for the different parts of the sky must all intersect in two points, the apex and the antapex. In applying this idea to the proper motions of about 2400 Bradley stars, divided into twenty-eight regions, Kapteyn derived the distribution of the proper motions corresponding to the center of the areas. The whole of the material was thus embodied in twenty-eight figures, like those in Figure 2, each of which shows at a glance the distribution of the proper motions for one particular region of the sky. This Figure 2 is the same as the one shown by Kapteyn at the Cape meeting of the British Association for the Advancement of Science in 1905. Not to overburden the plate, only ten of the twenty-eight regions are included. If the hypothesis of random distribution were true, all these figures should be symmetrical with respect to the line through the center of each field and the apex. It is clear that this is not the case: each figure shows two preferential deviations. Kapteyn showed that the assymetry as shown in the figure can be explained neither by an uncertainty in the precession, nor by systematic errors in the proper motions, nor by an erroneous position of the apex. As all the lines of favored directions for the two sets seem to converge, approximately, to two points, some 140° apart, the one 7° south of α Orionis, the other a few degrees south of η Sagittarii, Kapteyn came to the conclusion that we must have to do with two star streams, parallel to the lines joining our solar system and the two points mentioned.

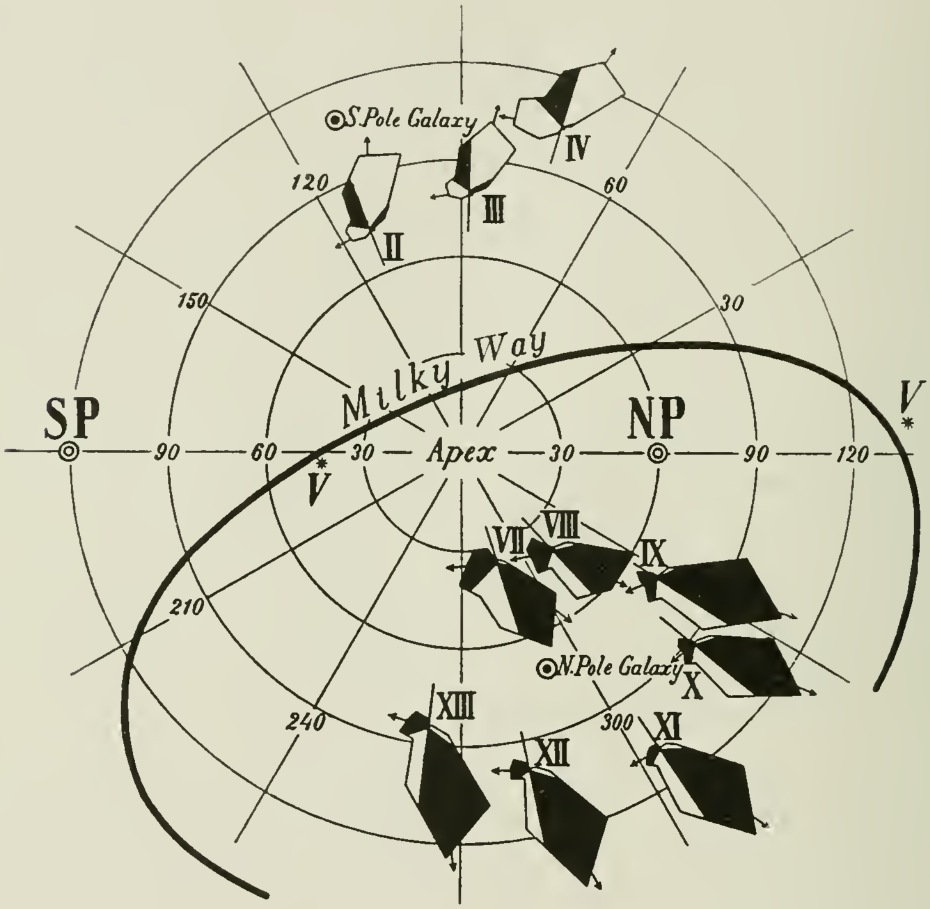

FIG. 2.—Distribution of proper motion in different parts of the sky which led to Kapteyn's discovery of the star-streams.

It is evident that such a discovery as that of the star streams would revolutionize the ideas of the structure of the universe. But at the same time it pointed out the necessity of collecting an increasing amount of data, in order to secure more reliable measures and especially data for the fainter stars. It was clear that the desire for such data could be satisfied only by the thorough co-operation of several institutions according to a well-organized plan. Kapteyn certainly was the right man to start such an organization. Through his work he had come into contact with most of the leading astronomers all over the world. His visits to America in 1904 and South Africa in 1905 gave splendid opportunity for discussing his plans with a number of eminent astronomers. In order to enable those who showed an interest in the matter to judge more thoroughly of the details, Kapteyn worked out a provisional plan; the result was a great deal of discussion and many useful suggestions. In 1906 Kapteyn published his famous *Plan of Selected Areas.* This pamphlet gives briefly but clearly, as only Kapteyn could give it, a program for the further attack on the structure of the universe. It includes not only the general plan but also in careful detail the methods of securing the necessary data: magnitude, proper motion, parallax, class of spectrum, and radial velocities for the stars in 252 well-selected regions. In the first and second reports (1911) Kapteyn was able to announce the formation of a committee to share the responsibility of advancing this plan. Its membership included Gill, Pickering, Hale, Küstner, Schwarzschild, Dyson, Adams, and Kapteyn, and it is sad to state that with Kapteyn one-half of its members have already gone forever. Yet the whole astronomical world is so convinced of the need of such a co-operative plan that it will undoubtedly be continued.

Next to the motions of the stars, their distribution in space interested Kapteyn most keenly. In this connection he derived the two well-known laws: the density-law and the luminosity-law, the former giving the density of stars per unit of volume and the change in the density with distance from the sun, and the latter, the percentage of stars equal in luminosity to the sun, and of those 10 times, 100 times, etc., as bright or as faint. Both are statistical laws; they do not give the distance and brightness of the individual stars, but how many stars there are at a certain distance and of a certain brightness. By successive steps these researches led Kapteyn to a conception of the distribution of the stars in space; they indicate that the stars are contained in a nearly ellipsoidal universe with an axial ratio of 5.1 with a decrease in the density away from the center and with the sun at a distance of about 650 parsecs from the center. In his last long paper on the subject, which with the modesty of the really great, was called "A First Attempt at a Theory of the Arrangement and Motion of the Sidereal System," Kapteyn had the satisfaction of giving a beautiful exposition of his life-work.

If a longer life had been granted to him, undoubtedly we would have seen him elaborate his beloved subject; yet as it is, it must have been a great satisfaction to him to reach this goal.

At about the time Kapteyn was spending his vacations in Leiden for the purpose of making his determinations of stellar parallaxes, he became acquainted and was soon on terms of warm friendship with the man who was then the leader in practical astronomy, David Gill, director of the observatory at the Cape of Good Hope. The story of the *Cape Photographic Durchmusterung* is well known to every astronomer. The difficulties met by Gill and Kapteyn would have disheartened most men. Kapteyn's famous letter of 1886 to Gill, offering his help in the following words, "However, I think my enthusiasm for the matter will be equal to (say) six or seven years of such work" has been widely quoted. It took about double that time, yet his enthusiasm did not fail, and the *Cape Photographic Durchmusterung* was completed with a thoroughness and accuracy which could be obtained only by two such masters. If we had no other work from his hand, Kapteyn's name would still take an honorable place in astronomical literature and would be mentioned with those of Argelander, Schönfeld, and Gould, names which every astronomer honors with gratitude. Yet in addition to this we have his discovery of the star streams, his plan of selected areas, his founding of the Groningen Astronomical Laboratory, now called "Astronomical Laboratory Kapteyn," which at the recent meeting of the International Astronomical Union, Baillaud duly called one of the three things which in his fifty years of astronomical life had revolutionized his science; and above all we have Kapteyn's investigations on the structure of the universe.

Truly Kapteyn belonged among the few really great men, whose death creates a vacancy which cannot be filled.

It seems superficial to enumerate here the many honors bestowed on him during his life. For completeness, however, we must mention them: Kapteyn received the honorary degree of D.Sc. from the Cape of Good Hope; of D.Sc. from Harvard University; of LL.D. from Edinburgh; he received the gold medal of the Royal Astronomical Society, the Watson and the Bruce medals and the prix de Pontécoulant; he was chevalier of the Legion of Honor of France, of the Netherlands Lion; he had the order "Pour le Mérite," and was commander in the Dutch order of Oranje-Nassau. Kapteyn was elected a member or associate of the following academies: Royal Astronomical Society, American Philosophical Society, National Academy of Sciences of Washington, Imperial Academy of St. Petersburg, Royal Academy of Dublin, Royal Academy of Edinburgh, British Association, Royal Swedish Academy, Royal Society of Sciences of Upsala, American Society, the Academy of Sciences in Paris, the Royal Society of London, the Academy of Sciences in Finland, and of the Royal Physical Association in Lund.

All through his life Kapteyn made friends; when he was young, among the older people, when older, among each new generation with which he came in contact. It was not difficult to become his friend; he saw always the best qualities in every person, the rest did not exist for him. There was always an atmosphere of happiness around him, in his daily life as well as in the scientific assemblies, where he was the center of gravity. His departure will be keenly felt in the astronomical world, but not there alone: many others will mourn the ending of this noble and happy life.

Especially in America, Kapteyn had numerous friends. From 1908 to 1914 he came to this country every summer to spend a few months at the Mount Wilson Observatory, of which institution he was Research Associate. Kapteyn and Mrs. Kapteyn thoroughly enjoyed their American trips, and these visits were no less appreciated by all with whom they came in contact.

Mrs. Kapteyn was born Catharina Elisabeth Kalshoven, and they were married in 1879. Their married life was singularly happy, and she has been devoted to the welfare of her husband and children, two daughters and a son: Jacoba Cornelia, wife of Professor W. Noordenbos, of Amsterdam; Henriette, wife of Professor E. Hertzsprung, of Leiden; and Gerrit Jacobus Kapteyn, who is a mining engineer.

How truly are his characteristics described by his friend Huizenga in the July number of the *Gids:* "When the right biographer for Kapteyn is found, the 'Life of Kapteyn' will be one of the most beautiful books that can be written."

Mount Wilson Observatory
Pasadena, California
August 1922

VISIBLE AND INFRA-RED RADIATION OF HYDROGEN

By FREDERICK SUMNER BRACKETT

ABSTRACT

Infra-red spectrum of hydrogen to $4.5\,\mu$.—The radiation from the central section of a long discharge tube, such as the one used by Wood to extend the Balmer series to the twentieth term, was analyzed by means of a rock-salt prism spectrometer, and readings were taken with an extremely sensitive vacuum thermo-junction. Besides some unidentified lines (Fig. 1), *five members of the Paschen series*, three of them new, were observed at the wave-lengths corresponding to the formula $\nu = N(1/3^2 - 1/m^2)$, where $m = 4, 5, 6, 7, 8$; also the *first two members of a new series* corresponding to $\nu = N(1/4^2 - 1/m^2)$, where $m = 5, 6$, were observed at 4.05 and $2.63\,\mu$. According to the Bohr theory these two series are due to electrons falling from outer orbits into the third orbit and fourth orbit respectively.

Variation of the relative intensity of Balmer and Paschen series lines of hydrogen with the current.—For the long discharge tube used, the first Paschen line was found to increase in intensity more rapidly than Hα, as the current was increased from one-ninth to one-half ampere through a section 7 mm in diameter.

INTRODUCTION

Two lines due to hydrogen were observed by Paschen[1] at the wave-lengths 18,751 A and 12,818 A. According to the Bohr theory these are due to an electron falling into the third from the fourth and fifth stable orbits in the hydrogen atom.

In view of the very low intensities of these spectral lines observed by Paschen, the detection of a series due to an electron falling into the fourth from orbits of greater quantum number has been considered improbable. In fact the lines mentioned above, forming the first two members of the Paschen series, were so faint that in order to observe them Paschen found it necessary to set the spectrograph in the correct position according to the wave-length predicted by Ritz in consequence of his combination principle.

By using a very long hydrogen tube Professor Wood[2] found it possible to abolish the secondary spectrum from the central position of the tube, and photograph the lines of the Balmer series down to the twentieth member. From the standpoint of the Bohr theory, this increase in the intensity of the higher members of the

---

[1] *Annalen der Physik*, **27**, 537, 1908.

[2] *Proceedings of the Royal Society*, **97**, 455, 1920; *Philosophical Magazine*, **42**, 729, 1921.

Balmer series might be attributed to increasing the probability of transitions between the orbits of higher quantum numbers. That being the case, we should expect an increase in the intensity of lines of other series which are also due to transitions of the electron between orbits of higher quantum numbers.

That this proved to be the case, and to a degree far greater than anticipated, is the essential feature underlying the success of the present investigation.

APPARATUS

The hydrogen tube of pyrex glass, used as the source, was about one meter in length. A central portion 25 cm long was viewed end on through an elbow in the tube. This portion of the tube was 7 mm in diameter (inside dimension). This small-size tubing was also used for a distance of about 10 cm on either side of the portion viewed. The remainder of the tube was made of larger diameter in order to reduce the resistance as much as possible. The electrodes were of thin aluminum foil rolled into hollow cylinders 8 cm long by 2 cm in diameter.

Hydrogen was introduced through a capillary sealed in near one electrode. The tube was exhausted by a Gaede mercury pump, communicating with the tube near the other electrode. During observation the pump was run continuously, the pressure depending upon the balance between the pump and the capillary intake.

Alternating high potential was supplied by a 6600-volt 5-kilowatt transformer operating on a 110-volt, 60-cycle primary circuit. The potential difference applied across the tube was varied by introducing resistance into the primary. The highest current maintained through the tube was a little more than half an ampere.

The dark space about the electrodes was about 3 mm in length, the positive column occupying almost the entire length of the tube. Striation appeared only in the portions of the tube of larger diameter, the central constricted portion being occupied by apparently continuous luminosity. The secondary spectrum was noticeable only near the electrodes. Throughout the greater part of the tube, the Balmer lines appeared with great brilliancy against a practically black background when the tube was viewed through a direct-vision prism.

The dispersion apparatus was a rock-salt monochromator of the Wadsworth type. Concave mirrors of 60-cm focal length were used for both collimator and telescope. The clear aperture of the prism was about 4 cm in diameter. Light only traversed the prism once, the simple form of apparatus being chosen in order to avoid scattered light. The slit widths were about 1 mm.

The detecting apparatus consisted of a single-junction vacuum thermo-couple, of the type constructed and previously used by Professor Pfund for measurement of stellar radiation. This was connected in series with a d'Arsonval galvonometer of sensibility about 5×10^{-10}.

A scale-distance of three meters was used, giving altogether an arrangement of extreme sensibility.

The light from the second slit was concentrated upon the blackened strip of the thermo-junction by means of a short-focus concave mirror. Both mirror and thermo-junction were protected by an asbestos housing. The leads to the galvanometer were carried through a metal conduit, grounded to prevent electrostatic effects. The galvanometer case, posts, etc., were heavily covered with cotton batting. The stability of this arrangement proved very satisfactory, deflections being reliable to 0.1 mm.

RESULTS

Part I. Distribution of intensity.—Figure 1 shows the distribution of intensity of radiation due to hydrogen in the infra-red between wave-lengths 0.5 μ and 4.5 μ.

In this diagram intensities have been plotted as the ordinates measured in millimeters of deflection of the galvanometer. It has been shown that intensities are proportional to galvanometer deflections for this thermo-couple for small deflections such as are obtained here. The abscissae are simply micrometer turns of the monochromator. The dispersion-curve based on five known points of the monochromator is shown superposed. Its ordinates are wave-lengths in microns indicated on the right. In order to read the wave-length of any point on the intensity-curve it is

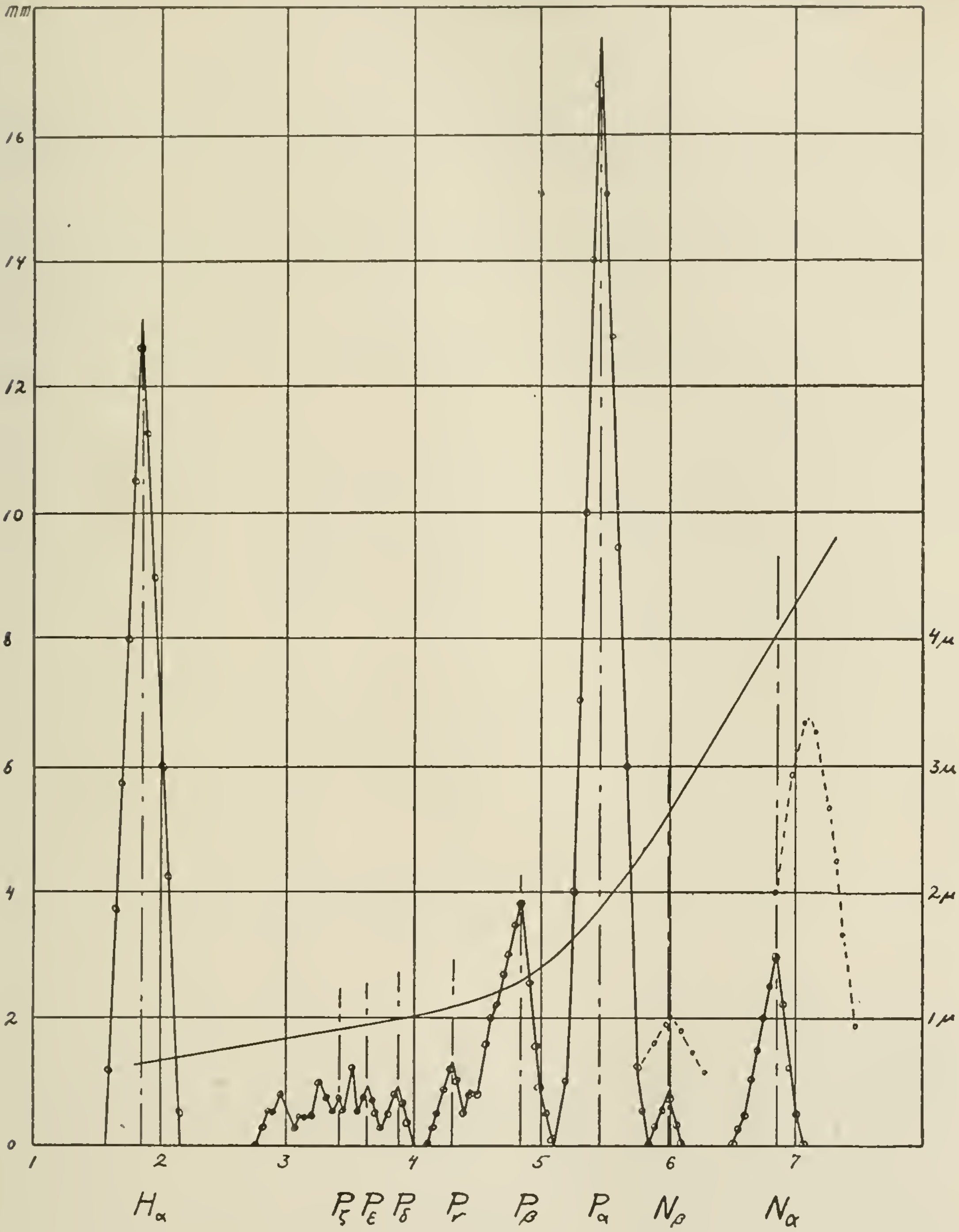

FIG. 1

merely necessary to find the point of the dispersion-curve having the same abscissa and read its ordinate at the right.

The maximum occurring at $4.05 \pm .03\ \mu$ and the second one at $2.63 \pm .02\ \mu$ are the first two members of a new series predicted from the Bohr theory by the formula

$$1/\lambda = 109{,}677.7\ (1/4^2 - 1/m^2);\ m = 5.6.$$

That is, they are attributed to an electron falling into the fourth from the fifth and sixth stable orbits of the hydrogen atom according to Bohr's model.

The largest maximum occurring at $1.88\ \mu$ is the first line of the Paschen series. It will be noted that it has an intensity greater than Hα (the last maximum on the left) in the ratio of about 4 to 3. The next four maxima are the next four members of the Paschen series.

The identity of the succeeding maxima is uncertain. Other lines are certainly present which do not belong to the Paschen series. The second maximum is probably Pζ.

These lines of the Paschen series are predicted from the Bohr theory by the formula

$$1/\lambda = 109{,}677.7\ (1/3^2 - 1/m^2);\ m = 4,\ 5,\ 6,\ 7,\ 8,\ (9),\ 10.$$

Line	Observed Wave-Length	Calculated Wave-Length
Pα	$(1.88\ \mu)$	$1.875\ \mu$
Pβ	$(1.28\ \mu)$	$1.282\ \mu$
Pν	$1.09 \pm .01\ \mu$	$1.094\ \mu$
Pδ	$1.01 \pm .01\ \mu$	$1.005\ \mu$
Pε	$0.95 \pm .01\ \mu$	$0.955\ \mu$

The dispersion-curve from which the wave-lengths have been determined is based upon five known points: $4.4\ \mu$ and $2.7\ \mu$ of the Bunsen flame (shown by dotted lines—scale reduced 100 times) and the three known hydrogen lines Pα, Pβ, and Hα. The values thus obtained should be quite satisfactory for purposes of identification, but of course have no great value from the standpoint of accurate wave-length measurement.

In view of the great intensity of the Paschen lines it is not surprising that many lines were readily observed which under ordinary conditions of excitation would not be detected. The readings shown on Figure 1 were taken in sequence, without setting upon known wave-lengths. The identity of the maxima was not realized until the dispersion-curve was later plotted.

Part II. Variation of intensity with current.—As it was noticed that the appearance of the tube changed decidedly with change in current, a set of intensity readings was taken on the first lines of three series—the Balmer, the Paschen, and the new series, when the current through the tube was varied from one-sixth of an ampere to over one-half an ampere. The curves obtained are shown in Figure 2.

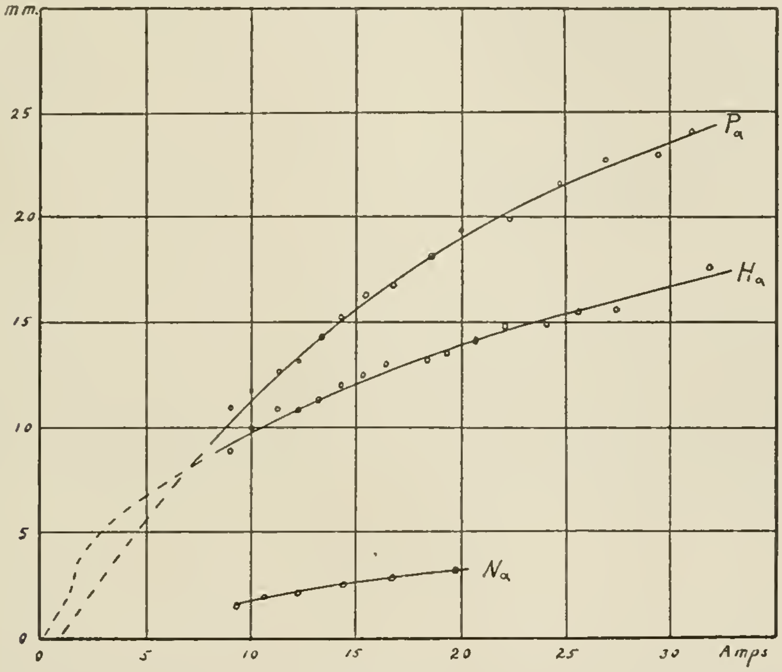

FIG. 2

The ordinates are intensities in millimeter deflections of the galvanometer, and the abscissae are current strengths through the primary of the transformer. The current through the tube is found with sufficient accuracy by dividing by 60. Readings on *a* of the new series are not shown for currents greater than 20 amperes primary, one-third ampere secondary, as radiation from the glass tube itself rendered them uncertain. No such effect was observed for lower currents or wave-lengths less than 3.5 μ. As a further precaution the tube was run only during the time of actual reading.

From this diagram, Figure 2, it will be noticed that although all three lines increase in intensity with increasing current, P*α* increases by far the most rapidly. Further readings (dotted portion of the curve) showed that at currents less than 7 amperes primary (about one-ninth ampere secondary) H*α* was more intense than P*α*.

At a current of 23 amperes through the primary we have the ratio of the intensity of P*α* to H*α* a little more than 4 to 3. According to the Bohr theory the energy lost by an electron undergoing transition from the fourth to the third orbit of the hydrogen atom will be

$$W_{P\alpha}=(1/3^2-1/4^2)\ Nh=7/144\ Nh,$$

while that lost in transition from the third to the second orbit would be

$$W_{H\alpha}=(1/2^2-1/3^2)\ Nh=20/144\ Nh,$$
$$W_{P\alpha}/W_{H\alpha}=7/20.$$

So the energy given out by an electron in transition from the fourth to the third orbit is only seven-twentieths of that given out by an electron falling from the third to the second orbit. Hence, in order to have P*α* more intense than H*α* in the ratio 4:3, there must be more atoms radiating P*α* than H*α* in the ratio of

$$\frac{4\times 20}{3\times 7}=\frac{80}{21}.$$

In view of the greater stability of the orbits of smaller quantum number and taking into account the principle of selection, we see that this is incompatible with what would be expected if radiation were resulting only from recombination of the atom and electron after ionization. We must therefore conclude that to a large extent radiation in such a long hydrogen tube arises from inelastic collision without ionization. In such a case we may have an abnormal concentration of energy in certain wave-lengths which would not be the case for recombination after ionization, inasmuch as the probability of an electron stopping in an orbit of high quantum number is much greater, where it is simply ejected to that orbit or one of slightly greater quantum number, than in the case where it is returning from ∞. This no doubt explains to a large extent the peculiar characteristics of the "long hydrogen tube," both in regard to the unusual intensity of the infra-red lines and also the higher members of the Balmer series.

All atoms which contribute to the radiation of the first Paschen line are left necessarily with the electron in the third orbit, whence it must proceed either to the second or the first orbit unless it is ejected to some orbit of greater quantum number by inelastic collision. Since considerably less than one-fourth of these atoms contribute to the radiation of $H\alpha$, we must conclude either that the second member of the Lyman series is radiated with great intensity, or that there must be multiple collisions to a large extent in such a tube.

It should be noticed that the higher members of the Paschen series occur in a region readily studied by photographic methods, plates hypersensitized by means of dicyanin being sensitive to $1.0\ \mu$. This work will be carried out in the near future.

CONCLUSION

1. The first two lines of a new series have been observed at wave-lengths $4.05 \pm .03\ \mu$ and $2.63 \pm .02\ \mu$, due, according to Bohr's theory, to an electron falling into the fourth from the fifth and sixth rings of the hydrogen atom.
2. Three and probably four additional members of the Paschen series have been observed.
3. The first Paschen line is more intense than $H\alpha$ in the ratio 4:3 under the conditions prevailing in the long tube for great current densities.

In this work I have been much indebted to Dr. Pfund, who proposed the problem and constructed the thermo-junction, the remarkable sensibility of which rendered the work possible.

It gives me great pleasure to express my appreciation to him, to Professor Wood for his interest and many suggestions, and to Dr. Ames for his generous support.

JOHNS HOPKINS UNIVERSITY
June 1922

A GENERAL STUDY OF DIFFUSE GALACTIC NEBULAE[1]

BY EDWIN HUBBLE

ABSTRACT

Suggested classification of nebulae.—Since the time of the Herschels, photography and spectroscopy have revolutionized the study of nebulae. The classification here suggested is based upon the fundamental differences between galactic and non-galactic nebulae. Galactic nebulae are subdivided into planetary and diffuse (luminous and dark), and non-galactic into spiral, elongated (spindle and ovate), globular, and irregular. The characteristics of each are discussed. The belief expressed by Curtis that all non-galactic nebulae are spirals is not justified by the facts.

Distribution of diffuse nebulae.—As shown in Figure 1 these nebulae are concentrated along two belts. One is the Milky Way and the other is approximately the belt of bright helium stars which defines the local cluster. Very few seem to occur in the vast regions between the Milky Way clouds and the local cluster.

Spectral characteristics of galactic nebulae and of associated stars.—(1) *Diffuse nebulae.* Some preliminary results, obtained with slitless spectrographs of various dispersions, are presented for sixty-two nebulae outside the Magellanic clouds, including the twenty-one whose spectra were previously known. They fall into two groups (Tables I and II): Group 1 contains thirty-three, giving predominantly continuous or absorption spectra; and Group 2, twenty-nine, giving predominantly emission spectra. The members of the "continuous" group have generally a smooth, cloudy structure and most of them are found in our local cluster, while those of the emission group are more likely to be filamentous and wispy and to lie in the Milky Way clouds. In the emission spectra the N_1 and N_2 lines are much weaker in comparison with $H\beta$ than in spectra of normal planetaries. (2) *Stars associated with diffuse nebulae* have been studied with slit spectrographs attached to the Mt. Wilson reflectors (Tables III and IV). Stars involved in nebulae having continuous spectra are nearly all of type B1 or later; but stars involved in emission nebulae nearly always have spectra earlier than B1, rarely showing any bright lines. (3) *Stars associated with planetary nebulae* show a corresponding relation. In fact, there is a steady progression in type from the Wolf-Rayet stars involved in small planetaries, through those involved in large planetaries, to the stars of types Oe5–B0 associated with extended diffuse nebulae of Group 1 and the stars of type B1 and later associated with diffuse nebulae of Group 2. A detailed discussion shows that, with the exception of the Cygnus loop and perhaps three other difficult or doubtful cases, each galactic nebula has associated with it one or more stars of a type conformable to its own spectral type. (4) This definite relation between the spectra of the nebulae and of the associated stars suggests that the *source of luminosity of the nebulae* is the radiation from those stars. According to this view, the nebulosity has no intrinsic luminosity but either is excited to emission by light from a star of earlier type or merely reflects light from a star of later type. From a consideration of the nebulosity around Rigel it appears that this luminosity may be excited at a distance of twenty light-years.

Nature of diffuse nebulosity.—From the foregoing results the nebulosity seems to consist of clouds of matter, molecules, dust, or perhaps larger particles, not hot enough to be self-luminous, but visible because of light excited by or reflected from involved or neighboring stars. Nebulae with continuous spectra seem usually more opaque than those giving emission spectra. Whether the association of such stars and nebulae is permanent or temporary is not yet known, but may be determined by studies of the radial velocities.

---

[1] *Contributions from the Mount Wilson Observatory*, No. 241.

Uncatalogued nebulae.—Five are listed: Table I, Nos. 4, 5, 15, and 21; Table II, No. 15. The third is a bright cometary nebula with a thirteenth-magnitude star at the apex; $\alpha = 6^h 3^m.1$; $\delta = +18°42'$ (1920).

Radial velocities of five stars associated with galactic nebulae.—Results are given for stars associated with N.G.C. 1514, 6514, 6523, and 7635. Of these B.D. $-23°13804$ and Boss 4560 are *binaries*.

CLASSIFICATION OF NEBULAE

The classification of nebulae from visual observations was of necessity based upon resolvability, brightness, size, and form. Thus Sir William Herschel distinguished between clusters and nebulae and devised, for the latter, three classes for brightness, a fourth for definite form, and a fifth for extra large size. It is true that he mentioned in his discussions the terms "milky nebulosity," "nebulous stars," and "stellar nebulae"; that his penetrating genius recognized the existence of nebulous fluid in the nebulous stars and probably in such milky nebulae as the great one in Orion, in contrast to the stellar nebulae or burred stars which he considered as distant clusters; that, in short, he did realize a distinction between planetaries and diffuse nebulae on the one hand and on the other the non-galactic nebulae; but throughout his researches he adhered strictly in catalogues and descriptions to the five classes: bright, faint, very faint, small with definite borders, and exceedingly large. This formal classification was elaborated by the simple system of abbreviation, still in general use, by which each object was described in considerable detail.

Sir John Herschel developed his father's system. His generation had discarded Sir William's idea of a nebulous fluid, as a direct result of the resolution of nebula after nebula by Lord Rosse's great mirrors. Even the Orion nebula, last stronghold of the nebulous fluid advocates, had been announced as resolved by the Parsonstown observers, and the central star in N.G.C. 1514, the great brightness of which as compared to the surrounding nebulosity had led Sir William to his belief in a nebulous fluid, was being explained not as a single star but as an exceptionally compact cluster of stars.

This state of affairs led Sir John Herschel[1] to avoid the discussion of physical distinctions among nebulae and to elaborate his father's formal classification in an ingenious manner. All nebulous objects were divided into regular and irregular, and the latter alone into nebulae and clusters, according to the difficulty of resolving them.

---

[1] *Cape Results* (1847), p. 137.

Regular nebulous objects were classified according to magnitude, brightness, roundness, condensation, and resolvability, with five degrees of each expressed by numbers. Thus a bright globular cluster would be 22322, meaning large, bright, round, condensed, and resolved. A small spindle might be classed as 43435, small, faint, elongated, considerably brighter center, irresolvable.

Irregular nebulae were classed as subregular, compact, branching, convoluted, cellular, fissured, and cometic, although Sir John remarks that these objects are so diverse that each one might well represent a separate class. Each subdivision was arranged in five orders of magnitude and brightness.

Here again is a tendency to distinguish between galactic and non-galactic objects, for the regular nebulae, although including the planetaries, for the most part make up the non-galactic nebulae, while the irregular are in general galactic nebulae.

This system of classification did not win a general acceptance because of its very elaboration and also because of the subsequent introduction of spectroscopy and photography. The new methods of research revolutionized the study of nebulae and the basis of nebular classification. Sir William Herschel's ideas were restored in part at least, for the existence of nebulous fluid in the form of gas or dust clouds in the planetaries and diffuse nebulae became a recognized fact. The old question of resolvability is now restricted to spirals and the kindred small non-galactic objects. There has slowly emerged a general recognition of the fundamental difference, hinted at by the Herschels, between planetaries and diffuse galactic nebulosities and the objects, spirals and others, that swarm in regions of high galactic latitude.

Curtis has expressed this new point of view by dividing nebulae into three classes—planetaries, diffuse, and spirals.[1] In explanation of the term "spiral" he states: "It is my belief that all the many thousands of nebulae not definitely to be classed as diffuse or planetaries are true spirals and that the very minute spirals appear as textureless discs or ovals solely because of their small (apparent) size."[1]

---

[1] *Adolfo Stahl Lectures* (1919), p. 98.

His argument for the truly spiral nature of all these non-galactic nebulae is this: "Were the great Nebula in Andromeda situated five hundred times as far away as at present, it would appear as a structureless oval 0ʹ.2 long, with very bright center, and not to be distinguished from the thousands of very small round or oval nebulae found wherever spirals are found. There is an unbroken progression from such minute objects up to the great Nebula in Andromeda itself. I see no reason to believe that these very small nebulae are of a different type from their larger neighbors."[2]

This argument is a daring extrapolation and is not justified by our present knowledge of nebular forms. Only a few hundred of the thousands of nebulae photographed show distinct traces of spiral arms. Objects of the most diverse forms, were they removed to the proper distances, would appear as faint "textureless discs or ovals" on the photographic plate. Curtis' extrapolation is not warranted unless all the larger objects examined show positive evidence in favor of, or at least no evidence against, a truly spiral structure.

Now the well-known irregular nebulae, N.G.C. 2366, 4214, and 4449, are unquestionably non-galactic and of considerable size, but by no stretch of the imagination, nor by any orientation, can these objects be termed true spirals. Yet many true spirals are recognized, which have diameters a tenth and less the diameters of these nebulae. It is possible of course to consider the irregular objects as rare exceptions to the general run of non-galactic nebulae.

Stronger evidence of non-spiral forms is found in a class of objects which may be termed globular nebulae. Some of the brighter examples of this type are M 49, 60, 84, 86, and 87, which average about two minutes of arc in diameter.[3] Repeated attempts with the 100-inch reflector under excellent observing conditions, using exposure times from one minute to nine hours, have failed to show any trace or suggestion of spiral structure in the objects mentioned. M 32, the smaller and brighter companion of the

---

[1] *Publications of the Lick Observatory*, 13, 12, 1918. [2] *Loc. cit.*

[3] M 60 and M 87 are shown in Plate III.

Andromeda nebula, is a slightly elongated variant of the globular type which also fails to show spiral characteristics under the resolving power of the 100-inch reflector. A long list could be compiled of non-galactic nebulae with diameters over a minute of arc which show no indication of spiral structure under the highest resolving power available. The number is comparable to that of the known spirals. A progression in size of these globular objects can readily be formed running from diameters of over two minutes of arc down to the limits of photographic plates. Toward the lower end of the sequence they merge into the spirals so that the two types become completely indistinguishable (Plate III).

These globular nebulae may be considered as belonging to the same family as the spirals—distribution, velocities, spectra, non-stellar nuclei, and symmetry of form suggest as much—but there is no shadow of evidence for calling them spirals in fact.

Curtis' classification, however, is easily the most significant that has been proposed up to date, and with some modifications would be acceptable as a system the general use of which should be urged. There appears to be a fundamental distinction between galactic and non-galactic nebulae. This does not mean that the latter class must be considered as "outside" our galaxy, but that its members tend to avoid the galactic plane and to concentrate in high galactic latitudes. The distinction seems to be fundamental in a physical sense as well as in distribution. Galactic nebulae are in general associated with stars; even the dark nebulosities are detected by their obscuration of stars. Non-galactic nebulae show no effect on stellar distribution in their neighborhood and have no stars definitely associated with them save those occasional novae which have flared up in a few spirals. The distinction can also be traced in form, texture, velocity, and spectrum, with little if any overlap. In fact, one can say that in no case, except possibly the Magellanic clouds and the similar object N.G.C. 6822, is there any question, from its photographic appearance alone, as to the class to which an individual nebula belongs.

Once this major division is recognized, the subclasses of galactic nebulae follow directly. They are *planetaries* and *diffuse* nebulae. Diffuse nebulae can be divided into luminous and non-luminous

PLATE III

North

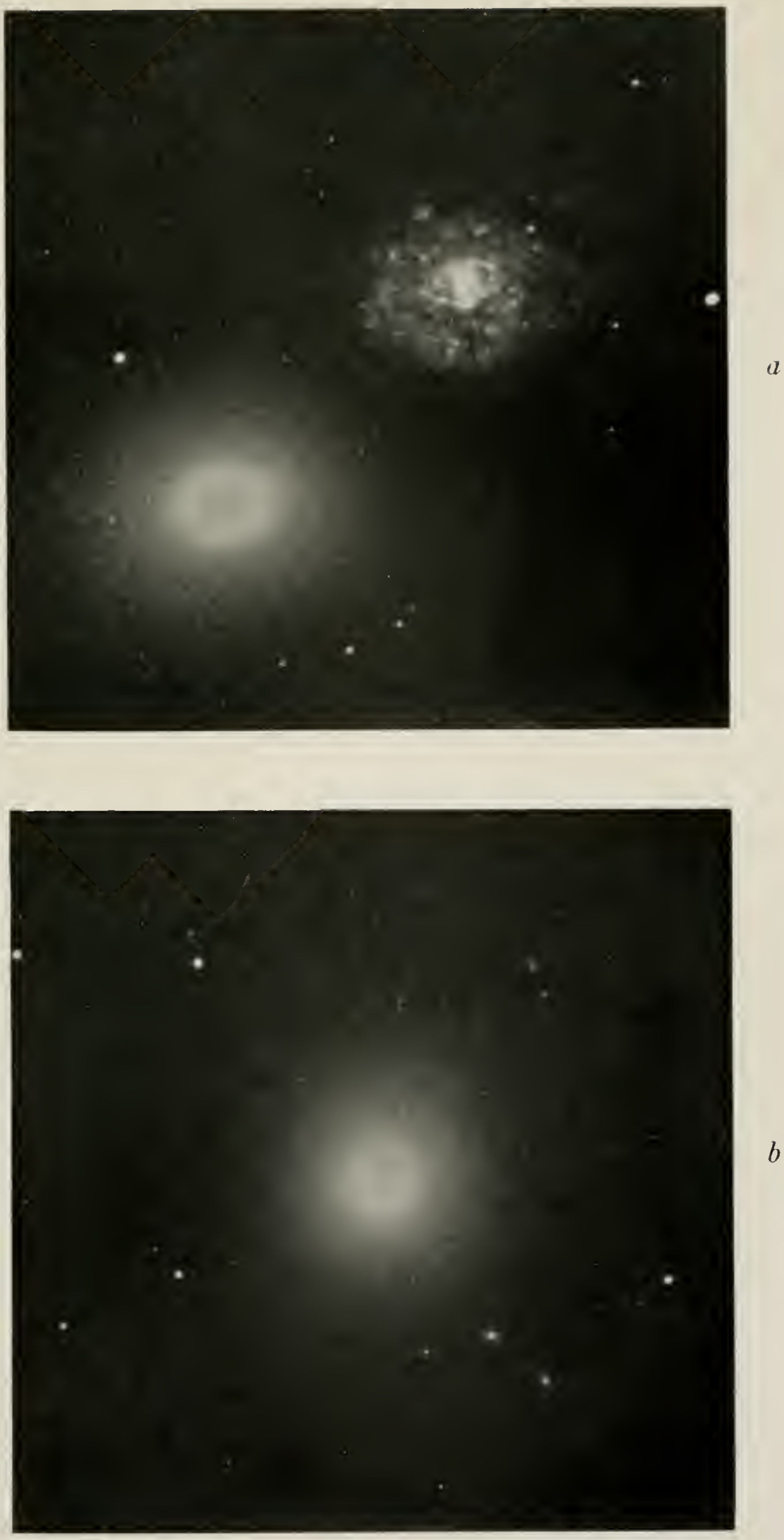

GLOBULAR NEBULAE

a. M 60, N.G.C. 4649 Globular 1 mm = 4″.2
N.G.C. 4647 Spiral
b. M 87, N.G.C. 4486 1 mm = 5″.2

Photographed with the 100-inch Hooker reflector

or dark nebulae. More detailed classification of these groups will depend upon form, spectrum, and relation to stars, and can well be left to special investigators.

Subdivision of non-galactic nebulae is a much more difficult problem. At present and for many years to come their classification must rest solely upon the simple inspection of photographic images, and will be confused by the use of telescopes of widely differing scales and resolving powers. Whatever selection of types is made, longer exposures and higher resolving powers will surely cause a reclassification of many individual nebulae, although the true spiral once recognized as such will maintain its class with all more powerful instruments, and irregular and globular types are not usually subject to change. Only a very low percentage of nebulae, and these the smaller ones, which appear globular with 24-inch apertures, resolve themselves into spirals or reveal ansae with a 100-inch aperture.

Globular nebulae have already been mentioned. The few known *irregular* nebulae are chaotic forms with non-stellar nuclei and coarse granular texture, and with spectra and radial velocities similar to those of the spirals. Examples are N.G.C. 2366, 4214, and 4449. They are easily distinguished from diffuse nebulae by their non-stellar nuclei and their texture, although analogies have sometimes been drawn between these irregular nebulae and the Magellanic clouds.

The gap between *spirals* and *globular* types is filled with the *elongated* nebulae. There are two distinct varieties of these, the one probably spirals on edge and the other akin to globular nebulae. They may be termed, respectively, spindles and ovate. The former, with sharp nuclei and tapering ansae, are familiar to all observers. The latter deserve some further comment. Examples of the ovate type are M 32 and M 59. They are similar to the globular nebulae in all save their elongated forms. Both are to be described as large and bright, yet even the 100-inch under the finest observing conditions with both long and short exposures reveals no trace or suggestion of spirality in either nebula. Whatever their past or future, their present state is not that of true spirals within the limits set by our observational data.

Spindles and ovate types merge into one another with decreasing linear size of the images on the plates, and the resulting confusion detracts from the value of the distinction for small objects or small-scale photographs. As a matter of fact each system of classification that can be devised for non-galactic nebulae will favor a certain range of resolving powers. The present one favors the largest reflectors. It is a compromise between Curtis' generalization and Wolf's specialization.[1]

Some light on the validity of this classification, and a scale for standardizing results from instruments of various dimensions, for statistical purposes at least, can be derived from photographs of rich fields of nebulae made with telescopes of different apertures and equivalent focal ratios, and with one telescope and differing exposure times. Classification of the nebulae for each exposure will indicate the percentage of objects of each type which are changed from one type to another with increasing exposure and resolving power. Preliminary investigations along this line have already been made, apertures from 10 to 100 inches being used.

The classification proposed for general use, together with typical objects for each class, is as follows:

	Examples
I. Galactic nebulae	
1. Planetary	N.G.C. 7662
2. Diffuse	
a) Luminous	N.G.C. 1976
b) Dark	Barnard 86
II. Non-galactic nebulae	
1. Spiral	M 101 (N.G.C. 5457, 8)
2. Elongated	
a) Spindle	HV 24 (N.G.C. 4565)
b) Ovate	M 59 (N.G.C. 4621)
3. Globular	M 87 (N.G.C. 4486)
4. Irregular	N.G.C. 2366

DISTRIBUTION OF GALACTIC NEBULAE

The distribution, spectra, and radial velocities of planetaries are now well known, due largely to the investigations carried out at the Lick Observatory. Large planetaries are distributed more or less uniformly over the sky, while the small ones concentrate sharply along the Milky Way and are especially numerous between eighteen and twenty hours of right ascension. It is reasonable to suppose that the apparent diameters and nuclear magnitudes are rough indications of distance and that, when real distributions are determined, the vertical deviations from the galactic plane will prove to be relatively small. Radial velocities of ninety-six planetaries corrected for the solar motion average 30 km or about five times the average for B stars. Their spectra are almost purely emission, the continuous spectrum being entirely negligible except for the region on the more refrangible side of the head of the hydrogen series. The ratio of intensities between the N_1, N_2, and $H\beta$ images is 10:3:1, with few exceptions.

---

[1] Wolf's classification of non-galactic nebulae is to be found in *Publicationen des Astrophysicalischen Instituts Königstuhl-Heidelberg*, Band III, No. 5, 1909.

Much less is known concerning the diffuse galactic nebulae. Their distribution in the sky is certainly not a simple concentration along the galactic plane. Figure 1 represents the distribution in galactic co-ordinates of all objects of this class, excepting those between galactic longitudes 200° and 300° which are too far south to be observed from Mount Wilson. Two distinct belts are defined —the Milky Way, and a belt inclined at about 20° to the Milky Way. This latter belt has approximately the same nodal points as those of the bright helium stars, although the inclination is considerably greater than that usually given for the stars. The data are not sufficient to determine a value for the dip.

Such a distribution emphasizes the relation between diffuse nebulosity and early type stars. The high inclination of the nebular belt suggests that these objects are comparable in distance with the brightest of the B stars and for the most part lie on the inner side of the ring. There is some evidence that the diffuse nebulae are concentrated in the local cluster and in the Milky Way clouds, and that vast regions between the two are practically devoid of nebulae. If this were not the case, we should expect to find the gaps between the two belts more generally filled, and also a greater dispersion among the galactic nebulae. Perhaps the strongest point in favor of such a distribution is the absence of nebulae with large positive galactic latitudes between longitudes 80° and 200°. In all these 120 degrees of longitude only one diffuse nebula has a latitude greater than +2°. This object is B.D. +23°1301 at +3°5, announced by Barnard as a nebulous star. The spectrum is B9, photo-visual magnitude 7.0, and hence it is probably relatively near. The greatest deviation from either plane is in the isolated group of dark and luminous nebulosity in Corona Australis, which includes the variable nebula, N.G.C. 6729. The distance of the group is of the order of one hundred parsecs,[1] so that it lies well within the local cluster, and its anomalous position in the sky must be due to perspective. The vertical distance from the galactic plane is about thirty parsecs.

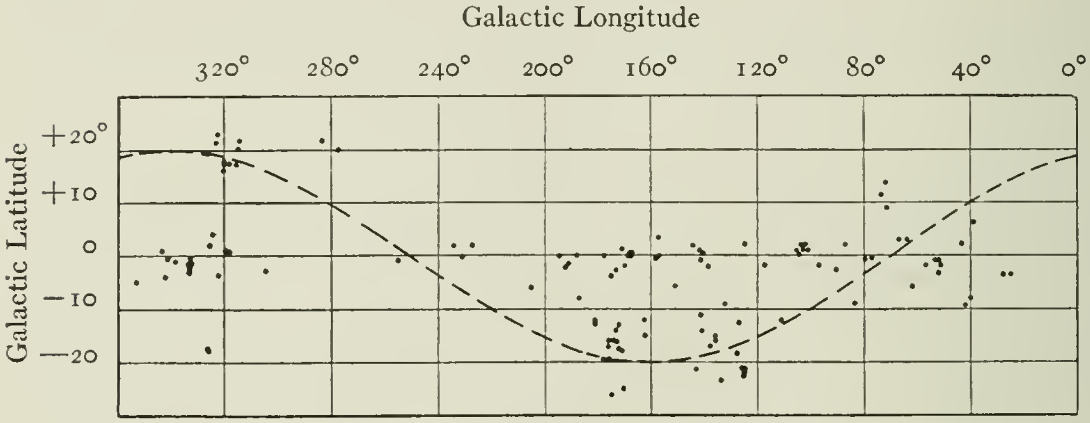

Fig. 1.—Distribution of diffuse nebulae in galactic co-ordinates

There is a decided tendency for diffuse nebulae to cluster. This is more pronounced among nebulae with predominantly continuous spectra than among those with emission spectra, and usually is accompanied by extensive dark nebulosity. Dark nebulae tend to follow the double distribution, although the scattering is greater and the gaps between the two belts are more generally filled than is the case with the luminous diffuse nebulae.

SPECTRA OF DIFFUSE NEBULOSITIES

Published results list emission spectra for thirteen diffuse nebulae as against continuous or absorption spectra for eight.[2]

---

[1] A distance of three hundred light-years is derived from the luminosity law applied to nebulous stars in the obscured areas, and from movements of luminosity in the nebula N.G.C. 6729 on the assumption that such movements have the velocity of light.

[2] This leaves out of consideration the nebulae in the Magellanic clouds.

This has somehow led to a presumption that an emission spectrum is a general characteristic of diffuse galactic nebulae.

Slit spectrograms of such faint objects will accumulate so slowly that it seems worth while to publish now some results from a preliminary survey with slitless spectrographs. Such instruments readily distinguish spectra which are predominantly emission from those predominantly continuous, although faint emission images on a strong continuous background cannot always be detected. Absorption lines are usually concealed in slitless spectra and the term "absorption spectrum" can be applied in general only to slit spectra. Several such spectra have been reported by Slipher and Pease, so that pure absorption spectra of diffuse nebulosities are as well established in fact as pure emission spectra of others. Indeed, it may be considered as better established, for it is more probable that all bright-line nebular spectra have some faint continuous background than that faint bright lines have been overlooked in absorption spectra of nebulae. The term "emission" will be used in discussing slitless spectra as an equivalent to "bright line" in slit spectra; the term "continuous," where neither bright nor dark lines can be seen; the term "absorption," where dark lines can actually be detected in either slit or slitless spectra. An unbroken series can readily be arranged from the slitless spectrograms, running from emission with no perceptible continuous spectrum to continuous with no emission. There is probably an uncertain number of objects listed as "continuous" in which faint emission images are present and not recognized, but in every case of previously known emission on a continuous background, the slitless spectra show unmistakable irregularities in distribution of density. In view of the uncertainty, however, the method adopted is to list the nebulae as giving predominantly continuous or predominantly emission spectra, and to call attention in notes to combinations of characteristics.

The various instruments employed in the survey are listed below and each is designated by a letter, by which it will be referred to in the course of this paper. It will be noticed that the range in the relation of scale to dispersion is sufficiently wide to accommodate itself to nebulae of all sizes. Seed 30 plates were used throughout with exposures ranging from two to nineteen hours.

A. Focal-plane spectrograph with slit removed, attached to 60-inch reflector, primary focus. Collimator and camera lenses about 6-inch focus. Dispersion, Hβ to Hϵ = 5.0 mm.
B. 15° objective prism on 10-inch Cooke astrographic lens, focus 45 inches. Hβ to Hϵ = 5.3 mm.
C. 6° objective prism on 10-inch Cooke lens. Hβ to Hϵ = 1.8 mm.
D. 39° objective prism on 4-inch lens, 7-inch focus, Hβ to Hϵ = 4.1 mm.
E. 25° objective prism on 4-inch lens, 7-inch focus, Hβ to Hϵ = 2.5 mm.
F. 25° objective prism on kinematograph lens F/1.8, 3-inch focus. Hβ to Hϵ = 1.0 mm.

Results from the survey are collected in two tables, one comprising nebulae which give predominantly continuous, and the other, those which give predominantly emission spectra. Nebulae whose spectra were previously known are included for the sake of completeness and are starred to indicate this fact. One nebula has thus been included which is too far south to be observed from Mount Wilson—N.G.C. 3372, the nebulosity around η Carinae. The two lists should contain all diffuse galactic nebulae for which spectrographic data are available, excepting those in the Magellanic clouds. The tables give in the first column a list number; in the second, the catalogue designation of the nebula; the third and fourth columns give galactic longitudes and latitudes; the fifth column, a rough indication of size on a scale of 1 to 5, the numbers increasing with the size; the sixth column, the instruments employed; the seventh, remarks and references.

Table I contains thirty-three objects having continuous spectra, eight of which were previously known as such. Of the latter, four give pure absorption spectra—the Pleiades, M 78, ρ Ophiuchi, and N.G.C. 7023.[1] N.G.C. 1977 and the two variable nebulae, N.G.C. 2261 and 6729, give faint bright-line images as well, and one, N.G.C. 2245, is known only through an objective prism spectrogram.

---

[1] Slipher reports that in the spectrum of N.G.C. 7023, "Bright Hβ seems to be present but not so obviously emissive as in the star" (*Publications of the Astronomical Society of the Pacific*, 30, 63, 1918). The involved star has bright reversed hydrogen lines. Hβ does not show on a spectrogram of the nebula made by Pease.

TABLE I

Diffuse Nebulae with Continuous Spectra

No.	Object	Galactic		Size	Instrument	Remarks
		Longitude	Latitude			
1.....	N.G.C. 1333	126°	−21°0	2	C	
2.....	I.C. 348	128	−17.5	2	A, B, C,	Also listed as I.C. 1985. B.D. +31°643, involved
3.....	Pleiades*	134	−22.0	5	C	See Slipher, *Lowell Bull.*, No. 55, 1912
4.....	....	136	−15.5	2	B, C	Uncatalogued nebula, $\alpha=4^h14^m$; $\delta=+28^\circ2'$ (1920)
5.....	....	141	−17.0	1	B, C	Uncatalogued nebula, $\alpha=4^h22^m.1$; $\delta=+24^\circ32'$ (1920)
6.....	N.G.C. 1579	132	− 9.0	2	C	
7.....	I.C. 2087	141	−14.0	1	B, C	
8.....	N.G.C. 1788	171	−24.5	2	A, B, C,	
9.....	I.C. 2118	175	−26.0	5	B, D, E	Great nebulosity north preceding Rigel
10.....	N.G.C. 1977*	175	−19.0	3	B, C	Dark helium and bright hydrogen. See Slipher, *A.S.P.*, **31**, 22, 1919
11.....	2023	173	−16.5	1	A, B, C	Nebulosity around B.D. −2°1345
12.....	2068*	173	−14.0	2	B, D, E	See Slipher, *A.P.S.* **31**, 212, 1919
13.....	....	172	−13.0	5	B, D, E	$\alpha=5^h45^m.5$; $\delta=+1^\circ$ (1920). Brightest portion of great "spiral" in Orion
14.....	2183	181	−11.0	1	A, B	
15.....	....	158	− 0.5	1	A, B	$\alpha=6^h3^m.1$; $\delta=+18^\circ42'$ (1920). Comet nebula uncatalogued
16.....	I.C. 446	168	+ 0.5	1	B, C	Also listed as I.C. 2167
17.....	447	168	0.0	2	B, C	Also listed as I.C. 2169
18.....	N.G.C. 2245*	169	+ 0.5	1	B, C	See *Ap.J.*, **44**, 196, 1916
19.....	2247	169	− 1.0	1	B	
20.....	2261*	171	+ 1.5	1	A, B, C	Faint emission on strong continuous spectrum. See *Lowell Bull.*, No. 81
21.....	....	193	− 1.5	1	B, C	Uncatalogued nebula about B.D. −12°1771
22.....	....	312	+17.0	3	B, F	Nebulosity about π Scorpii
23.....	I.C. 4592	322	+23.0	5	B, C, F	Nebulosity about ν Scorpii
24.....	4601	323	+21.0	2	B, C	Nebulosity about B.D. −19°4359 and B.D. −19°4361
25.....	4603	319	+17.0	4	B, C, F	Nebulosity about B.D. −24°12684
26.....	4604*	320	+18.0	4	B, C, F	Nebulosity about ρ Ophiuchi. See *Lowell Bull.*, No. 75, 1916
27.....	4605	320	+16.0	2	B, C, F	Nebulosity about 22 Scorpii
28.....	N.G.C. 6726, 7	327	−17.5	2	B, C	Nebulosity about B.D. −37°13023 and B.D. −37°13024
29.....	N.G.C. 6729*	327	−17.5	1	B, C	Faint emission on strong continuous spectrum. See *Lowell Bull.*, No. 81
30	6914	52	− 4.5	1	B, C	
31.....	7023*	72	+14.0	1	B, C	Slipher, *A.S.P.*, **30**, 63, 1918; Pease, *A.S.P.*, **27**, 240, 1915
32.....	7129	73	+ 9.0	1	A, B, C	
33.....	I.C. 5146	62	− 6.5	2	C	

NOTES

4. Photograph by Barnard, *Astrophysical Journal*, **25**, 219, 1907. This may be I.C. 359 whose position is given as 5^m preceding and 30′ south. No nebulosity is seen in that position.

5. In one of the dark lanes in Taurus.

7. In one of the dark lanes in Taurus. See Barnard, *Astrophysical Journal*, **25**, 218, 1906.

9. Faint extensions of this nebula stretch south and west to end in a faint obscuring cloud more than 35° from the galactic plane.

11. Wolf, *Astronomische Nachrichten*, **180**, 152, 1909, describes this as gaseous emission, but his observations undoubtedly apply to I.C. 434. See note on the latter nebula following Table II.

13. This is the brightest portion of the great loop encircling the belt and sword of Orion.

15. A bright uncatalogued nebula similar to N.G.C. 2245. A thirteenth-magnitude star is at the apex of the cometary form. It is surprising to find that so bright an object has been overlooked by observers.

21. Attention was called to this uncatalogued object in *Union Observatory Circular*, No. 7, 1911.

22. See Barnard's photograph in *Astrophysical Journal*, **23**, 144, 1906.

These nebulae show a decided tendency toward clustering, and can be divided as follows:

	Number
Taurus group	1– 7
Orion	8–14
Monoceros	15–21
Scorpius	22–27
Corona Australis	28–29
Cygnus	30–33

Their distribution in the sky, although affected by this grouping, is clearly not a simple concentration along the galactic plane. In Figure 2 they are plotted in galactic co-ordinates, and it is at

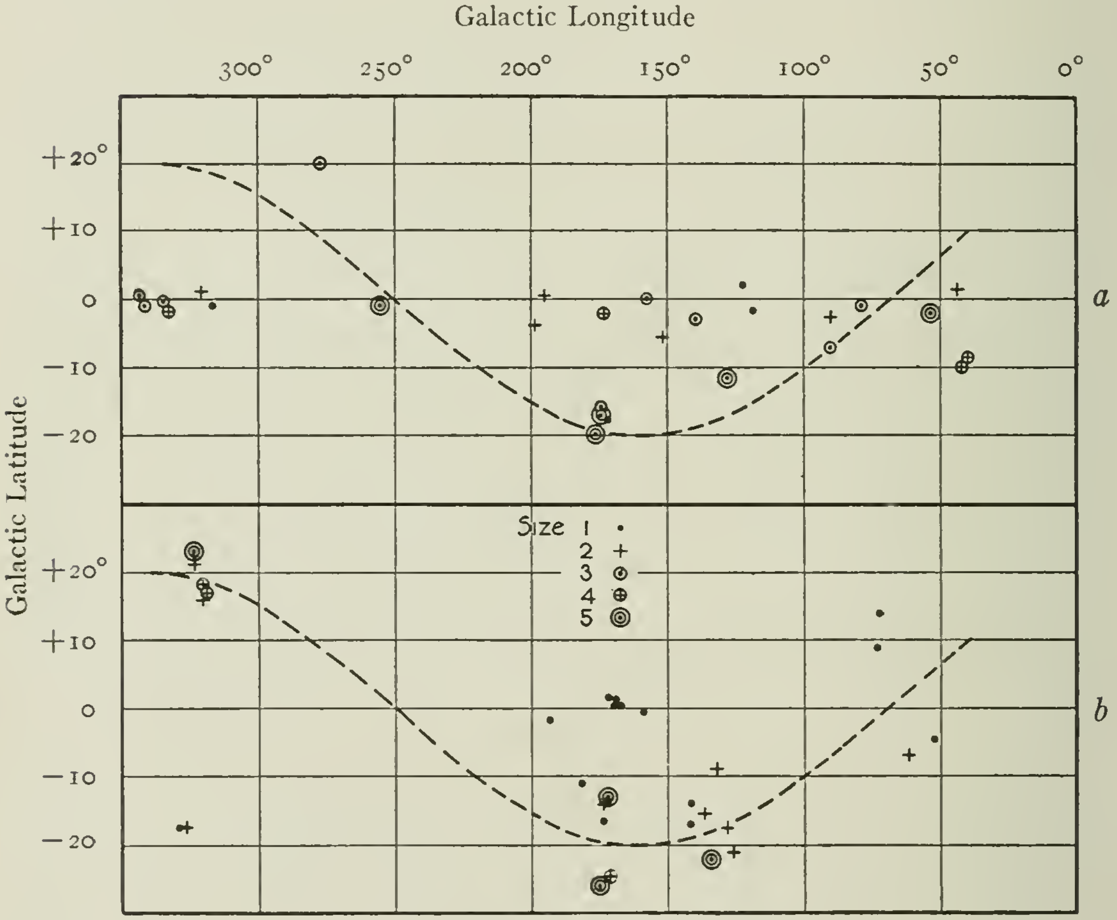

FIG. 2.—Distribution of diffuse nebulae

a. Nebulae with emission spectra

b. Nebulae with continuous spectra

once evident that most of them favor the tilted plane of bright helium stars. The Monoceros group and the isolated pair in

Corona Australis are the only exceptions. The latter, as has been mentioned, is relatively near; in fact, it is among our very nearest nebulous neighbors, and therefore can be properly assigned to the local cluster. The Monoceros group, on the other hand, may be truly galactic as judged by its position, the small size of its components, and the faintness of the stars involved.

Table II contains twenty-nine nebulae with emission spectra, thirteen of which were previously recognized as such. These objects show a greater preference for the galactic plane and less of a tendency to congregate into groups. They all lie close to the Milky Way, except the Cygnus nebula (N.G.C. 6960, 6992), N.G.C. 1499, 5128, and the Orion group. The largest objects in the galactic plane, however, fall at the nodal points of the belt of helium stars and might, from their position alone, be placed in either plane with equal reason. Starting from an assumption of double distribution, it is quite possible to divide the emission nebulae, assigning all five of the largest sizes, five out of thirteen of the graded sizes 4 and 3, and three out of eleven of the two smallest sizes, to the inclined plane. This distribution of sizes fits very well with the known fact that the local cluster of helium stars is nearer than the Milky Way clouds, and with the distribution in sizes of the "continuous" nebulae. Those assigned to the galactic plane have a very small dispersion and a mean galactic latitude of $-1^\circ\!.6$, which is exactly the latitude of the galactic circle as determined by Nort.[1] So close an agreement was of course unexpected, and lends some justification to the rather arbitrary division of nebulae between the two planes.

A study of the relative intensities of the monochromatic images in Table II leads to the interesting generalization that hydrogen in the extended nebulae as represented by $H\beta$ is much stronger compared to N_1 and N_2 than is the case in the planetaries. Wilson suggested this from the intensities in two extended nebulae, N.G.C. 1976 and 3372, and established the fact that emission nebulae in the Magellanic clouds occupy a position in this respect between the normal planetaries and the extended nebulae.

---

[1] *Recherches Astronomiques de l'Observatoire d'Utrecht*, 7, 1917.

TABLE II

DIFFUSE NEBULAE WITH EMISSION SPECTRA

No.	Object	Galactic		Size	Instrument	Remarks
		Longitude	Latitude			
1.....	N.G.C. 281	90°	− 7°0	3	B, C	One image, $N_1+N_2+H\beta$. Six hours with C much fainter than two hours' direct exposure
2.....	I.C. 59–63	90	− 2.5	2	B, C, D	Fan nebulae near γ Cass. D shows three images, $N_1+N_2+H\beta$(3), $H\gamma$(1), $H\delta$ (1)
3.....	N.G.C. 1491	118	− 1.5	1	C	Strong single image, $N_1+N_2+H\beta$
4.....	1499*	128	−11.5	5	B, C, D, E	Spectrum described in *A.S.P.*, **32**, 155, 1920. N_1+N_2 (2), $H\beta$ (2), 4686 (1), $H\gamma$ (2), $H\delta$ (1), $H\epsilon$ (1)
5.....	1624	122	+ 2.0	1	C	One image, $N_1+N_2+H\beta$
6.....	I.C. 405	139	− 3.0	3	C	Two images, $N_1+N_2+H\beta$ (2), $H\gamma$ (1). Faint continuous spectrum
7.....	N.G.C. 1952*	151	− 5.5	2	C	Four images, $N_1+N_2+H\beta$ (5), $H\gamma$ (2), $H\delta$ (0), 3727 (1). Strong continuous spectrum. See *L.O.B.*, **13**
8.....	I.C. 423	172	−17.5	1	B	Five images, N_1+N_2 (2), $H\beta$ (2), 4686 (1), 4363 (1), $H\gamma$ (2)
9.....	N.G.C. 1976*	176	−19.5	5	B, C, D, E	Orion nebula. See *L.O.B.*, **13**, and *A.S.P.*, **31**, 212, 1919
10.....	1982*	176	−19.0	2	B, C, D, E	Orion nebula. See *L.O.B.*, **13**, and *A.S.P.*, **31**, 212, 1919
11.....	I.C. 434*	174	−17.0	5	B	Bay nebula south of ζ Orionis. See Wolf, *A.N.*, **180**, 152. Five images, $H\beta$ (5), 4686 (2), $H\gamma$ (4), $H\delta$ (1), 3727 (2)
12.....	N.G.C. 2024	174	−16.0	3	B, D	N_1 (1), $H\beta$ (3), 4686 (2), $H\gamma$ (3), $H\delta$ (2), 3727 (2), faint continuous spectrum
13.....	2175	157	0.0	3	B, C	N_1 (1) $H\beta$ (3), $H\gamma$ (3)
14.....	2237	173	− 2.0	4	B, C, D	N_1+N_2 (2), $H\beta$ (1), $H\gamma$ (1)
15.....	....	198	− 4.0	2	C	One image, N_1+N_2
16.....	2359	194	+ 0.5	2	B, C	One image, N_1+N_2. Gaseous nature predicted from direct photographs by Pease, *Mt. Wilson Contr.*, No. 132
17.....	3372*	255	− 1.0	5	....	See *L.O..B*, **13**
18.....	5128	277	+20.0	3	C	$H\beta$ (2) 4686 (1), $H\gamma$ (2), $H\delta$ (1)
19.....	6302*	316	− 1.0	1	B	
20.....	6357	320	+ 1.0	2	C	One image, N_1+N_2
21.....	6514*	334	− 0.5	3	B, C	Trifid. See *L.O.B.*, **13**, N_1+N_2 (1), $H\beta$ (3), $H\gamma$ (2), $H\delta$ (1), 3727 (2)
22.....	6523*	333	− 0.5	4	B, C	M 8. See *L.O.B.*, **13**. N_1 (2), N_2 (1), $H\beta$ (4), 4363 (1), $H\gamma$ (3), $H\delta$ (1), $H\epsilon$ (1), $H\zeta$ (1), 3727 (2). Local variation to intensities
23.....	6611	343	+ 0.5	3	B	M 16. N_1+N_2 (1), $H\beta$ (3), $H\gamma$ (2). See *Mt. Wilson Contr.*, No. 177, p. 6
24.....	6618*	341	− 1.0	3	B	M 17. See *L.O.B.*, **13**, N_1 (4), N_2 (2), $H\beta$ (3), 4686 (0), 4361 (1), $H\gamma$ (3). Local variations
25.....	6888	43	+ 1.2	.....	B, C	$H\beta$ (2), $H\gamma$ (1), $H\delta$ (1), 3727 (2)
26.....	6960*	40	− 8.5	4	B	See Wolf, *A.N.*, **178**, 379; *ibid.*, **180**, 152
27.....	6992*	42	−10.0	4	B	See Wolf, *ibid.*, **178**, 152. Nos. 26 and 27, are really portions of one nebula—an enormous loop in Cygnus
28.....	7000*	53	− 1.0	5	B, C	Wolf, *Sitz. Heid. Akad. Wiss.*, **27**, 1, 1910
29.....	7635	79	− 1.0	3	A, B, C	$H\beta$ (5), $H\gamma$ (2), $H\delta$ (1), 3727 (4)

NOTES

Campbell and Moore were unable to see bright lines in N.G.C. 2024, 6992, and 7000. N.G.C. 6523, 6618, and 7635 each has at least one image of wave-length shorter than 3727.

7. The continuous spectrum in N.G.C. 1952 is so strong that the nebula might equally well be included in Table I.

11. I.C. 434. This is the remarkable Bay nebula stretching south from ζ Orionis, whose sharp edge on the following side is indented by a dark cloud billowing out from the obscured region bordering on the bright nebula. My plates give an emission spectrum which agrees with that described by Wolf in *Astro-*

nomische Nachrichten, **180**, 152, 1908, and ascribed by him to N.G C. 2023. N.G.C. 2023, however, is a typical nebulous star, B.D. $-2°1345$, in the obscured region following I.C. 434. The nebulosity around it has a strong continuous or rather an absorption spectrum with no trace of emission. Furthermore, Wolf's remarks "sudlich von ζ Orionis—umittelbar nordlich von die grossen Bucht . . . ." clearly apply to I.C. 434. In view of these facts, I assume the nebula whose spectrum Wolf describes in *Astronomische Nachrichten*, **180**, 152, is really I.C. 434 and so list that nebula as one whose spectrum was previously known. N.G.C. 2023 is listed among those giving continuous spectra which were not previously known.

13. Continuous spectrum fairly strong. Emission spectrum checked by a slit spectrogram.

15. This is an uncatalogued nebula described by Knox Shaw in *Helwan Bulletin*, No. 15. Discovery announced in *Union Observatory Circular*, No. 7, 1911.

28. N.G.C. 7635, formerly known as a nebulous star, appears to be a large planetary immersed in diffuse nebulosity. The brightest portions of the non-planetary nebulosity give the emission spectrum described.

The normal ratio N_1, N_2, and Hβ in the planetaries is 10:3:1. From the observations of Campbell and Moore and of Wilson, data can be gathered for extended nebulae as follows:[1]

	N_1	N_2	Hβ
N.G.C. 1976	10	3	5
3372	10	3	5
6514	3	1	10
6523	3	1	10
6618	10	3	5

Table II furnishes data of inferior accuracy, but strongly supporting those listed above.

	N_1+N_2	Hβ
N.G.C. 1499	1	2
I.C. 423	1	1
I.C. 434	0	5
N.G.C. 2024	1	3
2175	1	3
2237	2	1
5128	0	2
6611	1	3
6888	0	2
6960 6992	0	2
7000	0	2
7635	0	5

N.G.C. 1977 and 1982 are connected with N.G.C. 1976, the Orion nebula, and these, together with the outer region of the Orion nebula itself, show a decided weakening of the N_1 and N_2

---

[1] *Publications of the Lick Observatory*, 13.

lines, as compared to the 10:3:5 relation for the trapezium region. A spectrogram made at Mount Wilson with the slit east-west, just south of the B8 star B.D. $-5°1305$, 12′ south and preceding the trapezium, shows Hβ ten times as strong as N_1 and apparently just stronger than λ 3727.[1] It is interesting to note that the nebulosity condensing about the star shows a pronounced strengthening of the continuous spectrum without affecting the emission lines.

N.G.C. 281, 1491, 1624, 2359, 6357, and I.C. 59, 63, and 405 show such faint overlapping images that they cannot be separated into components for the estimation of relative intensities.

In no case, excepting N.G.C. 1952, is Hβ less than half the intensity of N_1. In this exceptional case, as studied from a slit spectrogram by Sanford, the local variations and overlap of double lines interfere with estimation of relative intensities and the only statement which can be made is that Hβ and N_2 are of about the same order of intensity.

The significance of this generalization is not clear as yet. Of the six giant planetaries[2] only one, N.G.C. 7635, shows the stronger Hβ, and the same ratio holds for small planetaries out of the Magellanic clouds discussed by Campbell and Moore. The most striking examples of these latter, N.G.C. 40, I.C. 418, N.G.C. 4361, and B.D. $+30°3639$, are in no way exceptional in appearance or in their nuclear spectra. The nuclei, however, are unusually bright as compared with the general average.

Among the non-galactic nebulae showing emission lines, two described by Campbell, N.G.C. 1068 and 4151, seem to have the normal planetary ratio, 10:3:1 for N_1, N_2, and Hβ, while three others described by Pease and by Slipher, M 33, N.G.C. 4214 and 4449 show the relatively stronger Hβ.

Tables I and II more than double the number of known emission spectra, and quadruple that of known continuous spectra. The latter now outnumber the former for separately catalogued objects; but in view of the greater tendency to group among the nebulae with continuous spectra, it is preferable to regard the numbers as about equal. As emission nebulae are much more easily identified for a given surface-brightness because of the discontinuous distribution of light in their spectra, it seems a reasonable extrapolation to assume that continuous spectra are actually more numerous than emission among the diffuse galactic nebulae.

---

[1] "Apparently" in that an ordinary lens and a Seed 30 plate were used. Quartz or U.-V. glass and Seed 23 plates would show λ 3727 as much stronger than Hβ.

[2] The term "giant planetary" is used to describe those with diameter greater than 2′. There are six such planetaries.

A study of direct photographs fails to give any necessary and sufficient criteria certain for predicting by inspection the nature of the spectrum of a given diffuse nebula. There are several general indications, but each has its exceptions. Filamentary and wispy nebulosity usually has an emission spectrum, as, for example, N.G.C. 1499, 1952, 1976, 2359, 6960, and 6992. This is not a necessary condition and is approximately satisfied in the "continuous" nebulosity about the Pleiades and 22 Scorpii; moreover N.G.C. 1952, the Crab nebula, has so strong a continuous background for its bright-line images that its spectrum could be classed as continuous almost as reasonably as emission. On the other hand, a smooth, cloudy structure is usually confined to "continuous" nebulosity, as in that about ν Scorpii and ρ Ophiuchi, but this again is approximated in the emission nebulae N.G.C. 2024 and the Trifid.

Nebulae with "continuous" spectra are usually associated with greater obscuration than are emission nebulae, although striking exceptions are found in Orion and N.G.C. 7000. It is of course a natural supposition that such vast bodies must be at least partly opaque, and that the "continuous" would be more so than the emission nebulae. Observation shows this to be the case. Obscuration is in fact a universal characteristic of diffuse galactic nebulae wherever the angular areas are large enough to warrant conclusions. The best direct evidence that I have found for transparency in any degree is presented by the helical nebula in Aquarius, N.G.C. 7293, the largest recognized planetary. Photographs made with the 100-inch reflector show three or four small non-galactic nebulae, including one spindle, within the luminous area of the planetary. The great size and galactic latitude of N.G.C. 7293 render it highly probable that the planetary is relatively near, at least nearer than the small nebulae, which, therefore, must be considered as shining through the planetary.

The brightest nebulae have emission spectra; the largest, continuous spectra. In general, however, the two classes mix pretty thoroughly when arranged in order either of size or of brightness. "Continuous" nebulae show a greater tendency to condense around stars, although most of the galactic nebulae have stars involved, and perhaps all have stars associated with them.

SPECTRAL TYPES OF STARS INVOLVED IN DIFFUSE NEBULOSITY

A study of the spectral types of such stars shows that those involved in "continuous" nebulae are of later types than those involved in emission nebulae. This conclusion is based on examination of slit spectrograms made with Cassegrain spectrographs on the 60-inch and 100-inch reflectors. One prism and an 18-inch camera were generally used, although for some of the faintest stars a 7-inch camera was necessary. Table III gives the types of stars involved in 29 of the "continuous" nebulae, which are designated by the list numbers of Table I.

Three cases are exceptional—the faint K8 star in No. 4, around which the nebulosity condenses so strongly and symmetrically that the star must be regarded as involved, and the nuclei of the two variable nebulae N.G.C. 2261 and 6729. V. M. Slipher reports the nuclear spectrum of N.G.C. 2261 as consisting of bright and dark lines agreeing closely with Nova Aurigae in its later stages. He suspected that the nucleus of N.G.C. 6729, R Coronae Australis, was similar, but three spectrograms made with the 100-inch reflector (7-inch camera) show a peculiar G-type spectrum with bright reversed hydrogen and enhanced iron lines. When these three cases are disregarded, the mean type of the other stars is about B4. None is earlier than B1.

There is a decided tendency toward uniformity of stellar type within the various groups. The Taurus group contains nothing earlier than B5. The Orion group is B2 and B3, with one exceptional B1 star in N.G.C. 1977, a nebula giving bright lines as well as a strong continuous spectrum. The stars in the Monoceros nebulae are B1 and B2, and those of the Scorpius group are B2 and B3 as in Orion, excepting the isolated case of I.C. 4601,

TABLE III

STARS INVOLVED IN NEBULAE WITH CONTINUOUS SPECTRA

No.	Nebula	Pv. Mag. of Stars	Spectrum of Stars	
1	N.G.C. 1333	10.6	B8	
2	I.C. 348	8.4	B6	B.D. +31°643
		9.8–11.6	B8–A2	9 stars
3	Pleiades	....	B5	Maia and Merope
4	....	12.5	K8	Probably a dwarf
6	N.G.C. 1579	12.0–12.2	A0–B5	2 stars
8	1788	10.0–13.0	B8–B8	2 stars
10	1977	4.6	B1	Boss 1364
11	2023	7.8	B2	B.D. −2°1345
12	2068	10.4–10.8	B5–B8	B.D. +0°1177
14	2183	14.0	B3	
15	....	13.5	B1	
16	I.C. 446	11.3	B1	
17	447	8.1	B1	B.D. +10°1159
18	N.G.C. 2245	10.7	B1	Bright Hβ suspected
19	2247	8.8	B2p	Bright Hβ and Hγ
20	2261	Var.	Pec.	Approximates a nova spectrum
21	....	8.2	B1	B.D. −12°1771
22	....	3.1	B2	π Scorpii
23	I.C. 5592	4.2	B2	ν Scorpii
24	4601	7.1–8.4	B8–A0	4 stars
25	4603	7.8	B2	B.D. −24°12684
26	4604	5.2–5.9	B2–B3	2 components of ρ Ophiuchi
27	4605	4.9	B3	22 Scorpii
28	N.G.C. 6726, 7	7.2–9.4	B9–B9	2 stars
29	6729	Var.	Gp	R Coronae Australis. Resembles T Tauri
30	6914	9.3–9.9	B5–B5	B.D. +41°3731 and B.D. +41°3737
31	7023	7.2	B2p	Bright Hβ and Hγ
32	7129	10.2–12.4	B3–B8	3 stars
33	I.C. 5146	10.0	B1	B.D. +46°3474

NOTES

4. Nebulous star north following Barnard's nebula.

15. Nucleus of cometary nebula resembling N.G.C. 2245. It is not catalogued.

17. There is a group of six stars in this nebula, some of which are certainly not involved.

24. Boss 4150, visual mag. 6.2, G5 giant, is involved in nebulosity connected with No. 24.

28. B.D. −37°13017 and 13018, visual mag. 6.5 and 6.7, B5 and B6, are involved in connecting nebulosity.

29. R Coronae Australis has bright unsymmetrically reversed hydrogen and enhanced iron lines on an absorption spectrum that is approximately a G-type but which has contradictory characteristics. The spectrum resembles that of T Tauri except that it has no bright H and K.

in which are involved four stars, B8 to A0. The Corona Australis group really comprises two double stars in addition to R. The types are B5, B6, B8, and B9, R itself being, as mentioned above, a peculiar later type.

The Monoceros group comprises all the "continuous" nebulae which can be assigned to the galactic plane with any degree of certainty. This distinction is emphasized by the fact that they contain, as a group, the earliest types of involved stars. The only other B1 star (excepting the transitional case of N.G.C. 1977 mentioned above) is central in I.C. 5146, the Cave nebula in Cygnus. This object is so near a nodal point of the inclined plane that it can be placed in either belt with equal justification. These facts raise a question as to whether or not there may be a real difference in type between stars involved in nebulae belonging to the galactic plane as compared with those belonging to the local cluster. The various groups differ so much among themselves, however, that no great weight can be assigned to results from one of their number. Moreover, there seem to be some later-type stars in the cluster around S Monocerotis and possibly in I.C. 447.

The K8 star in No. 4 is not unique. Heretofore it has been thought that all stars involved in nebulosity are B-type or earlier. The following list, which does not include several known cases of A stars, some of which are of the α Cygni type, shows that this is not rigorously true.

1. B.D. +31°597	K2 giant
2. B.D. +28°645	F8±
3. T Tauri	G peculiar with bright lines
4. No. 4	K8 dwarf
5. Boss 4150	G5 giant
6. R Corona Australis	G peculiar with bright lines

These six objects have all been photographed directly with the 100-inch reflector and, in each case, the nebulosity condenses about the star so obviously that there can be little doubt that the stars are really involved. Some may be cases of stars and nebulosity meeting in the course of the peculiar motions through space, but others, notably T Tauri and R Coronae Australis, must surely be inherently associated with the nebulosity surrounding them. None of them, however, shows any indications of nebulosity condensing into stars.

Absorption spectra of diffuse nebulae are reported by Slipher and by Pease as agreeing with the spectra of the brightest involved stars, as well as could be determined with the small dispersions employed. In this connection it is of interest to mention the following nebulae with predominantly continuous or absorption spectra which have bright-line stars involved.

Nebula	Star
Pleiades	Bright Hα in several of the brighter stars
N.G.C. 2247	Bright line B1p
N.G.C. 7023	Bright line B2p
N.G.C. 2261	Approximately a Nova spectrum[1]
N.G.C. 6729	G peculiar with bright hydrogen and enhanced iron lines

The spectrum of the Pleiades nebulosity has not yet been examined in the Hα region. No slit spectrogram has been obtained of N.G.C. 2247, and the objective-prism spectra could easily obliterate faint emission images. N.G.C. 7023 and 6729 are suspected, N.G.C. 2261 is definitely proved by Slipher, to have spectra corresponding in detail to the spectra of the stars involved. There is thus no evidence against, and some in favor of, the assumption that nebular spectra that are predominantly "continuous" are the spectra of reflected starlight.

Table IV indicates types of stars involved in nebulae with emission spectra. N.G.C. 3372, the η Carinae nebulosity, is not included because its position is such that no investigation could be made here concerning the question as to which stars are involved and which are not. η Carinae itself is usually accepted as being so involved, and if this is true, it is the one example known of a peculiar bright-line star in emission nebulosity. The Draper *Catalogue* lists two Wolf-Rayet stars within the limits of N.G.C. 3372, but there again the question of their being involved, or simply aligned, requires special investigation that cannot be carried out at Mount Wilson.

[1] *Lowell Observatory Bulletin*, No. 81, 1918.

There are two probable cases of Wolf-Rayet stars associated with diffuse nebulae having emission spectra. These are N.G.C. 2359 and 6888. Photographs of both nebulae have been published by Pease.[1] N.G.C. 2359 shows a ring and tangential streak suggesting the present form of the nebula surrounding Nova Persei No. 2. An eleventh-magnitude Ob star is approximately central in the ring and hence presumably associated with the nebula. N.G.C. 6888 is a segment of an ellipse with the Ob star B.D. +37°3821 of magnitude 7.1 near the center of the ellipse. The photograph suggests a ring of nebulosity of non-uniform brightness, inclined to the line of sight. Both nebulae have some resemblance to the planetaries or to a transitional type between planetary and extended forms. Both the nebular forms and types of stellar spectra suggest the possibility that these two nebulae are remnants of former outbursts of novae.

TABLE IV

STARS INVOLVED IN NEBULAE WITH EMISSION SPECTRA

No.	Nebula	Pv. Mag. of Stars	Spectrum of Stars	
1	N.G.C. 281	8.6–10.2 10.3–11.6	Oe5 Bo	4 components of B.D. +55°191 3 stars
3	1491	10.6	Bo	
5	1624	13.0–14.0	Oe5	3 stars. Magnitudes estimated
6	I.C. 405	5.8	Bop	Boss 1249
9	N.G.C. 1976	5.4–7.9	Oe5–Bo	4 components of Trapesium
10	1982	6.8	B1p	Bond 734. 4686 strong for type
13	2175	7.5	Oe5	B.D. +20°1284
14	2237	7.4–8.2	Oe5	4 brightest stars of the cluster
16	2359	11.0	Od	Magnitude estimated
21	6514	7.8–8.5	Oe5–Bo	2 components of B.D. −23°338
22	6523	6.1–6.9	Oe5–Bo	2 brightest stars in M 8. B.D. −23°13814–16
23	6611	8.3–9.2	Oe5–Bo	3 brightest stars in M 16.

NOTE

21. B.D. −22°4510, pv. magnitude 7.25, A3p (α Cygni type) is central in the northern lobe of the trifid nebula, N.G.C. 6514. The excessive color-index of this star, +0.80 magnitudes, together with the pronounced general absorption of the nebulosity, suggests that the star is actually within the nebula.

γ Cassiopeiae is probably associated with the emission nebulae I.C. 59 and 63. The star is clearly not involved, but the fan-shaped masses of nebulosity pointing toward that star suggest an intimate association. If this is true, γ Cassiopeiae is the one known case of a bright-line B-star associated with emission nebulosity. The type is called Bo peculiar.[1] ζ Orionis can with equal justification be considered as associated with N.G.C. 2024. In fact, all the belt stars of Orion might be thought of as associated with emission nebulosity, for the faint cloud in which they are immersed brightens in the portion known as I.C. 434, the bay nebula south of ζ Orionis, sufficiently to permit its spectrum to be identified as emission. These stars are of the Bo type.

---

[1] *Mt. Wilson Contr.*, No. 186; *Astrophysical Journal*, **51**, 276, 1920.

Another feature of the table is the marked tendency of Oe5 stars to form clusters in emission nebulae. Examples are N.G.C. 281, 1624, 2237, and 6611. Definite data are restricted to the brighter members of these clusters, but small dispersion spectrograms suggest that the fainter members are of somewhat later types and that the brighter ones alone determine the spectrum of the nebulosity.

N.G.C. 6618 (M 17) has no stars obviously involved, but there are indications of a cluster on its southern border. Two of the brightest of these are B8 and two fainter ones are Bo. General indications from focal-plane slitless spectrograms are that the two stars mentioned are the only late B-type stars in the group. A reasonable conclusion is that the two B8 stars are merely aligned, and that the group of fainter stars, if they are connected with the nebula, are of the usual type—Bo. The B8 stars are B.D. $-16^\circ 4827$ and $-16^\circ 4828$.

The main features of Table IV are the close limitation of the stars within the types Oe5 and Bo—at least for the brighter stars in each nebula—and the relatively rare occurrence of bright lines. These are four probable cases of emission nebulae associated with bright-line stars, but in no case do the spectra of star and nebula agree. The fact is well established that in the case of emission nebulae, the nebular spectrum and the spectra of stars involved or associated do not agree. This recalls Wright's remarks on the rare agreement between nebular and nuclear spectra among the planetaries.

---

[1] B.D. $-10^\circ 1848$ may be another case, but the spectrum of the nebulosity is so confused on my plates that the statement cannot be made definitely. The star is Bop with bright hydrogen lines.

The progression in stellar type from gaseous to "continuous" nebulae seems to be definitely established. There is no overlap save in N.G.C. 1982, which shows marked transitional characteristics in its spectrum. The sequence is well illustrated in the Orion nebulae of which the spectra have been investigated by Slipher and by Campbell and Moore.

N.G.C. 1976 gives a typical nebular emission line and a weak continuous spectrum. The trapezium stars are of type Oe5 and B0.[1]

N.G.C. 1982 gives a transitional spectrum. It is predominantly emission, but has a very considerable continuous background which intensifies in a marked degree about the involved star Bond 734. This is a B1 star, with λ 4686 unusually strong for the type. It might be called an early B1.

N.G.C. 1977. The spectrum is predominantly continuous with bright hydrogen and dark helium lines. No nebulium can be seen. The involved star, Boss 1364, is of type B1.

N.G.C. 2023. The spectrum is continuous with dark hydrogen and helium lines, and that of the involved star, B.D. −2°1345, is B2.

N.G.C. 2068 (M 78). The spectrum is continuous with dark hydrogen and helium lines and was classed by Slipher as probably late B. The stars involved are classed as B3 and B5, but subject to a rather large uncertainty. My own plates tend to place the nebular spectrum as not later than B5.

N.G.C. 2237 in Monoceros might be placed at the head of this sequence as it gives a pure emission spectrum with no continuous background perceptible. The four brightest stars involved, which have been investigated, all show fine Oe5 spectra.

SPECTRA OF PLANETARY NUCLEI

The progression is so pronounced that it seemed advisable to investigate the possibility of extending it into the other type of galactic nebulae, the planetaries. Wright has shown that some planetary nuclei have bright lines or bands, and that others do not. Where emission does occur it is probably of the Wolf-Rayet type. He has not published results for any of the nuclei of giant planetaries, and, as these seem to have the closest affinity to extended nebulae, their spectra have been observed at Mount Wilson.

---

[1] It has been previously mentioned that "continuous" nebulosity condenses strongly about the B8 star B.D. −5°1305 in the outer region of N.G.C. 1976, while the emission lines of the nebula are not affected by the star.

As an arbitrary division, those planetaries whose mean diameter exceeds two minutes of arc are called giants. There are six such, all within reach in this latitude.

N.G.C. 246
1514
3587 (Owl)
N.G.C. 6853 (Dumbbell)
7293 (Helix)
7635

Two of them have central stars bright enough for the Cassegrain spectrograph with one prism and an 18-inch camera on the 100-inch reflector. These are N.G.C. 1514 and 7635, whose central stars are, respectively, B.D. +30°623, 9.4 photo-visual magnitude, and B.D. +60°2522, 8.7 photo-visual magnitude. Their spectra are similar and of a type not covered by the Harvard classification. They show no bright lines or bands. The following dark lines are present.

Hβ
Hγ
Hδ
4542[1]
4200[1]
4026[1]
4686 faint and hazy
4471 just perceptible

To these may be added λ 4481 in B.D. +30°623 nearly as strong as λ 4542, and in B.D. +60°2522, λ 4147 stronger than λ 4471, and H and K faint and sharp. With these exceptions, the spectra could be described as Od with the bright lines suppressed to the extent of a trace of absorption in λ 4686. Their position is intermediate between the Wolf-Rayet type and Oe5. Radial velocities for four plates of each are +35.4 km for B.D. +30°623 and −34.5 km for B.D. +60°2522.

A single slit spectrogram of the central star in N.G.C. 246 made with one prism and a 7-inch camera shows a spectrum similar to B.D. +60°2522, the central star in N.G.C. 7635. In all three objects, the line λ 4542 is the strongest except the hydrogen lines.

By way of comparison, a spectrogram of the nucleus of the smaller planetary I.C. 2149 was obtained, using one prism and an 18-inch camera on the 100-inch reflector. This nucleus is one for which Wright reported a continuous spectrum with no bright lines. An exposure of eight hours gave a legible spectrum in spite of very poor seeing conditions. The rather faint continuous spectrum of the nucleus holds up unusually well toward the violet, and is crossed by the bright lines of the nebula, so sharp and narrow that their source is unmistakable. Only three dark lines can be detected. $H\beta$ and $H\gamma$ are very faint and hazy and almost obliterated by the strong bright nebular lines superposed. The third dark line is λ 4542, exceedingly faint, but free from any nebular line. No trace of λ 4686, either bright or dark, can be seen. Thus the nuclear spectrum, freed from the bright lines due to the nebula, is rather similar to a weak spectrum of the three central stars discussed above.

---

[1] The lines λλ 4542, 4200, and 4026 are those discovered by E. C. Pickering in the spectrum of ζ Puppis, for which he employed the designation Hγ′, Hδ′, and Hε′, respectively.

Slitless spectra have been obtained for the nuclei of all six of the nebulae. The dispersion is small, about 5.0 mm from $H\beta$ to $H\epsilon$, and conclusions based on them are not as certain as one would wish. All six are essentially similar; at least no difference could be made out on the small-dispersion plates. No bright lines or bands are seen, and all show the well-known strength in the ultraviolet which Wright first reported. This similarity of slitless spectrograms, together with the results of a detailed study of three higher-dispersion spectra taken with a slit, permits the assumption that we have in these central stars a class of objects intermediate between stars involved in extended emission nebulae and in the smaller planetaries.

Wright himself published observations of only two planetaries with mean diameters greater than one minute of arc. These are N.G.C. 4361 and 6720. In both cases the nucleus gave a continuous spectrum with no bright lines. His fifteen nebulae whose nuclei show no bright lines have a mean diameter of about 30″ as against 20″ for the fifteen whose nuclei do show bright lines, probably of the Wolf-Rayet type.[1]

The evidence, as far as it goes, points to a progression in spectral type of central or involved stars from the small planetaries to the large ones, and this progression joins immediately on to that of the extended nebulae. The complete sequence of stars involved in galactic nebulae can be represented as follows:

---

[1] *Publications of the Lick Observatory*, 13, 252, 1918.

Small planetaries	Wolf-Rayet
Large planetaries	Intermediate between Wolf-Rayet and Oe5
Extended emission nebulae	Oe5 and B0
Extended "continuous" nebulae	B1 and later

The overlap is surprisingly small and for the most part confined to nebulae with unusual forms or spectra. No conclusions have been formed as to the end of the sequence, although it may be significant that the stars of latest type seem to favor faint nebulosity and pronounced obscuration. N.G.C. 2359 and 6888, on the assumption that the Ob stars are truly associated, fall out of place. In both cases, however, there is evidence of a ring structure that suggests a nova origin or at least an affinity with the planetary type.

ASSOCIATION OF GALACTIC NEBULOSITY WITH STARS

This intimate relation between spectral type of nebula and of involved stars raises a presumption that one is a consequence of the other. It seems more reasonable to place the active agency in the relatively dense and exceedingly hot stars than in the nebulosity, and this leads to the suggestion that nebulosity is made luminous by radiation of some sort from stars in certain physical states. The necessary conditions are confined to certain ranges in stellar spectral type and hence are possibly phenomena of effective temperature. The nebulous material itself must be in a physical state sensitive to the stellar radiation, and close enough for the density of radiation to be effective. The abrupt transition from emission to "continuous" nebulosity between stellar types B0 and B1 suggests a critical point in the spectral sequence or possibly effective temperature below which stellar radiation is incapable of exciting nebulous material to emission luminosity. From thence down the spectral sequence the luminosity gives a continuous spectrum and probably partakes more and more of the nature of reflected light.

A theory of nebular luminosity built on these lines meets a first obstacle in the necessity for locating stars conspicuously associated with each galactic nebula, of the required spectral type, and properly placed to energize the nebulosity. Planetaries offer no great difficulty. There is doubt in some cases as to whether the nuclei are truly stellar, but there is usually a condensed center which may well conceal a star or take the place of a star as a center of radiation. In several extended nebulae, however, there is a conspicuous absence of any obviously dominating star or group of stars. Such of those as give continuous spectra show pronounced obscuration in and surrounding the nebulosity, and offer the possibility that stars capable of playing the required rôle are present but entirely or partially obscured. Nos. 4, 5, 6, and 7 in Table I are examples.

Emission nebulosity exhibits much less general absorption, possibly because the matter is in a more highly dissociated state. Here the assumption of obscuration generally fails, and the radiation centers must be sought among the multitude of stars always found within, or near to, the nebulosity. Such stars need not be apparently bright, for the apparent surface luminosity of nebulae is independent of the distance. Furthermore, several of the giant planetaries, for instance, N.G.C. 3587, 6853, and 7293, have bright nebulosity with central stars of the thirteenth to the fourteenth magnitude. Such objects then as N.G.C. 1499 and the nebula in Cygnus, N.G.C. 6960 and 6992, might, with no great stretch of the imagination, be considered as receiving affective radiation from some of the neighboring stars, after the manner in which N.G.C. 2024 probably receives its energy from ζ Orionis.

These suggestions may be applied to the nebulae considered in this paper. Table I contains only six nebulae with continuous spectra, which have no stars obviously involved or conspicuous on direct photographs for location and brightness. They are Nos. 4, 5, 6, 7, 9, and 13. The first four fall in the Taurus group and lie in regions of complete obscuration. Involved stars would need to lie on the near side or very close to the nearer surface of the nebulae in order to be seen at all. In two of these four cases, Nos. 4 and 6, faint stars are present which are almost certainly dimmed by intervening nebulosity. It is possible and even reasonable to assume that bright stars may be involved or associated with all four of these objects, but partially or completely hidden by the obscuring clouds.

No. 9 is the nebulosity north of and preceding Rigel. The form of the nebula approximates an arc with Rigel at the center. Moreover, several fan-shaped details are present which in each case point toward that star. In short, the nebula shows a considerable degree of radial symmetry with Rigel as the point of convergence. The spectral type of Rigel, B8p, and the absolute magnitude, −5.5 according to Kapteyn, are significant. The nebulosity extends to a distance of 2°5 from the star which, in terms of actual distance across the line of sight, is of the order of twenty light-years at the distance of Rigel. This seems an enormous distance over which to assume stellar radiation to be effective in illuminating nebulosity, but a comparison with the better-known Pleiades nebulosity indicates that the two cases are comparable, and Hertzsprung's[1] discussion of the Merope nebula lends considerable weight to the suggestion that reflected starlight can account for the whole of the nebular luminosity in that particular case. In terms of absolute magnitudes Rigel is about 4.7 magnitudes brighter than Merope and hence will have the same illuminating power at 8.7 times the actual distance of similar nebulosity from Merope; or since Rigel is about 1.5 times as distant as Merope from the earth, to an angular distance of about 5.8 times as seen from the earth. Nebulosity comparable in brightness to the nebulosity near Rigel exists nearer to Merope than to any other of the bright stars of the Pleiades, and it extends to a distance considerably more than 1/5.8 times its angular distance.

Inclusion of all the Pleiades stars will not entirely destroy the analogy. According to Trumpler's list of cluster stars, the equivalent brightness of the Pleiades cluster is of the order of magnitude 1.3 or about −3.7 absolute, and the center of the cluster is about 6′ west of Alcyone. Rigel then is 1.8 magnitudes brighter than the entire cluster and would have equal illuminating powers on nebulosity at about 1.4 times the angular distance of equivalent nebulosity from the center of the cluster. The equivalent distance in the Pleiades cluster is about 100.′ The actual nebulosity is rather sharply divided into bright inner clouds involving the more luminous stars and extending in parts to about 50′ from the center, and very faint exterior clouds extending to 3° or 3°.5 from the center. The position of the nebulosity near Rigel would seem to fall between these extremes. This discussion disregards inclinations to the line of sight of the direction from star to nebulosity, and hence leaves an element of uncertainty in the conclusion. It does seem plausible, however, to regard the relation of Rigel to its neighboring nebulosity in the same category as the relation between stars and nebulosities in the Pleiades cluster.

---

[1] *Astronomische Nachrichten*, **195**, 449 (No. 4679), 1913.

No. 13, the great loop, sometimes called the spiral, around the belt and sword of Orion, offers difficulties of another sort. The belt stars and the general aggregation of fainter stars in the vicinity are sufficiently bright to account for the nebular luminosity on the same basis as in the case of Rigel and the Pleiades, but the continuous spectrum of the nebulosity does not fit the Bo spectral types of the brighter belt stars. These same stars appear to produce an emission type of illumination in nebulosity immediately adjacent to them, N.G.C. 2024, I.C. 434, etc.; yet if they truly do illuminate the more distant loop, it is with a different light altogether. It may be that the physical state of the loop nebulosity is different from that in the closer objects—that the physical state of all nebulosity depends upon distance from, and spectral type of, associated stars. Or, again, the ability of stellar radiation to produce emission luminosity may be restricted to certain limits of distance which in this case are exceeded.[1]

The facts seem definite—the nebulosity close to the belt stars gives emission spectra while that far away gives a continuous spectrum. Several nebulae giving continuous spectra, as, for example, N.G.C. 2023, are nearer to the belt than is the loop, but they lie on the near side of an obscuring cloud which seems to veil them from the influence of the belt stars and permits them to shine by the undisturbed action of their own involved stars. Slipher suggested that spectra of the Orion nebulosities change from emission to continuous or rather to absorption, as one proceeds outward from a center—probably the great nebula around

[1] The brightest portion of the loop is nearest the belt stars. The distance across the line of sight to the nearest belt star—ζ Orionis—is about forty light-years.

θ Orionis, and these new observations may be but another application of some law. However this may be, the loop in Orion, if it does receive its light from the group of stars that includes the belt, is the one known example of a nebula giving a predominantly continuous spectrum, having as the brightest stars associated with it those of a type earlier than B1.

The result of this examination is as follows: twenty-six out of thirty-three nebulae giving predominantly continuous spectra have prominent stars obviously involved in the nebulosity; in six of the remaining cases more or less plausible means can immediately be suggested to account for the absence of dominating stars within the nebulae; and in the last case, exceptional in many respects, there exists at least possible means of accounting for the nebular illumination as originating in stars.

The case of the emission nebulae is nearly as strong. Among those listed in Table II the following do not have early type stars actually within their borders:

Nos. 2, 4, 7, 8, 11, 12, 25 (26 and 27), 28.

No. 2, I.C. 59, 63—the fan-shaped nebulae near γ Cassiopeiae. That star is obviously associated with, although not involved in, the nebula. The very form of the nebulosity seems determined by radiation or repulsive action from the star which lies at a center of radial symmetry with respect to the fans. The spectral type of γ Cassiopeiae, Bop with bright lines, conforms to the rule previously established concerning the relation between stellar and nebular spectra.

No. 4, N.G.C. 1499—ξ Persei is the brightest neighboring star. The nebula lies on a rough arc, concave to ξ Persei, which can readily be considered as occupying the center of the arc. The star is of type Oe5 and hence conformable to the nebular spectrum. No other star in the vicinity brighter than ninth magnitude has a spectrum earlier than B3.

No. 25, N.G.C. 6888—a long segment of an ellipse, of which B.D. $+37°3821$ occupies the center. The stellar type is Ob, hence the star and nebula seem to resemble N.G.C. 2359. No other star in the neighborhood has a spectrum earlier than B5. The only brighter star near is of K-type.

These three cases offer positive evidence of association of star and nebulosity. In each, one definite external star appears to dominate the nebula, its position approximating a center of radial symmetry, its spectral type conforming to the established rule. No rival claimants can be found for any of the positions.

No. 12, N.G.C. 2024—ζ Orionis, B0, a sort of super-giant with an absolute magnitude of −4.17 according to Kapteyn, is conveniently located to energize the nebula. Direct photographs give an instant impression that this star illuminates the nebula, although the details of nebulosity do not show such marked radial structure as is found in the three cases cited above.

No. 11, I.C. 434—the Bay nebula south of ζ Orionis. This seems part of a cloud involving the belt stars and σ Orionis. In this particular portion, both ζ and σ can be considered as sources of illumination, both from position and from spectral type.

No. 8, I.C. 423—a small loop between δ and ϵ Orionis, nearer the former. Both these stars from their spectral types can be considered as the energizing agents. Their positions bear no obvious relation to the figure of the nebula, but their distances are within reason unless greatly distorted by projection.

These three cases do not offer such definite evidence as the first three discussed. They pass from positive in No. 12 to suggestive in No. 8.

The last three cases, Nos. 7, 28, and 26 and 27, offer more serious difficulties. One indeed, 26 and 27, seems flatly to defy explanation on any observational basis.

No. 7, N.G.C. 1952, the Crab nebula, has two faint stars about centrally located. The brighter is of about 15.5 photographic magnitude and the other only slightly fainter. The nebular spectrum is strongly continuous with widely doubled bright lines. Curtis includes the nebula among the planetaries, although he calls it a doubtful classification. Exposure-ratio plates made at Mount Wilson indicate a decided negative color-index for the brighter star at least, and this, together with their approximately central position, permits the assumption that one or both are involved in or associated with the nebula. There are no bright stars in the neighborhood which can be considered as sources of energy, either from position or spectral type.

The question, then, is whether or not the faint central star or stars can dominate the nebula. The best answer is another analogy, this time with the Helical nebula in Aquarius, the giant planetary, N.G.C. 7293. This nebula has a diameter about three times that of the Crab and a central star about two magnitudes brighter. The relation between stellar magnitude and square of the radius are of the same order. If the Crab were at three times the distance of the Helical nebula the two objects would be comparable in size and brightness of their central stars. If the planetaries are energized by their central stars, then one may assume as a possibility that the same is true of the Crab nebula.

No. 28, N.G.C. 7000—the North America nebula. This object gives a considerable continuous spectrum with faint emission. Several stars from sixth to ninth apparent magnitude are involved, and heavy obscuration is evident around the borders, especially in the southern portion. The nebulosity is cloudy and devoid of filamentous detail. In a general way it recalls the appearance of the Trifid. The spectrum also has some resemblance to that of the Trifid, although this latter nebula has a stronger emission and a weaker continuous background. The stars involved in N.G.C. 7000 are all later than B1, and hence can account for only the continuous portion of the nebular spectrum.

Inspection of small-scale photographs of this nebula, for instance, those made by Barnard with the 6-inch Willard lens, suggests that α Cygni may be associated. The Trifid nebula offers a possible analogy, for in the north lobe of that object is a star of the same enhanced A-type as α Cygni. The star is B.D. $-22^\circ4510$, photo-visual magnitude 7.2, with a spectrum remarkably similar to that of α Cygni. The star has a color-index of about 0.8 magnitude and hence is regarded as involved in the nebulosity. The Trifid nebula gives an emission spectrum on a continuous background. The emission portion can be attributed to the Oe5 star B.D. $-23^\circ338$ in the southern lobe, but the lack of pronounced strengthening of continuous spectrum immediately contiguous to the star in the northern lobe suggests that the latter star may be responsible for part at least of the emission spectrum. The enhanced α Cygni type of stellar spectrum is so unique that unusual properties may be suggested for such stars without prejudice to the existing data. If the star, B.D. −22°4510, does produce some emission luminosity in the Trifid, then α Cygni can be considered a possible source of illumination in N.G.C. 7000.

α Cygni is some 5.5 magnitudes brighter than B.D. −22°4510; hence, if we assume the same absolute magnitude for both stars, α Cygni would have equal illuminating powers at about thirteen times the angular distance, or by figuring from the dimensions of the Trifid, to just under 2°. The nebulosity in N.G.C. 7000 actually does extend from 2°.5 to 3°.5 from α Cygni so that, disregarding inclinations to the line of sight, and remembering that nebulosity need not be similarly distributed in these objects, we can regard the distances in the two cases as roughly of the same order. It is necessary to emphasize that this discussion does not explain the luminosity of N.G.C. 7000, and that it does not even make out a strong case. The most that can be said is that a possibility is offered which derives some weight from analogy and which must receive some consideration before it can be definitely dismissed.

Nos. 26 and 27, N.G.C. 6960 and 6992, are portions of an enormous loop in Cygnus. This nebula apparently is the one absolute exception to the suggestion that all galactic nebulae have associated with them stars of spectral types conformable to the type of nebular spectrum. The spectrum of the loop in Cygnus appears to be almost purely emission, yet no stars earlier than B3 nor any stars of the enhanced α Cygni type can be located, which have any probable connection with the nebula. In fact no stars at all, brighter than 9.5 magnitude, can be suggested as associated with the nebulosity.

This discussion of emission nebulae indicates that seventeen out of the twenty-six objects in Table II have stars of conformable spectral types within and obviously associated with the nebulosity. Of the remaining nine objects, three give positive evidence of association with external stars, three suggest such association, two offer possibilities of association, and one seems flatly to contradict the idea of association.

Combining the results from Tables I and II there is one clear exception and three difficult or doubtful cases out of the sixty-two nebulae. Examination of an observing list of some one hundred and twenty-five extended galactic nebulae, all the known objects of this class north of −40° declination, shows no other exception and only one or two doubtful cases. The evidence then, with the single clear exception of the Cygnus loop, is very strongly in favor of the view that all galactic nebulae have associated with them stars of spectral types conformable to the types of the nebular spectra.

CONCLUSIONS

The general conclusion of this discussion is that all galactic nebulae are associated with stars and that the spectra of nebulae and associated stars have a definite relation. This suggests that galactic nebular luminosity has its source in stellar radiation. The phenomena are not simply those of reflected starlight, for in general the emission spectra of nebulae do not agree with the spectra of the associated stars. The reverse is true for diffuse nebulae with continuous spectra. In these cases the reflection theory appears to offer a reasonable explanation, or at least a working basis for further investigation. The mechanism of emission luminosity will probably find its explanation in the fact that it is always associated with the very hottest types of stars.

It is very doubtful whether or not a mass of diffuse nebulosity isolated in space and with no stars involved could hold together and at the same time shine by light generated by collisions of molecules. At temperatures corresponding to intensity-distribution or width of lines in nebular spectra, the average speeds of molecules would be so high compared to the velocities of escape that the nebulosities would probably dissipate rapidly. On the other hand, if molecular speeds were sufficiently small to admit of cohesion in the mass, the nebulosity would probably be too cold to radiate light. This argument suggests that diffuse nebulosity is not intrinsically luminous, but is rendered so by external causes. The only obvious external sources of energy are the stars actually involved in or neighboring to the nebulosity, and definite relations have now been found to exist between the radiations of such stars and nebulosity.

The resulting conception of diffuse galactic nebulae is that they are clouds of material (molecules, dust, or larger particles) illuminated by neighboring stars. The question as to whether the association is temporary or permanent can be answered by a comparison of radial velocities of stars and nebulae. Unfortunately the large majority of such stars are binaries which require a great deal of labor for determining the velocities of the systems. This is especially true of the Oe5 and B0 stars which are associated with the diffuse emission nebulae whose velocities are best determined.

The meager data available at present are indeterminant. Radial velocities are given by Campbell and Moore for six diffuse nebulae as follows:

N.G.C. 1976 (Orion)	+17.5 km
3372	+ 6.0
6514 (Trifid)	+11.0
6523 (M 8)	− 3.0
6618 (M 17)	+ 7.0

The brighter stars in N.G.C. 1976 are all binaries for which no velocities for the systems have been determined. The stars in N.G.C. 6618 are faint and no measures have been published as yet.

η Carinae, in N.G.C. 3372, gives for the hydrogen lines velocities differing from those of other emission lines. The mean of four spectrograms measured by Sanford[1] gives +33.8 km for hydrogen and −22.8 km for the other emission lines. It is just possible that the mean, +5.5 km, may have a significance when compared to the nebular velocity, +6.0 km.

The three brightest stars in N.G.C. 6514 have been observed at Mount Wilson. They are:

B.D. −22°4150, A3p	− 1.5 km, 3 plates
B.D. −23°13804 (brightest comp.), Oe5	− 4.7 km, 4 plates, range 26 km
B.D. −23°13804 (second brightest comp.), B1	+17.3 km, 3 plates, range 20 km
Mean	+ 2.9 km

The two brightest components of B.D. −23°13804 are undoubtedly binaries and the mean of the seven measures for the two, +6.3 km, is suggestive, but by no means conclusive, on the question of agreement between stellar and nebular velocities. B.D. −22°4510 is definitely not in agreement. Its high color-excess[1] may mean that it is seen through the entire nebula.

---

[1] *Lick Observatory Bulletins*, 8, 134, 1916.

One star in N.G.C. 6523 has been measured—Boss 4560, Oe5, magnitude 6.1. The spectrograms give a velocity of +12.6 km. As the range is 33 km, the star must be considered a binary.

Further data on this question are very desirable. A casual inspection of diffuse nebular structure and configurations of involved stars suggests that the association is for the most part temporary. This may be one fundamental distinction between diffuse nebulae and planetaries, for in the latter the central stars must be permanently associated with the surrounding nebulosity; otherwise their central positions could not in general be maintained.

Mount Wilson Observatory
May 1922

---

[1] The color-index is 0.8 magnitudes. See *Mt. Wilson Contr.*, No. 187, p. 15; *Astrophysical Journal*, **52**, 22, 1920.

INVESTIGATIONS ON PROPER MOTION

SEVENTH PAPER: INTERNAL MOTION IN THE SPIRAL NEBULA N.G.C. 2403[1]

By ADRIAAN VAN MAANEN

ABSTRACT

Spiral nebula N.G.C. 2403—Two pairs of plates covering eleven- and eight-year intervals, respectively, and all taken at the primary focus of the 60-inch reflector, were measured with the stereocomparator, and the motions of 76 points, presumably belonging to the nebula, were derived with respect to the mean motion of 24 comparison stars. The results for each point and star are shown by arrows on the accompanying *photograph*. *The proper motion of the nebula* as a whole comes out very small, namely, $\mu_\alpha = +0''.002$ and $\mu_\delta = 0''.000$. Taking the *inclination of the plane of the nebula* to the surface of the celestial sphere to be 48°, the *internal proper motions* in the plane of the nebula come out very similar to those found previously for M 33, 51, 81, and 101. The radial components are practically equal to the tangential components, both increasing with the distance from the center; the motions indicate an outward streaming along the spiral arms at a rate which increases from 0".015 per year at 1'.4 to 0".040 at 8'.9 (the average being 0".019), combined with an outward transverse motion of about 0".007 per year.

Proper motions of 24 comparison stars were also determined with a probable error of ±0".0038 per year. All but one or two have velocities less than 0".02 per year.

In January, 1921, Mr. Duncan succeeded in securing with the 60-inch Mount Wilson reflector several plates of the spiral nebula N.G.C. 2403 with exposure times ranging from one hour to four hours. For this object Mr. Ritchey had already taken plates in 1910, 1916, and 1917, and Mr. Pease had taken a photograph in 1912. Of these plates four were selected for measurement, and combined into two pairs for which the observing details are given in Table I.

TABLE I

	Date	Observer	Exposure	Quality
1	1910 Feb. 7	Ritchey	1^h	g
	1921 Jan. 4	Duncan	1^h	fg
2	1912 Nov. 8	Pease	$3\frac{1}{2}^h$	g
	1921 Jan. 5	Duncan	4^h	fg

---

[1] *Contributions from the Mount Wilson Observatory*, No. 242.

The nebula is described by Curtis[1] as "a bright, beautiful spiral 16′×10′. No nucleus apparent; many almost stellar condensations; of the general type of M 33." As the galactic latitude is not quite 30°, we have an abundance of stars which can be used for comparison purposes.

Seventy-six points, presumably belonging to the nebula, were measured, while for comparison purposes twenty-four stars from magnitude 13.5 to 17.0 were selected.

Both pairs of plates were measured with the new stereocomparator in four positions, with the direction east, west, north, and south successively coinciding with that of the increasing readings of the micrometer screw. For each pair the two measures in right ascension and those in declination were combined into one series of displacements; these values, $M\alpha_1$, $M\alpha_2$, $M\delta_1$ and $M\delta_2$, were reduced to proper motions by equations of the form:

$$\left.\begin{aligned} M_\alpha &= a+bx+cy+dx^2+exy+fy^2+m_\alpha \\ M_\delta &= a^1+b^1x+c^1y+d^1x^2+e^1xy+f^1y^2+m_\delta, \end{aligned}\right\} \qquad (1)$$

in which a, b . . . . f^1 are the plate-constants, x and y the co-ordinates of the objects measured, and m_α and m_δ the proper motions, expressed in parts of the micrometer screw. In order to reduce these motions to annual proper motions, expressed in thousandths of a second of arc, the quantities m_α amd m_δ for the first pair of plates must be multiplied by 0.765, for the second pair by 1.022.

The plate-constants were derived by least-squares solutions from the sets of twenty-four equations of form (1) for the comparison stars. The constants thus found were substituted in the equations of conditions (1) of all the objects measured. The annual proper motions are given in the fourth, fifth, sixth, and seventh columns of Table II. The second and third columns of this table contain the co-ordinates in x and y, expressed in minutes of arc, with a precision sufficient for identification.

Weights 2 and 1 were assigned to the two pairs respectively; the mean motions thus derived for the nebular points include the motion of the nebula as a whole with respect to the 24 comparison

---

[1] *Lick Observatory Publications*, 13, 24, 1918.

TABLE II

Co-ordinates and Annual Displacements

No.	x	y	$\mu_{\alpha 1}$	$\mu_{\alpha 2}$	$\mu_{\delta 1}$	$\mu_{\delta 2}$
a	−6'.7	+0'.9	+0".003	+0".007	−0".005	+0".003
b	−4.8	+4.9	+ 4	+ 5	+ 21	− 7
c	−2.0	+5.2	+ 3	− 1	− 5	+ 16
d	−2.4	+3.6	− 6	+ 14	− 40	− 27
e	−2.8	+1.7	− 7	− 34	+ 3	− 6
f	−4.1	−0.3	− 4	− 6	+ 10	+ 11
g	−4.9	−1.5	+ 5	+ 6	+ 6	+ 17
h	−5.1	−4.3	+ 2	− 10	− 5	− 8
i	−3.2	−4.9	− 2	− 5	− 3	+ 8
j	−1.9	−4.4	− 6	+ 2	− 5	− 10
k	−1.6	−2.0	− 2	+ 2	+ 5	− 10
l	−2.4	−1.2	− 4	+ 11	− 3	− 13
m	−0.4	−2.1	+ 5	+ 16	+ 10	− 3
n	−0.5	−1.2	+ 14	+ 7	0	+ 6
o	+0.9	−1.8	+ 1	− 6	+ 11	− 5
p	+3.6	−5.0	+ 8	+ 19	+ 6	0
q	+4.5	−4.7	− 7	− 10	− 5	+ 2
r	+5.4	−2.5	− 3	− 3	− 7	+ 3
s	+5.9	−1.6	+ 2	− 13	− 1	+ 1
t	+4.5	+0.7	+ 5	− 9	− 10	− 3
u	+5.5	+2.4	− 2	+ 17	+ 5	− 9
v	+1.9	−0.2	− 5	− 8	− 1	+ 23
w	+3.8	+4.1	+ 1	+ 12	+ 5	− 5
x	+0.6	+5.7	− 2	− 13	+ 5	+ 14
1	−7.0	−0.3	− 20	− 42	+ 26	+ 2
2	−7.0	−0.6	− 36	− 36	+ 24	+ 29
3	−2.8	+2.8	+ 7	− 28	+ 17	+ 5
4	−2.8	+2.7	− 18	− 15	+ 13	− 19
5	−2.8	+2.6	+ 17	− 11	+ 18	+ 29
6	−2.7	+2.7	+ 8	+ 3	+ 32	+ 63
7	−2.5	+3.0	+ 5	+ 13	+ 18	+ 13
8	−3.6	+1.2	0	− 11	+ 27	+ 26
9	−3.2	+0.9	+ 2	− 4	+ 14	− 22
10	−2.9	+0.6	− 19	− 28	− 1	+ 6
11	−2.3	−2.3	− 19	− 13	+ 9	+ 7
12	−2.0	−0.8	− 2	− 16	+ 26	− 11
13	−1.9	−0.4	− 32	− 37	+ 18	+ 34
14	−1.7	−0.4	− 3	− 30	+ 7	+ 23
15	−1.4	+0.4	− 7	− 23	+ 15	− 5
16	−1.9	+0.8	− 8	− 32	+ 8	0
17	−1.6	+1.7	+ 11	+ 18	+ 28	− 10
18	−1.6	+1.8	+ 20	− 1	+ 42	+ 10
19	−1.4	+1.8	+ 22	− 3	+ 8	+ 22
20	−1.6	+2.6	+ 18	− 9	+ 28	+ 4
21	−1.7	+2.7	+ 6	+ 23	+ 22	+ 44
22	−1.2	+3.3	+ 19	+ 11	− 1	− 6
23	−0.1	+5.0	+ 8	+ 41	+ 17	+ 4
24	−0.6	+3.7	− 1	+ 19	+ 8	− 20
25	−0.4	+3.6	+ 8	− 19	+ 56	+ 8
26	−0.4	+1.8	+ 16	+ 26	+ 28	+ 7
27	−0.5	+1.5	0	+ 32	+ 4	+ 8
28	−0.2	+1.7	+ 14	+ 12	+ 12	− 30

TABLE II—*Continued*

No.	x	y	$\mu_{\alpha 1}$	$\mu_{\alpha 2}$	$\mu_{\delta 1}$	$\mu_{\delta 2}$
29	−0′.1	+1′.7	+0″.021	+0″.018	+0″.015	−0″.002
30	0.0	+1.7	+ 7	+ 39	+ 14	− 17
31	−0.3	+0.7	+ 5	+ 42	− 5	+ 6
32	−0.6	+0.8	− 15	− 32	+ 30	+ 8
33	−0.3	+0.4	+ 2	+ 22	+ 22	+ 6
34	−0.2	+0.3	+ 5	+ 17	+ 5	+ 24
35	−0.3	−0.1	− 4	+ 1	− 4	− 3
36	−0.3	−0.3	− 11	− 34	+ 2	− 21
37	−0.4	−0.5	− 18	− 24	− 3	− 40
38	−0.5	−0.9	− 6	− 13	+ 13	− 40
39	−0.7	−1.1	− 24	− 29	+ 20	− 20
40	−0.2	−1.0	+ 4	− 22	+ 1	− 29
41	−0.1	−1.2	− 5	− 22	+ 1	− 29
42	0.0	−1.2	+ 10	− 12	+ 10	− 30
43	−0.2	−1.8	− 5	− 28	+ 8	− 7
44	+1.3	−4.4	+ 4	− 16	− 8	− 21
45	+1.5	−3.5	+ 4	− 23	− 11	− 22
46	+1.3	−2.3	+ 5	− 10	− 3	− 31
47	+1.4	−2.3	− 23	+ 23	− 17	− 29
48	+2.0	−2.3	+ 16	− 30	+ 2	− 34
49	+2.1	−2.3	+ 11	+ 11	+ 1	− 10
50	+2.1	−2.2	+ 13	− 6	0	− 24
51	+2.0	−2.1	+ 4	+ 8	− 3	− 8
52	+1.5	−1.5	+ 29	− 8	− 13	− 30
53	+1.4	−1.5	+ 12	− 61	+ 7	+ 5
54	+0.9	−1.0	− 2	+ 5	− 2	− 39
55	+0.9	−0.7	+ 21	+ 4	− 5	− 19
56	+0.7	+0.4	+ 5	− 3	− 4	− 30
57	+0.6	+1.2	+ 18	+ 28	− 8	− 4
58	+1.1	+1.4	− 4	+ 9	− 15	− 38
59	+0.7	+3.7	+ 24	+ 18	+ 20	− 2
60	+0.6	+3.6	+ 28	+ 41	+ 29	− 21
61	+1.4	+0.5	+ 8	+ 16	+ 2	0
62	+1.5	+0.7	+ 17	+ 27	− 8	− 9
63	+2.1	+0.1	+ 20	− 8	− 13	− 17
64	+2.3	0.0	+ 36	− 4	− 19	− 35
65	+2.8	−0.4	+ 2	+ 31	− 1	− 21
66	+2.9	−0.5	+ 15	+ 23	− 16	− 30
67	+2.3	−0.7	+ 12	+ 30	− 3	− 72
68	+2.8	−2.4	+ 8	− 29	− 5	− 20
69	+2.7	−2.8	− 12	− 34	− 23	− 41
70	+2.9	−3.5	+ 10	− 35	+ 5	− 20
71	+2.4	−4.1	− 11	− 22	− 7	− 45
72	+2.5	−4.2	+ 2	− 12	− 8	− 61
73	+2.7	−4.1	− 3	− 23	0	− 9
74	+4.7	+2.7	+ 34	+ 31	− 10	− 16
75	+4.5	−2.3	+ 26	+ 24	0	− 46
76	+6.2	−1.8	+ 16	+ 24	− 35	− 15

stars as well as the internal motions of the individual points. To derive the motion of the nebula as a whole, the same process was followed as for the nebulae formerly discussed.[1]

---

[1] *Mt. Wilson Contr.*, No. 118, p. 9; *Astrophysical Journal*, 44, 218, 1916.

a) The mean for all of the 76 points gives:

$$\mu_\alpha = +0''.002 \qquad \mu_\delta = +0''.001.$$

b) If the points are divided into four groups, corresponding to the four quadrants, the means of the two groups in opposite quadrants should give a good agreement. We find:

$$\text{Means for I and III} \quad \begin{cases} \mu_\alpha = +0''.000^5 \\ \mu_\delta = -0''.001 \end{cases}$$

$$\text{Means for II and IV} \quad \begin{cases} \mu_\alpha = +0''.003^5 \\ \mu_\delta = +0''.000^5 \end{cases}$$

The four quadrants combined give:

$$\mu_\alpha = +0''.002 \qquad \mu_\delta = 0''.000.$$

c) In order to avoid points far from the center, which have an asymmetrical distribution, we may use only those within a radius of $4'.2$. We find then:

$$\text{Means for I and III} \quad \begin{cases} \mu_\alpha = +0''.001 \\ \mu_\delta = -0''.002 \end{cases}$$

$$\text{Means for II and IV} \quad \begin{cases} \mu_\alpha = +0''.004 \\ \mu_\delta = +0''.001 \end{cases}$$

The four quadrants combined give:

$$\mu_\alpha = +0''.002^5 \qquad \mu_\delta = -0''.000^5.$$

Giving equal weights to each of the three methods used, we derive as the final motion of the nebula as a whole:

$$\mu_\alpha = +0''.002 \qquad \mu_\delta = 0''.000.$$

If now we subtract these quantities from the values μ_α and μ_δ for the nebular points, we obtain results which represent the internal motions and are given in the second and third columns of Table III and plotted in Plate IV. The plate also shows the motions of the 24 comparison stars as given in Table II; these stars are surrounded by a circle. The scale of the motions is indicated in the lower right-hand corner. The arrows represent the motions in about 1300 years. The probable errors of the

PLATE IV

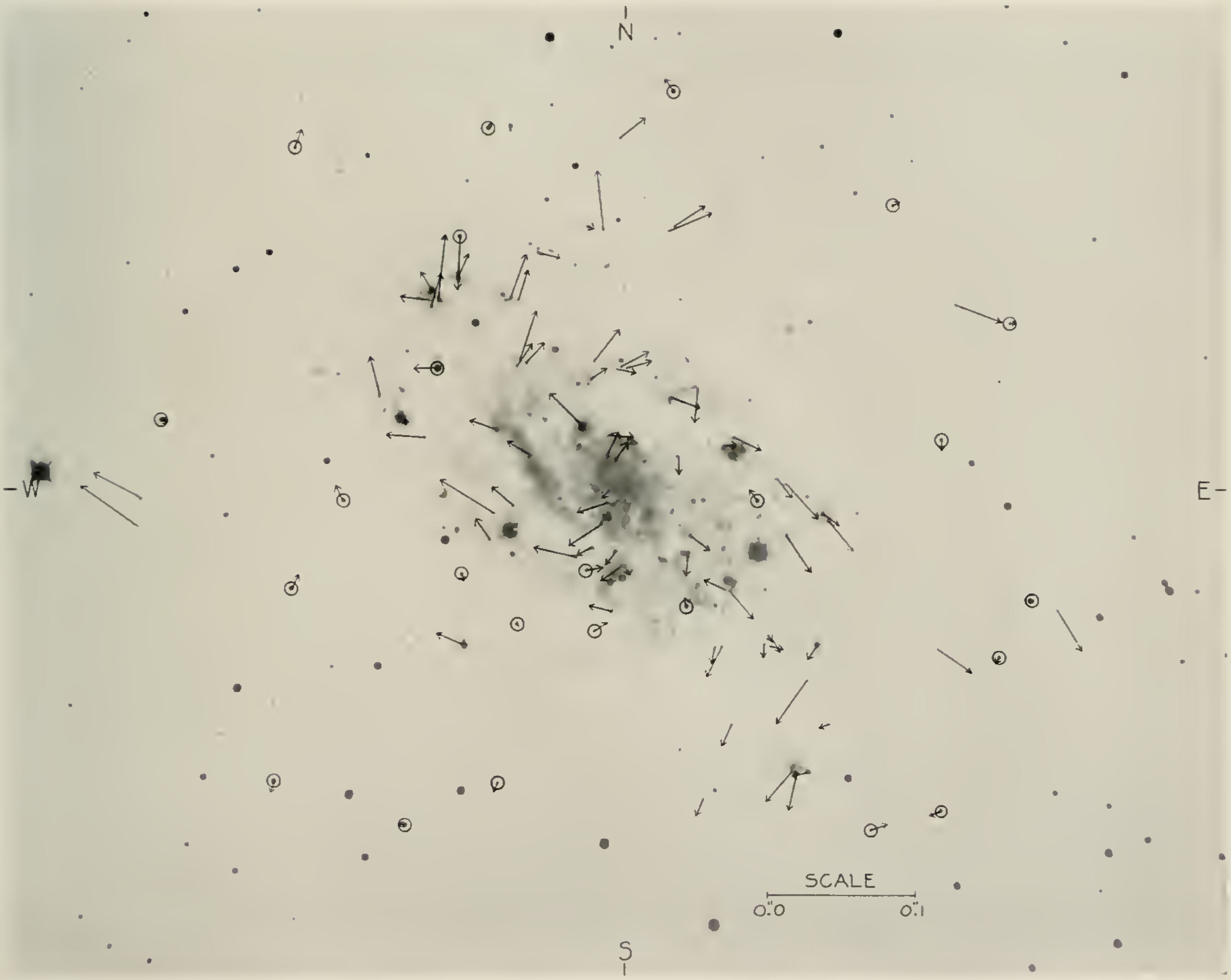

Internal Motions in N.G.C. 2403

The arrows indicate the directions and magnitudes of the mean annual motions. Their scale (0″.1) is indicated on the illustration. The scale of the nebula is 1 mm = 8″.1. The comparison stars are inclosed in circles.

TABLE III

Annual Internal Motions

No.	μ_α	μ_δ	Rotational	Radial	Stream	Transverse
1	−0″.029	+0″.018	+0″.022	+0″.028	+0″.034	+0″.012
2	−38	+26	+34	+32	+46	+8
3	−7	+13	+6	+12	+8	+10
4	−19	+2	−16	+12	−10	+18
5	+6	+22	+32	+10	+32	+6
6	+4	+42	+48	+30	+52	+20
7	+6	+16	+24	+10	+24	+6
8	−6	+27	+30	+4	+30	+4
9	−2	+2	+2	−2	+2	−2
10	−24	+1	−6	+30	−2	+30
11	−19	+8	+16	+8	+16	+8
12	−9	+14	+16	−2	+16	−6
13	−36	+23	+32	+28	+38	+20
14	−14	+12	+16	+8	+18	+4
15	−14	+8	+2	+16	+10	+14
16	−18	+5	−2	+18	+6	+16
17	+11	+15	+18	+6	+20	+2
18	+11	+31	+30	+20	+34	+16
19	+12	+13	+18	+4	+20	−2
20	+7	+20	+20	+20	+26	+14
21	+10	+29	+32	+28	+38	+20
22	+14	−3	+20	−4	+18	−6
23	+17	+13	+16	+24	+20	−22
24	+4	−1	+6	0	+6	0
25	−3	+40	−4	+50	+6	+50
26	+17	+21	+24	+32	+16	+36
27	+9	+5	+14	+8	+14	+10
28	+11	−2	+14	+2	+14	+2
29	+18	+9	+18	+20	+16	+22
30	+16	+4	+14	+16	+14	+18
31	+15	−1	+18	+2	+18	−2
32	−23	+23	−8	+26	+8	+26
33	+7	+17	+14	+16	+22	+4
34	+7	+11	+10	+14	+14	+10
35	−4	−4	0	+8	0	+8
36	−21	−6	+16	+18	+24	+10
37	−22	−15	+16	+34	+24	+28
38	−10	−5	+6	+10	+12	+4
39	−28	+7	+24	+14	+28	−4
40	−7	−9	+6	+12	+12	+6
41	−13	−9	+16	+16	+22	+2
42	+1	−3	−2	+4	+2	+6
43	−15	+3	+16	+2	+16	−6
44	−5	−12	+10	+18	+18	+10
45	−7	−15	+16	+18	+24	+4
46	−2	−12	+8	+10	+12	+6
47	−10	−21	+24	+16	+30	+2
48	−1	−10	−2	+8	+6	+6
49	+9	−3	+8	+8	+12	0
50	+5	−8	−8	+8	−4	+12
51	+3	−5	+4	+10	+10	+6
52	+15	−19	+2	+22	+18	+10

TABLE III—*Continued*

No.	μ_α	μ_δ	Rotational	Radial	Stream	Transverse
53	−0″.014	+0″.006	−0″.008	+0″.016	−0″.006	−0″.016
54	− 2	− 14	+ 16	+ 8	+ 16	− 8
55	+ 13	− 10	− 2	+ 16	+ 10	+ 12
56	0	− 13	+ 14	− 12	+ 10	− 16
57	+ 19	− 7	+ 22	+ 10	+ 22	+ 10
58	− 2	− 23	+ 14	− 30	+ 12	− 30
59	+ 20	+ 13	+ 18	+ 30	+ 24	+ 26
60	+ 30	+ 12	+ 28	+ 36	+ 32	+ 32
61	+ 9	+ 1	+ 4	+ 12	+ 6	+ 10
62	+ 18	− 8	+ 16	+ 16	+ 22	+ 10
63	+ 9	− 14	+ 14	+ 4	+ 14	− 4
64	+ 21	− 24	+ 26	+ 16	+ 30	− 2
65	+ 10	− 8	+ 6	+ 10	+ 12	+ 4
66	+ 16	− 21	+ 20	+ 14	+ 24	− 2
67	+ 16	− 26	+ 26	+ 18	+ 30	− 4
68	− 6	− 10	+ 16	+ 2	+ 14	− 6
69	− 21	− 29	+ 50	+ 10	+ 48	− 16
70	− 7	− 3	+ 12	0	+ 10	− 6
71	− 17	− 20	+ 36	+ 18	+ 40	− 2
72	− 5	− 26	+ 26	+ 24	+ 36	+ 6
73	− 12	− 3	+ 16	0	+ 14	− 8
74	+ 31	− 12	+ 26	+ 26	+ 30	+ 20
75	+ 23	− 15	− 4	+ 30	+ 26	+ 14
76	+ 17	− 28	+ 28	+ 20	+ 34	0

mean annual motions for the comparison stars are 0″.0036 in α and 0″.0039 in δ; for the nebular points, 0″.0071 in α and 0″.0082 in δ.

The plate indicates motions analogous to those found for M 101, 33, 51, and 81. They may be interpreted either as a rotation combined with a radial motion outward, or as a motion along the streamers outward. In order to investigate this it is necessary to take into account the inclination of the plane of the nebula to the tangential plane of the celestial sphere. It was estimated that the intersection of the two planes is in position angle 130° and that the inclination is about 48°. A diagram was constructed in which the foreshortening of the nebula was corrected; the motions in this diagram were then resolved into (*a*) rotational and radial components; (*b*) components along and perpendicular to the arms of the spiral (stream and transverse components). The results for the individual points derived from the diagram are in the last four columns of Table III, where the positive sign is used for motions in the direction north, east, south, west, and outward.

a) The mean rotational component is $+0''.015\pm0''.001$; the mean radial component, $+0''.014\pm0''.001$. There seems, however, to be a considerable increase of the motions with distance from the center; we have:

$r=1'.4$	$\mu_{\text{rot.}}=+0''.011$	$\mu_{\text{rad.}}=+0''.013$	$n=23$
3.1	+0.015	+0.011	37
5.1	+0.015	+0.019	11
7.3	+0.023	+0.023	3
8.9	+0.028	+0.030	2

The rotational components would correspond to hypothetical periods of from 50,000 to 120,000 years.

b) The mean stream component is $+0''.019\pm0''.001$, with a transverse component $+0''.007\pm0''.001$. With increasing distances from the center we find:

$r=1'.4$	$\mu_{\text{stream.}}=+0''.015$	$\mu_{\text{trans.}}=+0''.009$	$n=23$
3.1	+0.019	+0.004	37
5.1	+0.021	+0.012	11
7.3	+0.028	−0.001	3
8.9	+0.040	+0.010	2

The evidence is then, as in the cases of M 33, 51, 81, and 101, more in favor of a motion along the streamers of the spiral, combined with some radial motion outward, than of a rotational motion.

I wish to express my thanks to Messrs. Ritchey, Pease, and Duncan, who secured the plates used, and to Mrs. Marsh, of the Computing Division, for making all the necessary duplicate computations.

Mount Wilson Observatory
May 1922

INVESTIGATIONS ON PROPER MOTION

EIGHTH PAPER: INTERNAL MOTION IN THE SPIRAL NEBULA M 94=N.G.C. 4736[1]

By ADRIAAN VAN MAANEN

ABSTRACT

Spiral nebula M 94 (N.G.C. 4736).—This beautiful object has a large nucleus surrounded by many closely packed whorls. Comparison of two plates taken in 1912 and 1921 by Pease and Duncan, respectively, gives an annual *proper motion* of the nebula with respect to 14 comparison stars, of $\mu_\alpha = -0''.014$, $\mu_\delta = 0''.000$. The motions of 32 nebular points with reference to the nebula are shown on the *photograph*, Plate V. The *internal motion* seems to be a stream motion of $0''.021$ outward along the arms of the spiral, combined with an outward transverse motion of about $0''.009$. The motion is analogous to that found for M 33, 51, 81 and 101 and for N.G.C. 2403.

Parallaxes of spiral nebulae.—A discussion of the methods of derivation leads to the conclusion that the three most reliable are: (1) Jeans's filament method, (2) comparison of proper motions and radial velocities, and (3) comparison of internal proper motions and spectroscopic velocities. These methods point to *parallaxes* of from $0''.0001$ to $0''.0010$ and indicate that the distances and sizes of the nebulae are considerably less than those required by the island universe theory.

Curtis[2] describes this nebula as "a beautiful object. From the very bright, large nucleus spring many bright, closely packed whorls, forming a bright inner oval $2' \times 1'.5$ in p. a. about 110°. These inner whorls show many stellar condensations, whose sharpness and proximity to the nucleus would seem to make this one of the most favorable examples known for the investigation of motion in spirals. Fainter, closely packed, rather uniform outer whorls bring the nebula to a size of $5' \times 3'.5$."

Three plates of this field were available for measurement, taken in 1912, 1916, and 1921. The first plate, secured by Pease, February 20, 1912, with an exposure of 3^h45^m was compared with the one taken by Duncan on January 5, 1921, with an exposure of 2^h10^m. Fifteen stars of photographic magnitude 15.5 to 17.7 were selected for comparison purposes. One of these stars, *b*, was omitted in the reductions, as it showed a considerable proper motion; this star is a double having a companion of about the eighteenth magnitude at a distance of $\pm 5''$ in $p = \pm 355°$.

---

[1] *Contributions from the Mount Wilson Observatory*, No. 243.

[2] *Lick Observatory Publications*, 13, 33, 1918.

Thirty-two points presumably belonging to the nebula had measurable images on the plates; 19 of these belong to the inner whorls, while 13 are at greater distances from the center. Table I gives

TABLE I

Co-ordinates and Measured Annual Displacements

No.	x	y	μ_α	μ_δ
a	−4′.0	+5′.7	+0″.008	+0″.004
b	−4.8	+2.6	+ 59	− 118
c	−0.8	+3.0	0	− 14
d	−1.1	+2.7	− 12	− 6
e	−6.5	−1.8	− 10	− 3
f	−5.6	−2.9	+ 4	+ 5
g	−2.9	−2.7	+ 5	+ 8
h	−0.6	−3.3	+ 3	− 12
i	+1.6	−5.5	+ 8	− 3
j	+3.5	−4.5	− 18	+ 5
k	+8.2	−1.0	+ 1	+ 4
l	+2.8	−1.2	+ 12	+ 6
m	+6.6	+2.7	+ 8	− 20
n	+4.9	+4.7	− 3	+ 3
o	+3.0	+3.2	− 7	+ 26
1	−0.7	+0.6	+ 26	+ 9
2	−0.6	+0.6	+ 12	+ 3
3	−0.6	+0.4	− 34	+ 24
4	−0.6	+0.2	− 28	+ 28
5	−1.6	+0.4	− 49	+ 31
6	−1.9	−0.9	− 53	+ 11
7	−1.3	−0.9	− 70	+ 17
8	−0.9	−1.3	− 24	+ 20
9	−0.6	−1.5	− 50	− 6
10	−0.6	−0.1	− 26	+ 14
11	−0.1	−0.4	− 44	− 12
12	−0.2	−0.6	− 32	+ 4
13	+0.1	−0.5	− 19	− 3
14	0.0	−0.6	− 35	+ 18
15	+0.4	−0.5	− 41	− 21
16	+0.4	−0.6	− 34	− 28
17	+0.5	−0.8	− 24	− 30
18	+0.9	−0.6	+ 12	− 7
19	+0.8	−0.6	− 12	+ 9
20	+2.3	−1.1	− 3	− 30
21	+2.2	−0.8	− 7	− 8
22	+2.0	−0.6	− 10	+ 4
23	+0.9	+0.2	+ 3	+ 1
24	+0.7	+0.3	+ 24	− 19
25	+0.5	+0.5	− 7	− 12
26	+0.3	+0.6	+ 39	− 6
27	−0.1	+0.7	− 11	− 1
28	+1.0	+1.4	− 16	− 3
29	+0.7	+1.4	+ 16	+ 18
30	+3.0	+1.8	− 6	− 32
31	+2.0	+1.1	+ 31	− 6
32	0′.0	−1′.6	−0″.057	+0″.010

the position and the annual motions in right-ascension and declination of the objects measured. The results were obtained in the same way as for the spirals discussed in earlier papers.[1]

The measures were as a whole rather difficult; the exposures were too long to prevent the points in the inner whorls from showing large images imbedded in much nebulosity; on the other hand the exposures were too short to give strong enough images of the points in the outer whorls.

As in all other cases previously discussed, the motions thus found are relative to the comparison stars. In order to derive the internal motions the results must be freed from the total motion of the nebula. We have therefore followed the same process as for M 101, 33, 51, 81, and N.G.C. 2403.

All 32 points give for the mean motion of the nebula:

$$\mu_\alpha = -0\overset{''}{.}015 \qquad \mu_\delta = 0\overset{''}{.}000.$$

Dividing the points according to the four quadrants, we have:

Means for I and III,

$$\mu_\alpha = -0\overset{''}{.}016^5 \qquad \mu_\delta = +0\overset{''}{.}000^5.$$

Means for II and IV,

$$\mu_\alpha = -0\overset{''}{.}014^5 \qquad \mu\ = +0\overset{''}{.}001.$$

The four quadrants combined give:

$$\mu_\alpha = -0\overset{''}{.}015^5 \qquad \mu_\delta = +0\overset{''}{.}001.$$

Using only the 19 points of the inner whorls, we find:

Means for I and III

$$\mu_\alpha = -0\overset{''}{.}009^5 \qquad \mu_\delta = -0\overset{''}{.}001^5.$$

Means for II and IV

$$\mu_\alpha = -0\overset{''}{.}013^5 \qquad \mu_\delta = 0\overset{''}{.}000.$$

---

[1] *Mt. Wilson Contr.*, No. 118; *Astrophysical Journal*, **44**, 210, 1916; *Mt. Wilson Contr.*, No. 213; *Astrophysical Journal*, **54**, 237, 1921; *Mt. Wilson Contr.*, No. 214; *Astrophysical Journal*, **54**, 347, 1921; *Mt. Wilson Contr.*, No. 242; *Astrophysical Journal*, **56**, 200, 1922.

216

PLATE V

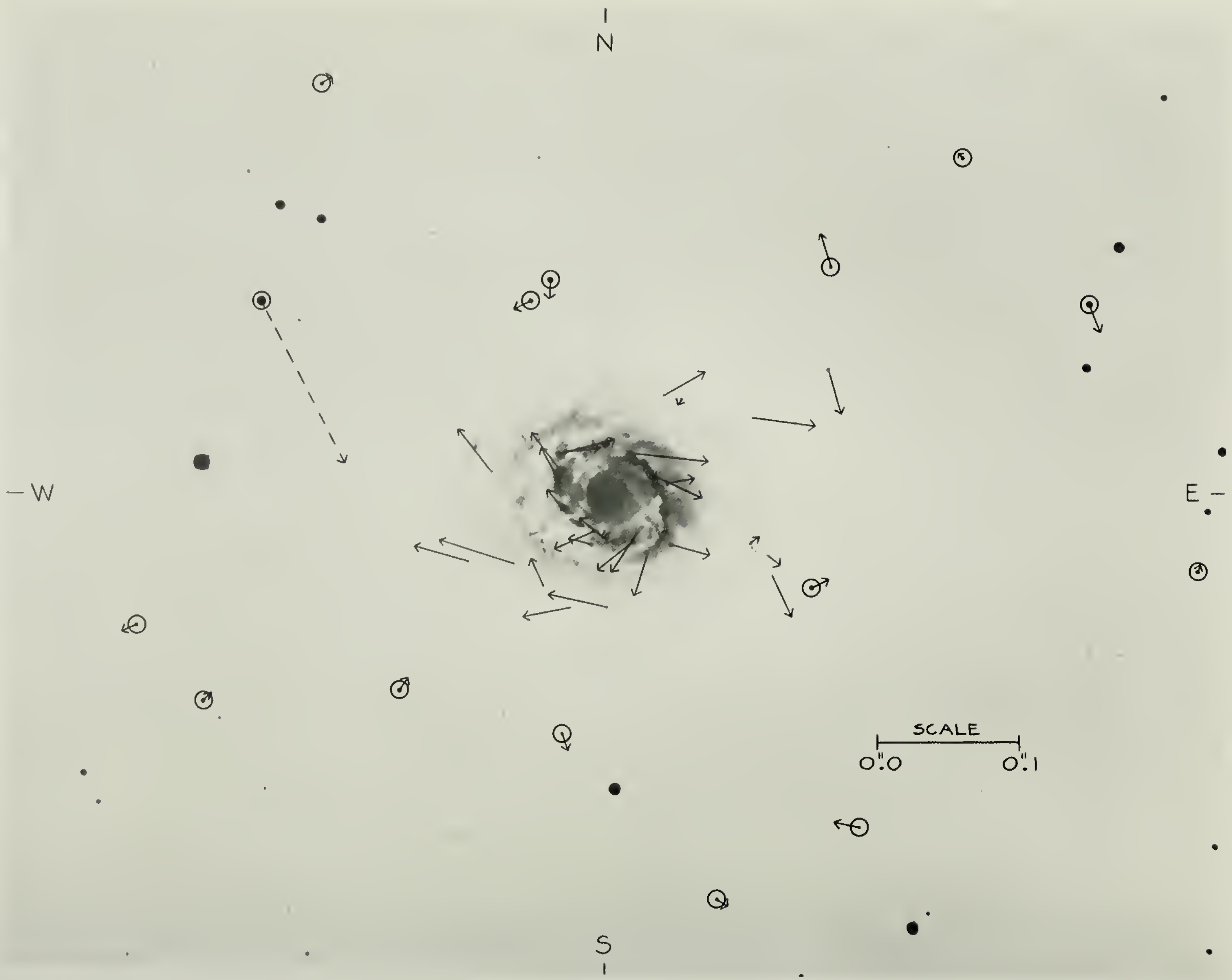

Internal Motions in N.G.C. 4736

The arrows indicate the directions and magnitudes of the annual motions. Their scale (0″.1) is indicated on the illustration. The scale of the nebula is 1 mm = 6″.7. The comparison stars are inclosed in circles.

The four quadrants combined give:

$$\mu_\alpha = -0''.011^5 \qquad \mu_\delta = -0''.001.$$

Giving equal weights to each of the three methods, we derive as the final motion of the nebula as a whole:

$$\mu_\alpha = -0''.014 \qquad \mu_\delta = 0''.000.$$

If now we subtract these quantities from the values μ_α and μ_δ for the nebular points, we obtain results which represent the internal motions. These are given in the second and third columns of Table II and plotted in Plate V. The plate also shows the motions of the 15 stars as given in Table I; the stars are surrounded by

TABLE II

ANNUAL INTERNAL MOTIONS

No.	μ_α	μ_δ	Rotational	Radial	Stream	Transverse
1	+0″.040	+0″.009	+0″.033	−0″.026	+0″.037	−0″.020
2	+ 26	+ 3	+ 23	− 15	+ 23	− 14
3	− 20	+ 24	+ 10	+ 29	+ 19	+ 24
4	− 14	+ 28	+ 22	+ 22	+ 26	+ 13
5	− 35	+ 31	+ 24	+ 39	+ 27	+ 37
6	− 39	+ 11	+ 24	+ 31	+ 30	+ 26
7	− 56	+ 17	+ 43	+ 38	+ 47	+ 33
8	− 10	+ 20	+ 20	− 10	+ 17	− 14
9	− 36	− 6	+ 30	+ 19	+ 31	+ 17
10	− 12	+ 14	+ 15	+ 9	+ 16	+ 7
11	− 30	− 12	+ 19	+ 25	+ 25	+ 18
12	− 18	+ 4	+ 17	+ 3	+ 17	0
13	− 5	− 3	+ 4	+ 3	+ 3	+ 4
14	− 21	+ 18	+ 21	− 17	+ 21	− 17
15	− 27	− 21	+ 33	+ 6	+ 31	+ 12
16	− 20	− 28	+ 32	+ 11	+ 30	+ 15
17	− 10	− 30	+ 24	+ 20	+ 23	+ 21
18	+ 26	− 7	− 10	+ 26	− 13	+ 25
19	+ 2	+ 9	− 9	− 3	− 9	− 1
20	+ 11	− 30	+ 21	+ 24	+ 24	+ 21
21	+ 7	− 8	+ 5	+ 10	+ 8	+ 8
22	+ 4	+ 4	− 5	+ 3	− 4	+ 5
23	+ 17	+ 1	+ 5	+ 17	+ 6	+ 17
24	+ 38	− 19	+ 34	+ 27	+ 33	+ 28
25	+ 7	− 12	+ 13	− 7	+ 14	− 3
26	+ 53	− 6	+ 53	+ 12	+ 54	0
27	+ 3	− 1	+ 3	− 3	+ 3	− 2
28	− 2	− 3	0	− 4	− 1	− 4
29	+ 30	+ 18	+ 19	+ 29	+ 27	+ 20
30	+ 8	− 32	+ 31	− 12	+ 29	− 16
31	+ 45	− 6	+ 28	+ 37	+ 32	+ 33
32	−0″.043	+0″.010	+0″.042	−0″.010	+0″.041	−0″.012

circles; the motion of star *b*, which was excluded for comparison purposes on account of its considerable proper motion, is indicated by a broken line. The scale of the motions is indicated in the lower right-hand corner of the plate.

The internal motions were then resolved into: (*a*) rotational and radial components; (*b*) components along and at right angles to the spiral arms (stream and transverse components).

The results are given in the fourth, fifth, sixth, and seventh columns of Table II.

a) The mean rotational component is $+0''.020 \pm 0''.002$, the mean radial component, $+0''.010 \pm 0''.002$. For the points belonging to the inner whorls, with a mean distance from the center $r = 0'.7$, the values are

$$\mu_{\text{rot.}} = +0''.018 \qquad \mu_{\text{rad.}} = +0''.007.$$

For those in the outer whorls, ($r = 2'.0$) we have

$$\mu_{\text{rot.}} = +0''.022 \qquad \mu_{\text{rad.}} = +0''.015.$$

b) The mean stream component is $+0''.021 \pm 0''.002$, the mean transverse component, $+0''.009 \pm 0''.002$; the results for the inner and the outer whorl separately are:

Inner whorls $\mu_{\text{stream}} = +0''.019$ $\mu_{\text{trans.}} = +0''.007$.
Outer whorls $\mu_{\text{stream}} = +0''.024$ $\mu_{\text{trans.}} = +0''.012$.

Although in N.G.C. 4736 the whorls are so closely packed and so nearly circular that the difference between rotation and stream-motion is necessarily small, yet the latter seems to interpret the motions a little more satisfactorily than the former. Analogous results were found for the other spirals, except that the resemblance to stream-motion is considerably stronger in all cases. From the material now available it seems therefore necessary to give up the idea that the motions found represent a rotation. In my first paper on the internal motions in spirals[1] I computed from the rotatory components the possible masses for the spirals; this example has later been followed by Lundmark,[2] McLaughlin[3] and others. Since now, however, it seems necessary to abandon the conception that we are dealing with rotation, we must at least for the present abstain from deriving conclusions as to the masses of the central bodies.

---

[1] *Mt. Wilson Contr.*, No. 118, 1916; *Astrophysical Journal*, **44**, 210, 1916.

[2] *Publications Society of the Pacific*, **34**, 113, 1922.

[3] *Popular Astronomy*, **30**, 294, 1922.

The problem of the distances of the spiral nebulae has been discussed by several astronomers during the last few years, principally by Curtis and Lundmark. In his exhaustive study, "The relations of the Globular Clusters and Spiral Nebulae to the Stellar System,"[1] Lundmark approaches the subject in not less than nine different ways. Some of these are based on the supposition that the spirals are comparable in size to the Milky Way system or to the Magellanic Clouds and thus start from assumptions which we are just trying to examine by deriving their distances. As examples we may quote Wolf's comparison of the caves in the Milky Way and in spiral nebulae and the hypothesis that the Magellanic Clouds are spiral nebulae. It is true that the large Magellanic Cloud resembles in appearance the nebula N.G.C. 4449, but then N.G.C. 4449 is far from a typical spiral. Curtis, for instance, describes this object as: "A very bright and interesting object, filling a space about $3'.5 \times 2'$. It is of exceedingly irregular structure, with many almost stellar condensations, and a bright nearly stellar nucleus. Of spiral type, as to nebulosity, but with very little evidence of spiral form."

Another derivation of the distances of spiral nebulae has been based on the appearance of novae in them. Assuming the absolute magnitudes of these novae to be the same as those in the Milky Way, a parallax can be derived. The assumption, however, that the novae in the Milky Way and those in the spirals have the same absolute magnitude is open to question. Of the 30 novae, more or less, which have been found in spirals, all but two (in N.G.C. 4321) appear in spirals showing a large amount of nebulosity. Attention has not before been called to this fact; why, for instance, has no nova ever been found in M 33, which resembles very much more Easton's structure of the Milky Way than does the Andromeda nebula? It is true that there exist a greater number of photographs of the Andromeda nebula; but of M 33 the Mount Wilson

---

[1] Dissertation, 1920. The work has been extended in several recent articles in the *Publications of the Astronomical Society of the Pacific*.

Observatory has available more than two dozen plates, all of which have been examined, principally by Messrs. Duncan and Humason, yet not a single nova has been found, while in the Andromeda nebula one in every two or three plates shows the image of a nova.

Of the other ways of determining the parallaxes of the spiral nebulae, the following may be mentioned.

a) The direct determinations seem to be unsatisfactory; the parallaxes derived by Barnard for the Andromeda nebula and by van Maanen for three spirals indicate that their parallaxes are smaller than the probable errors. This point might have been omitted if Bohlin[1] had not recently called attention to the large parallax derived by him for the Andromeda nebula, for which Barnard found $\pi = 0\overset{''}{.}000$ and van Maanen $+0\overset{''}{.}004$. Bohlin's measures are based on plates with the 6-inch Steinheil objective of the Stockholm Observatory, and it is well known from the researches of Kapteyn and others, that on plates taken with the smaller instruments, systematic errors of considerable size appear, especially if the hour-angles are large.

b) Star counts by Lundmark in the region of the Andromeda nebula show an increase of stars near the center; in M 33 there is no indication of an increase or a decrease in the number of stars as we approach the center of the plate. Lundmark concludes that these two spirals do not seem to absorb the light of stars as faint as magnitudes 16.5 and 15.7, respectively, and derives as a minimum parallax $0\overset{''}{.}000360$ and $0\overset{''}{.}000498$, respectively.

c) An ingenious method of determining the parallaxes of spiral nebulae was proposed by Jeans.[2] It is based on the conditions necessary for the breaking up of the line elements of the filaments thrown off by the nucleus. For M 101 Jeans thus derives a parallax of $0\overset{''}{.}001$. Although no great stress should be laid on this figure, it gives an indication of the order of magnitude of the distances.

d) Curtis has derived the proper motions of many of the spirals for which plates had been taken at the Lick Observatory. In his later papers, he does not use these motions, on the supposition that they are not real motions but due to the accidental errors of the measures. Lately, however, Lundmark has derived the motions of several spiral nebulae from the positions given in several catalogues. Comparing his motions with those of Curtis, I find, after the necessary corrections for a systematic difference, that they agree in sign in 62 per cent of the cases. As, moreover, the twelve values derived by van Maanen show an agreement in sign with Curtis' values in not less than 75 per cent of the cases, we must come to the conclusion that Curtis' results are not altogether due to the influence of accidental errors. Another point shows this too; from the radial velocities we find a relation between the size of the spirals and their motion, the smaller spirals having the larger motions. The results are given in the second column of Table III, while the third column gives the number of objects included. As we find an analogous relation for the proper motions, which are given in the fourth column, we must conclude that these are at least partly real.

---

[1] *Jubiläums Nummer, Astronomische Nachrichten*, 1921.

[2] *Problems of Cosmogeny and Stellar Dynamics*, p. 217 (1919).

TABLE III

Diameter	V	n	$\bar{\mu}$	n^1
	km/sec.			
>10′	339	5	0″.031	6
5′–10′	474	9	0.032	10
<5′	826	10	0.041	13

If then we use Curtis' mean motion of 0″.033 for the 66 largest spirals, and compare this value with the mean radial velocity, we derive a mean parallax of 0″.0003. Dr. Lundmark, who has recently computed the apices and mean parallaxes derived from Curtis' and his own proper motions, kindly allows me to mention his result in advance of publication. Using 800 km/sec. for Campbell's K-term in the solution he finds:

Mean parallax from 67 motions derived by Curtis, 0″.00010
Mean parallax from 82 motions derived by Lundmark, 0″.00011

The value of K is as yet very uncertain; smaller values of K will give larger parallaxes, and vice versa.

e) Finally we may compare the internal motions found by van Maanen with those derived by spectroscopic means; these amount to a few hundred kilometers per second; the comparison yields parallaxes of a few ten-thousandths of a second of arc, giving for the diameters of the spirals quantities from 10 to 300 light years.

Of the methods mentioned above, those under *c*, *d*, and *e* probably deserve the most credit. This material does not seem to warrant the acceptance of the island-universe theory. It is of course possible that later results may contradict this statement; but it seems well to point out that the evidence based on the best material at present available does not indicate that the spiral nebulae are comparable with our Milky Way system.

MOUNT WILSON OBSERVATORY
June 9, 1922

CORRIGENDA

ASTROPHYSICAL JOURNAL, **56**.

Page 129, Table I, column 6, line 6:
For 22,518.6 *read* 22,528.6.

Page 130, line 8 from bottom:
For initial energy *read* potential energy.

THE
ASTROPHYSICAL JOURNAL
AN INTERNATIONAL REVIEW OF SPECTROSCOPY
AND ASTRONOMICAL PHYSICS

VOLUME LVI NOVEMBER 1922 NUMBER 4

THE CEPHEID VARIABLE η AQUILAE

By CHARLES CLAYTON WYLIE

ABSTRACT

Cepheid variable η Aquilae; photometric study.—A series of 111 observations made with a photo-electric photometer during 1920, gives an accurate *light-curve* of this 4th magnitude star (Fig. 2 and Table IV). The range of variation is $1\overset{\mathrm{M}}{.}12$; the period is $7\overset{\mathrm{d}}{.}176$. The "secondary maximum" is confirmed as a pronounced halt in the decrease of light, from phase $1\overset{\mathrm{d}}{.}8$ to $2\overset{\mathrm{d}}{.}4$. Another fluctuation was indicated with maximum about phase $4\overset{\mathrm{d}}{.}3$. *Comparison with previous observations* suggests a shortening of the interval from minimum to maximum since 1900 and a gradually increasing period. Luizet's tabulation of residuals from a constant period is brought up to date (Fig. 3). There is no evidence of any decrease of period since observations began in 1784.

Change of period of Cepheid variables.—The increasing period of η Aquilae, which is contrary to the requirement of the *pulsation theory*, and the decreasing period of δ Cephei can perhaps be reconciled on the basis of the *binary theory* by assuming that η Aquilae rotates relatively faster than δ Cephei.

New variables.—*β Aquilae* seems to be a variable with a long or irregular period, for a progressive decrease of $0\overset{\mathrm{M}}{.}05$ was observed over an interval of three months (Fig. 1). The spectroscopic *binary δ Aquilae* is suspected of being an eclipsing variable with a range of about $0\overset{\mathrm{M}}{.}1$ but no period has been found.

A photo-electric study of η Aquilae, one of the best-known Cepheid variables, was undertaken at the University of Illinois in the hope that something of value might be contributed to the discussion of this type of variation. In particular, irregularities and secondary oscillations might be too small for certain detection by visual observers and yet be conspicuous in a photo-electric light-curve.

Observations were begun in July 1920 and carried through to November of that year. In all 111 observations were secured, one-third by Professor Stebbins and the remainder by myself. The variable and comparison stars are, in the Harvard system,

H.R. 7570, η Aquilae, magnitude 3.66–4.45, spectrum G.
H.R. 7377, δ Aquilae, magnitude 3.44, spectrum F.
H.R. 7602, β Aquilae, magnitude 3.90, spectrum K.

The Mt. Wilson spectral types are: η Aquilae, F9; δ Aquilae, A9; and β Aquilae, G7. An observation normally consisted of thirty-six measures taken in the following order: δ 3, η 3, β 6, η 3, δ 6, η 3, β 6, η 3, δ 3, one measure being a timing of the rate of motion of the electrometer thread between two scale divisions. Since δ Aquilae is brighter than β Aquilae, a neutral-tinted shade glass was used to reduce the light to approximate equality. Throughout this paper comparisons of other stars with δ Aquilae should be interpreted as comparisons with δ Aquilae observed through the shade glass, which reduced its light about $0^{M}.82$.

The differential correction for atmospheric extinction between η Aquilae and the comparison stars was taken from tables based on those in Müller's *Photometrie der Gestirne*. Nearly all observations were within the limits $19^{h}.0$ and $22^{h}.5$ sidereal time, during which interval the maximum tabular differential correction was for δ Aquilae, $0^{M}.018$, and for β Aquilae, $0^{M}.043$. The quantity from the table was multiplied by a factor depending on the transparency of the sky, which was obtained as in the work on σ Aquilae. The residuals from the preliminary curve were examined for a systematic hour angle correction; first, by plotting them for nights on which observations were carried on throughout nearly the entire three and a half hours during which the star could be observed; and second, by comparing residuals at different hour angles on different nights, using only the best nights. There was no indication of any appreciable systematic error remaining after the computed correction for differential extinction had been applied, although these corrections were larger than is usual in the work here.

The times were reduced to the sun, and the preliminary phases computed from the elements

$$\text{Maximum} = \text{J.D. } 2422606.562 + 7^{d}.176382 \cdot E$$

The period is that of Luizet,[1] without his harmonic term. A plot of the observations indicated that both comparison stars are probably variable. At certain times δ Aquilae was distinctly faint, in one case as much as one-tenth of a magnitude, and toward the end of the series β Aquilae was fainter than at the beginning.

In 1918 Messrs. Stebbins and Dershem used δ Aquilae as a comparison star for Nova Aquilae No. 3, and at that time it was suspected of variation.[2] It has been announced as a spectroscopic binary[3] of unknown period, and may be an eclipsing variable of small range. The other comparison star, β Aquilae, being of spectral type K, may be expected, if it varies at all, to be irregular.

As a first step toward unraveling the variations of the three stars, the observations where δ Aquilae was noticeably faint were marked. Then using only nights on which the transparency of the sky was good, and including no nights on which δ Aquilae had been marked faint at any time, the observed values of $\beta > \delta$ were plotted and a freehand curve drawn. The plotted values were compared with the curve, and one or two more rejections made on the ground that δ Aquilae was perhaps faint that night. The remainder were grouped into normal magnitudes which are given in Table II and plotted in Figure 1. From a freehand curve drawn through these normal magnitudes, the photo-electric reduction of β Aquilae to δ Aquilae could be obtained for the time of any observation.

The observed values of $\beta > \delta$ were compared with this curve, and from the residuals an unsuccessful attempt was made to get the period of variation of δ Aquilae. Phases were computed and the residuals plotted, at least around the supposed minima, for several different periods, but none was considered satisfactory. The range of variation is so small that it is probably better to await the determination of the period from spectroscopic observations.

Not knowing the variation of δ Aquilae, the following arbitrary rule was adopted. If any observed $\beta > \delta$ differed by more than $0^{\text{M}}040$ from the curve value, all comparisons with δ Aquilae were rejected on that night. If no residual exceeded $0^M.040$, but some exceeded $0^M.030$, the observations on that night were given half-weight. A few other observations had already been marked half-weight because of poor observing conditions.

---

[1] *Astronomische Nachrichten*, **163**, 361, 1903.

[2] *Astrophysical Journal*, **49**, 354, 1919.

[3] *Lick Observatory Bulletin*, **2**, 126, 1903; *Astrophysical Journal*, **39**, 265, 1914.

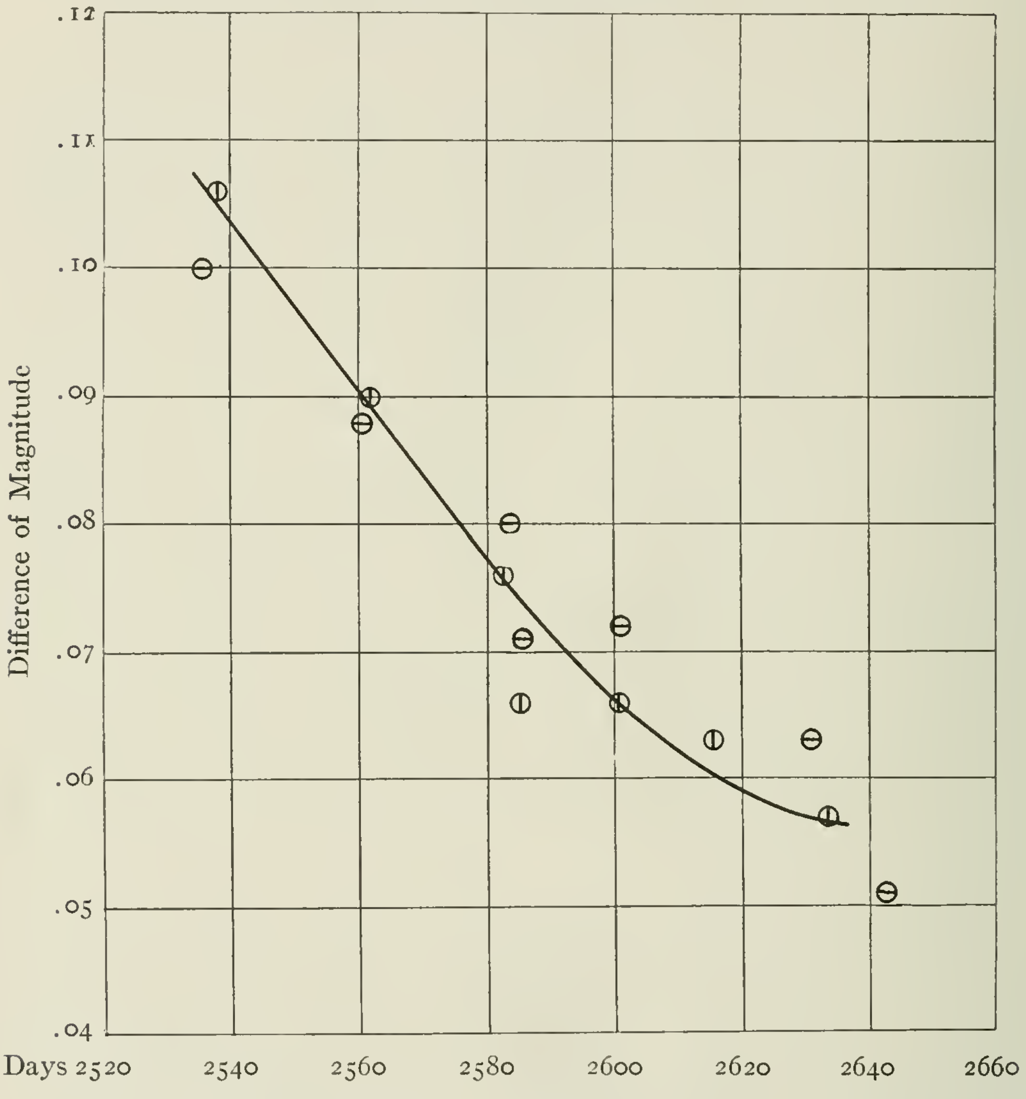

FIG. 1.—Variation of β Aquilae. Circles marked with vertical bars represent normal points from comparisons with δ Aquilae. Those marked with horizontal bars are from comparisons with η Aquilae.

Observations of $\beta > \eta$ were reduced to $\delta > \eta$ by applying the corrections scaled from Figure 1. Normal magnitudes for η were then formed, keeping the work on the two comparison stars separate, and a freehand curve drawn. As a check, the variation of β Aquilae was then determined by combining observed values of $\beta > \eta$ with the light-curve of η as based on δ, using only good nights. These computed values of $\beta > \delta$ as derived through η were assembled into normal magnitudes, which are plotted in Figure 1 for comparison with the values of direct observation. The satisfactory agreement shows that the progressive change between β and δ during the time of observation must be due to a variation of β, and that the light variation of η repeats itself from period to period within the limits of the present measures.

The times of maximum and minimum, and the amplitude of variation for η Aquilae were derived graphically from the normal magnitudes as follows:

Maximum, phase $0^{\mathrm{d}}.09$, magnitude $-0^{\mathrm{M}}.501$
Minimum, phase $5^{\mathrm{d}}.17$, magnitude $+0^{\mathrm{M}}.616$
Maximum–minimum $2^{\mathrm{d}}.10$, amplitude $1^{\mathrm{M}}.12$

The correction to the time of maximum from the preliminary ephemeris is then $+0^{\mathrm{d}}.09$. This was applied, giving the following elements which were adopted as final:

$$\text{Maxiumm} = \text{J.D. } 2422606.652 + 7^{\mathrm{d}}.176382 \cdot E$$

Table I gives the photo-electric observations of η Aquilae. The first column gives the Greenwich mean time of observation, and the second the phase computed from the final elements; the third column gives the difference between η Aquilae direct and δ Aquilae measured through the shade glass, and the fourth is the measured difference between η Aquilae and β Aquilae. A positive sign means in each case that the comparison star was brighter than η. Rejected observations are in parentheses, and half-weight observations are noted under remarks. Since the average time of observation is the same for each star, the differences β brighter than δ are obtained by subtracting the third column from the fourth.

The normal magnitudes, with phases from the final elements, are given in Table III, and plotted in Figure 2, where points from the two comparison stars are kept separate, and the rejected δ Aquilae observations are plotted as crosses. No β Aquilae observations considered satisfactory at the time of making have been rejected, so all comparisons with that star are incorporated in the normal points.

TABLE I

OBSERVATIONS OF η AQUILAE

Date, G.M.T.	Phase	Difference of Magnitude		Remarks
		δ	β	
2422523.712	3$^{\mathrm{d}}$.182	(+0$^{\mathrm{M}}$.282)	....	
.717	3.187	....	+0$^{\mathrm{M}}$.345	
.746	3.216	(+ .255)	....	
.751	3.221	....	+ .384	
2524.706	4.176	+ .448	+ .552	
.804	4.274	+ .455	+ .566	
2525.765	5.235	+ .588	+ .680	
2526.711	6.181	+ .138	+ .262	
2528.713	1.006	− .280	− .133	δ half-weight
.813	1.106	− .216	− .120	δ half-weight
2530.761	3.054	+ .211	+ .294	
2532.682	4.975	+ .606	+ .718	
2533.713	6.006	+ .270	+ .384	
.784	6.077	+ .189	+ .283	
2534.661	6.954	(− .566)	− .332	
.749	7.042	(− .536)	− .365	
.801	7.094	(− .500)	− .420	
2537.739	2.856	+ .116	+ .206	
2538.662	3.779	+ .366	+ .467	
.760	3.877	+ .377	+ .483	
2539.675	4.792	+ .566	+ .686	
.756	4.873	+ .591	+ .699	
2540.685	5.802	+ .404	+ .517	
.742	5.859	+ .364	+ .468	
2553.671	4.435	(+ .492)	+ .598	
.729	4.493	(+ .456)	+ .643	
2554.604	5.368	+ .563	+ .682	
.679	5.443	+ .559	+ .654	
2555.607	6.371	+ .005	+ .126	
2558.786	2.374	− .070	+ .036	
2559.717	3.305	+ .273	+ .370	
2561.731	5.319	+ .597	+ .681	
2566.622	3.032	+ .225	+ .296	
2567.599	4.009	+ .383	+ .506	δ half-weight
.738	4.148	+ .393	+ .496	δ half-weight
2570.594	7.004	− .443	− .381	
.659	7.069	− .470	− .427	
2573.709	2.943	+ .106	+ .220	δ half-weight
2580.585	2.642	− .008	+ .058	
.689	2.746	+ .053	+ .106	
2583.604	5.661	+ .499	+ .549	
.669	5.726	+ .471	+ .559	
.703	5.760	+ .424	+ .522	
2584.562	6.619	− .140	− .068	
.634	6.691	− .216	− .147	
.665	6.722	− .278	− .194	
.694	6.751	− .273	− .222	
2585.560	0.440	− .427	− .363	
.586	0.466	− .410	− .359	
.634	0.514	− .414	− .340	

TABLE I—*Continued*

Date, G.M.T.	Phase	Difference of Magnitude		Remarks
		δ	β	
2422585.649	$0^{\mathrm{d}}.529$	$-0^{\mathrm{M}}.389$	$-0^{\mathrm{M}}.328$	
.664	0.544	− .377	− .315	
.679	0.559	− .390	− .322	
2586.552	1.432	(− .127)	− .045	
.599	1.479	(− .123)	− .014	
.643	1.523	(− .122)	− .008	
.685	1.565	(− .119)	− .044	
2587.560	2.440	− .029	+ .042	
2588.549	3.429	+ .302	+ .392	
.620	3.500	+ .291	+ .391	
2592.557	0.260	(− .472)	− .378	
.617	0.320	(− .491)	− .371	
.656	0.359	(− .511)	− .362	
.676	0.379	(− .430)	− .382	
2593.543	1.246	....	− .082	β half-weight
.576	1.279	(− .158)	− .077	
.636	1.339	(− .194)	− .076	
.660	1.363	(− .151)	− .088	
2594.559	2.262	− .033	+ .048	Half-weight
2596.613	4.316	+ .465	+ .553	
2598.628	6.331	(+ .059)	+ .081	β half-weight
.648	6.351	(+ .040)	+ .094	
2599.615	0.141	− .469	− .417	δ half-weight
.662	0.188	− .500	− .398	δ half-weight
2600.545	1.071	− .208	− .144	
.599	1.125	− .188	− .131	
.644	1.170	− .203	− .135	
2601.569	2.095	− .074	+ .012	
.590	2.116	− .032	+ .029	
.636	2.162	− .068	+ .002	
.655	2.181	− .051	− .011	
2603.604	4.130	+ .433	+ .498	
2604.633	5.159	+ .616	+ .690	
2605.526	6.051	+ .250	+ .342	
.598	6.123	+ .191	+ .254	
2606.537	7.062	− .487	− .396	
.577	7.102	− .495	− .415	
2607.547	0.896	(− .304)	− .220	
.572	0.921	(− .337)	− .206	
.589	0.938	(− .315)	− .178	
2608.544	1.893	− .042	+ .018	
.587	1.936	− .054	+ .015	
.632	1.981	− .084	− .006	Half-weight
2609.581	2.930	+ .120	+ .215	
2614.545	0.718	− .346	− .286	
2615.535	1.707	(− .055)	+ .011	
.558	1.730	(− .107)	+ .009	β half-weight
2618.547	4.719	+ .566	+ .637	
.587	4.759	+ .558	+ .624	
2619.515	5.687	+ .481	+ .558	δ half-weight
.558	5.730	+ .437	+ .537	δ half-weight
2626.553	5.547	+ .542	+ .609	

TABLE I—*Continued*

DATE, G.M.T.	PHASE	DIFFERENCE OF MAGNITUDE		REMARKS
		δ	β	
2422627.540	$6^{d}.534$	$-0^{M}.073$	$-0^{M}.026$	
.558	6.552	− .074	− .032	
2628.542	0.360	− .450	− .367	
.565	0.383	− .476	− .392	
2632.561	4.379	+ .505	+ .558	
2633.515	5.333	+ .588	+ .648	
2641.535	6.175	+ .170	+ .210	
2642.531	7.171	− .485	− .449	
2649.494	6.958	− .422	− .387	

The adopted light-curve of η Aquilae is given in Table IV. It has not been drawn on Figure 2, as the observations themselves mark the course of the curve satisfactorily. Further, anyone examining suspected fluctuations will probably prefer a plot of the observations free from any evidence as to the judgment of others.

TABLE II

NORMAL MAGNITUDES OF β AQUILAE

Date, G.M.T.	Difference of Magnitude $\beta > \delta$	Number of Observations
2422537.7	$0^{M}.106$	7
2561.7	.090	4
2582.2	.076	4
2585.2	.066	10
2600.7	.066	8
2615.5	.063	1
2633.0	.057	2

A glance at the figure shows that the reality of a considerable "hump" cannot be questioned. Since absolutely all of the observations are represented in Figure 2, it is evident that the variations of β and δ do not affect the establishment of this secondary fluctuation. Luizet's[1] description of the irregularity, "comme un arrêt dans la diminution d'éclat de la variable," or the German "Stillstand," fits the photo-electric curve. The observations indicate a practically constant magnitude for about $0^{\mathrm{d}}.6$ beginning at phase $1^{\mathrm{d}}.8$. Some of the older curves from visual observations show a pronounced increase in brightness at this point. It was considered a real "secondary maximum," but most of the more recent light-curves have been drawn with no irregularity in the downward slope.[1] The modern tendency is to regard with suspicion permanent irregularities in curves by any but the most accurate photometric methods.[2] Photo-electric work has in general justified this skepticism, but in this particular instance we find confirmation of a secondary oscillation in Cepheid variation, while in addition to the pronounced secondary, there is indication of another fluctuation with maximum about phase four days. Lockyer believed the irregularities due to a secondary oscillation with period $1^{\mathrm{d}}.8$, one-

---

[1] *Astronomische Nachrichten*, 163, 364, 1903.

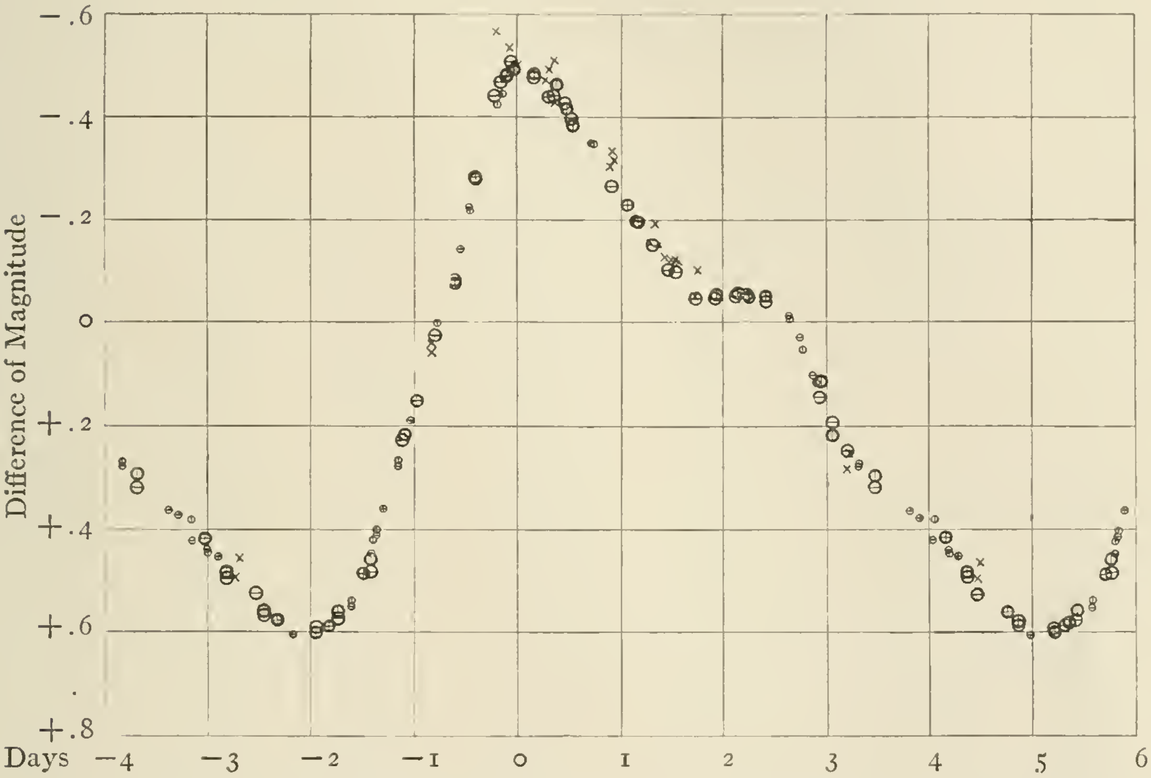

FIG. 2.—Normal magnitudes of η Aquilae. The smaller circles represent single observations and the larger circles normals of two or more observations. Comparison with δ Aquilae are marked with vertical bars and those with β Aquilae with horizontal bars. Rejected observations are plotted as crosses.

---

[1] *Ibid.*, 183, 265–278, 1909; 214, 195, 1921; *Mt. Wilson Contr.*, 7, 14, 1916.

[2] *Publications American Astronomical Society*, 4, 265, 1921.

fourth that of the principal light variation. But it is evident they cannot be represented by superposing a simple sine curve of any period on the principal variation. Using Lockyer's subperiod we might assume that the secondary oscillation rises to its strongest maximum about phase $2^{\mathrm{d}}.5$. A weaker maximum is reached at phase $4^{\mathrm{d}}.3$, the following minimum being coincident with the principal minimum. The two succeeding secondary fluctuations are negligible.

TABLE III

NORMAL MAGNITUDES OF η AQUILAE

PHASE	DIFFERENCE OF MAGNITUDE		NO. OBS.	PHASE	DIFFERENCE OF MAGNITUDE		NO. OBS.
	δ	β (reduced)			δ	β (reduced)	
$0^{\mathrm{d}}.164$	$-0^{\mathrm{M}}.484$	$-0^{\mathrm{M}}.474$	2	$4^{\mathrm{d}}.274$	$+0^{\mathrm{M}}.455$	$+0^{\mathrm{M}}.451$	1
0.313	....	− .440	3	4.348	+ .485	+ .494	2
0.372	− .463	....	2	4.464	....	+ .526	2
0.374	....	− .442	3	4.739	+ .562	+ .570	2
0.473	− .417	− .428	3	4.832	+ .578	+ .588	2
0.544	− .385	− .396	3	4.975	+ .606	+ .609	1
0.718	− .346	− .347	1	5.197	+ .602	+ .596	2
0.918	....	− .264	3	5.326	+ .592	+ .592	2
1.061	....	− .229	3	5.406	+ .561	+ .574	2
1.064	− .228	....	3	5.547	+ .542	+ .551	1
1.148	− .196	− .199	2	5.674	+ .490	+ .486	2
1.315	....	− .151	4	5.727	+ .460	....	2
1.456	....	− .104	2	5.728	....	+ .481	2
1.544	....	− .100	2	5.760	+ .424	+ .447	1
1.715	....	− .050	2	5.802	+ .404	+ .413	1
1.928	− .055	− .051	3	5.859	+ .364	+ .364	1
2.124	− .058	− .052	3	6.006	+ .270	+ .276	1
2.208	− .045	− .058	2	6.064	+ .220	+ .226	2
2.407	− .050	− .044	2	6.123	+ .191	+ .190	1
2.642	− .008	− .019	1	6.178	+ .154	+ .152	2
2.746	+ .053	+ .029	1	6.355	....	+ .026	3
2.856	+ .116	+ .100	1	6.371	+ .005	....	1
2.934	+ .115	....	2	6.543	− .074	− .086	2
2.936	....	+ .146	2	6.619	− .140	− .143	1
3.043	+ .218	+ .197	2	6.691	− .216	− .222	1
3.204	....	+ .250	2	6.736	− .276	− .283	2
3.305	+ .273	+ .279	1	6.956	....	− .440	2
3.464	+ .296	+ .320	2	6.958	− .422	....	1
3.779	+ .366	+ .362	1	7.004	− .443	....	1
3.877	+ .377	+ .378	1	7.023	....	− .468	2
4.009	+ .383	+ .421	1	7.064	− .481	− .477	2
4.136	+ .420	....	2	7.123	....	− .503	3
4.139	....	+ .422	2	7.136	− .490	....	2
4.176	+ .448	+ .437	1	....	....	....	....

As a matter of some interest, the light-curve was compared with the velocity curve as determined by Wright.[1] This shows that the pronounced halt in decreasing light is at apastron on the binary hypothesis, and just before the star reaches maximum volume on the pulsation hypothesis, following Eddington.

Possible variation from epoch to epoch of the light-curves of this and other Cepheids has been discussed by previous workers.[2] The photo-electric observations give evidence that there was no appreciable change in the form while the observations were in progress, and the curve is not greatly different from others published for this star. The maximum, however, is somewhat sharper, and the interval from minimum to maximum light is less than in recent curves. From those previously referred to, the values of this interval were found to be: in 1900, $2^{\mathrm{d}}38$; 1906–1907, $2^{\mathrm{d}}38$; 1917, $2^{\mathrm{d}}20$; and 1920, $2^{\mathrm{d}}10$. A decrease for the more recent series is noticeable, but in all strictness comparison should be made between curves determined with the same type of photometer.

TABLE IV

Light-Curve of η Aquilae

Phase	Difference of Magnitude	Phase	Difference of Magnitude
$-2^{\mathrm{d}}50$	$+0^{\mathrm{M}}56$	$1^{\mathrm{d}}50$	$-0^{\mathrm{M}}11$
−2.25	+ .60	1.75	− .06
−2.00	+ .61	2.00	− .05
−1.75	+ .57	2.25	− .05
−1.50	+ .49	2.50	− .03
−1.25	+ .33	2.75	+ .03
−1.00	+ .16	3.00	+ .21
−0.75	.00	3.25	+ .27
−0.50	− .20	3.50	+ .31
−0.25	− .41	3.75	+ .36
0.00	− .50	4.00	+ .40
+0.25	− .47	4.25	+ .45
0.50	− .40	4.50	+ .52
0.75	− .33	4.75	+ .57
1.00	− .24	5.00	+ .61
1.25	− .17	5.25	+ .60

---

[1] *Astrophysical Journal*, **9**, 62, 1899.

[2] Lockyer, *Dissertation*, pp. 78–86 (Göttingen, 1897); Luizet, *Astronomische Nachrichten*, **193**, 83, 1912; Shapley, *Mt. Wilson Contr.*, **6**, 179, 1915; Jordan, *Publications American Astronomical Society*, **4**, 265, 1921.

The variation of the period of η Aquilae has also been discussed. Lockyer,[1] from his discussion of observations of the past century, concluded it was variable. Luizet[2] also found a variation, and included a harmonic term in his value for the period, the value which has been used by most observers of η Aquilae in recent years. On the other hand[3] some have rejected the harmonic term. The elements are

$$\begin{aligned}\text{Maximum} &= \text{J.D. } 2396168.732 + 7^{\text{d}}.176382 \cdot E \\ &\quad + 0.14 \sin (0^\circ.044 \cdot E + 304^\circ) \\ \text{Maximum} - \text{minimum} &= 2^{\text{d}}.373\end{aligned}$$

Including the harmonic term the epoch of maximum derived from the photo-electric curve gives, as correction to the ephemeris, $-0^{\text{d}}.006$. This is good agreement, provided we go no farther, but for the minimum the correction is $+0^{\text{d}}.271$, which is not so satisfactory.

A more accurate determination of the length of the period in recent years was therefore made, using the photographic observations of Kohlschütter,[4] made in 1906–1907. The photographic and photo-electric amplitudes being practically the same, comparison of the curves is direct. Using Luizet's mean period between the two series normal magnitudes were formed from the photographic observations. Three observations were combined in a normal point except on the steep portion of the curve where two were used. This steep portion, between minimum and maximum, was used in the determination of the period, as the phase can be determined with more accuracy here than at the time of maximum or minimum.

A plot showed those points nearly a quarter of a day out of phase with the photo-electric curve, a graphical determination giving as a correction $0^{\text{d}}.22$. This gives as the correction to the period $+0^{\text{d}}.00032$, from which the value for the period between 1906 and 1920 is $7^{\text{d}}.17670$.

---

[1] *Op. cit.*, p. 91.

[2] *Op. cit.*, 163, 361, 1903.

[3] Hellerich, *Dissertation*, p. 6 (Bonn, 1913); Grouiller, *Bulletin Astronomique*, Deuxième Série, 1, 356, 1922.

[4] *Astronomische Nachrichten*, 183, 265, 1909.

This value for the length of the period is so much larger than the mean values of Lockyer and Luizet, obtained from a discussion of observations of the past century, that Luizet's tabulation of corrections to an ephemeris[1] from a constant period was brought up to date. Corrections computed from the light-curves of Kohlschütter and Lacchini,[2] and from the photo-electric light-curve, were added to the list. These residuals are plotted in Figure 3, points from maxima and minima being plotted separately. Normal points are formed, giving the determinations equal weight except that in the last point the photo-electric determination has been given double weight. The normal points are connected by a heavy line.

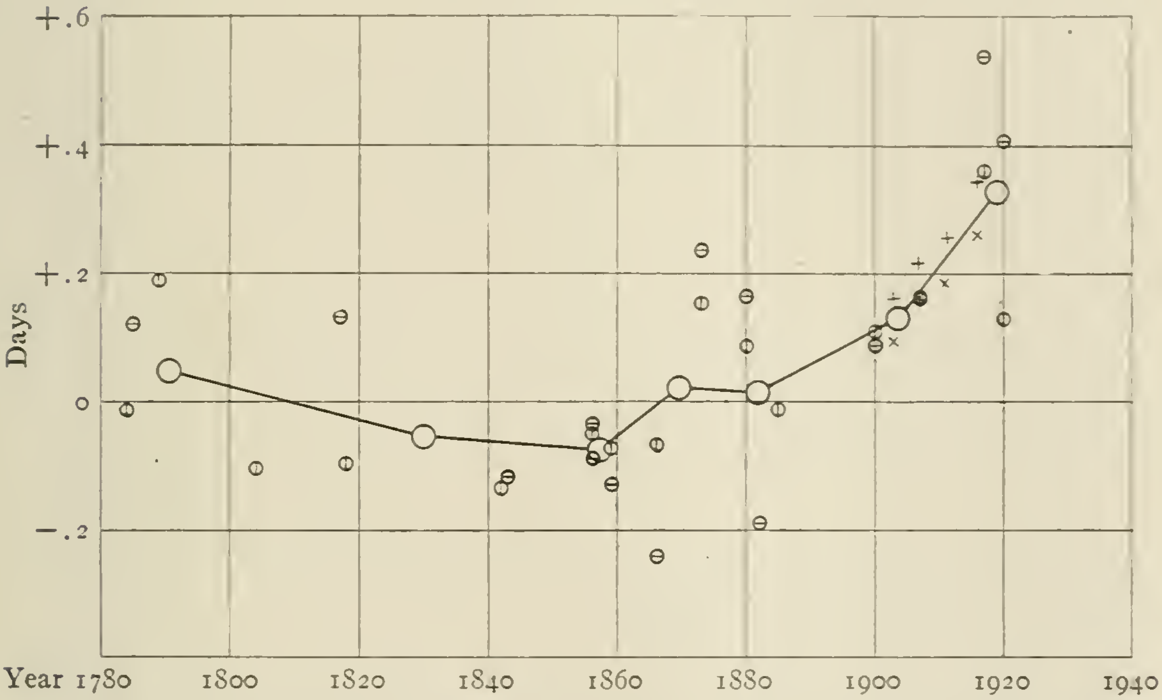

FIG. 3.—Variation in the period of η Aquilae. Points from maxima are marked with vertical bars and those from minima with horizontal bars. The large circles represent normal points. The results from Grouiller's recent values, which were not included in the normals, are plotted as plus signs and crosses, respectively.

Grouiller's monograph[3] on η Aquilae was received after the investigations of this paper were completed. His normal points from observations after 1900 are plotted on the figure as plus signs and crosses.

---

[1] *Op. cit.*, 163, 360, 1903.

[2] Lacchini, *Astronomische Nachrichten*, 214, 195, 1921.

[3] *Bulletin Astronomique*, Deuxième Série, 1, 331, 1922.

This line is distinctly concave upward, hence observational evidence indicates an increasing period at least in recent years. Certainly there is no evidence of an appreciable decrease at any time in the last 140 years. If the variation is harmonic, the available portion of the curve is too little to determine either the amplitude or the period with any accuracy. However, both must be much greater than the values found by Luizet.

The question of variation of period is of importance in Cepheid theory. The pulsation hypothesis demands a shortening of the period,[1] about 40 seconds annually for δ Cephei on the contraction theory of a star's energy. Similar conclusions follow on the rotation hypothesis, while according to the binary theory the period may either increase or decrease.[2] Tidal action should in general lengthen the period, if it is equal to or greater than the rotation period of the principal star. But if the satellite revolves in less than the rotation period, the orbital period should decrease.

There is evidence that the period of δ Cephei is decreasing.[3] If these suspected variations of period are accepted as real and attributed to tidal action, the deduction that η Aquilae probably rotates faster than δ Cephei follows.

Since either a rotation or a pulsation should affect the appearance of the spectral lines, the fact that the lines of η Aquilae are broader than those of δ Cephei is worthy of mention. δ Cephei[4] has the narrow well-defined spectral lines typical of giant stars, while the lines of η Aquilae,[5] also classed with the giant stars, "have the general characteristics of breadth and haziness, which tend to make them objectionable for purposes of accurate measurement." In a footnote to this reference the statement is made that "There is undoubtedly a resemblance between the spectra of η Aquilae and δ Cephei, the lines of the latter being, however, better defined, ..."

---

[1] Eddington, *Observatory*, **41**, 379, 1918; **42**, 339, 1919.

[2] Plummer, *Monthly Notices*, **80**, 507–509, 1920.

[3] Eddington, *op. cit.*, **42**, 338, 1919; Ludendorff, *Astronomische Nachrichten*, **212**, 185, 1920.

[4] Adams, *Observatory*, **42**, 167–168, 1919.

[5] Wright, *Astrophysical Journal*, **9**, 60, 1899.

SUMMARY

1. A series of photo-electric observations made in 1920 gives an accurate light-curve for η Aquilae.

2. The observations indicate a long period or irregular variation for β Aquilae. A progressive decrease of $0\overset{\mathrm{M}}{.}05$ is found for an interval of three months.

3. δ Aquilae, which has been announced as a spectroscopic binary of unknown period, is suspected of being an eclipsing variable with range about $0\overset{\mathrm{M}}{.}1$, but no period has been found.

4. The "secondary maximum" in the light-curve of η Aquilae is confirmed as a pronounced halt, or pause, in the decrease of light. Another fluctuation, with maximum about phase four days, is indicated.

5. Within the accuracy of the measures the light-curve did not change between July and November 1920. There has perhaps been a shortening of the interval from minimum to maximum since 1900, but accurate curves determined with the same photometric equipment and at different epochs are needed for a thorough investigation of this point.

6. The period, between 1906 and 1920, is determined by comparison with Kohlschütter's photographic observations. Luizet's tabulation of residuals from the constant period $7\overset{\mathrm{d}}{.}176382$ is brought up to date by including observations of 1906–1907, 1917, and 1920. Both methods of investigation favor an increasing period at present. The evidence is decidedly against a perceptible decrease in the period at any time since 1784.

7. The pulsation hypothesis demands a shortening of the period, while, according to the older binary theory, tidal action may increase or decrease the period. Other investigators have found evidence of a decrease in the period of δ Cephei.

Either pulsation or rotation should affect the spectral lines of a star. Attention is called to the evidence that the lines of η Aquilae are broader than those of δ Cephei, which have been examined for a pulsation effect.

University of Illinois Observatory
May 1922

THE ECLIPSING BINARY σ AQUILAE

By CHARLES CLAYTON WYLIE

ABSTRACT

Eclipsing variable star, σ Aquilae; photometric study.—A series of 97 observations with a photo-electric photometer during 1920 gives an accurate *light-curve* of this fifth-magnitude star (Fig. 1). It is found to be a normal eclipsing system with two minima and continuous variation, due to ellipticity, between eclipses. The range of variation is $0\overset{\mathrm{M}}{.}18$; the period is $1\overset{\mathrm{d}}{.}95026$. *The precision of the measurements* is such that the probable error of each of the 37 normals is $\pm 0\overset{\mathrm{M}}{.}006$. Because of the small range in partial eclipse, elements could not be determined from the light-curve alone; but since two spectra appear on the Allegheny plates of this binary, the spectroscopic orbit and estimates of relative intensity of the components enable the *elements and absolute dimensions for this system* to be given (Fig. 2 and Table VI).

Comparison star 22 Aquilae was constant within $0\overset{\mathrm{M}}{.}01$ or $0\overset{\mathrm{M}}{.}02$ from July to October 1920, but between 1918 and 1920 the observations indicate a change of $0\overset{\mathrm{M}}{.}02$ for either 22 Aquilae or σ Aquilae.

The variable radial velocity of σ Aquilae (H.R. 7474, magnitude 5.17, spectrum B8) was discovered at Mount Wilson in 1912, and the spectroscopic orbit was published by Jordan in 1916.[1] Jordan pointed out that the large value of K suggested an eclipsing system.

The spectra of two components appear on the plates of this star. Eclipsing binaries showing both spectra are the rare and favorable cases, since by combining the spectroscopic data with that from a good light-curve the dimensions of the system and the masses of the bodies can be found.

A short series of photometric observations was made on this star by Dr. Elmer Dershem at the University of Illinois in the summer of 1918. The reduction of these showed variation in light, which was announced by Professor Stebbins at the twenty-third meeting of the American Astronomical Society.[2]

A second series of observations was begun in June 1920 by Professor Stebbins and myself. This was carried to the middle of October, at which time ninety-seven observations, about equally divided between the two observers, had been secured.

With two or three exceptions each of these observations is the mean of three complete sets of measures, a set consisting of two readings on the comparison star, four on the variable, and then two more on the comparison star. Throughout the series, 22 Aquilae (H.R. 7303, magnitude 5.40, spectrum A0) was used as the comparison star.

---

[1] *Publications of the Allegheny Observatory*, 3, 189, 1916.

[2] *Publications of the American Astronomical Society*, 4, 115, 1919.

The differential correction for atmospheric extinction between σ Aquilae and 22 Aquilae was taken from tables based on those in Müller's *Photometrie der Gestirne.* It was less than $0^{\mathrm{M}}.015$ from sidereal time $17^{\mathrm{h}}.4$ to $21^{\mathrm{h}}.0$, and few measures were taken outside this limit. The correction to be applied was determined by multiplying the tabular value by a factor depending on the transparency of the sky, which was obtained in two ways: first, from the light effect of 22 Aquilae on the instrument, corrections for instrumental variation having been applied; and second, from the observer's estimate at the time of making the observation. The second method may seem somewhat crude, but the work at this observatory indicates that the estimate of an experienced observer deserves about the same weight as a result obtained by the first method. The factor for each observation was obtained by the two independent methods and the mean used. The two stars are of nearly the same spectral type, and as observations with large extinction have been rejected or given half-weight, errors due to uncertainty in this correction should be small.

The times were reduced to the sun, and the residuals from an approximate light-curve plotted using the total atmospheric extinction on σ Aquilae as abscissae. From this plot of the residuals it was decided to reject observations with an extinction greater than $0^{\mathrm{M}}.25$. Those with an extinction between $0^{\mathrm{M}}.18$ and $0^{\mathrm{M}}.25$ were given half-weight, and a few which had been marked weak for some other reason, such as smoke, were given weight one-half or three-fourths.

The center of eclipse was determined graphically, and from the epoch of the spectroscopic observations and the 1920 photometric series a correction to the Allegheny period of $+0^{\mathrm{d}}.00004$ was obtained. The available observations in 1918 were not sufficient for accurate determination of the epoch of eclipse, but a larger correction to the Allegheny period would bring them into better agreement with the 1920 series.

A plot of the residuals with the time as abscissa showed no evidence of variation in the comparison star throughout the 1920 series, but the 1918 observations were systematically high by two or three hundredths of a magnitude. Because of this, and the uncertainty in the period, the few observations of the earlier series were omitted in the formation of the normals.

By using the spectroscopic period, with the correction of $+0\overset{d}{.}00004$ derived above, and the photometric determination of epoch of eclipse the elements

$$\text{Minimum} = \text{J.D. } 2422486.797 + 1\overset{d}{.}95026 \cdot E$$

were obtained. These were adopted as final.

The photo-electric observations of σ Aquilae are given in Table I. The times were reduced to the sun, and the phases computed from the final elements given above. The difference of magnitude is the amount that σ was measured brighter than 22.

The observations of the 1920 series were then assembled according to phase and grouped into normal magnitudes. The rule was in general two observations to a normal during eclipse and three to a normal outside of eclipse. At one phase outside of eclipse two half-weight observations taken on the same night were rejected, as the others could be grouped into normals of approximately the same value. The thirty-seven resulting normal magnitudes and the residuals from the computed light-curve are given in Table II.

A plot of the normals showed a distinct ellipticity effect between minima. A periastron effect might also be suspected, but as the spectroscopic orbit is circular, this was considered error of observation. There is no appreciable reflection effect. The ellipticity factor z was obtained by Russell's graphical method, and the result used to determine the limits of the eclipses and check the definitive work which was as follows:

From normal magnitudes outside of eclipse the ellipticity effect was solved for, using the equation

$$m_0 - c \cos^2 \theta = m,$$

where m_0 denotes the maximum magnitude, m is the observed magnitude, θ is the phase from primary minimum, and c is a

TABLE I

OBSERVATIONS OF σ AQUILAE

Date, G.M.T.	Phase	Difference of Magnitude	Weight	Date, G.M.T.	Phase	Difference of Magnitude	Weight
1918 Series				2422533.615	$0^{\rm d}.017$	$(0^{\rm M}.267)$	....
(not used)				.629	0.031	(.274)	....
2421783.765	$1^{\rm d}.017$	$0^{\rm M}.353$	....	.647	0.049	.298	1/2
1785.759	1.061	.445	....	.661	0.063	.328	3/4
1786.764	0.115	.459	....	.681	0.083	.415	....
1787.773	1.124	.470	....	.692	0.094	.402	....
1793.728	1.229	.470	....	.734	0.136	.432	....
1802.771	0.520	.497	....	.744	0.146	.425	....
1804.742	0.541	.500	....	2534.603	1.005	.329	1/2
1805.740	1.539	.488	....	.619	1.021	.342	1/2
1806.751	0.600	.457	....	.633	1.035	.354	....
1813.679	1.677	.461	....	.694	1.096	.424	....
1817.665	1.762	.452	....	.710	1.112	.451	....
1827.644	0.040	.433	....	.724	1.126	.448	....
1828.649	1.045	.411	....	2537.710	0.211	.475	3/4
1837.631	0.275	.458	....	2539.609	0.160	.430	....
1845.611	0.454	.468	....	.624	0.175	.433	....
				2540.640	1.191	.455	....
1920 Series				.658	1.209	.440	....
2422486.810	0.017	.313	....	.711	1.262	.457	....
2498.774	0.279	.474	....	.722	1.273	.449	....
.840	0.345	.465	....	2553.690	0.589	.485	1/2
2506.763	0.468	.480	1/2	2554.647	1.546	.457	....
.797	0.502	.481	....	.662	1.561	.465	....
2508.796	0.551	.508	1/2	2559.690	0.738	.448	....
2509.826	1.581	.496	1/2	.699	0.747	.447	....
2514.737	0.641	.472	....	2561.694	0.791	.424	3/4
2517.711	1.665	.426	1/2	.706	0.803	.417	3/4
2521.768	1.822	.423	....	2566.690	1.887	.325	3/4
.797	1.851	.455	1/2	.708	1.905	.349	3/4
2522.711	0.814	.438	....	2567.680	0.926	.377	....
2523.646	1.749	(.405)	....	.697	0.943	.328	1/2
.672	1.775	.449	1/2	2570.619	1.915	.315	....
2524.679	0.832	.454	....	.638	1.934	.287	....
.733	0.886	.425	....	2574.614	0.059	.335	....
.750	0.903	.387	....	.634	0.079	.377	1/2
.767	0.920	.351	....	2583.630	1.273	.440	....
.782	0.935	.341	....	.645	1.288	.452	....
2525.697	1.850	.409	....	2584.600	0.293	.453	....
2526.651	0.854	.430	....	.614	0.307	.455	....
.668	0.871	.426	....	2585.606	1.299	.452	....
2528.750	1.003	.349	....	.622	1.315	.448	....
2529.681	1.934	.302	....	2587.601	1.344	.436	....
2530.615	0.917	.377	1/2	.615	1.358	.431	....
.637	0.939	.328	....	2588.592	0.384	.451	....
2531.614	1.916	.300	1/2	.605	0.397	.461	....
.672	0.024	.298	....	2589.574	1.366	.475	....
2532.642	0.994	.315	....	.594	1.386	.446	....
.701	1.053	.383	....	2593.594	1.485	(.432)	....
.734	1.086	.438	....	.608	1.499	(.424)	....
.751	1.103	.442	....	2595.595	1.536	.473	....

TABLE I—*Continued*

Date, G.M.T.	Phase	Difference of Magnitude	Weight	Date, G.M.T.	Phase	Difference of Magnitude	Weight
2422595.608....	$1^{\mathrm{d}}.549$	$0^{\mathrm{M}}.455$	....	2422605.563....	$1^{\mathrm{d}}.751$	$0^{\mathrm{M}}.441$	....
2596.554....	0.544	.462	....	.574....	1.762	.435	....
.566....	0.556	.460	....	2606.514....	0.752	.440	....
2600.581....	0.671	.441	....	2609.542....	1.830	.422	......
2603.577....	1.716	.430	....	.553....	1.841	.420	1/2
.587....	1.726	.423	....	....	....	....	....

constant. Twenty-one equations for the determination of m_0 and c gave

$$m_0 = 0^{\mathrm{M}}.467 \pm 0^{\mathrm{M}}.0025,$$
$$c = +0^{\mathrm{M}}.042 \pm 0^{\mathrm{M}}.0050,$$

from which $z = 0.075$. The ellipticity effect was removed from the observations by the formula

$$\text{Rectified magnitude} = m + 0^{\mathrm{M}}.042 \cos^2 \theta .$$

From a plot of the rectified magnitudes at secondary minimum the center of that eclipse was determined as phase $0^{\mathrm{d}}.980$, from which

TABLE II

NORMAL MAGNITUDES

Phase	Difference of Magnitude	Residual O−C	No. Obs.	Phase	Difference of Magnitude	Residual O−C	No. Obs.
$0^{\mathrm{d}}.020$.....	$0^{\mathrm{M}}.305$	$+0^{\mathrm{M}}.012$	2	$1^{\mathrm{d}}.013$.....	$0^{\mathrm{M}}.336$	$-0^{\mathrm{M}}.002$	2
0.056.....	.323	− .019	2	1.044.....	.368	− .006	2
0.069.....	.348	− .017	2	1.091.....	.431	+ .003	2
0.088.....	.408	+ .010	2	1.114.....	.447	+ .012	3
0.147.....	.429	− .004	3	1.200.....	.448	+ .005	2
0.190.....	.451	+ .012	2	1.268.....	.453	+ .001	2
0.293.....	.461	+ .009	3	1.280.....	.446	− .008	2
0.375.....	.459	− .003	3	1.319.....	.445	− .013	3
0.512.....	.473	+ .006	3	1.370.....	.451	− .012	3
0.563.....	.478	+ .013	3	1.543.....	.462	− .002	3
0.656.....	.456	.000	2	1.568.....	.475	+ .013	2
0.742.....	.448	+ .004	2	1.710.....	.426	− .019	3
0.779.....	.428	− .011	3	1.760.....	.440	+ .001	3
0.833.....	.441	+ .008	3	1.826.....	.422	− .009	2
0.878.....	.426	+ .005	2	1.848.....	.424	+ .006	3
0.908.....	.384	.000	2	1.896.....	.337	− .001	2
0.923.....	.364	− .002	2	1.915.....	.310	.000	2
0.938.....	.337	− .010	2	1.934.....	.294	+ .004	2
0.998.....	.332	+ .005	2	....	....	....	....

$e \cos \omega = +0.004$. The photometric observations are too few to show with certainty that the orbit is not perfectly circular. But the eccentricity of the spectroscopic orbit is given to only one decimal, and this value of $e \cos \omega$ seems possible. The observations about secondary minimum were therefore reflected about phase $0^{d}.980$ for further work.

From the rectified normals at both primary and secondary, elements were derived by Russell's method. It was found, however, that, as Russell has pointed out,[1] the value of k can be determined from partial eclipses of such small range only with the addition of data other than that derived from the light-curve. The assumption that the eclipses were grazing total and annular, with k about 0.33, gave the best representation of the light-curve. But this means a difference of over two magnitudes in the light of the components, while from the spectroscopic plates it is known to be much less. The estimate published with the spectroscopic orbit is a difference of $0^{M}.5$. A second independent estimate made by Jordan in April 1921 is $0^{M}.3$.

The second estimate was used, and from this, with $1-\lambda_1$ and $1-\lambda_2$ the photometric depth of minima, k, a_0, and χ were obtained. After a few approximations the following elements were adopted as satisfactory:

$\chi = 1.70$ $\quad C = 0.0799$ $\quad D = 0.0470$
$k = 1.00$ (adopted) $\quad 1-\lambda_1 = 0.121$ $\quad 1-\lambda_2 = 0.0905$.

Rectified primary minimum $= 0^{M}.327$.
Rectified secondary minimum $= 0^{M}.364$.

The adopted value for k corresponds to a difference of $0^{M}.31$ between the component stars, practically the second estimate. Using $k = 0.92$ the light-curve holds for the first estimate, $0^{M}.5$, so elements were computed for both values; but the masses of the component stars, and dimensions and inclination of the relative orbit, were found to be practically the same on the two assumptions, and only the results for $k = 1.00$ are given. An ephemeris was computed from the adopted elements, using Blazko's tables,[2] and independently by Russell's method as a check. The computed light-curve, Tables III and IV, is shown in Figure 1. The residuals

---

[1] *Astrophysical Journal*, 35, 331, 1912.

[2] *Annales de l'observatoire astronomique de Moscou*, 5, 104, 1911.

TABLE III

CONSTANTS OF THE LIGHT-CURVE

	Magnitude	Range	Light	Loss
Maximum	$0^{\mathrm{M}}.467$		1.000	
Primary minimum	0.285	$0^{\mathrm{M}}.182$	0.846	0.154
Secondary minimum	0.322	0.145	0.875	0.125
Rectified Curve				
Maximum	$0^{\mathrm{M}}.467$		1.000	
Primary minimum	0.327	$0^{\mathrm{M}}.140$	0.879	0.121
Secondary minimum	0.364	0.103	0.910	0.090

TABLE IV

LIGHT-CURVE

Phase	Difference of Magnitude	Phase	Difference of Magnitude
$\pm 0^{\mathrm{d}}.00$	$0^{\mathrm{M}}.285$	$0^{\mathrm{d}}.94$	$0^{\mathrm{M}}.345$
±0.02	.293	0.96	.328
±0.04	.316	0.98	.322
±0.06	.349	1.00	.328
±0.08	.384	1.02	.345
±0.10	.415	1.04	.370
±0.116	.430	1.06	.396
+0.15	.434	1.08	.419
0.20	.440	1.096	.430
0.30	.453	1.20	.443
0.40	.464	1.30	.457
0.488	.467	1.40	.466
0.60	.462	1.463	.467
0.70	.450	1.50	.467
0.80	.437	1.60	.459
0.864	.430	1.70	.447
0.88	.418	1.80	.434
0.90	.395	1.834	.430
0.92	.369		

from this curve are given in Table II, and from these we derive

$$\text{P.E. single normal} = \pm 0^{\mathrm{M}}.006\,.$$

The normal magnitudes are plotted as circles in Figure 1, the radius of each circle being equal to the computed probable error.

The data of the spectroscopic binary system,[1] are given in Table V. The value of sin i was known from the photometric elements. Combining this with the spectroscopic elements the absolute dimensions of the system and masses of the bodies were obtained. Following Russell,[2] the apparent diameter of the brighter star was computed from the magnitude and spectral type. From this and the actual diameter, the distance and parallax

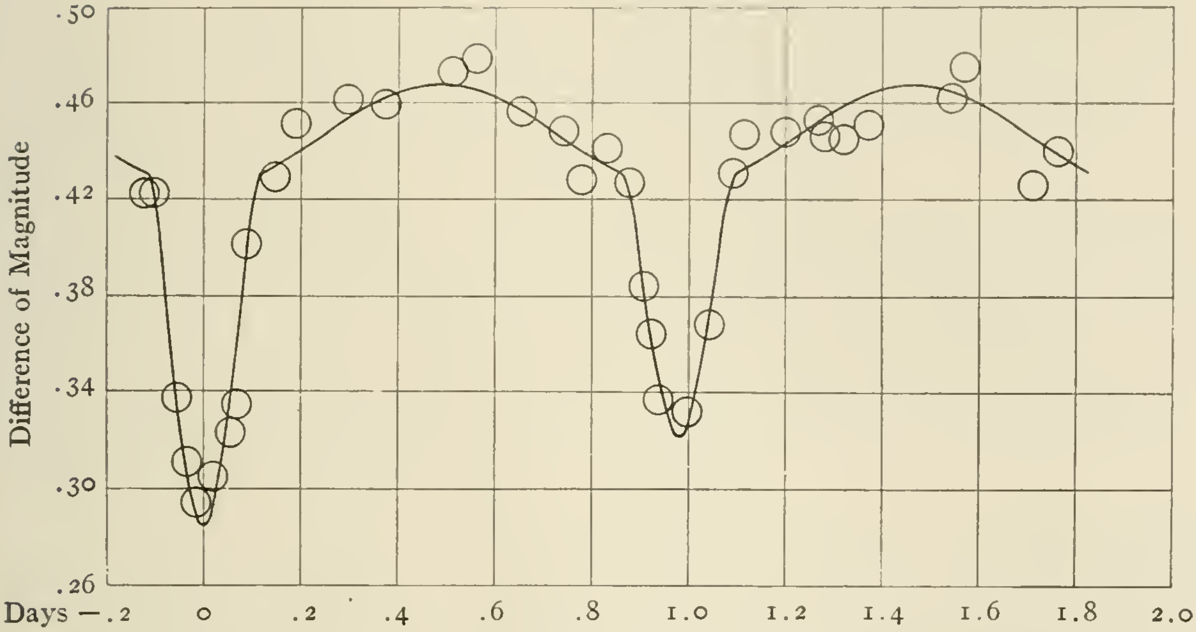

FIG. 1.—Light-Curve of σ Aquilae

TABLE V

SPECTROSCOPIC ELEMENTS OF σ AQUILAE (JORDAN)

P	$1^{\mathrm{d}}.95022$	$\pm 0^{\mathrm{d}}.0001$ (estimated)
μ	$184^{\circ}.595$	$\pm 0^{\circ}.0095$
e	0.0	±0.01
T (Max. vel.)	J.D. 2420054.331	$\pm 0^{\mathrm{d}}.0031$
γ	−5.00 km/sec.	±1.04 km/sec.
K_1	163.52 km/sec.	±1.35 km/sec.
$a_1 \sin i$	4,380,000 km	±3600 km
$m_1 \sin^3 i$	$5.3\odot$	
K_2	199 km/sec.	±4.1 km/sec.
$a_2 \sin i$	5,340,000 km	±110,000 km
$m_2 \sin^3 i$	$4.4\odot$	

---

[1] Jordan, *Allegheny Publications*, 3, 192, 1916.

[2] *Publications of the Astronomical Society of the Pacific*, 32, 315, 1920.

were obtained, the hypothetical parallax being 0″.006 corresponding to a distance of about 550 light-years.

The light elements are assembled in Table VI, and Figure 2 is the system represented by them. The ellipticity of the star disks has been neglected in the figure.

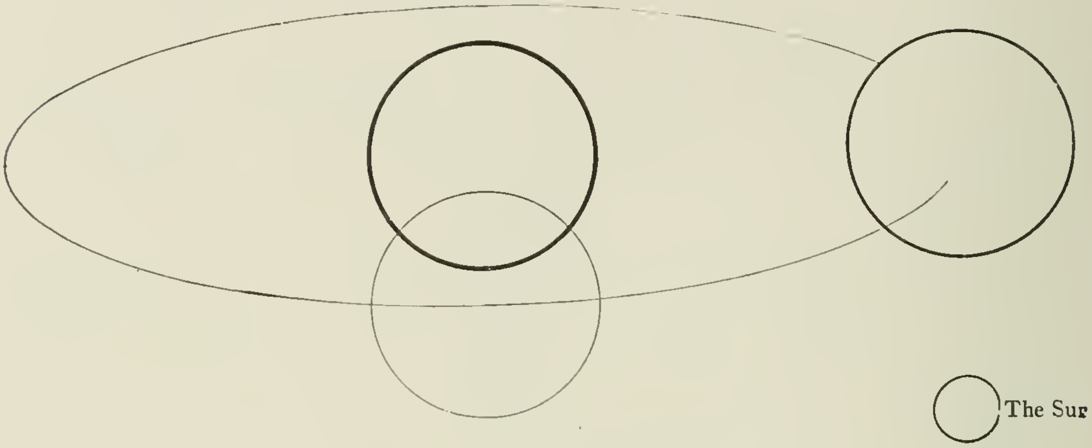

FIG. 2.—System of σ Aquilae

TABLE VI

ELEMENTS OF σ AQUILAE

Primary minimum, J.D. 242...........	......	2486.797 G.M.T
Period of revolution (photometric)......	P	$1^{d}.95026$
Phase of secondary minimum..........	......	$0^{d}.980$
Semi-duration of eclipse...............	......	$0^{d}.116$
Component of eccentricity............	$e \cos \omega$	+0.004
Cosine of inclination.................	$\cos i$	0.314
Ratio of radii........................	k	1.00
Ratio of axes.........................	b/a	0.955
Major semi-axis.......................	$a_1 = a_2$	0.242
Minor semi-axis.......................	$b_1 = b_2$	0.231
Light of brighter star................	L_1	0.572
Light of fainter star..................	L_2	0.428
Ratio of surface brightness...........	J_1/J_2	1.34
Magnitude of system..................	......	$5^{M}.17$
Magnitude of brighter star...........	......	$5^{M}.78$
Magnitude of fainter star............	......	$6^{M}.09$
From Allegheny spectroscopic elements	Sun = 1	
Major semi-axis.......................	$a_1 = a_2$	3.56
Minor semi-axis.......................	$b_1 = b_2$	3.40
Density of brighter star..............	ρ_1	0.150
Density of fainter star...............	ρ_2	0.125
Mean density of system...............	ρ_0	0.138
Mass of brighter star.................	m_1	6.19
Mass of fainter star..................	m_2	5.14
Parallax (from surface brightness)......	π	0″.006

SUMMARY

1. A series of observations made with a photo-electric photometer during 1920 gives the light-curve of σ Aquilae.

2. Using residuals from the computed curve the thirty-seven normal magnitudes show a probable error of $\pm 0^{M}.006$.

3. The comparison star 22 Aquilae was constant within the limit of the measures from July to October 1920, but a change of $0^{M}.02$ between 1918 and 1920 is indicated for either 22 Aquilae or σ Aquilae.

4. Because of the small range in partial eclipse, elements of σ Aquilae from the light-curve alone would be indeterminate, but since two spectra appear on the Allegheny plates, the information on this eclipsing system is unusually complete. The elements and absolute dimensions derived are given in Table VI, and the system is shown in Figure 2.

I am indebted to Professor Joel Stebbins for supervision and direction throughout these investigations, and for part of the observational data, and to Mr. J. K. Willy for checking some of the reductions.

University of Illinois Observatory
May 1922

A SPECTROSCOPIC METHOD OF DETERMINING THE ABSOLUTE MAGNITUDES OF A-TYPE STARS AND THE PARALLAXES OF 544 STARS

By WALTER S. ADAMS and ALFRED H. JOY[1]

ABSTRACT

Spectroscopic method of determining the absolute magnitudes of A-type stars.—In order to ascertain whether a spectroscopic method could be applied to these stars, spectrograms were obtained of nearly all the A-type stars in the Taurus and Ursa Major groups, fifty-six in all, whose absolute magnitudes are accurately known. The stars were then grouped (*a*) according to spectral type and (*b*) according to whether the lines were diffuse or sharp. A good correlation between magnitude and spectrum was found, the magnitude being brighter the earlier the spectral type and also brighter for spectra with sharp lines. The study was then extended to include all A-type stars for which both the spectral type and parallax were known, and the same correlation was found (see Fig. 1), the average difference being only $\pm 0''.0077$ for eighty-two parallaxes determined by group motion, and $0''.0131$ for 104 trigonometric parallaxes. The accuracy of parallax determinations by this method for A-type stars is thus of the same order as for stars of later types, and the method is evidently capable of considerable further refinement. A-type stars having "c" characteristics, such as α Cygni, require separate treatment, which may perhaps be based on the intensities of the well-known enhanced lines λ 4481 and λ 4233.

Spectroscopic parallaxes of 544 stars of type B7 to F2, determined on the basis of the foregoing results, are given in Table VI. When grouped according to their proper motions, the mean parallax of each group is found to increase from $0''.011$ for $\mu < 0''.010$ to $0''.037$ for μ about $0''.2$ (Fig. 2). This correlation is a very satisfactory confirmation of the accuracy of the method.

The spectroscopic methods used in the determination of the absolute magnitudes of stars of the later spectral types cannot in general be applied to those of the A-type of spectrum. With some notable exceptions, such as α Cygni and stars of similar spectra and those in which certain lines like λλ 4077, 4216, and 4481 are especially strong, the stars of this type do not show the large variations in the intensities of the lines which appear in the later types. They do, however, show very great differences in the appearance of the lines, in some stars such as Sirius the lines being sharp and well defined, and in others such as Altair very diffuse and vague. The importance of this characteristic will appear in the course of the discussion.

With a view to studying the nature of the spectra of stars of this type with known absolute magnitudes, spectrograms were obtained of nearly all the stars of type A which belong to the Taurus and the Ursa Major groups. The absolute magnitudes of these stars are known with a high degree of accuracy from the motions of the groups, and for many of the stars of the latter group trigonometric parallaxes are also available. A considerable range in absolute magnitude as well as in spectral type is found among these stars, and they afford, accordingly, excellent material for such an investigation.

---

[1] *Contributions from the Mount Wilson Observatory*, No. 244.

The first step in the study of these spectra, and as it proved the most important one, was an accurate classification of spectral type. Since the H and K lines of calcium, which form an important criterion in the classification of A stars by Miss Cannon and the other Harvard observers, are far to one side of the region of best definition on our spectrograms and do not appear at all on those taken with high dispersion, we have based our classification upon the intensities of the metallic arc lines showing in the stellar spectra. In this we were aided greatly by the use of the spectra of standard stars chosen from among those classified by Dr. Kohlschütter at this Observatory in the years 1912 to 1914. Spectra in which the helium lines do not appear and such prominent arc lines as λλ 4326 and 4384 are not present or are extremely faint are called A0. With increasing intensity of the arc lines the stars are classified as A1, A2, A3, etc. When the helium lines λλ 4026 and 4471 are just visible, the spectrum is classed as B9, and when λ 4471 and λ 4481 are equal, as B8. This system appears to be in good agreement with that of the Harvard observers and of Kohlschütter, a result which would naturally follow from the use of the standard types of the latter to check the results. A comparison of the spectral types as determined by Miss Cannon and by Kohlschütter has already been published by the Harvard College Observatory.[1]

In addition to the symbols indicating the spectral type the letters "n" for nebulous and "s" for sharp have been appended to indicate the character of the spectral lines. Thus the spectrum of Sirius is A2s and that of Altair A2n. Stars like α Cygni have the "c" characteristics noted by the Harvard observers and are indicated by cA2s, for example. The lines are always exceptionally sharp and the letter "s" is scarcely necessary. These stars are few in number and do not enter into the present discussion, but a brief reference is made to them at a later point.

---

[1] *Annals of the Harvard College Observatory*, 56.

If we separate the stars of the Taurus and Ursa Major groups into the successive spectral subdivisions obtained in this way, we find the results given in Table I. The absolute magnitudes are

TABLE I

Boss	*M*	Boss	*M*	Boss	*M*
Aon		A5n		A3s	
3117	+0.6	919	+3.0	1029	+1.3
3190	1.7	1086	2.8	2930	0.8
3752	0.4				
3961	0.3	A6n		A4s	
4009	0.6	1025	+3.2	553	+2.3
5573	1.7	1056	2.8	1046	0.7
A1n				3506	0.6
1024	+1.2	A7n			
1034	1.8	892	+3.2	A6s	
1220	0.5	991	2.5	1054	+2.1
3480	2.1	1022	2.1		
A2n		1058	3.2	A7s	
1033	+1.6	3360	2.8	1092	+2.3
1143	2.2			1122	1.9
2972	2.2	A8n		3475	2.3
A3n		1004	+2.8		
1026	+1.3	1007	2.4	A8s	
1047	2.3	1043	3.2	1114	+2.6
1051	2.8			1226	2.7
1087	1.6	Fon		2813	3.3
1194	1.6	935	+3.6	5425	1.9
A4n		1040	2.9	F1s	
1027	+2.8	A2s		961	+3.2
1067	1.9	1732	+1.3	1013	3.0
1090	1.6	3363	−0.2	1055	2.7
3382	2.7	3474	+0.6	F2s	
				1018	+2.8

those given by Rasmuson in his valuable memoir on moving clusters,[1] but a constant correction of +1.57 magnitudes has been applied to reduce to the unit of 10 parsecs instead of that of one siriometer as used by him. Six of the stars of the Ursa Major group are of type Aon and thus supplement in an important way those of the Taurus group which are of a more advanced type on the average.

---

[1] *Meddelanden från Lunds Astronomiska Observatorium*, Serie II, No. 26.

If these results are collected, we obtain the following mean absolute magnitudes for the various spectral subdivisions.

TABLE II

	M	No.		*M*	No.
A0n...........	+0.9	6	A2s..........	+0.6	3
A1n...........	1.4	4	A3s..........	1.0	2
A2n...........	2.0	3	A4s..........	1.2	3
A3n...........	1.9	5	A6s..........	2.1	1
A4n...........	2.2	4	A7s..........	2.2	3
A5n...........	2.9	2	A8s..........	2.7	4
A6n...........	3.0	2	F1s..........	3.0	3
A7n...........	2.8	5	F2s..........	2.8	1
A8n...........	2.8	3			
F0n...........	3.2	2			

Two conclusions may be drawn from an inspection of these results.

1. A definite progression is shown between absolute magnitude and spectral type, the stars of the more advanced types being the fainter. The change of absolute magnitude with type is most rapid among the earlier A stars and becomes comparatively slight in the later types.

2. The average absolute magnitude of the stars with sharp lines is in the case of the earlier A stars considerably brighter than that of the stars of the same types with diffuse lines. This difference becomes small for the later types.

The first of these results is in agreement with that found for the stars of the Taurus group in the case of the larger spectral divisions by Hertzsprung[1] and Kohlschütter,[2] who showed that for the successive spectral types A, F, G, and K the apparent magnitudes, and hence the absolute magnitudes for stars at the same distance, become progressively fainter. Without a more accurate knowledge of spectral type, however, it has not been possible hitherto to establish such a relationship for the subdivisions within the A type.

The second conclusion, that stars with sharp lines are brighter than stars of the same type with diffuse lines, is in accord with our knowledge of stars of the later types of spectrum. Thus the high luminosity of the Cepheid variables, the stars with the "c" characteristics of spectrum, and such objects as α Orionis and α Scorpii, is always found associated with narrow well-defined spectral lines. It is well known that the absorption spectrum of *o* Ceti changes from one with sharp lines at maximum of light to one with vague and diffuse lines near minimum. It seems altogether probable, as the measurement of stellar diameters has shown in a few cases, that the giant stars are large expanded bodies of gas of low density, a condition which favors the production of narrow lines, while the dwarf stars are smaller, more condensed bodies with atmospheres which show a much more rapid density gradient and so produce diffuse lines.

---

[1] *Astronomische Nachrichten*, 209, 119, 1919.

[2] *Ibid.*, 211, 297, 1920.

The results for the Taurus and Ursa Major groups proved to be of such interest that it seemed desirable to extend the investigation to include all the A-type stars for which reliable absolute magnitudes are available and for which photographs of spectra have been secured at Mount Wilson. The material used consists of 82 stars with absolute magnitudes derived from group motion and 104 stars with trigonometric parallaxes. Some of these are common to both lists so that the number of separate stars involved is 148. The absolute magnitudes of these stars have been taken from the lists of Rasmuson for the Taurus, Ursa Major, Perseus, Praesepe, and α Lyrae groups, and a few of his results have been included for other stars for which group motion seems to be clearly established. The trigonometric parallaxes are mainly from the Allegheny, McCormick, Mount Wilson, Sproul, Yale, and Yerkes observatories. These stars are all given in the general catalogue, Table VI of this article, with the corresponding trigonometric or group parallax, and so are not listed separately here. When an absolute magnitude has been derived both from group motion and from trigonometric parallax the arithmetical mean has been used.

All of these stars were classified independently by Adams and Joy, and in Table III are given the results for the two observers, collected according to spectral type and mean absolute magnitude.

TABLE III

	Adams		Joy			Adams		Joy	
	No.	*M*	No.	*M*		No.	*M*	No.	*M*
B9n......	12	+0.6	5	+0.5	B9s.....	3	−0.1	4	0.0
A0n......	16	0.9	28	1.0	A1s.....	4	+0.6	4	+0.6
A1n......	15	1.3	5	0.7	A2s.....	10	0.9	9	0.7
A2n......	12	2.0	11	1.9	A3s.....	8	1.4	4	1.6
A3n......	11	1.9	3	1.6	A4s.....	2	1.7	4	2.1
A4n......	13	2.1	7	2.2	A5s.....	4	2.0	3	1.4
A5n......	7	2.3	14	2.3	A6s.....	4	2.0	3	0.5
A6n......	6	2.6	10	2.3	A7s.....	2	2.9	2	2.3
A7n......	3	3.0	4	2.2	A8s.....	4	2.3	3	2.8
A8n......	2	2.8	9	2.6	A9s.....	1	3.8	1	3.0
A9n......	3	2.7	1	3.6	F0s.....	......	....	6	2.5
F0n......	......	....	2	2.9	F1s.....	4	2.0	1	3.0
F2n......	1	3.6	......	....	F2s.....	2	3.4	2	2.4
F3n......	......	....	2	3.0					

These results, although showing considerable variation in the number of stars of each subdivision as classified by the two observers, are in good agreement as regards the mean absolute magnitude for groups containing a fair number of stars. Most of the differences in classification represent variations of one or two subdivisions, as, for example, at A0n where several stars classified by Joy as of this type are called B9n by Adams.

TABLE IV

	Adams		Joy			Adams		Joy	
	No.	*M*	No.	*M*		No.	*M*	No.	*M*
B9n......	12	+0.58	5	+0.5	B9s.....	3	−0.1	4	+0.1
A0n......	16	0.87	33	0.92	A1s.....	4	+0.6	4	0.5
A1n......	15	1.34	......	....	A2.5s...	18	1.15	13	0.99
A2.5n....	23	1.96	14	1.85	A4.5s ..	6	1.9	7	1.8
A4.5n....	20	2.14	21	2.29	A7s.....	10	2.29	8	1.8
A6.5n....	9	2.7	14	2.29	F1s.....	......	....	10	2.71
A8n......	......	....	10	2.68	F2s.....	7	2.7	......	....
A9n......	6	2.9	......	....					
F1n......	......	....	4	2.9					

In order to facilitate the plotting of these quantities and partially to equalize the weights, the values have been further combined to form the mean results given in Table IV.

The curves plotted from these results are shown in Figure 1, and from these curves the values corresponding to each spectral subdivision have been determined as shown in Table V. Under O−C is given the difference between the values of the absolute magnitudes of Table III and those obtained from these curves. In other words, it shows to what extent the mean observed absolute magnitudes may be represented by a relationship based simply upon spectral type and the character of the spectral lines.

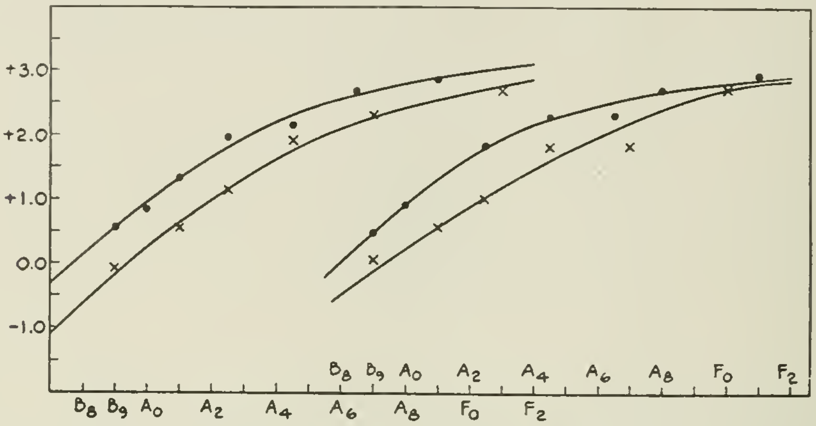

FIG. 1.—Curves showing the relationship between average absolute magnitude and spectral type for stars with parallaxes determined trigonometrically or from group motion. The points indicate groups of stars with diffuse (*n*) lines, the crosses sharp (*s*) lines. The curves on the left are for Adams, those on the right for Joy.

TABLE V

	ADAMS			JOY				ADAMS			JOY		
	M	O−C	No.	*M*	O−C	No.		*M*	O−C	No.	*M*	O−C	No.
B8n....	+0.2	......	.....	0.0	......	.....	B8s....	−0.7	......	.....	−0.5	......	.....
B9n....	0.6	0.0	12	+0.5	0.0	5	B9s....	−0.2	+0.1	3	−0.2	+0.2	4
A0n....	0.9	0.0	16	0.9	+0.1	28	A0s....	+0.2	......	.....	+0.2	......	.....
A1n....	1.3	0.0	15	1.3	−0.6	5	A1s....	0.6	0.0	4	0.5	+0.1	4
A2n....	1.7	+0.4	12	1.7	+0.2	11	A2s....	1.0	−0.1	10	0.8	−0.1	9
A3n....	2.0	−0.1	11	1.9	−0.3	3	A3s....	1.3	+0.1	8	1.2	+0.4	4
A4n....	2.2	−0.1	13	2.2	0.0	7	A4s....	1.7	0.0	2	1.5	+0.6	4
A5n....	2.3	0.0	7	2.3	0.0	14	A5s....	1.9	+0.1	4	1.7	−0.3	3
A6n....	2.5	+0.1	6	2.4	−0.1	10	A6s....	2.2	−0.2	4	2.0	−1.5	3
A7n....	2.7	+0.3	3	2.6	−0.4	4	A7s....	2.3	+0.6	2	2.2	+0.1	2
A8n....	2.8	0.0	2	2.7	−0.1	9	A8s....	2.4	−0.1	4	2.4	+0.4	3
A9n....	2.8	−0.1	3	2.7	+0.9	1	A9s....	2.5	+1.3	1	2.6	+0.4	1
F0n....	2.9	......	.....	2.8	+0.1	2	F0s....	2.6	......	.....	2.7	−0.2	6
F1n....	3.0	......	.....	2.8	......	.....	F1s....	2.7	−0.7	4	2.8	+0.2	1
F2n....	3.1	+0.5	1	2.9	+0.1	2	F2s....	2.8	+0.6	2	2.8	−0.4	2

This comparison shows clearly that the relationship between absolute magnitude and spectral type may be used to determine the mean absolute magnitudes of these groups of stars with a very satisfactory degree of accuracy. Since a large amount of the material consists of absolute magnitudes derived from the trigonometric parallaxes of stars which do not belong to recognized clusters, we may draw the important conclusion that this same relationship may be applied to A-type stars in general, as well as to such groups as those of Taurus and Ursa Major.

The vital question as to the application of this method to the case of individual stars is the next to be considered. If it can be so applied, it involves the conclusion that there is no dispersion in absolute magnitude among A-type stars which have very closely the same spectral type and the same spectral characteristics. This conclusion is perhaps not so radical as it appears at first, since the definition of spectral type and line-characteristics, if carried to extreme limits, might well serve to define the absolute magnitude of a star uniquely. Among stars of the M type, for example, the absolute magnitudes are determined by the relative intensities of certain pairs of lines. If these lines were used to define the spectral type, the latter could be used equally well to determine the absolute magnitude. With a few striking exceptions, such as the A-type companion of o^2 Eridani and some other stars to which reference will be made later, the A-type stars in general appear to be giant stars with no very wide dispersion in absolute magnitude. Within these limits, accordingly, it is quite conceivable that an accurate determination of the spectral characteristics might define the absolute magnitude.

The investigation of this question has been made in three ways:

1. Direct comparison with individual group parallaxes.
2. Direct comparison with individual trigonometric parallaxes.
3. Comparison of the average parallaxes and the average proper motion of 544 stars.

Since the results for the individual stars are all given in the catalogue appearing as Table VI, it seems unnecessary to repeat them here. The absolute magnitudes have all been determined by two independent observers and the parallaxes have then been combined. To illustrate: the spectral type of Boss 3474 (ζ^1 Ursae Majoris) as determined by Adams is A2s and by Joy A3s. Referring to Table V we find for these types the values +1.0 and +1.2 for the absolute magnitude. Combining with the apparent magnitude 2.4, we derive the parallaxes 0.″052 and 0.″057, or 0.″054 in the mean. Summarizing the results obtained in this way for 82 stars in Table VI with parallaxes derived from group motion, and 104 stars with trigonometric parallaxes, we secure the following comparison:

Group parallaxes: 82 stars; systematic difference, −0.″0014;
Average difference, ±0.″0077.

Trigonometric parallaxes: 104 stars; systematic difference, 0.″0000;
Average difference, +0.″0131.

These results compare very favorably with those obtained in the case of the later-type stars where the average difference between spectroscopic and trigonometric parallaxes is ±0.″015.

The agreement with the group parallaxes could, of course, be improved by a very slight readjustment of our reduction curves, but it has seemed preferable not to assign too great weight to these stars, both on account of the uncertainty still outstanding in the parallax of the Taurus group and because they represent a special selection of stars, while the trigonometric parallaxes are more representative of stars in general.

It is of interest to call attention to the results for the three most prominent stars in the list, Sirius (Boss 1732), Vega (Boss 4722), and Altair (Boss 5062). All three have well-determined trigonometric parallaxes, and in addition Sirius and Vega belong to recognized stellar groups and their parallaxes have been derived from group motion. The spectral types of these stars have been determined as A2s, A1s, and A2n, which give absolute magnitudes of +0.9, +0.55, and +1.7, and parallaxes of 0.″316, 0.″123, and 0.″145, respectively. The trigonometric parallaxes are 0.″374, 0.″110, and 0.″205, which correspond to absolute magnitudes of +1.3, +0.3, and +2.5. The group motion gives a parallax of 0.″380 for Sirius and 0.″104 for Vega. The correction of +0.4 to the spectroscopic absolute magnitude of Sirius required to bring it into agreement with observation is not excessive, and a change of type from A2s to A3s would account for nearly the entire difference. In the case of Altair, the correction of +0.8 magnitude is larger than would be expected, but it may find its explanation in the well-known fact that the spectral lines in this star are extraordinarily diffuse. In such cases the absolute magnitude may prove to be fainter than that of stars with the usual "n" characteristics, and further refinement of the method may show that these stars require separate treatment.

This method of determining parallaxes has been applied to the 544 stars listed in Table VI. In order to condense the results the separate determinations of the absolute magnitudes and parallaxes by the two observers have been combined. As a result, this makes a slight apparent discrepancy in a few cases between the absolute magnitude and the corresponding parallax. Since all of the stars in Table VI are designated by their numbers in Boss's Catalogue, it has not seemed necessary to add their positions. The successive columns of Table VI, therefore, give the Boss number, the apparent visual magnitude on the Harvard system,[1] the proper motion according to Boss, the spectral types by Adams and Joy, respectively, the mean of the absolute magnitudes, and the mean of the corresponding parallaxes. The parallaxes as derived from group motion, the trigonometric parallaxes, and the sources for both are added in the last three columns. The following letters are used to indicate the principal authorities for the trigonometric parallaxes: A, Allegheny; F, Flint; M, McCormick; S, Sproul; W, Mount Wilson; Y, Yale; Ye, Yerkes.

The third test of the applicability of the method to A-type stars consists in a comparison between the average of the proper motions and the average of the parallaxes of the stars in Table VI. With the large number of stars available, this comparison should prove especially valuable. The stars have been divided into groups according to their proper motions, with the limits indicated. The

---

[1] In the case of visual binaries the values of m refer to the brighter component. In the case of spectroscopic binaries, however, owing to the uncertainty in the relative brightness of the components it has seemed to us preferable for the present to leave the magnitudes without correction.

TABLE VI

Boss	m	μ	Spectrum A.	Spectrum J.	M	Spect. π	Group π	Trig. π	Auth.
10	2.2	0″.213	A1n	A0n	1.1	0″.060	....	....	
43	4.4	0.052	A1n	A2n	1.5	0.026	....	....	
50	4.5	0.081	A0n	A1n	1.1	0.021	....	0″.017	A
52	6.0	0.028	B9s	B8n	−0.1	0.006	....	....	
66	6.6	0.015	B7n	B9n	0.2	0.005	....	....	
68	5.4	0.016	B9n	A0n	0.8	0.012	....	....	
91	5.2	0.039	A1n	A3n	1.5	0.020	....	....	
154	5.5	0.027	A2s	A3s	1.1	0.014	....	....	
159	5.4	0.022	B9s	A0n	0.4	0.010	....	....	
166	6.8	0.006	A2n	A1s	1.1	0.008	....	....	
169	5.4	0.014	B9s	A0s	0.0	0.008	....	....	
198	5.9	0.006	A3n	A1n	1.6	0.011	....	....	
223	5.9	0.024	A4s	A7s	2.0	0.016	....	....	
224	5.5	0.039	B9s	A0s	0.0	0.008	....	....	
247	5.7	0.018	B9n	B9n	0.6	0.010	....	....	
252	5.7	0.326	A8n	A8n	2.8	0.026	....	....	
257	4.5	0.010	B8s	B8s	−0.6	0.010	....	0.010	Ye
263	5.5	0.038	B9s	B9s	−0.2	0.007	0″.010	....	Perseus
284	5.8	0.028	A2sp	B9s	0.4	0.008	....	....	
289	6.7	0.008	A0n	A0n	0.9	0.007	....	....	
295	5.3	0.056	A1n	A2n	1.5	0.018	....	....	
314	2.8	0.306	A3n	A3n	2.0	0.068	....	....	
340	5.8	0.025	B9n	A0n	0.8	0.010	....	0.017	W
347	6.2	0.011	B9n	A0n	0.8	0.008	....	....	
379	5.4	0.053	B9s	B9s	−0.2	0.008	0.013	....	Perseus
425	5.0	0.010	B8s	B8s	−0.6	0.008	....	....	
446	4.7	0.061	A4s	A5n	2.0	0.029	....	0.020	S, Ye
449	4.1	0.045	A1n	A0n	1.1	0.025	....	....	
463 Ft.	5.2	0.042	A3n	A2n	1.8	0.022	....	....	
466	5.4	0.023	A2n	A1n	1.5	0.016	....	....	
469	5.4	0.072	B9n	A0n	0.8	0.012	....	0.009	A, F, S, Y
490	6.7	0.035	A0n	A1n	1.1	0.008	....	....	
508	5.3	0.035	A0n	A0n	0.9	0.013	....	....	
521	5.7	0.015	A0n	A0n	0.9	0.011	....	....	
522	5.1	0.058	A1n	B9n	0.9	0.014	....	....	
526	5.3	0.012	A3s	A1s	0.9	0.014	....	....	
536	5.9	0.128	A9s	F0s	2.6	0.023	....	....	
550	4.8	0.015	A3s	A4s	1.4	0.021	....	....	
551	4.9	0.027	B9n	B9n	0.6	0.014	....	....	
553	5.8	0.076	A4s	A3sp	1.4	0.014	0.020	....	Urs. Maj.
616	6.3	0.040	A2s	A3s	1.1	0.010	....	....	
622	3.7	0.210	A0n	A0n	0.9	0.027	....	0.049	A, M, Y, Ye
644	4.3	0.213	A4n	A5n	2.2	0.039	....	0.022	A
666	5.3	0.054	A0n	A1n	1.1	0.014	....	....	
674N	5.3	0.017	A3s	A2s	1.0	0.014	....	0.018	S
674S	5.6	0.017	A3s	A2s	1.0	0.012	....	....	
682	5.5	0.017	B9n	B9n	0.6	0.010	....	....	
686	5.9	0.014	A5s	A4s	1.7	0.014	....	....	
696	4.2	0.150	A0n	A3n	1.4	0.028	....	....	
699	5.8	0.006	A1s	A0s	0.4	0.008	....	....	
715	5.6	0.038	B9n	B9n	0.6	0.010	0.009	....	Perseus
719	5.6	0.019	B9n	A0n	0.8	0.010	....	....	
721	5.5	0.083	A3n	A6n	2.2	0.022	....	....	
727	6.8	0.018	A0n	A0n	0.9	0.007	....	....	
731	5.5	0.039	A2s	A2s	0.9	0.012	....	....	
757	5.0	0.058	A1n	A0n	1.1	0.016	....	....	
777	5.9	0.011	A1s	A0s	0.4	0.008	....	....	
791	5.0	0.033	A0n	A0n	0.9	0.015	....	....	
800	5.6	0.017	A1n	A2n	1.5	0.016	....	....	
801	5.1	0.021	B8n	B9n	0.4	0.011	....	....	
802	5.5	0.040	B8n	B9n	0.0	0.008	0.009	....	Perseus
833	5.6	0.032	B9n	A0n	0.8	0.010	0.008	....	Perseus
845	5.6	0.055	A4s	A5s	1.7	0.017	(0.013)	....	Perseus
849	5.7	0.020	A4s	A5n	2.0	0.018	....	....	
878	5.1	0.042	A1n	A1n	1.3	0.017	....	....	
892	6.0	0.147	A7n	A7n	2.6	0.022	0.028	....	Taurus
896	4.9	0.005	B9n	B9n	0.6	0.014	....	....	
898	5.3	0.039	B8n	B9n	0.4	0.010	0.009	....	Perseus
901 Ft.	6.3	0.034	A0n	A0n	0.9	0.008	....	0.005	M
919	5.8	0.141	A5n	A5n	2.3	0.020	0.028	....	Taurus

TABLE VI—*Continued*

Boss	*m*	μ	Spectrum		*M*	Spect. π	Group π	Trig. π	Auth.
			A.	J.					
935	5.5	0″.159	F2n	A9n	2.9	0″.030	0″.034	....	Taurus
961	5.7	0.143	F1s	F1s	2.8	0.026	0.032	....	Taurus
974	5.1	0.004	A1n	A0n	1.1	0.015	....	....	
989	4.8	0.066	A5s	A5s	1.8	0.025	....	....	
991	5.6	0.112	A8n	A6n	2.6	0.025	0.024	....	Taurus
997	5.4	0.064	A1s	A0s	0.4	0.010	....	....	
1004	5.6	0.121	A6n	F0n	2.6	0.026	0.028	....	Taurus
1007	5.3	0.116	A9n	A8n	2.8	0.031	0.027	....	Taurus
1012	5.3	0.043	A1n	A0n	1.1	0.014	....	....	
1013	5.8	0.118	F1s	F1s	2.8	0.024	0.028	....	Taurus
1018	5.7	0.114	F1s	F3s	2.8	0.026	0.027	....	Taurus
1022	4.8	0.124	A6n	A8s	2.4	0.034	0.029	....	Taurus
1023	5.8	0.029	A3n	A3n	2.0	0.017	....	....	
1024	5.2	0.072	A1n	A0n	1.1	0.016	0.019	0″.015	Urs. Maj., M
1025	6.0	0.123	A5n	A6n	2.4	0.018	(0.029)	....	Taurus
1026	4.4	0.112	A3s	A4n	1.8	0.030	0.025	....	Taurus
1027	5.4	0.132	A3n	A5n	2.1	0.022	0.030	....	Taurus
1029	4.2	0.109	A3s	A4s	1.4	0.028	0.026	....	Taurus
1033	4.4	0.123	A2n	A3n	1.8	0.030	0.028	....	Taurus
1034	4.6	0.118	A0n	A2n	1.3	0.022	0.028	....	Taurus
1040	5.7	0.118	A9n	F0n	2.8	0.026	0.027	....	Taurus
1043	6.0	0.111	A8n	A8n	2.8	0.022	0.027	....	Taurus
1046	3.6	0.107	A3s	A6s	1.6	0.042	0.026	....	Taurus
1047	5.1	0.111	A2n	A4n	2.0	0.024	0.028	....	Taurus
1051	5.7	0.106	A3n	A4n	2.1	0.019	(0.026)	....	Taurus
1054	4.8	0.116	A5s	A7s	2.0	0.028	0.029	....	Taurus
1055	5.5	0.110	F1s	F0s	2.7	0.027	0.028	....	Taurus
1056	5.5	0.110	A5n	A8n	2.5	0.025	0.028	....	Taurus
1058	6.0	0.109	A5n	A8n	2.5	0.020	0.028	....	Taurus
1061	6.1	0.007	A3s	A5s	1.5	0.012	....	....	
1064	5.9	0.029	A2s	B9s	0.4	0.008	....	....	
1067	4.8	0.104	A2n	A5n	2.0	0.028	0.027	....	Taurus
1069	5.8	0.028	A3s	A4s	1.4	0.014	....	....	
1076	4.4	0.066	A3s	A0s	0.8	0.019	....	....	
1086	5.8	0.094	A4n	A6n	2.3	0.020	0.025	....	Taurus
1087	4.3	0.104	A3n	A4n	2.1	0.036	0.028	....	Taurus
1088	5.3	0.067	A4s	A6n	2.0	0.022	....	....	
1089	5.2	0.074	A4s	A6s	1.8	0.020	....	....	
1090	4.9	0.084	A3n	A5n	2.2	0.028	0.023	....	Taurus
1092	5.6	0.082	A5s	A8s	2.2	0.020	0.023	....	Taurus
1093	5.7	0.053	B9n	A0n	0.8	0.010	(0.012)	....	Perseus
1095	5.0	0.046	A4s	A5s	1.7	0.022	....	....	
1097	5.4	0.027	B9n	A0n	0.8	0.012	....	....	
1099	5.7	0.061	A0n	A0n	0.9	0.011	0.016	....	Perseus
1103	5.2	0.067	A0n	A0n	0.9	0.014	0.016	....	Perseus
1106	7.2	0.047	A1n	A0n	1.1	0.006	....	−0.014	S
1114	5.4	0.098	A8s	A8n	2.6	0.027	0.029	....	Taurus
1118	5.7	0.052	A1n	A1n	1.3	0.013	....	....	
1122	5.4	0.066	A7s	A7s	2.2	0.024	(0.020)	....	Taurus
1143	5.1	0.091	A2n	A2n	1.7	0.021	0.026	....	Taurus
1146	5.6	0.013	A2n	A0s	1.0	0.012	....	....	
1150	5.6	0.007	A1n	A0n	1.1	0.012	....	....	
1155	5.8	0.010	A2s	A1s	0.8	0.010	....	....	
1161	4.4	0.012	A2s	A2s	0.9	0.020	....	....	
1163	4.7	0.145	A1n	A0n	1.1	0.019	....	....	
1165	5.7	0.024	B9n	B9s	0.2	0.008	....	....	
1177	5.6	0.067	A2s	A2n	1.4	0.014	....	....	
1182	6.0	0.013	F1s	F2s	2.8	0.022	....	0.002	W
1194	4.7	0.082	A3n	A4n	2.1	0.030	(0.024)	....	Taurus
1220	2.9	0.118	A1n	A2n	1.5	0.052	(0.033)	....	Urs. Maj
1226	5.4	0.074	A7s	F0s	2.5	0.026	0.029	....	Taurus
1248	6.2	0.016	A2s	A1s	0.8	0.008	....	....	
1272	6.5	0.019	A4n	A5s	2.0	0.012	....	....	
1275	5.7	0.003	A1n	A2s	1.0	0.011	....	....	
1281	4.7	0.020	B9s	B9n	0.2	0.012	....	....	
1293	5.9	0.015	B9n	B9s	0.2	0.008	....	....	
1310	5.7	0.019	B9s	B9s	−0.2	0.007	....	....	
1318	5.5	0.031	A0n	B9n	0.7	0.011	....	....	
1320	5.9	0.039	B9n	A0n	0.8	0.010	....	....	
1366 Ft.	7.3	0.005	B9s	B9n	0.2	0.004	....	....	

TABLE VI—*Continued*

Boss	m	μ	Spectrum		M	Spect. π	Group π	Trig. π	Auth.
			A.	J.					
1378	5.6	0″.016	A7s	Fon	2.6	0″.025	....	....	
1411	5.5	0.009	A2s	A2s	0.9	0.012	....	0″.017	A
1423	5.7	0.059	A1n	A0n	1.1	0.012	....	....	
1424	5.5	0.010	F0s	F0s	2.6	0.026	....	....	
1427	6.4	0.007	A2n	A2n	1.7	0.011	....	....	
1433	6.0	0.024	A5s	A4s	1.7	0.014	....	....	
1453	4.9	0.014	A2s	A2n	1.4	0.020	....	....	
1478	2.8	0.047	A0np	A2np	1.5	0.055	0″.025	0.035	Urs. Maj., F, J, M
1482	2.7	0.105	A1s	A1s	0.6	0.037	....	0.019	A
1568	5.3	0.021	B8n	B9s	0.0	0.009	....	....	
1572	5.4	0.017	B9s	B9s	−0.2	0.008	....	....	
1575	4.4	0.022	A2s	A4s	1.2	0.024	....	0.026	M
1588	6.2	0.006	A1n	A1n	1.3	0.010	....	....	
1607	5.5	0.021	A7s	A6s	2.2	0.022	....	....	
1646	6.8	0.035	A2sp	A6sp	1.7	0.010	....	....	
1672	5.8	0.013	A1n	A0s	0.8	0.010	....	....	
1673	5.6	0.620	F2s	F3n	2.9	0.028	....	0.039	G, Y
1690	1.9	0.065	A2s	A2s	0.9	0.063	....	0.053	F, Ye
1716	5.3	0.015	A1n	A0n	1.1	0.014	....	....	
1732	−1.6	1.316	A2s	A2s	0.9	0.316	0.380	0.374	Urs. Maj., F, Gill, Ye
1751	5.7	0.023	B9s	B9s	−0.2	0.007	....	....	
1778	4.8	0.112	A4n	A5n	2.2	0.030	....	0.049	A
1880	5.8	0.011	B9n	A0n	0.8	0.010	....	....	
1886	3.6	0.068	A2n	A1n	1.5	0.038	....	0.038	A
1894	6.3	0.011	A9s	A8s	2.4	0.017	....	....	
1897	5.6	0.036	A6n	A6n	2.4	0.024	....	....	
1898	3.5	0.025	A3n	A6n	2.2	0.055	....	0.062	A, M
1903	7.4	0.048	A3n	A8n	2.4	0.010	....	0.009	A
1905	6.5	0.029	A0n	A0n	0.9	0.008	....	0.006	A
1930	5.3	0.028	A1n	A3n	1.6	0.018	....	....	
1952	4.2	0.236	A5s	A4s	1.7	0.032	....	0.055	A, Jo, M
1956	5.0	0.067	A1n	A3n	1.6	0.021	....	....	
1977	5.1	0.029	A0n	A0n	0.9	0.014	....	....	
1979 Br.	2.0	0.203	A2s	A3s	1.1	0.066	....	0.073	A, M, *et al.*
1984	5.8	0.016	B9n	A0n	0.8	0.010	....	....	
2045	5.3	0.027	B9n	A0n	0.8	0.012	....	....	
2051	5.1	0.017	A7n	A6n	2.6	0.031	....	....	
2054	6.2	0.020	A7n	A8n	2.7	0.020	....	....	
2078	5.0	0.047	A0n	A1n	1.1	0.016	....	....	
2121	6.2	0.017	A1n	A1n	1.3	0.010	....	....	
2122	5.9	0.011	A0n	A0n	0.9	0.010	....	....	
2178	6.4	0.017	A4s	A4n	2.0	0.012	....	....	
2185	5.5	0.005	A3n	A3n	2.0	0.019	....	....	
2237	4.0	0.071	A0n	A0n	0.9	0.024	....	....	
2240	6.3	0.011	A1n	A2n	1.5	0.011	....	....	
2241	6.3	0.011	A2n	A2n	1.7	0.012	....	....	
2246	5.4	0.070	A6s	A6s	2.1	0.022	....	....	
2287	5.6	0.027	A2s	A6s	1.5	0.016	....	....	
2295	4.2	0.074	B9n	A0n	0.8	0.020	....	....	
2305	6.7	0.036	A4n	A5n	2.2	0.013	0.011	....	Praesepe
2309	6.5	0.036	A2s	A2n	1.4	0.010	0.011	....	Praesepe
2311	6.3	0.036	A6n	A6n	2.4	0.017	0.011	....	Praesepe
2313	6.7	0.021	A4n	A7n	2.4	0.014	....	....	
2314	6.8	0.041	A6s	A6s	2.1	0.012	0.011	....	Praesepe
2328	5.7	0.011	A5s	A6n	2.2	0.020	....	....	
2343	6.0	0.005	A3n	A1n	1.6	0.016	....	....	
2353	5.7	0.098	A0n	A0n	0.9	0.011	....	....	
2357	5.2	0.046	B9n	A0n	0.8	0.013	....	....	
2381	5.7	0.045	A5n	A5s	2.0	0.018	....	....	
2400	5.2	0.062	A3s	A5n	1.8	0.022	....	....	
2404	3.1	0.502	A4n	A4n	2.2	0.066	....	0.090	Ab, F, Y
2407	4.3	0.054	A4s	A5s	1.7	0.030	....	....	
2417	5.8	0.007	A2n	A2n	1.7	0.015	....	....	
2423	5.7	0.004	A2n	A0n	1.3	0.014	....	....	
2424	3.7	0.073	B9n	A0n	0.8	0.026	....	....	
2429	6.3	0.008	A1n	A0n	1.1	0.009	....	....	
2443	4.5	0.134	A8s	F0s	2.6	0.041	....	....	
2461	5.9	0.100	A3n	A4n	2.1	0.018	....	....	
2465	5.3	0.052	A1s	A2s	0.7	0.012	....	....	
2476	4.9	0.086	A1n	A0n	1.1	0.018	....	....	

TABLE VI—*Continued*

Boss	*m*	μ	Spectrum		*M*	Spect. π	Group π	Trig. π	Auth.
			A.	J.					
2479.......	3.8	0″.338	A1n	A1n	1.3	0″.032	....	0″.017	A
2484.......	5.7	0.022	A1s	A3s	0.9	0.012	....	....	
2492.......	5.5	0.040	B9n	A0s	0.4	0.010	....	....	
2494.......	6.4	0.058	A2n	A5n	2.0	0.013	....	....	
2495.......	4.0	0.137	B9n	B9n	0.6	0.021	....	0.037	A, M
2540.......	3.8	0.117	A4n	A6n	2.3	0.050	....	0.033	A
2565.......	4.6	0.073	B9n	B9n	0.6	0.016	....	....	
2576.......	6.2	0.042	A1n	A1n	1.3	0.010	(0″.011)	....	Praesepe
2584.......	5.2	0.020	A5n	A6n	2.4	0.026	....	....	
2598.......	6.1	0.029	A3n	A3n	2.0	0.014	....	....	
2632.......	3.9	0.330	A4n	A7n	2.4	0.050	....	....	
2634.......	6.0	0.049	F1s	F1s	2.8	0.022	(0.011)	....	Praesepe
2637.......	5.0	0.009	A1s	A3s	0.9	0.015	....	....	
2641.......	6.0	0.033	A3n	A4n	2.1	0.016	....	....	
2642.......	5.3	0.194	A5n	A7s	2.2	0.024	....	....	
2647.......	5.9	0.204	A1s	A1s	0.6	0.008	....	0.035	A, Ye
2650.......	5.8	0.076	A0n	B9n	0.8	0.010	....	....	
2692.......	4.5	0.054	A2n	A3n	1.8	0.028	....	....	
2698.......	1.3	0.247	B6n	B9n	0.4	0.064	....	0.033	Y
2712.......	6.1	0.021	A1n	A0n	1.1	0.010	....	....	
2724.......	5.4	0.074	B9n	B9n	0.6	0.010	....	....	
2726.......	5.7	0.090	A3n	A3n	2.0	0.018	0.022	....	*a* Lyrae
2737.......	5.8	0.065	A1n	A2n	1.5	0.014	....	....	
2744.......	6.7	0.001	A1n	A0n	1.1	0.008	....	....	
2745.......	5.6	0.130	A2n	A2n	1.7	0.017	....	....	
2756.......	5.8	0.027	A1n	A3n	1.6	0.015	....	....	
2768.......	4.8	0.107	F1s	A8s	2.6	0.036	....	....	
2773.......	5.8	0.102	A1n	A2n	1.5	0.014	....	....	
2777.......	5.9	0.014	A3s	A2s	1.0	0.011	....	....	
2787.......	5.9	0.011	A2s	A1s	0.8	0.009	....	....	
2788.......	5.2	0.052	A0n	A0n	0.9	0.014	....	....	
2797.......	5.5	0.048	B8n	B8n	0.1	0.008	....	....	
2798.......	5.8	0.015	A0n	A0n	0.9	0.010	....	....	
2802.......	4.8	0.141	A4n	A4n	2.2	0.030	....	0.028	A
2808.......	5.6	0.040	B9n	A0n	0.8	0.010	....	....	
2813.......	5.2	0.074	A8s	A8s	2.4	0.027	0.043	0.034	Urs. Maj., A
2819.......	6.3	0.050	F0s	F3s	2.8	0.020	....	....	
2839.......	6.9	0.013	B9n	A0n	0.8	0.006	....	....	
2853.......	5.3	0.289	A6n	F0s	2.6	0.028	....	0.023	A, Jo
2866.......	5.4	0.049	B9n	A0n	0.8	0.012	....	....	
2887.......	6.1	0.021	A3n	A3s	1.6	0.012	....	....	
2909.......	4.5	0.077	B9n	A0n	0.8	0.018	....	....	
2930.......	2.4	0.089	A3s	A2s	1.0	0.054	0.046	....	Urs. Maj.
2940.......	6.1	0.071	A3n	A2n	1.8	0.014	....	....	
2951.......	6.4	0.004	A3s	A2s	1.0	0.009	....	....	
2956.......	5.6	0.004	A3s	A2n	1.5	0.016	....	....	
2972.......	2.6	0.207	A2n	A2n	1.7	0.066	(0.085)	....	Urs. Maj.
2974.......	3.4	0.106	A2s	A2s	0.9	0.032	....	0.021	A
2987.......	4.8	0.102	A0n	A1s	0.7	0.016	....	....	
2990.......	4.1	0.095	B9s	B9s	−0.2	0.014	....	....	
3023.......	5.3	0.052	B9n	A0n	0.8	0.012	....	....	
3052.......	6.4	0.035	A1n	A3n	1.6	0.011	....	....	
3055.......	4.8	0.061	B9n	A0n	0.8	0.016	0.015	....	*a* Lyrae
3063.......	5.5	0.154	A4n	A3n	2.0	0.020	....	....	
3088.......	5.1	0.068	A1n	A2n	1.5	0.019	....	....	
3097.......	5.2	0.050	A1n	A0s	0.8	0.015	....	....	
3101.......	2.2	0.511	A2n	A2n	1.7	0.079	....	0.114	F, S, Y
3117.......	2.5	0.094	A0n	A0n	0.9	0.048	0.041	0.011	Urs. Maj., F, M
3120.......	6.5	0.009	A1n	A0n	1.1	0.008	....	....	
3123.......	5.5	0.025	A3s	A3s	1.2	0.014	....	....	
3143.......	5.1	0.323	A6s	A6s	2.1	0.025	....	0.013	A
3150.......	6.0	0.044	A7s	A7s	2.2	0.017	....	....	
3173.......	6.3	0.013	A1n	A1s	0.9	0.008	....	....	
3178.......	6.8	0.006	F1s	A8s	2.6	0.014	....	....	
3183.......	5.8	0.096	A7s	A8s	2.4	0.020	....	....	
3190.......	3.4	0.110	A0n	A0n	0.9	0.032	0.045	....	Urs. Maj.
3202.......	5.9	0.030	A1n	A2n	1.5	0.013	....	....	
3206.......	6.2	0.038	A8s	A8s	2.4	0.017	....	....	
3208.......	6.3	0.067	F0n	A6n	2.6	0.019	....	....	
3229.......	6.0	0.084	A6n	A5n	2.4	0.019	....	....	

TABLE VI—*Continued*

Boss	m	μ	Spectrum		M	Spect. π	Group π	Trig. π	Auth.
			A.	J.					
3231	5.1	0″033	A3s	A2s	1.0	0″016	....	....	
3256	3.1	0.251	B9n	A0n	0.8	0.034	....	0″026	Ye
3257	5.7	0.060	A1n	A1n	1.3	0.013	....	....	
3266	5.4	0.020	A3s	A2s	1.0	0.014	....	....	
3276	6.1	0.023	A4s	A4s	1.6	0.012	....	....	
3277	5.4	0.084	B9n	B9n	0.6	0.010	....	....	
3284	6.7	0.019	A5s	A4s	1.7	0.010	....	....	
3290	5.9	0.040	A0n	A1n	1.1	0.011	....	....	
3309	4.9	0.135	B9n	B9n	0.6	0.014	....	....	
3310	5.5	0.078	B9n	B9n	0.6	0.010	....	....	
3323	5.2	0.112	A6n	A4n	2.4	0.027	....	....	
3329	6.0	0.054	A0n	A1n	1.1	0.010	....	....	
3332	5.8	0.022	A3n	A4n	2.1	0.018	....	....	
3334	6.4	0.068	A0n	A0n	0.9	0.008	....	....	
3337	5.6	0.051	A0n	B9n	0.7	0.010	....	....	
3338	6.2	0.055	A8s	A9n	2.5	0.018	....	....	
3339	5.8	0.095	A0n	A0n	0.9	0.010	....	....	
3343	5.9	0.101	A0n	A0n	0.9	0.010	....	....	
3360	6.3	0.067	A7n	A7n	2.6	0.018	0″019	....	Urs. Maj.
3363	1.7	0.115	A2s	A2s	0.9	0.069	0.042	....	Urs. Maj.
3371	2.9	0.237	A1s	A1s	0.6	0.034	....	0.044	Ye
3382	4.9	0.101	A4n	A5n	2.2	0.030	0.036	0.031	Urs. Maj., A
3392	5.1	0.027	B9n	B9n	0.6	0.012	....	....	
3409	4.4	0.057	A2s	A2s	0.9	0.020	....	0.011	M
3428^1	6.8	0.039	A1n	A1n	1.3	0.008	....	....	
3428^2	7.2	0.039	A1n	A3n	1.6	0.008	....	....	
3462	5.9	0.080	A5s	A5s	1.8	0.015	....	....	
3474	2.4	0.130	A2s	A3s	1.1	0.054	0.044	0.049	Urs. Maj., F, M, Pe, Y
3475	4.0	0.136	A8s	A5s	2.0	0.052	0.046	0.022	Urs. Maj., M
3478	5.8	0.014	A3s	A2s	1.0	0.012	....	....	
3480	4.0	0.123	A1n	A0n	1.1	0.026	0.042	0.037	Urs. Maj., A, M
3506	4.9	0.052	A3s	A5s	1.5	0.021	0.014	0.028	Urs. Maj., M
3507	6.3	0.067	A1s	A2n	1.2	0.010	....	....	
3518	4.9	0.104	A1n	A2n	1.5	0.021	....	0.052	S
3526	6.3	0.112	A7n	A5n	2.5	0.018	....	0.015	A, M, S, Ye
3539	5.7	0.060	B9n	A0n	0.8	0.010	....	....	
3540	6.4	0.055	A0s	A1s	0.4	0.006	....	....	
3546	6.2	0.053	B9n	A0n	0.8	0.008	....	....	
3580	6.6	0.033	A2n	A2n	1.7	0.010	....	....	
3585	6.0	0.038	A1n	A3n	1.6	0.013	....	....	
3612	4.3	0.032	A1n	A0n	1.1	0.023	....	....	
3652	6.6	0.065	A9s	F2s	2.6	0.016	....	0.025	A
3653	5.6	0.044	A0n	B9n	0.7	0.010	....	....	
3654	4.6	0.067	A4n	A5n	2.2	0.034	....	0.025	A
3663	5.8	0.055	A5s	A5n	2.1	0.018	....	....	
3666	4.3	0.238	A1n	A0n	1.1	0.023	....	0.041	A
3669	5.7	0.070	A3s	A3s	1.2	0.013	....	....	
3684	6.0	0.030	A0n	A0n	0.9	0.010	....	....	
3692 Br.	5.1	0.072	B9n	A0n	0.8	0.014	....	0.017	S, Ye
3692 Ft.	7.4	0.072	F0s	F2n	2.8	0.012	....	0.020	S, Ye
3706	6.2	0.098	A2n	A2n	1.7	0.013	....	....	
3719	6.6	0.088	A2n	A2n	1.7	0.010	....	0.011	A
3722	3.0	0.182	A3n	A3n	2.0	0.062	....	....	
3729	4.5	0.228	F0s	F0s	2.6	0.043	....	....	
3743	5.5	0.027	A0n	A0n	0.9	0.012	....	....	
3752	4.4	0.061	A0n	A0n	0.9	0.020	(0.016)	....	Urs. Maj.
3756	5.8	0.026	B9n	B9n	0.6	0.009	....	....	
3766 Br.	5.2	0.238	A5n	A5n	2.3	0.026	....	....	
3771 Ft.	5.1	0.049	A2n	A2n	1.7	0.021	....	0.019	A
3787	2.9	0.131	F1n	F1n	2.9	0.100	....	....	
3788	5.7	0.024	B9n	B9n	0.6	0.010	....	....	
3814	4.6	0.192	A4n	A4n	2.2	0.033	....	....	
3820	6.4	0.029	A1n	A1n	1.3	0.010	....	....	
3866	4.7	0.061	B9n	B9n	0.6	0.014	....	....	
3868	6.0	0.068	A0n	A0n	0.9	0.010	....	....	
3875	6.3	0.029	B9s	B9s	−0.2	0.005	....	....	
3883	5.3	0.078	A0n	A0n	0.9	0.013	....	....	
3885	5.6	0.109	A1n	A3n	1.6	0.016	....	....	
3902	6.1	0.029	A5s	A4n	2.0	0.016	....	....	
3911	5.5	0.017	A2n	A1n	1.5	0.016	....	....	

TABLE VI—*Continued*

Boss	*m*	μ	Spectrum		*M*	Spect. π	Group π	Trig. π	Auth.
			A.	J.					
3915	5.4	0″.051	A0n	B9n	0.7	0″.012	....	....	
3918	6.1	0.077	A5n	A5n	2.3	0.017	....	....	
3940	3.7	0.190	F2s	F2s	2.8	0.066	....	....	
3946	6.1	0.016	B9n	B9n	0.6	0.008	....	....	
3960 Br.	4.2	0.068	A4n	A7n	2.4	0.044	....	0″.013	A, Ye
3960 Ft.	5.2	0.068	A5n	A6n	2.4	0.026	....	0.019	A, Ye
3961	2.3	0.158	A0n	A0n	0.9	0.052	0″.050	0.059	Urs. Maj., Corona, F, M
3985	5.8	0.162	A7n	A5n	2.5	0.022	....	....	
3993	5.3	0.044	A3np	A2s	1.4	0.018	....	....	
3998	4.0	0.105	A0n	A1n	1.1	0.026	....	0.021	A, S, Ye
4007	5.6	0.033	A2s	A0n	1.0	0.012	....	....	
4009	3.7	0.091	A1n	A0n	1.1	0.030	0.023	0.035	Urs. Maj., A, M
4016	3.6	0.092	A0s	B9n	0.4	0.022	....	....	
4021	5.1	0.070	A1n	A3n	1.6	0.020	....	....	
4022	5.8	0.010	A6s	A8s	2.3	0.020	....	....	
4026	3.8	0.136	A6s	A4s	1.8	0.042	....	0.035	A
4028	5.2	0.099	A0n	A0n	0.9	0.014	....	....	
4037	5.4	0.046	B7n	B6n	−0.6	0.007	(0.012)	....	Scorpius
4041	5.9	0.034	B9n	A0n	0.8	0.010	0.009	....	Scorpius
4070	5.6	0.034	A1s	A1s	0.6	0.010	....	....	
4072	5.0	0.193	A5n	A8n	2.5	0.032	....	....	
4080	4.9	0.045	A0s	A2n	1.0	0.017	....	....	
4097	5.6	0.065	B9n	A0n	0.8	0.010	....	....	
4119	4.9	0.027	A3s	A3s	1.2	0.018	....	....	
4120	5.5	0.041	A1n	A3n	1.6	0.016	....	....	
4122	5.9	0.014	A2s	A3s	1.1	0.010	....	....	
4146	5.7	0.028	A2n	A2n	1.7	0.016	....	....	
4155	4.8	0.042	A3s	A4s	1.4	0.021	0.011	....	Scorpius
4163	4.8	0.172	A5n	A7n	2.4	0.034	....	0.031	A
4165	3.8	0.062	A3n	A0n	1.4	0.035	....	0.017	A
4176	6.2	0.022	A1n	B9n	0.9	0.008	....	....	
4181	5.0	0.261	A6n	A8n	2.6	0.034	....	0.045	G
4182	4.5	0.079	A2s	A2s	0.9	0.019	....	....	
4184	5.5	0.026	A1n	A0n	1.1	0.013	....	....	
4203	4.0	0.097	A1n	A1n	1.3	0.029	....	0.000	A, M, S, Ye
4206	4.6	0.033	A2s	A5s	1.4	0.022	....	....	
4210	5.6	0.023	A1s	A1s	0.6	0.010	....	....	
4213	5.0	0.042	B9n	A0n	0.8	0.014	....	....	
4221	5.8	0.021	A1n	A2n	1.5	0.014	....	....	
4229	5.6	0.024	B9s	A0n	0.4	0.009	....	....	
4260	6.0	0.003	B9n	A0n	0.8	0.009	....	....	
4285	5.6	0.029	A2s	A0n	1.0	0.012	....	....	
4291	6.4	0.011	A0n	A1s	0.7	0.008	....	....	
4300	5.4	0.098	A5s	A6n	2.2	0.022	....	....	
4332	5.3	0.012	A3s	A3s	1.2	0.016	....	....	
4338	6.2	0.038	B9n	B9n	0.6	0.009	....	....	
4348 Br.	6.3	0.055	A1n	A3n	1.6	0.012	....	....	
4353	6.0	0.032	A0n	A2n	1.3	0.012	....	....	
4360	3.3	0.093	A3s	A1s	0.9	0.033	....	....	
4376	3.2	0.165	A0n	A0n	0.9	0.035	....	0.028	A, M
4391	4.8	0.066	A0n	A0n	0.9	0.017	....	....	
4395	4.4	0.036	A0n	A1n	1.1	0.022	....	....	
4402	5.1	0.018	B9n	B9s	0.2	0.011	....	....	
4418	5.7	0.044	A4s	A3s	1.4	0.014	....	....	
4419	4.5	0.038	B9n	B9s	0.2	0.014	....	−0.004	A
4420	4.3	0.132	A6s	A7s	2.2	0.038	....	....	
4430	5.8	0.015	A1n	A0n	1.1	0.012	....	0.014	Ye
4442	5.7	0.108	A0n	A3n	1.4	0.014	....	....	
4449	6.6	0.015	B9s	A1s	0.2	0.005	....	....	
4458	5.0	0.158	A5n	A6s	2.2	0.027	....	0.019	A, F
4459	2.1	0.262	A0n	B9n	0.7	0.052	0.046	0.062	Corona, F, M, Y, Ye
4461	5.8	0.028	A5s	A8s	2.2	0.019	....	....	
4468	5.7	0.023	B9n	A0n	0.8	0.010	....	....	
4494	5.7	0.043	B9n	A0n	0.8	0.010	....	....	
4511	5.2	0.208	A1n	A0n	1.1	0.016	....	−0.001	A, Y
4514	6.4	0.009	A1sp	B9s	0.2	0.006	....	....	
4521	6.4	0.026	A0n	A2n	1.3	0.010	....	....	
4552	4.4	0.026	B9n	A0n	0.8	0.018	....	....	
4554	5.5	0.009	A9s	F2s	2.6	0.027	....	....	
4557	5.1	0.030	A1n	B9n	0.9	0.014	....	....	

TABLE VI—*Continued*

Boss	m	μ	Spectrum		M	Spect. π	Group π	Trig. π	Auth.
			A.	J.					
4581	3.7	0″.103	A5s	A5s	1.8	0″.042	....	0″.037	A
4592	5.2	0.027	A4s	A4s	1.6	0.019	....	....	
4640	6.5	0.010	B9n	A0n	0.8	0.008	....	....	
4643	5.5	0.057	A4s	A3s	1.4	0.016	....	....	
4669	5.7	0.034	A3s	A3s	1.2	0.013	....	....	
4685	5.2	0.035	B9n	A0n	0.8	0.013	....	....	
4702	5.4	0.007	B9s	B9s	−0.2	0.008	....	....	
4713	5.4	0.146	A5n	A8n	2.5	0.026	....	0.024	A
4719	5.8	0.026	A2s	A2s	0.9	0.010	....	....	
4722	0.1	0.346	A1s	A1s	0.6	0.123	0″.104	0.110	α Lyrae, F, J, Y, Ye
4748	6.0	0.057	A3n	A6n	2.2	0.018	....	0.000	Ye
4751 Br.	5.7	0.031	A3s	A6s	1.6	0.016	....	....	
4752	4.3	0.031	A5s	A8s	2.2	0.037	....	0.026	A
4754	5.9	0.022	A1n	A2n	1.5	0.013	....	0.030	A
4761	4.4	0.123	A2n	A5n	2.0	0.034	....	0.056	A
4777 Ft.	7.8	0.020	B8n	B8n	0.1	0.003	....	(−0.006)	Ye
4779	5.3	0.019	A0s	A1s	0.4	0.010	....	....	
4820	5.7	0.120	F2s	F2s	2.8	0.026	....	0.040	A, S
4821	5.8	0.002	B8n	B8n	0.1	0.007	....	....	
4824	3.3	0.008	B9sp	B9s	−0.2	0.020	....	0.012	M
4846	5.1	0.091	A2n	A4n	2.0	0.024	....	....	
4856	5.9	0.016	B9n	A0n	0.8	0.010	....	....	
4858	3.0	0.102	B9n	A0n	0.8	0.036	....	0.037	A, M
4866	5.7	0.056	A3s	A7s	1.8	0.016	....	....	
4867	5.5	0.098	A2n	A5n	2.0	0.020	....	....	
4899	5.6	0.044	A1n	A0n	1.1	0.012	....	....	
4914	5.1	0.011	A3n	A3s	1.6	0.020	....	0.011	A
4928	5.5	0.002	B9s	A0n	0.4	0.010	....	....	
4932	4.0	0.031	A4n	A7s	2.2	0.044	....	0.049	M
4947	6.0	0.019	A3s	A6s	1.6	0.014	....	....	
4953	3.4	0.265	A3n	A6n	2.2	0.058	....	0.057	A, M
4965	5.6	0.040	B9n	B9n	0.6	0.010	....	....	
4974	5.8	0.037	A0n	A0n	0.9	0.010	....	....	
4979	6.0	0.017	A0n	A0n	0.9	0.010	....	....	
4980	5.7	0.041	A0s	A0s	0.2	0.008	....	....	
4988	3.9	0.126	A1n	A0n	1.1	0.028	....	0.018	A, Ab
4998	4.9	0.004	B9n	B8n	0.3	0.012	....	....	
5007	5.9	0.006	B9np	A0n	0.8	0.009	....	....	
5024	5.4	0.032	A0s	A0s	0.2	0.009	....	....	
5042	6.1	0.017	A0s	B9s	0.0	0.006	....	....	
5048	3.0	0.065	A1n	A0n	1.1	0.042	....	0.055	S
5062	0.9	0.655	A2n	A2n	1.7	0.145	....	0.205	M, Y, Ye, *et al.*
5092	5.5	0.024	B9n	A2n	1.2	0.014	....	....	
5105	4.8	0.051	B9n	A0n	0.8	0.016	....	....	
5117	6.3	0.005	A1n	A0n	1.1	0.009	....	....	
5130	6.0	0.020	B9s	B9n	0.2	0.007	....	....	
5134	5.3	0.099	A6n	A6n	2.4	0.026	....	....	
5160	6.2	0.038	A0sp	A1n	0.8	0.008	....	....	
5171	3.4	0.032	B9s	B9s	−0.2	0.019	....	....	
5173	5.5	0.007	A1np	A0n	1.1	0.013	....	....	
5186	5.0	0.017	A0n	A0n	0.9	0.015	....	0.010	A, M
5188	5.0	0.094	A2n	A1n	1.5	0.020	....	....	
5211	5.5	0.046	A1n	A1n	1.3	0.014	....	....	
5220	6.1	0.022	A0n	A0n	0.9	0.009	....	....	
5224	5.4	0.018	B7n	B8n	−0.1	0.008	....	....	
5233	6.1	0.008	A0n	A0n	0.9	0.009	....	....	
5236	5.7	0.004	B7n	B8n	−0.1	0.007	....	....	
5244	5.0	0.026	A4n	A8n	2.4	0.031	....	0.024	M
5249	5.4	0.073	A1n	A0n	1.1	0.014	....	....	
5269	6.5	0.005	A1n	A0n	1.1	0.008	....	....	
5282	4.7	0.038	A1n	A4n	1.8	0.026	....	....	
5292	5.4	0.048	A2s	A2s	0.9	0.013	....	....	
5295	6.2	0.009	A0n	A0n	0.9	0.009	....	....	
5296	6.4	0.069	A3n	A5n	2.2	0.014	....	....	
5301	4.8	0.058	B9s	A1n	0.6	0.015	....	....	
5322	5.6	0.017	B8s	B9s	−0.4	0.006	....	....	
5337	3.8	0.044	A1n	A3n	1.6	0.037	....	0.023	M
5366	5.5	0.011	B9s	B9s	−0.2	0.007	....	....	
5371	4.8	0.051	A7n	F0s	2.7	0.038	....	0.010	M
5393	4.9	0.025	B9n	B9n	0.6	0.014	....	0.000	A

TABLE VI—*Continued*

Boss	m	μ	Spectrum		M	Spect. π	Group π	Trig. π	Auth.
			A.	J.					
5417	4.9	0″.060	A4s	A5s	1.7	0″.023	......	......	
5425	6.3	0.051	A8s	A8n	2.6	0.018	0″.013	......	Urs. Maj.
5443	4.8	0.169	A7s	A9s	2.4	0.034	......	0″.044	M
5465	5.4	0.015	B9s	B9s	−0.2	0.008	......	......	
5480	2.6	0.160	A2n	A0n	1.3	0.056	......	0.084	A, F, M
5491	5.1	0.054	A1s	A4s	1.0	0.016	......	......	
5498	5.7	0.124	A3n	A6n	2.2	0.020	......	......	
5511	5.5	0.206	A4n	A4n	2.2	0.022	0.052	0.037	α Lyrae, A, Jo
5525	5.4	0.018	B9n	B8n	0.3	0.010	......	......	
5532 Ft	8.0	0.012	A2n	A2n	1.7	0.005	......	(−0.011)	Ye
5548	6.0	0.008	B9n	A0n	0.8	0.009	......	......	
5550	6.3	0.026	A0n	A0n	0.9	0.008	......	......	
5555	5.3	0.100	A3n	A0n	1.4	0.018	......	......	
5558	5.8	0.117	A2n	A5n	2.0	0.018	......	......	
5573	6.0	0.052	A0n	A0n	0.9	0.010	0.013	0.010	Urs. Maj., M
5581	5.9	0.030	A2n	A4n	2.0	0.016	......	......	
5585	5.6	0.038	B9n	A2n	1.2	0.014	......	......	
5591	6.9	0.061	A5n	A8n	2.5	0.013	......	......	
5600	3.0	0.392	A3n	A5n	2.2	0.068	......	0.115	M
5626	6.5	0.001	B9n	A0s	0.4	0.006	......	......	
5639	6.0	0.009	B8s	B8n	−0.4	0.006	......	......	
5641	5.6	0.036	A0n	A0n	0.9	0.011	......	......	
5664	5.7	0.004	B7s	B6s	−1.2	0.004	......	......	
5667	5.5	0.007	B8n	B9n	0.4	0.010	......	......	
5669	5.6	0.039	B9n	A1n	1.0	0.012	......	......	
5709	4.4	0.026	A4n	F2n	2.6	0.043	......	0.005	A, M
5738	6.2	0.028	B8n	B9n	0.4	0.006	......	......	
5742	4.2	0.452	A6n	A6n	2.4	0.045	0.108	0.055	α Lyrae, A, M, S, Y, Ye
5780	6.2	0.004	A1n	A0n	1.1	0.009	......	......	
5803	4.9	0.030	A1s	B9s	0.2	0.012	......	......	
5818	5.5	0.014	A1n	A2n	1.5	0.016	......	......	
5847	6.1	0.019	A2s	A1s	0.8	0.009	......	......	
5848	5.2	0.019	A0n	A2n	1.3	0.017	......	......	
5858	4.8	0.036	A2s	A3s	1.1	0.018	......	......	
5879	5.7	0.037	A1n	A0s	0.8	0.010	......	......	
5904	3.5	0.052	A1n	A1n	1.3	0.036	......	......	
5967	5.3	0.024	B9n	B9n	0.6	0.011	......	......	
5969	5.6	0.015	A4s	A3s	1.6	0.015	......	......	
5973	5.2	0.017	A1n	A0n	1.1	0.016	......	......	
5996	5.9	0.012	A6s	A8s	2.3	0.019	......	......	
6011	6.2	0.017	A2s	A1s	0.8	0.008	......	......	
6020	6.5	0.233	A9n	F0s	2.8	0.018	......	0.016	W
6023	5.5	0.005	A2n	B9s	0.8	0.012	......	......	
6031	4.9	0.124	A3s	A3s	1.2	0.018	......	0.043	A
6063	5.5	0.042	A1n	B9n	0.9	0.012	......	......	
6075	5.3	0.016	B9n	B9n	0.6	0.011	......	......	
6113	5.8	0.027	A3n	A4s	1.8	0.016	......	......	
6128	5.4	0.033	A1n	A3n	1.6	0.018	......	......	
6133	6.2	0.013	A2s	A1s	0.8	0.008	......	......	
6139	6.1	0.014	A1s	A0s	0.4	0.008	......	......	
6166	5.7	0.007	A5s	A8s	2.2	0.016	......	......	
6168	6.1	0.013	B9s	B9s	−0.2	0.005	......	......	
6174	6.3	0.004	A4s	A3n	1.8	0.012	......	......	
6180	6.0	0.008	A2s	A1s	0.8	0.009	......	......	

results are given in Table VII and a curve drawn from them is shown in Figure 2.

Two results are given for the last group according as Boss 1732 (Sirius) is included or not. For statistical purposes it is, no doubt, better to omit it.

These values show an excellent degree of correlation between proper motion and parallax. The influence of occasional stars of small proper motion and large parallax, or large proper motion and small parallax, is not serious, because of the considerable number

TABLE VII

Limits of μ	No.	Av. μ	Av. π
<0″.010	49	0″.006	0″.011
0″.010 to 0″.019	83	0.015	0.012
0.020 to 0.029	72	0.025	0.014
0.030 to 0.039	56	0.035	0.014
0.040 to 0.049	39	0.044	0.016
0.050 to 0.069	74	0.059	0.019
0.070 to 0.099	55	0.084	0.020
0.100 to 0.149	68	0.118	0.029
0.150 to 0.250	30	0.196	0.037
>0″.250	18	0.430	0.071
	17	0.378	0.057

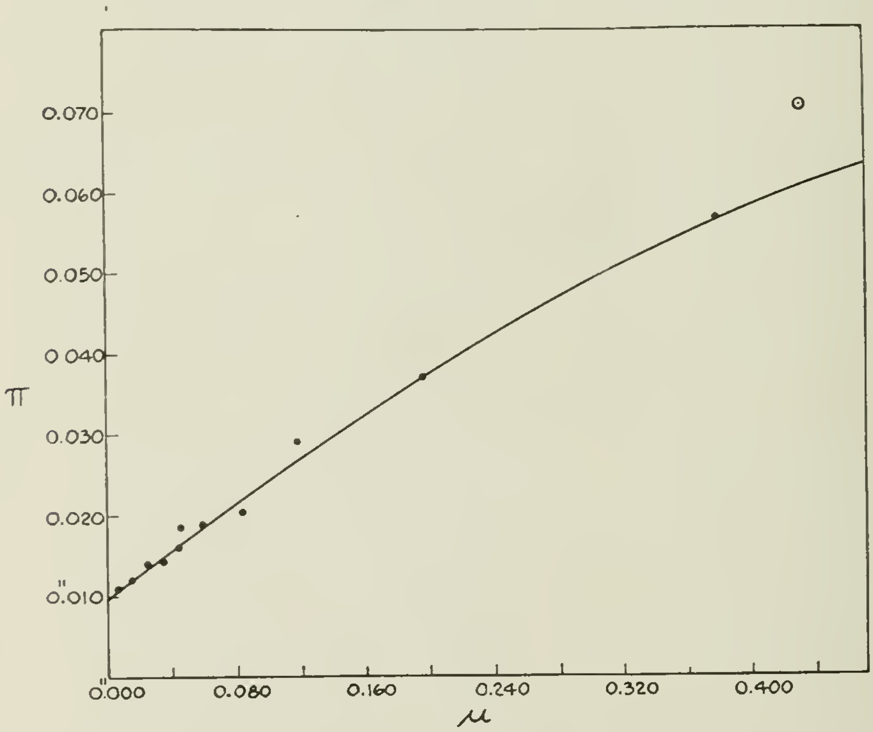

FIG. 2.—This curve shows the relationship between the average value of the proper motion and the average value of the spectroscopic parallax for the 544 stars of Table VI. The stars have been grouped according to the limits of proper motion given in Table VII. The point surrounded by a circle represents the value for the group of largest proper motion when Sirius is included; the neighboring point on the curve represents the same group when Sirius is omitted.

of stars in each group, the only important exception being that of Sirius. It is of interest to note that the curve would give an average parallax of 0″.009 for stars of zero proper motion, a result almost identical with that found by Strömberg[1] for stars of the later types of spectrum. Reference may also be made to the fact that the eighth group of stars, with proper motions between 0″.100 and 0″.149, while it includes most of the members of the Taurus moving cluster, also includes a large number of other stars. The parallax of 0″.029 is in good agreement with that of Rasmuson for the Taurus cluster, thus indicating that the latter stars do not differ materially in distance from other A stars having the same amount of proper motion.

We have referred previously to α Cygni (Boss 5320) and some other stars with similar spectral characteristics. Most of these are listed as "c" stars by Miss Cannon and have sharp narrow lines with the enhanced lines remarkably strong and prominent.

TABLE VIII

Boss	Spectrum	μ	b
478	A2s	0″.009	−3°
533	A1s	0.011	−3
534	A2s	0.005	−5
724	A2s	0.004	0
1268	A4s	0.016	−1
4503	A4s	0.015	−7
5320	A2s	0.001	+1
6111	A2s	0.010	0

Those at λλ 4233 and 4481 are especially striking, and it seems probable from a brief examination already made that these lines vary definitely with absolute magnitude. At present, however, we have no results based upon trigonometric measures or other data from which to determine absolute magnitudes which may serve as standards of reduction for the spectroscopic intensities. There can be little question that α Cygni is extremely bright, its absolute magnitude probably being of the order of −4 or −5. In spectral characteristics, great luminosity, small proper motion, and low galactic latitude these stars are associated with the Cepheid variables and stars of similar spectra and appear to form a continuation of the Cepheid chain of giant stars. Table VIII gives the stars of this type which we have found in our list. The galactic latitude is indicated by *b*.

---

[1] *Mt. Wilson Contr.*, No. 170.

The A-type companion of o^2 Eridani and probably the companion of Sirius appear to be cases of the rare phenomenon of A-type stars of very low luminosity. Three other stars of which we have spectrograms are much fainter than the vast majority of those of the A type. These are:

	m	Spectrum	μ	Trig. π	M
Lal. 5761	8.0	A2s	0".90	0".039	6.0
Lal. 28607	7.3	A2s	1.17	0.033	4.9
W. B. 23^h175	8.4	A2s	1.31	0.028	5.6

The last star is a double and the value of *M* refers to the combined magnitude.

The spectra of these stars are peculiar. The hydrogen lines are narrow and sharp, the metallic lines are very faint, and λ 4481 and λ 4233 are hardly visible. These latter lines, accordingly, show a behavior just the reverse of that in "c" stars like α Cygni. It is of interest to note that λ 4481 and λ 4233 are also very faint in the spectrum of the companion of o^2 Eridani.

Forty-five of the stars which appear in Table VI have been included in the list of 1646 stars[1] of the later spectral types for which absolute magnitudes derived by the spectroscopic method have been published. The latter values were obtained by an extrapolation of the reduction-curves for stars of the F type and have always been considered by us as subject to considerable uncertainty. A comparison of the results given in Table VI with those in the list of 1646 stars shows a mean difference of $0^M.5$, the absolute magnitudes in Table VI being the fainter. The difference is systematic although much of it is due to a small number of stars. We consider the parallaxes given in Table VI as superior to the earlier values and hope by means of these results to form a connection between the two systems which will render them consistent with one another.

---

[1] *Mt. Wilson Contr.*, No. 199; *Astrophysical Journal*, **53**, 13, 1921.

In conclusion, we may call attention to the agreement of the results of this investigation with those obtained by Lindblad[1] through a spectrophotometric study of the intensity of the continuous spectrum. Lindblad found that the region λ 3889–λ 3907, when compared with the adjacent region λ 3907–λ 3935, was relatively less intense in the spectrum of the intrinsically fainter stars. This effect he ascribed to the expansion of the wings of Hζ in such stars, as well as to the widening of certain of the arc lines of iron and silicon. In other words, the spectra of such stars are diffuse, and we obtain the same differentiation between the absolute magnitudes of stars with sharp and diffuse lines that has been found by other methods in the course of this investigation.

It is hardly necessary to state that the methods described in this communication can no doubt be greatly improved and refined. They appear capable, however, of yielding results of considerable value for the stars belonging to the largest of the spectral types. In addition, it seems probable that similar methods may be applied to the stars of the B type. It is well known from the work of several investigators that the stars of types B8 and B9 are considerably fainter intrinsically than those of the earlier divisions like B0 and B1. There is a strong probability, therefore, that a relationship between spectral type and absolute magnitude similar to that found for the A stars exists among those of type B.

SUMMARY

The principal results of this study may be summarized briefly.

1. A considerable number of A-type stars belonging to the Taurus and Ursa Major groups have been classified as accurately as possible into the subdivisions of this type and the spectra designated as nebulous or sharp according to the character of the lines.

2. From a comparison of the results a definite relationship between absolute magnitude and spectral type, as well as between absolute magnitude and the sharp or diffuse character of the lines, has been established.

---

[1] *Mt. Wilson Contr.*, No. 228; *Astrophysical Journal*, 55, 85, 1922.

3. Through an extension to stars with parallaxes determined by trigonometric methods, it is found that the same relationships are valid for stars outside of the moving clusters.

4. When this method for the determination of absolute magnitudes is applied to individual stars, a degree of accuracy is found quite comparable with that for stars of the later spectral types.

5. A catalogue of the parallaxes of 544 stars derived in this way is given.

6. A comparison between the average of the proper motions and the average of the parallaxes of these stars shows a satisfactory degree of correlation between the two.

7. The stars such as α Cygni having the so-called "c" characteristics require separate treatment. It seems probable that the intensities of the well-known enhanced lines λ 4481 and λ 4233 may be used as criteria for the determination of the absolute magnitudes of such stars. The same lines may perhaps be used for intrinsically faint A-type stars, in which these lines are very weak.

MOUNT WILSON OBSERVATORY
May 1922

THE DISTRIBUTION OF THE VELOCITIES OF STARS OF SPECTRAL TYPES F TO M[1]

By GUSTAF STRÖMBERG

ABSTRACT

Frequency-distribution of the velocity-vectors of stars of types F to M.—The three components of the velocities of about 1300 stars were computed from available data and referred to the galactic system of co-ordinates, assuming a solar motion of 20 km toward the apex $\alpha = 270^\circ$, $\delta = +30^\circ$. The frequency-distribution of the velocity-vectors in each of six groups, including, respectively, types A6–F9, F0–G5, G6–K1, K2–K9, Ma–Md, G0–M, and magnitudes 0–6, <3, <4, <4, <3, >3, was represented by a three-dimensional cosine-series with a large number of terms determined by harmonic analysis. From these results curves of equal frequency were drawn in the *xy*- and *yz*-planes (Figs. 1–6). It is evident from these that *giant stars* of types F2M form a single group or stream with an approximately ellipsoidal distribution, the shortest axis being nearly in the direction of the galactic pole. The elongation of the ellipsoid is greatest for the bright F stars and least for the late K and M stars, for which the distribution is nearly spherical. Among stars of spectral type F and magnitude 0 to 6 an additional stream was found moving nearly parallel with the Taurus group and including about one-fifth of the stars of this type. There is a marked asymmetry in the distribution of velocities, especially for the higher velocities. As a result, the most frequent velocity coincides neither with the mean velocity nor with the center of the velocity-ellipsoid, but has the values given in Table VII, being 13.4 km in the direction $\alpha = 86^\circ.2$, $\delta = -30^\circ.8$ (relative to the sun) for the giant stars. Another consequence of the asymmetry is that the constants of the ellipsoidal frequency-function depend somewhat on the method of computation on account of the difference in weighting the high velocities. The results of two methods are given (Tables IV, V, and VI). The *dwarf stars* also form a single group and show an ellipsoidal distribution of velocities, the most frequent velocity being 37.7 km in the direction $\alpha = 98^\circ.8$, $\delta = -17^\circ.4$ (relative to the sun).

Solar motion derived from the algebraic means of velocities of stars of types F to M is found to be dependent on the spectral types and absolute magnitudes of the group of stars used. Giant stars of later types give a somewhat higher declination of the apex (+44°) than stars of earlier types (+27°), while dwarf stars give +30°. The velocity from giants comes out 18.8 km while dwarfs give 31.7 km; in fact, stars of high velocity give, in general, a higher solar motion than slower stars, which indicates that the high-velocity stars have a systematic motion in a direction opposite to the sun's motion.

The large number of spectroscopic parallaxes recently determined by Mr. Adams and his collaborators[2] has made it possible to compute the absolute motions in space of about 1300 stars for which the proper motions and radial velocities are determined. The fact that the errors of the spectroscopic parallaxes are proportional to the parallaxes themselves makes them in general better adapted to this purpose than the trigonometric parallaxes. A large number of radial velocities have been determined at the Mount Wilson Observatory during recent years, and I am greatly indebted to my colleagues engaged in this work for permission to use these, as well as the spectroscopic parallaxes, in advance of publication.

---

[1] *Contributions from the Mount Wilson Observatory*, No. 245.

[2] *Ibid.*, No. 199; *Astrophysical Journal*, 53, 13, 1921.

The result of a study of the space-velocities, irrespective of their directions, was published in *Mount Wilson Contribution* No. 210; *Astrophysical Journal*, 54, 9, 1921. Since it is well known that the frequency of velocity-vectors of a given size is quite different in different directions, a detailed study has been made of the general distribution of the three-dimensional velocities. In order to obtain the general character of this distribution, the possible dependency of the velocity-distribution upon position in space was neglected. The known dependency of velocity upon absolute magnitude and spectral type has been taken into account to some extent by grouping the stars according to spectral type and for each type dividing them into two groups of different absolute magnitudes.

COMPUTATION OF THE VELOCITY-COMPONENTS

The three co-ordinates of a star relative to the sun and referred to the equatorial system are

$$\Xi = D\cos\alpha\cos\delta\,;\quad \mathrm{H} = D\sin\alpha\cos\delta\,;\quad \mathrm{Z} = D\sin\delta\,,$$

where α and δ are the right ascension and declination of the star and D its distance from the sun in kilometers. Differentiating these equations with respect to the time, we obtain the three velocity-components in the equatorial system relative to the sun:

$$\left.\begin{aligned}\xi &= \frac{d\Xi}{dt} = V\cos\alpha\cos\delta - \frac{k}{\pi}(\mu_\alpha\sin\alpha\cos\delta + \mu_\delta\cos\alpha\sin\delta)\\ \eta &= \frac{d\mathrm{H}}{dt} = V\sin\alpha\cos\delta + \frac{k}{\pi}(\mu_\alpha\cos\alpha\cos\delta - \mu_\delta\sin\alpha\sin\delta)\\ \zeta &= \frac{d\mathrm{Z}}{dt} = V\sin\delta + \frac{k}{\pi}\mu_\delta\cos\delta\end{aligned}\right\}\qquad(1)$$

where V is the radial velocity relative to the sun, μ_α and μ_δ are the proper motions in right ascension and declination expressed in seconds of arc per year, π is the parallax, and k is the mean distance earth–sun in kilometers divided by the number of seconds in a year. We have thus $k=4.737$ km year/sec.

The proper motions have been taken from Boss's *Catalogue* and corrected according to the formula:[1]

$$\Delta\mu_\alpha^{s} = +0^{s}.00021 - 0^{s}.00015 \sin\alpha \tan\delta$$

$$\Delta\mu_\delta'' = -0''.0023 \cos\alpha$$

For stars not in the Boss *Catalogue* the proper motions have in most cases been taken from the *Publications of the Cincinnati Observatory*, No. 18, Part IV, and in some cases, proper motions determined at Greenwich, and by Kapteyn, Roy, and others have been used. The radial velocities are from the lists published by the Lick, Mount Wilson, Yerkes, Cape, and other observatories, and in addition to these, use has been made of a large number of unpublished radial velocities determined at the Mount Wilson Observatory. The spectroscopic parallaxes have been used except in a few cases where the trigonometric parallaxes are large and well determined.

From this list of stars of known parallax, proper motion, and radial velocity, the following stars have been omitted: (1) the fainter components of binaries, the absolute magnitude used being that of the brighter component; (2) stars selected for observation on account of small proper motion, ninety-nine such stars being omitted; (3) spectroscopic binaries with large variation of the radial velocity for which the orbits are not determined. Many of the stars were of course selected for observation originally on account of large proper motion, but as this selection is mainly a selection of near and thus absolutely faint stars which have been treated separately, no omission is made for this reason. The inclusion of a large number of stars of large proper motion produces, however, an excess of stars of high speed among the giant stars.

SOLAR MOTION

If we form the means of the three velocity-components ξ, η, and ζ for a group of stars, we obtain the velocity of the "centroid" of this group of stars relative to the sun. The opposite vector is the velocity of the sun relative to this centroid. The polar coordinates of this vector are given by the equations:

---

[1] *Op. cit.*, p. xxviii.

$$\left.\begin{aligned} V_0 \cos A_0 \cos D_0 &= -\bar{\xi} \\ V_0 \sin A_0 \cos D_0 &= -\bar{\eta} \\ V_0 \sin D_0 &= -\bar{\zeta} \end{aligned}\right\} \qquad (2)$$

where A_0 and D_0 are the right ascension and declination of the sun's apex and V_0 is the solar velocity. Table I gives the results of this computation for different spectral types and absolute magnitudes. In this case all stars with a space-velocity higher than 100 km have been omitted.

TABLE I

Spectral Type	Absolute Magnitude	Number	A_0	D_0	V_0
A6 to F9.	≦3.0	153	269°	+27°	21.2
	≧3.1	133	274	+35	23.4
G0 to G9.	≦3.0	224	266	+32	19.9
	≧3.1	154	279	+23	40.2
K0 to K9.	≦4.0	325	282	+43	18.3
	≧4.1	112	286	+31	33.1
M.	<4.0	98	271	+44	16.2
	>6.0	16	354:	+68:	26.6:
A6 to M.	Giants	800	272.7	+36.9	18.8
A6 to M.	Dwarfs	415	280.8	+29.5	31.7

From Table I we see that for the giant stars the declination of the sun's apex shows a steady increase from +27° to +44°, which is in agreement with the results of several investigators who have determined its value from proper motions. This increase of the declination of the sun's apex with advancing spectral type was found by Dyson and Thackeray[1] to be especially pronounced among the faint stars in the zone +24° to +32°, and was attributed by them to an increase in the proportion of stars belonging to the second stream among stars of later types. That this explanation is in agreement with the results obtained in the present investigation will be seen later.

---

[1] *Monthly Notices of the Royal Astronomical Society*, **79**, 201, 1919.

Another conclusion to be drawn from Table I is that the dwarf stars apparently show a higher velocity for the sun than the giant stars. This result seems to explain the peculiar fact that the velocity of the sun as determined from the Mount Wilson radial velocities is somewhat larger than the original values of Campbell. The proportion of faint stars of large proper motion measured for radial velocity, most of which are dwarf stars, is fairly large among the stars observed at the Mount Wilson Observatory.

This increase in the velocity of the sun is especially marked if we group the stars according to space-velocity. This velocity, v, corrected for a standard solar motion of 20 km toward the point $\alpha=270°$, $\delta=+30°$, has been computed for each star according to the formula

$$v^2=\xi^2+(\eta-17.3)^2+(\zeta+10.0)^2.$$

Grouping the stars according to this space-velocity, v, and computing the solar motion for each group, we find a very great increase of the sun's motion with increasing space-velocity of the stars (Table II). This indicates that the stars of high velocity have a systematic motion opposite to the sun's motion, a result which was found by Adams and Joy[1] from a study of the space motion of thirty-seven stars of large radial velocity.

TABLE II

v	No.	A_0	D_0	V_0
km				km
0 to 60.	1026	272°1	+29°5	20.6
60 to 100.	210	295.4	+43.4	36.3
100 to 150.	50	288.9	+38.6	75.7
>150.	37	313.1	+53.8	209.1

DISTRIBUTION OF VELOCITIES

The solar motion is only one of a large number of characteristics which determine the general distribution of the velocities. To describe this distribution we may think of a certain number of stars starting at the same moment from a common origin with velocities equal and parallel to their velocities in space. After one second they will have spread out into a cluster, the mean density of which at a certain point is proportional to the probability that a star of this group has the velocity corresponding to the point in question. In studying this distribution two different types of frequency-functions have been used, viz., those based upon the two-drift theory of Kapteyn and the ellipsoidal theory of Schwarzschild. In order to make an inductive study of the distribution of the velocity-vectors without restricting ourselves to a special frequency-function, a more general type of function has to be used. One such function has been introduced by Charlier[1] for a "unitary statistical population" with three variables. The practical application of this function, however, requires the use of moments of high order, and this necessarily gives the stars of high velocity a much higher weight in the determination of the constants of the function than stars of low velocity. In the present case we are dealing with fairly small groups of stars and, on account of the selection of stars of large proper motion, too great a proportion of stars of high speed has probably been included. Hence it is especially important, at least when dealing with linear velocities, to use a function, the constants of which can be determined *directly* from the *numbers* of stars whose velocity-vectors lie between certain limits. To obtain the general character of the distribution of the velocities, we need, therefore, a general interpolation formula in three dimensions which can easily be integrated and whose constants can be determined simply from the integrated function. For this purpose use has been made of a three-dimensional cosine-series with the origin in the center of the limiting planes. Such a series can be written

---

[1] *Mt. Wilson Contr.*, No. 163; *Astrophysical Journal*, **49**, 179, 1919.

$$\left.\begin{aligned} F(xyz) = {} & a_0 + a_{100} \sin \alpha + a_{010} \sin \beta + a_{001} \sin \gamma + a_{200} \cos 2\alpha + a_{110} \sin \alpha \sin \beta \\ & + a_{101} \sin \alpha \sin \gamma + a_{020} \cos 2\beta + a_{011} \sin \beta \sin \gamma + a_{002} \cos 2\gamma \\ & + a_{300} \sin 3\alpha + a_{210} \cos 2\alpha \sin \beta + a_{201} \cos 2\alpha \sin \gamma + a_{120} \sin \alpha \cos 2\beta \\ & + a_{111} \sin \alpha \sin \beta \sin \gamma + \ldots\ldots \end{aligned}\right\} \quad (3)$$

---

[1] *Meddelanden från Lunds Observatorium*, Serie II, No. 9, p. 79, 1913.

where

$$\alpha=\frac{x\pi}{2c_1}, \qquad \beta=\frac{y\pi}{2c_2}, \qquad \gamma=\frac{z\pi}{2c_3}.$$

The six limiting planes are $x=\pm c_1$, $y=\pm c_2$, $z=\pm c_3$. The three angles α, β, and γ vary between the limits $-\pi/2$ and $+\pi/2$. The only assumptions made in using this frequency-function are that the number of velocity-vectors terminating in a cube *dx dy dz* varies continuously with x, y, and z, and that

$$\frac{dF}{dx}=0, \quad \frac{dF}{dy}=0, \quad \text{and} \quad \frac{dF}{dz}=0 \quad \text{for} \quad x=\pm c_1, \quad y=\pm c_2, \quad z=\pm c_3,$$

respectively.

The disadvantages of this function are that we must use a very large number of terms, and even then it may not be possible to represent the more rapid changes of the mean density of the velocity-cluster. The function is characterized by a large number of coefficients, and it is necessary to plot it graphically in order to gain an idea of its general character. It is, however, a convenient means for obtaining some information about the *actual* distribution of velocities, from which we can afterward decide what type of theoretical frequency-function can best be adopted.

The number of velocity-vectors of a group of stars terminating in a cube *dx dy dz* is expressed by

$$F(xyz)\,dx\,dy\,dz\,.$$

Integrating this function between the limits x_1, x_2; y_1, y_2; z_1, z_2, we find

$$\left.\begin{aligned}\int_{x_1}^{x_2}\int_{y_1}^{y_2}\int_{z_1}^{z_2} F(xyz)dx\,dy\,dz=A(A_0&+A_{100}\sin\bar{\alpha}+A_{010}\sin\bar{\beta}+A_{001}\sin\bar{\gamma}\\ &+A_{200}\cos 2\bar{\alpha}+A_{110}\sin\bar{\alpha}\sin\bar{\beta}+A_{101}\sin\bar{\alpha}\sin\bar{\gamma}\\ &+A_{020}\cos 2\bar{\beta}+A_{011}\sin\bar{\beta}\sin\bar{\gamma}+A_{002}\cos 2\bar{\gamma}+A_{300}\sin 3\bar{\alpha}\\ &+A_{210}\cos 2\bar{\alpha}\sin\bar{\beta}+\;.\;.\;.\;.\;)\end{aligned}\right\}\quad(4)$$

where

$$A=(x_2-x_1)(y_2-y_1)(z_2-z_1).$$

$$\bar{\alpha}=\tfrac{1}{2}(\alpha_1+\alpha_2)=\frac{\pi}{4c_1}(x_1+x_2)$$

$$\bar{\beta}=\tfrac{1}{2}(\beta_1+\beta_2)=\frac{\pi}{4c_2}(y_1+y_2)$$

$$\bar{\gamma}=\tfrac{1}{2}(\gamma_1+\gamma_2)=\frac{\pi}{4c_3}(z_1+z_2)$$

$$A_{lmn}=k_lk_mk_na_{lmn}$$

$$k_l=\frac{\sin\frac{l\Delta\alpha}{2}}{\frac{l\Delta\alpha}{2}}\;;\quad \Delta\alpha=\alpha_2-\alpha_1=\frac{\pi}{2c_1}(x_2-x_1)$$

$$k_m=\frac{\sin\frac{m\Delta\beta}{2}}{\frac{m\Delta\beta}{2}}\;;\quad \Delta\beta=\beta_2-\beta_1=\frac{\pi}{2c_2}(y_2-y_1)$$

$$k_n=\frac{\sin\frac{n\Delta\gamma}{2}}{\frac{n\Delta\gamma}{2}}\;;\quad \Delta\gamma=\gamma_2-\gamma_1=\frac{\pi}{2c_3}(z_2-z_1)\,.$$

As the unit of volume, we have for convenience used 1000 km^3; thus we have to replace the A just given by

$$0.001(x_2-x_1)(y_2-y_1)(z_2-z_1).$$

Starting with a group of N stars of a certain range in spectral type and absolute magnitude, we can compute how many rectilinear velocity-components fall inside a parallelopiped inclosed by the planes $x=x_1$; $x=x_2$; $y=y_1$; $y=y_2$; $z=z_1$; $z=z_2$. If N is the total number of stars in the group and n is the number of velocity-vectors terminating inside this parallelopiped, we have equations of condition of the form

$$N\int_{x_1}^{x_2}\int_{y_1}^{y_2}\int_{z_1}^{z_2}F(xyz)dx\,dy\,dz=NA(A_0+A_{100}\sin\bar{\alpha}$$
$$+A_{010}\sin\bar{\beta}+\;.\;.\;.\;.)=n. \qquad (5)$$

The computation of the constants of the series is very much facilitated by dividing the distances $-c_1$ to $+c_1$, $-c_2$ to $+c_2$, $-c_3$ to $+c_3$ into p_1, p_2, and p_3 equal parts, respectively, the p's being even numbers.

The solution of the equations of condition (5) is then simplified by the relationships

$$\left.\begin{aligned}
\Sigma \sin^2 \bar{\alpha} &= \Sigma \cos^2 2\bar{\alpha} = \Sigma \sin^2 3\bar{\alpha} = \Sigma \cos^2 4\bar{\alpha}, \text{ etc.} = \frac{p_1}{2} \\
\Sigma \sin^2 \bar{\beta} &= \Sigma \cos^2 2\bar{\beta} = \Sigma \sin^2 3\bar{\beta} = \Sigma \cos^2 4\bar{\beta}, \text{ etc.} = \frac{p_2}{2} \\
\Sigma \sin^2 \bar{\gamma} &= \Sigma \cos^2 2\bar{\gamma} = \Sigma \sin^2 3\bar{\gamma} = \Sigma \cos^2 4\bar{\gamma}, \text{ etc.} = \frac{p_3}{2}
\end{aligned}\right\} \qquad (6)$$

All the products in the least-squares solution vanish, and we have, for example,

$$NAA_0 = \frac{\Sigma n}{p_1 p_2 p_3}, \quad NAA_{100} = \frac{2\Sigma n \sin \bar{\alpha}}{p_1 p_2 p_3}, \quad NAA_{020} = \frac{2\Sigma n \cos 2\bar{\alpha}}{p_1 p_2 p_3},$$

$$NAA_{111} = \frac{8\Sigma n \sin \bar{\alpha} \sin \bar{\beta} \sin \bar{\gamma}}{p_1 p_2 p_3}, \quad NAA_{231} = \frac{8\Sigma n \cos 2\bar{\alpha} \sin 3\bar{\beta} \sin \bar{\gamma}}{p_1 p_2 p_3}.$$

When the coefficients A_{lmn} have been determined, the coefficients a_{lmn} are found from the equation

$$a_{lmn} = \frac{1}{k_l k_m k_n} A_{lmn}.$$

The total number of stars in the group has been reduced to 1000, and the series $F = a_0 + a_{100} \sin \alpha + a_{010} \sin \beta \; . \; . \; . \; .$, gives us then the number of velocity-vectors terminating in a cube of 10 km on the edge, the center of which is in the point x, y, z.

The fact that the motions of the stars are related to the plane of the galaxy makes it convenient to use galactic co-ordinates instead of equatorial. In order to have the origin near the center of the distribution, we have corrected all velocities for a standard solar motion of 20 km toward the point $A_0 = 270^\circ$, $D_0 = +30^\circ$. The pole of the galaxy is supposed to have the position $\alpha = 190^\circ.6$, $\delta = +27^\circ.2$ (Kapteyn).

If x, y, and z denote the galactic co-ordinates, we have the following equations of transformation:

$$\left.\begin{aligned} x&=+0.185\,\xi-0.983\,\eta+17.0 \\ y&=+0.449\,\xi+0.084\,\eta+0.889\,\zeta+7.4 \\ z&=-0.874\,\xi-0.164\,\eta+0.457\,\zeta+7.4 \end{aligned}\right\} \tag{7}$$

All constants derived from the frequency-functions are given in this system of co-ordinates. They can readily be converted into equatorial co-ordinates relative to the sun by aid of the equations

$$\left.\begin{aligned} \xi&=v\cos\alpha\cos\delta=+0.185x+0.449y-0.874z \\ \eta&=v\sin\alpha\cos\delta=-0.983x+0.084y-0.164z+17.3 \\ \zeta&=v\sin\delta \qquad\quad\;\, = \qquad\qquad +0.889y+0.457z-10.0 \end{aligned}\right\} \tag{8}$$

In Table III are given some data for the six different groups for which the coefficients in the series have been computed. The first two of these groups are overlapping. All terms up to the sixth order have been computed and in some cases terms of an even higher order. The total number of stars is in all cases reduced to 1000, and the unit of volume is 1000 km³. The most frequent velocity corresponds to the point of highest density in the velocity-cluster, and such a point is inclosed by non-intersecting surfaces of equal density. The intersections of these equi-frequential surfaces with any plane are closed curves surrounding the point or points of highest density.

TABLE III

	Group					
	I	II	III	IV	V	VI
Spectrum	A6 to F9	F0 to G5	G6 to K1	K2 to K9	Ma to Md	G0 to M
Absolute magnitude	0.0 to 5.5	≤2.9	≤3.9	≤3.9	<3	≥3.0
c_1	40	40	60	60	60	160
c_2	30	30	60	60	60	160
c_3	30	30	60	60	60	160
Number of stars	278	197	252	220	115	343
Number within limits	174	148	231	205	108	340
Taurus stars omitted	9	4	5	0	0	0

In Figures 1 to 6 are shown the intersections of the surfaces of equal frequency with the xy-plane (galactic plane) and the xz-plane. The x-axis is directed toward the intersection of the galactic plane with the equator (in Aquila). The velocity of the sun in this system of co-ordinates has the components +17.0, +7.4, and

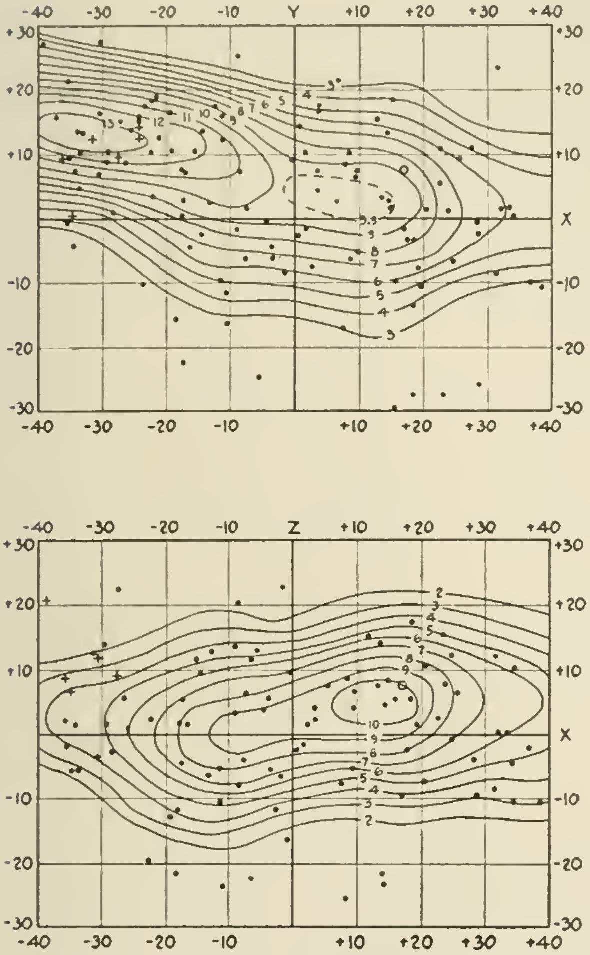

A6 to F9; M=0.0 to 5.5

FIG. 1

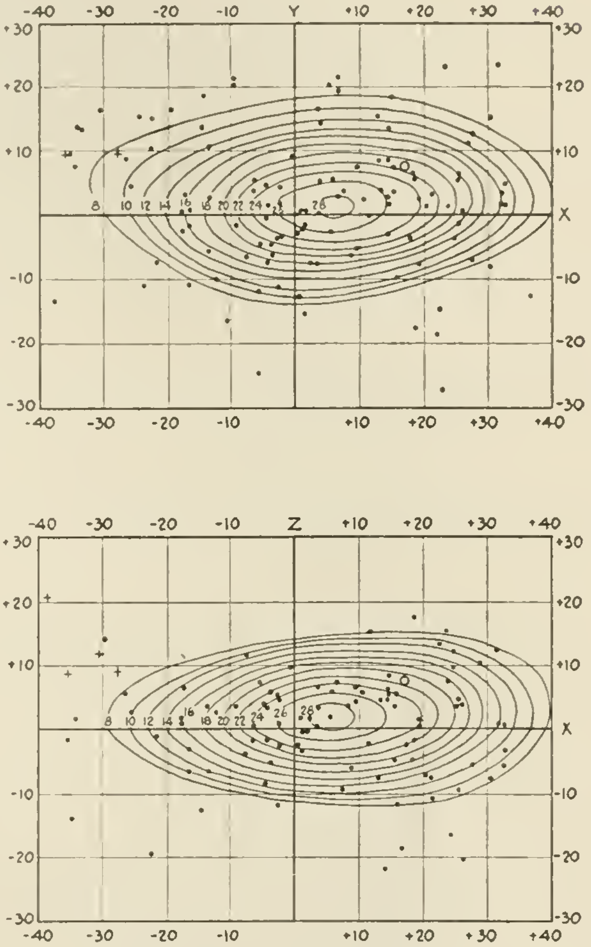

F0 to G5 M≦2.9

FIG. 2

+7.4 km, and is denoted by the symbol ⊙. The recognized members of the Taurus stream were omitted in the computation but are marked in the diagram by crosses. The dots in the diagrams represent the velocities of those stars whose velocity-components perpendicular to the plane of projection are small, the limits in Figures 1 and 2 being ± 10 km and in Figures 3 to 5, ± 20 km. For the dwarf stars in Figure 6 the projections in the xy- and xz-planes of the velocities of all the stars are given.

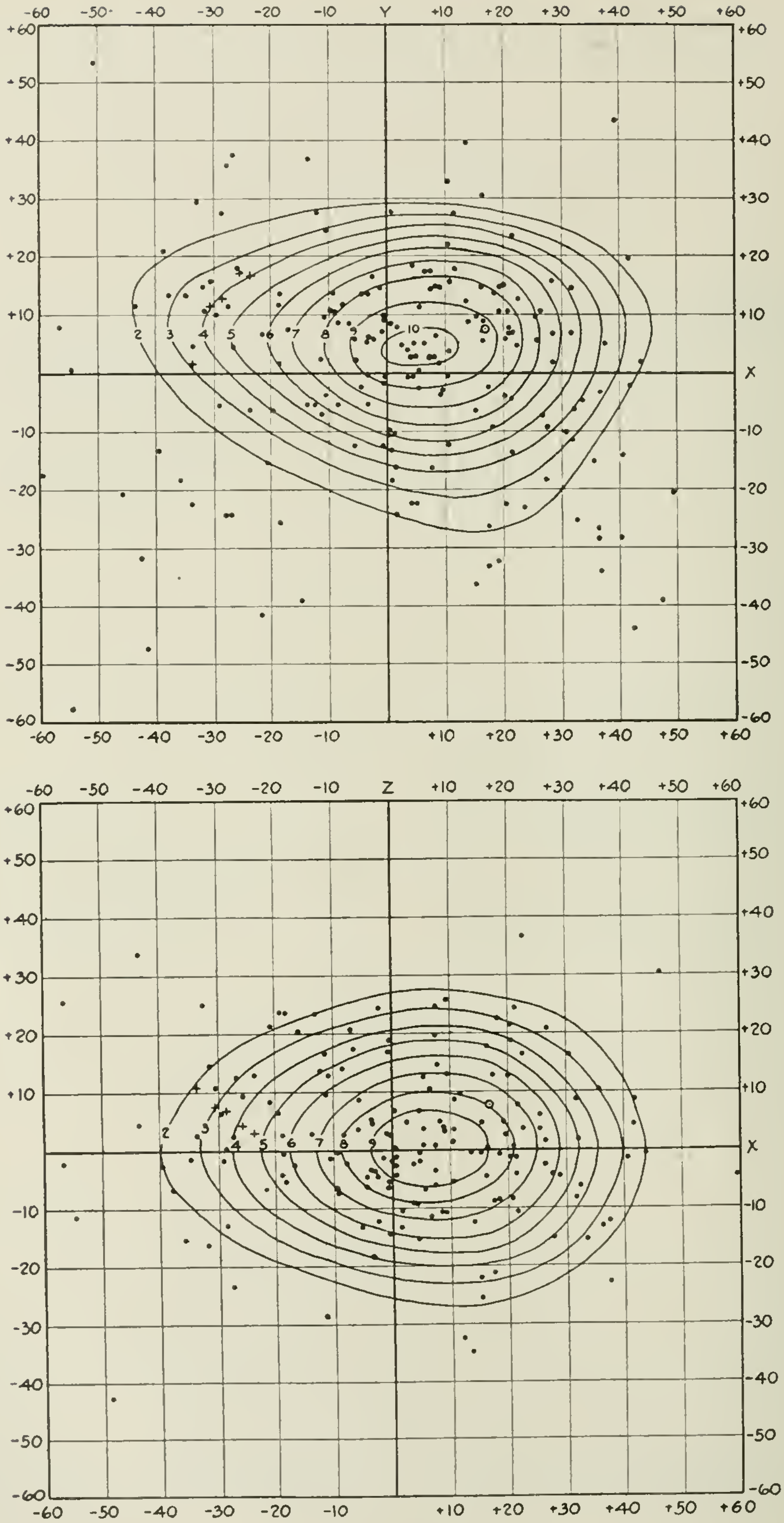

G6 to K1, M≦3.9

Fig. 3

A study of the diagrams in Figures 1 to 6 and the series upon which they are based leads to the following conclusions:

1. The giant stars of all types form a single "group" with an approximately ellipsoidal distribution, the longest and the intermediate axes in all cases lying very nearly in the galactic plane and coinciding approximately with the x- and y-axes. The shortest axis is nearly perpendicular to the galactic plane. The elongation of the ellipsoids is largest for the bright F stars and decreases for later types, the distribution being nearly spherical for the later K and the M stars.

2. The spread of the velocity-cluster increases with advancing spectral type and is much larger for the dwarf stars than for the giant stars.

3. The most frequent velocity does not coincide with the origin but lies for all the groups of giant stars in the first quadrant of the xy-plane and has the approximate values, $x=+5.8$, $y=+2.7$, $z=+1.7$ km. Relative to the sun this velocity is 13.4 km toward the point $\alpha=86°$, $\delta=-31°$.

4. If we exclude the very brightest F stars, many of which are Cepheid variables and stars of similar spectra, and take together stars of types A6 to F9, absolute magnitude 0 to 5.5, we find that these stars divide themselves into two streams. One of these coincides with the general group of giant stars, as can be seen from the agreement of its condensation point with that of the giant stars of other spectral types, while the other stream moves nearly parallel to the Taurus group. This latter stream comprises about 20 per cent of the ordinary stars of F type and its existence seems to indicate that a large number of stars of this spectral type in all regions of the sky are traveling with a velocity nearly identical with that of the Taurus group. Even among the brighter F stars, as well as among the G-type giants, the presence of members of this group is indicated by the protruding form of the equi-frequential surfaces in this region. This stream might be identified with Kapteyn's first drift, although the galactic latitude is not quite zero.

5. The dwarf stars, among which have been included stars of spectral types G0 to M of absolute magnitude fainter than 3.0, seem to form a group of their own as regards their motions. The

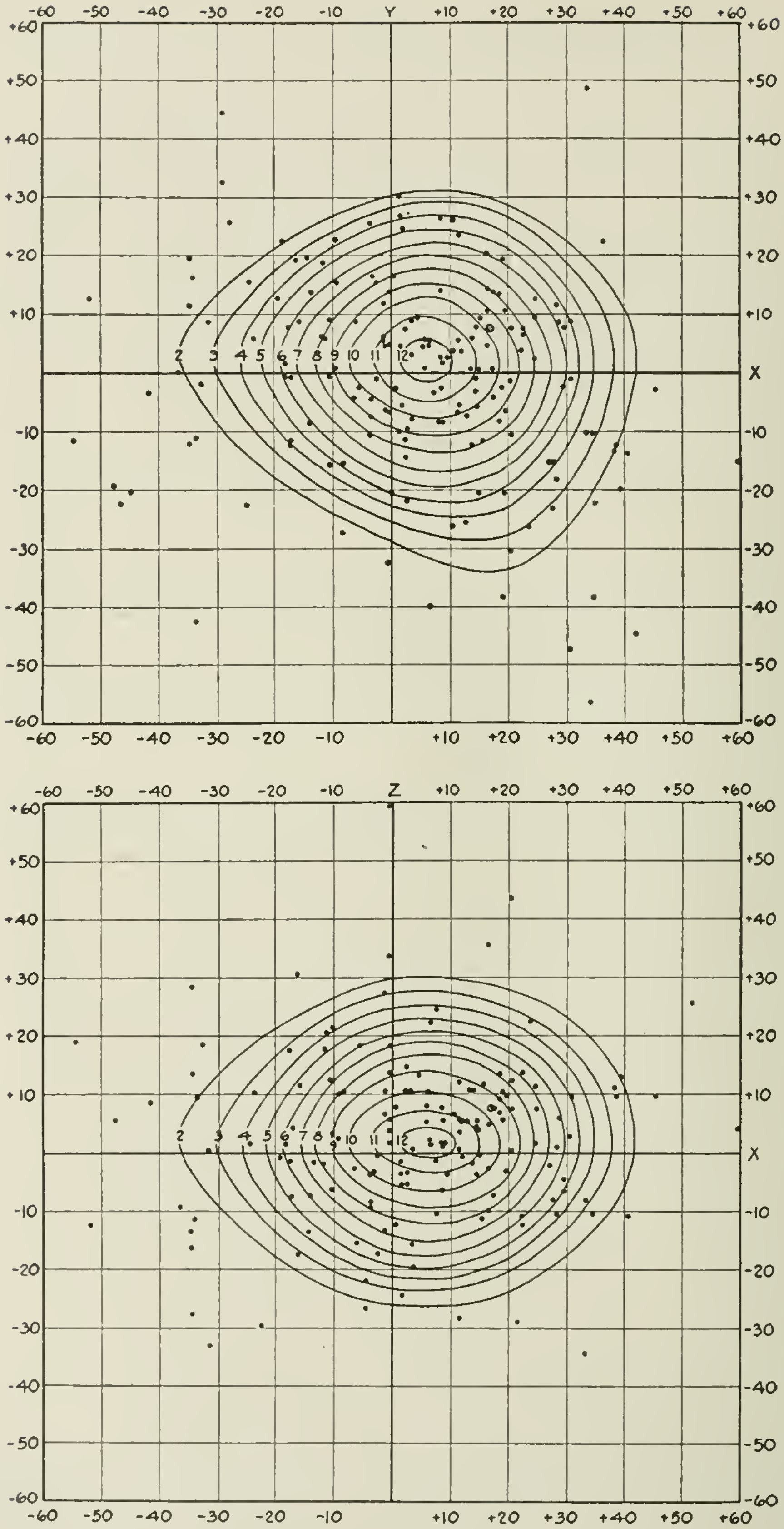

K2 to K9; $M \leqq 3.9$

FIG. 4

distribution of the velocities is ellipsoidal, with the major axis forming an angle of about 160° with the x-axis. The most frequent velocity is approximately $x = -19$, $y = -2$, $z = +1$ km, which nearly coincides with Kapteyn's first drift, while his second drift has been swallowed up by the ellipsoidal stream of giant stars.

6. There is a very marked asymmetry in the distribution of the velocities around the most frequent velocity-vector. The stars of high velocity show a tendency to avoid the first quadrant of the xy-plane. This produces a difference between the most frequent velocity and the mean velocity. The latter nearly coincides with the origin if the stars of very high speed are omitted, as was shown in the values for the solar motion given before. That this asymmetry is not due to any selection of stars of large proper motion moving opposite to the sun is shown by a study of the velocity-distribution of stars having very high speeds. In the diagram in Figure 7 arê plotted the projections in the xy-plane of the velocities of the stars having space motions larger than 100 km relative to the origin. The effect of the selection of large proper motions relative to the sun instead of to our adopted origin is then insignificant, and we find that, whatever the spectral type or the absolute magnitude, if the velocity of a star is great there is an avoidance of the first quadrant of the xy-plane.[1] No star of speed higher than 100 km is moving in this direction, a result in agreement with that found by Adams and Joy[2] for stars of high radial velocity.

Different methods can be employed to obtain the constants of the frequency-functions. For all groups of stars except Group I we may use the ellipsoidal theory to represent approximately the distribution. We then disregard the asymmetry already alluded to and the excess of stars of high velocity which has been found to exist when a comparison is made with the distribution of velocities as given by Maxwell's law.[3] The first method was to use the

---

[1] Dr. Merrill has called my attention to the fact that this asymmetry in the motion of stars of high velocity is also indicated by the high value of the solar motion as derived from Md stars and bright-line nebulae. The former have a residual radial velocity of 31 km and give a velocity of the sun of 56 km (P. W. Merrill, *Popular Astronomy*, **29**, 637, 1921). The latter have a residual radial velocity of 30 km and give a velocity of the sun of 29 km (*Lick Observatory Publication*, **13**).

[2] *Loc. cit.*

[3] *Mt. Wilson Contr.*, No. 210; *Astrophysical Journal*, **54**, 9, 1921.

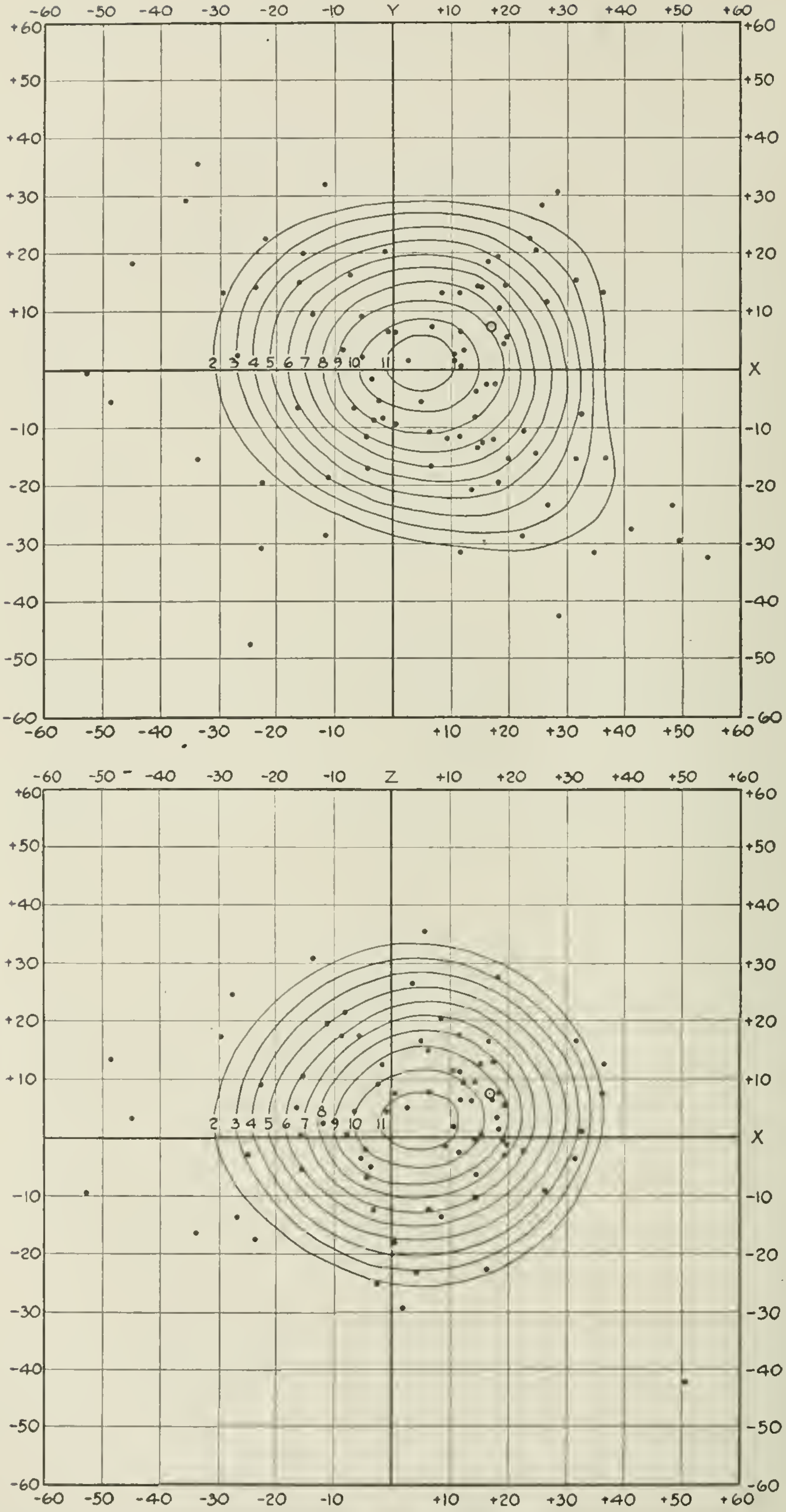

Fig. 5

trigonometric series already determined, and from the coefficients to derive the moments of first and second order. We thus diminish to a large extent the effect of the higher velocities, although in a somewhat arbitrary way.

The values of $\bar{x}$, $\bar{y}$, $\bar{z}$, $\overline{x^2}$, $\overline{yx}$, etc., can be found from the relations

$$\left.\begin{aligned} k\overline{x^l y^m z^n} &= \int_{-c_1}^{c_1}\int_{-c_2}^{c_2}\int_{-c_3}^{c_3} x^l y^m z^n F(xyz)\,dx\,dy\,dz \\ k &= \int_{-c_1}^{c_1}\int_{-c_2}^{c_2}\int_{-c_3}^{c_3} F(xyz)\,dx\,dz\,dy \end{aligned}\right\} \tag{9}$$

From the trigonometric series we find

$$\left.\begin{aligned} a_{000}\frac{\pi^2}{4c_1}\bar{x} &= a_{100}-\frac{a_{300}}{9}+\frac{a_{500}}{25}+\ldots+(-1)^{\frac{n-1}{2}}\frac{a_{n00}}{n^2} \\ a_{000}\frac{\pi^2}{4c_2}\bar{y} &= a_{010}-\frac{a_{030}}{9}+\frac{a_{050}}{25}-\ldots+(-1)^{\frac{n-1}{2}}\frac{a_{0n0}}{n^2} \\ a_{000}\frac{\pi^2}{4c_3}\bar{z} &= a_{001}-\frac{a_{003}}{9}+\frac{a_{005}}{25}-\ldots+(-1)^{\frac{n-1}{2}}\frac{a_{00n}}{n^2} \\ \overline{x^2} &= \frac{c_1^2}{3}-\frac{8c_1^2}{a_{000}\pi^2}\left[\frac{a_{200}}{2^2}-\frac{a_{400}}{4^2}+\ldots+(-1)^{\frac{n}{2}+1}\frac{a_{n00}}{n^2}\right] \\ \overline{y^2} &= \frac{c_2^2}{3}-\frac{8c_2^2}{a_{000}\pi^2}\left[\frac{a_{020}}{2^2}-\frac{a_{040}}{4^2}+\ldots+(-1)^{\frac{n}{2}+1}\frac{a_{0n0}}{n^2}\right] \\ \overline{z^2} &= \frac{c_3^2}{3}-\frac{8c_3^2}{a_{000}\pi^2}\left[\frac{a_{002}}{2^2}-\frac{a_{004}}{4^2}+\ldots+(-1)^{\frac{n}{2}+1}\frac{a_{00n}}{n^2}\right] \\ \frac{a_{000}\pi^4}{16c_1c_2}xy &= a_{110}-\frac{a_{310}}{9}-\frac{a_{130}}{9}+\frac{a_{510}}{25}+\frac{a_{330}}{81}+\frac{a_{150}}{25}+\ldots+(-1)^{\frac{m+n}{2}-1}\frac{a_{mn0}}{m^2n^2} \\ \frac{a_{000}\pi^4}{16c_1c_3}\overline{xz} &= a_{101}-\frac{a_{301}}{9}-\frac{a_{103}}{9}+\frac{a_{501}}{25}+\frac{a_{303}}{81}+\frac{a_{105}}{25}+\ldots+(-1)^{\frac{m+n}{2}-1}\frac{a_{m0n}}{m^2n^2} \\ \frac{a_{000}\pi^4}{16c_2c_3}\overline{yz} &= a_{011}-\frac{a_{031}}{9}-\frac{a_{033}}{9}+\frac{a_{051}}{25}+\frac{a_{033}}{81}+\frac{a_{015}}{25}+\ldots+(-1)^{\frac{m+n}{2}-1}\frac{a_{0mn}}{m^2n^2} \end{aligned}\right\} \tag{10}$$

From these moments we can determine the axes upon which we have to project the velocity-components in order to make the sum

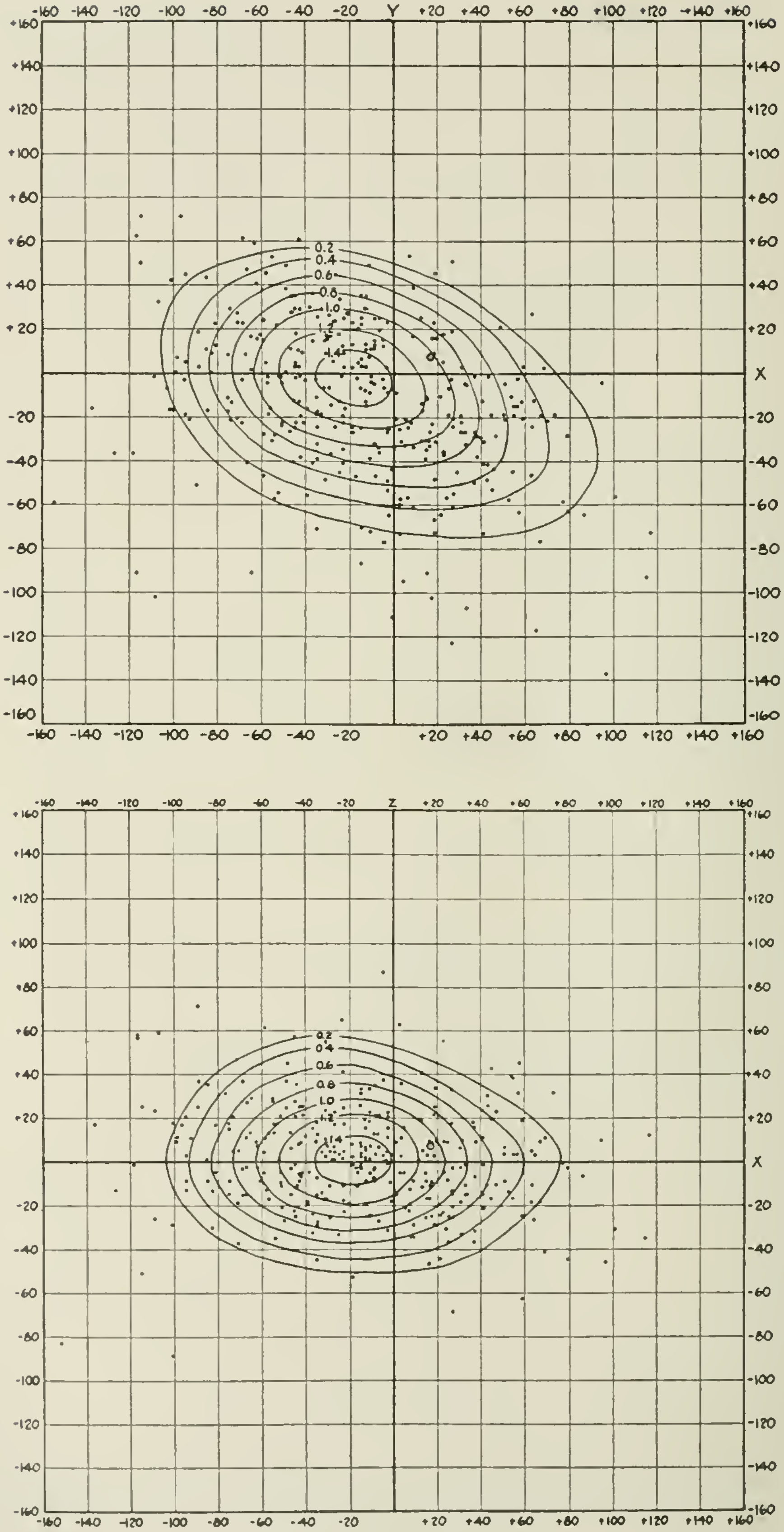

Go to Md ; M ≧ 3.0

FIG. 6

of the squares of the projected velocities a maximum or a minimum. We thus obtain the principal axes of the velocity-ellipsoids, except for the effect of the stars outside the planes $\pm c_1$, $\pm c_2$, and $\pm c_3$, which have been omitted. We should expect in this case to find the length of the axes somewhat smaller than if they had been computed directly from all the velocity-components. On the other hand, the directions of the axes can be determined with higher accuracy than if the high-velocity stars had been included. In Table IV are given the co-ordinates of the centroid as computed from the trigonometric series. For comparison the co-ordinates of the centroid computed directly from the velocity-components are added, as well as the co-ordinates of the axes of the velocity-ellipsoids. All of these results are in galactic co-ordinates.

TABLE IV

CONSTANTS OF VELOCITY-ELLIPSOIDS AS COMPUTED FROM MOMENTS AND REFERRED TO THE GALACTIC CO-ORDINATE SYSTEM

GROUP	CENTROID FROM TRIG. SERIES			CENTROID FROM VELOCITY COMP. OF STARS WITHIN LIMITS			CENTROID FROM VELOCITY COMP. OF ALL STARS		
	$\bar{x}$	$\bar{y}$	$\bar{z}$	$\bar{x}$	$\bar{y}$	$\bar{z}$	$\bar{x}$	$\bar{y}$	$\bar{z}$
	km	km	km	km	km	km	km	km	km
I	− 2.9	+ 3.0	0.0	− 4.3	+ 3.6	+0.3	−11.9	−14.8	+1.3
II	+ 3.3	+ 2.0	+0.1	+ 2.0	+ 2.0	+0.3	+ 1.4	− 3.4	−2.2
III	+ 1.6	− 0.1	+1.3	+ 0.6	+ 0.2	+1.5	− 1.7	− 2.4	+0.8
IV	+ 3.8	− 2.5	+2.4	+ 4.2	− 1.9	+2.0	+ 1.8	− 5.4	0.0
V	+ 5.5	− 2.2	+0.3	+ 5.7	− 2.0	+0.5	+ 5.1	− 5.7	+0.3
VI	−16.1	−12.4	+1.3	−15.3	−13.3	+0.9	−15.9	−16.9	+0.2

GROUP	MAJOR AXIS OF ELLIPSOID			INTERMEDIATE AXIS OF ELLIPSOID			MINOR AXIS OF ELLIPSOID		
	L	*B*	*a*	*L*	*B*	*b*	*L*	*B*	*c*
			km			km			km
II	173°	− 3	18.9	83°	+ 6°	13.5	238°	+83°	8.9
III	181	− 2	25.2	92	+16	20.2	265	+74	15.6
IV	158	+10	21.8	65	+16	18.8	280	+71	11.1
V	147	+11	23.5	54	+14	19.1	275	+72	16.1
VI	153	+ 5	51.3	63	+ 5	32.3	285	+83	22.6

The moments, however, are affected to an unequal extent by small changes in the larger and smaller velocities, and furthermore we have arbitrarily omitted stars of high velocity. This effect may be quite appreciable since we have reason to expect an excess of stars of high velocity compared with ellipsoidal distribution, and the influence of the asymmetry of the distribution may not be eliminated properly. Accordingly another method has been used which gives the constants of the ellipsoidal distribution directly from the observed *number* of velocity-components of definite size. Starting from approximate values of the constants of the function, we can compute corrections to these values from the differences between the observed and the computed number of velocity-vectors terminating in different regions of space. In order to simplify conditions we have to start from axes of co-ordinates which nearly coincide with the principal axes of the velocity-ellipsoids. We assume the following form for the frequency-function:

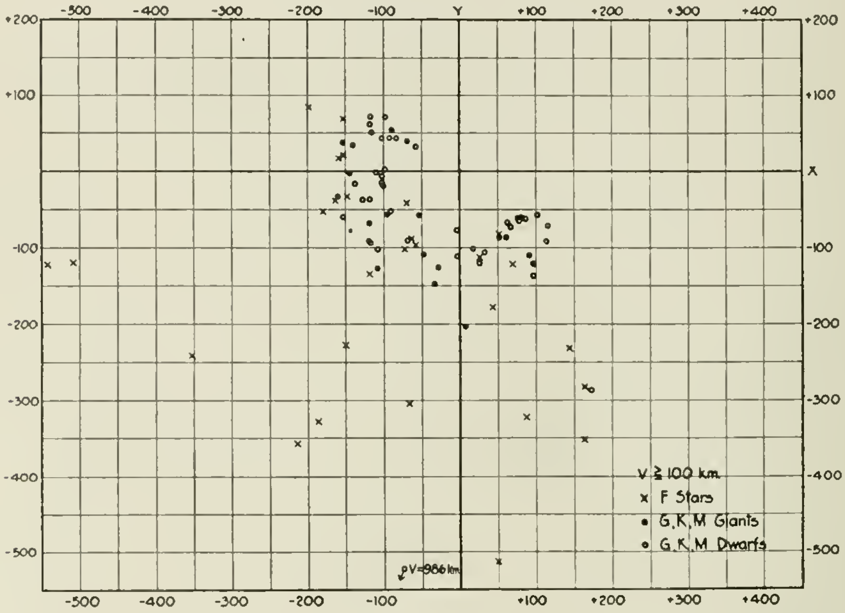

FIG. 7.—Projection on galactic plane of velocities of stars having speeds greater than 100 km per second.

$$F(x)dx\,dy\,dz = Ke^{-S}\,dx\,dy\,dz; \quad S = h_1^2\xi^2 + h_2^2\eta^2 + h_3^2\zeta^2 .$$

Integrating between infinite limits, we have for a total of 1000 stars

$$\int\!\!\int\!\!\int_{-\infty}^{+\infty} F(x)dx\,dy\,dz = K\frac{\pi^{3/2}}{h_1h_2h_3} = 1000$$

Thus

$$K = \frac{1000\, h_1 h_2 h_3}{\pi^{3/2}}\,.$$

The equation of the velocity-ellipsoid of Schwarzschild is then

$$\frac{\xi^2}{a^2} + \frac{\eta^2}{b^2} + \frac{\zeta^2}{c^2} = 1 = 2S$$

and for the axes of the ellipsoid, in other words, the dispersion (mean square deviation) along the principal axes, we have

$$a = \frac{1}{\sqrt{2h_1}}\,, \qquad b = \frac{1}{\sqrt{2h_2}}\,, \qquad c = \frac{1}{\sqrt{2h_3}}\,.$$

We shall assume that the axes of the system of co-ordinates are approximately parallel to the principal axes of the ellipsoids. This assumption can be made in all cases except for the dwarf stars. For these a recomputation of the distribution has been made relative to another co-ordinate system turned through an angle of $-24°$ about the z-axis.

The co-ordinates ξ, η, ζ in the system of co-ordinates which corresponds to the principal axes of the ellipsoids and the center of which coincides with the center of the ellipsoids are connected with the co-ordinate system used previously by the equations

$$\left.\begin{aligned}
\xi &= \alpha_1(x-x_0) + \alpha_2(y-y_0) + \alpha_3(z-z_0)\\
\eta &= \beta_1(x-x_0) + \beta_2(y-y_0) + \beta_3(z-z_0)\\
\gamma &= \gamma_1(x-x_0) + \gamma_2(y-y_0) + \gamma_3(z-z_0)
\end{aligned}\right\} \qquad (11)$$

x_0, y_0, and z_0 here denote the co-ordinates of the center of the ellipsoid; α_1, α_2, and α_3, the direction cosines for the ξ-axis, etc.

Assuming approximate value of h_1, h_2, h_3, x_0, y_0, z_0 and $\alpha_1 = \beta_2 = \gamma_3 = +1$; $\alpha_2 = \alpha_3 = \beta_1 = \beta_3 = \gamma_1 = \gamma_2 = 0$, we can compute the number of velocity-vectors that terminate in a parallelopiped limited by the six planes x_1, x_2; y_1, y_2; z_1, z_2, as well as its derivatives with regard to the constants of the frequency-function. If n_c is this number, we have

$$n_c = K\int_{\xi_1}^{\xi_2} e^{-h_1^2\xi^2}\,d\xi \int_{\eta_1}^{\eta_2} e^{-h_2^2\eta^2}\,d\eta \int_{\zeta_1}^{\zeta_2} e^{-h_3^2\zeta^2}\,d\zeta$$

$$= 125\,\Theta(\xi_1\xi_2)\,\Theta(\eta_1\eta_2)\,\Theta(\zeta_1\zeta_2) \qquad (12)$$

where

$$\Theta(\xi_1\xi_2) = \frac{2}{\sqrt{\pi}}\int_{h_1\xi_1}^{h_1\xi_2} e^{-t^2}dt\,;\quad \Theta(\eta_1\eta_2) = \frac{2}{\sqrt{\pi}}\int_{h_2\eta_1}^{h_2\eta_2} e^{-t^2}\,dt\,;$$

$$\Theta(\zeta_1\zeta_2) = \frac{2}{\sqrt{\pi}}\int_{h_3\zeta_1}^{h_3\zeta_2} e^{-t^2}dt\,.$$

The orientation of the ellipsoid can be determined by three independent quantities L_1, B_1, and B_2, of which L_1 and B_1 are the galactic longitude and latitude of the ξ-axis and B_2 the galactic latitude of the η-axis. These are all supposed to be fairly small quantities and correspond to small rotations about the z-, y-, and x-axis, respectively.

The equations of conditions then take the form

$$\left.\begin{array}{l}\dfrac{dn}{dh_1}\Delta h_1+\dfrac{dn}{dh_2}\Delta h_2+\dfrac{dn}{dh_3}\Delta h_3+\dfrac{dn}{dx_0}\Delta x_0+\dfrac{dn}{dy_0}\Delta y_0+\dfrac{dn}{dz_0}\Delta z_0 \\ \qquad\qquad +\dfrac{dn}{dL_1}L_1+\dfrac{dn}{dB_1}B_1+\dfrac{dn}{dB_2}B_2+n_c\kappa = n_0-n_c\,.\end{array}\right\} \qquad (13)$$

The observed number n_0 is reduced to a total of 1000 stars. Since we wish to determine the constants of the function from the distribution of velocities within a limited space, and do not wish to impose the condition that the number of stars of very high velocity is in exact agreement with the assumed distribution-law, we add the term $n_c\kappa$.

The expressions for the derivatives have been found to be the following:

$$\left.\begin{aligned}
\frac{dn}{dh_1} &= -\frac{250}{\sqrt{\pi}h_1}\Phi(\xi_1\xi_2)\Theta(\eta_1\eta_2)\Theta(\zeta_1\zeta_2)\\
\frac{dn}{dh_2} &= -\frac{250}{\sqrt{\pi}h_2}\Theta(\xi_1\xi_2)\Phi(\eta_1\eta_2)\Theta(\zeta_1\zeta_2)\\
\frac{dn}{dh_3} &= -\frac{250}{\sqrt{\pi}h_3}\Theta(\xi_1\xi_2)\Theta(\eta_1\eta_2)\Phi(\zeta_1\zeta_2)\\
\frac{dn}{dx_0} &= \frac{250h_1}{\sqrt{\pi}}\Psi(\xi_1\xi_2)\Theta(\eta_1\eta_2)\Theta(\zeta_1\zeta_2)\\
\frac{dn}{dy_0} &= \frac{250h_2}{\sqrt{\pi}}\Theta(\xi_1\xi_2)\Psi(\eta_1\eta_2)\Theta(\zeta_1\zeta_2)\\
\frac{dn}{dz_0} &= \frac{250h_3}{\sqrt{\pi}}\Theta(\xi_1\xi_2)\Theta(\eta_1\eta_2)\Psi(\zeta_1\zeta_2)\\
\frac{dn}{dL_1} &= \frac{250(h_2^2-h_1^2)}{\pi h_1h_2}\Psi(\xi_1\xi_2)\Psi(\eta_1\eta_2)\Theta(\zeta_1\zeta_2)\\
\frac{dn}{dB_1} &= \frac{250(h_3^2-h_1^2)}{\pi h_1h_3}\Psi(\xi_1\xi_2)\Theta(\eta_1\eta_2)\Psi(\zeta_1\zeta_2)\\
\frac{dn}{dB_2} &= \frac{250(h_3^2-h_2^2)}{\pi h_2h_3}\Theta(\xi_1\xi_2)\Psi(\eta_1\eta_2)\Psi(\zeta_1\zeta_2)\\
\Phi(\xi_1\xi_2) &= h_1\xi_1e^{-h_1^2\xi_1^2}-h_1\xi_2e^{-h_1^2\xi_2^2}\\
\Phi(\eta_1\eta_2) &= h_2\eta_1e^{-h_2^2\eta_1^2}-h_2\eta_2e^{-h_2^2\eta_2^2}\\
\Phi(\zeta_1\zeta_2) &= h_3\zeta_1e^{-h_3^2\zeta_1^2}-h_3\zeta_2e^{-h_3^2\zeta_2^2}\\
\Psi(\xi_1\xi_2) &= e^{-h_1^2\xi_1^2}-e^{-h_1^2\xi_2^2}\\
\Psi(\eta_1\eta_2) &= e^{-h_2^2\eta_1^2}-e^{-h_2^2\eta_2^2}\\
\Psi(\zeta_1\zeta_2) &= e^{-h_3^2\zeta_1^2}-e^{-h_3^2\zeta_2^2}
\end{aligned}\right\}\tag{14}$$

where ξ_1, ξ_2, η_1, etc., are determined by equation (11). Using the products of the functions Θ, Φ, and Ψ as coefficients, we secure a homogeneous set of equations of condition.

The distribution of velocities for Group I cannot be represented even approximately by an ellipsoidal frequency-function. In this case the sum of one ellipsoidal and one spherical frequency-function has been used, viz.:

$$F(xyz)=\mu Ke^{-S}+(1-\mu)Ke^{-h^2[(x-x_0^1)^2+(y-y_0^1)^2+(z-z_0^1)^2]}$$

$\mu/(1-\mu)$ is the relative proportion of stars belonging to ellipsoidal and to the spherical stream.

The new derivatives in this case are

$$\frac{dN_2}{dh}=-\frac{2N_2}{\sqrt{\pi}h}\left[\frac{\Phi(x_1^1x_2^1)}{\Theta(x_1^1x_2^1)}+\frac{\Phi(y_1^1y_2^1)}{\Theta(y_1^1y_2^1)}+\frac{\Phi(z_1^1z_2^1)}{\Theta(z_1^1z_2^1)}\right]$$

$$x_1^1=x-x_0^1\,,\quad y_1^1=y-y_0^1\,,\quad \text{etc.}$$

$$\frac{dn}{d\mu}=N_1-N_2\,,\quad n=n_c=\mu N_1+(1-\mu)N_2$$

$$\frac{dN_2}{dx_0^1}=\frac{250\,h}{\sqrt{\pi}}\Psi(x_1^1x_2^1)\Theta(y_1^1y_2^1)\Theta(z_1^1z_2^1),\ \text{etc.}$$

We have then

$$\mu\left[\frac{dN_1}{dh_1}\Delta h_1+\frac{dN_1}{dh_2}\Delta h_2+\ \ldots\ .\ +\frac{dN_1}{dB_2}B_2\right]$$
$$+(1-\mu)\left[\frac{dN_2}{dh}\Delta h+\frac{dN_2}{dx_0^1}\Delta x_0^1+\frac{dN_2}{dy_0^1}\Delta y_0^1+\frac{dN_2}{dz_0^1}\Delta z_0^1\right]$$
$$+\frac{dn}{d\mu}\Delta\mu+\kappa n_c=n_0-n_c\,.$$

The results of this computation are given in Table V. The probable errors in each case are given below the corresponding numerical values. According to the usual convention, that direction of the major axis is given which most nearly corresponds to 180° of galactic longitude in order to be comparable with Kapteyn's first stream. The dispersion along the two shortest axes in several cases is so nearly the same that only the direction of the major axis can be well determined.

The elements of the spherical stream of Group I are found to be,

$$x_0 = -31.1 \pm 1.4 \text{ km}$$

$$y_0 = +14.5 \pm 1.1$$

$$z_0 = +\ 3.0 \pm 0.7$$

$$a = \frac{1}{\sqrt{2h}} = 8.1 \pm 0.5$$

$$1 - \mu = 0.185 \pm 0.028.$$

Relative to the sun and in the equatorial system of co-ordinates, this condensation-point has the co-ordinates

$$\alpha = 92^\circ\!.3\,, \qquad \delta = +4^\circ\!.9\,, \qquad v = 48.7 \text{ km}$$

Boss's value[1] for the convergent point of the Taurus group is

$$\alpha = 91^\circ\!.8\,, \qquad \delta = +6^\circ\!.9\,, \qquad v = 45.6 \text{ km}\,.$$

We can thus identify this stream, which is superimposed on the general ellipsoidal distribution, with the Taurus stream, although these stars are scattered all over the sky. The percentage of stars belonging to this general Taurus stream is, as appears from the value of $1-\mu$, 18.5 ± 2.8 per cent of the stars of spectral type A7 to F9 and absolute magnitude 0.0 to 5.5. If we include in this group the nine recognized members of the Taurus stream which were omitted in the analysis, we find that 22 per cent of the stars of this type and absolute magnitude belong to the general Taurus stream. The spread corresponding to a dispersion of 8.1 km is no doubt due in part to errors in the quantities involved, but may also be due in part to an inherent dispersion of the velocities. Attention may be called to the fact that the dispersion of the velocities of the members of the Taurus stream has necessarily been estimated too low hitherto because of the selection of stars whose velocities are very nearly parallel. Even among the stars of type G there are several which belong to this general Taurus stream. This may be

---

[1] L. Boss, *Astronomical Journal*, **26**, 31, No. 604, 1908.

TABLE V

Constants of the Velocity-Ellipsoids as Computed from Distribution of Velocity-Vectors and Referred to the Galactic Co-ordinate System

Group	Center			Major Axis			Intermediate Axis			Minor Axis		
	x	*y*	*z*	*L*	*B*	*a*	*L*	*B*	*b*	*L*	*B*	*c*
	km	km	km			km			km			km
I.....	+ 5.39 ± 1.30	+0.80 ±0.35	+0.06 ±0.55	173°.6 ± 4.1	− 8°.5 ± 3.0	22.86 ± 1.04	....	....	12.25 ± 0.36	....	....	11.68 ± 0.45
II....	+ 5.49 ± 0.83	+1.52 ±0.65	+1.45 ±0.34	177.6 ± 3.4	− 0.1 ± 2.0	18.47 ± 1.13	87.6 ± 3.4	+ 9.1 ± 7.7	10.02 ± 0.43	+267.1 ± 3.4	+80.9 ± 7.7	7.92 ± 0.32
III...	+ 3.10 ± 1.02	−0.82 ±0.98	+0.68 ±0.53	181.0 ± 6.5	+ 4.1 ± 4.4	23.19 ± 0.87	....	....	16.49 ± 0.58	....	....	16.13 ± 0.69
IV....	+ 3.30 ± 0.81	−1.03 ±0.87	+2.50 ±0.33	153 ± 12	+ 2 ± 5	19.86 ± 0.67	....	....	15.93 ± 0.50	....	....	14.55 ± 0.99
V.....	+ 1.3 ± 2.1	−1.6 ±2.3	+5.5 ±1.3	142 ± 25	+27 ±22	18.8 ± 1.4	....	....	16.0 ± 1.4	....	....	15.2 ± 1.1
VI....	−17.0 ± 2.7	−6.8 ±2.2	+1.2 ±1.3	148.7 ± 4.6	+ 7.3 ± 2.4	48.97 ± 1.07	58.7 ± 4.6	+37.0 ±11.5	26.94 ± 0.86	255.3 ± 4.6	+52.4 ±11.5	21.80 ± 0.90

seen from the form of the equi-frequential surfaces as well as from an inspection of the points in the diagram.

In Table VI are given the same quantities as in Table V but referred to the equatorial system of co-ordinates, the center of the ellipsoids being referred to the sun.

TABLE VI

CONSTANTS OF THE VELOCITY-ELLIPSOIDS AS COMPUTED FROM THE DISTRIBUTION OF VELOCITY-VECTORS REFERRED TO THE SUN AND TO THE EQUATORIAL CO-ORDINATE SYSTEM

GROUP	CENTER			MAJOR AXIS		INTERMEDIATE AXIS		MINOR AXIS	
	α	δ	v	α	δ	α	δ	α	δ
			km						
I	84°0	−37°7	15.2	90°2	+ 1°7	....	....	....	....
II	88.0	−34.0	14.2	95.5	+ 2.1	3.0	+71.7	190.1	+18.1
III	91.7	−36.7	17.5	104.8	+ 1.0	....	....	....	....
IV	98.7	−35.7	16.8	89.4	+24.8	....	....	....	....
V	109.6	−29.5	18.2	105.7	+44.0	....	....	....	....
VI	102.4	−24.6	37.4	92.4	+31.1	252.4	+61.8	181.6	− 9.4

If we take the vectors opposite to those given in columns 2–4 of Table VI, we have the velocity of the sun referred to the center of the velocity-ellipsoid. For the giant stars this velocity is appreciably smaller than the velocity of the sun computed from the mean velocity. This result is due to the asymmetry of the distribution of the velocities taken in combination with the different weights given different stars in the use of quantities of zero order (numbers) and of first order (means). If the solar motion is used for the purpose of computing parallaxes from parallactic motion, the velocity based upon the means of the components should be employed.

Another consequence of this asymmetry is that the most frequent velocity does not correspond either to the mean velocity or to the center of the ellipsoidal distribution. From the diagrams we can easily estimate this most frequent velocity by determining the points of highest density of the general frequency-function. In Table VII these values are given both in galactic rectilinear co-ordinates relative to our adopted origin, and in equatorial polar co-ordinates relative to the sun.

TABLE VII

MOST FREQUENT VELOCITY-VECTORS

Group	x	y	z	α	δ	v
	km	km	km			km
I................	$+9$	$+3$	$+5$	100°	$-33°$	9.
II................	$+6.1$	$+1.1$	$+1.9$	90.4	-36.6	13.7
III................	$+6.0$	$+4.9$	$+0.4$	75.9	-24.6	13.2
IV................	$+5.8$	$+2.2$	$+2.0$	88.6	-32.2	13.5
V................	$+4.7$	$+1.0$	$+3.4$	97.9	-31.8	14.4
VI................	-19.0	-2.0	$+1.2$	98.8	-17.4	37.7
Giants (II to V)....	$+5.8$	$+2.7$	$+1.7$	86.2	-30.8	13.4

SUMMARY

The three components of the velocities of about 1300 stars of spectral types F to M have been computed from the proper motions, radial velocities, and parallaxes. The following are the principal results of the investigation:

1. The solar motion as derived from the algebraic means of the velocity-components is found to be dependent on the spectral types and absolute magnitudes of the stars to which it is referred. The giant stars of the later types give a somewhat higher declination of the sun's apex than the giant stars of earlier types. The dwarf stars give a much larger solar motion than the giant stars, and, in general, stars of high velocity give a larger motion than stars of low velocity.

The distribution of velocities of different groups of stars has been studied in different ways. The velocities are referred to the galactic system of stars and have been corrected for a standard solar velocity of 20 km toward the point $\alpha = 270°$, $\delta = +30°$.

In order to learn the nature of this distribution a very general type of frequency-function has been used, which in reality is an interpolation formula in three dimensions. The function is a three-dimensional cosine-series in which the coefficients are determined directly from the *number* of velocity-vectors within different limits. A very large number of terms has been determined by harmonic analysis, a synthesis has been made for the xy- and xz-planes, and curves of equal frequency have been drawn in these planes (Figs. 1–6 and Table III). From a study of these figures we can draw the following conclusions:

2. The giant stars of types F to M form a single group or "stream" with an approximately ellipsoidal distribution, the longest axis lying in the galactic plane and nearly coinciding with the x-axis, the line of intersection of the equator with the galactic plane. The shortest axis is nearly in the direction of the galactic pole. The elongation of the velocity-ellipsoid is largest for the bright F stars and smallest for the late K and M stars, for which the distribution is nearly spherical.

3. The most frequent velocity does not coincide with the origin, but for all groups of giant stars lies in the first quadrant of the xy-plane, and corresponds approximately to a velocity 13.4 km relative to the sun in the direction $\alpha=86^\circ\!.2$, $\delta=-30^\circ\!.8$. For the dwarf stars the most frequent velocity relative to the sun is 37.7 km in the direction $\alpha=98^\circ\!.8$, $\delta=-17^\circ\!.4$ (Table VII).

4. Among the stars of spectral types A7 to F9 and absolute magnitudes 0 to +6 there is in addition to the general group of giants another stream the motion of which coincides with that of the Taurus group. These stars are scattered all over the sky and comprise about 20 per cent of the stars of the above-mentioned spectral types and absolute magnitudes. Even among stars of somewhat later types there are stars belonging to this general Taurus group.

5. There is a marked asymmetry in the distribution of the velocities around the most frequent velocity-vector. Stars of high velocity show a tendency to avoid moving toward the first quadrant of the xy-plane. This asymmetry which is especially marked among the stars of very high velocity can be traced even among stars of ordinary velocity, thus producing a systematic difference between the most frequent velocity-vectors and the mean velocity.

6. Neglecting this asymmetry, the constants of the ellipsoidal frequency-function have been computed in two different ways: First, the method of moments was used, the moments being computed from the trigonometric series previously determined (Table IV). Second, the constants were determined from the distribution of velocities itself, approximate values for the constants being assumed and then corrected by values computed from the difference between the observed and the computed number of velocity-vectors

terminating in different parallelopipeds (Tables V and VI). The values computed in this way differ somewhat from those computed from the moments on account of the difference in weighting. The asymmetry in the distribution produces different values for the velocity of the sun, according as the latter is computed from the distribution of velocities itself, or from algebraic means. The first necessarily gives the smallest value for the sun's velocity, the latter the highest.

In the extensive computation involved in this investigation the author has received valuable help from the following members of the computing division: Mrs. Hannah M. Marsh, Miss Ada M. Brayton, and Miss Florence MacCreadie. Dr. Jean Paraskévopoulos of Athens and Professor D. T. Wilson of Cleveland also have taken part in the computations.

Mount Wilson Observatory
June 1922

THE APPLICATION OF VACUUM THERMOCOUPLES TO PROBLEMS IN ASTROPHYSICS[1]

By EDISON PETTIT and SETH B. NICHOLSON

ABSTRACT

Sensitive vacuum thermocouples.—Construction of the couple and cells is described. The couples were made of metal strips about 3 mm long, $\frac{1}{10}$ mm wide and $\frac{1}{120}$ mm thick, each overlapping junction being fused to a blackened tin disk receiver, $\frac{1}{2}$ mm in diameter and $\frac{1}{100}$ mm thick, each couple weighing only about $\frac{1}{30}$ mg. The sensitivity with a high vacuum (10^{-4} mm) was found to be from two to eleven times the value at atmospheric pressure, depending on the couple. To maintain the vacuum, metallic calcium was used. With a sensitive galvanometer (5×10^{-10} amp./mm) the *temperature sensitivity* obtained was 8×10^{-5} deg./mm, in one case. The *efficiency*, however, was very low, only about 10^{-6} of the incident energy being transformed into electrical energy. An ideal heat engine would be a hundred times more efficient.

Stellar radiation measurements.—Method of application of the vacuum thermocouple is described. The cell was mounted on a plate adapted to the Newtonian double-slide plate-holder of the 100-inch telescope, and connected by wires to a D'Arsonval galvanometer in the basement where the deflections were recorded on a moving plate, *Photographic records of the deflections for Vega, Arcturus, α Herculis, and R Hydrae*, with and without a water absorption cell, are reproduced (Plate VII).

Applications of thermocouple to solar energy measurements already made are the registration (1) of spectral energy distribution, (2) of drift curves across the disk in various wave-lengths, and (3) of total radiation curves across sun-spots and faculae.

Self-registering microphotometer is described in which the photo-electric cell is replaced by a vacuum thermopile. A suitable optical system enables the light through a slit 9 mm long and 0.1 mm wide to be integrated so as to eliminate the grain effect in the spectrograms measured.

Transmission curve for water, 1 cm thick, is reproduced.

Optical system for sensitive galvanometer.—By placing a spectacle lens of 6 m focus at the galvanometer and observing the image with cross-hair and eyepiece, a power of 350 could be used and the scale read accurately to 0.1 mm at 8 m.

In 1895 Lebedew[2] found that a thermocouple of iron-constantan was more sensitive in a vacuum than at atmospheric pressure. Since that time the thermocouple has been used both in vacuum and at atmospheric pressure by a number of physicists, for the study of radiation problems. The vacuum thermocouple has been applied to the study of stellar radiation with marked success by Pfund, and more recently by Coblentz. Pfund employed couples of 95Bi+5Sn against 97Bi+3Sb, and Coblentz employed Bi against 95Bi+5Sn and also Bi against Pt with success. The former[3] used charcoal heated by electric discharge, while the latter[1] employed metallic calcium, to maintain the vacuum.

---

[1] *Contributions from the Mount Wilson Observatory*, No. 246.

[2] *Annalen der Physik*, **56**, 12, 1895.

[3] *Allegheny Observatory Publications*, **3**, 45, 1913.

FORM OF CELL EMPLOYED

In the present investigation we have used the three types of cell shown in Plate VI. After considerable experimenting type 3 was adopted. The cell body and connecting tubes are made of Pyrex glass, the calcium tube *C* is of clear quartz, and the plug *P*, containing the platinum wires carrying the thermocouples, is of soda glass. The cell body *A* has an inside diameter of 42 mm and a wall 1.5 mm thick. The quartz tube *C* (14 mm inside diameter) is attached to the Pyrex tube by a ground joint and stop-cock grease, and sealed with red sealing wax. The metallic calcium is held in place by a wad of glass wool. The plug *P* carries three platinum wires to which two thermocouples are attached, at *T*. It is attached with a ground joint, sealed with stop-cock grease, and may be removed or replaced without destroying the thermocouples.

The cell *A* is fitted with two windows, W_1, W_2, of 10 mm clear aperture. The window W_1, which admits the radiation to the thermocouple, is closed with a quartz window 1.5 mm thick, the junction with the ground surface of the lip being made with stop-cock grease and protected by a rim of red sealing wax. In type 2 the window W_1 is of microscope cover-glass 0.12 mm thick. W_2 is closed with a piece of microscope slide-glass 1.28 mm thick. On looking through W_2 the thermocouple junction may be seen projected against the star image or other radiation entering W_1.

The advantages of this design of cell are as follows: (1) large bearing surfaces at the ground junctions of the plug and calcium tube; (2) a minimum exposure of contact surfaces at the windows; (3) couples may be withdrawn or replaced within the cell without danger of damage; (4) the blackened surfaces of the couples may be exposed to either window by simply rotating the plug, thus enabling the cell to be adapted to various apparatus.

PREPARATION OF THE THERMOCOUPLES

The choice of metals for the couples is dependent on a number of physical properties, which may be briefly enumerated as follows:

---

[1] *Bulletin Bureau of Standards*, 11, 185, 1915.

PLATE VI

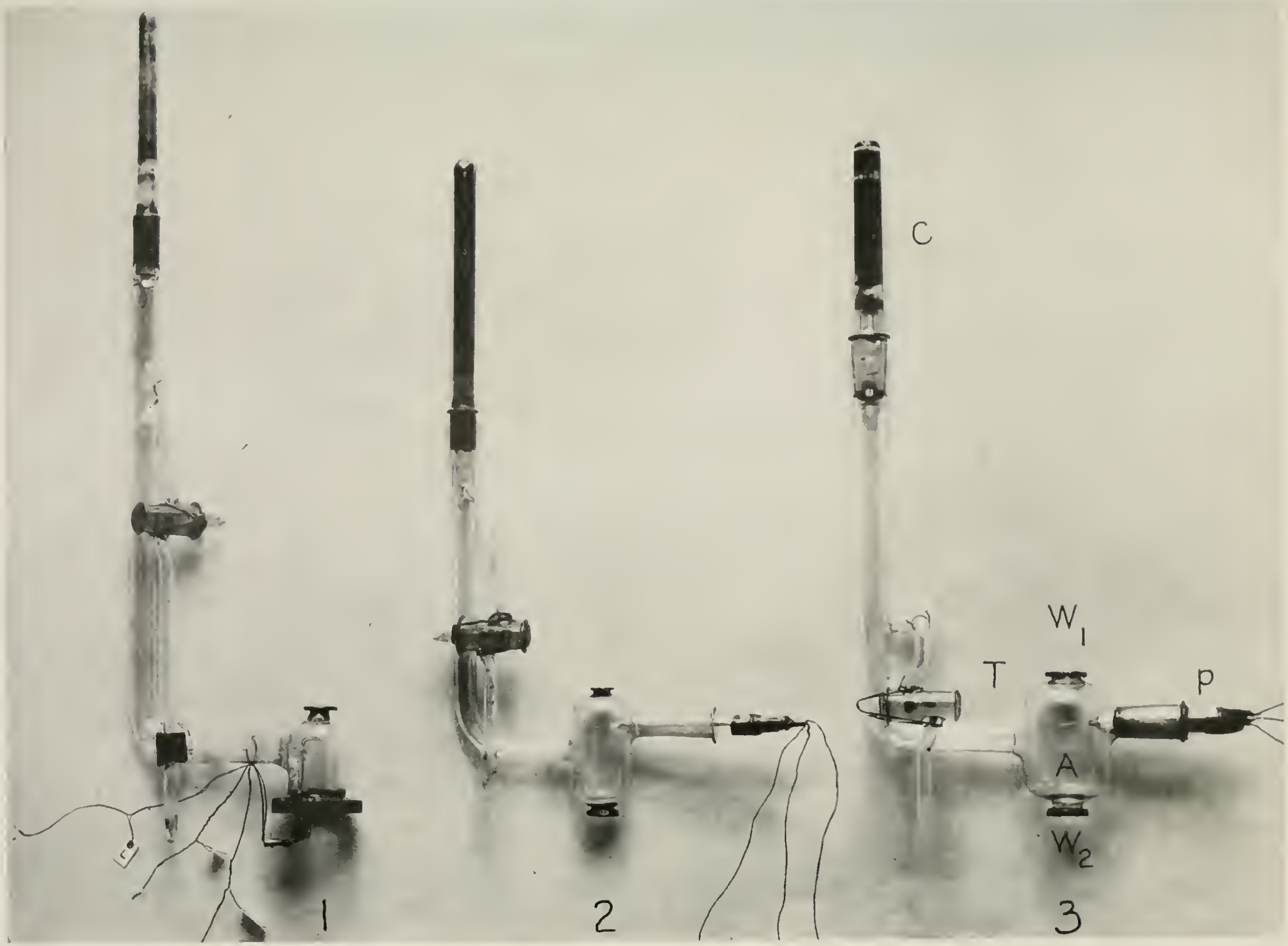

Types of Thermocouple Cells

(1) high electrical conductivity; (2) high thermoelectric power; (3) low heat conductivity; (4) low coefficient of brittleness; (5) approximately equal melting points; (6) low specific heat.

Of these six conditions (1) and (3) and also (2) and (4) are obviously antagonistic in nature. Generally the relative specific coefficients of thermal and electrical conductivity are nearly equal, and high thermoelectric power is associated with a crystalline structure making for great brittleness. There is a considerable range in the constants for some of the metals, especially those of more crystalline structure. This is due principally to two causes: differing conductivity and thermoelectric power in axial and equatorial directions, and impurities in the metal. Taking bismuth as an example, the thermoelectric power axially is $65 \times 10^{-6} V$/deg. C., and equatorially $45 \times 10^{-6} V$/deg. C. An impurity of $\frac{1}{3}$ of 1 per cent of tin will reduce the thermoelectric power to 0 relative to lead. The thermoelectric properties of alloys have been investigated by Mattheissen, Tait, Becquerel, Hutchins, and others, and it is found that most of the metals investigated are very sensitive to changes in the relative proportions of the alloy.

The current produced by the junction of a couple will depend on the thermoelectric power, p, the resistance, R, and the difference in temperature ΔT between the hot and the cold junction. The latter in turn depends on the specific heat of the junction, S; the mass, M; the quantity of heat, C, conducted away along the strips; the quantity C_1 conducted through the air; the quantity C_2 convected away; the quantity radiated, r; and the quantity incident on the junction, Q.

Then

$$I = \frac{kp}{SMR}[Q - (C_1 + C_2 + C + r)] \tag{1}$$

where I is the current and k is a constant depending on the units employed.

Obviously C_1, C_2 may be eliminated by placing the couple in a vacuum. Then r will depend only on the absolute temperature and C should be made as small as possible. In only a few cases, however, will this be of any advantage, since C and R are physically connected, and a decrease in C will correspondingly increase R.

The values of C and $1/R$ are both directly proportional to M, so that after a certain limit is reached, the only advantage in reducing M lies in the quickness of action of the couple in responding to changes in Q. Some advantage is gained, however, by placing at the junction of the two metals a thin plate of a third metal, functioning only as a receiver of the radiation and chosen so that the specific heat will be low. If the plate is very thin and M is small, then its conductivity is unimportant.

The thermoelectric power, p, is itself dependent on the absolute temperature at which the thermocouple is working. Generally this is high for low temperatures and decreases for the higher temperatures, passing through zero and reversing sign at the "temperature of inversion." Considerable advantage would be gained in operating the couple at the temperature, let us say, of liquid air, but the difficulties attending this modification of the apparatus have thus far prevented its successful application.

We have employed chiefly the following metals: Bi, 95Bi+5Sn, Pb, Sn, Pt, Au, Cu, 806Sb+696Cd, Ag, 97Bi+3Sb, Te. When the metals are easily fusible, the simplest method of producing fine flat strips suitable for thermocouples is that first proposed by Pfund. About 10 gm of the metals to be fused and alloyed are placed in a Rose's crucible and heated in a current of hydrogen, which prevents oxidation from destroying the ratios of the metals introduced. The molten metal is then dashed with all possible force perpendicularly on a large plate of window glass. The spattered metal is thus transformed into a spray of fine radiating wires. An abundant supply of strips 0.005 mm or more thick and 0.05 mm or more wide is thus obtained.

The operation of forming the junctions is carried out on a large sheet of plate glass. As one must everywhere avoid adhesion when working with such small masses, the glass is kept warm by laying it on the planed surface of a large iron casting which has previously been heated. A sheet of white paper lies between the glass and the casting.

Because of its low specific heat and melting point, tin or ordinary tinner's solder is chosen for the receivers. Shavings of the metal are rolled out into thin sheets; these are cut into narrow strips, which are cut into small pieces by means of a scalpel. The latter are fused with a bit of rosin by touching them with a loop of nichrome wire heated by a current of electricity. This immediately produces a minute sphere of the metal, which when pressed flat by a plate of glass produces a thin disk suitable for the receivers. By trial it is found that a sphere 0.15 mm in diameter can be pressed into a receiver 0.5 mm in diameter, which is almost as thin as can be handled. It is easy to find the length of strip necessary for these spheres, which can then be produced in quantity. After several dozens of them have been fused with a bit of rosin, the latter is dissolved away with amyl alcohol and the disks made as needed.

The operation of forming the couples, such as are shown in Figure 1, is carried out about as follows: The strips to be employed are removed from the glass plates carrying the spattered metals by means of a razor blade attached to a convenient handle. These strips are first examined under a microscope to detect any defects which might weaken them, and then laid so that the ends overlap. One of the prepared receivers is then laid over the junction without rosin or other soldering flux. A strip of mica 12×30×.02 mm, bent in the middle so as to keep the center raised 1 or 2 mm above the glass is then laid over the junction and held down with the finger and two 10-gm weights laid close on either side of the couple to keep the mica in contact with it. The welding together of the junction and receiver is accomplished by touching the mica directly above the receiver with the electrically heated loop of nichrome wire. The loop must be heated just below redness and only the briefest

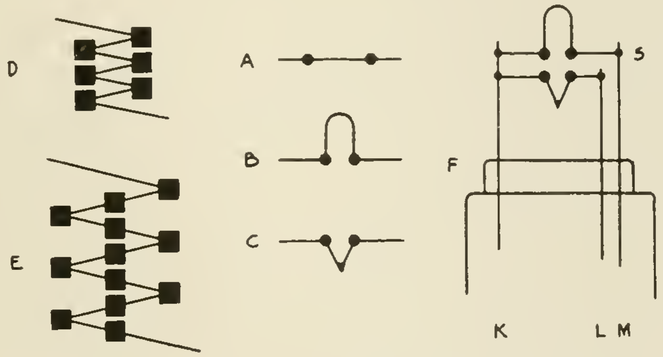

Fig. 1.—Types of thermopiles and thermocouples

possible contact made with the mica. Only one junction at a time is welded, otherwise one may adhere to the glass and the other to the mica, in which case it is impossible to remove the mica without destroying the couple.

The receivers are painted with a mixture of lampblack, two parts; platinum black, one part; turpentine, five parts; and alcohol, twenty parts. This paint, put on with a fine camel's hair brush, forms a black mat surface which will dry quickly.

In Figure 1 are shown five forms of thermocouple; *A*, *B*, and *C* are compensated junctions adapted to stellar observations, *D* and *E* are piles adapted to spectroscopic work, and *F* shows the method of mounting the couples on the platinum wires *K*, *L*, *M*. Forms *B* and *C* have been adopted for stellar observations, since the deflections may be doubled by shifting the junctions alternately on the star image as first applied by Pfund. In *B* the middle strip is folded into a U form in order to bring the junctions close together and leave a space between them, but for some of the more brittle metals which cannot be folded without breaking them, type *C* is used, where two short strips are welded together in V form. Type *D* is a pile which we have used on the registering microphotometer, and *E* is another type of pile first employed by Rubens[1] in 1898 for spectroscopic work at atmospheric pressure, and used more recently by Coblentz[2] in a vacuum.

The platinum wires *K*, *L*, *M* (Fig. 1, *F*) are flattened out on the free ends and solder is run over them on one side. After being washed in alcohol, the thermocouples are laid in place and small disks of solder, *S*, formed in the same manner as above described for the receivers, except that they are flattened out without first removing the rosin, are laid upon the ends of the couples where they cross the platinum wires at *S*. The solder on the platinum wires is then melted by touching it with the nichrome loop.

The masses of the couples so constructed are exceedingly small. The mass of the entire couple *A*, *B*, or *C* is approximately $\frac{1}{30}$ to $\frac{1}{40}$ mg, while the mass of the portion heated by the incident stellar radiation is only 0.012 mg. The metal strips forming the couple are each approximately 3 mm long and 0.008×0.10 mm in cross-section, and the receivers are $\frac{1}{2}$ mm in diameter by 0.009 mm thick. The resistance of course depends on the metals employed, but generally is 8 to 20 ohms.

---

[1] *Zeitschrift für Instrumentenkunde*, **18**, 65, 1898.

[2] *Scientific Papers, Bureau of Standards*, **17**, 188, 1921.

VACUUM EFFECTS

Lebedew[1] determined the law of sensitivity change with change in pressure for a constantan-platinum couple, and found that for the blackened couple the increase was 7.4 times and for the unblackened couple 34 times, for the highest vacuum attained, estimated less than 0.0001 mm. Pfund[2] found an increase of "six times," and Coblentz[3] a "four and one-half fold" increase. In the present investigation we have found increases of two to eleven fold for the vacuum effect.

The effect of the vacuum on the sensitivity does not appear to be the same for all thermocouples, even of the same construction and materials, though the effect of differing materials seems to be the most pronounced. Graphs of the galvanometer deflection against the pressure for three thermocouples are given in Figure 2. It will be seen that the vacuum has little effect upon the sensitivity until the region of 1 mm mercury pressure is reached. Then for the Ag-Te couple the entire increase takes place between 1 mm and 0.01 mm, while the Bi-Bi Sn couple shows an increase of 20 per cent between 0.01 mm and 0.0001 mm. From this it appears that the vacuum which must be maintained in order to keep the sensitivity constant depends on the metals employed in the thermocouple. Thus for Ag-Te couples a vacuum of 0.01 mm is sufficient; but for Bi-Bi Sn this vacuum would occur on a steep part of the curve and in order to insure constant sensitivity a vacuum of 0.0001 mm should be maintained.

A general explanation of the character of the curve is easily given. It is known that the thermal conductivity of a gas is independent of the pressure until the region of 1 mm is reached, when it begins to drop rapidly to zero as the mean free path of the molecules becomes comparable to the dimensions of the container.

---

[1] *Annalen der Physik*, **9**, 209, 1902.

[2] *Physikalische Zeitschrift*, **13**, 870, 1912.

[3] *Bulletin of the Bureau of Standards*, **11**, 636, 1915.

The thermal conductivity also depends on the nature of the gas; for hydrogen it is much greater than for any other. This should make a thermocouple less sensitive in this gas than in air, say. Figure 2 shows how this effect appears in the sensitivity curves when this gas is employed.

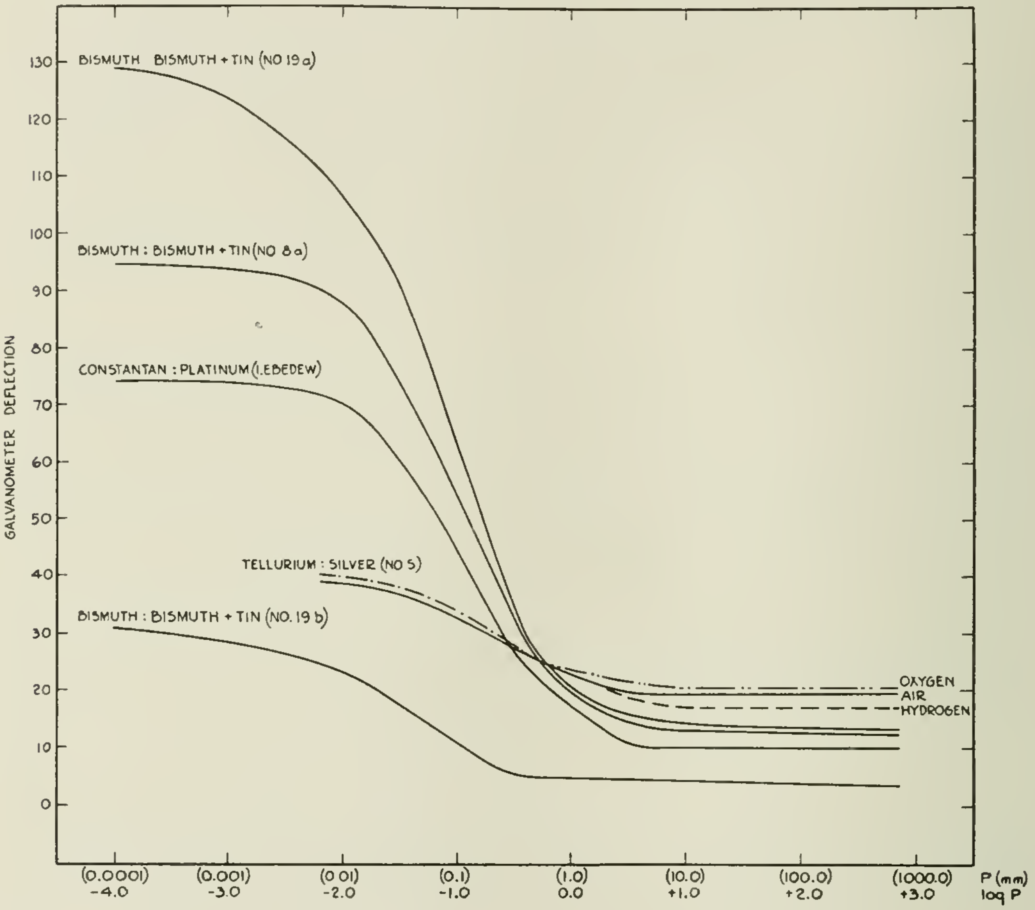

FIG. 2.—Variation of thermocouple sensitivity with pressure

The use of metallic calcium to maintain the vacuum has been studied by both Soddy[1] and Coblentz.[2] The calcium is heated while the pump is in operation to remove the hydrocarbon vapors. We have found it necessary to pump a considerable time to remove these gases completely. After the vacuum has been raised by the pump to a desired limit, it may thereafter be brought back to this point by merely heating the calcium tube to a low red heat with a small electric heater or lamp. After the lamp is removed the absorption of the gases continues for about twenty minutes until the tube has cooled considerably.

---

[1] *Proceedings of the Royal Society*, A, 78, 429, 1907.

[2] *Op. cit.*, 11, 625, 1915.

Coblentz uses a discharge between two platinum terminals inserted in that part of the tube connecting the calcium tube to the thermocouple cell, to test the degree of evacuation obtained while heating the calcium. Since our cells are made of Pyrex glass, it was not feasible to use sealed-in electrodes for this purpose; outside electrodes were therefore substituted. It was found, however, that after the discharge passed, the sensitivity decreased to about 30 per cent to 50 per cent and remained at this level for some hours. On opening the stop-cock to the pump which was maintained at about 0.001 mm pressure, the sensitivity immediately rose to normal again, and this could be repeated at will. Apparently the discharge did not produce a change in pressure, for none was detectable on opening the stop-cock to the gauge. On this account, the discharge test was discarded and tests of the sensitivity by use of a standard lamp were substituted. This is more satisfactory in another way, for it gives a quantitative test of the sensitivity which the discharge test does not give, and all that is necessary is to heat the calcium tube till the sensitivity rises to normal.

SOME PROPERTIES OF VACUUM THERMOCOUPLES

In thermocouples of these small dimensions some interesting properties were observed. Generally in a compensated couple, such as Figure 1 (*A*, *B*, *C*), the two junctions do not give the same deflections, i.e., the compensation is not exact. One case was observed in a couple of Bi-Bi Sn where the deflections for the two junctions were 125 mm and 25 mm and both in the same direction, the current flowing normally across the first junction and in reverse across the second. How this could occur we are unable to explain. As a rule, however, the compensation is so complete that, while observing star deflections, we can turn on all the lights in the dome, without disturbing the galvanometer. With this couple the Peltier effect was quite pronounced. When a deflection was observed with the first junction, the galvanometer mirror swung rapidly at first, then suddenly slowed down and crept up to maximum over 8 or 10 mm, but when a deflection was observed with the second junction the galvanometer mirror over-ran its maximum 2 or 3 mm and returned to normal deflection after one or two seconds.

The absorbing power of the black paint of course depends on the wave-lengths of the incident radiation, being somewhat greater for the shorter waves. Coblentz has found that the reflecting power of this paint is only about 2 per cent. Tests were made with both blackened and unblackened sides of the receivers turned to the window admitting the radiation. The ratio of deflections for the unblackened side to the blackened side was $\frac{1}{3}$ to $\frac{1}{4}$. It was thought that the sensitiveness of the couple might be increased by blackening, on both sides, the entire couple and strips except the receiver, but the effect was very slight. Several couples were repainted after testing, but this seemed to have little effect on the sensitivity.

The efficiency of a thermocouple is exceedingly low. An approximate value of this quantity may be obtained from data relating to the sensitivity tests of No. 19, for example. This efficiency is the ratio between the electrical energy produced and the quantity of the incident radiation, expressed in the same units. If W is the wattage of the lamp, D its distance from the couple, r the radius of the receiver of the thermocouple, R its resistance, i the galvanometer sensitivity in amperes, S the observed deflection, then the efficiency is

$$E=\frac{4R(DSi)^2}{Wr^2}\,. \tag{2}$$

Now for No. 19, $W=90$, $r=\frac{1}{4}$ mm, $R=20$ ohms, $D=3000$ mm, $S=125$ mm, $i=4.75\times 10^{-10}$ amp./mm. Hence, $E=4.5\times 10^{-7}$, i.e., only about half a millionth of the incident radiation actually produces deflection in the galvanometer. Of course we are assuming a uniform distribution of radiation about the lamp, and neglecting the heat convected away from it, as well as the absorption of the air through which the beam must pass. For a value of E so small, however, these quantities could hardly affect the order of the result.

We may approach the problem in another way. The receiver of the thermocouple will continue to increase in temperature until the heat lost and converted into electrical energy equals the amount being absorbed from the incident ray. The ratio of the heat converted into electrical energy to the total heat received is the desired value of E. As was seen in equation (1), since the thermocouple is in a vacuum, the only sources of lost heat are the quantity C, conducted away by the strips, and the quantity radiated, r.

In order to determine these values, let us assume the temperature at which the couple is working to be 20° C., and that a difference of 1° C. between the two junctions is produced by the incident radiation. Let us take couple No. 19 already cited. Since the area of the receiver is about $\frac{1}{5}\times 10^{-2}$ sq. cm, and since, as already seen, it radiates about $\frac{1}{3}$ as much from the unblackened as from the blackened side, then Stefan's law becomes

$$r=\tfrac{4}{3}\times\tfrac{1}{5}\times 10^{-2}\times 1.28\times 10^{-12}(T_1^4-T^4)\text{ cal./sec.}=$$
$$3.4\times 10^{-15}(T_1^4-T^4)\text{ cal./sec.}\qquad(3)$$

and since $T_1=293$ and $T=292$, then

$$r=3.4\times 10^{-7}\text{ cal./sec.}$$

The amount conducted away varies directly as the cross-section of the metal strips A, and inversely with their length L, the constant of proportionality K being the amount conducted through one centimeter cube in one second per degree centigrade. This constant for bismuth is 0.02 cal./sec. Since there are two strips 3 mm long at each junction, one of which contains only 5 per cent tin, we may compute the heat conducted through one strip and call the total amount just double this. Hence the amount of heat conducted away is

$$C=\frac{2KA}{L}\text{ cal./sec.}=2\times 0.02\times 0.000008\times 3\text{ cal./sec.}$$
$$=9.6\times 10^{-7}\text{ cal./sec.}\qquad(4)$$

Now the amount of heat, I, converted into electricity, expressed in cal./sec., varies directly with the square of the thermoelectric power p, the square of the difference in temperature ΔT, and the reciprocal of the resistance R, the constant of proportionality being the Joule equivalent, 0.24. Since $\Delta T = 1^\circ$ C., p = about 50×10^{-6} volts, and $R = 20$ ohms, we have

$$I=\frac{0.24(p\Delta T)^2}{R}\text{ cal./sec.}=\frac{0.24\times(50\times10^{-6})^2}{20}\text{ cal./sec.}=3\times10^{-11}\text{ cal./sec.}$$

The efficiency then is

$$E=\frac{I}{r+C+I}=\frac{3\times10^{-11}\text{ cal./sec.}}{3.4\times10^{-7}+9.6\times10^{-7}+3\times10^{-11}\text{ cal./sec.}} \tag{5}$$

or

$$E=2.3\times10^{-5}.$$

These low values of the efficiency computed here are in part due to the small range in temperature over which the thermocouple works. From the principle of Carnot's Cycle it is known that the efficiency of the theoretically perfect heat engine is

$$E=\frac{T_1-T}{T_1}. \tag{6}$$

The efficiency of the thermocouple, then, considered as a converter of available heat, may be obtained by multiplying the values of E found in equations (2) and (5) by the reciprocal of equation (6). For equation (2) the value of T_1 is the room temperature at which the thermocouple was tested, which was 293° C. absolute. The difference in temperature (T_1-T) between the hot and cold junction for this thermocouple will be shown in equation (7) to be 16×10^{-5} deg. C. per mm deflection. Since in equation (2) the deflection was 125 mm, then $(T_1-T)=2\times10^{-2}$. The value then of $T_1/(T_1-T)$ is 1.5×10^4. Multiplying the value of E obtained in equation (2) by this coefficient, we obtain for the relative efficiency $E=6.7\times10^{-3}$. For the value of E in equation (5) $T_1=293$, $T=292$, which gives for the coefficient 2.93×10^2. Multiplying the value of E in equation (5) by this quantity we obtain for the relative efficiency $E=6.7\times10^{-3}$. It is, then, theoretically possible to construct a thermocouple over one hundred times as sensitive as No. 19 considered here.

Ganot states that Clamond's thermoelectric battery of Fe-Sb Zn heated directly with coal gas under favorable conditions has an efficiency of $E=5\times10^{-3}$.

Some attempts to prevent the losses by radiation have been made by placing the couple at the center of curvature of a hemispherical mirror, the radiation being admitted through a hole in its center. We have not found it possible to apply this principle with the present apparatus since a slight displacement of the junction would render the mirror inactive. Again this would be effective on only one junction. The effect of a hemispherical mirror would be to reduce the losses by radiation to that emitted by the unblackened surface of the receiver, which is approximately one-fourth of the whole amount. Reducing the value of r in equation (5) to one-fourth of its value, we obtain a value for E which is just five-fourths its original value. Hence we may say that the effect of a hemispherical mirror is to increase the sensitivity one-fourth, assuming the mirror to reflect perfectly and the central hole to be of negligible area. In the case of the stellar thermocouples, Figure 1, *B* and *C*, the increase would be only one-eighth when the method of double deflections is used.

It is of interest to know the temperature sensitivity of the thermocouple. This may be determined from the current relations in the circuit.

Let us determine what change in temperature of the receiver will be required to give a deflection of 1 mm on the scale. If we let

P = the potential produced in the circuit expressed in volts
p = the thermoelectric power of the junction in volts
i = the sensitivity of the galvanometer in amperes/mm
R = the total resistance of the circuit
Δt = the required change of temperature in deg. C.
T = temperature of cold junction

then all the constants are known for any particular couple. Let us take No. 19 cited above. Here p normally should be about $150 \times 10^{-6}\ V$, but on account of the impurity of the bismuth, probably it is not greater than about $60 \times 10^{-6}\ V$. $i = 4.75 \times 10^{-10}$ amp., $R = 20$ ohms. Then

$$\Delta t = \frac{P}{p} = \frac{iR}{p} = \frac{4.75 \times 10^{-10} \times 20}{60 \times 10^{-6}} = 16 \times 10^{-5} \text{ deg. C.} \qquad (7)$$

and with a more sensitive galvanometer this figure could easily be pushed to one-millionth of a degree.

Since deflections of about 150 mm are employed ordinarily on recording apparatus, the difference in junction temperature must be approximately 2.4×10^{-2} deg. C. at maximum working deflection for the galvanometer employed. We may now form an estimate of the speed of action of the couple.

We may state the speed of action in terms of the time required for the heat to travel from the blackened face of the receiver to the junction on the rear side and reach a state of steady flow. The increase $\Delta t_2=2.4\times10^{-2}$ deg. C. is that reached by the rear side of the receiver after the steady state is established. To determine the time required, it will be necessary to know the increase in temperature of the front (blackened) face also. This is given by

$$W=\frac{k(\Delta t_1-\Delta t_2)}{u} \text{ or } (\Delta t_1-\Delta t_2)=\frac{Wu}{k} \qquad (8)$$

where W is the rate at which heat flows through unit cross-section, k is the conductivity, $\Delta t_1-\Delta t_2$ is the difference of temperature between the two faces and u is the thickness of the receiver in cm. Now $W=(C_1+R_1)/A$, where C_1 = heat conducted away along the two strips, R_1 = heat radiated from the rear face, and A is the area of the receiver in square centimeters.

Now taking couple No. 19 again as an example,

$$\begin{aligned} C_1&=\Delta t_2 C \text{ [where } C \text{ is the value in eq. (4)]}\\ &=2.4\times10^{-2}\times9.6\times10^{-7}\text{ cal./sec.}=2.3\times10^{-8}\text{ cal./sec.} \end{aligned} \qquad (9)$$

The amount radiated from the rear face is given by

$$R_1=\tfrac{1}{3}\times\tfrac{1}{5}\times10^{-2}\times1.28\times10^{-12}[(T+\Delta t_2)^4-T^4]\,. \qquad (10)$$

Let $T=293°$ C. then

$$R_1=\frac{1.28\times10^{-14}}{15}\times2.4\times10^6=2.0\times10^{-9}\text{ cal./sec.,}$$

hence the total loss is 2.5×10^{-8} cal./sec. and the value of W is

$$W=2.5\times10^{-8}\times5\times10^2\text{ cal./sec.}=1.25\times10^{-5}\text{ cal./sec.} \qquad (11)$$

and from equation (8)

$$\Delta t_1 - \Delta t_2 = \frac{1.25 \times 10^{-5} \times 10^{-3}}{16 \times 10^{-2}} = 7.8 \times 10^{-8} \text{ deg. C.} \qquad (12)$$

This is the stable condition and is reached only after an indefinite period of time. Since $\Delta t_1 - \Delta t_2$ is insignificant compared to the value of $\Delta t_2 = 2.4 \times 10^{-2}$ deg. C., we may neglect it in the following computation. Let us inquire what time will be required for the rear face to reach a temperature 99 per cent of the steady state, i.e., the time required for the thermoelectric current to reach 99 per cent of its value under the influence of the incident radiation. We have Fourier's equation for the flow of heat

$$\frac{\Delta t_2}{\Delta t_1} = 99 \times 10^{-2} = \frac{2}{\sqrt{\pi}} \int_{\frac{u}{2h\sqrt{t}}}^{\infty} e^{-\beta^2} d\beta \qquad (13)$$

Since $u = 10^{-3}$ cm, $h^2 = 0.4$, this gives us

$$t = 6.2 \times 10^{-3} \text{ sec.}$$

It follows then that the lag of the thermocouple is negligible when applied to recording apparatus. If we multiply the equation (10) by the factor 4, we obtain the total radiation from both faces of the receiver. This gives us 8×10^{-9} cal./sec. as the loss by radiation. This is only one-third the loss by conduction along the strips, which is 23×10^{-9} cal./sec. Hence the desirability of using substances of low heat conductivity for the strips.

APPLICATIONS TO THE ASTROPHYSICAL PROBLEMS

1. *Stellar radiation problems.*—To observe the total radiation from stars, the thermocouple is mounted on a plate provided with a low-power eyepiece and water cell which can be moved in front of the thermocouple or moved away by means of a lever on the face of the plate. The apparatus is adapted to the Newtonian double-slide plate holder of the 100-inch telescope. A four-wire cable 135 feet long connects the thermocouple with the galvanometer room in the basement of the dome. Two of these wires are used for the thermo-

couple circuit, and the other two connect the observer at the telescope with the observer at the galvanometer by telephone. The deflections are obtained by orienting the thermocouple so that the line connecting the two receivers is parallel to one of the guiding screws, and by shifting the receivers alternately upon the star image with a half-turn of this screw.

In order to test the fundamental sensitivity of the thermocouple during the observations, an electric lamp (100-watt "Peerless" mazda) is placed on a bracket in the Cassegrain plate holder. The light from this lamp is reflected from the Cassegrain flat to the Newtonian flat and is received by a small lens at the Newtonian plate holder and projected on the thermocouple. When not in use, the lens may be swung aside and the lamp turned off.

Two types of galvanometer have been employed, viz., Leeds and Northrup high sensitivity D'Arsonval No. 2285, and more recently the Coblentz-Thompson galvanometer of the same make. Of the D'Arsonval galvanometers, two of different electrical properties have been used. No. (1) has a period of 4.44 seconds, resistance of 9.1 ohms, and mirror sufficiently flat to use a scale at 8 m, which gives a sensitivity of 4.75×10^{-10} amp./mm. No. (2) has a period of 6.5 sec., resistance of 17.4 ohms, and sensitivity of 3.1×10^{-10} amp./mm with scale at 8 m.

This latter galvanometer had a mirror $\frac{5}{16}$ inch in diameter with very good figure when tested in the Pasadena laboratory, so good in fact that a scale could be read at 11 m. When the galvanometer was taken to Mount Wilson and set up in the 100-inch dome at a temperature of 34° F., the figure became so bad that a scale could scarcely be read at 1 m, and the projected image of a lamp filament at a distance of 4 m was a band 7 mm broad with sharp edges and dark center. On removing the galvanometer to Pasadena the figure was restored. The mirror was then detached and the beeswax which covered the entire back and was used as a cement to attach it to the moving coil was removed, and the mirror attached to the coil again by a bit of universal wax placed in the center of the back. This procedure effectually removed the annoying change in figure of the mirror, which has since performed admirably, although subjected to temperatures below freezing.

No. (1) was placed under a bell jar and subjected to variations in pressure. No change in sensitivity was observed, even when the pressure was reduced to 10^{-3} mm. At this pressure the period was reduced 4 per cent, while an enormous drift was introduced which could not be removed even by grounding various parts of the galvanometer.

Both visual and photographic methods have been employed to observe the galvanometer deflections. Visually two methods have been used. When the scale was at 8 m the highest power telescope it was found feasible to employ was approximately 45. But by placing a spectacle lens of 6 m focus directly in front of the galvanometer mirror and observing the image with an eyepiece with cross-hair in the field, a power of 350 could be employed advantageously, and the scale read with accuracy to tenths of a millimeter.

When visual observations are made, the drift of the galvanometer is difficult to allow for. This drift can be reduced to a minimum by inclosing the thermocouple cell in a wad of cotton wool, and surrounding the galvanometer by a double wall box, the space also being filled with cotton. With this arrangement the observed drift of the D'Arsonval galvanometer is at most only 1 or 2 mm per minute, and is often absent. By taking the observations at regular intervals, keeping the star on the receiver in the meantime, an approximate value of the drift may be obtained.

The method which we have adopted at Mount Wilson consists in recording photographically the deflections and drift. The photographic plate 7×17 inches, or 8×10 inches, is carried by a slide moving in cast-iron ways, which is driven by a screw so that the film is always in the focal plane of a cylindrical lens of semicircular cross-section, $\frac{1}{2}$-inch aperture and 8 inches long, set with its axis at right angles to the motion of the plate. The image of a straight filament lamp, formed by the spectacle lens before the galvanometer mirror, is at right angles to the axis of the cylindrical lens. That portion, then, which the lens intercepts, will form a point image on the plate, which in turn registers the motion of the galvanometer. The plate is driven 2 cm a minute by a motor-driven gear from which a large range of speeds can be had.

Plate VII is a reproduction of photographic records of Vega (mag. 0.1), Arcturus (mag. 0.2), α Herculis (mag. 3.0), and R Hydrae (mag. 8.0), respectively, made with this apparatus on the same night and reduced to one half the original scale. The larger deflections, on the left, for each star were taken without a water cell, those on the right with a water cell 1 cm thick interposed in the beam. The increasing absorption of the water cell with the advance in spectral type is well shown, as is also the increase in total radiation for a given magnitude. The effects of poor seeing are well shown in the deflections for α Herculis without the water cell.

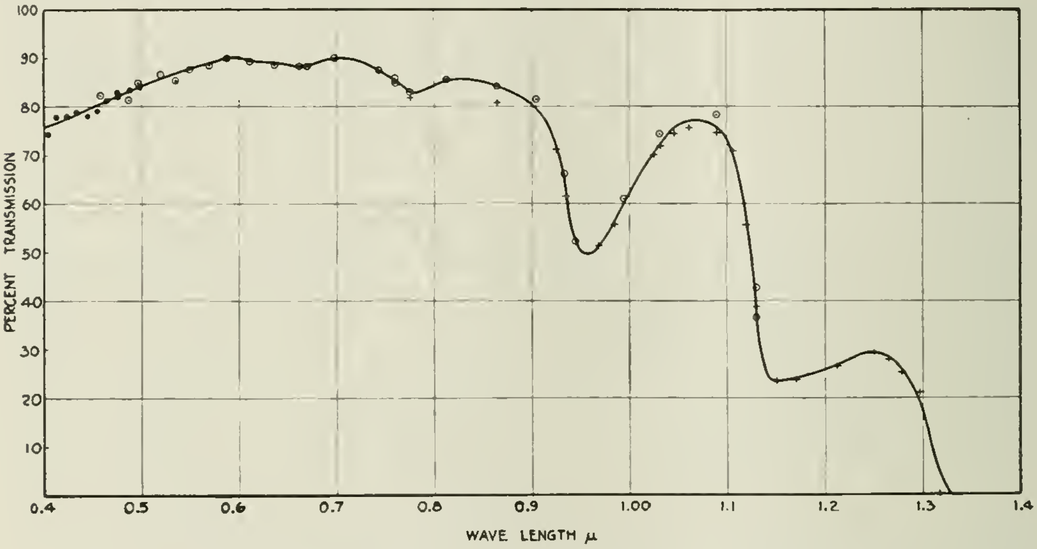

Fig. 3.—Transmission of a water cell 1 cm thick, having windows of microscope cover-glass 0.12 mm thick.

The water cell employed in these observations consists of a brass cylinder 1 cm long with microscope cover-glasses 0.12 mm thick cemented to the two ends. The transmission curve of this cell, filled with distilled water, as observed with the thermocouple in the Pasadena laboratory, is shown in Figure 3. From the curve it will be seen that very little energy is transmitted beyond 1.1 μ and none at all beyond 1.4 μ. It will also be noted that star deflections observed through the water cell cannot exceed 90 per cent of the deflections observed without it.

2. *Solar applications.*—The problems to which we have thus far applied the thermocouple may be listed as follows: (1) registration of the spectral energy curve of the sun; (2) registration of drift

PLATE VII

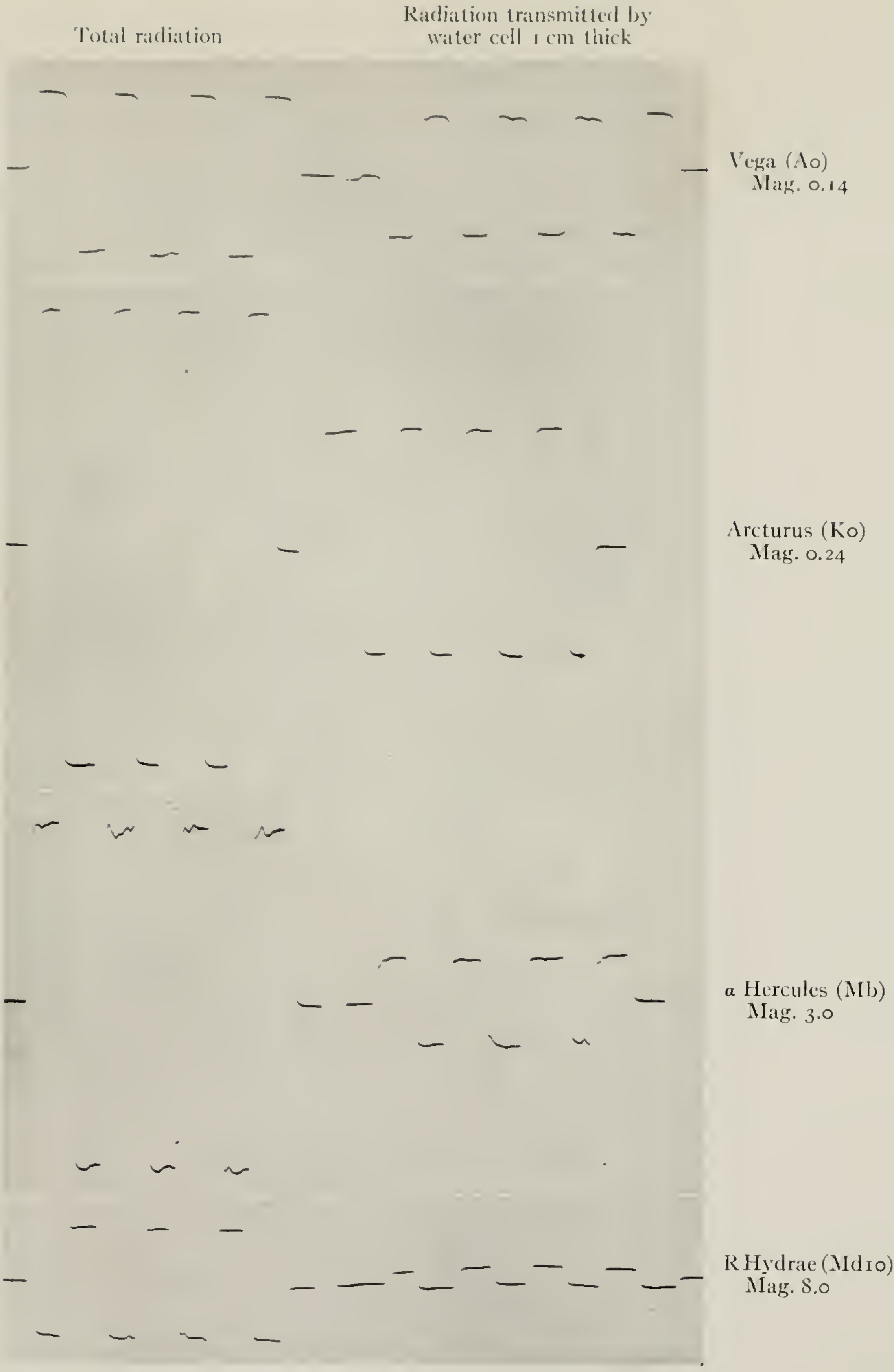

Photographic Records of Galvanometer Deflections Made by Stars of Various Spectral Types

curves across the disk in various wave-lengths; (3) energy relations across sun-spots and faculae.

The apparatus employed in these investigations consists of the photographic registering apparatus already described. For studying the energy relations across spots and faculae the apparatus is mounted on the head of the spectrograph of the 150-foot tower telescope. The thermocouple is contained in a wooden case carried horizontally by a screw-driven plate, which is connected by a back gear to the driving shaft of the photographic registering apparatus. A paper-covered metal shield, perforated with a needle point, is attached to the thermocouple case directly above one of the receivers in such a way that the needle hole can be adjusted by means of a screw so that the light from the solar image passing through it will fall on the receiver. An aperture in the side of the case, closed by a cork, enables the observer to effect this adjustment.

The spot is now brought by the slow motions of the coelostat in line with the pin hole, and the photographic registering apparatus set in motion. By means of the back gear, the ratio is so adjusted that the thermocouple is driven about 1 cm while the photographic plate travels 20 cm. The galvanometer, which is set on an arm of the spectrograph head, is connected to the photographic registering apparatus by means of an aluminum box 1 m long, which shuts out the light of the room from the cylindrical lens. By this apparatus the total radiation curve across the spot is obtained. By rotating the spectrograph head, curves may be obtained across the spot in any direction.

THE REGISTERING MICROPHOTOMETER

In 1912 Koch first introduced the principle of the registering microphotometer, using a photo-electric cell and string electrometer as the registering device. The curves were photographically registered on a falling plate controlled by clock work. In 1915 Stetson[1] modified the apparatus by substituting a thermopile and galvanometer for the photo-electric cell and electrometer, thus making the apparatus simpler and freer from the annoyances to which the photo-electric cell is subject. Stetson's apparatus was read visually and was not a self-recording apparatus. In 1921 Moll[1] applied the self-registering principle to the thermocouple, the negative and plate being driven by hand. In both Stetson's and Moll's apparatus the thermocouple operated at atmospheric pressure.

---

[1] *Astrophysical Journal*, **43**, 253, 1916.

The new registering microphotometer now in use at Mount Wilson was built in the Pasadena shop after designs by Mr. Babcock and set in operation in 1914. The photo-electric cell and string electrometer were employed by him as in Koch's apparatus. The modifications introduced by Babcock consisted in (1) moving the plate by a motor-driven screw, (2) providing for plates 15 cm × 100 cm, (3) introducing a gear shift between the moving microscope stage and plate screw so that a number of magnifications of motion between the negative and moving plate could be used, (4) use of a cylindrical lens in place of a slit before the moving plate, and (5) taking all light used in the apparatus from one Nernst filament. The modifications introduced by us consist in (1) replacing the photo-electric cell and electrometer by a vacuum thermopile and D'Arsonval galvanometer, (2) the use of both sunlight and a nitrogen-filled straight-filament lamp as sources of illumination, (3) adding a second microscope for setting purposes, (4) introducing an adjustable second slit before the thermopile, (5) projecting an illuminated slit upon the photographic film as in Moll's apparatus instead of limiting a large beam by means of a slit directly above the film as in Koch's machine, and (6) the introduction of parallel silvered plates into the barrel of the microscope to increase the field of the objective and the deflections of the galvanometer.

Plate VIII shows the machine as it is now used, arranged for solar illumination. The whole instrument rests on a cast-iron bed-plate *AB*, 12 ft. long and 28 in. wide, which stands on a cement pier. The photographic registering device *C* and the traveling microscope stage *D* are connected by the shift-gear box *G* and driven by the motor *M*. The plate carrier *K* carries the plate *P* horizontally past the cylindrical lens *L*, and is moved by the long screw *Sc* of 2 mm pitch in the casting below. By means of two mirrors the

---

[1] *Proceedings of the Physical Society of London*, **33**, 207, 1921.

PLATE VIII

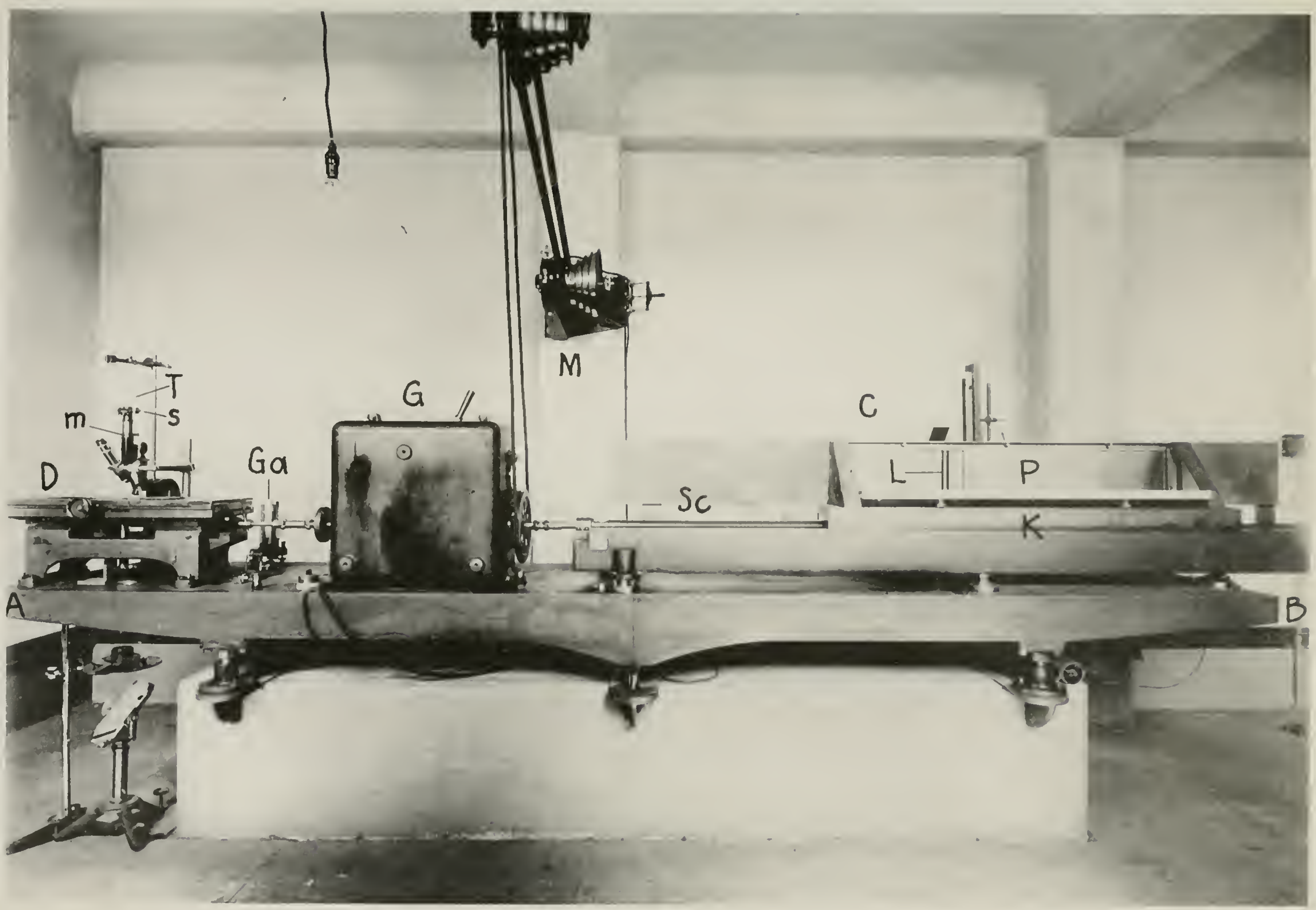

The Registering Microphotometer

image formed by the galvanometer mirror is made to play up and down along the cylindrical lens, and thus the curves are produced. The microscope stage *D* rests on four steel balls and is driven by a screw of 1 mm pitch connected to the gear box *G*, in the same direction as the photographic plate *P*. By means of the gear box *G* the ratio of speeds between *C* and *D* may be varied from two to fifty fold. The microscope *m* contains at its upper end an adjustable slit *S* above which the thermopile *T* is placed. Lead-wires from the thermopile are connected with the registering galvanometer *Ga* on the bed plate of the instrument. A motor is also provided to drive the machine at high speed so that the plate may be returned to starting position when several curves are being compared. In this way all the runs may be made in the same direction, thus eliminating the lag of the galvanometer, due to its period.

In securing a curve representing the energy relations across a spectral line in a photograph, it is obvious that in order to avoid distortions of the curve it will be necessary to employ as narrow an element of the line as possible. This means, in effect, that the magnification of the microscope *m* should be large and that the second slit *S*, which limits the beam reaching the thermopile, should be narrow. There is, however, a limit to the width of the slit *S*, since too narrow a slit will introduce irregularities due to the clustering of silver grains in the film, or dust and defects in the film. With the present apparatus these irregularities begin to appear when the slit width is reduced to about 0.1 mm for the negatives employed. For very fine-grained plates this limit can of course be further reduced.

In order to remedy this defect it will be necessary to integrate over a greater length of line than is available with Koch's arrangement. The device adopted to facilitate this is shown in the diagram of the optical system now employed (Fig. 4). Artificial light or sunlight passes through a condenser and falls on a slit S_1, an image of which, formed by the objective O_1, is projected on the spectral line *L* of the negative on the moving microscope stage. An image of this illuminated portion of the spectral line *L* is projected by the microscope objective O_2 on to the second slit S placed just in front of the thermopile T. By means of the two parallel mirrors M_1, M_2 the portions of the beam which would otherwise fall outside of the field are thrown back upon the thermopile and become effective. From tests it was found that the 40 mm objective employed had fair field over 10°, so that a spectral line 9 mm long could be employed. By adjusting the length of the slit S_1, or the distance from the mirrors M_1, M_2 to the objective O_2, the field may be limited to this value. The full lines indicate the path of the rays in the present arrangement, and the dotted lines the same for the arrangements of Koch and Moll.

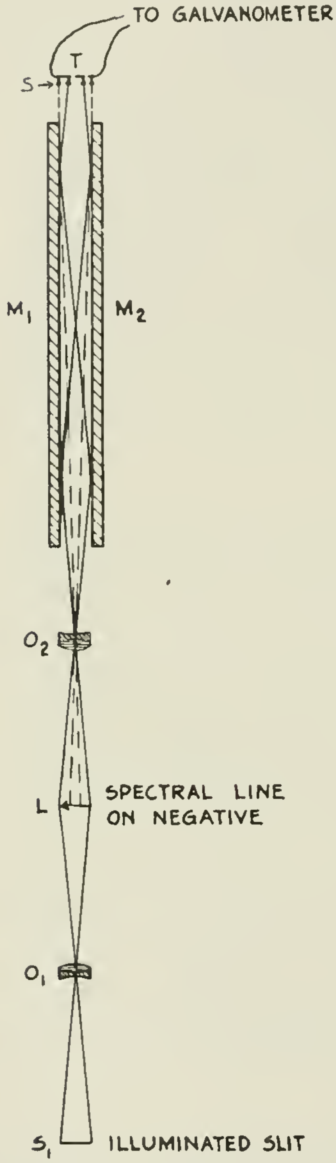

Fig. 4—Optical system of the registering microphotometer.

By adjusting the width of the first slit S_1, only that portion of the spectral line L is illuminated which is included in the image which passes through the second slit at S. This device employed by Moll reduces the scattering of the light in the film, but probably its greatest advantage is in eliminating the use of the first slit just above the moving plate at L, thus facilitating the adjustment of the negative.

When the thermocouple is employed to replace the photo-electric cell on the registering microphotometer, no means is available for compensating the apparatus against changes in the intensity of the illumination used. No mention of this is made in the descriptions of the apparatus employed by Stetson and Moll, who used storage batteries as a source of current for the illumination. While we cannot compensate the thermopile, we may, at the same time, however, register the variations in the illumination by projecting a portion of the beam incident on the first slit S_1, on a second thermopile and registering the fluctuations in intensity on the photographic plate by means of a second galvanometer of the same period as the one employed with the first thermopile T. The results of investigations with the apparatus and methods here described will appear in a future paper.

MOUNT WILSON OBSERVATORY
July 1922

THE ELECTRIC FURNACE SPECTRUM OF IRON IN THE ULTRA-VIOLET, WITH SUPPLEMENTARY DATA FOR THE BLUE AND VIOLET[1]

By ARTHUR S. KING

ABSTRACT

Electric furnace emission and absorption spectra of iron in the ultra-violet, for various temperatures from 1400° to 2600° C.—This paper supplements one published in 1913 on the iron furnace spectrum from λ 3884 to λ 7208. Furnace emission spectra extend into the ultra-violet only as far as the continuous spectrum of a black body at the same temperature. It has now been found, however, that by using a very hot source, such as a gas-filled tungsten lamp or a series of fine wires exploded by Anderson's method, absorption spectra corresponding to either low or high temperatures of the vapor may be obtained extending to λ 2298 or beyond. The relative intensities in absorption spectra are the same as in emission spectra of the same temperature. A large number of spectrograms have been made in the first and second orders of a 15-foot concave grating. Tables I–III contain the *temperature classification of 904 lines, λ 2298 to λ 3878*, and the relative intensities in the arc and in high, medium, and low temperature furnace spectra, either emission or absorption, upon which the classification is based. For iron, the low-temperature lines, classes I and II, are well developed at 1600°, the medium, class III, at 2000°, and the high-temperature lines, class IV, at 2300°. About sixty lines, of various classes, are relatively very weak in the arc; they are denoted by I A, II A, etc. *A revised classification of 262 lines, λ 3884 to λ 4531*, based on later spectrograms, is given in Table IV; and Table V contains a list of the most persistent low-temperature lines, the twenty-one from λ 3745 to λ 4482 emitted by the vapor at 1400°, as photographed by long exposure with a 1-meter concave grating. On Plate XI a high-temperature absorption spectrum is shown between two arc spectra.

Discussion of the significance of the temperature classification of spectral lines.—Work with various metals indicates a parallelism between the successive temperature excitation stages and the radiation stages as the potential is increased in low-voltage vacuum arcs. For high boiling-point metals, the classification can perhaps be more readily made by the furnace method. To assist in the correlation of the two types of classification, elements which may have their spectra excited in either way should be carefully studied in both ways.

A paper on the electric furnace spectrum of iron from λ 3884 to λ 7208 was published by the writer[2] in 1913. The present paper begins at the violet limit of the former investigation and extends the study to λ 2298, which is as far as it has been possible to obtain lines by means of the furnace. Within this range, the lines given in tables of arc wave-lengths are covered with reasonable completeness, the missing lines generally being very faint in the arc or of the enhanced-line type, both of these classes requiring, as a rule, the stronger excitation of the electric discharge. As in other studies of furnace spectra, the purpose has been to show the changes in relative line intensity through various furnace temperatures and into the conditions of the arc, and from these data to classify the lines according to the temperatures at which they first appear and their rates of growth as the temperature rises.

---

[1] *Contributions from the Mount Wilson Observatory*, No. 247.

[2] *Ibid.*, No. 66; *Astrophysical Journal*, 37, 239, 1913.

The temperature stages for this purpose must be selected for each element according to the observed changes in its spectrum, and it is desirable that at each stage there be a marked change from the spectrum at the stage below. For iron, the low-temperature spectrum was found to be well developed at 1600° C. and the plates for this group of lines were taken from 1600° to 1700°. For the medium temperature, at which another set of lines appears, about 2000° was used. The high-temperature spectrum develops at about 2300° and still higher temperature has little effect beyond increasing the reversals and giving general intensification. Nevertheless, temperatures of 2500° to 2600° were used for most of the high-temperature spectra, in order to obtain the full effect of the conditions corresponding to this stage.

The same methods of classification have been used as in previous studies, but an important new feature is the use which has been made of absorption spectra, obtained by methods described in recent papers,[1] and by others still more recently developed.

It was noted in the first paper on the iron spectrum, and has been many times confirmed for this and other spectra, that at a given temperature of the furnace the emission spectrum stops at a point in the ultra-violet somewhat short of the limit of the continuous spectrum given by a black body at the same temperature. A close approach to such a black body is easily obtained by placing a graphite plug in the central part of the tube and heating the furnace to the temperature previously used for the emission spectrum.

A limit is thus set to the wave-length range within which the furnace at a certain temperature can give emission lines, and if appearance at this temperature is the criterion indicating that lines belong to a certain class, all lines of shorter wave-length automatically go into a higher class. It is often the case, however, that the lines of shorter wave-length, when produced by the furnace at a higher temperature or in the arc, show no features that would distinguish them from those in the region given by the low-temperature furnace. This forced distinction, due to the fact that the furnace cannot emit beyond a certain point, was noted in the study of the spectrum of calcium, strontium, barium, and magnesium.[1]

---

[1] *Mt. Wilson Contr.*, Nos. 174, 233; *Astrophysical Journal*, 51, 13, 1920; 55, 380, 1922.

In the present investigation, trials were made to see if iron vapor at low temperature would absorb radiation of shorter wave-length than it was able to emit. This proved to be the case. When a beam of white light from a very hot source was passed through the moderately heated furnace, iron absorption lines appeared as far in the ultra-violet as the solid body was able to build up a continuous spectrum; and by using successively hotter sources behind it, the furnace at 1600° C. gave absorption lines as far as λ 2298. The emission spectrum at this temperature ends at λ 3440, though this is due partly to the fact that for a considerable range below this, no low-temperature lines occur.

There seems to be no reason why ultra-violet absorption lines obtained in this way should not be classed as low-temperature lines. A stellar spectrum produced by sufficient difference of temperature between the body of the star and cool iron vapor surrounding it should show no difference (disregarding atmospheric absorption) between these lines and the low-temperature lines of the visible spectrum.

It has therefore been considered legitimate to use the absorption spectrum for a certain temperature stage as a means of extending the data beyond the point where the emission lines die out. This has resulted in a division of the tabulated lines into three sections. In Table I, from λ 2298 to λ 2808, the comparison is between the absorption spectra at high and low temperatures. Both of these extend to shorter wave-lengths than the corresponding emission spectra. At high temperature, however, it has been possible to force the emission spectrum to λ 2462. The relative intensities of emission and absorption lines with the furnace at high and low

---

[1] *Mt. Wilson Contr.*, No. 150; *Astrophysical Journal*, 48, 13, 1918.

PLATE IX

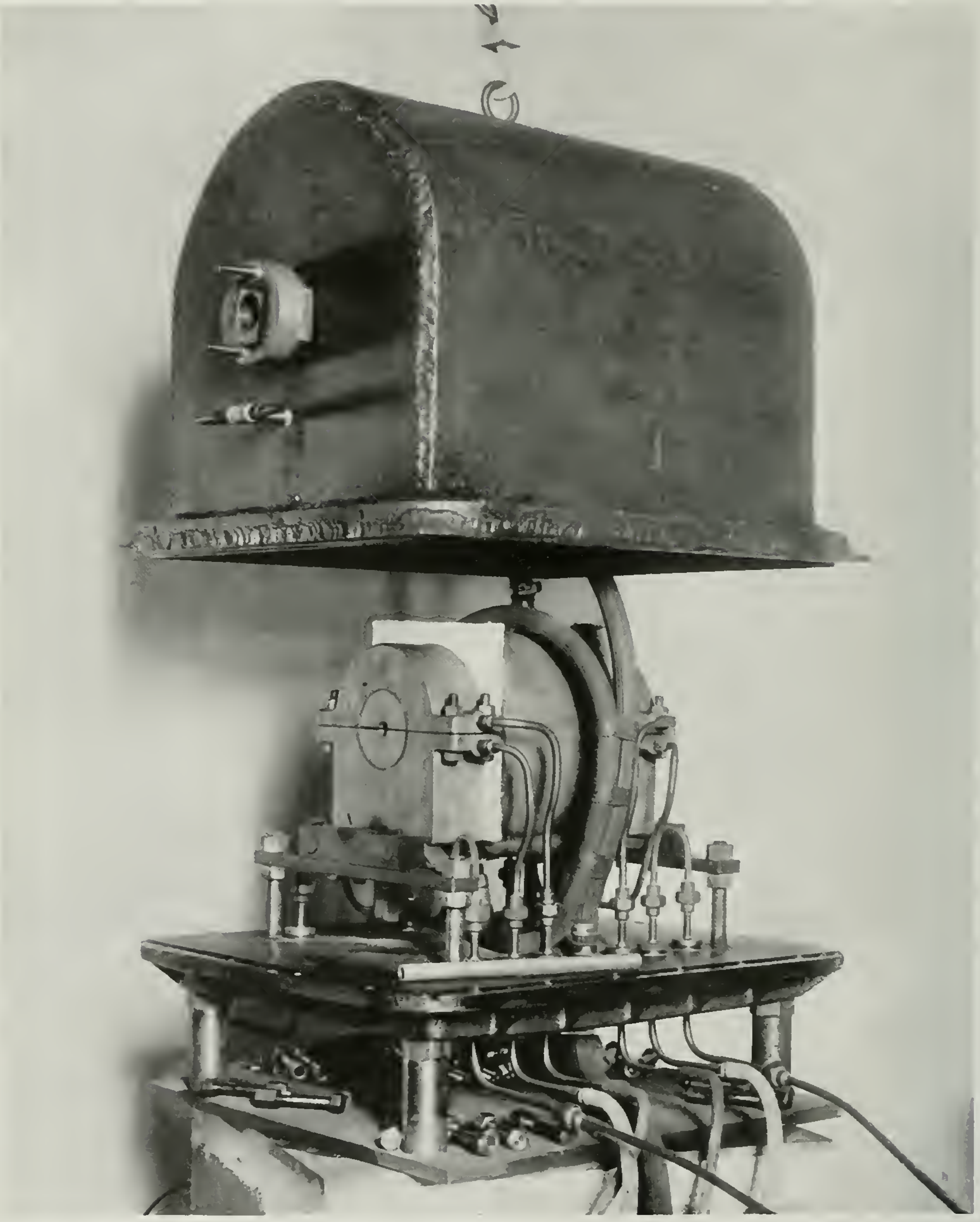

Vacuum Electric Furnace

temperatures were so nearly the same as to justify printing only a single list. Table II includes data from λ 2813 to λ 3437. The high- and medium-temperature columns are for emission lines, but intensities of the low-temperature lines are to be obtained only from the absorption spectrum. Table III, for the range λ 3440 to λ 3788, makes use of emission spectra at the three temperature stages, though in compiling it constant reference was made to the reversibility of lines as shown by their strength in absorption spectra.

EXPERIMENTAL METHOD

a) *Furnaces.*—Two electric furnaces have been employed. The first, in which the tube with its supports is inclosed in a strong cylindrical chamber, adapted for high pressure as well as vacuum, was used throughout the previous investigations. The other is for pressures not above the atmospheric limit, and consists of a heavy sheet-iron hood which is lowered upon a base-plate through which the connections for electric current and water pass to the supports of the furnace tube. These supports are hollow bronze blocks, water-cooled, and bored to hold cylindrical graphite bushings which make direct contact with the tube. The latter is of Acheson graphite, and various forms have been used in special experiments, but the size regularly employed has been of 13-mm bore, 19-mm outside diameter, and 30-cm length. The heated portion of the tube between the contact blocks is about 20 cm long. A tubular water jacket of cast iron, of 17.5 cm internal diameter, surrounds the furnace tube, so that no cooling of the outer inclosure is required. This furnace, and also the older one, were usually pumped out to a pressure of less than 1 cm of mercury, but numerous experiments were made at atmospheric pressure. An illustration of this furnace with the hood raised is shown in Plate IX.

Iron in powdered form was placed in the heated portion of the tube. A preliminary heat was given at a temperature sufficient to melt the iron, which then stuck to the wall of the tube, probably forming a carbide. A supply of iron thus remained in place during the life of the tube, and no fresh charging was needed. The presence of air appeared to cause a more vigorous combination of the metal with the material of the tube.

Alternating current of from 10 to 30 volts was usually employed on the furnace tube; but in the later work, direct current from a 500-kw generator was often used. This was especially useful in experiments with the furnace at atmospheric pressure, as the temperature changes caused by the thinning tube could be compensated by a close control of the voltage.

b) *Production of absorption spectra.*—Three methods of obtaining absorption spectra were used during the investigation. A very useful method was to place a cylindrical plug of graphite near the center of the tube and observe the absorption produced by iron vapor in front of this plug. Very high black-body temperatures are obtainable in this way, the plug frequently being heated above 3200° C., the highest temperature readable on the pyrometer. With this arrangement, however, it is a question as to the temperature of the vapor which absorbs. As in previous work with this method, the spectrum indicated a difference of about 400° between the plug and the absorbing layer, which would mean that the relatively cool vapor near the end of the tube is effective, while the main mass of vapor in the tube is too hot to give the required gradient. This method, especially when the tube was made thinner near the middle, so that the plug was much hotter than the main length of the tube, gave good results for the high-temperature absorption spectrum. An absorption spectrogram for which the plug was held at a temperature of 3000° gave lines as far as λ 2447, the relative intensities showing no important difference from an emission spectrum at 2600°. In another test, the emission spectrum at 2400° was compared with absorption spectra for which the plug was held closely at 2400°, 2600°, and 2800°, respectively. The 2800° spectrum was identical in all essential features with the emission spectrum at 2400°. At low temperatures, however, it is desirable to know as accurately as possible the temperature of the absorbing vapor. For this purpose it is best to use an open tube, the temperature of whose wall can be closely measured, and pass through the tube a beam of light from a source so much hotter that the vapor in the main section of the tube can be safely assumed to be in a condition to absorb. This was arranged by placing a 900-watt gas-filled lamp, operating at 30 amperes, behind the furnace, and directing its beam through the tube. The rated temperature of the tungsten spiral in this lamp is 2900° C. To get the full benefit of the lamp in the ultra-violet region, a side tube closed by a quartz window was set in the bulb, which was then refilled with pure nitrogen.

A third method was to use as a source of continuous spectrum the light from exploding wires inclosed in a block of wood. This has been shown by Anderson[1] to give excellent absorption spectra of the material of the wire, extending far into the ultra-violet. Dr. Anderson kindly operated the explosion apparatus and the light was passed through the furnace heated at various temperatures. As it is necessary to use metals giving as few lines as possible in the region to be studied, wires of aluminium and of lead were tried. The latter was most nearly free from disturbing lines, both of the metal itself and of iron impurities, and a number of furnace absorption lines were added to the list obtainable by the other methods. The explosion method promises to be generally useful, the chief drawback, aside from the disturbing lines in the source, being the very large number of explosions required (on account of their almost infinitesimal duration) to build up a continuous spectrum with a high-dispersion spectrograph.

c) *Photography of the spectrum.*—The spectrograms for the various furnace temperatures were made as far as possible with the vertical concave-grating spectrograph of 15-foot radius. All of the photographs used for the final intensity estimates were made in this way, except when wire explosions were used as an absorption source, a 1-meter concave grating giving high intensity beyond λ 3000 then being employed. The second order of the 15-foot instrument, giving a scale of 1.86 A per millimeter, was used as far as λ 2800, while the first order was used for the shorter wave-lengths. Many spectrograms, especially for low-temperature spectra, were made with the 1-meter spectrograph and used for checking those of the higher dispersion. These were particularly useful in deciding whether certain lines can be brought out at a given temperature, since a long exposure with this instrument may be depended on to show lines which with higher dispersion are under-exposed.

---

[1] *Mt. Wilson Contr.*, No. 178; *Astrophysical Journal*, 51, 37, 1920.

EXPLANATION OF THE TABLES

Tables I, II, and III contain in the first column the wave-lengths of iron lines on the international system. These are for the most part according to the measurements of Burns,[1] rounded off to two decimal places, though in some cases values from the table of iron lines given by Kayser[2] have been used. Lines in the arc tables which are not given by the furnace even at high temperature are entered only when they offer a striking contrast with neighboring lines which in the arc are of equal intensity or even weaker, but which appear distinctly in the furnace. This rule is not followed closely in the region of wave-lengths shorter than λ 2500, where a large proportion of the strong arc lines are of polar type and are usually absent from the furnace spectrum.

The arc intensities in the tables are graded so that a large proportion of the lines are given values comparable with those for the high-temperature furnace. In the ultra-violet, the arc spectrum taken close to the poles is very different from that emitted by the central region, and it is the lines of the latter which in the main make up the furnace spectrum. The photographs for estimation of arc intensities were therefore made with the slit across the image of the arc and about midway between the poles. For the arc, as for the emission furnace, "r" and "R" refer to degrees of reversal, while a line of nebulous structure is denoted by "n."

In the gradation of furnace intensities, "tr" indicates that a trace is visible on a strongly exposed spectrogram, while a line distinctly outlined is given intensity "1." Lines of strength above 20 are likely to show some degree of reversal, and before this intensity is reached, the line has a softened appearance which may be mistaken for faintness. Some plates out of the large collection for each temperature stage usually showed the true condition of the line. The scale for absorption lines was made as closely comparable as possible with that for emission lines.

The "arc type," in the fifth column of Table I, refers to the relative strength of a line at the center and near the poles of the arc. Type "C" is strong in the center of the arc, while type "C–P"

---

[1] *Lick Observatory Bulletin*, 8, 27 (No. 247), 1913.

[2] *Handbuch der Spektroscopie*, 6, 896.

TABLE I

Temperature Classification of Iron Lines, λ 2298–λ 2808

λ (I.A.)	Arc Intensity	Furnace Intensities		Arc Type	Class
		High-Temp. Absorption	Low-Temp. Absorption		
2298.18	10r	4	2	C	II
2299.25	2	1	......	C	III
2303.57	3	2	1	C	II
2309.00	2	1	......	C	III
2313.12	2	1	......	C	III
2320.37	2	1	......	C–P	III
2354.88	3	2	1	C–P	II
2368.60	10	1	......	C–P	III
2373.74	15	2	1	C–P	II
2382.04	20	2	1	C–P	II
2438.19	2	1	......	C	III
2447.72*	4	4	?	C	II ?
2453.48	5	1	......	C	III
2457.60	6	3	1	C–P	II
2462.19	4	4	......	C	III
2462.65	10r	12	3	C	II
2465.16*	6	3	......	C–P	III
2468.89	4	2	......	C–P	III
2472.37	5	2	......	C–P	III
2472.90	12R	20	4	C	II
2473.07	?			C	II
2476.67	3	2	......	C	III
2479.48	6	10	2	C	III
2479.78	20R			C	II
2483.28	60R	40	10	C	II
2483.54	10			C	II ?
2484.19*	15R	8	2	C	II
2488.15	40R	30	8	C	II
2489.76*	15r	8	2	C	II
2490.66	30R	20	4	C	II
2491.16	20R	15	4	C	II
2496.54	6	1	......	C–P	III
2498.90	10	tr	......	P	IV
2501.14	20R	15	3	C	II
2507.90	6	2	......	C–P	III
2510.84	15R	12	2	C	II
2512.37	5r	3	tr	C	III
2518.11	12r	10	2	C	II
2522.86	40R	30	5	C	II
2524.29	8r	5	2	C	II
2527.44	15r	12	3	C	II
2529.27	10r	8	tr	C	III
2529.83	3	2	......	C	III
2530.70	3	2	......	C	III
2533.80	4	tr	......	C	IV
2535.61	8r	6	......	C	III
2540.98	10R	10	1	C	III
2542.11	6	tr	......	C–P	IV
2543.93	6	tr	......	C–P	IV
2544.72	6	tr	......	C	IV
2545.98	10r	10	1	C	III
2549.62	10r	10	1	C	III
2552.63	2	2	......	C	III
2556.87	1	1	......	C	III
2576.70	4	2	......	C–P	III
2582.31	6	1	......	C	III
2584.54	8	3	......	C–P	III
2585.89*	20	1	......	P	IV
2588.01*	8	1	......	C	III
2594.05	1	1	......	C	III
2594.16	1			C	III
2599.58	6	3	......	C–P	III
2605.69	6	1	......	C–P	III
2606.84	6	3	......	C–P	III
2610.76	1	1	......	C	III
2612.79	2	2	......	C	III
2614.51	1	1	......	C	III
2618.03	5	2	......	C–P	III
2618.72	2	2	......	C	III
2623.38	2	2	......	C	III
2623.54	5	2	......	C–P	III
2629.60*	2	2	......	C	III
2632.25	4	2	......	C–P	III
2632.60	2	4	......	C	III A
2635.82	8	4	......	C–P	III
2636.49	1	1	......	C	III
2641.65	4	2	......	C	III
2644.01	8	3	......	C–P	III
2645.43	1	2	......	C	III A
2647.57	3	4	......	C	III
2651.72	2	1	......	C	III
2656.15	3	tr	......	C	III
2660.41	1	1	......	C	III
2662.07	3	2	......	C	III
2666.41	2	1	......	C	III
2666.82	8	4	......	C–P	III
2666.97	3			C	III
2667.92	1	2	......	C	III A
2669.50*	2	......	......	C	IV
2673.22	1	tr	......	C	III
2679.07	10	3	......	C–P	III
2680.46	2	1	......	C	III
2689.22	8	3	......	C–P	III
2689.84	2	tr	......	C	III
2690.07	2	2	......	C	III
2695.04	1	tr	......	C	III
2697.03	2	tr	......	C	III
2699.11	6	2	......	C–P	III
2706.02	4	tr	......	C	IV
2706.59	8	3	......	C–P	III
2708.58*	4	......	......	C	IV
2710.55	2	tr	......	C	III
2711.66	4	2	......	C–P	III
2714.88	1	tr	......	C	III
2715.33	1	tr	......	C	III
2717.79	2	1	......	C	III
2718.45*	6	?	......	C–P	III ?
2719.04	60R	60	10	C	II
2719.43*	3	?	......	C	III ?
2720.91	40r	40	6	C	II
2723.58	15	15	3	C	II
2724.96*	10	3	......	C–P	III
2726.06	6	2	......	C–P	III
2728.03	3	2	......	C	III
2728.83	2	2	......	C	III
2730.98	2	2	......	C	III
2733.58	15	5	1	C	II
2734.01	2	tr	......	C	III
2734.27	2	tr	......	C	III
2735.48*	8	5	......	C–P	III
2735.61*	8			C	III
2737.31	20r	20	2	C	II

TABLE I—*Continued*

λ (I.A.)	Arc Intensity	Furnace Intensities		Arc Type	Class	λ (I.A.)	Arc Intensity	Furnace Intensities		Arc Type	Class
		High-Temp. Absorption	Low-Temp. Absorption					High-Temp. Absorption	Low-Temp. Absorption		
2742.02	2	1	......	C	III	2769.67	1	1	......	C	III
2742.26	20	30	5	C–P	III	2772.08	20	6	2	C–P	II
2742.41	30r			C	II	2772.11	1		......	C	III
2743.57	3	1	......	C–P	III	2773.23	2	tr	......	C	III
2744.07	10	8	2	C	II	2774.73*	3	2	......	C	III
2744.53	8	2	......	C–P	III	2778.08	3	5	......	C	III
2746.99*	20	2	......	P	III	2778.23	20			C–P	III
2750.15	25r	20	4	C	II	2778.85	3	3	......	C	III
2753.69	3	2	......	C	III	2780.70	1	tr	......	C	III
2754.03	3	2	......	C	III	2781.84	4	2	......	C	III
2754.43	2	1	......	C	III	2787.94	5	8	......	C–P	II
2756.33	20	10	6	C	I	2788.11	30		2	C	II
2757.32	10	3	......	C–P	III	2792.40	1	1	......	C	III
2759.82	4	2	......	C	III	2795.01	3	2	......	C	III
2761.79*	18	3	......	C–P	III	2797.78	15	3	......	C–P	III
2762.03	15	3	......	C–P	III	2799.15	1	tr	......	C	III
2763.11	4	2	......	C	III	2804.52	20	3	1	C–P	II
2764.33	3	1	......	C	III	2806.99	20	3	1	C–P	II
2766.91	2	2	......	C	III	2807.24	2	1	......	C	III
2767.52*	20	3	......	P	III	2808.33	2	1	......	C	III

2447.72	Probably present at low temperature close to Pb absorption line. Blends in arc with close polar line to red.
2465.16	Some strengthening at pole in arc. Possibly blend with polar line.
2484.19	Blend in arc with polar line to red.
2489.76	Blend in arc with polar line to red.
2585.89	Strong throughout arc, enhanced at poles.
2588.01	Blend in arc with polar line to red.
2629.60	Close blend in arc with polar line.
2669.50	Appears faintly in high-temperature emission spectrum.
2708.58	Appears faintly in high-temperature emission spectrum.
2718.45 2719.43	Blend in furnace with λ 2719.04.
2724.96	Blends in arc with polar line λ 2724.89.
2735.48–.61	Furnace line is chiefly λ 2735.61.
2746.99	Strong throughout arc, enhanced at poles.
2761.79	Slightly strengthened at poles.
2767.52	Much enhanced at pole.
2774.73	Blend in arc with polar line to violet.

indicates that the line is emitted with little change of intensity from center to pole. Polar lines, denoted by "P," are rarely visible in the furnace spectrum.

The classification of lines given in the last column of each table has been carried out in the same manner as in previous papers, except that class I B of the former paper on the iron spectrum is here replaced, as has been the case for the other metals studied, by class I.

Classes I and II are low-temperature lines, but those of class I maintain their strength at low temperature longer than do the lines of class II. These classes include practically all of the lines which

TABLE II

TEMPERATURE CLASSIFICATION OF IRON LINES, λ 2813–λ 3437

λ (I.A.)	Arc Intensity	Furnace Intensities			Class
		High-Temp. Emission	Med.-Temp. Emission	Low-Temp. Absorption	
2813.29	30R	8	5	3	II
2815.51	3	2	......	......	IV
2817.51	6	5	2	......	III
2820.81	2	2	......	......	IV
2823.28	20	4	3	1	II
2825.56	20	6	3	2	II
2825.69	6	2	1	1	II
2827.89	5	3	2	......	III
2828.81	7	3	2	......	III
2832.43	25r	4	3	1	II
2835.46	6	4	4	4	I
2838.12	10	5	3	......	III
2840.42	6	4	2	2	II
2843.63	10	3	2	......	III
2843.97	20r	6	5	2	II
2845.60	8	6	3	......	III
2846.83	3	1	......	......	IV
2848.71	5	3	1	......	III
2851.80	15r	5	3	1	II
2858.90	5	3	2	1	II
2862.50	4	2	......	......	IV
2863.43	8	3	1	......	III
2863.87	8	6	3	3	I
2866.63	7	3	2	......	II
2867.31	3	1	......	......	IV
2867.57	3	1	......	......	IV
2868.44	3	1	......	......	IV
2869.31	10	6	6	6	I
2872.34	7	4	4	......	III
2874.18	10	8	6	6	I
2875.31*	5	3	......	......	IV
2877.30	8	4	2	......	III
2880.58	2	1	......	......	IV
2880.76*	5	......	......	......	V
2883.73*	4	......	......	......	V
2886.32	3	1	......	......	IV
2887.81*	5	......	......	......	V
2893.76	1	2	......	......	IV A
2893.88	2	1	......	......	IV
2894.51	10	3	1	......	III
2895.04	8	3	1	......	III
2899.42	8	3	......	......	IV
2901.38	5	4	......	......	IV
2901.92	5	2	......	......	IV
2907.52	5	......	......	......	V
2912.16	20r	12	10	8	I
2912.26	3	3	......	......	IV
2914.31	3	1	......	......	IV
2918.03	10	1	......	......	IV
2918.35	3	1	......	......	IV
2920.69	5	4	......	......	IV
2923.29	7	1	......	......	IV
2923.85	7	1	......	......	IV
2925.36	4	......	......	......	V
2925.90	4	3	......	......	IV
2926.58*	10	tr	......	......	V
2929.01	25r	15r	10	8	I
2929.12	6	4	......	......	IV
2929.62	2	1	......	......	IV
2936.90	60R	50r	20r	15	I
2937.81	10n	1	......	......	IV
2941.34	15r	15r	10	8	I
2944.40*	6	......	......	......	V
2945.07	3	1	......	......	IV
2947.66*	6	......	......	......	V
2947.88	60R	50R	20r	15	I
2948.44	4	1	......	......	IV
2949.21*	8	......	......	......	V
2950.25	20n	3	......	......	IV
2953.49	5	1	......	......	IV
2953.78*	5	......	......	......	V
2953.94	50R	35R	15r	10	II
2954.66	5	2	......	......	IV
2957.37	30R	25R	12r	8	II
2960.00	10	3	......	......	IV
2960.30	1	1	......	......	IV
2965.26	20	15r	10	6	II
2965.82	2	1	......	......	IV
2966.90	125R	100R	40R	20	II
2969.36	5	3	2	1	II
2969.48	10	6	4	4	I
2970.11	40R	30R	10r	10	I
2970.52*	4	......	......	......	V
2972.28	3	1	......	......	IV
2973.14	60R	50R	20r	15	I
2973.24	60R	50R	20r	15	I
2976.13	5	2	......	......	IV
2980.54	5	1	......	......	IV
2981.45	20r	15r	12	8	I
2981.86	6	4	......	......	IV
2983.57	125R	100R	30r	25	I
2984.83*	10	6	1	......	IV
2985.55	4	......	......	......	V
2986.46	3	5	5	1	III
2987.29	10	8	6	1	III
2988.47	2	3	......	......	IV
2990.39	6	4	......	......	IV
2991.65	5n	3	......	......	IV
2994.43* 2994.50*	100R	80R	40R	35	I
2996.39	5	2	......	......	IV
2999.52	30R	30R	12	5	II
3000.45	8	8	3	......	III
3000.95	100R	80R	30r	25	I
3002.65*	5	......	......	......	V
3003.03	10	10	6	tr	III
3005.31	3	1	......	......	IV
3007.15	8	8	3	......	III
3007.28	12r	10r	7	5	I
3008.14	60R	50R	20r	12	I
3009.10	5	3	......	......	IV
3009.58	25r	20r	10	3	II
3011.48	7	3	......	......	IV
3014.18	3	5	......	......	IV
3014.92	1	2	......	......	IV A
3015.93	4	1	......	......	IV
3016.18	12	8	8	tr	III
3017.63	15r	30R	15r	10	I A
3018.99	15r	12r	10	1	III
3020.50	100R	75R	30R	10	II
3020.64	200R	150R	80R	50	I
3021.08	150R	100R	40R	30	I
3024.04	15r	30R	15r	10	I A
3025.28	3	5	2	......	III
3025.64	15	8	1	......	IV
3025.85	50R	50R	25r	20	I

TABLE II—*Continued*

λ (I.A.)	Arc Intensity	Furnace Intensities			Class	λ (I.A.)	Arc Intensity	Furnace Intensities			Class
		High-Temp. Emission	Med.-Temp. Emission	Low-Temp. Absorption				High-Temp. Emission	Med.-Temp Emission	Low-Temp. Absorption	
3026.47	15	10	8	1	III	3165.86	4	2	......	......	IV
3029.24	3	3	......	......	IV	3166.44	6	3	......	......	IV
3030.15	15	8	1	......	IV	3168.86	2	1	......	......	IV
3031.22	12	6	......	......	IV	3171.35	5	1	......	......	IV
3031.64	15	10r	10	tr	III	3171.66	2	1	......	......	IV
3037.39	80R	60R	30r	20	I	3172.07	2	1	......	......	IV
3037.78	2	5	tr	......	IV A	3175.45	12	6	tr	......	IV
3040.43	15	10	8	1	III	3176.37	2	1	......	......	IV
3041.64	10	6	1	......	IV	3178.01	10	5	1	......	IV
3041.75	15	10	8	......	III	3178.55	2	1	......	......	IV
3042.03	15	8r	8	......	III	3178.97	3	1	......	......	IV
3042.67	15	10r	8	......	III	3179.54	3	1	......	......	IV
3045.08	5	4	3	......	III	3180.22	20	7	1	......	IV
3047.61	100R	80R	40r	25	I	3180.76	5	10	10	3	II A
3053.07	5	2	......	......	IV	3181.53	4	1	......	......	IV
3055.27	12	6	2	......	III	3182.08	3	1	......	......	IV
3057.45	40R	20R	10r	5	II	3182.99	3	1	......	......	IV
3059.09	100R	80R	40r	25	I	3184.63	3	1	......	......	IV
3060.99	4	3	......	......	IV	3184.90	7	15r	8	7	I A
3066.49	3	3	......	......	IV	3186.75	3	......	......	......	V
3067.12	8	6	tr	......	IV	3188.59	4	2	......	......	IV
3067.25	30r	15r	8	4	II	3188.84	7	3	......	......	IV
3068.18	8	8	1	......	IV	3191.67	7	15r	10	10	I A
3075.73	25r	15r	8	3	II	3192.81	8	5	tr	......	IV
3078.02	4	8	1	......	IV A	3193.21	10	25r	10	10	I A
3078.44	3	1	......	......	IV	3193.31	8	5	......	......	IV
3083.75	20	12	6	2	II	3194.42	3	1	......	......	IV
3091.58	20	12	6	2	II	3196.09	2	1	......	......	IV
3092.79*	2	2?	?	......	III ?	3196.15	2				IV
3093.81	3	6	......	......	IV A	3196.94*	20	8	6	4	II
3098.19	6	2	......	......	IV	3199.53	15	8	6	3	II
3099.90	20	20	8	2	II	3200.48	15	5	tr	......	IV
3099.97	15		8	2	II	3200.79	2	6	4	tr	III A
3100.31	20	12	8	2	II	3202.56	2	1	......	......	IV
3100.67	20	15	8	2	II	3205.40	15	5	tr	......	IV
3112.08	3	1	......	......	IV	3207.09	2	1	......	......	IV
3116.63	12	8	6	......	III	3208.48	4	1	......	......	IV
3117.63	1	3	1	......	III A	3209.33	6	2	......	......	IV
3119.50	6	4	......	......	IV	3210.25	8	4	......	......	IV
3120.44	6	3	......	......	IV	3210.83	10	4	tr	......	IV
3125.66	15	10	7	......	III	3211.49	4	1	......	......	IV
3126.17	8n	1	......	......	IV	3211.69	8	1	......	......	IV
3128.88	1	1	......	......	IV	3211.87	4	1	......	......	IV
3129.33	5	5	tr	......	IV	3212.00	10	5	1	......	IV
3132.51	4n	......	......	......	V	3214.04*	20	8	2	......	III
3134.11*	10	8	5	......	III	3214.39	8	15r	8	8	I A
3139.91	4n	......	......	......	V	3215.94	12	5	1	......	IV
3140.39	5n	......	......	......	V	3217.39	10	5	tr	......	IV
3142.45	6	2	......	......	IV	3219.58	12	5	1	......	IV
3142.89	5	2	......	......	IV	3219.82	10	8	3	......	III
3143.24	2	5	3	......	III A	3221.94	2	1	......	......	IV
3143.98	8	1	......	......	IV	3222.07	20	6	4	......	III
3144.49	6n	1	......	......	IV	3225.79	25	8	5	......	III
3151.34	10	2	......	......	IV	3226.73	2	5	2	......	III A
3153.21	5	3	......	......	IV	3227.07	3	1	......	......	IV
3154.51	2	1	......	......	IV	3227.76	15	6	1	......	IV
3155.29	2	1	......	......	IV	3227.81					
3156.27	5n	1	......	......	IV	3228.26	5	3	......	......	IV
3157.04	8	5	......	......	IV	3228.92	3	1	......	......	IV
3157.88	6	3	......	......	IV	3229.13	4	8	8	3	II A
3160.65	10	5	......	......	IV	3230.21	6	3	tr	......	IV
3161.37	4	4	tr	......	IV	3230.98	10	5	tr	......	IV
3161.95	8	4	tr	......	IV	3233.06	8	1	......	......	IV
3162.34	2n	1	......	......	IV	3233.98	12	6	tr	......	IV
3165.01	3	1	......	......	IV	3234.62	7	15r	8	8	I A

TABLE II—*Continued*

λ (I.A.)	Arc Intensity	Furnace Intensities			Class	λ (I.A.)	Arc Intensity	Furnace Intensities			Class
		High-Temp. Emission	Med.-Temp. Emission	Low-Temp. Absorption				High-Temp. Emission	Med.-Temp. Emission	Low-Temp. Absorption	
3236.23	8	20r	10	10	I A	3342.30	4	......	......	......	V
3239.45	15	8	1	......	IV	3346.94	1	1	......	......	IV
3243.41	3	1	......	......	IV	3347.93	6	4	......	......	IV
3244.19	15	8	1	......	IV	3351.53	2	1	......	......	IV
3246.02	8	12	10	8	I	3351.75	3	1	......	......	IV
3246.49	3	1	......	......	IV	3354.07	3	1	......	......	IV
3246.97	6	3	......	......	IV	3355.24	6	1	......	......	IV
3247.30	3	1	......	......	IV	3356.33	1	2	......	......	IV A
3248.22	10	5	......	......	IV	3356.41	3	2	......	......	IV
3249.20	3	1	......	......	IV	3359.50	2	5	2	......	III A
3250.63	4	2	......	......	IV	3366.79	5	1	......	......	IV
3251.24	8	1	......	......	IV	3366.87	5	2	......	......	IV
3252.93	4	1	......	......	IV	3369.57*	8	3?	2?	......	III
3253.61	4	1	......	......	IV	3370.79	10	6	tr	......	IV
3254.37	10	2	......	......	IV	3372.08	3	1	......	......	IV
3257.24	2	1	......	......	IV	3378.68	6	3	......	......	IV
3257.60	8	4	tr	......	IV	3379.02	6	4	......	......	IV
3260.00	6	2	......	......	IV	3380.12	8	4	......	......	IV
3260.28	4	1	......	......	IV	3382.41	3	2	......	......	IV
3262.28	4	1	......	......	IV	3383.70	5	4	tr	......	IV
3264.52	5	2	......	......	IV	3383.99	8	6	1	......	IV
3265.06	8	15r	10	8	I A	3387.41	2	1	......	......	IV
3265.63	15	6	2	......	III	3389.75	2	1	......	......	IV
3268.25	5	2	......	......	IV	3392.02	2	tr	......	......	IV
3271.01	15	6	2	......	III	3392.31	8	6	tr	......	IV
3276.48	4	2	......	......	IV	3392.66	15	9	3	......	III
3278.74	4	1	......	......	IV	3394.59	5	5	tr	......	IV
3280.27	8	2	......	......	IV	3396.98	4	8	5	......	III A
3284.60	5	3	......	......	IV	3397.64	2	4	1	......	III A
3286.03	2	1	......	......	IV	3399.34	15	8	2	......	III
3286.76	20	8	4	......	III	3401.52	6	10	9	......	III
3288.97	2	1	......	......	IV	3402.26	5	2	......	......	IV
3291.00	5	3	......	......	IV	3404.30	3	7	3	......	III A
3292.03	8	2	......	......	IV	3404.36	6	5	1	......	IV
3292.60	8	5	1	......	IV	3406.45	3	1	......	......	IV
3298.14	6	5	1	......	IV	3406.81	6	5	1	......	IV
3305.98	20	8	4	......	III	3407.47*	20	15	7	......	III
3306.36	20	8	4	......	III	3410.18	3	tr	......	......	IV
3307.24	5	1	......	......	IV	3411.36	3	2	......	......	IV
3310.35	4	1	......	......	IV	3413.14	15	10	4	......	III
3314.75	7	2	......	......	IV	3415.54	4	4	......	......	IV
3317.13	3	2	......	......	IV	3417.85	12	7	2	......	III
3319.26	2	1	......	......	IV	3418.51	10	6	2	......	III
3322.50	5n	1	......	......	IV	3422.50	3	1	......	......	IV
3323.74	7	3	......	......	IV	3422.67	7	5	1	......	IV
3324.54	4	2	......	......	IV	3424.29	10	8	2	......	III
3325.47	4	2	......	......	IV	3425.02	4	2	......	......	IV
3328.87	5	1	......	......	IV	3426.39*	5	10	6	......	III A
3331.62	3	1	......	......	IV	3426.65	5	6	tr	......	IV
3335.78	4	1	......	......	IV	3426.99	2	4	2	......	III A
3337.67	6	3	......	......	IV	3427.13	20	8	6	......	III
3339.20	2	1	......	......	IV	3428.20	8	6	2	......	III
3340.57	6	4	......	......	IV	3431.83	3	1	......	......	IV
3341.91	5	10	10	......	III A	3437.05	3	1	......	......	IV
3342.23	5	2	......	......	IV						

2875.31 Blend in arc with polar line.
2880.76, 2883.73 Strong polar lines.
2887.81 Not a polar line, though absent in furnace.
2926.58, 2944.40, 2947.66, 2949.21, 2953.78, 2970.52 Polar lines.
2984.83 Blend in arc with polar λ 2984.79.
2994.43–.50 λ 2994.43 is chief part of blend, which shows in furnace as a reversed line with violet side strongest.
3002.65 Polar line.
3092.79 Blend with strong Al line.
3134.11 Blend Ni. but arc and furnace lines chiefly Fe.
3196.94 Blend Ni on red side.
3214.04 Apparently a close double with components of equal strength.
3369.57 Blend Ni. Probable intensity of Ni line subtracted.
3407.47 Probably double.
3426.39 Double with faint violet component.

TABLE III

TEMPERATURE CLASSIFICATION OF IRON LINES, λ 3441–λ 3878

λ (I.A.)	Arc Intensity	Furnace Intensities (Emission)			Class	λ (I.A.)	Arc Intensity	Furnace Intensities (Emission)			Class
		High Temp.	Med. Temp.	Low Temp.				High Temp.	Med. Temp.	Low Temp.	
3440.61	150R	125R	125R	125r	I	3552.84	3	2	......	......	IV
3440.99	75R	75R	75r	60	I	3553.74	6	2	......	......	IV
3442.36	5	4	tr	......	IV	3554.12	4	12	10	1	III A
3442.68	3	8	5	......	III A	3554.52	2	2	......	......	IV
3443.88	50r	50R	50r	50	I	3554.92	40	15	3	......	III
3445.16	20	8	4	......	III	3556.88	7	10	tr	......	IV
3447.28	8	6	1	......	IV	3558.52*	30	30R	20	10	II
3450.33	10	7	1	......	IV	3559.51	2	1	......	......	IV
3451.62	2	1	......	......	IV	3560.71	5	1	......	......	IV
3451.92	10	7	1	......	IV	3565.38	60r	60R	60r	50	II
3452.28	10	12	8	1	III	3565.58	3	2	......	......	IV
3458.31	4	2	......	......	IV	3567.05	2	1	......	......	IV
3459.92	4	1	......	......	IV	3568.98	4	2	......	......	IV
3462.35	2	1	......	......	IV	3570.10	100R	100R	100r	75	I
3463.31	2	2	......	......	IV	3570.24	20	10	4	......	III
3465.86	60r	60R	60r	50	I	3571.23	2	4	......	......	IV A
3466.50	3	6	4	......	III A	3572.00	6	5	......	......	IV
3468.85	4	2	......	......	IV	3573.40	2	tr	......	......	IV
3469.83	2	1	......	......	IV	3573.84*	3	4	......	......	IV
3471.27	5	3	......	......	IV	3573.89*	4				IV
3471.34	6	3	......	......	IV	3575.25	2	1	......	......	IV
3475.45	70r	75R	75r	60	I	3575.38	4	4	2	......	III
3475.65	6	6	tr	......	IV	3575.98	2	1	......	......	IV
3476.71	40	40R	40	40	I	3576.76	2	1	......	......	IV
3483.01	3	6	5	tr	III A	3581.20	250R	200R	150R	150r	I
3485.34	7	6	tr	......	IV	3581.65	1	1	......	......	IV
3489.67	4	2	......	......	IV	3582.20	5	2	......	......	IV
3490.58	100r	100R	75r	75	I	3583.32	2	1	......	......	IV
3495.29	8	4	......	......	IV	3584.66	8	7	1	......	IV
3497.11	10	10	2	......	III	3584.79	1	1	......	......	IV
3497.84	40	40R	40r	40	I	3584.96	4	2	......	......	IV
3500.57	2	2	......	......	IV	3585.32*	30	30R	15	10	II
3504.87	2	2	......	......	IV	3585.71*	20	20R	15	8	II
3505.07	2	1	......	......	IV	3586.12	10	6	......	......	IV
3506.50	6	4	......	......	IV	3586.99*	30	25R	18	12	II
3508.49*	5	3	......	......	IV	3587.25	2	1	......	......	IV
3513.82	30	25R	20	10	II	3587.42	2	1	......	......	IV
3516.41	5	1	......	......	IV	3587.75	3	2	......	......	IV
3521.26*	25	20R	20	10	II	3588.62	3	3	......	......	IV
3521.84	2	4	......	......	IV A	3588.92	2	1	......	......	IV
3524.08	3	3	......	......	IV	3589.11	8	12r	12	2	III
3524.24	4	6	tr	......	IV	3589.45	3	2	......	......	IV
3526.02	1	1	......	......	IV	3594.63	8	6	tr	......	IV
3526.07	20	30R	30r	30	I	3595.29	2	1	......	......	IV
3526.17	15	15r	10	6	II	3596.20	1	1	......	......	IV
3526.38	4	3	......	......	IV	3597.05	3n	1	......	......	IV
3526.47	4	5	tr	......	IV	3598.71	1	2	......	......	IV A
3526.67	5	4	......	......	IV	3599.63	3	tr	......	......	IV
3527.80	4	4	......	......	IV	3602.10	1	3	......	......	IV A
3529.82	6	8	3	......	III	3602.46	2	1	......	......	IV
3530.38	2	2	......	......	IV	3602.54	3	2	......	......	IV
3533.00	5	4	......	......	IV	3603.20	10	7	1	......	IV
3533.20	10	7	......	......	IV	3603.82	1	1	......	......	IV
3536.55	15	10	1	......	IV	3605.45*	15	12	tr	......	IV
3537.50	1	1	......	......	IV	3606.68	20	10	4	......	III
3537.73	3	3	......	......	IV	3608.15	3	2	......	......	IV
3537.89	4	4	......	......	IV	3608.86	100r	80R	60r	60	I
3540.13	3	3	......	......	IV	3610.15	20	9	2	......	III
3540.71	3	8	6	......	III A	3610.71	2	1	......	......	IV
3541.09	15	10	1	......	IV	3612.08	8	3	......	......	IV
3542.08	15	10	1	......	IV	3612.94	1	4	......	......	IV A
3542.24	1	1	......	......	IV	3614.56	2n	tr	......	......	IV
3545.64	5	4	......	......	IV	3616.58	3n	tr	......	......	IV
3549.87	4	4	1	......	III	3617.32	2	tr	......	......	IV
3552.11	1	1	......	......	IV	3617.79	12	6	tr	......	IV

TABLE III—*Continued*

λ (I.A.)	Arc Intensity	Furnace Intensities (Emission)			Class	λ (I.A.)	Arc Intensity	Furnace Intensities (Emission)			Class
		High Temp.	Med. Temp.	Low Temp.				High Temp.	Med. Temp.	Low Temp.	
3618.39	2	2	......	......	IV	3686.00	15n	7	1	......	IV
3618.77	125R	100R	80r	80	I	3686.26	2	2	......	......	IV
3621.46	15	8	1	......	IV	3687.10	2	3	......	......	IV
3622.01	12	7	1	......	IV	3687.46	40r	40R	40	30	I
3623.19	8	7	1	......	IV	3687.66	4	3	1	......	III
3623.45	1	1	......	......	IV	3689.46	12	6	1	......	IV
3623.78	2	1	......	......	IV	3690.73	4	1	......	......	IV
3625.15	6	3	......	......	IV	3693.02	1	tr	......	......	IV
3628.09	1	1	......	......	IV	3694.00	20	8	1	......	IV
3630.35	4	2	......	......	IV	3695.05	8	4	......	......	IV
3631.09	7	4	tr	......	IV	3697.44	6n	3	......	......	IV
3631.46	125R	100R	75r	75	I	3698.61	2	1	......	......	IV
3632.04	10	5	......	......	IV	3699.14	1	tr	......	......	IV
3632.55	3	1	......	......	IV	3701.08	20	9	1	......	IV
3632.98	3	2	......	......	IV	3702.03	3	2	......	......	IV
3633.84	1	tr	......	......	IV	3702.49	1	2	......	......	IV A
3634.34	6n	1	......	......	IV	3703.56*	5	?	?	......	IV ?
3634.68	4n	tr	......	......	IV	3703.70	3	1	......	......	IV
3635.19	2	6	1	......	IV A	3703.82	3	1	......	......	IV
3636.19	2	3	......	......	IV	3704.46	10	4	tr	......	IV
3636.65	1	tr	......	......	IV	3705.57	100r	100R	80r	80	I
3636.99	2	1	......	......	IV	3707.05	8	3	......	......	IV
3637.25	1	1	......	......	IV	3707.83	20	20r	20	20	I
3637.86	3n	tr	......	......	IV	3707.92	8	10	5	......	III
3638.30	12	7	tr	......	IV	3709.25	75r	40R	30	15	II
3640.39	15	10	1	......	IV	3711.23	3	2	......	......	IV
3643.62	2	1	......	......	IV	3711.41	2	tr	......	......	IV
3643.72	1	1	......	......	IV	3715.92	4	4	tr	......	IV
3645.09	2	1	......	......	IV	3716.45	12	6	tr	......	IV
3645.49	1	1	......	......	IV	3718.41	3	2	......	......	IV
3645.83	6	2	......	......	IV	3719.94	250R	300R	300R	300r	I
3647.43	3	1	......	......	IV	3721.28	2	2	......	......	IV
3647.85	100R	100R	75r	75	I	3721.40	1	1	......	......	IV
3649.31*	5	20r	25	20	I A	3721.51	2	1	......	......	IV
3649.51	12	10	1	......	IV	3722.57	50r	100R	80r	80	I A
3650.03	4	2	......	......	IV	3724.38	8	8	2	......	III
3650.28	5	5	1	......	IV	3726.92	6	4	tr	......	IV
3651.47	20	12	2	......	IV	3727.10	4	2	tr	......	IV
3653.76	1	1	......	......	IV	3727.62	50r	40R	30	20	II
3655.47	4	2	......	......	IV	3727.81	3	2	......	......	IV
3656.23	3n	tr	......	......	IV	3728.67	1	1	......	......	IV
3657.14	1	tr	......	......	IV	3730.39	3	2	......	......	IV
3657.89	1	1	......	......	IV	3730.95	2	1	......	......	IV
3659.52	8	6	1	......	IV	3731.37	2	1	......	......	IV
3663.46	1	1	......	......	IV	3732.40	10	10	6	1	III
3664.56	2	1	......	......	IV	3733.32	40r	80R	60r	60	I A
3666.24	1	tr	......	......	IV	3734.87	300r	150R	100R	100r	II
3667.28	3n	1	......	......	IV	3735.33	6	4	......	......	IV
3668.00	1	tr	......	......	IV	3737.14	150R	200R	200R	200r	I
3669.16	3	tr	......	......	IV	3738.31	10	4	......	......	IV
3669.53	10	8	1	......	IV	3739.11	1	1	......	......	IV
3670.04	3	2	......	......	IV	3739.32	1	1	......	......	IV
3670.09	3	2	......	......	IV	3739.54	3	2	......	......	IV
3670.81	1	1	......	......	IV	3740.26	3	2	......	......	IV
3672.69	1	1	......	......	IV	3742.62	4	3	......	......	IV
3674.77	2	1	......	......	IV	3743.36	20	40R	25	20	II A
3676.31	6	6	tr	......	IV	3743.47*	6	?	?	......	IV ?
3677.31	2	tr	......	......	IV	3744.10	4	3	......	......	IV
3677.63	12	9	1	......	IV	3745.56	100R	150R	150R	150r	I
3678.86	3	3	......	......	IV	3745.90	40r	80R	80r	75r	I A
3679.92	40r	100R	80r	80	I A	3746.48	1	1	......	......	IV
3680.69	2n	tr	......	......	IV	3746.93	6	4	......	......	IV
3680.80	1	tr	......	......	IV	3748.26	60R	125R	100r	100r	I A
3681.77	1	tr	......	......	IV	3748.49*	7	?	?	......	IV ?
3682.24	20	8	tr	......	IV	3748.96	5	3	......	......	IV
3683.06*	10	20r	20	20	I A	3749.49	200R	125R	80r	50	II
3684.11	15	8	1	......	IV	3753.61*	8	5?	3?	......	III

TABLE III—*Continued*

λ (I.A.)	Arc Intensity	Furnace Intensities (Emission)			Class
		High Temp.	Med. Temp.	Low Temp.	
3754.50	1	1	......	......	IV
3756.07	1	2	......	......	IV A
3756.94	4	1	......	......	IV
3757.46	1	tr	......	......	IV
3758.23	150R	125R	75r	40	II
3760.05	8	6	3	......	III
3760.53	6	5	2	......	III
3761.41	1	1	......	......	IV
3763.79	100r	80R	50	30	II
3765.54	20	6	1	......	IV
3766.67	1	tr	......	......	IV
3767.19	80r	60R	40	25	II
3768.03	3	3	tr	......	IV
3770.00	4	1	......	......	IV
3770.31	3	1	......	......	IV
3770.41					IV
3773.69	1	tr	......	......	IV
3774.83	5	4	tr	......	IV
3776.46	6	5	tr	......	IV
3777.45	2	1	......	......	IV
3778.52	4	tr	......	......	IV
3779.42	3	1	......	......	IV
3779.50	2	1	......	......	IV
3781.19	2	3	tr	......	IV
3782.46	1	tr	......	......	IV
3785.95	6	4	tr	......	IV
3786.18*	4	1	......	......	IV
3786.68	8	8	8	2	III
3787.88	50	30R	20	20	II
3789.18	3	1	......	......	IV
3790.09	12	10	10	6	II
3790.76	1	2	tr	......	IV A
3792.16	2	2	......	......	IV
3792.83	1	1	......	......	IV
3793.35	1	1	......	......	IV
3793.87	1	1	......	......	IV
3794.34	8	4	1	......	III
3795.00	60	40R	30	25	II
3797.52	12	4	1	......	III
3798.51	40	30R	20	20	II
3799.55	50	40R	20	20	II
3801.68	3	2	......	......	IV
3801.81	1	tr	......	......	IV
3805.35	12	5	tr	......	IV
3806.22	2	tr	......	......	IV
3806.70	10	4	1	......	III
3807.54*	7	8?	3?	......	III
3808.73	4	3	......	......	IV
3810.76	2	tr	......	......	IV
3811.89	2	tr	......	......	IV
3812.97	40	25R	20	20	II
3813.06*	5?	?	......	......	IV
3813.64	2	1	......	......	IV
3813.89	2	......	......	......	V
3814.53	5	10	8	2	III A
3815.84	100r	50R	30	20	II
3816.34	4	5	1	......	IV
3817.64	3n	1	......	......	IV
3820.43	250R	200R	200R	60	II
3821.18	10	4	tr	......	IV
3821.84	3	2	......	......	IV
3824.08	1	1	......	......	IV
3824.31*	2	?	......	......	IV ?
3824.44	50r	100R	100r	100r	I A
3825.89	200R	125R	80r	40	II
3826.84	1	1	......	......	IV
3827.57	1	1	......	......	IV
3827.83	75r	50R	30	20	II
3829.46	1	1	......	......	IV
3830.76	1	1	......	......	IV
3830.87	1	1	......	......	IV
3833.31	5	5	1	......	IV
3834.23	100r	80R	60	30	II
3836.34	4	2	......	......	IV
3837.14	1	1	......	......	IV
3839.26	7	3	......	......	IV
3840.44	80r	60R	40	25	II
3841.05	80r	25r	25	15	II
3843.26	8	4	tr	......	IV
3846.41	2	tr	......	......	IV
3846.81	8	2	......	......	IV
3849.97	40	40r	30	25	II
3850.82	12	15r	20	10	II
3852.58	6	6	1	......	IV
3856.37	50r	100R	100r	100	I A
3859.22	10	6	2	......	III
3859.91	300R	250R	200R	200r	I
3861.34	2	1	......	......	IV
3863.75	2	1	......	......	IV
3865.53	30	40r	25	20	II
3867.22	7	4	......	......	IV
3867.93	1	tr	......	......	IV
3869.56	3	2	......	......	IV
3869.59					IV
3871.75	4	3	......	......	IV
3872.51	60	60R	35	20	II
3872.92	1	tr	......	......	IV
3873.77	8	8	1	......	IV
3876.04	4	15	12	1	III
3878.02	60	60R	40	20	II
3878.58	100r	100R	100r	75r	II

3508.49 Probably double.
3573.84–.89 Blend in furnace. Violet component appears strongest.
3521.26, 3558.52, 3585.32–.71, 3586.99 Become very faint at 1600°.
3605.45 Blend Cr on violet side.
3649.31 Between Classes I and II. Weak at 1600°.
3583.06 Blend V on red side.
3703.56 Blend V.
3743.47 Blend with preceding line.
3748.49 Blend with preceding line.
3753.61 Blend V. Probable intensity of V line subtracted.
3786.18 Probably double.
3807.54 May be partly V.
3813.06 Blend with preceding line.
3824.31 Blend with following line.

reverse readily in the furnace or in the arc with moderate current. The distinction between the two classes will be considered further in the discussion. Lines of class III are absent or at least very faint at low temperature, and first appear distinctly at medium temperature. There is much variety among these lines, but a large proportion show a rapid increase in intensity through the high-temperature stage and under the conditions of the arc. Class IV lines require strong excitation and usually appear only at high temperature, though perhaps faintly at medium temperature. Most of the fainter arc lines belong in this class, but many lines of intensity 10 or higher in the arc require the high-temperature furnace for their appearance. Class V lines appear in the arc but are absent from the furnace. Lines of this character are listed in Tables I–III only when they show considerable strength in the arc. Their number is relatively few, since polar lines are seldom included, and, except for these, class V is made up chiefly of very faint arc lines.

"A" after the class number denotes that the line is relatively weak in the arc. The selection depends to some extent on the average intensity adopted for arc and furnace spectra. In the tables, a line whose arc intensity is not more than half of that for the high-temperature furnace is placed in this division.

An asterisk after the wave-length refers to a note at the end of the tables.

REVISED CLASSIFICATION OF BLUE AND VIOLET IRON LINES

Table IV contains 262 lines, from λ 3884 to λ 4531, which are within the range covered by the former paper. A revision of the classification seemed desirable to make this portion of the spectrum uniform with the ultra-violet region treated in the present paper. This is chiefly on account of the change in the temperature steps, 1600°–1700° now being used for the low temperature stage instead of 1800°–1900°. Twenty-six lines not in the former list are included in Table IV, and ninety lines have their classes changed. About half of the changes are from class V to class IV, due to improved high-temperature spectrograms, which show distinctly many faint lines not obtained before with the furnace. Of the remaining changes, a few are due to errors incident to the first attempt at a

TABLE IV

Classification of Iron Lines, λ 3884–λ 4531

λ	Class	λ	Class	λ	Class	λ	Class
3884.37	IV	3971.33	III	4143.42	III	4267.83	IV
3885.51	III	3973.66	V	4143.87	I	4268.75	IV
3886.29	I	3976.62	IV	4147.68	III	4271.17	III
3887.05	I	3977.75	III	4149.37	V	4271.76	II
3888.52	II	3981.78	III	4152.18	II A	4282.41	III
3888.83	IV	3983.96	III	4153.92	IV	4285.45	IV
3890.84	IV	3985.39	IV	4154.50	III	4291.47	I A
3891.93	V	3986.18	IV	4154.82	IV	4294.13	II
3893.40	IV	3989.86	V	4156.81	III	4298.04	IV
3893.92	IV	3990.38	V	4157.81	IV	4299.25	III
3894.01	III	3994.12	V	4158.81	V	4305.46	IV
3895.66	I	3995.99	IV	4170.91	IV	4307.91	II
3897.45	IV	3997.40	III	4172.13	IV	4309.38	IV
3897.89	IV	3998.06	III	4172.75	II A	4315.09	III
3898.01	II	4001.67	III	4173.32	IV	4325.77	II
3899.03	IV	4005.25	II	4173.93	II A	4337.05	II
3899.71	I	4006.31	IV	4174.92	II A	4351.55	IV
3900.52	V	4006.63	IV	4175.64	III	4352.74	III
3902.95	II	4007.27	IV	4176.57	IV	4358.51	IV
3903.90	IV	4009.72	III	4177.60	II A	4367.58	IV
3906.48	I	4014.54	III	4181.76	III	4367.91	III A
3907.47	III	4017.15	III	4182.39	IV	4369.78	III
3907.94	IV	4021.87	III	4184.89	III	4375.93	I
3909.67	V	4024.75	V	4187.05	III	4383.55	II
3909.83	III	4030.51	IV	4187.81	III	4387.90	IV
3910.85	IV	4032.64	III	4191.45	III	4388.42	IV
3913.64	III	4043.90	IV	4195.34	IV	4389.25	II A
3916.74	IV	4044.62	IV	4196.22	IV	4390.96	IV
3917.19	II	4045.82	II	4198.31	III	4404.75	II
3918.42	IV	4058.23	IV	4199.10	III	4415.13	II
3918.65	IV	4058.77	IV	4199.97	I A	4422.57	III
3920.26	I	4062.45	III	4202.03	I	4427.31	I
3922.92	I	4063.60	II	4203.99	III	4430.20	IV
3925.65	IV	4066.98	III	4206.70	I A	4430.62	III
3925.95	IV	4067.28	III	4207.13	IV	4433.22	IV
3927.93	I	4067.99	III	4208.61	V	4435.15	II A
3930.30	I	4070.78	III	4210.36	III	4439.89	IV
3932.64	IV	4071.75	II	4213.65	IV	4442.35	III
3933.61	IV	4074.79	IV	4215.42	IV	4442.84	IV
3935.82	III	4076.64	IV	4216.19	I	4443.20	III
3937.33	IV	4078.36	IV	4217.56	IV	4445.43	I A
3940.89	II	4079.25	IV	4219.36	IV	4447.14	IV
3942.45	IV	4079.85	IV	4220.34	IV	4447.73	III
3943.35	IV	4080.23	IV	4222.23	III	4454.39	III
3944.90	IV	4083.78	IV	4224.17	IV	4459.13	III
3945.12	IV	4084.51	IV	4224.51	IV	4461.66	I
3947.00	IV	4085.01	IV	4225.46	IV	4462.01	IV
3947.54	IV	4085.31	IV	4225.96	IV	4464.77	IV
3948.11	IV	4095.98	IV	4226.43	IV	4466.56	II
3948.78	IV	4098.19	IV	4227.45	III	4469.39	IV
3949.96	III	4100.75	II A	4229.75	III	4476.02	III
3951.17	IV	4104.14	V	4232.72	IA	4479.61	IV
3952.61	IV	4107.50	III	4233.61	III	4480.14	IV
3953.16	IV	4109.81	IV ?	4235.95	III	4482.18 }	I
3955.37	IV	4114.45	IV	4237.16	III A	4482.26 }	
3956.46	IV	4118.56	IV	4238.04	IV	4484.24	IV
3956.68	III	4120.21	IV	4238.83	IV	4485.67	IV
3957.04	IV	4121.81	IV	4239.85	III	4488.92	IV
3963.12	V	4122.52	IV	4245.26	III	4489.74	I A
3964.52	V	4126.19	IV	4247.44	III	4490.09	IV
3966.07	III	4127.62	IV	4248.22	IV	4494.57	III
3966.63	IV	4132.06	II	4250.13	III	4525.15	IV
3967.43	IV	4132.91	III	4250.79	II	4528.62	II
3967.97	IV	4134.68	IV	4258.39	I A	4531.16	II
3969.26	II	4137.00	IV	4260.49	III		
3970.39	IV	4139.94	II A	4266.97	IV		

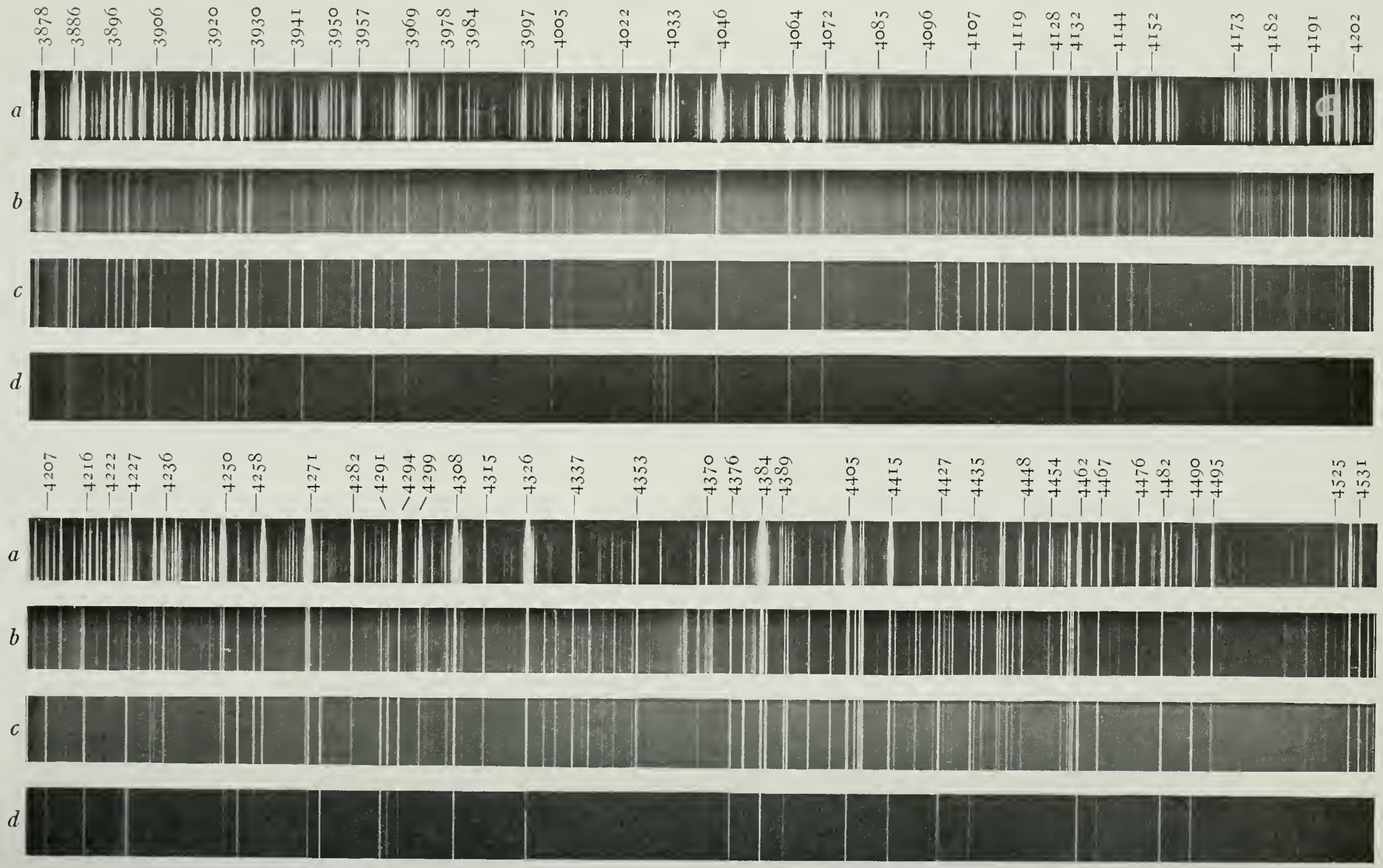

Arc and Furnace Spectra of Iron in Violet and Blue

a Arc spectrum; *b, c, d* Furnace spectra at 2600°, 2000°, 1650° C., respectively classification of this kind, but most of the alterations result from the new low-temperature stage. A line may retain at 1800°–1900° an intensity sufficient to place it in class I if this were the low temperature selected; but a temperature drop of 200° may weaken it so that it clearly belongs in class II, possibly verging on class III. Naturally some lines still strong at 1600° may weaken rapidly below this, and the most pronounced low-temperature lines reduce to the small number in Table V (see p. 337) emitted at 1400°. The 1600°–1700° stage emits, however, a set of lines retaining fair intensity under as weak excitation as is ordinarily usable for the iron spectrum in the laboratory, and the high-temperature lines have had an opportunity to drop out in the range below 2000°.

As the gradation of intensities for the lines included in Table IV is shown in the 1913 paper, it was considered sufficient in this revision to print the classes only. Beyond λ 4600 into the red, the later photographs confirm the earlier so closely as to classes that it seems unnecessary to go over the ground.

Table IV is supplemented by a reproduction of this region in Plate X. Three furnace spectra for temperatures of 2600°, 2000°, and 1650°, respectively, are given with a strong arc spectrum, the latter just sufficing to show some of the more pronounced lines of the sort which are relatively stronger in the furnace than in the arc. The strong lines emitted in the furnace and not in the iron arc are due chiefly to titanium and vanadium. λ 4227 of calcium is strong in the medium- and low-temperature spectra.

DISCUSSION OF RESULTS

a) *Distinctive features of classes I, II, and III.*—The difference between classes I and II is not as decided in the ultra-violet as in the visible region and for many purposes the two classes may perhaps be considered together as the low-temperature group. In segregating the lines in this paper, the absorption spectrum at low temperature has been of much service. It was considered that lines appearing in absorption at a temperature as low as 1600° were at least in class II, and those which maintained their intensity to the greatest extent were placed in class I. In the portion covered by the low-temperature emission spectrum, as far as λ 3440, the appearance of the lines both in emission and absorption was considered. The experiments of Hemsalech[1] with the flame spectrum of iron showed that, of the stronger lines, a portion are emitted with relatively high intensity in the outer mantle of the flame, while others require the stronger excitation found on the boundary of the cone. The lines of these two classes correspond closely, in the region common to both investigations, with classes I and II, respectively, of the furnace lines. The susceptibility to reversal in either the high-temperature furnace or the arc often distinguishes between these two classes. Of the two emission lines having approximately the same width, one may show a wider reversal. In a low-temperature absorption spectrum it will be distinctly the stronger line. This indication that the line maintains its strength in the lower-temperature absorbing vapor distinguishes the class I line. The contrast between λ 3734.87 and λ 3737.14 illustrates this point. The first, having in the arc much greater brightness in proportion to its width, is given the higher intensity. In the low-temperature furnace, the second is much the stronger. In the visible region, the quartet of class I lines λλ 3920–3930 contrasts in the same way with the class II triplets having stronger lines at λ 4045 and λ 4384.

Class III lines, by reason of their absence from low-temperature vapors, do not show reversal in the furnace emission spectrum, and in the absorption spectrum, when the furnace is hot enough to absorb these wave-lengths, their weakness in comparison with lines of classes I and II is very pronounced. The rapid development of class III lines is the chief cause of the very different appearance of the low- and high-temperature spectra; while in the arc, the fact that the class III lines are often among the strongest in the spectrum and classes IV and V have become prominent makes the arc spectrum of iron very different from that of the furnace.

b) *Lines appearing at 1400° C.*—It may be of interest to record a list of the most persistent low-temperature lines of iron. By means of long exposure with a 1-meter concave grating spectrograph, the emission lines listed in Table V were obtained. The furnace temperature was held close to 1400° C. The film was of the Eastman portrait variety, showing little sensitiveness beyond the blue. The twenty-one lines which appear are all pronounced members of class I, except that a bare trace is visible of λ 4384, the strongest of the class II lines. The absence of the triplets to which λ 4384 and λ 4046 belong is one of the striking features of this very low-temperature emission. λ 4376 is under these conditions the strongest line of the spectrum.

---

[1] *Philosophical Magazine*, 33, 1, 1917.

TABLE V

Persistent Low-Temperature Lines of Iron

λ	Intensity	λ	Intensity
3745.56	1	3920.26	8
3820.43	1	3922.92	8
3824.44	2	3927.94	8
3825.89	1	3930.30	8
3856.37	4	4216.18	2
3859.91	4	4375.93	10
3878.58	5	4383.55	tr
3886.29	6	4427.31	8
3895.65	5	4461.65	4
3899.70	5	4482.18	2
3906.47	2		

c) Lines relatively weaker in arc than in furnace.—In all of the furnace spectra thus far studied, attention has been drawn to this type. Such a line may be extremely weak in the arc and still strong in the furnace. The type may be found in any temperature class and its occurrence points to a difference, as yet obscure, between the arc and furnace excitations. These lines, designated by "A" after the class number, may reverse at high temperature, in which case they remain strong at low temperature and belong in class I A. Those which do not reverse are of two types. The type prevailing in the ultra-violet usually comes under class III A, becoming very faint at low temperature. The other type consists of I A lines, which are narrow at all temperatures, but remain strong at low temperature. These appear to be confined to the visible region, where λλ 4200, 4258, 4291, 5225, 5247, 5250.2, 5255 may be noted as conspicuous examples.

d) Relation to arc types.—It has been noted that lines appearing in the furnace spectrum are likely, in the arc spectrum, to show strongest in the region of the arc away from the poles. It was possible to photograph the spectral region below λ 2800, covered in Table I, so as to show this change from center to pole, as the astigmatism of the concave grating is small for this part of the spectrum. Plate XI reproduces a section of this region, a high-temperature furnace absorption spectrum being placed between two arc spectra, the upper being the integrated spectrum of the central and polar vapors, and the lower taken with the axis of the arc along the slit. In the upper strip it may be seen that some lines relatively faint in the arc, such as λ2750 and λ2756 are distinct in the furnace, being radiated chiefly by the vapors away from the pole, while the adjacent strong lines λ2749 and λ2755, with major emission at the poles, are absent in the furnace. Strong furnace lines are wide and frequently reversed in the hood of vapor above the center of a vertical arc, and fade rapidly toward the lower pole, where polar conditions are more concentrated. Lines of the intermediate type, designated in Table I as "C–P," of about the same strength from center to pole, are usually present in the furnace, but relatively weaker than lines which are more closely confined to the center.

d) Probable relation to ionization phenomena.—The trend of recent investigations has been to show a parallelism between the excitation stages given by different temperatures and those produced by various voltages in studies of ionization potentials. As no work has been done with iron vapor as to the effect of different voltages, nothing definite can be said for this spectrum, but for metals which have been studied in both ways, there has as yet been no contradiction of the view that the two modes of excitation result, at corresponding points, in the same radiative processes. In other words, temperatures can be selected to bring out successive groups of lines in the same way that various voltages may be used, as in the recent work of Foote, Meggers, and Mohler.[1] On account of the high vaporization point of substances such as iron, the classification of many spectra can be carried out best by the furnace method, but the close connection of the critical voltages with the quantum theory, in the results obtained by the voltage method, makes desirable a study of the correspondence for those elements

---

[1] *Philosophical Magazine*, 42, 1002, 1921; *Astrophysical Journal*, 55, 145, 1922.

PLATE XI

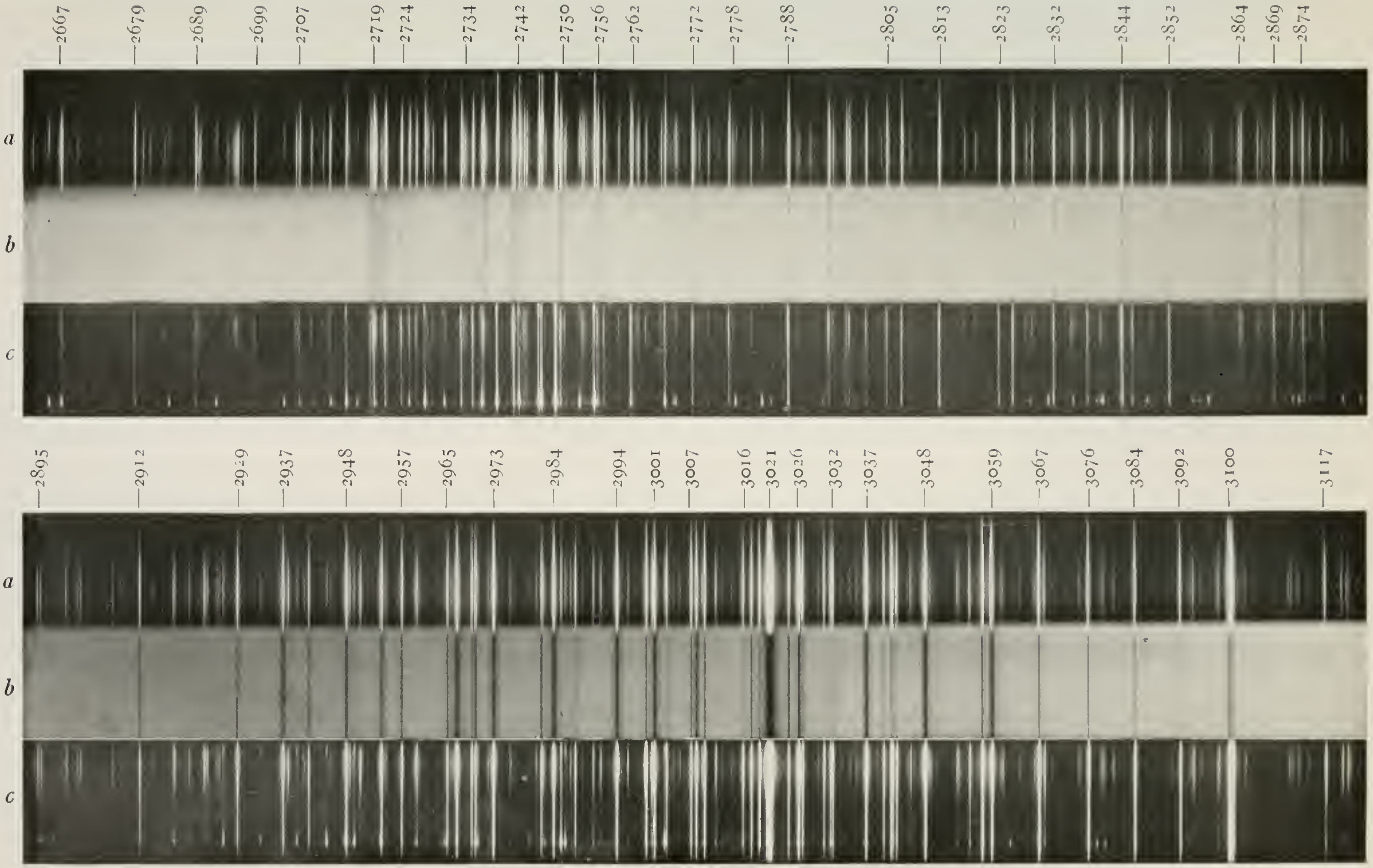

ARC AND FURNACE SPECTRA OF IRON

a Arc spectrum of combined central and polar vapors; *b* Absorption spectrum of high-temperature furnace; *c* Arc spectrum showing radiation by central vapor, and (below) in region close to positive pole

which may have their spectra excited in either way. The short extension into the ultra-violet of the furnace spectrum has prevented the observation of many important low-temperature lines as long as emission spectra only were employed. The methods here described for the production of the low-temperature absorption spectrum of iron can be applied with other elements to the grouping of their lines at various temperatures through the range from perhaps λ 2300 into the infra-red.

Mount Wilson Observatory
August 1922

CHANGES IN THE SPECTROGRAPHIC ELEMENTS OF Y SAGITTARII[1]

BY JOHN C. DUNCAN

ABSTRACT

Changes in the spectrographic elements of Y Sagittarii.—A velocity curve of this Cepheid variable, derived from 17 single-prism spectrograms made at Mount Wilson and three triple-prism spectrograms made at Mount Hamilton in 1921, is compared with the curve derived from 26 single-prism spectrograms made at Mount Hamilton in 1908 (Fig. 1). Elliptic elements for both years are given. The velocity of the system is found to have changed from +3.6 to −5.9 km/sec., while the eccentricity in 1921 appears to be double its value in 1908. Other elements also seem to have changed, but less markedly.

Y Sagittarii is a well-known variable star of the δ Cephei class. The variability of its brightness was discovered by Sawyer in 1886, and that of its radial velocity by Curtiss in 1904. A preliminary velocity curve and elliptic elements, derived from observations made with the single-prism spectrograph of the Lick Observatory in 1908, were published by me in 1909.[2] Last winter my attention was called by Mr. Joy to the fact that observations made at Mount Wilson in 1918 gave a velocity some twenty kilometers below that shown by my curve of 1908, and I then undertook a new determination of the curve.

The star was placed by Mr. Adams on the observing list of the 60-inch and 100-inch reflectors, and in the spring and summer of 1921 seventeen one-prism spectrograms were secured. An approximate curve derived from these observations showed unmistakably a velocity of the system several kilometers less than that of 1908. This difference seemed too great to be due to the use of different spectrographs and methods of measurement, but that question was nevertheless referred to Director Campbell, who very kindly had three plates made with the three-prism spectrograph and measured at the Lick Observatory, the dates of the plates corresponding to salient points of the curve. These plates agree very well with the Mount Wilson plates, and in the final determination of the elements were given additional weight on account of their high dispersion. Data concerning the 1921 plates, and also three plates made at Mount Wilson in 1918 and one in 1919, are given in Table I. Plates with numbers preceded by γ were made with the 60-inch telescope; by C, with the 100-inch. The phase (days since maximum brightness) is computed from the elements of Hellerich.[1]

---

[1] *Contributions from the Mount Wilson Observatory*, No. 248. Read at the Swarthmore meeting of the American Astronomical Society, December, 1921.

[2] *Lick Observatory Bulletin*, 5, 82, 1909.

TABLE I

Plate	Date, G.M.T.	J.D. 2420000+	Phase	Vel.	O.−C.	Wt.
γ 7145	1918 July $19^{d}19^{h}22^{m}$	1794.807	3.912	0.0	−12.1	.....
γ 7157	July 21 17 27	1796.727	0.059	−23.0	+ 0.1	.....
γ 7206	Aug. 17 16 20	1823.681	3.919	+ 2.2	−10.0	.....
γ 8710	1919 Sept. 13 15 00	2215.625	3.281	− 3.3	− 7.3	.....
γ 10002	1921 Mar. 17 01 10	2766.048	5.244	− 9.8	− 1.6	1
γ 10011	Mar. 18 01 05	2767.045	0.468	−28.4	− 5.9	1
C 952	Mar. 20 00 42	2769.029	2.452	− 0.9	+ 4.3	1
γ 10088	Apr 17 00 19	2797.013	1.569	−10.0	+ 3.8	1
γ 10127	Apr. 25 23 26	2805.976	4.759	+18.7	+ 3.4	1
γ 10136	Apr. 27 23 53	2807.995	1.005	−19.9	− 1.2	1
γ 10165	May 25 19 57	2835.831	5.748	−14.4	+ 8.1	1
γ 10166	May 25 20 45	2835.865	5.782	−15.5	+ 7.3	1
γ 10178	May 26 22 28	2836.936	1.079	−25.9	− 7.8	1
γ 10204	June 15 22 07	2856.922	3.745	+ 9.3	− 0.6	1
γ 10207	June 16 21 11	2857.883	4.706	+19.8	+ 3.4	1
γ 10216	June 19 21 30	2860.896	1.946	−10.0	+ 0.2	1
γ 10221	June 20 19 45	2861.823	2.873	− 3.9	− 3.2	1
γ 10233	June 22 21 09	2863.881	4.931	0.0	− 9.1	1
C 1174	July 24 19 42	2895.821	2.232	−10.4	− 2.9	1
Lick	July 26 18 43	2897.780	4.191	+15.0	− 0.7	3
C 1185	July 26 18 54	2897.787	4.198	+11.0	− 4.8	1
γ 10337	July 26 19 07	2897.797	4.208	+12.8	− 3.1	1
Lick	Aug. 14 17 13	2916.717	0.035	−21.5	+ 1.4	3
Lick	Aug. 16 17 06	2918.712	2.030	− 8.6	+ 0.8	2

The velocity is in each case the mean result of measures by two or more observers. The residuals O.−C. are taken from the 1921 velocity curve shown in Figure 1.

Although the binary hypothesis of Cepheid variation is not universally accepted, the usual elliptic elements seem still to be the best means for numerically representing the observed variations in radial velocity; and I accordingly give these elements, leaving their interpretation on the pulsation and other hypotheses to the reader. Corrections to the preliminary elements of 1908 (except the period) were computed by least squares. These corrections were in every case smaller than their probable errors. The period found from photometric observations by Hellerich was adopted. A least-squares solution was made for the elements of 1921, using the seventeen plates made at Mount Wilson and the three made at Mount Hamilton. The results are shown in Table II.

---

[1] Inaugural Dissertation, Berlin, 1913.

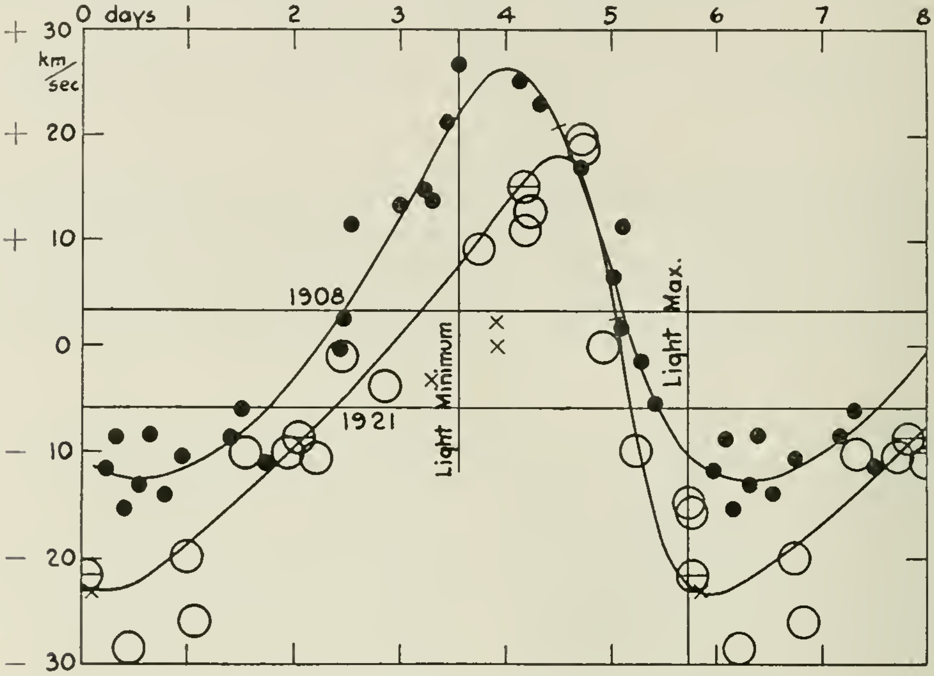

FIG. 1.—Velocity curves of Y Sagittarii, 1908 and 1921

TABLE II

	1908	1921	Difference
P		5.773268 days (Hellerich)	....
K	19.3 ± 0.8 km/sec.	20.6 ± 0.8 km/sec.	+ 1.3 ± 1.2 km/sec.
γ	+3.6 ± 1.2 km/sec.	−5.9 ± 1.5 km/sec.	− 9.6 ± 1.9 km/sec.
ω	43°0 ± 13°8	74°5 ± 6°2	+31°5 ± 15°1
e	0.21 ± 0.04	0.42 ± 0.04	+0.21 ± 0.06
T	4.51 ± 0.21	5.05 ± 0.08	+0.54 ± 0.22
$a \sin i$	1 500 000 km	1 354 000 km	−146 000 km
$\frac{m_1^3 \sin^3 i}{(m+m_1)^2}$	0.004☉	0.003☉	....
ϵ	±2.4 km/sec.	±3.1 km/sec.	....

The time T of periastron passage is counted in days from the time of light-maximum. The interval from light-maximum to velocity minimum was 0.64 days in 1908 and 0.19 days in 1921; the interval from light minimum to velocity maximum was 0.27 and 0.72, respectively—the former interval having diminished and the latter increased, each by 0.45 days. The observations, and the velocity curves representing the above elements, are plotted in Figure 1. The Lick observations of 1908 are indicated by filled circles; those of 1921 by barred rings; the Mount Wilson observations of 1921 by plain rings; and those of 1918 and 1919 by crosses.

The most important changes found are those in the velocity of the system and in the eccentricity, which are so large as to leave little doubt of their reality. From the large negative residuals of the observations made near light minimum in 1918 and 1919, one might infer that the curve has differed more from its position of 1908 at some intermediate epoch than in 1921. It seems evident that the star will repay further observation.

WHITIN OBSERVATORY
WELLESLEY, MASSACHUSETTS
February 1922

PREPARATION OF ABSTRACTS

Every article in the *Astrophysical Journal*, however short, is to be preceded by an abstract which should be submitted by the author with the manuscript. In order that the abstract may aid the reader by furnishing an index and brief summary of the contents of the article, and may also be suitable for reprinting in an abstract journal, it should be of the type of those which have been appearing in the *Astrophysical Journal* since 1920. It is requested that the abstracts be prepared in accordance with the following:

DIRECTIONS AND RULES

1. *Notes.*—Read the article carefully, taking rough notes covering all the new information reported, keeping a specially sharp lookout for new incidental results and suggestions not directly related to the main subject.

2. *Subtitles.*—Write, first, a title describing the group of results forming the main contribution of the article, including all that belong together. If there are in addition results which do not come under that title, gather them into as few groups as possible and formulate a complete and precise title for each. For examples of such subtitles see the italicized parts of the abstracts for 1920.

The subtitles should together form a complete index of the new information; that is, they should include every measurement, observation, method, suggestion, and theory which is presented as new and of value in itself. They should be complete in themselves and independent of the main title of the article.

3. *Text.*—Write a paragraph summarizing the main group of results and including the corresponding subtitle either all at the beginning or with parts scattered through the text; and then do likewise for the other groups.

The text should summarize the author's conclusions and should transcribe all numerical results of general interest, including all that might be looked for in a table of astronomical and physical constants, with an indication of the accuracy of each. It should give all the information that anyone, not a specialist in the particular field involved, might care to have in his notebook.

Complete sentences should be used except in the case of subtitles. The abstract should be made as readable as the necessary brevity will permit. Italicize subtitles but no other words or phrases.

4. *Final checking.*—Re-read the article so as to check the abstract and correct any omissions and mistakes; read the subtitles by themselves to see that they properly index the information; and read the abstract to see whether it cannot be condensed and its English be improved.

These rules, and the abstracts which have appeared up to this time, have been prepared by Dr. Gordon S. Fulcher, recently of the National Research Council, now of Corning, New York. The editors desire formally to express their obligation and that of all readers of the *Journal* to Dr. Fulcher for the patience and skill which he has shown in revising, according to the technical standards, the abstracts sent in by authors, and in many cases in writing entirely new abstracts where the authors had neglected our request for abstracts. It will in future be absolutely impossible for Dr. Fulcher to continue this labor of love. Meantime, authors are notified that their articles cannot be accepted unless accompanied by adequate abstracts, and if articles are sent without abstracts, otherwise acceptable for publication, they will not be forwarded to the printer for composition until the abstracts are received.

A SELECTED LIST OF ONE HUNDRED SLIDES

Great Nebula in Andromeda

This "hundred list" is issued for the benefit of institutions or individuals desiring a small collection thoroughly representative of present astronomical science.

Send for our circular, "A Selected List of One Hundred Slides."

The price of the lantern slides is 75 cents each, except those which are colored (which are $1.50 for more than one color, or $1.10 for a single color); but for this special collection of one hundred slides, as here listed, the price is $62.50, a saving of approximately $12.00. Carriage is charged to the purchaser.

THE UNIVERSITY OF CHICAGO PRESS
CHICAGO - - - - - - - - - - ILLINOIS

Cambridge University Press

Series Spectra. Being a Supplementary Chapter (XV) to *Modern Electrical Theory.* By N. R. Campbell, Sc.D. Demy 8vo. Price on application. Cambridge Physical Series.

Physics: The Elements. By N. R. Campbell, Sc.D., F.Inst.P. Large royal 8vo. $12.50.

Problems of Cosmogony and Stellar Dynamics. Being an Essay to which the Adams Prize of the University of Cambridge for the year 1917 was adjudged. By J. H. Jeans, M.A., F.R.S. With 5 plates. Large royal 8vo. $7.00.

An Introductory Treatise on Dynamical Astronomy. By H. C. Plummer, M.A., Andrews Professor of Astronomy in the University of Dublin, and Royal Astronomer of Ireland. With 8 text-figures. Large royal 8vo. $6.00.

Space, Time, and Gravitation. An outline of the general Relativity Theory. By A. S. Eddington, M.A., M.Sc., F.R.S., Plumian Professor of Astronomy and Experimental Philosophy, Cambridge. With a frontispiece. Demy 8vo. $5.00.

The Absolute Relations of Time and Space. By Alfred A. Robb, Sc.D., D.Sc., Ph.D. Demy 8vo. Price on application.

FETTER LANE, LONDON, E.C. 4: C. F. CLAY, Manager

The Stone of the Sun and the First Chapter of the History of Mexico

By ENRIQUE JUAN PALACIOS

Translated by FREDERICK STARR

This famous stone in the Archaeological Museum of Mexico has been the cause of much idle speculation and the object of no little intelligent study.

In his translation Professor Starr says, "As a specimen of native American art it is of extraordinary interest; as a mass of symbols, in which the astronomical and chronometric knowledge of the ancient Mexicans is, in a sense, summarized, it is of the highest importance." Continuing he says that it had long been his purpose to print a study guide of the stone for the use of his students, but that the work of Palacios was so well done he decided to translate instead.

The monograph contains illustrations of several different portions of the stone.

Paper, 75 cents, postpaid 79 cents

THE UNIVERSITY OF CHICAGO PRESS
CHICAGO - - - - - - ILLINOIS

Stellar Spectra for Educational Purposes

¶ In response to requests, the Yerkes Observatory has prepared a set of 24 copies of stellar spectrograms obtained with the Bruce spectrograph attached to the 40-inch telescope. These are suitable for measurement in a laboratory course in astronomy, or for detailed study by the spectroscopist.

¶ The dispersion used is adapted to the character of the spectrum, fourteen having been made with one-prism, two with two prisms, and eight with three prisms. The plates (4×2 inches) cover the principal types of spectra from AO to MO, together with a spectrum of the Orion nebula, two of Nova Aquilae, and four giving different velocities of a suitable spectroscopic binary. A print is supplied, identifying the principal lines in the comparison spectrum, which was either that of titanium or of titanium and iron, and the data necessary for the reduction of the measures is given, together with the results obtained from the originals at the Yerkes Observatory. The spectra are reproduced in the negative form, by contact, and are intended to represent the originals faithfully.

¶ It is believed that this collection furnishes the material necessary for a year's work in stellar spectroscopy at institutions not having the requisite instrumental equipment, and will sufficiently acquaint the student with the classification of stellar spectra.

The price of the set is $12.00, plus postage

THE UNIVERSITY OF CHICAGO PRESS
CHICAGO - - - - - - - - ILLINOIS

THE ORIGIN OF THE EARTH

By THOMAS C. CHAMBERLIN
Professor Emeritus in the Department of Geology
The University of Chicago

One of "The University of Chicago Science Series"

FROM THE PREFACE

"In telling the story of this search for the mode by which the earth came into being, we have let the incidents that led the inquiry on from one stage to another fall in with the steps of the inquiry itself. It is in keeping with the purposes of this series of booklets that the motives which set researches going should have their place with the quests that arose from them. . . . . The final story of the birth of the earth will come only after a time, when the vestiges of creation have been more keenly discerned and more faithfully rendered than is possible now."

Cloth, $1.75, postpaid $1.85

THE UNIVERSITY OF CHICAGO PRESS
CHICAGO - - - - - - - ILLINOIS

The BOOK *of* LAKE GENEVA

By DR. PAUL B. JENKINS

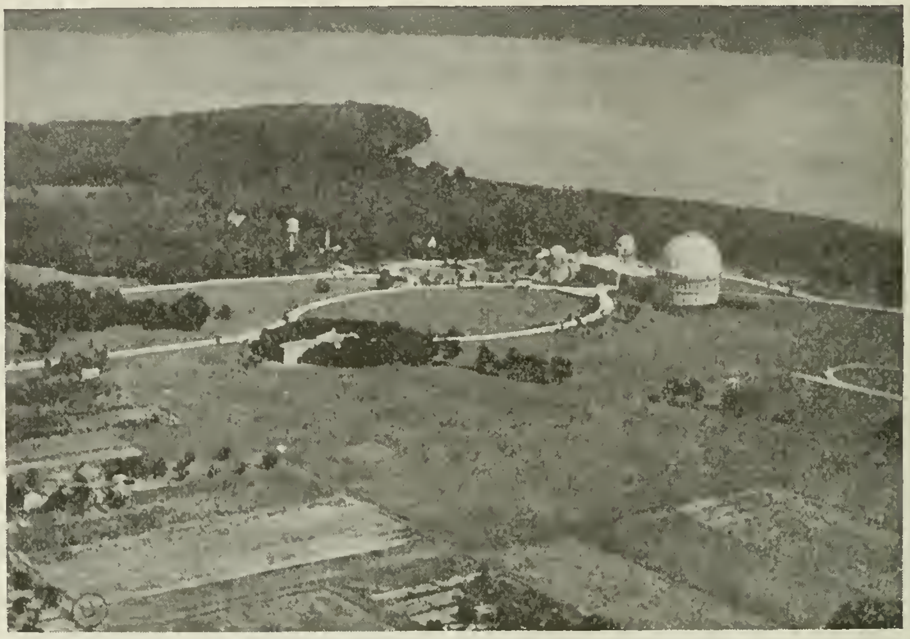

J. W. MCCARTNEY

Yerkes Observatory of the University of Chicago

¶ If you have a home at Lake Geneva, Wisconsin, or have ever visited there you will want this handsome volume. It is a swiftly-moving story of the history of the lake, a nature-guide for the tourists who visit it, and a splendidly illustrated gift book, describing the homes and institutions on its shores. Your dealer has it on sale or you may purchase direct from us.

$4.00 net, postpaid $4.12

Published for the Chicago Historical Society by

THE UNIVERSITY OF CHICAGO PRESS

THE
ASTROPHYSICAL JOURNAL
AN INTERNATIONAL REVIEW OF SPECTROSCOPY
AND ASTRONOMICAL PHYSICS

VOLUME LVI DECEMBER 1922 NUMBER 5

ASTRONOMICAL PHOTOGRAPHIC PHOTOMETRY AND THE PURKINJE EFFECT. II[1]

By F. E. ROSS

ABSTRACT

Photographic photometry of stars.—The four methods in use are outlined and the principles underlying each are pointed out. The *turbidity method* depends on the increase of size of image with intensity. The Greenwich formula connecting the diameter of the image with the star's magnitude is shown to fail for images less than 50 μ in diameter and a new formula which holds for all cases is suggested: $\sqrt{(d+h)} = a+b \log I$, where a, b, and h are constants. On the assumption that the growth of the image is due to diffuse scattering and reflection of the light, formulae for the intensity of this light at any distance from the edge are deduced and sections of images are given which show both theoretical and actual equiluminous surfaces (Fig. 1, and Pl. XII). However, it is found by experiment that the rate of growth or turbidity (Δ) is not constant but increases with the intensity, for instance from 9 to 12 μ when the intensity is multiplied three hundred fold. This effect is of importance in accurate measurements, since if it is not allowed for, deduced relative magnitudes will vary with the time of exposure. Data are also given showing marked variations of turbidity with the kind of plate (Table IV) and with the telescope used, but if the optical system is well corrected the optical turbidity should be negligible. The probable error of this method is about $0\overset{\mathrm{M}}{.}1$ for very sharp images but may be reduced considerably by using plates of greater turbidity and with small inherent irregularity. In the *densitometric method*, which involves the measurement of out-of-focus images, the probable error is small except that due to inherent plate irregularities, so the more these are reduced the greater will be the relative accuracy of this method. The variation of turbidity with wave-length, the *photographic Purkinje effect*, is of great importance. The results obtained are reviewed, but because of the complexity of the effect no general conclusions can as yet be given. An explanation is suggested for Abney's discovery that for some plates the least gradation is for the wave-length of maximum sensitivity.

Transmission of some photographic plates to white, blue, green, and red light is given (Table I). While Block and Renwick have found that the absorption is not exponential, for very thin films the law (Bouguer's) may hold, at least approximately.

Photographic turbidity for spectrum lines is found to be the same as for circular images of the same width.

---

[1] Communication No. 150 from the Research Laboratory of the Eastman Kodak Company.

There are in use at present four methods of astronomical photographic photometry. These are, in historical sequence:

A. Measurement of diameters of stellar images.

B. Measurement of densities or degree of blackness of out-of-focus images.

C. Eye comparisons of blackness and size of image with a sequence of images of known light value.

D. Measurement of total obstructance of the photographic image to radiation, as in the thermoelectric method of Stetson.

The usefulness of any photometric method depends primarily upon its sensitivity, which mathematically can be defined as the ratio of effect to stimulus. In the case of method A, the sensitivity is the ratio of the increase in diameter of a focal image to the logarithm of the exposure, called "astrogamma." In method B, it is the ratio of the increase in density to the logarithm of the exposure, usually called "gamma" or gradation. In D it is the ratio of the increase in the mass of exposed and developed grains in a focal image to the logarithm of the exposure. C is essentially the same as D, but is limited in practice to faint images. Method A depends for its efficacy on the sidewise scatter of light in the emulsion. Method B depends largely on the depth penetration of the light. Methods C and D depend upon a combination or addition of A and B, and accordingly make use of the *total* action of the light, which A or B do not. Their sensitivity is therefore higher and they must moreover be considered more logical methods than A or B.

Distribution of light in the emulsion.—The increase in density of a photographic image and the increase in size are phenomena partly of common origin. The increase in size of an image in the case of a perfectly sharp image is due to multiple reflection, refraction, and diffraction of the image-forming light by the grains of silver halide, which, in thickly packed layers, constitute the emulsion. The light is thus deflected from its original direction perpendicular to the plate in a succession of steps until its direction of flow, measured by normals to the equiluminous surfaces, lies in the plane of the emulsion perpendicular to the geometrical edge of the image. The equiluminous surfaces *A* . . . . *N* (Fig. 1) which lie under the image itself are parallel to the surface of the emulsion, and can obviously be joined or linked with the equiluminous surfaces which lie off the edge. The photometric characteristics of the density of an image, upon which method B is based, are determined, in part at least, by the surfaces *A* . . . . *N*, while method A is based upon the characteristics of the surfaces *A* . . . . *R*.

There are a variety of factors which govern the penetration of light in an emulsion. Among these may be mentioned the size, shape, packing, orientation, and optical properties of the silver halide grain, optical properties of the embedding gelatine, wavelength and composition of the light, and thickness of the emulsion layer. Concerning the specific action of each of these factors, little or nothing is known, although the subject is of great importance from many points of view.

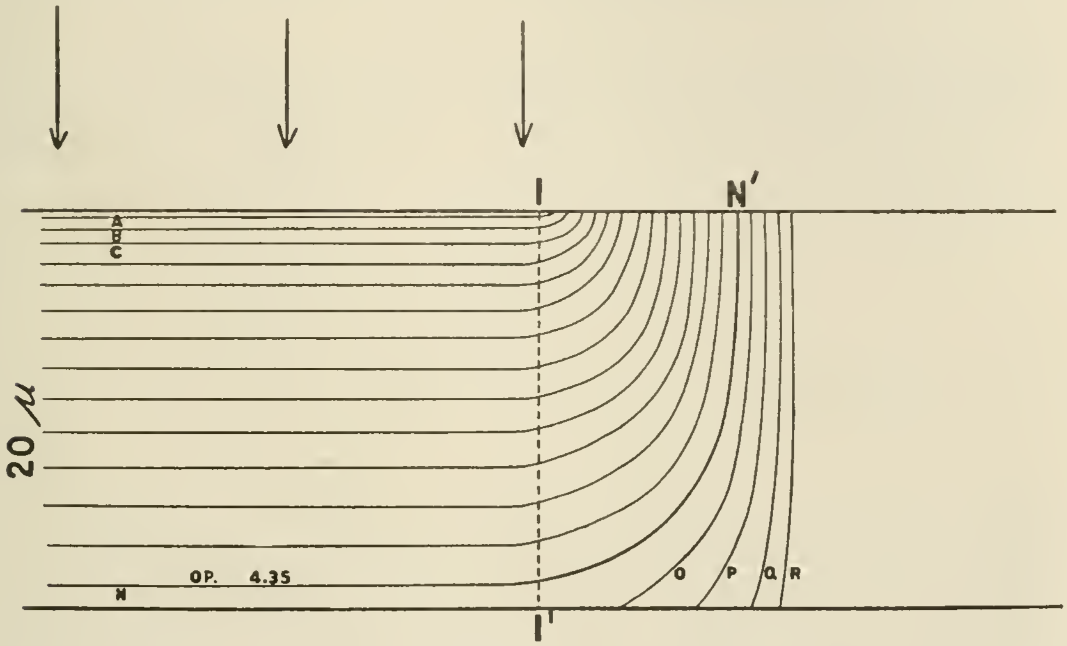

FIG. 1.—Equiluminous surfaces at edge of a sharp image

The silver halide grains which are contained in the high speed emulsion are in great measure in the form of plates or tablets which must be oriented nearly parallel to the surface of the emulsion.[1] Such emulsion would accordingly be expected to show very little side scatter and a high direct or specular transmission. If there were no reflections or diffraction in the passage of the light through the emulsion, the transmission would follow Bouguer's law, which states that equal thicknesses absorb equal percentages of the incident light. The subject has been investigated theoretically and experimentally by Bloch and Renwick[1] who found considerable deviation from Bouguer's law. Calling D the effective density where $D = \log_{10}$ opacity, and putting W = weight of silver bromide in mg per cm^2 they find for a typical fast emulsion:

---

[1] L. Silberstein, "The Orientation of the Grains in a Dried Photographic Emulsion," *Jour. of the Optical Society of America*, 2, 171, 1921, and 3, 363, 1921.

$$\left.\begin{array}{ll}\text{White light illumination:} & D=0.66\ W^{0.64} \\ \text{Violet light illumination:} & D=1.123\ W^{0.82}\end{array}\right\} . \qquad (1)$$

With Bouguer's law holding, the exponent of W should be unity. A strong color effect is shown, as was to be expected.

For the average fast emulsion $W=1$ very nearly. Accordingly the corresponding opacities from (1) are:

	Opacity	Transmission
		Per Cent
White light	4.58	21.8
Violet light	13.3	7.5

These values show that the penetration of light in an emulsion is extremely sensitive to wave-length variations. Abney found from photographic tests that an ordinary Kodak film transmitted 22 per cent of the incident light agreeing with the results from Bloch and Renwick for white light.

Values of the transmission of various types of plates have been determined photographically in this laboratory by E. Huse for the three primary colors and for white, with results shown in Table I. The receiving medium in all cases was a Wratten and Wainwright panchromatic plate.

The blue, green, and red in Table I refer to the transmission of Wratten and Wainwright filters C, B, and A respectively. White refers to the acetylene flame screened with Wratten and Wainwright filter No. 79.

---

[1] "The Opacity of Diffusing Media," *Photographic Journal*, 40, 49, 1916.

Data on the optical behavior of emulsion film are given by Nutting.[1] The distribution curves of reflected and transmitted light, drawn from his data, are shown in Figure 2. According to these results approximately 57 per cent of the incident light is reflected and 35 per cent transmitted.

TABLE I

TRANSMISSIONS

Plate	White	Blue	Green	Red
	Per Cent			
Seed 30	22	8	39	41
Seed 23	18	8	32	39
Seed process	34	11	40	36
Seed lantern	41	25	43	44
Std. orthonon	13	....	26	30
W. and W. panchromatic	10	5	12	23

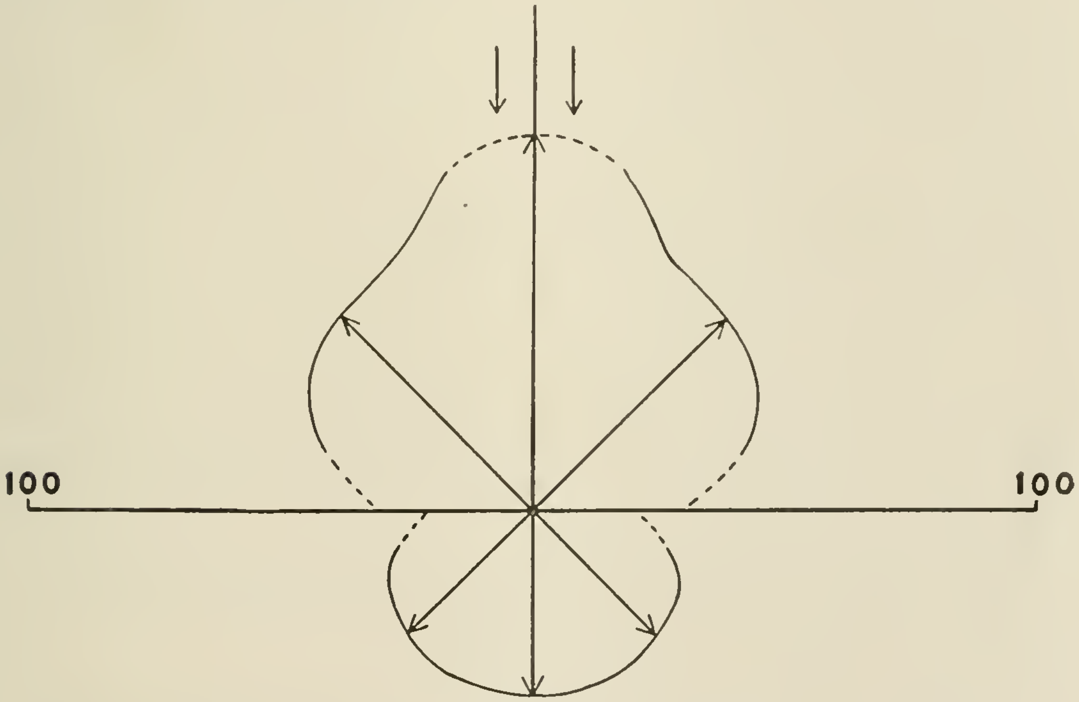

FIG. 2.—Distribution curves (reflection and transmission) of a photographic emulsion, Nutting's data, from visual measurement.

The equiluminous surfaces *A* . . . . *N* (Fig. 1) are drawn to scale from the first of equation (1). The illumination at each surface is 90 per cent of that at the preceding surface, so that each layer absorbs 10 per cent of the light incident upon it. It is seen that the effective densities decrease downward in the film, it requiring a progressively greater thickness to produce the 10 per cent drop in illumination. Assuming the total thickness of the emulsion 20 μ, it can be calculated from equation (1) that 38 per cent of the total light absorbed is absorbed in a layer 2 μ thick adjoining the surface, while only 3 per cent is absorbed in a similar layer at the bottom. Assuming Bouguer's law to be the correct one, these numbers become 18 and 5 per cent respectively.

---

[1] "The Optical Properties of Diffusing Media," *Transactions of the Illuminating Engineers Society*, **10**, 353, 1915.

It remains to trace the course of the equiluminous surfaces upon entering the shadow adjacent to the image, where they must rise to the surface. Their course will evidently depend upon the degree of sharpness of the image under consideration. The nearly ideal case of an exceedingly sharp image such as is produced by contact printing will be chosen. It is a simple matter to calculate the light-intensity at any point in the shadow from the rate of spreading of the image, assuming Bouguer's law to hold in this region, which is approximately true, as will be shown later. Thus it is found, assuming light of wave-length 4600 A, that a 10 per cent drop in illumination occurs uniformly in a horizontal distance of 0.71 μ. Scaling off this distance in succession from the point I toward N in Figure 1, the exit points for the complete series of equiluminous surfaces $A \ldots . N$ are obtained. The intermediate portions of the curves lying to the right of II' can be only roughly sketched. To obtain their true form would require an intricate mathematical investigation which would be without profit, on account of the many parameters of unknown relative values.

The formula proposed by Tugman[1] for the light-intensity in the shadow adjacent to an image, namely

$$I=I_0 e^{-K(x+y)} ,$$

where x is the distance from the edge and y the distance below the surface, obviously does not hold. A much more complicated relation is necessary. The rate of diminution of intensity downward appears to follow a different law than the law of sidewise drop in intensity. From Figure 1 it is seen that in the ideal case chosen

---

[1] "Resolving Power of Plates," *Astrophysical Journal*, 42, 341, 1915.

PLATE XII

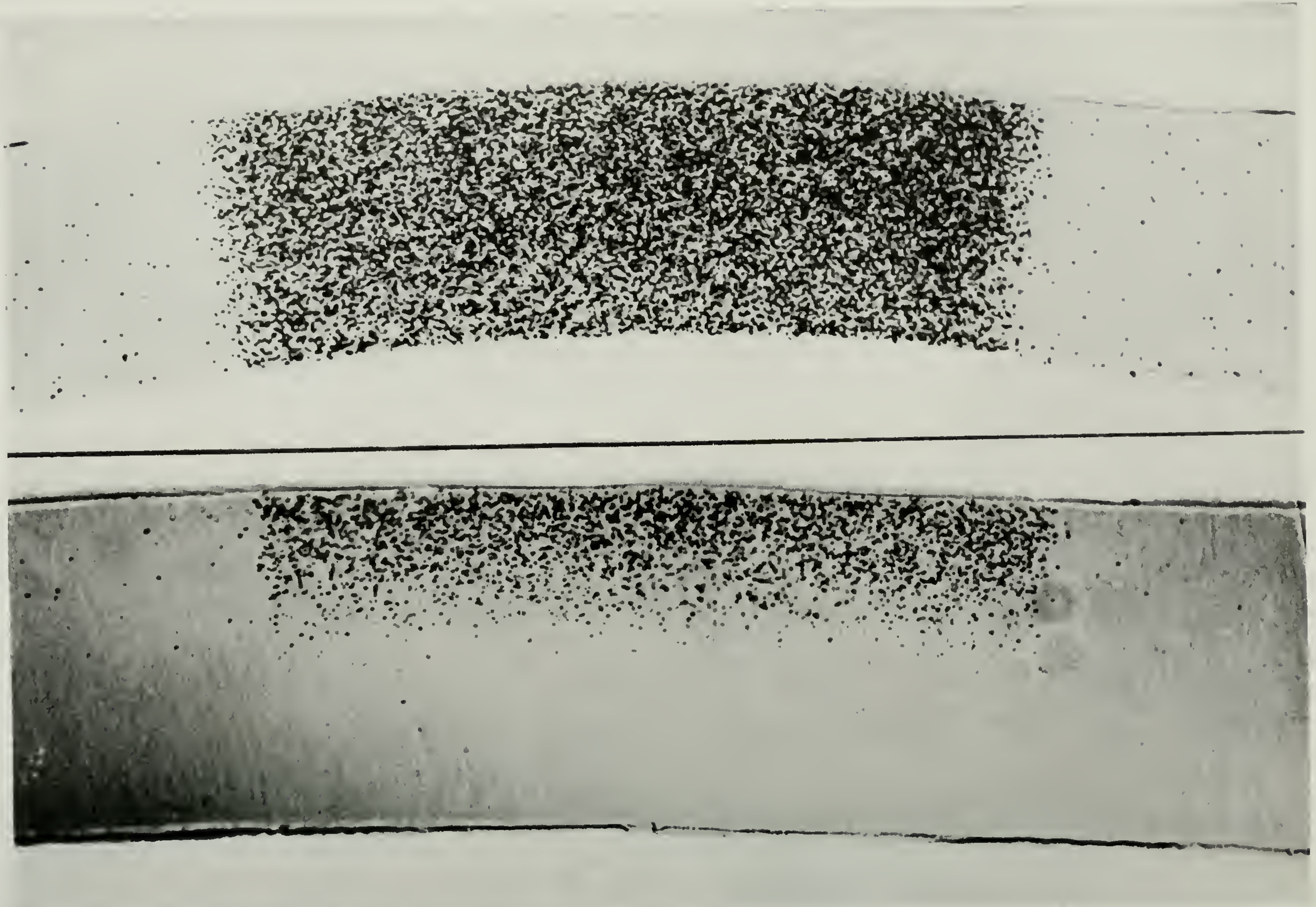

Magnified Sections of a Sharp Slit Image

Upper, fully exposed; lower, light exposure the equiluminous surfaces which lie off the edge of the image are much more closely packed than those lying under the image. This can be explained as a color absorption effect. The light which is traveling parallel to the surface of the emulsion must, on account of its being composed largely of diffracted light, be of shorter average wave-length than the light passing normally through the emulsion. The opacity in this direction will accordingly be higher, resulting in a compression of the series of equiluminous surfaces. In the case of images formed by optical systems, the degree of compression will vary widely with the sharpness or perfection of the image. The horizontal system under the image will be independent of all conditions except composition of the imaging light and its converging angle. For parallel light the opacity should be higher and the penetration less than for light impinging in a wide cone, corresponding to the condition of diffuse illumination. It will be observed that the equiluminous surfaces are shown rising to the surface in a nearly vertical direction. That they actually are of this form in the case of very sharp images seems to be proved by the photomicrograms of an image in which a small amount of spreading has taken place (Pl. XII). The image appears to have expanded as much in the lower layers as in the upper. The section was made while the strips were swollen (with dilute alcohol), the vertical scale being approximately ten times the horizontal. Other cases have been obtained in which the inclination is of intermediate types, corresponding to images of an inferior degree of sharpness. In general it can be stated that the form and orientation of the surfaces of equal illumination are the resultant of the surface distribution due to the optical system and the emulsion distribution due to the spreading of the image-forming light. The problem is thus an exceedingly complicated one. Further difficulties are introduced if the anomalies of development taking place at the edge of an image are considered.

The principles underlying the two methods of astronomical photometry will now be considered. In the densitometric method photometric measurement is limited by the amount of silver which can be deposited in the film perpendicular to the surface, which depends upon penetration of the light and of the developer. When a long working-range of moderate sensitivity is desired, it is of advantage to have the specific opacity of the emulsion as high as possible and considerable dispersion in grain sensitivity. If, on the other hand, high sensitivity in photometric measurement is desired regardless of a short working-scale, an emulsion of low specific opacity of uniform sensitivity, but rich in silver, is preferable. In the second method of astronomical photometry, in which the increase in size of a small image is made use of, obviously a much wider range of intensities can be measured. The sensitivity of both methods is subject to control in a variety of ways; that of the densitometric method depends upon gamma or contrast, upon developer and development time, and upon the wave-length of light used; that of the size-of-image method depends upon the emulsion, the wave-length of light, but not to any extent upon developer or development time. An additional important factor in determining the sensitivity of the second method is the optical sharpness of the image, which in the case of astronomical observations depends to a great extent upon the steadiness of the air. Perfectly steady air is a detriment to accurate photometric work of this kind, on account of the sharp images, which increase in size at such a slow rate with respect to increase in intensity that a correspondingly low sensitivity is produced. Accordingly a telescope of long focus is preferable in this case to one of short focus, on account of its greater magnification of atmospheric disturbances and, in addition, on account of its optical aberrations, which in general are proportional to focal length (see p. 363).

The writer has reviewed in another place the formulae connecting photographic density and exposure.[1] Astronomers rightly are generally interested in such formulae only to the extent that photographic exposure E involves the stellar magnitude M and exposure time t. This relationship, undoubtedly involving the fundamental law of photographic action, has been given three forms: (1) the reciprocity law; (2) Schwarzschild's law; (3) Kron's law. In order to show that these laws are fundamentally at variance, it is only necessary to point out that according to the reciprocity law, the photographic efficiency is *constant* for all light-intensities.

---

[1] "On the Relation between Photographic Density, Light-Intensity, and Exposure Time," *Journal of the Optical Society of America*, 4, 255, 1920.

In the case of Schwarzschild's law, the efficiency *increases uniformly* as the light-intensity increases, while in the case of the Kron law, there is an *optimal intensity*, or a light-intensity at which the energy applied has greater efficiency than when applied at any other intensity, greater or smaller. It is thus seen how radically different the three laws are, laws which undoubtedly have root in important physical or chemical phenomena of which we are at present in ignorance. Since they all have been found to be of undoubted applicability in numerous cases, it must be concluded that special circumstances alter the photographic action, throwing it to one or the other of the three *modi operandi*, in a manner which we are unable at the present time to conceive.

The mathematical relation between the diameter of photographic star images and stellar magnitude and exposure time appears to have attracted the attention of astronomers even before the introduction of the dry plate. The earliest formula by Bond in 1857 is:

$$d^2=Q+Pt. \qquad (2)$$

To see how closely this formula fits the modern dry plate, some measures by the writer are plotted in Figure 3, according to this formula. It is seen that the linear relation is far from being realized except for a very short range of 1 to 4 (1.5 magnitudes). Bond notes that the sensitiveness of his plate increased toward the end of the exposure, a fact which appears capable of explaining his comparatively unique formula.

About 1890 a number of formulae applicable to the dry plate were proposed by Scheiner, Charlier, and others, which involved roots of the intensity and exposure time. Among others, the square and fourth root were adopted. As in the case of the Bond formula, these formulae are compared with the same data as in Figure 3. In addition formulae involving the sixth and eighth roots are shown on the same diagram (Fig. 4). It will be noticed that as the root increases the relation becomes more nearly linear, exception being made of the smaller measured diameters. If the lenses used were of poor quality and other conditions were such that it was not possible to obtain small star images such as are obtained at the present day, it is not surprising that equations of this type were obtained. In the modern development of the subject, working along more correct lines, investigators have introduced logarithmic functions of time and intensity in their equations, instead of those quantities themselves and their roots. This procedure is based on the principle that equal fractional or percentage variations in exposure produce

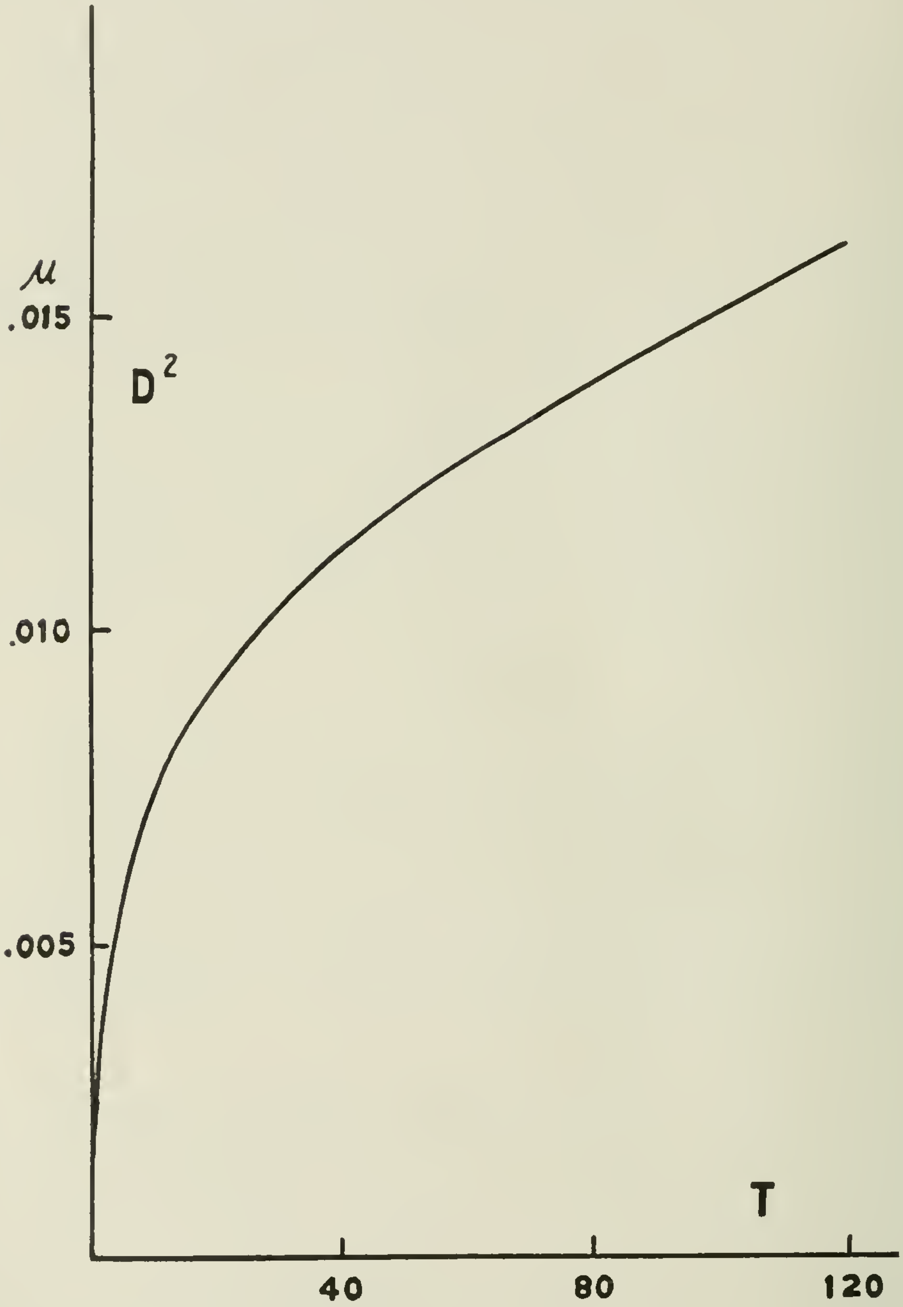

FIG. 3.—Comparison of Bond's formula for diameter of images with measures on modern dry plate.

equal effects on the photographic plate, at least in its useful exposure region. Scheiner's formula,

$$d = a + b \log I, \tag{3}$$

is of this type. It has been shown to follow mathematically if the distribution of light at the edge of an image is of the simple form of Bouguer's law,

$$I = I_0^{-\kappa x}. \tag{4}$$

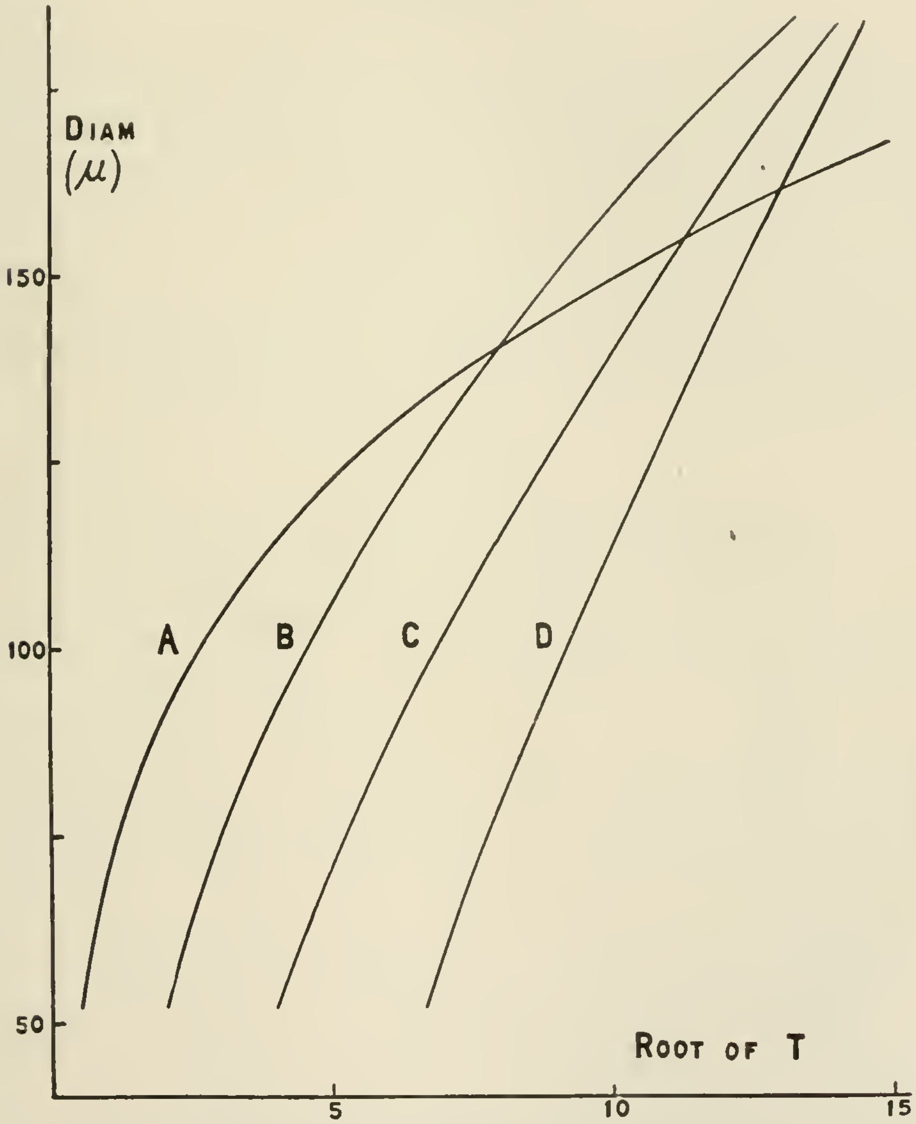

FIG. 4.—Diameters of images plotted against *A*, square; *B*, fourth; *C*, sixth; and *D*, eighth root of *t*.

This form of the intensity function has been adopted in deriving the series of equiluminous surfaces adjacent to the edge of an image (Fig. 1). It was soon found, however, that for the higher light-intensities and longer exposures this simple formula no longer applied. It was superseded by the Greenwich formula which is equivalent to

$$\sqrt{d}=a+b \log I. \tag{5}$$

The relation between b and κ is

$$\kappa=\frac{2}{\text{mod.}}\cdot\frac{1}{b}.$$

This formula appears to satisfy the demands of most photometric work. So far as the writer is aware no question has been raised as to its applicability to very small star images such as are frequently obtained under the best conditions with well-corrected telescopes of not too great focal length.

In Table II the series of measured diameters adopted in the previous comparisons is used. The error of the Greenwich formula for diameters below 50 μ is seen to be very pronounced.

TABLE II

GREENWICH FORMULA COMPARED WITH OBSERVATION

Exposure Time	Measured Diameter	Diameter Greenwich Formula	Error of Formula
	μ	μ	μ
1ˢ0	19	30	+11
1.9	29	36	+ 7
3.8	39	43	+ 4
7.5	47	51	+ 4
15.0	57	58	+ 1
30.0	68	67	− 1
60.0	77	77	0
120.0	86	86	0
240.0	97	97	0
480.0	109	108	− 1
960.0	120	120	0
1920.0	130	131	+ 1

The diameters in Table II are plotted in Figure 5 according to the Scheiner equation (*A*) and the Greenwich equation (*B*). The Scheiner equation fits the observations, except in the case of the larger diameters. On the other hand the Greenwich equation is seen to be very seriously in error for the smaller diameters. It is not surprising that this error is not generally in evidence, since the images which have been usually obtained in photometric work have not been sufficiently small, owing either to length of focus, poor optical corrections, or bad seeing.

The modification which is necessary in the Greenwich formula to make it fit the observations is quite obvious. It is only necessary to add a constant h to the measured diameter, the equation thus becoming

$$\sqrt{d+h}=a+b\log I\,. \tag{6}$$

Curves C, D, and E (Fig. 5) show the result for $h=50$, 100, and 150 respectively. In the last case, for $h=150$, the representation is entirely satisfactory. The correct value of h in any given case may be sufficiently well determined in a few minutes by graphical methods.

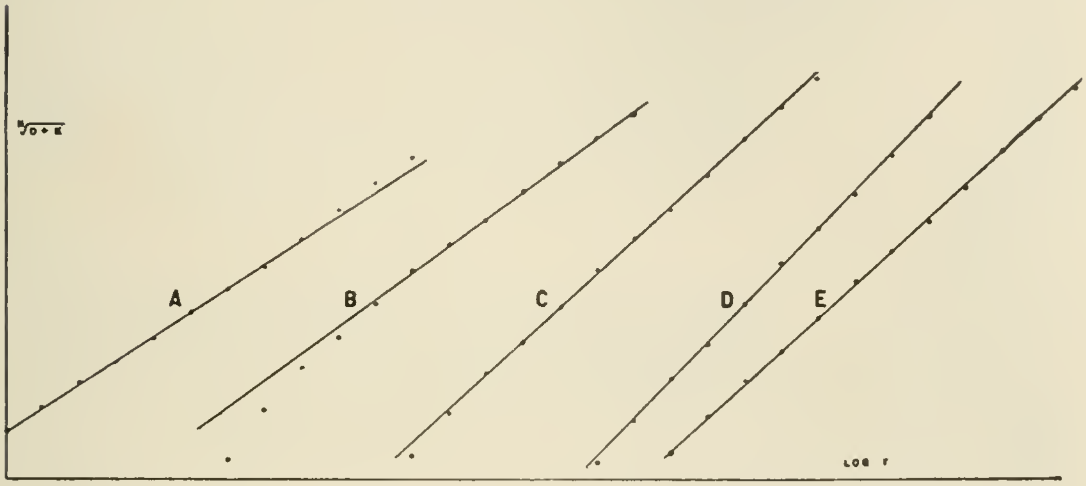

FIG. 5.—Diameters plotted against log t according to the Scheiner (A), Greenwich (B), and new formula (C, D, E).

The problem of image growth will now be treated mathematically, in so far as this is practicable. It was formerly supposed that the growth of images was a chemical phenomenon, grains of silver bromide being supposed to develop by infection from neighboring grains. While there may be a certain measure of truth in this supposition, in so far as secondary actions are concerned, e.g., development of clumps of grains as a unit, it is not necessary to resort to hypotheses of this nature to explain the phenomenon, for the evidence shows that there is sufficient scattered light, in the region immediately surrounding an image, to account for its spread or increase in size. It is quite impossible to deduce mathematically the curve of light distribution in a direct manner, on account of the number of separate factors entering, very few of which can be expressed in any kind of mathematical form. Attempts at solving the problem must therefore be restricted to the other end, working backward from photographic effect to light distribution, ignoring secondary development disturbances.

Let the light-intensity over the uniformly illuminated central stellar disk be denoted by I_0; the diameter of the disk by g, which depends on the optical system and upon the seeing, and in nowise upon the photographic plate. Let the light-intensity at a distance x from the edge of the uniformly illuminated central disk be denoted by I. Assuming Scheiner's equation of image growth, it has been shown that the light distribution is given by

$$I=I_0e^{-\kappa x}\,. \tag{7}$$

Assuming the Greenwich equation, the equation for light distribution can be shown to reduce to

$$I=I_0e^{-\kappa\left[\sqrt{x+g/2}-\sqrt{g/2}\right]}\,. \tag{8}$$

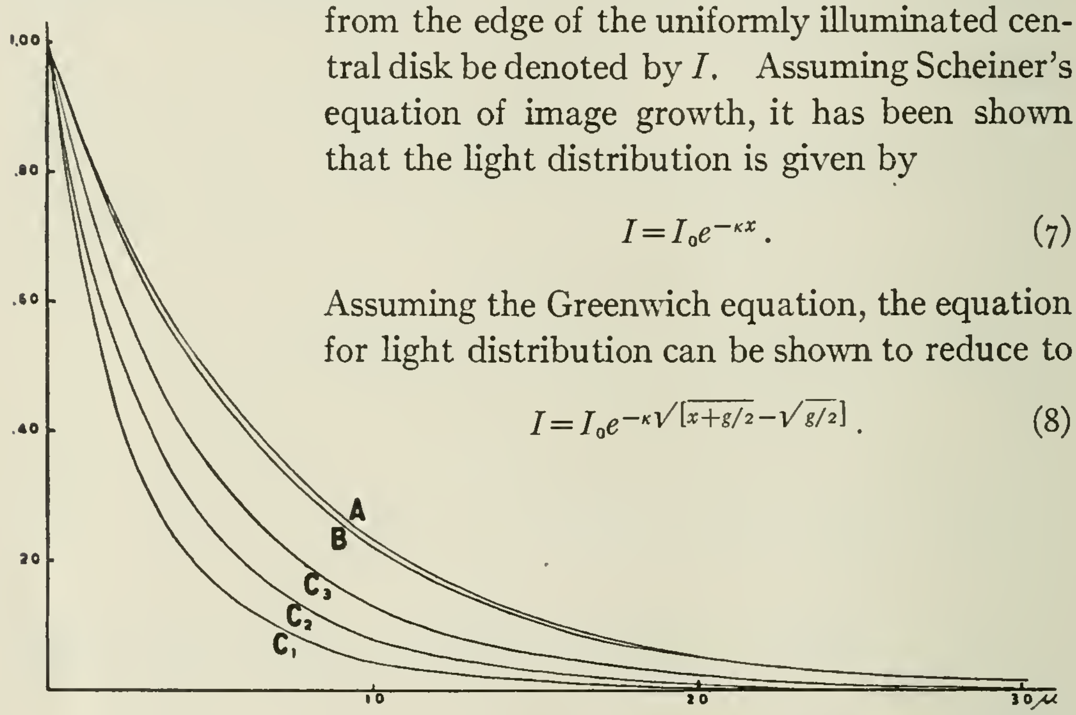

Fig. 6.—Light intensities near edge of an image: Scheiner formula, *A;* new formula, *B;* Greenwich formula, C_1, C_2, and C_3, for increasing values of g.

The new equation (6) leads to the distribution

$$I=I_0e^{-\kappa\left[\sqrt{x+\frac{g+h}{2}}-\sqrt{\frac{g+h}{2}}\right]}\,. \tag{9}$$

The curves of light distribution for the three cases of the Scheiner, Greenwich, and revised Greenwich formulae, computed from the foregoing equations, are given in Figures 6 and 7, using constants determined from Figure 5. Figure 6 is for the region within 30 μ of the edge of the image; Figure 7 for the region 50 μ to 100 μ. The curves show the characteristic differences known to exist. For example, the Scheiner and the new formula agree near the edge of the image, as was to be expected, but diverge widely at greater distances. The Greenwich formula appears to stand alone at all distances, but in the region of greater distances this divergence is only apparent, for if in Figure 8 the ordinates of the Greenwich formula are multiplied by 5.9 the two curves are made to coincide.

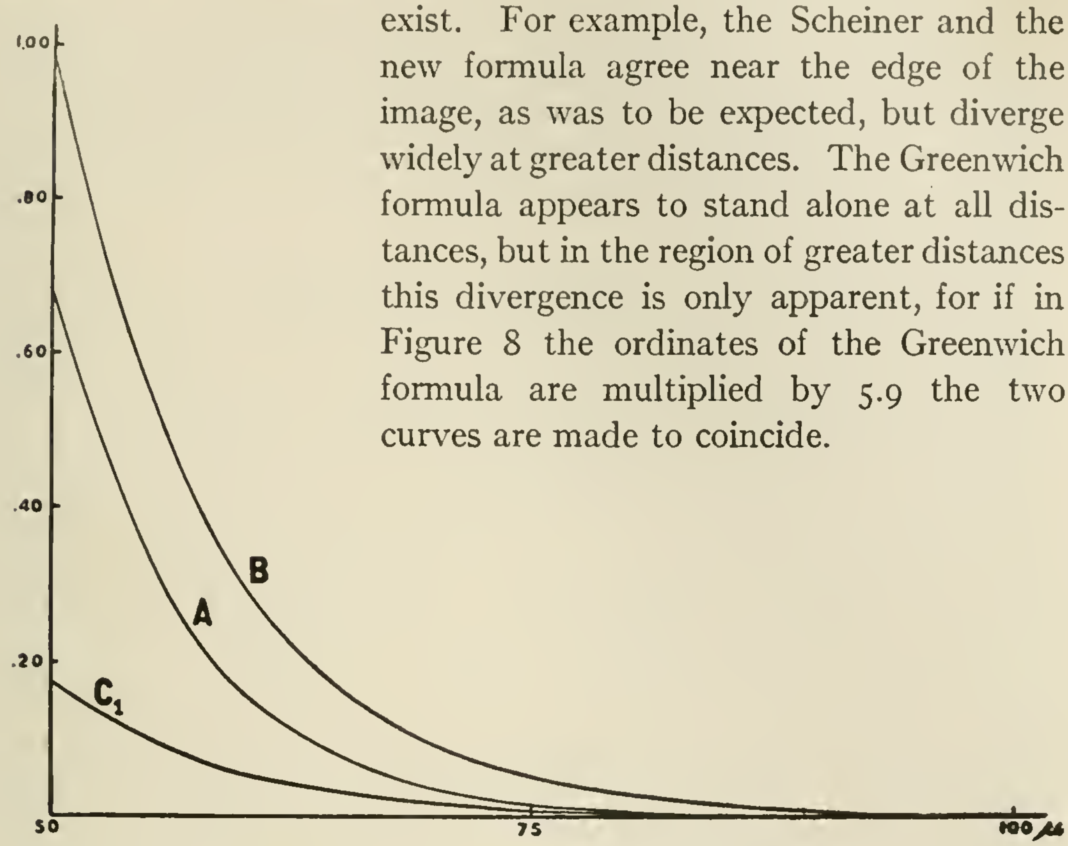

FIG. 7.—Relative light intensities, 50–100 μ from edge of image. Continuation of Figure 6.

Cause of the deviation from the Scheiner equation.—Some experiments have been made with the object of throwing light on the increase in the rate of growth of images with increased exposure. The data obtained by Bloch and Renwick (p. 348) on the opacity of emulsions are suggestive and useful in this connection. Using their equation for white light,

$$D = 0.66\, W^{0.64}\,,$$

where D is the optical density of a film and W the mass of silver bromide. Calling x the distance below the surface,

$$W = a \cdot x,$$

where a is a constant. Also

$$D = \log \frac{I_0}{I}\,,$$

whence

$$I = I_0 e^{-\kappa x^{0.64}} . \tag{10}$$

This equation, which purports to give the distribution of light downward in an emulsion, is quite similar to the sideways light distribution (eq. 8) which was derived from the Greenwich formula, the only essential difference being in the exponent of x, which is 0.64 instead of 0.50.

Consider two round images of equal intensity on the photographic plate, with diameters respectively of the order of .05 mm and 1 mm, for example. If the physical constants of the emulsion are known, the light distribution is mathematically determinable, but, as pointed out above, the solution has never been attempted. Nevertheless, it is easy to see in a general way that the light distribution should not be the same for the two images, an equality which would be required by Bouguer's law. The falling off in intensity in the case of the larger image should be less rapid, on account of reinforcing illumination filtering out from the central region of the image. This reinforcement must be less effective in the case of the smaller image. The same reasoning applies to a certain extent in the case of two true star images formed by stars very unequal in magnitude, and is materially strengthened when expansion of the disks caused by atmospheric unsteadiness is taken into account. Accordingly, with increase in intensity, an increase in the rate of growth, such as is tacitly assumed in the Greenwich and the new equation, is to be expected. But the fact that the Greenwich equation is greatly in error for the small diameters must be remembered. It should be noted that Bloch and Renwick's equation (p. 348) was not based on data from extremely thin emulsions, so there is no experimental evidence that it actually holds for the top layers of an emulsion. Its applicability as embodied in the Greenwich equation, to the limited region immediately bordering the true edge of an image, is accordingly open to question.

Figure 8 shows the intensity of light distribution downward in an emulsion, computed from Bloch and Renwick's equation. W is taken as unity, which is a close approximation, and the thickness of the emulsion is taken equal to 20 μ. The distribution curve for

Bouguer's law is also shown for comparison. Assuming each layer of grains equal to 2 μ in depth, it is seen that the absorption in the first layer of grains at the surface is twice as much from Bloch and Renwick's equation as it is from Bouguer's. The same steep drop in vertical transmission is shown by Bloch and Renwick's curves as is shown by the sideways transmission curve computed from the Greenwich equation (Fig. 6). Reasoning from analogy, it is probable that in the first few layers of an emulsion the transmission downward is more nearly in accord with Bouguer than with Bloch and Renwick.

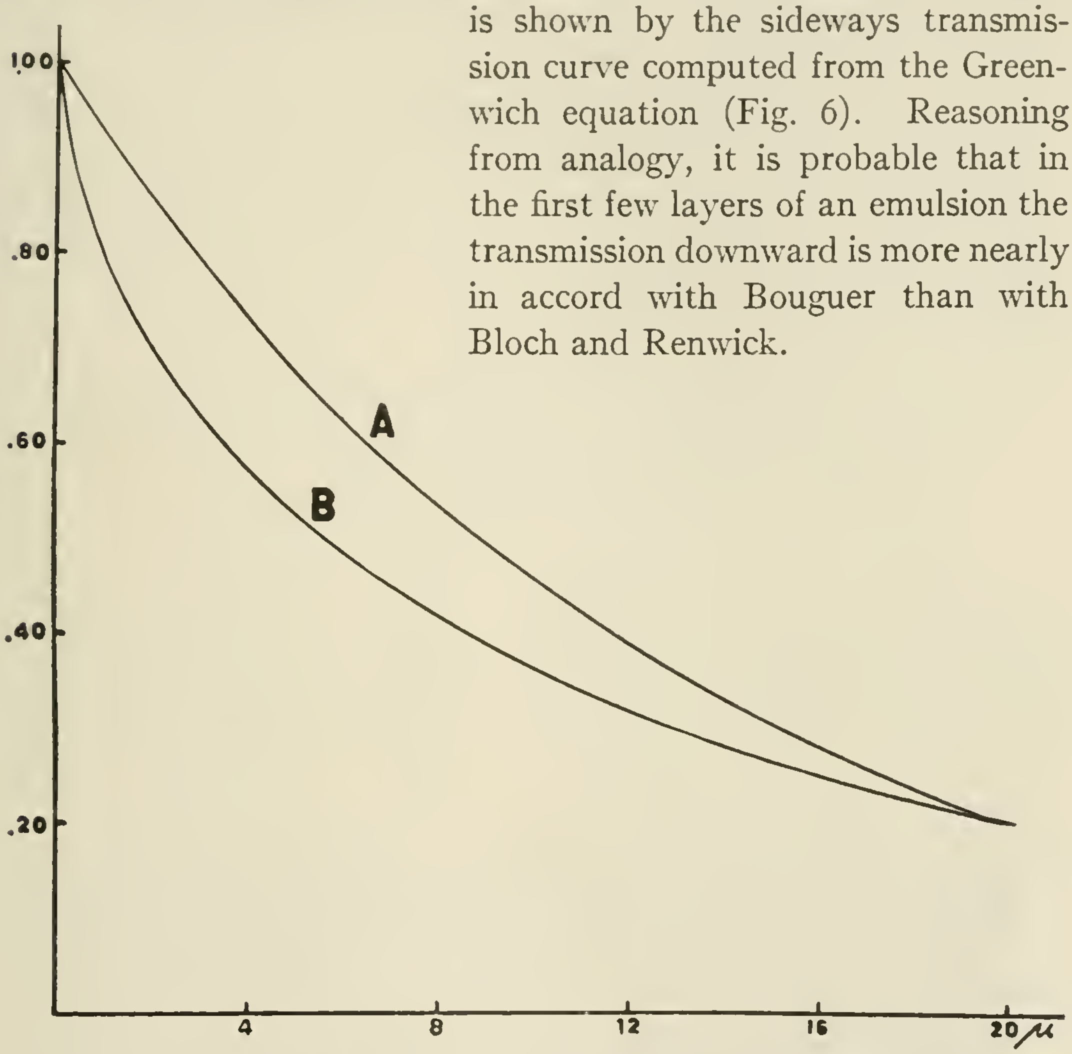

FIG. 8.—Light intensity at various depths in an emulsion according to Bouguer's (*A*) and Bloch and Renwick's (*B*) formulae.

To obtain data with respect to the dependence of Δ, the rate of growth, on the size of the unexpanded or optical image, a series of measurements was made, the results of which are contained in Table III. A test object having a series of nine circular apertures varying in diameter from 0.16 mm to 2.3 mm was photographed in the precision reducing camera, exposure times ranging from

1 second to 32 minutes, from which Δ was computed for each aperture. The plate used was Seed 23, quality of light, white.

In the case of the images of the five smallest apertures, no departure from Scheiner's law was apparent over an exposure range of 1 second to 32 minutes, or 1 to 1920. For the largest aperture, No. 9, the strictly linear relation (Scheiner's) held over a range of 1 second to 8 minutes or 1 to 480. Using the same test object and reducing the intensity of the light fifty times diminished Δ about 10 per cent for the larger holes, but had no effect on Δ for the smaller apertures. In addition it was found that for this case of diminished light-intensity there was neither increase nor decrease of the range over which the linear relation holds.

TABLE III

VARIATION OF Δ WITH SIZE OF IMAGE

Aperture	Diameter of Image (Geometrical)	Diameter of Image (Lightest Exposure)	Δ
	mm	mm	μ
1	.004	.010	9.0
2	.006	.012	9.2
3	.008	.015	9.5
4	.011	.018	9.7
5	.014	.020	9.9
6	.017	.031	10.8
7	.025	.046	11.2
8	.034	.058	11.5
9	.057	.085	11.9

In obtaining turbidity values for a very intense diffraction image, the diffusing screen between the light source and the test object was removed, and the light adjusted in position until it was in line with aperture No. 1 and the center of the lens. Under these conditions an exposure of 1 second gave an image of diameter 64 μ, which is as large as that previously obtained with a 6-minute exposure through the same aperture. From this it can be calculated that the increase in intensity is 300 times (6.2 magnitudes). The value of Δ was found to have increased from 9.0 to 12.5, which is approximately the value for aperture No. 9. However, the shape of the curve was quite different, the linear relation between diameter and exposure time holding only over the very limited range from 1^s to 30^s. Since in this experiment there has been no change in the size of the geometrical image, nor in the character of the aberration or diffraction pattern, the conditions are analogous to the practical astronomical case of photographing a field of stars of varying brightnesses. The conclusion is that under these circumstances the *deduced relative magnitudes are dependent on the exposure time*, Δ being a function of the star's magnitude. This phenomenon is similar to the Purkinje or color-gradation change. In accurate astronomical photometry it is not to be overlooked.

The dependence of Δ upon telescope and plate is shown in the three paragraphs below which were communicated by J. A. Parkhurst, of the Yerkes Observatory, from a thesis of Miss Alice Farnsworth.

Forty-inch refractor.—The focal length is 62.5 feet. Size of minimum image, approximately .080 mm. There does not appear to be any straight-line portion to the diameter-magnitude curve. The following are the values of Δ, the plate being Cramer Iso.

Diameter mm	Δ mm
.080	.020
.500	.050

Δ having been defined as the increase in diameter for doubling of the exposure time, if the value is desired for unit increase in stellar magnitude, the values given must be multiplied by the ratio of 0.4 to log 2.

Twelve-inch aperture of 2-foot reflector.—The focal length is 93 inches. Size of minimum image, .017 mm. In the case of this telescope the relation between diameter and magnitude, as well as between diameter and log exposure time appear to be linear over the unusually wide range of approximately 8 magnitudes. The deduced values of Δ are:

Plate	Δ mm
Seed 30	.011
Cramer Isochromatic	.020

Ultra-violet 6-inch camera.—The focal length is 32 inches. Size of minimum image, .014 mm. The characteristics are the same as those of the reflector noted above. The values of Δ are:

Plate	Δ mm
Seed 30	.013
Cramer Isochromatic	.020

Probable errors.—The accuracy with which stellar magnitudes can be calculated by the turbidity of "growth of image" method depends upon two factors: (*a*) accuracy with which the diameters of the star disks can be measured, (*b*) magnitude of Δ. These are not independent, however, since the accuracy of measurement depends on the sharpness, which is a function of the turbidity. Calling the diameter d, and the magnitude m,

$$d=a+\frac{\Delta}{\log 2}\log I,$$

$$m=b+2.5\log I,$$

giving the increment or probable error relation

$$\delta m=\frac{0.75}{\Delta}\delta d. \tag{11}$$

For very sharp images the probable error δd is approximately ± 1 μ. Taking Δ equal to 10 μ, this relation gives $\delta m=\pm.075$ mag. Since the irregularities of the photographic emulsion are known to have an inherent probable error of approximately ±.06 mag., the total probable error in this case becomes ±.096. For larger values of Δ, the images become less sharp, so that δd increases, but not in the same ratio. For example, taking $\Delta=50$ μ, we should expect d to be approximately ±2 μ, giving $\delta m=.030$ mag. In this case the total error is ±.067 mag. The advantage of greater turbidity which is gained both by proper choice of telescope and of emulsion is apparent.

The densitometric method, or measurement of density D for out-of-focus images, leads to a greater accuracy than can be attained by the turbidity method. In this case

$$D=a+\gamma\log I,$$

giving

$$\delta m=\frac{2.5}{\gamma}\delta D.$$

The error in magnitude thus is inversely proportional to γ or the contrast of the emulsion. If the exposures are properly made,

$\gamma = 1.5\pm$ for a fast plate, δD will vary but will not differ greatly from .01. Accordingly from the formula $\delta m = .017$ mag. In extreme cases, where contrasty plate and developer is used, $\gamma = 3.5$, giving $\delta m = .007$ mag. The inherent plate errors must of course be added to these values. According to recent tests by H. T. Stetson[1] a means has been found of reducing the plate error to one-half of its former amount. This will increase the value of the densitometric and the Stetson methods in stellar photometry relatively to the turbidity method.

Turbidity of fine-grain plates.—Table IV gives turbidity values of Seed lantern and yellow-dyed Seed lantern plates. The same test object as before was used. A considerable decrease in turbidity for yellow-dyed plates is apparent. The unexpected result is obtained that there is no difference between the turbidity of Seed 23 (Table III) and of Seed lantern.

TABLE IV

TURBIDITY

APERTURE	GEOMETRICAL DIAMETER OF IMAGE	SEED LANTERN		YELLOW-DYED SEED LANTERN	
		Threshold Diameter of Image	Δ	Threshold Diameter of Image	Δ
	mm	mm	μ	mm	μ
1	.004	.007	8.0	.005	....
2	.006	.007	8.2	.005	....
3	.008	.007	8.5	.006	....
4	.011	.009	9.0	.008	....
5	.014	.011	10.4	.010	....
6	.017	.018	11.1	.014	5.1
7	.025	.021	11.3	.020	6.5
8	.034	.030	11.5	.025	6.9
9	.057	.056	11.6	.053	8.2

Relative turbidity of star images and spectral lines.—In order to compare turbidities in this case, it is evident from the preceding that the images must be of approximately the same width. A test object was made having a slit aperture 1 mm in width with circular holes of the same width arranged on each side of the slit. This was photographed in the reducing camera in the usual way on a Seed 23 plate. The results are as follows:

---

[1] *Popular Astronomy*, **29**, 287, 1921.

	Star Images	Slit
Width of image (1 sec. exposure)....	.082 mm	.068 mm
Observed Δ (exp. range 1^s to 120^s)..	8.2 μ	8.2 μ

A violet combined with an aesculine filter was used, which accounts for the small values of Δ compared with those in Table III, in which unscreened white tungsten light was used. The values of Δ for star images and slit are seen to be the same. This is contrary to expectation, for it was supposed that the slit would show greater turbidity, on account of the reinforcing illumination from a greater extent of illuminated area, just as it was found that larger star images, for this same reason, showed greater turbidity than small images.

Variation of Δ with wave-length.—The values of Δ for a number of plates differing in type were determined in the precision camera behind a series of color filters. Typical curves have been given in a former publication.[1] Δ has been found to be smallest in the violet, agreeing with theory. Curves of these types are of importance with respect to the photographic Purkinje phenomenon considered in the following section.

The extent to which the measured values of Δ depends on the optical system and on its accuracy of focus has not yet been determined. In the case of printing by contact (of a specially prepared metallic slit) with the emulsion, it can be taken for granted that the "optical" turbidity is negligible, so that the measured turbidity should be that of the emulsion itself. By comparing values thus obtained with those obtained in conjunction with optical instruments, the relative importance of optical and emulsion turbidities may be judged. Determinations of Δ for contact slit images were made for various wave-lengths on Seed 23 and Seed panchromatic plates. The printing light was derived from a monochromatic illuminator. The Δ-wave-length curves resulting are shown in

---

[1] F. E. Ross, "Photographic Photometry and the Purkinje Effect," *Astrophysical Journal*, 52, 90, 1920.

Figure 9. Comparing with the values in Table III, there is seen to be substantial agreement. The conclusion is that for well-corrected optical systems the optical turbidity is negligible. The extremely small turbidity in the violet ($\Delta = 5\ \mu$) is noteworthy. It must not be overlooked that this is of profound importance in the Purkinje effect, whether considered from the standpoint of the turbidity or densitometric method of photometry.

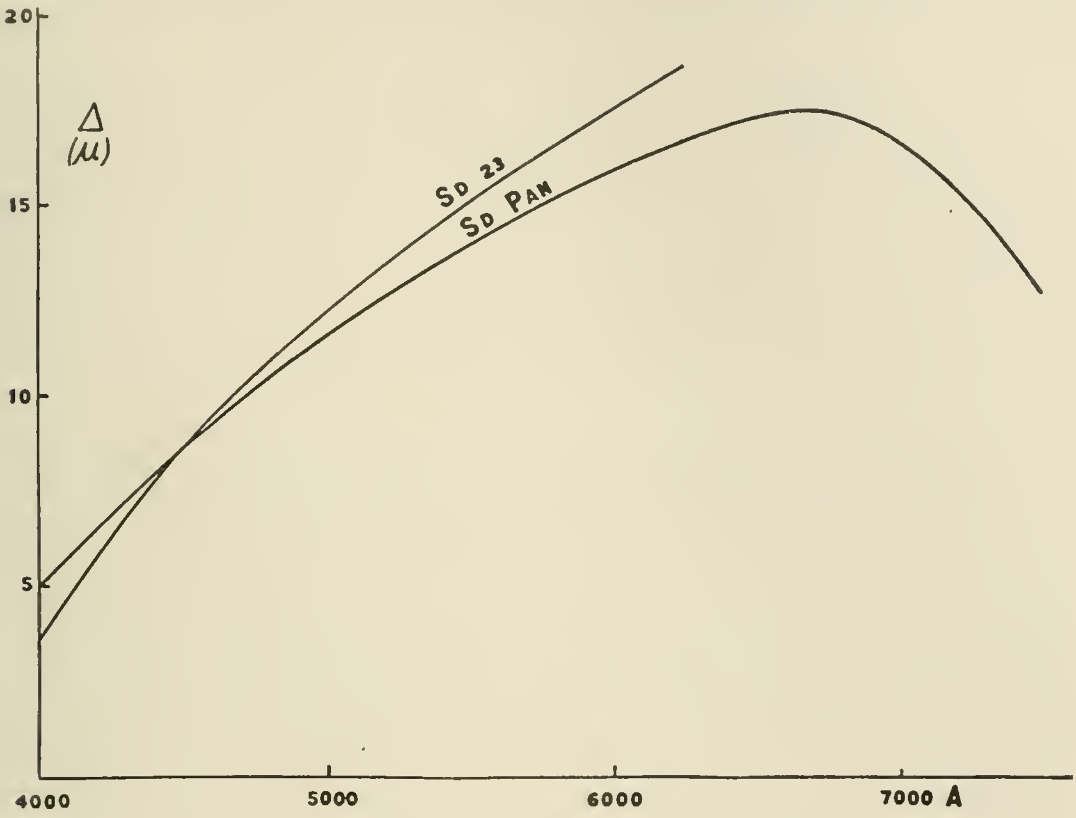

FIG. 9.—Turbidity depending on wave-length

PHOTOGRAPHIC PURKINJE EFFECT

A brief historical account will be given of the photographic Purkinje phenomenon, the change of gradation or contrast with change of color. That there is an appreciable effect of this kind appears to have been discovered nearly simultaneously by Sir W. Abney[1] and J. Precht[2] in 1899. Precht discovered the phenomenon through comparing densitometric results obtained by using as sources of illumination a benzene lamp and an amyl-acetate lamp, respectively poor and rich in actinic rays, it is claimed. He concluded: (1) "Die relative chemische Helligkeit zweier Lichtquellen ist abhängig vom absoluten Intensität." (2) "Die relative chemische Helligkeit zweier Lichtquellen ist abhängig vom absoluten Wert der Expositionszeit."

---

[1] "On the Variation in Gradation of a Developed Photographic Image When Impressed by Monochromatic Light of Different Wave-Lengths," *Proceedings of the Royal Society*, 61, 300, 1901.

[2] "Photographisches Analog zu Phanomen von Purkinje," *Arch. wiss. Photographie*, 1, 277, 1899.

C. Jones[1] made a careful study of the phenomena at about the same period. He concluded that in general the gradation increases continuously from the ultra-violet to the red. An exception is found when development is in pyro-ammonia, in which case the gradation curve was found to be reversed.

The following quotation from Abney clearly summarizes his conclusions:

> Nearly two years ago, in an article in *Photography* I indicated that a variation in gradation due to differences in the monochromatic light in which the exposure was made did exist, and some six months ago Mr. Chapman Jones, in a paper communicated to the Royal Photographic Society, independently announced the same result from experiments made principally with orthochromatic plates with light passing through various colored media and he generalized from his experiments that the smaller the wave-length the less steep was the gradation, the ultra-violet rays giving the least steep and the red the most steep gradation. My experiments which at that time had been partially completed did not bear out this generalization to the full when pure silver salts were used, and my subsequent measurements with them show that the least steep gradation is that given by the monochromatic light to which the simple silver salt experimented with is most sensitive, and that the gradation becomes steeper as the wave-length of light employed departs in either direction in the spectrum from this point, the steepest gradation being given by the extreme red. The case of orthochromatic plates in which is a complex mixture of silver salt and dye is necessarily less simple, involving consideration of the localities in the spectrum to which the dye or dyes, together with that of the silver salt, are most sensitive. For this reason the simple salts have been experimented with in preference to the more complicated organic compounds. It may be thought that these results might be peculiar to the salt of silver experimented with. A further series of experiments were conducted with the chloride of silver in gelatine. The maximum sensitiveness of these plates was found to be near H ($\mu = 3968.6$ A) in the solar spectrum. The gradation was found to be least at this point and increased when rays on each side of this point were

---

[1] "The Effect of Wave-Length on Gradation," *Photographic Journal*, 24, 279, 1900.

employed to act on the film. In the blue, near the F line, where the sensitiveness of the plate was very small, the gradation was excessively steep, as it also was in the extreme ultra-violet.

Abney's conclusion, that the least gradation is at the point of maximum sensitivity, is a beautiful and somewhat startling theorem. Abney himself appears at a loss to account for it. "What scientific explanation there is of this difference in true gradation factor is hard to say." The following explanation is proposed by the writer. It has been shown in a previous paper[1] by the writer that for emulsions composed of grains of equal sensitivity the gradation or gamma is a maximum, and that as the number of groups of grains of varying sensitivity increases, gamma decreases. A simple case in point is the mixture on one plate of a fast and a slow emulsion. It appears quite probable that in the case of the emulsions studied by Abney, a greater number of groups, with no inert grains, come into action at the wave-length where the general sensitivity is a maximum. This should result in a lower gamma, as just shown.

Contrary to the results quoted so far, G. Leimbach[2] obtains no change of gradation with wave-length. "In Bereiche der normalen Belichtung wachst die Schwarzung mit zunehmender Belichtungszeit nach demselben Gesetz, "or," Die Gradation ist für alle Wellenlangen die selbe."

The astronomical importance of the subject is well illustrated in the attempts which have been made to prove from photographic data that light suffers an appreciable absorption in its passage through space, which were based upon the assumption that the photographic gradation is the same for all colors. That the data do not allow such conclusions to be drawn has been shown by J. A. Parkhurst[3] and by H. E. Ives.[4] From his own investigation of the subject Parkhurst concludes ". . . . Experiment with the photographic color-filter furnishes no evidence for or against an absorption or scattering of light in space." Ives shows that a conclusion of selective space-absorption of light is based upon the assumption that the gradation of the photographic plate is the same for all colors. Ives's paper on the subject is of importance in indicating causes underlying the phenomenon, and in giving reasons for the contradictions found by different investigators. He concludes that the factors of importance in determining the variation of gradation with wave-length are (1) penetration of the dye in the film; (2) penetration of the light; (3) penetration of the developer. He notes the important fact that when plates are color sensitized by bathing, the penetration of the dye into the emulsion is superficial. In the case of plates color sensitized by the manufacturer, the dye is incorporated in the emulsion before coating, so that the light-sensitive layer is much thicker and consequently a much higher gradation is obtained. "With a Cramer instantaneous isochromatic plate, the red gradation was steeper than the blue. With a Seed 26, bathed for two minutes in a 1:100,000 solution of pinacyanol, the blue gradation was steeper than the red." Ives suggests that Leimbach's negative result was due to surface development, since he developed in ferrous oxalate developer for a short time only.

---

[1] *Loc. cit.*, p. 265.

[2] "Die Absolute Strahlungsempfindlichkeit von Bromsilberplatten gegen Licht verschiedener Wellenlange," *Zeitschrift für wissenschaftliche Photographie*, 7, 181,1901.

[3] "The Evidence from Photographic Color Filters in Regard to the Absorption of Light in Space," *Astrophysical Journal*, 30, 331, 1909.

[4] "Some Photographic Phenomenon Bearing upon Dispersion of Light in Space," *ibid.*, 31, 157, 1910.

J. A. Parkhurst[1] has sought to determine directly the change of gradation of the photographic plate for stars of different classes or colors. He finds a difference of 1.5 per cent in the direction of higher gradation for the red stars, but concludes: "We, therefore, reach the conclusion that for Seed 27 plates and for extra-focal images the slight systematic effect which may be present is nearly or quite masked by the accidental errors arising principally from the lack of uniformity in the film."

No attempt has been made in the foregoing review to enumerate all the investigations bearing upon this very important subject. The contradictions and confusion are evident without further citation. Careful study of the methods employed by the various investigators does not in general disclose any lack of care in details or narrowness in treatment. Without any pretense to being exhaustive, many of the investigations were admirably planned and carefully carried out. Assuming as we must therefore that no flagrant errors were made by any or by all of the investigators, the only possibility of accounting for the discrepancies appears to be to assert that the wave-length effect upon gradation is strongly variant with the particular emulsion, and to a possibly lesser extent with developer and development conditions. It cannot be said that this dependence was not present in the minds of many of the investigators for, in several cases, a large number of plates of various kinds, including blue sensitive, isochromatic and panchromatic were used. Also more than one developer was in general employed.

---

[1] "A Property of the Photographic Plate Analogous to the Purkinje Effect," *Astrophysical Journal*, 49, 202, 1919.

H. E. Ives (p. 370) has pointed out why no general statement of the gradation wave-length effect can be made, and enumerated some of the important causes of variation in results obtained. Besides those mentioned by him, there are doubtless others. There is, for instance, the Eberhard effect, or retardation of development dependent upon the *density* of an image and upon its *size*. Since astronomers are concerned in general only with very minute images, it is quite clear that laws of photographic action worked out in the laboratory where much larger density areas are in general employed, are not entirely applicable.

The tendency of a photographic plate to reversal, a phenomenon which, according to the views of some investigators, begins at the first moment of exposure and gains strength with its advance, must have an important bearing upon the gradation of the plate. Abney has shown that pre-exposure of a plate to red light accelerates the reversal tendency. It is quite clear from this therefore that the composition of the incident light must have an indirect or catalytic action on the plate, aside from its direct latent-image forming characteristics. Accordingly, the *quality* of the light used by the experimenter has an indirect effect on gradation and can account for some of the differences obtained. That the reversal action is of importance in practical photography is shown by the experiments of Channon[1] on exposures of great length.

Consideration of the action of reducers gives a helpful point of view. It is well known that the action of some reducers is confined to the surface of the image, while others appear to act uniformly through the depth of the image. This differential action depends upon relative rates of diffusion of reactants and reaction products compared with the velocity of the chemical actions. Similar principles can be conceived to hold in ordinary development. In fact the Eberhard effect is accounted for chemically in this way. Accordingly rates of diffusion through gelatine, with the many chemical factors which control and change it, become important factors in depth development, which has been shown to play an important part in gradation phenomena.

---

[1] "Studies in Photographic Science," *Photographic Journal*, 50, 164.

Rochester, N.Y.
May 23, 1922

THE SPARK SPECTRUM OF GALLIUM IN AIR AND IN HYDROGEN

BY ELIAS KLEIN

ABSTRACT

Spark spectrum of gallium, 2177 to 6414 A, in air and hydrogen, was photographed with the aid of a Littrow type spectrograph, and the wave-lengths of 83 gallium lines, 14 of them questionable, are given accurate to about ±0.05 A. Of these 23 had been measured by Uhler and Tanch and 26 by Saunders, but 48 are new. The spark in hydrogen was tried because the spark in air oxidizes the gallium and then the spectrum becomes less rich in lines. To eliminate lines due to possible impurities, spark spectra of Cu, Fe, Pb, In, Zn, and Sn were photographed next to the gallium spectrum.

APPARATUS AND METHODS

The spectral regions studied were photographed with a large quartz spectrograph, of the Littrow type, made by the Adam Hilger Company, Ltd., London. For this instrument the spectrum range between λ 2000 and λ 8000 is divided into three portions which are approximately: λλ 2000–2500; λλ 2500–3400; λλ 3400–8000. The dispersion for the middle of each of the above regions is roughly, 2 A per mm; 6 A per mm; 15 A per mm.

The gallium used for the spark in air was prepared and purified by Professor Uhler according to the method of Browning and Uhler.[1] A bead of this metal, about 3 mm in diameter, was placed in a small cavity made in the end of a copper rod 10 mm in diameter. This served as the lower electrode. The upper electrode was a No. 5 copper wire filed to a point. For the spark in hydrogen (discussed later) the gallium was electrolytically deposited from a decidedly alkaline solution of gallium chloride. The original solution contained indium sulphate, gallium chloride, and ammonium formate, the indium having been removed first by electrolysis. The gallium thus obtained was placed in a quartz tube which was evacuated and heated with a blast lamp to the softening point of the quartz. The pumps were kept in operation during this process. Owing to the very low vapor pressure of gallium most of the metals (Zn, Pb, Sn, In) which occur as impurities in it are distilled on the cooler portions of the tube (and the trap joining it) at a much lower temperature than the boiling point of gallium. Thus the gallium is purified and remains in liquid form at the bottom of the tube.

---

[1] Uhler and Browning, *American Journal of Science*, 41, 351; 42, 397, 1916.

The spark in air as well as that in hydrogen was produced by a 500 watt transformer (powerfactor 1/3) rated at 15,000 volts and made by the American Transformer Company. The primary current, 110 volts 60 cycles, varied from six to fifteen amperes, depending upon the metals used in the spark gap. In parallel with the spark gap, which was about 5 mm, was connected a Leyden jar battery of capacity approximately .005 μf. The current in the oscillatory circuit, as measured by a hot wire ammeter, was over 10 amperes. The period of this circuit (gap in air) was about 10^{-6} seconds.

The time of exposure for the spark varied from 5 to 20 minutes in air, and from 20 minutes to 2 hours in hydrogen. Slit widths of 0.02–0.04 mm were used throughout this work.

Generally Seed plates Nos. 26 and 30 were used and found quite satisfactory. For the region between λ 6000 and λ 8000 special plates were obtained from the Eastman Kodak Company, through the courtesy of Dr. C. E. K. Mees. These plates served their purpose admirably. A simple hydrochinone developer according to L. E. Jewell[1] was used throughout.

The spectra of copper and iron were used for standard comparison. The most likely impurities (other than copper and iron) in the metal used for the present investigation are lead, indium, zinc, and tin. The spectra of these metals were photographed above and below the gallium spectrum in each case, without displacing the plate. This method of eliminating foreign lines saved much time in the final measurements of the plates. All the plates were measured with a Gaertner engine which had been modified and tested by Professor Uhler.

SPARK IN HYDROGEN

It was originally intended to get the spark spectrum of gallium in air only, and several plates were taken for each region, thus covering the entire range of the spectrograph. Upon studying the plates in detail it was observed that, in general, in any given region of the spectrum the same sample of gallium radiated a decreasing number of lines with successive exposures of identical duration. This was due to the fact that the gallium oxidized very readily but superficially when heated, and that the oxide of gallium (Ga_2O_3) apparently radiated only the strongest lines of the metal. This difficulty could have been overcome by continually removing the outer oxide layer, thus bringing the metallic surface into sparking communication with the upper electrode. This method, however, was considered impracticable because of the great scarcity of the metal, and the long, troublesome process of again reducing the oxide of gallium to the metallic form. Besides, one is never certain, by this method, that he has got all the lines gallium is capable of radiating under the given sparking conditions, although it later appeared that some of the exposures in air showed as many lines as those in hydrogen. It was necessary, therefore, to seek an oxygen-free medium for the gallium spark. Nitrogen proved undesirable, due to its many bands which masked the fainter gallium lines. Helium, as supplied by the Navy Department, was found to contain too much nitrogen to be useful in this investigation. Commercial electrolytic hydrogen, as supplied by the Tariffville Oxygen Company, Connecticut, proved quite pure and gave satisfactory results.

---

[1] L. E. Jewell, *Astrophysical Journal*, 11, 242, 1900.

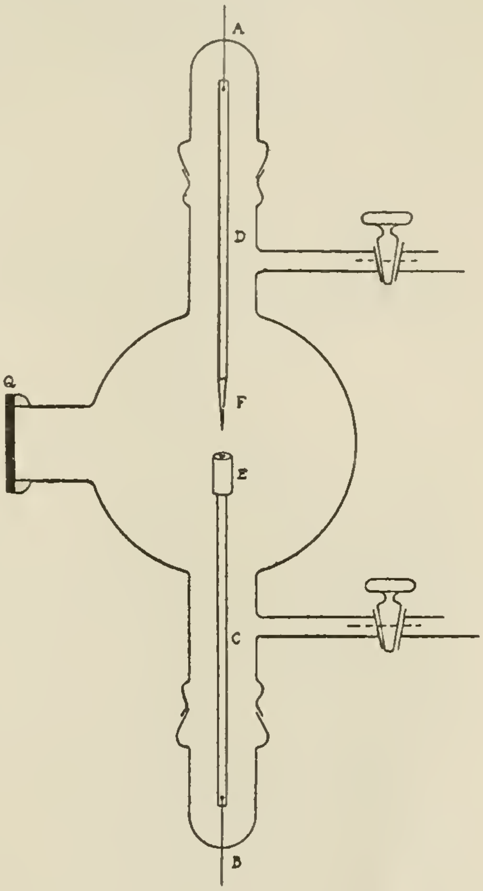

Fig. 1

The spark chamber employed was as shown in the accompanying sketch. It consisted of a glass bulb about six inches in diameter. Into the ground-joint tubes were sealed platinum wires, *A*, *B*. To the inner ends of these were joined aluminum rods, *B*, *C*. *E* is a short copper rod having a cavity in its upper end where the gallium was placed. *F* is a No. 5 copper wire. The quartz plate, *Q*, was cemented to the bulb with sealing wax.

The chamber and system of drying bulbs to which it was attached were evacuated to a pressure of about 10^{-5} cm of mercury by means of a Western Electric diffusion pump, and a Gaede rotary pump. The apparatus was then filled with dried hydrogen to atmospheric pressure and was cut off from the supply tank by means of a stop-cock. During each exposure a fan cooled the bulb to keep the pressure constant and the sealing wax about the quartz window from melting.

DETERMINATION OF WAVE-LENGTHS

The wave-lengths of gallium were computed by means of the simplified Hartmann dispersion formula,

$$\lambda=\lambda_0+\frac{C}{N_0-N}\,.$$

The constants λ_0, C and N_0 were calculated from the superimposed copper or iron spectrum. The interval for which these constants were determined never exceeded 200 A units. In most cases 50 or 100 A were used. Each set of plates, those taken in hydrogen as well as those taken in air, were measured, and independent computations of wave-lengths were made for each.

The wave-lengths given in the following table are the averages of the two sets of computations. Faint lines, the wave-lengths of which agreed with those of more intense lines in the spectrum of a common element, were considered as impurities. Questionable lines are indicated as such, and should be interpreted as faint lines whose wave-lengths do not agree with suspected impurity lines by 0.05 A or 0.10 A. The limit of accuracy of the wave-lengths shown in the table is approximately 0.05 A.

Column two contains a list of wave-lengths of the gallium spark spectrum which Professor F. A. Saunders had occasion to measure recently and which he very generously turned over to the author for comparison. A Hilger Quartz Spectrograph Type "C" was used for photographing these lines. The gallium contained traces of copper, chromium, and manganese.

TABLE I

Table of Wave-Lengths in International angstroms

No.	Uhler and Tanch Arc in Air	Saunders Spark	Present Work Spark	Estimated Intensity	Remarks
1.	2171.9				
2.			2176.76	3	broad, hazy
3.	2195.665		2195.63	2	H_2 plates only
4.			2205.91	2	hazy
5.	2211.753				
6.	2218.039				
7.	2236.103		2236.17	3	fairly sharp
8.	2255.034	2255.60*	2255.29	2	hazy
9.	2259.227	*	2259.24	1	faint
10.		2266.86*	2266.84	2	diffuse
11.		*	2285.19	2	hazy H_2 plates only
12.	2294.202	2294.17*	2294.19	2	diffuse
13.	2297.869	2297.90*	2297.89	2	fair
14.	2338.293	2338.25	2338.24	3	broad
15.	2338.596				
16.			2359.48(?)	1	H_2 plates only
17.	2371.325	2371.30	2371.29	3	sharp
18.	2418.699	2418.72	2418.69	4	sharp
19.			2422.61	3	broad, diffuse
20.			2423.14	2	hazy, diffuse
21.		2424.27	2424.29	3	fairly sharp
22.	2450.078	2450.02	2450.04	6	diffuse
23.	2500.187	2500.18	2500.17	7	diffuse
24.	2500.714	2500.74	2500.72	3	diffuse
25.			2588.92(?)	3	hazy H_2 plate only
26.			2589.73(?)	2	hazy H_2 plate only
27.			2602.04	2	very hazy
28.	2659.873	2659.90	2659.89	7	fair
29.		2700.55	2700.56	4	sharp
30.		2702.39	2702.42(?)	1	faint on H_2 plate only
31.	2719.664	2719.76	2719.59	8	fairly sharp
32.		2780.22	2780.12	9	very broad
33.		2830.24	2830.19	1	very faint
34.			2836.87	1	very faint
35.	2874.240	2874.35	2874.24	9	diffuse
36.		2929.81	2877.50(?)	3	sharp
37.	2943.639	2943.60†	2943.59	10	diffuse
38.	2944.175	2944.27†	2944.18	9	diffuse
39.		2987.97	2987.99	4	diffuse
40.		2997.93	2997.99	3	diffuse
41.		3004.14	3004.10	6	fairly sharp
42.			3015.60	2	very hazy
43.		3024.38	3024.33	1	faint
44.		3058.13	3058.15	3	diffuse
45.			3058.92	1	faint H_2 plate only
46.		3064.88	3064.45	2	sharp
47.			3072.14	3	fair
48.		3074.22	3075.87	2	fair
49.			3093.22(?)	2	sharp
50.			3124.90	1	faint
51.			3181.44	2	diffuse

TABLE I—*Continued*

No.	Uhler and Tanch Arc in Air	Saunders Spark	Present Work Spark	Estimated Intensity	Remarks
52			3189.01	1	faint
53			3190.46(?)	2	sharp
54			3192.86(?)	2	sharp
55			3375.32	7	diffuse
56			3417.12	5	hazy
57			3473.39	1	faint
58			3479.46	5	diffuse
59			3517.21	4	diffuse
60			3576.96	5	fairly sharp
61			3650.73(?)	1	faint hazy
62			3701.61	2	faint hazy
63			3730.03	6	diffuse may be doublet
64			3806.87	4	diffuse
65			3944.29	2	sharp
66	4032.975		4032.98	10	fair hazy edges
67			4069.52(?)	2	diffuse
68	4172.048		4172.05	10	fair
69			4250.67	3	diffuse
70			4254.13	2	hazy and diffuse
71			4256.17	2	hazy
72			4261.93	4	hazy
73			4616.43(?)	2	fairly sharp
74			4417.69(?)	2	fairly sharp
75			4820.59	2	sharp
76			4864.92	4	diffuse
77			4995.61	3	sharp
78			5338.88(?)	2	diffuse
79			5360.09	4	diffuse—looks like doublet
80			5844.22(?)	4	very diffuse
81			5992.34	3	hazy
82			6396.61	5	fair
83			6414.01	4	fair

* Iron standards are very weak here. Precision reduced.

† Not completely resolved. Might be a pair.

The agreement between columns two and three, although by no means perfect, is as close as could be expected when the following factors are taken into consideration. (1) The difficulty in setting on the lines because of the continuous background, especially on the plates taken with gallium in hydrogen which required long exposures; and, the easy reversals of the gallium lines. (2) The difference in dispersion between the two instruments used. Lines 47 and 48 have probably coalesced into one line on the plate of Professor Saunders. The mean position of these two lines is about 3074.00 which is no further away from 3074.22 than is line 46 from the corresponding line of Professor Saunders. He designates 3074.22 as "very hazy."

The author has so far been unable to extend the gallium series beyond those shown by Paschen and Meissner,[1] and Uhler and Tanch.[2]

The author is indebted to Professor H. S. Uhler for suggesting the problem and for the interest he showed during the progress of this investigation.

Sloane Laboratory
Yale University
August 1921

---

[1] *Annalen der Physik*, 43, 1223, 1914.

[2] *Astrophysical Journal*, 55, 291, 1922.

THE ABSENCE OF OXYGEN AND WATER-VAPOR LINES FROM THE SPECTRUM OF VENUS[1]

By CHARLES E. ST. JOHN AND SETH B. NICHOLSON

ABSTRACT

Absence of oxygen and water-vapor lines from the spectrum of Venus.—It has been generally assumed that the atmosphere of Venus is like our own, containing both oxygen and water vapor, but the spectroscopic evidence for this assumption is very doubtful. Recently spectrograms have been made with the Snow telescope and the Littrow grating spectrograph at times when the relative velocity of Venus and the earth was sufficient to separate completely corresponding lines produced by the two atmospheres. Special attention was given to the lines of water vapor near λ 5900 and to the bands a and B due to oxygen. No trace of any line due to the planet's atmosphere was observed. It is estimated that in the path traversed by the solar light through Venus' atmosphere there must be less than the equivalent of one meter of oxygen, less than one-thousandth of that in our atmosphere, and less than one millimeter of precipitable water vapor.

Atmosphere of Venus.—Various observational facts and theories concerning this atmosphere *are discussed.* Although the new data prove that there is no appreciable amount of oxygen or water vapor above the visual surface of Venus, nothing is definitely known about the elevation of this surface above the presumably solid surface of the planet, or whether this reflecting layer is composed of cirro-strati, of haze, or of clouds of dust produced by violent atmospheric circulation.

It has been generally assumed in the literature on planetary atmospheres that the atmosphere of Venus is similar to our own; in particular, that oxygen and water vapor are present. Secchi,[2] 1868, noted in the spectrum of Venus a nebulous band on the red side of the D line and also one to the violet, the δ of Brewster. He observed these with Venus at a high altitude and when the air was so dry that he assumed that they were not of telluric origin. Huggins[3] had previously, 1863, studied the spectrum of Venus, Mars, Jupiter, and Saturn. Of Venus he says:

> The light of Venus gives a spectrum of great beauty. The line D was seen double, B, C, and numerous solar lines to a little beyond G, were distinctly visible; and the principal of these were measured and found to agree with corresponding lines in the solar spectrum. Lines other than these, and in the position in which the stronger atmospheric lines present themselves, were carefully looked for, but no satisfactory evidence of any such lines has been obtained.

---

[1] *Contributions from the Mount Wilson Observatory*, No. 249.

[2] *Spettrie Protuberanze*, p. 24, 1869.

[3] *Philosophical Transactions of the Royal Society*, 154, 422, 1864.

PLATE XIII

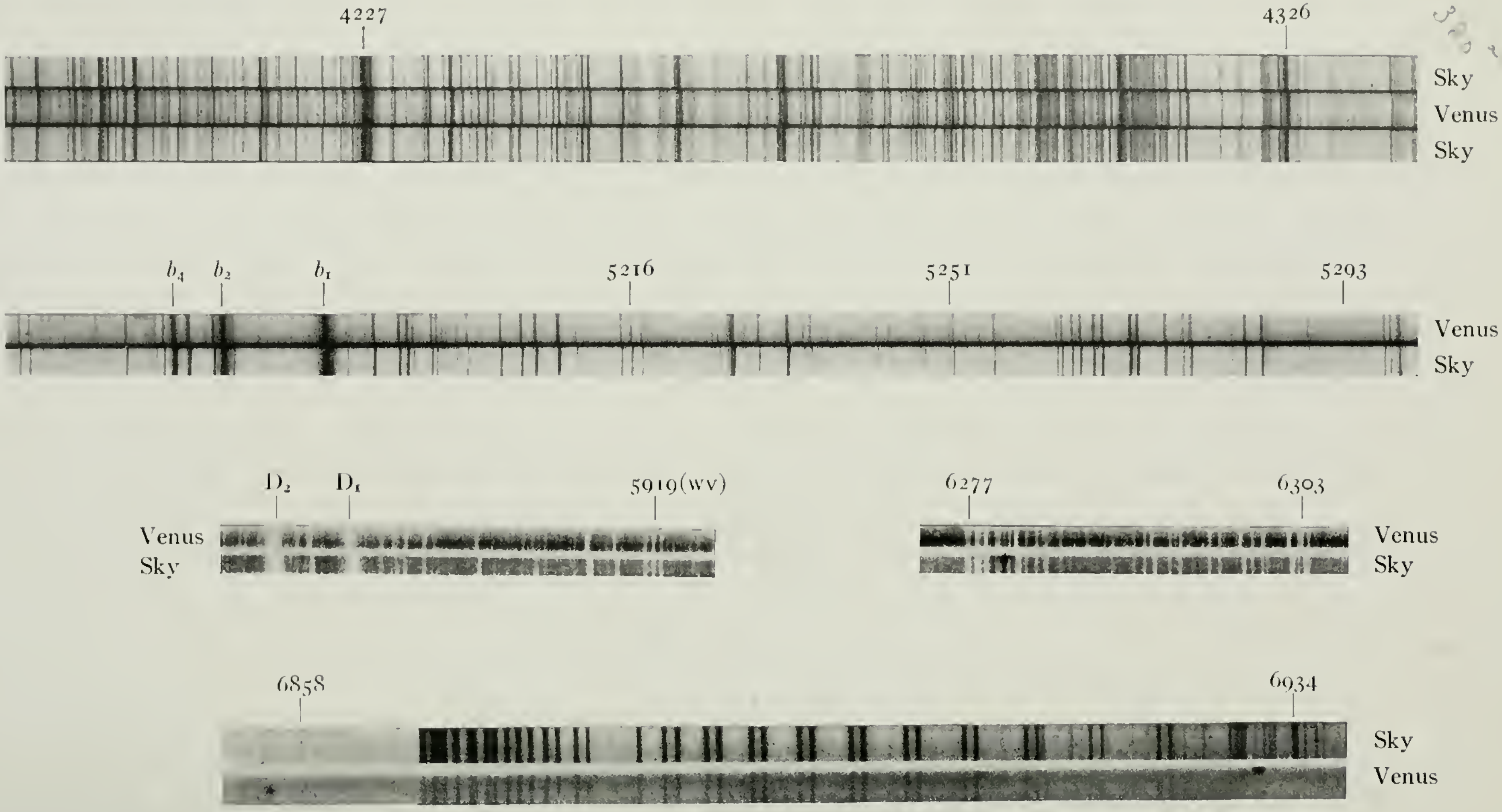

Spectra of Venus and Sky

The basis of the assumption permeating the literature on planetary atmospheres is found in the observations of Vogel.[1] Of his observations on the oxygen band at λ 6275 and the water-vapor bands at λλ 5945 and 5925 he says:

> Die Venus stand bei den Beobachtungen so hoch, dass man nicht annehmen kann, dass unser Atmosphäre einen merklichen Einfluss auf das Venusspectrum ausgeübt habe, die Linien oder Streifen sind daher entschieden dem Venusspectrum eigen und deuten auf die absorbirende Wirkung einer Atmosphäre.

Scheiner[2] in his review of the question sums up as follows:

> There seems to be no doubt that the telluric lines appear stronger in the less refrangible portions of the spectrum of the planet than in the solar spectrum. There can therefore be no doubt that the atmosphere of Venus exerts an absorption similar to that of our own, and hence the nature of the two atmospheres must be similar. . . . . We may safely assume that the clouds of Venus consist of condensed aqueous vapor, thus again resembling those of the earth.

Arrhenius[3] is still more specific and states that:

> The humidity (on Venus) is probably about six times the average of that on the earth or three times that in the Congo where the average temperature is 26° C. The atmosphere of Venus holds about as much water vapor 5 km *above* the surface as does the atmosphere of the earth *at* the surface. We must therefore conclude that everything on Venus is dripping wet. The vegetative processes are greatly accelerated by the high temperature. Therefore the life time of organisms is probably short.

The fallibility of these older visual observations, in which conclusions are drawn from estimates of the relative intensities of integrated groups of lines in the spectrum of Venus and of the moon or sky, is shown by comparing Vogel's observations in the green region with our spectrograms of Venus and the sky. Vogel notes, among others, groups at λ 5216 and λ 5251 as strengthened in the spectra of Venus, and Scheiner accepts the observations as definite proof of the similarity of the atmosphere of Venus and the earth. Arrhenius' conception of supertropical moisture and luxuriance of vegetation is founded likewise on these older observations. These groups are resolved on the Mount Wilson spectrogram, Plate XIII, and our examination shows no strengthened lines in the spectrum of Venus. The lines of both groups are identified as iron lines of intensity 2 and 3 on the Rowland scale. The degree of dependence that can be placed upon the Mount Wilson spectrograms may be inferred from observations at λ 5293 of some lines which are marked Awv? and 00 intensity in the Rowland table. These were clearly displaced in the spectrum of Venus, with no lines visible in the undisplaced positions. An examination of juxtaposed spectra of the east and west limbs of the sun confirms this evidence that the lines are entirely solar and not atmospheric.

---

[1] *Untersuchungen über die Spectra der Planeten*, pp. 10–16, 1874.

[2] *Astronomical Spectroscopy*, pp. 197–198, 1894.

[3] *The Destinies of the Stars*, pp. 250–251, 1918.

These older visual observations depended on estimating the relative intensities of integrated groups of lines in the spectra of Venus and skylight. Lowell[1] suggested measuring the position of the oxygen and water-vapor lines to see whether they were affected by the Doppler shift, and V. M. Slipher obtained spectrograms of Mars and the moon and of Venus and the sky with a dispersion of 50 A per mm at 6100 A.[2] Of the spectrograms of Mars, Lowell says:

> The results at first seemed significant. To the writer's eye the shift of the solar lines under the microscope was perceptible though slight and in the shift the *a* band seemed to share. The lines of water vapor near D though present in both spectra were not strong enough to make much deduction possible.

Of Venus he says,

> Here again eye estimates by the writer subscribed to a shift in the *a* band, the water vapor lines, very faint, concurring; . . . . As regarded differences in density, none was perceptible between either the Martian and the lunar or the solar and Venusian, either in the oxygen *a* band or the water vapor lines near D. Water vapor is probably non-existent on the illuminated side of Venus and extremely scarce on Mars. As for oxygen the results above show that the spectroscopic method is hardly a delicate enough one in this respect to decide the question.

And Slipher remarks:

> Examination and measurement of them led to the same uncertain results as in the case of those of Mars. Although this attempt has failed to detect aqueous vapor in Mars and Venus, the conclusion should not be drawn that it

---

[1] *Lowell Observatory Bulletin*, No. 17, 1905.

[2] Campbell and Albrecht in observations on Mars quite independently applied the Doppler-Fizeau method to a planetary atmosphere. *Lick Observatory Bulletin*, **6**, 11 (No. 180), 1910.

does not exist in their atmospheres, nor that it will always remain impossible to discover it spectrographically.

This brief account reviews the spectroscopic evidence upon which the current views in respect to the constitution of the atmosphere of Venus were founded when we began our observations in March, 1921, and indicates the extreme detail reached in their interpretation. At the Berkeley meeting of the Astronomical Society of the Pacific in August, when we reported our results, Dr. Slipher also reported results of his recent observations in which he used relative intensity as a criterion, and obtained similar negative results.

INSTRUMENTAL METHODS

The spectrograms were obtained with the Snow telescope and the Littrow grating-spectrograph.[1] To Professor Wood we are greatly indebted for the loan of a large grating very bright in the first order. It was ruled by Anderson and has a surface of 95×170 mm. The dispersion in the first order of the 18-foot spectrograph is 3 A per millimeter. For the α band and the 5900 region the plates were Seed 23's, sensitized to red light by pinacyanol. Ilford Special Rapid panchromatic plates, hypersensitized with ammonia, were used for the B band, λ 6867.

The wave-lengths of eight water-vapor lines near D and of seven oxygen lines in the α band were measured on five spectrograms of Venus and on three of the sky, using I.A. wave-lengths of solar lines, corrected for motions, for standards of reference. On three of the spectrograms of Venus the wave-lengths of the water and oxygen lines were referred also to iron arc lines; the spectrum of the arc was put on intermittently during the long exposures on Venus. On a fourth spectrogram of the sky they were referred to the lines of a simultaneously exposed iron arc. The wave-lengths thus found were compared with the wave-lengths of the same telluric lines, obtained under much higher dispersion, given in Table I.

From the variation among the differences, Rowland *minus* International (R−I in Table I), the relatively low accuracy of measurement of water-vapor and oxygen lines is apparent, even on spectrograms with a scale of 0.72 A per millimeter. For the oxygen line λ 6278, which is double on the Mount Wilson plates, the mean wave-length of the two components is used for the comparison with the Rowland value. In such a series of measurements as is presented in this paper, where the scale is 3 A per millimeter, a precision in the final means greater than 0.005 A is hardly to be expected. The results of the measurements are shown in the eighth column of Table II under Δλ, the Δλ being the difference between the observed wave-lengths and those of Table I.

---

[1] *Mt. Wilson Contr.*, No. 208; *Astrophysical Journal*, 54, 381–382, 1921.

TABLE I

Wave-Lengths of the Comparison Lines

Water Vapor* I.A.	R−I	Oxygen† I.A.	R−I
5885.982	+0.211	6278.106	+0.197
87.227	0.218	81.186	0.201
87.665	0.215	81.963	0.201
5909.001	0.212	92.171	0.202
19.058	0.218	92.967	0.203
19.646	0.214	95.186	0.203
24.276	0.214	95.968	+0.202
32.097	+0.219		

* *Mt. Wilson Contr.*, No. 223; *Astrophysical Journal*, 55, 36, 1922.

† Unpublished results by St. John and Babcock.

Because of the dearth of reference lines, a different method of measurement was adopted for the oxygen lines in the B band, λ 6867. The positions of nineteen oxygen lines in the spectra of Venus were compared with their positions in the spectra of the sky taken under similar spectrographic conditions. The scale readings of the solar lines on the spectrograms of the planet were corrected for the relative velocity of Venus and the earth. The average difference between these adjusted scale readings and those of the same lines on the sky spectrograms was then applied to all lines, thus bringing the readings of the solar lines into mean agreement on the two spectrograms. In the absence of absorption by oxygen in the atmosphere of Venus, the oxygen lines should now have the same scale readings in the two spectra; on the other hand, the presence of absorption should register as a displaced component of the oxygen lines, broadening or doubling them, according to the relative velocity. Spectrograms were taken with Venus east and west of the sun, the range in velocity corresponding to a Doppler

TABLE II

OBSERVATIONAL DATA

Plate	Subject	1921	P.S.T.	z sec z	Velocity E−V	Doppler Shift	Δλ	Lines Meas.	Refer. Lines	Phase
					km	A	A			
V 274....	Venus	Feb. 24	5^h36^m–9^h00^m	67° 2.56	−12.87	−0.254 −0.270	+0.015 −0.010	water vapor α, oxygen	arc sun	98°0
275....	Sky	Feb. 25	4 30	76° 4.13	....	....	+0.003 −0.001	water vapor α, oxygen	sun	....
276....	Venus	Feb. 25	5 40 −9 00	68° 2.67	−12.84	−0.253 −0.269	+0.014 −0.004	water vapor α, oxygen	arc sun	98°7
277....	Sky	Feb. 27	4 58	81° 6.39	....	....	−0.006 +0.001	water vapor α, oxygen	sun	....
278....	Venus	Feb. 27	5 37 −9 00	68° 2.67	−12.79	−0.252 −0.268	−0.012 −0.015	water vapor α, oxygen	arc sun	100°3
279....	Sky	Feb. 28	3 49	68° 2.67	....	....	−0.009 −0.013	water vapor α, oxygen	arc	....
280....	Sky	Feb. 28	4 10	71° 3.07	....	....	−0.014 −0.021	water vapor α, oxygen	sun	....
282....	Venus	Feb. 28	7 20 −9 05	76° 4.13	−12.76	−0.252 −0.268	−0.005 −0.006	water vapor α, oxygen	sun	101°1
285....	Venus	Mar. 1	7 19 −9 00	76° 4.13	−12.73	−0.267	−0.005	α, oxygen	sun	101°8
289....	Venus	Mar. 3	6 16 −9 00	69° 2.79	−12.69	−0.249	+0.026	water vapor	sun	103°4
301....	Venus	Mar. 24	5 55 −8 35	70° 2.92	−10.99	−0.252	+0.00	B, oxygen	sun	125°1
303....	Venus	Mar. 27	5 45 −8 38	71° 3.07	−10.38	−0.238	0.00	B, oxygen	sun	129°0
359....	Venus	Aug. 13	15 0 −23 0*	31° 1.17	+12.44	+0.286	−0.00	B, oxygen	sun	67°1

* Exposure interrupted; total 7^h10^m.

shift of 0.538 A. The results of the comparison are given in the eighth column of Table II, where the $\Delta\lambda$ for these plates is the difference Venus *minus* sky.

OXYGEN

Five spectrograms of Venus were taken in the region of the a band when the relative velocity of Venus and the earth was -12.8 km, the corresponding Doppler shift being 0.268 A to the violet, an amount sufficient to separate completely the terrestrial components from those of Venus. Although some solar lines of intensity 000 are faintly visible on these spectrograms, no lines are observable where they should appear if produced by oxygen in Venus' atmosphere. The measured wave-lengths of the oxygen lines present on the spectrograms of Venus and the sky and the magnitude of their deviations from the wave-lengths of Table I show, moreover, that the oxygen lines produced by the earth's atmosphere in the spectrum of the planet are not measurably shifted by blending with lines originating in the atmosphere of Venus and wide enough to overlap those of terrestrial origin.

The B band is producible by a much smaller quantity of oxygen than the a band and therefore furnishes a more sensitive test. King has recently shown that 39.4 m of air at 72 cm pressure, equivalent to 8 m of oxygen, give the lines of the B band faintly.[1] His solar spectrograms indicate that the lines of the B band produced by 39.4 m of air are comparable in intensity with solar lines of intensity 00 on the Rowland scale. On the spectrograms of Venus in this region lines of intensity 1 have about the same visibility as the limiting lines on King's spectrograms. To obtain an estimate of the length of an oxygen column which would produce the lines of the B band with an intensity of 1, we have made use of a valuable paper by Jewell[2] on the variation of the intensity of water-vapor lines with the quantity of water vapor traversed and of the change in intensity of the oxygen line λ 6287.953 with zenith distance. Jewell determined the intensities of Fraunhofer lines—000 to 6— in terms of the Fe line λ 5930.406. Graphs from these data show that the intensity intervals from 000 to 6 are roughly equal, and that the intensity of the water-vapor line λ 5919.860 is strictly proportional to the amount of water vapor traversed (Figs. 1, 2). A similar proportionality is shown to hold for the oxygen line λ 6287.953 and is assumed to hold for the oxygen lines of the B band. The interval from 00 to 1 is approximately 0.16 of the intensity of the Fe line λ 5930. This is equivalent to an increase in the length of path of 16 per cent. Hence the lines of the B band would probably appear on the spectrogram of Venus if the absorbing column contained the equivalent of 9.2 m of oxygen under ordinary conditions of pressure.

---

[1] *Mt. Wilson Contr.*, No. 232; *Astrophysical Journal*, **55**, 411, 1922

[2] *Astrophysical Journal*, **4**, 324, 1896.

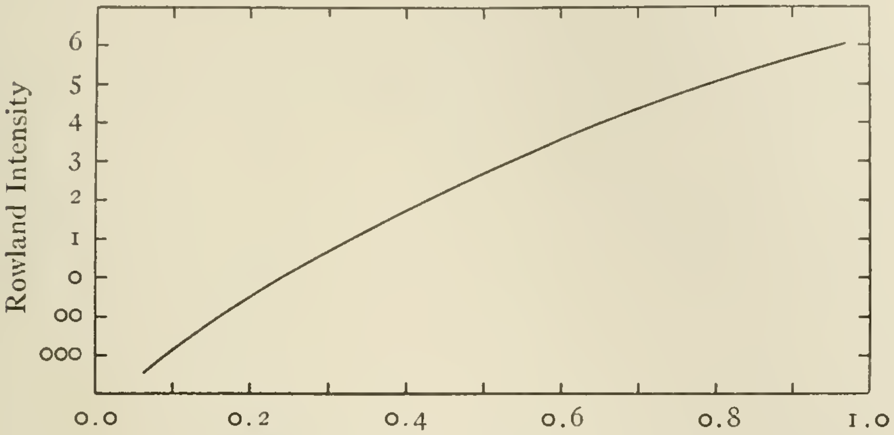

FIG. 1.—Rowland intensities in terms of λ 5930 taken as unity

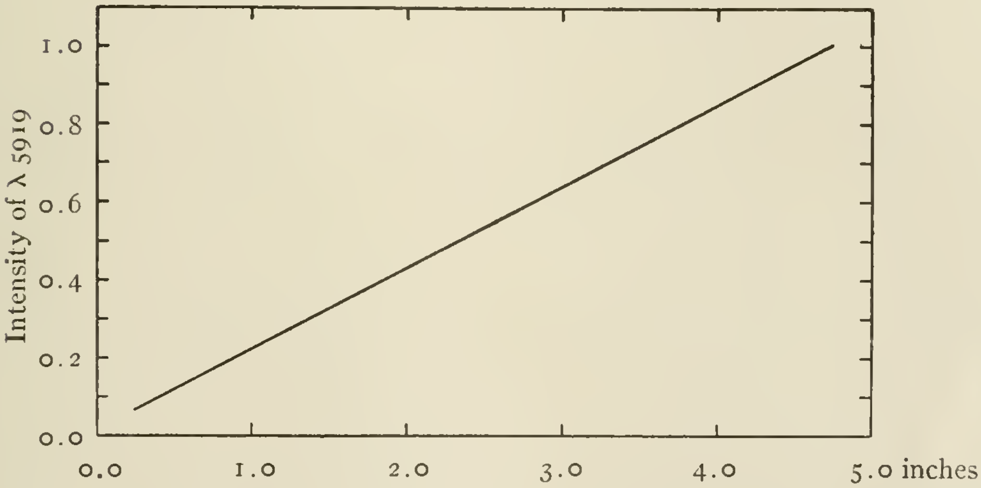

FIG. 2.—Intensity at the zenith of λ 5919 (wv) in terms of λ 5930 (Fe) for various amounts of precipitable water in the atmosphere expressed in inches.

Two spectrograms of Venus showing the B band, March 24 and March 27, 1921, were taken when the relative velocity was −10.68 km, the equivalent Doppler effect being −0.245 A. A similar spectrogram was taken August 14, when the relative velocity was +11.36 km, the Doppler displacement being +0.286 A. With the scale of 3 A per millimeter, the doublets of the B group are widely separated, but in the interspaces no lines are visible, where lines due to oxygen absorption in the atmosphere of Venus should appear, though solar lines of intensity 0 are present. Whether lines originating in the planet would be completely separated from the terrestrial lines by shifts of 0.264 A and 0.286 A depends on the widths of the lines. It is evident that at most only a small amount of oxygen is traversed in the atmosphere of Venus, and lines produced by it would be faint and narrow. On a plate of the B band taken by King with an air path of 39.4 m, the mean width of the single lines is 0.19 A. The mean width of these lines on plate V 359 is 0.27 A, and the Doppler shift +0.29 A, so that the edges of the lines would be separated by 0.06 A. Spectrograms V 301 and V 303 are not so suitable for this purpose, as the continuous background is fainter and the lines somewhat wider and the Doppler shift smaller than for V 359. When, however, the positions of the oxygen lines in these spectrograms are compared with their positions in the sky spectrograms, the measures show a displacement of 0.003 A to the red, whereas the Doppler shift would be 0.245 A to the violet. On V 359, the measured displacement is 0.002 A to the violet, with a possible Doppler shift of 0.285 A to the red. If, therefore, for any cause the lines of the B band produced by small amounts of oxygen on Venus are somewhat wider than those produced in the laboratory, the results show that there is no measurable influence of overlapping of the edges of the terrestrial lines by undetected Venus components.

The length of the path traversed through Venus' atmosphere in a layer of a given radial depth depends upon the phase angle of the planet and the position on the disk of the point from which the light is observed. For a point on the line perpendicular to the terminator and limb, whose distance from the limb in units of the length of that line is d, the zenith distances of the earth, z_e, and of the sun, z_s, are given by

$$\sin z_e = 1 - d - d \cos i ,$$

$$z_s = i - z_e$$

where *i* is the phase angle. Table III gives the total length of the path traversed by the solar beam for different phase angles and different distances from the limb in units of the radial depth. The secant equation used here is of course not applicable just at the limb and terminator.

TABLE III

$\sec z_e + \sec z_s$

d	*i*		
	70°	100°	130°
(Limb) 0.0	∞	∞	∞
0.1	3.0	3.7	5.5
0.2	2.6	3.2	4.8
0.3	2.4	3.1	4.8
0.4	2.5	3.2	5.0
0.5	2.6	3.5	5.6
0.6	3.0	4.0	6.6
0.7	3.5	5.0	8.2
0.8	4.7	6.9	11.6
0.9	8.1	12.9	22.9
(Terminator) 1.0	∞	∞	∞

At the middle point of the visible disk, corresponding to the center of the spectral band, the path for plates V 301 and V 303 was 5.2 times the radial depth of the layer penetrated, and for V 359 it was 2.5 times the depth. On the basis that lines of intensity 1 would be produced by 9.2 m of oxygen, it follows for V 301 and V 303 that the quantity of oxygen traversed did not exceed the equivalent of a column 2 m long under standard conditions. For light from near the terminator the path traversed in Venus' atmosphere is much longer. With the slit normal to the terminator, as in these observations, one edge of the spectrum corresponds to this longer path. For spectrograms V 301 and V 303 the path for the light at the point halfway between the center and edge of the spectrum was 7.5 times the radial depth of the layer. The edge of the spectrum shows no trace of oxygen lines due to absorption in the planet's atmosphere. Absorption capable of producing lines of intensity 1 would be expected if an oxygen layer equivalent to 1 m under normal pressure had been traversed in the passage through the atmosphere of Venus. As the oxygen in the earth's atmosphere is equivalent to a column 1500 m long, it follows that the oxygen in the path through Venus' atmosphere was less than one-thousandth of that in the terrestrial atmosphere.

WATER VAPOR

Five spectrograms of Venus taken when the relative velocity of Venus and the earth was −12.8 km, the corresponding Doppler shift being −0.252 A, form the basis of the investigation on water vapor. The relative velocity was sufficient to separate completely lines produced by absorbing gases common to both atmospheres. No traces of lines due to the planet's atmosphere are discernible on the spectrograms.

An upper limit for the amount of water vapor in the atmospheric layer on Venus penetrated by the solar beam may be found by the following considerations. Spectrogram V 282 was taken at mean zenith distance 76°. The average quantity of precipitable water above Mount Wilson is 0.69 cm[1] (the mean for the days of observation was 0.72 cm). The water-vapor line λ 5919.860 was of intensity about 5 on the Rowland scale, and telluric water-vapor lines of intensity 000 and 00 can be identified on the spectrum of Venus. Had a like quantity of water vapor been present in the planet's atmosphere above the reflecting surface, the intensity of the component of λ 5919.860 due to Venus should have been about 4 as against 5 for the terrestrial line, since the water-vapor masses traversed would have been 2.5 cm for Venus and 2.9 cm for the earth, the two respective paths being 3.6 and 4.1 times that for zenith distances 0. For the point half-way between the center of the disk and the terminator the water mass traversed would have been 4.2 cm, corresponding to solar intensity 7 for the water-vapor line λ 5919.860. These results are deduced from the graphs of Jewell's data. Terrestrial water-vapor lines of 00 intensity are easily seen on the plate, but no line is visible 0.25 A to the violet of the terrestrial line λ 5919.860, in which position 0.7 cm of water above the apparent surface of Venus would have produced a line of intensity 7. As the water vapor traversed in the atmosphere of Venus was not sufficient to produce the line λ 5919.860 with intensity 00, there must have been less than 1 mm of water in the layer of the planet's atmosphere traversed by the solar beam, for a line of intensity 00 is produced by 16 per cent of the water vapor necessary for a line of intensity 7.

---

[1] *Annals of the Astrophysical Observatory*, 3, 189, 1913.

Measurements of the wave-lengths of eight water-vapor lines were made on the five spectrograms of Venus and on four of the sky. The wave-lengths in Table I were obtained from solar spectrograms with a dispersion four times that used in this investigation. For these closely crowded lines the mean excess of 0.008 A shown by the Venus measures in Table II, when they are compared with the values given in Table I, represent probably the systematic errors associated with the measurement of spectral lines not well separated and varying in intensity from time to time as is characteristic of atmospheric lines. The difference is positive, whereas it should be negative if there were a measurable effect due to partial superposition of lines produced by water vapor in Venus' atmosphere.

DISCUSSION

These observations indicate that the previous spectroscopic evidence for oxygen and water vapor in the atmosphere of Venus, depending upon visual observations of a change in line intensity, is not reliable, that in fact there is no acceptable spectroscopic evidence of the presence of either. On the other hand, they do not show the complete absence of water vapor and oxygen from the planet's atmosphere, but that, to the depth penetrated by the solar beam, they are not present beyond a definite low limit.

Previous to Russell's[1] investigation in 1898 the accepted view as to the extent of Venus' atmosphere made it much denser than our own.[2] Russell showed that the prolongation of the cusps, formerly attributed to refraction, was mainly due to diffuse reflection of light by the planet's atmosphere. He concluded that the horizontal refraction at the apparent surface cannot exceed 12′ as against 34′ for the earth, and that there is no satisfactory evidence that the atmosphere of Venus at the apparent surface is more than one-third as dense or extensive as the earth's at sea-level. The entire height above the apparent surface he thinks may be thirty miles as compared with the earth's forty, thus implying a pressure at this surface of perhaps one-tenth that of the earth's atmosphere at sea-level. He attributes the prolongation of the cusps visible in daylight to a hazy layer of fog or dust lying below the 4100-foot level, a haze-bank whose upper boundary presents a more or less abrupt decrease in haziness, and whose lower portions may at times be obscured by low mountains, evidenced by irregularities in the thin circle of illumination on the side opposite the sun when Venus is at inferior conjunction.

---

[1] *Astrophysical Journal*, 9, 284, 1899.

[2] Young, *Manual of Astronomy*, p. 356, 1912.

A. W. Clayden[1] makes a strong presentation of the view that Venus has a moisture-laden atmosphere as dense and extensive as that of the earth. He decides on a long period of rotation, but one less than 225 days. He assumes that a high and heavy layer of pillared cumuli covers the cyclonic areas of low pressure and rising vapor, that over the regions of greater pressure the anticyclonic circulation results in lower detached masses of cumuli between which we see perhaps the shaded surface of the planet, and that a filmy veil of cirrus produces the prolongation of the cusps.

If, as suggested by Russell, the pressure at the visible surface is only one-tenth of an atmosphere, then the atmosphere of Venus is much poorer in oxygen than the earth's atmosphere, as the quantity of oxygen in Venus' atmosphere above the visible surface is less than the equivalent of 1 m, while in our atmosphere above the level of similar pressure there are 104 m of oxygen. If the reflection takes place at the upper surface of a 4100-foot haze-bank, which Russell suggests may be partially cut off at times by low mountains and therefore may not be far above the actual surface of the planet, then the oxygen above this low level is less than one-thousandth of that in the earth's atmosphere above Mount Wilson, elevation 1739 m.

If, on the other hand, it be assumed, as by Clayden, that the atmosphere of Venus is similar in composition and extent to ours, it follows that the reflected sunlight has not penetrated to a point less than 43 km from the real surface of the planet and has traversed but an insignificant path through its atmosphere, since in the earth's atmosphere there is above the 43 km level the equivalent of a meter of oxygen under normal pressure, an amount capable of registering on our spectrograms. The question of the depth to which the solar beam penetrates the planet's atmosphere and the probability that it reaches a point much nearer the real surface than 43 km are considered in detail in the discussion of water vapor.

---

[1] *Monthly Notices*, 69, 195, 1909.

TABLE IV

AMOUNT OF OXYGEN ABOVE A GIVEN ELEVATION

Elevation	Pressure	Oxygen
km	mm	m
0	760	1490
5	405	722
10	201	324
15	90	135
20	41	54
25	19	23
30	8.6	10.0
35	3.8	4.2
40	1.6	1.76
45	0.85	0.73
50	0.40	0.30

Any conclusion as to water vapor must rest upon the nature and temperature as well as the elevation of the apparent surface at which diffuse reflection takes place. The high albedo has been considered evidence of a cloudy surface, but the equally high reflecting power of Vesta indicates that this evidence is not definitive, since for Vesta there is no question of a cloudy surface. Russell[1] gives a Bond albedo of 0.59 for Venus. Using 65 per cent as the reflecting power of a cloudy surface, Abbot and Fowle[2] found 0.60 as the corresponding albedo for a cloud-covered earth. Aldrich[3], under more favorable conditions of observation, obtained 78 per cent as the reflecting power of clouds, from which the albedo calculated in the same manner is 0.75 for a cloud-covered earth. Russell says that the Bond albedo A should not be used for comparison with the observed reflecting power of terrestrial substances, but a quantity p, which he defines in an article on the albedo of

[1] *Loc. cit.*, p. 190.

[2] *Annals of the Astrophysical Observatory*, 2, 161–163, 1908.

[3] *Smithsonian Misc. Collections*, 69, 10, 1919.

planets and satellites.[1] For Venus p is 0.49 while for clouds it is 0.78. Both the reflecting power and the Bond albedo are considerably less than would be expected if Venus is completely cloud covered.

The conditions of Venus' atmosphere depend in large measure upon the period of rotation, the temperature, and the temperature gradients, all undetermined quantities. The period of rotation is quite probably not less than fifteen days, the limit shown by Slipher's observations with which our own agree. With a period of rotation equal to that of the orbital revolution, it is reasonable to assume, as Arrhenius suggests,[2] that water vapor and all other constituents of an atmosphere would collect and be congealed on the side of the planet turned away from the sun where a temperature near absolute zero would prevail. But the illumination of the whole circumference of the disk when Venus is at inferior conjunction, attributed to scattering and refraction, shows the presence of an atmosphere of considerable extent. These considerations give grounds for assuming that the period of rotation is shorter than that of the orbital revolution and hence is between the extremes of 15 and 225 days. For an intermediate period of rotation, an atmosphere would be present over the region of insolation, subject probably to violent disturbances near the terminator. This would be in harmony with Quenisset's[3] observations, both photographic and visual, of extensive and rapid changes in the obscuring envelope, indicating a shallow atmosphere.

The region of maximum cloudiness in the terrestrial atmosphere is mainly below 4000 m,[4] coinciding roughly with the average altitude of the zero isotherm, which is 3000 m.[5] The corresponding region of cloudiness in the atmosphere of Venus would be where the temperature and humidity conditions are similar. According to Abbot and Fowle,[6] the mean temperature of the earth's surface is

---

[1] *Astrophysical Journal*, 43, 191, 1916.

[2] *Worlds in the Making*, p. 61, 1908.

[3] *Comptes Rendus*, 172, 1645, 1921.

[4] Humphreys, *Physics of the Air*, p. 309, 1920.

[5] Hann, *Handbook of Climatology*, p. 250, 1903.

[6] *Annals of Astrophysical Observatory*, 2, 173–175, 1908.

287°.2 A, but the temperature of the true radiating surface of the earth as a planet is 263° A, this surface being chiefly the water-vapor layer at an elevation of 4000 m or more above sea-level. The elevation of a water-vapor radiating surface on Venus, however, would probably be greater owing to higher temperature. Using 2.5 calories as the solar constant, Poynting[1] gives the average temperature of an ideal planet at Venus' distance from the sun as 342° A, and at the earth's distance as 290° A. With 287°.2 A for the temperature of the earth the temperature of Venus becomes 337° A.

If the surface temperature of Venus be taken as 337° A and a temperature gradient of 6° per kilometer be assumed in Venus' atmosphere, such as obtains on the earth, the elevation of the zero isotherm would be 11 km, that of a water-vapor radiation surface 12 km, and that of the isothermal layer 19 km, which are to be compared with 3, 4, and 11 km for the earth.

The conditions at Mount Wilson offer favorable opportunities to study the increase in the relative humidity of the air above a cloudy surface. The velo cloud,[2] as the Spanish called the "high fog" of southern California, often covers the valleys to a height of 1200–3000 feet, especially during the months of May and June. For nine clear days in May and eight in June, 1921, the mean vapor pressure on Mount Wilson was 3.25 and 4.05 mm, respectively, while for nine days in May and twenty-one in June, with clear sky above and the velo cloud 4000 feet below and two to five miles distant, the respective vapor pressures were 4.65 and 5.28 mm, about 35 per cent greater. In the case of Venus' atmosphere with a water-vapor content sufficient to form a continuous layer of cumulus clouds exposed to nearly twice the intensity of the solar radiation at the earth, the water vapor above the dense cloud layer would probably exceed the increase at Mount Wilson when velo clouds are 4000 feet below and several miles away. This increment is two or three times the quantity our spectrograms should record. Granting the probable circulation in the planet's atmosphere suggested by Clayden, it seems also probable, especially over the anticyclonic

[1] *Collected Scientific Papers*, p. 315, 1920.

[2] Carpenter, *The Climate and Weather of San Diego*, 1913.

areas, that the solar beam would penetrate a region of the atmosphere where water vapor would be encountered in detectable quantity. The spaces not only above, but especially between the columnar cloud masses, must be more or less moisture laden, since, under the powerful solar radiation, evaporation and convection into the neighboring drier regions would take place as over the velo clouds, and under the downward anticyclonic flow, the clouds would be carried into regions of higher temperatures and more or less dissipated. The results would be an atmosphere of high humidity over extensive areas more or less open to observation, as the high cirrus assumed by Clayden would offer little obstruction.

If the dusky markings upon which investigators have based the observations interpreted as showing short rotation periods are actual surface features of the planet, or if they are a transient thinning of a cloudy envelope, it is probable that we there see down to levels at which the humidity would be high in an atmosphere so heavily moisture laden that the planet is enveloped in a blanket of clouds. Spectrogram V 274 was taken eight hours later than Quenisset's photographs showing extensive dusky areas, but no traces of water-vapor lines are discernible on any part of the spectral band.

If the brilliant white spots from which the long rotation period has been deduced really belong to the planet's surface, and, as suggested, are snow-covered mountain peaks extending into the upper atmosphere, it seems probable that water vapor would be spectroscopically detectable by its absorption lines were they to stand free from the corresponding terrestrial lines, as they would in our spectrograms. It is to be considered also that the spectrograms were taken in light of long wave-length, for which scattering is relatively small and the consequent penetration into a hazy atmosphere great. In the case of the oxygen lines, near λ 6900, the depth from which the light is reflected is well below the apparent visual surface.

If, however, the reflecting surface consists of a permanent layer of cirro-stratus, the quantity of water vapor traversed by the reflected beam would be small, as cirro-strati are formed in the upper troposphere where the temperatures are very low. These low temperatures practically insure that cirro-strati consist of ice crystals, but as at such low temperatures there is little water to condense, their structure is necessarily more or less tenuous and fibrous and consequently the reflected light will have penetrated the layer to a great depth. Above such a cloud-surface there would be the thinner cirrus to which the prolongation of the cusps is due, and the still higher atmosphere which produces by refraction the illumination around the planet's circumference observed at inferior conjunction.

Reflection from a layer of cirri gives the shortest possible path for the light in the planet's atmosphere. The water vapor above the cirrus level may be insufficient for detection by observations on the lines in the rain-band. The spectrographic test for oxygen by observations on the B band is, however, much more sensitive. In the earth's atmosphere above the cirrus level there is the equivalent of 274 m of oxygen at sea-level; above 19 km, the elevation assumed for the cirrus level on Venus, there is still the equivalent of 65 m, but our observations show that oxygen on Venus above the reflecting surface is less than 2 per cent of this amount.

It is of interest to consider some alternatives to water-vapor clouds. It is possible that a very small quantity of water vapor would produce an impenetrable haze-bank if the atmosphere of Venus contained minute hygroscopic centers of condensation capable of producing cloud particles in an atmosphere where the humidity is much below that which otherwise would be essential to cloud formation.[1] With such a hazy atmosphere on Venus, analogous to but denser than the dry-weather haze that sometimes obscures the valley or lies along the lower reaches of the distant mountains viewed from Mount Wilson, the surface of the planet might appear much as we see it. To an observer on the planet's surface transmitted light would be rich in long wave-lengths, as to us when the earth's atmosphere is laden with volcanic dust. To an outside observer the color would depend upon the proportion of the light scattered in its atmosphere to that reflected from its surface.

Under the probable extremes of temperature on the opposite hemispheres of Venus it is conceivable that the violent atmospheric circulation would cause clouds of dust to be permanent features of the planet's atmosphere, dust composed of highly reflecting material such as that to which the high reflecting power of Vesta is due. Wilsing and Scheiner[1] give for liparitic pumice a reflecting power of 0.56, for rock salt 0.44, and for granular limestone 0.42. These are comparable with 0.49 for Venus and 0.48 for Vesta. It is to be observed, however, that the presence of two of these substances would imply the action of water at the time of their production or segregation. The dust storms that sometimes prevail for days over the deserts and occasionally sweep through the mountain passes suggest vividly the possibilities on a dry and wind-swept planet.

---

[1] Humphreys, *Physics of the Air*, p. 92, 1920.

Whether or not light reflected from the continually evaporating surfaces of clouds produces sufficient water vapor to give its absorption lines with observable intensity is a question whose answer would aid greatly in determining the character of the apparent surface of Venus and in solving the puzzling problems of its atmosphere. We hope later to obtain more observational data as to the humidity around and above clouds, and to extend the spectrographic observations to the water-vapor band near λ 7200, as the lines of this band are producible by smaller amounts of vapor and would furnish a more sensitive test of its presence. Other and quite as important information would be obtained from the relative color indices of Venus and terrestrial clouds and from direct photographs through violet and infra-red filters[2] as used by R. W. Wood for Jupiter and Saturn. These would show the apparent surfaces at widely different levels and offer the possibility of reaching the actual surface through the thinner portions of the atmospheric veil.

It has been too easily assumed, perhaps, that the atmospheric conditions on our nearest planetary neighbors are similar to those on the earth, and that on Venus development has followed along similar lines and by like stages as on the earth. It was long ago suggested by Koene,[3] of Brussels, that all free oxygen may have been formed from carbonic acid in the air. Arrhenius says that we may take it as established that the masses of free oxygen in the air and of free carbon in the sedimentary strata approximately correspond to each other, and that probably all the oxygen of the air owes its existence to plant life.[1] That a similar production of oxygen has apparently not taken place on Venus suggests that some condition is wanting. Possibly a deficiency of water has prevented or hindered the freeing of oxygen through vegetation, or it may be that the exacting conditions for the origin of life have not been satisfied so that the existing atmosphere may consist of other permanent or semipermanent gases such as nitrogen or carbon dioxide.

---

[1] *Potsdam Publications*, 20, Part IV, 1909.

[2] *Mt. Wilson Contr.*, No. 113; *Astrophysical Journal*, 43, 310, 1916.

[3] *Mémoires de Chimie*, 1856.

MOUNT WILSON OBSERVATORY
July 1922

---

[1] *Worlds in the Making*, pp. 58, 59.

THE SOURCE OF LUMINOSITY IN GALACTIC NEBULAE[1]

By EDWIN HUBBLE

ABSTRACT

Relation of the luminosity of galactic nebulae to the magnitudes of associated stars. (1) *Diffuse nebulae.* If, as has been suggested, these nebulae owe their luminosity to radiations from associated stars, then the angular extent of nebulosity should increase with the apparent brightness of the stars. More precisely, if we assume that the clouds of nebulosity are illuminated by stellar light whose intensity varies inversely as the square of the distance from the stars; that each part of a nebula reflects or re-emits, without change in actinic value, all the starlight intercepted by it; and that the light from the stars themselves reaches us undimmed by absorption, then the square of the maximum angular extent of nebulosity a, for an exposure E, should be proportional to E times the apparent luminosity of the star I, or $a^2/E=a_1^2/60=I\times$ const., or $m+5\log a_1=B$, where a_1 is the angular distance reduced to a uniform exposure of 60^{m}. For a Seed 30 plate and a focal ratio of 5 to 1, B is equal to 11.6 or 10.6, according as the line joining the star to the faint nebulosity is perpendicular to the line of sight or has the mean inclination corresponding to random direction. To test this equation, data for eighty-two nebulae were plotted, $\log a_1$ against m. The points lie near the line: $m+4.9\log a_1=11.0$, thus showing that the inverse-square law holds closely and that the other assumptions are approximately correct. The mean deviation of the points from the line, over an interval of 14 magnitudes, is only $\pm 0\overset{\mathrm{m}}{.}8$; but thirteen points lie above the limiting theoretical curve. The probable explanation is that in these cases the apparent brightness of the stars is diminished through absorption by nebulosity between the star and the observer, that is, the third assumption is not wholly justified. This is borne out by the fact that these stars show a color excess which is usually greater than the residual magnitude. While most of the nebulae have continuous spectra, in eighteen cases the spectra are emission, and thus differ widely from the spectra of the associated stars. Since the corresponding points show no systematic deviation from the theoretical curve, the luminosity must be due to re-emission of light of the same total actinic value, rather than to reflection, and this suggests the possibility that the light producing the continuous spectrum is also re-emitted. The great loop in Cygnus is a conspicuous exception, since no sufficiently bright star is in evidence. The star, perhaps, is hidden or dimmed by nebulosity. Reduced to absolute magnitudes, the foregoing equation becomes $M+5\log l=2.5\log E-5.52$, where l is the linear distance in parsecs from star to nebulosity and E is in minutes. For Rigel, $M=-5.6$, an equivalent exposure of thirteen hours shows nebulosity, presumably made luminous by it, extending to $12\overset{\circ}{.}5$, or ninety-three light-years. (2) *Planetary nebulae.* When certain systematic corrections suggested by observations made at Mount Wilson are applied to data given by Curtis for the limiting exposure times and the apparent magnitudes of the nuclei for fifty-six objects, the angular distance A_1 of the brightest details of luminosity from the central stars, reduced to uniform exposure time on the assumption of an inverse-square law of luminosity with respect to the central stars as sources, varies with the photographic magnitude of the central stars according to the equations: $m+(5.3\pm0.4)\log A_1=17.9$, or $m+5\log A_1=17.6\pm0.2$. The first of these is the correlation curve derived from the data; the second, the curve having the theoretical slope which best represents the plotted points. The correlation between m and $\log A_1$, however, is not nearly as close as in the case of the diffuse nebulae. The residuals, for instance, seem to be related to the type of planetary, averaging $+1.8$ for the ring type, and -1.5 for globular

---

[1] *Contributions from the Mount Wilson Observatory*, No. 250.

objects. The corresponding theoretical equation, based on the assumption stated above for diffuse nebulae, but for an exposure time of six seconds, is: $m+5 \log A = 13.6 \pm 0.3$. Hence, the observed luminosity per unit area is about four magnitudes brighter than the theoretical. The discrepancy for these nebulae may be due to a difference between the spectra of the nebulosity and of the nuclei, the latter having relatively much more energy in the ultra-violet; or it may indicate that the radiations which excite the luminosity are chiefly corpuscular.

Revised photographic magnitudes of the nuclei of planetary nebulae.—The values given by Curtis for fifty-six objects seem to require a systematic correction of

$$+0.173m-3.37.$$

New cometary nebulae at $\alpha = 6^h 3^m$, $\delta = +18°42'$ (1920) shows striking similarity to the variable nebula N.G.C. 2261, although variability has not yet been established.

I. DIFFUSE GALACTIC NEBULAE

This paper gives the results of an attempt to test the theory that stellar radiations are the source of luminosity of galactic nebulae. V. M. Slipher[1] found that in the case of Merope, Maia, ρ Ophiuchi, N.G.C. 2068 and N.G.C. 7023 the absorption spectrum of the nebulosity agreed, approximately at least, with the spectra of the brightest involved stars. On this ground he suggested that these nebulosities at least are shining by reflected light from the involved stars. Hertzsprung[2] made a quantitative test of this suggestion in the case of the Pleiades nebulosity by determining the surface brightness at several points in the nebulosity and comparing the results with those derived by spreading the light of the stars over spherical shells of radii equal to the distances from the stars to the points of nebulosity whose surface brightness he had measured. He found the nebulosity to be from 4 to 5 magnitudes fainter than would be expected on a theory of total reflection, and concluded that, if a suitable albedo were assumed, the reflection of star light could account for the nebular luminosity. H. N. Russell[3] has accepted the idea of reflection for diffuse nebulae with continuous spectra, and has advanced the theory that galactic nebulae with emission spectra, diffuse as well as planetaries, are excited to luminosity by radiations from involved or neighboring stars.

The writer has found that particular stars can be selected which are obviously involved in or conspicuously associated with practically every known diffuse nebulosity. The spectra of these stars bear a definite relation to the spectrum of the associated nebulosity, such that if the stellar spectra are earlier than B1, the nebular spectrum is emission, and, if the stellar spectra are later than B1, the nebular spectrum is continuous. Nebulosity associated with stars of the critical type B1 usually possesses a spectrum of mixed characteristics. The transition in nebular spectra from emission to continuous, although rapid, is quite smooth. It is not abrupt. The only pronounced exception to the rule of spectral relation is the possibility that stars with highly enhanced spectra of the α Cygni type may be associated with nebulosity whose spectrum is predominantly emission. α Cygni itself and B.D. $-22^\circ 4510$, of the same type, appear to be associated with N.G.C. 7000 and N.G.C. 6514, respectively. Bright-line stars associated with emission nebulae are the exception and not the rule. Wolf-Rayet stars associated with diffuse nebulosity are rare. In the northern skies only two cases are known—N.G.C. 2359 and 6888. Both show some affinity with planetaries or with nova phenomena.

---

[1] *Lowell Observatory Bulletin* No. 55, 1912; 75, 1916; *Astronomical Society of the Pacific*, **30**, 63, 1918; **31**, 212, 1919.

[2] *Astronomische Nachrichten*, **195**, 449, 1913.

[3] *Proceedings of the National Academy of Sciences*, **8**, 115, 1922; *Observatory*, **44**, 72, 1921.

This definite spectral relation suggests that nebular luminosity depends to a certain degree at least on stellar radiations, and an attempt has been made to test this quantitatively. The method employed was to determine the surface brightness of diffuse nebulosities giving continuous spectra, by means of the limiting exposure times necessary to just register the nebulosity under standard conditions. Preliminary results from a small number of objects demonstrated that the brightness and extent of the nebulosity are definitely related to the magnitude of the associated stars, and that existing photographs could be used to establish the relationship. Accordingly Table I was constructed from an examination of the plates already available. In the first column is given the catalogue designation of the nebulae; in the second column, the spectral type of the nebulae, E and C for observed emission and continuous spectra, e and c for the same characteristics, not observed, but inferred from the spectral types of associated stars, according to the rules given in the preceding paragraph; in the third column the apparent photographic magnitudes, m, of the associated stars, combined, if a group of stars appears; in the fourth, the spectral type of the associated stars; in the fifth, the color excess[1] of these stars; in the sixth, the exposure time, E, in minutes, of the plates examined; in the seventh, the greatest angular distances, from the stars, in minutes of arc, at which nebulosity could be detected. For a group of stars involved in nebulosity, a was measured from the mean position of the stars. In most cases of this sort the extent of the groups of stars is small compared to the extent of nebulosity. In the eighth and ninth columns are given the quantities $\log E$ and $\log a$; in the tenth, the corrected quantity $\log a_1$, representing $\log a$ reduced to a uniform exposure time of 60 minutes; in the eleventh, the designations of the stars whose magnitudes are given in the third column; in the twelfth column the instruments employed in obtaining the photographs examined.

The data are fairly homogeneous, as the plates used were all Seed 30's, most of them taken with the 60-inch and 100-inch reflectors, both of focal ratio 1 to 5. Several were taken with a Tessar Ic lens, called "Kodax" in the eleventh column, and with a 10-inch Cooke astrographic lens, both of which have focal ratios 1 to 4.5. In these cases the values of $\log E$ were corrected by the quantity $+0.12$ in order to reduce them to the Newtonian reflector system. A few measures are from photographs by Barnard, made with the 10-inch Bruce lens of focal ratio 1 to 5, and designated "Barnard" in the twelfth column. A small correction should be applied to $\log E$ in these cases in order to allow for the light cut off by the Newtonian flat, but the amounts and the numbers are so small that they have been disregarded.

The photographic magnitudes for stars brighter than 6.0 are from visual magnitudes found in the *Harvard Annals*, to which have been applied both color indices and color excess. Magnitudes of the fainter stars are from polar comparisons made by the writer, and are on the Mount Wilson scale.

The quantities used in the following discussion, m, a, and E, are quite independently determined, and there is no reason to suspect

---

[1] The color excesses are taken from *Mt. Wilson Contr.* No. 187; *Astrophysical Journal*, 52, 8, 1920; and from further unpublished measures by Seares and Hubble. The latter values are provisional. Final values will appear in a joint paper to be published shortly.

TABLE I

Object	Spec. Nebula	*m*	Spec. Star	*CE*	*E* min	*a*	Log *E*	Log *a*	Log a_1	Star	Instrument
B.D. +64°13	c	10.4	B2	0.65	100	1′.5	2.000	0.176	0.065	.....	60-inch
N.G.C. 281	E	7.3	Oe5	0.10	210	14	2.322	1.146	0.874	B.D. +55°191	60-inch
I.C. 59, 63	E	2.2	B0p	0.00	60	33	1.898	1.518	1.458	γ Cassiopeiae	10-inch
B.D. +60°596	c	9.7	B2	0.40	120	3	2.079	0.477	0.326	.....	60-inch
N.G.C. 1333	C	10.9	B9p	0.30	180	4	2.255	0.602	0.364	.....	60-inch
B.D. +31°597	c	8.6	K2g	0.00	60	2	1.778	0.301	0.301	.....	100-inch
+29°565	c	9.6	A5	0.33	120	4.3	2.079	0.634	0.483	.....	60-inch
Merope	C	4.0	B5	0.00	120	25	2.079	1.398	1.247	.....	60-inch
Pleiades	c	1.2	.....	0.00	615	270	2.789	2.431	1.926	Entire cluster	Barnard
I.C. 348	C	9.0	B6–A1	0.80	180	2.3	2.255	0.362	0.124	B.D. +31°643	100-inch
N.G.C. 1491	E	11.3	B0	1.00	120	1.8	2.079	0.255	0.104	.....	60-inch
1499	E	3.7	Oe5	0.00	120	70	2.199	1.845	1.634	ξ Persei	10-inch
1514	E	9.7	Odp	0.70	90	1.8	1.954	0.255	0.167	B.D. +30°623	100-inch
I.C. 359?	C	13.5	K8d	0.00	240	0.4	2.380	−0.398	−0.699	.....	100-inch
N.G.C. 1624	E	12.0	Oe5	.....	120	1.5	2.079	0.176	0.025	.....	60-inch
1788	C	10.2	B8	0.22	90	3	1.954	0.477	0.389	B.D. −3°1013	60-inch
I.C. 405	E	5.8	B0p	0.30	90	11.5	1.954	1.061	0.973	Boss 1249	60-inch
2118*a*	C	0.2	B8p	0.00	60	180	1.898	2.255	2.195	Rigel	10-inch
2118*b*	c	0.2	B8p	0.00	600	750	2.898	2.875	2.315	Rigel	Kodax
N.G.C. 1976	E	4.8	Oe5, B0	.....	90	35	2.074	1.544	1.396	Trapezium	10-inch
1977	C+E	4.6	B1	.....	120	20	2.079	1.301	1.150	c′ Orionis	100-inch
I.C. 431	c	7.6	B2	0.17	120	3	2.079	0.477	0.326	B.D. −1°1001	100-inch
432	c	6.9	B2	0.05	120	4	2.079	0.602	0.451	−1°1005	100-inch
N.G.C. 2023	C	7.9	B2	0.30	90	6.8	1.954	0.832	0.744	−2°1345	60-inch
2024	E	1.4	B0	0.00	90	33	1.954	1.518	1.430	ζ Orionis	100-inch
I.C. 435	C	8.2	B3	0.20	90	4	1.954	0.602	0.514	B.D. −2°1350	60-inch
N.G.C. 2068	C	10.8	B5	1.00	120	4.5	2.079	0.653	0.502	+0°1177	60-inch
2071	C	10.8	B9	0.80	120	2	2.079	0.301	0.150	+0°1181	60-inch
Orion	c	1.4	B0	0.00	600	240	2.898	2.380	1.820	ζ Orionis	Kodax
Cometary Neb.	C	13.2	B1	.....	60	1.5	1.778	0.176	0.176	.....	100-inch
N.G.C. 2170	c	11.0	B1	1.02	90	1.5	1.954	0.176	0.088	B.D. −6°1415	60-inch

B.D. −6°1417	c	10.2	B5	0.55	90	3.1	1.954	0.491	0.403	......	60-inch
−6°1418	c	9.9	B5	0.65	90	1.5	1.954	0.176	0.088	......	60-inch
N.G.C. 2182	c	9.0	B3	......	120	2.0	2.079	0.301	0.150	B.D. −6°1431	60-inch
2183	C	14.0	B3	......	120	0.5	2.079	−0.301	−0.452	......	60-inch
2185	C	12.9	B3	......	120	1.3	2.079	0.114	−0.037	......	60-inch
B.D. −6°1444	c	10.8	B3	......	120	0.5	2.079	−0.301	−0.452	......	60-inch
N.G.C. 2175	E	7.3	Oe5	0.20	240	14	2.380	1.146	0.845	B.D. +20°1284	60-inch
2237	E	5.3	Oe5	0.00	180	35	2.375	1.544	1.246	*m* for group	10-inch
I.C. 446	C	11.8	B1	0.80	120	1.8	2.079	0.255	0.104	......	60-inch
447	C	7.7	......	......	120	7.5	2.199	0.875	0.664	*m* for group	10-inch
N.G.C. 2245	C	11.2	B1p	0.88	45	1.3	1.653	0.114	0.177	......	60-inch
2247	C	9.2	B2p	0.68	60	2.5	1.778	0.398	0.398	B.D. +10°1772	100-inch
2282	c	10.1	B2	0.35	90	2	1.954	0.301	0.213	+ 1°1503	60-inch
I.C. 2177	E	7.3	B0p	0.70	120	9	2.079	0.954	0.803	−10°1848	60-inch
B.D. −12°1771	C	8.1	B1	0.20	40	1.8	1.602	0.255	0.343	......	60-inch
−23°5277	c	9.2	B9	......	90	2.5	1.954	0.398	0.310	Triple star	60-inch
−23°5296	c	9.0	B1	......	90	2.5	1.954	0.398	0.310	......	60-inch
π Scorpii	C	2.8	B2	......	400	113	2.602	2.053	1.641	......	Barnard
I.C. 4592	C	3.9	B2	......	180	80	2.255	1.903	1.665	ν Scorpii	Barnard
4601*a*	C	7.1	B9, A0p	0.20	300	13	2.477	1.114	0.765	B.D. −19°4358, 9	100-inch
4601*b*	C	7.1	B8, A0	0.32	300	13	2.477	1.114	0.765	−19°4361	100-inch
σ Scorpii	c	3.2	B1	0.48	270	140	2.431	2.146	1.819	......	Barnard
I.C. 4604	C	5.1	B2, B3	0.50	270	60	2.431	1.778	1.451	ρ Ophiuchi	Barnard
4605	C	4.7	B3	0.12	270	50	2.431	1.699	1.372	22 Scorpii	Barnard
N.G.C. 6514	E	7.0	Oe5	......	90	10	1.954	1.000	0.912	B.D. −23°13804	60-inch
6523	E	5.4	Oe5, B0	......	90	12	2.074	1.079	0.931	*m* for group	10-inch
I.C. 4678	c	10.4	B3	0.50	60	2.3	1.778	0.362	0.362	B.D. −23°13906	100-inch
1274*a*	c	8.7	B1	0.35	60	2.7	1.778	0.431	0.431	−23°13997	100-inch
1274*b*	c	9.2	B1	0.35	60	2.5	1.778	0.398	0.398	−23°13998	100-inch
N.G.C. 6589	c	9.8	B2	0.42	90	1.9	1.954	0.279	0.191	−19°4940	100-inch
6590	c	10.5	B3, B5	0.40	90	2.1	1.954	0.322	0.234	−19°4946	100-inch
I.C. 1284	c	7.7	B2	0.50	90	5	1.954	0.699	0.611	−19°4953	100-inch
N.G.C. 6611	E	7.3	Oe5	......	90	6	1.954	0.778	0.690	*m* for group	60-inch
I.C. 1287	c	6.1	B2	0.62	270	25	2.551	1.398	1.011	Boss 4687	10-inch

TABLE I—*Continued*

Object	Spec. Nebula	m	Spec. Star	CE	E	a	Log E	Log a	Log a_1	Star	Instrument
N.G.C. 6726, 7	C	7.1	B9	0.10	60	3.8	1.778	0.580	0.580	B.D.−37°13023,4	100-inch
6729	C	10.0	Gp	......	60	1	1.778	0.000	0.000	R Cor. Aust.	100-inch
6888	E	6.7	Ob	......	180	8	2.255	0.903	0.665	B.D. +37°3821	60-inch
I.C. 4954, 5*a*	c	13.7	B3	1.10	60	0.4	1.778	−0.398	−0.398	....	60-inch
4954, 5*b*	c	12.2	B3	0.90	60	0.6	1.778	−0.222	−0.222	....	60-inch
4954, 5*c*	c	14.4	A3	0.55	60	0.2	1.778	−0.699	−0.699	....	60-inch
N.G.C. 6914*a*	C	8.9	B3	0.00	180	3.0	2.255	0.477	0.239	B.D. +41°3737	60-inch
6914*b*	C	9.2	B4	0.00	180	2.5	2.255	0.398	0.160	+41°3731	60-inch
γ Cygni, *a*	......	3.0	F8p	0.00	180	115	2.375	2.061	1.763	....	10-inch
γ Cygni, *b*	......	3.0	F8p	0.00	180	75	2.375	1.875	1.577	....	10-inch
N.G.C. 7000	C+E	1.8	A3p	0.00	180	220	2.375	2.342	2.044	α Cygni	10-inch
7023	C	7.4	B2p	0.55	120	6	2.079	0.778	0.627	B.D. +67°1283	60-inch
B.D. +57°2309	c	6.5	B2p	......	120	9	2.079	0.954	0.803	....	60-inch
+67°1332	c	8.2	B4	0.05	90	4	1.954	0.602	0.514	....	60-inch
N.G.C. 7129	C	10.5	B3	0.60	60	1	1.778	0.000	0.000	....	60-inch
I.C. 5146	c	10.4	B1	0.97	120	5	2.079	0.699	0.548	B.D. +46°3474	60-inch
N.G.C. 7635	E	8.5	Odp	0.20	90	6	1.954	0.788	0.690	+60°2522	100-inch

The actual E is given for 10-inch and Kodax plates, but 0.12 is added to the value of log E in these cases to reduce to the Newtonian reflector system.

Pleiades. Trumpler's value of m for the entire cluster is used, and a color index of −0.10 is applied. E and a are taken from Barnard's photograph of the exterior nebulosity. *Publications Lick Observatory*, **11**, Plate 15, 1913.

I.C. 359? A nebulous star north following the nebula at $\alpha = 4^h14^m$, $\delta = +28°5'$ (1920), described by Barnard in *Astrophysical Journal*, **25**, 223, 1907, and which may be I.C. 359.

I.C. 2118. "*a*" refers to the brighter portion north preceding Rigel. "*b*" is the extreme limit of the faint extensions that trail off south preceding for several degrees into Eridanus.

Orion. Refers to the great exterior loop around the belt and sword of Orion. The following side of the loop was used and was referred to ζ Orionis as the nearest of the extremely bright stars. This procedure is questionable in detail but probably permissible in determining orders of magnitude.

Cometary Nebula. A bright uncatalogued cometary nebula at $\alpha = 6^h3^m$, $\delta = +18°42'$ (1920).

π Scorpii. E and a are from Barnard's photographs reproduced in *Astrophysical Journal*, **23**, 144, 1906.

I.C. 4592, 4604, 4605. E and a are from Barnard's photographs reproduced in *Astrophysical Journal*, **31**, 8, 1910.

N.G.C. 6729. This is the variable nebula about R Coronae Australis. The star is also variable and the measures refer to a particular date.

large systematic errors. The range in m is from 0.2 to 14.4; in a from $0\overset{'}{.}2$ to $750'$; in E from 40 min. to 790 min. The mean errors in m are estimated as about 0.1, and in a about 5 per cent. The actual observed E, is, of course, exact to the minute, but differences in sky conditions, state of mirrors, plates, and development, suggest a mean error in the equivalent exposure time of the order of 5 per cent.

The nebulosity fades more or less smoothly with increasing distance from the stars, and the points for which a was measured represent in general the limiting surface brightness which registers on the particular plate examined. If the exposures were all of the same duration, under uniform conditions, a comparison of m with a should then indicate the relation existing between nebular and stellar luminosity. If this relation were due to a reflection of star light, and the albedo of the nebulosity were constant, the relation would be expressed by $m+5\log a=K$ where K is a constant depending on the albedo, the limiting surface brightness shown on the photographs, and the distribution of angles which the directions, stars to points, measured for a, make with planes perpendicular to the lines of sight.

As a first step in the investigation, m was plotted against $\log a$, disregarding the differences in exposure times. This plot is shown in Figure 1. The extent of nebular illumination is clearly a function of the stellar luminosity, and the relation is approximately linear. A curve with a slope, or coefficient of $\log a$, equal to 5 can be fitted to the plot in the form

$$m+5\log a=11.9 \tag{1}$$

so as to represent the points fairly well. Considering the great differences in exposure times, and the fact that measures on the brighter stars are as a rule from longer exposures than those for the fainter stars, Figure 1 is pretty fair evidence that nebular luminosity obeys the inverse-square law with the associated stars as sources of illumination.

This assumption affords a simple method of referring the data to a homogeneous system by reducing $\log a$ to $\log a_1$, corresponding to a uniform exposure E_0, or inversely, reducing $\log E$ to $\log E_1$, corresponding to a uniform angular distance a_0. Let I and I_0 be the minimum intensities registered in exposure times E and E_0,

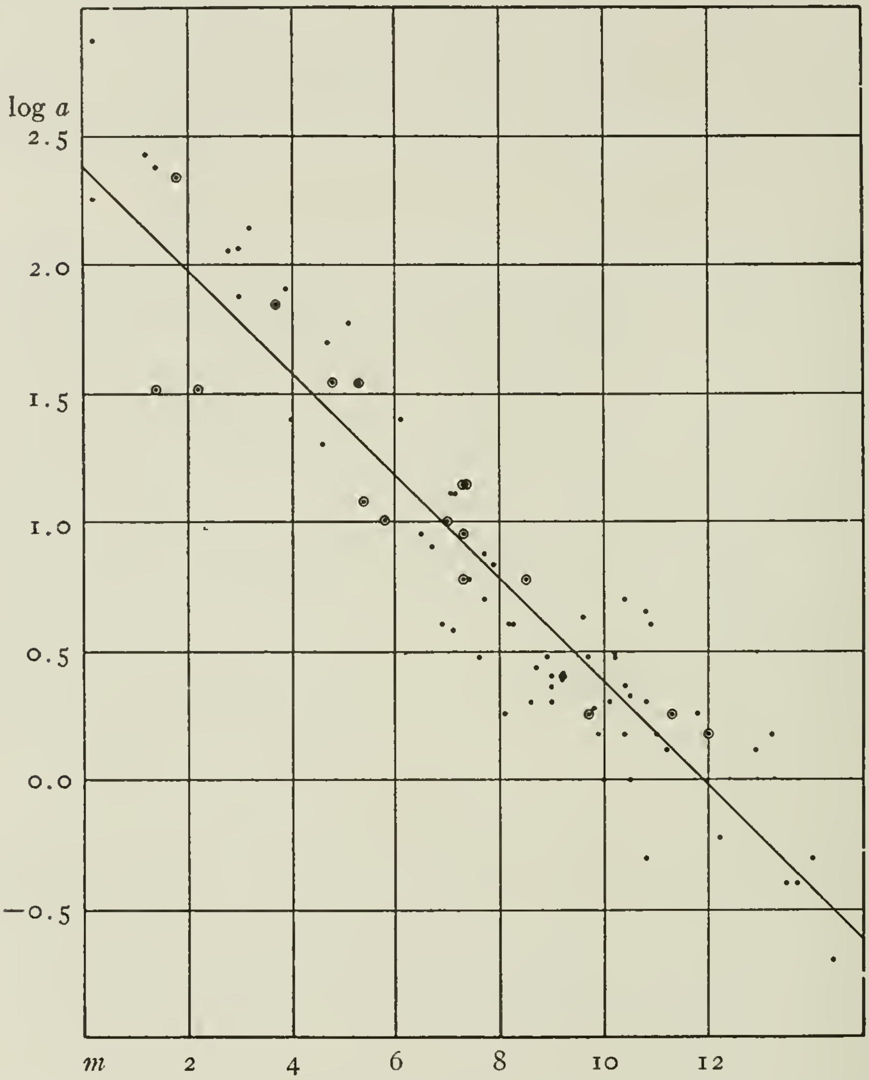

FIG. 1.—Photographic magnitudes of stars associated with diffuse nebulae (abscissae), plotted against the logarithm of the greatest angular extent of nebulosity from these stars (ordinates). The data are from Table I. Differences in exposure times of the plates examined are disregarded. The line represents the equation $m+5 \log a=11.9$. The coefficient of log a indicates that the nebular luminosity obeys the inverse-square law with respect to the stars as sources.

p Schwarzschild's exponent in the reciprocity law. Then, assuming the inverse-square law to hold rigorously for nebular illumination,

$$\left(\frac{a}{a_1}\right)^2=\frac{I_0}{I}=\left(\frac{E}{E_0}\right)^p \tag{2}$$

$$\log a_1=\log a+\frac{p}{2}(\log E_0-\log E) \tag{3}$$

likewise

$$\log E_1 = \log E + \frac{2}{p}(\log a_0 - \log a) \tag{4}$$

The magnitudes m can be plotted either against $\log a_1$, angular distances corresponding to a uniform exposure time, or against $\log E$, the brightness corresponding to a uniform distance; but with the scale properly chosen, the two figures would be identical, because of the relation derived from (3) and (4):

$$\log E_1 + \frac{2}{p} \log a_1 = \log E_0 + \frac{2}{p} \log a_0 = \text{Constant}$$

Log E_0 has been chosen as 60 minutes of time and $\log a_0$ as one minute of arc, and p has been assumed as unity. Thus,

$$\log a_1 = \log a + \tfrac{1}{2}(1.778 - \log E) \tag{5}$$

$$\log E_1 = \log E - 2 \log a \tag{6}$$

$$\log E_1 = 2 \log a_1 = 1.778 \tag{7}$$

Log a_1 was chosen as the quantity to be plotted against m in order that the result might be compared with Figure 1. The question of the proper value of p raises a serious theoretical difficulty which is minimized in the actual plotting by the use of a value for E_0 near the mean E, so that $\log E_0 - \log E$ in equation (5) is small. The various values of p used in discussions on stellar photometry range from about 0.75 to 1.00. No values have been directly determined for long exposures on nebular surfaces under actual observing conditions and there is very little basis on which to select the most probable value. However, the greatest difference in any particular $\log a_1$ as determined by equation (5) for the extreme values of p, is about 0.12. The mean difference is less than 0.04, which is of the same order of accuracy as the original data. These considerations seemed to justify the selection of $p = 1.00$ as the simplest procedure. The effect of using other values can be determined later, should the matter prove important.

Figure 2 shows the plot of $\log a_1$ against m. A least-squares solution gave for the adjusted curve

$$m+(4.90\pm0.13)\log a_1=11.02\pm0.10 \tag{8}$$

The simple mean of $m+5\log a$ is 11.10, and the corresponding curve differs from that of (8) by less than a tenth of a magnitude over the entire range of 14.2 magnitudes. The average deviation in m for both curves is about 0.8 magnitudes. The deviation of the coefficient of $\log a_1$ in (8) from the expected value of 5.0 is within the errors of observation.

A theoretical value can be computed for the constant on the right side of equation (8), by assuming the inverse-square law to hold rigorously and by assuming further that all the starlight intercepted by the nebulosity is re-emitted. Consider a point of nebulosity at distance a in minutes of arc from the star. The surface brightness of this nebulosity is determined on the above assumption by spreading the luminosity of the star over a spherical shell of radius a. Expressed in magnitudes per square second of arc, this surface brightness will be $m+2.5\log 4\pi(60a)^2$ or $m+11.64+5\log a$. Seares has determined the limiting surface brightness of an exposure of one minute on a Seed 30 plate, using a reflector of focal ratio 1 to 5.[1] This quantity, expressed in magnitudes per square second of arc, is 18.8±0.3. It applies approximately to all photographic instruments of an equivalent focal ratio. For an exposure of sixty minutes corresponding to the values of $\log a_1$, the limiting surface brightness is $18.8+2.5\,p\times1.778$ or $18.8+4.45\,p$. Equating these two expressions,

$$\left.\begin{aligned} m+5\log a_1&=7.16+4.45\,p\\ &=11.61 \text{ for } p=1.00\end{aligned}\right\} \tag{9}$$

Assuming a random distribution of directions from star to nebulosity, the mean a observed, projected on a plane perpendicular to the line of sight, should be less than the true a by the factor $\pi/2$. This difference can be corrected by increasing m by $5\log\pi/2=0.98$. Equation (9) then becomes

$$\left.\begin{aligned} m+5\log a_1&=6.18+4.45\,p\\ &=10.63 \text{ for } p=1.00\end{aligned}\right\} \tag{10}$$

---

[1] *Mt. Wilson Contr.* No. 191; *Astrophysical Journal*, 52, 162, 1920.

If the assumption that the light emitted by the nebulosity exactly equals the starlight intercepted is correct, then equation (10) should represent the points in Figure 2, and equation (9) should play the rôle of an upper limit to the points. The agreement between (10) and (8) is close enough to raise a strong presumption that the assumption just mentioned is justified by the facts. Thus

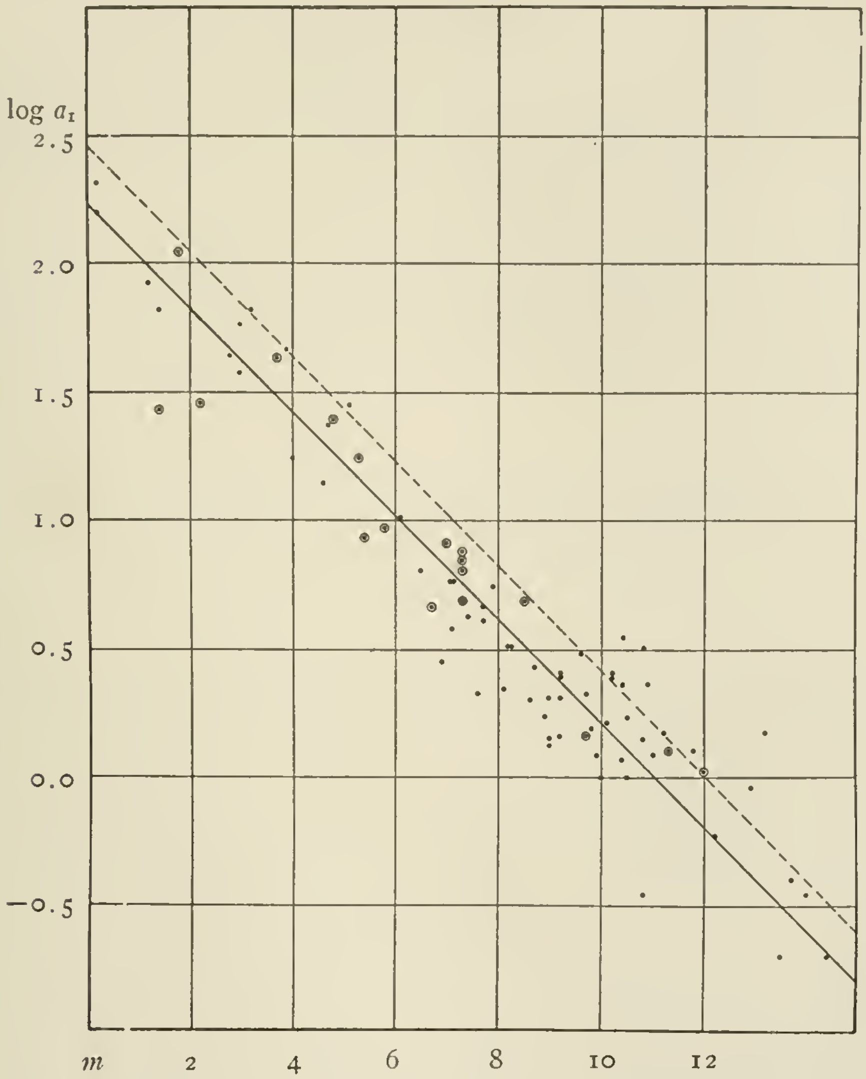

FIG. 2.—The same as Fig. 1, except that log a has been reduced to log a_1, corresponding to a uniform exposure time of one hour on Seed 30 plates with a reflector of focal ratio 1 to 5. The full line represents the curve $m+4.90 \log a_1=11.02$ derived from a least-squares solution. The broken line represents a limiting curve parallel to the full line, displaced 0.98 to the right.

(8) Observed.............. $m+4.90 \log a_1=11.02 \pm 0.10$

(10) Theoretical............ $m+5.00 \log a_1=10.63 \pm 0.3$

The difference in slopes can scarcely be shown on the plot, and the difference in the constants on the right side of the equations is just the sum of the probable errors. It should be noted further that the constant in (8) falls nearly half-way between those for equations (9) and (10), the theoretical limiting curve and the mean curve on the assumption of random distribution of the directions from star to points measured for a. Any deviation from random distribution in the observed data would fall in this direction, for in each case the maximum a was consciously sought.

Observations and theory can also be compared by using $\log a$ and $\log E$ directly in a generalized form of equation (10). Assuming again that the total amount of starlight intercepted is re-emitted by the nebulosity

$$\left.\begin{aligned} 18.8\pm0.3+2.5\log E &= m+11.64+5\log a \\ m+5\log a-2.5\log E &= 7.16\pm0.3 \text{ (limit)} \\ &= 6.18\pm0.3 \text{ (mean)} \end{aligned}\right\} \qquad (11)$$

The left side can be computed from the original data and proves to be 6.65±0.07 with an average residual of about 0.82. This lies almost exactly half-way between the theoretical limiting and mean values, and supports the suggestion that the data deviate from a random distribution in the direction of large angles to the line of sight. If the coefficient of $\log a$ in equation (11) be replaced by 4.90, as indicated in equation (8), the constant becomes 6.57.

This is not an independent method, for equations (9) and (10) reduce to equation (11) when the value of $\log a_1$ given in equation (5) is substituted into (9) and (10). The difference in the constant, $11.02-6.57=11.10-6.65=4.45$, is the quantity $2.5\,pE_0$ when p is taken as unity.

Equation (11) expresses a direct relation between the original data and should be the nicest method of procedure in the investigation. It is not well suited to least-squares solutions, however, because $\log a$ and $\log E$ are not independent. This difficulty is obviated by the transformation into equations (9) and (10).

Within the limits of error, equation (8) agrees with the theoretical mean curve expressed by equation (10). Disregarding for the moment possible deviations from random distribution in the data, a limiting curve should appear on the plot parallel to the mean curve and displaced 0.98 magnitudes toward the side of increasing m. Any points falling to the right of this limit require explanation, for they indicate that the nebulosity is too bright or the stars too faint for a strict agreement with the theory that diffuse nebulosity re-emits exactly the light it receives from associated stars. Such a limiting curve has been sketched as a broken line on the plot in Figure 2, and several points do fall beyond. The general evidence is very strong against the nebulosity being too bright, i.e., that it emits more light than it intercepts from the star, and such an explanation should be appealed to only as a last resource.

The most probable solution appears to be the diminution of the stars' apparent brightness by nebulosity intervening between them and the earth. This is a well-known phenomenon among stars involved in nebulosity and makes itself felt in the abnormally large color indices which such stars as a general rule possess. The color excess, measured color index *minus* that normal to the spectral type of the star observed, is probably due to scattering of starlight by intervening nebulosity. If scattering is responsible for the color excess, then the true photographic magnitude of the star, as seen free from its screen of nebulosity, would be brighter than the observed value by about twice the color excess.

The nebulosity responsible for the observed scattering is obviously between the star and the earth. If the path from star to point of nebulosity measured for a were reasonably free from intervening nebulosity, such a correction should certainly be applied to the observed m. If, on the other hand, the nebulosity responsible for the scattering is distributed symmetrically about the stars, then the observed m is just that which is effective in illuminating the exterior points of nebulosity which were measured.

An examination of the points falling beyond the limiting curve indicates that as a rule they are measured from stars with large color excesses, and that a correction figured on this basis will throw them on the safe side of the curve. The stars from which these 13 points were measured, with D their distance in magnitudes beyond the limiting curve and *CE* their measured color excesses, are listed below:

Star	*D*	*CE*
σ Scorpii	0.10	0.48
ρ Ophiuchi	0.15	0.50
B.D. +46°3474	1.05	0.97
B.D. +01177	1.20	1.00
B.D. −31013	0.10	0.22
B.D. −61417	0.20	0.55
B.D. −2312906	0.15	0.50
N.G.C. 1333	0.65	0.30
N.G.C. 2245	0.05	0.88
I.C. 446	0.30	0.80
N.G.C. 1624	0.10	....
N.G.C. 2185	0.70	....
Cometary Nebula	2.05	....

Color excesses are not available for the last three objects. N.G.C. 1624 is a small group of Oe5 stars involved in emission nebulosity. The combined magnitude is from estimated individual magnitudes and may be a few tenths in error. The stars in the last two nebulae show considerable color visually, and analogy with other objects of a similar nature suggests large values for the color excess. The cometary nebula is an uncatalogued object in a region of pronounced obscuration at $\alpha = 6^h3^m$, $\delta = +18°42'$ (1920) which shows a striking similarity to the variable nebula N.G.C. 2261. It is being followed for variability, but thus far without positive results. The color excess may not be large enough to account for the large *D*, but a small amount of general absorption could be postulated to make up the balance.

It is reasonable to suppose that in these 13 cases, the nebulosity responsible for the color excess is for the most part between the star and the observer, and that relatively little is between the star and point of nebulosity measured for *a*. An idea of how general is this dissymmetry of distribution about the stars of nebulosity responsible for the scattering can be derived from a study of relations between the residuals in Figure 2 and the color excesses. Measures of this last quantity are available for 63 points. There is no systematic difference in distribution between these and the points for which color excesses have not been measured. The residuals may therefore be taken directly from Figure 2. A least-squares solution of the observational equations $x+y\,CE=$ Residual in m, gives

$$R\pm 0.08=0.90\,CE-0.32 \tag{12}$$

If the scattering nebulosity were always symmetrically distributed about the stars, the coefficient of CE should be zero; if it were always between the star and observer and never between star and points measured for a, the coefficient should be approximately 2. An excess in scattering nebulosity between stars and points measured for a, over that between star and observer, would reduce the measured a and this effect could not be distinguished from that due to inclinations of the directions from star to measured points. The observed value of the coefficient of CE, namely 0.90, seems to indicate that the scattering nebulosity is distributed, not symmetrically, but rather at random about the stars. Corrections computed from equation (12) would provide only for the scattering nebulosity between star and observer in excess of that symmetrically distributed. It would reduce the constant in equation (8) by the quantity 0.32 and the resulting value, 10.70, would be in excellent agreement with that expected from theory, namely 10.63. Similar nebulosity not in the line of sight would reduce the true values of a, and a correction would in the mean tend to compensate the correction suggested by equation (12). The scattering effect probably will not seriously affect the mean values in Figure 2, although it offers a ready explanation for individual residuals.

A supplementary table of data was constructed from a homogeneous series of exposures made for the purpose of determining surface brightness of nebulosity from minimum exposure times necessary to show the nebulosity. The number of objects was small, but the results agree satisfactorily with those from Table I. The summation of $m+5\log a-2.5\log E$ is 6.50 ± 0.18, in good agreement with the theoretical value of 6.18 ± 0.30. The curve adjusted for the slope corresponding to the inverse-square law of luminosity is $m+5\log a_1=10.95\pm 0.18$. The correlation curve is $m+4.38\log a_1=10.54\pm 0.20$; but the points are not well distributed for a good determination of the slope, and the small value of the coefficient of log a_1 cannot seriously affect the general conclusions. The plot of log a_1 against m is shown in Figure 3.

The data in Table II are entirely independent of those in Table I except the values for m. Different points were measured for a, and the exposure times average about one-sixth of those in Table I. The range in E for the two tables is especially significant, running in the first from 40 minutes to over 10 hours and in the second from 7 seconds to 50 minutes. Individual comparisons of log a_1 have no meaning, for inclinations of the directions from star to measured points cannot be determined independently. The systematic difference in log a_1 is 0.015, or about $3\frac{1}{2}$ per cent, which is satisfactorily small and indicates that the distribution of directions and of scattering nebulosity is comparable in the two systems of data.

TABLE II

Object	m	CE	Spec. Star	E	a	Log E	Log a	Log a_1	Instrument
				min.					
N.G.C. 1333	10.9	0.30	B9p	3.0	0'.15	0.477	−0.824	−0.174	60-inch
Merope *a*	4.0	0.00	B5	1.0	1.67	0.000	0.222	1.111	60-inch
Merope *b*	4.0	0.00	B5	0.25	0.40	−0.602	−0.398	0.792	60-inch
I.C. 348	9.0	0.80	B6–B9	4.0	0.32	0.602	−0.495	0.093	60-inch
359	13.5	0.00	K8d	50	0.17	1.699	−0.778	−0.738	100-inch
N.G.C. 1788	10.2	0.22	B8	1.0	0.17	0.000	−0.778	0.112	60-inch
I.C. 2118	0.2	0.00	B8p	30	135	1.597	2.130	2.220	10-inch
N.G.C. 2023	7.9	0.30	B2	0.33	0.33	−0.477	−0.477	0.651	60-inch
I.C. 435	8.2	0.20	B3	3.0	0.40	0.477	−0.398	0.252	60-inch
N.G.C. 2068	10.8	1.00	B5	0.50	0.40	−0.301	−0.398	0.641	60-inch
2071	10.8	0.80	B9	1.0	0.30	0.000	−0.523	0.376	60-inch
Orion	1.4	0.00	B0	30	210	1.597	2.322	2.412	10-inch
N.G.C. 2245	11.2	0.88	B1p	0.25	0.17	−0.602	−0.778	0.412	60-inch
2247	9.2	0.68	B2p	0.13	0.083	−0.875	−1.079	0.247	100-inch
I.C. 4592	3.9	......	B2	40	45	1.722	1.653	1.681	10-inch
4603	8.4	0.85	B2	30	10	1.597	1.000	1.090	10-inch
4604	5.1	0.50	B2–B3	20	25	1.421	1.398	1.577	10-inch
4605	4.7	0.12	B2	10	4.5	1.120	0.653	0.982	10-inch
N.G.C. 6726	7.2	0.10	B9	0.33	0.13	−0.477	−0.875	0.252	100-inch
6727	9.1	0.80	B9	0.60	0.13	−0.222	−0.875	0.125	100-inch
6729	10.0	0.50	Gp	0.25	0.10	−0.602	−1.000	0.190	100-inch
N.G.C. 7023	7.4	0.55	B2p	0.17	0.20	−0.778	−0.699	0.569	60-inch
7129	10.5	0.60	B3	0.33	0.072	−0.477	−1.176	−0.048	60-inch

The actual E is given for 10-inch plates, but 0.12 has been added to the value of log E to reduce to the Newtonian reflector system.

Merope *a* refers to the well-known wispy nebulosity, while *b* refers to the small bright cometary nebulosity about 30″ south of the star.

I.C. 359. The catalogue designation is uncertain. The position is given in the notes to Table I.

Orion refers to the brightest portion of the great exterior loop at about $\alpha = 5^{h}45^{m}.5$, $\delta = +1°$ (1920).

The general conclusion from this investigation is that, within the errors of observation, the data can be represented on the hypothesis that diffuse nebulae derive their luminosity from involved or neighboring stars, and that they re-emit at each point exactly the amount of light radiation which they receive from the stars. Where stars of sufficient brightness are lacking in the neighborhood, or, if present, are not properly situated to illuminate the nebula as seen from the earth, the clouds of material present themselves as dark luminosity.

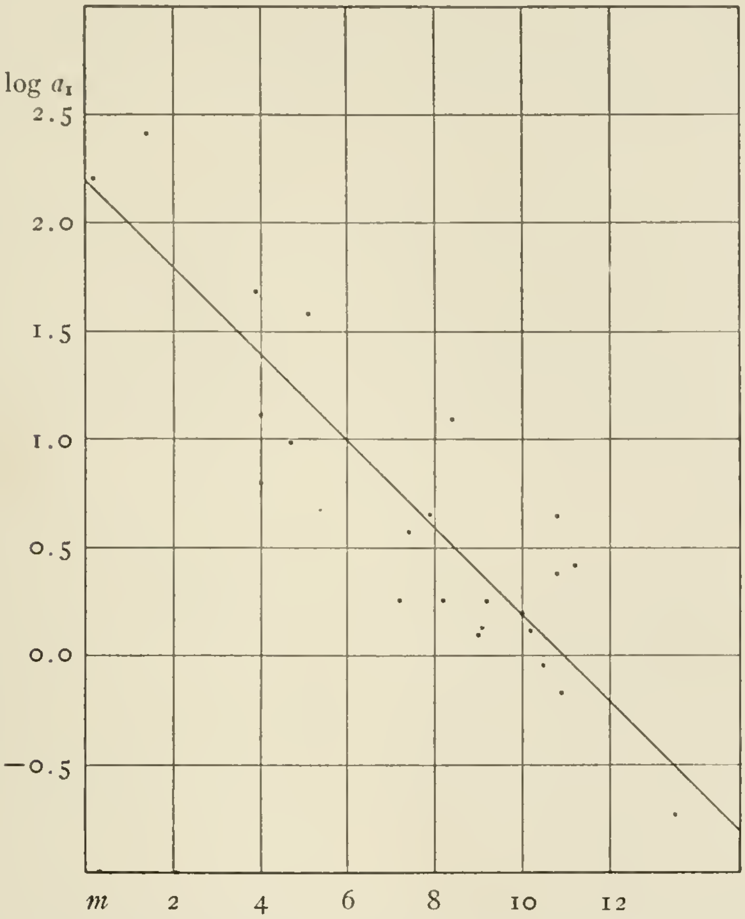

FIG. 3.—Photographic magnitudes of stars associated with diffuse nebulae (abscissae), plotted against the logarithm of the greatest angular extent of nebulosity from these stars (ordinates). The data are from Table II, derived from minimum exposures necessary just to register the brightest portions of the nebulae. Log a has been reduced to log a_1 corresponding to a uniform exposure of one hour on Seed 30 plates with a reflector of focal ratio 1 to 5. The straight line represents the equation $m+5 \log a_1 = 10.95$.

Eighteen of the objects listed in Table I show spectra which are predominantly emission. The points corresponding to these objects are mingled among the others in a thoroughly homogeneous manner and show no systematic characteristics whatsoever. Such a result was unexpected. The associated stars in these cases, with the exception of the Ob star B.D.+37°3821 in N.G.C. 6888, are of the usual Oe5 and B0 types,[1] hence the nebular luminosity cannot be a phenomenon of simple reflection, but must result from some process of absorption and re-emission of stellar radiation. The data indicate that within the spectral limits to which Seed 30 plates are sensitive the continuous radiations from the stars are absorbed by the nebulosity and completely re-emitted as discontinuous radiations within the same range of wave-lengths. This may be a mere coincidence, but the idea is suggestive and should be investigated in detail.[2]

The fact that the emission nebulae do not shine by simple reflected starlight raises a question as to the process of illumination in the nebulae which show continuous or absorption spectra. The evidence given by V. M. Slipher as to the agreement between spectra of nebulae and of associated stars in the cases of Merope and Maia, ρ Ophiuchi, N.G.C. 2068, and N.G.C. 7023, is in favor of the reflection theory.

Analogy with emission nebulae, however, suggests the possibility that the process may be one of absorption and re-emission. This view is supported by the manner in which emission nebulae with no perceptible continuous spectrum merge smoothly into "continuous" with no emission as the spectral types of the dominating stars pass from Oe5 to the middle B's. It is extremely difficult, in the reflection theory, to account for the absence of strong continuous spectrum from purely emission nebulae. One must suppose that the physical state of this type of nebulosity is quite different from that of "continuous" nebulosity, being such that reflection is not possible. Further, it would lead to the logical conclusion that the physical state of nebulosity depends upon and is determined by the spectral type of the associated stars. Such a relation is not impossible, for the intensity of stellar radiation, closely associated with spectral type, must play a large rôle in determining the distribution of nebulous particles of various sizes, and thus indirectly bear upon the distribution of spectral characteristics throughout a given nebula. It seems impossible at present to strike a balance between the two views concerning the mechanism of illumination, but it is worth mentioning that the analogy of emission nebulae is quite as strong an argument against, as the agreement of spectra is in favor of, the theory of pure reflection.

---

[1] γ Cassiopeiae and B.D. $-10°1848$ in I.C. 59, 63, and I.C. 2177 respectively show weak hydrogen emission lines.

[2] Plots similar to Fig. 2 were constructed for each of the various stellar spectral types in Table I; no systematic differences were found to exist.

Another striking characteristic of Figure 2 is the relatively small spread in the points and especially the complete absence of points falling far below the mean curve. The average deviation is about 0.8 in m or 0.16 in log a_1. The greatest single deviation to the left is 2.6 magnitudes or 0.53 in log a_1. A simple inspection of photographs shows at once that nebulosity as a rule is not symmetrically distributed about stars. Nevertheless Figure 2 indicates that as a rule nebulosity is found at the extreme limits to which a star will illuminate it sufficiently to be photographed with exposures of several hours duration. The explanation is probably to be found in relations between pressure and illumination effects of the stellar radiations on nebulous material of the sizes responsible for the nebular luminosity.

Several of the objects in Table I are of considerable interest individually. γ Cygni for instance is a pseudo-Cepheid with a spectral type F8p. The radiative symmetry of the several neighboring patches of nebulosity raises a strong presumption that they are associated with the star, and this is supported by the positions of the corresponding points in Figure 2. The same can be said concerning α Cygni and the North America nebula, N.G.C. 7000, as well as β Orionis and the nebula I.C. 2118 with its long extension into Eridanus. N.G.C. 1514 is really a giant planetary, conspicuous for the exceptionally bright central star.

One well-known galactic diffuse nebula is a conspicuous exception. The only object investigated for which no obviously dominating star could be located and for which no pronounced obscuration was conveniently situated to hide such a star, is the great loop in Cygnus of which N.G.C. 6960 and 6992 are brighter portions. These portions give emission spectra as could be expected from their filamentary structure. They are opposite one another at the ends of the longer diameter of the loop. Barnard's photograph reproduced on Plate 80 of the *Lick Publications*, Volume XI, shows the configuration. The major axis is roughly $2^\circ\!.5$. One would expect to find a star of spectral type B0 or earlier approximately central, and hence about a degree and a quarter from the outer edges of the nebula. From Figure 2, the apparent photographic magnitude should be around 2.0, with a probable error of less than a magnitude. In the immediate vicinity no early-type stars can be found as bright as 9.0, the limit to which the search was pushed. The evidence from the other diffuse nebulae is too strong to admit the Cygnus loop as a real exception, shining by its own intrinsic luminosity, and explanation must be sought wherever possible. The obvious assumption is that there is a small cloud of dark nebulosity immediately in front of a central star, sufficiently opaque to dim the star by several magnitudes but inconspicuous on small-scale photographs.

Photographs of the central region made with the 100-inch reflector show no certain traces of such dark areas, and general obscuration cannot be present for at least one spiral nebula is shown on the plates. There is considerable filamentous nebulosity in this region, of much the same structural characteristics as the bordering patches of nebulosity known as N.G.C. 6960 and 6992. This suggests that the nebula as a whole may be an ellipsoidal shell rather than a simple loop. B.D. $+30^\circ 4199$, the brightest star within the loop, which is not far from the center, has enough nebulosity immediately around it to be called a nebulous star. Its visual magnitude is given in the B.D. as 7.0, and its spectrum is of highly enhanced type similar to that of α Cygni. It is just possible that this star, dimmed several magnitudes by general absorption of intervening nebulosity, is the source of illumination of the loop. This would be analogous to the association of α Cygni itself and the similar star B.D. $-22^\circ 4510$ with emission nebulosity.

Another point worth mentioning is that, using the observed magnitude for B.D. $+30^\circ 4199$, the relation between m and a for the loop would be of the same order as those for the Crab nebula (N.G.C. 1952), the Dumbbell nebula (N.G.C. 6853), and the Helical nebula in Aquarius (N.G.C. 7293). These objects appear to form a separate group, and speculation concerning their exceptional nature may well be deferred until the luminosity of planetaries has been investigated in a quantitative manner.

An interesting application of the conclusions arrived at in this paper can be made in the case of the spiral M 33. The bright knot in the spiral known as N.G.C. 604 has an emission spectrum of the galactic diffuse nebular type. That is to say, hydrogen is so strong as compared to nebulium that $H\beta$ is of about the same intensity as N_1. This is a general rule among diffuse emission nebulae, but is exceptional among the planetaries. Three of four stars involved in N.G.C. 604 strengthen the analogy with galactic diffuse nebulae. If we assume the same conditions to hold in N.G.C. 604 as in the galactic nebulae, these stars must be considered as probably Bo or Oe5, and Kapteyn's value of -2.5 for the mean absolute magnitude of Bo stars can be used with some degree of justification to estimate the parallax. The apparent magnitudes of these stars have not been measured, but a casual inspection of plates made with various instruments and exposures suggests that the order of magnitude of the brightest is about 15. An exposure of two hours shows nebulosity extending to about $10''$ from the brightest star, so the corresponding point in Figure 2 would fall very close to the mean curve, and the analogy with galactic nebulae is still further strengthened. Since the brightest star alone is used, Kapteyn's value for the mean absolute magnitude can scarcely be considered too bright. The resulting modulus, $m-M$, of 17.5 corresponds to a parallax of $0\overset{''}{.}000032$ or a distance of about 30,000 parsecs. If absorption were present, dimming the apparent brightness of the star, the distance would be correspondingly decreased. Measures of the color index would probably determine this point.

The general equations (11) expressing the relations between m, a, and E can be transformed into corresponding relations between M, the absolute magnitude (photographic in this case) and l, the greatest linear distance in parsecs to which luminous nebulosity extends, by means of

$$m=M-5-5\log\pi$$
$$a=3438\,\pi\,l$$

The expression for a is approximate, the exact relation being $l=2/\pi\sin a/2$, but the difference within the range covered by a is practically negligible. Substituting into the limiting general equation (11),

$$M+5 \log l = 2.5 \log E - 5.52 \tag{12}$$

It follows that for exposures of about 160 minutes on Seed 30 plates with reflectors of focal ratios 1 to 5, representing therefore a limiting surface brightness of $18.8+2.5 \log 160 = 24.32$ magnitudes per square second of arc, the simple relation holds,

$$M+5 \log l = 0 \tag{13}$$

This will represent average conditions of direct nebular photography. A short table of corresponding values will emphasize the enormous distances involved.

	Parsecs		Light Years
For $M=-5$	$l=10$	or	32
-2.5	3.2		10
0	1.0		3
$+2.5$	0.31		1
5	0.1		0.3
10	0.01		0.03

The sun, with a photographic absolute magnitude around 5.65, would be capable of illuminating a surface to a brightness of 24.32 magnitudes per square second of arc at a distance of 0.074 parsecs = 0.24 light years = 1.5×10^4 astronomical units, or 470 times the mean distance of Neptune.

The greatest value of l encountered among the nebulae is for the nebulosity preceding Rigel. The absolute photographic magnitude of the star is about -5.58.[1] An exposure of ten hours with a 1.5-inch Tessar Ic lens of focal ratio 1 to 4.5 corresponds roughly to an exposure of thirteen hours with the reflectors, and from equation (13) the value of l should be about 29 parsecs or 93 light years. On the plate, nebulosity can be traced south preceding Rigel to a distance of nearly $12^\circ\!.5$. Using Kapteyn's value of $0''\!.0069$ for the parallax of Rigel, this corresponds to a distance of nearly 31 parsecs or a hundred light years.

---

[1] Kapteyn's value of -5.5 for the visual absolute magnitude is corrected for the normal color index of a B8 star.

II. PLANETARIES

The fidelity with which the luminosity of diffuse nebulae having emission spectra obeys the laws derived from data obtained mainly from nebulae with continuous spectra, suggests the possibility of applying the methods developed in the preceding discussion to an investigation of luminosity relations in the planetaries. Spectra of the nuclei or central stars of these objects are predominantly continuous. Emission bands are frequently present, but, except for three or four objects, the energy in these bands is a negligible fraction of the energy in the complete spectrum. The law is definitely established that the spectra of nucleus and of nebulosity are dissimilar. In these respects the spectral relations between nebulosity and central stars are analogous to those in the case of the diffuse nebulae having emission spectra.

In other respects, however, the analogy fails to hold. The emission lines N_1 and N_2 are as a rule much stronger in the planetaries than in the diffuse nebulae. Since they are situated very near the red limit of sensitivity of Seed 30 plates, the tendency is to destroy the similarity of intensity distribution between stellar and nebular spectra which appears to hold for diffuse emission nebulae and which permits these objects to obey the same luminosity laws as diffuse nebulae with continuous spectra. Moreover, the extraordinary intensity in the ultra-violet region of the spectra of planetary nuclei introduces a new element into the luminosity relations which may differentiate them from those found among diffuse nebulae.

Difficulties are to be expected in an investigation of luminosity relations between stars with predominantly continuous spectra and nebulosity with complicated emission spectra, and, in the absence of definite theories of the mechanism of nebular illumination, the results will be in the nature of general tendencies rather than precise laws. Provisional results, however, should at least indicate some of the special features to be considered in a later and more thorough investigation.

Curtis'[1] descriptive catalogue of planetaries visible in the northern skies furnishes fairly homogeneous data for 78 objects. For each nebula he gives an illustration, an estimate of the photographic magnitude of the central star, the measured dimensions of the nebulosity, and estimates of its brightness expressed by the relative exposure necessary to register the brightest nebular feature on Seed 27 plates at the primary focus of the Crossley reflector.

---

[1] *Lick Observatory Publications,* 13, Part III, 1918.

In Table III are collected the data for the 56 objects in Curtis' catalogue which have more or less conspicuous central stars. The first column gives the designation; the second, the estimated magnitude m of the central star; the third, the angular distance, A, in seconds of arc measured from the central star to the brightest details of the nebulosity, which, as well as could be determined, are those details for which the relative exposure times are given by Curtis; the fourth, the relative exposures, e; the fifth and sixth columns, the logarithms of A and e, respectively; the seventh, the quantity $\log A_1$, the significance of which will be explained later. The values of m and e are those given by Curtis. When A is given by Curtis, his value is listed in Table III; otherwise it is estimated from the illustrations accompanying the catalogue.

An inspection of the table indicates no trace of correlation between m and $\log A$, but considerable, though vague, evidence of a relation between m and $\log e$. The most conspicuous feature, however, is a rather definite relation between m and a combination of $\log A$ and $\log e$, in the sense that bright central stars are usually associated either with bright and small or with faint and very large nebulae. Furthermore, a study of the illustrations establishes the fact that, where multiple rings are present in a nebula, the order of brightness is usually inversely that of the radii or distances from the central star, and that, in the structureless disks, there is a tendency for the brightness to diminish outward from the central star. These facts, together with the conclusions derived from the discussion of diffuse nebulae, suggest a reduction of $\log A$ to $\log A_1$ corresponding to a uniform relative exposure, on the assumption that the central stars are the sources of luminosity and that, for a homogeneous distribution of nebulosity, the inverse-square law is rigorously obeyed.

TABLE III

PLANETARY NEBULAE

Object	m	A	e	log A	log e	log A_1
N.G.C. 40	10	17″	4	1.23	0.60	0.93
246	9.5	100	100	2.00	2.00	1.00
650, 1	16	40	20	1.60	1.30	0.95
I.C. 1747	14	6	15	0.78	1.18	0.19
351	14	4	2	0.60	0.30	0.45
N.G.C. 1501	12	24	25	1.38	1.40	0.68
1514	8.8	60	80	1.78	1.90	0.83
1535	10	10	2	1.00	0.30	0.85
J 320	12	3.5	0.8	0.54	−0.10	0.59
I.C. 418	9	7	0.2	0.85	−0.70	1.20
N.G.C. 1952	15.2	50	60	1.70	1.78	0.81
2022	13	11	5	1.04	0.70	0.69
I.C. 2149	12	3	0.3	0.48	−0.52	0.74
N.G.C. 2371, 2	12	17	15	1.23	1.18	0.64
2392	9	9	5	0.95	0.70	0.60
2438	16	30	50	1.48	1.70	0.63
2452	19	8	20	0.90	1.30	0.25
2610	15	18	60	1.26	1.78	0.37
3242	9	13	3	1.11	0.48	0.87
3587	12	100	100	2.00	2.00	1.00
4361	10	20	30	1.30	1.48	0.56
I.C. 3568	11	5	0.2	0.70	−0.70	1.05
N.G.C. 6058	12	10	30	1.00	1.48	0.26
I.C. 4593	10	5	2	0.70	0.30	0.55
N.G.C. 6210	11	4	0.3	0.60	−0.52	0.86
6309	13	5	4	0.70	0.60	0.40
6369	16	14	70	1.15	1.85	0.23
6439	18	2	8	0.30	0.90	−0.15
6445	19	18	20	1.26	1.30	0.61
6543	9.2	8	0.2	0.90	−0.70	1.25
6563	18	18	60	1.26	1.78	0.37
6572	9	3	0.1	0.48	−1.00	0.98
6567	14	3	0.6	0.48	−0.22	0.59
6578	15	4	8	0.60	0.90	0.15
6620	15	2.5	4	0.40	0.60	0.10
6629	13	7	10	0.85	1.00	0.35
6720	13	30	6	1.48	0.78	1.09
6751	12	10	20	1.00	1.30	0.35
6772	18	26	250	1.41	2.40	0.21
6778	14	9	15	0.95	1.18	0.36
6781	14	50	80	1.70	1.90	0.75
6803	13	2.7	0.3	0.43	−0.52	0.69
6804	12	20	25	1.30	1.40	0.60
6818	14	10	0.7	1.00	−0.15	1.07
6826	9	11	1	1.04	0.00	1.04
6853	12	90	20	1.95	1.30	1.30
6891	10	3.5	2	0.54	0.30	0.39
6894	16	22	70	1.34	1.85	0.42
6905	13	18	20	1.26	1.30	0.61

TABLE III—*Continued*

Object	m	A	e	$\log A$	$\log e$	$\log A_1$
N.G.C. 7008	12	40	20	1.60	1.30	0.95
7009	11	12	0.2	1.08	−0.70	1.43
7026	14	3	0.8	0.48	−0.10	0.53
7139	18	35	300	1.54	2.48	0.30
7293	11	300	150	2.48	2.18	1.39
7354	16	8	15	0.90	1.18	0.31
7662	11.5	8	0.2	0.90	−0.70	1.25

These assumptions lead to a reduction formula analogous to equation (3). Let the uniform relative exposure be unity and let the exponent p also be taken as unity. Then

$$\log A_1 = \log A - \tfrac{1}{2} \log e \tag{14}$$

Log A_1 is listed in the seventh column of Table III.

Figure 4 shows the plot of m against $\log A_1$ for the 56 planetaries in Table III. Some degree of correlation is obvious, but the coefficient is so small that a least-squares solution in the form used in the investigation of diffuse nebulae does not give satisfactory results. Accordingly the data were treated by the method of correlations. The two regression curves are

$$RC \text{ of } m \text{ on } \log A_1 \; . \; . \; . \; . \; m + 4.63 \log A_1 = 16.03 \tag{15}$$

$$RC \text{ of } \log A_1 \text{ on } m \; . \; . \; . \; . \; m + 13.35 \log A_1 = 21.84 \tag{16}$$

Coefficient of correlation 0.59

$$\sigma_m = 2.80 \qquad \sigma_{\log A_1} = 0.356$$

The correlation ratio of equation (15) is 0.61, and of (16), 0.64. Attention should be called to the fact that the regression curve of m on $\log A_1$, determined by plotting the mean m for groups of $\log A_1$, is not a straight line but a rather well-defined curve convex to the origin of co-ordinates and hyperbolic in form. The correlation ratio is computed from this curve. The reason for such a curve is to be found in the distribution of errors, especially the systematic errors in m and e, which will be discussed later. Equation (15) is the straight line which best fits the points of the regression curve. The regression curve of log A_1 on m is a straight line.

The best simple expression for the relation between m and log A_1 is probably the curve of symmetry, or the bisector of the acute angle between the lines represented by equations (15) and (16). This

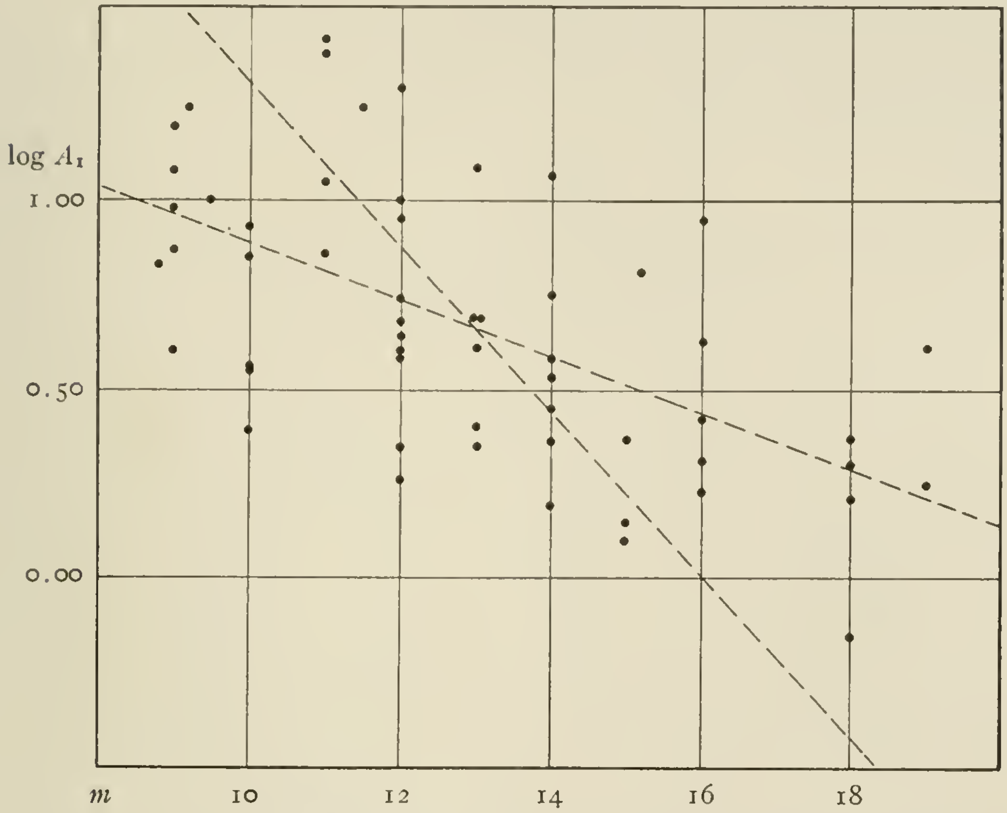

FIG. 4.—Plots of m, the photographic magnitude of central stars in planetary nebulae, against log A_1, where A_1 is the angular extent of nebulosity from the central stars reduced to a uniform exposure time. The data are taken from Table III. The broken lines are the regression curves.

reduces the sum of the perpendicular distances from the points to the line to a minimum. The bisector is

$$m+(6.91\pm0.6)\log A_1=17.55\pm0.22 \qquad (17)$$

The data are not of a high order of accuracy but the mean values should be significant. The distances A must be essentially free from serious systematic errors, although the accidental errors are probably large as compared to the values of A, especially in the many very small nebulae.

The relative exposure, *e*, seems to be fairly reliable for large and faint nebulae, but is probably too large for the small and bright objects as compared with larger-scale photographs made with the 60-inch and 100-inch reflectors. This may be due to the known dependency of minimum visibility on surface area, and to the difficulty on small-scale photographs of distinguishing the star image from bright nebulosity in its immediate neighborhood. Such errors would be especially serious in the case of stars involved in very small dense nebulae.

TABLE IV

COMPARISON OF MOUNT WILSON LIMITING EXPOSURE TIMES WITH CURTIS' RELATIVE EXPOSURES

OBJECT	E	e	$R=\frac{E}{e}$
	a) Large and Faint Nebulae		
	sec.		
N.G.C. 246	600	100	6.00
1514	300	80	3.75
3587	600	100	6.00
6445	150	20	7.50
6853	120	20	6.00
6894	480	70	6.86
7293	900	150	6.00
Mean	....	....	6.02±0.28
	b) Small and Bright Nebulae		
	sec.		
N.G.C. 3242	1	0.3	3.33
I.C. 3568	4	2.0	2.00
4593	6	2.0	3.00
N.G.C. 6210	1.5	0.3	5.00
6572	0.4	0.1	4.00
6720	10	6	1.67
7009	0.8	0.2	4.00
7662	0.8	0.2	4.00
Mean	....	....	3.38±0.33

Minimum exposures in seconds of time required just to register the brightest details of nebulosity on Seed 30 plates at the primary focus of the 60-inch reflector have been derived by the writer for 15 planetaries. These are compared with Curtis' values of *e* in Table IV. The first column designates the nebulae, the second gives the minimum exposures E in seconds of time derived from the Mount Wilson plates, the third gives Curtis' values of e, and the fourth contains the ratios $R=E/e$ which represents the minimum exposure, expressed in seconds, made on Seed 30 plates with the 60-inch reflector, corresponding to Curtis' unit of relative exposure.

The values of e for N.G.C. 3242 and I.C. 3568 have been arbitrarily changed by shifting the decimal points one place to the left and to the right, respectively. Curtis' value of 3 for N.G.C. 3242 is unquestionably a misprint for 0.3, since he remarks that the inner ring shows in 10 seconds on a Seed 23 plate. His description of I.C. 3568 places its brightness about equal to that of I.C. 4593. The value $e=6$ for N.G.C. 6720, the ring nebula in Lyra, is surprisingly high. The nebula may be photographed in 10 seconds with the 60-inch, and a rather strong image registers in 15 seconds.

The unit of relative exposure corresponds to an exposure of 10 seconds on a Seed 27 plate with the Crossley reflector. A standard region in the Orion nebula near the trapezium shows well under these conditions.[1] When one considers the more favorable focal ratio of the 60-inch reflector, and the difference in intensities between that "just perceptible" and that "well shown," the ratio $E/e=6.0$ found for the large faint nebulae seems to be a reasonable value. The relative speeds of the two instruments, allowing for the fact that the Crossley plates are made at the direct focus without the use of a Newtonian flat, is about 1.18 in favor of the 60-inch. The factor due to the different standards of intensities used in the two series is a matter of conjecture and can be variously estimated at from 1.25 to 1.50, in the sense that the smaller intensities, and hence shorter exposures, are employed by the writer. Using a mean value of 1.38 for this factor, and considering the difference in speed between Seed 27 and Seed 30 plates to be negligible, the computed ratio E/e should be about $10\div 1.18\times 1.38=6.14$. This agrees with the observed value, 6.0, for the large faint nebulae and indicates that the discrepancy between the ratios of the two lists in the preceding table is due to errors in the small bright objects.

The evidence seems rather definitely in favor of a systematic error in e for the very bright nebulae, but the data are not sufficient to determine the limitations of the error. A correction would decrease e for these objects and hence increase $\log A_1$. Since the bright nebulae as a rule have bright central stars, the effect would be to raise the upper ends of the correlation curves compared to the lower ends, and to decrease the value of the coefficient of $\log A_1$ in equation (17). It is probable that the systematic error in e is not serious for values of e greater than 2.0. The effect on equation (17) can be estimated by applying to each e a uniform correction equal to 2 or less and considering any errors in the larger e's as accidental. As there are only four objects with e greater than 2 and less than 5, beyond which the systematic error is almost certainly negligible, this course seems justifiable. The correction to be applied is computed from the mean of the values for the bright nebulae in Table IV, disregarding N.G.C. 6720, the discrepancy in which may be considered as an accidental error. Each e equal to 2 or less must then be divided by $6.2 \div 3.62 = 1.72$. Log e is accordingly decreased by 0.24, and $\log A_1$ increased by 0.12. This correction is applied to eighteen objects. The mean $\log A_1$ of Table III, 0.667, will be increased by $0.12 \times 18/56 = 0.039$. The corrected mean value will be 0.706. The mean m will remain the same, hence the corrected curve must pass through the point $m = 12.95$, $\log A_1 = 0.706$. For the objects in which e has been corrected, the mean m is low, 11.3, and no m is greater than 14. Likewise the mean $\log A_1$ is high, 0.86, and only two are less than 0.50. The result is that the intersection of the curve with the m-axis at $m = 17.55$ will be very little disturbed. The corrected curve will pass close to this point and through the point $m = 12.95$, $\log A_1 = 0.706$. The equation of the corrected curve will therefore be approximately

---

[1] Curtis, *op. cit.*, p. 59.

$$m + 6.52 \log A = 17.55 \qquad (18)$$

Curtis' magnitudes are estimates and therefore subject to rather large accidental errors. In addition, there is a pronounced systematic error for the brighter stars, in the sense that they are estimated too bright.

Van Maanen has given photographic magnitudes of the central stars of the planetaries which he has measured for parallax.[1] The method he employs is to count the numbers of stars equal to or brighter than the ones in question on his parallax plates and to extract the corresponding magnitude from van Rhijn's[1] tables of average stellar densities for given galactic latitudes. This procedure is subject to considerable accidental error in individual cases, especially of the brighter stars, for the field used is small enough to be seriously affected by local irregularities in stellar distribution. In the mean, however, they should be reliable within the limits of Curtis' accidental errors.

---

[1] *Mt. Wilson Contr.* No. 237, 1922.

The writer has derived provisional photographic magnitudes for several central stars, using the method of polar comparisons, with exposures timed to show a minimum of nebulosity. In general each of the values depends upon a single plate and they are not, therefore, very reliable. They should, however, be of the same order of accuracy as van Maanen's determination, and both series can be used to reduce Curtis' measures to the scale of the polar sequence. The data are given in Table V. Van Maanen's value of 8.0 for the central star in N.G.C. 1514 is omitted for the reason that the star is too bright for a good determination of the magnitude by the method of star counts.

The mean difference, van Maanen − Curtis, is 1.3, corresponding to a mean magnitude (Curtis) of 11.5. The mean, Hubble − Curtis, is 1.4 for a mean magnitude (Curtis) of 12.0. Between Curtis' magnitudes and the differences vM − C and H − C, called Δ, the combined data give a coefficient of correlation of 0.44, which has very little significance. The mean point of the material is at m (Curtis) $= 11.7$, $\Delta = +1.35$. This probably represents a systematic error in Curtis' values amounting to -1.35 at his magnitude 11.7. It is improbable that the error should be uniform over the range of m covered by Table III. A more reasonable assumption is that the error vanishes near the limiting magnitude obtainable with the Crossley in an exposure of moderate length. This supposition is supported by the two faint central stars in Table V for which Δ is negligible. If this is the case, the correction to Curtis should be represented approximately by a straight line drawn through the mean point of the data of Table V, rejecting the two faint stars in N.G.C. 6445 and 6772, and cutting the axis of m at an arbitrarily chosen point, say m equals 19.5. The formula expressing Δ, the correction to be added to Curtis' m, is then

---

[1] *Groningen Publications*, No. 27, Table IV, 1917.

$$\Delta = -0.173\, m + 3.37 \tag{19}$$

The effect of this assumed correction would be in the nature of a rotation of the correlation curves of Figure 4 in a clockwise direction around the points where they cross the abscissa $m = 19.5$. Equation (18) corrected in this manner becomes

TABLE V

PHOTOGRAPHIC MAGNITUDES OF PLANETARY NUCLEI

Object	Curtis	van Maanen	Hubble	vM−C	H−C	H−vM
N.G.C. 40	10	11.6	....	1.6	....	....
1501	12	13.0	....	1.0	....	....
1514	8.8	....	9.7	....	0.9	....
2022	13	14.2	....	1.2	....	....
2371, 2	12	13.5	....	1.5	....	....
2392	9	10.0	....	1.0	....	....
3242	9	....	11.7	....	2.7	....
3587	12	....	14.3	....	2.3	....
I.C. 3568	11	....	12.0	....	1.0	....
4593	10	....	10.2	....	0.2	....
N.G.C. 4361	10	....	12.8	....	2.8	....
6210	11	11.7	....	0.7	....	....
6445	19	....	19	....	0.0	....
6543	9.2	11.3	....	2.1	....	....
6572	9	10.8	10.2	1.8	1.2	−0.6
6720	13	14.7	14.7	1.7	1.7	0.0
6772	18	....	18.1	....	0.1	....
6804	12	13.4	....	1.4	....	....
6853	12	....	13.6	....	1.6	....
6905	13	14.5	....	1.5	....	....
7008	12	12.8	....	0.8	....	....
7009	11	....	11.7	....	0.7	....
7026	14	15.1	....	1.1	....	....
7293	11	....	13.3	....	2.3	....
7662	11.5	12.9	12.5	1.4	1.0	−0.4
Mean	11.7	....	....	1.34	1.36	....

$$m + 5.40 \log A_1 = 17.88 \tag{20}$$

This curve is probably a fair representation of the data, disregarding the probable misprints in the decimal points for e in the cases of N.G.C. 3242 and I.C. 3568. Taking these into account and correcting Curtis' values of m and e for the systematic errors suggested by the Mount Wilson observations, the recomputed correlation curves are:

RC of m on $\log A_1$ .... $m+3.71 \log A_1=16.73$

RC of $\log A_1$ on m .... $m+9.21 \log A_1=20.70$

Correlation curve .... $m+(5.33\pm0.4) \log A_1=17.88\pm0.18$ (21)

Coefficient of correlation 0.64

$$\sigma_m=2.28 \qquad \sigma_{\log A_1}=0.389$$

The plot corresponding to the corrected data is shown in Figure 5.

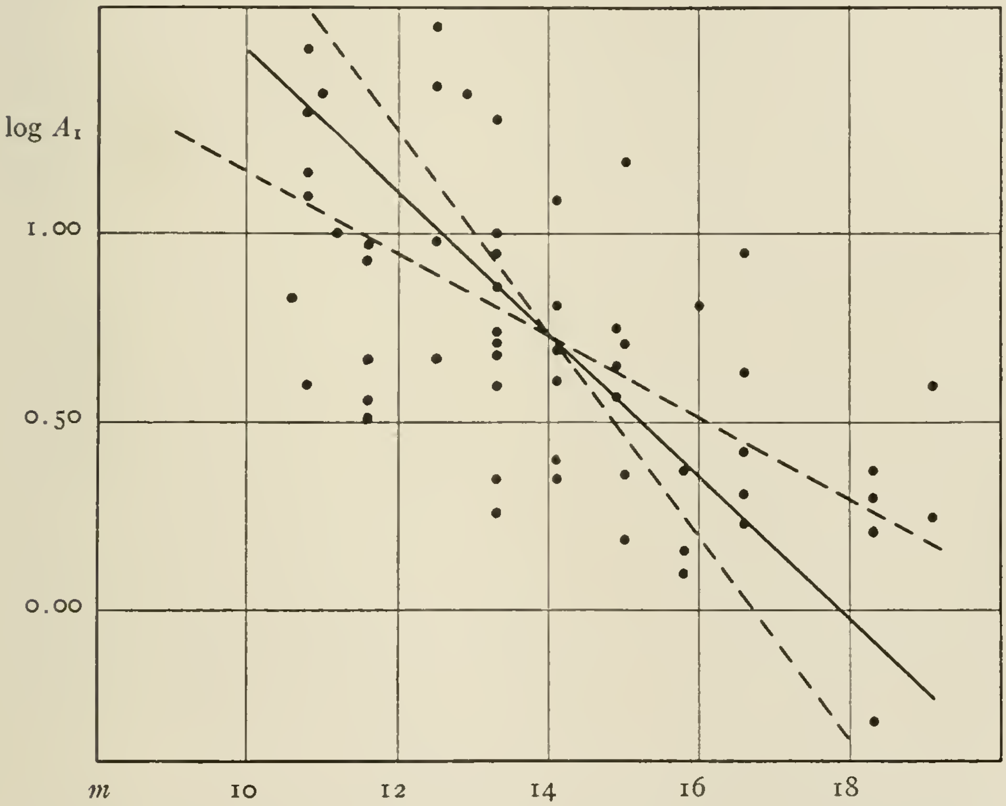

FIG. 5.—The same as Fig. 4, the data having been corrected for probable systematic errors. The full line represents the correlation curve for an equal weighting of the regression curves.

A curve passing through the mean m and $\log A_1$ and having the slope to be expected on the assumption of an inverse-square law of luminosity can be represented by the equation

$$m+5 \log A_1=17.64\pm0.17 \qquad (22)$$

The two equations (21) and (22) agree within the limits of errors over the range covered by the data.

The general conclusion is in favor of the theory that the planetaries as well as the diffuse nebulae derive their luminosity from radiations of associated stars, and that the inverse-square law is at least one important factor in determining the distribution of luminosity throughout the nebulae. The complicated discontinuous nebular spectra of the planetaries, the great intensity in the ultraviolet of the continuous nuclear spectra, and the obvious concentration of luminous nebulosity in restricted zones, probably disturb the simple application of the inverse-square law sufficiently to account for the large residuals found in the present investigation.

There are some indications that the residuals computed from equations (21) and (22) may be related to the various types of planetaries. The four ring nebulae, N.G.C. 2438, 6720, 6894, and 7293, all show large positive residuals, averaging +1.80, while the globular objects I.C. 3568, 4593 and N.G.C. 6439, 6572, 6578, 6620, and 6629 all show large negative residuals, averaging −1.50. It is possible that when more precise data are available, a complete sequence can be established involving relations between residuals, on the one hand, and, on the other, spectral characteristics of nuclei and of nebulosity, color indices of nuclei, and structure of nebulosity.

It is worth mentioning at this point that when referred to B.D. +30°4199 as the central star, the loop in Cygnus discussed in the first part of this paper takes its place among the ring nebulae. The maximum distance A, measured to the following edge of N.G.C. 6992, which registers in an exposure of forty minutes, is $90'$. $m+5\log A_1=7.2+12.0=19.2$. The residual, $19.2-17.6=+1.6$, is of the order of that for the other ring nebulae.

Assuming the inverse-square law to hold rigorously with respect to the central stars as sources in the case of the planetaries, and assuming further that, within the range of wave-lengths to which the fast Seed plates are sensitive, the light emitted by the nebulosity is exactly that which it intercepts from the stars, a theoretical relation can be derived analogous to that in equation (9). Assumptions of random distribution in direction from stars to points of nebulosity measured for A are not necessary, for the symmetrical forms of the planetaries indicate that in general the directions of greatest extent of nebulosity from the central stars lie close to the plane perpendicular to the line of sight. The surface brightness of nebulosity on the above assumptions, expressed in magnitudes per square second of arc, is found by distributing the light of the star over a spherical shell with a radius equal to the distance to the point of nebulosity considered. Let this distance, A, be expressed in seconds of arc. Then

$$S.\,B. = m + 2.5 \log 4\pi A^2 = m + 5 \log A + 2.75 \tag{23}$$

The unit of relative exposure corresponds to an exposure of six seconds with the 60-inch reflector, or, if Seares's value for the limiting surface brightness just registered in an exposure of one minute is used[1] to a limiting surface brightness of $18.8 \pm 0.3 + 2.5 \log 0.1 = 16.3 \pm 0.3$. Substituting this value for $S.B.$ into equation (23),

$$m = 5 \log A = 13.55 \pm 0.30 \tag{24}$$

which expresses the relation between m and $\log A$, where A is measured from the star to the most distant nebulosity which just shows in an exposure of six seconds.

A comparison between this equation and the observational equations (21) and (22) shows a discrepancy in the constants amounting to from 4.1 to 4.3±0.6 magnitudes, in the sense that in general the observed nebulosity extends to a greater distance from stars of a given magnitude than the assumptions permit. Expressed in another way, the nebulosity at a given distance from the star is about 4.1 to 4.3±0.6 magnitudes per square second of arc brighter than can be accounted for on the assumption that, within the range of the fast Seed plates, the light emitted by the nebulosity is exactly the starlight intercepted. This may well account for the apparent absence of central stars or nuclei from some of the planetaries.

No adequate explanation of this discrepancy can be made without a knowledge of the mechanism by which the nebular illumination is excited, but a few suggestions may aid in formulating the problem. The source of illumination is rather definitely established as located in the central stars. The diffuse nebulae with emission spectra fail to show this discrepancy although it seems reasonable to suppose that the mechanism of illumination is much the same. The most striking difference between the nebular spectra of the planetaries and the emission spectra of diffuse nebulae is found in the much greater strength of the nebulium lines N_1 and N_2 in the planetaries. These lines are situated very close to the limits of sensitivity toward the red of the Seed 30 plates, and thus tend to destroy that equivalence of intensity distribution which the spectra of emission diffuse nebulae appear to share with the spectra of their associated stars, and by virtue of which they actually follow the same luminosity laws as do the diffuse nebulae with continuous spectra. The strengthening of the nebulium lines in the planetaries is accompanied by no corresponding strengthening of the continuous spectrum of the nuclei in this region. The maximum intensity of the continuous nuclear spectrum is shifted to the violet as compared with that of the stars associated with diffuse nebulae, and this in effect decreases the relative intensity in the region of the nebulium lines. If the nebular emission lines were considered as integrated from the continuous spectrum in their immediate vicinity, then the strong nebulium lines would represent a considerable part of the green region to which the Seed 30 plate is relatively insensitive. Such a supposition, if it were physically possible, could account for only a small part of the discrepancy, for these two lines seldom furnish more than a third of the nebular luminosity, as is shown by Wright's measures of relative intensities of nebular images made on spectrograms obtained with a slitless quartz spectrograph and a reflecting telescope, which are comparable with the direct photographs used in deriving the data of the present discussion.[1]

Another difference between planetaries and diffuse nebulae is found in the greater intensity of the ultra-violet continuous spectrum of the planetary nuclei as compared to that of the stars associated with diffuse nebulosity. The nuclear spectra are in general predominantly continuous. When corrected for atmospheric absorption, the energy curve of the continuous spectrum rises more and more steeply with decreasing wave-length up to the limits of reflectivity of silvered mirrors. Wright remarks, "Where the maximum is cannot be conjectured." It is certainly at a wave-length less than 3300 A. Thus the nebulosity receives a vast amount of energy in stellar radiations in a region of the spectrum which plays but a minor rôle in the determination of photographic magnitudes. It is entirely conceivable that the energy in these continuous radiations may be absorbed by the nebulosity and, by some mechanism analogous to that of fluorescence, be re-emitted as discontinuous radiations of longer wave-lengths. If this were the case, the m in equation (20) would be replaced by one of smaller numerical value representing a sort of ultra-violet magnitude, and the discrepancy in the constants would be materially reduced, if not entirely eliminated. Following this line of thought, the suggestion arises that the nebulium lines may possibly reveal themselves as fluorescent spectra of hydrogen or helium or a mixture of the two.

---

[1] *Lick Observatory Publications*, 13, Part VI, 1918.

There exist in the solar system itself possible analogies to the mechanism by which emission luminosity may be excited in nebulosity by radiations emanating from a continuous source. Chief among these are the terrestrial aurorae, the solar corona, and the comets. In each of these cases, radiations of some sort emanating from the sun excite matter in a gaseous state to luminosity of a discontinuous nature. The prevailing opinion concerning the aurora is that the phenomenon is due to the ionization of atmospheric gases by high-speed charged particles.

H. N. Russell[1] has made suggestions of a similar nature to account for the spectrum of emission nebulae. Such a mechanism would account for the inverse-square law quite as well as a mechanism based on ethereal radiations, and would probably find no serious obstacle in the excessive luminosity of the planetaries. Furthermore, this explanation was also formulated from independent considerations, namely, the relations which Russell found to exist between relative sizes of monochromatic images of individual planetaries and ionization potentials of the radiations forming the images.

---

[1] *Observatory*, 44, 72, 1921. Russell states that the luminosity of gaseous nebulae is probably due to ionization of the gases by radiations from associated stars, and that the radiations may be either ethereal or corpuscular.

Relations of a similar nature are suspected in the monochromatic images of diffuse nebulae with emission spectra. In these cases, however, the quantitative agreement between nebular and stellar luminosity, both for purely emission nebulae and for those with mixed spectra, appears to favor the notion of ethereal radiations. This agreement may of course be due to the nature of the relations between intensities of corpuscular radiations and spectral types or temperatures of the stars.

Mount Wilson Observatory
August 1922

NOTE ADDED DECEMBER 21, 1922

The stars within the great loop of nebulosity around the belt and sword of Orion sum up to an integrated apparent photographic magnitude of about 0.0. The loop extends to about 5°.7 or 342′ from the estimated center of gravity of the stars considered, and registers very nearly to this limit in exposures of about three hours. Therefore $m+5 \log a_1 = 11.5$, a value more representative than that derived from considering ζ Orionis alone.

New material on about 40 per cent of the objects in Curtis' list of planetary nebulae confirms the suggested systematic corrections for m and e as being of the right order of magnitude.

ORBIT OF THE ECLIPSING BINARY TW ANDROMEDAE[1]

By MARTHA BETZ SHAPLEY

ABSTRACT

Uniform and darkened orbits of the eclipsing binary TW Andromedae.—Orbits were calculated from 86 photographic observations made at Mount Wilson from 1914 to 1916. The adopted elements of light variation are

$$\text{Min.} = \text{J. D. } 2420051.618 + 4^{\text{d}}.122745\ E$$

The principal eclipse is total and there is some evidence of variation of the large, faint component. The *color index* at maximum is +0.57 mag., at minimum +1.36 mag. When reduced to the photographic scale by proper allowance for color, 74 photovisual observations, as well as the photographic measures, are well represented by the curves shown in Figs. 1 and 2, corresponding to the orbits whose elements are given in Table VI.

Photographic and photovisual observations of the eclipsing variable star TW Andromedae were made by Mr. Shapley with the 60-inch reflector at Mount Wilson during the years 1914 to 1916. Miss Davis assisted in measuring and reducing the 160 multiple-exposure photographs, which contain a total of 540 images of the variable.

TABLE I

COMPARISON STARS FOR TW ANDROMEDAE

Star	Photographic Magnitude	Photovisual Magnitude	Color Index
B.D.+31°5023	10.70	9.99	$+0^{\text{m}}.71$
$23^{\text{h}}57^{\text{m}}$, +32°13′ (1900)	11.69	10.93	+0.76
B.D.+32°4755	9.27	8.81	+0.46

The magnitudes of the comparison stars, Table I, were standardized by means of the North Polar Standards.[2] Tables II and III contain the photographic and photovisual observations. The apertures employed range from nine inches to sixty inches; the exposure times from thirty seconds to two minutes.

---

[1] *Contributions from the Mount Wilson Observatory*, No. 254.

[2] Seares, *Mt. Wilson Contr.*, No. 97; *Astrophysical Journal*, 41, 206, 1915.

TABLE II

PHOTOGRAPHIC OBSERVATIONS OF TW ANDROMEDAE

J.D. and Gr. H.M.T.	No. Exp.	Phase	Mag.	J.D. and Gr. H.M.T.	No. Exp.	Phase	Mag.
2420393.646....	5	$-0\overset{\mathrm{d}}{.}160$	10.26	2420455.651....	4	$+0\overset{\mathrm{d}}{.}005$	12.22
393.653....	5	−0.153	10.34	455.662....	4	+0.016	12.24
393.660....	5	−0.146	10.51	455.671....	4	+0.025	12.33
393.667....	5	−0.139	10.59	456.611....	5	+0.965	9.62
393.678....	5	−0.128	10.81	456.618....	4	+0.972	9.58
396.703....	4	+2.897	9.73	456.623....	4	+0.977	9.48
397.756....	5	−0.173	10.32	456.629....	4	+0.983	9.46
397.770....	5	−0.159	10.26	458.617....	4	+2.970	9.84
397.786....	5	−0.143	10.53	458.626....	4	+2.979	9.76
397.797....	5	−0.132	10.51	459.578....	4	−0.192	9.82
397.812....	5	−0.117	10.70	459.584....	4	−0.186	10.13
397.837....	5	−0.092	11.26	459.590....	4	−0.180	10.02
397.863....	5	−0.066	11.66	459.597....	4	−0.173	10.18
397.876....	5	−0.053	11.88	459.602....	4	−0.168	10.23
397.889....	5	−0.040	12.09	459.607....	4	−0.163	10.17
397.903....	5	−0.026	11.98	459.615....	4	−0.155	10.31
397.916....	5	−0.013	12.00	459.624....	4	−0.146	10.24
397.929....	5	0.000	12.06	459.637....	4	−0.133	10.51
397.944....	5	+0.015	12.29	459.647....	4	−0.123	10.67
397.958....	5	+0.029	12.16	459.656....	4	−0.114	10.68
397.973....	5	+0.044	12.12	459.667....	4	−0.103	10.88
397.986....	5	+0.057	11.77	459.679....	4	−0.091	11.04
398.003....	5	+0.074	11.53	459.689....	4	−0.081	11.35
398.017....	5	+0.088	11.32	459.698....	4	−0.072	11.52
398.031....	5	+0.102	11.03	459.727....	4	−0.043	11.98
398.035....	5	+0.107	10.88	459.736....	4	−0.034	12.04
422.707....	3	+0.042	12.29	459.745....	4	−0.025	12.12
422.734....	3	+0.069	11.56	517.669....	4	+0.181	10.01
422.746....	4	+0.081	11.38	517.676....	4	+0.188	9.91
422.757....	4	+0.092	11.21	517.687....	4	+0.199	9.71
422.777....	4	+0.112	10.81	517.694....	4	+0.206	9.65
422.787....	4	+0.122	10.53	517.704....	4	+0.216	9.64
422.797....	4	+0.132	10.36	517.712....	4	+0.224	9.73
422.811....	4	+0.146	10.52	2421050.911....	3	+1.589	9.86
425.622....	4	+2.957	10.07	050.924....	3	+1.602	9.88
425.631....	4	+2.966	10.00	051.864....	3	+2.542	9.68
425.675....	4	+3.010	9.68	051.889....	3	+2.567	9.84
425.683....	4	+3.018	9.55	052.863....	3	+3.541	9.78
425.692....	4	+3.027	9.56	052.891....	3	+3.569	9.78
425.699....	4	+3.034	9.59	053.867....	3	+0.422	9.78
425.707....	4	+3.042	9.57	053.876....	3	+0.431	9.80
425.716....	4	+3.051	9.56				
455.623....	4	−0.023	12.25				
455.632....	4	−0.014	12.16				
455.642....	4	−0.004	11.99				

TABLE III

PHOTOVISUAL OBSERVATIONS OF TW ANDROMEDAE

J.D. and Gr.H.M.T.	No. Exp.	Phase	Mag.	J.D. and Gr. H.M.T.	No. Exp.	Phase	Mag.
2420396.687....	3	$+2^{d}.871$	9.06	2420458.622....	3	$+2^{d}.975$	9.23
397.749....	3	−0.180	9.71	458.631....	3	+2.984	9.31
397.762....	3	−0.167	9.67	459.582....	3	−0.188	9.34
397.776....	3	−0.153	9.64	459.587....	3	−0.183	9.36
397.790....	3	−0.139	9.78	459.594....	3	−0.176	9.45
397.803....	3	−0.126	9.76	459.599....	3	−0.171	9.54
397.819....	3	−0.110	10.02	459.605....	3	−0.165	9.44
397.858....	3	−0.071	10.45	459.610....	3	−0.160	9.54
397.870....	3	−0.059	10.40	459.619....	3	−0.151	9.51
397.883....	3	−0.046	10.57	459.628....	3	−0.142	9.49
397.897....	3	−0.032	10.85	459.642....	3	−0.128	9.63
397.910....	3	−0.019	10.78	459.651....	3	−0.119	9.87
397.923....	3	−0.006	11.19*	459.660....	3	−0.110	10.03
397.936....	3	+0.007	10.77	459.674....	3	−0.096	10.23
397.952....	3	+0.023	10.87	459.685....	3	−0.085	10.25
397.966....	3	+0.037	10.68	459.694....	3	−0.076	10.42
397.979....	3	+0.050	10.64	459.702....	3	−0.068	10.63
397.995....	3	+0.066	10.60	459.731....	3	−0.039	10.90
398.009....	3	+0.080	10.40	459.740....	3	−0.030	10.77
398.024....	3	+0.095	10.15	459.749....	3	−0.021	10.88
422.728....	3	+0.063	10.82	517.673....	3	+0.185	9.47
422.740....	3	+0.075	10.64	517.681....	3	+0.193	9.23
422.752....	3	+0.087	10.35	517.691....	3	+0.203	9.31
422.769....	3	+0.104	10.08	517.698....	3	+0.210	9.13
422.783....	3	+0.118	9.81	517.708....	3	+0.220	9.19
422.792....	3	+0.127	9.71	517.715....	3	+0.227	9.38
422.801....	3	+0.136	9.72	2421050.906....	2	+1.584	9.08
425.626....	3	+2.961	8.85:	050.919....	2	+1.597	9.18
425.635....	3	+2.970	9.13	051.857....	2	+2.535	9.27
425.679....	3	+3.014	9.07	051.885....	2	+2.563	9.13
425.686....	3	+3.021	9.08	052.858....	2	+3.536	9.13
425.696....	3	+3.031	9.02	052.886....	2	+3.564	9.28
425.703....	3	+3.038	9.20	053.872....	2	+0.427	9.16
425.712....	3	+3.047	9.08	053.881....	2	+0.436	9.23
425.721....	3	+3.056	9.16				
425.799....	4	+3.134	9.16				
456.615....	3	+0.969	9.02				
456.621....	3	+0.975	9.10				
456.626....	3	+0.980	9.11				
456.632....	3	+0.986	9.02				

---

* Rejected observation, abnormality unexplained.

The period used for the reduction is that derived by van der Bilt.[1] To satisfy the Mount Wilson observations, a correction of $-0^d.004$ has been made to the initial epoch, giving the adopted elements:

$$\text{Min.} = \text{J.D. } 2420051.618 + 4^d.122745 \text{ E.}$$

The individual photographic observations are plotted in Figure 1 with the curve computed from orbital elements, based on the assumption of disks of uniform brightness. The scattering of the observations at the bottom of the minimum is believed to be due, in part at least, to actual fluctuations in the light of the presumably very red faint component, which alone is visible at the time of principal eclipse.

TABLE IV

PHOTOGRAPHIC NORMAL POINTS FOR TW ANDROMEDAE

Number	No. Obs.	Mean Phase	Mean Mag.	O–C, Darkened
1	13	$0^d.018$	12.14	$0^m.00$
2	5	.044	12.07	+0.05
3	5	.068	11.61	0.00
4	5	.087	11.27	+0.01
5	5	.103	10.96	−0.01
6	5	.121	10.68	−0.01
7	5	.136	10.50	0.00
8	5	.149	10.38	+0.02
9	5	.165	10.25	+0.05
10	5	.182	10.05	−0.01
11	5	0.207	9.71	−0.19
12	23	....	9.70	0.00

Tables IV and V contain the mean magnitudes, photographic and photovisual, after reflecting all observations on to one branch of the curve. The first normal group of each table contains the observations during the phase of totality; the last includes all observations outside the minimum.

The orbits are based on the photographic light curve.[2] Uniform and darkened elements were computed, and, together with other data concerning the system, are arranged in Table VI. The mean densities are not corrected for probable unequal distribution of mass.

The photographic normals are plotted as dots in Figure 2, where the co-ordinates are, respectively, light intensity, corresponding to

---

[1] *Astronomische Nachrichten*, **196**, 396 (No. 4703), 1913.

[2] A provisional orbit has been published by Stewart in *Astrophysical Journal*, **42**, 315, 1915.

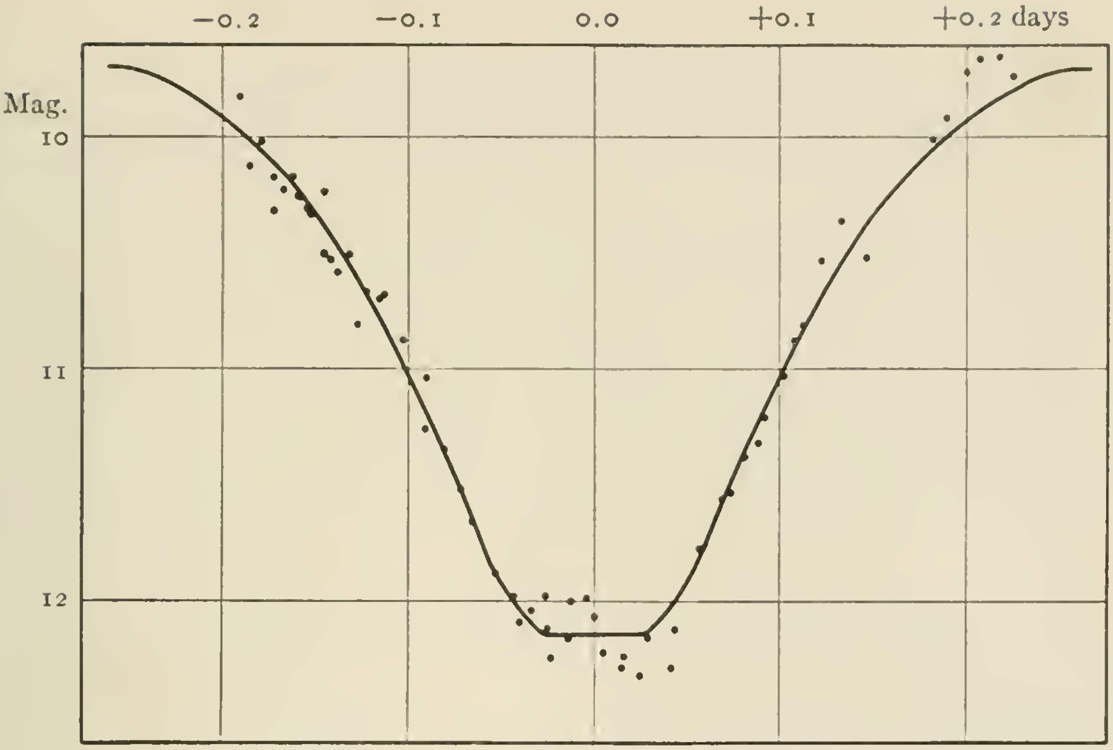

FIG. 1.—Photographic observations and computed uniform light-curve for TW Andromedae.

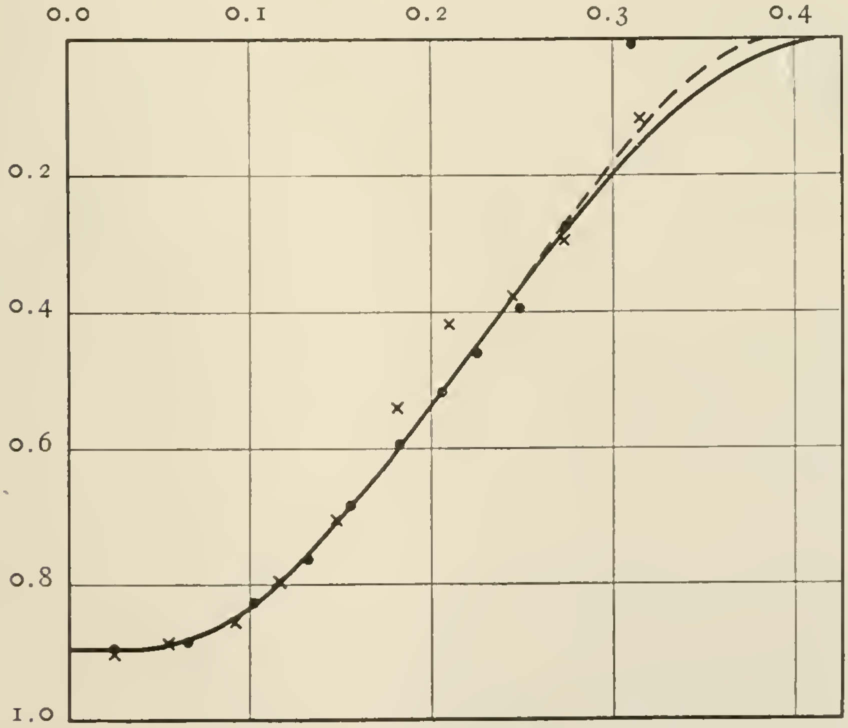

FIG. 2.—Computed intensity-curves for TW Andromedae. Ordinates are losses of light-intensity, $1-l$; abscissae are sines of phase angles.

TABLE V

PHOTOVISUAL NORMAL POINTS FOR TW ANDROMEDAE

Number	No. Obs.	Mean Phase	Mean Mag.	O-C, Darkened
1	4	$0^{d}.018$	10.82	$+0^{m}.04$
2	5	.037	10.75	−0.01
3	5	.061	10.62	+0.03
4	5	.077	10.43	0.00
5	5	.098	10.17	−0.02
6	5	.120	9.83	−0.11
7	5	.139	9.63	−0.13
8	5	.163	9.57	0.00
9	5	.182	9.47	+0.02
10	5	0.211	9.25	−0.04
11	24	....	9.13	0.00

TABLE VI

ORBITAL ELEMENTS AND OTHER DATA FOR TW ANDROMEDAE

Right Ascension	$23^{h}58^{m}10^{s}$ 1900	
Declination	$+32°17'.3$	
Period	$4^{d}.122745$	
Nature of eclipse	Total	
	Pg.	Pv.
Magnitude at maximum	9.70	9.13
Magnitude at minimum	12.14	10.78
Range at primary minimum	$2^{m}.44$	$1^{m}.65$
Light of brighter star	0.894	0.781
Light of fainter star	0.106	0.219
Color index at maximum	$+0^{m}.57$	
Color index at minimum	+1.36	
	Uniform	Darkened
Inclination of orbit	81°40′	86°2′
Least distance of centers	0.145	0.069
Semi-duration of primary eclipse	$0^{d}.256$	$0^{d}.285$
Semi-duration of totality	$0^{d}.026$	$0^{d}.023$
Computed range at secondary minimum	$0^{m}.02$	$0^{m}.06$
Radius of brighter star	0.127	0.174
Radius of fainter star	0.275	0.252
Ratio of radii	0.46	0.69
Most probable density of brighter star	0.193	0.075
Most probable density of fainter star	0.019	0.025
Radius of brighter star in terms of sun's radius	1.73	2.36
Radius of fainter star in terms of sun's radius	3.74	3.42
Distance of centers in terms of sun's radius	13.6	13.6
Ratio of surface brightness in photographic light	40.	17.7
Photovisual absolute magnitude of brighter star	1.4	0.7
Photovisual absolute magnitude of fainter star	2.9	2.2
Hypothetical parallax	0″.003	0″.002

the mean magnitude, and the sine of the orbital longitude, corresponding to the mean phase. The full-line curve is computed from the darkened elements; the broken curve, representing the uniform orbit, coincides with it throughout more than half the eclipse.

The photovisual normals have been reduced to the photographic light-curve by applying as a factor the ratio of photographic to photovisual range at primary minimum; they are represented by crosses in Figure 2. It is clear from the plot that the orbit derived from photographic observations satisfactorily represents both the photographic and photovisual data, when allowance is thus made for the difference in the color of the two components.

Cambridge, Massachusetts
March 1922

ORBITS OF THE SPECTROSCOPIC BINARIES LALANDE 13792 AND AOe 12584[1]

By R. F. SANFORD

ABSTRACT

Orbits of the spectroscopic binaries Lalande 13792 and AOe 12584.—Both binaries are dwarfs, with absolute magnitudes of about +5. The elements of each, determined from more than twenty spectrograms, are respectively: P, 32.8092 and 5.4145 days; e, 0.080 and 0.000; K, 27.5 and 64.9 km/sec; γ, +19.7 and −97.4 km/sec. In the case of AOe 12584, the lines of the secondary show faintly and give for K, +74.0 km/sec, and for the functions $m \sin^3 i$ and $m_1 \sin^3 i$ the values 0.803 and 0.704⊙. The large space velocity of AOe 12584, like that of Lalande 29330, is directed away from the quadrant which the apices of other stars of large space motion in general avoid.

Differences between dwarf and giant binaries.—The six spectroscopic binaries of the dwarf division whose orbits have been determined by the writer display smaller eccentricities for a given period group than do giant binaries, as has been shown by R. E. Wilson from data relating to both visual and spectroscopic binaries. Furthermore, they have a mean period much shorter than that of the majority of giants of the same spectral division.

The orbits of nine spectroscopic binaries determined by the writer at the Mount Wilson Observatory have appeared in two previous papers.[2] In the introduction to the first of these may be found explanations of the tables of observations, methods of obtaining and correcting the preliminary elements, and the formation of the velocity curves. In general these statements apply to the two spectroscopic binaries whose orbits are presented in the present contribution. All of the data in Table I are taken from the list of spectroscopic parallaxes of 1646[3] stars. The last column shows

TABLE I

Name	Mag.	α(1900)	δ(1900)	Spectral Class	Vis. Abs. Mag.	μ	π Sp.	No. Rev.
Lal. 13792=H.D. 54371...	7.0	$7^h\ 3^m.5$	+25°54′	G5	4.8	0″.225	0″.036	26
AOe12584=H.D. 107760..	8.2	12 17.9	+73 48	G6	5.4	0.49	0.028	340

H.D.=Henry Draper Memorial Catalog.

---

[1] *Contributions from the Mount Wilson Observatory*, No. 251.

[2] *Ibid.*, Nos. 201, 221; *Astrophysical Journal*, **53**, 201, 1921; **55**, 30, 1922.

[3] *Mt. Wilson Contr.*, No. 199; *Astrophysical Journal*, **53**, 13, 1921.

the number of revolutions of each star in its orbit between the first and last observation of velocity recorded in the tables of observations.

LALANDE 13792 (B.D.+25°1594)

This star was placed on the spectroscopic observing list to increase the data for the curves used for the determination of absolute magnitudes, since the parallax, $0''.031$, derived at the Allegheny Observatory, together with the apparent magnitude, showed it to be a star of low absolute magnitude. The annual proper motion, $0''.225$, is in keeping with this conclusion. The parallax derived by the spectroscopic method is $0''.036$, in good agreement with the trigonometric value. The variability in radial velocity was strongly suspected from the measures of the third plate, and definitely confirmed by that of the fourth. Twenty-two spectrograms have been secured. (Table II.)

TABLE II

OBSERVATIONS OF LALANDE 13792

Plate No.	Date	G.M.T.	Phase	Velocity	O−C
				km/sec	km/sec
γ 8947	1920, Jan. 6	22^h02^m	$13^d.588$	+ 1.4	−3.0
9070	Mar. 11	18 32	12.825	+ 5.2	+3.5
9600	Sept. 29	0 07	17.202	+19.2	−0.6
9715	Nov. 3	0 35	19.411	+32.6	+3.0
9733	Nov. 21	0 55	4.616	+ 1.8	+3.0
9836	Dec. 27	23 50	8.762	− 5.8	+1.5
9941	1921, Feb. 23	20 14	0.994	+13.4	−4.3
10007	Mar. 17	17 50	22.894	+33.3	−9.2
C 955	Mar. 20	17 10	25.866	+51.2	+3.8
γ 10102*	Apr. 19	16 23	23.025	+47.7	+4.9
10111*	Apr. 21	17 42	25.080	+37.7	−9.2
10681	Dec. 8	1 00	25.719	+53.6	+6.2
10754*	1922, Jan. 12	22 26	28.803	+47.4	+3.9
C 1527	Jan. 13	23 43	29.956	+39.5	−0.2
γ 10766	Jan. 15	17 13	31.586	+31.9	+0.9
10825	Feb. 14	18 32	28.831	+38.1	−5.3
C 1567	Feb. 15	19 00	29.851	+41.6	+1.9
γ 10846	Feb. 18	15 24	32.701	+26.0	+1.5
10861	Mar. 6	18 26	16.018	+12.0	−2.5
C 1596	Mar. 8	19 25	18.060	+27.6	+4.0
γ 10918	Mar. 17	17 35	26.982	+47.2	+0.1
11004	May 4	16 14	9.308	−10.6	−3.8

* Given weight ½ in least-squares solution.

The estimated spectrum is G5, with lines of satisfactory quality. There is no certain evidence of the spectrum of the secondary star. It was found possible to assemble all the velocities upon a satisfactory preliminary curve with 32.8092 days as the period. The twenty-six orbital revolutions which separate the first and last observations make an interval so long that only very small changes in the period could be made without seriously disturbing the velocity-curve. Hence this period has been considered final.

Preliminary elements derived by Russell's method and by the graphical method of Lehmann-Filhés were in substantial agreement, the latter giving

PRELIMINARY ELEMENTS

P	32.8092 days
e	0.052
ω	$99\overset{\circ}{.}7$
K	+28.3 km/sec
T	J.D. 2423073.7
γ	+21.2 km/sec

An ephemeris computed with these elements gave the residuals for the velocities. Three plates as indicated in Table II were assigned weight one-half on account of their poor quality. All others were given weight unity.

The final elements result from the correction of the preliminary value by two least-squares solutions, the second being undertaken because of rather large differences between the residuals derived from the elements as first corrected and those derived by substitution of the unknowns in the conditional equations. Although the

FINAL ELEMENTS AND PROBABLE ERRORS

P	32.8092 days
e	0.080±0.039
ω	$82\overset{\circ}{.}1 \pm 26\overset{\circ}{.}1$
K	27.5±1.0 km/sec
T	J.D. $2423071.941 \pm 2\overset{d}{.}334$
γ	+19.7 km/sec
$a \sin i$	12,383,000 km
$\frac{m_1^3 \sin^3 i}{(m+m_1)^2}$	0.0705 $\odot$

quantity Σpv^2 for the final elements, which is seventy-two per cent of its value for the preliminary elements, scarcely differs from that for the elements as first corrected, the ephemeris and conditional equations give residuals that are in satisfactory agreement; moreover, the probable errors for ω and T have been materially reduced, although those for K and e remain as before. The probable error for a velocity of unit weight is ±3.0 km/sec.

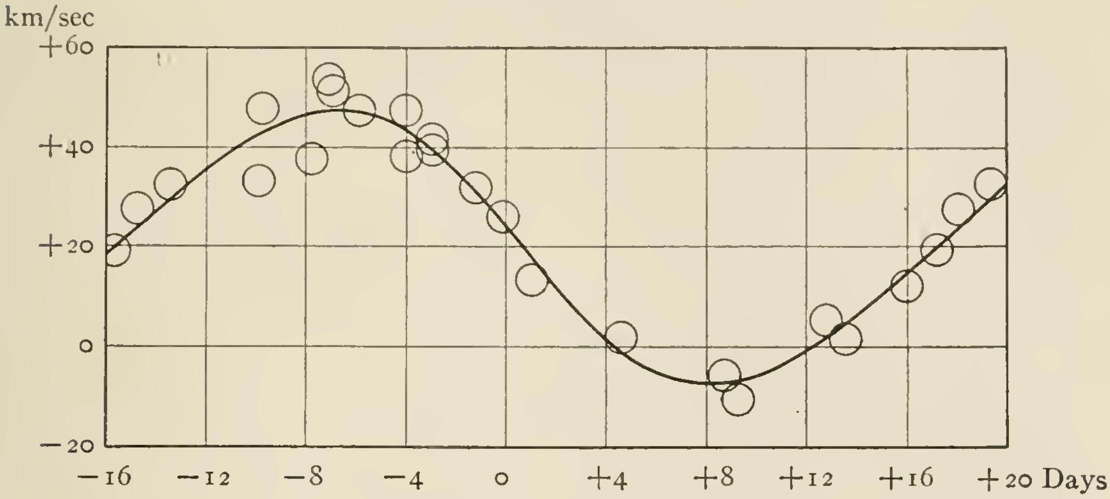

FIG. 1.—Velocity-curve of Lalande 13792

In the radial-velocity diagram (Fig. 1) the velocity of the system has not been represented in the usual way, since its value, +19.7 km/sec, is so nearly that of the line whose ordinate is +20 km/sec that, with the scale used, no distinction could be made between the two.

AOe 12584 (B.D.+74°493)

This star was placed on the Mount Wilson observing list for the determination of absolute magnitudes by the spectroscopic method because of its large annual proper motion (0″.49) and its apparent magnitude (8.2), which suggested low luminosity. The observations gave an absolute magnitude of +5.4, spectral class G6, and the second spectrogram revealed the variation in its radial velocity. Twenty-four plates (Table III) have been secured with the 60-inch reflector, using a one-prism spectrograph provided with a camera of 18-inches focus, except that for the second, third, and fourth plates a camera of 7-inches focus was used. These have been assigned half weight. The northerly declination of this object puts it beyond the reach of the Hooker telescope, the use of which would have been advantageous, for with the 60-inch reflector, even under fair conditions, it has been necessary to use exposures of about three hours. Under poor conditions, which are likely to occur at the season when the star is best placed for observation, longer exposures have been necessary and some plates are rather underexposed. Weights have been assigned accordingly. The spectrum shows a satisfactory set of lines for measurement when the velocity is near that of center of mass. But the secondary spectrum is bright enough to render the spectral lines of the primary less distinct by the superposition of the continuous spectrum when the radial velocities of the two components differ. Measures of the radial velocity of the secondary have been made on several plates, as Table III shows, but are not considered suitable to the

TABLE III

OBSERVATIONS OF AOE 12584

PLATE NO.	DATE	G.M.T.	PHASE	VELOCITY		O–C PRIM.	WT. PRIM.
				Prim.	Second		
				km/sec	km/sec	km/sec	
γ 5704......	1917, Apr. 4	$20^{\text{h}}20^{\text{m}}$	$2^{\text{d}}.042$	−152.9	....	− 9.0	0.5
6929*.....	1918, May 24	17 25	1.001	− 70.3	....	+ 1.2	0.5
8170*.....	1919, May 13	19 25	3.139	−170.6	....	−16.2	0.5
8292*.....	June 13	17 23	1.567	−106.1	....	+ 7.2	0.5
9056......	1920, Mar 8	20 30	5.385	− 33.1	−163.2	− 0.5	1.0
10000......	1921, Mar. 16	21 02	4.803	− 44.1	−149.1	+ 4.0	1.0
10008......	Mar. 17	20 23	0.362	− 37.7	−168.0	+ 0.4	1.0
10100......	Apr. 18	19 49	5.267	− 38.6	−156.6	− 5.2	0.5
10113......	Apr. 21	21 00	2.901	−151.8	− 28.0	+ 8.9	1.0
10125......	Apr. 25	20 18	1.457	−102.1	....	+ 3.1	1.0
10148......	May 14	18 45	4.148	− 96.4	....	− 5.6	1.0
10152......	May 15	19 22	5.174	− 37.2	−167.8	− 2.3	1.0
10200......	June 14	18 10	2.637	−169.4	....	− 7.3	0.5
10202......	June 15	18 00	3.630	−123.8	− 33.6	+ 4.7	0.5
10206......	June 16	17 58	4.629	− 59.1	....	− 1.5	0.5
10210......	June 18	17 39	1.200	− 87.6	....	− 1.7	1.0
10220......	June 20	17 36	3.199	−158.5	− 31.0	− 6.4	1.0
10251......	July 11	17 23	2.532	−158.0	− 33.6	+ 2.9	1.0
10255......	July 12	17 10	3.523	−119.3	....	+16.1	1.0
10262......	July 13	17 07	4.521	− 59.1	−135.4	+ 5.2	1.0
10277......	July 16	17 06	2.105	−148.8	− 27.7	− 1.7	1.0
10862......	1922, Mar. 6	21 45	2.474	−158.6	− 27.2	+ 1.3	0.5
10963......	Apr. 7	19 26	1.891	−137.4	....	− 2.1	0.5
11000......	Apr. 18	18 29	2.021	−143.7	− 20.2	− 0.8	1.0

* Taken with 7-inch camera.

determination of any element except the amplitude and the relative masses of the two components, to be referred to later.

A set of preliminary elements, derived after twenty spectrograms had been secured, has already been published.[1] One branch of the velocity-curve was later strengthened by four additional plates, after which a second set of elements was derived.

PRELIMINARY ELEMENTS

	(1)	(2)
P	$5^{\mathrm{d}}.414$	$5^{\mathrm{d}}.41454$
e	0.000	0.025
ω		204°
K	64 km/sec	67 km/sec
K_1	70 km/sec	
T	J.D. 2422798.875	2422856.162
γ	−97.5 km/sec	−97.8 km/sec

The differences are slight, when it is considered that for circular elements the epoch is arbitrary and that K_1 has been left for determination in a more accurate way.

The second set indicated a slight eccentricity, the reality of which it seemed more satisfactory to leave to the outcome of a least-squares solution. Since 340 revolutions separate the first and last observations, the period has been taken as definitive. If K_1 is derived independently, and ω_1 for the secondary is taken as $\omega+180°$, there remain only five elements to be corrected by the method of least-squares.

As often happens when the eccentricity is small, two of the resulting normal equations were practically identical. Hence only four, instead of five unknowns, could be determined satisfactorily. In this case, instead of corrections to ω and T, a correction to u, the argument of latitude, results. As a matter of fact, three sets of corrections have been derived, (*a*) one which corrects all five elements, (*b*) another set which corrects three elements and the argument of latitude, u, and (*c*), a set like the second, except that it is based upon the twenty-two spectrograms that remain after the rejection of two (γ 8170 and γ 10255) with large residuals. The value of Σpv^2 for the elements thus corrected becomes less and less, both for all the observations and for the twenty-two considered in the last set. In other words, the rejection of the two observations showing large residuals leads to corrections which do not materially affect the size of these residuals and does improve the representation of the remaining observations.

---

[1] *Publications American Astronomical Society*, 4, 283, 1921.

A comparison of the residuals derived from an ephemeris based upon set (*c*) with those derived from substitution into the conditional equations showed that the elements might be further improved. Since these corrections had reduced the eccentricity to 0.005, this element was assumed to be zero and another least-squares solution for corrections to γ, K, and T was made, T now being referred to the time of the smallest negative velocity of the primary. After these corrections had been applied, ephemeris and conditional equations gave practically identical values for the residuals. Hence these elements are considered definitive.

K_1 has been determined from the relation $K_1 = K\left(\frac{V_1-\gamma}{V-\gamma}\right)$ in which V is the computed velocity for the primary, V_1 is the observed velocity of the secondary, and γ and K are elements of the primary. The weights assigned depend on the number of lines measured in determining V_1.

FINAL ELEMENTS AND PROBABLE ERRORS

P	$5^{\mathrm{d}}.41454$
K	64.9 ± 1.3 km/sec
K_1	74.0 km/sec
T	J.D. $2422853.120 \pm 0^{\mathrm{d}}.020$
γ	-97.4 km/sec
$a \sin i$	4,833,000 km
$a_1 \sin i$	5,510,000 km
$m \sin^3 i$	$0.803 \odot$
$m_1 \sin^3 i$	$0.704 \odot$

Reference to set (1) of the preliminary elements will show how closely they agree with the final elements, and that the choice of set (2) was not a happy one, although for this case the eccentricity was not arbitrarily assumed to be zero.

If all twenty-four plates are considered, the probable error of a single determination of radial velocity of unit weight is ±4.0 km/sec, and ±2.9 km/sec if based upon the twenty-two plates finally used. The probable errors for the elements are based on the larger of these two values, which is also used as radius for the circles representing the individual velocities in the diagram in Figure 2. The barred circles refer to velocities derived from the three spectrograms taken with low dispersion to which reference has already been made. The larger circles represent the velocities for the secondary star as far as they were measured. Their evident inaccuracy did not seem to warrant the inclusion of a velocity-curve for them.

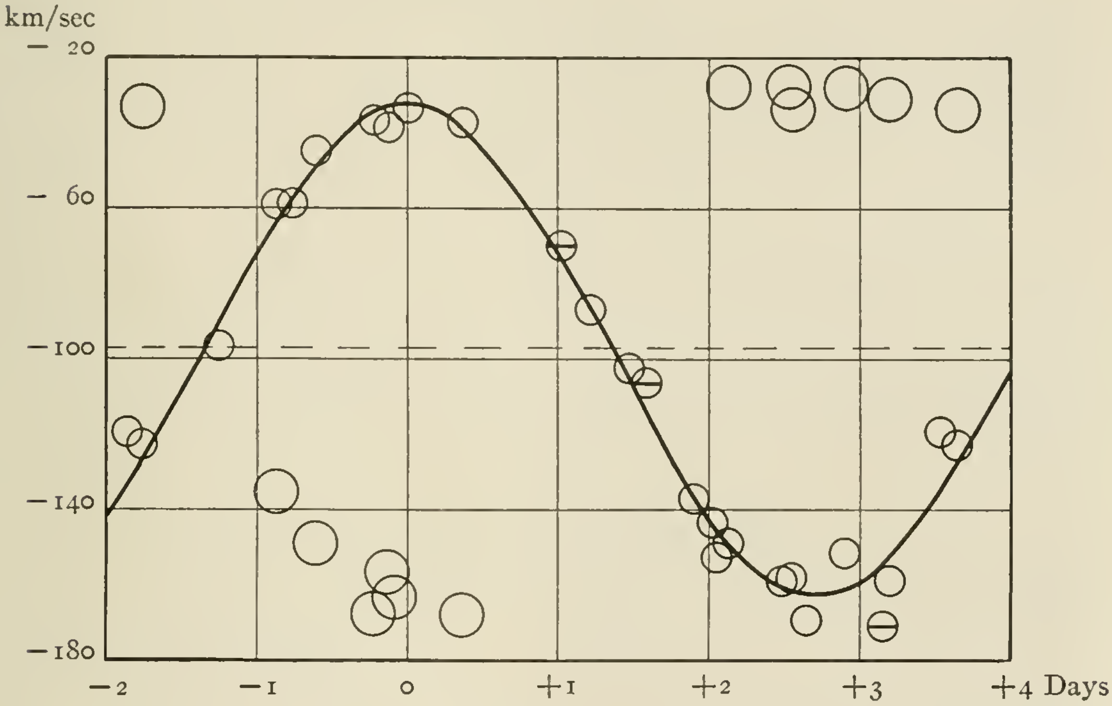

FIG. 2.—Velocity-curve of AOe 12584

Including the two binaries discussed in this paper, six of a total of eleven whose orbits have been derived by the writer at Mount Wilson have absolute magnitudes that place them in the dwarf division. Since binary stars of low luminosity are relatively few in number, it is of interest to collect certain elements for these six stars, as has been done in Table IV.

Attention has already been called to the fact that the dwarf binary Lalande 29330[1] has a period and an eccentricity both of which are small for a star of its spectral class when compared with mean values based upon hitherto existing material, relating, for the most part, to giant stars. Forming mean values of spectral class, period, eccentricity and absolute magnitude for the six binaries, we find the data of the first line of Table V. This is followed by the similar data for class G stars taken from a table by Aitken.[2]

TABLE IV

Name	App. Mag.	Sp. Class	Abs. Mag.	P	e	K	γ	$a \sin i$	$\frac{m_1^3 \sin^3 i}{(m+m_1)^2}$
						km/sec	km/sec	km	⊙
OΣ 82.....	7.0	F9	4.1	$4\overset{d}{.}0000$	0.060	36.1	+37.4	1.98×10^6	0.0193
Lal. 29330..	8.5	K0	6.0	4.2850	0.089	38.1	−60.6	2.24×10^6	0.0244
Lal. 49867..	7.3	K2	6.0	6.7217	0.059	38.5	−19.8	3.55×10^6	0.0396*
AOe 12584..	8.2	G6	5.4	5.4145	0.000	64.9	−97.4	4.83×10^6	....
75 Cancri...	6.0	G2	4.1	19.4589	0.206	20.2	+12.3	5.26×10^6	0.0157
Lal. 13792..	7.0	G5	4.8	32.8092	0.080	27.5	+19.7	12.38×10^6	0.0705

* Given erroneously as 0.0125 ⊙ in *Mt. Wilson Contr.*, No. 201.

TABLE V

Spectral Class	Period	Eccentricity	Abs. Mag.
G4..............	12 days	0.082	+5.1
G...............	267 days	0.129	Mostly giants

When it is considered that the first line shows mean values for stars whose spectral classes range from F9 to K2, and that in the table from which the second line is taken the value of *e* is larger for the spectral divisions which precede and follow G, it appears that in Table V we again have evidence that dwarf binaries have shorter periods and smaller eccentricities than do giant stars of approximately the same spectral class.

Dr. R. E. Wilson has also discussed the period-eccentricity relation[3] for binary stars, and as far as his data go, finds that for the same average period dwarf stars have an average eccentricity smaller than that of the giants. In order to display this feature, the material in Table I of his paper corresponding to that in Table IV above is reproduced in Table VI. The first column gives his number of the period group, the range in each of which is given in the second column. Then follow pairs of columns which show the mean eccentricity and the number of stars for giants and for dwarfs, and, finally a pair which give the same data derived from the six binaries in Table IV.

---

[1] *Mt. Wilson Contr.*, No. 201; *Astrophysical Journal*, **53**, 212, 1921.

[2] *The Binary Stars*, p. 199, 1918.

[3] *Astronomical Journal*, 33, 147, 1921.

TABLE VI

Group	Period	Giants		Dwarfs		Dwarfs (Sanford)	
		e	No.	*e*	No.	*e*	No.
2........	4– 8 days	0.114	19	0.020	3	0.052	4
3........	8– 25 days	0.250	22	0.132	4	0.206	1
4........	25–100 days	0.468	15	0.010	1	0.080	1

It is readily seen that the eccentricities for the first column of dwarfs are systematically smaller than those for giants, which is borne out rather well by the spectroscopic binaries whose eccentricities are displayed in the next to the last column.

Both Aitken[1] and Wilson[2] have called attention to an apparently abrupt change in the mean eccentricity for the stars with periods between 25–100 days.

Although the data for such a conclusion are meager indeed, the same phenomenon is shown in the last column of eccentricities, but it is by no means certain from either the fifth or seventh columns that there is a minimum in the eccentricity-period relation for group 4 or a maximum for group 3. Two more dwarf binaries for which I have nearly enough material for orbits will add one star each to groups 2 and 3 and will have eccentricities consistent with the values given in this seventh column. Orbital elements of dwarf spectroscopic binaries falling in groups 3 and 4 are therefore especially to be desired in order to settle (*a*) the reality of this departure from a smooth curve in the period-eccentricity relation, and (*b*) whether the departure means a maximum for group 3 or a minimum for group 4.

[1] *The Binary Stars*, p. 197, 1921.

[2] *Astronomical Journal*, 33, 147, 1921.

It is of interest to note that two of the binaries of Table IV, Lalande 29330 and AOe 12584, have large velocities of the center of mass (γ). Their space motions place them in that group of stars of large space-velocity whose motions have been discussed by Adams and Joy[1] and later more completely by Strömberg,[2] and whose apices are directly away from the quadrant of avoidance shown to exist by these investigators.

Mount Wilson Observatory
September 1922

---

[1] *Mt. Wilson Contr.*, No. 163; *Astrophysical Journal*, **49**, 179, 1919.

[2] *Proceedings of the National Academy of Sciences*, **8**, 141, 1922.

STELLAR SPECTRA OF CLASS S[1]

I. GENERAL DESCRIPTION

By PAUL W. MERRILL

ABSTRACT

Class S stars.—A number of red stars have spectra similar to that of R Geminorum, which differs from the recognized types of the Harvard classification. It is proposed to group them into an additional class with the symbol S. *A provisional list* of 22 S stars is given, including the following *long-period variables: X and R Androm., R and T Camelop., V Cancri, R Can. Min., U and S Cassiop., R Cygni, R and T Gemin., RW Librae, R Lyncis, R Orionis, T Sagittarii, and S Urs. Maj. Characteristic spectral features* are shown by typical spectrograms and by a table of forty-three lines from λ 4500 to λ 4860, particularly a complicated structure between λ 4630 and λ 4660. The absorption lines λ 4554 (Ba) and λ 4607 (Sr) are unusually strong, and there is an absorption band in the red extending from λ 6470 to longer wave-lengths. A remarkable feature is the presence of enhanced lines of iron, λλ 4584, 4924, and 5018, as emission lines. As in the case of class M stars, the variables alone show strong bright hydrogen lines (type Se); $H\beta$ is more intense than $H\gamma$, and the lines are narrow. A list of the plates obtained at Mount Wilson, together with the dates, phases, and notes as to the individual spectra, are given. *The relationship to other classes* is discussed. While the S stars appear to be more closely related to giant Ma stars than to any other type, they probably do not belong in either the G-R-N or the G-K-M branch, but form a third branch. The recognition of these stars as a distinct group should aid in the general study of long-period variables.

In Secchi's classification of stellar spectra, made nearly sixty years ago, there are two great groups of orange and red stars, namely, types III and IV. Both types are marked by characteristic absorption bands which face in opposite directions in the two types. Those of type III are now known to be due to titanium oxide, and those of type IV to carbon. In the more detailed system of classification developed at the Harvard College Observatory, these groups, called classes M and N respectively, have been subdivided, but stars with intermediate spectra have not been found. No object is known to show both carbon and titanium bands; these spectral features seem to be mutually exclusive. Accordingly there is no place for the carbon stars in the spectral progression which runs without a break through the sequence of classes B, A, F, G, K, and M, since the latter end of this chain is characterized by increasing strength of the titanium bands. The alternative arrangement for class N is a side branch paralleling the main sequence in the K-M region. The discovery of the class R stars, which in color and spectroscopic details are intermediate between classes G and N, strongly supports this view.[1]

---

[1] *Contributions from the Mount Wilson Observatory*, No. 252.

Among the long-period variables there are a number which are not clearly of either class M or class N, and which have been variously classified by the Harvard observers. The following statement in regard to these stars is found in the introduction to the *Henry Draper Catalogue:*

> Several spectra which have hitherto been called Md1 or Md2, in which Hβ is the strongest bright line, are found to be peculiar and are designated Pec. in Table I. The variable stars R Andromedae, U Cassiopeiae, S Cassiopeiae, R Lyncis, R Canis Minoris, T Geminorum, and R Cygni may be given as examples. These spectra do not show the titanium bands having bright edges at 4762, 4954, and 5168 as in all divisions of Class M, but more nearly resemble the spectrum of π^1 Gruis, which may be placed in a subdivision of Class R, assuming some peculiarities.

Few observations of any of these stars have been made with slit spectrographs until recently. Spectrograms of R Cygni were secured by Wright[2] in December, 1911. They showed a complicated spectrum most of whose details could not be identified. Several stars of this type were included in the radial velocity observations of long-period variables[3] made by the writer at Ann Arbor from 1913 to 1915, but in only one case was the exposure sufficient to show the absorption spectrum; R Lyncis, photographed in February, 1915, was found to have a spectrum resembling that of R Cygni as observed by Wright.

Since resuming the investigation of long-period variables at Mount Wilson, I have photographed a number of objects which have spectra of the same type as R Cygni and R Lyncis. They have been recognized as forming a special group distinct from either class M, N, or R. The designation class "S" has been suggested for them by the action of the International Astronomical Union at the Rome meeting in May, 1922.

---

[1] The relationships between classes G, R, and N have been thoroughly discussed by Rufus, *Publications of the Observatory, University of Michigan*, **2**, 103, 1916.

[2] *Monthly Notices*, 72, 548, 1912. The preceding article gives an account of visual observations by Espin.

[3] *Publications of the Observatory, University of Michigan*, **2**, 45, 1916.

It is the purpose of this article to furnish a description of spectra of class S together with some remarks on the relationship to other classes. The general conclusion may be anticipated here by stating that the S stars probably form a third branch of the spectral sequence in addition to the G-K-M and the G-R-N branches. (See page 473.)

In Table I is given a first list of stars of class S. The observations upon which the inclusion of each star depends may be inferred from Table II, which gives a record of the Mount Wilson spectrograms, and from the Harvard notes and the brief discussions of each star which follow. It is highly probable that future observations will disclose additional stars of class S, especially among the long-period variables. It is less likely, though not impossible, that one or two stars of Table I will be shown by improved observations to belong to some other spectral class.

TABLE I

Provisional List of Stars of Class S

Name	H.D.	R.A. 1900	Dec. 1900	Mag.	Spect.	Period days
X Androm.	1167	$0^h10^m.9$	+46° 27′	8.1–14.2	Se	346.5
R Androm.	1967	0 18.8	+38 1	5.6–14.0	Se	410.7
U Cassiop.	4350	0 40.8	+47 43	8.0–16.	Se	276.0
S Cassiop.	7769	1 12.3	+72 5	7.6–14.5	Se	609.5
T Camelop.	29147	4 30.3	+65 57	7.0–13.5	Se	370
R Orionis	31798	4 53.6	+ 7 59	8.7–13.5	Se?	378.5
	35155	5 17.6	− 8 45	7.0	S	....
R Lyncis	51610	6 53.0	+55 27	7.0–13.8	Se	379.2
R Gemin.	53791	7 1.3	+22 52	6.4–13.8	Se	370
R Can. Min.	54300	7 3.2	+10 11	7.2–10.0	Se	337.7
	58881	7 22.4	−11 31	9.0	S	....
T Gemin.	63334	7 43.3	+23 59	8.0–13.5	Se	288.1
	63733	7 45.3	−18 45	8.5	S	....
V Cancri	70276	8 16.0	+17 36	7.5–13.0	Se	272.1
S Urs. Maj.	110813	12 39.6	+61 38	7.3–12.5	Se	226.5
	121447	13 50.3	−17 45	8.1	S	....
R Camelop	127226	14 25.1	+84 17	7.9–13.7	Se	269.5
RW Librae	136734	15 17.2	−23 42	8.6–11.7	Se	490 (about)
	172804	18 37.1	+ 6 43	9.1	S	....
T Sagittarii	....	19 10.5	−17 9	7.2–12.0	Se	381.3
R Cygni	....	19 34.1	+49 58	6.6–13.9	Se	426
π^1 Gruis	....	22 16.6	−46 27	6.6	S	....

Table II contains a record of most of the Mount Wilson spectrograms of stars of class S. They were secured with one-prism slit

TABLE II

Journal of Observations

Star	Plate	Date	Mag.	Phase	Intensities			Remarks
					Hβ	Hγ	Hδ	
				days				
X Androm.	C 1454	1921, Nov. 13	9.5	−16	12	2	.....	
	C 1462	Nov. 14	9.5	−15	4	0.5	.....	
R Androm.	γ 8725	1919, Oct. 3	7.5	−25	5	2	1	
	C 130	Oct. 15	7.5	−13	4	2	2	
	C 137	Oct. 16	7.5	−12	6	3	3	
	C 1499	1921, Dec. 15	7.5	−16	12	5	5	
U Cassiop.	C 1449	1921, Nov. 12	8.2	− 4	8	4	4	
	C 1455	Nov. 13	8.2	− 3	9	4	3	
S Cassiop.	γ 10755	1922, Jan. 13	8.9	+22	7	2	.....	
T Camelop.	γ 11245	1922, Aug. 9	8.8	−36	5	2	.....	Obs. by Hoge
H.D. 35155	C 672	1920, Sept. 26	7.0	.....	.....	.....	.....	
R Gemin.	γ 8727	1919, Oct. 3	7.4	−27	8	3	0.5	
	C 127	Oct. 14	7.0	−16	10	5	2	
	C 133	Oct. 15	7.0	−15	12	6	2	
	C 144	Oct. 17	7.0	−13	12	6	2	
	C 681	1920, Sept. 28	7.2	−30	8	3	.....	
	C 821	Dec. 27	8.3	+60	10	4	0.5	
	C 1339	1921, Sept. 21	8.1	−50	4	0.5	.....	
	γ 10524	Oct. 10	7.2	−31	12	5	1	
	C 1402	Oct. 13	7.1	−28	.....	.....	.....	Red region
	C 1408	Oct. 14	7.1	−27	.....	.....	.....	Red region
	C 1456	Nov. 13	7.2	+ 3	15	7	2	
	C 1501	Dec. 15	7.3	+35	12	7	2	
	C 1502	Dec. 15	7.3	+35	.....	.....	.....	Green region
R Can. Min.	C 294	1920, Mar. 3	8.0	−10	15	5	0.5	
	C 299	Mar. 4	8.0	− 9	15	5	0.5	
	γ 9047	Mar. 7	8.0	− 6	8	3	.....	
	C 909	1921, Feb. 25	8.3	+20	15	7	2	
	γ 9990	Feb. 28	8.3	+23	.....	.....	.....	Red region
	C 1522	1922, Jan. 12	8.5	−33	6	3	.....	
T Gemin.	C 968	1921, Mar. 28	9.1	−23	2	0.5	0.5	
	C 1009	Apr. 29	8.6	+ 9	10	5	3	
H.D. 63733	C 1464	1921, Nov. 14	8.5	.....	.....	.....	.....	
V Cancri	C 194	1919, Nov. 9	8.0	+10	15	7	2	
	γ 8875	Nov. 13	8.0	+14	7	3	1	
	γ 8883	Nov. 14	8.0	+15	6	3	0.7	
	γ 10132	1921, Apr. 27	7.9	− 3	10	5	0.7	
	γ 10757	1922, Jan. 13	7.9	−12	9	5	0.7	
	C 1552	Feb. 11	7.8	+17	15	8	3	
S Urs. Maj.	C 369	1920, Apr. 8	8.5	−31	7	3	.....	
	C 373	Apr. 10	8.5	−29	11	5	.....	
	γ 9252	June 3	8.2	+25	6	3	.....	
	γ 9848	Dec. 29	8.4	+25	6	4	1	
	C 866	1921, Jan. 28	8.8	−52	4	2	.....	
	C 1553	1922, Feb. 11	8.5	−28	7	3	.....	
	C 1626	Mar. 19	7.6	+ 8	9	6	1	
H.D. 121447	C 1706	1922, May 16	8.1	.....	.....	.....	.....	
R Camelop.	γ 8266	1919, June 9	8.2	+ 7	4	2	.....	
	γ 8272	June 10	8.2	+ 8	2−	1	.....	
	γ 8345	July 8	8.9	+36	2	1	.....	
	γ 11077	1922, May 17	8.2	−18	4	2	0.4	
H.D. 172804	C 472	1920, June 6	9.1	.....	.....	.....	.....	Obs. by Sanford

TABLE II—*Continued*

Star	Plate	Date	Mag.	Phase	Intensities			Remarks
				days	Hβ	Hγ	Hδ	
T Sagittarii............	C 1059	1921, June 20	8.5±	+39	7	3	1	
		1922, July 13	9.1	+65	6	2	.....	
R Cygni..............	C 965	1921, Mar. 27	7.3	+31	15	6	2	
	C 966	Mar. 27	7.3	+31	.....	.....	.....	Red region
	C 1007	Apr. 28	8.9	+63	15	5	2	
	C 1038	May 26	9.2	+91	15	5	2	
	γ 11079	1922, May 17	6.8	+ 4	10	4	1	
	γ 11117	June 14	8.0	+32	15	5	2	
	C 1784	July 11	8.9	+59	15	6	2	

spectrographs with 18-inch camera-lens foci, and are of the usual photographic region unless otherwise noted in the remarks. The γ plates were secured with the 60-inch reflector; the C plates with the 100-inch Hooker reflector. The column headed "Phase" gives the number of days before (−), or after (+), the nearest maximum. The intensities of the bright hydrogen lines are estimates of the strength of the lines on the negatives, no allowance having been made for instrumental or other observational effects. Hβ is usually overexposed and the estimates of this line are doubtless only rough approximations.

X ANDROMEDAE, H.D. 1167

Remark in *H.D.:*

> On a photograph taken November 8, 1904, the spectrum was estimated Mb, having Hγ and Hδ bright, and equal in intensity.

The Mount Wilson plate taken on November 13, 1921, shows a spectrum similar to that of R Andromedae (C 137), but resembling still more closely R Geminorum (C 133) and S Ursae Majoris (C 373). The M bands are not recognizable and must be very weak, if present at all. Of the bright hydrogen lines, Hδ is not seen, Hγ is a fairly strong narrow line, and Hβ is overexposed. The intensities of Hβ and Hγ are perhaps as six or eight to one. This estimate is best made from the plate taken on the following night, which has much less exposure, and on which the strong bright Hβ line is the only outstanding feature; Hγ is clearly seen but is very weak.

It is evident that at the 1921 maximum the spectrum differed very greatly from that at the date of the Harvard observations which was less than a month after the 1904 maximum. Changes of this character are of the highest interest as bearing on the relationships between classes M and S. It is hoped to discuss them in a subsequent contribution, after more observational data have been secured.

R ANDROMEDAE, H.D. 1967

Remark in *H.D.:*

> The spectrum is very peculiar, and does not appear to be of any division of Class M. In the continuous portion between Hβ and Hγ it resembles the spectrum of π^1 Gruis, R.A. $22^h16^m.6$, Dec. $-46°27'$, and should probably be placed in some division of Class R. The continuous portion of the spectrum is very faint in the region having shorter wave-length than Hγ. The hydrogen lines Hβ, Hγ, Hδ, and Hζ are bright. Hβ is about 0.3 as bright as Hγ and Hδ which are nearly equal.

If we applied to S-type stars the criteria of absolute magnitude developed by Adams and Joy for K and M stars, R Andromedae would appear to be of high luminosity (perhaps comparable with K and M giants), since λ 4215 is strong and λ 4455 weak. The bright hydrogen lines are very conspicuous. The Harvard and the Mount Wilson observations agree in making bright Hζ stronger than Hϵ. This circumstance is discussed on page 471. Several narrow maxima are present in the continuous spectrum, some of which, at least, are doubtless true emission lines. Among these are the enhanced iron lines λλ 4584, 4924, 5018. (See page 472.)

U CASSIOPEIAE, H.D. 4350

Remark in *H.D.:*

> The spectrum resembles that of R Andromedae, H.D. 1967, and does not appear to be of Class M. Hγ and Hδ are bright. On a photograph taken July 10, 1894, these two lines are of equal brightness, but on photographs of October 8, 1896, and December 1, 1905, Hδ is from 3 to 6 times as bright as Hγ.

The spectrum shows considerable difference from that of R Andromedae (C 137) and more nearly resembles that of R Geminorum (C 133). There is a definite indication of the titanium band at λ 4954, and possibly a trace of the one at λ 4761.

S CASSIOPEIAE, H.D. 7769

Remark in *H.D.:*

The spectrum is peculiar, and does not appear to be of Class M, but to resemble in characteristics that of R Andromedae, H.D. 1967. On several photographs examined the brightness of Hβ varies from 2 to 10 times that of Hγ.

On the Mount Wilson spectrogram, γ 10755, bright Hβ is several times as strong as Hγ. The continuous spectrum is very weak but traces of the principal S features are seen.

T CAMELOPARDALIS, H.D. 29147

Remark in *H.D.:*

The spectrum resembles Class R, in having the strong absorption band 4640–4750, and other dark bands between Hβ and Hγ. It is very faint in the region of shorter wave-length than Hγ.

The only Mount Wilson plate is underexposed but several of the chief S features can be identified.

R ORIONIS, H.D. 31798

Remark in *H.D.:*

The line Hβ is bright. The spectrum shows strong dark bands and may belong to Class R.

H.D. 35155

Remark in *H.D.:*

The spectrum resembles that of π^1 Gruis in the region from Hβ to Hγ.

Omitting the bright hydrogen lines, this spectrum is on the whole a very good match for that of R Geminorum (C 133), although a few of the less conspicuous absorption lines are weaker than in R Geminorum and there are slight differences in the characteristic S structure near λ 4650. The titanium bands are more prominent, that at λ 4954 being fairly strong, with indications of others.

R LYNCIS, H.D. 51610

Remark in *H.D.:*

The spectrum does not appear to be of Class M, but to resemble that of R Andromedae, H.D. 1967. The lines Hβ, Hγ, and Hδ are bright. On photographs taken November 27, 1905, and December 12, 1907, the line Hγ was the strongest bright line. Hβ and Hδ were respectively 0.4 and 0.1 as strong as Hγ.

The Ann Arbor observations indicated that this spectrum is similar to that of R Cygni as observed by Wright. See *Publications of the Observatory, University of Michigan*, **2**, 52, 65, 1916.

R GEMINORUM, H.D. 53791

Remark in *H.D.:*

> The spectrum is peculiar and resembles that of Class R rather than Class M. Two dark bands are present between Hβ and Hγ. On photographs taken October 25, 1906, and October 12, 1910, Hγ is bright. The spectrum is not seen in regions of shorter wave-length than 4300.

As compared with R Andromedae there is a general similarity but many differences are obvious. Bright Hδ is much weaker relatively to Hγ than in R Andromedae. The continuous spectrum does not extend as far toward the violet. The absorption line λ 4554 is much stronger and broader. There are numerous differences in the relative intensities of lines and in the details of band structure. The spectrograms of the red region record Hα as a bright line, and show the strong absorption band at about λ 6470, which was photographed by Wright in the spectrum of R Cygni (*Monthly Notices*, **72**, 548, 1912).

R CANIS MINORIS, H.D. 54300

Remark in *H.D.:*

> The spectrum is peculiar and resembles that of R Andromedae, H.D. 1967. On photographs taken February 3, 1897, February 1, 1910, and January 24, 1911, the line Hγ is bright.

The spectrum differs somewhat from that of R Geminorum, and decidedly from that of R Andromedae. As compared with R Geminorum (C 133) there are some dissimilarities in the details of the band absorption near λ 4645, and a feature at λ 4736 is quite different. The plate of the red region is badly underexposed but shows the Hα line to be bright.

H.D. 58881

Remark in *H.D.:*

> The spectrum is not seen in the region of shorter wave-length than 4200. It resembles that of π^1 Gruis. Bright and dark bands are situated between Hβ and Hγ.

T GEMINORUM, H.D. 63334

Remark in *H.D.:*

On a photograph taken February 8, 1893, the spectrum is peculiar and probably resembles that of R Andromedae, H.D. 1967. It is very faint except in the region between Hβ and Hγ. The lines Hγ and Hδ are bright.

The spectrum is much like that of R Geminorum, though not an exact duplicate.

H.D. 63733

Remark in *H.D.:*

In the region of 4700, the spectrum resembles that of π^1 Gruis, R.A. $22^h16^m.6$, Dec. $-46°27'$. It is very faint from Hγ to the end of shorter wave-length.

Except for the bright hydrogen lines, which are missing, this spectrum is a rather close match for that of R Geminorum (C 133).

V CANCRI, H.D. 70276

Remark in *H.D.:*

On a photograph taken March 30, 1892, the lines Hβ and Hγ are nearly equally bright, and the spectrum is very faint from Hγ to the end of shorter wave-length. The spectrum may resemble that of R Andromedae, H.D. 1967.

This spectrum is much like that of R Geminorum, but the band absorption is slightly weaker.

S URSAE MAJORIS, H.D. 110813

Remark in *H.D.:*

On photographs taken February 22, 1906, and April 26, 1909, the spectrum is of a peculiar class, and resembles that of R Andromedae, H.D. 1967. The line Hγ is bright. A bright band is situated at about 4645.

This spectrum is much like that of R Geminorum. Certain changes dependent on the light phase have been observed and will be described in another contribution.

H.D. 121447

Remark in *H.D.:*

The spectrum is not seen in the region having shorter wave-length than 4200. It bears some resemblance to the spectrum of π^1 Gruis between Hβ and Hγ.

With the exception of the bright hydrogen lines, which are missing, this spectrum is a fair match for that of R Geminorum

(C 133), although there are some differences in the relative intensities of certain features. The band absorption is weaker.

R CAMELOPARDALIS, H.D. 127226

Remark in *H.D.*:

> On a photograph taken May 20, 1890, the spectrum is peculiar with bright and dark bands between Hβ and Hγ, and resembles that of R Andromedae, H.D. 1967. The lines Hβ, Hγ, and Hδ are bright. The relative intensities are 2, 10, and 2.

All of the Mount Wilson plates are underexposed. The continuous spectrum is too faint to classify with certainty, but it is probably of class S.

RW LIBRAE, H.D. 136734

Remark in *H.D.*:

> On a photograph taken June 3, 1907, the spectrum has the lines Hβ, Hγ, and Hδ bright. The intensities are 8, 10, and 3, respectively. The continuous spectrum is much stronger between Hβ and Hγ than in other portions. It is not well defined but probably resembles that of R Andromedae, H.D. 1967.

H.D. 172804

Remark in *H.D.*:

> The spectrum is faint. It may resemble that of the variable star 043065, T Camelopardalis, H.D. 29147.

With the exception of the bright hydrogen lines, which are missing, this spectrum closely resembles that of R Geminorum, but there is more contrast in certain features. The band absorption is probably stronger than in any other non-variable S-type star observed at Mount Wilson. Parts of the spectrum are much like that of π^1 Gruis, but a band-head near λ 4736 is lacking. The plate of H.D. 172804 was secured by Mr. Sanford in connection with his program for class R stars. I am indebted to him for permission to make use of it.

T SAGITTARII *191017*

Remark in *H.A.*, 56, page 211:

> The spectrum changes from Md0 to Md4, on 8 plates. Hδ apparently changes from 30 to 70. On two plates the spectrum is peculiar, and on one plate it is Class Md peculiar.

On the Mount Wilson plates the continuous spectrum is too faint to classify with certainty but is probably of class S.

R CYGNI 193449

Remark in *H.A.*, 56, p. 211:

> The spectrum of this star is peculiar, and shows changes on the various photographs.

This spectrum resembles that of R Geminorum (C 133) more than that of R Andromedae (C 137), but has the band absorption somewhat stronger than in R Geminorum. Photographs of the spectrum of R Cygni were secured by Wright in December, 1911, and are described in the *Monthly Notices*, 72, 548, 1912. The Mount Wilson plate of the red region is underexposed, but shows a strong bright Hα line and the prominent band at about λ 6470 as observed by Wright. Visual observations by Espin, recorded in the *Monthly Notices*, 72, 546, 1912, indicate that during the latter part of 1911 the spectrum varied as the brightness increased. The recent Mount Wilson photographs, including some not listed in Table II, also show very considerable changes in some features of the spectrum. They are briefly described in the *Publications of the Astronomical Society of the Pacific*, 33, 206, 1921. A more complete discussion of the changes is reserved for another paper.

π^1 GRUIS

Remark in H.A., 56, page 219:

> The spectra of T Camelopardalis and π^1 Gruis resemble each other and are very peculiar. The absorption band between 4640 and 4750, is present, and almost all of the continuous spectrum between this band and Hγ is cut out by other strong absorption bands.

This star is too far south for the Mount Wilson telescopes, but slit spectrograms taken at the Lick Observatory station at Santiago, Chile, in July and September, 1915, have been made available to me through the kindness of Dr. Campbell and Dr. Moore. This spectrum is the only one thus far observed with slit spectrographs which resembles R Andromedae more than R Geminorum. Several bright lines or maxima are weaker in π^1 Gruis than in R Andromedae, but on the whole the similarity is very close, with, of course, the exception of the bright hydrogen lines which are seen only in R Andromedae. The general similarity of the absorption-band spectra of these two stars was clearly brought out by Miss Cannon through a comparison of the Harvard objective-prism plates. See *Publications of the American Astronomical Society,* Twenty-third Meeting, Ann Arbor, 1919.

GENERAL DISCUSSION

The resemblance between classes R and S which appears from objective prism observations, is seen by means of slit spectra to be of the most general character only. The band in the blue is of decidedly shorter wave-length in class S, and there is throughout this region a marked lack of correspondence in the spectral details. On the other hand some of the characteristic S features are recognizable in the spectra of many giant stars of classes K and M, being more strongly developed in some stars than in others. From the comparisons which have thus far been made it appears that in general S stars are more closely related to giant Ma stars than to those of other types.

Perhaps the most characteristic feature of the S spectrum is a complicated structure in the region λ 4630 to λ 4660. This apparently consists of both absorption and emission lines and probably also contains one or more band-heads in absorption. A fairly definite idea of this portion of the spectrum may perhaps be gained by comparing the illustrations with the data in Table III. An absorption band in the red with its head near λ 6470 and extending toward longer wave-lengths is probably characteristic of class S, and may prove a useful criterion for classification.

The wave-lengths in Table III depend upon measurements of one-prism spectrograms of several variables of class Se. In the second column, *a* denotes absorption line, *e*, emission line or maximum, *bh*, band-head. The values given in the table were computed upon the assumption that the *e* features have the same velocity displacement as the bright hydrogen lines, and that they are systematically 0.2 A toward the violet from the absorption lines. Thus the emission lines and maxima were corrected for the apparent velocities obtained from the bright hydrogen lines, while

468?

PLATE XIV

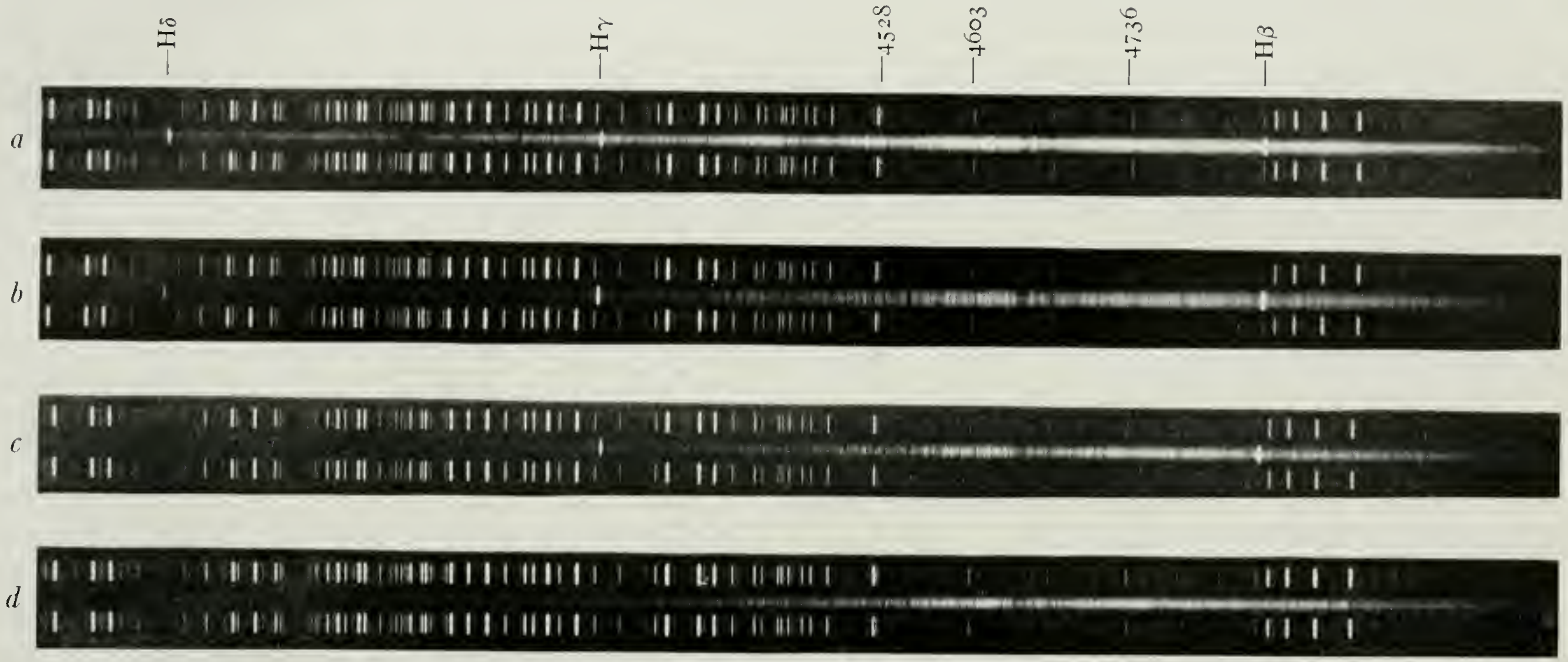

One-prism Spectrograms of Stars of Class S

(*a*) R Andromedae, October 16, 1919.
(*b*) R Geminorum, October 15, 1919.
(*c*) S Ursae Majoris, April 10, 1920.
(*d*) H. D. 35155, September 26, 1920.

TABLE III

CHIEF FEATURES IN CLASS S SPECTRA λ 4500–λ 4860

I.A.	Character	Intensity	Identification
4506.6	*a*	3	....
11.4	*e*	var.	....
12.8	*a*	2	Ti?
21.4	*e*	var.	....
23.1	*a*	2	Ba?
27.4	*a*	2−	Ti?
35.5	*a*	3	Ti+?
40.3	*a*	1−	....
54.0	*a*	5	Ba
62.9	*a*	1	....
68.9	*e*	....	....
71.3	*a*	2	Mg+?
80.6	*a*	1	Va
83.6	*e*	var.	Fe Enh.
86.2	*a*	2	V
88.3±	*e*	....	....
94.3	*a*	2	V
4606.8	*a*	3	Sr+?
08.7	*e*	....	....
13.1	*a*	1	....
14.9	*e*	....	....
16.1	*a*	2−	Cr?
18.2	*e*	....	....
19.2	*bh*	....	....
20.2	*a*	2	....
31.5	*e*	....	....
34.1	*a*	2	....
36.6	*e*	....	....
37.5	*bh*	....	....
44.3	note	....	....
52.4±	*e*	....	....
75.1	*a*	1	Ti?
88.0	*a*	2	....
4707.1	*a*	1	....
09.9	*a*	1	....
58.6	*a*	1	....
84.1	*a*	1	....
99.8	*a*	2	Ti?
4811.7	*a*	1−	....
15.6	*a*	1	....
23.6	*a*	1−	Mn?
28.0	*a*	2	....
32.0	*a*	2	....

NOTES TO TABLE III

4511.4 *e*. This has been observed as a bright line in the spectra of four Md variables.

4521.4 *e*. This has been observed as a bright line in the spectrum of one Md variable.

4644.3. Center of broad absorption space.

4652.4 *e*. Broad or double.

4828.0 *a*, 4832.0 *a*. These lines are very persistent although of moderate strength.

4448.2. A maximum, possibly a bright line, has been measured in this position on twelve plates.

an additional correction of −0.2 A was given to the absorption lines. The need of this correction was indicated by measurements of a few plates in the region λ 4100–λ 4500. The relative displacement of bright and dark lines is analogous to that well known in Md spectra. The proper amount of the correction for the S spectra is possibly somewhat greater than 0.2 A but the data are too meager to yield a precise value. In one N variable Moore[1] found a corresponding displacement of 0.2 A. In Md variables it appears to be a function of the light period, being 0.25 to 0.3 A for the average period of the Se stars.

Continuous spectrum.—These stars are red, the color-indices of the variables probably being as great as that of the Md variables, namely, 1.8 magnitudes. As compared with Ma stars, the continuous spectrum falls off toward the violet from about λ 4500, and with greater rapidity after λ 4430.

Absorption lines.—Table III shows the chief absorption lines in the region λ 4500–λ 4860. The strength of the barium line λ 4554 makes it an outstanding feature. This line and λ 4607 (Sr) are much stronger than in classes K and M. The strength of λ 4496, compared to the neighboring line, λ 4494, is also notable. Only two or three spectrograms are available for the study of the region from λ 4450 toward the violet. Judged from these, the absorption spectrum in this region is more like that of class M than at the longer wave-lengths. In several portions of the spectrum there is, in fact, a considerable degree of correspondence between absorption lines in classes S, M, and N, in spite of their notable differences.

Bright lines.—The wave-lengths marked *e* in Table III refer to rather broad[2] maxima which vary in prominence in different spectra (especially λλ 4511.4, 4521.4, and 4583.6). In some spectra they are scarcely distinguishable from portions of continuous spectrum lying between absorption lines or spaces; in other spectra they appear to be outstanding bright features, decidedly above the general intensity of the neighboring continuous spectrum. Thus, while the designation *e* in the table may be considered merely as describing the more conspicuous maxima, it is believed by the writer that they probably correspond to actual emission. This is borne out for λ 4583.6, which is identified with the enhanced iron line λ 4583.8, by the presence of similar lines at λλ 4924, 5018, corresponding to other well-known enhanced iron lines.

---

[1] *Lick Observatory Bulletin*, 10, 160, 1921.

[2] Exception should be made for λ 4511.4 and λ 4521.4, as these wave-lengths correspond to fairly narrow lines, the former appearing nearly monochromatic.

As in class M[1], stars showing bright hydrogen lines are long period variables. The bright hydrogen lines have quite different properties, however, in the two classes. In class S the less refrangible lines are stronger, but they rapidly decrease in intensity in passing toward the ultra-violet.[2] The relative intensities of $H\beta$, $H\gamma$, and $H\delta$ are shown in Table II.[3] The lines to the violet of $H\delta$ are usually too weak to be observed, even when $H\beta$ is strongly overexposed. In fact, $H\epsilon$ has never been seen on the Mount Wilson plates of S spectra. In one or two stars, however, the bright $H\zeta$ line has been recorded here and also at Harvard. Thus, in these cases at least, $H\zeta$ is stronger than $H\epsilon$. As is well known, this is also true in Md stars. It is particularly interesting to find it so in S spectra, where the Balmer series has widely different characteristics, as this circumstance lends support to the not wholly acceptable conclusion that $H\epsilon$ is actually emitted, but subsequently weakened through the absorption of overlying calcium vapor. $H\alpha$ is bright on the few plates of the red region thus far secured.

---

[1] Certain M stars recently found to have bright lines either do not vary in magnitude, or vary irregularly through a small range. Some of these stars are dwarfs (Adams and Joy, *Publications of the Astronomical Society of the Pacific*, **32**, 158, 1920, and **34**, 174, 1922), and others (*ibid.*, **34**, 175, 1922), while evidently giants, have spectra differing markedly from that of *o* Ceti and other well-known Md variables. Considering only stars whose underlying spectrum is similar to that of the typical M giants, we find what seems to be a perfect correspondence between variability and the presence of bright hydrogen lines.

[2] This is also true of the hydrogen lines in the peculiar M stars referred to in the preceding footnote, but, as these lines are reversed or somewhat widened, their appearance is different from the narrow hydrogen lines in S stars. See *Publications of the Astronomical Society of the Pacific*, **34**, 175, 1922. As observed with one-prism dispersion, the $H\gamma$ and $H\delta$ lines of S spectra appear monochromatic. On most of my negatives $H\beta$ is too strong to judge of its real character. It may be slightly widened.

[3] Comparable estimates of the intensities of the bright hydrogen lines in Md spectra may be found in Table III, *Mt. Wilson Contr.*, No. 200; *Astrophysical Journal*, **53**, 191, 1921.

In comparing the relative intensities of the bright hydrogen lines as given by remarks in the Harvard publications with those of the Mount Wilson plates as shown in Table II, there seem to be many striking differences, but allowance must be made for the fact that in many cases the Harvard observations were made with emulsions much less sensitive to the $H\beta$ region (relatively to $H\gamma$ and $H\delta$) than those now in use. I do not know whether or not a difference in focus between these lines on the Harvard plates could have effected the apparent relative intensities.

An unexpected feature is the presence of the enhanced lines of iron, λλ 4584, 4924, 5018. We have been accustomed to think of enhanced lines as being prominent in classes A to G, especially in the intrinsically brighter stars, and becoming inconspicuous in the later (redder) spectral classes. The presence of the above-mentioned lines in these red S variables, as well as the observations by Adams, Joy, and Humason of enhanced lines in certain peculiar M stars,[1] represents, in our present limited knowledge of stellar conditions, an anomalous circumstance which invites investigation.

The mean period of sixteen class S variables is 364 days. This is about the same as that of the Md stars having the more advanced spectra. The data for the Md stars in the following small table are taken from *Harvard Annals*, **76**, Table IX.

Class	Number	Period
Md 3, 4, 5	90	260
Md 6, 7	70	302
Md 8, 9, 10	67	355
Se	16	364

The recognition of the S stars as a distinct group may remove part of the difficulty in studying the relationship between spectral type and period among the long period variables.

The evolutionary relationship of class S stars to those of other classes, as well as the dependence of spectral modifications upon absolute luminosity, present highly interesting problems for future investigation.

---

[1] *Publications of the Astronomical Society of the Pacific*, **34**, 175, 1922.

It seems probable that the S stars form a third division of the giant sequence, and that they are related more closely to M than to N stars. Whether or not stars exist having spectra intermediate between Mb, Mc, and the advanced S type remains to be determined, but it is suspected that it may be possible at least to fill the gap between Ma and the early S spectra. A tentative notion of the spectral relationships among red stars is represented by the diagram in Figure 1.

Many questions are suggested which cannot profitably be discussed here. One noteworthy circumstance, however, may be pointed out, namely, that along each of the three branches, M, N, and S, there is an increasing tendency toward variability in light, and toward the presence of bright lines in the spectra. Certain facts[1] might be interpreted as indicating that the general cause of the light variations is essentially the same in both Md and Se stars, with the possibility that the differences in spectrum are due either to differences in conditions which are not important in controlling the amount of light radiated, or to differences in chemical composition. Dr. Shane, who made a special study of N-type variables,[2] is of the opinion that the main causes underlying the light variations are probably common to both Md and N stars. It is not easy to say, however, just what generalizations may properly be drawn from the analogies between the M, N, and S branches. The effective temperatures are probably not the same,

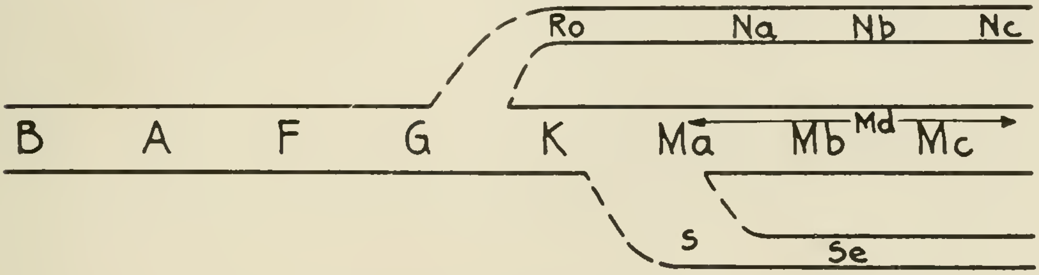

FIG. 1.—Hypothetical relationships of red stars

as several lines of evidence, especially the measurements of heat indices[1] by Nicholson and Pettit, indicate that the effective radiating temperature of the variables similar to *o* Ceti is decidedly lower than that of other red stars.

---

[1] Observations of R Cygni bearing on this matter are briefly discussed in the *Publications of the Astronomical Society of the Pacific*, 33, 206, 1921.

[2] *Lick Observatory Bulletin*, 10, 79, 1920.

It is hoped to treat the radial velocities of Se stars, the red portions of the S spectrum, the variable spectra of certain S stars, and the general relationship between classes M and S in future contributions.

MOUNT WILSON OBSERVATORY
August 17, 1922

---

[1] *Publications of the Astronomical Society of the Pacific*, **34**, 181, 1922.

THE BEHAVIOR OF SPECTRAL LINES AT THE POSITIVE POLE OF THE METALLIC ARC[1]

By PAUL W. MERRILL

ABSTRACT

Classification of arc lines by relative strengthening at the positive pole.—In the Pfund type of arc there is a small well-defined region of luminous vapor just above the point where the core of the arc enters the molten bead which forms the positive electrode, and at the boundary of this region many spectral lines change suddenly in intensity to a greater or less degree. By keeping the core of the arc steady and focusing it on the slit of a 30-foot Littrow spectrograph, plates were obtained from which it was possible to group about 500 *iron lines* from λ 3849 to λ 5763 into six classes: change imperceptible (0), slight (1), small (2), sufficient to double the intensity (3), great (4), or very great (5). The *relationship to the furnace classification* of King was studied for each group. In general the strengthening at the pole is greater for the high-temperature lines, the average class for King's classes I, II, and III being, respectively, 0.2, 1.0, and 1.9. But the average for classes IV and V is only 1.8, and for the diffuse lines of these classes, only 1.3. Lines of each temperature class are also found in each of the positive-pole classes 0, 1, and 2; hence the correlation is only fair, although probably as close as can be expected with such different modes of excitation. The strengthening of the enhanced lines is very marked (average class being 4), so that positive pole observations may be useful in distinguishing these lines. The classifications of 180 *cobalt lines* and of some *nickel lines* show the same general relationships as were found for the iron lines.

An interesting recent development in spectroscopy has been the increasing importance attached to the classification of spectral lines according to their behavior under various conditions of excitation. This has been due in part to the desire to provide an improved basis for the interpretation of spectroscopic observations of various light sources, particularly of celestial objects, and in part to the wide discussion of the quantum and ionization theories of the emission of spectral lines.

It has long been recognized that the relative intensities of lines in light from different portions of the electric arc afford a means by which the lines may be grouped. Most of the spectroscopic investigations of the structure of the arc have been concerned with the carbon arc, but a number have dealt with arcs between metallic electrodes. Among the phenomena observed in metallic arcs, one of the most interesting and important is, that near the poles, especially the positive pole, lines appear which are absent or very weak in the center of the arc or in integrated arc light, but which are characteristic of the disruptive spark. Photographs made by the writer in 1919 exhibited this property of enhanced lines very clearly, and also showed systematic effects for other types of lines. The general results of a study of these photographs[1] are described in the present paper.

---

[1] *Contributions from the Mount Wilson Observatory*, No. 253.

Iron was the element most extensively observed in this investigation. The arc used was of the Pfund type, the upper, negative electrode consisting of an iron rod, the lower, positive electrode of a drop of molten iron oxide. A copper rod hollowed out at the upper end served as a holder for the iron oxide and made possible an arc with a spheroid of oxide slightly smaller than usual. With currents of about two amperes the arc burned steadily with a small, sharply-defined, circular, bright area on the molten surface, from which the core of the arc proceeded. It proved important for the present purpose to have this positive "bead" localized and steady, for the vapors immediately surrounding it were the source of the special phenomena described in the following paragraphs. The general appearance of this portion of the arc is well shown in the illustrations accompanying papers on the iron arc by St. John and Babcock.[2]

An image of the arc was projected in such a way that the line joining the electrodes coincided with the slit of the 30-foot Littrow spectrograph. In the photographs thus obtained each spectral line represents the emission of that radiation along the axis of the arc. The actual arc length was about 5 mm, the magnification of the image three times. Currents ranging from 1.5 to 3.2 amperes at 250 volts were employed.

The particular subject dealt with in the present paper is the increase in the intensity of spectral lines at the bright end of the arc core just off the positive pole. The effects at the positive pole are more sharply localized than those at the negative pole. Most lines show a continuous increase in intensity on passing from the

---

[1] Reported upon at the Pasadena Meeting of the Pacific Coast Section of the American Physical Society, June, 1919; *Physical Review*, 14, 271, 1919.

[2] *Mt. Wilson Contr.*, Nos. 106, 137; *Astrophysical Journal*, 42, 231, 1915; 46, 138, 1917.

PLATE XV

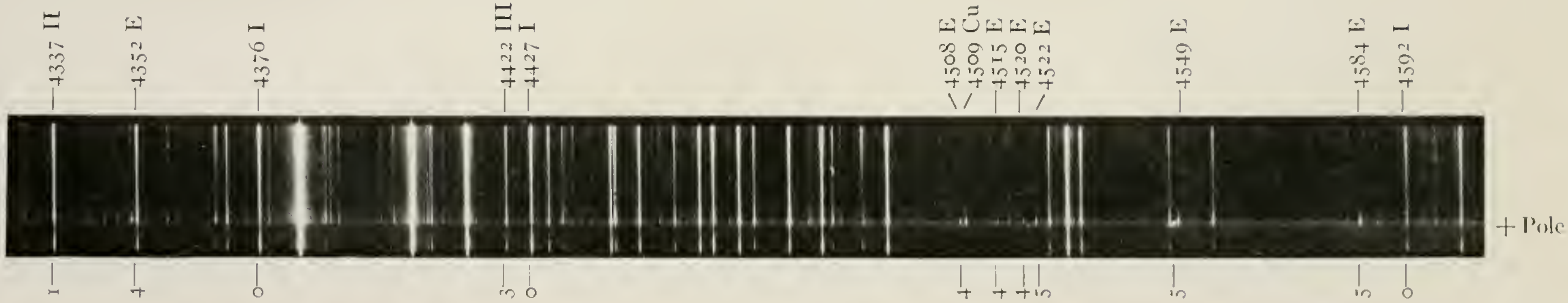

Spectrum of the Iron Arc

Showing behavior of the lines at the positive pole. The figures above the spectrum indicate the wave-length and temperature class; those below the degree of strengthening at the positive pole. The extensions of the lines below the narrow strip of continuous spectrum marking the positive pole are due largely to reflection of the main portion of the arc from the molten spheroid of oxide forming the positive terminal.

center to the negative pole, but on approaching the positive pole, there is, for an affected line, a sudden increase in intensity at a point corresponding to the boundary of a small bright volume contiguous to the pole.

Nearly 550 iron lines between wave-lengths 3849 A and 5763 A were classified according to the increase of intensity at the positive pole on the following basis:

0 no increase
1 slightest observable increase
2 small increase
3 considerable increase (intensity about doubled)
4 great increase
5 very great increase

The relationship of this classification to other classifications of the same lines is exhibited in Table I, which gives for each class the number of lines of each degree of pole strengthening. Thus the numbers in the first row indicate that out of sixty-three class I lines fifty-one were not strengthened, ten were very slightly strengthened, and two showed a somewhat greater increase at the positive pole. The Roman numerals I–V refer to the temperature classes determined by King[1] from data obtained by use of the electric furnace; *E* indicates enhanced lines, and *e*, lines with a negative pole effect.[2] In compiling the numbers for this table it was noticed

TABLE I

Positive Pole Strengthening of Iron Lines

Class	0	1	2	3	4	5	Total	Average
I	51	10	2	......	......	......	63	0.2
II	18	15	10	3	......	......	46	1.0
III	3	24	50	14	......	......	91	1.9
IV	4	29	65	21	3	......	122	2.0
IV*n*	3	16	15	......	......	......	34	1.4
V	......	15	24	2	......	......	41	1.8
V*n*	1	19	6	......	......	......	26	1.2
e	......	1	4	8	1	......	14	2.6
E	......	....	1	8	12	7	28	3.9

---

[1] *Mt. Wilson Contr.*, Nos. 66, 247; *Astrophysical Journal*, **37**, 239, 1913; **56**, 318 1922.

[2] St. John and Babcock, *Mt. Wilson Contr.*, No. 202; *Astrophysical Journal*, **53**, 260, 1921.

that many of the lines which fell in columns 0–2 of rows IV and V were broad or nebulous. Accordingly all lines of these classes that are so marked, either by King[1] or Burns,[2] were separated and placed in rows IV*n* and V*n*.

The chief facts brought out by this study may be seen by inspection of Table I. To facilitate comparison of the various types of lines, the average value of the pole strengthening for each has been placed in the last column. The progression in these average values is shown by the following grouping:

Class	I	II	IV*n*, V*n*	III, IV, V	*e*	*E*
Number..................	63	46	60	254	14	28
Average strengthening.....	0.2	1.0	1.3	1.9	2.6	3.9

The *e* lines in the green, λ 5364–λ 5598, are of special interest. They are in furnace class V and are greatly strengthened at the positive pole. In confirmation of the observations of St. John and Babcock it was noted that at the positive pole these lines are distended toward shorter wave-lengths. The *d* lines in the regions λ 5232–λ 5624 are in class IV and in group 2 as regards pole strengthening.

The enhanced lines, designated by *E*, are from Lockyer's table, with a few additions from other sources. The degree of strengthening at the positive pole seems to be approximately proportional to the amount of enhancement in passing from arc to spark, but the data at hand do not allow any precise determination of this relationship. They suggest that there is a sequence of types of lines from I at one end to enhanced lines at the other; that classes I, II, and III follow in regular order, but that classes IV and V contain two types of lines, one type continuing the sequence I–III and connecting it with the enhanced lines, the other type similar to the nebulous lines in regard to furnace behavior and pole strengthening but not separated from the others by the present treatment of the data. If these remaining lines, which really belong to the subgroup represented by "*n*," were removed, it is possible that the pole values for the remainder of the group would rise, and perhaps take an appropriate position between classes III and *E*. To make a complete separation of the classes IV and V into two subgroups would be rather difficult, because the characteristics of the two apparently overlap. That is to say, while subdivisions are indicated with definite differences between them, lines intermediate in their characteristics may not be lacking. It would appear rather arbitrary to attempt a division on the basis of the pole data alone. Probably the division based on the sharpness of the lines could be carried farther. The results would be of value when correlated with pole data. The *e* lines are peculiar in that, although lacking in sharpness, they have high pole strengthening.

---

[1] *Loc. cit.*

[2] *Lick Observatory Bulletin*, 8, 27, 1913.

TABLE II

Pole Strengthening of Individual Iron Lines

λ Rowland	Furnace	Positive Pole	λ Rowland	Furnace	Positive Pole
3950.102	III	1	4260.640	III	2
3951.311	IV	2	4308.081	II	0
3966.212	III	2−	4291.630	IA	0
3966.778*n*	IV	2	4294.301	II	1
4100.901	IIA	0	4415.293	II	0+
4107.649	III	3−	4427.482	I	0
4177.698	IIA	0	4459.301	III	3
4181.919	III	3	4461.818	I	0
4199.267	III	2	4489.911	IA	0
4202.198	I	0	4494.738	III	1
4206.862	IA	0	4528.798	II	2
4210.494	III	2	4531.327	II	0
4216.351	I	0	4919.174	III	2
4219.516	IV	4	4939.868	I	0
4232.887	IA	0	5050.008	III	2
4233.772	III	1+	5051.825	I	0
4250.287	III	1	5166.454	IA	0
4250.945	II	0+	5171.778	II	1
4271.325	III	1+	5341.213	II	1
4271.934	II	1	5371.734	I	0

It may be of interest to cite several examples of individual lines showing different behavior at the positive pole. For this purpose I have chosen pairs of lines in King's list of "Neighboring Lines Which Are Differently Affected in the Furnace."[1] This will be sufficient to exhibit typical behavior of the various classes, and also some of the common variations. Comparison with Table I will show which lines represent average values and which deviations. λ 4219.516 is included by Gale and Adams in the list of enhanced lines.

Cobalt.—Estimates of the strengthening of cobalt lines at the positive pole of the arc were made in the same manner as for iron. For the summary in Table III 180 lines between the wave-lengths 3845 and 4629 A were used.

The bright volume of vapor immediately above the spot on the positive pole in the cobalt arc is not so sharply localized as with iron, and more lines show a gradual strengthening toward the positive pole, so that the appearance of the photographs is slightly different and in some cases the estimates less definite than for iron. The main features of the phenomena are the same, however, and the mean values of pole strengthening for the different furnace classes are nearly the same as for iron.

TABLE III

POSITIVE POLE STRENGTHENING OF COBALT LINES

Class	0	1	2	3	4	Total	Average
I	25	12	2	....	....	39	0.4
II	2	15	8	4	....	29	1.5
III	....	11	45	9	....	65	2.0
IV	....	2	9	2	....	13	2.0
V	1	5	7	1	....	14	1.6
E	2	1	9	5	3	20	2.3

The enhanced lines in the last row are all of Lockyer's list which have been observed. Some of these lines which give small pole strengthening do not seem to be characteristic enhanced lines. If this row were restricted to well-marked cases of enhancement, a value of 3 or 4 would be found instead of 2.3.

Not many lines in the cobalt spectrum have been noted as hazy. Four class V lines of this character give a mean value of pole strengthening less than that of the whole class. Thus the meager data available agree with iron in this particular also.

---

[1] *Mt. Wilson Contr.*, No. 66; *Astrophysical Journal*, **37**, 239, 1913.

A smaller amount of data for *nickel* indicates that the same general relationships exist for this element also.

The fact that grouping the spectral lines of three elements according to their behavior at the positive pole of the arc gives a classification which runs parallel to the temperature classification is of interest in showing that the inherent differences of the various classes of lines are such as to allow them to be distinguished in sources other than those upon which the classification was based. The chief factor which differentiates the various classes of lines is, presumably, the degree of excitation required for their production. To what extent the physical conditions at the center and at the positive pole of the arc are identical with those in the furnace at low and at high temperatures is difficult to judge, but we may at least say that the relative effects upon the atom, as regards radiation, are comparable.

That the unsharp lines are subject to a smaller increase of intensity at the positive pole than are sharp lines of corresponding temperature classes is an outstanding fact for which a certain explanation is not now available. It may be that the unsharp lines represent vibrations lacking in stability, being easily perturbed, as shown by the lack of homogeneity, and that under the more intense conditions at the pole these vibrations can be executed by relatively few electrons.

The ease and definiteness with which enhanced lines can be distinguished at the positive pole suggest that arc observations should be given consideration in the formation of lists of enhanced lines. A particular advantage is that the criterion is not the strength at the pole, but the increase in intensity (amounting practically to a discontinuity) at a definite point in passing from the center to the positive pole. This can be shown by a single photograph, and the selection of enhanced lines should be less arbitrary than when based upon a comparison of the relative strength of lines in separate arc and spark exposures.

The type of observations described in the present paper is possible only on a steady arc, such as the Pfund form of iron arc. Several of the metals can be made to burn in this fashion, and perhaps methods can be developed by which the arcs of numerous elements can be sufficiently controlled to permit the gathering of similar data. With proper precautions, valuable results can probably be obtained for certain elements by using iron electrodes containing small amounts of the elements in question.

At present, positive pole phenomena would seem to be most useful in their bearing on problems connected with the classification of spectral lines, but they may also prove valuable in studying the temperature and electrical conditions at different points in the arc.

Mount Wilson Observatory
August 1922

GEOMETRICAL PROOF FOR THE WADSWORTH CONSTANT DEVIATION SYSTEM[1]

By R. C. GIBBS and J. R. COLLINS

ABSTRACT

Axis of rotation for Wadsworth constant deviation system.—In order that there may be no lateral shift of the emergent ray, the Wadsworth constant deviation system should be rotated about the intersection of the plane of the mirror and the plane bisecting the angle of the prism, as an axis. *A geometrical proof of the location of the axis* is presented which is much shorter than the analytical one given by Wadsworth.

In the Wadsworth constant deviation system, a triangular prism and mirror are mounted on the same rotating table. If a parallel beam of white light is incident upon the prism so that some color passes through the prism at minimum deviation and is reflected by the mirror, then, as the prism and mirror are rotated together about *any* axis that is perpendicular to the principal plane of the prism and to the path of the incident beam, the path of the emergent beam for whatever color is passing through at minimum deviation remains fixed in direction.

Let OP represent the direction of the incident beam, PQ that of the refracted beam, and QD that of the reflected or emergent beam. By an analytical method, Wadsworth[2] determined the particular axis about which the prism and mirror may be rotated without producing a sidewise displacement of the emergent beam. Using the direction of the incident beam as one of his co-ordinate axes he assumed an axis of rotation as at R and determined in turn the equation of *SQ*, a line lying in the plane of the mirror, that of *PQ*, and that of *QD*. This enabled him to find the co-ordinates of D and to write an equation for the perpendicular distance, p, from the origin O to QD as follows:

$$p=2a\cos^2\beta/2+2b\sin\theta/2+2d\cos(\theta+\Phi),$$

---

[1] The proof here given in full was presented at the Toronto meeting of the American Physical Society in December 1921, and a brief abstract of it appears in the *Physical Review* (2), **19**, 4, 381.

[2] *Astronomy and Astrophysics*, **13**, 835, 1894.

where a is the perpendicular distance from R to the incident beam, b that from R to PS which is the bisector of the prism angle, and d that from R to the plane of the mirror.

It is readily seen that in order for p to remain constant b and d must both be equal to zero. Therefore, if the emergent beam is to suffer no shift, the system must be rotated about S, the intersection of the bisector of the angle of the prism and the plane of the mirror.

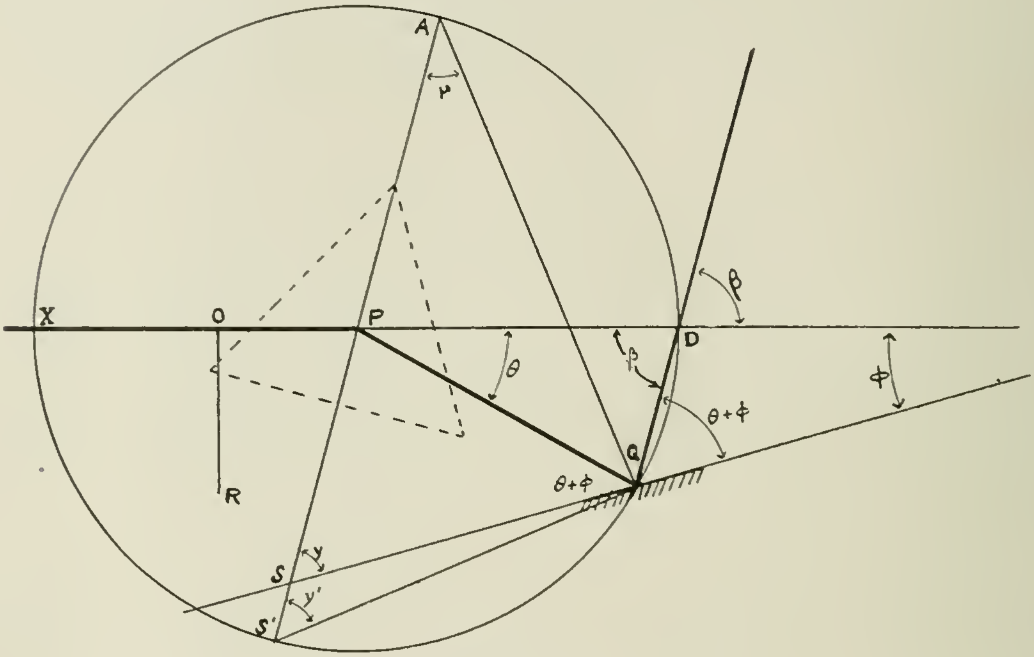

FIG. 1

Although the essential steps in this method are simple and straightforward, yet many of the transformations are necessarily long. By following a method similar to that used by E. Bloch[1] in finding the corresponding axis of rotation for a constant deviation prism of the Pellin-Broca type, the location of this axis may be determined by means of a short geometrical proof.

Describe a circle through D and Q having its center on PS, cutting PS at A and S' and the incident ray at X.

$$\text{Arc } XS' = \text{arc } S'Q.$$

---

[1] *Journal de Physique*, 7, 145, 1917.

Therefore $\beta/2$ is measured by $S'Q/2$ and $\mu=\beta/2$.

$$\gamma'=90-\beta/2$$

$$\gamma=180-\left(\frac{180-\theta}{2}+\theta+\Phi\right)=90-\left(\frac{\theta}{2}+\Phi\right).$$

$$\beta=\theta+\Phi+\Phi=\theta+2\Phi$$

Therefore

$$\gamma=90-\beta/2=\gamma'$$

and S' coincides with S. S therefore lies on the bisector of β for all positions of the rotating system.

Since β is constant and since one of its sides is the fixed incident ray, the bisector of β remains fixed in direction.

If then the system is rotated about an axis through S, the bisector of β will not shift and consequently the emergent ray will not shift.

There is no other axis of rotation for which this condition is satisfied, for, if the system is rotated about any other axis than the one through S, S will shift. Hence the bisector of β would shift and therefore the emergent ray would shift. By imposing other conditions for drawing the circle, it is possible to reach the same conclusion by other slightly different though similar procedures.

CORNELL UNIVERSITY
December 1921

Reviews

The Telescope. By Louis Bell. New York: McGraw-Hill Book Co., 1922. 8vo, pp. ix+287, figs. 190, plate 1. $3.00 (English price, 15*s.*) net, postpaid.

There are several small handbooks on the telescope, but the writer knows of nothing in English which brings together in compact form so much of information, suggestion, and helpful advice for the users of telescopes as are to be found in Dr. Bell's book. The author is well qualified for the preparation of such a book, being widely known for his studies of various optical as well as electrical problems. His purpose, as stated in the Preface, is "to bring the facts regarding the astronomer's chief instrument of research somewhere within grasp and up to the present time." Some of the material brought together here would not be readily accessible to the ordinary reader, and the references given at the close of a few of the chapters will be of value to those who wish to make a further study of the subjects treated. Similar lists of references might well have been added to other chapters.

The frontispiece is a fine engraving of Galileo's telescopes. The first two chapters trace the evolution of both refracting and reflecting telescopes, with a discussion as to their relative merits. The author dismisses with little comment the claim recently made that Bacon used telescope apparatus, although he admits that the great philosopher had clear ideas of refraction and that suggestions in his manuscript may have led to the making of spectacles, which were common long before the combination of lenses necessary for the refracting telescope was discovered. The processes of making, testing, and working optical glass are next described, the object being to give to the reader "a better understanding of the difference between the optical glass industry and the fabrication of commercial glass, and . . . . a fuller realization of how fine a work of art is a finished objective or mirror as compared with the crude efforts of the early makers or the hasty bungling of too many of their successors."

The fourth chapter deals with the properties of objectives and mirrors. The problems of spherical and chromatic aberration are considered, and the conditions that must be fulfilled if both are eliminated. A glance at the diagram of the spectrum (fig. 60), illustrating the irrationality of dispersion, should make clear to any reader what is accomplished by combining lenses of crown and flint glass.

The consideration of various kinds of eye-pieces, with the advantages and disadvantages of each, is postponed until after a discussion of telescope mountings. Several varieties of mountings are described, from the simplest altazimuth for a small portable to the adaptation of the "English equatorial" mount used for the Hooker 100-inch telescope on Mount Wilson. Accounts are also given of special forms of mounting so designed that the observer may be protected, as the Gerrish polar telescope at Harvard, the Porter polar reflector, and the Hartness turret telescope. The amateur who has mechanical ability and wishes to make a mounting for his own instrument will find many suggestions here.

A few pages are devoted to hand telescopes and binoculars, special attention being given to the use of Porro prisms for field glasses and binocular telescopes.

In a chapter on accessories to the telescope we find described diagonal eye-pieces for observation of sun and stars, different kinds of micrometers and photometers. The necessity of a good clock drive whenever micrometer measures are to be made or photographs taken is emphasized and several forms are explained, the Gerrish electric control used successfully at the various Harvard stations being specially noted.

The last pages of the book are filled with practical suggestions. Excellent advice is given to the prospective purchaser of a telescope, and explicit directions for the testing of a small lens or mirror. The description of the Hartmann and Foucault tests will give the amateur an insight into methods used for larger instruments. The observer whose object glass needs a thorough cleaning will find here such detailed directions that he need not fear to remove his lenses from their cell, while methods of re-silvering mirrors are given for the owner of a reflector. The directions for adjusting the polar axis of a small equatorial could be followed easily, and the diagram (fig. 170) showing the position of the pole throughout the twentieth century with reference to Polaris and the two stars BD 88° 112 and BD 89° 13 is especially good. Various devices for protecting the telescope are described, from the simplest possible removable covering up to the revolving dome usually found in a fixed observatory.

The suggestions in the Appendix as to what may be done by a faithful observer with a very modest telescopic equipment are for the most part good, but surely the author does not mean to imply that the unknown rotation period of the planet Neptune might be found in this way!

The volume is a neat and attractive one, the type is good, the illustrations numerous and excellent. The author's statements are usually clear, but occasional obscure sentences occur and a number of slips and typographical errors mar the book. For instance, "A *seventh* century astronomer and his telescope" (see p. 15) would be a decided anachronism, and on page 204 the figure labelled "Ordinary striae" has evidently been interchanged with the one illustrating "A bad case of striae." Such errors will undoubtedly be corrected when a new edition is published.

A. S. Y.

Geschichte und Literatur der veränderlichen Sterne. By G. Müller and E. Hartwig. Leipzig: Poeschel & Trepte. Band II, 1920, 4to, pp. 468; Band III, 1922, 4to, pp. 137.

The first volume of this important publication of the Astronomische Gesellschaft appeared in 1918, and was reviewed at length in this *Journal*, **49**, 286, 1919. That review applies equally to the second volume, which includes the stars from right ascension 15^h to 23^h, thus completing the first part of the work. There are two appendices: the first, written by E. Zinner and G. Van Biesbroeck, giving the history and literature of thirty-two Novae which appeared between the years 1572 and 1912; and the second, written by C. Hoffmeister, dealing with Variables in Clusters.

The third volume contains the Catalogue, which arranges in form for ready reference the essential items from the earlier volumes. The data for each star occupy twenty-two columns of the double quarto page, giving the place for 1900 and the epoch of the chart, precession, color and spectrum, magnitude at maximum and minimum, calendar and Julian date of maximum epoch, mean period with interval from minimum to maximum, class of variation, volume in Hagen's *Atlas*, discovery name and date, and remarks. An appendix gives corresponding data for 320 variables and fifteen novae confirmed between 1915 and 1920. There is also an index of variables arranged by constellations, a table of light-equation for 276 variables of short period, a table of Julian days from 1600 to 2000, and a table for conversion of hours and minutes to decimals of a day.

This work is indispensable for astronomical libraries and observers of variable stars.

The price to American buyers is $4.50 each for Volumes I and II; $3.60, for Volume III. Members of the Gesellschaft are given a discount of one-third from these prices.

J. A. Parkhurst

INDEX TO VOLUME LVI

SUBJECTS

PAGE

Aberration Experiment, Einstein's. *C. V. Raman* 29
Abstracts, Preparation of 344
TW Andromedae, Orbit of Eclipsing Binary. *Martha Betz Shapley.* . 439
η Aquilae, Cepheid Variable. *Charles Clayton Wylie* 217
σ Aquilae, Eclipsing Binary. *Charles Clayton Wylie* 232
Astrophysics, Application of Vacuum Thermocouples to Problems in. *Edison Pettit* and *Seth B. Nicholson.* 295
Binaries Lalande 13792 and AOe 12584, Orbits of Spectroscopic. *R. F. Sanford* 446
Binary TW Andromedae, Orbit of Eclipsing. *Martha Betz Shapley.* . 439
Binary σ Aquilae, Eclipsing. *Charles Clayton Wylie* 232
Cells, Voltage-Current Relation in Central Anode Photo-Electric. *Herbert E. Ives* and *Thornton C. Fry* 1
Corrigenda 216
Deviation System, Geometrical Proof for the Wadsworth Constant. *R. C. Gibbs* and *J. R. Collins* 483
Einstein's Aberration Experiment. *C. V. Raman* 29
Errata 216
Gallium in Air and in Hydrogen, Spark Spectrum of. *Elias Klein* . . 373
Gravitation, Majorana's Theory of. *A. S. Eddington* 71
Helium as Function of Pressure, Width of Lines of. *Lloyd W. Taylor* . 16
Helium, Spectrum of Neutral. (*See also* Corrigenda, p. 216.) *Ludwik Silberstein* 119
Hydrogen, Quantum Theory of Spectrum of. *H. A. Wilson* . . . 34
Hydrogen, Visible and Infra-Red Radiation of. *Frederick Sumner Brackett.* 154
Index 489
Infra-Red Radiation of Hydrogen. *Frederick Sumner Brackett.* . . 154
Interferometer, Determination of Wave-Lengths of 118 Titanium Lines by. *Frederick L. Brown* 53
Interferometer Observations of Double Stars. *Paul W. Merrill* . . 40
Iron in Ultra-Violet, Electric Furnace Spectrum of. *Arthur S. King* . 318
Kapteyn, J. C., 1851–1922. *A. van Maanen* 145
Magnitudes for Stars near North Pole, Revised. *Frederick H. Seares* . 97
Magnitudes of A-Type Stars and Parallaxes of 544 Stars, Spectroscopic Method of Determining Absolute. *Walter S. Adams* and *Alfred H. Joy.* 242

PAGE

Majorana's Theory of Gravitation. *A. S. Eddington* 71

Nebula M 94=N.G.C. 4736, Internal Motion in. *A. van Maanen* . . 208

Nebula N.G.C. 2403, Internal Motion in Spiral. *A. van Maanen* . . 200

Nebulae, Study of Diffuse Galactic. *Edwin Hubble* 162

Nebulae, Source of Luminosity in Galactic. *Edwin Hubble* . . . 400

North Polar Sequence, Further Evidence on Brightness of Stars of. *Frederick H. Seares* and *Milton L. Humason* 84

North Pole, Revised Magnitudes for Stars near. *Frederick H. Seares* . 97

X Ophiuchi, Variable Double Star. *C. H. Gingrich* 132

Orbit of Eclipsing Binary TW Andromedae. *Martha Betz Shapley*. . 439

Orbits of Spectroscopic Binaries Lalande 13792 and AOe 12584. *R. F. Sanford* 446

Parallaxes of 544 Stars, Spectroscopic Method of Determining the Absolute Magnitudes of A-Type Stars and. *Walter S. Adams* and *Alfred H. Joy* 242

Parallaxes of Stars in Region of B.D.+31°643. *C. H. Gingrich* . . 139

Photometry and Purkinje Effect, II, Astronomical Photographic. *F. E. Ross* 345

Proper Motion, Investigations on. Seventh and Eighth Papers. *A. van Maanen* 200, 208

Purkinje Effect, II, Astronomical Photographic Photometry and. *F. E. Ross* 345

Quantum Theory of Spectrum of Hydrogen. *H. A. Wilson* . . . 34

Reviews:

Louis Bell. *The Telescope* (A. S. Y.) 486

G. Müller and E. Hartwig. Geschichte und Literatur der veränderliche Sterne (J. A. Parkhurst) 488

Y Sagittarii, Changes in Spectrographic Elements of. *John C. Duncan* . 340

Sequence, Further Evidence on the Brightness of Stars of North Polar. *Frederick H. Seares* and *Milton L. Humason* 84

Spectra of Class S. *Paul W. Merrill* 457

Spectral Lines at Positive Pole of Metallic Arc. *Paul W. Merrill* . . 475

Spectral Types F to M, Distribution of Velocities of Stars of. *Gustaf Strömberg* 265

Spectrographic Elements of Y Sagittarii, Changes in. *John C. Duncan*. 340

Spectrum of Gallium in Air and in Hydrogen, Spark. *Elias Klein* . . 373

Spectrum of Helium as Function of Pressure in Source, Width of Certain Lines of. *Lloyd W. Taylor* 16

Spectrum of Hydrogen, Quantum Theory of. *H. A. Wilson* . . . 34

Spectrum of Iron in Ultra-violet, with Supplementary Data for the Blue and Violet, Electric Furnace Spectrum of. *Arthur S. King* . . 318

Spectrum of Neutral Helium. (*See also* Corrigenda, p. 216.) *Ludwik Silberstein* 119

PAGE

Spectrum of Strontium, Revision of Series in. *F. A. Saunders* . . . 73

Spectrum of Venus, Absence of Oxygen and Water-Vapor Lines in. *Charles E. St. John* and *Seth B. Nicholson* 380

Star X Ophiuchi, Variable Double. *C. H. Gingrich* 132

Stars, Interferometer Observations of Double. *Paul W. Merrill* . . . 40

Stars and Parallaxes of 544 Stars, Spectroscopic Method of Determining Absolute Magnitudes of A-Type. *Walter S. Adams* and *Alfred H. Joy* 242

Stars in the Region of B.D.+31°643, Parallaxes of. *C. H. Gingrich* . . 139

Stars near North Pole, Revised Magnitudes for. *Frederick H. Seares* . 97

Stars of Spectral Types F to M, Distribution of Velocities of. *Gustaf Strömberg* 265

Stars of North Polar Sequence, Further Evidence on Brightness of. *Frederick H. Seares* and *Milton L. Humason* 84

Strontium, Revision of Series in Spectrum of. *F. A. Saunders* . . . 73

Thermocouples to Problems in Astrophysics, Application of Vacuum. *Edison Pettit* and *Seth B. Nicholson* 295

Titanium Lines by Means of Interferometer, Determination of Wave-Lengths of 118. *Frederick L. Brown* 53

Ultra-Violet, with Supplementary Data for the Blue and Violet, Electric Furnace Spectrum of Iron in. *Arthur S. King* 318

Vacuum Thermocouples to Problems in Astrophysics, Application of. *Edison Pettit* and *Seth B. Nicholson* 295

Variable η Aquilae, Cepheid. *Charles Clayton Wylie* 217

Variable σ Aquilae. *Charles Clayton Wylie* 232

Variable TW Andromedae, Orbit of. *Martha Betz Shapley* . . . 439

Velocities of Stars of Spectral Types F to M, Distribution of. *Gustaf Strömberg* 265

Venus, Absence of Oxygen and Water-Vapor Lines in Spectrum of. *Charles E. St. John* and *Seth B. Nicholson* 380

Wadsworth Constant Deviation System, Geometrical Proof for. *R. C. Gibbs* and *J. R. Collins* 483

Wave-Lengths of 118 Titanium Lines by Means of Interferometer, Determination of. *Frederick L. Brown* 53

INDEX TO VOLUME LVI

AUTHORS

PAGE

Adams, Walter S., and Alfred H. Joy. A Spectroscopic Method of Determining the Absolute Magnitudes of A-Type Stars and the Parallaxes of 544 Stars 242

Brackett, Frederick Sumner. Visible and Infra-Red Radiation of Hydrogen 154

Brown, Frederick L. Determination of the Wave-Lengths of 118 Titanium Lines by Means of the Interferometer 53

Collins, J. R., and R. C. Gibbs. Geometrical Proof for the Wadsworth Constant Deviation System 483

Duncan, John C. Changes in the Spectrographic Elements of Y Sagittarii 340

Eddington, A. S. Majorana's Theory of Gravitation 71

Fry, Thornton C., and Herbert E. Ives. Voltage-Current Relation in Central Anode Photo-Electric Cells 1

Gibbs, R. C., and J. R. Collins. Geometrical Proof for the Wadsworth Constant Deviation System 483

Gingrich, C. H. Parallaxes of Stars in the Region of B.D.+31°643 . 139

Variable Double Star X Ophiuchi 132

Hubble, Edwin. General Study of Diffuse Galactic Nebulae . . . 162

Source of Luminosity in Galactic Nebulae. 400

Humason, Milton L., and Frederick H. Seares. Further Evidence on the Brightness of the Stars of the North Polar Sequence . . . 84

Ives, Herbert E., and Thornton C. Fry. Voltage-Current Relation in Central Anode Photo-Electric Cells. 1

Joy, Alfred H., and Walter S. Adams. A Spectroscopic Method of Determining the Absolute Magnitudes of A-Type Stars and the Parallaxes of 544 Stars 242

King, Arthur S. The Electric Furnace Spectrum of Iron in the Ultra-Violet, with Supplementary Data for the Blue and Violet . . . 318

Klein, Elias. Spark Spectrum of Gallium in Air and in Hydrogen . 373

Merrill, Paul W. Behavior of Spectral Lines at the Positive Pole of the Metallic Arc 475

Interferometer Observations of Double Stars 40

Stellar Spectra of Class S 457

Nicholson, Seth B., and Edison Pettit. Application of Vacuum Thermocouples to Problems in Astrophysics 295

PAGE

NICHOLSON, SETH B., and CHARLES E. ST. JOHN. Absence of Oxygen and Water-Vapor Lines in the Spectrum of Venus 380

PARKHURST, J. A. Review of: *Geschichte und Literatur der veränderliche Sterne.* G. Müller and E. Hartwig 488

PETTIT, EDISON, and SETH B. NICHOLSON. Application of Vacuum Thermocouples to Problems in Astrophysics 295

RAMAN, C. V. Einstein's Aberration Experiment 29

ROSS, F. E. Astronomical Photographic Photometry and the Purkinje Effect, II 345

ST. JOHN, CHARLES E., and SETH B. NICHOLSON. Absence of Oxygen and Water-Vapor Lines in the Spectrum of Venus 380

SANFORD, R. F. Orbits of the Spectroscopic Binaries Lalande 13792 and AOe 12584 446

SAUNDERS, F. A. Revision of the Series in the Spectrum of Strontium . 73

SEARES, FREDERICK H. Revised Magnitudes for Stars near the North Pole 97

SEARES, FREDERICK H., and MILTON L. HUMASON. Further Evidence on the Brightness of the Stars of the North Polar Sequence . . 84

SHAPLEY, MARTHA BETZ. Orbit of the Eclipsing Binary TW Andromedae 439

SILBERSTEIN, LUDWIK. On the Spectrum of Neutral Helium. (*See also* Corrigenda, p. 216) 119

STRÖMBERG, GUSTAF. The Distribution of the Velocities of Stars of Spectral Types F to M 265

TAYLOR, LLOYD W. Width of Certain Lines of the Spectrum of Helium as a Function of Pressure in the Source 16

VAN MAANEN, A. Internal Motion in the Spiral Nebula N.G.C. 2403 . 200
  Internal Motion in the Spiral Nebula M 94=N.G.C. 4736 208
  J. C. Kapteyn, 1851–1922 145

WILSON, H. A. Quantum Theory of the Spectrum of Hydrogen . . 34

WYLIE, CHARLES CLAYTON. Cepheid Variable η Aquilae 217
  Eclipsing Binary σ Aquilae 232

YOUNG, ANNE S. Review of: *The Telescope.* Louis Bell . . . 486

BINDING [illegible] MAY 1 1 19

QB
1
A9
v.55-56
[redacted]
cop.3
Physical &
Applied Sci.
Serials

The Astrophysical journal

PLEASE DO NOT REMOVE
CARDS OR SLIPS FROM THIS POCKET

UNIVERSITY OF TORONTO LIBRARY

STORAGE